A TREATISE ON

APPLIED HYDRAULICS

By the same Author

HYDRAULIC MEASUREMENTS

CENTRIFUGAL AND OTHER ROTODYNAMIC PUMPS

LAND, WATER AND FOOD

A TREATISE ON

APPLIED HYDRAULICS

by

HERBERT ADDISON

O.B.E., M.Sc., M.I.C.E., M.I.Mech.E.

Formerly Professor of Hydraulic Machines
at the Fouad I University
Giza, Egypt

★

FOURTH EDITION

REVISED AND ENLARGED

REPRINTED

ASIA PUBLISHING HOUSE

BOMBAY CALCUTTA NEW DELHI MADRAS

1959

FIRST PUBLISHED 1934
SECOND EDITION 1938
REPRINTED 1941
THIRD EDITION 1944
REPRINTED 1948
REPRINTED 1950
FOURTH EDITION 1954
REPRINTED 1956
REPRINTED 1959

PRINTED IN GREAT BRITAIN
AT THE ABERDEEN UNIVERSITY PRESS LIMITED
ABERDEEN, SCOTLAND

PREFACE

SINCE the first edition of this book was prepared twenty years ago, the art of Hydraulic engineering and the sciences on which it depends have alike made uninterrupted progress. These advances—advances in the design and construction of hydraulic machines and of hydraulic structures—have been recorded in numerous specialised technical books and papers. Yet this extension of knowledge has not lessened the need for a general book such as this one. On the contrary, the author believes that students and engineers are glad to have a text-book which limits itself to direct explanations of hydraulic principles, while yet serving as a guide to sources where more detailed information may be found.

In the present edition, therefore—the Fourth Edition—little change has been made in the style of presentation that has found favour with readers of earlier editions. Naturally, the subject matter has been carefully revised, nor has the resulting increase in bulk been in any way disproportionate to the widening of the field that must be covered. As it now stands, then, the book epitomises the author's experience in the lecture room and the laboratory during thirty years of instruction and research.

Only one specifically new section has been introduced : it is a brief collection of biographical notes about some of the outstanding personalities whose efforts did so much for the advancement of Hydraulics. But while we all—readers and author alike—are indebted to these pioneers, the author cannot forget that he is under another obligation also : he gratefully acknowledges the debt he owes to the various firms, organisations and individuals who so kindly assisted in the preparation of this book in all its stages.

HERBERT ADDISON

LONDON, 1952.

CONTENTS

(Paragraph headings are given on the first page of each chapter)

PART I

FUNDAMENTAL PRINCIPLES

PART II

PRACTICAL APPLICATIONS

PART I

FUNDAMENTAL PRINCIPLES

CHAPTER I

LIQUIDS AND THEIR PROPERTIES

1. Introductory. Hydraulics may be defined as the application of the principles of Hydrostatics and Hydrodynamics to practical engineering problems. In general these problems comprise the design, construction, and operation of devices for controlling water in various ways: for regulating its flow in natural waterways, for conducting it along pipes and channels, for developing water power from rivers and lakes, and for raising water from one level to another. When required, these devices must also be adapted for dealing with other liquids as well, e.g. oils, spirits, etc.

2. Units of Measurement. Systems of units suited to various countries and to various kinds of hydraulic calculations are classified in Table 1 (overleaf). For converting from one system to another, the complete *Table of Conversion Factors* may be used: it is found on page **693**, at the end of the book, immediately following the *Key to Symbols* on page 691.

3. Liquids and their Properties. In ordinary usage there is no difficulty in recognising a liquid or in distinguishing liquids from solids and gases. A solid has a fixed shape which it retains whatever we do to it; a billiard ball is a sphere, and no ordinary forces that we can apply to it will sensibly alter its shape. But we do not associate liquids with the notion of shape; on the contrary, a liquid takes instead the shape of whatever vessel it is poured into. If the volume of liquid is less than that of its containing vessel, there will be a horizontal

TABLE I.

UNITS OF MEASUREMENT USED IN HYDRAULICS.

Quantity to be Measured.	Symbol.	System of Units.	
		Foot.	Metric.
Weight .	W	Pound (lb.). Ton = 2240 lb.	Kilogram (kg.). Metric ton = 1000 kg.
Force .	P	The weight of 1 lb.	The weight of 1 kg. Dyne.
Mass * .	M	Slug.	Gram (gm.).
Length .	L l	Foot (ft.).	Centimetre (cm.). Metre (m.). Kilometre (km.).
Volume .	Q q	Cubic foot (cu. ft.). Imperial gallon (gall.) = 0·1605 cu. ft.	Cubic centimetre (cu. cm.). Litre (lit.) = 1000 cu. cm. Cubic metre (cu. m.). = 1000 litres.
Time .	t T	Second (sec.). Minute. Hour.	Second. Minute. Hour.
Rate of flow	Q q	Cubic feet per second (cusec. or c.f.s.). Gallons per minute.	Cubic centimetres per second (cu. cm./sec.). Litres per second (lit./sec.). Cubic metres per second (cu. m./sec. or m.^{3}/sec.).
Energy .	E	Foot-pound (ft.-lb.).	Kilogram-metre (kg. m.).
Power .	P	Horse-power (h.p.) = 550 ft. lb./sec.	Metric horse-power = 75 kg. m./sec.
Temperature	T t	Degree Fahrenheit, °F.	Degree centigrade, °C.

* In all systems the relation between weight and mass is :—

$$\text{Mass} = \frac{\text{Weight (= force of gravity)}}{\text{Acceleration due to gravity}} = \frac{W}{g}.$$

Thus :—

$$\text{Mass in slugs} = \frac{\text{pounds weight}}{\text{32·2 ft. per sec. per. sec.}}.$$

$$\text{Mass in grams} = \frac{\text{dynes}}{\text{981 cms. per sec. per. sec.}}.$$

Note : The units pound (mass) and poundal (force) are not used in this book.

free surface exposed to the atmosphere. Gases, on the other hand, always completely fill the vessels which hold them.

In the following paragraphs the further properties of liquids of which the engineer must be cognisant are briefly examined.[1]

4. Density of Liquids. The density of a liquid may be expressed either as the

Specific weight, or weight per unit volume $= w$,

or as the

Specific mass, or mass per unit volume $= \rho$.

The relation between the two is invariably :—

$$\rho = w/g.$$

Thus, specific *weight* of water at atmospheric temperature,

$w = 62{\cdot}4$ lb. per cubic foot,

or 981 dynes per cubic centimetre.

Specific *mass* of water at atmospheric temperature,

$\rho = 62{\cdot}4/32{\cdot}2 = 1{\cdot}94$ slugs per cubic foot,

or 1·00 grams per cubic centimetre.

Alternatively, liquid density may be expressed as a *ratio* between the specific weight of the given liquid and the specific weight of some standard liquid, e.g. distilled water at a temperature of 4° C. This ratio is termed the *specific gravity* (S.G.) of the liquid.

In particular industries, e.g. the petroleum industry, special arbitrary scales of density are often used.

5. Variations in Liquid Density.[2] These may be caused either by changes of *temperature,* or by changes of *pressure* (§ 17).

(i) *Effect of temperature.* The change produced by heating *water* is shown by the appropriate graph in Fig. 1, from which it is seen that at 212° F. (100° C.) the density of water is nearly 5 per cent. less than it is at 32° F. (0° C.). This reduction proceeds still more rapidly at higher temperatures, thus :—

Temperature of water (degrees) Fahr.	39	122	212	302	392	482
Temperature of water (degrees) Cent.	4	50	100	150	200	250
Relative density at saturation pressure	1·000	0·989	0·957	0·917	0·865	0·797

[1] See Bibliography, page 695.

The density of an *oil* or a *spirit*, besides being in general lower than that of water (see Table III, § 9), usually responds in a more uniform way to temperature changes. Over quite a wide range of temperature, a given *rise* of temperature produce as *constant* diminution of the density of a specified liquid. For liquids such as lubricating oils, this relationship can be expressed :—

$$dS = - A \, . \, dt,$$

where dt = change of temperature (deg. F.),

dS = corresponding change in specific gravity,

A = a constant having a value of the order of 0·00035 to 0·00040.

(ii) *Effect of Pressure.* Although for many purposes liquids may be regarded as incompressible, yet they do in fact yield slightly under pressure. The characteristic of the liquid which determines the amount of elastic yield is termed the *Bulk Modulus* or the *Elastic Modulus* of the liquid : [3] it is comparable with the Modulus of Elasticity of a solid, and is denoted by the symbol K.

If q = original volume of liquid,

dp = change of pressure,

dq = corresponding change of volume,

Then
$$\frac{dq}{q} = \frac{dp}{K}.$$

In other words, if the liquid could be imagined to remain perfectly elastic, the Bulk Modulus K represents the pressure per unit area required to compress the liquid to zero volume.

TABLE II.

Liquid.	Mean Pressure (lb./sq. in.) (psi.)	Bulk Modulus K (lb./sq. in.) (psi.)
Water	Atmospheric	200,000
	50	250,000
	Above 100	300,000
Crude oil	Above 400	250,000
Petrol (gasoline)	Above 400	150,000

Table II gives some approximate values of K, suitable for general use, for liquids at atmospheric temperature.

Since the Bulk Modulus of *water* is only slightly affected by temperature changes, it is convenient to remember that its value may safely be taken as 300,000 psi., or 21,000 kg./sq. cm. This means that an increase of pressure of 3000 psi. is required to increase the density of water by *one* per cent.

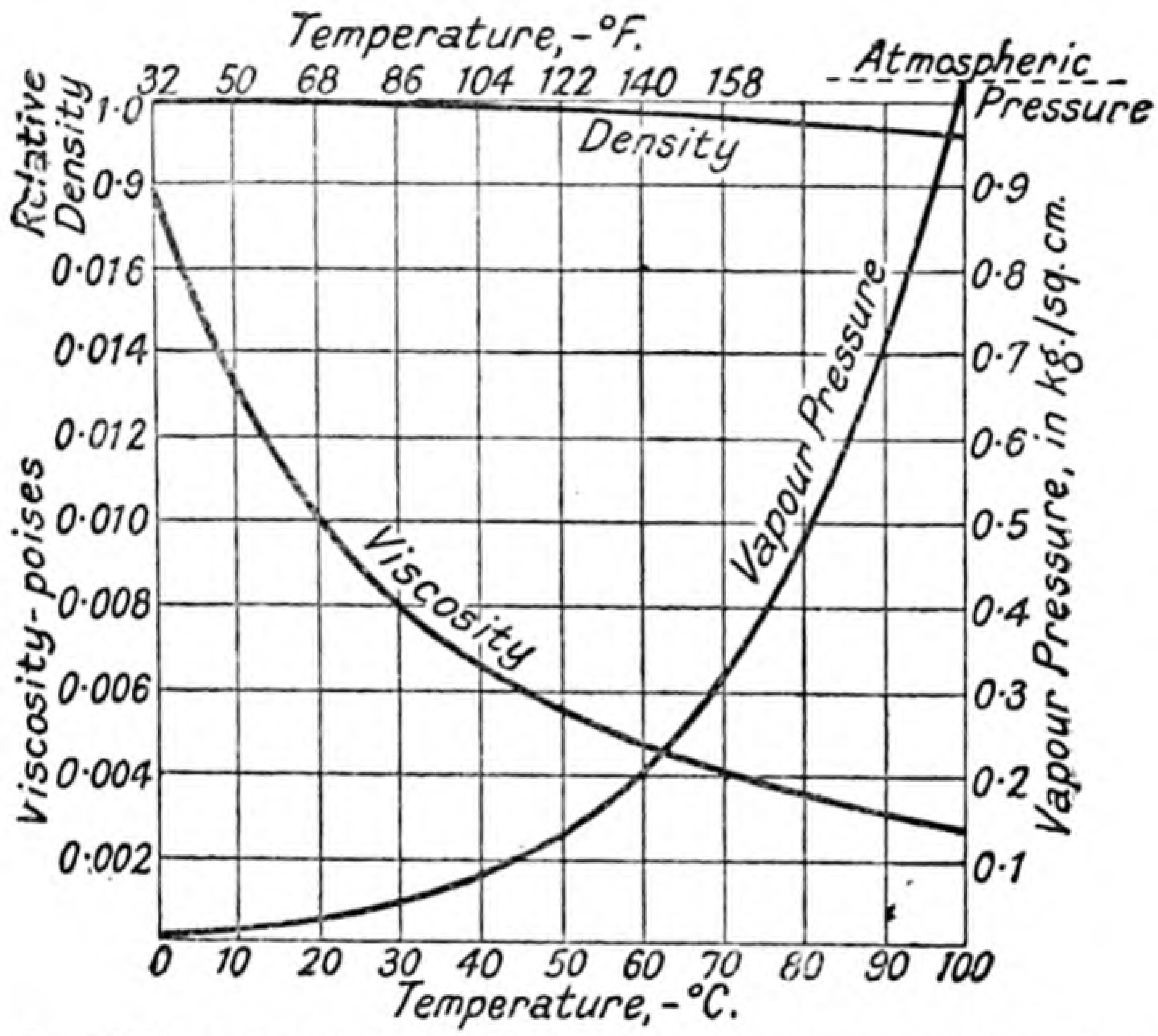

FIG. 1.—Effect of temperature on physical properties of water.

The Bulk Modulus of *oils*, etc., is substantially *reduced* as the temperature *rises*, or as the mean *pressure* falls below the values given in Table II.

6. Surface Tension. Although in general terms we regard a liquid as being unable to maintain any fixed shape unless supported by the walls of a containing vessel, yet it is not difficult to recall instances of small amounts of liquid which do unaided preserve a very definite form. Such are drops of water hanging from an imperfectly closed tap, which behave as though each were enclosed in a thin bag or membrane similar to a minute toy india-rubber balloon. The property of liquids which permits of this formation is known as *surface tension*; it is on account of surface tension that a vessel with a horizontal brim may be filled more than brimful with water, the same invisible "skin" which sustains the drops also restraining the excess water from spilling over.

If we consider an imaginary line drawn along this "skin" or surface, there will be a tendency for opposing forces to tear the surface apart along this line. It is the *force per unit length* acting across the line, which serves as a measure of surface tension. Some approximate values, for common liquids at a temperature of 68° F. in contact with air, are :—

Liquid.	Surface Tension in Dynes per centimetre.
Water	73
Oils	about 30
Mercury	510

These figures show how small are the forces involved in surface tension effects : along a line 200 ft. long in a water/air surface, the total tension would amount to 1 lb. weight only.

In addition to the formation of drops of water mentioned above, other examples of surface tension are given by bubbles of air or vapour in water, and drops of oil in water.

Only occasionally is it necessary to take surface tension effects *numerically* into account in hydraulic calculations ; the height of liquids standing in gauge tubes is one example (§ 372 (i)).

7. Viscosity. An essential property of a liquid is that it will flow, but since "thin" liquids such as water or alcohol flow much more easily than "thick" liquids such as syrup or heavy oil, each liquid must have some characteristic property which controls its rate of flow. This property is termed viscosity—it is the property in virtue of which the liquid resists any deforming force—it gives a measure of the reluctance of the liquid to yield to shear. That there is a connection between the deforming force and the *rate* of yielding to it is easily seen by trying to pull a spoon vertically out of a jar of thick syrup. Hardly any effort is needed if the spoon is raised slowly, but if the spoon is jerked up sharply the liquid is so unwilling to release it that the jar and its contents may be lifted bodily off the table.

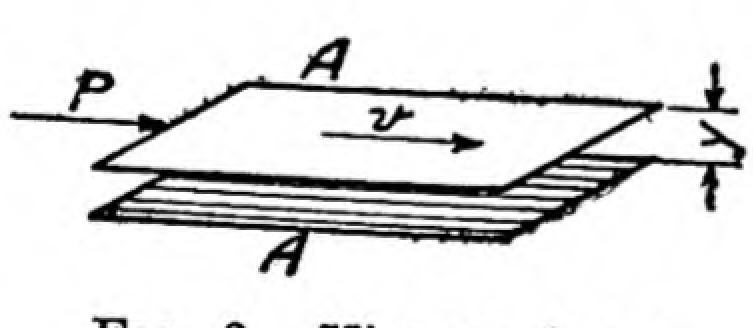

FIG. 2.—Viscous shear.

The forces called into play in overcoming viscosity may be studied by imagining a very thin layer of liquid sandwiched between two flat parallel plates as in Fig. 2. To cause the upper plate to slide over the lower one, thus shearing the intervening film of liquid, a tangential force P must be applied, which is found to have the value

$$P = \mu A \frac{v}{y} \quad . \quad . \quad . \quad . \quad (1\text{-}1)$$

where A denotes the area of each of the plates,
v ,, the velocity of one plate relative to the other,
y ,, the thickness of the film of liquid,
and μ (*mu*) is the *viscosity* of the liquid, sometimes termed the *coefficient of viscosity*, or the *dynamic viscosity*, or the *absolute viscosity*.

If A, v, and y each have the value unity, μ will numerically be equal to P, whence the definition that "the viscosity of a liquid is the numerical value of the tangential force on unit area of either of two parallel planes at unit distance apart, when the space between these planes is filled with the liquid in question and one of the planes moves with unit velocity in its own plane relatively to the other."

As to the manner in which the liquid behaves when undergoing viscous shear, we may regard the film in Fig. 2 as being itself made up of innumerable parallel sheets or laminæ of liquid of infinitesimal thickness, sliding one over the other. The lower plate being at rest, the lowermost lamina is also imagined to be at rest, the uppermost lamina has the same velocity v as the upper plate, and the intermediate ones have velocities proportional to their distances from the lower plate. Thus the velocity of the lamina distant y_1 from the lower plate would be $y_1 \cdot \frac{v}{y}$, where $\frac{v}{y}$ is termed the *velocity gradient.*

The *intensity of viscous shear*, or *viscous shear stress*, τ, *at a* point in a liquid at which the velocity gradient is $\frac{dv}{dy}$, can evidently be put in the form

$$\tau = \frac{P}{A} = \mu \cdot \frac{dv}{dy} \quad . \quad . \quad . \quad (1\text{-}2)$$

An alternative way of describing viscous properties is to use the term *kinematic viscosity*. The *kinematic viscosity* of a liquid is represented by ν (*nu*) $= \frac{\mu}{\rho}$, where μ denotes the viscosity, and ρ (*rho*) denotes the specific mass of the liquid. § 4.

8. Units of Viscosity. From equation 1-1 it is seen that *viscosity* μ must be expressed in terms of $\frac{\text{force} \times \text{time}}{\text{area}}$. Thus in the C.G.S. system of units in which the unit of force is the dyne, the unit of viscosity would be $\frac{\text{dyne} \times \text{second}}{\text{sq. cm.}}$: the name given to this unit is the *poise*.

The *centipoise*, written *cp.*, is 1/100 of a poise.

In foot units the unit of force is the weight of one pound, and viscosity must therefore be expressed in terms of $\frac{\text{lb.} \times \text{sec.}}{\text{sq. ft.}}$ There is no specific name for this unit.

To convert viscosity in poises (C.G.S. units) to viscosity in foot units, multiply by 0·00209. **(Example 1.)**

Kinematic viscosity has the form

$$\nu = \frac{\text{viscosity}}{\text{specific mass}} = \frac{\left(\frac{\text{force} \times \text{time}}{\text{area}}\right)}{\left(\frac{\text{mass}}{\text{volume}}\right)}.$$

But Force can be expressed : mass × acceleration,

or
$$\text{mass} \times \frac{\text{length}}{(\text{time})^2}.$$

Whence :—

$$\text{Kinematic viscosity} = \frac{\left[\frac{\text{mass} \times \left(\frac{\text{length}}{(\text{time})^2}\right) \times \text{time}}{(\text{length})^2}\right]}{\left[\frac{\text{mass}}{(\text{length})^3}\right]}$$

$$= \frac{(\text{length})^2}{\text{time}} = \frac{\text{area}}{\text{time}}.$$

It is because of the simplicity of this relationship that kinematic viscosity is a more convenient quantity than dynamic viscosity, § 7.

In the foot system of units, kinematic viscosity is expressed in *square feet per second.*

In the C.G.S. system, the unit of kinematic viscosity is the *stoke*, viz : one square centimetre per second.

The *centistoke* is 1/100 of a stoke.

To convert values of kinematic viscosity in *stokes* to kinematic viscosity in foot units, multiply by 0·00108.

9. Variations in Viscosity. (*a*) The general effect of *temperature* on the viscosity of liquids is known to us [4] from common observation : to *reduce* the viscosity—to make the liquid flow more easily—we must heat it. Likewise we should imagine that the viscosity of a heavy oil would be much higher than the viscosity of water. These impressions are given numerical form in Table III, and in the Viscosity curve for water in Fig. 1. It is worth remembering that for rough estimates, the value both of the viscosity and of the kinematic viscosity of water at ordinary atmospheric temperatures is 0·01 in C.G.S. units. But the corresponding values in foot

TABLE III.

VISCOSITY OF LIQUIDS AT DIFFERENT TEMPERATURES (IN POISES).

Liquid.	Approximate S.G.	μ = Viscosity in Poises at stated Temperature in degrees Centigrade.					
		0°.	20°.	40°.	60°.	80°.	100°.
Water . .	1·00	0·0179	0·0101	0·0066	0·0048	0·0036	0·0028
Alcohol . .	0·79	0·0177	0·0120	0·0083	0·0059		
Paraffin (kerosene)	0·81	0·032	0·020	0·013	0·009		
Petrol (gasoline) .	0·75	0·0071	0·0055	0·0044	0·0036		
Motor-car engine lubricating oil (light) . .	0·94		3·55	0·72	0·28	0·14	0·07
Do. do. heavy .	0·94			2·52	0·73	0·31	0·17

units are 0·0000209 and 0·0000108 respectively, from which it is clear that the C.G.S. system is usually to be preferred when viscosity is to be taken numerically into account.

(*b*) The effect of *pressure* on the viscosity of *water* is inappreciable—at least for pressures below 1000 atmospheres (15,000 psi). But *oils* are much more sensitive: their viscosity invariably *rises* as the pressure increases.[5] At a pressure of 1000 psi. the oil viscosity may be 10 per cent. or 15 per cent. greater than its value at atmospheric pressure, while if the pressure rises to 15,000 psi. there may be a ten-fold increase in viscosity.

These changes can be expressed by the general approximate equation :—

$$\eta/\eta_o = e^{\phi(p - p_o)}$$

where η = viscosity in centipoises at absolute pressure p kg./sq. cm.

η_o = viscosity in centipoises at absolute pressure p_o kg./sq. cm.

ϕ = a coefficient whose value may range from 0·001 to 0·004, depending upon the kind of oil.

e = base of Napierian logarithms = 2·7183.

The *measurement* of viscosity is described in §§ 370-371, where various arbitrary scales of viscosity, e.g. the Redwood scales, are mentioned.

The general *effect* of viscosity is always to damp down relative motion between different parts of a liquid, and if no external energy is supplied, viscosity will invariably in time reduce the liquid to a state of quiescence. The energy absorbed in overcoming viscous resistance is wholly transformed into heat energy; thus viscosity plays a part in hydraulics analogous in many ways to mechanical friction. Nevertheless it is convenient in many problems of hydraulic flow to regard water as a "perfect" liquid having zero viscosity, and then later to apply a correction factor to allow for the viscous forces which, although small, do exist.

10. Vapour Pressure. Vapour always tends to be liberated from the free surface of liquids, exerting a definite pressure which depends on temperature; the relation between the temperature and the vapour pressure (or "vapour tension")

of water is represented by the appropriate graph in Fig. 1, § 5. The practical effect of this pressure is to reduce the height of the column of water that can be sustained by atmospheric pressure (§ 16), and thus to limit the permissible suction head on pumps and turbines.

Water will boil even at atmospheric temperatures if the absolute pressure to which it is subjected is reduced down to the vapour pressure corresponding to the temperature. This generation and sudden collapse of bubbles of vapour may result in the destructive phenomenon of cavitation erosion (§ 134).

The volatility of spirits, e.g. alcohol, petrol (gasoline), etc., is a consequence of their relatively greater vapour pressure, as compared with that of water.

The actual loss of water by evaporation [(6)] from the surfaces of reservoirs, lakes, etc., varies from a negligible amount in very cold, damp weather up to nearly ½ in. depth daily in dry, tropical climates.

11. Impurities in Liquids. As the engineer is very rarely called upon to handle pure water, he must take cognisance of the various ways in which dissolved or suspended solids, gases, or other liquids will modify the properties of the water. In particular, he must so construct the pipes and vessels with which the impure water comes in contact that they are not damaged by chemical or electrolytic action.

Dissolved Solids. These usually have the effect of increasing the *density* of water,[(7)] raising its *boiling-point*, and lowering its *freezing-point.* Thus the specific gravity of sea-water may rise to 1·03 or more ; moreover, in order to withstand its corrosive action, sea-water pumps should preferably be made of non-ferrous alloy (brass, bronze, etc.) rather than of iron.

Dissolved Liquids. Quite small traces of dissolved acids may enable water to set up serious electrolytic effects. The acidity or alkalinity of water, whether due to free acids or not, can conveniently be expressed in terms of the hydrogen-ion content (*p*H value) of the water. Knowing this value, the designer is helped to choose materials likely to have the necessary endurance.

Concentrated acids can only be handled at all if the pumps, pipes and containers are lined with special materials such as lead, stoneware, etc.

Dissolved Gases. Water at atmospheric pressure and 32° F. will dissolve about 3 per cent. of its own volume of *air* ; this air may be driven out of solution either by heating the water or by reducing the pressure on it. The liberation of air bubbles at low pressures—particularly at sub-atmospheric pressures—is a fruitful source of annoyance ; unless measures are taken to vent the free air or otherwise dispose of it, these small accumulations may hamper or entirely stop the working of pumps, falsify the readings of gauges, and display a surprising range of mischievous activities. Dissolved air has so destructive an effect on high-pressure steam boilers that most rigorous control must be exercised to ensure that only air-free water is fed into them.

Entrained Gases. Small bubbles of gas—usually air—may be entrained by flowing water, oil, etc., and may persist for quite a long time before they finally escape.[8] Until they do, these bubbles may influence the apparent density, compressibility, etc., of the liquid.

Suspended Solids are found in nearly all natural rivers and water-courses, ranging in size from boulders down to impalpable mud and silt, § 200. These solids can, if necessary, be removed from the water by various processes of straining, sedimentation, and filtration. Channels such as sewers and irrigation canals must be so designed that the suspended solids are carried along and not deposited on the bed of the waterway. Pumps must be specially constructed to withstand the mechanical or abrasive effect of heavily-charged waters, especially if the suspensions are sharp and gritty, as they often are in industrial and metallurgical processes.

The presence of solids in suspension may affect the laws of flow when a liquid passes along a channel or through a pipe (§ 160 (iii)). In extreme cases, where the mixture has the consistency of a paste, its viscous properties are profoundly modified. Behaving as a *non-Newtonian* liquid—a name given to distinguish the paste from the true Newtonian liquids described in §§ 7-9—its viscosity is not a constant at a given temperature, but it depends upon the apparent rate of shear, i.e. upon the velocity gradient.[9]

CHAPTER II

LIQUIDS AT REST; STATIC PRESSURE, ETC.

12. Static Pressure. If a rectangular vessel be filled with a liquid at rest (Fig. 3), the total downward force exerted by the liquid on the horizontal base of the vessel will be equal to the total weight of the liquid. Let this weight $= W$. If A be the area of the base, then the force per unit area exerted on the base by the liquid will be $W/A = p$. This force per unit area p is known as the *unit pressure* or the *specific pressure* or the *intensity of pressure* or the *static pressure* or the *hydrostatic pressure*.

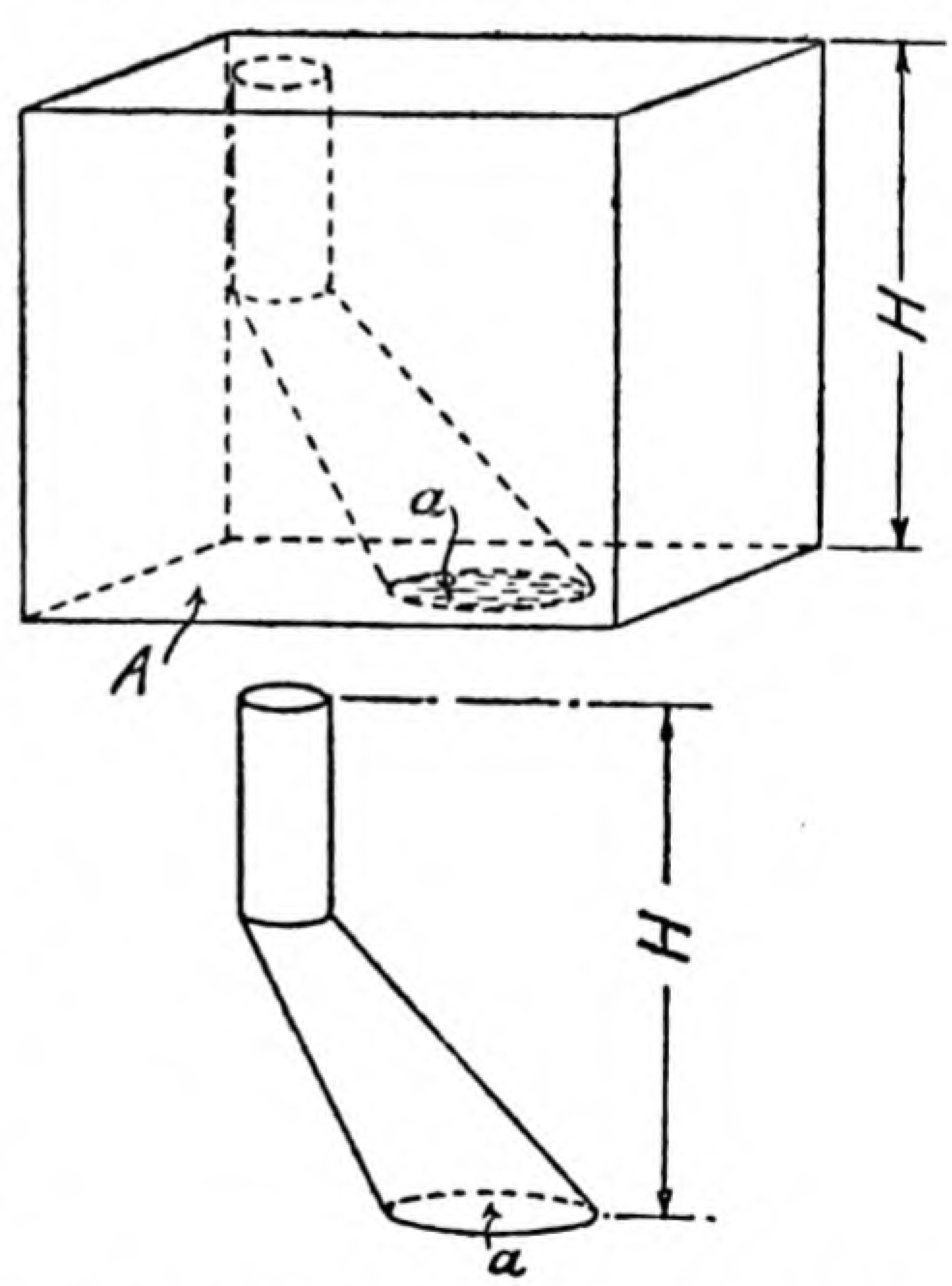

FIG. 3.—Pressure under head H.

Further, if H be the depth of the liquid, and w its density in terms of weight per unit volume, then $W = wAH$ and $p = wAH/A = wH$. The same reasoning would apply to any horizontal plane passing through the liquid; if the plane is at a distance h vertically below the free surface, then the pressure at any point in this plane is

$$p = wh \qquad \qquad (2\text{-}1)$$

Consider now a very small cubical element of liquid, with its upper and lower faces horizontal, at a mean distance h below the surface. Since this cube is at rest, there must be an upward force acting on it exactly equal to the downward force as calculated above; moreover, these opposed forces would certainly flatten out the cube unless there were equally intense horizontal forces supporting the vertical faces of the cube. Similarly, by imagining the element to be turned successively in different directions, we reach the conclusion that the pressure at a point in a liquid at rest is the same in all directions.

A more precise examination of the forces acting on the element shows that only in the limiting case of an infinitely small distance between the upper and lower faces is it true to say that on both these faces the same pressure prevails. As soon as this distance has an appreciable value, it is manifest from equation (2-1), and from the pressure gradient shown in Figs. 5 and 6, that the pressure on the lower face of the element is *greater* than the pressure on the upper face. It is the resulting upward differential thrust that opposes the downward force of gravity acting on the element.

It is self-evident that the pressure exerted by a liquid on a plane area must be *normal* to the area. The pressure could only have a component parallel with the plane if the liquid were in shear, but since the liquid is at rest, viscous or shearing forces cannot exist, therefore such parallel components are impossible.

13. Static Head. The vertical distance h between any selected point in a liquid at rest and the free surface exposed to the atmosphere is spoken of as the *head* of liquid above the point. Alternatively we might say that at the selected point the head or the *static head* or the *pressure head* is h. The connection between head and intensity of pressure is given by equation 2-1 above, viz. $h = \frac{p}{w}$.

It is by no means essential that there should be a continuous *vertical* column of liquid between the free surface and the point at which the head or pressure is measured, nor has the shape of the vessel any influence on the pressure. Consider any small area a as shown by hatching on the base of the vessel (Fig. 3). Now let this area be surrounded by a tube of any sort extending up to the surface—in the diagram an irregular

inverted funnel is suggested. Clearly the mere lowering into position of this contrivance can have no effect on the pressure on the hatched area ; nor will this pressure be altered if we run off the exterior liquid surrounding the funnel and thus leave the funnel, its contents, and the area at its base isolated as shown in the lower part of Fig. 3.

Extending this reasoning, it can be stated that in any system of freely inter-communicating tanks, reservoirs, or passages filled with liquid at rest, all parts of the liquid in a given horizontal plane will be subjected to the same head, this head being measured vertically from the plane passing through the free surface, no matter how far distant horizontally the free surface may be. Even if there is no visible or existing free surface, as may happen in a system of piping in which the pressure is maintained artificially by a pump, it is simple to calculate where the free surface would be if an open pipe could be connected to the system high enough for a free surface to be formed.

14. Gauge and Absolute Pressures. In the preceding paragraphs it has been stated that the pressures under discussion are those due to the liquid *only ;* they are thus often spoken of as *gauge* pressures, because they have the values that would be indicated by ordinary types of pressure gauge (§§ 372-374). To obtain the total unit pressure from all causes, or *absolute pressure,* we must add to the gauge or hydrostatic pressure the pressure which the atmosphere is exerting on the surface of the liquid.

The mean pressure of the atmosphere at sea-level is usually assumed to be 14·7 lb./sq. in. (1·03 kg./sq. cm.) ; it is equivalent to a head of 33·9 ft. (10·3 metres) of water, or to a head of 29·9 ins. (76·0 cms.) of mercury ; or to 1013 millibars (1 millibar (mb.) = 1000 dynes/sq. cm.). The effect of altitude on mean barometric pressure is shown in the accompanying table.

Altitude above sea-level	Feet. Metres.	0 0	3280 1000	6560 2000	9840 3000	13,120 4000
Barometric pressure expressed in head of water.	Feet. Metres.	33·9 10·3	30·2 9·2	26·6 8·1	23·6 7·2	20·7 6·3

In hydraulic calculations, gauge pressures are commonly used—unless otherwise stated the values in this book refer to pressures above or below atmosphere.

15. Negative Pressure and Negative Head. If the absolute pressure at a point in a hydraulic system is less than the pressure of the atmosphere, we say that at such a point there exists a *negative pressure* or *negative head.* Fig. 4 shows the conditions in which a pressure of this kind might be produced; here a tube dips at its lower end beneath the surface of the liquid in a small reservoir. If the upper end of the tube be open to the atmosphere, the liquid at A will stand at the same level inside the tube as it does outside; if, now, air is pumped from the upper end, the liquid will rise in the tube—we say that the pump is drawing or sucking the liquid up. Nevertheless we know that what is actually happening is that the atmospheric pressure acting on the free surface of the liquid in the reservoir is forcing or pushing the liquid up the tube. Under ideal conditions, in which the pump could produce a perfect vacuum and the liquid had zero vapour pressure, the liquid would rise to a maximum height equivalent to the true height of the barometer.

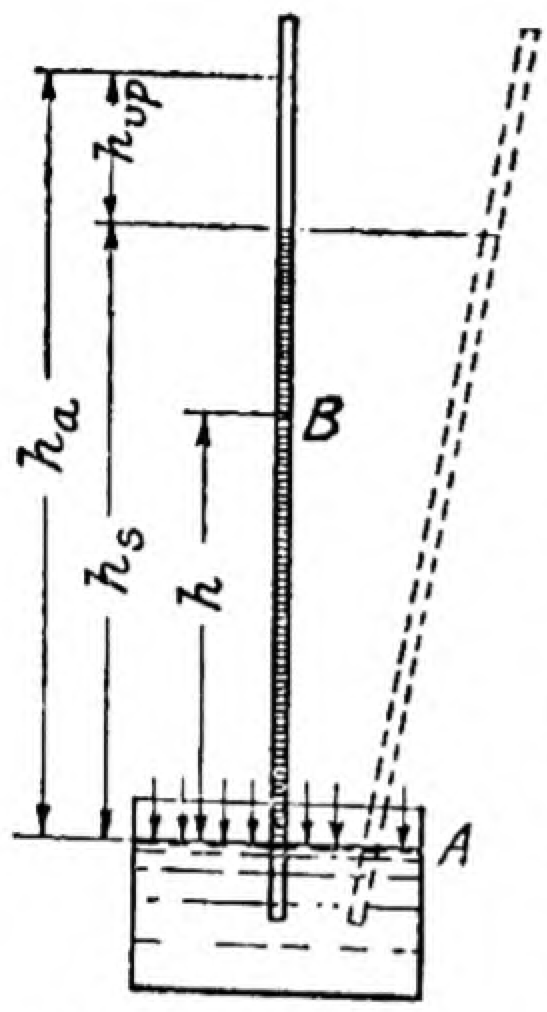

FIG. 4.—Negative head.

At any point B in the column of liquid there will now be a negative pressure, which may be computed as follows: At a point A inside the tube at reservoir level, the absolute pressure must be equal to the pressure of the atmosphere $= p_a$; the static pressure due to the column of liquid between B and A is wh, where w is the density of the liquid and h is the vertical distance BA; therefore the absolute pressure at A, viz. p_a, must be greater than the absolute pressure at B, p_b, by an amount wh. Hence $p_a = p_b + wh$, or $p_b = p_a - wh$. The *gauge* pressure at B is thus $(p_a - wh) - p_a = -wh$, and the head at B is $-\left(\frac{wh}{w}\right) = -h$. Such negative heads are also spoken of as *vacuum* heads or *suction* heads.

It is evident, then, that the definition offered at the

beginning of § 13 is quite a general one ; if the selected point is *below* the free surface of the liquid, h is positive and the head is positive ; if the point is *above* the free surface, h is negative and the head is negative.

16. Limiting Values of Negative Head. The maximum attainable negative head depends upon the barometric pressure and upon the vapour pressure of the liquid. In Fig. 4, if h_a is the height of the column of liquid equivalent to the barometric pressure, corrected for altitude, and h_{vp} is the head equivalent to the vapour pressure of the liquid at the appropriate temperature and in the appropriate units, then the limiting height of column will be $h_s = h_a - h_{vp}$. No matter for how long the exhausting pump connected to the top of the tube were worked, the liquid would never rise to a greater height than h_s—continued pumping would merely draw off more and more vapour from the liquid surface inside the tube. If the liquid were heated, the column would fall due to the increase in vapour pressure (§ 10), until at boiling-point the head h_s would have diminished to zero. (See vapour pressure curve for water, Fig. 1, § 5.)

The inclined tube shown in broken lines in Fig. 4 has been added as a reminder that such inclination has no effect on the conclusions just reached, so long as all distances are still measured *vertically*. **(Example 5.)**

17. Units of Pressure and of Head. Positive pressures are usually stated in terms of pounds per square inch (lb./sq. in. ; psi.), or of kilograms per square centimetre (kg./sq. cm.), or of atmospheres. A pressure of 1 kg./sq. cm. = 14·22 lb./sq. in. = 0·97 atm.

Heads, either positive or negative, are expressed in feet, centimetres or metres.

Negative, vacuum or suction heads are also stated in terms of inches (or centimetres) head of mercury.

The numerical relationships between the various systems of units are given in the general conversion table, page 693, but it is worth memorising that at normal atmospheric temperature :

1 ft. head of fresh water is equivalent to a pressure of
62·4 lb./sq. ft. = 0·434 lb./sq. in.

1 metre head of fresh water is equivalent to a pressure of
1000 kg./sq. metre = 0·1 kg./sq. cm.

If any hydraulic problem offers a choice of a solution in terms of pressure or in terms of head, it is frequently advisable to work in terms of *head*; in any event it is important to remember that in formula 2-1, if w is expressed in lb./cu. ft., and h in feet, then the units of p will be pounds per square *foot*, viz. 144 × lb./sq. inch.

18. Calculation of Total Thrust on Immersed Plane Surfaces. Knowing how to calculate the hydrostatic pressure at any point in a liquid, we can find the total resultant thrust exerted by the liquid over the whole of a given immersed surface by a process of summation. If the area is horizontal, the total downward thrust on it has been shown to be represented by wHA (§ 12).

To deal with a vertical area, e.g. the vertical face $ABCD$ of the tank full of liquid shown in Fig. 5, we consider first a very small element of area a, distant h below the free surface. The static thrust on this element, wha, is identical in value with the weight of liquid contained within the small horizontal prism of area a and length h indicated in broken lines. Thus the total thrust on the whole area $ABCD$ will be equal to the sum of the weights of all the small prisms similar to the one just described; and this sum is simply the weight of liquid contained within the (imaginary) wedge $ABCDEF$, of which the inclined face makes an angle of 45° with the horizontal. In brief,

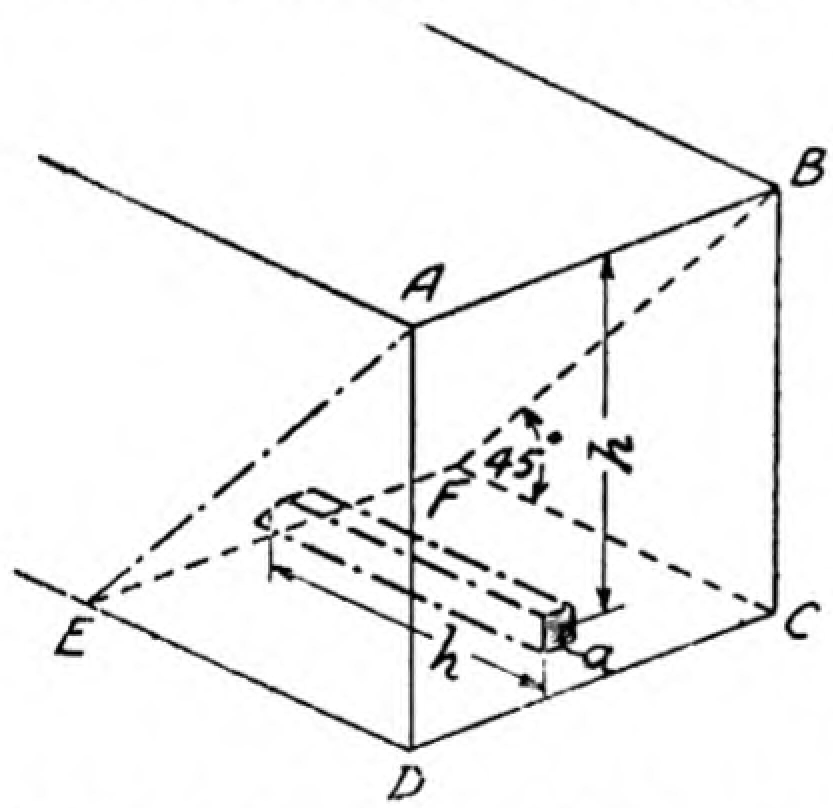

FIG. 5.—Thrust on vertical surface.

Total hydrostatic thrust P = total weight of wedge.

In calculating the total thrust on any selected area of the vertical side of the vessel, e.g. on the door RST shown by hatching in Fig. 6, it is now necessary to find the weight of liquid contained within the appropriate *prism*. This prism has the same cross-section as the door; it is bounded perpendicularly at one end by the door and at the other end by the plane inclined at 45° which passes through the intersection of the plane containing the door, and the water surface.

The *line of action* of the total resultant thrust passes horizontally through the centre of gravity of the wedge or the prism ; the point at which this line of action cuts the area under discussion—point CP in Fig. 6—is termed the *centre of pressure* of the area.

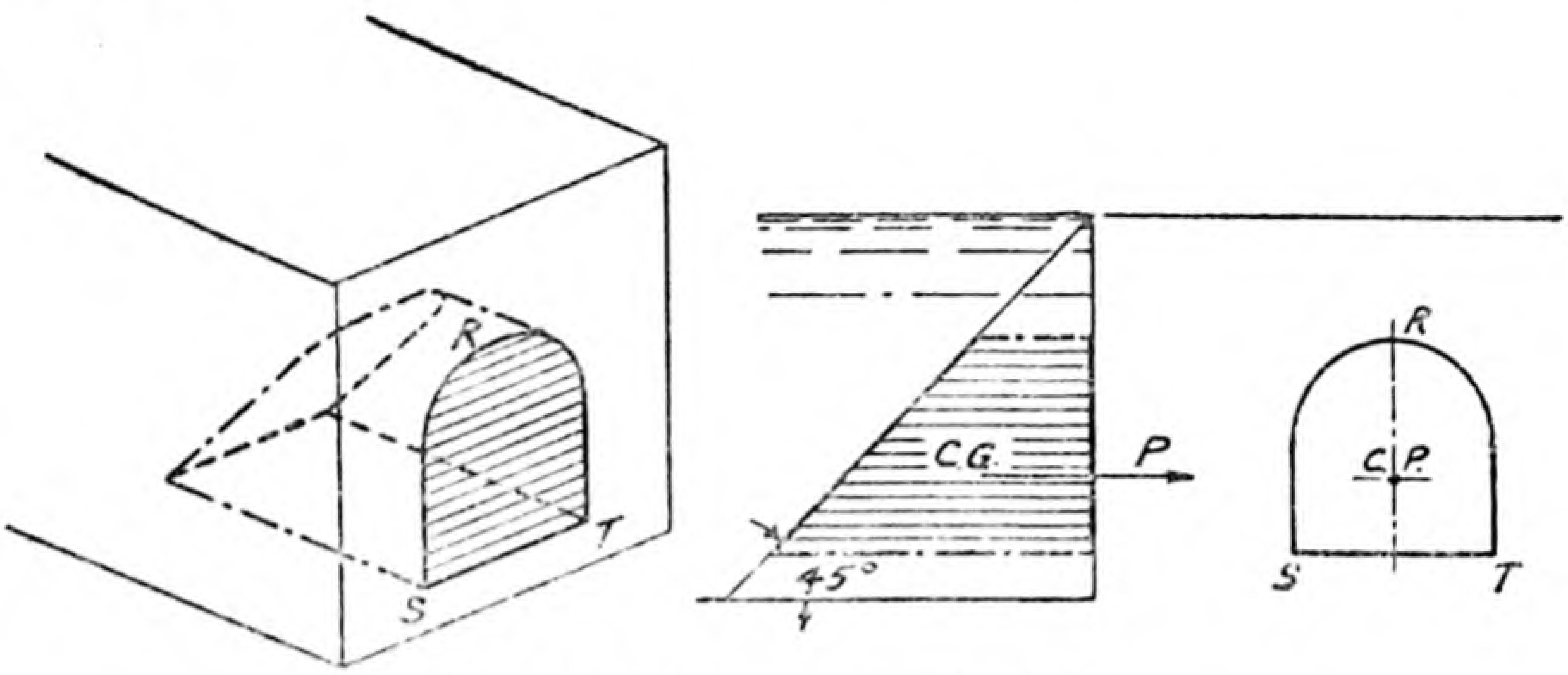

Fig. 6.—Thrust on vertical door.

19. Analytic Method of Calculating Static Thrust. Considering the general case of a lamina lying in a plane making an angle θ with the free surface of the liquid (Fig. 7), the total hydrostatic thrust on the hatched element, of area $b \cdot dx$, is—

$$\text{pressure} \times \text{area} = wh \cdot b \cdot dx = w \cdot x \;\sin\; \theta \cdot b \cdot dx.$$

Therefore P = total thrust on whole surface $= w \sin\theta \cdot \Sigma b \cdot x \cdot dx$.

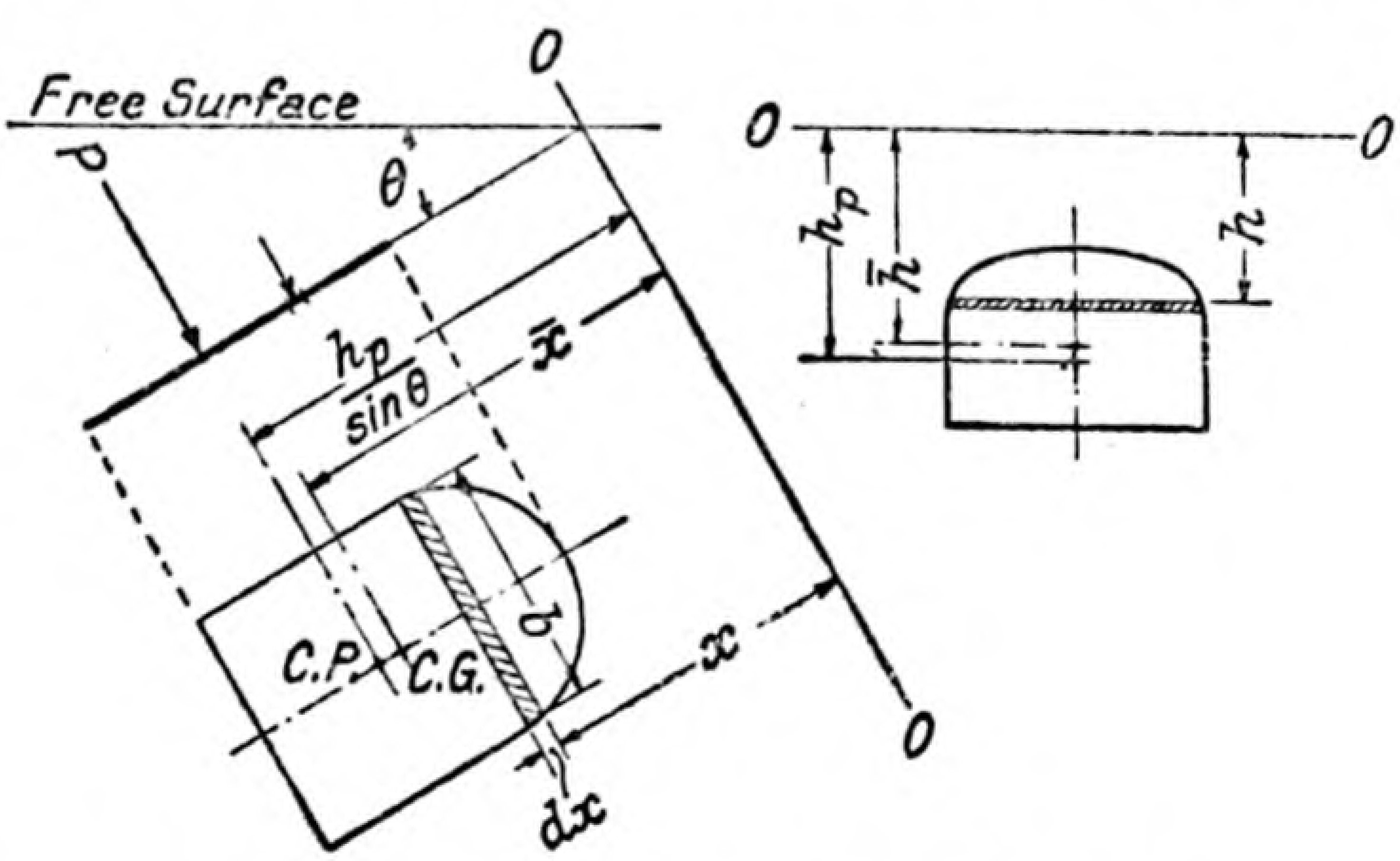

Fig. 7.—Static thrust on inclined surface.

But $\Sigma b \cdot x \cdot dx$ represents the total area A of the lamina $\times$ distance $\bar{x}$ of its centre of gravity from OO. Therefore

$$P = w \sin\theta \cdot A \cdot \bar{x} = wA\bar{h} \quad . \quad . \quad (2\text{-}2)$$

where $\bar{h}$ is the distance of the centre of gravity of the lamina vertically below the free surface. Alternatively,

total thrust = area × intensity of pressure at C.G. of area.

It will be observed that so long as the C.G. of the lamina remains in the same horizontal plane, the total thrust P remains unaltered, no matter how the lamina is turned or tilted.

The calculation of the position of the centre of pressure proceeds thus: Taking moments about OO (Fig. 7), the moment of the thrust on the elementary strip $= w \,.\, x \sin \theta \,.\, b \,.\, dx \,.\, x$, and the sum of the moments of the thrusts on all similar strips $= w \,.\, \sin \theta \Sigma b x^2 dx$, which also = moment of total static thrust.

Now $\Sigma b \,.\, dx \,.\, x^2$ is the moment of inertia I_o of the lamina about OO, therefore moment of total static thrust

$$= w \sin \theta \,.\, I_o \quad . \quad . \quad . \quad . \quad \text{(I)}$$

But, also, moment of total static thrust $= P \,.\, \dfrac{h_p}{\sin \theta}$

$$= wA\bar{h}\frac{h_p}{\sin \theta} \quad . \quad \text{(II)}$$

where h_p is the vertical depth of the centre of pressure below the free surface.

Equating (I) and (II),

$$h_p = \frac{I_o \sin^2 \theta}{A\bar{h}} \quad . \quad . \quad . \quad . \quad . \quad . \quad \text{(2-3)}$$

$$= \frac{\text{2nd moment of area about } OO \times (\sin \theta)}{\text{1st moment of area about } OO}.$$

It is often convenient to substitute in this equation

$$I_o = I_G + \frac{A\bar{h}^2}{\sin^2 \theta},$$

where I_G is the moment of inertia of the area about its centre of gravity. The vertical distance of the centre of pressure *below the centre of gravity* is represented by $\dfrac{I_G \sin^2 \theta}{A\bar{h}}$, which becomes less and less (for a given value of θ) as the area is more and more deeply submerged.

Note that when the area is in a vertical plane, $\sin\theta = 1$, and therefore $h_p = \dfrac{I_0}{A\bar{h}}$. **(Example 6.)**

20. Graphical Method of Determining Position of Centre of Pressure. This method, being adapted for locating the centre of pressure both in a horizontal and in a vertical direction, is specially useful if the area is unsymmetrical about a vertical axis. If OO (Fig. 8) is the line in which the plane containing the lamina cuts the liquid surface, a horizontal datum line XX is drawn through the centre of gravity of the area.

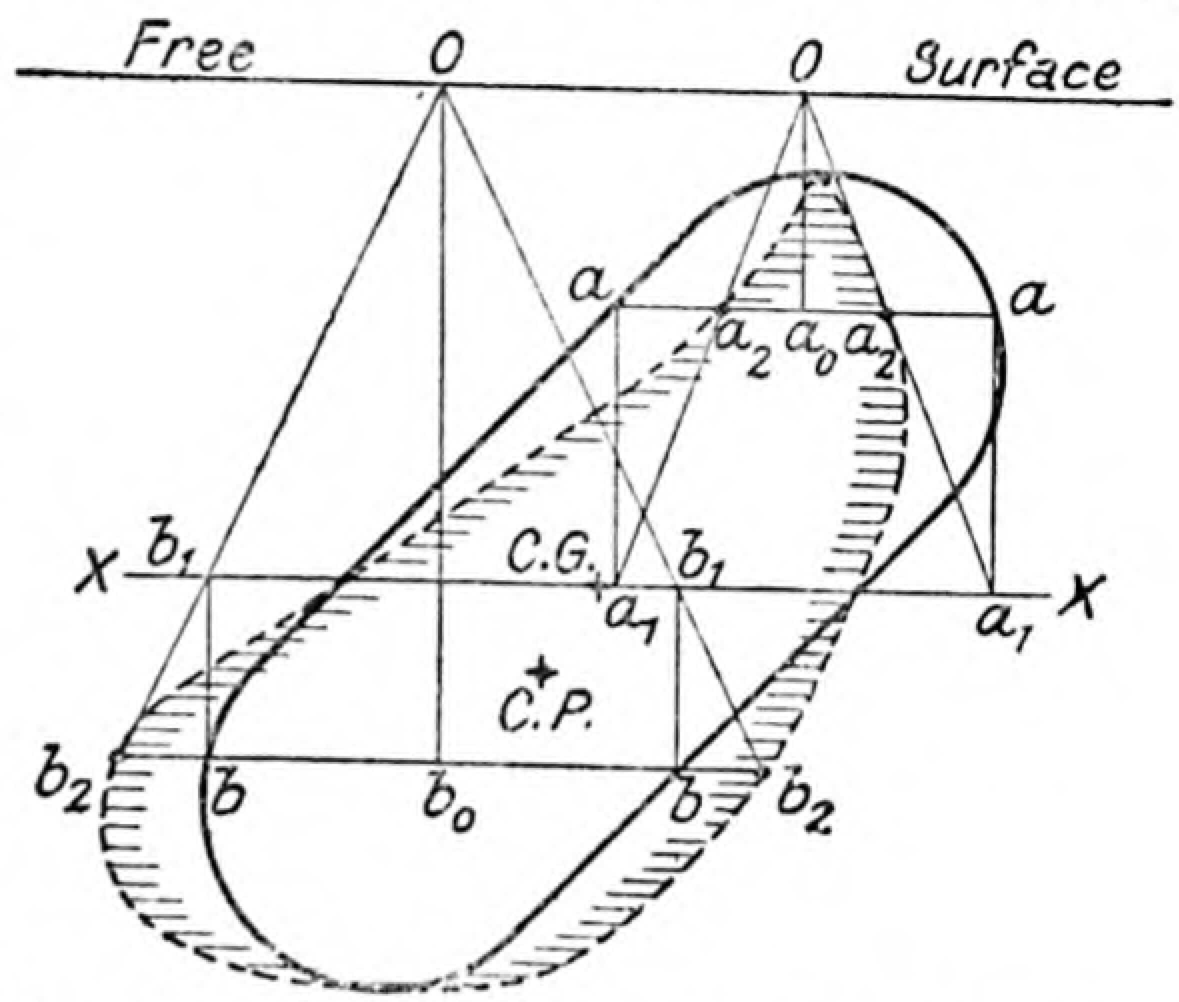

FIG. 8.—Centre of pressure of irregular area.

Each horizontal element in turn is bisected as at a_o, b_o, and a perpendicular carried up through each mid-point to the line OO. Perpendiculars aa_1, bb_1 are also dropped from the ends of the elements on to the datum line XX. Then the lengths a_2a_2, b_2b_2 intercepted on the elements by the lines

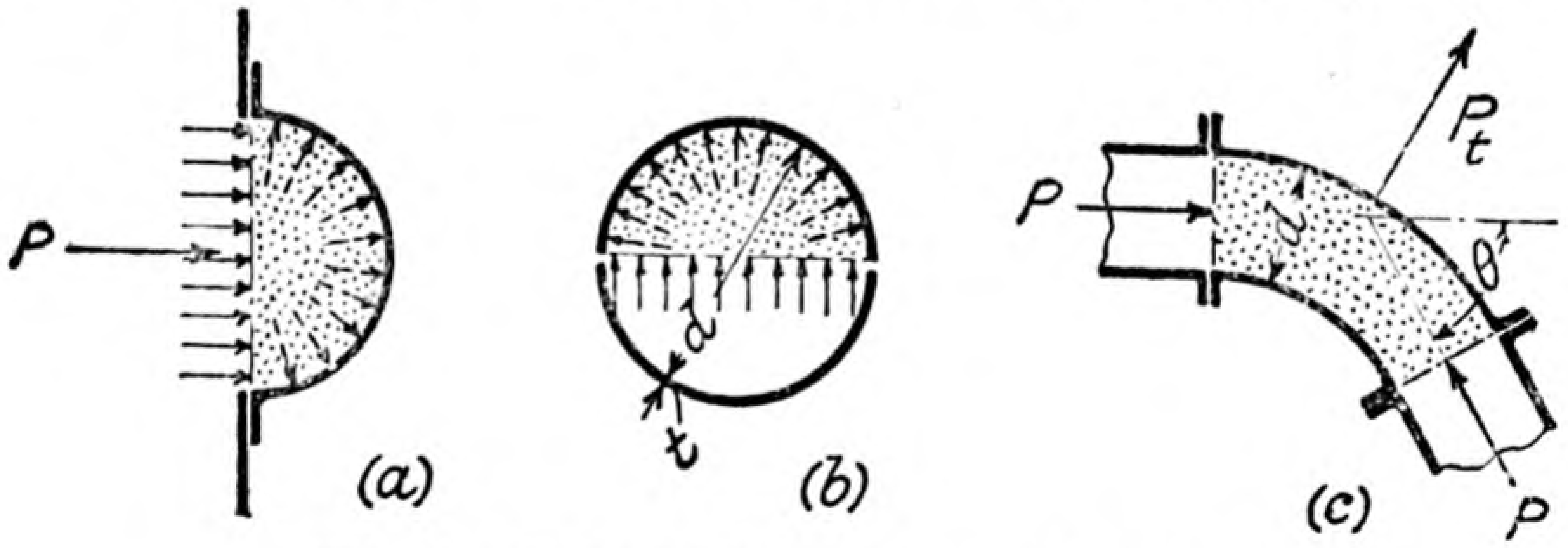

FIG. 9.—Forces acting on curved surfaces.

Oa_1 and Ob_1 represent to scale the static thrusts on the elements. A smooth curve drawn through all the points corresponding to a_2, b_2, etc., results in the distorted figure shown hatched in Fig. 8: the position of the *centre of gravity* of this hatched figure is then also the position of the *centre of pressure* of the original area shown in full lines.

21. Resultant Thrust on Curved Surfaces. Where curved surfaces are concerned it is usually sufficient to know

the sum of the components, in a given direction, of the individual thrusts produced by the pressure p on different parts of the surface. In calculating, for example, the size and number of bolts required to secure the flanged hemispherical cover shown in Fig. 9 (a), it is only necessary to know the total thrust P, and therefore we merely calculate the static thrust on any convenient *plane* normal to P. The arrows representing the actual pressures on different parts of the cover, shown in broken lines, do not interest us ; it is the arrows shown in full lines that must be taken into account.

Similarly, the circumferential or hoop tensile stress f_t in the walls of a pipe of diameter d and thickness t is computed thus :

Total static thrust on a diametral plane of length l

$$= p \, . \, d \, . \, l \quad \text{(Fig. 9 } (b)).$$

Resisting force $= 2 \, . \, t \, . \, l \times$ tensile stress.

$$\text{Equating, stress } f_t = \frac{pd}{2t} \qquad \textbf{(2-4)}$$

(It is here assumed that the stress is uniformly distributed, viz. that the pipe is a " thin " cylinder and not a " thick " one.[10])

(Example 8.)

The forces at a pipe bend (Fig. 9 (c)) afford another illustration. The static thrusts P, P on planes normal to the pipe axes each have the value $\frac{\pi}{4} d^2 \, . \, p$, therefore the total resultant force on the bend, which must be resisted by an anchorage or by the flange bolts, is

$$P_t = 2P \sin \frac{\theta}{2} = P\sqrt{2(1 - \cos \theta)}.$$

This method of treatment is, of course, only applicable so long as the pressure in the pipe is so great that it can be considered uniform over the areas under discussion, the liquid shown stippled in the figure serving only to transmit thrust as though it were solid matter. On the other hand, if it were required to calculate the total thrust, say, on the curved face of a dam, it would be necessary actually to find the individual thrusts on a succession of small elements. **(Example 7.)**

22. Methods of Resisting Static Pressure. Some of the principles utilised when designing engineering structures which have to withstand the static pressure of liquids are

suggested in Fig. 10. In the vertical steel-plate water-tank, (i), the plates of the *cylindrical* shell are in tension only, and thus self-supporting, their thickness being proportioned in accordance with equation (2-4), § 21. But a *rectangular* tank, (ii), requires a system of stays to prevent outward bulging or collapse of the sides; horizontal stays of tie-bars (a) may tie one side to the opposite side, or diagonal stays (b) may transmit the load from the side of the tank to the bottom.[11] The entire weight of the tank and its contents is

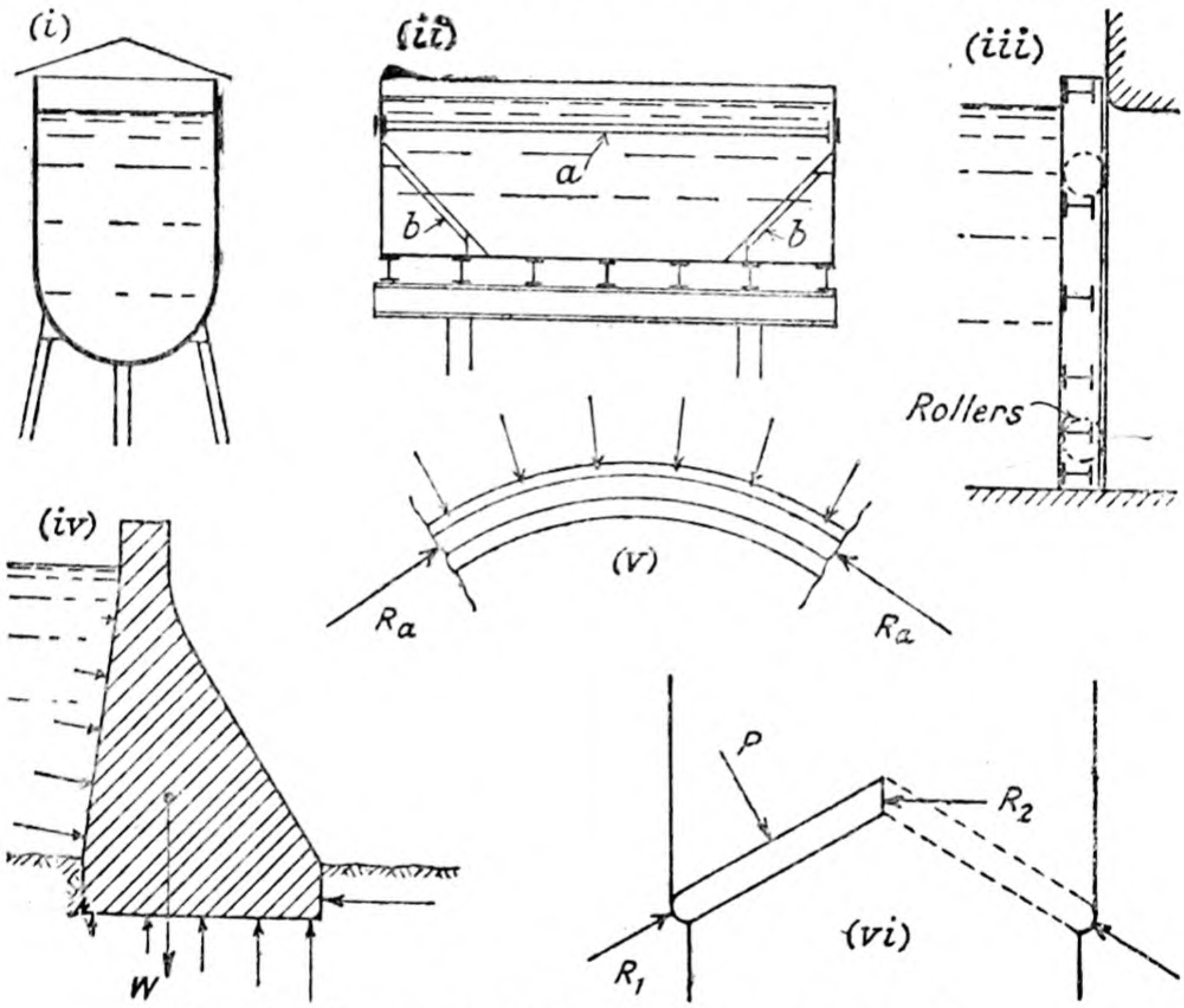

FIG. 10.—Structures designed to resist static pressure.

transmitted through a grid of steel floor-beams to vertical columns, and so to the ground. In the *sluice-gate* shown at (iii), the horizontal I-beams supporting the skin-plates are pitched closer together at the bottom than at the top, in accordance with the law connecting pressure with depth. Rollers running on vertical rails fixed to the piers reduce friction when the gate has to be lifted (§§ 191–194).

A more complex system of forces and reactions keeps a *concrete* or *masonry dam* in equilibrium. When the dam is of the straight *gravity* type, (iv), the overturning moment exerted

by the water pressure is resisted by a righting moment of which the two elements are the downward weight of the masonry W, and the resultant upward reaction of the rock foundation acting against the base of the dam. In an *arched dam* built across a narrow gorge, as shown in plan in Fig. 10 (v), additional resistance to the thrust of the water is given by the reactions R_a, R_a, of the rock walls of the gorge which serve as abutments to the arch. Similar conditions prevail in the conventional type of hinged *lock-gates*, (vi); here we see that the hydrostatic thrust P on the leaf shown in full lines is resisted by the reaction R_1 of the hinge and by the reaction R_2 of the opposite gate.

23. Resultant Static Thrust on Floating Bodies. A floating body at rest is prevented from sinking by the vertical components of the static pressure acting on the various parts of the immersed surface. In order to maintain equilibrium, the resultant upthrust U must act vertically, it must pass through the centre of gravity G of the body, and it must be equal in magnitude to the weight W of the body. That the upthrust and the weight of the body are each identical with the weight of liquid displaced can be realised by imagining the floating body to be removed, and the cavity left in the liquid to be exactly filled again by pouring into it the necessary quantity of additional liquid (Fig. 11). In the diagram, the cavity is shown at (i), and the mass of liquid that would just fit into it is shown at (ii). Since a given point x is equally distant below either of the free liquid surfaces, it follows that the external and the internal pressures at the point are equal and opposite; consequently the line of action of the resultant external pressure components, viz. the upthrust U, must pass through the centre of gravity B of the *displaced liquid*. The point B is termed the *centre of buoyancy*.

The equilibrium between the weight of the body and upthrust is not necessarily stable. For example, a casual glance at Fig. 11 (*i*) might suggest that here the equilibrium is very unstable; since the point of application of W, viz. the centre of gravity of the body, G, lies above the point of application B of the upthrust U, it seems natural that as soon as the body is tilted by the slightest amount, it will continue to heel more and more rapidly until it eventually capsizes. But, in fact, this may not happen at all. The reason is that when the

vessel tilts, the centre of buoyancy *does not remain in the same relative position* but shifts transversely, e.g. from position B to position B' (Fig. 11 (iii)). Here it is evident that the upthrust acting through the *new* centre of buoyancy B' is exerting a righting moment and will tend to bring the vessel back to the upright position again. It is found that what really has a controlling influence on the stability of the floating body is the position of the point M. This point, known as the *metacentre*, represents the intersection of the

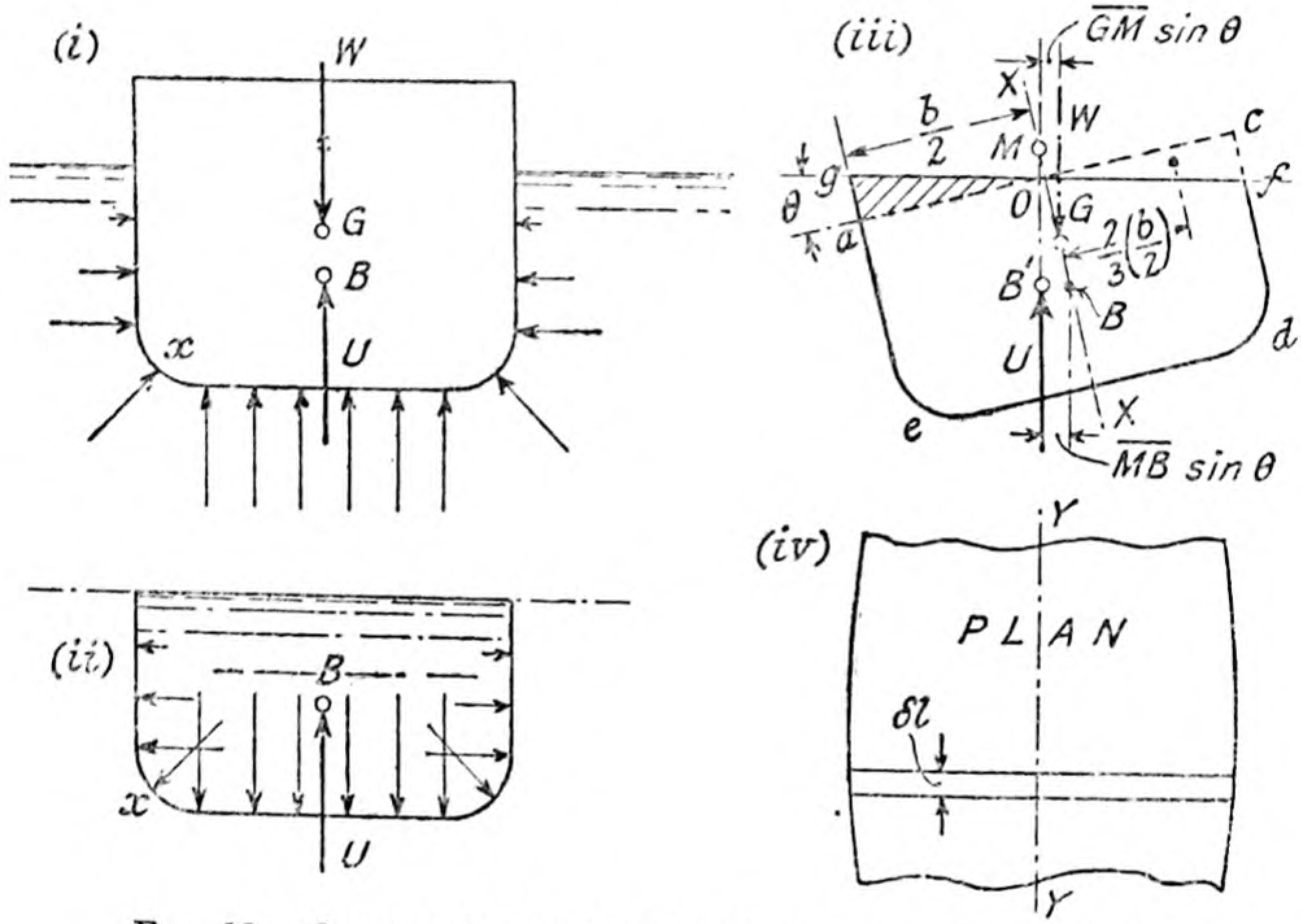

Fig. 11.—Overturning and righting forces on a floating body.

axis XX of the body, with the new line of action of the upthrust U corresponding with a very small angle of heel θ. If the metacentre M is *above* the centre of gravity G, as it is in the diagram, then the equilibrium will be stable, and as soon as the disturbing force is withdrawn the vessel will roll to and fro and eventually settle down in its original position. But if the metacentre is *below* the centre of gravity, then the slightest disturbance will make the vessel capsize. The distance GM is termed the *metacentric height.*

24. Computation of Metacentric Height. Assuming that the vessel is being deliberately held over in the tilted position by the action of some external overturning moment,

e.g. wind pressure, centrifugal force (of a ship steaming in a curved path), the pull of mooring ropes, or a thwartship movement of cargo, we proceed to compute the opposing or righting moment called into play by the alteration in the shape of the volume of displaced water. Let us consider first a thin transverse vertical lamina of the water, having a thickness in a fore-and-aft direction of δl, Fig. 11 (iv). Before heeling, the lamina had the shape *acde*; after heeling, the shape is *gfde*. The one shape can be transformed into the other by moving the wedge *Ocf* across into the vacant space *Oga*, which it will exactly fill. If $b = 2 \,.\, Oc$ represents the water-line width of the lamina, then the weight of each wedge is $w \,.\, \frac{1}{2} \,.\, \frac{b}{2} \,.\, \frac{b}{2} \tan\theta \,.\, \delta l$, and the moment of the wedge about the central point O is $\frac{wb^2}{8} \,.\, \tan\theta \,.\, \delta l \left(\frac{2}{3} \,.\, \frac{b}{2}\right)$. The transposition of the wedge is thus responsible for a righting moment of double this amount, viz.

$$\frac{wb^3}{12} \,.\, \tan\theta \,.\, \delta l.$$

To find the total righting moment M_r contributed by all the elementary wedges from the stem to the stern of the vessel, we must integrate, thus

$$M_r = \int_L^O \,.\, \frac{wb^3}{12} \,.\, \tan\theta \,.\, \delta l,$$

where L represents the length of the water-line section. If the vessel is indeed of the shape of an ordinary ship or boat, then the imaginary solid comprising the sum of the wedges may be visualised as resembling a division of an orange. Now the term $\int_L^O \frac{b^3}{12} \,.\, \delta l$ itself represents the moment of inertia I of the water-line section about its longitudinal axis YY, where "water-line section" means the plane area of the opening made by the vessel in the free water surface, as indicated in the plan view, Fig. 11 (iv). It therefore follows that $M_r = wI \tan\theta$.

We can also write down another expression for the righting moment. It is the moment created by the transverse shift of the centre of buoyancy from B to B'; since, by definition, the

metacentre M lies vertically above B', then $M_r = wV\overline{MB}\sin\theta$, where V is the total volume of displaced water, i.e. W/w or U/w.

Equating the two values of the righting moment M_r, we have

$$wI \tan\theta = wV.\ \overline{MB}\sin\theta.$$

But since, for a very small value of the angle θ, $\sin\theta = \tan\theta$, it becomes possible to write

$$\overline{MB} = I/V.$$

If the distance BG of the centre of gravity G of the vessel above or below the centre of buoyancy B is known, we finally arrive at the desired value of the metacentric height, thus

$$\overline{GM} = I/V \pm \overline{BG}. \quad . \quad . \quad . \quad (2\text{-}5)$$

Corrections are manifestly necessary to this expression if the angle of heel is considerable.

Energy of Liquids

25. Pressure Energy of Liquids. To show the manner in which liquids are regarded as possessing *pressure energy* in virtue of their pressure head, we may consider a vessel (Fig. 12) having in its side a very small horizontal cylinder fitted with a frictionless piston. The head of liquid above the piston being h, the area of the piston being a, and the liquid having density w, a force $P = wha$ must be exerted on the piston to hold it in position against the thrust of the liquid. If now the piston be allowed to yield to the thrust through a small distance dl, the work done against the force P is $P\ .\ dl$.

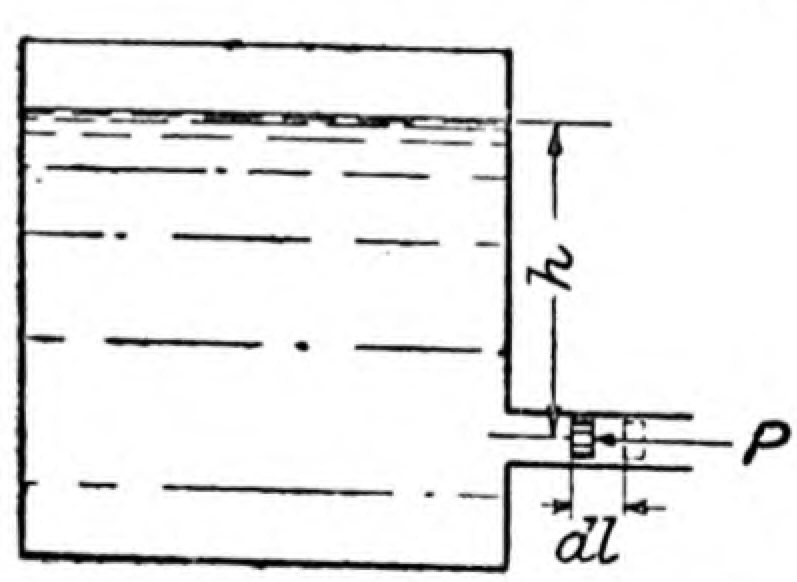

FIG. 12.—Illustration of pressure energy.

To perform this amount of work, a weight of liquid $w\ .\ a\ .\ dl$ has entered the cylinder; we therefore say that the energy given up by weight $w\ .\ a\ .\ dl$ of liquid is $P\ .\ dl = w\ .\ h\ .\ a\ .\ dl$, and thus that the energy per unit weight of liquid is $\dfrac{w\ .\ h\ .\ a\ .\ dl}{w\ .\ a\ .\ dl} = h$. This energy per unit weight is termed the *pressure energy* of the liquid; it is numerically equal to the head, and is expressed in the same units. It is, nevertheless,

helpful to remember that the statement (e.g.) "the pressure energy of water under a head of 2·8 feet is 2·8 feet" is merely an abbreviated way of saying "the pressure energy of water under a head of 2·8 feet is 2·8 foot-lb. per lb."

26. Potential or Position Energy of Liquids. A liquid is regarded as possessing potential or position energy by reason of its vertical height above the earth's surface or above some arbitrary horizontal datum plane. The relation between position energy and pressure energy is illustrated in Fig. 13, which represents a pipe of varying section connected at its upper end to a tank and plugged at its lower end, the free surface of liquid in the tank being at a distance z vertically above the datum plane.

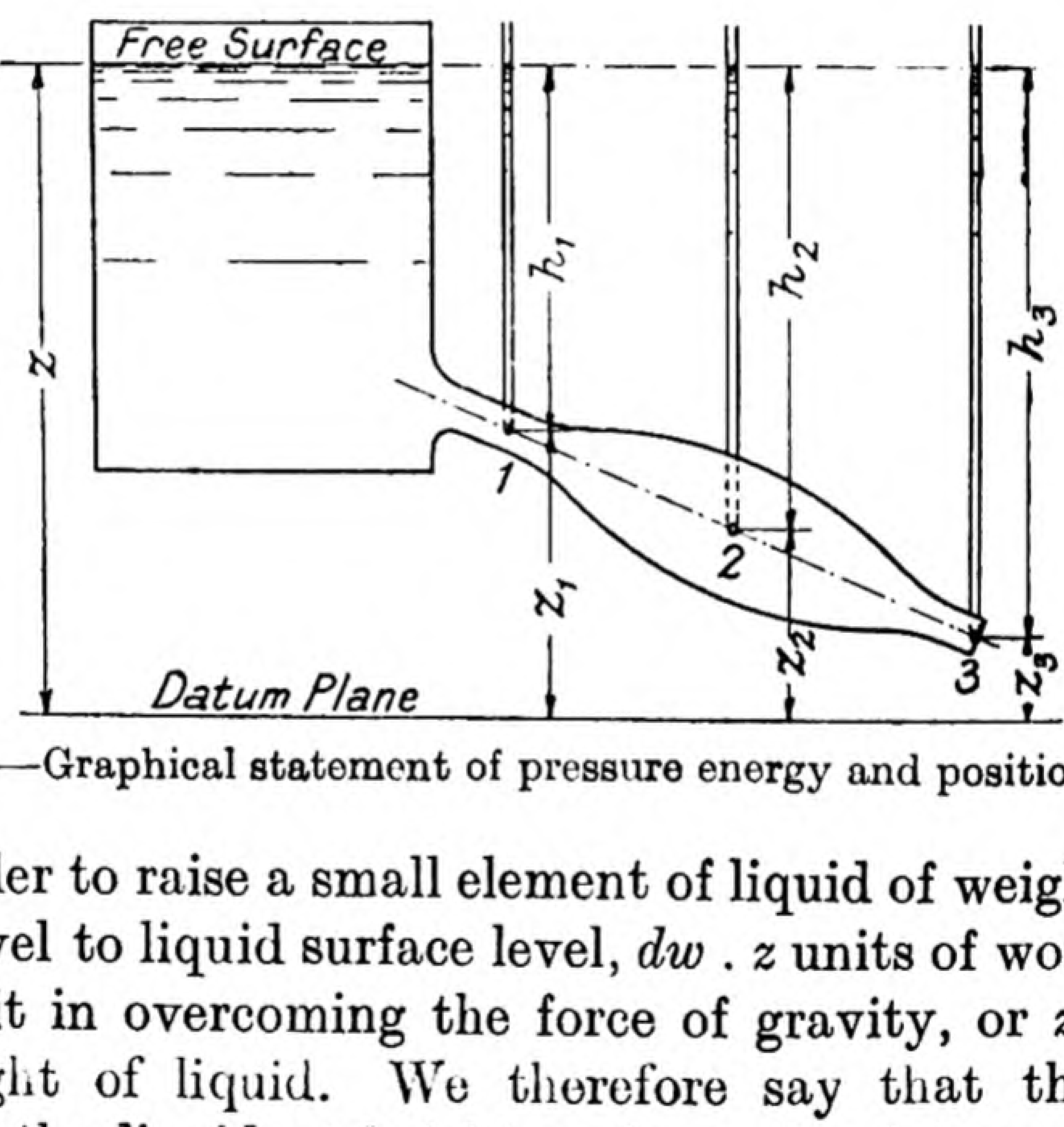

FIG. 13.—Graphical statement of pressure energy and position energy.

In order to raise a small element of liquid of weight dw from datum level to liquid surface level, $dw \, . \, z$ units of work must be done on it in overcoming the force of gravity, or z units per unit weight of liquid. We therefore say that the *position energy* of the liquid at height z above the datum plane is z. Similarly the position energy at points 1, 2, and 3 is z_1, z_2, and z_3 respectively. Another name for position energy is *geodetic head.*

Now the pressure energy at points 1, 2, and 3 respectively will be represented by the heights h_1, h_2, and h_3 of the columns of liquid standing in the gauge tubes connected with those points, and since the liquid is at rest the tops of all the columns will lie in the plane of the free surface. Evidently, therefore, $z = z_1 + h_1 = z_2 + h_2 = z_3 + h_3$; that is, the total

energy of the liquid is the same at all points. Naturally this must be so, for if at one point the liquid had more energy than at another, it would certainly try to move from the region of high energy to the region of low energy. It is for this reason that the free surface of a liquid at rest must necessarily be horizontal; if for any reason a hump or hollow were formed, it would be quickly levelled out in order to fulfil the condition of uniformity of energy at all points in the mass of the liquid.

27. Elastic Energy of Liquids. In just the same way that energy is absorbed in compressing a gas, so also is energy required to raise the pressure of a liquid contained in a closed vessel. But because of the very small compressibility of the liquid (§ 5), its elastic energy is correspondingly small. Let us now suppose that liquid completely fills the vessel shown in Fig. 12, that the vessel has a rigid closed top, and that no deformation of the sides can occur. Then the system would resemble a boiler or the like being subjected to a hydraulic test by means of a test-pump (**Example 8**). Let the total weight of liquid in the system be W, of normal density w and Bulk Modulus K. A small movement dl of the little piston will diminish the volume of the liquid by an amount $a \,.\, dl$, and the corresponding pressure rise will be $p = \dfrac{a \,.\, dl}{W/w} \,.\, K$ (§ 5).

The thrust P on the piston will vary from zero at the beginning of the stroke to $p \,.\, a$ at the end of the stroke (neglecting the pressure due to the head h). The total work done on the piston and the energy given to the liquid is consequently $p \,.\, a \,.\, \frac{1}{2}dl$. But from above, $a \,.\, dl = \dfrac{W}{w} \,.\, \dfrac{p}{K}$. Substituting,

$$\text{total work done} = \frac{1}{2} \,.\, \frac{p^2}{K} \,.\, \frac{W}{w}, \text{ and}$$

$$\textit{elastic energy per unit weight of liquid} = \frac{p^2}{2wK}. \qquad \textbf{(2-6)}$$

What happens to the small volume of liquid $a \,.\, dl$ displaced by the movement of the piston? If the vessel is open-topped, as in Fig. 12, the net effect is to raise the surface level by a very small amount; at the end of the operation, the quantity $a \,.\, dl$ can be looked upon as being spread in a very thin layer on top of the existing mass of liquid, which has itself suffered no change. We can therefore quite reasonably think of the quantity $a \,.\, dl$ as being lifted

bodily through a height h, the entire energy absorbed in the process being given to this small volume *alone*. But in the alternative conditions of the closed vessel which we have just been studying, the energy expended on the piston is shared by the *whole mass* of liquid in the vessel.

A pictorial statement of the distinction between pressure energy and elastic energy is given in Fig. 14. The two identical vessels each have a pressure gauge which registers a pressure p. In the vessel (i) the pressure is generated by the head of liquid H in the upper open-topped reservoir and its communicating pipe; in the closed vessel (ii) the *same* pressure p has been built up by pumping liquid into the vessel through the cock C and then closing and sealing the cock. Is the energy of the liquid near the top of the vessels the same? By no means. Undoubtedly in both instances there is elastic energy $p^2/2wK$, but in addition the open vessel (i) has pressure energy $H = p/w$ also, the ratio between elastic energy and pressure energy being $\dfrac{p^2/2wK}{p/w} = \dfrac{p}{2K}$. If, for example, the head H were 100 ft., this ratio would have the extremely minute value of 1/13800.

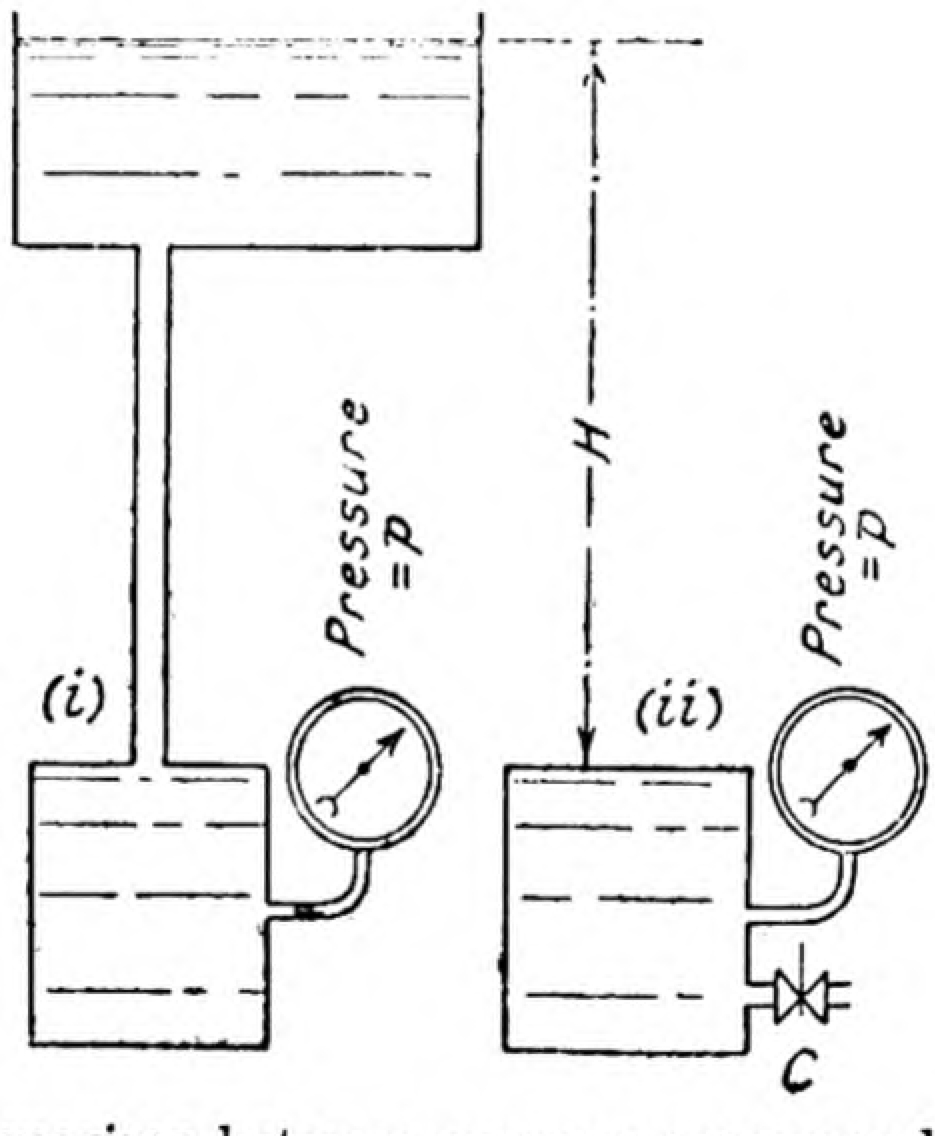

FIG. 14.—Comparison between pressure energy and elastic energy.

In many hydraulic calculations, then, the elastic energy of liquids is *entirely negligible*. Only when inertia pressure or water-hammer in pipes comes into play (§§ 116-118) does elastic energy assume a predominant role.

CHAPTER III

LIQUIDS IN MOTION

28. Forces Acting on Flowing Liquids. If we study the equilibrium of a small submerged element of a liquid at rest, we find that the only forces acting on it are (i) its weight, acting vertically downwards, and (ii) the various static thrusts acting on its faces. The element does not move upwards or downwards because the *difference* between the thrusts on the lower and upper faces exactly neutralises the weight; it does not move sideways because the static pressure is uniform on all sides (§ 12). Suppose now that the element begins to move. Remembering that it must obey the same laws of motion as a solid element, we conclude that force must have been applied to generate acceleration. Moreover, the only way of applying force to the element is by modifying the pressures exerted on it by the surrounding liquid. If the acceleration is horizontal, we can say that the originating force is the result of pressure differences on the sides of the element, in just the same way that the force that resists gravity depends upon pressure differences on the top and bottom of the element. As explained in § 35, it is quite easy to work out the relationship between pressure difference and acceleration when conditions are suitable; for the moment, it is sufficient for us to be on the alert in watching for such pressure changes when liquids are retarded or accelerated. An important consequence is that the pressure at a point in a moving liquid may now *no longer depend solely* on the depth of the point below the free surface, § 12.

If the liquid element is moving faster or slower than its neighbours, then tangential or shearing *viscous* forces will also be set up (§ 7), whose intensity will depend upon the

relative speeds of the elements—the velocity gradient—and upon the nature of the liquid.

The relative importance of the two types of force, (*a*) inertia or acceleration forces; and (*b*), viscous forces, varies very widely. Sometimes, as in the types of flow described in Chapter IV, viscous forces are so relatively unimportant that for preliminary calculations they may be disregarded altogether. Their effects can afterwards be taken into account when necessary by means of correcting factors. But when, on the other hand, liquids flow through closed or open conduits (Chapters V and VI), viscous effects are predominant and their intensity and distribution can often be precisely calculated.

By the use of the *Reynolds number* (§§ 64, 94), a numerical value may be given to the relative influence of inertia forces and viscous forces in stipulated conditions of flow.

29. Types of Flow. The innumerable small elements that together constitute a flowing stream, in closed as well as in open passages, may group themselves in a variety of ways. They may be regarded as moving in regular formation just as disciplined soldiers do, or on the other hand they may swirl and jostle rather like the individuals in a disorderly mob. Some characteristic flow patterns are shown schematically in Fig. 15.

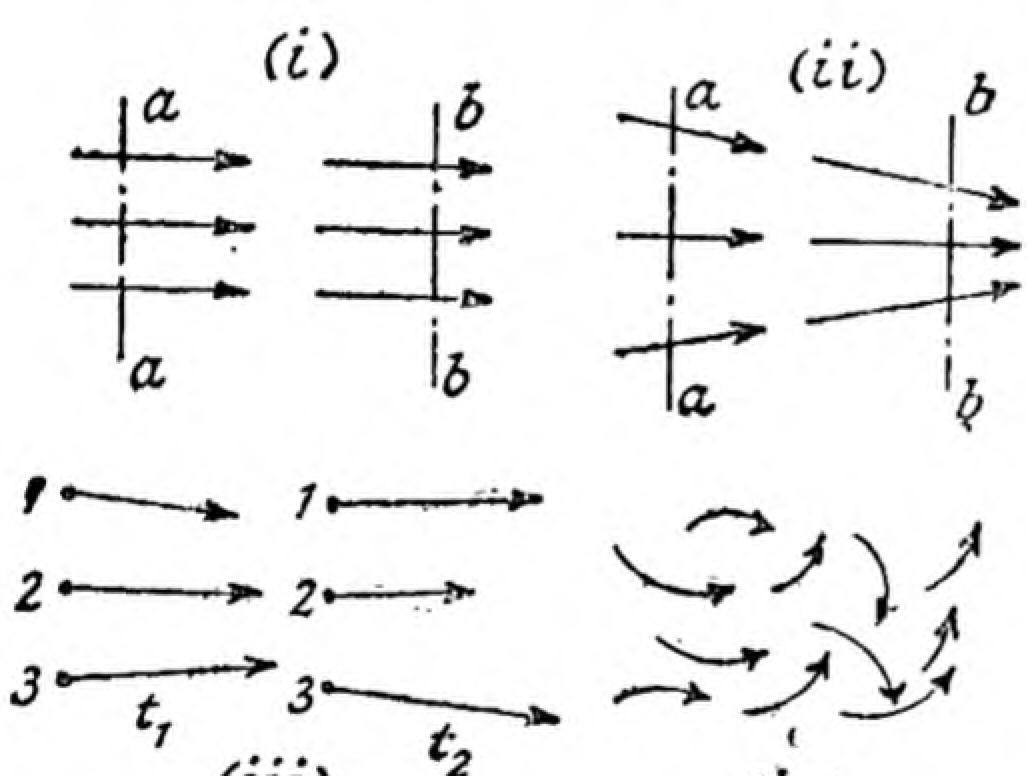

FIG. 15—Types of flow.
(*i*) Steady, uniform.
(*ii*) Steady, non-uniform.
(*iii*) Unsteady.
(*iv*) Turbulent.

(i) *Steady, Uniform Flow.* Here is the perfect type of military regularity. The liquid elements travel along straight, parallel tracks, and the successive elements passing a given point all have the same speed and direction; but it is not essential that the speed along one track should be the same as in adjoining tracks. All that is required is that conditions at one transverse plane, as at *aa* in the diagram, should be in all respects identical with those at another plane *bb*. Such precision of movement is actually found to occur in small pipes

at low velocities (§ 65), and a near approach to it is realised when free jets issue from well-formed orifices (§ 43).

(ii) *Steady, Non-uniform Flow.* If the liquid elements move in converging paths, as at (ii), evidently their velocities must increase as the elements pass from plane *aa* to plane *bb*, and the conditions at the two planes can no longer be identical. The flow is therefore said to be *non-uniform.* Nevertheless, at a given point in either plane the velocity remains unvarying in magnitude and direction, and thus the flow is still described as *steady.* Alternative titles are *stream-line* or *continuous.* Although the actual flow conditions in converging nozzles and the like (§ 42) approach quite closely to the ideal just described, yet if the direction of flow were reversed, causing the liquid paths to diverge, then inherent tendencies come into play which destroy the stability of the regime (§§ 39, 90).

(iii) *Unsteady Flow.* The system of representing this type of motion, Fig. 15 (iii), is a little different from what has heretofore been used. The diagram shows, at a number of points in the *same* plane, the conditions at two *different* moments of time. The intention is to emphasise the variability of the flow ; at each of the points 1, 2, and 3, the velocity has changed both in magnitude and direction during the short interval between t_1 and t_2. Naturally the same haphazard changes will be occurring at any other planes, and thus we can say that the liquid now shows very few signs of orderly progression. It *does* progress—in this instance from left to right—and that is as much as we can say for it. Nevertheless these are the conditions that the engineer nearly always has to deal with.

(iv) *Turbulent Flow.* This term is used in two senses. In discussing problems of pipe flow (Chapter V), it is convenient to describe the motion of the liquid as turbulent if it departs in the slightest degree from complete regularity or steadiness. In this sense unsteady flow, (iii), is always classed as turbulent flow. There is also a more general sense. Liquid motion is said to be turbulent when the elements are in an extreme state of disarray, and when their velocity fluctuations are particularly violent and erratic ; rotary or eddying movements are nearly always strongly developed. An attempt to depict such conditions is found in Fig. 15 (iv). We may expect to meet this

final limit of unsteadiness whenever a jet of liquid impinges into a more slowly-moving mass of liquid (§§ 39, 45).

30. Representations of Turbulent Flow. Since steady flow is the exception and unsteady and turbulent flow the rule, we cannot be content to dismiss turbulence as being by its nature unpredictable and amenable to no fixed laws. Some possible approaches to law and order are suggested in Fig. 16. At (*a*) we attempt to plot the actual track followed by a selected liquid element, recording also the instantaneous velocity vectors at successive points. System (*b*) corresponds to the method of plotting unsteady motion followed in Fig. 15 (iii); at a given instant we plot the velocities of a number of elements passing a given transverse plane. At (*c*) we fix our attention on a *single* point in the passage, and by means of vectors we record the velocity at that point at the end of successive short intervals of time. Each of these vectors in turn, v_{t_1}, v_{t_2}, etc., may be resolved into two components, (i) an *invariable* mean component u, parallel to the general direction of flow, and (ii) a *fluctuating* component. In diagram (*d*) these are represented by the vectors AC and BC respectively; the three-dimensional nature of the components of turbulence BC is more clearly conveyed by Fig. 55. We might thus regard the uniform component AC as the steady speed of a ship, and the components BC as representing the relative movements of the passengers on the ship. No matter how actively they play deck-tennis or waltz, or run up and down stairs, the daily distance travelled over the earth's surface is in no way affected. In a similar way, hydraulic calculations may often be simplified by ignoring the turbulent components of the liquid motion and by taking account only of the mean velocity u. This procedure will be adopted in the following further examination of flow phenomena.

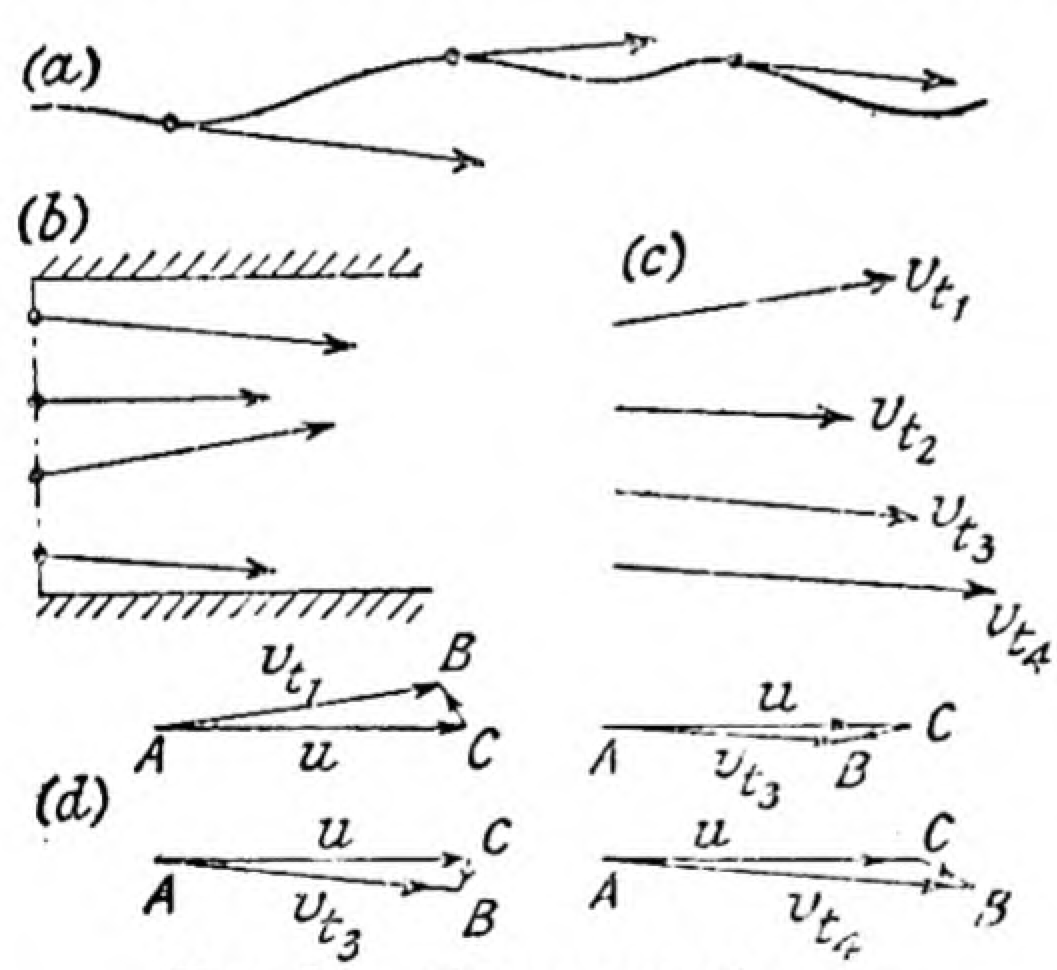

FIG. 16.—Representations of turbulent flow.

31. Rate of Flow of a Liquid. The volume of liquid flowing past a given transverse plane in unit time is spoken of as the *rate of flow* or *discharge* of the liquid ; it is usually expressed in terms of cusecs (cu. ft. per sec.), gallons per min., litres per sec., etc., and is denoted by the symbols Q or q.

If the rate of flow past the given plane is variable, Q may represent either the average rate of flow over a period of time, or the instantaneous limiting value of $\frac{dC}{dt}$, where dC is the small volume flowing past the plane in a small interval of time dt.

Knowing the discharge q and the cross-section a of the waterway in a plane normal to its length, the mean velocity v of the water is q/a ; conversely the discharge q through a pipe of diameter d, through which water is flowing with mean velocity v, is $\frac{\pi}{4}d^2v$. Although it is often easy to find experimentally the values of q and of v—for example, by collecting in a measuring-tank the liquid issuing from the pipe—this information tells us nothing about the *velocity distribution* at different points in the cross-section of the passage. Only in rare instances is the distribution uniform, Fig. 17 (i), such that all over the cross-section the local velocity u is identical with the mean velocity v. More often the local velocity varies from point to point, as in diagram (ii) ; here the *mean* velocity v has the value $\frac{\int u \, . \, \delta a}{a}$, where δa represents the area of the small elements of which the total cross-sectional area a is made up. By plotting actual velocity u against distance measured along a diameter, a *velocity distribution curve* is obtained (Fig. 54, § 71). It is to be noted that in turbulent motion, the symbol u represents the local mean velocity at a *point*, § 30, whereas v represents the mean velocity over the *whole section*.

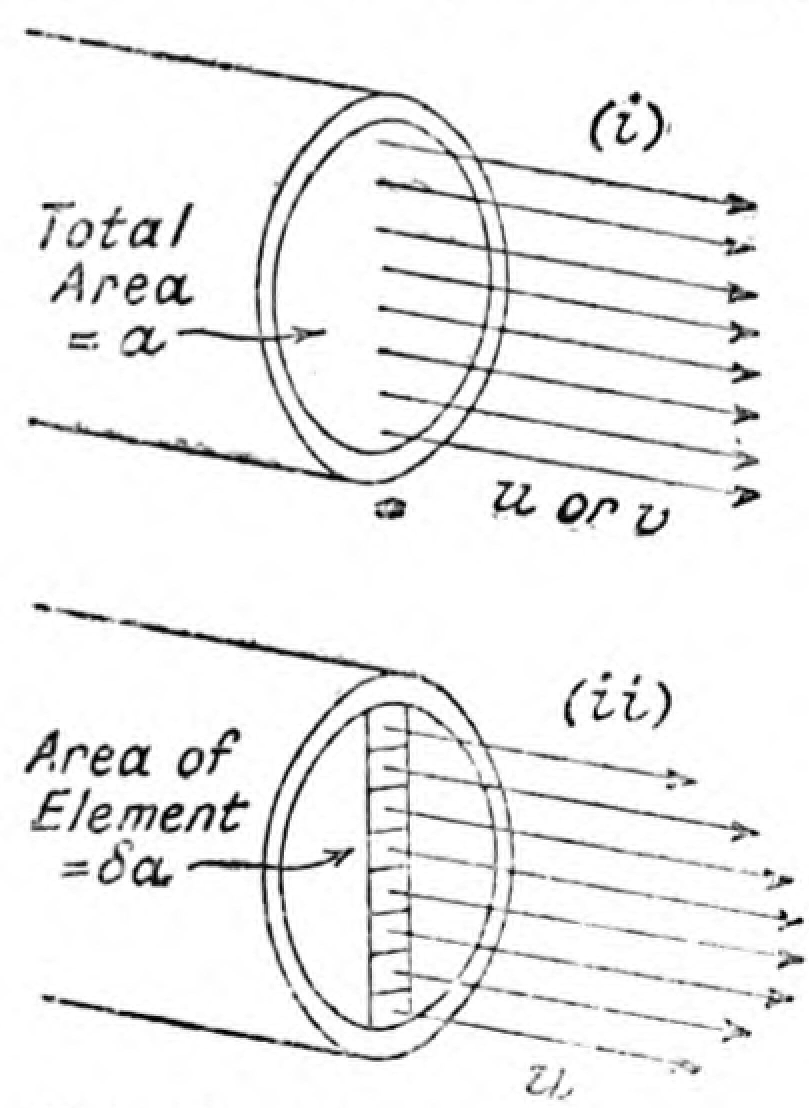

FIG. 17.—Types of velocity distribution.

32. Velocity Energy of Liquids. Just as a solid body of weight W moving with velocity V possesses kinetic energy represented by $\frac{WV^2}{2g}$, so a quantity of liquid of weight W moving with velocity V has kinetic or velocity energy $\frac{WV^2}{2g}$, or an amount of energy per unit weight of $\frac{V^2}{2g}$. This energy per unit weight, usually termed the *velocity energy* or the *kinetic energy* of the liquid, is expressed in the units of length which enables it to be added to pressure energy h or position energy z:

$$\left(\frac{V^2}{2g} = \frac{\frac{\text{length}^2}{\text{time}^2}}{\frac{\text{length}}{\text{time}^2}} = \text{length}\right).$$

Engineers frequently use the terms " pressure *head*," " position *head*," velocity or " kinetic *head*," interchangeably with the terms pressure energy, velocity energy, etc., generally used in this book.

The term *specific energy* is sometimes used to denote the total energy of a liquid per unit weight, viz. the sum of position energy, pressure energy, and velocity energy.

(*Note.*—With non-uniform velocity distribution, Fig. 17 (ii), the average velocity energy over the whole cross-section will not be $\frac{v^2}{2g}$, but will be $K' . \frac{v^2}{2g}$, where K' is a coefficient varying in value from 1·1 or 1·2 to 2·0, depending upon the nature of the flow. The reason is as follows :

The weight of liquid per second flowing past a small element of area da is $w . da . u$. The corresponding kinetic energy per second is $w . da . u . \frac{u^2}{2g}$.

The mean velocity energy per unit weight over the whole section is $\frac{\int w . da . \frac{u^3}{2g}}{w a v}$, which must necessarily be greater than $v^2/2g$. Moreover, even this correction neglects the velocity energy of the turbulent velocity components BC, § 30. Nevertheless, for ordinary purposes the nominal value for velocity energy $v^2/2g$, may be accepted.)

33. Conversion of Energy. An apparatus similar to the one shown in Fig. 13, § 26, may be used to show how transformations of energy occur as liquids flow through closed

passages. Here in Fig. 18 the plug at the end of the pipe is removed to allow the liquid to flow, and an inlet pipe provided for maintaining a constant level in the reservoir. One of the fundamental principles of Hydraulics, *Bernoulli's Theorem*,* states that in such a system the total energy of a perfect liquid under ideal conditions *does not change* as it flows from point to point; that is, that at any selected point in the system, the sum of position energy, pressure energy, and velocity energy will be equal to the sum at any other point.

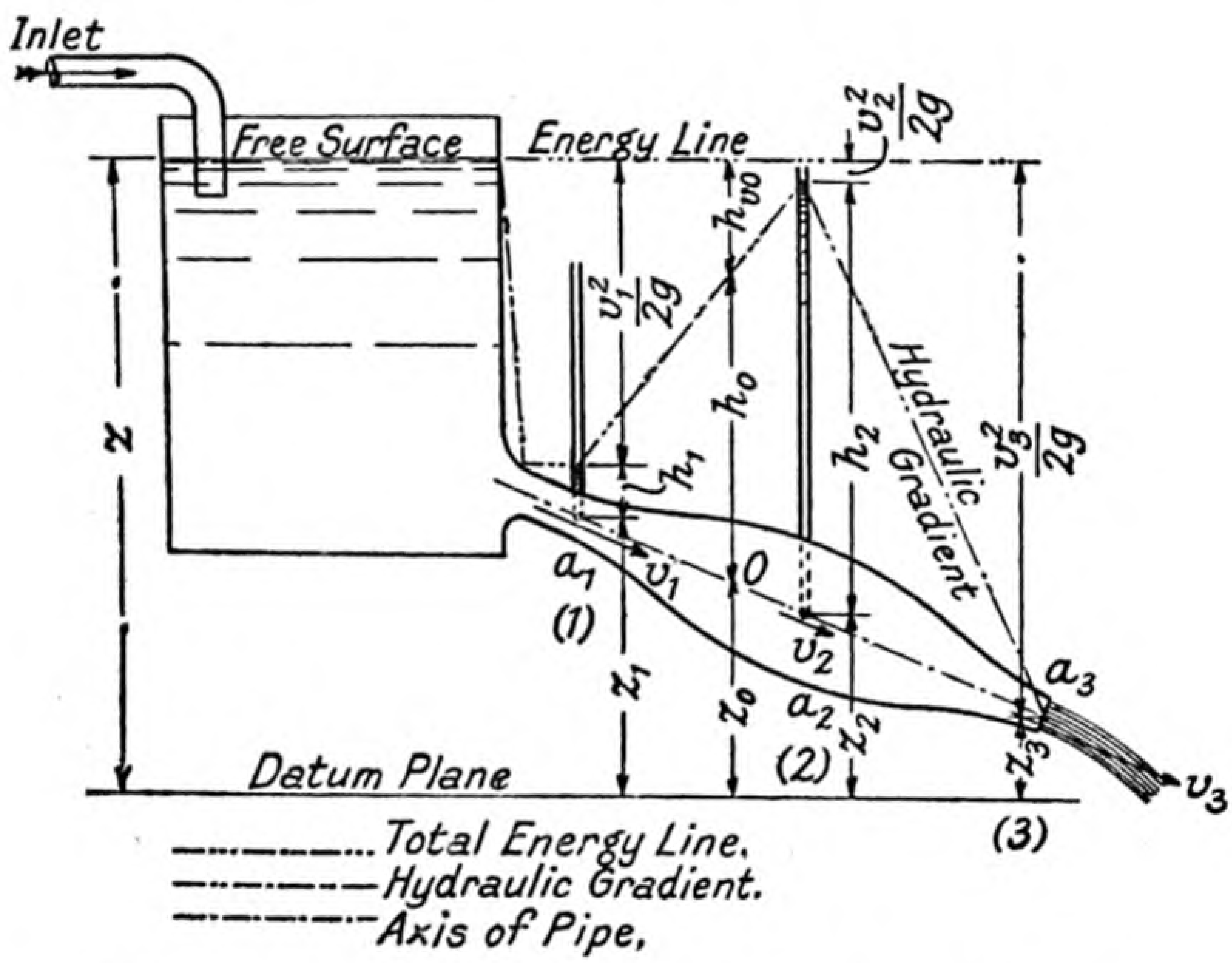

FIG. 18.—Graphical statement of Bernoulli's theorem.

The total energy at different points in the pipe axis may be tabulated as shown below.

	Position Energy.	Pressure Energy.	Velocity Energy.
Free surface .	z	Zero	Zero
Point 1 . .	z_1	h_1	$v_1^2/2g$
,, 2 . .	z_2	h_2	$v_2^2/2g$
,, 3 . .	z_3	Zero	$v_3^2/2g$

* Personal information will be found in the section entitled *Some Brief Biographical Notes*, p. 712.

There it is seen how a total amount of energy (per unit weight of liquid) z can exist wholly in the form of position energy at the free surface, as position energy, pressure energy, and velocity energy at points 1 and 2, and as position energy and velocity energy at point 3.

According to Bernoulli's theorem, then,

$$z = z_1 + h_1 + v_1^2/2g = z_2 + h_2 + v_2^2/2g = z_3 + v_3^2/2g \quad \textbf{(3-1)}$$

(Example 12.)

34. Graphical Plotting of Energy. If the total discharge through the pipe (Fig. 18) is known and also the cross-sectional areas, a_1, a_2, a_3, then the velocities v_1, v_2 and v_3, and consequently the velocity heads, can at once be calculated. The pressure heads at the respective points can be read off directly from the gauge glasses connected to these points, so that all the information is available for plotting the heads to scale in the manner shown in Fig. 18. To complete the diagram the *total energy line* is drawn, connecting the ordinates representing total energy, and the *hydraulic gradient* is added connecting the tops of the water columns.

We now have a complete graphical statement of Bernoulli's theorem. On any vertical at any point 0 on the axis of the pipe, the intercept h_{vo} between the total energy line and the hydraulic gradient represents to scale the *velocity energy* at the point, the intercept h_o between the hydraulic gradient and the pipe axis represents the *pressure energy*, and the intercept z_o between the pipe axis and the datum line represents the *position energy*. Since the total energy at all points is assumed to be uniform, the total energy line is horizontal.

As these conceptions are of the utmost value in many hydraulic problems, the reader is invited to memorise the code of dot and dash lines used in Fig. 18, which will be consistently employed in this book. The subscripts $_1$, $_2$, $_3$, etc., will also be used in future to distinguish the pressures, areas, velocities, etc., at the points 1, 2, 3, etc., just as they are here.

It remains to be pointed out that the validity of Bernoulli's theorem, in the simplified form just presented, depends on the following assumptions, viz.: (1) no dissipation of energy occurs in the system whether arising from viscous shear or from any other cause, (2) at any given point the velocity remains uniform

and is uniform all over the cross-section at that point, § 29 (i), and (3) the motion of the liquid is everywhere parallel with the pipe axis. Although none of these requirements can in fact be fulfilled, the theorem, suitably corrected, remains the basis for a variety of hydraulic flow calculations.

35. Relation Between Acceleration and Pressure Gradient. The changes in the state of the liquid depicted in Fig. 18 provide a good opportunity of verifying the statements made in § 28. We have certainly found that the pressure head in a moving liquid no longer depends solely on the depth below the free surface, for as soon as flow began in the pipe of varying section, the liquid columns in the gauge tubes fell from the levels shown in Fig. 13 to those shown in Fig. 18, *although the elevation of the free surface was in no way altered.* We observe, too, that a falling pressure gradient corresponds with a rising velocity and *vice versa.* By throwing this relationship into mathematical form we arrive at an alternative statement of Bernoulli's theorem, thus:

Let us consider a small transverse slice of a stream of liquid moving along a converging passage, Fig. 19, e.g. a part of the passage between points (2) and (3), Fig. 18. Its (very small) thickness is δl, and the areas of the two faces are respectively a and $a + \delta a$. Because of the falling pressure gradient, there is a difference of pressure head δh between the two faces, and the equivalent resultant thrust $P_1 - P_2$ imparts to the element an acceleration $\frac{dv}{dt}$.

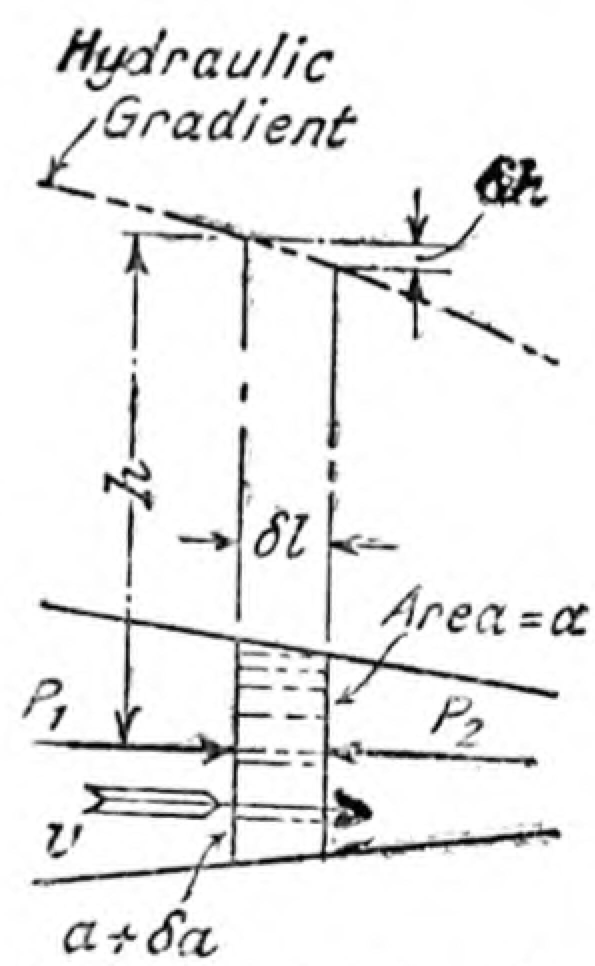

FIG. 19.—Acceleration of a liquid element.

Under limiting conditions this axial thrust or accelerating force has the value $w\,.\,dh\,.\,a$. Writing, therefore, the fundamental equation of motion, Force = Mass × Acceleration, and inserting appropriate values, we have

$$w\,.\,dh\,.\,a = \frac{w}{g}\,.\,a\,.\,dl\,.\,\frac{dv}{dt}$$

or

$$\frac{dv}{dt} = g\,.\,\frac{dh}{dl}. \qquad \text{(3-2)}$$

Expressed in words, this means that the acceleration of the element is equal to the acceleration of gravity g, multiplied by the slope of the hydraulic gradient. Alternatively, the acceleration of the element is comparable with the acceleration of a solid object sliding freely down a (frictionless) plane having the same slope as the hydraulic gradient.

Rewriting equation (3-2), and giving the term dh its correct negative sign, yields the form

$$dv \, . \frac{dl}{dt} = -\, g \, . \, dh,$$

or

$$v \, . \, dv + g \, . \, dh = 0.$$

A final integration results in a simplified form of the Bernoulli equation, thus :

$$\int v \, . \, dv + \int g \, . \, dh = \frac{v^2}{2} + gh,$$

or

$$\frac{v^2}{2g} + h = \text{constant.}$$

Inclination of the passage will have no influence on the general law, for the changes in position energy thereby introduced will be exactly neutralised by the equal and opposite changes in pressure energy.

Although the converging stream of liquid has hitherto been supposed to be bounded by the metallic walls of a conical pipe, the energy equation is in no way dependent upon this condition. The boundaries might equally well be the imaginary ones such as those that form a *stream tube* in a mass of liquid (§ 36).

(Example 13.)

36. Stream-lines : Stream-tubes. The preceding paragraphs have concerned themselves only with the bulk flow of liquid ; there has been little attempt to trace the paths of individual elements. In pursuing this further enquiry it is helpful to return again to the apparatus shown in Fig. 18, of which a part is reproduced to a larger scale in Fig. 20. An element of liquid in the free surface at A will ultimately find its way into the mouth of the passage at point (1). What path will it follow ? Can the element wander at will, or is it constrained to follow one particular path ? The answer is, that in the idealised conditions now assumed to prevail, the element has no choice : by a suitable graphical process, we can plot—at least in

principle—the track that each element must move along. This track is termed a *stream-line*. One of these is suggested by the line AA in Fig. 20; another by the line BB; so that in the end we could form an image of a very large number of stream-lines completely filling the inlet tank of the apparatus, each beginning at the free liquid surface and all converging on to the mouth of the passage.

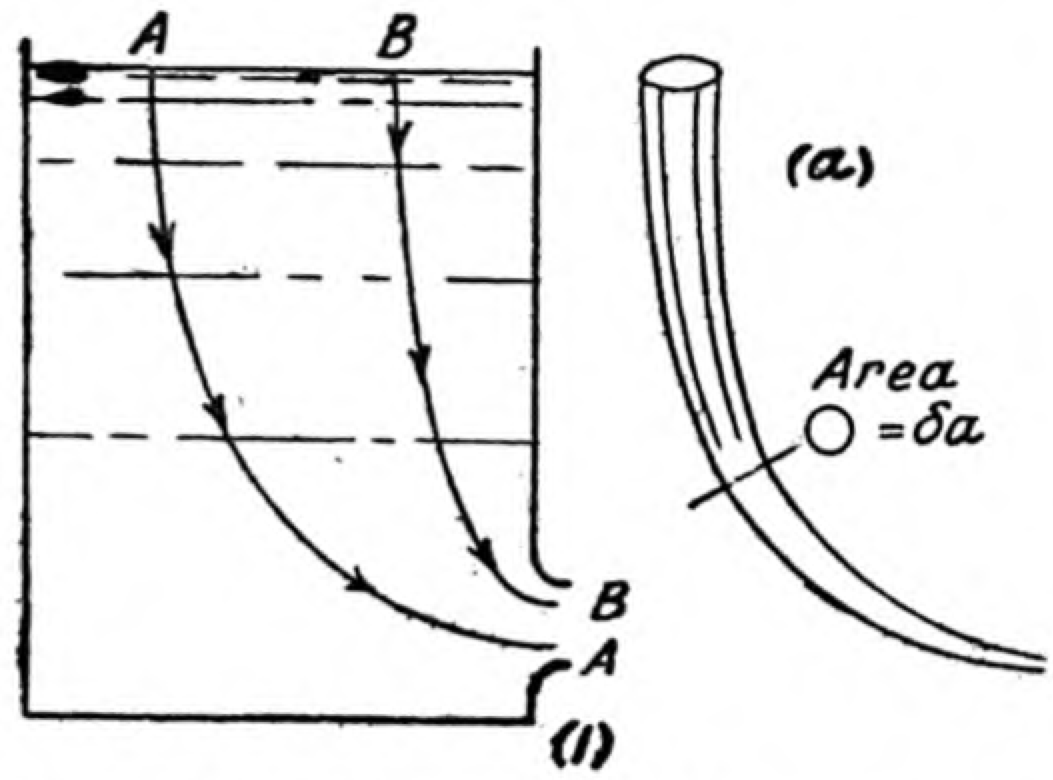

FIG. 20.—Stream-lines and stream-tube.

The next step is to select bundles of stream-lines which would themselves form a very small closed passage. One such passage, known as a *stream-tube*, and corresponding to the line AA, is shown in isolation in Fig. 20 (a). Within the imaginary and invisible walls of this stream-tube a small but finite quantity of liquid can be assumed to flow; at each point the liquid velocity would depend upon the cross-section δa of the stream-tube, just as the gross mean velocity did in the much larger passage, Fig. 18. The total discharge q traversing the system will be the sum of the individual discharges dq in the stream-tubes.

The flow-net. To complete the process by which the true shape of stream-lines may be established, a further set of lines must be added: they are termed *equi-potential lines*. The combination of stream-lines and equi-potential lines is termed the *flow-net*. A simple illustration is seen in Fig. 21 (I).

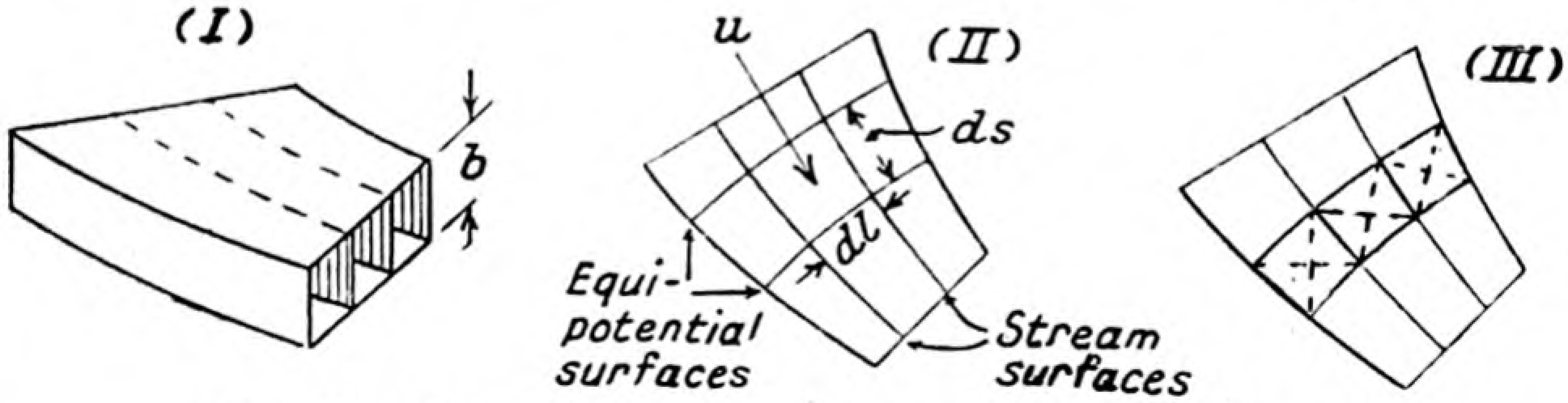

FIG. 21.—Stream surfaces and equi-potential surfaces.

It relates to two-dimensional flow along a curved passage of uniform width b. The cross-section of the passage is divided into three stream-tubes each of rectangular section: the

stream surfaces, or the walls of the stream-tubes, are intersected by two equi-potential surfaces, Fig. 21 (II). These surfaces, and the lines which represent them in plan, are sketched in according to any plausible or provisional ideas; and the problem now is, how to adjust and correct them in order to give the final and correct form ?

Four conditions must be fulfilled :—

(i) Each equi-potential line must cut each stream-line perpendicularly.

(ii) Each stream-tube must convey the same elementary discharge dq as any other, viz. the total flow q must be equally shared between the stream-tubes.

(iii) At any point the transverse spacing dl of the stream surfaces, or the transverse width of the stream-tube, must be *inversely* proportional to the velocity u in the stream-tube at that point.

(iv) At any point the transverse spacing ds of the equi-potential lines must be *inversely* proportional to the velocity at that point.

If dl and ds are both inversely proportional to local velocity, evidently the ratio dl/ds is constant throughout the flow-net. Also, if we cared to make the ratio dl/ds unity, and to choose a fine enough mesh for the flow-net, each of the small quadrilaterals that compose it would be a tiny square. Here then is the test for checking the first or provisional attempt at sketching the flow-net, Fig. 21 (II). Clearly it does not satisfy the conditions. A second attempt, Fig. 21 (III), is a good deal nearer the mark, for if the constituent quadrilaterals are not squares, at least they can be considered as similar quadrilaterals.

37. Velocity Potential and its Significance. Having now established a simple form of flow-net and thereby traced the shape of the stream-lines which are what really interest us, should we not now enquire : are the equi-potential lines or surfaces of any further use, or can they be discarded as the builder dismantles the scaffolding when the house is finished ? What kind of potential do they indeed represent ? In this connection the word is perhaps a trifle misleading : it may recall the term potential *energy*, § 26. In fact there is *no such*

connection. The expression *velocity potential*, denoted by the symbol ϕ, is defined as the integrated value of the product $u\,(ds)$ as a liquid element traverses a stream-tube. In passing from one equi-potential surface to a closely adjacent one, Fig. 21 (II), the liquid will experience a change of velocity Potential $d\phi$. Now as the velocity in the stream-tube at this point is u, and the distance travelled by the element is ds, then by definition the change of velocity potential $d\phi$ can also be written $u\,.\,(ds)$, or $d\phi = u(ds)$. Hence total change of velocity potential over a particular stream-line $= \phi = \int u(ds)$.

On this understanding, equi-potential surfaces are those which link together all points at which the velocity potentiol is the same. Thus we observe that, no matter at what position the liquid passes from one equi-potential surface to the next, Fig. 21 (II), the increase of velocity potential $d\phi$ is uniform. Since $d\phi = u(ds) = (dq/dl\,.\,b)\,.\,ds$; and since dq is constant and (ds/dl) is constant, § 36, evidently $d\phi$ must be constant.

Here, in conclusion, is a summary of the changes of various kinds that a liquid element will undergo as it flows along a converging stream-tube such as those in Fig. 21 (II) :—

Its velocity will *increase*.

Its total energy will remain *constant*, § 33.

Its pressure energy will *diminish*.

Its velocity potential will *increase*.

But whereas velocity and pressure have a physical meaning—they can be detected and measured by suitable instruments—velocity potential is purely a mathematical conception.

In other types of flow, however, equi-potential lines may have quite a positive physical significance. Consider, for instance, a topographical map depicting a tract of hilly country. The contour lines on this map are lines of equal *gravitational* potential; the courses of the natural streams show the tendency of the water to run down-hill, at right angles to the contour lines. In conjunction, the streams and the contour lines form a crude kind of flow-net.

There is another kind of hydraulic flow in which the equi-potential lines are in effect lines of equal *pressure-head;* this condition may be found when liquids percolate through permeable materials, §§ 96, 209.

Again, when an electrical current flows through a homogeneous conductor, e.g. a liquid electrolyte, the equi-potential lines here are lines of equal *electrical* potential.

While these various analogies may have useful practical applications, it is important to remember that they all differ in one important respect from the basic condition stated in §§ 36, 37, viz.: uniformity of total energy.

38. Examples of Flow-nets. Even if, as so often happens in hydraulic apparatus, the flow-net should comprise very numerous stream-lines and equi-potential lines, the method of construction explained in § 36 can still be applied. An example is illustrated in Fig. 22, which represents two-dimensional flow into a passage of rectangular cross-section.(12) The first step here is to try to find a position where the stream-lines are parallel, for at that position the equi-potential surfaces will be plane surfaces and we shall find *straight* equi-potential lines. If at such a plane, as at OO in Fig. 22, we make the further reasonable assumption that the local velocity u is uniform across the section, then the stream-surfaces will be equally spaced. By working upstream, sketching the stream-surfaces and the equi-potential lines, and gradually correcting them as in § 36, the desired flow-net is finally plotted. Fig. 22 shows an intermediate stage in this process. If three-dimensional flow is in question, a modified treatment is required, as in § 147 (i).

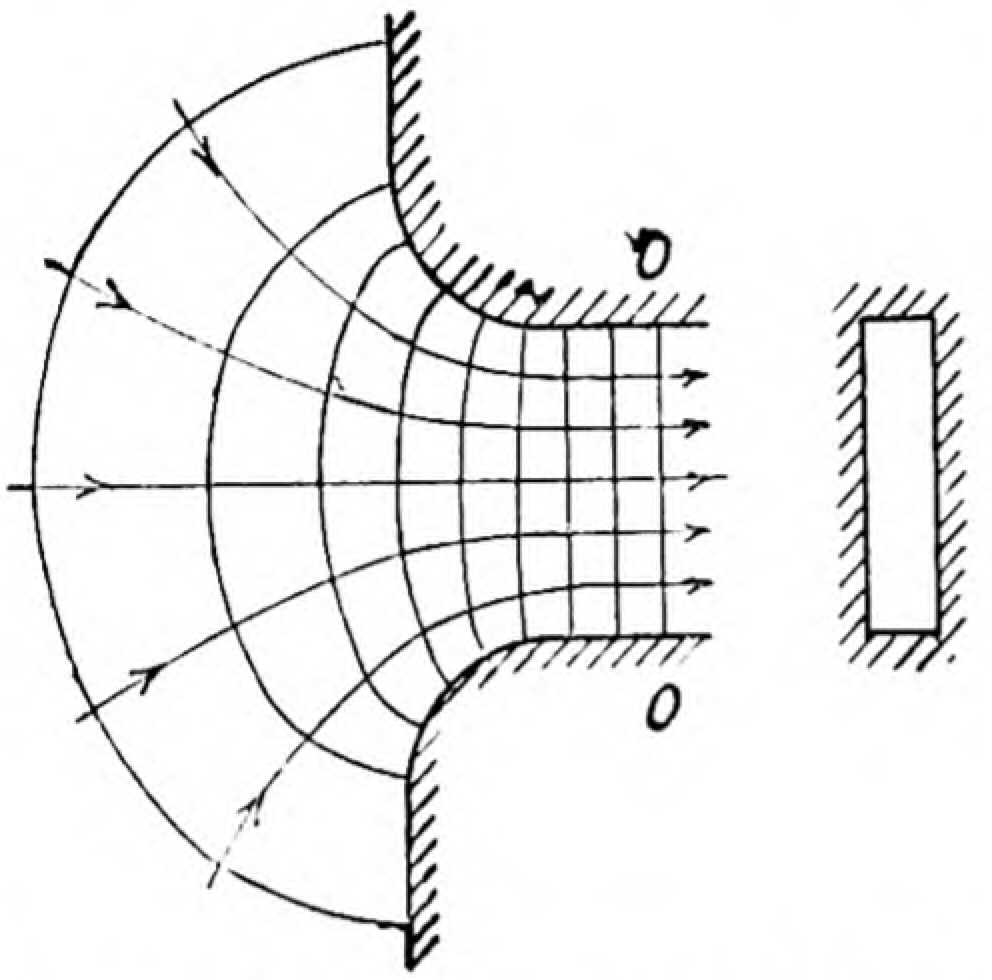

FIG. 22.—Provisional sketch of flow-net

Quite a different type of two-dimensional flow is suggested in Fig. 23. Instead of being confined within the walls of a passage, the liquid flows freely along an open stream; immersed in the stream is a fixed solid object, and we desire to know how this object will divert the liquid filaments in its vicinity. The result of plotting part of the flow-net to a larger scale is seen in Fig. 24 (*a*), which relates to a cylindrical-shaped solid, set transversely across the stream. A study of the flow-net

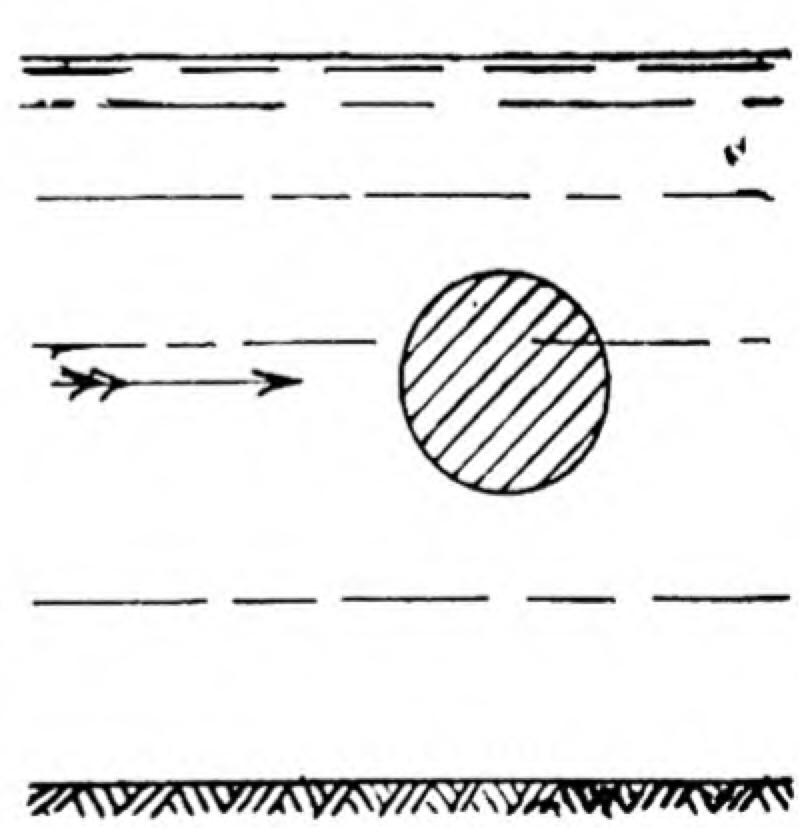
FIG. 23.—Flow past immersed solid.

yields highly interesting information. If we examine first a liquid element moving along the horizontal axis OO, we note that the spacing of the equi-potential surfaces it crosses rapidly *widens*, implying that the liquid is losing speed. Still keeping the element under observation as it now begins to travel round the surface of the cylinder, we see that the equi-potential lines become more closely-pitched, denoting a rapid increase in the liquid velocity.

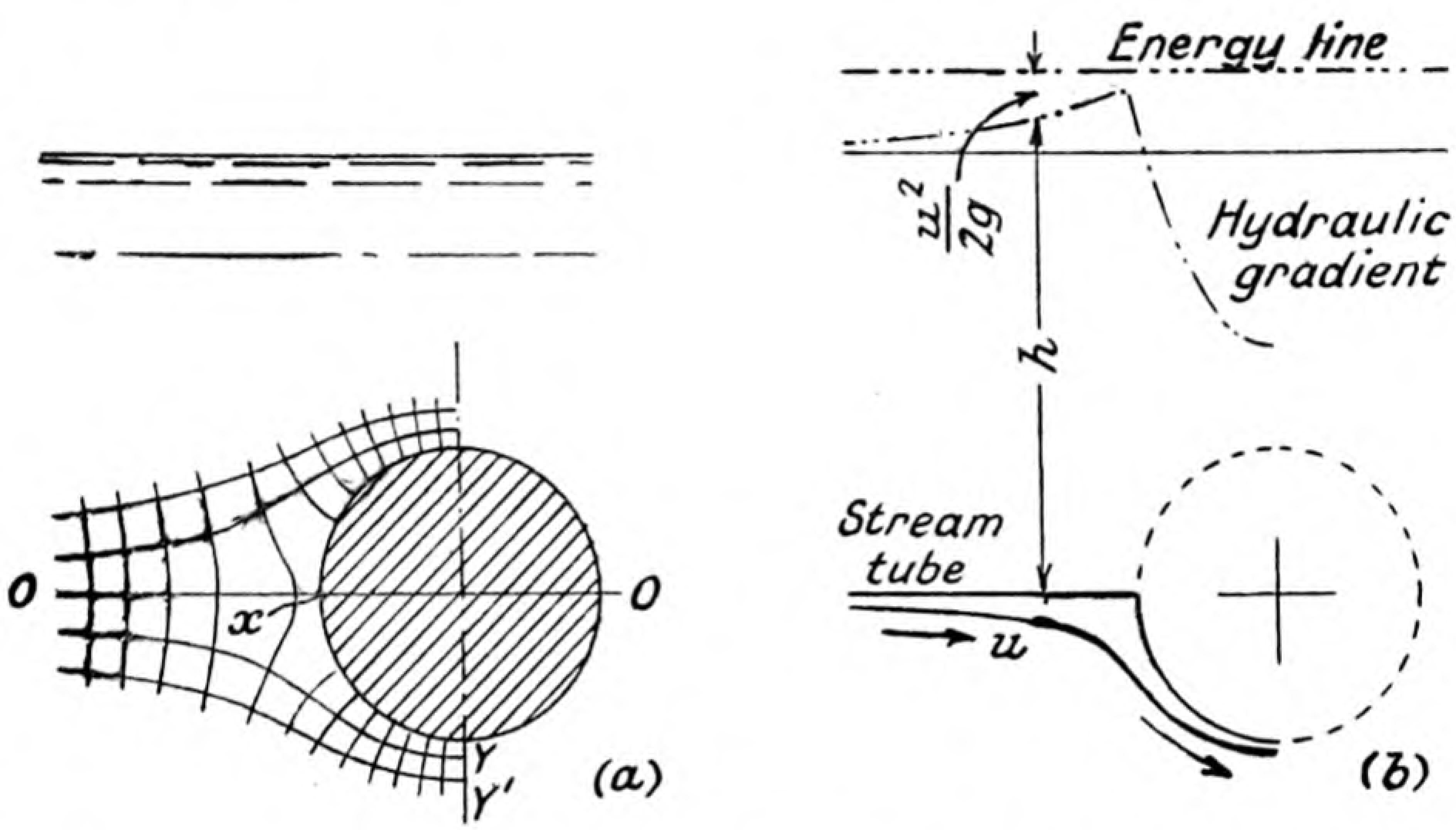

FIG. 24.—Influence of immersed solid, as shown by (*a*) flow-net, (*b*) hydraulic gradient.

Another type of exploration would lead along the vertical equi-potential line YY′. As we move away from the solid cylindrical surface, the pitch of the stream-surfaces increases—they become more widely-spaced. This means that the velocity becomes progressively less, § 36.

The utility of the flow-net is still not exhausted. Not only does it offer a ready means of ascertaining the liquid velocity at any point in the system, but it can give information too about the *pressure-head* of the liquid. Since idealised conditions are here supposed to prevail, the total energy of the liquid is assumed to be constant, § 33, and therefore Bernoulli's theorem can be applied to any stream-tube. In turn, this implies that for each stream-tube the *hydraulic gradient* can be plotted, § 34. An example is seen in Fig. 24 (*b*), which relates to the stream tube OxY in Fig. 24 (*a*). As we should expect, the pressure-head rises to a maximum at the point at which the

liquid element makes contact with the solid surface ; it falls again as the element picks up speed.

39. Energy Dissipation by Turbulence. What would be the effect of *reversing* the direction of flow throughout the system depicted in Fig. 22 ? Would the liquid elements emerging from the narrow passage carry out an orderly deployment, each going back on its original track and so re-creating the pattern of stream-lines shown in the diagram ? Ordinary observation tells us that in fact they would do nothing of the kind. On the contrary, we should expect the emerging liquid elements to preserve a sort of mass formation, thrusting their way through the bulk of liquid in the wide part of the passage and then gradually dispersing. The effect is suggested on a smaller scale in Fig. 25.

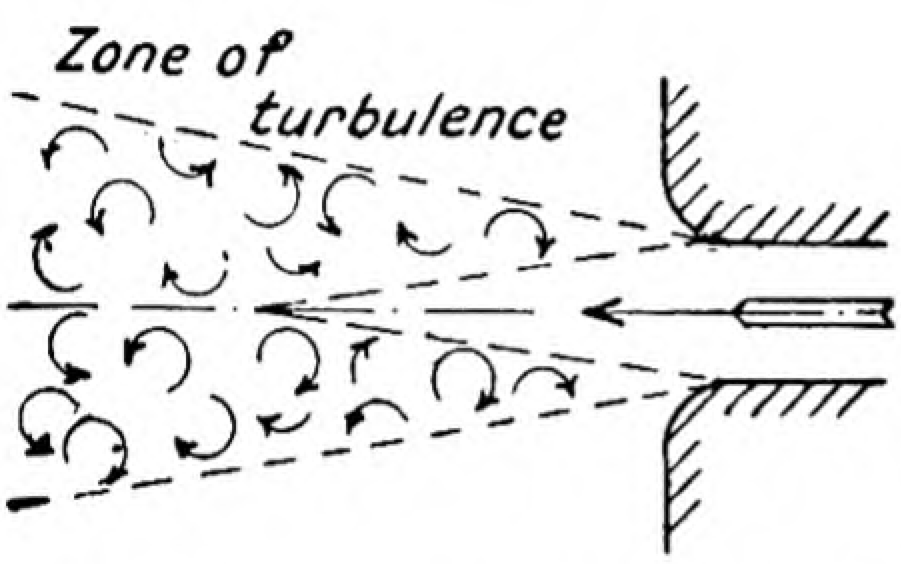

FIG. 25.—Energy dissipation by turbulence.

Here is an instance of the extreme condition of turbulence described in § 29 (iv). Yet by regarding only the mean motion of the elements, § 30, we can discern some sort of general pattern. Along the axis or core of the main stream or jet, Fig. 25, the *mean* velocity falls. Transversely, in any plane normal to the axis, the mean velocity likewise diminishes as we proceed outwards.(13) The zone of intense turbulence is confined within the limits sketched in the diagram ; but as this mass of violently eddying liquid moves onwards, it influences also the adjacent and nominally stationary liquid, from which elements are torn to mingle with the jostling throng of elements already present.(14)

In almost every way, then, the flow pattern now under study is different from those patterns that form the subject-matter of §§ 33-38. There the type of liquid motion could be described as steady, and usually non-uniform flow § 29 ; viscous effects were disregarded, and uniformity of total energy was assumed. But now, in Fig. 25, viscous influences are predominant ; the violent shearing action between adjacent liquid elements must incite viscous resistances, § 7, which ultimately involve a rapid dissipation of energy, § 9.

In such conditions there can no longer be any question of thinking about stream-lines, velocity potential, or flow-nets : all such conceptions would be wholly meaningless.

The simple example of violent turbulence illustrated in Fig. 25 is only one of many forms that may occur. In the conditions shown in Fig. 24, § 38, the potential flow defined by the flow-net would likewise break down into intense eddying in the regions to the right of the vertical YY—or even before that, § 127. The whole process is associated with the *separation of the boundary layer*, § 90. But exceptional conditions may exist, with very viscous liquids moving at low velocities, in which a regular, orderly flow pattern persists even in those regions where we should expect a state of extreme turbulence.

40. Non-dimensional Expressions. Although this chapter, and other chapters in Part I of this book, are intended to deal only with fundamental principles, yet even now it is not too soon to try to predict what complexities may arise in Part II of the book, where specific problems of hydraulic engineering will be examined. Not only will these problems involve a variety of expressions such as those for velocity, depth, diameter, viscosity, energy, etc., etc., but a wide variety of units may be chosen (§ 2), e.g. gallons per minute, dynes per square centimetre, feet per second, kilogram-metres per second, and the like. To simplify so far as is practicable such computations, two processes are found to be advantageous :

(i) To break down into their basic form the various factors involved.

(ii) To classify into *non-dimensional groups* these fundamental terms. As these groups will be pure numbers or ratios, their numerical values will be quite independent of the system of units preferred, provided that *consistent* units are chosen.

As an example of the first process, we may review the treatment of kinematic viscosity given in § 8, and the study of velocity energy in § 32. Instead of writing in full the terms "length", "force", etc., we could use some equivalent arrangement of the fundamental physical concepts

length, represented by L,
mass, represented by M,
time, represented by T.

More complex expressions could be built up from these basic terms, thus :—

Area could be expressed by . $(\text{length})^2 = L^2$

Velocity . . . . . $\dfrac{\text{length}}{\text{time}} = \dfrac{L}{T}$

Force . . . mass × acceleration $= \dfrac{ML}{T^2}$

Kinematic viscosity . . . . $\dfrac{\text{area}}{\text{time}} = \dfrac{L^2}{T}$

Viscosity . . . $\dfrac{\text{force} \times \text{time}}{\text{area}} = \dfrac{\dfrac{ML}{T^2} \cdot T}{L^2} = \dfrac{M}{LT}.$

If these *dimensional* terms are suitably combined, the desired *non-dimensional* numbers or parameters are finally obtained. Useful examples are the *Froude number*, § 52, the *Reynolds number*, § 94, the *Cavitation number*, § 135, and the *Shape number*, § 318.

The operation of assembling into these groups the fundamental terms involved is facilitated by the process of *Dimensional Analysis*.[15]

CHAPTER IV

FLOW THROUGH ORIFICES AND OVER WEIRS

41. Free-flow Devices. The present chapter is devoted to the study of specific types of flow having a basic resemblance to that depicted in Fig. 18, § 33. From an open-topped reservoir or tank in which a steady surface-level is maintained, the liquid is allowed to escape through an opening of accurately defined shape and size, and it then flows freely away at atmospheric pressure. Each liquid element is assumed to be under the influence only of (i) the force of gravity, (ii) pressure-differences which impart acceleration or retardation to it (§ 35). A direct application of Bernoulli's theorem (§ 33) will provide the desired ideal relationship between head and discharge, which can afterwards be corrected, in the light of experiment, to compensate for the observed effects of viscosity and surface tension. A precise knowledge of these relationships is of great practical value because of the frequent use of orifices and weirs for measuring the rate of flow of liquids (Chapter XIX).

42. Flow through Bell-mouthed Circular Orifice. Water issuing horizontally from a circular rounded orifice in the vertical side of a tank (Fig. 26) takes the form of a smooth parallel jet of the same diameter as the opening, curving downwards under the action of gravity. At a point (1) inside the tank on the axis of the orifice, sufficiently distant from the opening for the water to be sensibly at rest, the position energy relative to a datum plane containing the axis is zero, the pressure energy is h, and the velocity energy is zero ; at

a point (2) exactly at the mouth of the orifice, where the jet has attained its full velocity of efflux v, the position energy is zero, the pressure energy is zero (the water now being at atmospheric pressure), and the velocity energy is $v^2/2g$. Then by Bernoulli's theorem,

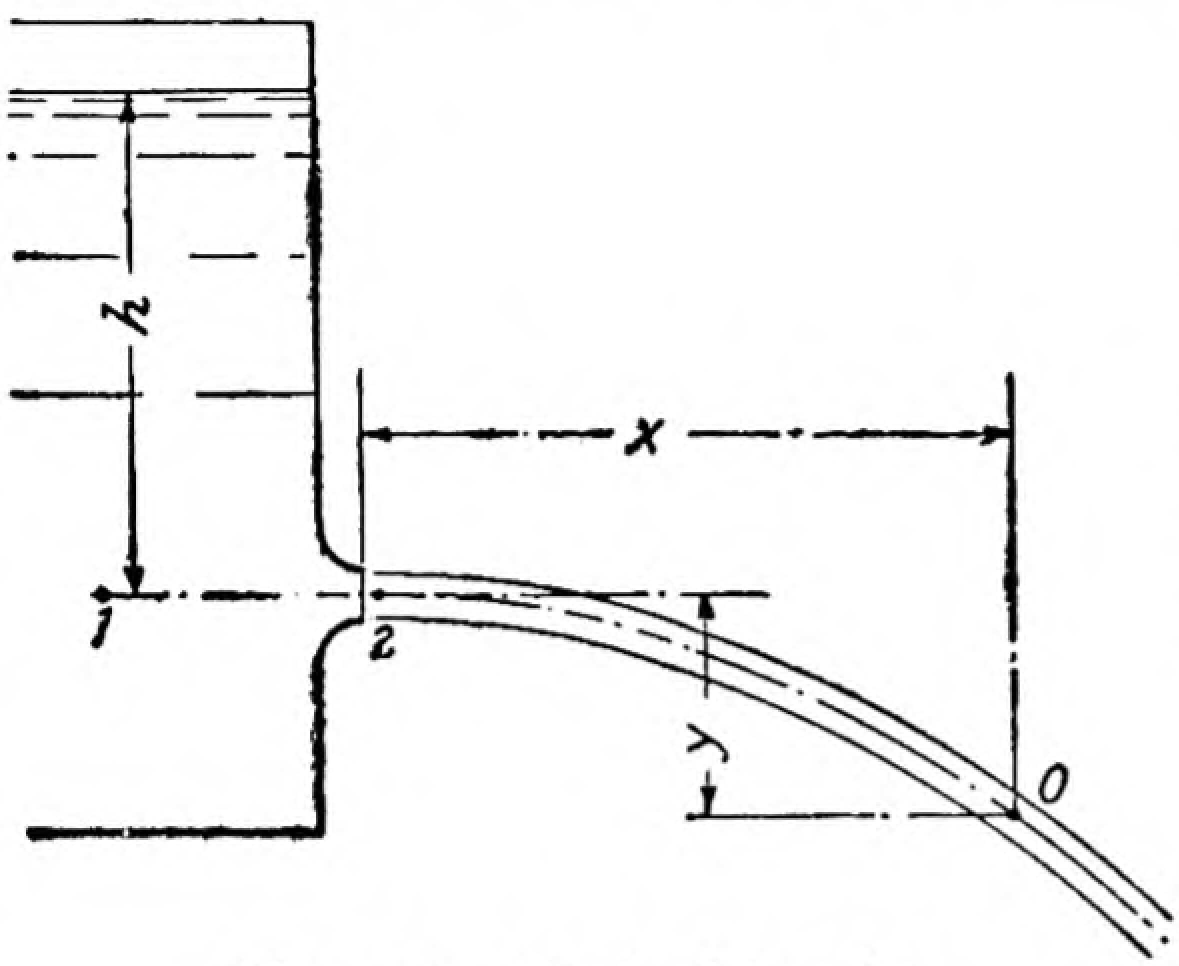

FIG. 26.—Path of free jet.

$$0+h+0=0+0+v^2/2g,$$

or $$v = \sqrt{2gh} \quad \textbf{(4-1)}$$

This ideal velocity v is sometimes called the *spouting velocity* corresponding to the head h; it is the velocity that a solid body would acquire after falling freely *in vacuo* through a height h.

Due to friction between the jet and the walls of the orifice, the *actual velocity* of efflux v_a is slightly less than the ideal velocity. The ratio $\frac{\text{actual velocity}}{\text{ideal velocity}} = \frac{v_a}{v}$ has a maximum value of about 0·99 for large orifices and it falls to 0·95 or less for orifices of $\frac{1}{2}$ in. diameter or so under heads of a foot or less. This ratio $\left(\frac{v_a}{v}\right)$, denoted by C_v, is known as the *coefficient of velocity* of the orifice. A method of measuring the actual velocity, and thus of evaluating C_v, is indicated in Fig. 26; it consists in measuring the co-ordinates x and y of a point 0 in the core of the jet. In time t a particle of water issuing from the orifice with horizontal velocity v_a will traverse a horizontal distance $x = v_at$, and during the same interval t it will fall freely under gravity through a vertical distance $y = \frac{1}{2}gt^2$, whence $v_a = x\sqrt{\frac{g}{2y}}$. The principle of the Pitot tube may also be used, as in Fig. 101, § 120.

The *discharge* through the orifice, q, is represented by $a \,.\, v_a$, where a is the area of the orifice and also in this case the area of the jet. The ratio

$$\frac{\text{actual discharge}}{\text{ideal discharge}} = \frac{q}{a\sqrt{2gh}}$$

is termed the *coefficient of discharge*, C_d, of the orifice—in the present instance it is identical in value with the coefficient of velocity C_v.

Prolongation of the bell-mouthed orifice into a *nozzle* as used, for example, on fire-hoses has little effect on the value of the coefficients C_v and C_d, which vary from 0·98 to 0·95 or less according to the size and shape of the nozzle. **(Example 15.)** It is to be noted in this connection that a jet directed vertically upwards from such a nozzle will not reach a height equal to the static head that produces flow; owing to friction in the nozzle, to friction between the jet and the surrounding air, and to the breaking up of the jet into spray, the water may only be thrown to a height equal to $\frac{3}{4}$ of the head.[16]

43. Circular Sharp-edged Orifice. To avoid the uncertainty attending the use of the bell-mouthed orifice, whose coefficients depend unduly on the precise curvature, the sharp-edged orifice is often preferred, in which the water flows only over a flat surface before breaking into a free jet (Fig. 27). To make sure that the liquid does not touch any other solid surface, the outlet side of the orifice plate is relieved or chamfered as shown in the illustration. This diagram likewise gives an impression of the stream-lines (§ 36) along which the liquid elements approach the orifice.

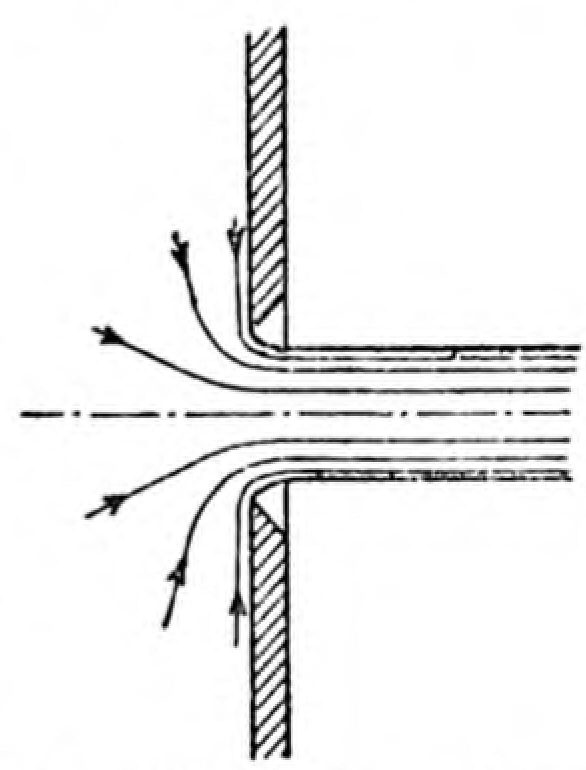

Fig. 27.—Sharp-edged orifice.

After leaving the edge of the opening, the jet rapidly contracts and only attains a parallel form at a distance of about 0·5 diameters from the plane of the orifice; the point at which the parallel part of the jet begins is termed the *vena contracta*. Thereafter, at least in favourable conditions, the jet appears to the eye nearly as rigid and immovable as a curved glass rod: we can easily believe that the flow is as steady, uniform, and uniformly distributed as it is possible to achieve, § 29 (i).

The ratio

$$\frac{\text{contracted area of jet}}{\text{area of orifice}} = \frac{a_a}{a} = C_c,$$

is termed the *coefficient of contraction* of the orifice. The value of a_a, and thus of C_c, may be obtained by actually

measuring the diameter of the jet with micrometer screws, or it may be computed from a knowledge of C_v and C_d, as shown below. It is then found that C_c is of the order of 0·63. The coefficient of velocity, as determined by the method described in the previous paragraph, ranges in value from 0·99 to 0·95 or less.

The discharge through the sharp-edged orifice is the product of the area of the *jet* and the velocity of the jet, that is, $q = C_c a \times C_v\sqrt{2gh}$; but also $q = C_d a\sqrt{2gh}$, therefore $C_d = C_v \times C_c$. The coefficient of discharge C_d is the easiest of all the coefficients to measure, for it entails only direct observations of h and of q. **(Example 16.)** As a result of very many such observations,[17] it is possible to state that so long as the orifice has a diameter of 0·2 ft. (6 cms.) or more, and works under a head of 1·5 ft. (45 cms.) or more, C_d for water at atmospheric temperatures has a very nearly constant value of 0·597. For smaller orifices, other temperatures, lower heads, or other liquids, the following formula, which takes into account all these variables, may tentatively be used :—

C_d for sharp-edged orifice

$$= 0{\cdot}592 + \frac{4{\cdot}5}{\sqrt{R_n}} \qquad . \quad . \quad . \ (4\text{-}2)$$

where R_n is the nominal Reynolds number (§ 64)

$$= \frac{vd}{\nu} = \frac{\sqrt{2gh} \times \text{diam. of orifice}}{\text{kinematic viscosity}}.$$

(*Note :* The various types of coefficient, e.g. the coefficient of discharge C_d, are examples of the non-dimensional expressions mentioned in § 40, thus :—

$$C_d = q/(a\sqrt{2gh}) = \frac{\dfrac{L^3}{T}}{L^2\sqrt{\dfrac{L}{T^2}}\,.\,L} = 1$$

or C_d is dimensionless, or a pure number.)

44. Energy of a Jet. Knowing the velocity v and the area a of a jet, the rate at which it carries away energy is readily calculated. The weight of liquid flowing per second is wav; the velocity energy per unit weight is $v^2/2g$; hence total energy per second $= wav \times \dfrac{v^2}{2g} = \dfrac{wav^3}{2g}$. Putting $W = wav =$ weight of liquid per second, then energy per second $= \dfrac{Wv^2}{2g}$.

If this energy is expressed in ft. lb./sec., the corresponding horse-power is $\dfrac{\text{energy per second}}{550}$.

If the energy is expressed in kg. m./sec., the corresponding metric horse-power is $\dfrac{\text{energy per second}}{75}$.

The method by which the jet may be made to yield up such energy is described in §§ 123 and 124.

45. Submerged Orifices. An orifice which, instead of discharging freely into air, projects its jet into water on the downstream side, is said to be drowned or submerged. These conditions are represented in the diagram (Fig. 28). Due to the inter-action—the drag or friction—between the jet and the water surrounding it, the jet is quickly checked and in time "smothered," its diameter increasing and its boundaries becoming ill-defined until at some distance from the orifice the average velocity on the axis has fallen almost to zero, § 40.

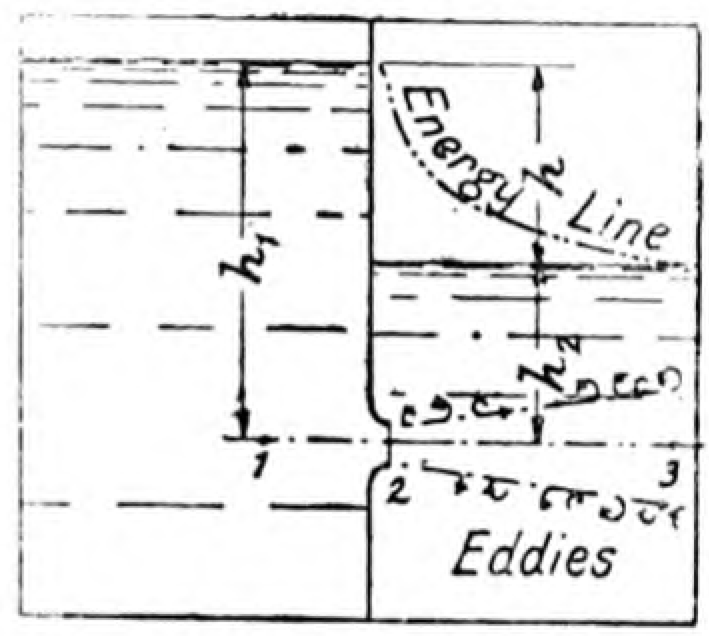

FIG. 28.—Submerged orifice.

Because of the intensity of the turbulence, energy is rapidly dissipated. This is denoted in Fig. 28 by the quick descent of the total energy line; while at point 1 the total energy is h_1, and at point 2 it is $h_1 = h_2 + v_2{}^2/2g$, yet at point 3 it is h_2 only. It is to be noted that since $v_2{}^2/2g = h_1 - h_2 = h$, the ideal velocity v_2 at the orifice depends upon the *difference* in water level between the two tanks, irrespective of the position of the orifice. The coefficient of discharge C_d for a submerged orifice may be slightly less than for a similar orifice freely discharging into air.

46. Submerged Orifice Discharging into Pipe. Although thewhole of the water in the downstream tank in Fig. 28 is visibly in a state of slow, swirling motion, yet at a sufficiently great distance from the orifice the average velocity in the direction of the jet is sensibly zero. If, on the other hand, the jet discharges into a pipe as in Fig. 29, the water on the downstream side now has a mean velocity v_3. It is therefore reasonable to say that if in Fig. 28 the loss of energy depends upon the *difference* between the velocity of the jet

and the mean velocity of the water into which it impinges, viz. upon $(v_2 - 0)$, then in Fig. 29 the energy loss will depend upon $(v_2 - v_3)$, and will be represented by

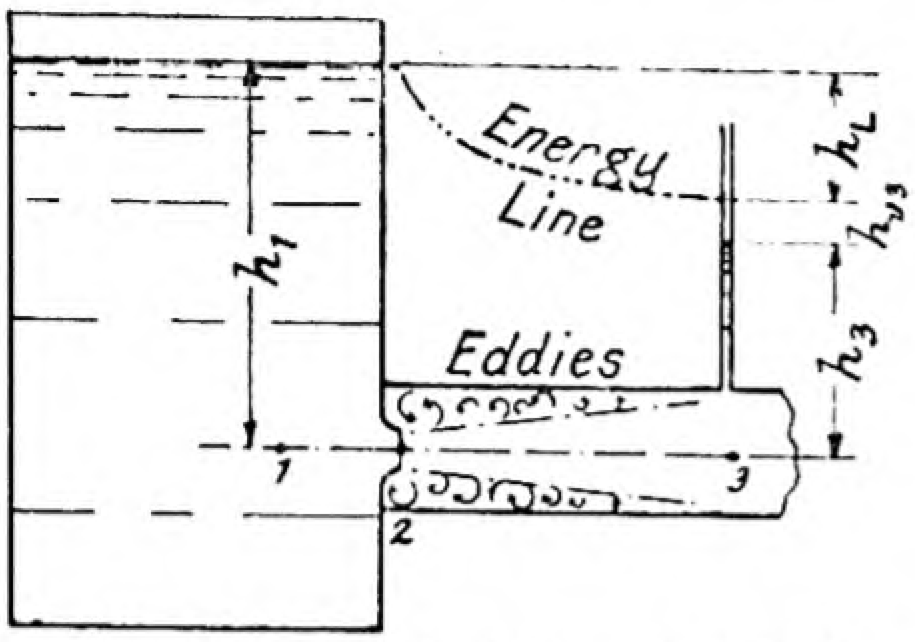

FIG. 29.—Illustration of eddy loss.

$$h_L = \frac{(v_2 - v_3)^2}{2g}. \quad . \quad \textbf{(4-3)}$$

The total energy line shows that at point 1 the energy is h_1, while at point 3 it has fallen to $h_3 + h_{v3}$, where $h_{v3} = \frac{v_3^2}{2g}$, the difference having been lost in initiating eddies in the zone surrounding the jet.

An alternative derivation of equation (4-3) is given in § 136.

47. Bell-Mouthed Orifice with Diverging Mouth-Piece. The flow through orifices is sensibly affected by adding a mouthpiece, tail-pipe or ajutage. Applying Bernoulli's theorem to the points 1, 2, and 3 (Fig. 30 (*a*)), in which a diverging taper pipe is shown affixed to a bell-mouthed orifice, we have, under ideal conditions,

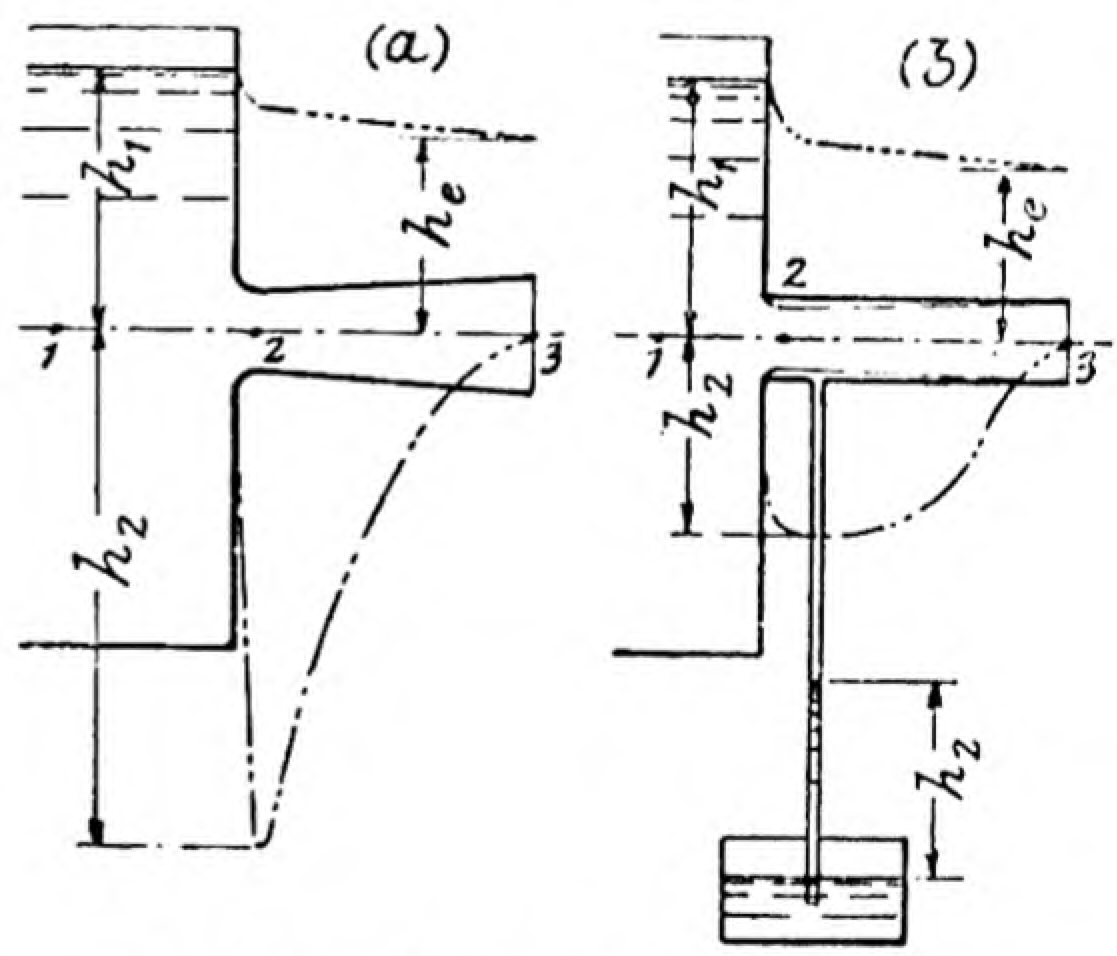

FIG. 30.—External mouthpieces: (*a*) Diverging; (*b*) Parallel.

$$h_1 = h_2 + \frac{v_2^2}{2g} = \frac{v_3^2}{2g}.$$

Since v_2 is clearly greater than v_3, the head at 2 is negative; the water here can be regarded as being pushed through the orifice by the positive head h_1, and drawn or pulled through by the negative head h_2. Consequently the discharge through the orifice is *increased* by the addition of the tail-pipe, in the ratio (under ideal conditions) of

$$\frac{a_3\sqrt{2gh}}{a_2\sqrt{2gh}}, \quad \text{viz.} \quad \frac{a_3}{a_2}.$$

The friction and eddy losses that do in fact occur in the orifice and in the mouthpiece depend upon the length and the

angle of divergence of the tail-pipe (§ 87 (*b*)); they are rarely less than 16 per cent. of the static head h_1, for a mouthpiece of the proportions shown in Fig. 30 (*a*). Accepting this value, the true expression connecting head with velocity will therefore be $h_1 = v_3^2/2g + 0{\cdot}16h_1$, from which $v_3 = 0{\cdot}92\sqrt{2gh_1}$. If the coefficient of discharge C_d of the orifice is based on the outlet area a_3, its value may thus be 0·92, but if C_d is based on the orifice area a_2, its value is $0{\cdot}92\dfrac{a_3}{a_2}$, which may be considerably greater than unity.

48. Plain External Mouthpiece, or Pipe Extension. Here (Fig. 30 (*b*)) a short length of parallel pipe of the same diameter as the orifice and not less than four diameters long is attached to a plain sharp-edged orifice in the side of the tank. The jet contracts and forms a vena contracta just as though the pipe were not there; then the jet expands and issues from the pipe "full-bore" in a stream of the same diameter as the pipe. Between the vena contracta and the pipe walls a zone of violently eddying water is formed, precisely as in Fig. 29, which continuously abstracts energy from the jet at a rate indicated by formula 4-3 above (§ 46).

Bernoulli's equation must therefore be modified thus: Total energy at 1 = Total energy at 2 = Total energy at 3 + loss of energy between 2 and 3,

or
$$h_1 = h_2 + \frac{v_2^2}{2g} = \frac{v_3^2}{2g} + \frac{(v_2 - v_3)^2}{2g}.$$

Taking a coefficient of contraction C_c for the orifice of 0·61,

then
$$v_2 = \frac{v_3}{0{\cdot}61},$$

therefore
$$h_1 = \frac{v_3^2}{2g} + \frac{\left(\dfrac{v_3}{0{\cdot}61} - v_3\right)^2}{2g}$$

whence $v_3 = 0{\cdot}84\sqrt{2gh_1}$. Owing to additional losses [18] in the pipe and in the orifice, the actual value of the coefficients of discharge and of velocity, $C_d = C_v = \dfrac{v_3}{\sqrt{2gh_1}}$, are about 0·82.

(*Note.*—Under high heads it may be possible for the jet to spring clear of the walls of the mouthpiece without touching them, in which case the flow through the orifice is unaffected by the mouthpiece.)

49. Internal Mouthpiece, or Borda's Mouthpiece. (*a*) *Jet springing clear.* In the Borda mouthpiece the pipe projects internally into the tank (Fig. 31). To calculate the coefficient of contraction when the jet springs clear (Fig. 31 (*a*)), we consider a circle of area a on the left-hand wall of the tank,

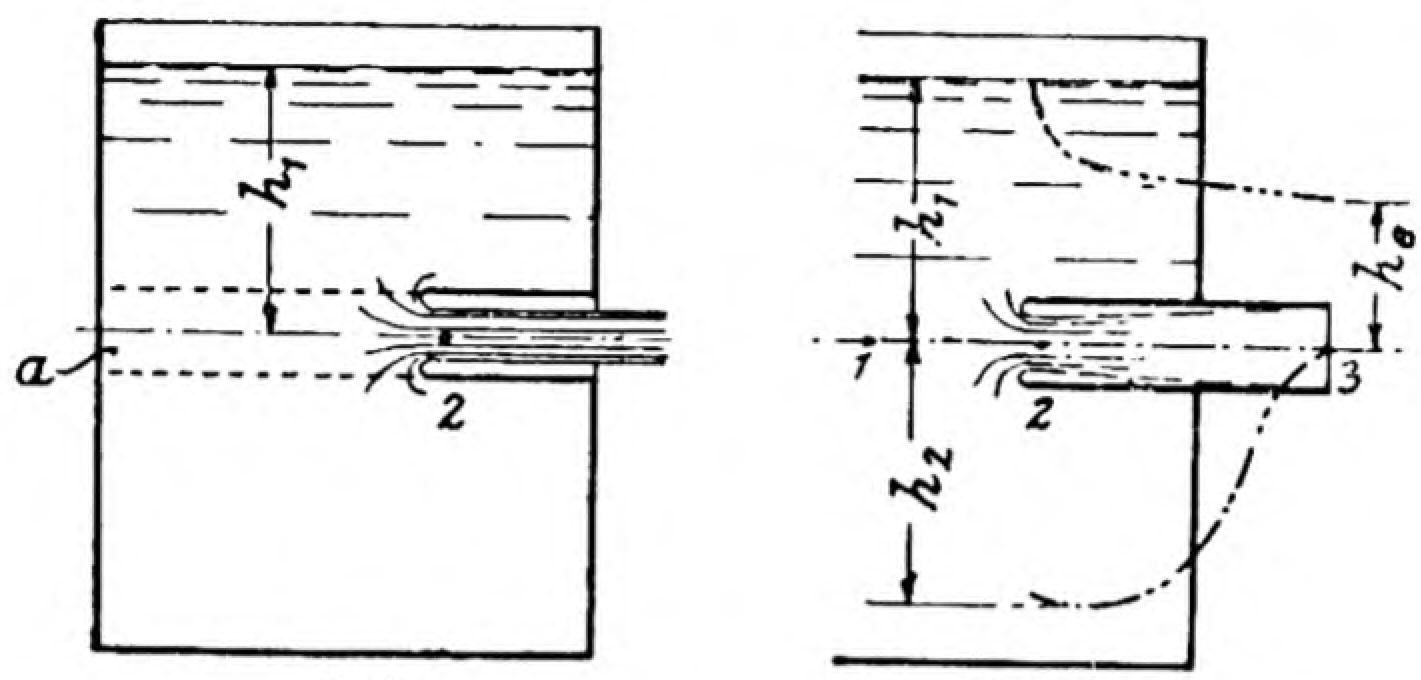

FIG. 31.—Internal mouthpiece: (*a*) Running clear; (*b*) Running full.

exactly opposite the orifice, so that if the mouthpiece were prolonged it would meet the wall in this circle. The static thrust on the area a is $P = wah_1$; but on the right-hand wall there can be no counterbalancing thrust because of the hole in this wall. It is the unbalanced reaction wah_1 which can be regarded as imparting acceleration to the water. (See also § 122.)

The mass of water entering the mouthpiece per second is $\dfrac{wC_c av_2}{g}$, therefore the change of momentum per second imposed on the water by the force wah_1 is $\dfrac{wC_c av_2}{g} \times v_2$. Equating,

$$wah_1 = \frac{wC_c av_2^2}{g}, \quad \text{from which} \quad C_c = \frac{h_1}{\dfrac{v_2^2}{g}}.$$

But from the energy equation, we know that $h_1 = \dfrac{v_2^2}{2g}$.

$$\text{Substituting, we find} \quad C_c = \frac{\dfrac{v_2^2}{2g}}{\dfrac{v_2^2}{g}} = 0{\cdot}5.$$

Thus the jet running clear in a Borda mouthpiece has an area one-half that of the pipe.

(*Note.*—The reason why the above method cannot be used for finding the value of C_c for a plain sharp-edged orifice (§ 43) is illustrated in Fig. 32. Because of the inwardly flowing streams converging radially over the orifice plate, there is a zone immediately surrounding the opening in which the pressure has already been reduced below the full static head h; these pressure-changes along a stream-tube are suggested in Fig. 24 (*b*), § 38. Consequently the unbalanced reaction producing horizontal acceleration of the main liquid stream is wah, *plus* a reaction equivalent to the reduction in pressure in the zone surrounding the orifice.

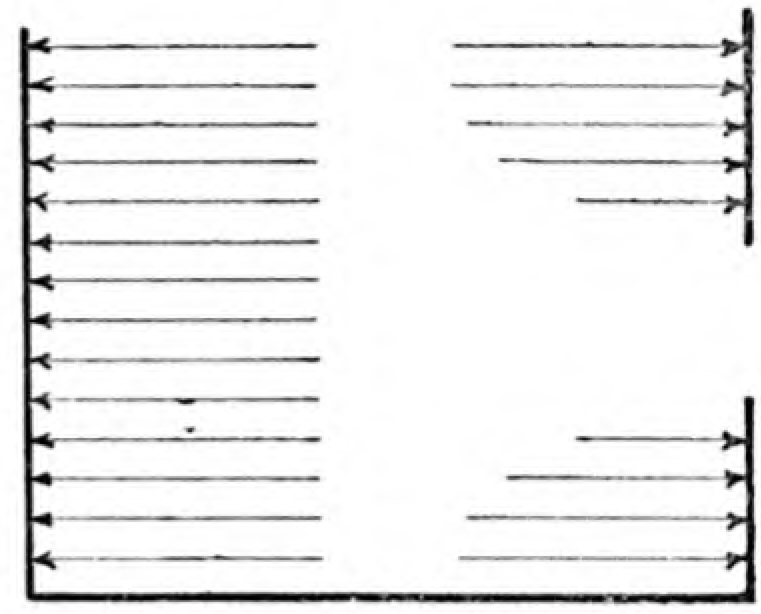

FIG. 32.—Pressure distribution near orifice.

There is no such zone in the side of the tank containing the Borda mouthpiece, for here, still water is everywhere in contact with the tank walls; pressure changes take place well towards the middle of the tank.)

(*b*) *Mouthpiece running full.* If once the jet touches the inner wall of the pipe, it expands and fills the pipe, which then runs full-bore (Fig. 31 (*b*)). The coefficient of discharge can then be calculated in the same way as in § 48 above, except that now $v_2 = \dfrac{v_3}{0{\cdot}50}$. The value of C_d is thus found to be 0·71, but its measured value may be 0·75 or more.

When an internal or an external mouthpiece runs full, the appearance of the jet is very different from that of the jet issuing from a properly-operated sharp-edged orifice, § 43. The violent state of turbulence generated in the mouthpiece is made manifest by the milky look of the water and by the tendency of the jet to break up into a diverging stream of individual drops.

50. Comparison of Mouthpieces. The lengths of the ordinates h_e (Figs. 30 and 31), representing the total energy at the outlet of the mouthpieces, afford a measure of the comparative efficiency of the various forms of tail-pipe. As the efficiency $\left(\dfrac{h_e}{h_1}\right)$ is readily seen to be equal to $C_d{}^2$, the relative efficiencies are: for the taper "stream-lined" mouthpiece 84 per cent., for the external mouthpiece 67 per cent., and for the Borda mouthpiece 56 per cent. But the superiority of the taper mouthpiece does not depend on this figure 84 per cent. alone; in addition we must take into account the increased discharge area a_3 of this mouthpiece compared with the area a_3 of the other two.

It will be noticed that adding an external mouthpiece or a Borda mouthpiece will increase the discharge of a sharp-edged orifice, in the ratio of about $\frac{0 \cdot 82}{0 \cdot 60}$ and $\frac{0 \cdot 75}{0 \cdot 60}$ respectively.

The hydraulic gradients sketched in Figs. 30 and 31 show that there is a negative head, § 15, in each of the tail-pipes. The existence of this negative head—the head that "pulls" the water through the orifice and so increases its discharge—can be demonstrated by connecting to the throat of the tail-pipe, as in Fig. 30 (*b*), a glass tube dipping at its lower end into a vessel of water. The height h_2 to which the water rises in the tube can be calculated from the energy equation established in the preceding paragraphs,

$$h_2 = h_1 - \left(\frac{v_2{}^2}{2g}\right), \quad \text{or} \quad h_2 = h_1 - \frac{\left(\frac{v_3}{C_c}\right)^2}{2g}.$$

For the external mouthpiece, h_2 is thus found to be $-0 \cdot 80h_1$, and for the internal mouthpiece, $-1 \cdot 24h_1$. Due to the losses in the orifices themselves, the observed values of h_2 are a little less than these. In no circumstances, of course, can they exceed the limits specified in § 16.

51. Principle of Geometrical Similarity. In this paragraph it is our object to compare the performances of openings and orifices of the same geometrical *shape* but of different *sizes.* The orifice in the large tank in Fig. 33 has a diameter D and works under a head H; the orifice in the small tank has a diameter d and it works under a head h. Putting n for the ratio $\frac{D}{d}$, geometrical similarity is said to exist if $\frac{H}{h} = n$, and if any one dimension in the large tank is n times the corresponding dimension in the small tank.

Will the trajectories of the jets also be similar? From § 42 we have $V = X\sqrt{\frac{g}{2Y}}$, and $v = x\sqrt{\frac{g}{2y}}$; also, under ideal conditions, $V = \sqrt{2gH}$, and $v = \sqrt{2gh}$.

Therefore
$$\frac{V}{v} = \sqrt{\frac{H}{h}} = \sqrt{n}.$$

Consequently $$\frac{X\sqrt{\dfrac{g}{2Y}}}{x\sqrt{\dfrac{g}{2y}}} = \sqrt{n}, \quad \text{and thus} \quad \frac{X^2}{x^2} \cdot \frac{y}{Y} = n.$$

Hence, if $$\frac{X}{x} = n, \quad \frac{Y}{y} \text{ also} = n.$$

The paths of the jets, then, *are* similar. If the left-hand diagram were re-drawn to a reduced scale of $\frac{1}{n}$, it would exactly coincide with the right-hand diagram. Thus, we may be justified

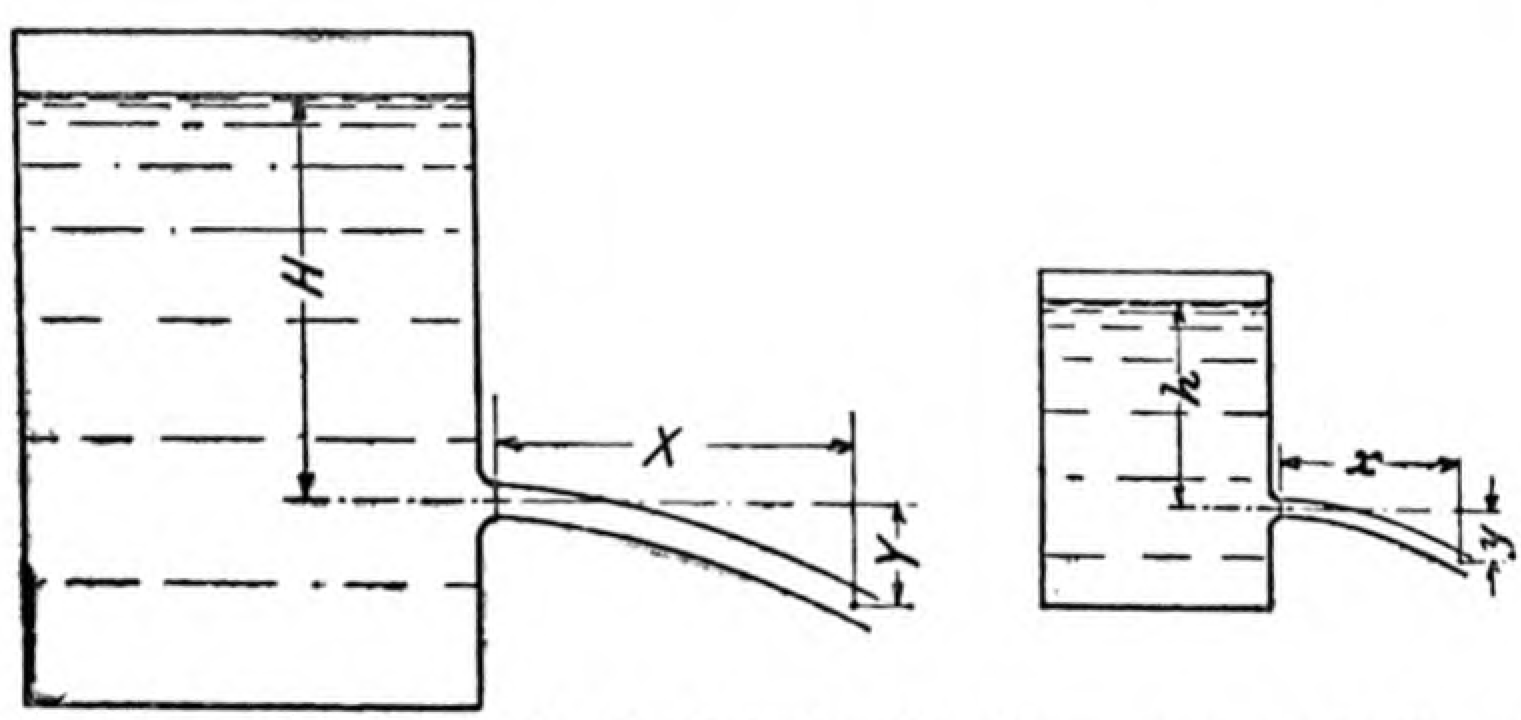

FIG. 33.—Geometrically similar jets flowing from geometrically similar orifices.

in assuming that in all other respects the jets are similar, that they both have the same ratio $\frac{\text{diameter of jet}}{\text{diameter of orifice}}$ and that consequently they have the same coefficients C_c, C_v and C_d.

The performances of the orifices may now be tabulated as follows:

	Large.	Small.
Head.	H.	h.
Diameter of orifice.	D.	d.
Area of orifice.	$A = \frac{\pi}{4}D^2$.	$a = \frac{\pi}{4}d^2$.
Area of jet.	C_cA.	C_ca.
Velocity of jet.	$V = C_v\sqrt{2gH}$.	$v = C_v\sqrt{2gh}$.
Discharge.	$Q = C_cAV$	$q = C_cav$
	$= C_d\frac{\pi}{4}D^2\sqrt{2gH}$.	$= C_d\frac{\pi}{4}d^2\sqrt{2gh}$.

The ratio of the *areas* is thus $\dfrac{D^2}{d^2} = n^2$.

The ratio of the *velocities* is thus

$$\frac{V}{v} = \frac{C_v\sqrt{2gH}}{C_v\sqrt{2gh}} = n^{\frac{1}{2}}.$$

The ratio of the *discharges* is thus

$$\frac{Q}{q} = \frac{C_d\frac{\pi}{4}D^2\sqrt{2gH}}{C_d\frac{\pi}{4}d^2\sqrt{2gh}} = n^2\sqrt{n} = n^{\frac{5}{2}}.$$

If the orifices are of so simple a form, and work under such conditions that the effects of viscosity are inappreciable, then the ideal relationships here established are found to hold good, very nearly indeed, in practice. For example, they would be valid for the sharp-edged orifices having a constant coefficient of discharge mentioned in § 43. On the other hand, it is shown in § 95 that if the passages under comparison are relatively long and narrow, so that friction losses are to be taken into account, then the exact relationships $\dfrac{V}{v} = n^{\frac{1}{2}}$, and $\dfrac{Q}{q} = n^{\frac{5}{2}}$, cannot possibly be realised.

Nevertheless the principle of geometrical similarity, suitably corrected, is of the highest practical value in forecasting, by means of experiments on scale models, the behaviour of large sluices, turbines, pumps, etc.[19]

52. The Froude Number. In the preceding paragraph it was shown that one condition for geometrical similitude was that

$$V/\sqrt{2gH} = v/\sqrt{2gh}.$$

Since, by definition, $H/D = h/d$, the equation can be simplified into the form :

$$\frac{V}{\sqrt{gD}} = \frac{v}{\sqrt{gd}}.$$

Examining these expressions, we find that they are *dimensionless*, § 40 ; each of them is represented by a pure number.

This number is termed the *Froude* number. It serves as a criterion which, when applied to two geometrically-similar

systems, determines whether or not geometrical similitude of flow may be expected. In general terms, if V is any representative velocity in the system, and D a representative dimension, then if the Froude numbers $V/\sqrt{gD}$ have identical values in the two systems, there will be similarity of flow pattern: this similitude will extend to abstractions such as flow-nets, § 38, as well as to visible liquid surfaces.

At this stage it is illuminating to examine again the fundamental assumptions on which the present chapter is based, § 41. Only two types of force were accepted, (i) the force of gravity, (ii) forces related to acceleration or retardation of liquid elements. With the help of the analysis used in § 49 (*a*) we may now assign mathematical values to such forces: a gravitational force was represented by wah, and an inertia force by wav^2/g. The ratio between them is thus $\dfrac{\left(\dfrac{wav^2}{g}\right)}{wah}=\dfrac{v^2}{gh}$; which is of the same form as the Froude number $v/\sqrt{gd}$. In other words, the Froude number itself serves as a measure of the relative importance of the inertia or acceleration forces as compared with the gravitational forces in a system.

It is easy to visualise the effect of changing the Froude number in given circumstances. Suppose, for instance, that the head in the large tank in Fig. 33 were to be considerably increased, thereby *increasing* the Froude number. The jet, now moving much more rapidly, would spring out almost horizontally; its velocity energy would be so relatively great that the gravitational force acting upon the liquid would be ineffective in trying to pull the jet down into its original shape depicted in Fig. 33.

53. Comparison between Orifices and Weirs. The essential difference between an orifice and a weir is implicit in the expressions: water flows *through* an orifice but *over* a weir. Yet the same apparatus may serve either as an orifice or as a weir. In Fig. 34(*a*), water is seen flowing through a circular aperture called an orifice; but if because of a diminution of discharge the water surface falls below the top of the aperture (Fig. 34(*b*)), the aperture is then called a weir. Small weirs in thin vertical plates are often termed *notches*. Another change in terminology is that the stream of water which is known as the jet when issuing from an orifice becomes the *nappe*, *sheet*, or *vein* when flowing over a weir. Under very

low heads the nappe tends to cling to the downstream face of the weir plate, Fig. 42; the following discussion of weir discharges refers only to the normal flow when the nappe springs clear as shown in Fig. 34 (*b*).

The large orifice (Fig. 34(*a*)) may well be looked upon as a transitional stage between the small orifices dealt with in the preceding paragraphs, and the weir. In such an orifice it would manifestly be wrong to assume, as has hitherto been done,

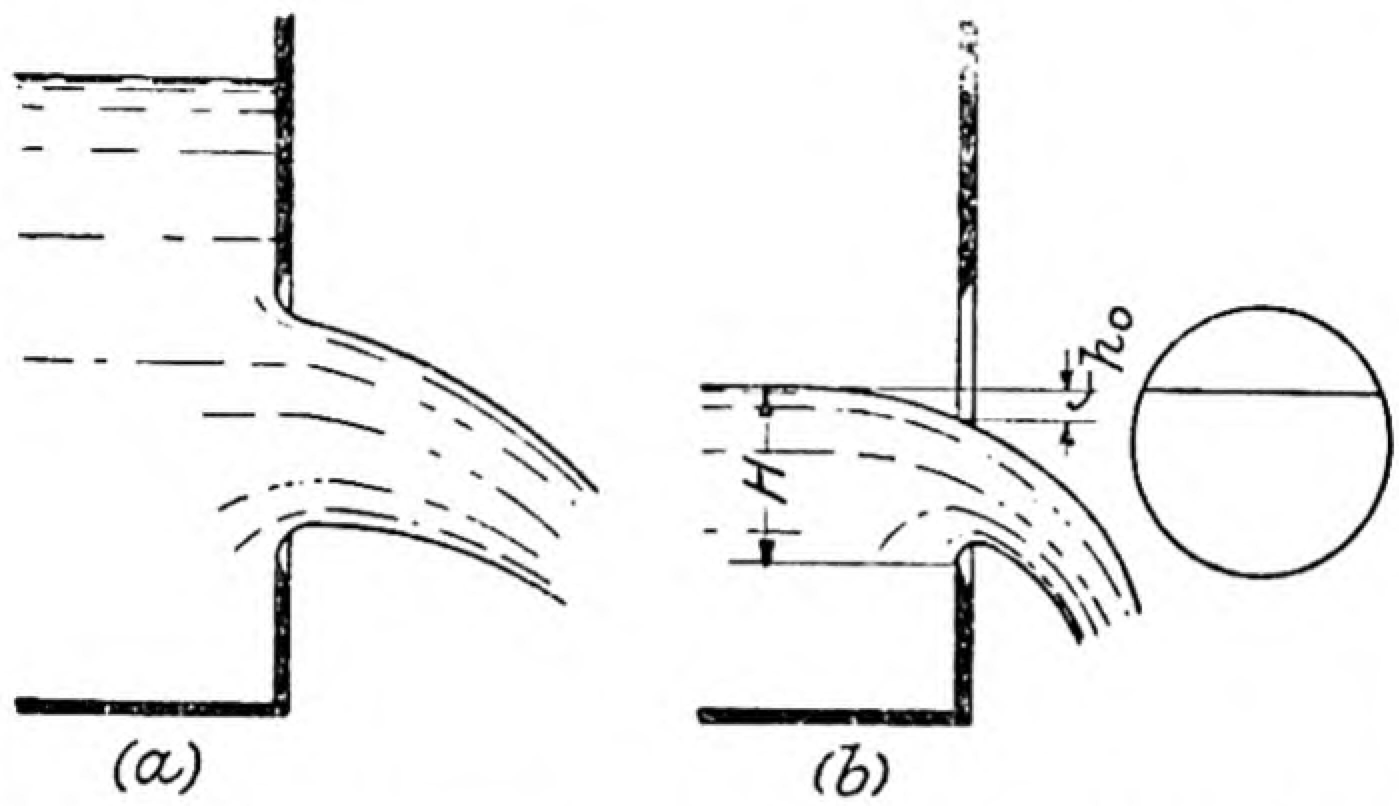

FIG. 34.—Circular aperture acting as (*a*) orifice; (*b*) weir.

that the average velocity throughout the cross-section of the jet is the same as the velocity at the axis. The correct way to deal with the variations in velocity between the top and the bottom of the opening, due to the difference in pressure head at these points, would seem to be to divide the cross-section into a number of small elements, treat each of these as a small orifice acting under its appropriate head, and then to obtain the total flow by summing the individual discharges. In practice, however, the conditions are rarely simple enough for this procedure to be followed (§§ 191-194).

Referring now to Fig. 34 (*b*), the water can only have acquired the velocity necessary to carry it over the weir at the expense of pressure or position energy; this is indicated by the amount h_0 by which the water in the plane of the weir plate has fallen below the still water level. But it would not be admissible to equate h_0 to the average velocity energy of the nappe at this point, because, on account of the curved paths in which the water is moving, and the resulting influence of centrifugal force (§ 139), the height $(H - h_0)$ no longer truly represents its pressure energy. We therefore

make no attempt to measure h_o. Instead, the height H from the lowest point of the opening to the (assumed) *still* water surface is measured and is spoken of as the head over the weir. Although circular weirs of the sort here mentioned are occasionally used, the types now to be described are generally preferred because of the relative simplicity of the important relationship connecting the head H with the discharge. Instruments suitable for measuring the head H are described in Chap. XIX.

In weir flow the type of acceleration of the liquid elements described in § 49 can be made visible to the eye. A fragment of paper dropped on to the water surface a little distance upstream from the weir is seen to float along quite sedately until it nears the plate itself; then it gradually gathers speed and finally dives swiftly downwards.

54. Sharp-edged Triangular Weir. The flow through this simple weir or notch (Fig. 35) lends itself well to investigation by the principle of geometrical similarity, § 51. Considering

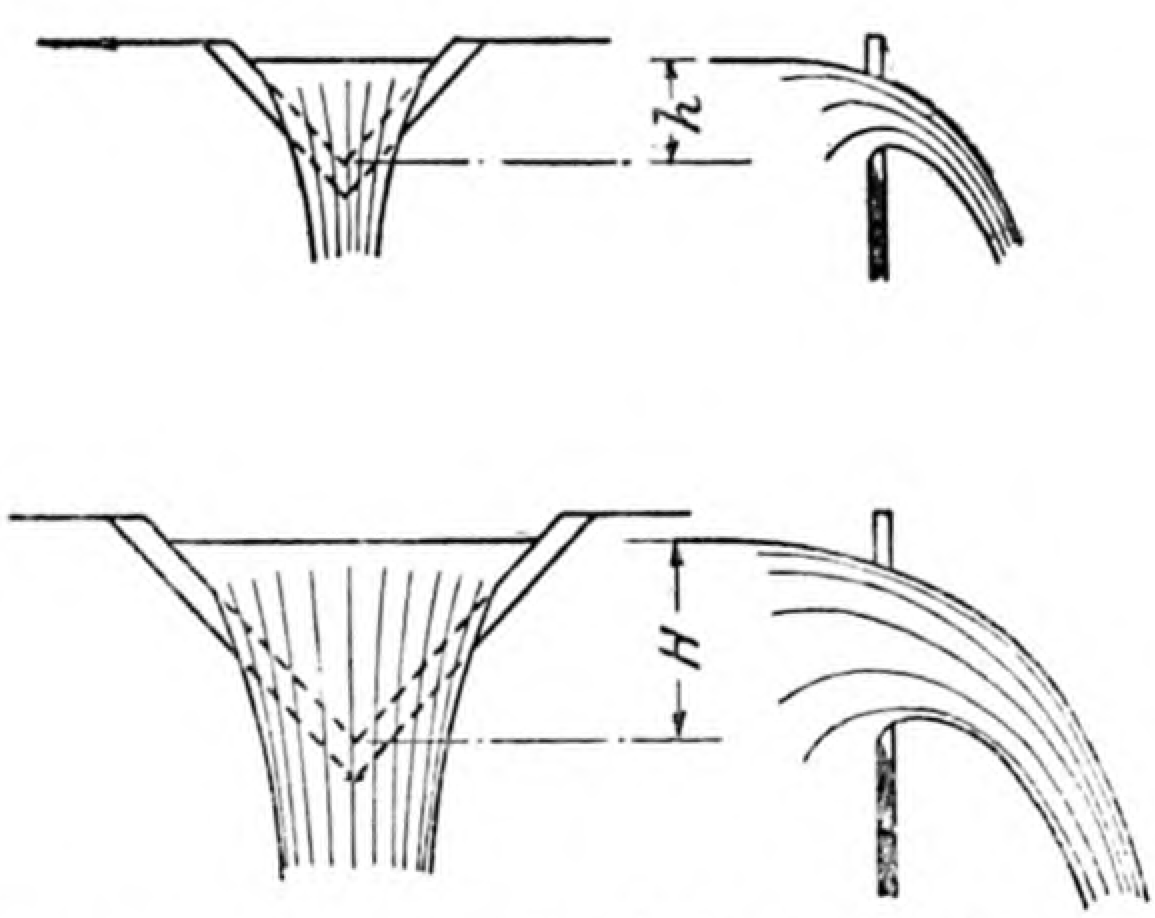

FIG. 35.—Geometrically similar triangular weirs.

two such notches of the same base angle but of different sizes, the nappes under ideal conditions should be geometrically similar, and thus if h and H are the respective heads and q and Q the discharges, then $\left(\frac{H}{h}\right)^{\frac{5}{2}} = \frac{Q}{q}$. But in any one notch the nappe under any one head will be similar to the nappe under any other head, and therefore discharge $Q =$ a constant $\times H^{\frac{5}{2}}$.

Alternatively the discharge may be assessed by the integration method outlined in § 53 above. We first consider a

small horizontal elementary strip in the plane of the weir plate, of breadth b and height dh (Fig. 36), and calculate what the discharge dq would be through an orifice of these dimensions under head h, viz.

$$dq = C_d b \,.\, dh \,.\, \sqrt{2gh} = C_d \,.\, 2(H - h) \tan \frac{\theta}{2}\, dh \,.\, \sqrt{2gh}.$$

The total discharge over the weir will then be

$$Q = \int_0^H C_d \,.\, 2(H - h) \tan \frac{\theta}{2} \,.\, \sqrt{2gh} \,.\, dh$$

$$= \frac{8}{15} C_d \,.\, \tan \frac{\theta}{2} \sqrt{2g} \,.\, H^{\frac{5}{2}}. \quad (4\text{-}4)$$

This relationship is of the same form as that established by the principle of similarity, above.

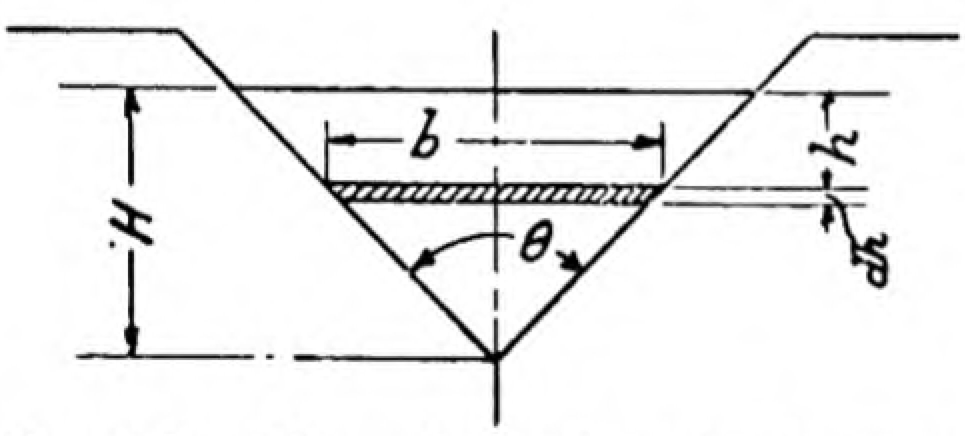

Fig. 36.—Flow through weir element.

For heads above 0·2 ft. (6 cms.), the value of the coefficient of discharge C_d for a right-angled weir, $\theta = 90°$, has a nearly constant value of 0·593. Inserting this value in the equation above, and expressing H in feet and Q in cusecs, we obtain

$$Q = 2{\cdot}53\, H^{\frac{5}{2}} \text{ (very nearly)}.$$

If H is in cms. and Q in litres/sec.,

$$Q = 0{\cdot}0140\, H^{\frac{5}{2}}.$$

To allow for the slight variations to which C_d is subject on account of viscosity and surface tension, a more general relationship is

$$Q = 2{\cdot}48\, H^{2\cdot48} \quad (Q \text{ in cusecs, } H \text{ in ft.})$$

or $$Q = 0{\cdot}0146\, H^{2\cdot48} \quad (Q \text{ in litres/sec., } H \text{ in cms.}).$$

Both in this and in the following paragraphs, the values for discharge coefficients relate only to water at atmospheric temperatures.

55. Rectangular and Trapezoidal Weirs. Here the weir has a straight horizontal sill or crest. The discharge

through a horizontal element of a rectangular weir (Fig. 37), of breadth b and height dh, is $dq = C_d \, . \, b \, . \, dh \, . \, \sqrt{2gh}$, hence the total discharge Q over the weir is

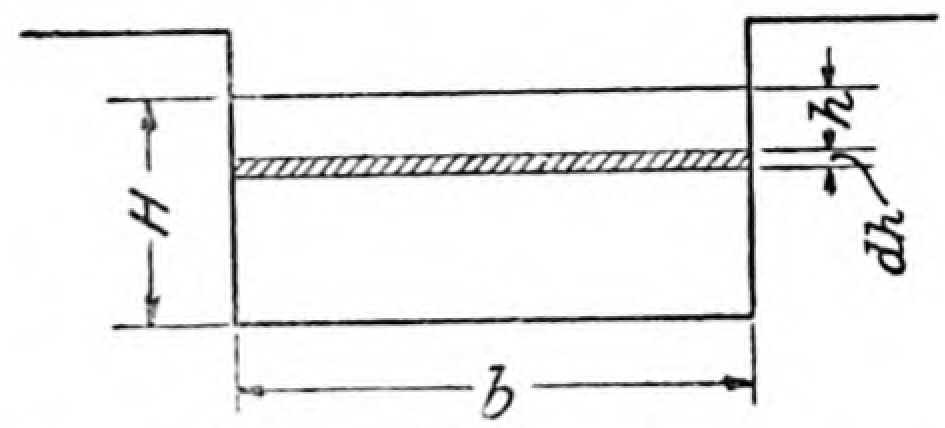

Fig. 37.—Rectangular weir.

$$Q = \int_0^H C_d b \, . \, \sqrt{2gh} \, . \, dh$$

$$= \tfrac{2}{3} C_d \, . \, b \, . \, \sqrt{2g} \, . \, H^{\frac{3}{2}}. \quad \textbf{(4-5)}$$

If the weir is sharp-edged both along the crest and at the ends (Fig. 38 (I)), the nappe is said to have both bottom and end contractions. The effect of the end contractions becomes

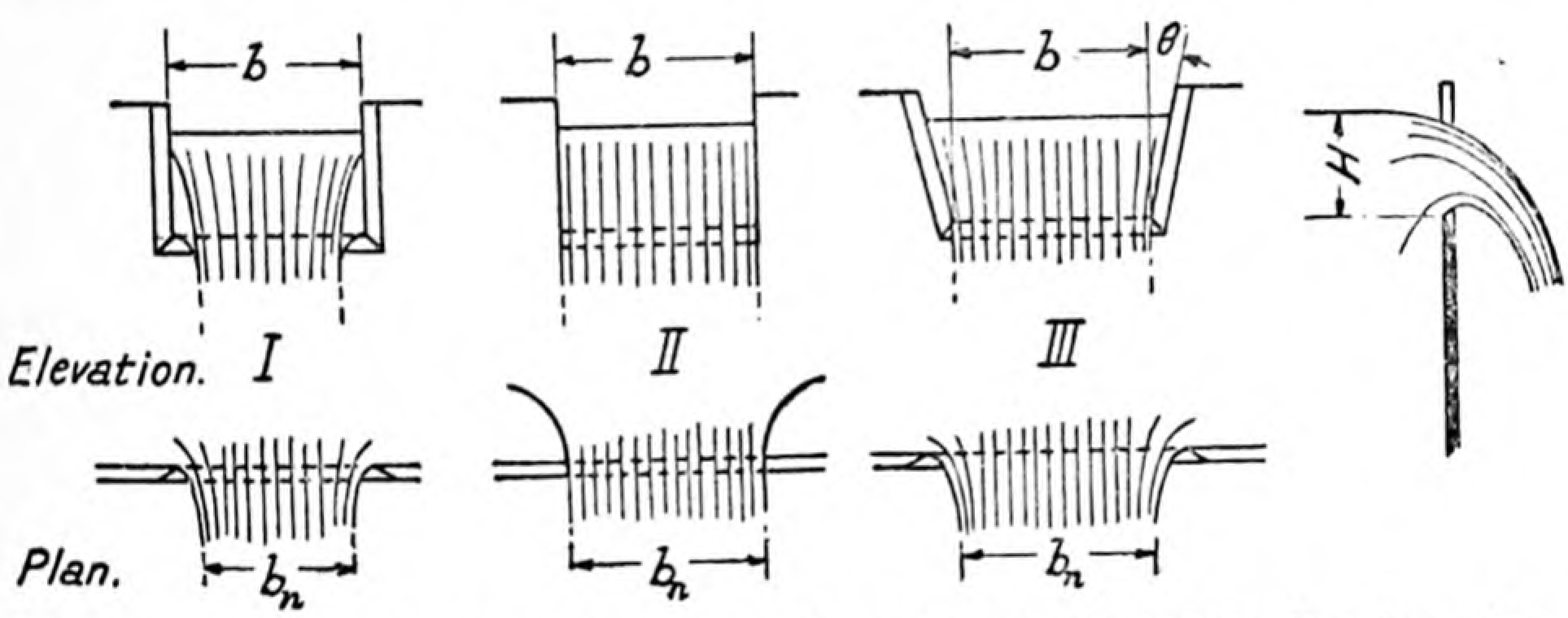

Fig. 38.—*I.* Fully contracted rectangular weir; *II.* Suppressed rectangular weir; *III.* Trapezoidal weir.

greater as the head increases, i.e. the breadth b_n of the nappe diminishes; to compensate for this, a variable coefficient C_d must be used in formula 4-5 above, thus

$$C_d = 0{\cdot}623 \left(\frac{b - \frac{H}{5}}{b} \right).$$

This is Francis' formula, which gives results correct within 2 per cent. or so, provided the breadth b is not less than three times the head H.

A weir sharp-edged at the bottom only (Fig. 38 (II), or Fig. 40) is spoken of as a weir with suppressed end contractions, or briefly as a *suppressed rectangular weir*. As the nappe always has the same breadth as the weir, i.e. $b_n = b$, the coefficient of discharge C_d has an approximately uniform value of 0·623. **(Example 17.)**

Another way of securing a nearly uniform coefficient, even with a weir having bottom and end contractions, is to splay out the ends by a sufficient amount from the vertical to neutralise the effect of the end contractions. Such a *trapezoidal* or *Cippoletti* weir (Fig. 38 (III)) then behaves just like a rectangular weir with suppressed end contractions, provided the angle of splay θ is 14°, corresponding to a deviation from the vertical of 1 in 4. With the trapezoidal weir the value of C_d to be used in formula 4-5 above is 0·632.

56. Velocity of Approach Correction. It has been emphasised that the head H used in weir formulæ should be measured in still water. What, then, must be done if the

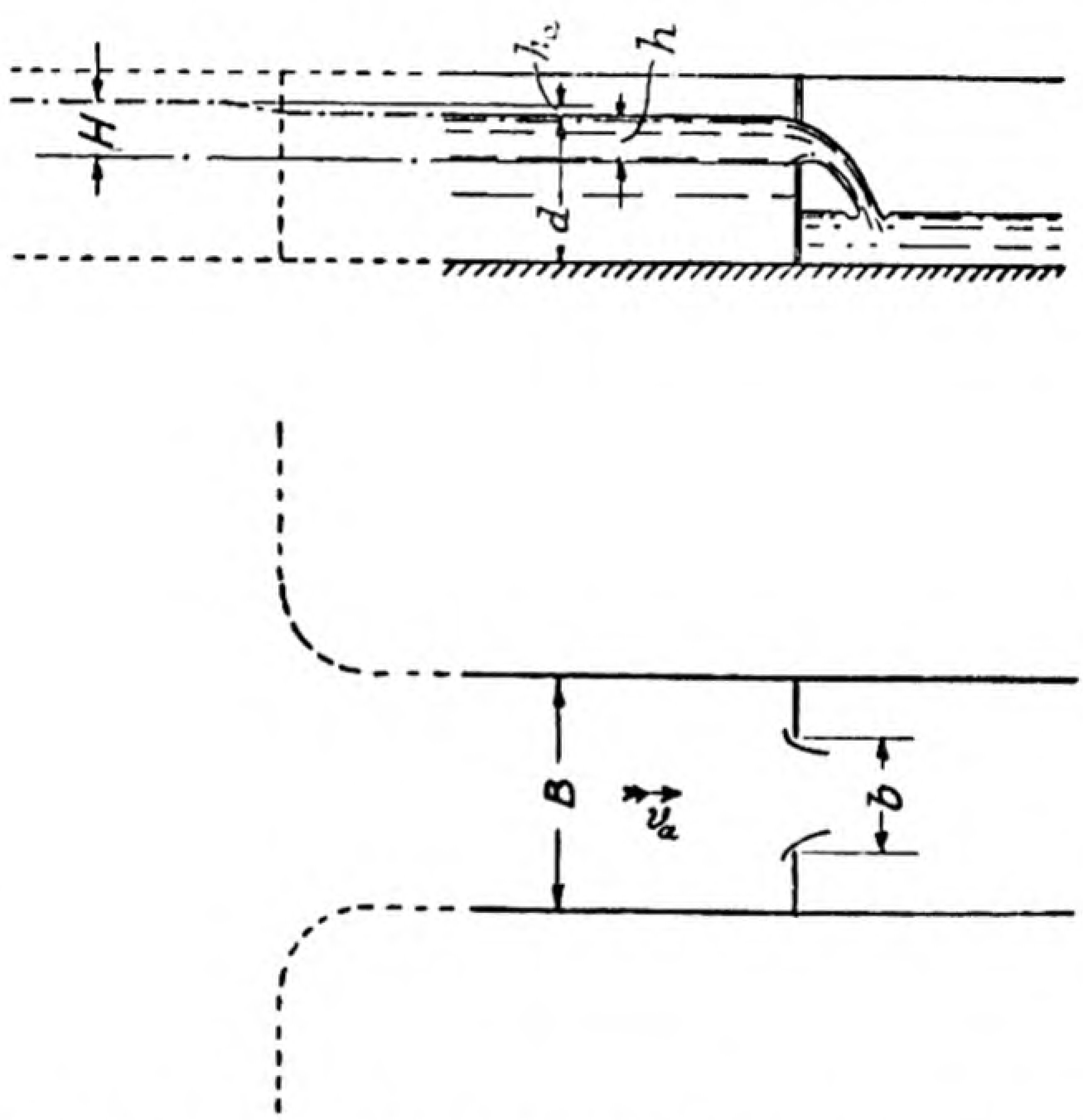

FIG. 39.—Effect of velocity of approach on weir performance.

approach channel is so narrow that the water at the measuring point already has an appreciable velocity? The solution to this problem is indicated in Fig. 39.

If the discharge over the weir Q were known, together with the breadth B and the depth d of the channel, the mean *velocity of approach* v_a would be represented by $\frac{Q}{Bd}$, and the corresponding *head of approach* h_a would be $v_a^2/2g$. Thus at some imaginary point a little further upstream where the channel might widen out into a pond, the still water head H

would be the measured head h plus the velocity head h_a. If no approach channel intervened between the imaginary pond and the weir, we should in the ordinary way use the value H in the appropriate weir formula; the effect of the approach channel is merely to introduce a transitional stage in which a small part of the original energy of the water is converted into velocity energy before the remainder of it is so converted in the nappe.

In actual fact, on account of the variations in the velocity at different points in the channel cross-section (§ 103), the true head of approach h_a is found to be something of the order of $1{\cdot}5\frac{v_a^2}{2g}$; consequently the value of H to be used in formula 4-5 is $\left(h + 1{\cdot}5\frac{v_a^2}{2g}\right)$, where h is the head over the weir measured at a point in the channel at which the *mean* velocity is v_a.

When using the Francis formula for the coefficient of discharge, however, the velocity of approach correction is applied by substituting for the term $H^{\frac{3}{2}}$ in formula 4-5, § 55, the term

$$\left[\left(h + \frac{v_a^2}{2g}\right)^{\frac{3}{2}} - \left(\frac{v_a^2}{2g}\right)^{\frac{3}{2}}\right],$$

so that the complete formula for a rectangular weir with *end contractions*

is $$Q = \tfrac{2}{3} \times 0{\cdot}623\left(b - \frac{H}{5}\right)\sqrt{2g}\left[\left(h + \frac{v_a^2}{2g}\right)^{\frac{3}{2}} - \left(\frac{v_a^2}{2g}\right)^{\frac{3}{2}}\right].$$

The corresponding formula for a *trapezoidal weir* (Fig. 38 (III))

is $$Q = \tfrac{2}{3} \times 0{\cdot}632b\sqrt{2g}\left[\left(h + \frac{v_a^2}{2g}\right)^{\frac{3}{2}} - \left(\frac{v_a}{2g}\right)^{\frac{3}{2}}\right].$$

(Example 18.)

57. Approach Channel of the Same Breadth as the Weir. The most reliable kind of measuring weir is a sharp-crested, suppressed, rectangular weir built across a channel of the same breadth b as the weir. By this means the conditions prevailing when the weir formulæ were originally established can be accurately reproduced, with a reasonable probability that the same coefficients will apply. These coefficients can now be expressed in terms of the measured head h over the

weir, and of the height P of the weir crest above the channel bed (Fig. 40).

Bazin's values for the coefficient of discharge C_d are

$$C_d = \left(0{\cdot}607 + \frac{0{\cdot}0148}{h}\right)\left[1 + 0{\cdot}55\left(\frac{h}{P+h}\right)^2\right]$$

if h and P are in feet,

or $$C_d = \left(0{\cdot}607 + \frac{0{\cdot}00452}{h}\right)\left[1 + 0{\cdot}55\left(\frac{h}{P+h}\right)^2\right]$$

if h and P are in metres.

Rehbock's values for the coefficient C_d are

$$C_d = \left(0{\cdot}605 + \frac{1}{320h - 3} + \frac{0{\cdot}08h}{P}\right)$$

if h and P are in feet,

or $$C_d = \left(0{\cdot}605 + \frac{1}{1050h - 3} + \frac{0{\cdot}08h}{P}\right)$$

if h and P are in metres.

In every case these values are used directly in formula 4-5, § 55, the measured head h being inserted *without further correction* in place of H; for the special virtue of Bazin's and Rehbock's treatment is that the velocity of approach and all other corrections are included in the numerical coefficient.

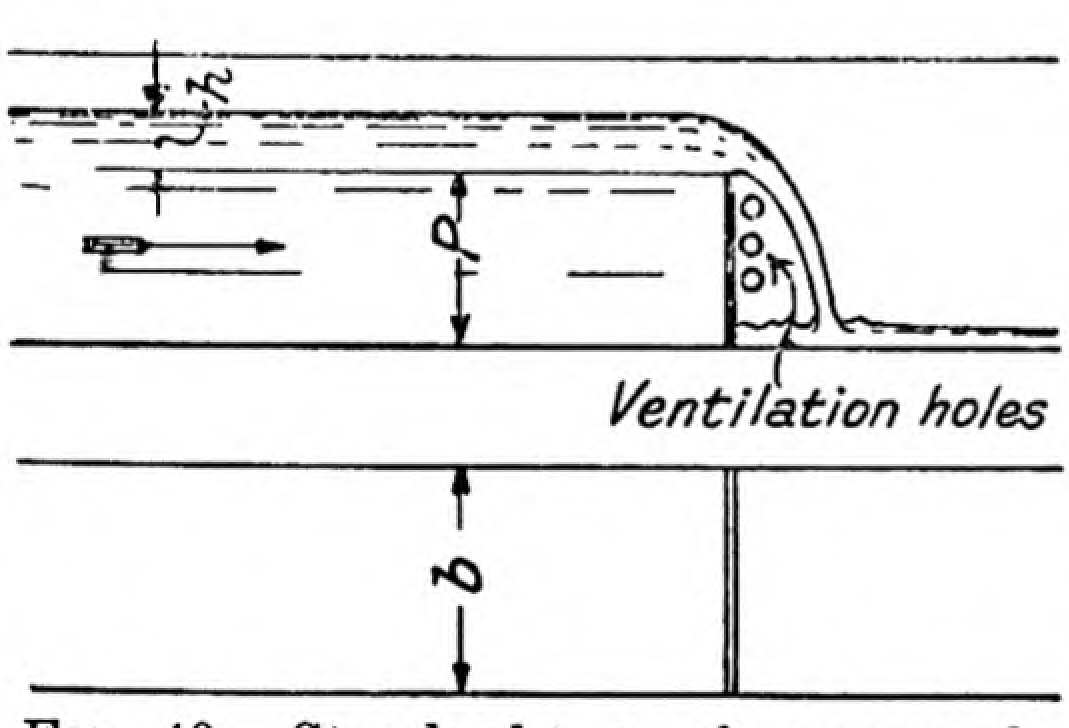

FIG. 40.—Standard type of suppressed rectangular measuring weir.

In Fig. 41 values of C_d according to Bazin and to Rehbock are plotted for heights of weir of 1 ft. and 2 ft. The interesting manner in which C_d falls to a minimum value under heads of rather less than a foot is noticeable, and also the disparity between the two sets of values. The probability is that for small weirs, working under low heads, such as are used in laboratories, the Rehbock formula is the more reliable, while for larger outdoor measurements Bazin's values are more likely to be right.

The *ventilation holes* shown in Fig. 40, communicating with

the space under the nappe, are quite indispensable ; they are pierced through the sides of the channel just downstream of

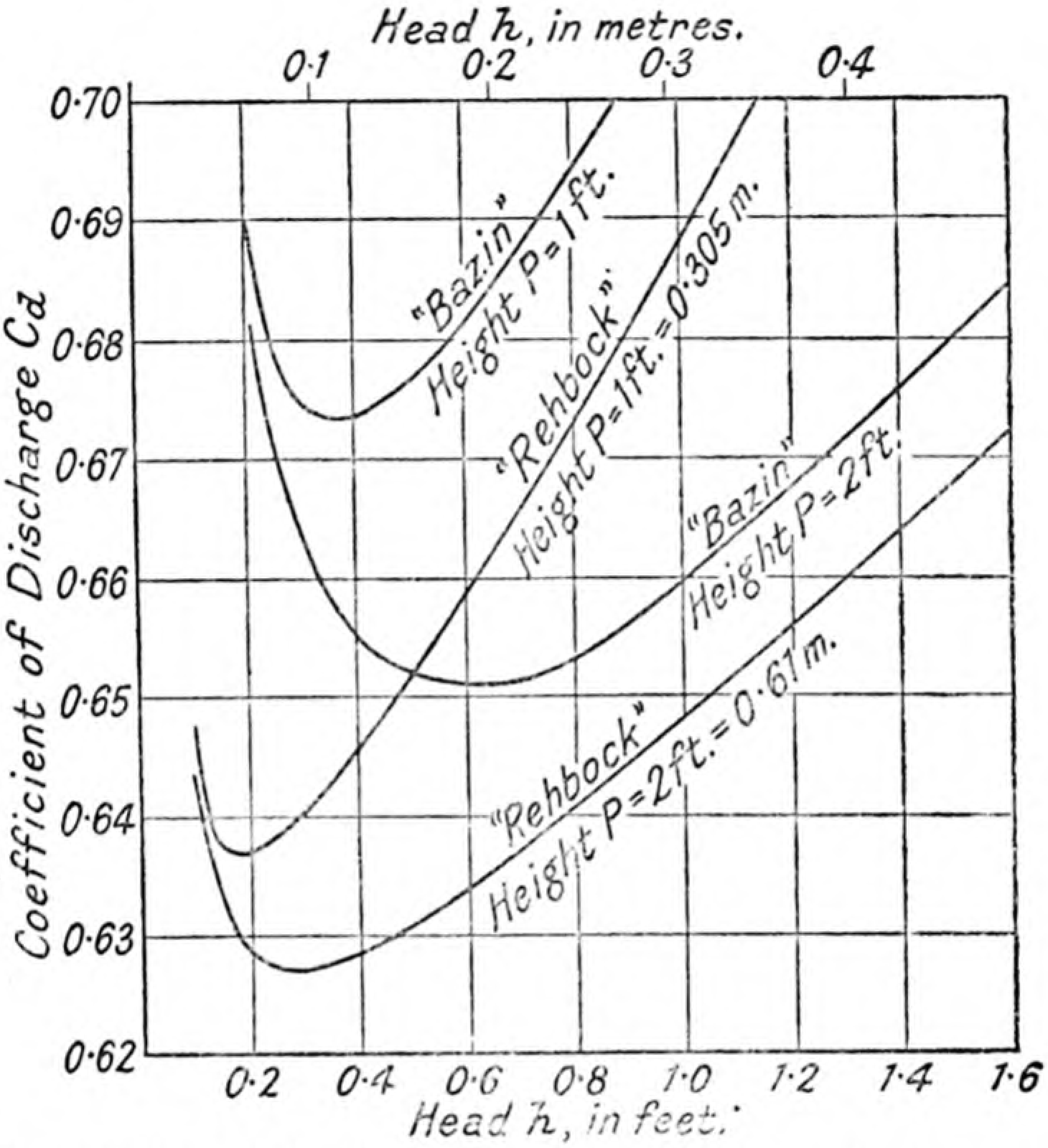

Fig. 41.—Bazin and Rehbock coefficients for sharp-edged, suppressed, rectangular weirs.

the weir plate. The space enclosed between the side walls, the weir plate, and the nappe otherwise acts as a closed box with a transparent side made of water. Air is gradually exhausted from this space by the flowing water, resulting in the formation of a negative head which causes a greater discharge over the weir than ought truly to occur under the measured head h. The ventilation holes ensure that the space is always maintained at atmospheric pressure.

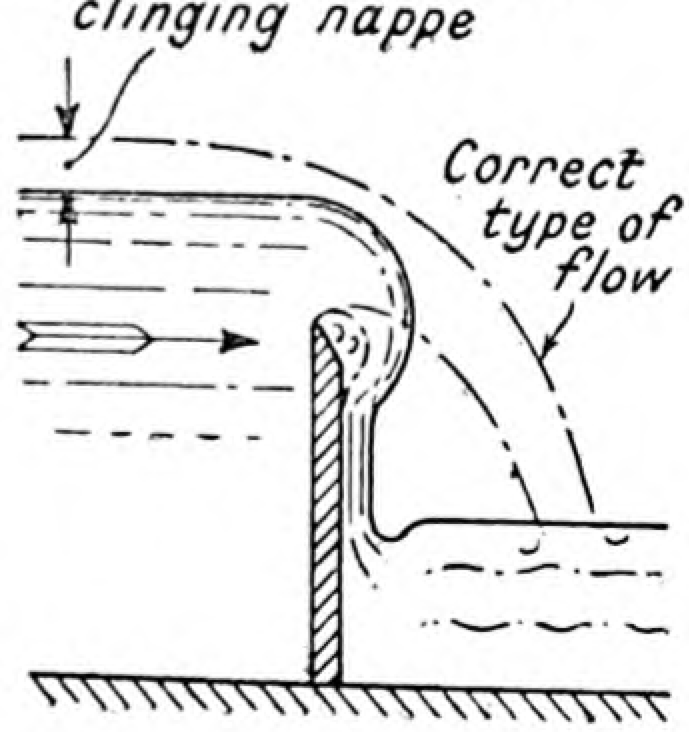

Fig. 42.—Clinging nappe.

The *clinging nappe* mentioned in § 53 and illustrated in Fig. 42 must specially be guarded against when suppressed weirs are used. So long as it persists, measurements of head are quite meaningless. But if the observer rubs his finger just once over the sharp edge of the weir-plate, the clinging nappe will instantly break down and the clear-springing nappe will establish itself.

Formulæ for suppressed weirs, as for all other standard types, are only valid if the weir plate itself is perfectly smooth and vertical, wholly free from any roughnesses or projections such as bolt-heads, etc.

58. Wide-crested or Flat-topped Weir. The objections to using the drop in surface level h_o (Fig. 34 (*b*)) as a measure of the discharge over a weir, disappear if the water in this region flows in a nearly parallel sheet as it does in a flat-topped weir (Fig. 43). Applying Bernoulli's equation to the points 1 and 2, we have

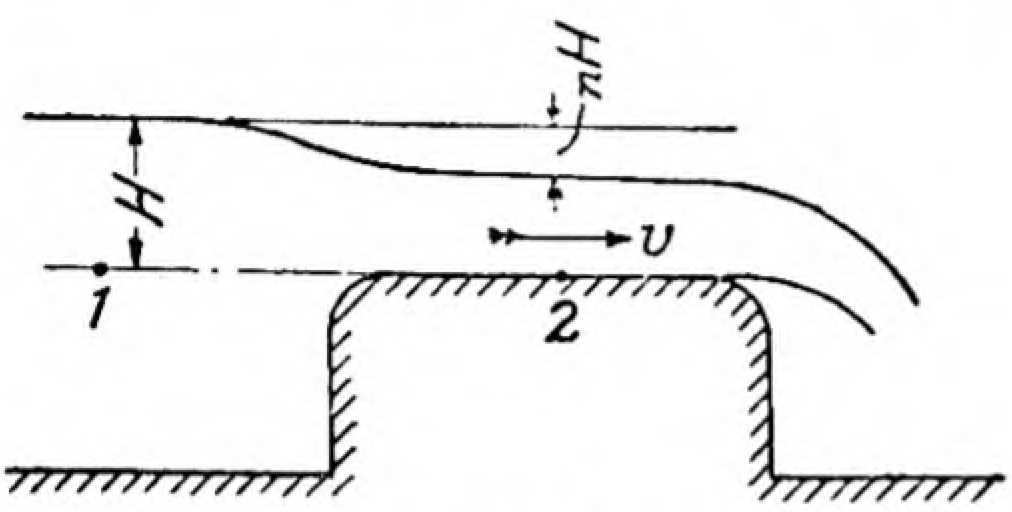

FIG. 43.—Broad-crested weir.

$$H = (H - nH) + \frac{v^2}{2g},$$

whence $v = \sqrt{2gnH}$, and

$$Q = C_d b(H - nH)\sqrt{2gnH}.$$

The thickness of the sheet $(H - nH)$ will adjust itself in such a way as to give maximum discharge over the weir, the corresponding value of n being obtained by differentiation, thus

$$\frac{dQ}{dn} = K(\tfrac{1}{2}n^{-\frac{1}{2}} - \tfrac{3}{2}n^{\frac{1}{2}}) = 0,$$

from which $n = \frac{1}{3}$. Substituting,

$$Q = C_d \,.\, b \,.\, \sqrt{2g} \,.\, H^{\frac{3}{2}} \,.\, \tfrac{2}{3}\sqrt{\tfrac{1}{3}}$$

or

$$Q = C_d \,.\, 0{\cdot}385b\sqrt{2g} \,.\, H^{\frac{3}{2}} \qquad . \quad . \quad (4\text{-}6)$$

Under favourable conditions the value of C_d may rise to 0·98, the precise figure depending both on the shape of the weir and on the head.[20]

(*Note.*—In the above analysis it has been unnecessary to take into account the velocity variation throughout the nappe that occurs with sharp-edged weirs—§§ 54 and 55—for now the water velocity is assumed to be uniform at all points in a given cross-section of the nappe. On the other hand, the velocity of approach correction, § 56, is essential.)

59. Submerged Weirs. The weirs so far discussed are referred to as *clear overfall weirs*, because the water on the downstream side never rises above the crest level and therefore never interferes with the flow. If the downstream level rises above this limit the weir is said to be *submerged* or *drowned*, and there will be a possibility that the downstream depth of water as well as the upstream depth will influence

the discharge. Considering a sharp-edged rectangular weir working under an upstream head h_u (Fig. 44), the discharge per unit length of crest under clear-overall conditions can be represented by the area ADBEC, which is a graphical integration of the expression $\int \sqrt{2gh}\,.\,dh$ (§ 55). If now the weir be submerged to a depth h_d, then the submerged filaments of the nappe will all have the velocity due to the head $(h_u - h_d)$, and the discharge per unit crest length will be reduced to the value represented by the hatched area ADEC ; in other words, drowning has reduced the discharge by an amount proportional to the area DBE.

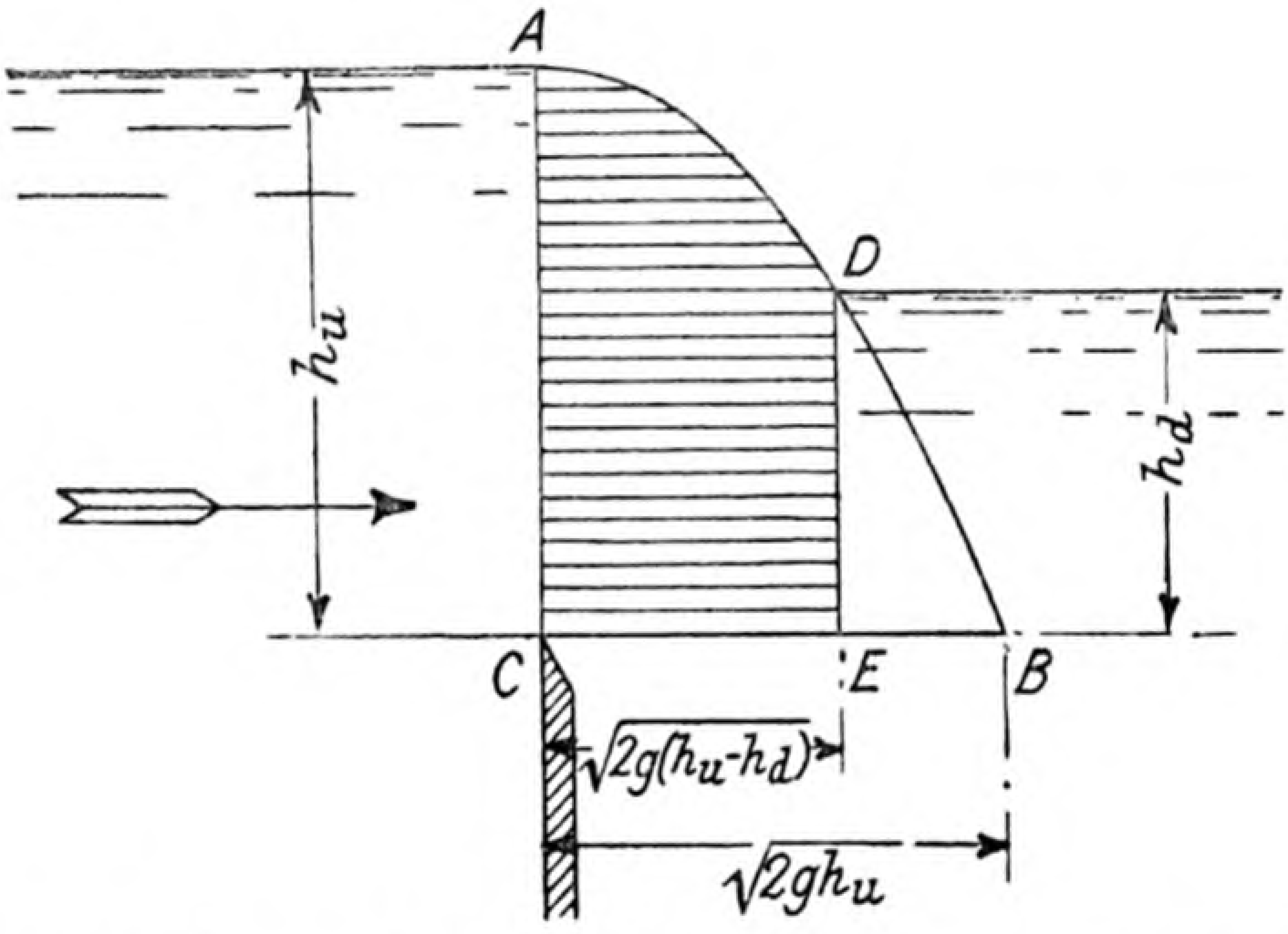

FIG. 44.—Diagram showing effect of submergence on weir flow.

Actually, as explained in § 189, the effect of drowning is often less than this, on account of the tendency of the water to form a standing wave downstream of the weir.[21] With some types of weir the flow remains unaffected even if the submergence rises to 70 per cent. of the upstream head. The corresponding figure for the flat-topped weir (§ 58) is about 66 per cent.

60. Application of the flow-net. The aim of the preceding paragraphs has been to develop simple weir formulæ which, when linked with appropriate empirical coefficients, will be adapted to immediate practical use. No rigorous treatment has been enforced, and indeed assumptions have been made that are undeniably crude. For instance, it would appear from Fig. 44 that the water surface upstream of the weir remained

level as far as the point A; but in fact the water at that point has already begun its curved downward path, Fig. 34. Before leaving this question for the time being, it may therefore be helpful to return to the basic principles that control the flow, § 36; for a flow-net when applied to a weir should be just as illuminating as one applied to an orifice. In order that the necessary condition of two-dimensional flow may be fulfilled, we may choose a suppressed rectangular weir, § 57. Although the corresponding flow-net, Fig. 45, can only be constructed at the cost of much labour, it does show very graphically how the liquid elements in an ideal system would move.[22]

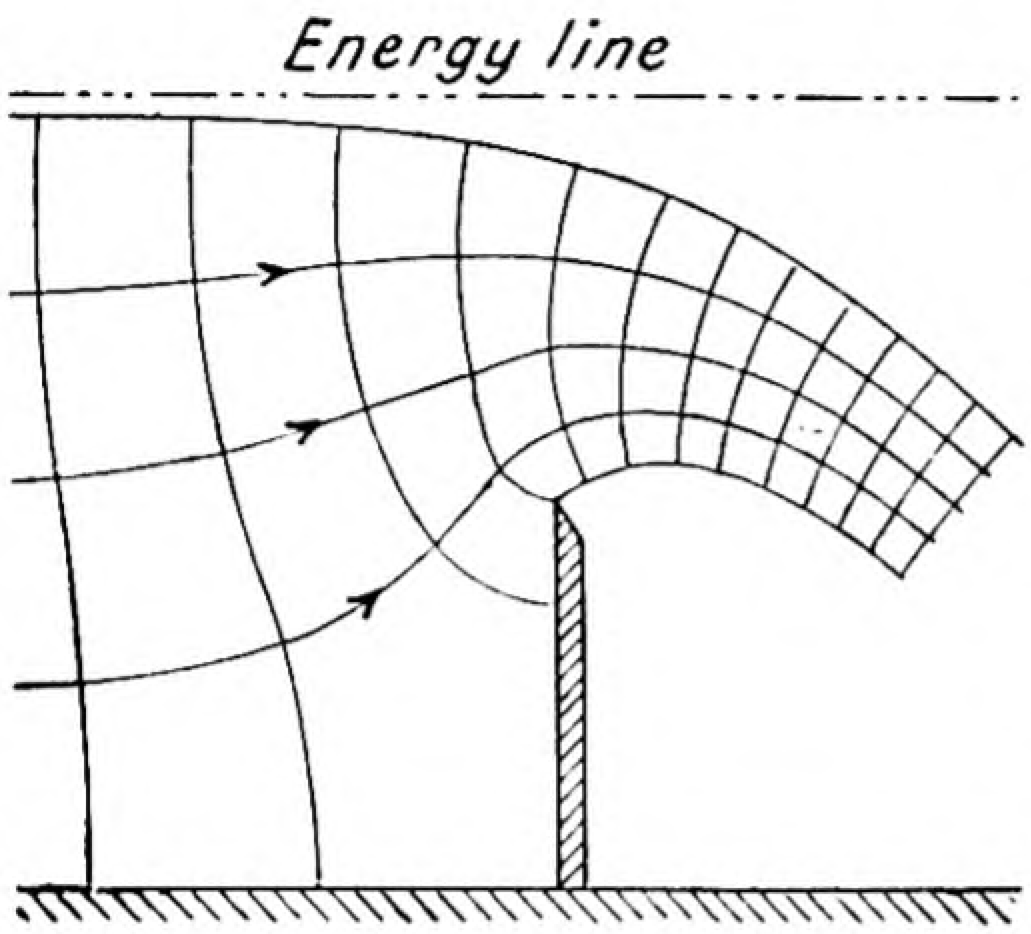

FIG. 45.—Construction of flow-net for suppressed rectangular weir.

61. Flow under Variable Head. The time taken to lower the surface level in a tank or reservoir due to flow through an orifice or over a weir can be found by a process of integration. Consider a rectangular or circular tank of cross-section A (Fig. 46), in which the surface level is to be lowered from H_1 to H_2 by the discharge of the contents through an orifice of area a and coefficient of discharge C_d in the bottom of the tank. At the moment at which the head has fallen to h, the rate of flow through the orifice is $q = C_d a\sqrt{2gh}$, and in the small interval of time dt during which the level falls a distance dh the quantity discharged is $q \,.\, dt$.

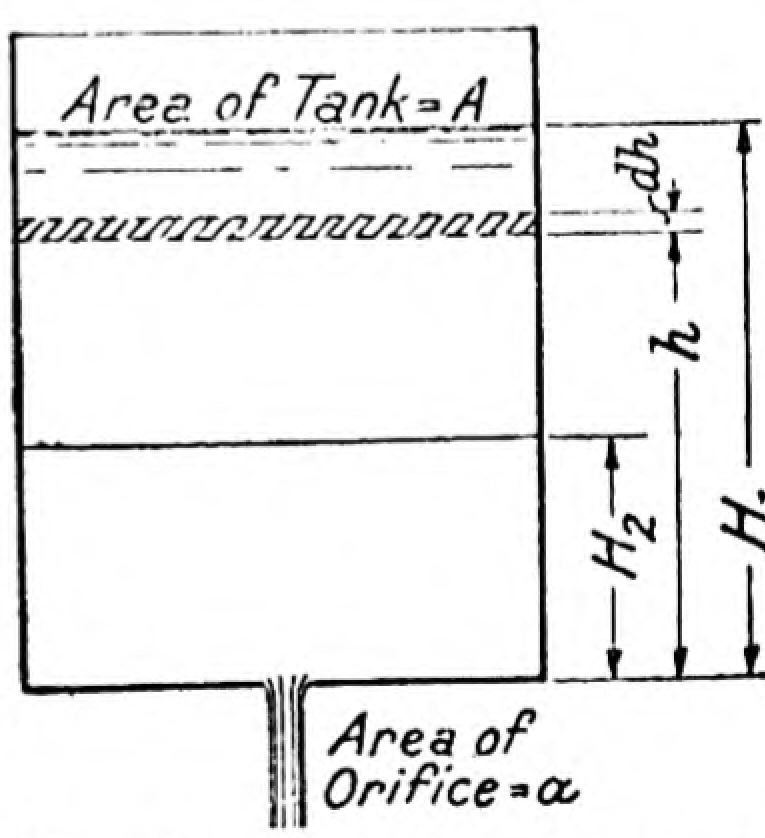

FIG. 46.—Lowering the liquid level.

But this discharge in time dt is also represented by the layer of liquid shown hatched in Fig. 46, of which the volume is Adh. Equating, we have $Adh = q \,.\, dt = C_d a\sqrt{2gh} \,.\, dt$, from

which $$dt = \frac{Adh}{C_d a\sqrt{2gh}},$$

whence total time T

$$= \int dt = \int_{H_2}^{H_1} \frac{Adh}{C_d a\sqrt{2gh}} = \frac{2A}{C_d a\sqrt{2g}}[H_1^{\frac{1}{2}} - H_2^{\frac{1}{2}}].$$

If the sides of the tank are not parallel, so that the area A of the water surface varies with the depth, the problem can nevertheless be solved, provided that A can be expressed in terms of h, and that the resulting expression for dt is integrable.

(Example 19.)

CHAPTER V

FLOW THROUGH CLOSED CONDUITS

62. The General Problem. When a liquid flows through a closed passage of appreciable length, e.g. a long, horizontal pipe of uniform circular cross-section, it is no longer possible to maintain, as we have hitherto done, that viscous forces acting on the liquid elements are relatively trifling. On the contrary, they appear to be the only forces that can influence the flow. So far as we can see, neither the velocity energy nor the position energy of the liquid varies from one part of the pipe to another; *yet the liquid steadily loses energy as it flows along.*[23] The only way in which energy can disappear in this fashion is by overcoming viscous resistances. Of course when we say that energy has disappeared we know perfectly well where it has got to: it has all been transformed into heat energy (§ 9). But we can never, for any effective purpose, get it back again.

The pressure and energy changes involved in pushing the liquid along the passage are shown diagrammatically in Fig. 47. The length l of pipe is chosen at such a distance from the pipe

inlet that the regime of flow has become uniform, so that conditions at point 2 are as nearly as possible identical with those at point 1. The relative heights h_1 and h_2 of the measuring columns in the glass gauge tubes indicate that in the length of pipe l the liquid, while moving with mean velocity v, has lost an amount $h = (h_1 - h_2)$ of pressure energy. The same information is given by the slope of the energy line and hydraulic gradient. But between the falling gradient here depicted, and the idealised falling hydraulic gradient shown in Figs. 18 and 19, a fundamental distinction is to be noted. In the second instance we received something in return for the loss of pressure energy—we got an increase in velocity energy. In the present instance we get *nothing*.

What the engineer requires in his daily work are simple relationships between the pipe length l, the pipe diameter d, the mean velocity of the liquid v, and the head loss h. But these modest demands can rarely be satisfied; more often than not the relationships are extremely complex. After many years of analysis and research, mathematicians and experimenters have still been unable to offer clear, unassailable solutions that will serve for all the varied problems of pipe flow. Thus the treatment given in the following pages is a simplification adapted only to immediate practical needs.

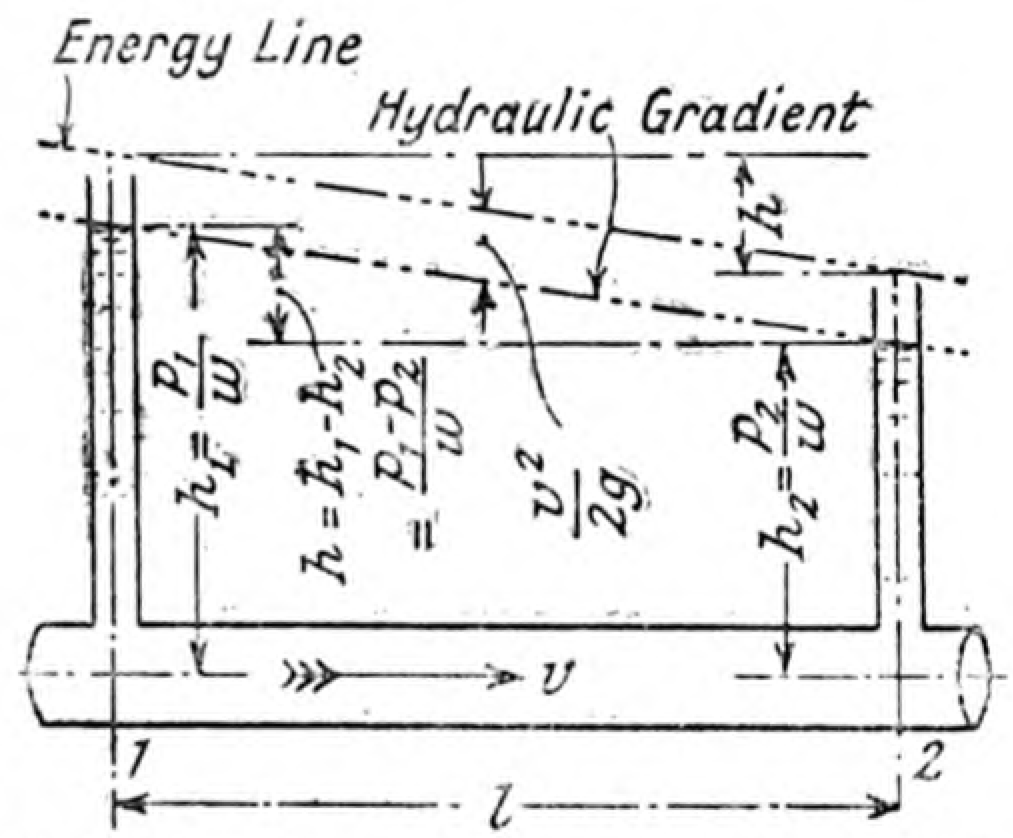

Fig. 47.—Energy loss in closed conduit.

63. The Experimental Evidence. The main facts on which theories of pipe flow must be based can be summarised thus:—

(i) *Relation between velocity and head loss.* In a system such as is shown diagrammatically in Fig. 47 it is quite easy to measure experimentally the value of the mean velocity v and of the head loss h. By making these measurements at various rates of flow, a series of values may be gathered which, when plotted, will yield a graph of the type OA reproduced in Fig. 48 (i). This particular curve relates to the flow of water at

atmospheric temperature through a smooth brass pipe 2·50 cms. diameter and 600 cms. long. The curve is not a continuous one. At very low velocities the head loss is found to be directly proportional to the velocity. At higher speeds the curve becomes nearly parabolic in shape, viz. $h \propto v^n$, where ^{n} is an exponent lying within the range 1·75 — 2·0. There is an intermediate region where the head loss may vary in an unpredictable manner. These three types of relationship are more evident if the plottings are made to logarithmic scales, as in Fig. 48 (ii).

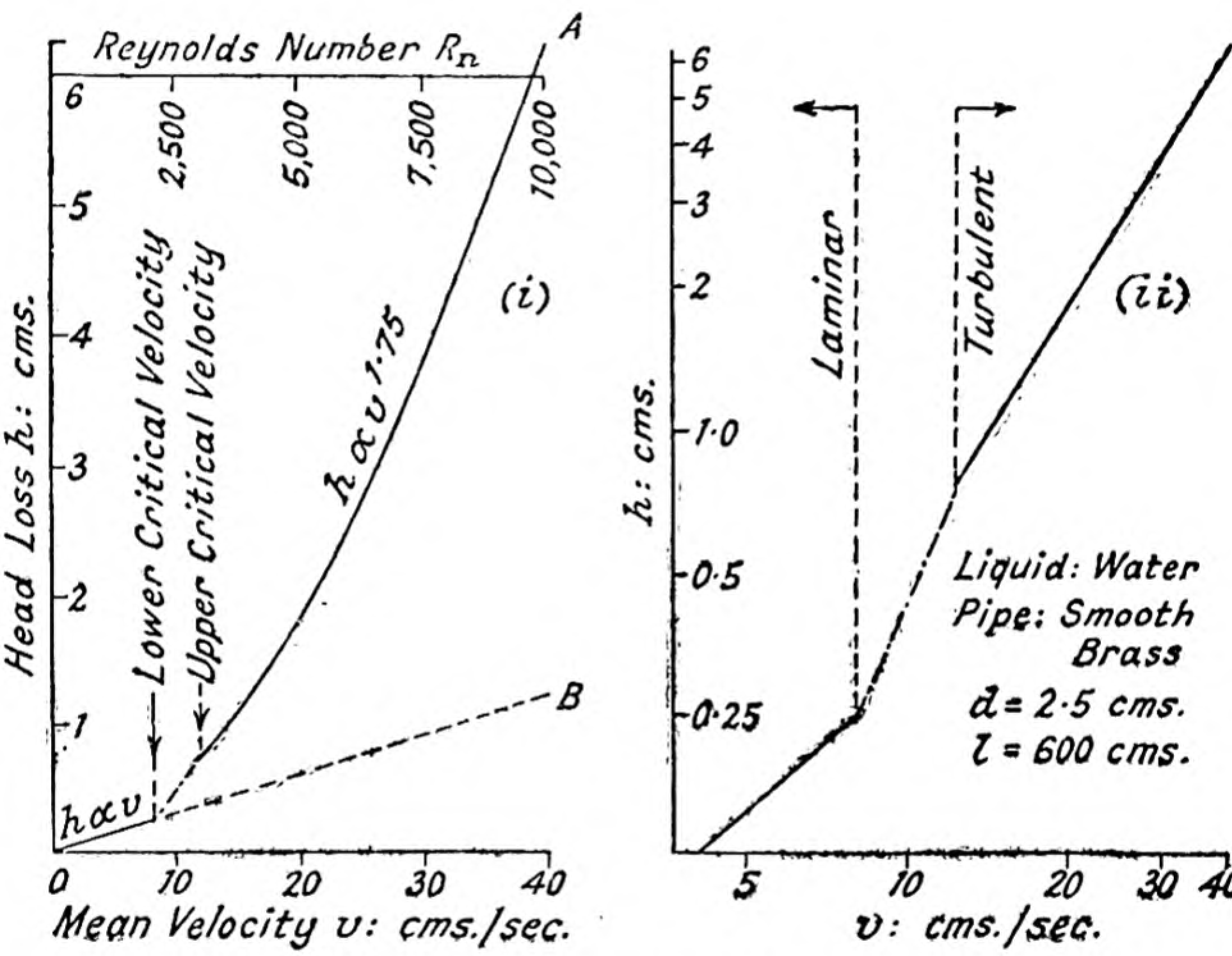

FIG. 48.—Relation between mean velocity and head loss.
(i) Linear scales. (ii) Logarithmic scales.

Variations in the viscosity of the liquid will have a marked effect on the energy loss at low velocities, but a much smaller effect at high velocities. Roughening the pipe walls, on the other hand, does not affect the flow at low velocities, but it may do so at high velocities.

(ii) *Observed behaviour of liquid elements.* If a liquid such as water is allowed to flow through a glass tube, and if one of the liquid filaments is made visible by means of dye, then by watching this filament we may get valuable insight into the

actual behaviour of the liquid as it moved along.[24] The equipment first used by Professor Osborne Reynolds for this celebrated experiment is shown diagrammatically in Fig. 49. After the water in the supply tank has stood for several hours to allow it to come completely to rest, the outlet valve is slightly opened. The central thread of dye carried along by the slow stream of water in the glass tube is seen to be nearly as steady and well-defined as the indicating-column in an alcohol thermometer, (i). But when, as a result of further opening of the valve, the water velocity passes a specific limit, a change becomes manifest: the rigid thread of dye begins to break up and to grow momentarily ill-defined, (ii). Finally, at high velocities the dye mixes completely with the water and the coloured mixture fills the tube, (iii).

Another indication of instability at high rates of flow is the behaviour of the gauge columns used for measuring pressure-heads in systems such as are shown in Fig. 47. The tops of the columns are not motionless, but pulsate irregularly through a range of possibly several millimetres.

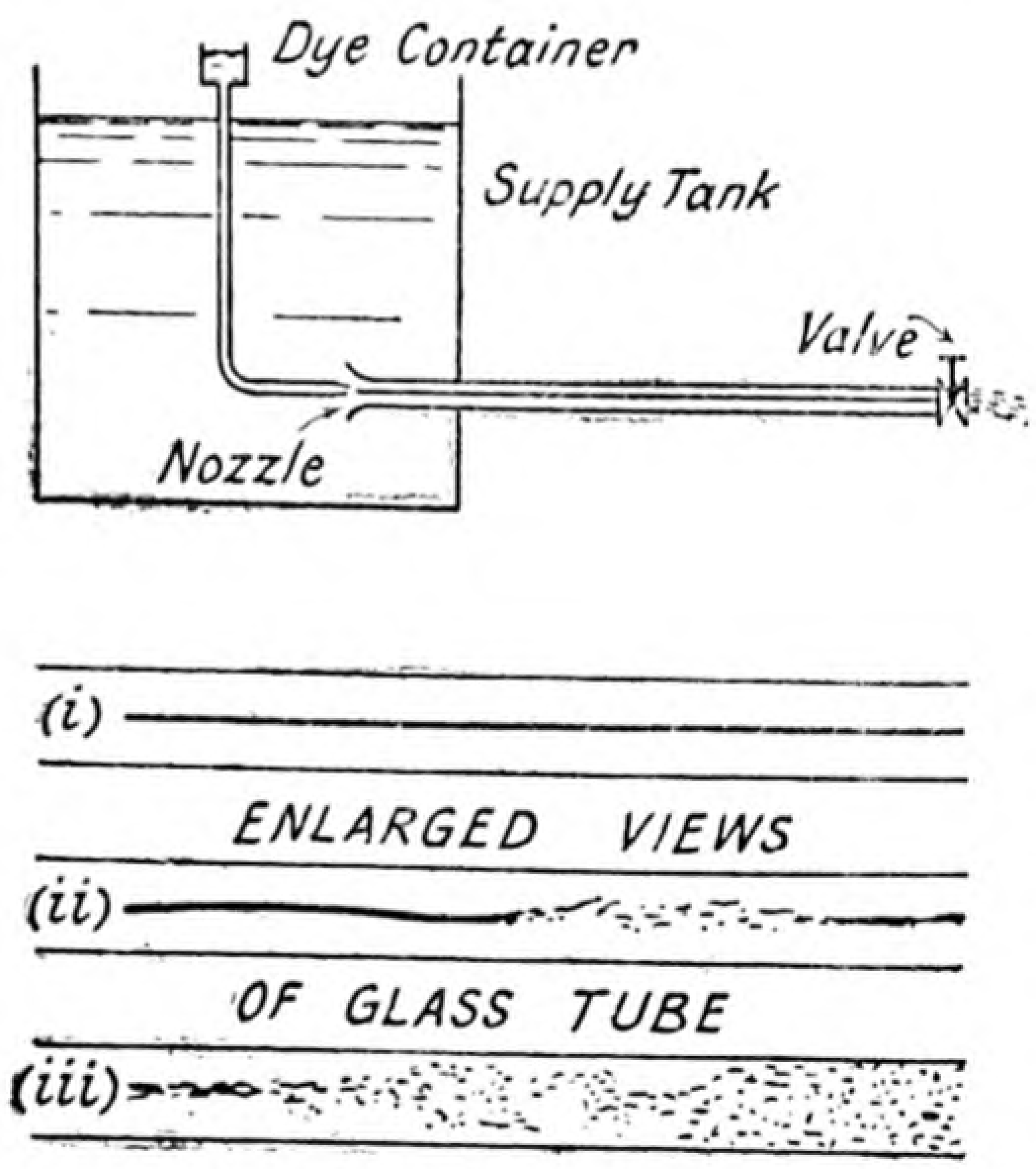

Fig. 49.—Osborne Reynolds' experiment.

(iii) *Velocity distribution.* At low rates of flow the measured maximum velocity at the pipe axis is double the mean velocity v; at high discharges the velocity-distribution curve is much flatter, somewhat resembling the diagram, Fig. 17 (ii).

(iv) *Heat transfer.* If a metallic pipe be surrounded by a water-jacket through which hot water is circulated, it may be found that the liquid flowing through the pipe picks up heat much more readily if it flows quickly than if it flows slowly. One would have expected just the reverse, viz. that the longer time the liquid spends in traversing the heated zone, the hotter it would become.

64. Laminar and Turbulent Flow: Critical Velocity. We are obliged, then, to recognise at least two quite distinct types of pipe flow: one that is characteristic of small pipes, low velocities, and viscous, sluggish liquids, and another that seems to be associated with large pipes, high velocities, and low viscosities. The two regimes are designated by any of the following terms :—

Low Velocity Type.	*High Velocity Type.*
Viscous.	Turbulent.
Laminar.	Unsteady.
Steady.	Sinuous.
Stream-line.	
Continuous.	

The justification for these titles has already been explained in § 29, or it will be found in the succeeding paragraphs.

The velocity at which the flow in a pipe changes from the one type of motion to the other, known as the *critical velocity*, can be approximately predicted by the use of the *Reynolds number* or Reynolds criterion, § 94. This is the numerical value of the expression

$$\frac{\text{mean velocity in pipe} \times \text{diameter of pipe}}{\text{kinematic viscosity of liquid}},$$

viz. Reynolds number $= \dfrac{vd}{\nu} = R_n$.

(Note that R_n is a *pure number* which is independent of the system of units, so long as these are consistently chosen, e.g. v in cm./sec., d in cm., and ν in sq. cm./sec., or v in ft./sec., d in ft., and ν in sq. ft./sec, § 40.

As will be shown later, the conception of the Reynolds number is of great service also in predicting the behaviour of flowing liquids in various other circumstances.

In dealing with the flow through orifices, nominal values of R_n may be used, based on the ideal velocity through the orifice and on the diameter of the orifice, § 43.)

If the Reynolds number describing the flow of a particular liquid in a particular straight, circular pipe has a value less than 2000, the flow will in general be *stream-line*, or *viscous*, etc.; if the Reynolds number is greater than 2800, the flow will almost certainly be *turbulent;* if R_n lies between these values, the flow may be either the one or the other. Thus the critical velocity has no fixed value, but is dependent on d and v. The value of the critical velocity corresponding with $R_n = 2000$

is called the lower critical velocity; that corresponding with $R_n = 2800$ is the higher critical velocity.

The reason why the Reynolds number alone does not provide an indisputable criterion to the state of flow is that circumstances such as the shape of the pipe and the initial condition of the liquid have some influence on the matter. Irregularities in the pipe or increases in diameter, e.g. tapering enlargements, always lower the critical velocity; tapering reductions in diameter as in a nozzle usually increase the critical velocity. In the pipes used for conveying water in ordinary engineering practice the flow is almost invariably *turbulent.*

65. Characteristics of Laminar Flow. The observed behaviour of liquids under conditions of viscous flow can be explained on the hypothesis that the liquid moves in the form of concentric cylinders or shells sliding one within the other

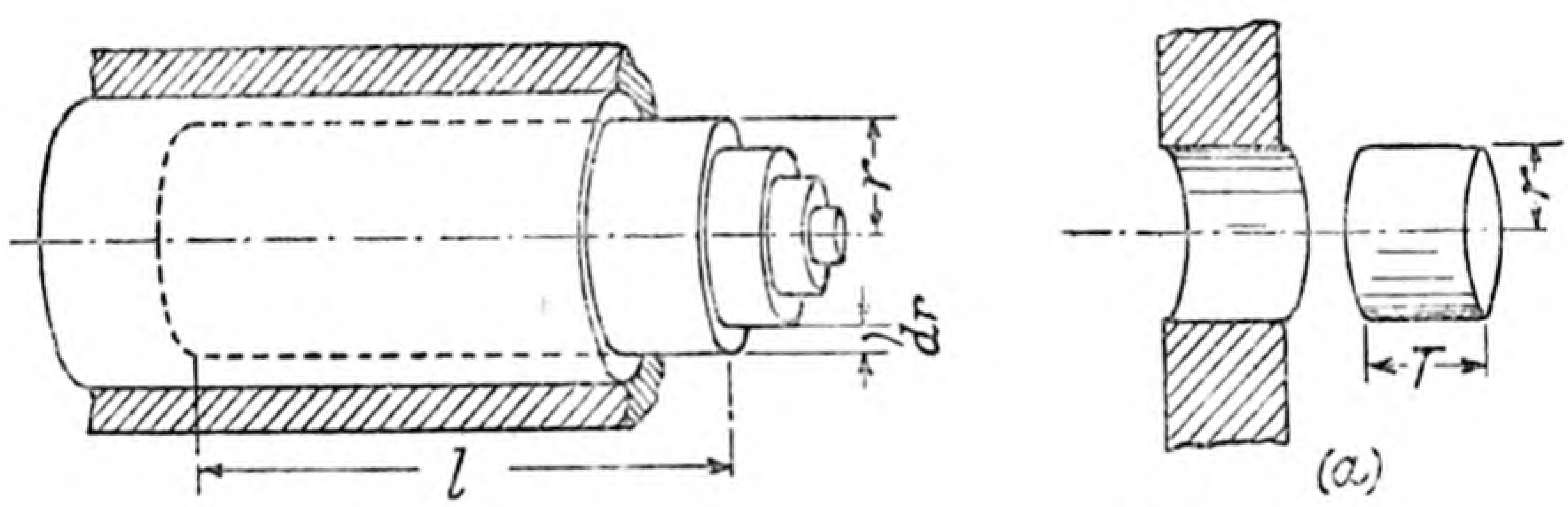

FIG. 50.—Laminar flow in circular pipe of radius R.

like the sections of a telescope (Fig. 50); these shells correspond exactly with the laminæ referred to in § 7 rolled up into tubes—hence the term *laminar* flow. The force necessary to push one of these shells through the shell immediately surrounding it is analogous to the force required to punch a hole through a plate (Fig. 50 (*a*)). If the plate is of thickness T, the hole is of radius r, and the shearing strength of the metal is f_s, then the force will be $f_s \, . \, 2\pi rT$; similarly, if the length of one of the shells of liquid is l, its radius is r, its velocity is u, the velocity gradient at its external surface is $\frac{du}{dr}$, and the viscosity of the liquid is μ, then the force required to overcome viscous shear is

$$P = \mu \, . \, 2\pi rl \, . \, \frac{du}{dr}. \quad (\S\ 7.)$$

Now the force available for overcoming the resistance of the shell is the difference in the static thrusts on the two ends of the shell itself and on all those within it, viz. $P = (p_1 - p_2) \cdot \pi r^2$, where p_1 and p_2 are the respective pressures at the upstream and downstream ends of the shell. (Fig. 47.)

Similarly, the *shear stress* at the surface of the shell, corresponding to the stress f_s above, is

$$\tau = \frac{(p_1 - p_2)\pi r^2}{2\pi r l} = \frac{(p_1 - p_2)r}{2l} \quad . \quad . \quad (5\text{-}1)$$

Equating now the two values for the differential total axial thrust P, we have

$$\mu \cdot 2\pi r l \cdot \frac{du}{dr} = (p_1 - p_2)\pi r^2$$

or
$$du = \frac{p_1 - p_2}{l} \cdot \frac{1}{2\mu} \cdot r \cdot dr.$$

We next assume that the velocity of the outermost shell, of radius R, in contact with the pipe wall, is zero. Thus when $r = R$, $u = 0$, and the equation can be integrated thus :

$$\int du = \frac{p_1 - p_2}{l} \cdot \frac{1}{2\mu} \cdot \left[\frac{r^2}{2}\right]_r^R$$

or
$$u = \frac{p_1 - p_2}{l} \cdot \frac{1}{4\mu}(R^2 - r^2) \quad . \quad . \quad (5\text{-}2)$$

The discharge or rate of flow corresponding to a single shell of radius r, thickness dr, and velocity u is $dq = 2\pi r \cdot dr \cdot u$; therefore the total discharge Q flowing through the pipe is

$$\int dq = \int_0^R 2\pi r \cdot dr \cdot u$$

$$= \int_0^R 2\pi r \cdot \frac{p_1 - p_2}{l} \cdot \frac{1}{4\mu}(R^2 - r^2)dr \text{ (from equation 5-2 above)}$$

$$= 2\pi \cdot \frac{p_1 - p_2}{l} \cdot \frac{1}{4\mu} \cdot \frac{R^4}{4}$$

or
$$Q = \frac{\pi d^4}{128\mu} \cdot \frac{p_1 - p_2}{l} \quad . \quad . \quad . \quad . \quad . \quad (5\text{-}3)$$

where d is the pipe diameter. **(Example 27.)**

The *mean* velocity v of the liquid, Q/A, reduces to the

form $$\frac{\pi d^4}{128\mu} \cdot \frac{p_1 - p_2}{l} \Big/ \frac{\pi}{4} d^2$$

or $$v = \frac{d^2}{32\mu} \cdot \frac{p_1 - p_2}{l} \quad . \quad . \quad . \quad (5\text{-}4)$$

From this equation an expression for the pressure drop is derived, viz.

$$p_1 - p_2 = \frac{32\mu l v}{d^2} \quad . \quad . \quad . \quad (5\text{-}5)$$

The corresponding head loss or energy loss (Fig. 47), is

$$h = \frac{p_1 - p_2}{w} = \frac{32\mu}{w} \cdot \frac{lv}{d^2} = 32\frac{\nu}{g} \cdot \frac{lv}{d^2}.$$

66. Application of Laminar Flow Formulæ. Measurement of the discharge and pressure drop in pipes in which laminar flow is known to occur demonstrates that the purely analytical relationships just arrived at are accurately fulfilled. This agreement not only justifies the hypotheses on which the formulæ were founded, but it permits the formulæ to be used directly for practical calculations without any correction or adjustment. The experimental fact that head loss varies directly as mean velocity or as discharge (§ 63 (i)) is in accordance with formulæ 5-3 and 5-4. The assumption that the liquid actually in contact with the pipe wall is at rest, and does not rub along the surface, is supported by the knowledge that wall roughness has no effect on the flow (§ 63 (i)), and that heat transfer is slow (§ 63 (iv)); a stationary film of liquid may well be expected to serve as an insulating sheath retarding the passage of heat from the external water-jacket to the internal liquid. As regards velocity distribution (§ 63 (iii)), here again the analytical results are acceptable. On inserting in equation 5-2 the value $r = 0$, we find that the local velocity u at the pipe axis is twice as great as the mean velocity v computed from formula 5-4. (See also Fig. 54, § 71.)

67. Turbulent Flow. The problem of extracting any orderly information from the random and disorderly movements of a swirling assembly of liquid elements looks rather daunting. As soon as the upper critical velocity is overstepped we can no

longer count on the smooth regularity that characterises purely laminar flow ; though, on the other hand, we have no cause to believe that the transition is sudden. In fact, the onset of turbulence as the mean velocity progressively increases is a gradual process, beginning first in the region of the pipe axis and spreading outwards. Even in fully-developed turbulent flow, at the highest velocities, there is evidence that a very thin zone of laminar flow may still persist near the pipe wall (§ 78). But for the moment it will be advisable to put aside such speculations for detailed study later on (§ 74) ; just now we intend to concentrate attention on the liquid actually touching the pipe wall. We shall make the rough assumption that in turbulent flow the liquid is rubbing against the wall, and that the resistance it experiences is at the root of the energy loss that we have to try to evaluate. The frictional resistance per unit area of wetted surface is of the same nature as the shear stress τ for which an expression was given in formula 5-1, § 65, except that it cannot now be directly attributed to laminar viscous effects. Using the symbol τ_0 to represent the *limiting stress at the pipe wall*, at which $r = R$, we find that

$$\tau_0 = \frac{(p_1 - p_2)R}{2l} = \frac{whR}{2l},$$

(Fig. 47), an expression in which all the terms are readily measurable. Utilising the experimental knowledge that head loss h varies as v^n (§ 63 (i)), we can write—

Frictional resistance per unit area at *unit mean velocity*

$$= F = \textit{coefficient of surface friction} = \frac{whR}{2lv^n} \quad . \quad (5\text{-}6)$$

The variations in the value of F, obtained by direct measurement of the factors h, v, etc., will show the influence of various kinds of pipe surfaces, various liquids, etc. There is also the attractive possibility that F for a given class of surface may be measured in other ways, e.g. by observing the force needed to tow a thin plate through still water ; but it will be found that this line of approach is beset by difficulties (§ 127). In any event the mathematical dimensions of the coefficient of surface friction are complex, § 40, making it desirable to evolve other coefficients for use in practical computations.

68. Formulæ for Turbulent Flow. (i) *Darcy Type.* This very useful formula depends upon the use of a *pipe coefficient* f which is derived from the coefficient F as follows :—

$$f = F \cdot \frac{2g}{w}.$$

The particular advantage of this modification is that the new coefficient f is *non-dimensional*—it is a pure number having the same value no matter what mutually consistent system of units is chosen, § 40. Variations in velocity, roughness or diameter are reflected in the corresponding value of the pipe coefficient ; but often the law of variation is quite a simple one (§ 69).

Substituting appropriate values in equation 5-6, § 67, and assuming that the exponent n has the value 2, we obtain for a pipe of diameter d :—

$$\frac{wf}{2g} = \frac{wh}{2lv^2} \cdot \frac{d}{2}$$

from which

$$h = \frac{4fl}{d} \cdot \frac{v^2}{2g} \qquad . \quad . \quad . \quad (5\text{-}7)$$

Engineers find it convenient to have the head loss expressed in this way, in terms of the nominal velocity energy $v^2/2g$ of the flowing liquid, but mathematicians prefer the variant

$$-\delta p = \lambda \cdot \rho \cdot \frac{l}{d} \cdot \frac{v^2}{2}$$

in which δp is the pressure drop, and λ is a coefficient having the value $\lambda = 4f$.

(ii) *Chezy type.* This formula permits the mean velocity v to be expressed in terms of the hydraulic mean depth and of the virtual slope. It is thus particularly suited for passages of non-circular or irregular shape.

The *hydraulic mean depth* or *mean hydraulic radius*, denoted by the symbol m (or alternatively by r or R), has the value $m = A/P$, where A is the cross-sectional area of the waterway and P is its *wetted perimeter*. Evidently for a circular pipe running full, $A = \frac{\pi}{4}d^2$, $P = \pi d$ and $m = \frac{d}{4}$.

The *virtual slope*, denoted by i (or sometimes by S) is the friction loss per unit length of pipe, i.e. $i = h/l$. For a horizontal straight pipe the virtual slope is the slope of the *hydraulic gradient* (Fig. 47) ; but it is specially to be noted that there is usually no relation at all between the *virtual* slope and the *actual* slope of the pipe axis.

Instead of using the pipe coefficient f, we employ another derivative of the coefficient of surface friction F. Designated the *Chezy coefficient* C, it has the value

$$C = \sqrt{\frac{w}{F}} = \sqrt{\frac{2g}{f}}.$$

By once more assigning the arbitrary value 2 to the exponent n, we can now rearrange equation 5-6 in the form

$$v^2 = \frac{w}{F} \cdot \frac{d}{4} \cdot \frac{h}{l}.$$

Then, on inserting the values $h/l = i$, and $d/4 = m$ (for a circular pipe of diameter d running full), we obtain the Chezy equation

$$v = C\sqrt{mi} \quad . \quad . \quad . \quad (5\text{-}8)$$

Empirical suggestions for estimating the value of C are given in § 156. It is to be noted that this coefficient is *not* a pure number; its value changes not only with pipe diameter, and often with pipe velocity, but also with the system of units. If, however, we write $v = C_0\sqrt{gmi}$, then this modified coefficient C_0 is non-dimensional.

(iii) *Exponential formulæ.* By expressing head loss in the form

$$h = \frac{f_1 l v^n}{d^x} \quad . \quad . \quad . \quad . \quad (5\text{-}9)$$

we gain respite from fluctuating coefficients which seem to be at the mercy of every change in flow conditions. *Within a restricted range* of velocities, diameters, etc., the coefficient f_1 and the exponents n and x are *invariable* for a specified class of pipe surface ; but the coefficient is no longer dimensionless, § 40. Suitable choice of values for the exponents enables the formula to describe all types of flow, laminar as well as

turbulent, so long as a given kind of liquid is used. Thus, if $n = 1$ and $x = 2$, equation 5-9 becomes identical in structure with equation 5-5, § 65. If $n = 1{\cdot}75$ and $x = 1{\cdot}25$, the exponential equation represents turbulent flow at low Reynolds numbers through smooth pipes. If $n = 2$, then we may be sure that turbulent flow through rough pipes is in question. Values of f_1 are tabulated for practical use in § 157.

69. Resistance Coefficients for Smooth Pipes. If the pipe surface is manifestly smooth to the touch, e.g. if it is of lead or drawn brass, then it is found that the value of the pipe coefficient f, § 68 (i), depends *only on the numerical value of the Reynolds number* describing the flow (§ 64). The relationship is plotted in the graph, Fig. 51. Although it was analytic

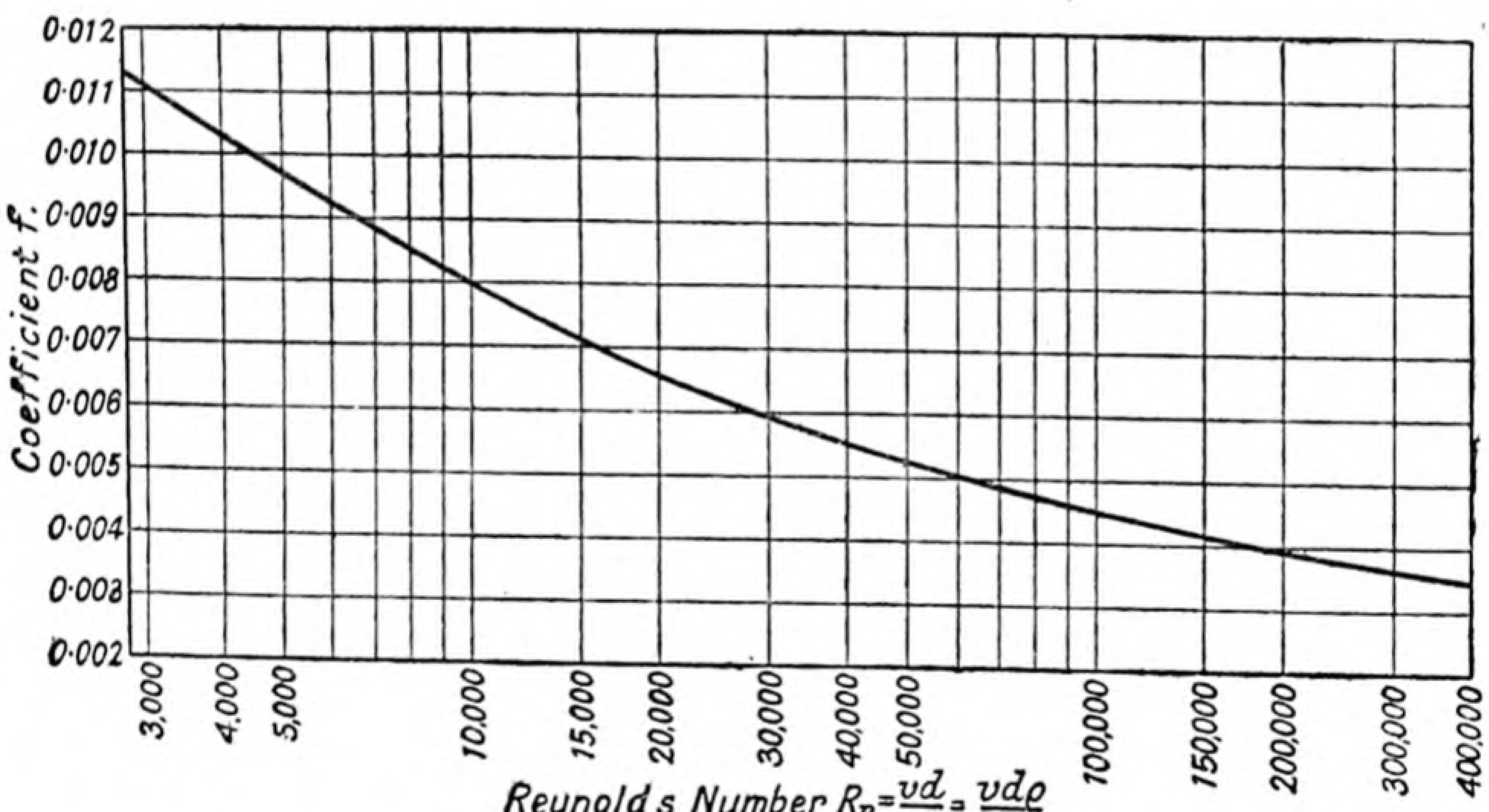

FIG. 51.—Relation between Reynolds number and pipe coefficient for smooth circular pipes.

reasoning which first suggested this exceedingly fruitful system of plotting the variables concerned, the actual shape of the curve is the result wholly of experimental observations. Having established the shape in this way, it becomes possible to develop mathematical expressions which more or less accurately fit the curve. **(Example 28.)**

Within a range of Reynolds number 3000 to 150,000, the relationship $f = 0{\cdot}08\, R_n^{-0{\cdot}25}$ is adequate. It will be observed that the values $n = 1{\cdot}75$ and $x = 1{\cdot}25$, § 68 (iii), are based on this evaluation of f.

For the whole range of Reynolds numbers yet explored, from 3000 to 30,000,000, alternative expressions are—

$$f = 0{\cdot}0008 + 0{\cdot}055 R_n^{-0{\cdot}237}$$

$$f = \frac{0{\cdot}0773}{\left[\log_{10} \frac{R_n}{7}\right]^2}$$

$$\frac{1}{\sqrt{f}} = 4 \log_{10} \left[\frac{R_n\sqrt{f}}{1{\cdot}25}\right].$$

It is important to realise the remarkable range of this simple interconnection between f and R_n. It takes into account not only variations of diameter and velocity, but also changes in the density and viscosity of the fluid. Not only, therefore, is it valid for water, oil, spirits, etc., but also for gases such as air. The general form of the relationship—a relation between two non-dimensional quantities—is typical of the correlations that are found to be of the greatest utility in hydraulic analysis and calculation, § 40.

(The above formulæ relate to straight pipes of circular cross-section. For curved pipes, and for rectangular passages, see Bibliography [25], [26], [27].)

70. Resistance Coefficients for Rough Pipes. Most of the pipes used in engineering, e.g. iron or steel water mains, are certainly not smooth to the touch; after years of service they may be very rough indeed. If, as a result of measuring h, l, d, and v when water flows through such pipes, we compute the values of the coefficient f and plot them against the corresponding Reynolds numbers, then we ought not to be surprised if the uniformity illustrated in Fig. 51 is now no longer realised. Instead of the plotted points falling on a single graph, each particular pipe seems to have its own particular graph, as shown in Fig. 52. The only general impressions that can be gathered from a study of the graphs are: (i) For a given Reynolds number, the coefficient for a rough pipe is invariably *greater* than it is for an equivalent smooth pipe. Although sometimes the difference between two values is trivial, yet in extreme cases the "rough" coefficient may be three or four times as great as the "smooth" coefficient. (ii) On the whole, small and rough pipes have higher coefficients than larger pipes of lesser roughness (*see also* Fig. 136, § 154).

If, on the other hand, the roughness is of a nature that can be controlled and measured, then the experimental figures become more tractable. Such, for example, are the results

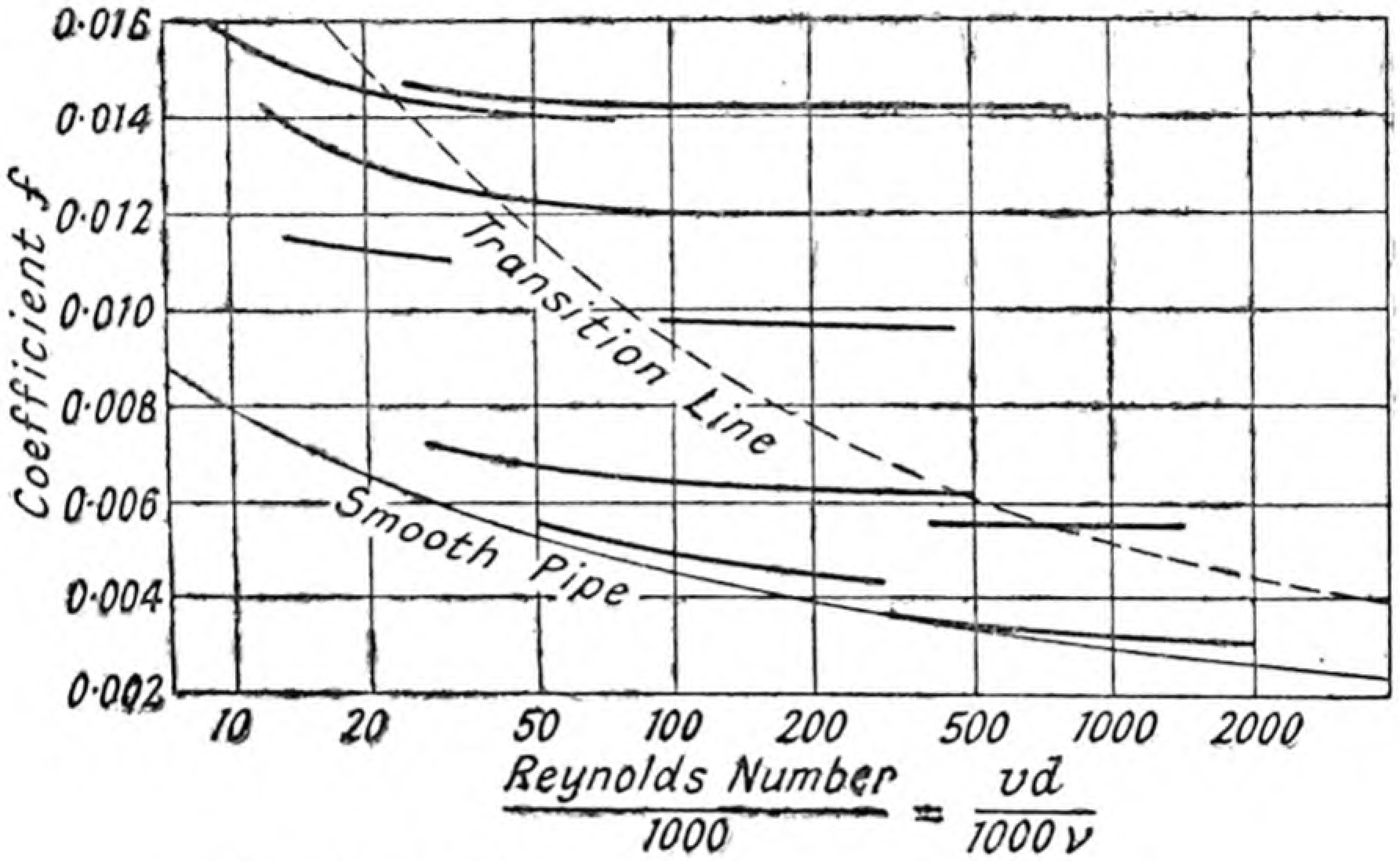

Fig. 52.—Coefficients for commercial rough pipes.

collected by J. Nikuradse in a celebrated series of observations on pipes whose internal surfaces were coated with carefully-graded sand grains.[28] So long as the *relative roughness* remained the same, viz. the ratio between the size of the sand grains, k,

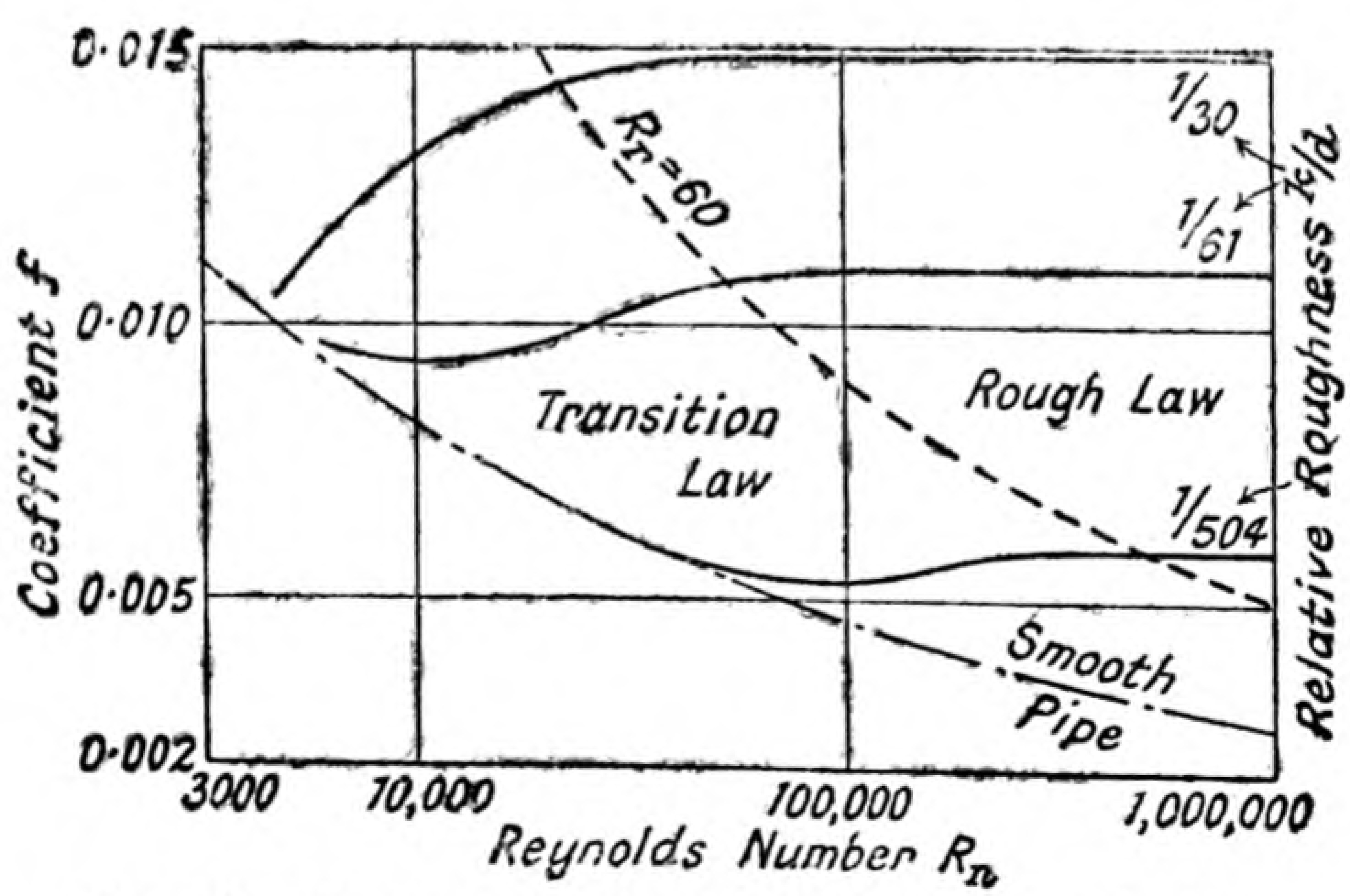

Fig. 53.—Coefficients for artificially-roughened pipes.

and the pipe diameter, d, then a *single curve* connecting R_n and f would serve for all sizes of pipe. A few of these curves are reproduced in Fig. 53, each one being distinguished by a number proportional to the relative roughness, k/d.

Explanations of these experimental facts are offered in §§ 79-81, and empirical rules for estimating the effect of roughness will be found in Chapter IX.

(Examples 29, 30, 31.)

71. Velocity Distribution in Circular Pipes. Knowledge of the manner in which the local velocity changes from point to point across a diameter is valuable in two ways: it gives insight into the general behaviour of the flowing liquid, and it materially assists in the practical measurement of pipe discharge. It is therefore no longer admissible to be deterred by the apparent state of perpetual disorder that reigns within the main stream of liquid. Indeed, as soon as we leave the friendly security of the pipe wall and plunge, like an explorer, fearlessly into the interior, we find that things are not nearly as chaotic as we had imagined. Beneath the superficial irregularity of turbulent motion there lies a quite clear and unmistakable flow pattern; at each point on the pipe diameter the observed *average* velocity component u along the pipe axis (§ 30) is rigidly related to the *mean* pipe velocity $v = q/A$ and to the relative position of the point.

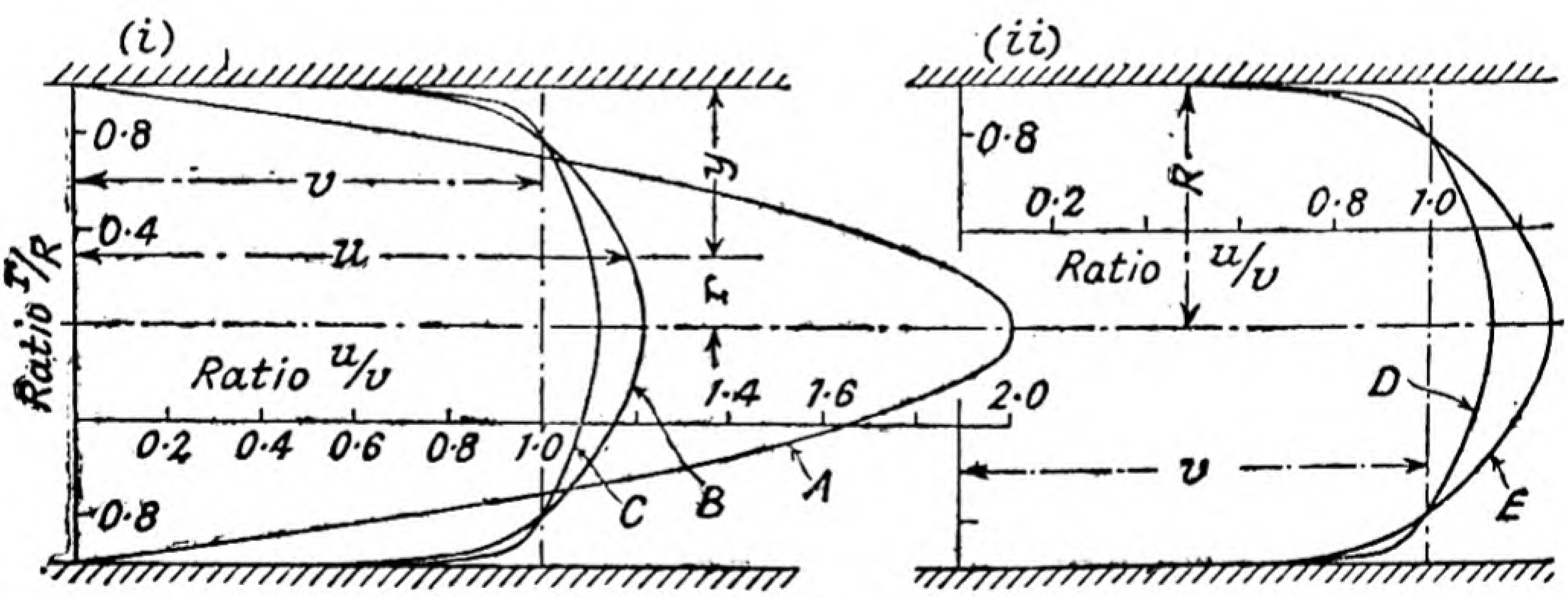

FIG. 54.—Examples of velocity profiles in circular pipes.

(i) A. Laminar flow, $R_n < 2000$.
(i) B. Smooth pipe, $R_n = 10{,}000$.
(i) C. Smooth pipe, $R_n = 3{,}000{,}000$.
(ii) $R_n = 500{,}000 \begin{cases} \text{D. Smooth, } f = 0{\cdot}0034. \\ \text{E. Very rough, } f = 0{\cdot}012. \end{cases}$

Laminar flow. As there are here no irregularities that might mask the velocity-distribution relationship, we find as we should expect that the curve is a parabola, Fig. 54 (i), *A*. It is the direct graphical interpretation of equation 5-2, § 65.

Turbulent flow. Just as various mathematical expressions can be constructed to fit the experimentally-determined curve between R_n and f, Fig. 51, so there are a number of analytical relationships that will agree with the experimental curves between the radius r of a point and the local mean velocity component u. One of the most useful of these is

$$\frac{du}{dy} = \frac{2 \cdot 5}{y}\sqrt{\frac{\tau_0}{\rho}} \quad . \quad . \quad . \quad (5\text{-}10)$$

in which y is the distance of the point from the pipe wall (i.e. $y = R - r$), and τ_0 is the shear stress at the pipe wall (§ 67). By inserting in the expression for τ_0 the value of h derived from equation 5-7, it can quickly be seen that equation 5-10 can be re-written

$$\frac{du}{dy} = \frac{2 \cdot 5v}{y}\sqrt{\frac{f}{2}};$$

and when this is integrated we are left with the result

$$u = v\left[1 + \sqrt{\frac{f}{2}} \cdot \left(3 \cdot 75 - 5 \cdot 75 \log_{10}\frac{R}{y}\right)\right] \quad . \quad (5\text{-}11)$$

Within the range of *controlled laboratory experiments,* equation 5-11 is universally true, both for *rough* and for smooth pipes. The curves plotted by its use in Fig. 54 enable interesting comparisons to be made. For a given *smooth* pipe the velocity-distribution curve is flatter at high Reynolds numbers than it is at low numbers; for a given *Reynolds number* the appropriate curve is flatter for a smooth pipe than for a rough pipe.[29]

It is to be remembered that these simple formulæ are limited in their application in the following ways :—

(i) They only apply to those sections of a uniform circular pipe, at some distance from the inlet, at which a permanent regime of flow has been established.

(ii) They do not apply to points very close to the pipe wall (§ 78).

(iii) They may not agree with conditions in large pipes.

(The fundamental importance of the laws of velocity distribution will now be apparent. Whereas in laminar flow the parabolic (radius : velocity) relationship follows directly from the laws of viscous shear, the corresponding relationships for turbulent flow must be determined *experimentally.* But in

either case when once the velocity distribution is known, an integration process will yield the rate of discharge in the pipe. This, in turn, permits the pipe coefficient f to be evaluated. In such a manner it has been possible to predict, by purely mathematical processes, the shape of the $R_n : f$ curve plotted in Fig. 51, using equation 5-10 as a basis. Satisfactory concordance is found between the predicted and the experimental curve. The statement in § 69 relative to Fig. 51 nevertheless remains true: analysis must have a basis of experimental evidence *in some form or other* before the diagram can be drawn.)

72. Distribution of Turbulence. Having now discovered that the mean velocity components conform to regular rules in spite of the turbulent nature of the flowing stream, we may take a further step: we may try to find out whether the variable turbulent components (§ 30) are similarly amenable to law and order. Studying now a three-dimensional picture, Fig. 55, in place of the elementary two-dimensional diagram (d) in Fig. 16, we observe that the actual *instantaneous* velocity AB at a point A may be resolved into a mean component AC, parallel with the pipe axis, together with one or more of the three variable or turbulent components CB, CD, and CE. Of these, CB and CD are parallel to two adjacent sides of the square passage (normal to the pipe axis), while CE is parallel with the pipe axis. The whole essence of turbulence is that the *average* value of each of the turbulent components, taken over a long period and taking account of sign, is zero. Expressed in another way, we can say that at the point O, the instantaneous velocity is the vectorial resultant of the mean velocity u (viz. the velocity that would be measured with a Pitot tube (§ 380) and plotted in velocity distribution curves such as Fig. 54), and the instantaneous turbulent components u_{tx}, u_{ty} and u_{tz} taken along three axes mutually at right angles. But can we measure these components? In simplified conditions this is not impossible. A special microscope with travelling eye-piece is used to observe brightly illuminated particles suspended in the

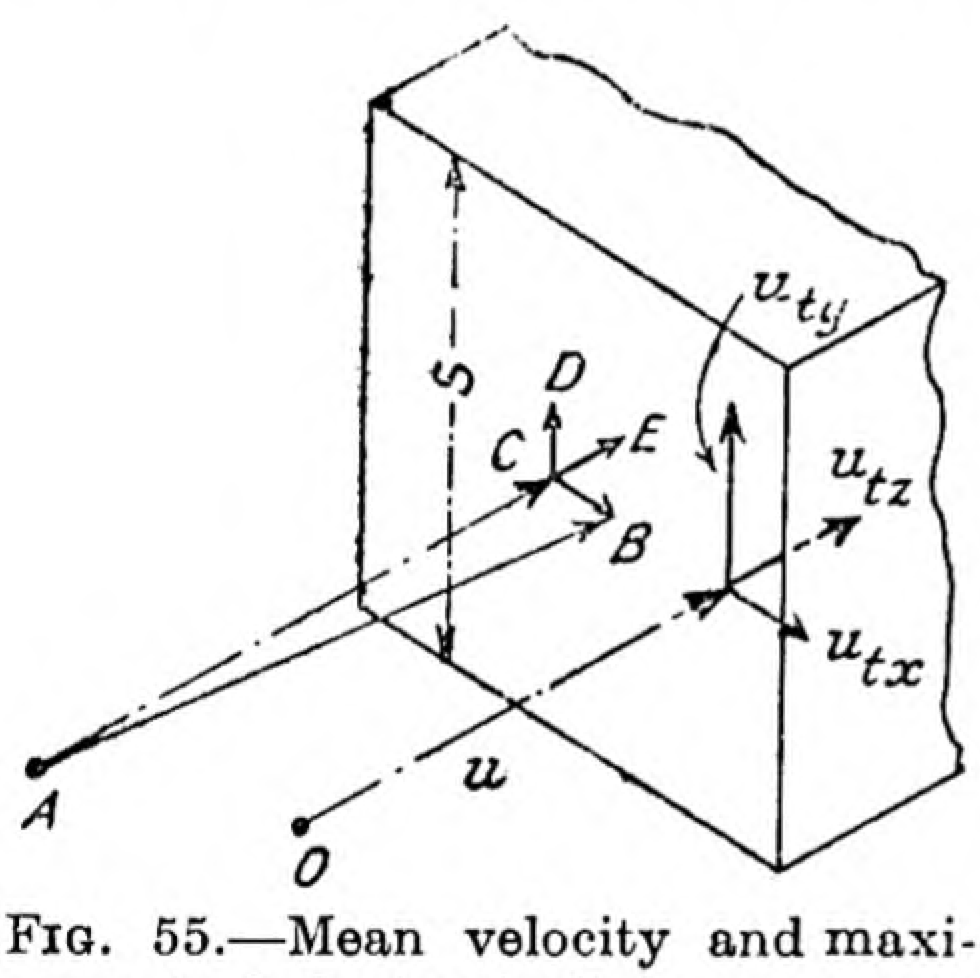

FIG. 55.—Mean velocity and maximum turbulent velocity components in square passage.

liquid.[30] Analysis of the results shows that in a small square pipe of 0·89-inch side, the *maximum* values of the turbulent components at the pipe axis was about 0·15 v, where v is the mean velocity over the whole section. At a point 0 distant $0{\cdot}1 \times s$ from the pipe wall, the maximum value of the transverse component u_{tv} was nearly 0·4 v. At any point in the cross-section the mean value of each of the components, *disregarding* sign, was about one-quarter of the corresponding maximum value. As the vectors in Fig. 55 are plotted roughly to scale, this diagram shows at a glance that turbulence is not uniformly distributed; the relative magnitude of the turbulent components varies from point to point, and the turbulent motion is *more* violent at some distance from the pipe axis than it is at the axis itself.

73. Distribution of Pressure and of Total Energy. In developing formulæ for pipe flow it was assumed without question that uniform pressure prevailed at all points across a given section of the passage (see Fig. 57, § 76). What authority have we for so doing? The only experimental evidence is what is given by the glass gauge tubes, Fig. 47, and they only tell us what is the pressure at holes in the pipe wall. As yet we know nothing about the pressure inside the pipe, away from the walls. However, special pressure measurements designed to explore the whole area of a cross-section have proved that the original assumption was justified; for all ordinary engineering purposes, the pressure across a diameter of a uniform circular straight pipe *is* uniform.[31]

As regards *total* energy, this can readily be measured: in fact, values of mean velocity at a point are deduced from such measurements (§ 380). By subtracting pressure energy from total energy assessed in relation to the proper datum, velocity energy is known, its distribution being of some such form as is illustrated in Fig. 71.

74. Theories of Turbulent Flow. This chapter has been devoted thus far to a résumé of the experimental evidence that has emerged from a study of flow in closed passages, and to a collection of formulæ by which this evidence is made available for daily use. But little attempt has been made to *explain* the observed characteristics of pipe flow. No answer has been vouchsafed to such questions as:—

(i) With a given liquid flowing in a given pipe, why should there be a change of regime when the mean velocity exceeds a certain limit ? Why should not the original laminar flow persist even at the highest velocities ?

(ii) Why should the resistance to flow be so much greater in the turbulent regime than in the laminar regime ? The term *viscous* suggests to us sluggishness and reluctance to move ; yet, if we re-examine Fig. 48 (i), § 63, we see that if the original laminar flow had been maintained up to the limits of the diagram, as indicated by the broken line OB, then the resistance or head loss would only have been about one-fifth of the actual loss denoted by point A. The disparity becomes rapidly more marked at higher velocities.

(iii) What gives the velocity-distribution curves, Fig. 54, § 71, their characteristic shapes ?

(iv) Why should various types of wall roughness have such seemingly incalculable effects on the flow in the pipe ?

These are questions that have engaged the highest powers of such pioneer investigators as Osborne Reynolds, Professor Prandtl, Professor von Karman, and Professor G. I. Taylor. As mentioned in § 62, complete and rigid solutions are not yet forthcoming ; but from the theories now current a few of the simpler ones may be summarised as being likely to interest readers of this work.

75. The Momentum Transfer Theory. The first step demanded by this hypothesis is to assume that the telescopically-sliding shells of liquid postulated n § 65 can still be imagined to exist. The only new principle now involved, as compared with laminar conditions, is that as the shells move onwards their constituent elements of liquid are continually changing. Because of the radial or transverse turbulent components of velocity, such as u_{tx} in Fig. 55, elements of liquid are incessantly *drifting sideways* out of one shell and across into a neighbouring shell. Each shell might thus be likened to a motor-bus traversing a busy urban route ; although the loaded bus always contains, say, forty passengers, yet the individuals who make up this total will be in constant flux as some passengers get out and others get in at every stopping-place. On this basis, then, the difference between laminar flow and turbulent

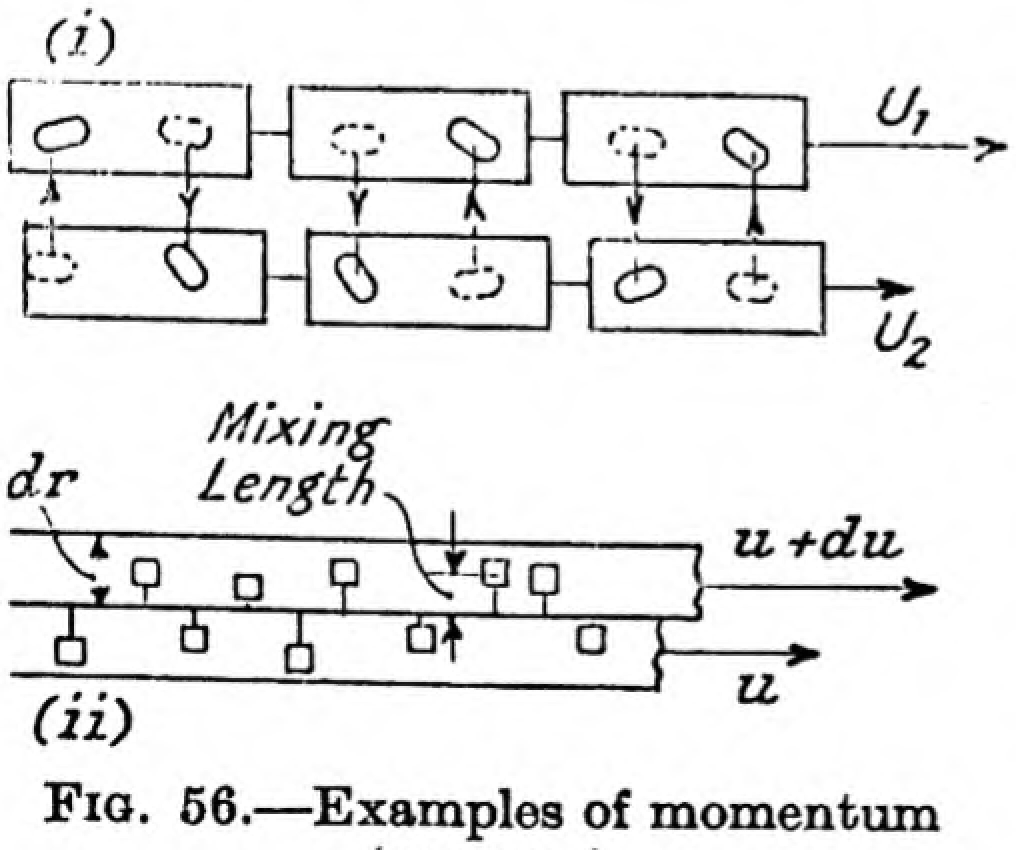

FIG. 56.—Examples of momentum transport.

flow lies here: that whereas in the one, the shells slide smoothly and evenly one within the other, in the second case the shells seem to stick, bind, or seize. Some quite unmistakable additional resistance must be at work, otherwise how can we account for the departure of line OA from line OB in Fig. 48 (i)?

According to the theory of *momentum transfer* or *momentum transport*, the cause of the additional resistance is the interchange of *momentum* resulting from the transverse velocity components. In the simplified example of momentum transfer symbolised in Fig. 56 (i), two trains of flat trucks are seen moving along parallel railway tracks, one having a speed U_1, and the other a slower speed U_2. So long as there is no communication between the trains, each is powerless to influence the other. Now suppose that on each truck there is a cargo of heavy sacks and a crew of labourers whose job it is to pitch the sacks from one train across to the other. A sack of weight W thrown from the fast train, on the point of alighting on the slow train, will still have preserved its original forward momentum $W/g \,.\, U_1$. After coming relatively to rest on a slow truck its momentum will now only be $W/g \,.\, U_2$; the *difference of momentum has been yielded up* to the slow train. In effect, the slow train has been pushed forwards. In a similar manner, the sacks thrown in the reverse direction will have a braking action on the fast train. The harder the men work, the more powerful will be the accelerating or retarding forces, and the more the speeds of the trains will tend to be equalised. Yet if each man keeps pace with his opposite number, there will be no *net* transfer of sacks; the average cargo on each train remains unchanged. It is only *momentum* that has been transferred.[32]

In terms of road transport we may replace the two trains by vehicles moving along a highway. Properly taught and experienced drivers should have no trouble in keeping slow and fast vehicles each in their respective slow and fast traffic lanes. But if impatient or incompetent drivers began to weave from one lane across into the other, the original orderly velocity distribution would be broken down and the whole jostling mass of traffic would move onward at nearly uniform speed. Although the exact equivalent of momentum transfer is here absent, yet we can see clearly enough that any type of transverse mixing is inimical to orderly and differentiated progress.

Passing now to the shells of turbulent liquid shown in longitudinal section in Fig. 56 (ii), individual elements or packets are represented by little squares. These liquid elements, moving transversely under the impulsion of turbulent components of velocity, correspond with the sacks thrown by the labourers. It is the transfer of momentum so generated that tends to damp down the velocity difference du existing between adjacent shells, and gives the effect of making one shell try to move at the same speed as its neighbour.

76. Eddy Viscosity. The name given to this interlocking action of momentum transfer is *eddy viscosity* or *virtual viscosity*. It is denoted by the symbol η. The corresponding apparent shear stress at the surface of contact of adjacent shells is known as the *Reynolds shear stress*, and is denoted by τ_r. The relation between these two quantities is identical with the relation between absolute viscosity and viscous shear stress, equation 1·2, § 7. Instead of writing $\tau = \mu \,.\, \dfrac{du}{dy}$, we now write $\tau_r = \eta \,.\, \dfrac{du}{dy}$. Now the total shear stress at radius r, no matter how it is produced, can be computed from equations 5·1, § 65, viz. $\tau_t = (p_1 - p_2) \,.\, r/2l$. But the total shear stress τ_t is also the sum of the viscous shear and the Reynolds shear, i.e. $\tau_t = (\mu + \eta)\dfrac{du}{dy}$. If in a given instance the velocity-distribution curve is available, then the velocity gradient

du/dy can quickly be measured and the value of the eddy viscosity η calculated. The successive steps in the calculation are shown graphically in Fig. 57. Beginning at (i) with a shell of liquid of radius r and length l, subjected at its two ends to the known pressures p_1 and p_2, we pass on to (ii) where the total shear stresses τ_t are plotted. The straight-line representation of equation

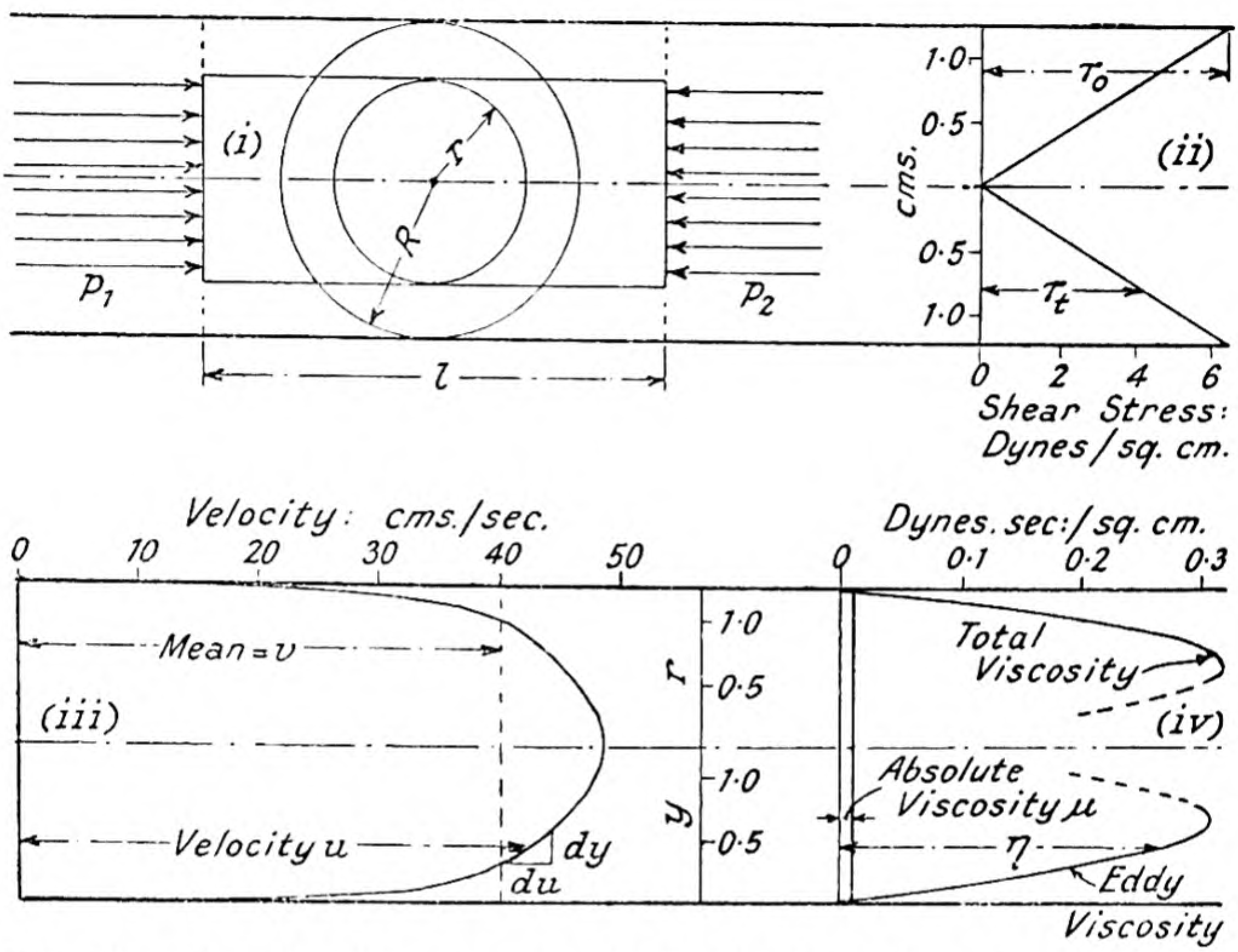

FIG. 57.—Flow of water, at mean velocity of 40 cms./sec., in smooth pipe 2·5 cms. diameter. Graphs show distribution of (i) pressure, (ii) shear stress, (iii) velocity, (iv) viscosity.

5·1, applicable for all types of flow, is clearly to be seen. From the velocity-distribution curve, (iii), which in this instance is identical with B, Fig. 54 (i), we construct the apparent viscosity-distribution curve, (iv). Deducting from the total viscosity the absolute viscosity μ, we are left with the desired eddy viscosity η.

We have here, then, a complete description of the flow conditions represented by the point A in Fig. 48 (i). Because of the relatively low value of the Reynolds number, the absolute viscosity is still not altogether negligible in comparison with the eddy viscosity. Remembering that the latter value mounts rapidly with rising Reynolds numbers, while the former remains unaltered, one would expect that at high rates of flow in large, smooth pipes, the absolute viscosity of the liquid would have virtually no effect on the frictional resistance. But this is not so, for the reasons explained in § 78; the pipe wall is shielded from the full effects of eddy viscosity by a laminar boundary film.

The term *kinematic eddy viscosity*, represented by ϵ, is used to denote the expression: $\dfrac{\text{eddy viscosity}}{\text{specific mass}}$, viz. $\epsilon = \eta/\rho$. These relationships are the exact counterparts of those that connect viscosity with kinematic viscosity, § 7.

77. The Mixing Length. Although the conception of eddy viscosity is itself highly important because of its utility as a sort of statistical measure of turbulence, its own variability tends to mask the rigidity of the underlying framework or pattern we are trying to expose. Professor Prandtl has therefore developed the complementary notion of the *mixing length.* It would really be more accurate to speak of the mixing *distance ;* for this new conception is concerned with the transverse distance represented in Fig. 56 (ii). The mixing distance, then, is defined as the average distance a small packet or element of liquid will move, when drifting sideways from one shell to an adjacent one, before acquiring the velocity of its new surroundings. The more briskly the element moves—the greater the turbulent component u_{tx} in Fig. 55—the more deeply the element can be expected to penetrate into its new resting-place. Returning again to a study of the crews on the trains symbolised in Fig. 56 (i), we readily observe that a sack flung transversely from one train will slide *sideways* as well as longitudinally after alighting on the truck which receives it. Moreover, the transverse distance it covers before it stops sliding serves as a measure of the momentum which the labourer imparted to it. Yet this distance *alone* tells us nothing about the propulsive or braking effect that momentum transfer is exerting on the trains ; the utmost efforts of the men will be entirely unavailing if the trains are going *at the same speed.* Longitudinal drag, whether between trains or between shells, depends both upon the transverse distance and upon velocity difference, viz. upon l_m and du in Fig. 56 (ii).

According to the Prandtl hypothesis, the Reynolds shear stress τ_r is chosen to represent longitudinal drag, and it is related to the mixing length l_m and to the velocity gradient in the following manner :—

$$\tau_r = \rho \, . \, l_m{}^2 \left(\frac{du}{dr}\right)^2 .$$

In specified conditions of flow, values of velocity-gradient and of Reynolds shear can be computed just as they were in § 76. Numerical values of l_m can consequently be extracted, and when these are plotted as in Fig. 58 a relationship of remarkable simplicity is revealed. At any rate within the range of

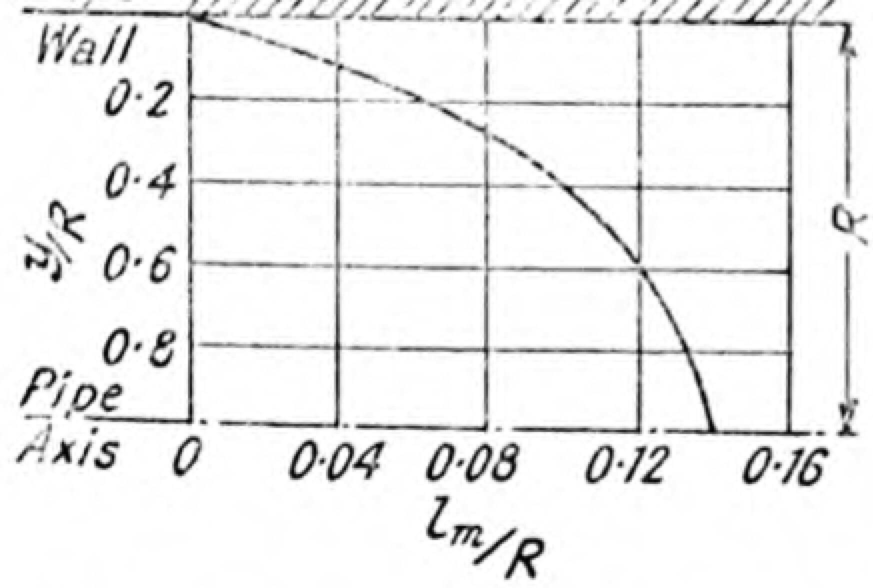

FIG. 58.—Plot of mixing length.

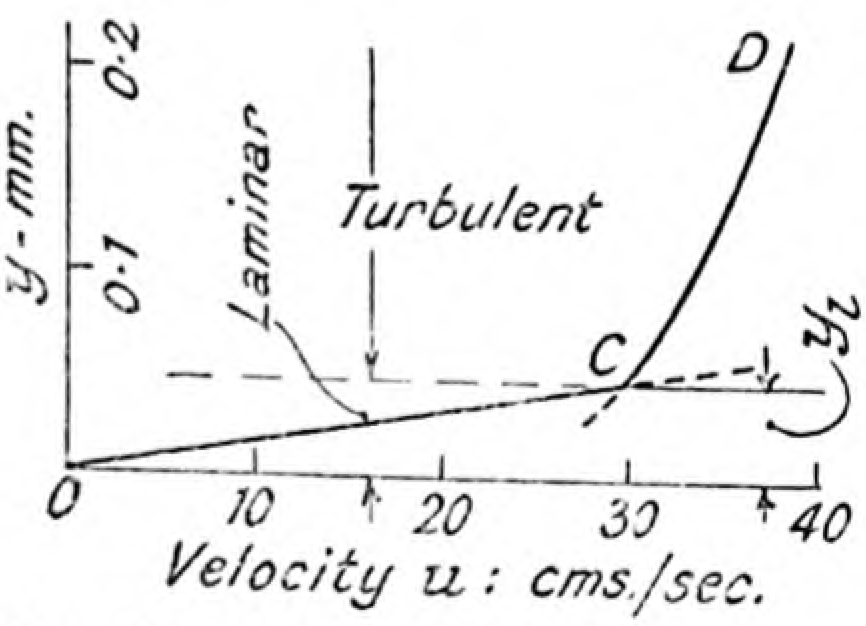

FIG. 59.—Velocity distribution near pipe wall.

controlled laboratory conditions, the ratio between the mixing length l_m and the radius r depends *only* upon the relative distance y/R from the pipe wall. The correlation has been verified both for rough and for smooth pipes, for Reynolds numbers above 100,000. Here, then, is another example of a relationship between two non-dimensional expressions which, although based on experimental evidence—the observed shape of velocity-distribution curves —could never have taken form without prolonged analytical preparation.

It remains to be added that the mixing distance is not intended to be more than a convenient abstraction. As yet we cannot identify actual elements of liquid and measure how far they do travel sideways. At least we can be certain that their motion will be vastly more complex than that of the sacks. These move freely through air (though doubtless there will be not a few collisions in mid-air); but the liquid elements have to thrust and jostle their way through other elements that hamper them on all sides. Nor has this two-dimensional treatment taken any account of the components u_{t_y} and u_{t_z} in Fig 55, which continually excite disturbances in the surrounding liquid even if they appear to have no direct concern with momentum transfer between shells.

78. Flow Conditions at the Pipe Wall. In the light of the various facts and hypotheses now at our disposal, we can return to the crucial problem of what actually goes on close to the pipe wall.[33] Is the provisional assumption that the liquid really rubs against the wall any longer tenable? One thing is certain: if the liquid does behave in this way, the velocity gradient at the pipe wall must be infinitely great, for there is a finite change in u in an infinitely small change in y. Admittedly the velocity-distribution equation 5-10, § 71, appears to support this belief; but then this relationship was never intended to apply to the liquid actually touching the wall. On the contrary, if a special technique of velocity-measurement is applied to this zone, the conception of rubbing friction cannot be upheld. As nearly as we can tell, the liquid elements that touch the solid boundary of the passage are *at rest*, and the elements within a very short distance from the boundary are moving at a speed that is very nearly proportional to the distance y.

The laminar boundary layer. We are led to believe, then, that throughout a very thin laminar boundary layer which forms a kind of lining to the pipe, the flow conditions are identical with those prevailing in purely laminar flow, § 65. The shear stress at the pipe wall, τ_0, is the result purely of viscous shear. Unquestionably it is in this region that we should expect to find minimum Reynolds shear, for both Figs. 57 (iv) and 58 trend positively towards the values $\eta = 0$ and $l_m = 0$ when $y = 0$. An impression of the composite nature of the finally acceptable velocity-distribution curve is given in Fig. 59, which reproduces with a suitably magnified scale of y a part of curve (iii), Fig. 57. The part OC of the curve within the boundary layer, is of the parabolic form described by equation 52; § 65; the part CD naturally conforms to the turbulent law represented by equations 5-11, § 71. Because of the very small thickness of the laminar layer, the error involved in assuming OC to be a straight line is negligible. Its equation can then be taken to be $u = y \cdot \frac{\tau_0}{\mu}$. This enables the position of the point of intersection C to be calculated, which in turn yields the value—

$$\text{Thickness of laminar boundary film} = y_l = 11{\cdot}6\frac{\nu}{v_f} = 11{\cdot}6\frac{\nu}{\sqrt{\frac{f}{2}}}.$$

(*Note.*—The expression $v\sqrt{\frac{f}{2}} = \sqrt{\frac{\tau_0}{\rho}}$, denoted by the symbol v_f or v_*, is known as the *friction velocity* or the *shear force velocity*.)

Although Fig. 59 is not intended to affirm that there is indeed an abrupt transition from one type of flow to the other, yet the following paragraphs show what interesting consequences are linked with the conception of the laminar layer. It may here be noted that even at the low mean velocity of

40 cms./sec. the film is less than half a millimetre thick, and that as the mean pipe velocity rises the film becomes progressively thinner. Fig. 59, like the diagram (Fig. 57 (iii)) on which it is based, refers in general to *smooth* pipes only.

79. Specification of Wall Roughness. With one more weapon in our armoury—a well-founded belief in the properties of the laminar boundary layer—we can attack the remaining and the most resistant problem of pipe flow. It is the problem of assessing and defining the roughness of the boundary when the closed conduit is no longer smooth.[34] The engineer's requirements are pictorially expressed in Fig. 60. If diagram (iv) is a magnified section of the pipe wall, e.g. the wall of a cast-iron pipe, he wants to know by how much the frictional resistance of such a pipe will be augmented as compared with an equivalent smooth pipe. Is there any possibility of telling him, by physical examination and measurement of the material alone ? Can we gauge the effect on the flowing liquid of these random and irregular projections that in the aggregate constitute the "roughness" of the pipe ?

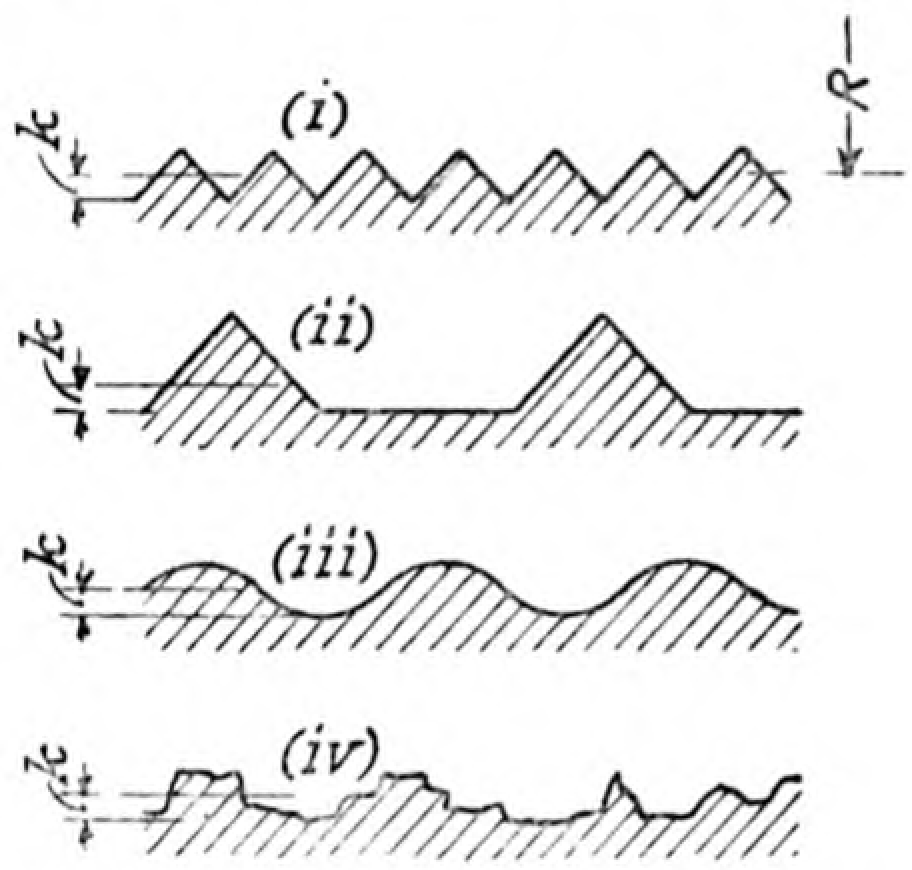

Fig. 60.—Wall roughness.

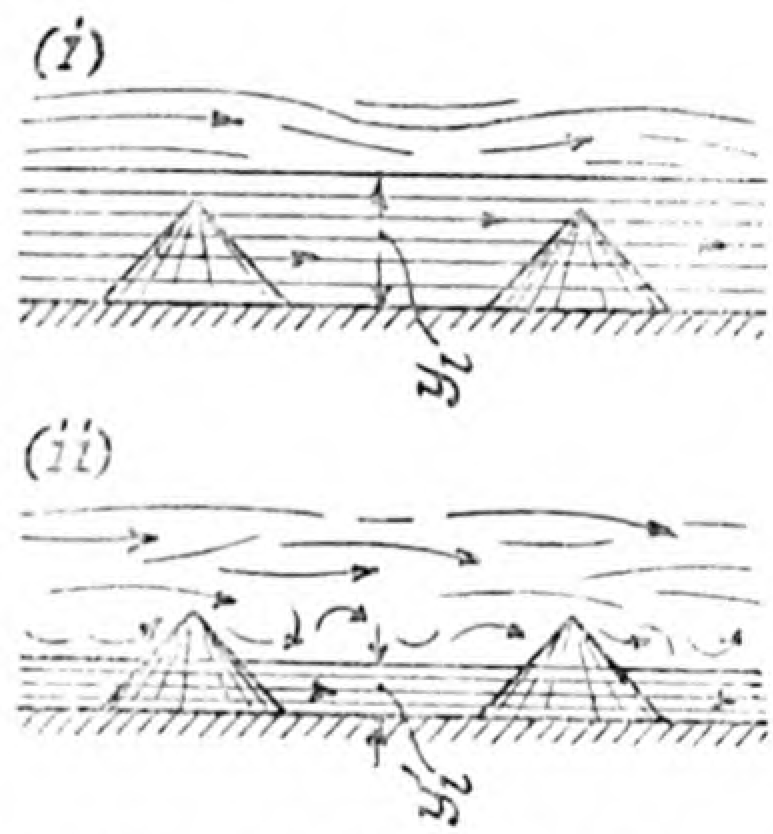

Fig. 61.—Relation of wall roughness to laminar boundary layer.

Put in this form, the problem is as yet insoluble. We can understand why by trying to substitute formalised and regular projections, such as might conceivably have the same effect as the actual random ones. Various forms of circumferential grooves are suggested at (i), (ii), and (iii) in the diagram ; they all have the same mean height k as the specified roughnesses (iv). Yet who could possibly say which of the three would most accurately simulate the type of surface, (iv), we shall be forced to use in practice ? This does not mean that the whole system of comparing commercial pipes with arbitrary standard types of roughness must be abandoned ; it means that the comparison must be carried out in another way. Returning to the basic diagram, Fig. 47, we must actually measure the hydraulic resistance losses in a variety of conditions, and we must establish by analysis a method of interpreting the results.

80. The Reynolds Roughness Number. Although direct inspection of various forms of roughness projection, Fig. 60, all of equal mean height, will not yield a trustworthy estimate of the appropriate value of the pipe coefficient f, yet it seems fairly clear that (*a*) the frictional resistance will depend not upon the *absolute roughness* k, but upon the *relative roughness* k/d, and (*b*) the type of roughness, whether sharp and angular or smooth and wavy, will influence the resistance. If, for example, the mean height in Fig. 60 has the value $k = 2$ mm., we can well believe that roughness on such a scale would

create a serious impediment to flow if the pipe diameter d were 10 mm., but would have only a trifling effect in a pipe 1000 mm. diameter.

In order to establish the indispensable correlation between the pipe size, the pipe surface, the properties of the liquid flowing through it, and the pipe coefficient f, a flow criterion supplementary to the Reynolds number is found useful. It is the *Reynolds roughness number* R_r, and is built up thus:

$$R_r = \frac{v_f k}{\nu} = v\sqrt{\frac{f}{2}} \cdot \frac{k}{d} \cdot \frac{d}{\nu} = R_n \cdot \sqrt{\frac{f}{2}} \cdot \frac{k}{d}.$$

This non-dimensional quantity is the product of three non-dimensional terms each of which may be expected to influence the flow, viz. the Reynolds number itself, a derivative of the pipe coefficient, and the relative roughness. By writing the absolute roughness k in the form $R_r \cdot \frac{\nu}{v_f}$, and comparing it with the thickness y_l of the laminar boundary layer in an equivalent smooth pipe, thus,

$$\frac{k}{y_l} = \frac{R_r \cdot \frac{\nu}{v_f}}{11{\cdot}6 \frac{\nu}{v_f}} = \frac{R_r}{11{\cdot}6}$$

the very significant fact emerges that what the Reynolds roughness number really represents is the *ratio* of the absolute roughness to the laminar film thickness.

A physical interpretation of this ratio is suggested in Fig. 61. It shows a magnified section of a pipe wall in which the roughness projections are symbolised by conical studs. When the pipe velocity is low we shall expect a low Reynolds number, a low Reynolds roughness number and a relatively thick laminar boundary film; indeed, the film is so thick that it quite submerges the roughnesses, as depicted in diagram (i). In other words, the projections *do not sensibly interfere with the flow*, and they are therefore powerless to modify the value of the pipe coefficient. The rough pipe behaves exactly like a smooth pipe. Now let the mean velocity in the same pipe be increased, so increasing the ratio between k and y_l. The resulting flow picture, Fig. 61 (ii), reminds us of a tidal estuary from which the stream is swiftly ebbing. The rocks which were submerged at the top of the flood, (i), are now exposed, and the racing waters visibly swirl around them. But we must not get carried away by imagery of this sort. In the occurrences we are actually studying, that are on a scale comparable with the lines of type used in this paragraph, the point to grasp is that in diagram (ii) the roughnesses project into the zone of turbulent motion, and that they there generate *additional* turbulence. Moreover, the liquid film next to the pipe wall is now so torn and dishevelled that we had better refer to it as an imaginary laminar layer.

81. Smooth-law, Transitional, and Rough-law Flow. Can we produce a rough pipe which will, in fact, display the variations in behaviour equivalent to the idealised states shown in Fig. 61? Yes: test results from such a pipe have already been reproduced in Fig. 53. Consider the artificially-coated pipe having a value k/d of $\frac{1}{504}$; at low Reynolds numbers its characteristic line merges into the smooth-pipe graph transferred from Fig. 51, but when R_n approaches 1,000,000 the line is horizontal. The first state, which may be termed *smooth-law flow*, is linked with Fig. 61 (i). The value of the pipe coefficient f is *independent* altogether of the size and form of the roughness projections; it is controlled solely by the value of the Reynolds number R_n.

This means that variations in density or viscosity of the liquid may play their part in determining frictional resistance.

The fact that in the *rough-law* regime the pipe coefficient has an invariable value is proof that (*a*) the characteristics of the liquid are wholly without effect on the flow, (*b*) the value of the exponent n in equation 5-9, § 68 (iii), is 2·0, (*c*) for the specified class of artificial roughness, nothing can alter the value of f except a change in the relative roughness k/d. Fig. 61 (ii) is certainly a convincing guide here. If the mean velocity and the imaginary laminar film thickness remain the same, it is easy to understand why an increase in the size of the projections will engender still more turbulence and still higher energy losses, which must infallibly be reflected in an augmented value of the pipe coefficient.

Conditions in the *transitional* regime are manifestly the most complex of all, for it seems as though any change in either the liquid or the passage will affect the resistance to flow. But at least we can de-limit the zone of uncertainty. A fairly definite boundary in Fig. 53 marks off the lower limit of rough-law flow. Both this boundary and the upper limit of smooth-law flow relating to *this special type* of sand-grain roughness, can be expressed in terms of the Reynolds roughness number thus :

Smooth-law flow	R_r below 4.
Transition flow	R_r between 4 and 60.
Rough-law flow	R_r above 60.

Or, using the ratio $k/y_l = R_r/11{\cdot}6$ developed in § 80, we find transitional flow beginning as soon as the diameter of the sand grains exceeds about one-third the thickness of the laminar layer, and persisting until the imaginary laminar layer is only one-fifth the sand-grain diameter.

Such rigid demarcations cannot reasonably be looked for when the indeterminate roughnesses of commercial pipes are in question.[35] Yet the individual graphs in Fig. 52 do display comparable tendencies to those in Fig. 53 ; on the right of the transition-line reproduced from Fig. 53, the curves have a horizontal trend, while to the left they look as if they might eventually meet the smooth-pipe curve.

82. Universal Graphs for Turbulent Flow in Rough Pipes. If it is true that within the rough-law regime the value of the pipe coefficient depends only on the relative roughness k/d, then it should be possible to plot the relationship. For the type of artificial roughness that gives the effects reproduced in Fig. 53, the connection is shown in Fig. 62 ; this is plotted quite directly by reading off values of f corresponding to (say) R_n = 1,000,000 in Fig. 53, and setting them up against corresponding values of k/d. Here again is an experimentally-determined curve for which a mathematical expression can be found. In this instance the expression is

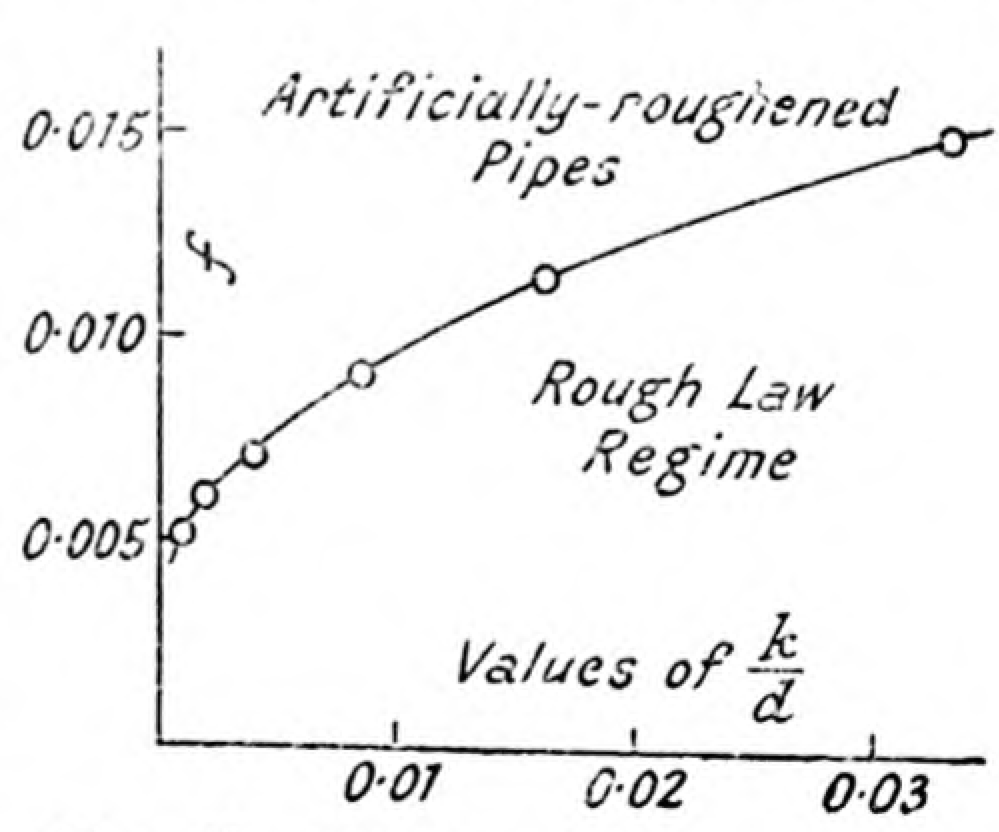

FIG. 62.—Relation between relative roughness and pipe coefficient.

$$\frac{1}{\sqrt{f}} = 4 \log_{10} 3{\cdot}7\frac{d}{k}.$$

From this it follows that if we use a new non-dimensional coefficient f_0 to represent rough pipe performance having the value

$$f_0 = 4 \log 3{\cdot}7\frac{d}{k} - \frac{1}{\sqrt{f}} \quad . \quad . \quad . \quad . \quad (5\text{-}12)$$

then f_0 will always have the value zero *so long as the rough-law* regime is in operation.

As for the *smooth-law* regime, we know that values of f applicable to smooth pipes can now be used. Choosing from § 69 the form

$$\frac{1}{\sqrt{f}} = 4 \log_{10}\left(\frac{R_n\sqrt{f}}{1{\cdot}25}\right) = 4 \log_{10}\left(R_r \cdot \frac{d}{k}\sqrt{\frac{2}{f}} \cdot \frac{\sqrt{f}}{1{\cdot}25}\right),$$

and substituting in the equation for f_0, we obtain

$$f_0 = 2{\cdot}08 - 4 \log_{10} R_r.$$

If values of coefficient f_0 are finally plotted against the Reynolds roughness number R_r, as in Fig. 63, a single *horizontal* line will represent rough-law flow, and a single *inclined* straight line will represent smooth-law flow. What is remarkable is that values of f_0 corresponding to transitional flow also fall on a single curve: it is the curve I in Fig. 63. The diagram is therefore as universal in its way as is Fig. 51. Whereas Fig. 51 consisted of a single curve

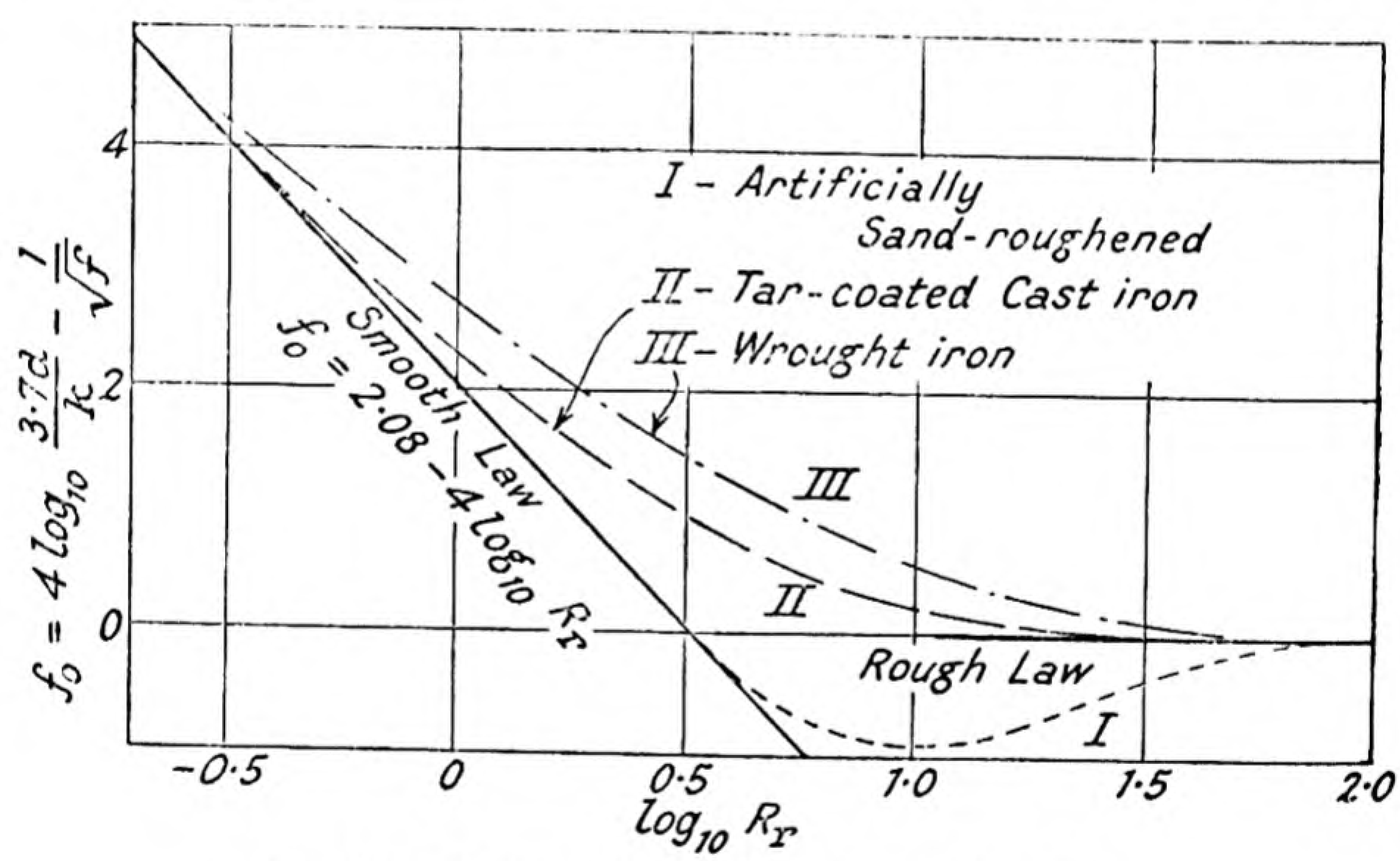

FIG. 63.—Universal plotting of turbulent flow.

applicable to any kind of liquid flowing in any kind of straight, circular, smooth pipe, so Fig. 63 (I) may provisionally be accepted for any liquid in any pipe having roughnesses in the form of a *particular kind of sand grain*. The limits of transitional flow $R_r = 4$ and $R_r = 60$ (§ 81) are here marked by the points at which the transitional curve becomes tangential to the smooth-law and the rough-law straight lines respectively.

Similar curves describing the behaviour of the pipes actually used in engineering would be of the utmost value; but the difficulty here is that the absolute roughness k cannot be measured (§ 79) as it could when actual sand grains were concerned. However, the system of estimating the equivalent

value of k outlined below has given promising results: (i) For various pipes of the selected class, e.g. cast-iron, values of the pipe coefficient f are collected from actual observation of head loss and velocity, and plotted as in Fig. 52. (ii) From the parts of the graphs which lie—or can be assumed to lie—within the rough-law zone, known values of f and d are inserted in the rough-law equation 5-12, and corresponding values of k computed. The mean value of k is accepted as the absolute roughness and is used thenceforward throughout the whole range of pipe performance. (iii) With the help of the observed values of the pipe coefficient f, values of the Reynolds roughness number R_r and of the reduced coefficient f_0 are worked out and plotted as in Fig. 63. A smooth curve is finally drawn through the points.[36]

From the actual examples II, III, of such curves reproduced in Fig. 63, it is to be noted that in the transitional zone they have quite a different shape from the curve I relative to artificial roughening. Moreover, this zone extends to much lower values of R_r, so that in some instances the smooth-law region is never reached at all. The limitations of the method should be fully realised. Thus, we adopt the rough-law equation 5-12 not because we know it is the true one but because we know no other. Nevertheless, we have at last found some way, even if an imperfect one, of describing the type of roughness associated with a particular material. Instead of describing it by a scale drawing of the projections themselves, we use in conjunction a nominal linear dimension and a curve such as I, II, and III in Fig. 63.

83. A Pictorial Comparison. In interpreting diagrams such as Figs. 52, 53, and 63, it is helpful to recognise a very real physical difference between the two types of wall roughness in question: "artificial" roughness and what may be termed "natural" roughness. With the one type of roughness, *geometrical similarity of form* may be realised; with the other, it cannot.

If spherical sand grains are used to create the artificial roughness, then the pipe walls could be represented by diagrams such as Fig. 64 (i) and (ii). Although the two pipes are of different diameters, yet the grain diameters are likewise unequal: since the ratio k/d is equal to K/D, the pipes have the same relative roughness. The two passages are geometrically similar, § 51, and it is therefore not surprising that there should be similarity of performance, viz. a single curve in Fig. 53 will serve for both pipes.

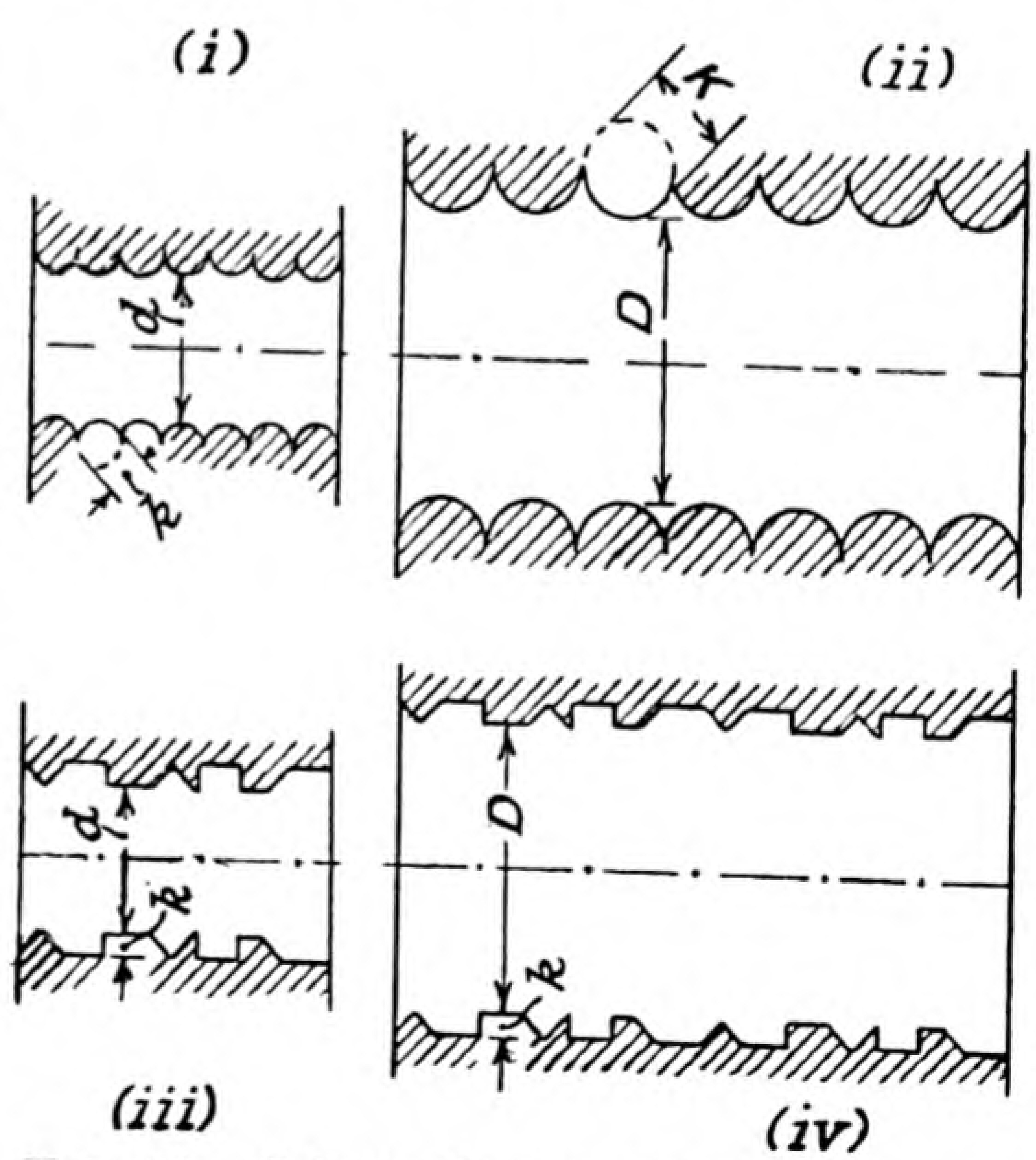

Fig. 64.—Schematic comparison between:
(i), (ii) artificial roughness,
(iii) (iv) natural roughness.

Turning now to "natural" roughness—say the roughness of cast iron—this might be represented in the formal way suggested in Fig. 64 (iii) and (iv). The point here is that the projection height k is *independent* of the pipe diameter: it is constant. Since k/d can no longer be equal to k/D, geometrical similarity is no longer

possible. It is for this reason that in a diagram such as Fig. 52, each diameter of pipe must have its own curve.

As for the connection between these considerations and the shape of the "universal" curves in Fig. 63, it is the irregularity of the "natural" roughness that seems to be the potent factor. At least it is known that only a completely uniform roughness distribution will yield the drooping curve marked (I) in this diagram.

84. Review of Turbulent Flow Theories. By selecting and arranging *in the most favourable manner* the experimental facts available, it has been possible to establish the plausible and consistent hypotheses outlined in the preceding paragraphs. But they are not the only theories. However, the general picture is sufficiently sharp and clear. The break-down of purely laminar flow begins when an element of liquid near the axis of the passage first drifts sideways into a region of lower velocity. There is no reason why it should not make this exploration, deprived as it is of directional guidance because of its remoteness from the pipe boundary. As soon as momentum transport begins, there is an increased tendency towards turbulent disturbance which is propagated throughout greater areas of the cross-section. With rising mean velocity there is a growing turbulent core of liquid surrounded by a dwindling laminar belt which shrinks to a thin film, of which vestiges may persist even at very high velocities. It is always the pipe wall which serves as the last refuge of laminar flow.

The rapid rise in frictional resistance as turbulence sets in may be attributed to the deformation of the velocity-distribution curve. At least in a smooth pipe it is the slope of this curve alone, at the pipe wall, that determines the intensity of viscous shear and therefore the force needed to push the liquid through the pipe. Under the effect of momentum transport, the central shells of liquid tend to become locked more and more firmly together; and the corresponding regions of the velocity-distribution curve must of necessity become flatter. The flatter the central parts of the curve become, the steeper must be the slope of the outer parts near the boundary.

An important consequence of the turbulent mixing process is that it affects not only the liquid elements themselves, but any attribute or property that the elements carry with them. If they have a burden of suspended silt, § 111, the silt will be transported sideways just as momentum is transported, § 75. If each liquid element is charged with heat, there will likewise be a transverse movement of heat; here lies the explanation of the rapidity of heat transfer that we find in turbulent flow conditions, § 63 (iv).

85. Secondary Losses in Closed Passages. Only rarely is it possible to provide a straight, uniform circular pipe for conveying a liquid from one point to another. On the contrary, the pipe may have to be bent so that it can be carried round corners, and it may contain junctions and changes of section of various kinds. All such departures from uniformity impose an additional energy loss on the flowing liquid which augments the loss due to frictional resistance. In a long pipe, however, these new losses are relatively small compared with frictional losses, and for this reason, they are sometimes termed *secondary losses*. An alternative title is *eddy loss*. It is convenient to group them into three categories : (i) those at inlet to the pipe, (ii) those due to changes of section of the waterway in a straight passage, and (iii) those due to actual bends or deviations of the pipe axis.

In a general way we can say that secondary losses are the result of fully-developed turbulence such as was illustrated in Figs. 15 (iv) and 25, §§ 29, 39. They can thus be expressed basically in terms of (i) the nominal velocity energy of the liquid, $v^2/2g$, and (ii) a coefficient of loss C_l depending upon the particular shape of the passage. But, since the velocity distribution of the liquid may be entirely upset as it traverses the change of section, important changes in pipe-wall conditions may also be expected. These will be reflected in a modification of wall resistance over the whole length of waterway whose regime is disturbed—a distance that may amount to ten or twenty pipe diameters. All the factors which influence frictional loss in straight uniform pipes—dimensions, wall roughness, mean velocity, nature of liquid—may thus have similar but greatly reduced effects on secondary losses. These variations will for the moment be disregarded, the question being examined in greater detail in §§ 93, 95.

Because secondary losses of energy are often associated with what is termed separation of the boundary layer, § 90, they are sometimes referred to as *separation* losses.

86. Loss at Entry.—If the entrance to the pipe is rounded or bell-mouthed (Fig. 65 (*a*)), the loss of energy incurred is

$$h_L = 0{\cdot}04\left(\frac{v^2}{2g}\right),$$

where v is the mean velocity in the pipe.

If the entrance is sharp or square-edged (Fig. 65 (*b*)), there will be a local contraction of the stream and a loss of energy due to the resulting re-expansion, which was found by § 46

to be $$\frac{\left(\frac{v}{C_c} - v\right)^2}{2g},$$

C_c being the coefficient of contraction at the vena contracta. The resulting value of h_L is usually taken to be

$$h_L = 0{\cdot}5\frac{v^2}{2g}.$$

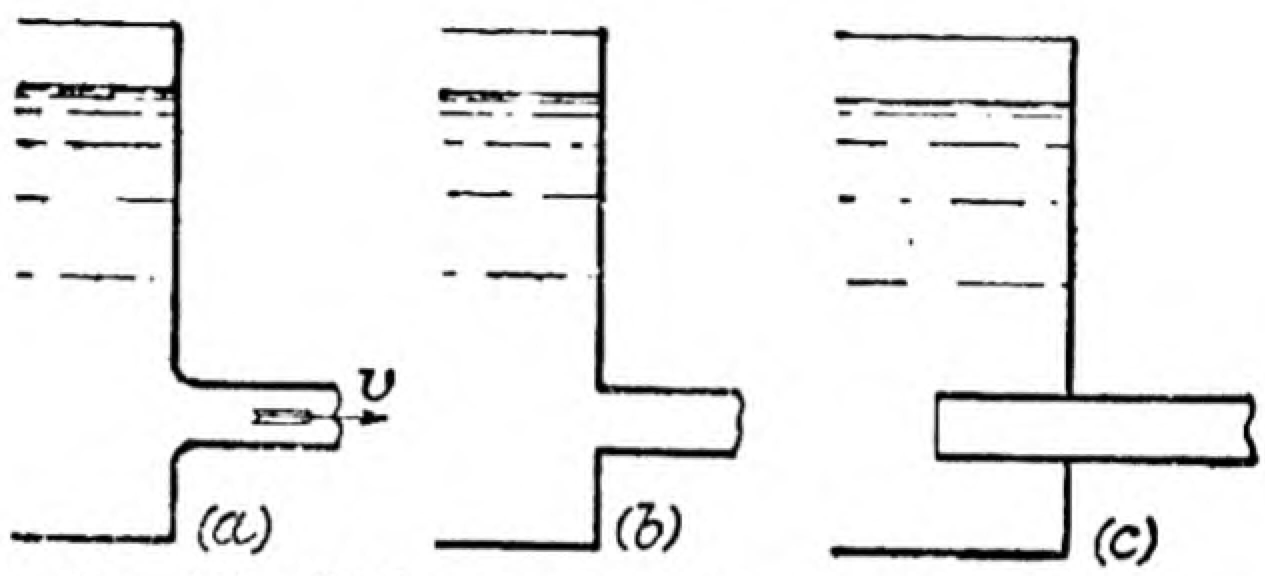

FIG. 65.—Liquid from reservoir entering circular pipe.

A re-entrant pipe (§ 49 (*b*)), will impose a still greater loss, viz.

$$h_L = 0{\cdot}7\frac{v^2}{2g}$$

or more (Fig. 65 (*c*)). In the three types of pipe entry, then, the respective values of coefficient of loss C_l are approximately: (*a*) 0·04, (*b*) 0·5, (*c*) 0·7.

87. Losses Due to Change of Section.

(*a*) *Sudden enlargement.* When the stream of liquid moving with velocity v_1 impinges on a stream moving with a lower velocity v_2 (Fig. 66), we find by applying formula 4-3, § 46, that the loss of energy is about

$$h_L = \frac{(v_1 - v_2)^2}{2g} \quad \text{(see also § 136).}$$

Observe that although the total energy line drops by an amount h_L, the hydraulic gradient *rises* by an amount h_g, showing that the pressure *increases* as a liquid flows past a sudden enlargement.

(*b*) *Tapered enlargement.* By the use of a tapered enlargement (Fig. 67), the eddies indicated in Fig. 66 can to a

large extent be suppressed, the energy loss diminished, and the rise in pressure increased.[37] Minimum loss is secured by making the rate of straight taper

$$\frac{\text{increase of diameter}}{\text{increase of length}} = \frac{1}{10},$$

whereupon

$$h_L = 0{\cdot}14\frac{(v_1 - v_2)^2}{2g}$$

approximately, or only 14 per cent. of the corresponding loss in a sudden enlargement. Making the taper more gradual increases the loss because of the increased friction; making it steeper does not induce the stream to expand more rapidly, but merely provides dead space in which eddies can form and so increase the "separation" loss, § 90.

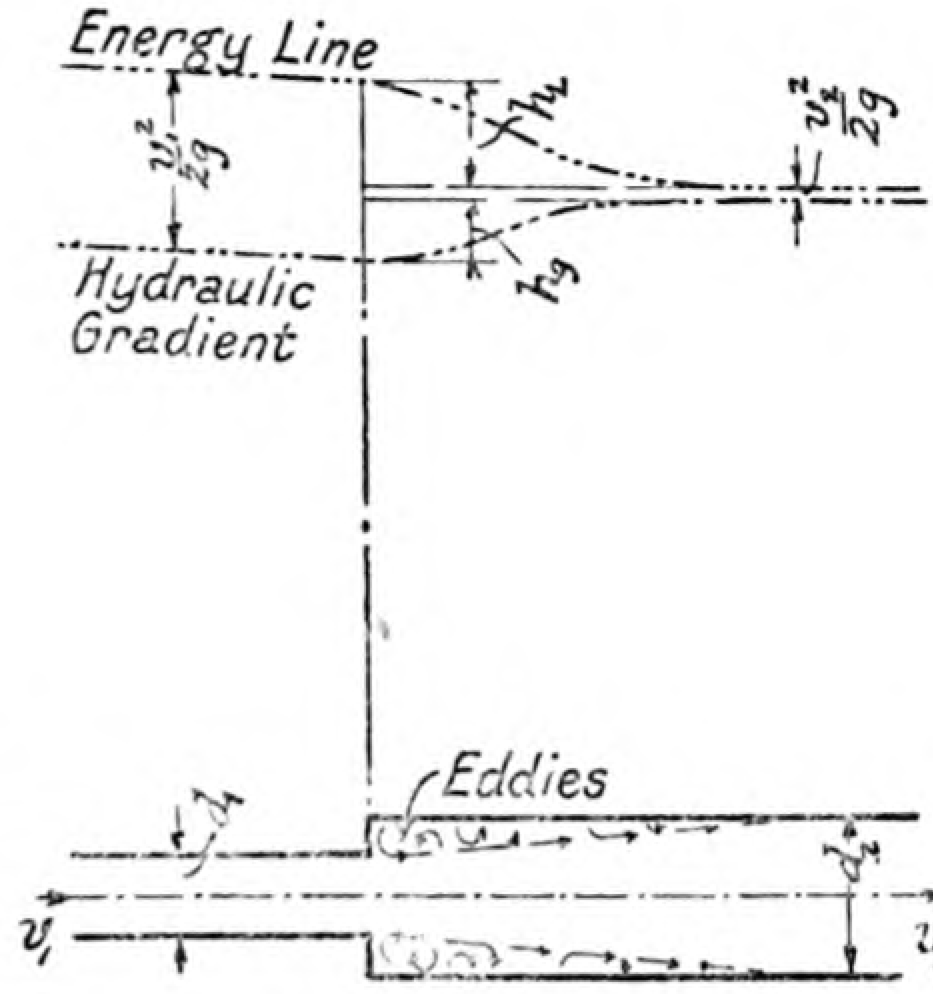

FIG. 66.—Change in regime at sudden enlargement.

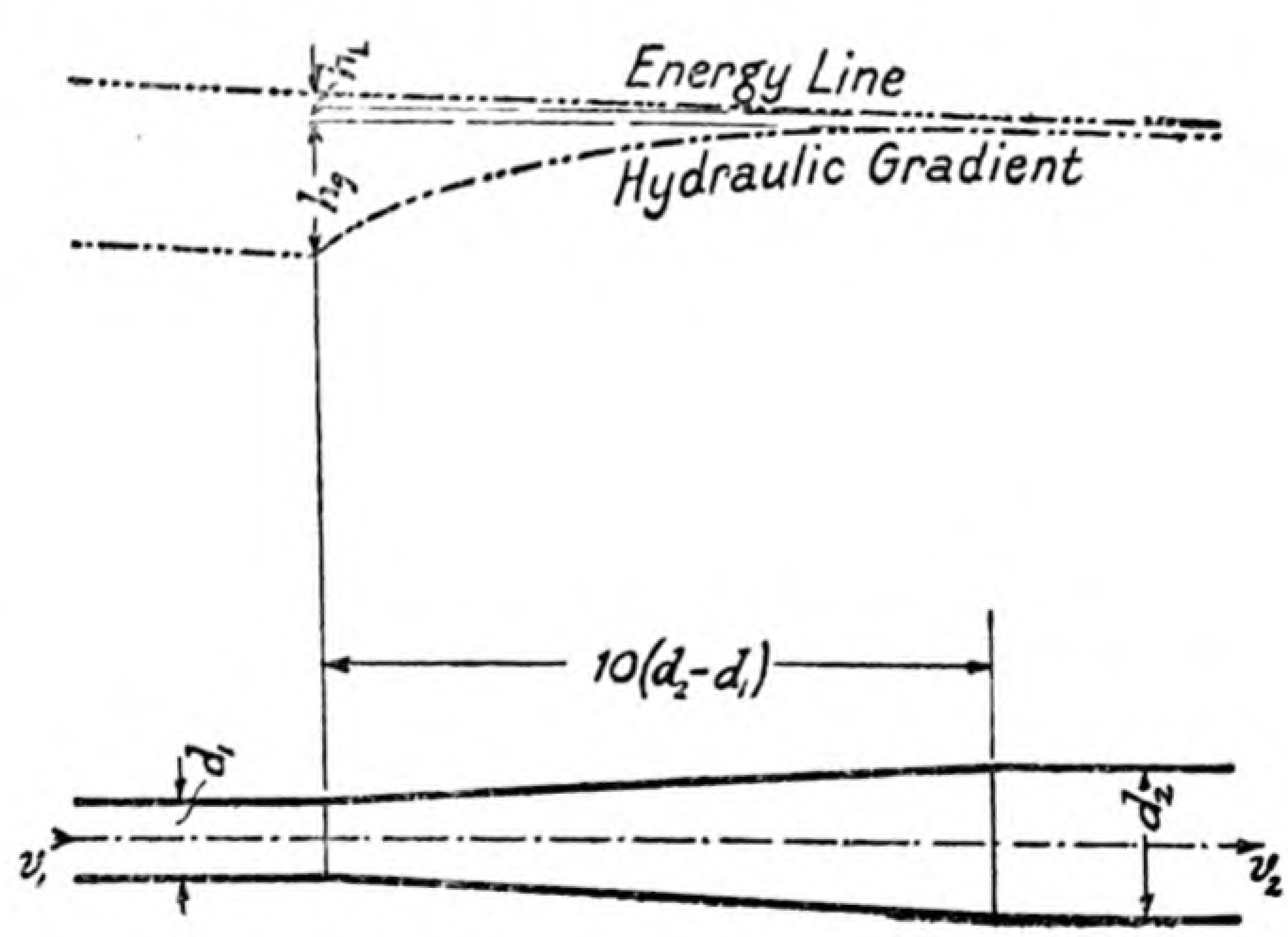

FIG. 67.—Recuperation of pressure head in tapered enlargement.

But a slight reduction in the value of h_L can be attained by making the enlargement trumpet-shaped, the rate of taper increasing as the diameter increases.

(c) *Sudden contraction.* The loss of energy here (Fig. 68) is of the same nature as in the external mouthpiece, § 48, and in the sharp-edged pipe entry, Fig. 65 (b). So long as the

diameter of the large section of the pipe is relatively big enough to permit full contraction to occur in the small section, the loss of energy is taken to be

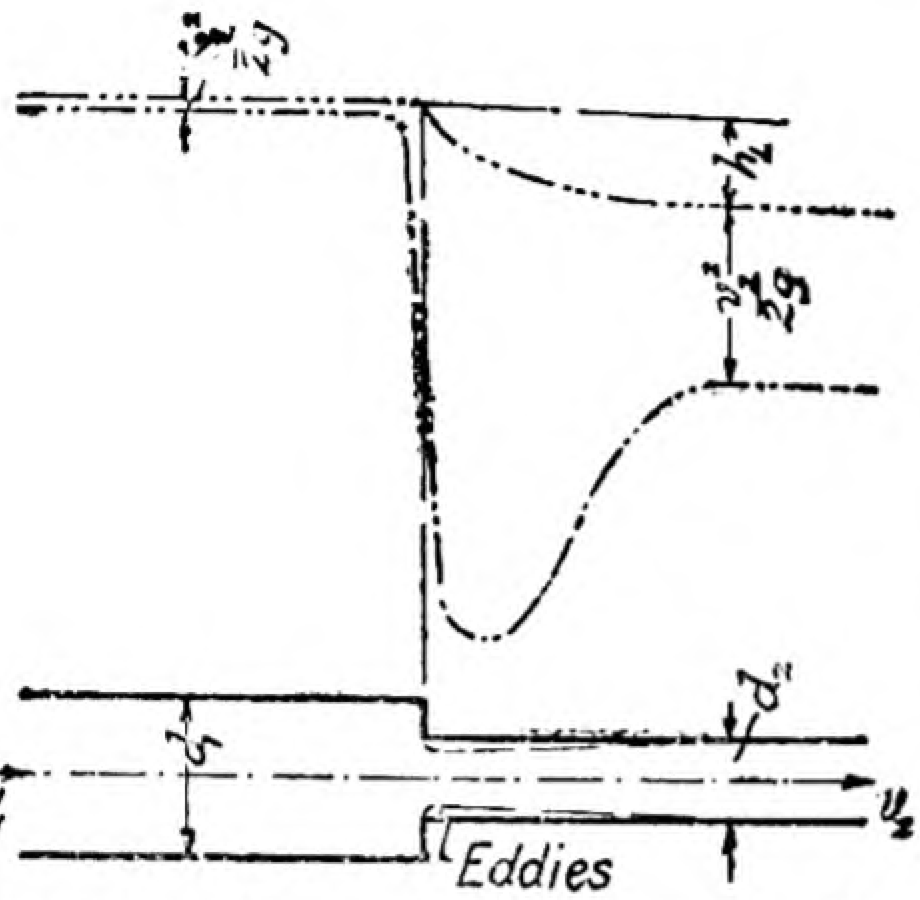

Fig. 68.—Loss in sudden contraction.

$$h_L = 0{\cdot}5\frac{v_2^2}{2g}.$$

If d_1 is only slightly greater than d_2, the coefficient of contraction will be decreased and the energy loss correspondingly reduced.

(*d*) *Pierced diaphragm, or orifice.* Here also (Fig. 69) the loss of energy is due to the eddying set up as the stream expands from the contracted area $C_c a$ at the vena contracta, immediately downstream of the orifice, to the full pipe area A. If v is the velocity in the pipe, equation 4-3, § 46, shows that

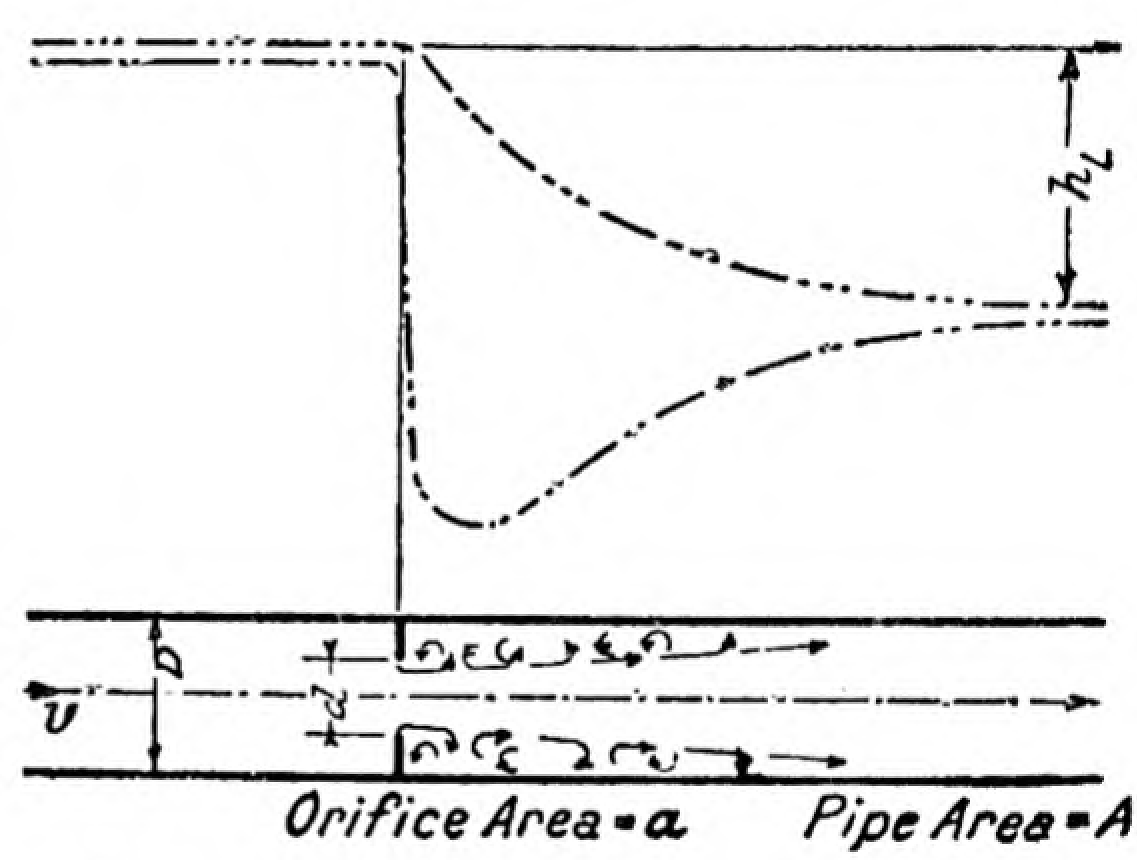

Fig. 69.—Pressure drop at orifice in circular pipe.

$$h_L = \frac{\left[\left(v \cdot \frac{A}{C_c a}\right) - v\right]}{2g}$$

$$= \frac{v^2}{2g}\left(\frac{A}{C_c a} - 1\right)^2.$$

For approximate calculations C_c may be taken as 0·65.

A partially closed *valve* in a pipe acts as an orifice of variable shape and variable area. By adjusting it to give the necessary value of $\frac{A}{a}$, any desired amount of energy may be dissipated (§§ 92, 169).

88. Losses Due to Change of Direction. The paths of the main streams of liquid sketched in Fig. 70 suggest that in bends, elbows, and tee-pieces the eddy loss is of the same nature as it is in a sudden enlargement (§ 87 (*a*)); there is a stationary zone of eddying liquid that not merely obstructs

the flow, but continually abstracts energy from the useful or effective stream that sweeps past it. Even if the bend is of so large a radius that this gross type of turbulence is minimised, yet the flow pattern will remain favourable to the *separation of the boundary layer* that is described in § 90. Because of the free vortex flow in the bend, § 141, the liquid near the walls will encounter a rising pressure gradient at points S and S in Fig. 70, with a possibility of increased energy loss due to turbulence. It follows that it is exceptionally difficult to

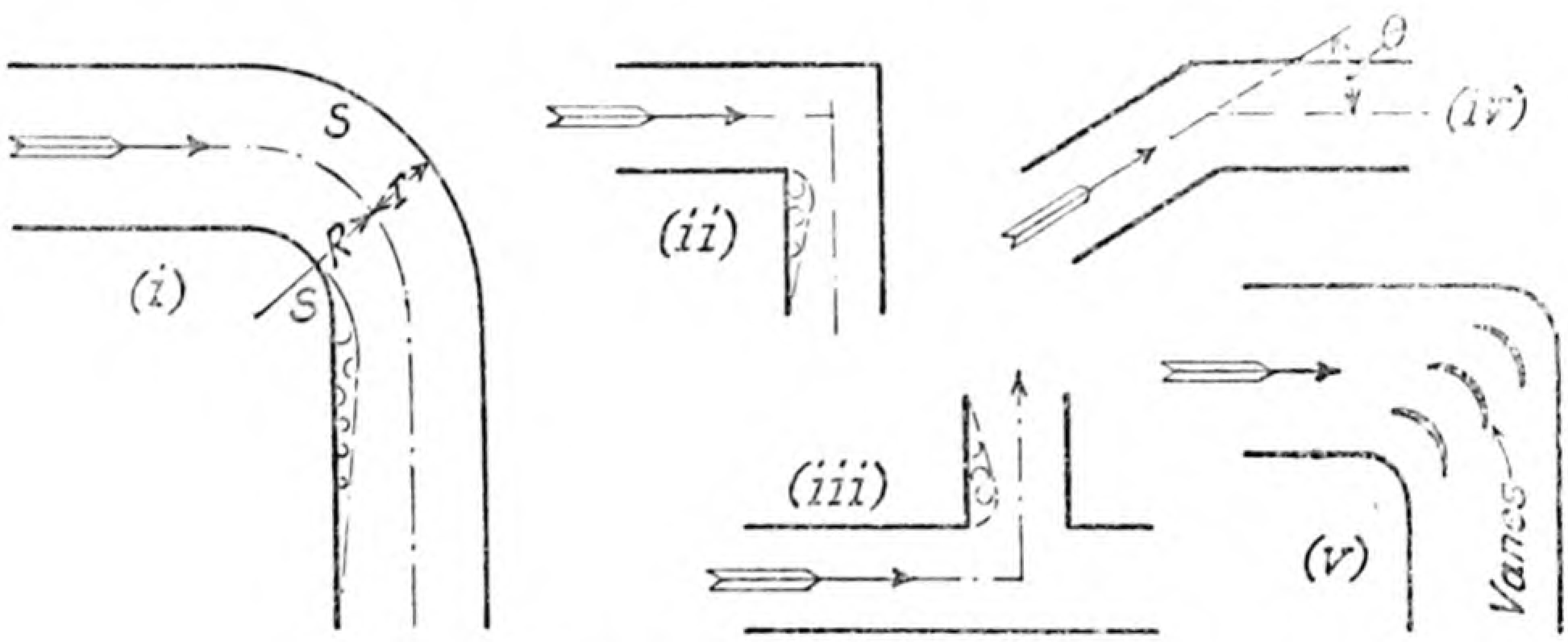

FIG. 70.—Types of elbows, bends, etc.

isolate the loss in the bend itself from the overall losses in the conduit of which it forms a part. The following values for the coefficient C_l in the equation $h_L = C_l \cdot \frac{v_2}{2g}$ are therefore approximations only.[38]

For the *bend*, (i) so long as the radius R of the pipe axis is not less than $5r$, where r is the pipe radius, then

$$C_l = 0{\cdot}2 \text{ to } 0{\cdot}3.$$

For the right-angle *elbow* or *tee-piece*, (ii) or (iii),

$$C_l = 1{\cdot}0.$$

For the *obtuse-angled* elbow, (iv),

$$C_l = \sin^2\theta,$$

where θ is the angle of deviation.

These rather serious losses can be reduced [39] by using a grid of deflecting vanes extending across the passage, as at (v), Fig. 70. The change in direction of the pipe axis can then be accomplished with a value of C_l hardly greater than 0·15.

89. Efficiency of Energy Transformation. It is useful at this stage, in the light of the information given in the preceding paragraphs, to compare the efficiency of the two principal types of energy transformation that occur in hydraulic flow. When pressure energy is converted into velocity energy, as for example in a nozzle or at the bell-mouthed entrance to a pipe, the loss has been shown to be about 4 per cent. ; that is, of the total pressure energy yielded up, 96 per cent. has been recovered again in the form of velocity energy The efficiency of conversion is therefore 96 per cent.

One of the most efficient devices for reversing the process —for converting velocity energy into pressure energy—is a taper pipe of the sort shown in Fig. 67. During a gradual reduction of velocity from v to (say) $\frac{v}{4}$, the velocity energy yielded up is $\frac{v^2}{2g} - \left(\frac{v}{4}\right)^2 \Big/ 2g = 0{\cdot}94\frac{v^2}{2g}$, and the energy wasted, even under the most favourable conditions (§ 87 (*b*)), is about

$$0{\cdot}14\,\frac{\left(v - \frac{v}{4}\right)^2}{2g} = 0{\cdot}079\,\frac{v^2}{2g}.$$

The energy loss is thus 8·4 per cent. of the velocity energy supplied, and the efficiency of transformation is 91·6 per cent.

These figures fairly represent the relative difficulty of the two sorts of conversion : *pressure* energy can easily and efficiently be transformed into velocity energy, but to transform *velocity* energy into pressure energy involves more serious losses.

The actual seat of these energy losses may be located if we take the trouble to study the *changes in velocity distribution* that accompany changes in the cross-section traversed by the flowing liquid.[40] These changes are shown pictorially in Fig. 71. Liquid with normal velocity distribution and mean velocity v_1 approaches either (i) a tapered contraction or (ii) a tapered enlargement. As indicated by the hydraulic gradient, the nominal variation of pressure head is δh, downwards or upwards as the case may be. From the known local velocity u at various radii, the corresponding velocity head can be worked out, and a curve between relative radius r/R and velocity head can be plotted as at (1), diagram (iii). Since, in traversing the tapered length, every liquid element undergoes the same energy interchange δh, we may add this amount to or subtract it from the curve (1) and thus produce the curves

(2) and (3); these then represent curves of distribution of velocity energy at the reduced and enlarged sections respectively. Finally, from the values of $\frac{u_2^2}{2g}$ and $\frac{u_3^2}{2g}$ we may compute desired values of u_2 and u_2 and plot them in diagrams (i) and (ii).

At once it is apparent that the tapered reduction has made the velocity distribution *more uniform,* while the enlargement has *intensified* the velocity variations. In other words, in the one case the ratio : maximum velocity/mean velocity has diminished, while in the other it has increased. What is still more significant is that near the walls of the enlarged section (ii) the velocity has been brought down to zero—the liquid has actually come to rest. An analytical proof that this is likely to happen is provided by equation 3-2, § 35. If this is written in the form $\delta u = g \cdot \delta h/u$, we see that near the pipe wall where the local velocity u is small, the velocity *variation* δu is relatively large, and may easily be as great as u itself.

90. Separation of the Boundary Layer. Manifestly the collection of stationary elements just described is going to cause serious disturbances to the main stream of flowing liquid, and especially to the boundary layer (§ 78). A kind of traffic block has occurred; consequently the elements following on behind are deflected away from the wall as suggested in Fig. 71 (iv), and there

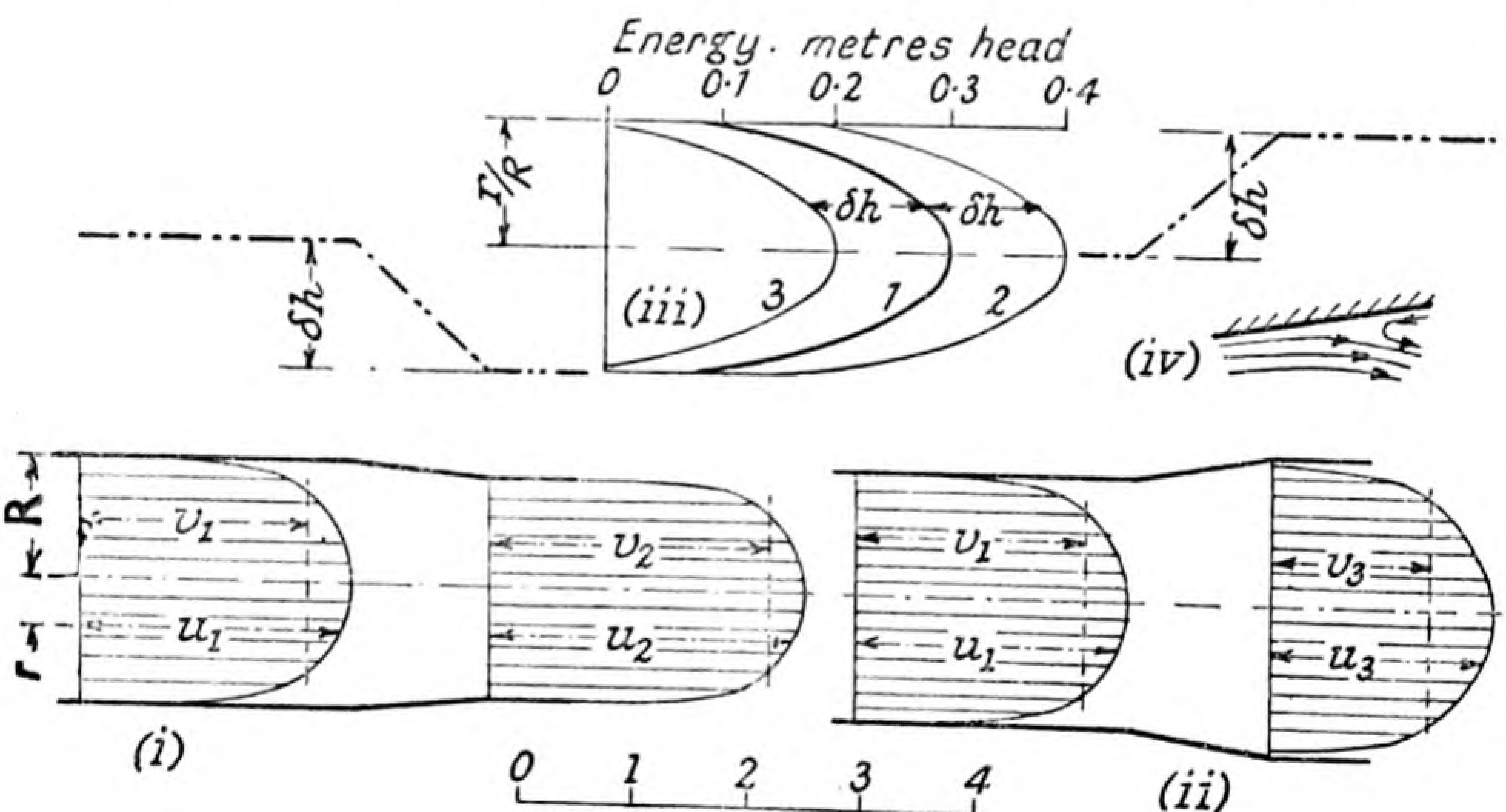

FIG. 71.—Effect of change of section on (i) (ii) velocity profile, (iii) energy profile.

is a confused transverse drift, downstream of the disturbance. This phenomenon, designated the *separation of the boundary layer,* convincingly explains the inevitable eddy losses that occur when liquid near a solid boundary passes into a region of *increasing* pressure. It makes clear, too, the statement in § 64 that diverging boundaries tend to lower the critical velocity, by reason of the added danger of turbulence they introduce. If we like to replace the liquid elements in Fig. 71 (ii) by motor vehicles ascending the steep hill shown in profile by the rising hydraulic gradient, we get a very graphic impression of the turmoil that would ensue when the slowest vehicle nearest the kerb failed to make the grade and finally stalled.

Since the essence of the process of boundary layer separation is a collapse of order into disorder, it is idle to hope that the process can be represented in any rigid geometrical form. But a generalised pictorial approach to the problem is offered in Fig. 72. Liquid is moving from left to right, traversing on its way a curved part of the solid boundary which may either be the transition section of a tapered enlargement in a pipe, Fig. 71 (ii), or the outlet area of a pipe bend, say, point S in Fig. 70 (i). Originally there is a normal type of boundary layer, as in Fig. 59; its thickness is y_l, and in the adjacent liquid the local velocity is u. The effect of the curved boundary is to reduce the local velocity to u', and to thicken very markedly the boundary layer itself. Finally, at the right-hand side of the diagram, the distortion of the velocity distribution curve is so serious that negative velocity components have appeared; the boundary layer has been wholly disrupted, and in its place we find the state of turmoil and confusion indicated on a smaller scale in Fig. 71 (iv).

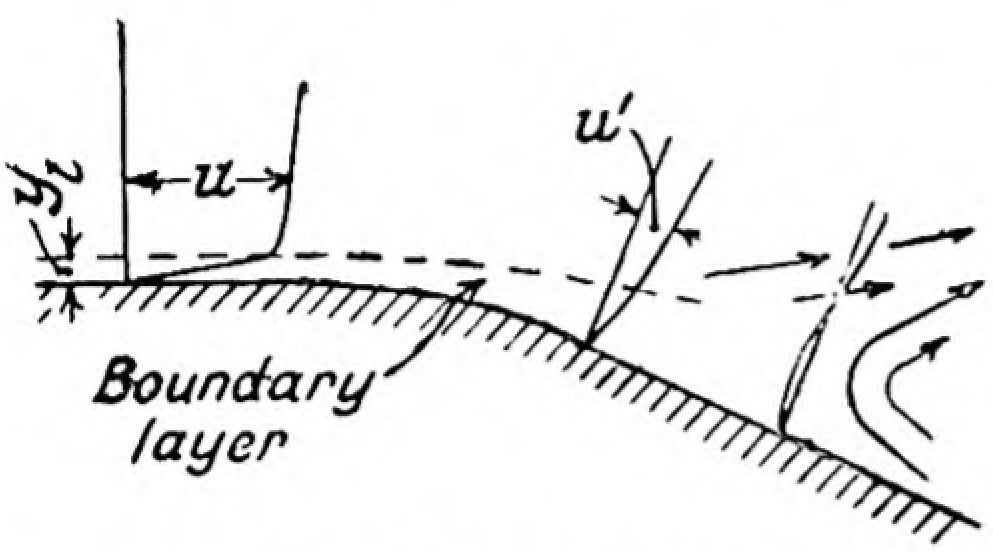

FIG. 72.—Break-up of boundary layer

91. Transmission of Pressure Energy.

In considering the efficiency with which energy can be transmitted along pipes, the velocity energy is generally so small compared with the pressure energy that it can be ignored. Referring to Fig. 73, the energy of the liquid is reduced by friction from h_1 at point 1 to h_2 at point 2. If W is the weight of liquid flowing per second along the pipe, the total energy input per second is Wh_1, and the energy per second delivered to point 2 is Wh_2. The efficiency of the pipe as a transmission device is thus

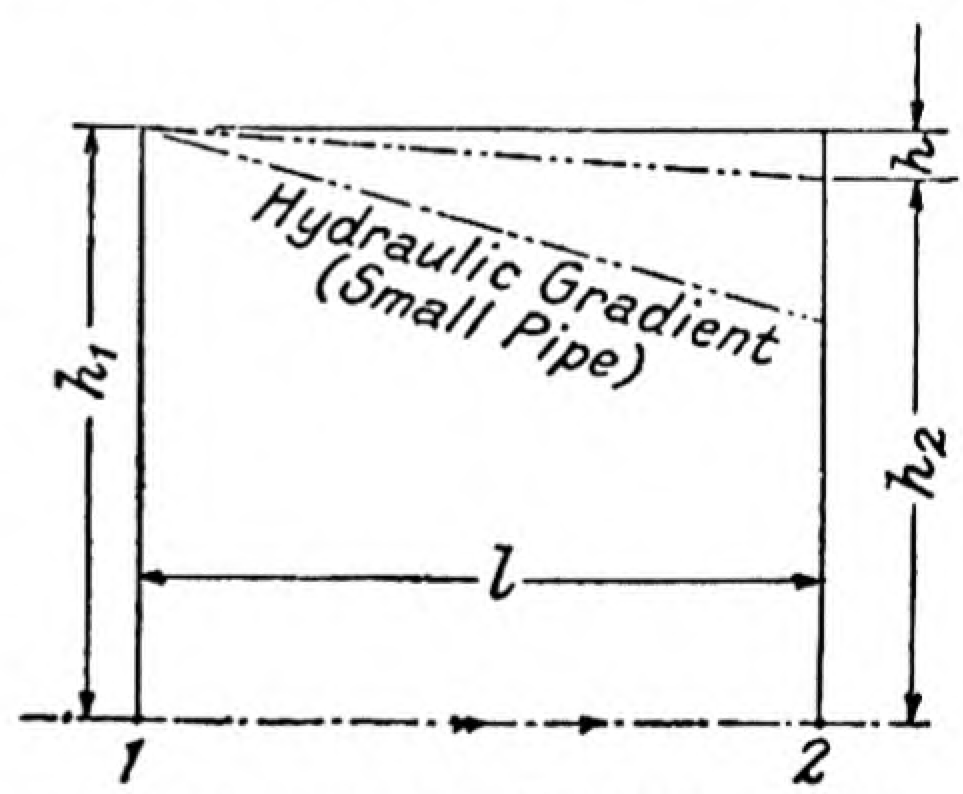

FIG. 73.—Hydraulic transmission of energy.

$$\frac{Wh_2}{Wh_1}=\frac{h_1-h}{h_1},$$

where h is the friction loss.

For a given energy output $= Wh_2 = \frac{\pi}{4}d^2wvh_2$, and a given initial head h_1, it is evident that a specified quantity of energy per second may be transmitted from 1 to 2 either through a

large diameter, costly pipe, or through a small, cheap pipe. Since the friction loss h has the value $\frac{4fl}{d} \cdot \frac{v^2}{2g}$, § 68, the term $\frac{v^2}{d}$ will be much greater for the small pipe than for the large pipe : the energy loss will therefore be greater, as indicated by the steeply sloping hydraulic gradient in Fig. 73, and the efficiency of transmission will be less.

If W is expressed in lb./sec. and h_2 in ft., then the *water horse-power* delivered at point 2 is

$$\frac{Wh_2}{550} \qquad . \quad . \quad . \quad (5\text{-}13)$$

If W is expressed in kg./sec. and h_2 in metres, the equivalent metric water horse-power is $\frac{Wh_2}{75}$.

The total loss of energy per second in friction in a given pipe is represented by

$$Wh = \frac{\pi}{4}d^2 \cdot v \cdot w \cdot \frac{4fl}{d} \cdot \frac{v^2}{2g}$$
$$= \text{constant} \times fv^3.$$

If the pipe is rough, the variations in f will be small, hence friction horse-power loss varies approximately as the *cube* of the velocity, v.

92. Destruction of Energy. The most effective way of reducing the energy of the liquid flowing along a closed passage is to dissipate the surplus energy by instituting violent eddying motion. This can be done either by using a pierced diaphragm having a fixed area of opening (Fig. 69), or by interposing a valve in which the area can be regulated (§ 169). Such a valve can serve (i) to control the discharge in the passage, (ii) to control the pressure, or (iii) to regulate both simultaneously. It is true that in the first type of control, which is illustrated in Fig. 74 (i), there is very little actual destruction of energy in the control mechanism. Here the liquid issues from the constant-level reservoir through so short a pipe that friction losses are virtually negligible ; the discharge varies directly with the area of opening, or nearly so, as the valve gate is progressively closed. Conditions closely resemble those for free-flow orifices, §§ 42, 43. In Fig. 74 (ii) we imagine a pump to be

delivering a *constant* discharge q through the pipe and valve; by manipulation of the valve gate, we control the value of the coefficient of loss $\left(\frac{A}{C_c a} - 1\right)^2$, § 87 (*d*), and thus bring the head loss to the amount h_{L1} or h_{L2}, or any other desired value. This method of pressure-control by *throttling* is extremely convenient in practice.

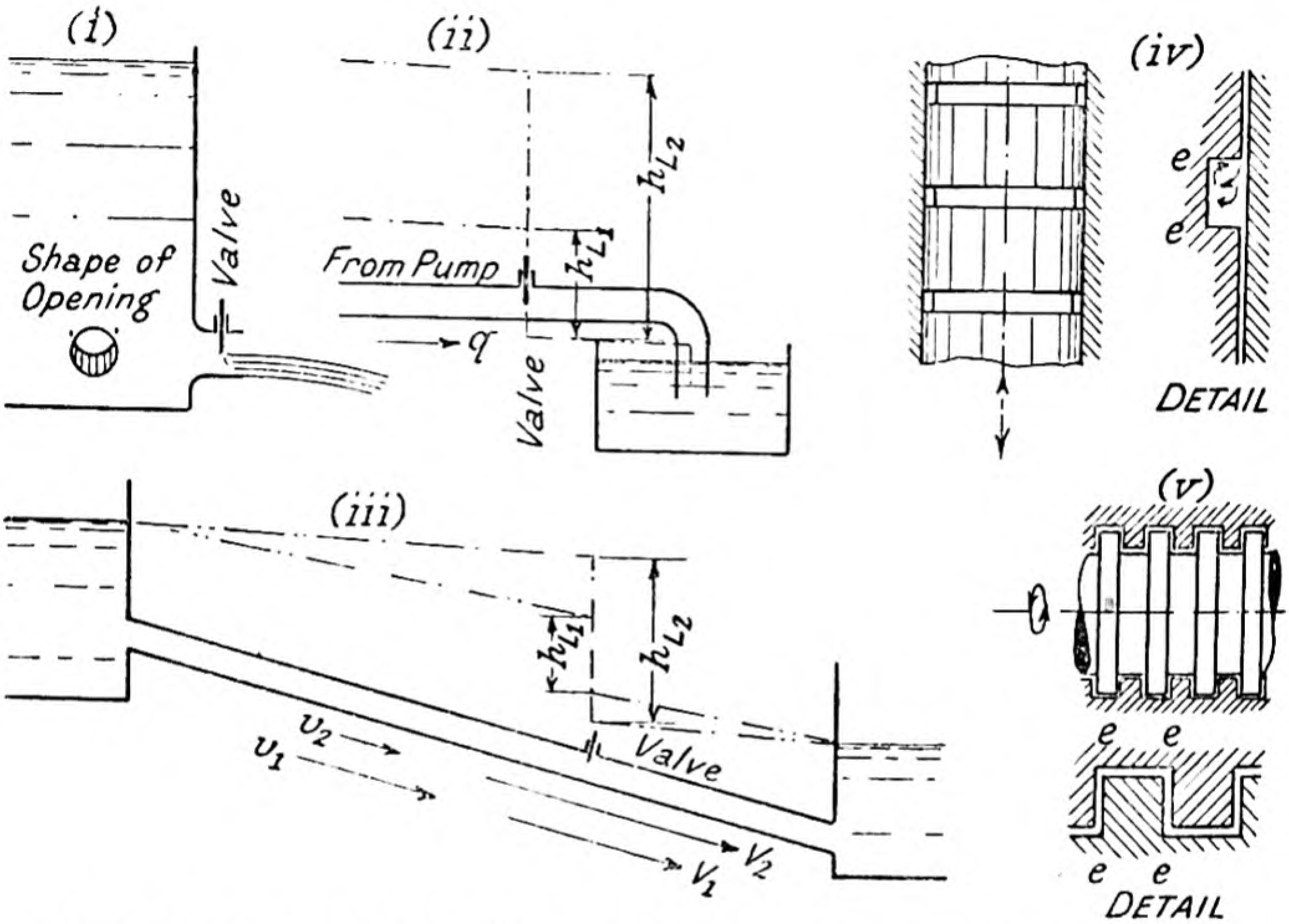

FIG. 74.—Energy destruction at (i) (ii) (iii), valve, (iv) grooved plunger, (v) labyrinth gland.

More ordinary conditions are depicted in Fig. 74 (iii), where the primary object of the regulating-valve is to control the rate of flow of water from the upper reservoir to the lower one. This can only be achieved by adjusting the area through the valve which in turn augments or diminishes the pressure-head drop h_{L1} or h_{L2}. When the valve is fully open, virtually the whole of the available head is dissipated in pipe friction, the hydraulic gradient has its maximum inclination and the rate of flow reaches its highest value (§ 68 (ii)). When the valve is fully closed the hydraulic gradient is horizontal. It will be observed that the *smaller* the velocity v in the pipe, the *greater* must become the velocity V through the valve opening itself.

The principle of deliberately setting up turbulence as a means of controlling flow is applicable to passages of annular as well as of circular form. Fig. 74 (iv) shows a plunger or spindle which is required to reciprocate longitudinally through a cylindrical opening; there is a pressure-difference between the two ends of the plunger, and it is desired to reduce, as far as practicable, leakage of liquid between the moving surfaces. Naturally, the clearance between the two must first be reduced to the minimum; thereafter the resistance to flow can be still further increased, and the leakage loss diminished, by cutting annular grooves in which secondary losses of energy can be provoked. If the shaft is a revolving instead of a reciprocating one, then the system of annular collars working *without metallic contact* inside a grooved housing, Fig. 74 (v), is known as a *labyrinth gland.* Although there must inevitably be a steady leakage of liquid from the high-pressure to the low-pressure end of the gland, this can be brought within stipulated limits by using a sufficient number of collars. The zone of eddying at each abrupt change of direction $e \, . \, e \, . \, e$. exacts its toll of energy as the liquid leaks past.

93. Principle of Dynamical Similarity. It is here our purpose to try to discover for geometrically-similar *closed* passages a criterion of performance which will serve in much the same way as the Froude number serves for free-flow conditions. That criterion, § 52, expressed the relative importance of inertia forces as compared with gravitational forces.

Turning now to closed passages, we have to remember that gravitational forces are here without effect on the liquid; instead, the motion of the liquid elements is controlled only by (i) acceleration or inertia forces, and (ii) viscous forces (§ 28). Either from § 35 or § 49 it may be seen that typical inertia forces may be expressed in the form: $\frac{w}{g} \, . \, a \, . \, v^2$, while the characteristic viscous force is: $\mu \, . \, a \, . \, \frac{v}{y}$ (§ 7). Arranging the two typical forces as a ratio, thus:

$$\frac{\frac{w}{g} \, . \, a \, . \, v^2}{\mu \, . \, a \, . \, \frac{v}{y}} \qquad . \quad . \quad . \quad (5\text{-}14)$$

we find that the ratio reduces to the form $\frac{vy\rho}{\mu}$, which in general terms can be written: $\frac{\text{velocity} \times \text{length}}{\text{kinematic viscosity}}$. By substituting for the term *length* a diameter d, we observe that in fact the *ratio between the forces is the Reynolds number* $R_n = \frac{vd\rho}{\mu} = \frac{vd}{\nu}$ (§ 64). **(Example 32.)**

If, in two geometrically similar closed passages, the Reynolds numbers are identical, we say that *dynamical similarity* exists; and the test of dynamical similarity is that inertia and viscous forces should stand in a common ratio. As the paths traced out by the liquid elements depend wholly on the resultant of the forces acting on them, the consequence of dynamical similarity should be that the flow patterns in the two systems are identical. Just as the visible jets issuing from free flow orifices can be adjusted to have similar shapes, § 51, so we may imagine the invisible and much more complicated tracks of liquid elements in closed passages to be identical in their general proportions. Just as similarly shaped jets led us to expect identical coefficients of discharge, so we may accept dynamical similarity as a guarantee of identical *coefficients of loss*. Comparing, for example, passages of varying section such as those shown in Figs. 65-68, then appropriate values of $C_l = h_L \Big/ \frac{v^2}{2g}$ will be numerically equal if the Reynolds numbers are equal. Naturally for *rough* passages the stipulated condition of geometrical similarity can only be fulfilled if the type of roughness and the relative roughness $\frac{k}{d}$ are identical in the two passages.

94. General Significance of the Reynolds Number. With a firmer knowledge of the fundamental meaning of the Reynolds number, it is now profitable to examine anew the various duties that have already been assigned to it.

(i) *Critical velocity.* That R_n is a pure number, § 64, is evident the moment we realise that it represents a *ratio* between two types of force. Its non-dimensional nature is equally well revealed by the theory of dimensions, § 40, thus:

$$\frac{vd}{\nu} = \frac{\dfrac{\text{length}}{\text{time}} \times \text{length}}{\dfrac{\text{area}}{\text{time}}} = \frac{\dfrac{L}{T} \times L}{\dfrac{L^2}{T}}.$$

A *high* numerical value indicates that the upper term—the inertia-force term—of the basic ratio [eqn. 5-14] is preponderant; a *low* value tells us that the lower or viscous-force term is relatively more important. Naturally, then, it is to be expected that a very low Reynolds number will be associated with laminar flow, in which inertia forces have been very much reduced. And, remembering that the essence of turbulence is the confused intermingling of rapidly-moving elements, incessantly subjected to violent accelerations and retardations, we can regard $R_n = 3{,}400{,}000$ (say) as the most concise way of expressing a very advanced state of *turbulent* flow.

(ii) *Velocity profiles.* The dependence of velocity distribution upon the Reynolds number, Fig. 54, § 71, serves as an effective analogy with the identically shaped jets shown in Fig. 33. This similarity of shape of jet had been brought about by correctly adjusting the *Froude* numbers. By suitably adjusting flow conditions in pipes to give identical *Reynolds* numbers we get similarly shaped velocity profiles; even if the flow patterns themselves cannot be made manifest to us, the diagrams which represent them have the desired resemblance.

(iii) *Overall losses in closed passages.* It should now be apparent that the graphs, Figs. 51 and 53, representing flow in pipes are no more than special cases of a whole general family of curves expressing a relation between Reynolds number and hydraulic resistance of some form or another. We may, therefore, enlarge the meaning of the expression for the coefficient of loss $C_l = h_L \Big/ \dfrac{v^2}{2g}$ (§ 85), to embrace the *total* resistance in the conduit. For circular straight pipes the term $\dfrac{4fl}{d}$ in equation 5-7 is only another way of writing the coefficient of loss C_l. By rearranging the expression in the form $4 \cdot \dfrac{l}{d} \cdot f$, it very conveniently exposes the two constituents of the coefficient of loss: (i) a term descriptive of the geometrical *form*

of the passage—in this case the ratio l/d which expresses its proportions, and (ii) a term such as f which shows how the resistance depends upon the inter-relation between the dimensions of the passage and the nature of the liquid (§ 85). It is the Reynolds number which has the unique privilege of displaying this inter-relation in the most compact form.

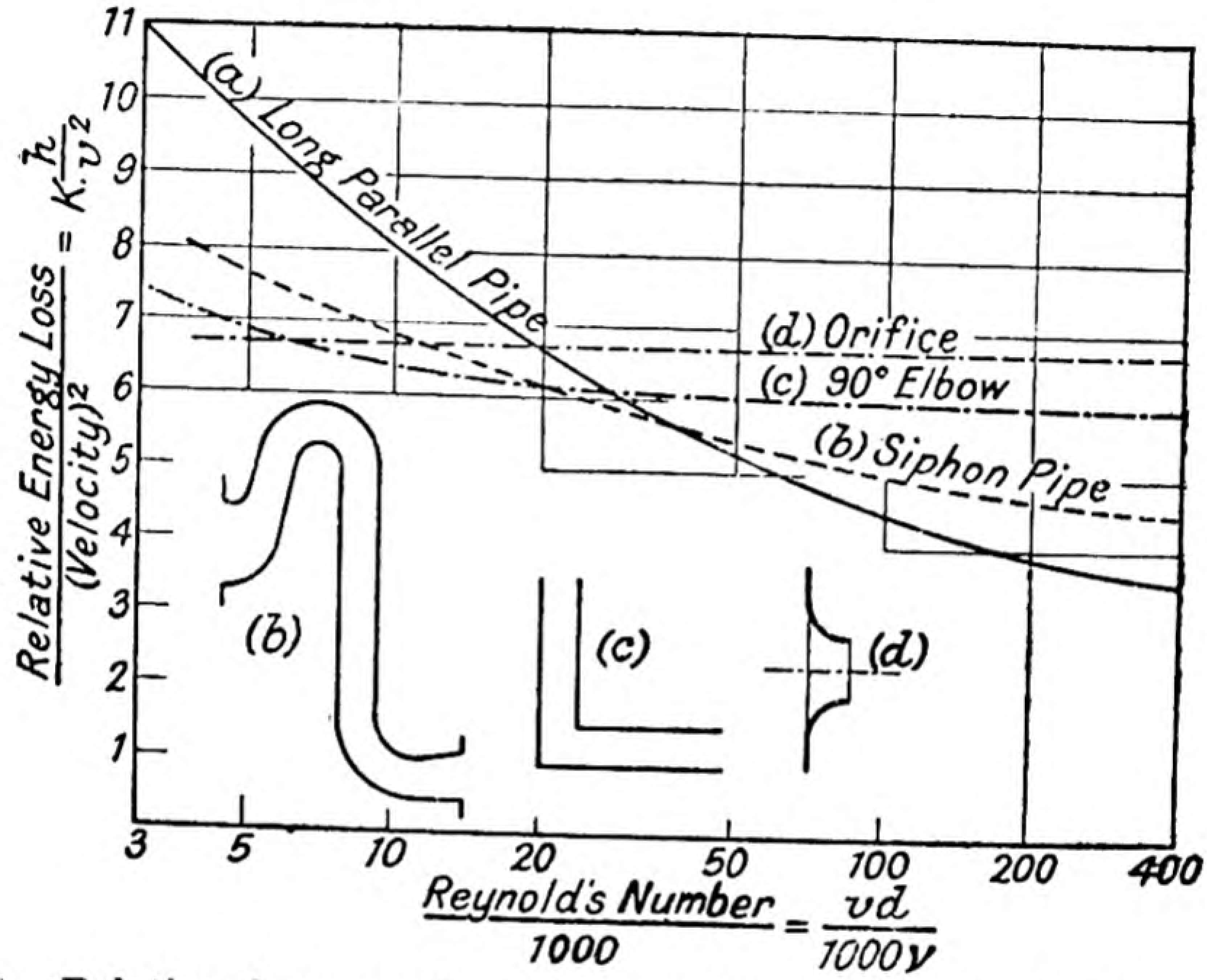

FIG. 75 —Relation between Reynolds number and energy loss for various types of smooth passages.

As the geometrical shape varies, so does the shape of the graph between R_n and hydraulic resistance vary. The difference between the geometrical shape and texture of the wall of a smooth pipe as compared with a rough pipe is reflected in the variations noticeable in Figs. 51 and 53. In general we shall expect to find that the resistance in relatively long and narrow passages, in which wall friction constitutes the major part of the total energy loss, is more dependent on the Reynolds number than is the resistance in very short passages. In an orifice, for example, § 87 (*d*), virtually the entire loss is the result of turbulence. These characteristic relationships are graphically displayed in Fig. 75; here the vertical scale of relative resistance or energy loss is graduated in arbitrary units, in order that the *shapes* of the graphs can conveniently be compared. As we progress from the long, smooth pipe to the orifice of negligible length, the typical curves progressively flatten out.

95. Applications of Dynamical Similarity. Let us assume that in order to predict the total energy loss as water flows through the pipe "special" shown in Fig. 76, a scale model is constructed. It is required to find the conditions

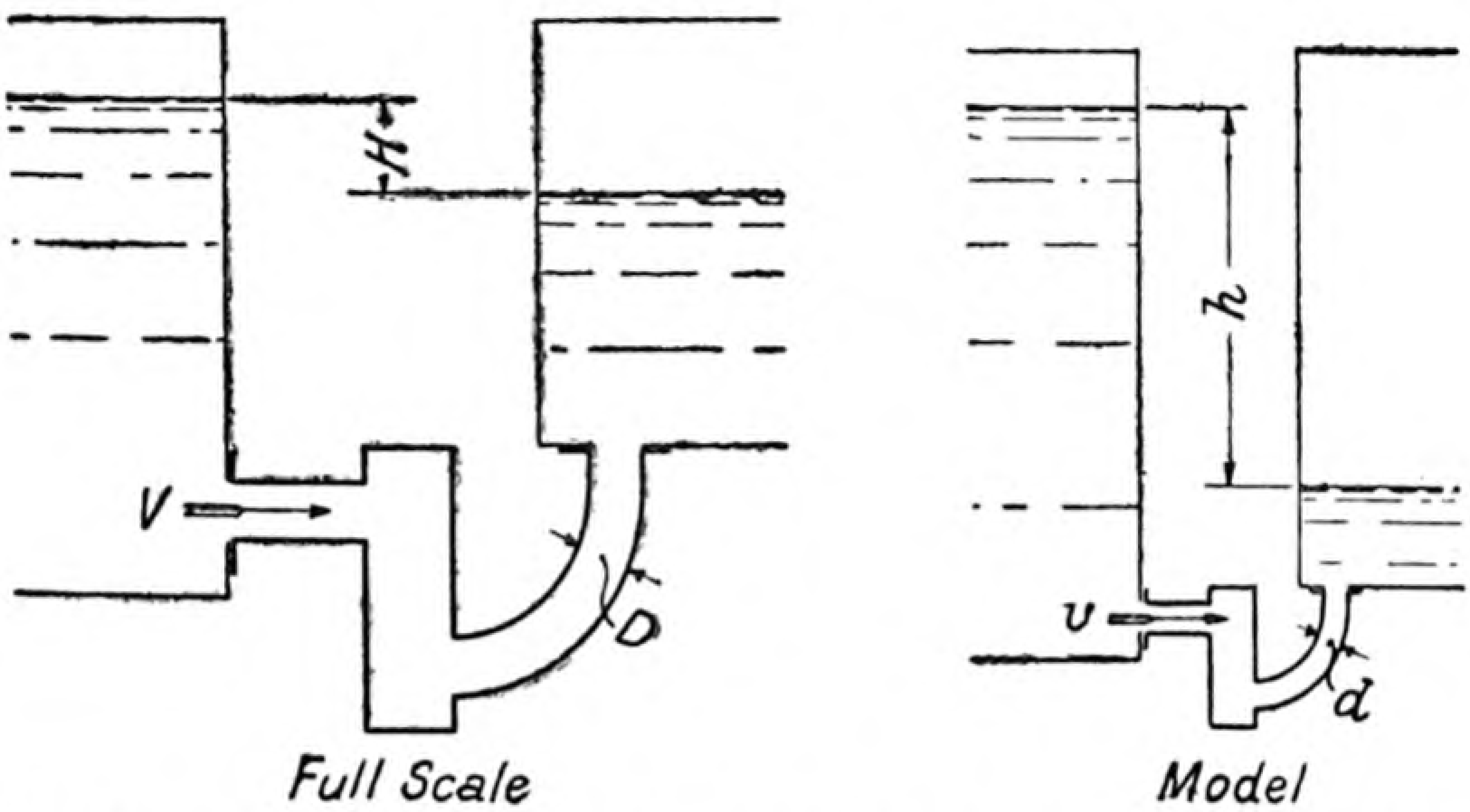

FIG. 76.—Demonstration of dynamical similarity in geometrically similar passages.

under which the model must be tested to ensure that the measured head loss h under a measured discharge q will give a reliable guide to the full-scale loss. Applying the principle of dynamical similarity, these conditions are:

$$\text{(i)}\ \frac{H}{V^2} = \frac{h}{v^2}, \quad \text{and} \quad \text{(ii)}\ \frac{VD}{\nu} = \frac{vd}{\nu_o}$$

If water is used both for the model and for the full-scale pipe, $\nu_o = \nu$, therefore $VD = vd$, whence $\frac{h}{H} = \left(\frac{D}{d}\right)^2$. The necessary head h for the model must therefore be *greater* than the full-scale head H (Fig. 76). By maintaining this relationship between the heads, very close agreement between the values of $\frac{H}{V^2}$ and $\frac{h}{v^2}$ can be relied upon, so long as both the model and the full-scale pipes have *perfectly smooth walls* (or have the same relative roughness $\frac{k}{d}$), and are built with the same degree of accuracy in every detail.

Dynamical similarity is usually impossible of achievement in passages and openings having a free surface exposed to the atmosphere, e.g. sluices and flat-topped weirs, in which the head producing flow must bear a fixed relationship to

the dimensions of the opening. Here the requirements of dynamical similarity, viz. $\frac{h}{H} = \left(\frac{D}{d}\right)^2$, are flatly opposed to the necessities of geometrically similar heads, $\frac{h}{H} = \frac{d}{D}$. The result is shown diagrammatically in Fig. 77, where geometrically similar smooth pipes with nozzle outlets are seen discharging under

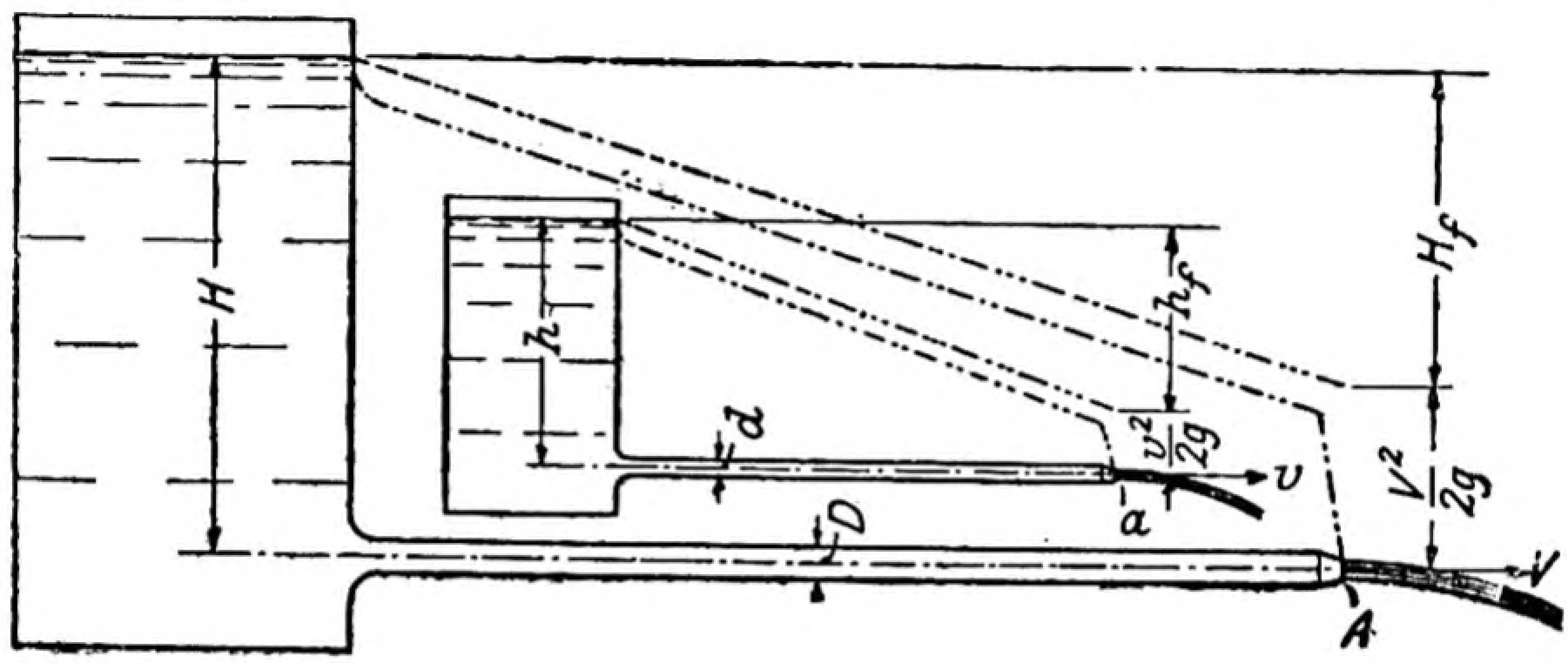

FIG. 77.—Demonstration of scale effect.

geometrically similar heads. Since both v and d are individually smaller than V and D, then R_n for the small pipe is less than R_n for the large pipe, f_o is therefore greater than f, $\frac{h_f}{h}$ is greater than $\frac{H_f}{H}$, consequently $\frac{v^2}{h}$ is smaller than $\frac{V^2}{H}$. The lack of dynamical similarity is made visible to the eye by the disparity between the virtual slopes in the two pipes.

In such cases the ratio $\frac{Q}{q} = \frac{H^{\frac{5}{2}}}{h^{\frac{5}{2}}}$ (§ 51) is not realised: the discrepancy is spoken of as the *scale effect*. The scale effect, which generally manifests itself in a lowering of the value of the coefficient of discharge C_d for a small passage as compared with the value for a large one, will evidently be most serious in forms of opening that are relatively long and narrow.[41] **(Example 33.)**

Naturally, a scale effect may also arise if in rough-walled passages the relative roughness is not maintained uniform at corresponding points in the two systems. But to say that identical Reynolds numbers and identical Froude numbers cannot simultaneously exist is not an invariable truth. The

foregoing reasoning on which such a supposition was based ignored the possibility of varying the *kinematic viscosity* of the fluid and controlling the Reynolds number, and therefore the resistance, in that way. By using different fluids in the two systems under comparison, the scale effect may be eliminated. This expedient has highly important practical advantages (§ 332).

96. Flow through Irregular Passages, i.e. Granular Material. The method illustrated in Fig. 75 of plotting total relative hydraulic resistance against Reynolds number becomes particularly useful when very complicated passages are concerned. Such are the irregular passages or pores through which a liquid seeps when traversing a bed of sand as in a filter or as in the porous subsoil surrounding a well.[42] We can hardly begin to try to measure the length and diameter of each of these multitudinous waterways, or to ask with any confidence how existing flow formulæ should be applied to such discouraging conditions. A more reasonable line of approach is to concern ourselves with the bulk flow only, and to regard the grains which occupy the gross area of waterway as enormously increasing the pipe friction. Thus, if in Fig. 78 (i) a length l of the passage of diameter d is filled with the granular material, the remainder of the passage remaining unobstructed, then if v is the mean velocity in the *unobstructed* passage we might express the energy loss h by an expression analogous to the Darcy quadratic equation 5-7, § 68. In place of the pipe coefficient f, we should use another non-dimensional coefficient f_p. What would the value of this new coefficient depend upon? It would certainly depend largely upon the size and character of the grains; for the actual resistance of the passage walls might in comparison be negligible. The smaller the grains, the more angular their shape, and the more closely they were packed together, the greater would be the total resistance or head loss h.

Porosity and its influence. Considering for the moment uniform spherical grains of diameter δ, it can quickly be shown how the manner of packing will affect the form of the intervening passages through which the liquid actually flows. The influence of the *shape* of the grains can be studied later. If we imagine the spheres to be packed by hand, one by one, then two limiting geometrical arrangements are possible; they can

be expressed by the use of a *porosity* factor α, which is the ratio

$$\alpha = \frac{V_v}{V_t} = \frac{\text{total volume of voids or interstices}}{\text{total volume into which the grains are packed}}.$$

Thus, if in Fig. 78 (i) there were n spherical grains of diameter δ, then V_t would have the value $\frac{\pi}{4}d^2l$, and V_v would have the value $\frac{\pi}{4}d^2l - n\frac{\pi\delta^3}{6}$. Straightforward geometry shows that in

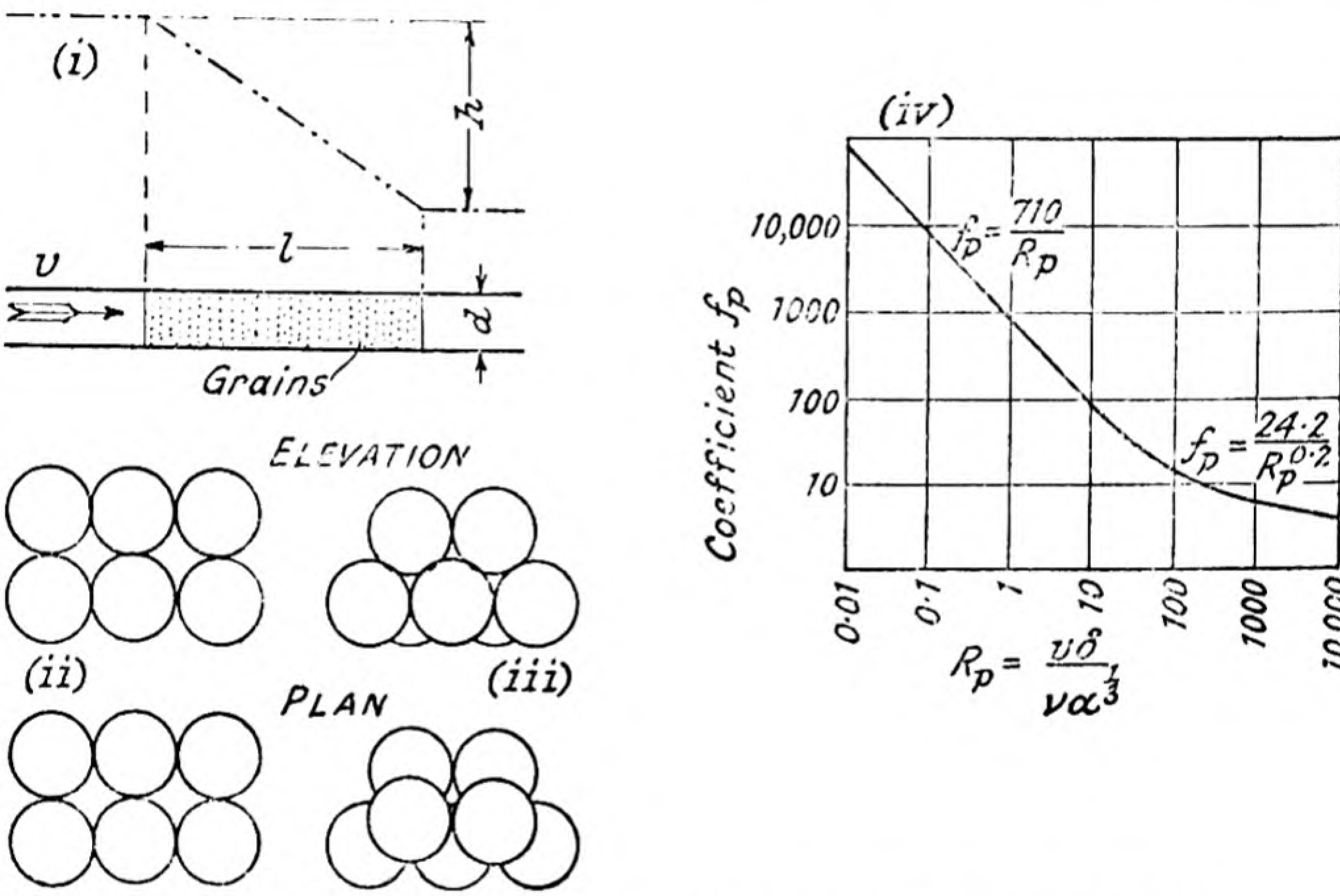

FIG. 78.—Flow through assembly of uniform spherical grains.

the rectangular system of packing, (ii), in which each sphere touches six other spheres, the porosity is 0·47; whereas in the triangular pattern, (iii), where each sphere touches twelve others, the porosity is 0·23. The porosity found in an actual assemblage of spherical grains, in which the individual constituents are jammed one against the other in all manner of random ways, will depend upon how the container was tapped or shaken as the grains were shovelled in. We know that the value of α will lie somewhere between 0·47 and 0·23, but we have no means of calculating it. On the other hand, we can very easily *measure* the porosity, e.g. by finding out how much water will be needed to fill the pores.

The importance of this information lies here: it tells us the aggregate volume of all the small and intricate passages through which the liquid seeps; or in other words, the volume V_v represents the combined length of all the passages multiplied by their mean cross-sectional area. Thus the porosity can be regarded as a link, even if an indefinite one, between the known velocity v in the unobstructed waterway, Fig. 78 (i), and the unknown velocity through the interstices which we can be sure is what finally determines the head loss h. The exact nature of the link must depend upon experimental evidence, but we can see at once that if v, l, d, and δ are kept unchanged, then a diminution of α will *reduce* the net area for flow, and therefore increase the head loss. Two alternative methods of computing the head loss, based upon different interpretations of the porosity factor, are summarised in the following paragraphs.

97. Quadratic Formulæ for Granular Material. (i) This treatment, being based on the velocity head of the liquid in the unobstructed passage, has affinities with corresponding pipe formulæ, with the estimation of coefficient of loss (§ 85), and with the conception of the drag coefficient of immersed solids (§ 127). Re-writing formula 5-7 in the form

$$h = \frac{f_p l}{\delta \alpha^{\frac{5}{3}}} \cdot \frac{v^2}{2g} \qquad . \quad . \quad . \quad (5\text{-}15)$$

we are then enabled to calculate, from known experimental values of h, l, v, δ, and α (Fig. 78), the corresponding values of the non-dimensional coefficient f_p. Similarly, the value of the Reynolds *permeability number* $R_p = \dfrac{v\delta}{\nu\alpha^{\frac{1}{3}}}$ may be computed. Plotting the one set of values against the other, the points are found to lie on a single curve as reproduced in the diagram (iv). The agreement holds good for spheres ranging in diameter from 0·04 inch to 0·62 inch, and for viscosities from 0·01 poises to 1·8 poises.[43] It is this curve, analogous to those plotted in Fig. 75, that was referred to at the beginning of § 96; its likeness to the curve representing the resistance of isolated spheres (Fig. 114) is very marked.

For values of R_p below about 5, the graph is a straight line which is the equivalent of the equation $f_p = \dfrac{710}{R_p}$: the

relationship is the counterpart of the equation $f = \dfrac{16}{R_n}$, which results from applying equation 5-7 to laminar flow conditions, showing that within this range the flow through the pores of the granular mass is *viscous*. For values of R_p above 500 the graph has a smaller slope; its equation $f_p = \dfrac{24 \cdot 2}{R_p^{0 \cdot 2}}$ at once invites comparison with the relationship $f = \dfrac{0 \cdot 08}{R_n^{0 \cdot 25}}$ for turbulent flow in smooth pipes (§ 69).

To adapt the curve, Fig. 78 (iv), to non-spherical grains, e.g. graded sand grains of fairly uniform size, the values of f_p should be multiplied by a "shape factor" varying from 1·2 to 1·9, and depending upon the angularity and proportions of the particles.

(ii) Another quadratic equation is

$$h = f_r \cdot \frac{l}{\delta} \cdot \frac{v^2}{g} \qquad \ldots \qquad (5\text{-}16)$$

where the coefficient f_r can be given a value which takes into account (*a*) porosity, (*b*) the effect of the walls of the container, (*c*) the shape of the particles, (*d*) variations in particle size if the material is non-homogeneous.[44]

For the simplest case of uniform spherical grains, of diameter δ, disposed to give a porosity factor of 0·4, then the non-dimensional coefficient f_r is found to have the value

$$f_r = \frac{1000}{R_e} + \frac{60}{\sqrt{R_e}} + 12$$

where R_e is a type of Reynolds number represented by $\dfrac{v\delta}{\nu}$. This treatment gives values for the head loss h which do not necessarily accord exactly with those derived from equation 5-15. There is a significant reason for this discrepancy. All equations which purport to describe the flow through granular material cannot do more than represent statistical probabilities: they show what is likely to happen, not what must inevitably happen. Although in two comparable beds of material the porosity may be the same, yet the grains may have fortuitously disposed themselves so that in one bed the flowing liquid has an

easier path than in the other. The corresponding variations in the coefficient f_r may be most marked within the range of Reynolds number $R_e = 1$ to $R_e = 1500$, especially if the grains are of random shape, i.e. non-spherical.

98. Linear Permeability Equations. If the flow through the pores is viscous, viz. if the Reynolds permeability number R_p is less than about 5 (§ 97), then we can write down the most elementary form of flow equation :

$$v = k_o \cdot \frac{h}{l} \quad . \quad . \quad . \quad (5\text{-}17)$$

where k_o is a *permeability factor* valid only for a given size of grain packed in a specified manner, and for a stated kind of liquid. It will be observed that the factor k_o has the dimensions $\frac{L}{T}$, viz. it represents a velocity.

A re-arrangement that takes into account all the variables except shape is

$$h = \frac{k'\nu l v}{g\delta^2} \cdot \frac{(1-\alpha)^2}{\alpha^3} \quad . \quad . \quad (5\text{-}18)$$

in which the coefficient k' is now *non-dimensional.* When applied to graded sand grains of diameter 1·0 to 0·2 mm., this formula gave a value of k' of about 360. It is instructive to compare the formula with the modified form of equation 5-5, § 65, $h = \frac{32\nu l v}{gd^2}$, which described laminar flow through parallel circular pipes. The method of interpretation of porosity utilised in formula 5-18 is attributed to J. Kozeny.[45] With suitable correction, it can be applied to the extremely fine passages in masses of clay, and also to granular material of varying grain diameter.

(The various terms chosen to represent the effect of porosity, viz. α , $\alpha^{\frac{1}{3}}$, $\frac{(1-\alpha)^2}{\alpha^3}$, all have some analytical justification ; further observations alone will show which have the soundest experimental support.)

CHAPTER VI

FLOW ALONG OPEN CHANNELS

99. Transition from Closed to Open Conduits. The transition from pipe flow to channel flow is analogous to the change from orifice conditions to weir conditions (§ 53). It is illustrated in Fig. 79. So long as the surface level in the downstream reservoir is kept above the top of the passage, (i), then the laws applicable to closed conduits will prevail. But if the level is lowered sufficiently, (ii), then a free liquid surface exposed to the atmosphere will form throughout the passage. The flow will then be typical of the familiar motion of water in natural streams and rivers and in artificial canals.[46] However, as the submerged part of the pipe perimeter has seemingly been very little affected, we can hardly believe that the general characteristics of flow have been fundamentally altered. On the contrary, it seems likely that the reasoning applied to closed passages in Chapter V will, when appropriately modified, be serviceable here also. What are these emendations?

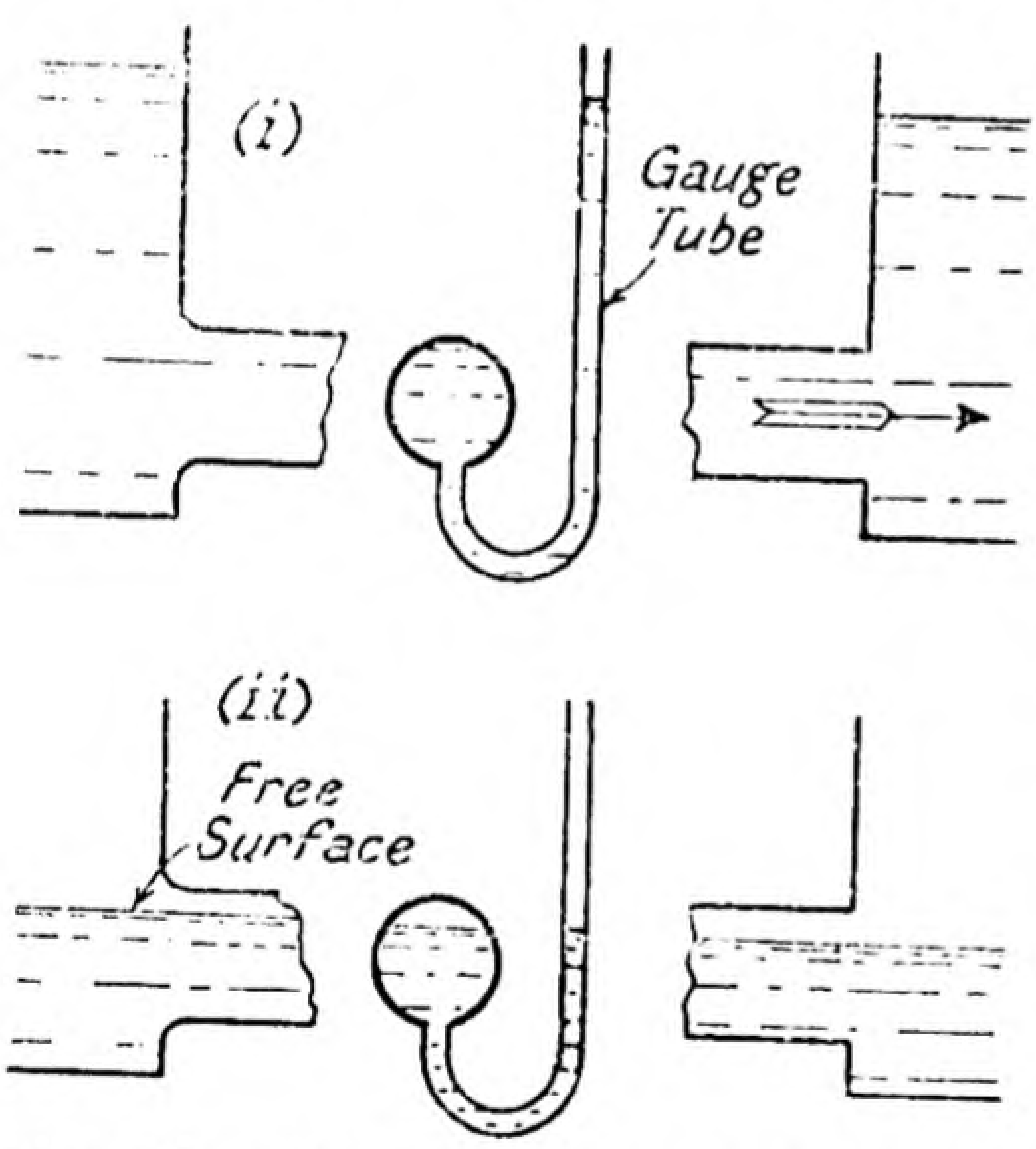

FIG. 79.—Circular passage acting as (i) closed conduit; (ii) open channel.

(i) No longer may we say that the virtual slope or slope of the hydraulic gradient has no basic relationship to the slope of the channel bed. As Fig. 79 (ii) clearly shows, the water surface itself serves as the hydraulic gradient, and the slope of this surface must be closely linked with the bed-slope; indeed, when uniform flow prevails the two slopes are invariably identical.

(ii) In a circular closed passage the shear stress τ_0 or wall resistance per unit area at a given cross-section is uniform around the entire periphery (§ 67). There are two reasons why that cannot be so in an open channel. Across the whole of the free liquid surface there can manifestly be no shear stress whatever (unless the wind is powerful enough to generate one); and even at the wetted surface of rectangular and polygonal channels, it is found that the shear stress is less at the corners than it is at the middle of the straight sides. Associated with this lack of uniformity is a type of transverse velocity component which may cause whole masses of liquid to move along with a slow helical or cork-screw motion.

(iii) The distribution of the turbulent velocity components will be less regular than was found in pipe flow, § 72. For example, only two-dimensional turbulence can occur at the water surface; if there were a third or vertical component in this region we should see the water dancing up and down.

(iv) When applying the Reynolds criterion, § 64, to channel flow, an actual dimension such as width or depth would not fairly serve as the representative term expressing length. Instead, we must use the hydraulic mean depth m (§ 68 (ii)), inserting it in the expression $R_{nc} = \frac{vm}{\nu}$, where R_{nc} may be called the Reynolds channel number.

Other differences between pipe and channel flow will become manifest during the course of this chapter.

100. Types of Channel Flow. *Stream-line and turbulent.* Although true stream-line flow, § 64, is known to exist in open channels, it can only be detected at all with the help of every refinement of laboratory technique.[47] So long as the Reynolds channel number R_{nc} is less than about 300, then it seems highly probable that the head loss is directly proportional to the mean

velocity, just as it is in a circular pipe (equation 5-5, § 65). But such conditions are altogether outside the experience of the practising engineer, who will be concerned exclusively with *turbulent* channel flow. This may be said to begin effectively when R_{nc} exceeds 5000; and even a number as low as this can only be realised in such a tiny channel, a few inches in width, that it would seem to be far beneath the notice of an engineer accustomed to think in terms of a Thames or a Potomac. Although, therefore, no further reference will be made in this book to viscous flow in channels, it is to be remembered that this type might occur in the scale models that are as valuable for elucidating problems of channel flow as they are for the conditions described in §§ 51 and 95.

Uniform and non-uniform. An extension of the definition of uniform flow offered in § 29 (i) is now to be adopted. In a

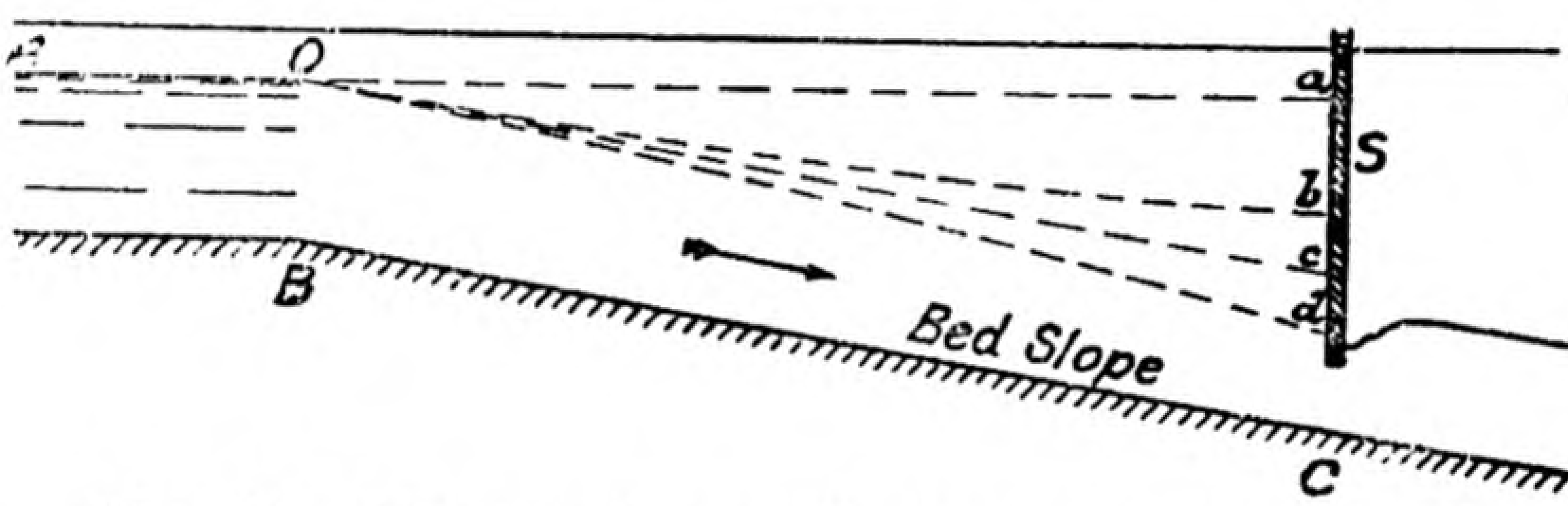

FIG. 80.—Water surface profiles in rectangular channel.

channel the flow is said to be uniform if the *mean* local velocity u, at corresponding points in the cross-sections under comparison is unvarying; the turbulent components are disregarded as they were in § 30. Whereas uniform or non-uniform flow in this sense can be imposed at will on the liquid in a closed passage by controlling the pipe cross-section, e.g. by making the pipe parallel or tapered, the pertinent factor in a channel is the relation between depth and discharge.

Considering a channel BC of uniform width and bed-slope leading from a reservoir in which the water level AO (Fig. 80) is kept steady, it is easy to see that the water surface slope in the channel can be modified at will by regulating the sluice S at the outlet or "tail." When the sluice is shut there will be no flow along the channel and its surface slope will be zero (Oa). A small sluice opening will allow a small discharge, the characteristics of flow being a greater depth at the tail

than at the head of the waterway, and a curved water surface concave upwards (*Ob*).

Further progressive opening of the sluice will eventually bring about a critical stage at which the water surface *Oc* is straight and parallel with the bed *BC*, the water depth is uniform throughout, and the cross-sectional area and mean velocity v are the same at all stations in the channel. We then say that *uniform flow* is in operation. If the tail-water level is still further drawn down by additional opening of the sluice, the water surface profile again becomes curved (*Od*), but now the convexity is upwards. The types of flow represented by *Ob* and *Od* in Fig. 80 are manifestly *non-uniform.*

Although uniform flow will only occur if it is specifically made to occur, or if the channel is so long that the flow automatically settles down to uniform conditions, it is nevertheless usually assumed, unless otherwise stated, that the flow in open streams is uniform.[48]

(*Note.*—For the sake of clarity, the vertical scale of diagrams such as Fig. 80 and its successors is *greatly exaggerated.* If the bed-slope and water-slope were given their natural or true inclinations, say 1/5000, it would be quite impossible to distinguish the corresponding lines from horizontal straight lines.)

101. Uniform Flow. Adopting the conception of surface friction formulated in § 67, and using the symbols of § 68 (ii),

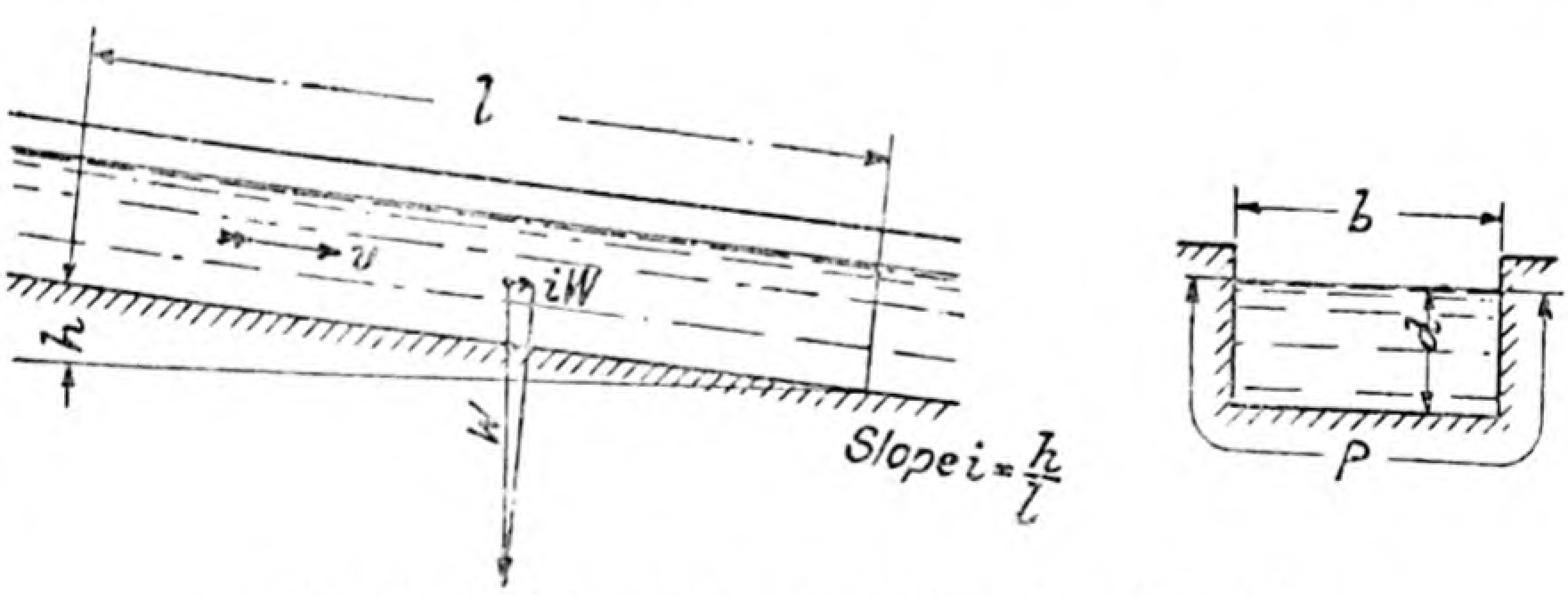

FIG. 81.—Uniform flow in rectangular channel.

we can say: In a length l of a rectangular channel of uniform slope i and wetted perimeter P (Fig. 81), in which the mean velocity of the water is v, the area in contact with the water is Pl, and consequently the frictional resistance $= F \, . \, P \, . \, l \, . \, v^n$. The available force for overcoming this resistance is the component, parallel with the bed of the channel, of the total

weight W of the water contained in length l, viz. iW. Equating, $iW = F \,.\, P \,.\, l \,.\, v^n$, or $i \,.\, wAl = F \,.\, P \,.\, l \,.\, v^n$, whence

$$v^n = \frac{w}{F} \cdot \frac{A}{P} \cdot i.$$

Assuming $n = 2$, and writing $\sqrt{\frac{w}{F}} = C$, the Chezy equation is reached,

$$v = C\sqrt{mi} \quad . \quad . \quad . \qquad \textbf{(6-1)}$$

This treatment of flow in bulk, and its representation in Fig. 81, gives a reassuring sense of reality to the conception of wall friction. If we like to compare the whole mass of water sliding down the channel with the hull of a ship sliding down the launching ways, a further comparison suggests itself. The frictional resistance between the moving and the fixed surfaces is manifested by the smoke that arises from the ways. Through the medium of viscous shear, heat is likewise generated as the liquid rubs against the sides of the channel ; but it is virtually impossible to measure the resulting extremely small temperature rise of the liquid.

The discharge Q flowing down the channel $= Av =$ (in a rectangular channel) $bdv = bdC\sqrt{\frac{bd}{b + 2d} \cdot i}$. If the depth d is small compared with the width b, it is seen that Q varies approximately as $d^{\frac{3}{2}}$. Thus a channel resembles a rectangular weir in this respect, that an increase in depth or in head not only increases the velocity of the water but also the area of the waterway, hence the relationship $Q = K$ (depth)$^{\frac{3}{2}}$ common to both. But on the other hand, orifices and pipes have an invariable cross-section, and so the quantity discharged by either depends more or less accurately on (head)$^{\frac{1}{2}}$. (**Example 44.**)

102. Resistance Coefficients for Channels. Because of the much greater experimental difficulties in evaluating the flow coefficients for channels as compared with pipes,[49] it has not yet been found possible to present the relevant information with the precision suggested by Figs. 51 and 53. Nevertheless, it is convenient to retain the coefficient f as a measure of performance for open as well as for closed passages. Remembering that in a closed circular passage, $m = d/4$, we may adapt the formula 5-7 for present purposes by rewriting it $h = \frac{f \,.\, l}{m} \cdot \frac{v^2}{2g}$. For hydraulically *smooth* channels, the relationship between the coefficient f and the Reynolds channel number R_{nc} may be

expected to have the tendencies described in § 69. For a range of $R_{nc} = 5000 - 10{,}000$, it has been verified [47] that

$$f = 0{\cdot}023 R_{nc}^{-0{\cdot}15}.$$

For *rough* channels, it seems likely that rough-law conditions will apply. So long as the Reynolds roughness number $= \dfrac{v_f k}{\nu}$ is greater than 60 (§§ 79-81), then the value of the coefficient depends only on relative roughness and not at all on velocity and viscosity.

The connection between f and the Chezy coefficient C has already been defined, § 68 (ii); it is $f = \dfrac{2g}{C^2}$. The various ways of expressing the shear force velocity or friction velocity, § 78, are also instructive in this connection:

$$v_f \text{ or } v_* = \sqrt{\frac{\tau_0}{\rho}} = v\sqrt{\frac{f}{2}} = \sqrt{gmi} = v\frac{\sqrt{g}}{C}.$$

There still remains the question of the *shape* of the cross-section. Will this have any effect on the flow coefficient? An infinite number of channels—curved, rectangular, or trapezoidal in section—might be made having identical values of m and i and roughness k; would a single value of C or f suit them all equally well? Evidence is uncertain here. If there is any difference, it may be that semi-circular channels have a slightly smaller resistance—a lower f and a higher C—than other shapes have in comparable conditions.

The empirical formulæ favoured by engineers for evaluating the Chezy coefficient or its equivalent in specified circumstances are summarised in Chapter X.

103. Velocity Distribution in Channels. In a very shallow, wide rectangular channel the variations of shear stress τ_0 mentioned in § 99 (ii) would presumably be very small if we studied only the central part of the cross-section. We might therefore expect that the velocity profile in this region would be of the form expressed in equation 5-10, § 71. But in normal streams of finite (width : depth) ratio we are left to seek guidance from various empirical rules.[50] The distribution in a given instance is represented graphically either by a set of velocity profiles of which one is reproduced in Fig. 82 (i), or by a series

of *isovels* or lines of equal velocity such as are shown in Fig. 82 (ii). If, along a vertical line AA in the transverse cross-section of the stream (ii), we measure the velocity at a number of points and plot corresponding offsets horizontally, then the velocity profile (i) results; as the position of the vertical AA is shifted, so will the shape of the velocity-distribution curve alter. In the diagram (i) the local velocity u is expressed in terms of the mean velocity *along the vertical*, v_m, which will only by chance have the same value as the mean velocity *over the whole section*, v. In Fig. 82 (ii) the isovels are related to the *maximum* local velocity, u_m.

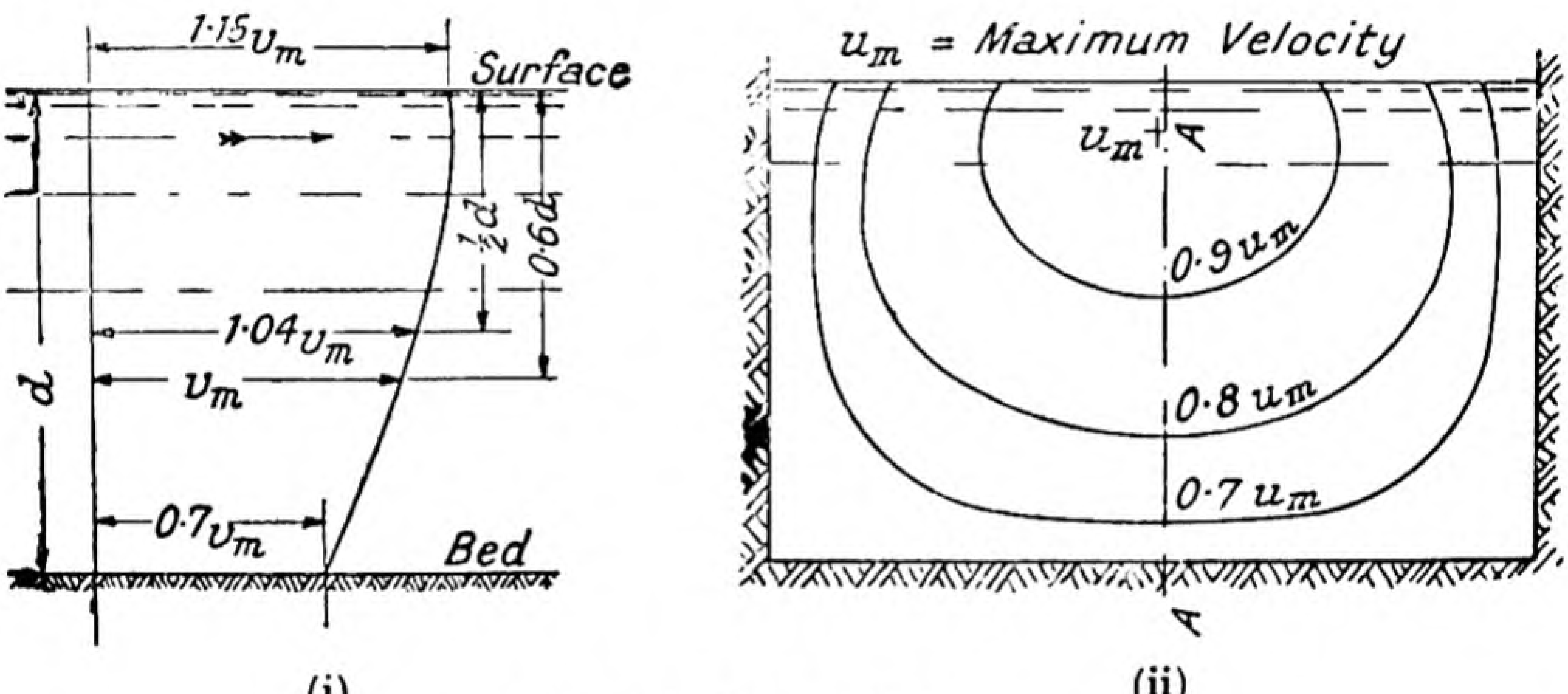

FIG. 82.—{(i) Velocity profile / (ii) Isovels} in open channel.

Opinion is fairly unanimous on the following questions :—

(*a*) *Surface velocity* u_s. The ratio u_s/v_m, which in diagram (i) is given an average value of 1·15, may vary within limits of at least 1·1 to 1·2. But it is significant that, for a given absolute roughness of channel bed, the ratio tends to diminish as the channel depth increases; whereas for a stipulated depth, the value increases as the roughness increases. In the one case, the profile becomes flatter; in the other, it becomes more curved. These tendencies agree exactly with those described in § 71 and illustrated in Fig. 54.

(*b*) *Position of filament of maximum velocity.* Only in channels that are relatively very wide and shallow is the maximum local velocity u_m found to occur at the highest point of the vertical, i.e. at the free surface. As the width : depth ratio b/d grows progressively less, so does the point at which the maximum velocity is registered gradually sink below the

surface, until when the channel is deeper than it is wide the point may be a distance $d/4$ from the surface.

(c) *Position of mean filament.* At one particular point on the velocity profile the local velocity u must evidently be equal to the mean velocity v_m. The position of this point has considerable practical importance in stream gauging; the distance $0{\cdot}6d$ from the surface, Fig. 82 (i), is found to apply with some degree of consistency. But a more reliable relationship is $v_m = \dfrac{u_{0\cdot2} + u_{0\cdot8}}{2}$ where $u_{0\cdot2}$ and $u_{0\cdot8}$ are the local velocities at distances respectively $0{\cdot}2d$ and $0{\cdot}8d$ below the water surface.

(d) In regard to the *bottom velocity* recorded in the diagram as $0{\cdot}7v_m$, this is to be looked upon as a nominal figure only; it is the velocity at a point as near to the bottom as we can get, using normal measuring equipment (§ 381). We can be sure that the water actually touching the channel bed is moving very much more slowly than this; indeed, very careful laboratory observations prove that in these artificial conditions the velocity profile terminates at the zero point just as it does in the ideal diagram, Fig. 59. There may be a boundary layer in a channel just as there is in a pipe.

104. Non-uniform Flow. Non-uniform flow in an open channel having uniform bed-slope i is invariably characterised

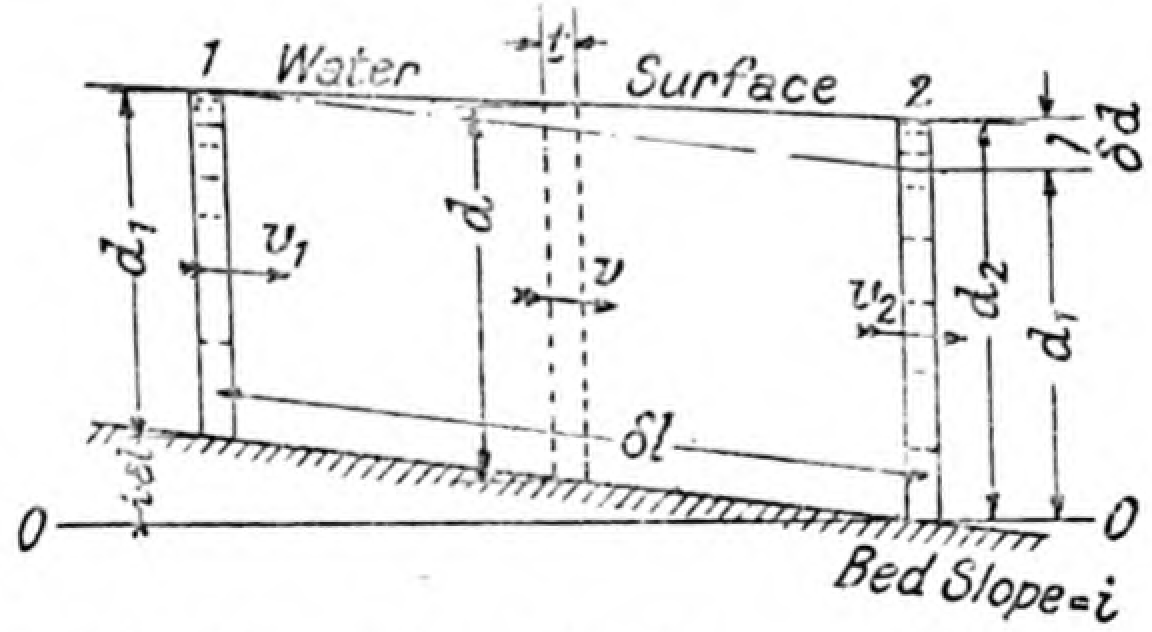

Fig. 83.—Non-uniform flow in rectangular channel.

by a curved water surface profile. By choosing a sufficiently short length of the channel, however, such as δl in Fig. 83, it becomes permissible to assume that the water surface between points 1 and 2 is straight. Due to the increase in depth δd, the mean velocity v_2 is less than v_1; if the channel is rectangular in cross-section, the average velocity v, at a station midway

between 1 and 2, at which the depth is d, will be $v_1 . \frac{d_1}{d}$ or $v_2 . \frac{d_2}{d}$, from which

$$v_1 = v . \left(\frac{d}{d - \frac{\delta d}{2}}\right), \quad \text{and} \quad v_2 = v\left(\frac{d}{d + \frac{\delta d}{2}}\right).$$

Let the cross-section of the channel, and its wetted perimeter, at the station midway between 1 and 2 be A and P respectively, F being the coefficient of surface friction (§ 101).

We proceed to examine the energy changes incurred by a thin transverse slice or lamina of water, of average thickness t, as it travels from point 1 to point 2; if t is made equal to $\frac{1}{wA}$, the lamina will contain unit weight of water. At point 1 the total energy of the lamina is $i . \delta l + d_1 + \frac{v_1^2}{2g}$; at point 2 it is $d_2 + \frac{v_2^2}{2g}$ (taking the plane OO as the datum plane). The energy loss is thus

$$i . \delta l + d_1 - d_2 + \frac{v_1^2}{2g} - \frac{v_2^2}{2g}.$$

Substituting the values derived above for v_1 and v_2, we have energy loss

$$= i . \delta l - \delta d + \frac{v^2}{2g}\left[\left(\frac{d}{d - \frac{\delta d}{2}}\right)^2 - \left(\frac{d}{d + \frac{\delta d}{2}}\right)^2\right]$$

$$= i . \delta l - \delta d + \frac{v^2}{gd} . \delta d \quad . \quad . \quad . \quad . \quad . \quad . \quad \text{(I)}$$

since δd is very small compared with d.

Now the average frictional resistance between the channel bed and the edges of the lamina is $F . P . t . v^n = F . P . \frac{1}{wA} . v^n$. The energy absorbed in overcoming this resistance as the lamina moves through a distance δl is

$$\frac{F}{w} . \frac{P}{A} v^n \delta l \quad . \quad . \quad . \quad . \quad \text{(II)}$$

Equating I and II, assuming $n = 2$, and writing $\frac{w}{F} = C^2$ as in § 101, we have

$$i\,.\,\delta l - \delta d + \frac{v^2}{gd}\,.\,\delta d = \frac{F}{w}\,.\,\frac{P}{A}\,.\,v^2\delta l = \frac{v^2}{C^2 m}\,.\,\delta l$$

or
$$i\,.\,\delta l - \frac{v^2}{C^2 m}\,.\,\delta l = \delta d\left(1 - \frac{v^2}{gd}\right),$$

whence
$$\frac{\delta d}{\delta l} = \frac{i - \frac{v^2}{C^2 m}}{1 - \frac{v^2}{gd}} \quad . \quad . \quad . \quad (6\text{-}2)$$

which is the fundamental equation governing non-uniform flow.

105. Interpretation of Non-uniform Flow Equation. The importance of equation 6-2 lies in the simplicity with which it expresses, at any selected station in a stream, the slope of the water surface *with respect to the bed*, in terms of the water depth and the mean velocity. Thus, knowing the depth and cross-section of the waterway at any point, and the discharge flowing along it, the equation shows us at once whether or not the flow is uniform, and if it is not, whether the water depth diminishes or increases in a downstream direction.

(Example 45.)

(i) If the value of $\frac{\delta d}{\delta l}$ is found to be zero, the flow must be *uniform*, for if the water surface has zero slope with respect to the bed, then the depth, cross-section, velocity, etc., must remain constant. For $\left(\frac{\delta d}{\delta l}\right)$ to be zero, $\left(i - \frac{v^2}{C^2 m}\right)$ must be zero, or $v = C\sqrt{mi}$. Here is an alternative derivation of the Chezy equation.

(ii) If the numerator of equation 6-2 has a positive value, then the water depth will increase continuously as points further and further downstream are chosen, and the longitudinal profile of the water surface will be a curve, concave upwards, to which the name *backwater curve* is given (§ 184).

(iii) If the numerator of the equation is negative, then the water depth diminishes in a downstream direction, the surface curve being now convex upwards and being styled a *falling surface* curve or a *drop-down* curve (§ 186).

(iv) So far, it has been assumed that the denominator $\left(1 - \frac{v^2}{gd}\right)$ of the equation 6-2 has had a positive value. Should it by any chance have the value zero, corresponding with a value of $v = \sqrt{gd}$, then $\frac{\delta d}{\delta l}$ will have the seemingly anomalous values of $+\infty$ or $-\infty$, according to the sign of the numerator: that is, the water surface will be vertical.

(v) If both numerator and denominator have negative values, then the quotient $(\delta d / \delta l)$ will have a positive value.

The following paragraphs show how these diverse results are capable of reasonable explanation.

106. Critical Depth in a Flowing Stream. If a fixed discharge Q be passed along a rectangular channel of width b, the mean velocity v and depth d at any given point must be linked up by the equation $Q = bdv$; or putting $q = \frac{Q}{b} =$ *discharge per unit width*, then $v = \frac{q}{d}$. The total energy per unit weight of liquid (referred to the channel bed as datum) is thus

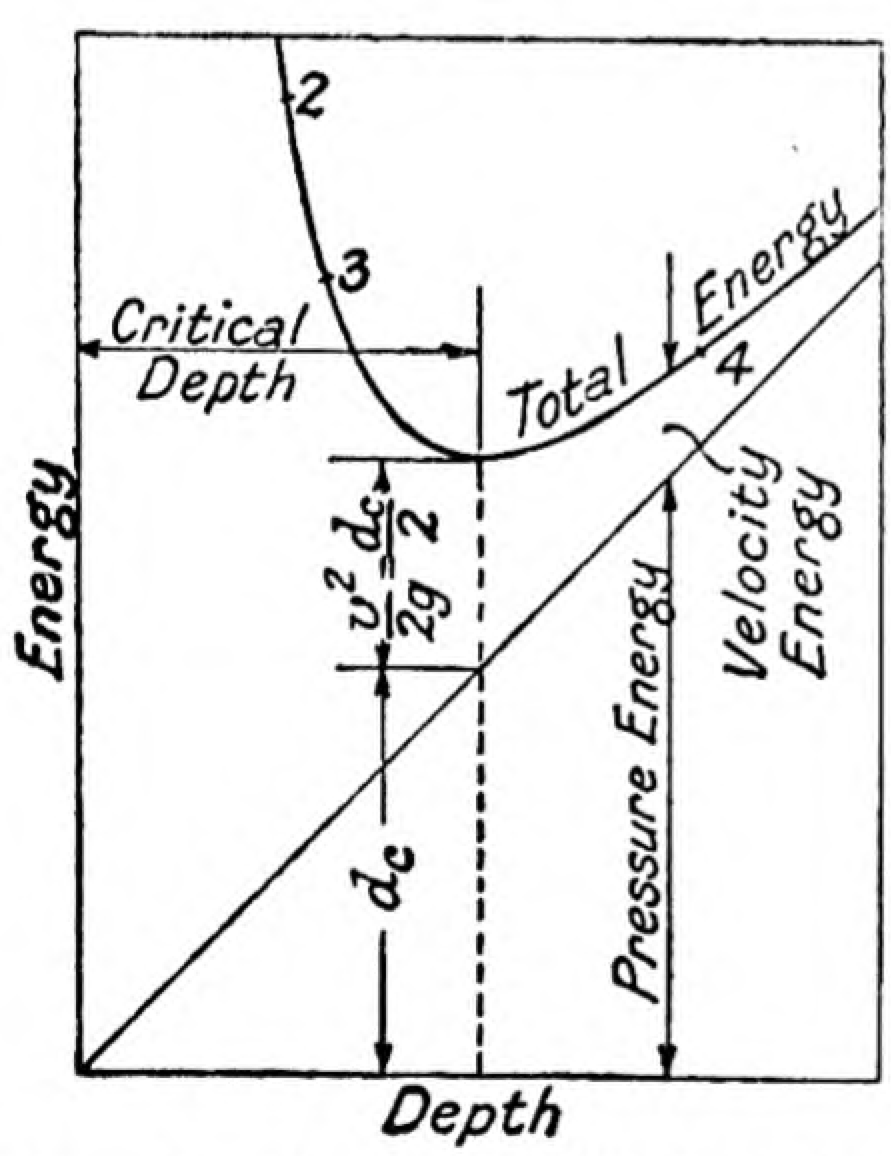

FIG. 84.—Energy plotted against stream depth.

$$\left(d + \frac{v^2}{2g}\right) = d + \frac{q^2}{d^2 \cdot 2g}.$$

If the values of total energy so calculated are plotted against depth, a curve of the sort reproduced in Fig. 84 is obtained; it shows that the energy of the water is at a minimum when the velocity energy is one-half of the pressure energy, viz. when $\frac{v^2}{2g} = \frac{d}{2}$ or when $v = \sqrt{gd}$. The depth $d_c = \sqrt[3]{\frac{q^2}{g}}$ at which this occurs is called the *critical depth*. It is the depth at which the Froude number, § 52, attains the value unity.

The conditions are critical in this sense, that water flowing

along a channel cannot change its depth from below to above the critical value, or vice versa, without its water surface passing through some state of discontinuity—some break, drop, or jump—which is the visible expression of the values $\frac{\delta d}{\delta l} = \frac{+\infty}{-\infty}$ referred to in § 105 above; for it will be observed that these values are reached just when the water reaches the critical depth $d_c = \frac{v^2}{g}$.

107. "Shooting" Flow. When the depth of a stream is below the critical value, the flow is sometimes described as "*shooting*" flow; when the depth is above the critical value, the flow is called "*streaming*" flow. Fig. 85 shows the nature of the discontinuities that are necessary to change the flow from one kind to another. Here we see a rectangular channel with a horizontal bed, provided with a sluice gate S. At section 1 the water "streams" along quite gently, the smallness of the velocity energy h_{v1} relative to the depth d_1 indicating that d_1 is well above the critical value.

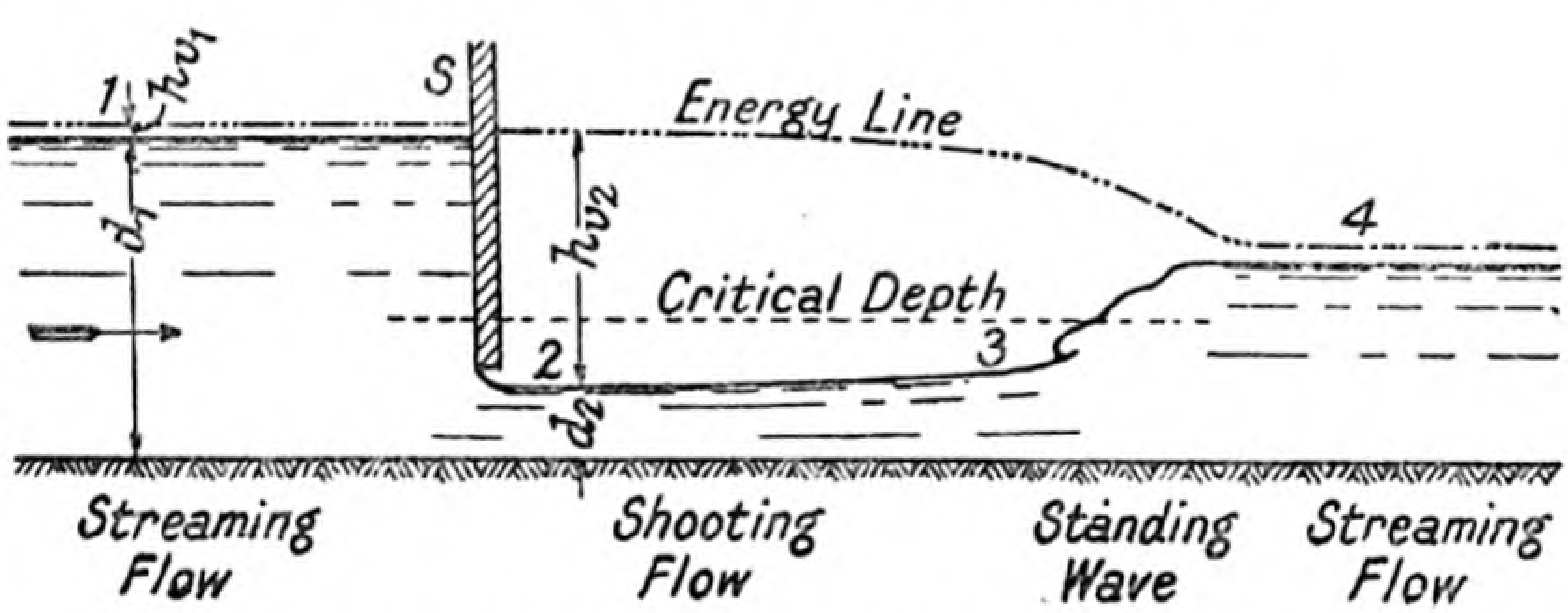

FIG. 85.—Changes of state during flow beneath a sluice gate.

In passing under the sluice gate, most of the pressure energy of the water is converted into velocity energy, so that h_{v2} is considerably greater than $\frac{1}{2}d_2$. The flow is now certainly "shooting" flow, and the appearance of the water as it issues at high velocity beneath the gate undoubtedly justifies the title. So far the energy loss sustained by the water has been trivial; but the high velocity with which the stream now passes down the channel from point 2 to point 3 imposes serious friction losses on it, as indicated by the fall of the energy line in Fig. 85. The corresponding part 2-3 of the curve (Fig. 84), moreover, shows that a

diminution of energy must be accompanied by an *increase* in depth; the fact that the water surface now rises is also apparent from § 105 (v), for since both numerator and denominator of the basic equation are under present conditions negative in value, the fraction has a positive value. Inspection of equation [6-2] further makes it clear that as the depth increases, the value of $\frac{\delta d}{\delta l}$ also increases and rapidly approaches the value $+\infty$.

108. The Standing Wave. The appearance of the water surface corresponding to the value $\frac{\delta d}{\delta l} = +\infty$ is suggested in Fig. 85 and is depicted in the photograph (Fig. 184). The confused, turbulent region in which the water surface suddenly rises is called the *standing wave* or *hydraulic jump;* such a discontinuity is essential, in the conditions here assumed, in order to permit the flow to change again from the "shooting" regime to the "streaming" regime. The total energy of the water at 4 (Figs. 84 and 85) being less than it is at 3, the water disposes of its surplus energy by initiating violent eddying motion just as it does at a sudden enlargement in a pipe (§ 87 (*a*)). The maximum *height* of a standing wave, viz. the maximum increase in depth of the stream in which it occurs, may be calculated by the method explained in § 137.

109. "Streaming" Flow. Normally the water depth in rivers and canals is very much above the critical depth—

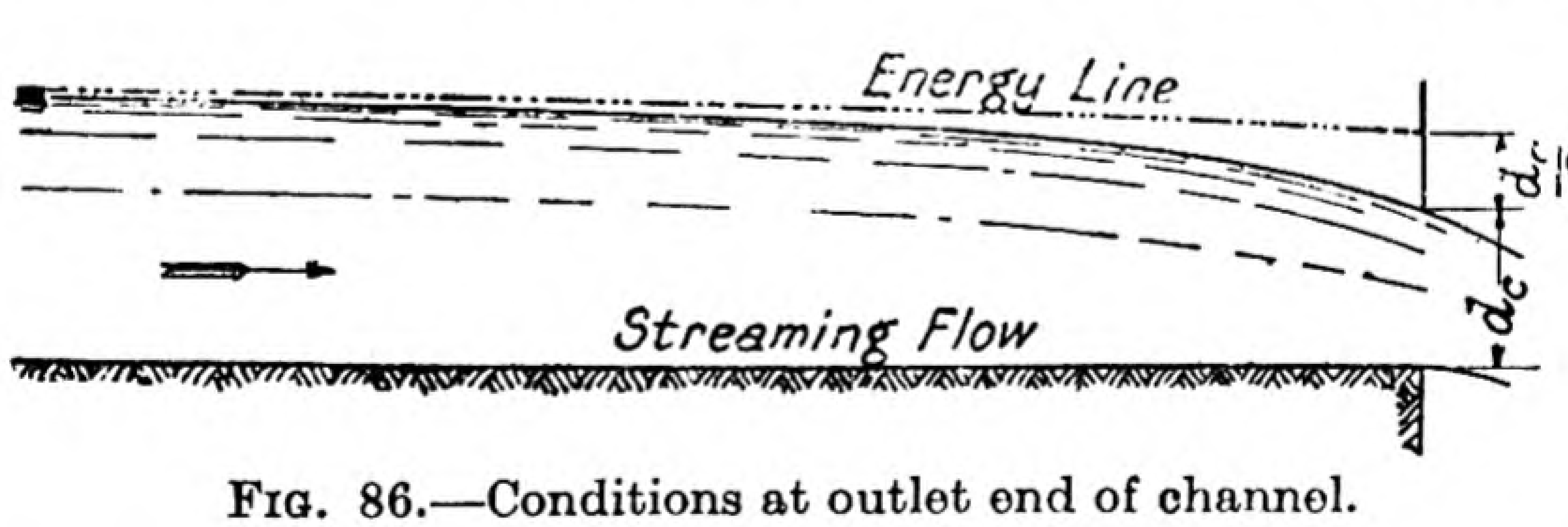

FIG. 86.—Conditions at outlet end of channel.

streaming flow is the rule, and shooting flow is the exception. In the case of a uniform rectangular channel with a horizontal bed, discharging freely into the atmosphere at the downstream end (Fig. 86), it is impossible for the water to be drawn down to the critical depth before it reaches the downstream end. As the water continually parts with its energy to overcome

friction losses, it must carefully husband its store so that it only arrives at the condition of minimum energy, i.e. it only attains the critical depth, at the end of its journey.

Consideration of equation 6-2, § 104, shows that under present conditions the value of $\frac{\delta d}{\delta l}$ is negative, and is continually increasing ; the water slope thus becomes progressively steeper, and as the depth approaches the critical depth at the outlet end of the channel, the very rapid drop in the water surface corresponds with the ideal value of $\frac{\delta d}{\delta l} = -\infty$. It is instructive to note that at the moment of emerging into the atmosphere, the water is (ideally) in the same state as the water flowing over a flat-topped weir (§ 58), viz. the velocity energy is equal to one-half the pressure energy.

(*Note.*—Referring to Fig. 86, it can be shown that in fact the critical depth is reached just before the water reaches the end of the channel, but at a distance from the outlet that, in relation to the scale of this diagram, would be inappreciable. The curvature of the filaments of water at this station, moreover, represents a further departure from the ideal conditions on which equation 6-2 was based.)

110. Comments on Various Types of Channel Flow. In summarising the information given in the preceding paragraphs, it may again be pointed out that the flow in open channels is invariably assumed to be turbulent, sinuous, or unsteady ; for most practical purposes, stream-line or viscous flow (§ 65) may be regarded as non-existent. Whether the flow is *uniform* or *non-uniform* depends purely upon whether or not the water surface is parallel to the channel bed. Whether the flow is *streaming* or *shooting* depends upon whether the water depth is above or below the critical depth. Thus we may have either uniform streaming flow, or non-uniform streaming flow, or uniform shooting

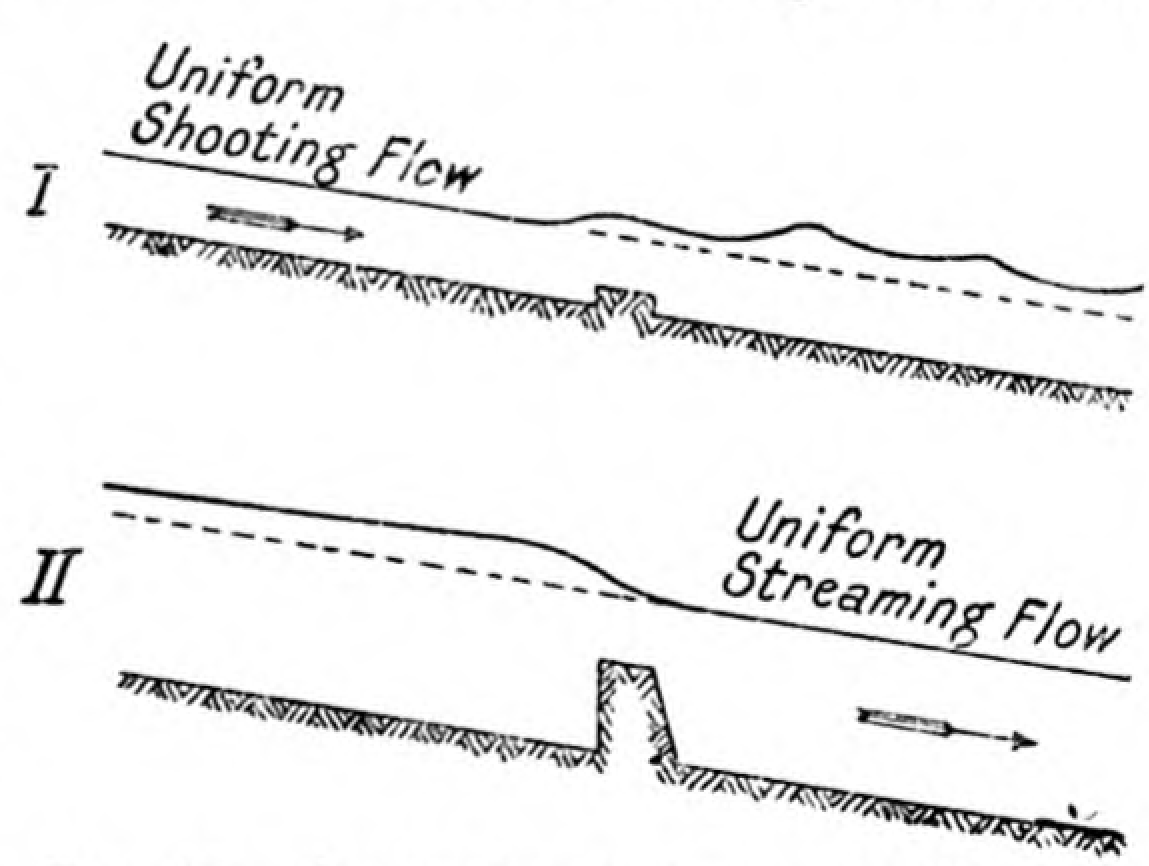

FIG. 87.—Comparison between shooting and streaming flow.

flow, or non-uniform shooting flow. Of these, it is uniform streaming flow that most often occurs (or is assumed to occur) in practice.

If, in a channel in which uniform flow is in operation, the stream is obstructed by a weir or other fixture which causes a loss of energy, "shooting" water will behave quite differently from "streaming" water. In the first case (Fig. 87 (i)), no effect will be produced on the regime *upstream* of the obstruction, but the water depth *downstream* will increase; quite probably the water will not immediately settle down to uniformity of flow, but will dispose itself in the form of a series of standing waves. On the other hand, streaming water is unaffected *downstream* of the obstruction (Fig. 87 (ii)), but the water surface *upstream* is raised; thus the water surface drops in passing the obstruction. The conditions nevertheless remain perfectly stable, and at a sufficiently great distance upstream, the non-uniform flow imposed by the weir gradually merges into uniform flow (§ 184).

Note.—The distinguishing terms "shooting" and "streaming" are only two among a number that have been proposed. Some of these variants are given below; it will be noted that the prefixes "super" and "sub" relate rather to the velocity than to the depth, and thus the meaning of the terms must be clearly memorised.

Water depth *below* critical depth.	Water depth *above* critical depth.
Shooting	Streaming
Rushing	Flowing
Rapid	Tranquil
Supercritical	Subcritical
Superundal	Subundal

111. Turbulent Mixing in a Flowing Stream. Since so many resemblances have already been observed between the behaviour of liquid elements in closed conduits and those in open channels, it is now desirable to examine still another one. This concerns the process of turbulent mixing of elements described in § 75. As applied to a flowing stream, such a process could be represented schematically in the way suggested in Fig. 88. Considering any small element of liquid A, this

might have not only its horizontal mean local velocity component u—the velocity that alone has hitherto been studied in this chapter—but also an additional momentary transverse turbulent component (§ 72). In consequence, the selected element might move from A to A', viz. it would be lifted from beneath to above some reference or datum plane OO. Another element B might likewise descend from B to B'.

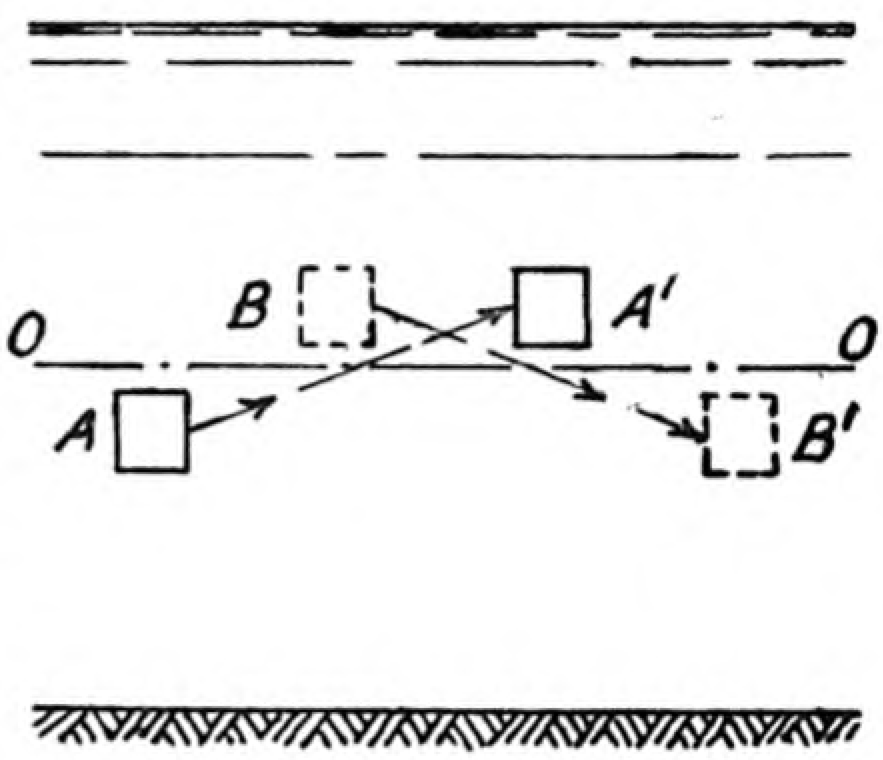

FIG. 88.—Interchange of liquid elements.

If pure water were concerned, this intermingling would be of interest only because of its influence upon the eddy viscosity which is itself the major cause of the resistance to flow of the whole bulk of liquid (§ 76). But most natural rivers and many artificial canals do not carry pure or even clear water: they carry a mixture of water and *suspended solids*—silt, mud, sand, etc. (§ 11). Yet these solids are upheld only by the motion of the water, for as soon as the water comes to rest the solid particles begin to settle towards the bed of the channel. After a sufficient length of time they would form a layer covering the channel bed, leaving only clear water above. What characteristic of the liquid motion is it, then, that enables the particles to resist the law of gravity? We can show that if the conditions are suitable, the turbulent mixing process itself would suffice. In the ensuing discussion, the term "silt" will be used in a general sense, to cover all types of suspended solid particles, e.g. sand grains, smaller grains of mud, etc.

112. Influence of Silt Concentration. A study of Fig. 88 quickly shows that it is the type of "distribution" of the silt throughout the body of liquid that will determine the effectiveness of the turbulent mixing process. If the distribution were uniform—if each unit volume of liquid contained the same number of silt particles—then there would be no net change in the intensity of silt concentration above and below the datum line OO. On the whole, just as much silt would be carried downwards as was carried upwards. But meanwhile the pull of gravity is ceaselessly at work on the particles:

the particles would therefore gradually settle: the stream could not carry them along.

Let us now assume another type of silt distribution, as shown in Fig. 89 (*a*). Here the water below the datum plane OO is more heavily charged than the water above the line. In consequence, the movement of the liquid element AA' transports silt from a region of high concentration to one of low concentration, while the movement of BB' is in the reverse direction. Before long, as the process continues and as each of the migrating elements becomes absorbed into its new surroundings, there will be a tendency for a progressive *dilution* of the heavily-charged lower layer, and for a *strengthening* of the upper or lightly-charged layer of water. Just as turbulent mixing tended to damp out variations of mean velocity (§ 75), so here it tends to smooth out variations of silt concentration. On the other hand, we have to remember the pull of gravity on the particles: it tends to reverse the process, viz. to carry the silt downwards. At a particular stage, we could imagine the two opposing influences to be in equilibrium, resulting in the establishment of a steady regime of silt concentration.[51]

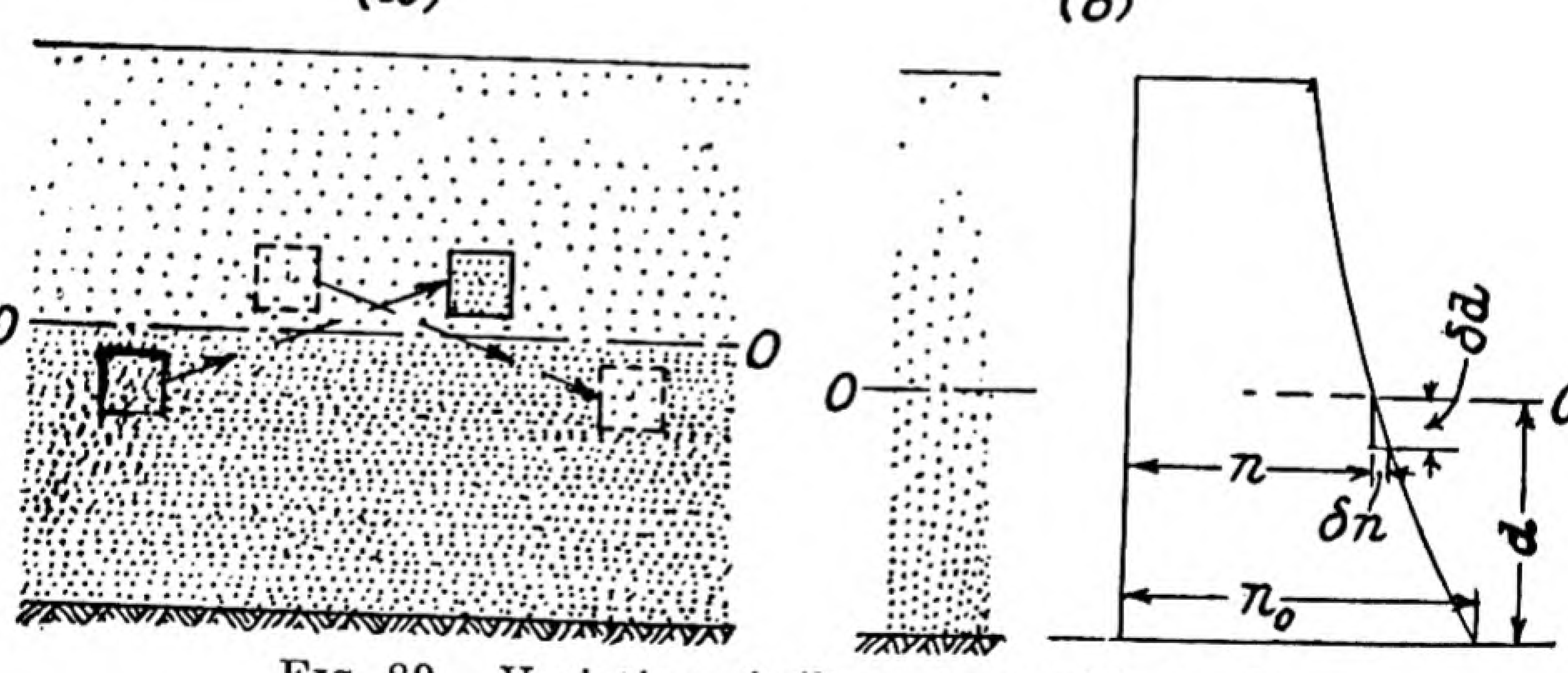

FIG. 89.—Variation of silt content with depth.

113. General Laws of Silt Transport. In an actual stream it is hardly likely that there will be any abrupt transition in silt concentration of the sort indicated in Fig. 89 (*a*); we are much more likely to find a gradual variation which can be represented by a silt-distribution curve, Fig. 89 (*b*). The shape of this curve can be established, at least in idealised conditions, as follows:—

Let n = silt concentration at a height d above the stream bed.

n_o = silt concentration at the stream bed (both expressed in terms of weight of silt particles per unit volume of liquid).

U = rate of descent of particles in *still* water, or terminal velocity, § 129.

ϵ = the kinematic eddy viscosity of the flowing water at height d (§ 76).

Considering unit area of a horizontal plane OO at height d, Fig. 89 (*b*), the *downward* gravitational influence on the silt particles will cause them to traverse this unit area at a rate

$$(U \times n) \text{ weight per unit time} \qquad . \quad . \quad \text{(I)}$$

The *upward* movement due to turbulent mixing will depend upon the gradient of the silt-distribution curve, $\delta n/\delta d$, and upon the intensity of the turbulent mixing process; to represent this turbulence intensity we may use the kinematic eddy viscosity ϵ (§ 76). Thus *upward* rate of silt movement per unit area

$$= \epsilon \, . \frac{\delta n}{\delta d} \text{ weight per unit time} \qquad . \quad . \quad \text{(II)}$$

A steady condition of equilibrium between downward and upward influences will occur when (I) = (II), or

$$U \, . \, n = -\epsilon \, . \frac{\delta n}{\delta d} \qquad . \quad . \quad . \quad \textbf{(6-3)}$$

Integration of this equation will yield the desired shape of the silt-distribution curve.

If the crude assumption were permitted that the kinematic eddy viscosity remained uniform throughout the depth of the stream, then the silt-distribution curve would have a simple logarithmic shape, as in Fig. 89 (*b*); its equation could be written

$$\log_e n_o - \log_e n = \frac{Ud}{\epsilon} \qquad . \quad . \quad \textbf{(6-4)}$$

Even in this simplified form we see that equation 6-3 does conform with our common knowledge of silt suspension. If

the silt particles are relatively large, the terminal velocity U will be considerable and the curve will be sharply inclined away from the vertical : that is, the water near the stream bed will be much more heavily charged with silt particles than the surface water is. But if the silt is very finely divided, or alternatively if the turbulence is intense—which corresponds with a rapidly-flowing stream and a high value of the kinematic eddy viscosity ϵ—then the silt will be fairly evenly distributed throughout the stream depth. **(Example 46.)**

These general impressions still remain acceptable if we now take into account the variations of ϵ with depth d. By analogy with closed conduit flow, § 76, we can be sure that such variations will certainly occur, and they will modify the shape of the silt-distribution curve, Fig. 89 (b). Still other factors combine to influence the behaviour of suspended material in the rivers and canals that the engineer is called upon to control, § 200.

CHAPTER VII

DYNAMIC PRESSURE OF LIQUIDS

114. Types of Dynamic Pressure. Whenever the velocity of liquid elements is suddenly changed in magnitude or direction, forces are called into play analogous to those that resist acceleration or retardation in the motion of solid bodies (§ 28). These forces manifest themselves by changes of pressure in the liquid itself, and by corresponding changes in the resultant thrust that the liquid exerts on the solid boundaries that contain it. The fundamental connection between change of velocity and change of pressure was studied in § 35 ; the specific types of *inertia pressure* or *dynamic pressure* that are now to be examined include :

(i) Acceleration or retardation of columns of liquid in closed conduits, e.g. water hammer effects.

(ii) Impact of free jets of liquid on solid surfaces.

(iii) Impact of liquid streams on submerged solids.

(iv) Impact of one liquid stream on another.

The term *kinetic pressure* is sometimes used as a synonym for *dynamic pressure.*

115. Inertia Pressure in a Pipe due to *gradual* closure of a valve. Typical conditions producing inertia pressure are

represented in Fig. 90, where the velocity in the pipe AB extending from a reservoir can be controlled by a valve at B. For a given valve opening a steady pressure head Ba will be established at B, and there will be a normal hydraulic gradient Oa drooping from A to B. If now the valve be closed at a suitable rate, the pressure head at B will rise by an amount h_i, with a corresponding displacement of the whole hydraulic gradient from Oa to Ob. This state of affairs persists until the valve is fully shut, whereupon the hydraulic gradient, which by this time has an *upward* slope Oc, suddenly drops to the horizontal Oe, and the pressure head throughout the pipe is stabilised at a value equal to the static head in the reservoir. The additional pressure head h_i is the *inertia head*, and the equivalent pressure p_i is the *inertia pressure*.

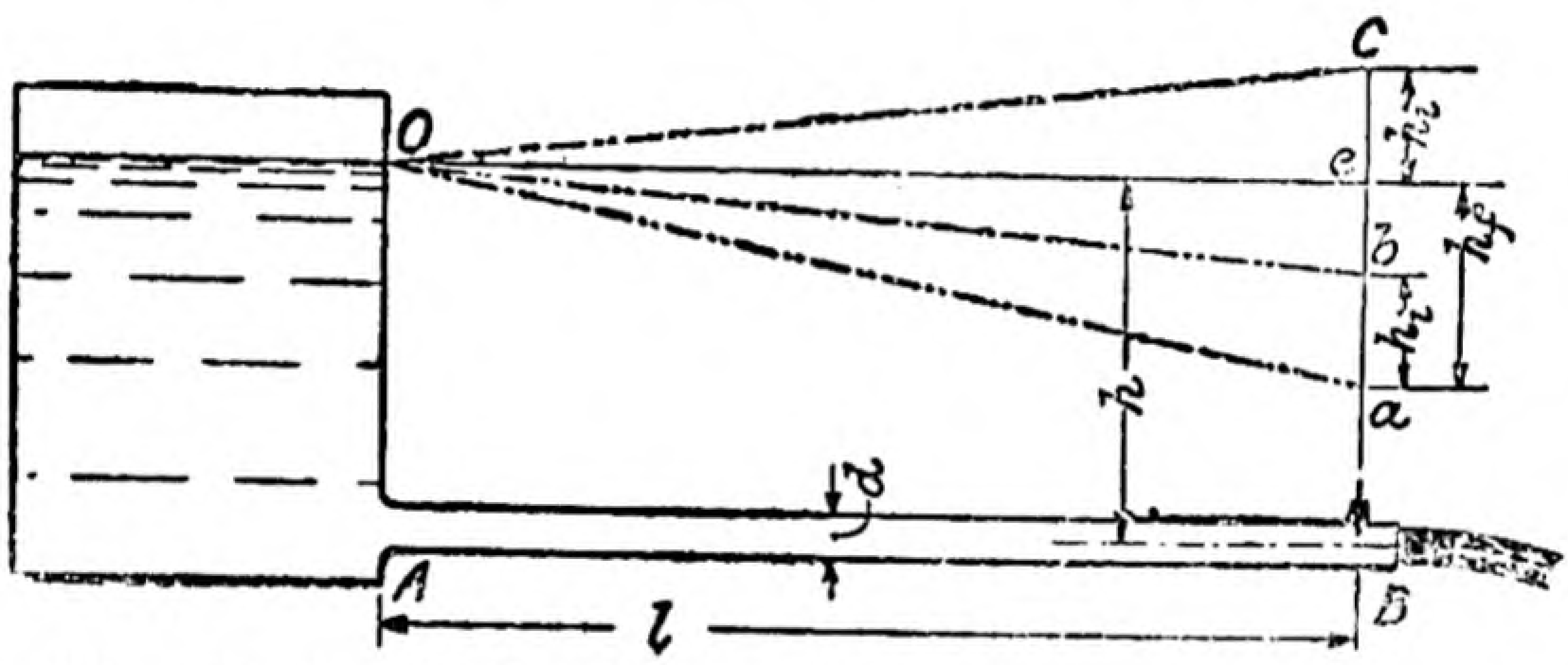

FIG. 90.—Effect on hydraulic gradient of gradual retardation of liquid column.

It will be assumed that the rate of closure is adjusted so as to bring the column to rest, with uniform retardation, from an initial uniformly-distributed velocity v, in time t secs. The total mass of liquid contained in the pipe of length l and diameter d is $\frac{w}{g} \cdot \frac{\pi}{4} \cdot d^2 l$. The rate of retardation of the column is $\frac{v}{t}$. The axial force available for producing retardation is (inertia pressure $\times$ pipe area) $= p_i \cdot {}^{\pi}d^2$. Inserting these values in the equation

$$\text{force} = \text{mass} \times \text{retardation}$$

we have
$$p_i \frac{\pi}{4} d^2 = \frac{w}{g} \cdot \frac{\pi}{4} d^2 l \times \frac{v}{t}$$

whence $$p_i = \frac{wlv}{gt} = \text{inertia pressure,}$$

also $$\frac{p_i}{w} = h_i = \frac{lv}{gt} = \text{inertia head} \quad . \quad . \quad (7\text{-}1)$$

These values relate to the point B (Fig. 90); by selecting other points in the pipe, it is quickly seen that the inertia pressure is proportional to the distance of the point from A, and that therefore the modified hydraulic gradient is always a straight line. The maximum pressure head from all causes, being represented by (static head − friction head + inertia head), will naturally occur at the moment when friction head is least, viz. just before the valve is fully shut. This is made

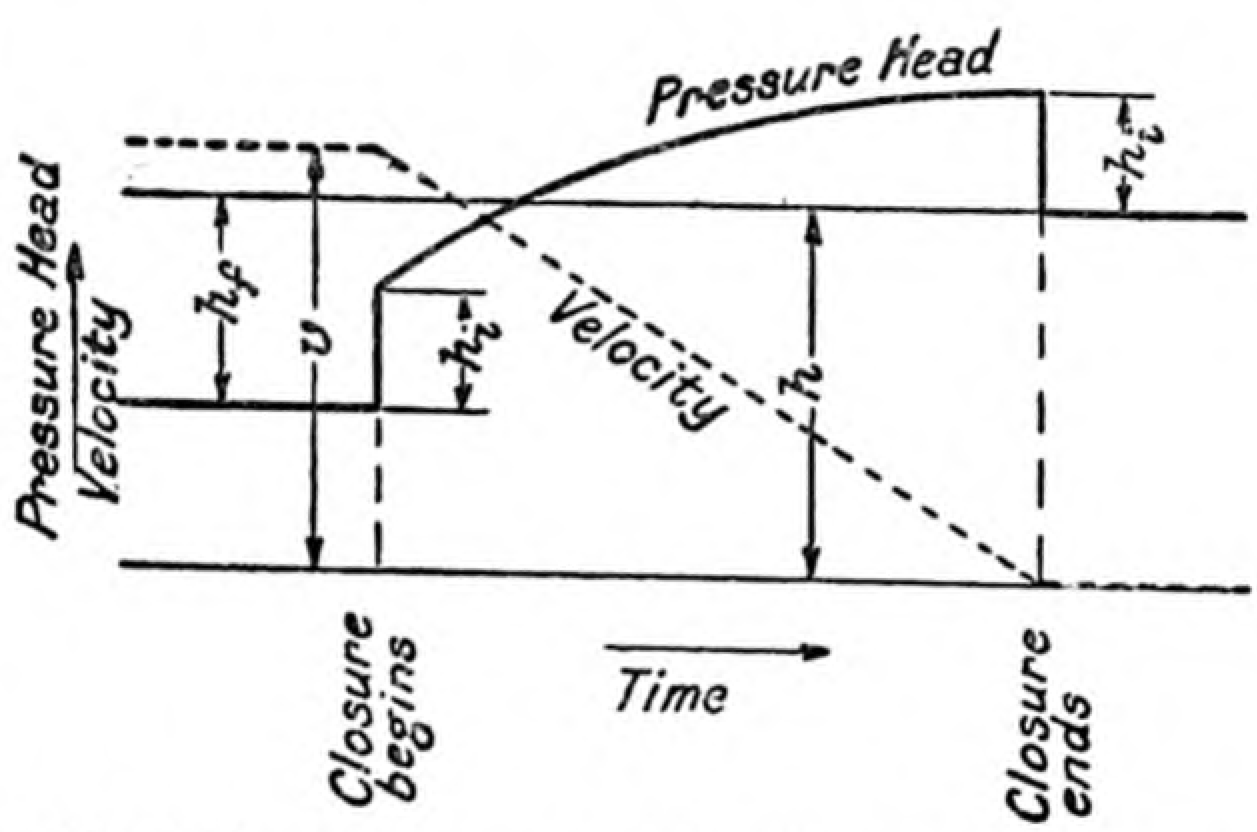

FIG. 91.—Variations in pressure and velocity during valve closure.

clear by the graph (Fig. 91), in which total pressure head and velocity are plotted against time, for a point in the pipe adjacent to the valve. (But note that secondary pressure oscillations may modify the shape of this graph—§ 118.)

Gradual *opening* of the valve, from a partially closed position, will permit the column of liquid to accelerate and so induce a *negative* inertia head.

The inertia head produced by *variable* retardation or acceleration of the column will also be variable, its value at any moment being obtainable from the modified form of formula 7-1

$$h_i = \frac{l}{g} \cdot \frac{dv}{dt}. \qquad \textbf{(Example 51.)}$$

The resemblance of this equation to equation 3-2, § 35, is specially to be noticed.

116. Effect of Instantaneous Closure of Valve. Inspection of equation 7-1 shows that if the time of closure t is zero, the inertia head should rise to infinity; but as experimental observation proves that on the contrary the pressure rise following very rapid valve closure is quite finite and measurable, we conclude that some essential factors have been omitted from the reasoning on which the equation was based. These factors are: (i) the compressibility of the liquid (§ 5 (ii)), and (ii) the elasticity of the pipe walls; together they make it *impossible for the liquid column to be stopped instantaneously*, even if it were possible to shut the valve instantaneously. Thus, if the head of a train of loosely-coupled trucks is suddenly checked (Fig. 92), the following trucks still keep on moving until all the "play" between them has been taken up. Only then is the whole train at a standstill.

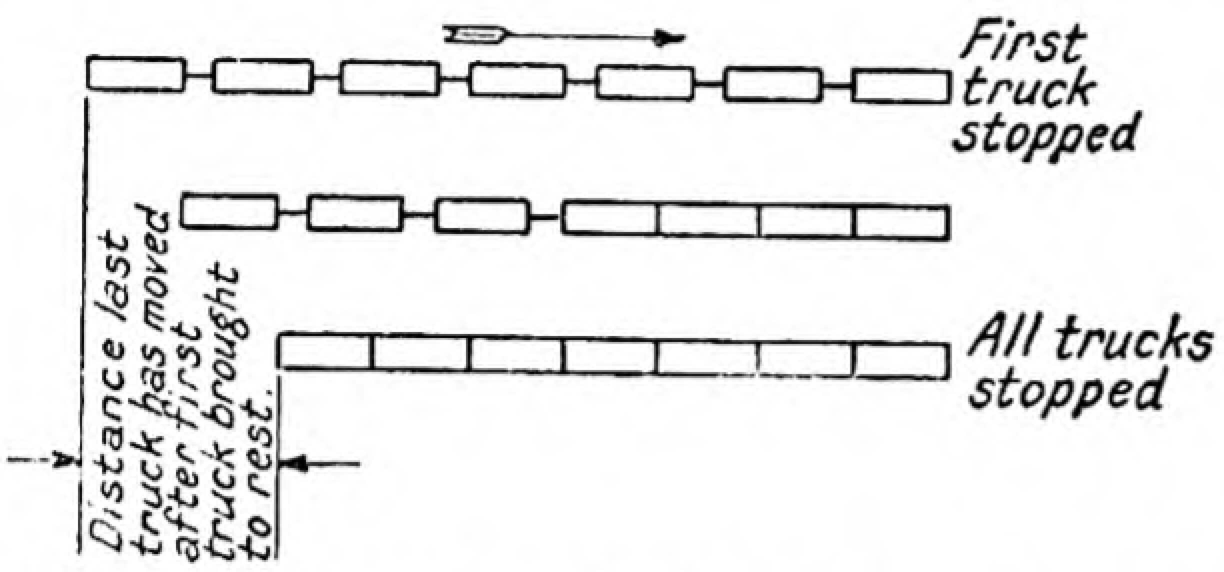

FIG. 92.—Stopping of a loosely-coupled train.

Using this analogy, the true sequence of events in the pipe may now be studied (Fig. 93). At (*a*) the water column is seen advancing with normal velocity v under normal pressure p at the moment before the valve at B is instantaneously shut. As the friction head will be very small in comparison with the inertia head, we shall neglect it. At (*b*), immediately after valve closure, a wave of inertia pressure, as shown by the step in the hydraulic gradient, has begun to sweep with velocity v_0 along the pipe, compressing the water distinguished by stippling, and expanding the pipe; meanwhile the water to the left of the wave front has continued to move on *as though nothing had happened*. At (*c*) the wave has advanced still further, while at (*d*) the entire pipe is full of water *at rest* under a pressure $p + p_i$, the whole of the pipe walls being distended under this pressure.

The result is that in the interval of time dt required to stop the water column, a transverse plane Xa at the end of the column has been able to move through a distance dl to a new position Xd; in other words, the compression of the water

column together with the distension of the pipe walls have made room for an amount of water dQ (indicated by hatching) to enter the pipe *after* the valve has been shut.

Let dq_c = the volume by which the water column is compressed due to pressure p_i.

dq_e = the additional volume provided by the stretching of the pipe walls under pressure p_i.

dD = the resulting increase in pipe diameter.

dt = time for pressure-wave to traverse the pipe.

T = the wall thickness of the pipe.

E = Young's modulus for the material of the walls.

K = Bulk modulus for the liquid.

f_t = tensile hoop stress in pipe walls due to p_i.

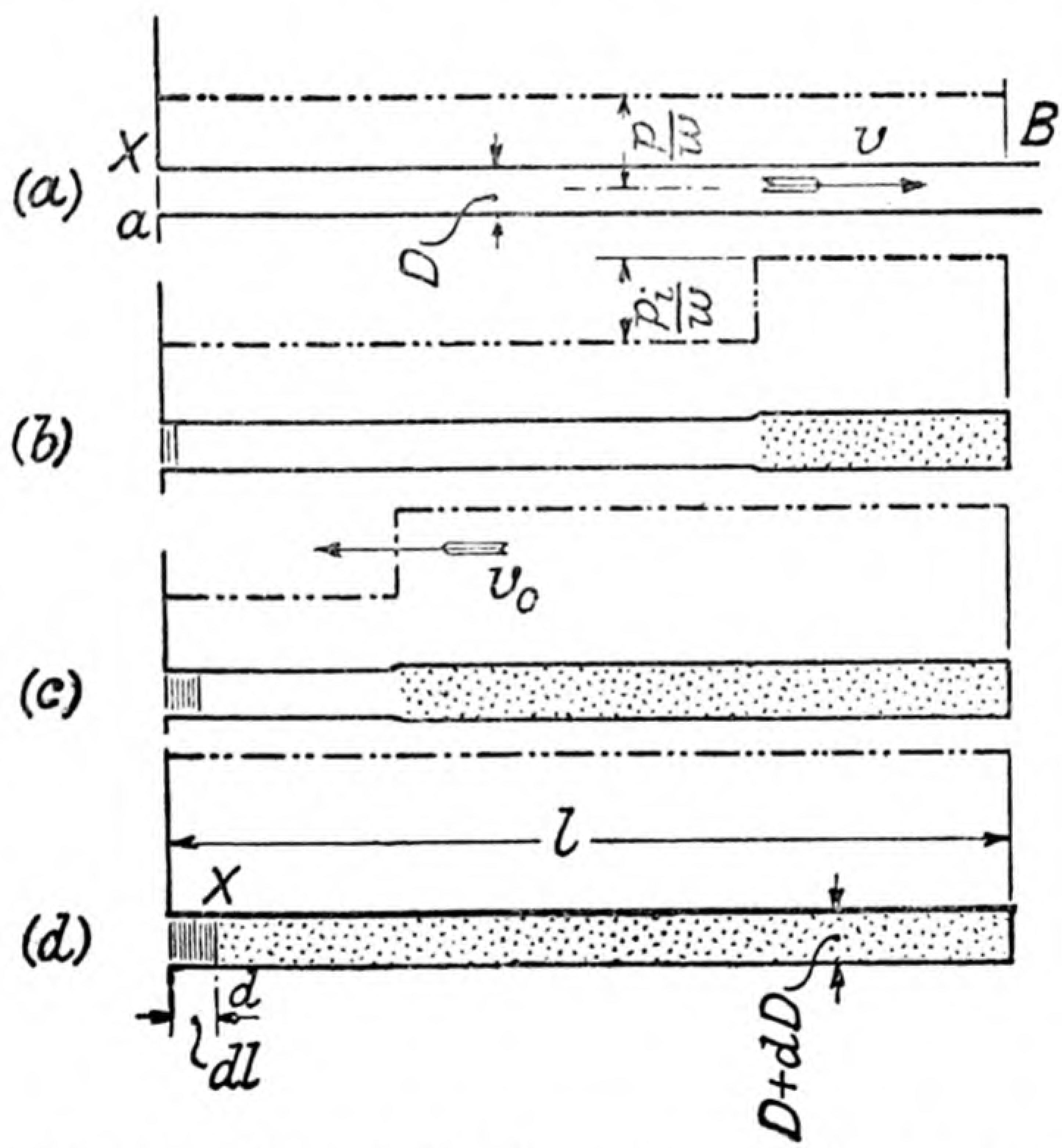

FIG. 93.—Transmission of pressure wave along a pipe.

Now $$dQ = \frac{\pi}{4}D^2 dl,$$

$$dq_c = \frac{p_i}{K} \cdot \frac{\pi}{4}D^2 l \quad (\S\ 5)$$

and $$dq_e = \left[\frac{\pi}{4}(D + dD)^2 - \frac{\pi}{4}D^2\right]l = \pi D \cdot \frac{dD}{2} \cdot l.$$

But also $$f_t = \frac{p_i D}{2T} \quad \text{(equation 2-4, § 21)}$$

and again $$f_t = \frac{dD}{D} \, . \, E.$$

Therefore $$dD = \frac{p_i D}{2T} \cdot \frac{D}{E},$$

whence $$dq_e = \frac{p_i D^2}{2TE} \cdot \frac{\pi D l}{2}. \qquad \textbf{(Example 8.)}$$

Writing now the fundamental equation

$$dQ = dq_c + dq_e,$$

and substituting the values just obtained, we have

$$\frac{\pi}{4} D^2 dl = \frac{p_i}{K} \cdot \frac{\pi}{4} D^2 l + \frac{p_i D^2}{2TE} \cdot \frac{\pi D l}{2}$$

or $$dl = p_i l \left[\frac{1}{K} + \frac{D}{TE}\right].$$

But $$dl = v \, . \, dt,$$

therefore $$p_i = \frac{v \, . \, dt}{l\left(\frac{1}{K} + \frac{D}{TE}\right)} \quad . \quad . \quad . \quad \text{(I)}$$

This expression still contains one unknown, dt, but it can be eliminated by using formula 7-1, § 115, *which is now strictly applicable :* the term dt does truly represent the time to bring the column to rest.

Thus $$p_i = \frac{wlv}{g \, . \, dt},$$

wherefore $$dt = \frac{wlv}{g \cdot p_i}.$$

Substituting this value in equation I above gives us

$$p_i = \frac{wv^2}{gp_i\left(\frac{1}{K} + \frac{D}{TE}\right)},$$

whence $$\textit{inertia pressure} = p_i = \frac{v}{\sqrt{\frac{g}{w}\left(\frac{1}{K} + \frac{D}{TE}\right)}} \quad . \quad . \quad \text{(7-2)}$$

As the value of the term $\frac{D}{TE}$ is usually small compared with the value of $\frac{1}{K}$, it may be neglected for approximate calculations, leaving the equation in the form

$$p_i = v\sqrt{\frac{wK}{g}} \qquad . \quad . \quad . \quad (7\text{-}3)$$

which is independent of the dimensions of the pipe and indeed of everything except the initial velocity of the liquid and its physical characteristics.

The *velocity of the compression wave* v_o is represented by

$$v_o = \frac{l}{dt} = \sqrt{\frac{g}{w\left(\frac{1}{K} + \frac{D}{TE}\right)}}.$$

If the simpler form $v_o = \sqrt{\frac{gK}{w}}$ is adopted, v_o is seen to be identical with the *velocity of the propagation of sound* in the liquid.

By substituting the equivalent value of v_o in equation 7-2, we obtain a very convenient expression for the inertia head, viz.:

$$h_i = \frac{p_i}{w} = \frac{vv_o}{g} \qquad . \quad . \quad . \quad (7\text{-}4)$$

This is often known as the Allievi formula.

Particular care is necessary in choosing the *units* to be used in these formulæ. Assuming the liquid to be water, if v is expressed in ft./sec., D and T in ins., and K and E in lb./sq. in., formula 7-2 reduces to

$$p_i \text{ in lb./sq. in.} = \frac{v}{8{\cdot}63\sqrt{\frac{1}{300000} + \frac{D}{TE}}},$$

and formula 7-3 reduces to p_i in lb./sq. in. $= 63{\cdot}4\ v$. If v is expressed in m./sec., D and T in cms., and K and E in kg./sq. cm., formula 7-2 reduces to

$$p_i \text{ in kg./sq. cm.} = \frac{v}{9{\cdot}9\sqrt{\frac{1}{21000} + \frac{D}{TE}}},$$

and formula 7-3 reduces to p_i in kg./sq. cm. $= 14{\cdot}6\ v$. The velocity of sound in water = velocity v_0 of compression wave (approx.) may be taken as 4700 ft./sec. or 1430 m./sec.

(Example 52.)

117. Pressure Oscillations following Instantaneous Closure. It is now necessary to trace the behaviour of the water column onwards from the point of time represented in Fig. 93 (*d*). Here a most important distinction is to be observed between this column and the column shown in Fig. 90, § 115. Under the conditions of gradual retardation, the whole of the kinetic energy of the water due to its velocity v is assumed to have been destroyed by pipe friction and by eddying in the partially closed valve, etc., so that the moment the valve is fully shut the water in the pipe becomes inert.

It is quite otherwise under the conditions of instantaneous closure. No energy has yet been destroyed—it has been employed in compressing the water and distending the pipe in exactly the same way that the energy of a weight is employed in compressing the spring on which it falls. The instant it comes to rest the weight begins to rebound—the energy momentarily given to the spring is yielded up again.

(By equating in this manner the velocity energy of the moving liquid column to the elastic energy of the stationary column, we find an alternative derivation of equation 7-3, thus.

The kinetic energy per unit weight is $\dfrac{v^2}{2g}$.

The elastic energy per unit weight is $\dfrac{p_i^2}{2wK}$ (§ 27). Therefore $\dfrac{v^2}{2g} = \dfrac{p_i^2}{2wK}$

(neglecting the resilience of the pipe walls), or $p_i = v\sqrt{\dfrac{wK}{g}}$.)

Evidently, then, the water column will only remain instantaneously in the state represented in Fig. 93 (*d*). It, too, will rebound; the energy temporarily stored in the compressed water and the stretched pipe walls will be reconverted into velocity energy; the operations described in § 116 will be reversed, until after a further period of time dt the return pressure wave has reached the valve and the whole column has reverted to its original state except that it is now moving with velocity v *away from* the valve.

The next stage in the cycle consists in the transmission

of a wave of *negative* inertia pressure, of intensity ($-\ p_i$), from the valve to the open end of the pipe and back again. In an interval of time $4dt$, then, the cycle is completed, the water once more travelling towards the valve with velocity v under pressure p. If it were not for friction and other losses, the cycle would be repeated indefinitely, as shown in Fig. 94, but actually the pressure oscillations rapidly diminish in intensity and finally die out.

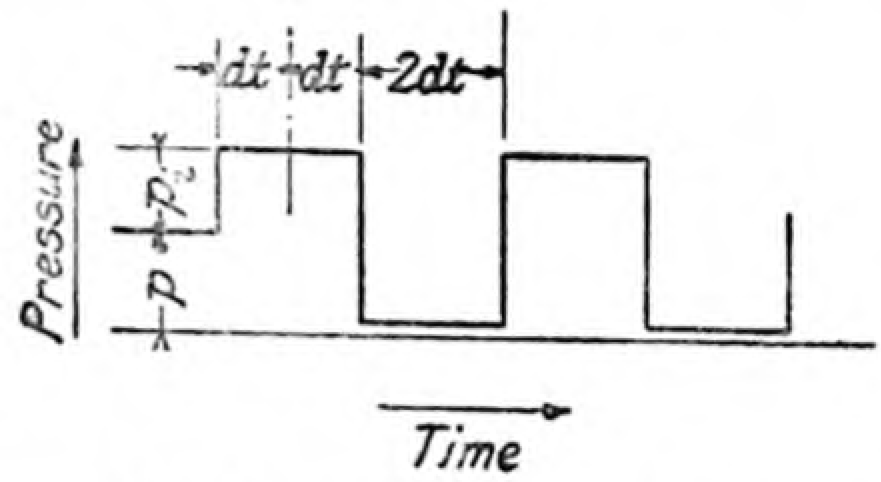

FIG. 94.—Ideal wave form.

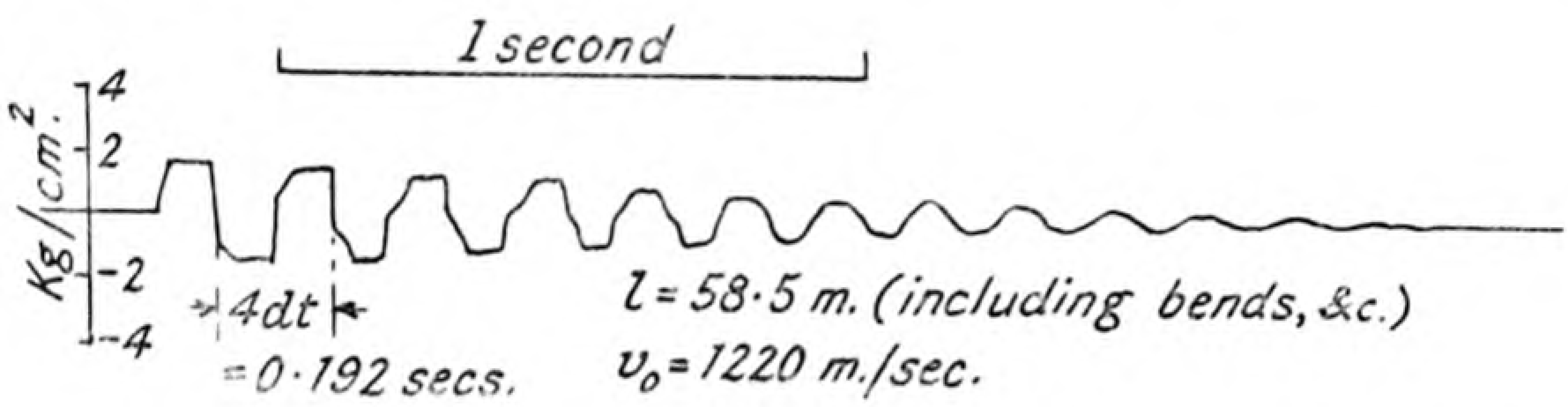

FIG. 95.—Autographic time-pressure record, at end of $1\frac{1}{4}''$ pipe.

An actual time-pressure record, showing the damping effect of friction, etc., is reproduced in Fig. 95.

Evidently if the positive inertia pressure p_i is greater than the absolute pressure in the pipe before valve closure, viz. if $p_i > p_a + p$, then it is impossible for the full negative inertia pressure $-\ p_i$ to be realised, for to do so would bring the resulting absolute pressure below zero. In such cases there is a rupture of the water column moving away from the valve during the negative part of the wave, and a vacuous space is momentarily formed near the valve, in which the absolute pressure is the vapour pressure of the water. The duration of the negative wave is thus increased, and the general shape of the time-pressure curve is modified, as suggested in Fig. 96. Both in this figure and in Fig. 94 the curves relate only to points close to the valve; for other points the wave form is different (§ 175).

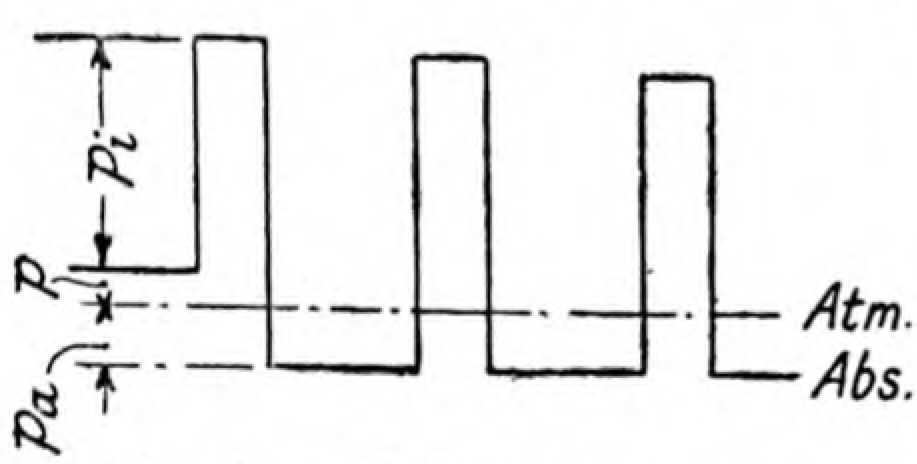

FIG. 96.—Modified wave form.

118. Rapid but not Instantaneous Closure. The pressure changes in the pipe near the valve if closure is effected rapidly, in time τ, can be studied by considering the valve to be closed in a succession of steps—say n small movements; after each very small interval of time, of duration τ/n, the valve is imagined to be instantaneously moved by the small

amount required to impart to the water column a sudden reduction in velocity δv, so generating an inertia pressure δp Each small valve movement will thus set up a pressure wave of the same form as, but of much less amplitude than, the one shown in Fig. 94, and the total inertia pressure in the pipe at any moment can be found by summing the individual pressure increments, as is done in Fig. 97. If the number of movements n be infinitely great, then the steps in the graph will be smoothed out, and the time-pressure curve will have the form indicated in (e.g.) Fig. 98 (II); the various curves in this diagram show how the time of closure τ influences the resultant wave form. In particular, they show that if the liquid

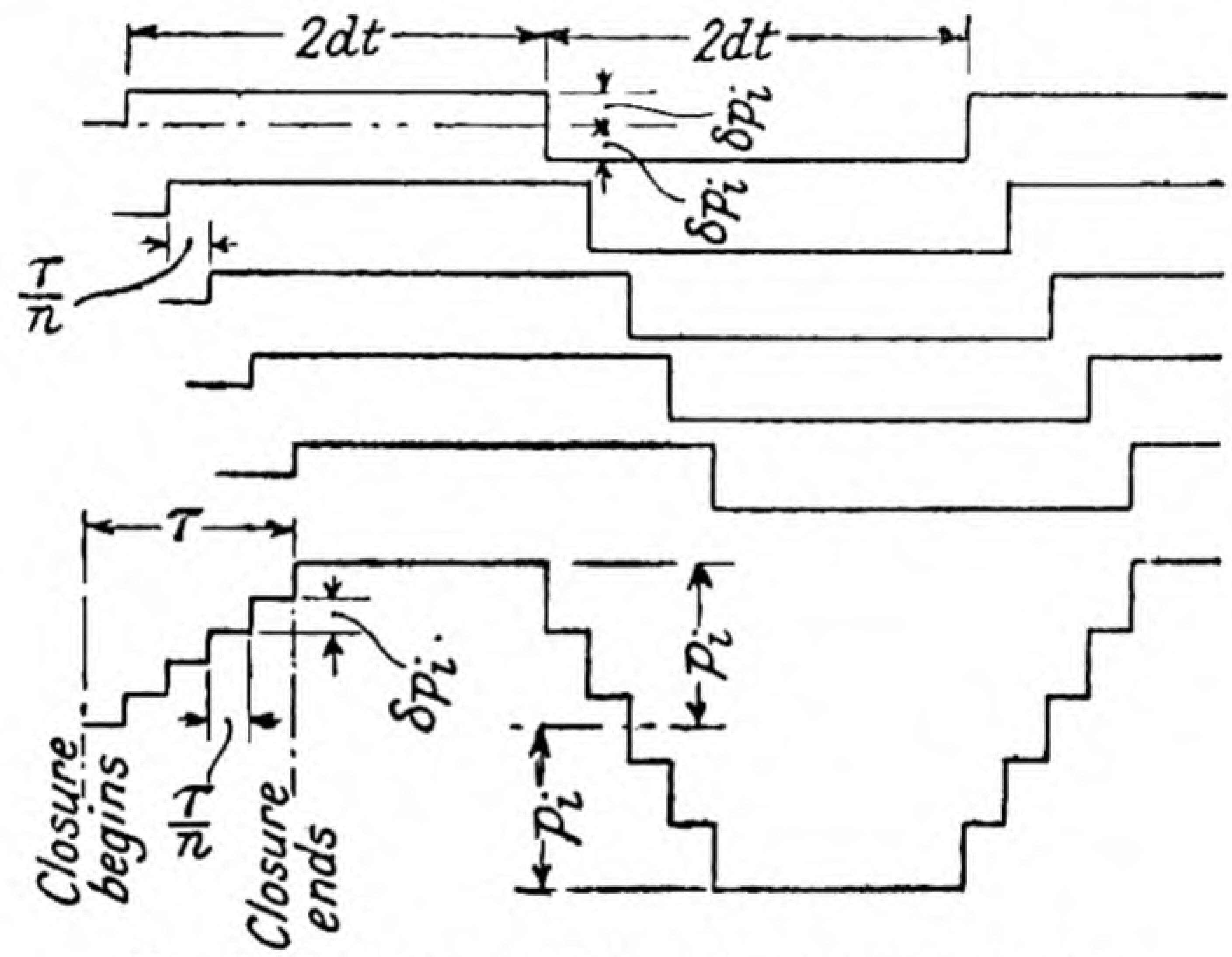

FIG. 97.—Superposition of pressure waves.

column is retarded uniformly and brought to rest in a time *not greater than* 2*dt*—if, that is, the valve closure is completed before the first pressure wave has travelled to the open end of the pipe and back again—then the maximum inertia pressure near the valve will have the *same value for rapid closure as it has for instantaneous closure*, and therefore formulæ 7-2 and 7-3 are applicable.

If, however, the time of valve closure τ is greater than $2dt$, then the maximum inertia pressure p_{ir} can be computed thus: Until the arrival at the valve of the first return pressure wave, the rate of increase of total inertia pressure at the valve is p_i/τ, and therefore after an interval $2dt$ the pressure will have attained the value $p_i \times \frac{2dt}{\tau}$. This represents the

maximum value, for, as seen in Fig. 98 (IV), the inertia pressure thereafter diminishes again, subsequently fluctuating between the values p_{ir} and 0, with a periodicity of $4dt$. Under the conditions specified, then, $p_{ir} = p_i \times \frac{2dt}{\tau}$, where p_i represents the inertia pressure corresponding to instantaneous closure.

Although so far the special case of *uniform* retardation of the water column has been considered (which it is important to note is *not* realised by uniform valve movement—§ 172), the method illustrated in Fig. 97 is manifestly applicable to

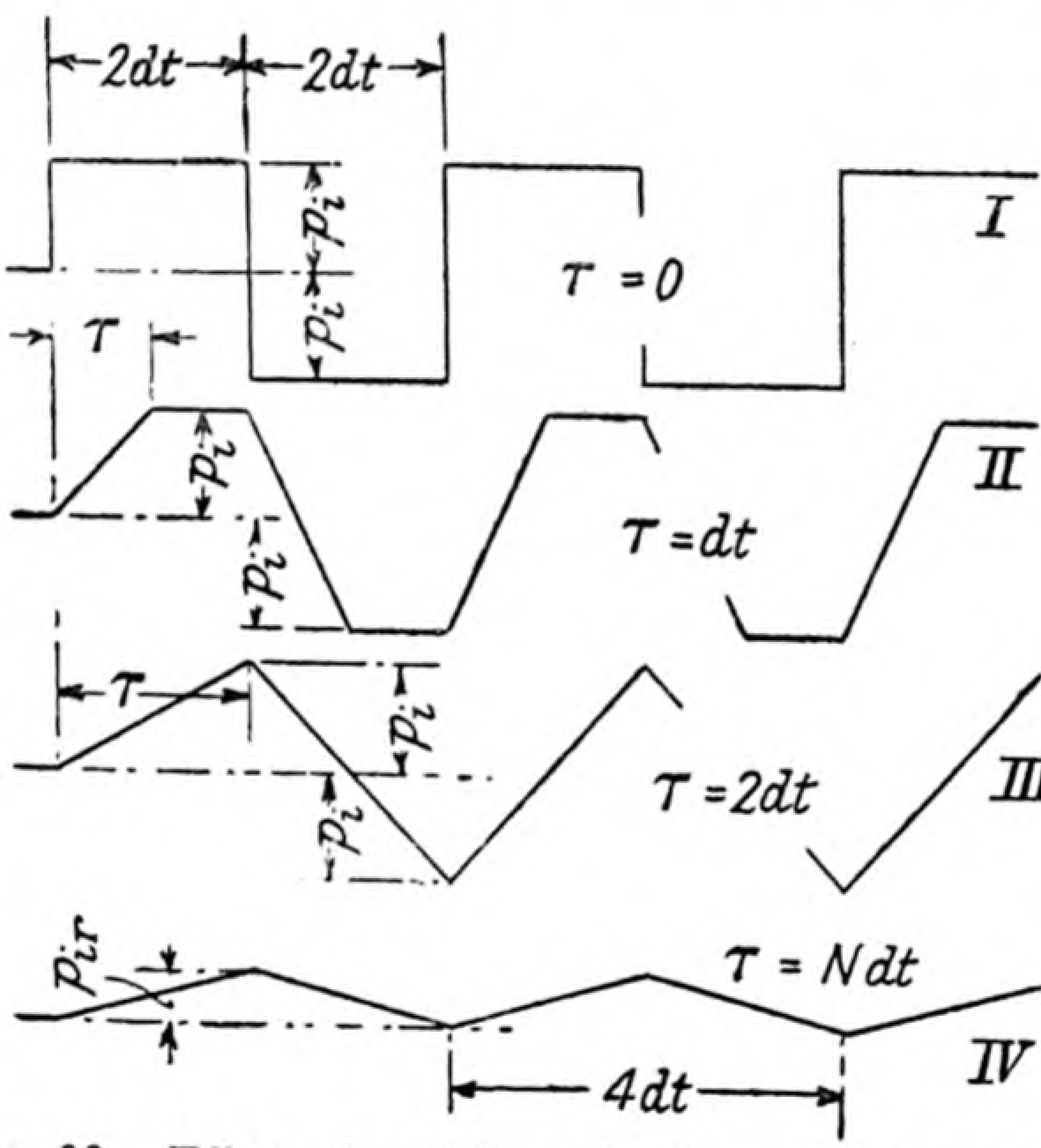

FIG. 98.—Effect of rapidity of valve closure on shape of pressure wave, for uniform retardation.

any conditions in which the law connecting retardation with time is known (§ 176).

Comparing the result just obtained with the result yielded by formula 7·1, § 115, which both relate to non-instantaneous closure, it will be found that an anomaly remains to be explained. From § 116, $p_i = \frac{wlv}{g \cdot dt}$, and therefore

$$p_{ir} = \frac{wlv}{g \cdot dt} \cdot \frac{2dt}{\tau} = \frac{2wlv}{g\tau}.$$

But formula 7·1 gives: inertia pressure $= wlv/g\tau$, or only one-half of the previous value. The explanation is suggested in Fig. 99, in which the high-frequency waves shown in Fig. 98 are superposed upon the time-pressure curve of Fig. 91. Here it is evident that the *maximum* momentary inertia pressure is twice the mean pressure, just as the two formulæ indicate.

But the high-frequency fluctuations are by no means inevitable; they are no more than a consequence of the sudden application of the retardation represented in Fig. 91. If the time : velocity graph had changed its slope *gradually* instead of rapidly, so smoothing out the sharp kinks at the beginning and end of the closing period, then the corresponding time-pressure diagram might more truly represent what actually happens than Fig. 99 does. An

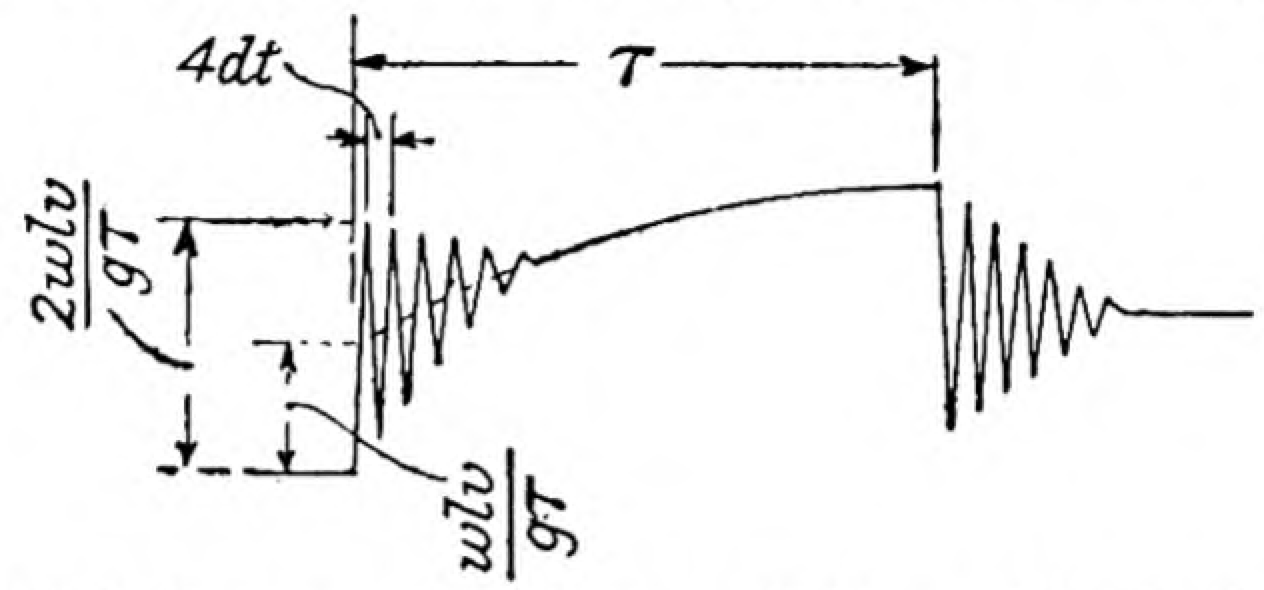

FIG. 99.—High-frequency pressure oscillations at beginning and end of valve closure.

analogy from railway travel is provided by Fig. 92; if a passenger train is now in question instead of a freight train, it is easy to recollect what occurs if the draw-gear and buffing-gear are inadequately damped, and if the driver handles his brakes unskilfully. When the train starts or stops, there may be a disagreeable periodic lurching of the carriages, of which Fig. 99 may serve as a diagram.

(*Note.*—The term *water-hammer* is often used to describe these phenomena, discussed in the previous paragraphs, which result from velocity variations in pipes. But naturally the formulæ that have been derived are not limited only to the flow of water. If other liquids such as oils are in question, it may happen that viscous effects will modify the shape of the pressure-wave, but they will not influence either the maximum pressure or the periodicity.[52])

119. Inertia Forces Due to Radial Acceleration. Having now studied some of the effects of *linear* acceleration in closed conduits, we pass on to an example of the influence of *radial* acceleration when liquids travel in curved paths.

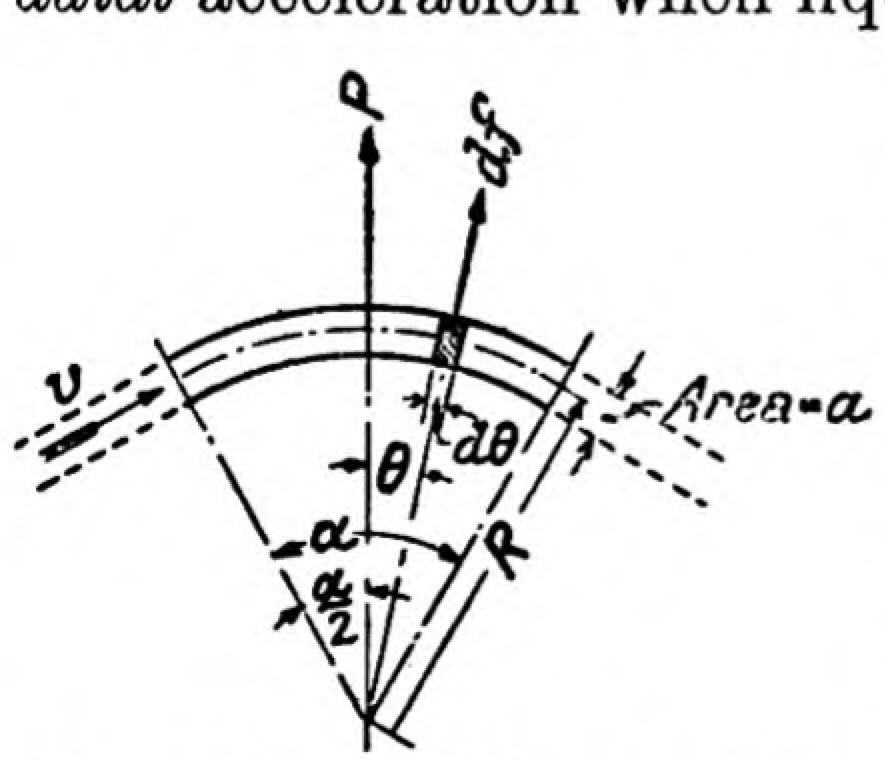

FIG. 100.—Radial acceleration.

Water moving with uniform speed v along a pipe curved to a radius R is subjected to a radial acceleration $\frac{v^2}{R}$, and a corresponding inertia force is generated. But instead of producing an increase in the average intensity of pressure of the water, the inertia force causes the water to transmit to the pipe itself a resultant dynamic thrust P (Fig. 100).

The weight of a small element of water, of cross-section a, subtending a small angle $d\theta$ at the centre of the bend, is $w \, . \, R \, . \, d\theta \, . \, a$.

The centrifugal force df acting on this element = mass × radial acceleration

$$= \frac{w}{g} . R . d\theta . a . \frac{v^2}{R}.$$

The component of this force acting in direction P

$$= \frac{w}{g} . Rd\theta . a . \frac{v^2}{R} \cos\theta.$$

The resultant dynamic thrust is therefore

$$P = \int_{-\frac{\alpha}{2}}^{+\frac{\alpha}{2}} \frac{w}{g} . av^2 \cos\theta d\theta$$

$$= \frac{w}{g} . av^2 . 2 \sin\frac{\alpha}{2}$$

$$= \frac{W}{g} . v\sqrt{2(1 - \cos\alpha)} \quad . \quad (7\cdot5)$$

where W is the weight of liquid flowing through the pipe per second, and α is the angle through which the liquid is deflected in passing round the bend.

Alternative approaches to this problem are to be found in § 121 (c) and § 141.

Impact of Free Jets.

120. Intensity of Dynamic Pressure. When a free jet of liquid issuing from a nozzle or the like (§ 42) impinges on a fixed or moving solid object, two new features of the retarding process are to be taken into account: (i) both before and after impact, the liquid is at atmospheric pressure; (ii) although the initial velocity and cross-section of the liquid stream may accurately be known, its final state may often be difficult to define. Simple conditions which permit a direct computation of the intensity of dynamic pressure are illustrated in Fig. 101; here a glass tube drawn out into the form of a fine nozzle is presented axially to a horizontal jet projected from an orifice. A liquid element in

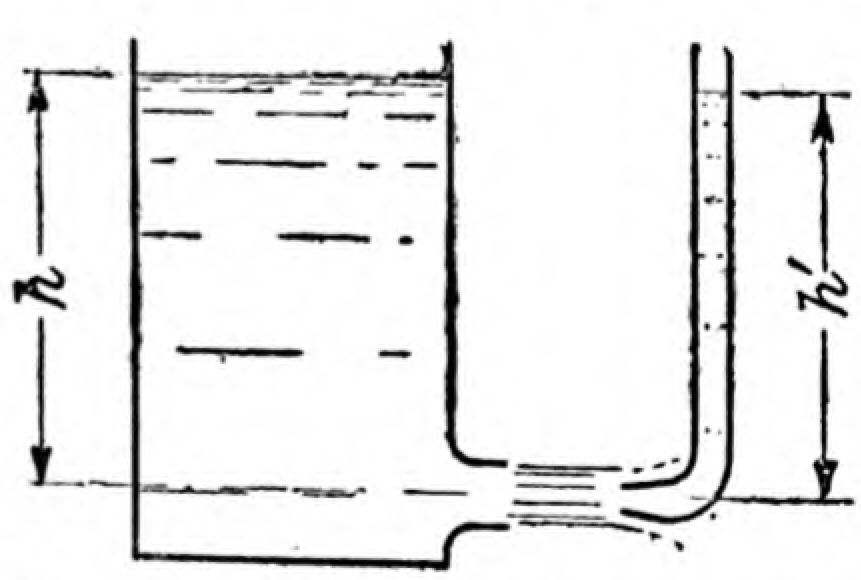

Fig. 101.—Principle of Pitot tube.

the axis of the jet, originally travelling with velocity U, will be brought completely to rest by the time it reaches the mouth of the glass tube. As no energy losses have been incurred, we conclude that the velocity energy has all been converted into pressure energy, and that consequently the dynamic pressure exerted on the stationary liquid in the tube is

$$p_i = \frac{wU^2}{2g}.$$

If the measured vertical height to which the liquid rises in the tube is h', we can compute the velocity U if this were not already known ; for evidently $U = \sqrt{2gh'}$. Here is the basis for a very valuable technique of velocity-measurement (§ 380). The observed height h' is slightly less than the original head h above the orifice because of the energy loss in the orifice itself (§ 42).

If now the jet were to be directed normally against a fixed flat plate, Fig. 102, only at one point on the plate can we say with confidence that the dynamic pressure is $wU^2/2g$. It is the point at which the axis of the jet intersects the surface of the plate. We call it the *stagnation point*, because we can imagine that here the liquid elements are indeed brought completely to rest. The pressure p_i at this point, which would be registered by a pressure-gauge communicating with a small hole drilled through the plate, is likewise termed the *stagnation pressure*. As we proceed outwards from this central point, the measured dynamic pressure on the plate declines more and more from its maximum value of $wU^2/2g$.

Without a knowledge of the pressure-distribution, we cannot find the total dynamic thrust on the plate by the integration process that served for computing the total static thrust, § 19. Instead, the principle of change of *momentum* is utilised ; the rate of loss of momentum suffered by the whole mass of liquid as a result of the impact will provide a direct measure of the force exerted by the liquid.

121. Dynamic Thrust of a Jet on Fixed Surfaces.

(*a*) *Plane surface normal to jet* (Fig. 102).

Let a represent the cross-sectional area of the jet.
U „ „ mean velocity of the jet.
W „ „ weight of liquid per second delivered by jet.

Mm_1 represent the momentum per second of the jet, in direction of thrust P, before impact.

Mm_2 ,, ,, momentum per second of the liquid, in direction of thrust P, after impact.

P ,, ,, dynamic thrust exerted on fixed surface.

Now Mm_1 = mass of water delivered per second × component of its velocity in direction P

$$= \frac{W}{g} \times U.$$

After impact the water slides away in all directions over the plate, but none of it, except for the small amount that may splash back, has a velocity component *in direction P*.

Therefore $$Mm_2 = \frac{W}{g} . O = 0.$$

Since force = rate of change of momentum
= change of momentum per second,

then

$$\text{dynamic thrust} = Mm_1 - Mm_2 = \frac{W}{g} . U - O = \frac{W}{g} . U$$

or $$P = \frac{W}{g} . U. \qquad (7\text{-}6)$$

Writing $W = waU$, then $P = \dfrac{waU^2}{g}$.

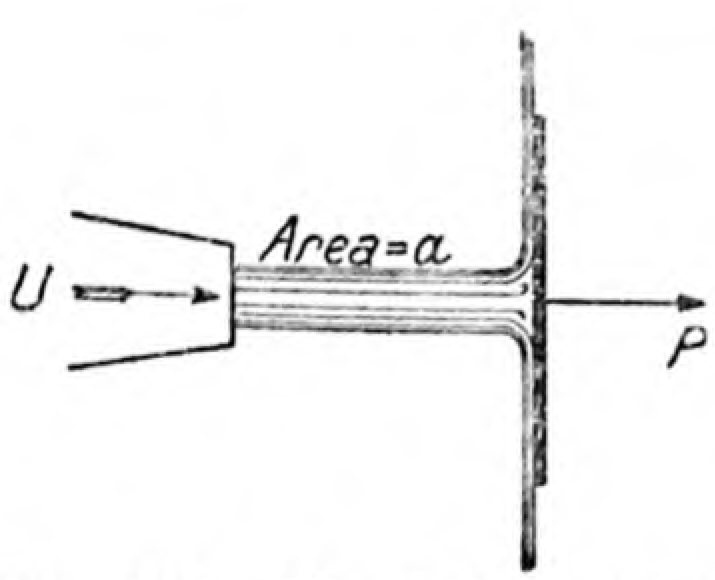

FIG. 102.—Normal impact of jet.

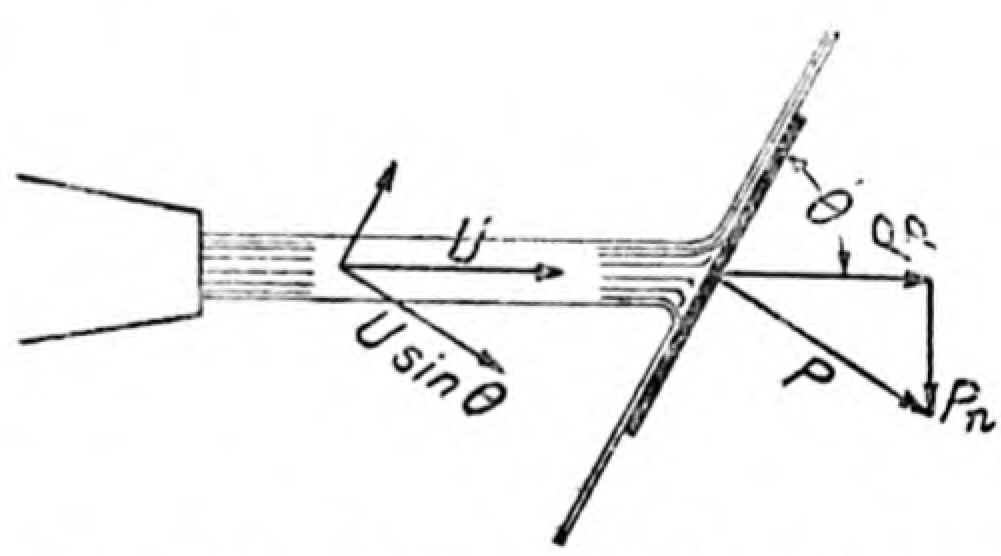

FIG. 103.—Impact on inclined surface.

(*b*) *Plane surface inclined at angle θ to the jet* (Fig. 103).

Here the water sliding over the plate after impact almost certainly will have a mean velocity component parallel with U, and no means seem to be available in the first instance for evaluating it. We therefore resolve the jet velocity into two components, of which one, $U \sin \theta$, is normal to the plate and the other, $U \cos \theta$, is parallel with the plate; this latter can

forthwith be ignored, as it cannot possibly produce a normal thrust on the plate.[53]

The normal velocity component is inserted in place of U in formula 7-6 above, whence

$$P = \frac{W}{g} . U \sin \theta.$$

The total dynamic thrust P can then be resolved if desired into a thrust P_p parallel with the jet, and a thrust P_n normal to the jet, where

$$P_p = \frac{W}{g} U \sin \theta \sin \theta = \frac{W}{g} U \sin^2 \theta,$$

and $$P_n = \frac{W}{g} U \sin \theta \cos \theta.$$ **(Example 53.)**

(c) *Curved surface on which the jet impinges tangentially* (Fig. 104). Under ideal conditions the liquid slides over the

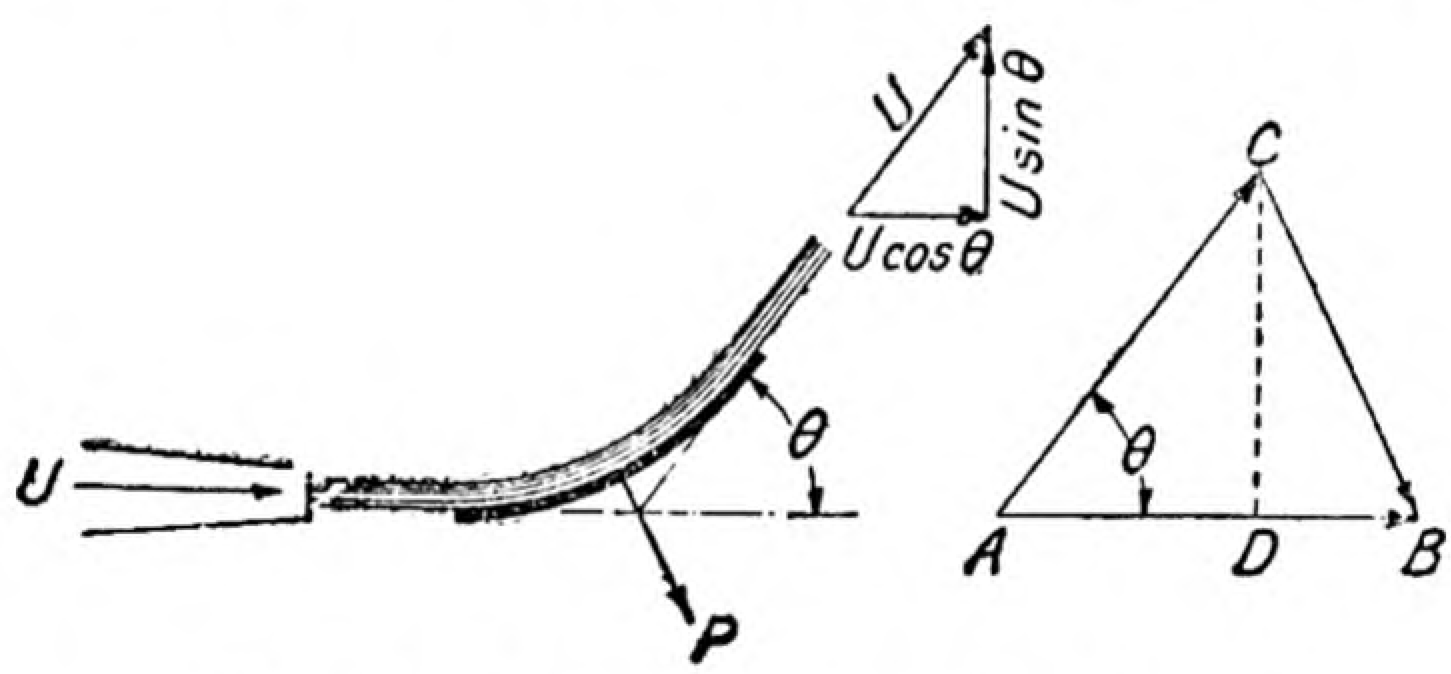

FIG. 104.—Impact on curved surface.

surface without friction, and leaves the vane with the speed U with which it enters it. Thus

$$Mm_1 = \frac{W}{g} . U, \quad \text{and} \quad Mm_2 = \frac{W}{g} . U \cos \theta,$$

whence $$P_p = Mm_1 - Mm_2 = \frac{W . U}{g} - \frac{WU}{g} . \cos \theta$$

or $$P_p = \frac{W}{g} . U(1 - \cos \theta) \quad . \quad . \quad . \quad . \quad (7\text{-}7)$$

where P_p represents the dynamic thrust *in the direction of the jet.*

The thrust P_n normal to the jet will be given by the expression $O - \frac{W}{g} . U \sin \theta = - \frac{W}{g} . U \sin \theta$, the negative sign indicating that the thrust in Fig. 104 is exerted downwards.

The total resultant thrust, viz. the resultant of P_p and P_n, is readily shown to have the value

$$P = \frac{W}{g} \cdot U\sqrt{2(1 - \cos\theta)}.$$

These results may also be obtained vectorially. Setting off to scale the distance AB (Fig. 104) to represent the initial momentum per second $\frac{W}{g} . U$, and AC to represent the final momentum per second $\frac{W}{g} . U$, the vector difference CB will represent the change of momentum per second, which is numerically equal to the total resultant thrust. Thus CB represents to scale the thrust P, DB represents P_p, and CD represents P_n.

These methods of treating the problem may be compared with the method used in § 119 for solving a precisely similar problem.

It is interesting to note that when $\theta = 180°$, a given jet can develop (in ideal conditions) just double the thrust on a curved surface that it can exert in a flat plate.

Coefficient of impact. The observed or measured dynamic thrust P_a exerted by a jet is rarely identical in value with the thrust P calculated from the formulæ just developed; the ratio $\frac{P_a}{P}$ is termed the *coefficient of impact*, C_i. For normal impact on flat plates, C_i has a value of about 0·95. In impact on curved surfaces, the effect of friction in retarding flow over the surface will tend to give C_i a value greater than unity if θ is very small, because friction reduces vector AC (Fig. 104), and therefore increases vector DB. For values of θ greater than 90°, friction will reduce DB and thus give values of C_i less than unity.

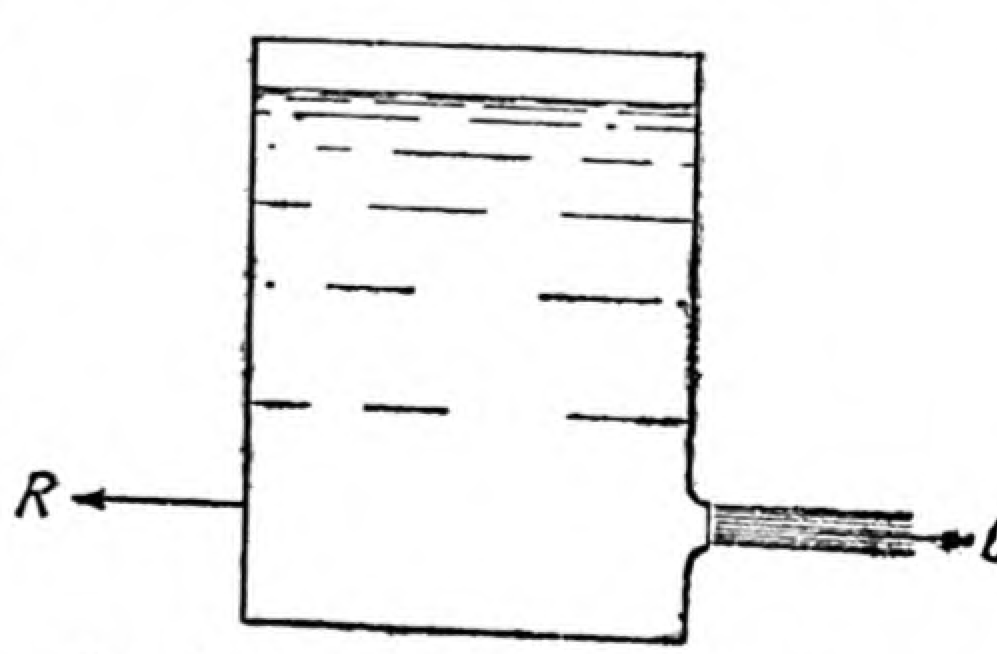

FIG. 105.—Reaction on side of tank.

122. Reaction from a Jet. Since a jet impinging on a plate can exert a thrust P, the existence of an equal and opposite reaction R is to be expected. Fig. 105 shows how

the reaction is applied to the vertical wall of a tank; if such a tank were mounted on wheels, it would travel along—a kind of hydraulic rocket car—from right to left. To calculate the reaction R in the case of a stationary tank, we consider the change of momentum per second from the moment the liquid is at rest in the tank to the moment it has attained full jet velocity U. Thus

$$R = Mm_1 - Mm_2 = 0 - \frac{W}{g}U = - \frac{W}{g} . U,$$

the negative sign showing that the direction of R is opposite to the direction of U. What happens to the jet afterwards—whether it strikes a plate or not—cannot influence the reaction in any way.

§ 49 explains how the reaction R may also be regarded as the unbalanced *hydrostatic* thrust on an area of the left-hand wall of a tank corresponding with the area of the right-hand wall which is relieved of static thrust by reason of the aperture through which the jet emerges.

123. Work Done by a Jet: (*a*) when impinging normally on a series of *flat* moving vanes.

As soon as a plate subjected to the dynamic thrust of a jet is allowed to yield to the thrust, work will be done on the plate: energy (§ 44) will be transferred from the jet to the plate. In Fig. 106 it is assumed that the wheel to which the plates—now called *vanes, blades* or *paddles*—are radially attached is so large in diameter that the jet can always be regarded as impinging on them normally. Let the mean tangential velocity of the vanes be v.

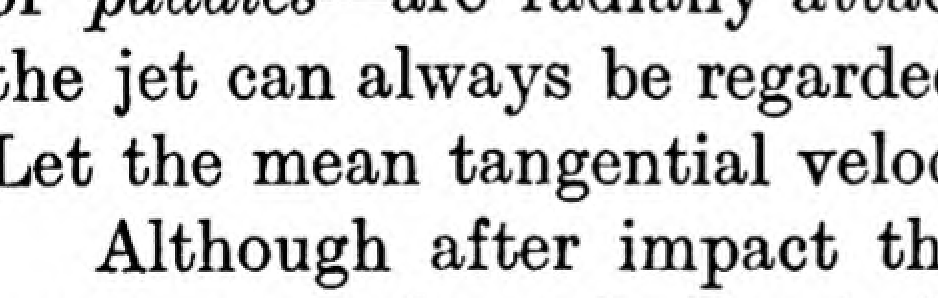

FIG. 106.—Impact on radial vanes.

Although after impact the water slides radially over the vanes precisely as it does in Fig. 102, yet it now shares their forward velocity v; thus the tangential thrust P exerted on the vanes is

$$Mm_1 - Mm_2 = \frac{W}{g} . U - \frac{W}{g} . v = \frac{W}{g}(U - v).$$

The work performed per second, E_o, by this thrust is represented by $P \times$ distance through which the vanes are moved per second, i.e. $E_o = \frac{W}{g}(U - v)v.$

Evidently for a given jet velocity U the value of E_o will depend upon the value of v, falling to zero when $v = 0$ or $v = U$, and rising to a maximum at some intermediate value of v. By differentiating and equating $\frac{dE_o}{dv}$ to zero, the maximum value of E_o is found to be $\frac{1}{2} \cdot \frac{WU^2}{2g}$, when $v = \frac{1}{2}U$.

Now the energy per second delivered by the jet is $\frac{WU^2}{2g} = E_i$, and therefore the efficiency of the apparatus regarded as a machine, viz. $\frac{E_o}{E_i}$, cannot exceed 0·5 or 50 per cent. That the efficiency has such a low value, even under the ideal conditions here assumed, is not surprising when it is remembered that the whole of the energy still retained by the water on leaving the vanes is completely thrown away.

124. Work Done by a Jet: (*b*) when impinging tangentially on a series of *curved* moving vanes.

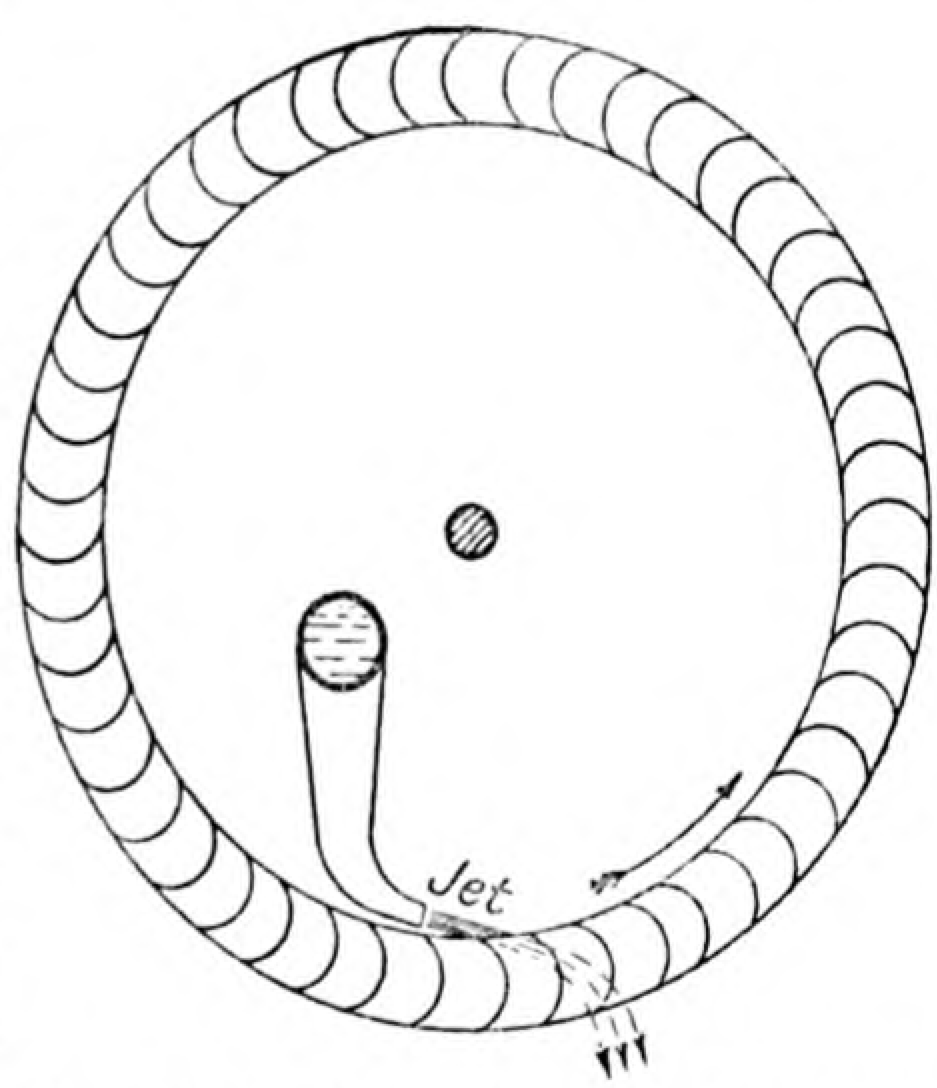

FIG. 107.—Impact on moving vanes.

Since the thrust on a stationary curved vane may be as much as double the corresponding thrust on a flat plate (§ 121), it is reasonable to suppose that the efficiency of the elementary turbine described above could be improved by substituting, as in Fig. 107, curved vanes for flat ones. To ensure that the water slides tangentially on to the blades, thereby avoiding loss of energy due to shock, it is essential that the velocity of the water *relative to the blades* should have a direction parallel to the leading edge of the blades. We therefore construct the "inlet velocity triangle," ABC, Fig. 108, in which AB represents to scale the velocity v of the vanes, AC represents the velocity U of the jet, and in which consequently the vector difference BC represents the *relative*

velocity of the water as it slides over the surface. The condition to be fulfilled is that the "inlet blade angle" α shall be identical with the angle α in the vector diagram.

In the ideal state of affairs here assumed, the water will be subjected to no frictional loss during its passage over the blades, and will therefore leave them with the same relative velocity v_r as that with which it entered; but the *absolute* velocity U_1, relative to the earth, with which the water escapes will be the vector sum of v and v_r, represented by the vector

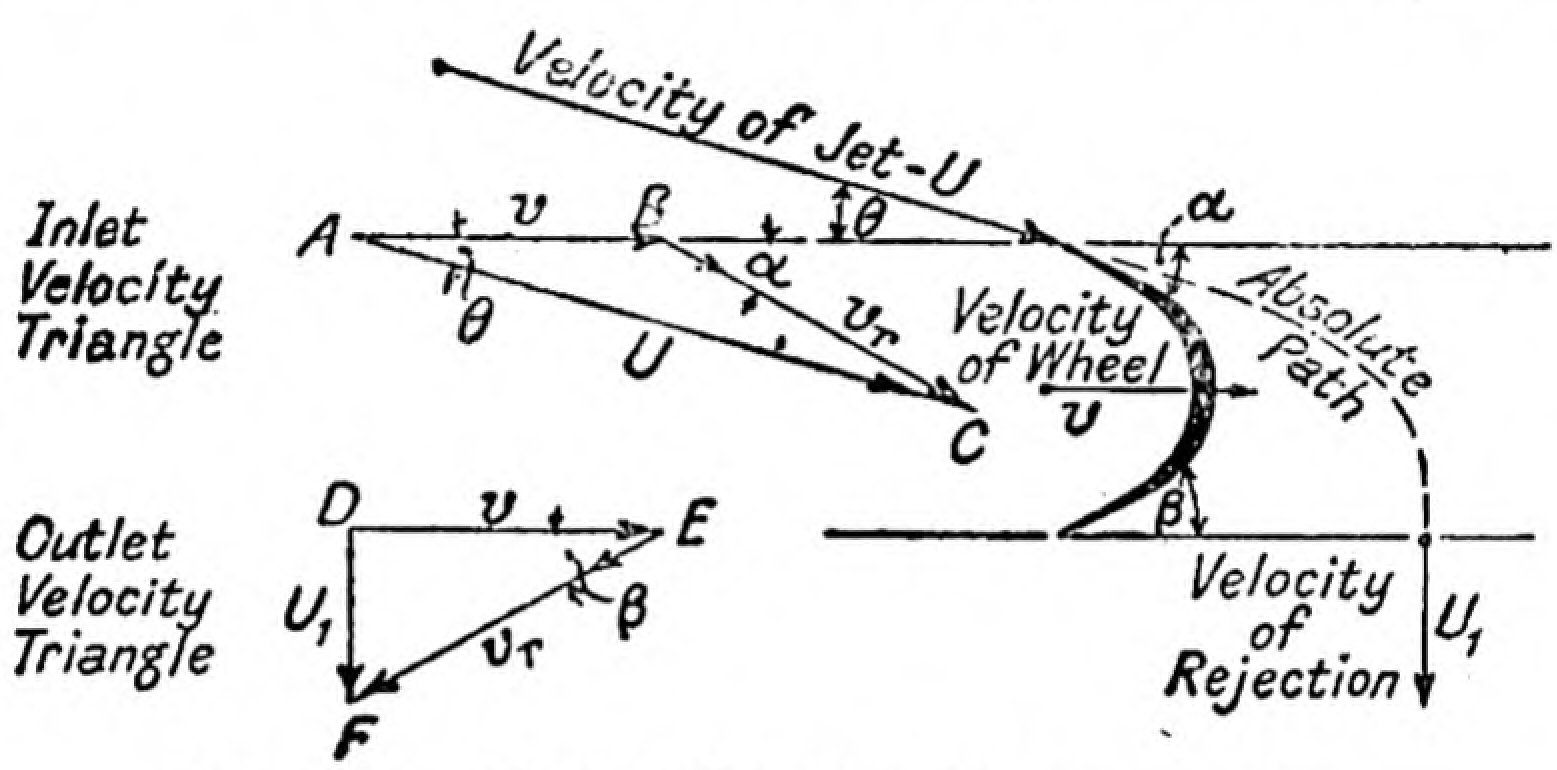

FIG. 108.—Vector diagrams for curved vanes.

DF in the "outlet velocity triangle" *DEF*. If the component of the initial absolute velocity U, in the direction of v, be denoted by V, and the component of U_1 in direction v be denoted by V_1, the dynamic thrust on the vanes is seen to be $\frac{W}{g} \cdot (V - V_1)$, and the work done per second on them, E_o, is $\frac{W}{g} \cdot (V - V_1)v$.

Alternatively we may say that the energy per second E_o given to the blades is the difference between the incoming energy and the outgoing energy per second, viz.

$$\frac{W \cdot U^2}{2g} - \frac{W \cdot U_1^2}{2g}.$$

The efficiency of the apparatus $\frac{E_o}{E_i}$ is thus seen to have the value $\frac{U^2 - U_1^2}{U^2}$, which can be brought as near as we please to unity by making U_1 sufficiently small. **(Example 54.)**

By plotting the position in space of a particle of water as it slides over a blade, the *absolute path* of the water is

obtained, as shown by the broken line in Fig. 108. The diagram makes it clear that the effect of interposing the ring of moving vanes is to bend the jet from an inclined to a more or less vertical direction, reducing its speed from U to U_1, while leaving its *pressure* unaltered.

125. Work Done by the Reaction of a Jet. This may be demonstrated by the little apparatus shown in Fig. 109. Known as *Barker's Mill*, it consists of a cylindrical vessel mounted in bearings and having at its lower end two or more radial pipes terminating in orifices from which jets may be projected tangentially. An inlet channel at the upper end feeds water into the apparatus at the rate required to maintain a steady head h above the orifices or nozzles.

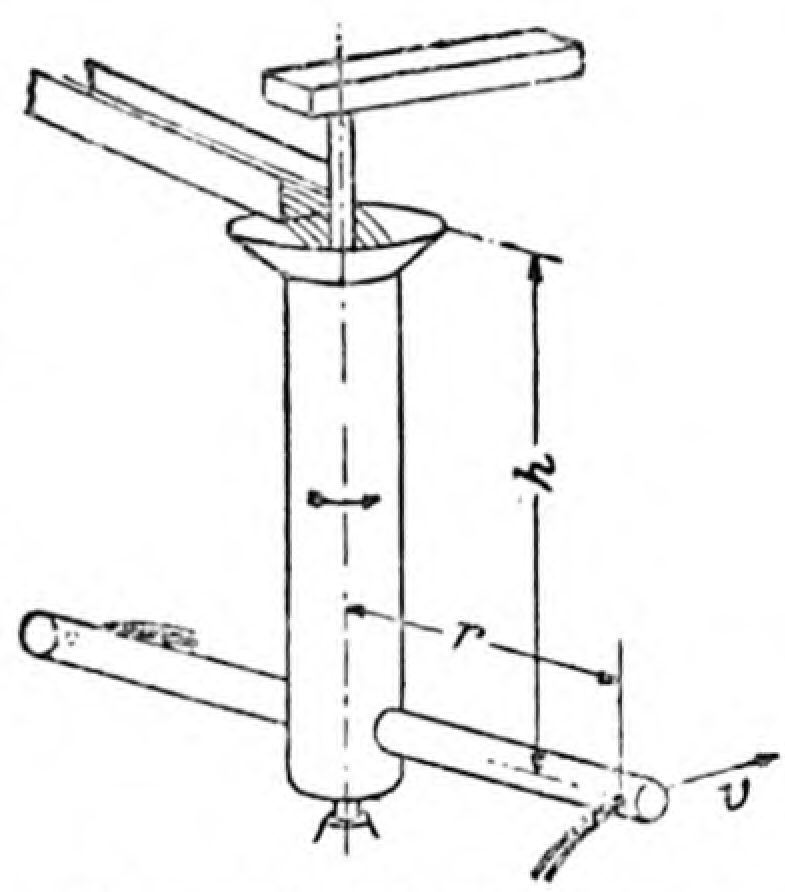

FIG. 109.—Barker's Mill.

If the mill rotates at a speed giving the nozzles a tangential velocity v, the forced vortex in the radial pipes (§ 143) will impose a centrifugal head $h_c = \frac{v^2}{2g}$ on the water in the pipes, resulting in a total head producing flow through the nozzles of $\left(h + \frac{v^2}{2g}\right)$. The velocity of efflux, or the relative velocity of the water V_r with respect to the nozzles, is thus

$$V_r = \sqrt{2g\left(h + \frac{v^2}{2g}\right)}, \quad \text{whence} \quad h = \frac{V_r^2 - v^2}{2g}.$$

Now the velocity of rejection—the absolute velocity U_1 of the water immediately after leaving the nozzles—is $(V_r - v)$. Consequently the tangential reaction exerted on all the nozzles by a total weight of water per second W flowing through them is $\frac{W}{g} \cdot [0 - (V_r - v)] = -\frac{W}{g} \cdot (V_r - v)$, (§ 122), and the corresponding energy output per second is

$$E_o = \frac{W}{g} \cdot (V_r - v)v.$$

As the energy input per second E_i is $Wh = W\dfrac{(V_r^2 - v^2)}{2g}$, (from above), the efficiency of the machine is

$$\eta = \frac{E_o}{E_i} = \frac{\frac{W}{g}(V_r - v)v}{W\left(\frac{V_r^2 - v^2}{2g}\right)} = \frac{2v}{V_r + v}.$$

This expression, it will be noticed, is of quite a different form from the expression for the efficiency of machines depending on the *impact* of jets (§§ 123 and 124). So far from reaching a maximum efficiency at a finite speed, the Barker's Mill ideally can only arrive at an efficiency of unity when its speed v is infinity. Nevertheless the basic principle of operation — the generation of dynamic thrust as a result of change of momentum—is the same in the two machines. This is easily recognised when the two are superposed, as in Fig. 110. By holding the upper ring of nozzles stationary and allowing the jets to play on the lower ring of vanes, the apparatus is made to act as an impact or *impulse* machine ; when the nozzles are released and allowed to revolve, we have a *reaction* machine (Chapter XIII).

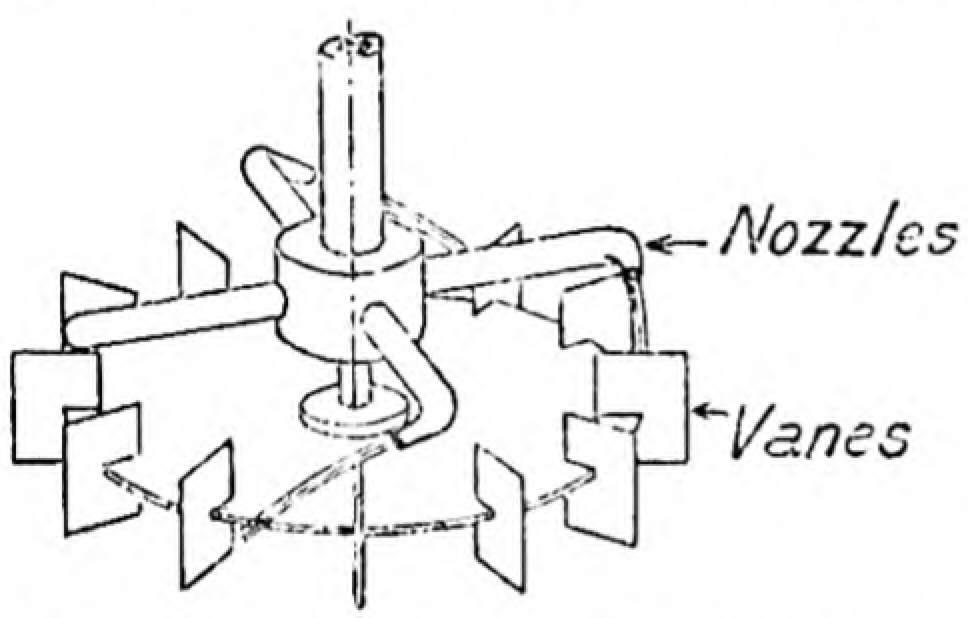

FIG. 110.—Elementary reaction turbine (above), and impulse turbine (below).

The principle of Barker's Mill may often be seen embodied in the rotary sprayers used for watering lawns.

DYNAMIC PRESSURE ON TOTALLY-IMMERSED SOLIDS.

126. Analysis of the Problem. When we attempt to apply to a solid *immersed below the surface of a flowing stream* the methods for determining dynamic thrust that have hitherto been found serviceable, we come upon various new complexities :

(i) The total angle through which the individual liquid filaments are deflected becomes indeterminate, making it impracticable to apply directly the principle of change of momentum to them.

(ii) When once the liquid elements that form a free jet have passed beyond the downstream edge of a vane or plate, they have no further opportunity of influencing the forces acting on the plate. But if the plate is immersed, then liquid filaments may curl round behind it and there exert a type of suction or negative pressure.

(iii) Especially if the submerged solid is relatively long and narrow, frictional resistance against its surface may play a dominant role; this frictional drag cannot then be dismissed merely by applying a coefficient of impact (§ 121).

(iv) The position of the object in relation to the surface, sides, or bed of the stream may affect the value of the dynamic thrust it sustains.

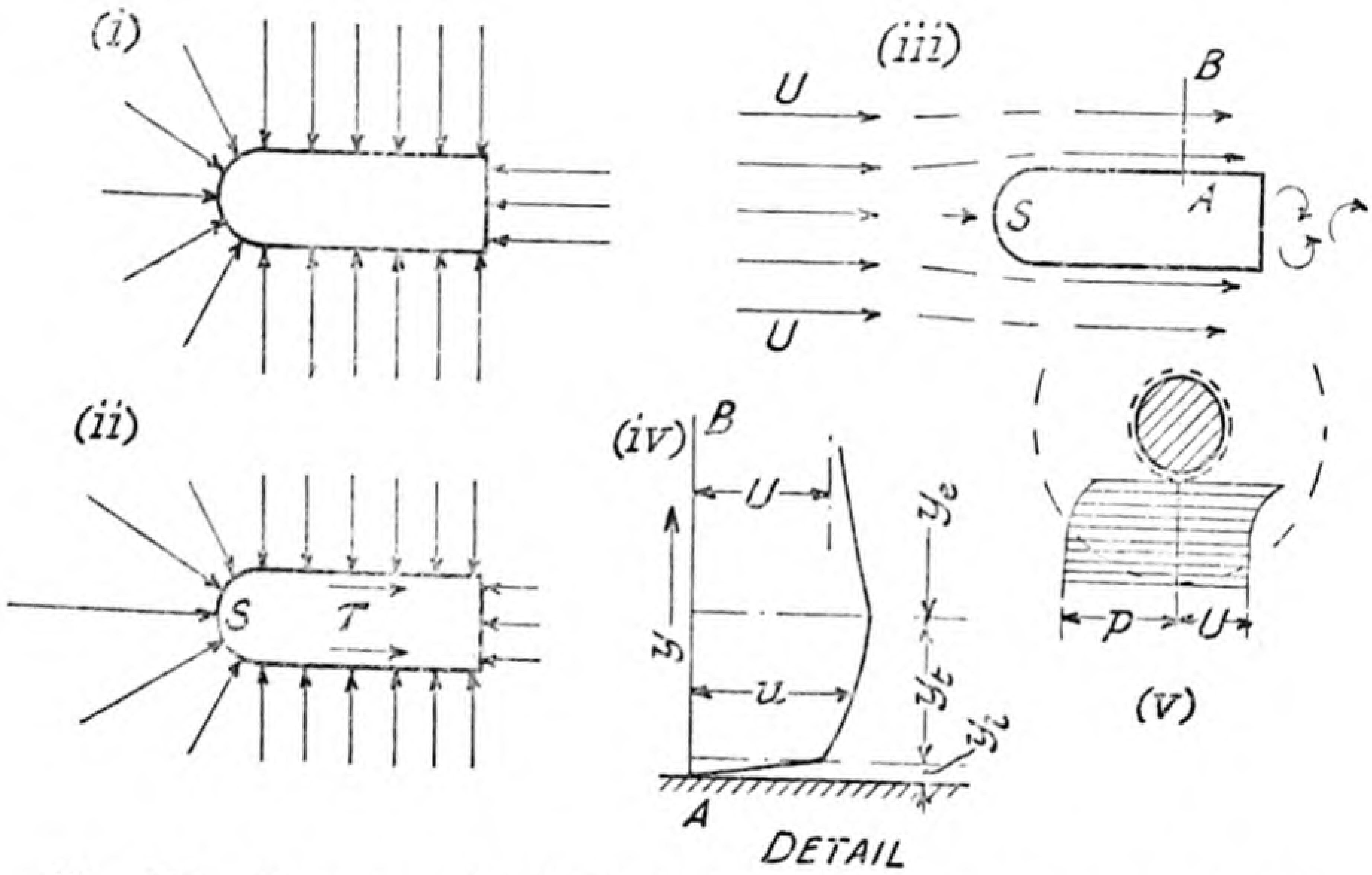

FIG. 111.—Pressure and velocity distribution near an immersed solid.

The fresh line of approach thus rendered desirable is symbolically illustrated in Fig. 111. The diagrams are intended to show: (1) How the pressure-distribution over the immersed solid is modified when the surrounding liquid begins to move; and (2) How the regime of flow of the liquid is distorted by the interposition of the solid. Choosing a solid of generalised form —in this instance a blunted cylinder presented axially to the current—we see that in diagram (i) the lengths of the arrows correspond with the uniform pressure-distribution associated with a liquid *at rest* (Chapter II). (The diameter of the solid may be assumed to be small in relation to the depth of

immersion.) When the liquid begins to move from left to right, (ii), the effect is to *increase* the pressure over the nose of the object, to *diminish* slightly the pressure over the sides, and to *reduce* considerably the pressure over the flat base. Still more significant is the appearance of tangential or shear forces $\tau\tau$. The combined result is to subject the solid to a horizontal thrust or *drag* which would sweep it downstream unless it were anchored in some way or other.

Changes in the regime of the flowing liquid are suggested in Fig. 111 (iii). Before entering the zone of disturbance set up by the solid, all the parallel filaments are imagined to be moving with uniform velocity U. Of these, the axial one that impinges normally on the nose of the solid will be brought to a standstill at the stagnation point S (§ 120); the others will be deflected through varying angles and through varying transverse distances. The composite nature of this envelope of distorted flow can be realised by examining the conditions at successive points along a radial line such as AB, diagram (iii), of which an enlarged view is given in diagram (iv). There is first a thin *boundary layer* or sheath in which the velocity rises from zero at the surface A to a maximum value U_b which is greater than the original undisturbed velocity U. It is in this region that the viscous or the Reynolds shear stresses are developed (§ 76) which are the cause of the frictional drag on the surface of the solid. The flow may be wholly viscous, wholly turbulent, or generally turbulent with a laminar sub-layer of thickness y_l (§ 78) as indicated in diagram (iv). Energy dissipation is regarded as taking place wholly in the boundary layer and in the turbulent, eddying wake that trails for a long distance downstream of the solid.(54)

Beyond the boundary layer is a zone of *uniform energy*; here energy conversion occurs but not energy destruction. In this zone, the assumed conditions are identical with those studied in § 38, Fig. 24. As suggested in Fig. 111 (v), the pressure rises and the velocity falls as we proceed outwards, until eventually we reach a region where the pressure and velocity are unaffected by the proximity of the solid.

127. Form Drag, Surface Drag, and Total Drag. The use of terms that continually recall problems of pipe flow should encourage us to make a more thorough-going comparison. A

coat-sleeve with its internal lining can serve as an image of flow in closed passages : turn the coat inside out, and there is the external boundary layer or lining ready for inspection just as it is in Fig. 111 (iv). If it was convenient to make an arbitrary separation of energy losses in pipes into frictional and secondary losses (§ 85), it should be equally advantageous to distinguish between the *surface* or frictional *drag* on an immersed solid, resulting from tangential or shear forces, and *form drag* which depends upon the re-distribution of normal pressures as a result of momentum changes and eddying. Similarly, also, the numerical value of the Reynolds number (§§ 93, 94) will guide us in assessing the relative importance of the two types of drag.[55]

Pictorial representations of surface drag and form drag, either separately or in combination, are offered in Fig. 112. The object is here imagined to be made up of two laminæ which can be shaped as required—they may be

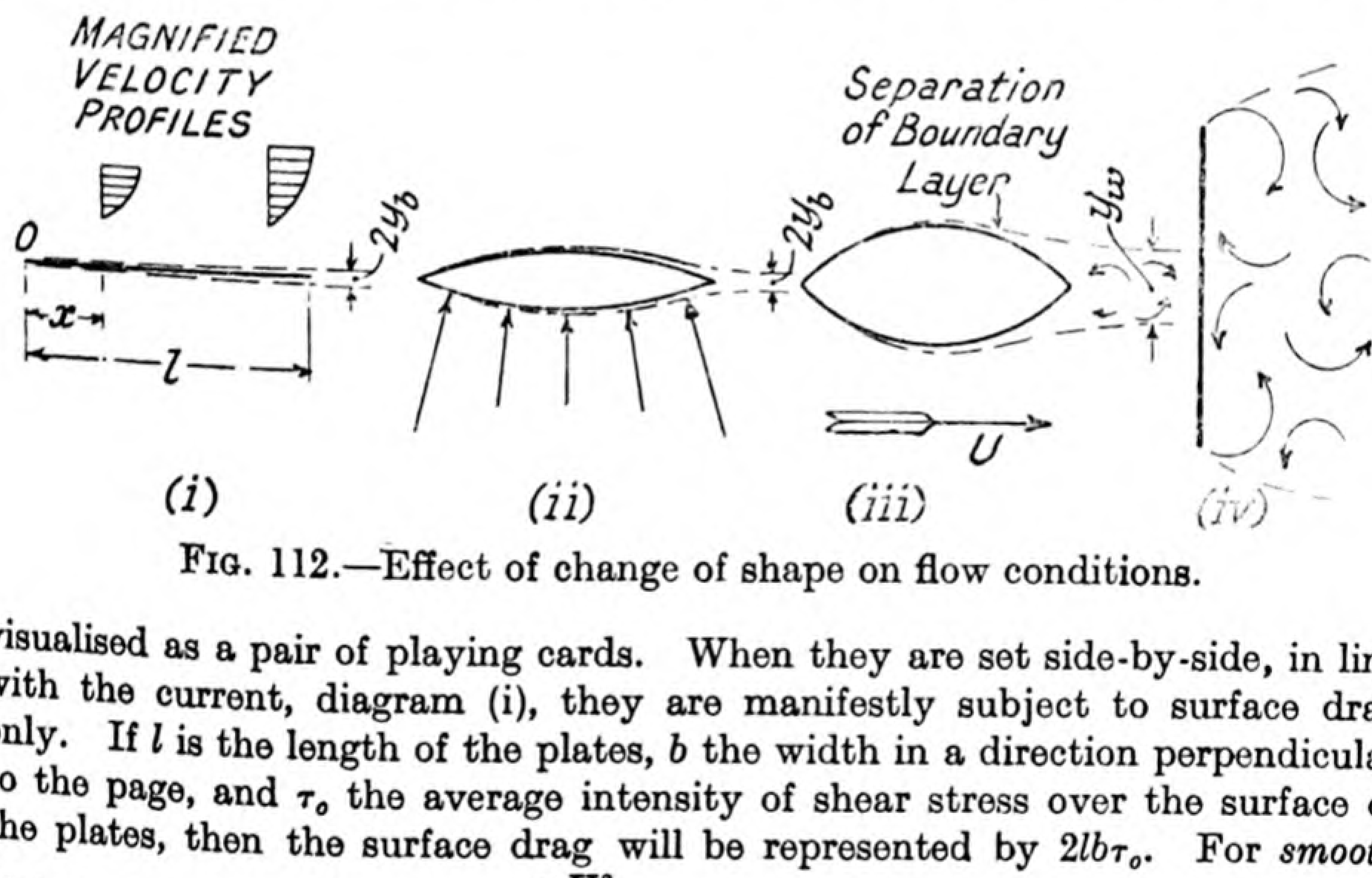

FIG. 112.—Effect of change of shape on flow conditions.

visualised as a pair of playing cards. When they are set side-by-side, in line with the current, diagram (i), they are manifestly subject to surface drag only. If l is the length of the plates, b the width in a direction perpendicular to the page, and τ_o the average intensity of shear stress over the surface of the plates, then the surface drag will be represented by $2lb\tau_o$. For *smooth* plates, we may write $\tau_o = f_d \cdot \frac{wU^2}{2g}$, where f_d is a coefficient analogous to the pipe coefficient f (§ 68). Accepting the expression $\frac{Ul}{\nu}$ as an appropriate form of the Reynolds number R_n, we may use it to evaluate the coefficient f_d thus :

$$f_d = 0{\cdot}074R_n^{-0{\cdot}2}.$$

In only one marked respect do these relationships differ from the corresponding ones applicable to pipe flow (§ 69); whereas the length of closed conduit subject to examination was so far distant from the entry that the values of τ_o and f were assumed to have settled down to steady values, this condition cannot be realised along the surfaces depicted in Fig. 112 (i). On the contrary, the intensity of the shear stress has a maximum value at the leading edge O, and thereafter rapidly diminishes. This is a consequence of

the growth in thickness of the turbulent boundary layer, and of the corresponding easing of the velocity gradient at the surface. The two magnified velocity profiles help to make this clear. Alternatively, the substitution of x instead of l in the above expressions will indicate numerically the greater average intensity of shear over the front area of the plates as compared with the average over the whole area.[56]

Suppose now that the two laminæ are caused to buckle outwards a little, which might be done by pressing the edges of our two playing cards between finger and thumb. Within certain limits, diagram (ii), this will have *no effect* either on the *boundary layers or on the drag*. Here, then, is an object of definite form which unquestionably disturbs the flow filaments yet is not subjected to form drag ; the object has been almost perfectly " stream-lined ". But when the convexity becomes excessive, (iii), then flow conditions deteriorate ; the boundary layers break away and they thicken into a turbulent wake, these changes being signalised by a sharp rise in the total drag. *Form drag* is beginning to take effect. The separation of the boundary layers is attributable to the causes explained in § 90. Considering a liquid filament moving past the object just outside the boundary layer, we observe from a comparison of Figs 111 (iii) and 112 (ii) that near the leading edge the pressure falls and the velocity rises ; but later on, as the arrows representing pressure in Fig. 112 (ii) indicate, there is a pressure rise as the filament velocity drops back to normal. It is such regions of increasing pressure that inevitably encourage separation. In diagram (ii) the boundary layers held out against this tendency ; in diagram (iii) they have succumbed. The thickness of the turbulent zone has increased from $2y_b$ to y_w.

In the final stage, (iv), the plates are set transversely across the stream. Surface drag has disappeared, for whatever shear forces are present can have no component in the direction U. But the eddying wake has now extended to a width even greater than that of the plates, affording a graphic impression of how serious the form drag must now be.

128. Evaluation of Total Drag on Symmetrical Solids. Instructive though these conceptions of surface drag and form drag may be, they are usually of less practical consequence than a knowledge of the *total drag*. The total drag P will depend upon the size, shape, roughness, and orientation of the solid body, upon the velocity U of the approaching liquid stream, and upon the Reynolds number describing the flow. If the solid is assumed to be located some distance away from the surface or the boundaries of the stream, the disturbances mentioned in § 126 (iv) may henceforward be disregarded. The customary manner of expressing the total drag is

$$P = C_D \,.\, w \,.\, a \,.\, \frac{U^2}{2g} \quad . \quad . \quad . \quad (7\text{-}8)$$

where

C_D is a *drag coefficient* whose numerical value depends upon the shape, roughness, etc., of the solid, and

a is the projected cross-sectional area of the solid on a plane transverse to the direction of the velocity U.

It will be realised that the drag coefficient represents the ratio between (i) the actual or observed dynamic thrust on the solid, and (ii) the ideal thrust that would be exerted on the projected area a if the stagnation pressure (§§ 120, 126) prevailed over its whole extent. The similarity in general structure between formula 7·8 and the alternative form of equation 7·6 (§ 121) is a reassuring confirmation of the reasoning employed.

(Example 55.)

Ref. No. Fig. 113.	Description.	Proportions.	Range of Reynolds' Number (§ 129).	Approx. Value of Drag Coefficient C_D.
i	Thin circular flat disc, normal to stream	—	> 1000	1·12
ii	Thin rectangular flat plate, normal to stream	$\frac{l}{c} = 5$	> 1000	1·2
iii	Thin rectangular flat plate, flow around ends suppressed	$\frac{l}{c} = 5$	> 1000	1·95
iv	Sphere	—	1000–200,000	0·4–0·5
v	Circular cylinder, axis normal to stream	$\frac{l}{d} = 5$	1000–100,000	0·75
vi	Circular cylinder, flow around ends suppressed	$\frac{l}{d} = 5$	1000–200,000	1·0–1·2
vii	Circular cylinder, axis parallel to stream	$\frac{l}{d} = 5$	> 1000	0·9
viii	Stream-lined solid	$\frac{l}{d} = 5$	> 200,000	0·06–0·10

Experimentally observed values of drag coefficients, applicable within a limited range of Reynolds number to various symmetrical smooth bodies, are given in the above Table and in Fig. 113.

Points requiring comment are :—

(i) *End effect.* Why should the drag coefficient of a plate or cylinder set transversely across a stream depend on its *aspect ratio*, or ratio of dimension l to dimension c or d? By studying the distribution of dynamic pressure over such objects, § 130, we observe that near the edges the pressure dies away. The same thing will happen near the ends, from which we conclude that the average intensity of pressure over a strip near the end of the transverse plate or cylinder will be less than it is near the middle. If the plate is relatively long and narrow—if it has a large aspect ratio l/c—the resulting effect on the drag coefficient will be inappreciable; but over a short, squarish plate the transverse "leaking" away of pressure may be serious. If the plate or cylinder extends completely across the stream, which in Fig. 113 (iii) and (vi) is imagined to be bounded by parallel walls,

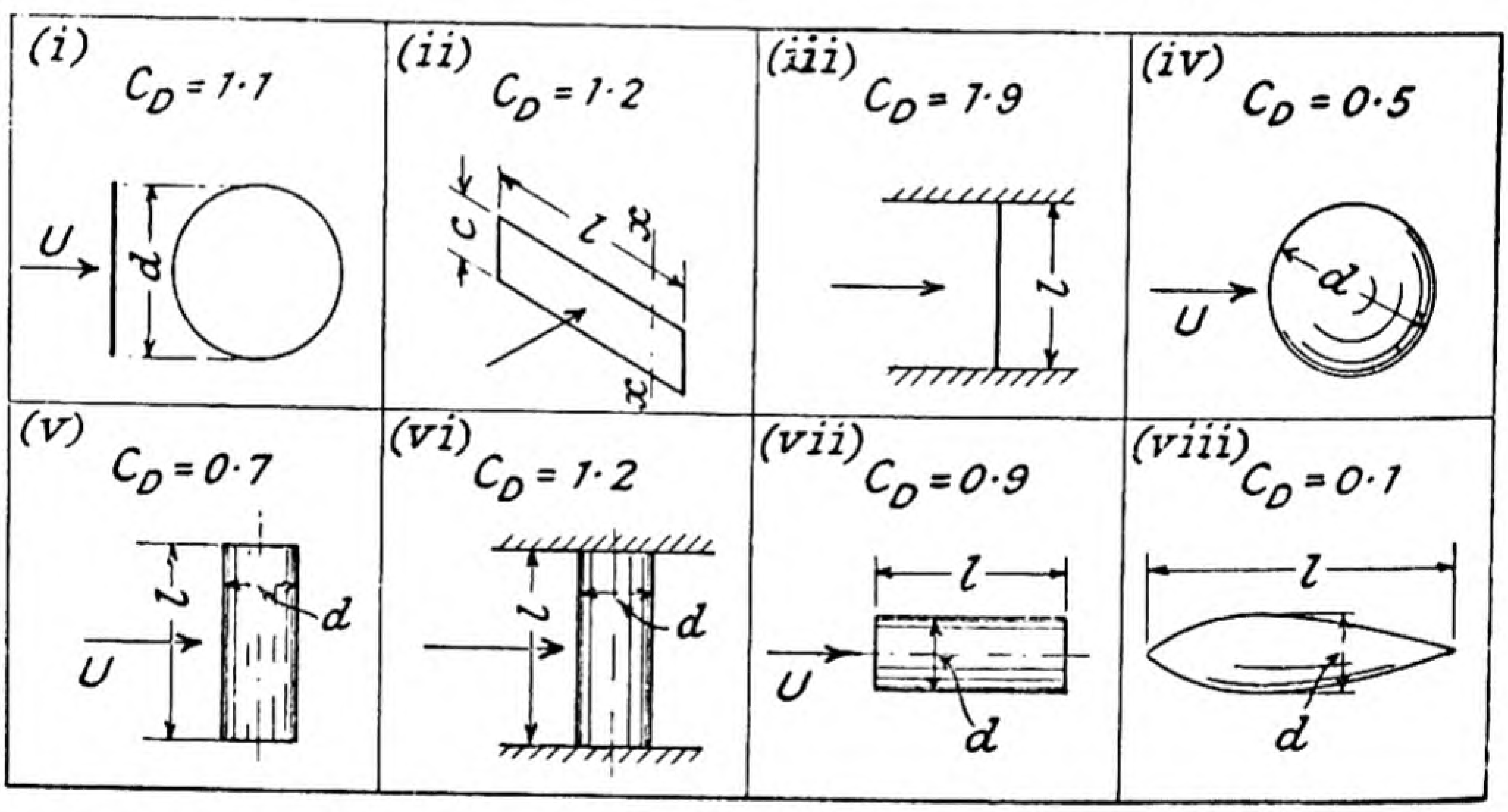

FIG. 113.—Approximate values of drag coefficients for smooth solids. (See Table.)

then the end effect is completely suppressed: the flow is two-dimensional only. The general problem has certain affinities to the suppression of rectangular weir contractions, § 55.

(ii) *Stream-lining.* Using this term in its proper sense, we note that the stream-lining of the cylinder, Fig. 113 (vii), (viii), has reduced the total resistance to about one-tenth of its original value. The reduction of energy loss consequent upon the suppression of eddying recalls the comparable effect of stream-lining a sudden pipe enlargement (§ 87): here is another instance of pipe-flow turned inside-out.

(iii) *Fixed or moving object?* Since it is the velocity of the liquid relative to the object that determines the intensity of the thrust it sustains, it is immaterial—at least in principle—whether the object is at rest relatively to the earth or whether the liquid is at rest and the object is pushed or towed through it.

129. Relationship between Drag and Reynolds Number. Before plotting for immersed solids the graphs that gave such fruitful results for closed conduits, § 94, we must establish a uniform convention for expressing the Reynolds number. For the smooth spheres and cylinders now in question, the diameter d will serve as the representative length term, wherefore $R_n = \frac{Ud}{\nu}$. There should be no surprise when it is found that experimental values of drag coefficient plotted against R_n produce curves, Fig. 114, that so closely resemble those already reproduced in Figs. 75 and 78. As before, dynamical similarity of flow for geometrically similar smooth solids will occur at identical values of the Reynolds number. It will naturally be understood that the values of drag coefficient stated in Fig. 113 and in the descriptive Table relate only to the range in which the curves in Fig. 114 are sensibly horizontal.

What might be termed the lower critical velocity for *spheres*—the velocity at which turbulent effects are completely damped out and viscous drag is supreme (§ 64)—occurs at the value $R_n = 0{\cdot}1$. Below this value the logarithmic plot of C_D against R_n is a straight line whose slope is expressed by $C_D = 24/R_n$. Inserting appropriate values from equation 7-8 yields the form $P =$ total drag on sphere $= 3\pi\mu dU$,

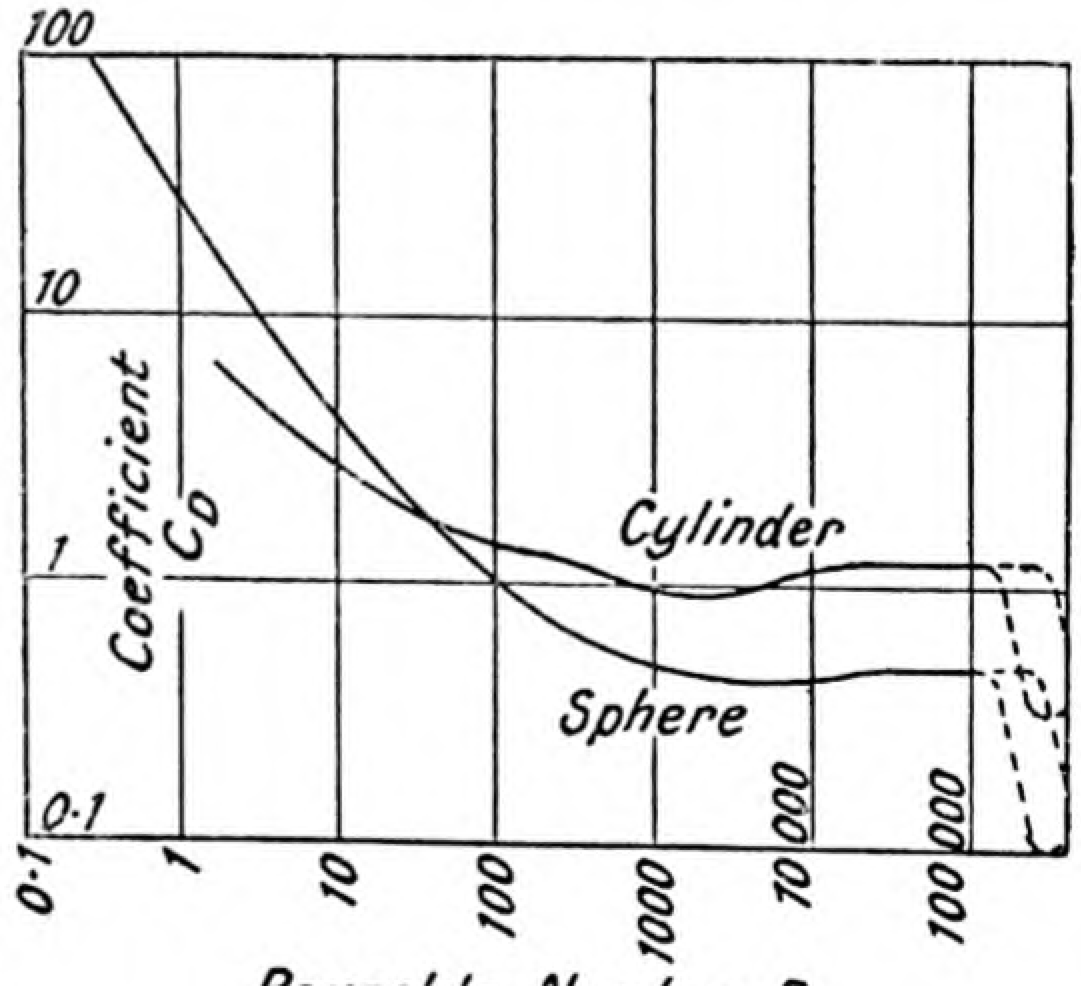

FIG. 114.—Variation of drag coefficients.

which is an expression of *Stokes' Law.* This linear connection between force and velocity is in accord with the laws of laminar flow through pipes, equation 5-5, § 65.

Terminal velocity. The measurement of the extremely small dynamic thrusts here involved is carried out indirectly by observing the *terminal velocity* of the small sphere when falling freely through a mass of stationary liquid. When acceleration has ceased and the speed of descent has attained its uniform value or terminal velocity U, then the total drag must exactly balance the apparent weight of the sphere. If

σ is the specific mass of the sphere,
ρ is the specific mass of the liquid,

then
$$U = \frac{gd^2(\sigma - \rho)}{18\mu}.$$

It is an apparent anomaly that although within this range of viscous flow the sphere seems to move through the liquid without the least disturbance—the liquid closes in behind it just as the body of a snake closes in behind the egg it is swallowing—yet in fact disturbances are propagated throughout a considerable distance But they are not turbulent or eddy disturbances: there is nothing in the nature of a wake (Fig. 112). The nature of the corrections that must be applied if the containing vessel is of restricted dimensions is suggested in § 370 (ii).

130. Pressure-distribution on Immersed Solids. The total absolute normal pressure per unit area at any point on the surface of a solid moving relatively to the surrounding liquid is made up of: (i) the static pressure of the liquid, (ii) the pressure of the atmosphere, and (iii) the dynamic or kinetic pressure resulting from momentum changes induced in the liquid. Here we are concerned only with the last item; we must remember that it is represented by the positive or negative *difference* between the total pressure at the selected point, and the total pressure at any point in the same horizontal plane in the undisturbed mass of flowing (or stationary) liquid. The conception of stagnation pressure is here as valid as it was when studying the dynamic effects of free jets (§ 120); we may thus very conveniently use it as a standard of reference, introducing a *coefficient of dynamic pressure*, C_k, to show the relation between the pressure at the point under observation, and the pressure at the stagnation point, e.g. at the point S, Fig. 111 (ii). Thus,

$$p_k = \text{dynamic or kinetic pressure} = C_k \cdot \frac{wU^2}{2g}.$$

Some actual types of pressure-distribution may now be traced.

(i) *Flat rectangular plate normal to stream.* By taking observations along a line such as xx in Fig. 113 (ii), and setting off the dynamic pressures as in Fig. 115 (i), we get a clear picture of the importance of the negative dynamic pressure at the back of the plate; the direction of the arrows, *away* from the downstream surface, indicates that the resultant *pull* is augmenting the *push* exerted on the front of the plate. The maximum value of C_k on the front

is 1·0, while at the back C_k has a fairly uniform value of 1·4. Integration of the pressure-distribution curve or pressure profile should yield the maximum value of C_D = drag coefficient = 1·95.

(ii) *Circular cylinder.* As Fig. 115 (ii) suggests, the predominating influence of suction or negative dynamic pressure is more marked now even than it was for a flat plate. At the point of the circumference directly facing the current, the stagnation pressure prevails and $C_k = 1·0$; but as we proceed round the periphery the pressure rapidly fades away. Only over about 1/6 of the circumference do we find a positive pressure; over the remaining part the dynamic pressure is negative. At first sight it is certainly unexpected to find a negative pressure over areas of the cylindrical surface that are inclined towards the current; yet as soon as we realise that the flow lines hereabouts are disposed in a kind of free vortex pattern (§ 140) it becomes less difficult to accept the notion of low pressures at the interior surfaces of curved streams.

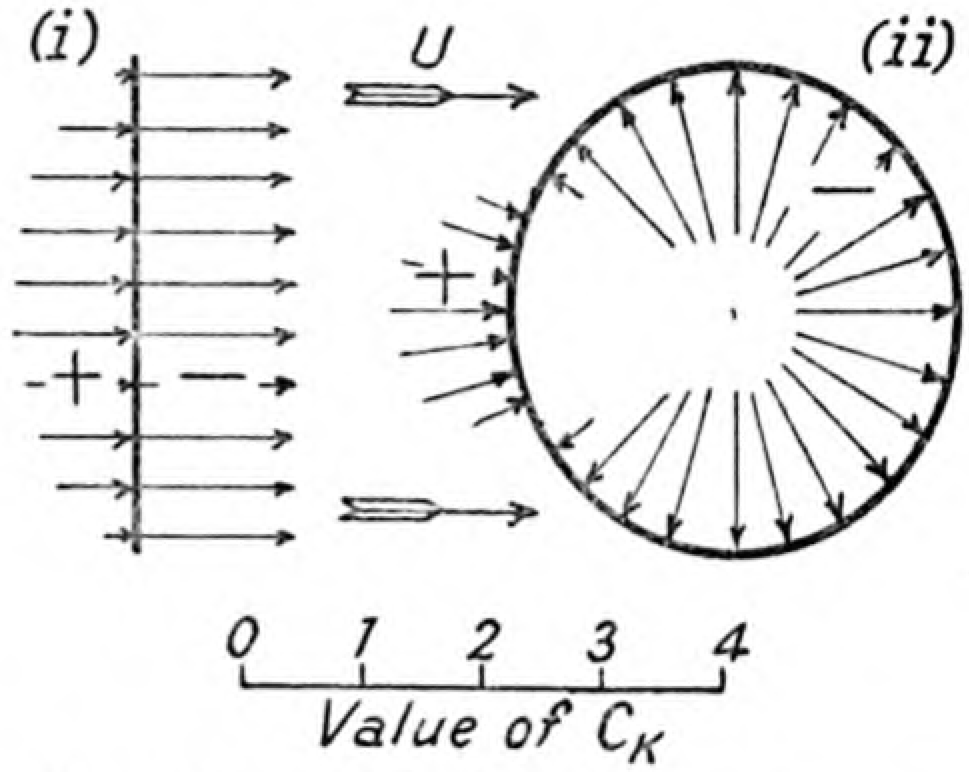

FIG. 115.—Distribution of dynamic pressure: (i) plate, (ii) cylinder.

Indeed, such low pressure zones were specifically shown in Fig. 24, § 38, which relates to exactly the conditions now in question.

(iii) *Stream-lined solid.* Accepting Fig. 112 (ii) as a crude presentation of the absolute pressure-distribution over a typical stream-lined object, we observe that at corresponding areas near the nose and near the tail, the absolute pressures appear to be equal. Thus if it were not for the distortion introduced by the boundary layers, the resultant thrust in the direction of U would be zero, i.e. the form drag would be zero. This is no longer even approximately true for the imperfectly stream-lined solid, Fig. 112 (iii); because of the separated and thickened boundary layer, the absolute pressure on the tail area has fallen off relatively to the pressure at the nose. It is this difference which lies at the root of form drag in such conditions.

131. Dynamic Thrust in Inclined Surfaces. Leaving now the consideration of symmetrical solids set axially with the current, we come upon conditions resembling those illustrated in Figs. 103 and 104; if a plate or blade is set obliquely across the flowing stream, then there will be a transverse component of the thrust corresponding to P_n (§ 121). When immersed solids are in question it is usual to designate this component the *lift*, denoted by the symbol L; the *drag*, now denoted by D, is regarded as the component of the total dynamic thrust P which is parallel with the original velocity vector U. For a blade of aerofoil section the relative magnitudes of lift and drag are indicated in Fig. 116 (A). Their numerical values

are computed from the expressions—

$$\left.\begin{aligned}\text{Lift} &= L = C_L \,.\, bc \,.\, \frac{wU^2}{2g} \\ \text{Drag} &= D = C_D \,.\, bc \,.\, \frac{wU^2}{2g}\end{aligned}\right\} \quad . \quad . \quad (7\text{-}9)$$

These, it will be noticed, are a little different from equation 7-8; the representative area bc is no longer the projected area on a plane transverse to the flow, but is related to the *chord* or *blade width* c. The small-scale plans in Fig. 116 make it clear

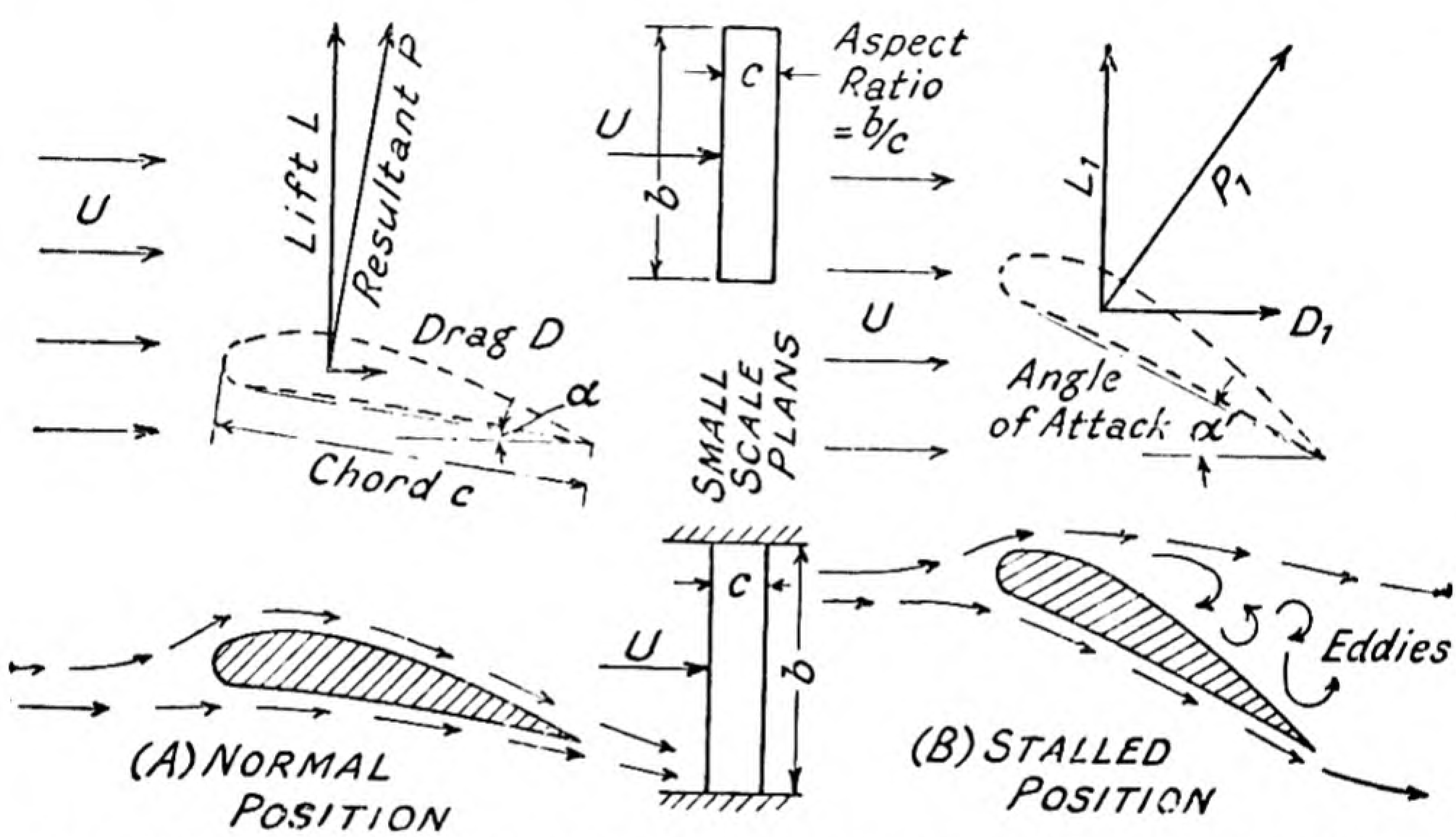

FIG. 116.—Forces on aerofoil in (A) normal position, (B) stalled position.

that the dimension b is what we should call the *span* of an aeroplane wing. The upper view shows a wing of finite aspect ratio (§ 128 (i)); in the lower view the "end effect" is eliminated and conditions are equivalent to an infinite aspect ratio.[57]

A new term has now to be introduced when evaluating the lift coefficient C_L and the drag coefficient C_D; it is the *angle of attack* α, or the angle between some arbitrarily chosen reference line on the blade cross-section, and the direction of the velocity vector U. As before, C_L and C_D will depend upon blade shape, surface roughness, Reynolds number, and aspect ratio (§ 128); but it is the angle of attack which has the overmastering effect. The typical graphs in Fig. 117 show the opposing trends to which the lift coefficient and the drag coefficient are subjected. As we should expect, the connection between small variations of α and changes of C_L recalls the

corresponding correlation between θ and P_n, § 121 (*c*); but as α progressively mounts, the slope of the graph falls away; the lift coefficient reaches a maximum value and then actually diminishes. Meantime the drag coefficient, which at first was relatively insensitive to changes of α, now climbs more and more rapidly.

These tendencies are expressed vectorially in Fig. 116; comparing diagrams (A) and (B), we see that as the angle of attack rises from α to α_1, the lift declines from L to L_1, while

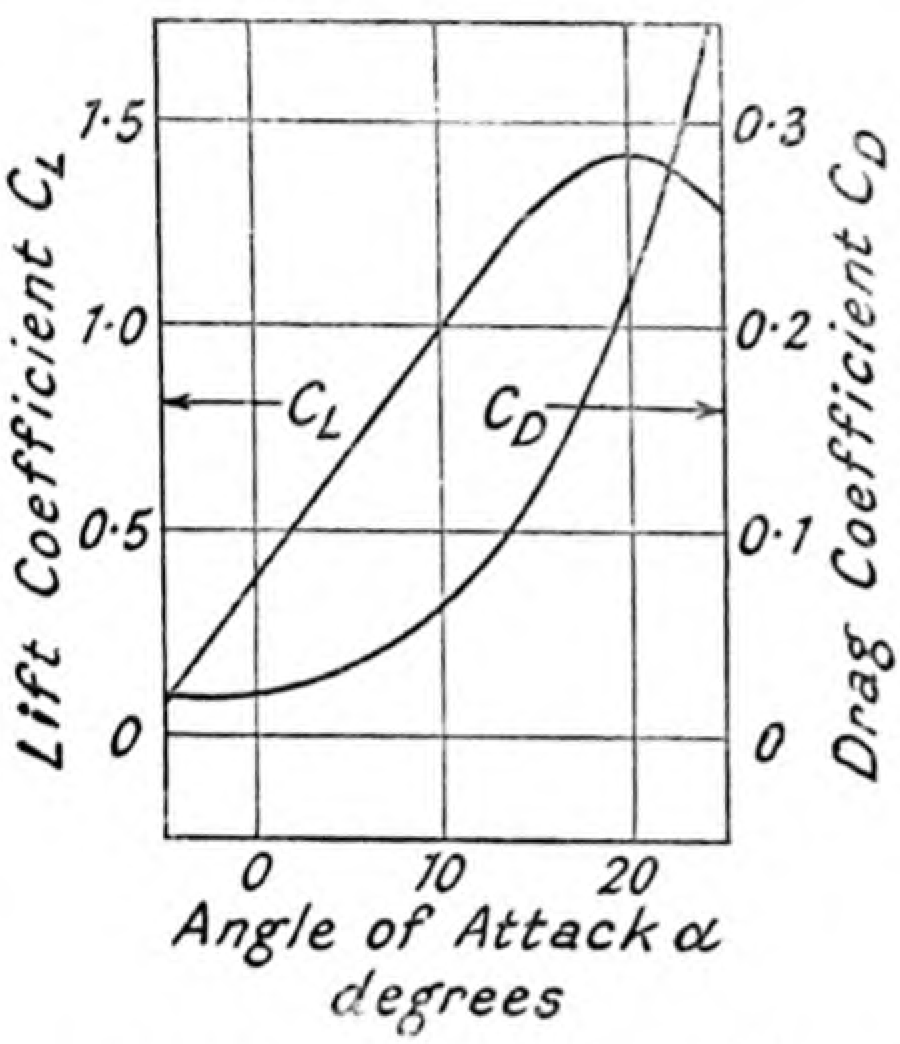

FIG. 117.—Typical aerofoil performances.

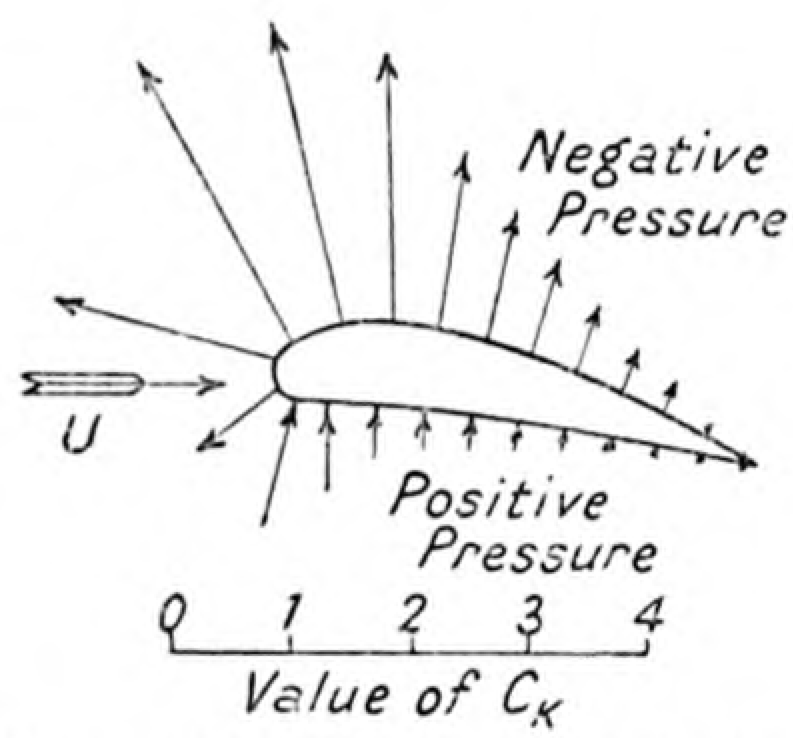

FIG. 118.—Pressure-distribution on aerofoil.

the drag rises from D to D_1. Once more it is the separation of the boundary layer which is responsible (§§ 90, 127); with increasing angles of attack, the flow filaments outside the boundary layer are no longer able to follow the profile of the blade surface. The consequent onset of eddying depicted in diagram (B) fully accounts for the deterioration in the blade performance. When the blade has been tilted so sharply that the lift has reached its maximum and has begun to fall again, the blade is said to be *stalled*.

The pressure-distribution diagram, Fig. 118, shows that on inclined surfaces, no less than on symmetrical ones, it is the negative dynamic pressures that account for the greater part of the total dynamic thrust. In this particular example, the numerical value of the negative dynamic pressure near the leading edge of the upper surface of the blade is more than double the stagnation pressure.

In a book devoted exclusively to Hydraulics and not to Aerodynamics, it would be quite proper to use the term " hydrofoil ", rather than aerofoil, for the inclined surfaces just discussed. The study of the forces and pressures acting upon such solids, or upon any solids immersed in a flowing stream, is not dependent upon the type of stream. It need not be an open channel having a free surface exposed to the atmosphere. Indeed, when making experimental observations it may be much more convenient to mount the object in a closed conduit. Water can be forced through such a " water tunnel " at controlled rates, and the absolute pressure can likewise be independently controlled.[58]

132. Distribution of Absolute Pressure. In the diagrams that illustrate the preceding paragraphs, e.g. Figs. 111, 115, and 118, a system of vectors has been chosen to represent the pressure at any point on the surface of the immersed solid. According to one convention, the length of the arrows showed to scale the gauge pressure, while in another context the arrows showed the kinetic or dynamic pressure, § 130. For studying certain kinds of problem, still another method of presentation is advantageous ; it is based upon the treatment outlined in § 38, Fig. 24(*b*). Either by constructing the flow net as there explained, or by actual pressure-measurements, the type of diagram shown in Fig. 119 is obtained. The immersed object indicated to a greatly enlarged scale by the broken line is the cylinder with blunted nose already mentioned in § 126. Absolute pressures (§ 14), are set off against a datum line of zero pressure ; the pressure line represents the absolute pressure prevailing at points on the surface of the solid at the same elevation as its axis.

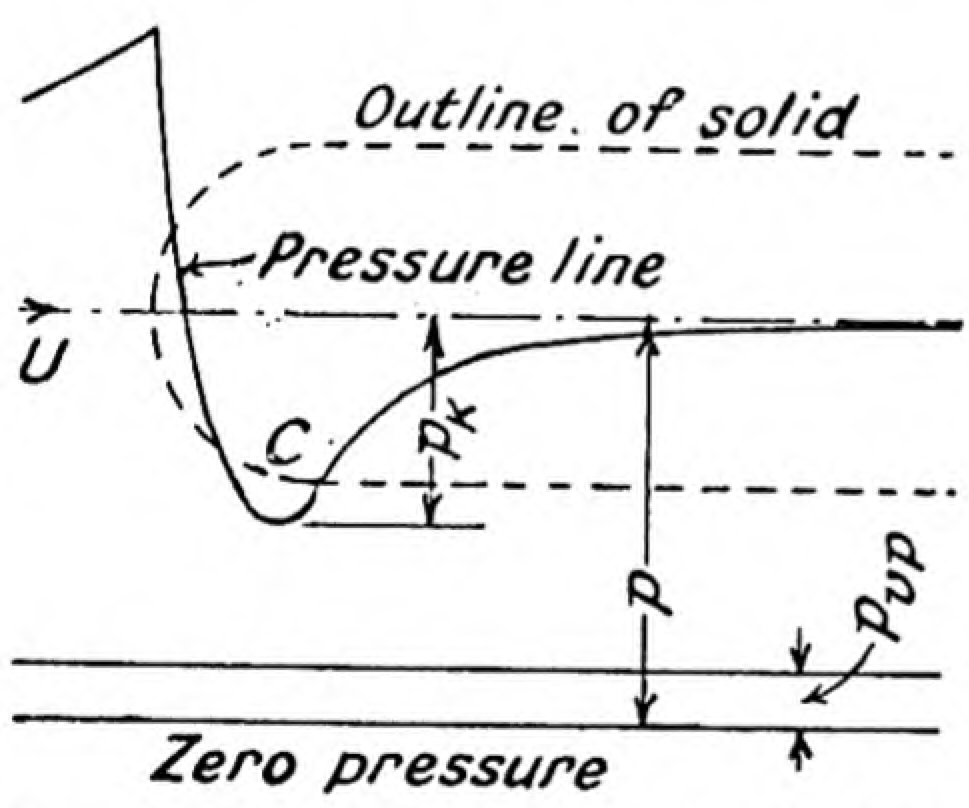

FIG. 119.—Distribution of absolute pressure on cylindrical solid set axially to stream.

Comparing this diagram with the original one, Fig. 111 (ii), we now find that the latter only displayed in a rough or provisional way the pressure-distribution over the solid surface. Both diagrams correctly show the stagnation pressure or maximum pressure at the nose of the solid ; but the corrected diagram Fig. 119 reveals a most important new trend—it is the pronounced downward sweep of the pressure-line as the

liquid elements travel round the nose of the object. A quite significant *negative* kinetic pressure p_k is thereby generated; or in other words the absolute pressure falls to a value considerably below that prevailing in the undisturbed liquid. As will be explained in § 135, this dip in the pressure-line may have a critical importance.

In regard to the relation between Fig. 119, which we may now regard as a true record of pressure-measurement, and the type of diagram, Fig. 24, which depended upon the form of the flow-net, it is to be remembered that the one involves a real liquid in which viscous forces operate, whereas in the other diagram they were ignored.

Cavitation Phenomena.

133. Causes of Cavitation. Cavitation is the name given to the phenomena that occur at the solid boundaries of liquid streams when the negative pressure rises to its limiting value. As explained in § 16, this limiting negative pressure is the one at which the *absolute* pressure is equal to the vapour pressure of the liquid at the prevailing temperature. No lower pressure can possibly be attained; any attempt to reduce the absolute pressure still further merely makes the liquid boil more briskly. How can the motion of liquids create these considerable negative heads? The pressure profiles reproduced in Figs. 115, 118 and 119 suggest one possibility. If, in a given horizontal plane in a liquid stream, the gauge pressure in the undisturbed stream is p_g and the negative dynamic pressure at the surface of an immersed solid is p_k, then the absolute pressure at the selected point on the surface is $p_a + p_g - p_k$. It is only a matter of stipulating a high enough stream velocity U to ensure that $p_a + p_g - p_k$ is brought down to the value of the vapour pressure p_{vp}. **(Example 56.)**

The study of flow in closed passages has likewise revealed numerous opportunities of generating negative heads. Consider, for example, the diverging mouthpiece illustrated in Fig. 30, § 47; here is a negative head h_2 which can be made as great as we wish just by increasing the outlet area a_3. In Figs. 68 and 69, § 87, the hydraulic gradients similarly make a downward sweep whose extent is quite within our control. Now, in Fig. 120, the negative head produced downstream of

a partially closed valve is related to a free liquid surface, thus permitting a graphical statement of the connection between the head h_a corresponding to atmospheric pressure, the head h_{vp} corresponding to vapour pressure, and the limiting negative head h_n. The stage is set for cavitation to begin. What kind of performance may we expect? The performers will be bubbles: bubbles of air and bubbles of vapour. Any reduction of pressure is likely to liberate from solution small amounts of dissolved air and other gases (§ 11); a reduction of pressure on the scale we now have in mind will release in far greater numbers bubbles of *vapour*.

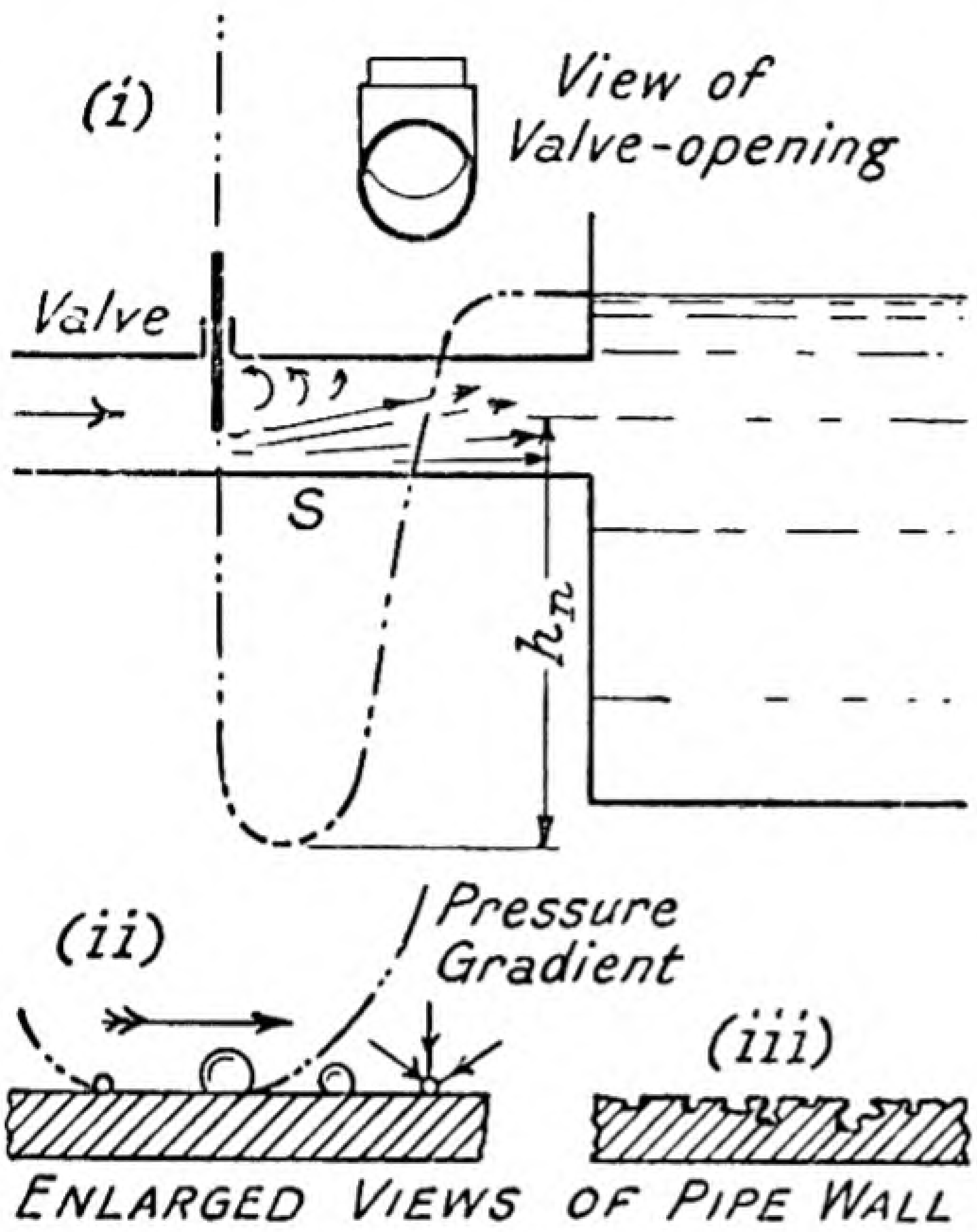

FIG. 120.—Cause and effect of cavitation.

The stage itself is the area S of the inner surface of the pipe immediately downstream of the valve—enlarged views of it, before and after the performance, are given in diagrams (ii) and (iii). Evidently it is no light comedy the actors are going to present, but rather a tragedy of destruction.

134. Effects of Cavitation. By plotting in diagram (ii), Fig. 120, the absolute pressure gradient in relation to a datum which is set a distance p_{vp} below the pipe surface, we can see how the rapidly moving liquid elements enter and leave a zone of pressure in which boiling will certainly occur. Vapour bubbles will grow while the liquid traverses this zone; they will collapse immediately they pass beyond it.[59] The life of the bubbles is thus very transient indeed: it may occupy 1/100 of a second or less. It is exactly this rapidity of collapse which charges the tiny bubbles, only a few millimetres in diameter, with their malign potentialities. The symbolical picture of the death of a bubble at the right of diagram (ii) shows clearly enough that the liquid advancing into the cavity left by the bubble will have a component normal to the pipe wall, and it is not difficult to imagine

that when the liquid elements are ultimately stopped by the solid surface a species of *water hammer* will be induced (§§ 114-118). But what is difficult to realise, and what can only be demonstrated by mathematical analysis, is that movements on so insignificant a scale may be capable of generating *infinitely great* inertia pressures.[60] It is true that the very high pressures that are, in fact, experienced only operate over extremely minute areas; but as the collapse of each bubble is thus the occasion of a very small but very real hammer-blow delivered to the metal forming the pipe wall, it is only a matter of having enough bubbles acting over a sufficiently long period for destruction of the metal to begin. An impression of the pitted, devastated appearance of metal subjected to prolonged attacks of this kind is offered in Fig. 120 (iii), and in Fig. 408, § 348. Quite probably the process is accelerated by the newly released oxygen in the *air* bubbles.

It is the cavities filled with vapour, then, that earn for these phenomena their title of cavitation. If the surfaces that form the seat of cavitation belong to immersed solids (§§ 130, 131), there is a double justification for interpolating this description in a chapter devoted to dynamic pressure: dynamic effects first of all create the low-pressure conditions favourable to bubble-formation, and it is in the superimposed dynamic sequence of bubble-collapse that damage to the metallic surface originates.

The results of allowing cavitation to arise may thus be summarised[61] :—

(i) The metallic or concrete walls that contain the liquid streams may be damaged or ultimately completely destroyed (§§ 282, 348).

(ii) Audible crackling or rattling may be noticed, which may grow into dangerous vibration when large structures are involved.

(iii) The milky appearance of the liquid, brought on by the generation of vapour bubbles, is an indication of a transitory reduction of density.

(iv) The entire system of pressure- and velocity-distribution near the affected region may be distorted (§§ 281, 335).

To eliminate or minimise these evils, it is manifestly desirable either to rearrange water-levels, pressures, or velocities in

order to raise the minimum absolute pressure, or else to use specially resistant metals, e.g. stainless steel or chrome-nickel steel, in the threatened areas. As will now be shown, there is also the valuable possibility of improving the *shape* of the solid surfaces.

135. The Cavitation Number. Since the most destructive effects of cavitation occur actually at the solid boundaries in contact with the liquid, these phenomena can only properly

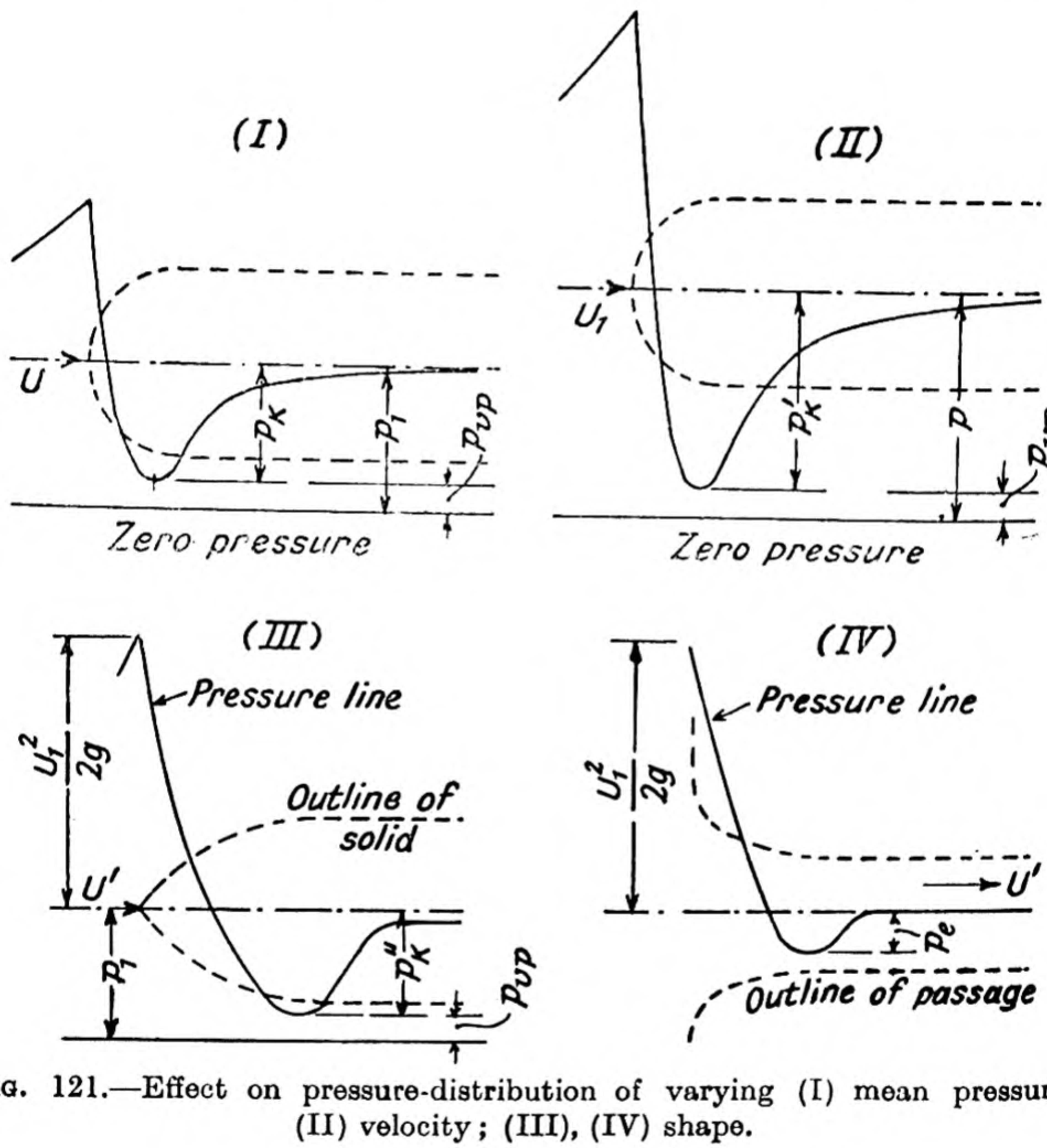

FIG. 121.—Effect on pressure-distribution of varying (I) mean pressure, (II) velocity; (III), (IV) shape.

be controlled if we know the true distribution of absolute pressure at these boundaries. In this respect the pressure-line sketched in Fig. 120 (i) was inadequate, because it only described the mean flow. We therefore turn to diagrams such as Fig. 119, where the variables in question are graphically set out for our inspection. This particular diagram, relating

to an immersed solid, shows that there is little risk of cavitation: even over the area C of the solid which is exposed to the lowest absolute pressure, there is a comfortable margin between this minimum and the vapour pressure p_{vp}. What happens if conditions are altered? Two possibilities are presented in Fig. 121. In diagram (I), where the solid and the shape of the pressure-line are identical with those of Fig. 119, the only change has been in the absolute pressure at the solid axis: this has been reduced from the value p to the value p_1. But this change has brought about momentous consequences, for the margin available in Fig. 119 has now disappeared: the pressure-line touches the vapour-pressure line, and the critical stage has been reached at which cavitation will begin.

In Fig. 121 (II) it is the approach velocity of the liquid that has been adjusted: it has increased from the value U in Fig. 119 to U_1 in diagram (II), the pressure p at the axis remaining unchanged. Yet the result is the same as before: as a consequence of the magnified dip in the pressure-line, its lowest point has touched the vapour-pressure line and cavitation conditions have been established.

Here, then, are two alternative methods of dealing with an identical immersed solid which create identical cavitation conditions. We may therefore reasonably expect to find some identical mathematical relationship which will describe both methods; and it should preferably be a non-dimensional one, § 40. A very convenient expression is termed the *cavitation number* or criterion or parameter. It is represented by the symbol σ_k, and has the form

$$\sigma_k = \frac{p - p_{vp}}{\left(\dfrac{wU^2}{2g}\right)}$$

where p denotes the absolute pressure in the undisturbed flow of liquid,

p_{vp} denotes the vapour pressure of the liquid,

and U denotes the velocity in the undisturbed liquid.

The significance of the cavitation number can be understood by comparing it with another non-dimensional criterion, the coefficient of dynamic pressure, C_k, which has the value

$p_k \Big/ \frac{wU^2}{2g}$ (§ 130). If in the present context we agree that C_k and p_k will refer to the maximum negative dynamic pressure anywhere on the surface of the immersed object, it follows that at the critical stage represented in Figs. 121 (I) and (II) we may write

$$p_k = p - p_{vp}.$$

But

$$p_k = C_k \cdot \frac{wU^2}{2g},$$

and

$$p - p_{vp} = \sigma_k \cdot \frac{wU^2}{2g},$$

from which it follows that $\sigma_k = C_k$. But since C_k is by definition constant for the given solid, the limiting value of σ_k is likewise constant: it applies impartially to the two diagrams (I) and (II). As for the conditions in Fig. 119, the descriptive cavitation number is there much higher, showing that cavitation is *less* likely to occur.

A particular advantage of the treatment developed in this paragraph is that it reveals the very important influence of the *shape* of the solid surface in question. If the nose of the solid were to be modified, e.g. made more pointed, then the downward dip of the pressure-line, Fig 121 (II), might be reduced—with a corresponding decline in the risk of cavitation. Such an improvement is shown in Fig. 121 (III), where, for the same velocity as in diagram (II), a lower absolute pressure p_1 is permissible.

A final diagram, Fig. 121 (IV), serves as a comment on the original diagram of the series, Fig. 120. Here is a pressure line which does indeed represent conditions at the wall of the passage; the passage in this instance being the entry to a closed conduit, as in Fig. 65 (*a*), § 86. The shape of the pressure line could be predicted by the use of a flow-net as in Fig. 22, § 38, and it could likewise be traced by electrical analogy methods that are now frequently used.[62]

Impact of One Liquid Stream upon Another.

136. Dynamic Pressure at a Sudden Enlargement in a Pipe. When a stream of water emerges with velocity v_1

from a pipe of diameter d_1 and area a_1, and impinges on the mass of water moving with a smaller velocity v_2 in a larger pipe d_2, of area a_2 (Fig. 122), it is possible here also to calculate the resulting rise of pressure p_i, by the principle of change of momentum. Let us consider the water contained between the two transverse planes XX and YY. Since this water is being neither accelerated nor retarded, the total thrust P_x on section XX must be equal to the total thrust P_y on section YY (friction being neglected).

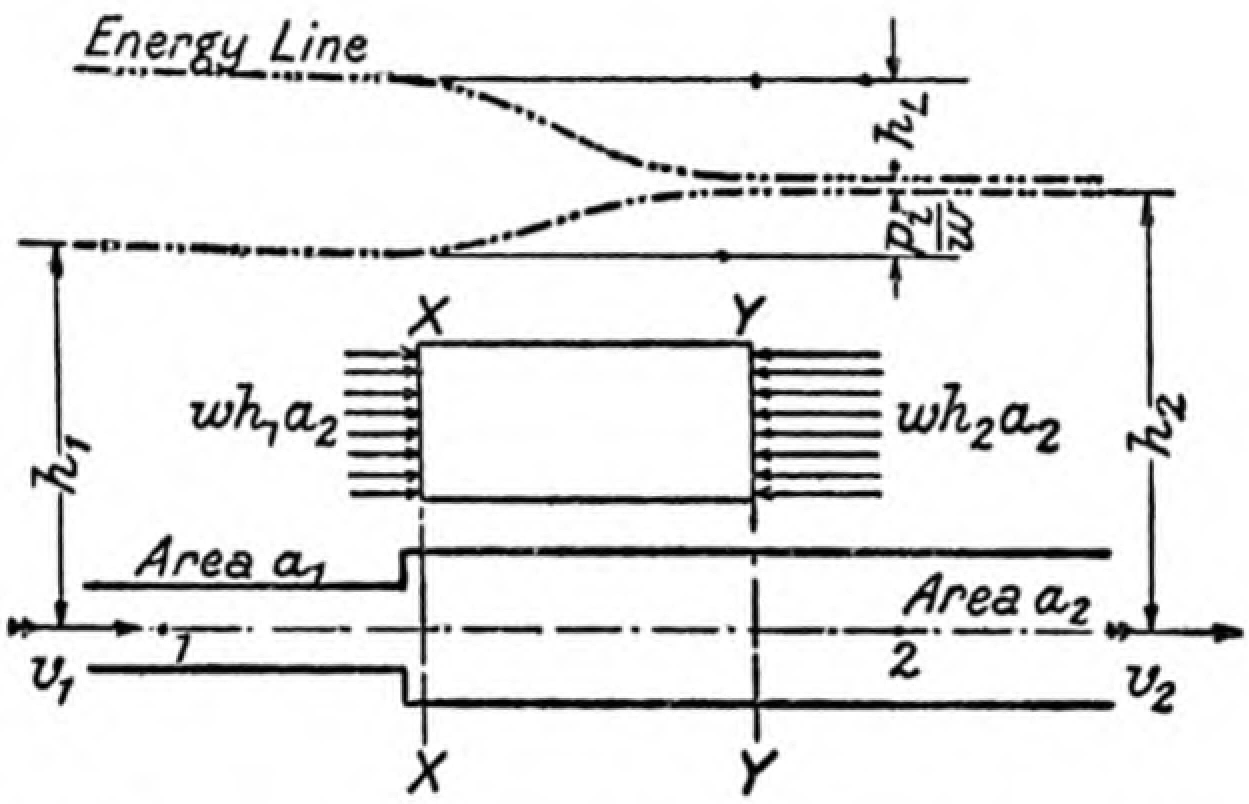

FIG. 122.—Pressure and energy changes at a sudden enlargement.

Now if h_1 and h_2 are the respective static heads at the two sections, the static thrust wh_2a_2 on section YY is manifestly greater than the static thrust wh_1a_2 on section XX, therefore equality between P_x and P_y is established by using the conception of a dynamic thrust P_d, such that $P_x + P_d = P_y$.

As before, dynamic thrust P_d = change of momentum per second

$$= \left(\frac{w}{g} \cdot v_1a_1\right)v_1 - \left(\frac{w}{g} \cdot v_2a_2\right)v_2.$$

But because of the constancy of discharge through the pipe,

$$Q = a_1v_1 = a_2v_2,$$

whence $$P_d = \frac{w}{g} \cdot (v_1 - v_2)a_2v_2.$$

Inserting this value in the equation $P_x + P_d = P_y$, we obtain

$$wh_1a_2 + \frac{w}{g}(v_1 - v_2)a_2v_2 = wh_2a_2,$$

whence $$w(h_2 - h_1) = \frac{w}{g} \cdot v_2(v_1 - v_2) = p_i,$$

which is the increase in pressure at the sudden enlargement. (Example 57.)

At once the loss of energy h_L can be calculated. Applying Bernoulli's equation to points 1 and 2,

$$h_1 + \frac{v_1^2}{2g} = h_2 + \frac{v_2^2}{2g} + h_L,$$

whence $$h_L = \frac{v_1^2}{2g} - \frac{v_2^2}{2g} - (h_2 - h_1).$$

Substituting the above value for $(h_2 - h_1)$,

$$h_L = \frac{v_1^2}{2g} - \frac{v_2^2}{2g} - \frac{v_2(v_1 - v_2)}{g} = \frac{(v_1 - v_2)^2}{2g}$$

which agrees with equation 4-3, § 46.

(*Note.*—Although this analysis yields results which compare reasonably well with experimental values, it is founded on dubious assumptions. As is shown in Fig. 66, the transition from velocity v_1 to velocity v_2 is not carried out suddenly ; it rather takes the form of a gradually expanding stream surrounded by a zone of eddies. Thus the statement in the first part of this paragraph, that the water is being neither accelerated nor retarded, does not necessarily apply to individual elements of water.

137. Dynamic Pressure at a Sudden Enlargement in the Cross-section of an Open Stream. The reasoning followed in the preceding paragraph can readily be adapted to the problem of finding the height of a standing wave in an open channel (§ 108). Let d_1 and d_2 now represent the upstream and downstream depths respectively in the channel (Fig. 123), which may be assumed to be of rectangular cross-section of unit width, the discharge being denoted by q.

As before, dynamic thrust P_d exerted on the water between sections XX and YY

$$= \left(\frac{w}{g} \cdot v_1 d_1\right)v_1 - \left(\frac{w}{g} \cdot v_2 d_2\right)v_2$$

$$= \frac{w}{g} \cdot v_1^2 \cdot d_1 - \frac{w}{g} \cdot v_1 d_1 \cdot \frac{v_1 d_1}{d_2} \text{ (because } v_1 d_1 = v_2 d_2 = q),$$

$$= \frac{w}{g} \cdot v_1^2 d_1\left(1 - \frac{d_1}{d_2}\right).$$

The static pressure, however, is now no longer uniform over section XX or YY; it varies with the depth as shown by the hatching (§ 18). Hence

$$P_x = \text{static thrust on section } XX = \frac{wd_1}{2} \cdot d_1,$$

$$P_y = \text{static thrust on section } YY = \frac{wd_2}{2} \cdot d_2.$$

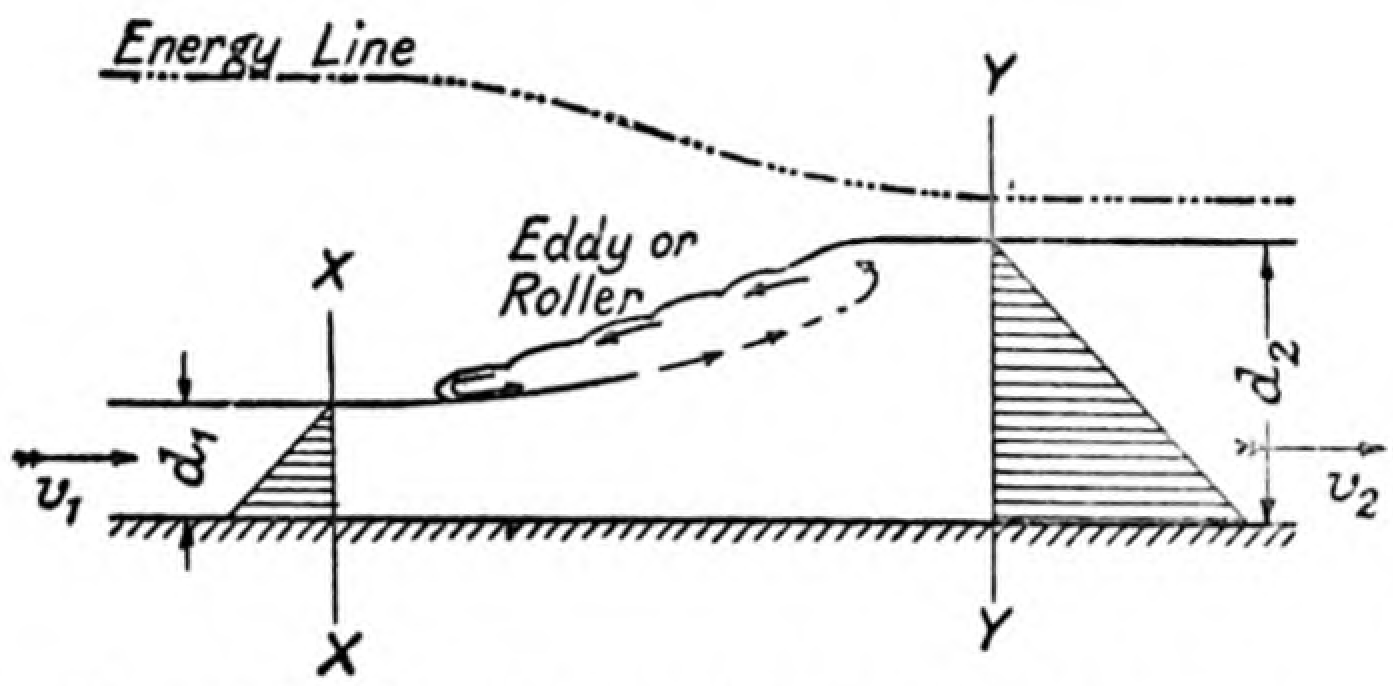

FIG. 123.—Calculation of height of standing wave.

Writing again the fundamental equation $P_x + P_d = P_y$, and inserting the appropriate values, we have

$$\frac{wd_1^2}{2} + \frac{w}{g} \cdot v_1^2 d_1\left(1 - \frac{d_1}{d_2}\right) = \frac{wd_2^2}{2}$$

which reduces to the form

$$d_2^2 + d_1 d_2 - \frac{2v_1^2 d_1}{g} = 0.$$

Solving this equation, we obtain

$$d_2 = -\frac{d_1}{2} + \sqrt{\frac{2v_1^2 d_1}{g} + \frac{d_1^2}{4}} \quad . \quad . \quad (7\text{-}10)$$

which represents the maximum downstream depth of water that can be associated with an upstream depth d_1 and upstream velocity v_1. Values calculated from this equation agree fairly well with observed values of the downstream depth.

(Example 58.)

It was made clear in § 108 that a standing wave can only be formed if d_1 is less than the critical depth—that is, if "shooting" flow is in operation upstream of the wave.

Formula 7-10 confirms this, for if we substitute in it the value for v_1^2 corresponding to the critical depth, viz. $v_1^2 = gd_1$, the value of d_2 is seen to fall to that of d_1—the standing wave disappears.

The shape of the total energy line in Fig. 123 serves as a reminder that although a standing wave enables the water surface in a stream to rise, the operation inevitably involves dissipation of energy.[63]

CHAPTER VIII

RADIAL AND ROTARY MOTION OF LIQUIDS

In this chapter a number of the fundamental equations developed in earlier chapters are applied to the special conditions arising when liquids move towards or revolve around a central point or axis.

138. Radial Flow. In Fig. 124 (*a*), water is seen flowing from a cylindrical reservoir, through the annular space formed

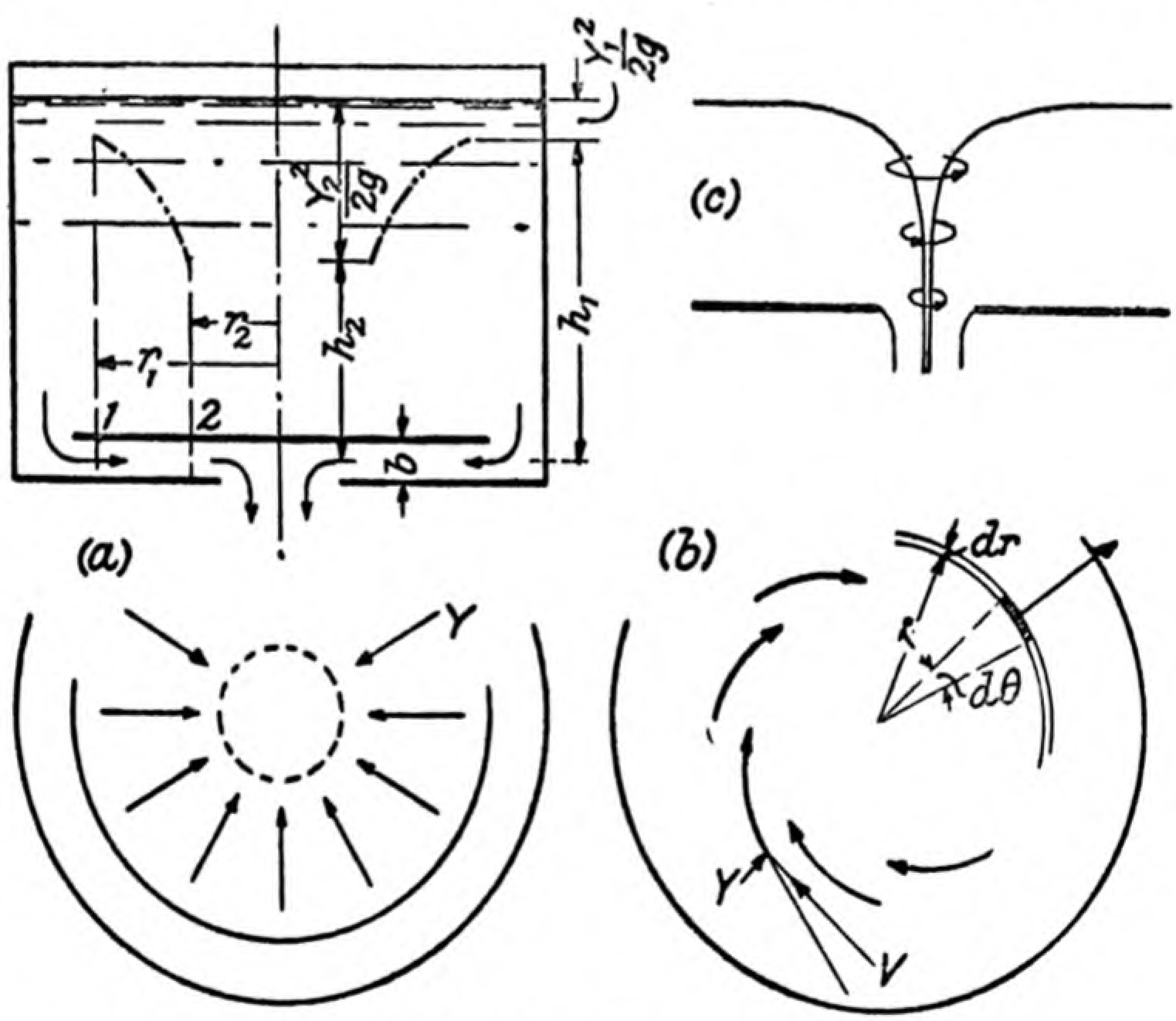

FIG. 124.—Radial and spiral flow.

by the bottom of the reservoir and a flat circular plate fixed at a distance b above it, and escaping through an opening below. The relationship [Discharge = Area × Velocity] must apply here as it does in linear flow, provided that the area in question is normal to the velocity. Since in Fig. 124 (*a*) the water is flowing

radially inwards, the only kind of area that will fulfil this condition is a cylindrical one : at any radius r the area available for flow is $2\pi rb$, and the velocity Y will be represented by $\dfrac{\text{discharge}}{2\pi rb}$. To this radial velocity the specific name *velocity of flow* is given.

As the water flows inwards its velocity will increase and consequently, there being no energy changes under ideal conditions, its pressure energy will diminish. Applying Bernoulli's theorem to points 1 and 2 (§ 33),

$$h_1 + \frac{Y_1^2}{2g} = h_2 + \frac{Y_2^2}{2g} = h_2 + \frac{Y_1^2}{2g}\left(\frac{r_1^2}{r_2^2}\right)$$

$$(\text{since } q = 2\pi r_1 b Y_1 = 2\pi r_2 b Y_2)$$

from which the drop in pressure head is seen to be

$$h_1 - h_2 = \frac{Y_1^2}{2g}\left[\frac{r_1^2}{r_2^2} - 1\right]. \quad . \quad \quad . \quad \textbf{(8-1)}$$

The hydraulic gradient on a cross-section through the vertical axis of the system will have the form shown in the figure.

The relationship Yr = constant is evidently only true for flow between parallel plates ; if the plates are suitably " dished," the velocity of flow, and therefore the pressure head, can be made uniform at all points. **(Example 68.)**

139. Vortex Flow. If the water flowing between the plates (Fig. 124 (*b*)) has a spiral motion, at the same time moving towards the axis and revolving around it, the flow is expressed in terms of its radial and tangential components. The radial component of the velocity at any point is termed, as before, the velocity of flow ; the tangential component is termed the *velocity of whirl* and is denoted by the symbol V. The pressure changes associated with the *radial* velocity components may be calculated in the manner just explained ; to these must be added the pressure changes due to the *tangential* velocity components.

Let us consider a very thin ring or annulus of rotating liquid, of mean radius r, radial thickness dr, and axial width b (Fig. 124 (*b*)), moving with mean tangential velocity V. Selecting a small element of this ring subtending at the centre an angle $d\theta$, we can say that :

The volume of the element is $rd\theta \, . \, dr \, . \, b$.
The weight of the element is $w \, . \, rd\theta \, . \, dr \, . \, b$.
The centrifugal force acting on the element is

$$\frac{w}{g} \, . \, rd\theta \, . \, dr \, . \, b \, . \, \frac{V^2}{r}.$$

What is it that resists the centrifugal force? What compels the element to follow its circular path in preference to a straight path? Manifestly such an inward thrust can only be derived from a difference of pressure head dh generated between the inner and outer faces of the element; the intensity of this thrust will be

$$- rd\theta \, . \, b \, . \, w \, . \, dh.$$

Equating the two forces which must of necessity be in equilibrium, we have

$$\frac{w}{g} \, . \, rd\theta \, . \, dr \, . \, b \, . \, \frac{V^2}{r} = - rd\theta \, . \, b \, . \, w \, . \, dh,$$

from which
$$- dh = \frac{V^2}{r} \, . \, \frac{1}{g} \, . \, dr \quad . \quad . \quad . \quad \text{(8-2)}$$

Before integrating in order to evaluate the total change of pressure head between the inner and outer boundaries of the rotating mass of liquid, we must know what is the law connecting the radius r with the velocity of whirl V. If the relation is such that the specific energy of the liquid is uniform throughout, then *free vortex flow* is said to be in operation; another type of velocity distribution gives us *forced vortex flow* (§§ 142-144).

By putting equation 8-2 into the form $\frac{V^2}{r} = g \, . \, \frac{dh}{dr}$, we are offered another instructive example of the way in which liquid elements are controlled by the pressure gradients of the fields in which they lie. The static pressure gradient in a liquid at rest keeps each element motionless against the downward pull of gravity (§ 28); the pressure gradient along a horizontal converging passage is responsible for the *linear* acceleration of the element (§ 35); and now we observe that in vortex motion there is a connection between pressure gradient and *radial* acceleration. The relationships, too, are identical. Equation 3-2 and the modified form of equation 8-2 are alike expressions of the law that the acceleration is equal to $g \times$ the slope of the hydraulic gradient.

140. Free Vortex Motion. There is little need for hesitation in accepting the condition of uniform energy distribution stipulated for this type of flow. Apart from friction and eddy

losses, which we quite habitually disregard for preliminary calculations, why should the liquid gain or lose energy as it flows through the vortex? But we are obliged to admit that the tangential velocity V of the ring or annulus, Fig. 124 (*b*), cannot be uniform over the entire radial distance dr; the velocity must be *greater* at the inner periphery of the annulus than it is at the outer periphery. Let the change in velocity be dV. The corresponding change in velocity energy will be $\frac{(V + dV)^2 - V^2}{2g}$ which, in the limit, has the value $\frac{V \, . \, dV}{g}$. Equating increase in velocity energy to loss in pressure energy while passing from the outer to the inner faces, we have $dh = \frac{V \, . \, dV}{g}$. But equation 8-2 has already given us a value for dh, from which we find

$$- \frac{V^2}{r} \, . \, \frac{1}{g} \, . \, dr = \frac{V \, . \, dV}{g},$$

and in turn

$$- \frac{1}{r} \, . \, dr = \frac{1}{V} dV.$$

Integration finally yields the result

$$\int - \frac{1}{r} \, dr = \int \frac{1}{V} dV, \quad \text{or} \quad \log r + \log V = \text{constant},$$

proving that the law connecting radius and velocity is

$$Vr = \text{constant}.$$

If the whirl velocity V_1 corresponding to a radius r_1 be given, we can write

$$Vr = V_1 r_1, \quad \text{or} \quad V = \frac{V_1 r_1}{r}.$$

Inserting this value for V in equation 8-2 gives

$$- dh = \frac{V_1^2 r_1^2}{g} \, . \, \frac{1}{r^3} \, . \, dr,$$

from which the desired value of the total change of pressure head, $h_1 - h_2$, between radii r_1 and r_2, is obtained, thus :

$$h_1 - h_2 = \int dh = \frac{V_1^2}{2g} \left[\frac{r_1^2}{r_2^2} - 1 \right]. \qquad . \quad . \quad (8\text{-}3)$$

Alternatively, if V_2 is the whirl velocity at radius r_2, then

$$h_1 - h_2 = \frac{V_2^2}{2g} - \frac{V_1^2}{2g}.$$

A familiar example of free vortex flow occurs when water escapes from an orifice in the bottom of a tank (Fig. 124 (*c*)), the lowering of the water surface itself demonstrating the connection between increased velocity of whirl and diminished pressure head. It is specially to be noted that in these conditions the values of flow coefficients quoted in §§ 42, 43 *no longer hold good.*

When water flows outwards instead of inwards, under conditions either of radial or spiral flow, the ideal energy equations will be unaltered, but the actual rise of pressure head will be less than the equivalent drop accompanying inward flow, because of the relatively greater losses inevitable in converting velocity head to pressure head (§ 89).

141. Free Vortex Flow in Pipe Bends. The free vortex flow that takes place when a liquid flows around curved passages such as bends in a pipe line causes a redistribution of pressure and velocity, as shown in Fig. 125 ; as the pressure head rises

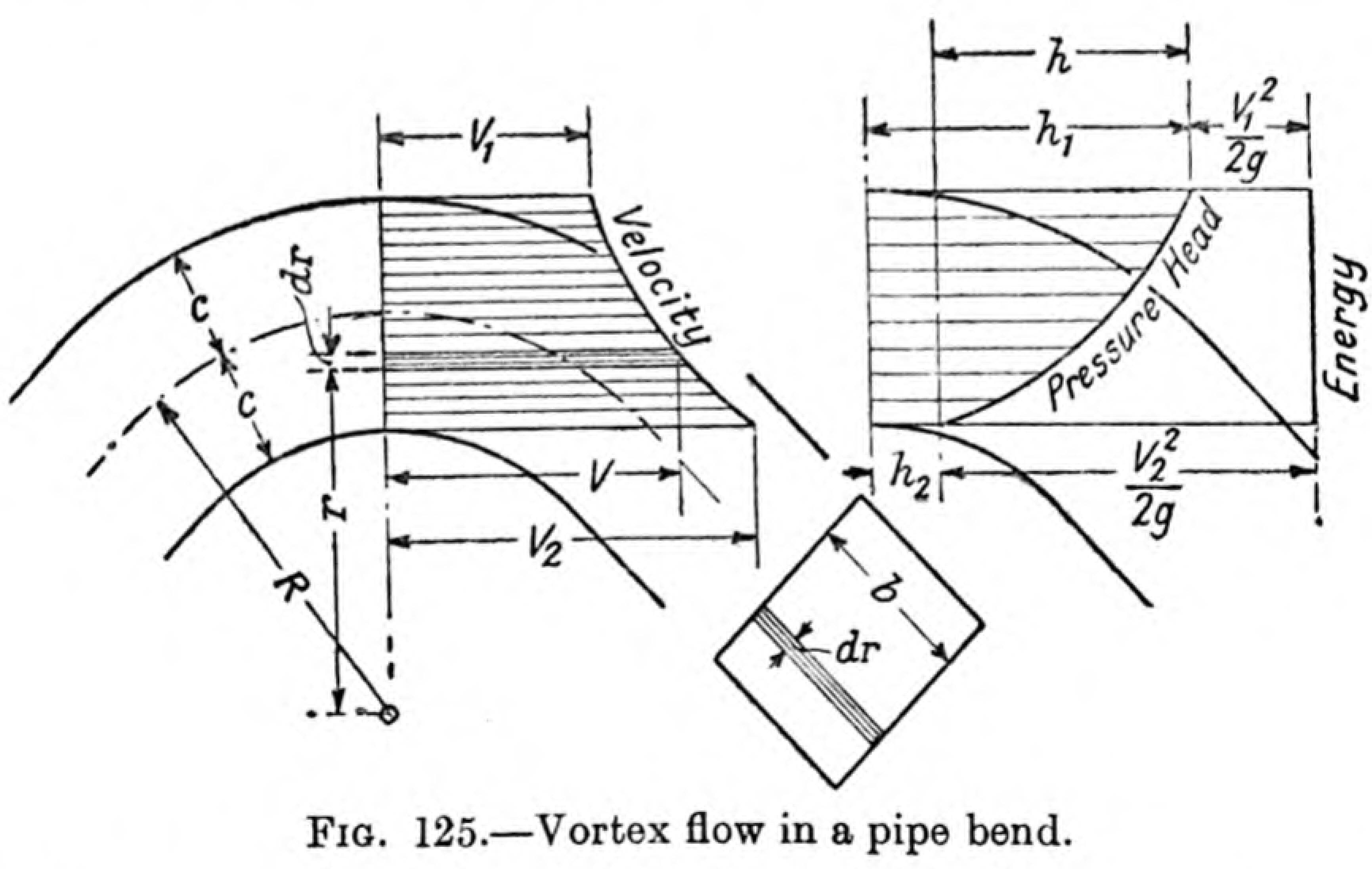

FIG. 125.—Vortex flow in a pipe bend.

from h_2 at the inside of the bend to h_1 at the outside, the velocity of whirl falls from V_2 to V_1, the total energy remaining uniform. Denoting the radius of the centre-line of the bend by R, the radial width of the passage by $2c$, and the constant product of V and r by K, so that $K = Vr$, then the free vortex

equation 8-3 may be put into the form

$$h = \text{differential head} = h_1 - h_2 = \frac{1}{2g}\left[\left(\frac{K}{R-c}\right)^2 - \left(\frac{K}{R+c}\right)^2\right],$$

which reduces to
$$\frac{K^2}{2g} \cdot \frac{4Rc}{(R^2 - c^2)^2},$$

whence
$$K = \sqrt{2gh} \cdot \frac{R^2 - c^2}{2\sqrt{Rc}}.$$

For a waterway of rectangular section, of transverse width b, the discharge dq flowing through a small element of area $b \cdot dr$ (Fig. 125) will be $V \cdot b \cdot dr$, or $dq = K \cdot b \cdot dr/r$. On integrating this expression to obtain the total discharge q flowing round the bend, we obtain

$$q = \int_{R-c}^{R+c} K \cdot b \cdot \frac{dr}{r} = 2{\cdot}3026Kb\,[\log_{10}(R+c) - \log_{10}(R-c)].$$

Inserting now the value of K, from above, we find

$$q = \sqrt{2gh} \cdot \frac{R^2 - c^2}{2\sqrt{Rc}} \cdot 2{\cdot}3026b\,[\log(R+c) - \log(\mathrm{R} - c)].$$

Similarly, it may be shown that if the bend is of circular cross-section, of radius c, then

$$q = \sqrt{2gh} \cdot \frac{R^2 - c^2}{\sqrt{Rc}} \cdot \pi[R - \sqrt{R^2 - c^2}].$$

Owing to the effect of wall friction and to secondary types of flow within the passages, the observed pressure and velocity distributions in curved passages do not quite conform to the ideal patterns just described; but the equations nevertheless give useful guidance concerning the correlation between discharge and differential head.[(64)]

(*Note.*—It has already been suggested (§ 88) that one source of the loss of energy sustained by water traversing a pipe-bend is the additional eddying set up downstream of the bend, as the free vortex flow gives place to the normal velocity distribution corresponding to uniform turbulent flow in straight pipes.

It will also now be evident that in § 119 the effect of free vortex motion was ignored; the error is inconsiderable so long as the pipe diameter is small in comparison with the bend radius.)

142. Forced Vortex Motion. This is the name given to rotary or spiral motion when the velocity of whirl is *directly* proportional (instead of being inversely proportional) to

the radius, i.e. $\frac{V}{r}$ = constant. A forced vortex is formed in a vessel containing water revolving about a vertical axis (Fig. 126); after a time, viscous resistances will damp out all relative motion, and the vessel, together with its contents, will rotate as a single body, in which naturally the tangential velocity at any point is proportional to the radius. Because of centrifugal force, the free water surface is not horizontal — it forms a paraboloid of revolution.

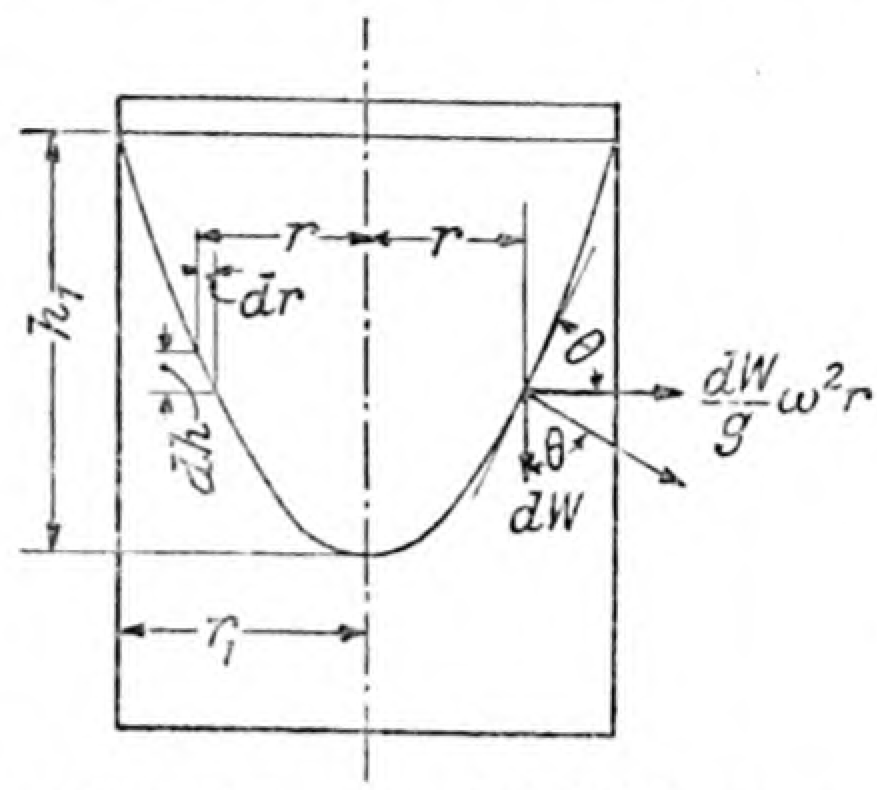

FIG. 126.—Paraboloidal water surface.

This is a result of the condition that the water surface at any point must be normal to the total resultant force acting on a particle of water at that point. Considering a very small element of water of weight dW in the water surface at radius r, the downward force on this element is its weight dW, and the centrifugal force acting radially outwards is $\frac{dW}{g} \cdot \omega^2 r$, where ω is the angular velocity of the vessel and contents. The total resultant force will thus have an inclination θ to the vertical, and the water surface, being normal to the total resultant force, will have the same inclination to the horizontal (Fig. 126).

The inclination can also be expressed:

$$\tan \theta = \frac{\frac{dW}{g} \cdot \omega^2 r}{dW} = \frac{\omega^2}{g} \cdot r,$$

also $$\tan \theta = \frac{dh}{dr},$$

whence $$dh = \frac{\omega^2}{g} r \cdot dr.$$

Integrating, $$h_1 = \int dh = \frac{\omega^2}{2g} \cdot r_1^2,$$

proving that, as indicated above, the axial cross-section of the water surface is a parabola. **(Example 69.)**

143. Flow Under Forced Vortex Conditions. It is quickly apparent that the energy distribution in a forced vortex is quite different from what it is in a free vortex; since water near the outside of the vessel (Fig. 126) has both a higher velocity and a greater pressure than water in the same horizontal plane near the centre, its total energy must be considerably greater. Hence water can only be made to move from the inner to the outer part of a forced vortex by giving it energy from some external source, and similarly water moving inwards will yield up energy.

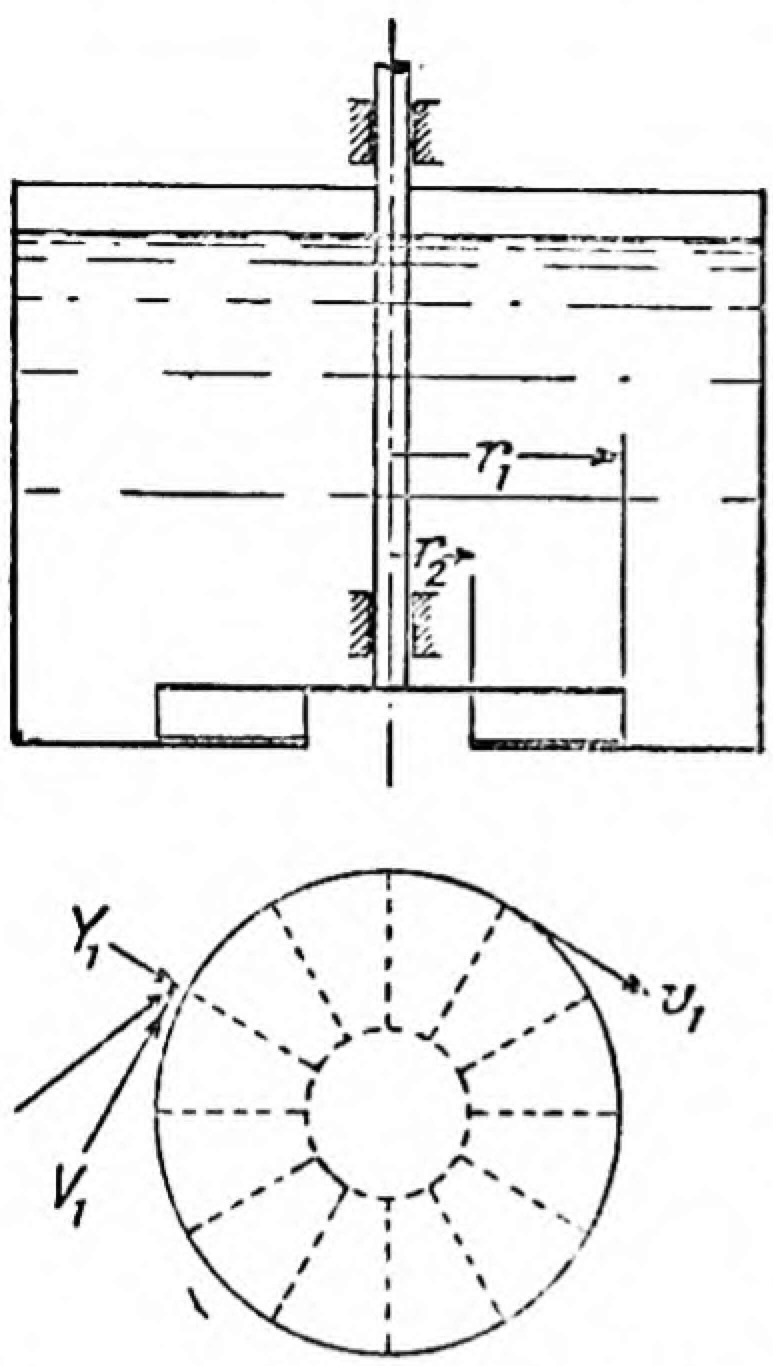

FIG. 127.—Apparatus for generatng forced vortex mot on.

Fig. 127 shows how the apparatus described in § 138 may be modified to permit it to absorb the energy liberated when flow through a forced vortex takes place. The upper disc is now attached to a vertical shaft so that it may be free to revolve, and radial blades or paddles are fixed to its under side in order to compel the water forcibly to accept the velocity of whirl appropriate to the radius (see [233] § 336).

Inserting now the value $V = \dfrac{V_1}{r_1} . r$ in equation 8-2 § 139,

we obtain $$-\,dh = \frac{1}{g} \cdot \frac{V_1^{\,2}}{r_1^{\,2}} r^2 \cdot \frac{1}{r} \cdot dr.$$

Integration yields $$\int dh = h_1 - h_2 = \frac{1}{2g} \cdot \frac{V_1^{\,2}}{r_1^{\,2}} (r_1^{\,2} - r_2^{\,2}),$$

from which $$h_1 - h_2 = \frac{V_1^{\,2}}{2g}\left(1 - \left(\frac{r_2}{r_1}\right)^2\right) = \frac{V_1^{\,2}}{2g} - \frac{V_2^{\,2}}{2g} \quad . \quad (8\text{-}4)$$

which confirms the result obtained in the preceding paragraph. This type of pressure-distribution, applicable when the radial velocity component Y_1 is negligibly small, is depicted in Fig. 129 (I). (Example 70.)

144. Work Done by or on Water when Flowing through a Forced Vortex. The energy liberated during inward flow under forced vortex conditions manifests itself in the generation of dynamic pressure on the blades attached to the disc (Fig. 127).

The calculation of the dynamic thrust and of the work done on blades having (assumed) rectilinear motion was based on change of *linear* momentum (§ 123); by analogy, therefore, the work done on blades having rotary motion will depend upon changes of *angular* momentum.

Considering a general case, let

V_1 = velocity of whirl of water at outer periphery of forced vortex immediately before impinging on blades. (This whirl component is imparted to the water by suitable external fixed blades.)

v_1 = peripheral velocity of outer edges of rotating blades.

V_2 = velocity of whirl of water at inner periphery of vortex immediately after leaving blades.

v_2 = velocity of inner edges of blades.

r_1 = outer radius of wheel.

r_2 = inner radius of wheel.

ω = angular velocity of wheel.

W = weight of water flowing per second through wheel.

Now the angular momentum of the water per second, or the moment of momentum per second, immediately before entering the wheel $= \frac{W}{g} \cdot V_1 r_1$, and the angular momentum of the water per second immediately after leaving the wheel

$$= \frac{W}{g} \cdot V_2 \cdot r_2.$$

Therefore change of angular momentum per second

$$= \frac{W}{g} \cdot (V_1 r_1 - V_2 r_2),$$

which equals the torque or twisting moment exerted on the wheel.

Also work done per second on wheel

$$\begin{aligned}
&= \text{torque} \times \text{angular velocity} \\
&= \frac{W}{g}(V_1 r_1 - V_2 r_2)\omega \\
&= \frac{W}{g}\left(V_1 r_1 \frac{v_1}{r_1} - V_2 r_2 \frac{v_2}{r_2}\right) \\
&= \frac{W}{g}(V_1 v_1 - V_2 v_2),
\end{aligned}$$

143. Flow Under Forced Vortex Conditions. It is quickly apparent that the energy distribution in a forced vortex is quite different from what it is in a free vortex; since water near the outside of the vessel (Fig. 126) has both a higher velocity and a greater pressure than water in the same horizontal plane near the centre, its total energy must be considerably greater. Hence water can only be made to move from the inner to the outer part of a forced vortex by giving it energy from some external source, and similarly water moving inwards will yield up energy.

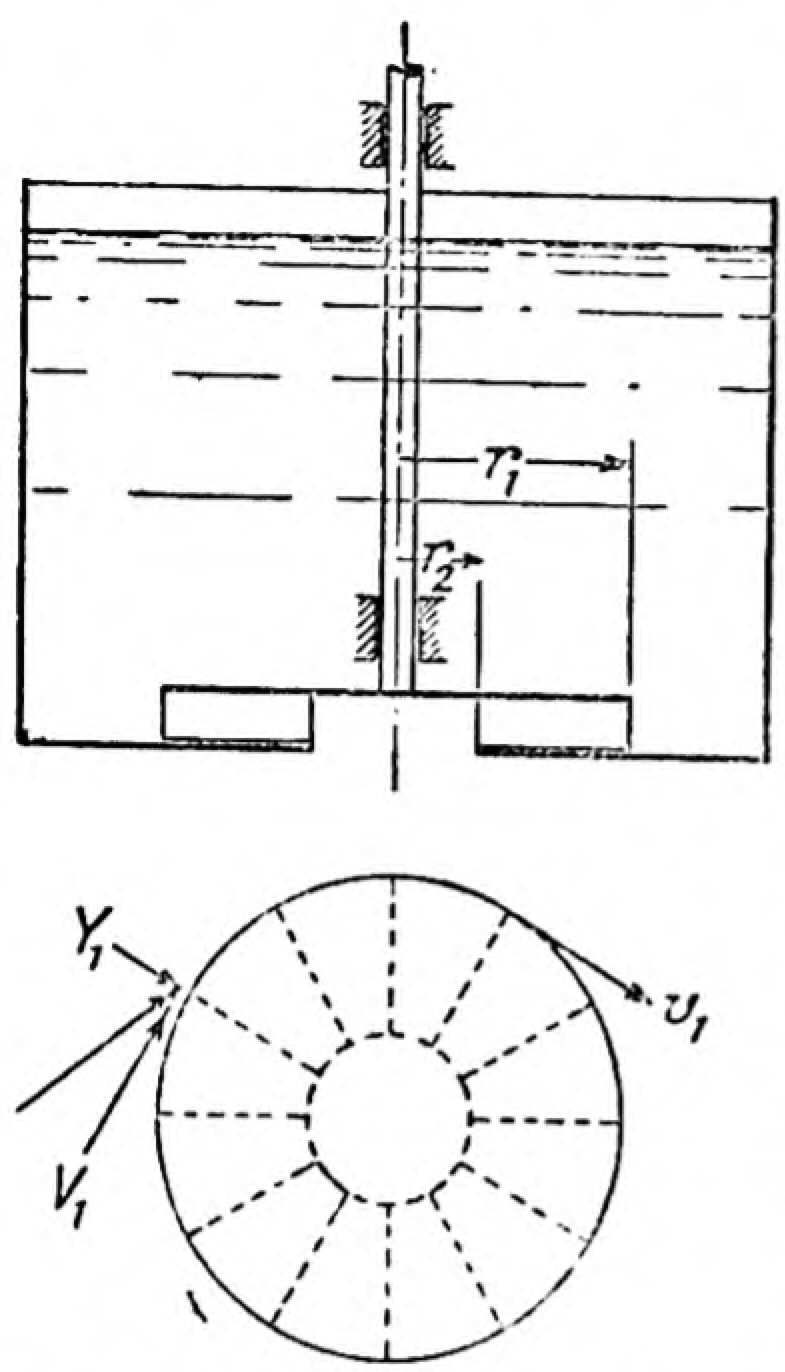

FIG. 127.—Apparatus for generatng forced vortex mot on.

Fig. 127 shows how the apparatus described in § 138 may be modified to permit it to absorb the energy liberated when flow through a forced vortex takes place. The upper disc is now attached to a vertical shaft so that it may be free to revolve, and radial blades or paddles are fixed to its under side in order to compel the water forcibly to accept the velocity of whirl appropriate to the radius (see [233] § 336).

Inserting now the value $V = \frac{V_1}{r_1} . r$ in equation 8-2 § 139,

we obtain $$-\,dh = \frac{1}{g} \cdot \frac{V_1^{\,2}}{r_1^{\,2}} r^2 . \frac{1}{r} . dr.$$

Integration yields $$\int dh = h_1 - h_2 = \frac{1}{2g} \cdot \frac{V_1^{\,2}}{r_1^{\,2}} (r_1^{\,2} - r_2^{\,2}),$$

from which $$h_1 - h_2 = \frac{V_1^{\,2}}{2g}\left(1 - \left(\frac{r_2}{r_1}\right)^2\right) = \frac{V_1^{\,2}}{2g} - \frac{V_2^{\,2}}{2g} \quad . \quad \textbf{(8-4)}$$

which confirms the result obtained in the preceding paragraph. This type of pressure-distribution, applicable when the radial velocity component Y_1 is negligibly small, is depicted in Fig. 129 (*I*). **(Example 70.)**

144. Work Done by or on Water when Flowing through a Forced Vortex. The energy liberated during inward flow under forced vortex conditions manifests itself in the generation of dynamic pressure on the blades attached to the disc (Fig. 127).

The calculation of the dynamic thrust and of the work done on blades having (assumed) rectilinear motion was based on change of *linear* momentum (§ 123); by analogy, therefore, the work done on blades having rotary motion will depend upon changes of *angular* momentum.

Considering a general case, let

V_1 = velocity of whirl of water at outer periphery of forced vortex immediately before impinging on blades. (This whirl component is imparted to the water by suitable external fixed blades.)

v_1 = peripheral velocity of outer edges of rotating blades.

V_2 = velocity of whirl of water at inner periphery of vortex immediately after leaving blades.

v_2 = velocity of inner edges of blades.

r_1 = outer radius of wheel.

r_2 = inner radius of wheel.

ω = angular velocity of wheel.

W = weight of water flowing per second through wheel.

Now the angular momentum of the water per second, or the moment of momentum per second, immediately before entering the wheel $= \frac{W}{g} . V_1 r_1$, and the angular momentum of the water per second immediately after leaving the wheel

$$= \frac{W}{g} . V_2 . r_2.$$

Therefore change of angular momentum per second

$$= \frac{W}{g} . (V_1 r_1 - V_2 r_2),$$

which equals the torque or twisting moment exerted on the wheel.

Also work done per second on wheel

$$\begin{aligned} &= \text{torque} \times \text{angular velocity} \\ &= \frac{W}{g}(V_1 r_1 - V_2 r_2)\omega \\ &= \frac{W}{g}\left(V_1 r_1 \frac{v_1}{r_1} - V_2 r_2 \frac{v_2}{r_2}\right) \\ &= \frac{W}{g}(V_1 v_1 - V_2 v_2), \end{aligned}$$

or work done per unit weight of water flowing through wheel

$$= \frac{V_1 v_1 - V_2 v_2}{g} . \quad . \quad . \quad . \quad (8\text{-}5)$$

This energy, less the energy wasted in friction, etc., is transmitted through the shaft to whatever apparatus for absorbing or utilising energy is coupled to it.

Formula 8-5 can be applied to general questions involving energy generated by dynamic pressure, e.g. to the problems discussed in §§ 123-125, even though the flowing water may not be in the form of a complete vortex.

The formula is, of course, equally applicable to outward flow through a forced vortex, except that in this case the expression $\frac{W}{g}(V_1 v_1 - V_2 v_2)$ represents the rate at which energy must continually be fed into the wheel *via* the shaft. The use of curved blades instead of radial ones will not affect the validity of the above relationship, but it may alter the relative values of V_1, V_2, etc.

145. Tangential Acceleration. The equation (8-5) that has just been established—one of the numerous expressions attributed to the mathematician Euler—is of fundamental importance ; it serves as a guide to the performance of a whole group of hydraulic machines[65] such as rotodynamic pumps and turbines, chapter XII. Here in this paragraph we wish to make a further study of the connection between the energy of the liquid flowing through the wheel, and the torque or twisting moment exerted upon the shaft. How in fact is this torque exercised ? There can only be one way : a *pressure-difference* must exist between the two sides of each of the radial blades shown in Fig. 127, and in consequence there arises a resultant *tangential thrust* on each blade. Although this seems to be a new type of dynamic thrust, we can well believe that it is in some way connected with the acceleration or retardation of liquid elements, just as other kinds of dynamic pressure were (§§ 115, 126).

The acceleration now to be examined is a *tangential* acceleration ; it arises whenever in a moving system there is a combination of angular velocity and radial velocity. An

example is illustrated in Fig. 128, where a solid object is shown sliding radially along a straight uniform rod. Pivoted at one end, the rod rotates about its pivot with uniform angular velocity ω. The solid, of weight W, moves outwards with a uniform velocity Y relative to the rod.

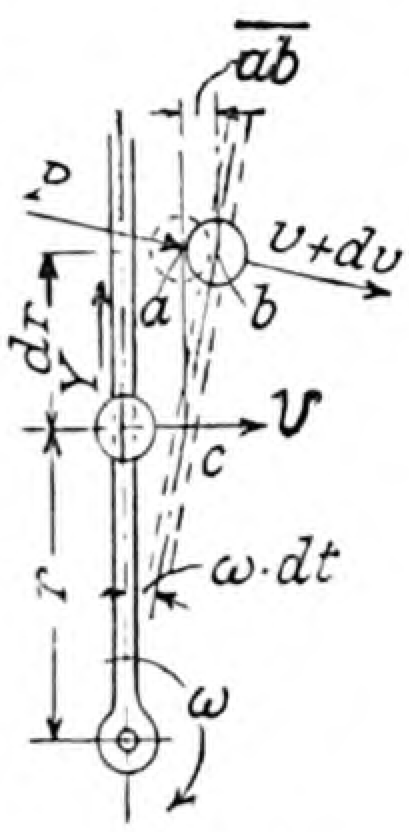

FIG. 128. Coriolis acceleration.

Suppose that when it is at radius r the object has a tangential velocity v. After a small interval of time dt, during which the object will have moved along the rod a distance dr, its tangential velocity will have increased to $(v + dv)$. But if, instead of this, the rod had been hinged at point c so that the part ca had moved parallel with itself, then at the end of interval dt the solid would only have arrived at point a instead of at point b: there would have been no change in the tangential velocity of the object. In order now to restore the rod to its original straightness, the object must be moved through an additional tangential distance ab; this can only be done if the rod exerts on the object a tangential force P, thereby impressing on it a *tangential acceleration* denoted by α.

This tangential acceleration can be evaluated thus:—
The angular distance traversed by the rod in time dt is $\omega \,.\, dt$, therefore the linear distance ab is represented by

$$dr \,.\, \omega\, dt \,. = Y \,.\, dt \,.\, \omega\, dt.$$

Inserting now appropriate values in the Newtonian equation

$$\text{Distance} = \tfrac{1}{2}\,(\text{acceleration}) \times (\text{time})^2,$$

we have $$\overline{ab} = \tfrac{1}{2}\alpha(dt)^2,$$

or $$Ydt \,.\, \omega dt = \tfrac{1}{2}\alpha(dt)^2,$$

from which

$$\alpha = \text{tangential acceleration} = 2Y\omega \qquad . \qquad . \quad \textbf{(8-6)}$$

This expression, which represents the simplest type of tangential acceleration, is associated with the name of the French mathematician *Coriolis.*

146. Coriolis Acceleration, Torque, and Blade Pressure. The validity of equation 8-6 is in no way dependent upon the moving object being a solid object: we may quite legitimately apply the equation to an element of liquid, e.g. the liquid enclosed between two blades of the rotor shown in Fig. 127, § 143. Considering such an element, now identified by hatching in Fig. 129, we note that it has the following characteristics: Radial thickness $= dr$; axial width $= b$; circumferential length $= l = 2\,\pi r/n$ (where n is the number of blades); volume $= l\,.\,b\,.\,dr$; weight $= w\,.\,l\,.\,b\,.\,dr$; radial velocity $= Y$; angular velocity $= \omega$. According to equation (8-6), therefore, the element will be subjected to a tangential acceleration α of intensity $2Y\omega$.

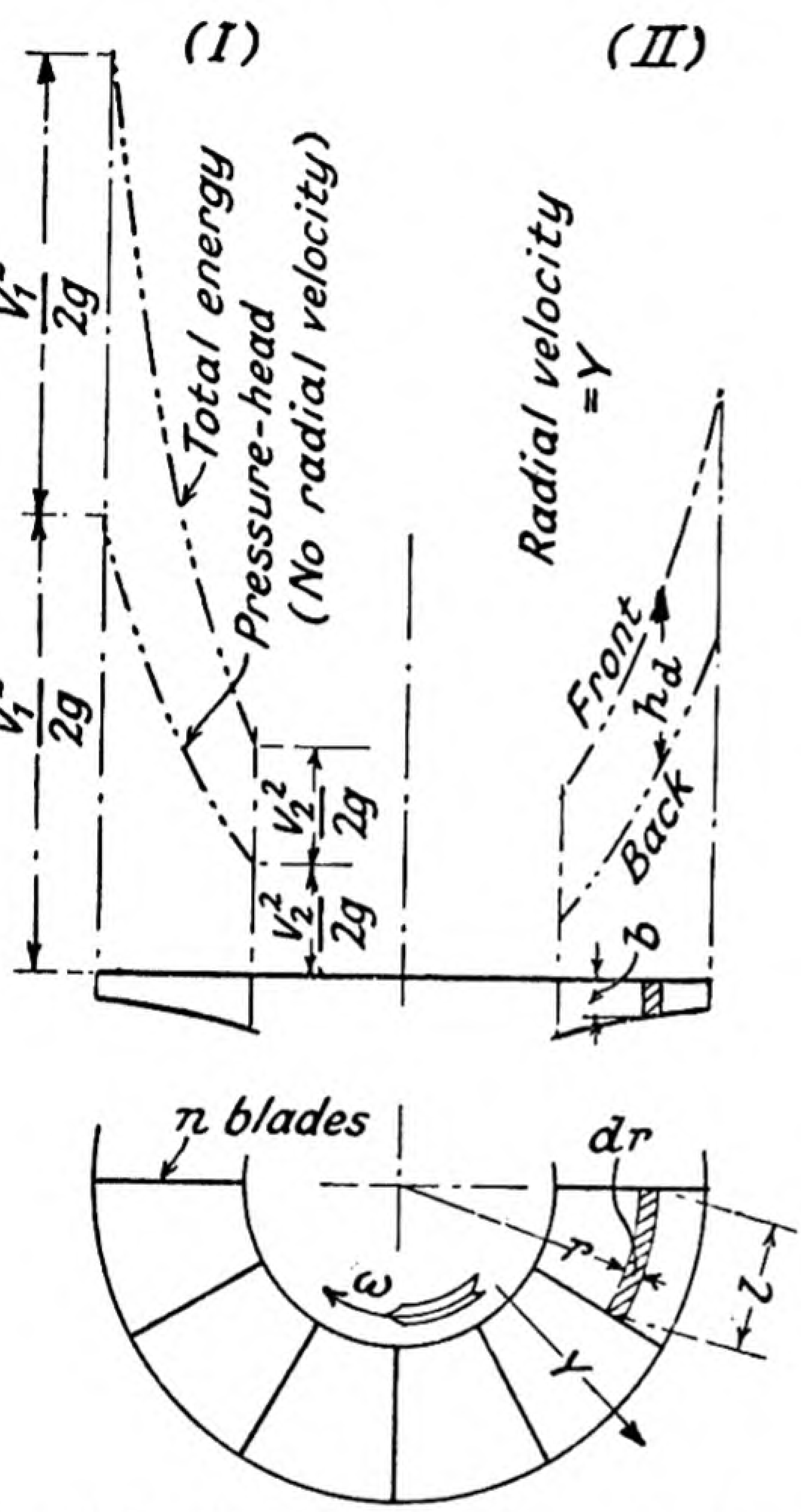

FIG. 129.—Distribution of pressure-head and of total energy in rotating passages.

Now if, because of its small length, we disregard the curvature of this little column of liquid, we may liken it to the liquid column enclosed within the pipe shown in Fig. 90, § 115; both columns experience acceleration in the direction of their lengths, and therefore in both cases the derived form of equation (7-1) is applicable, viz.

$$\text{Inertia pressure} = (w\,.\,l/g) \times \text{acceleration.}$$

Since in the present instance the acceleration has the value $2Y\omega$, we may write :—

$$p_d = \text{pressure difference between front and back of blade}$$
$$= (wl/g)\,.\,2Y\omega \qquad (8\text{-}7)$$

If at each point along a blade, this pressure-difference were computed and multiplied by the corresponding blade area, then by summation the gross tangential thrust on the blade could be found. An equivalent integration would yield the torque on the blade, and in turn the torque on the shaft; in ideal conditions it would be found that this torque agreed exactly with the value computed from equation (8-5). **(Example 71.)**

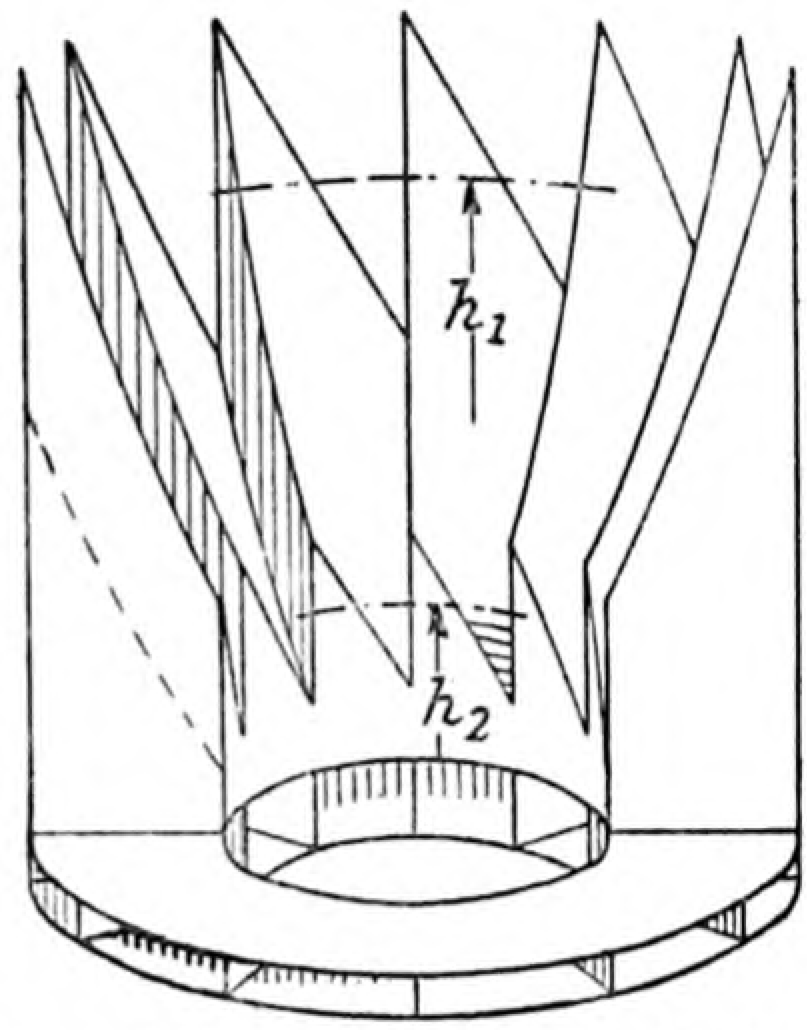

Fig. 130.—Idealised enveloping surface corresponding to Fig. 129 (*II*).

It is now possible to form a complete picture of the ideal distribution of pressure-head within the passages of a wheel or rotor such as was first mentioned in § 143. If we were to erect at each point a vertical whose height represented to scale the ideal pressure-head at that point, Fig. 129 (*I*), then *if there were no flow* through the wheel the enveloping surface would have the form of a paraboloid of revolution comparable with what was shown in Fig. 126. But there would be no actual energy transfer. If next we assume outward flow through the rotor passages, which implies that the shaft is continuously giving energy to the liquid, Fig. 129 (*II*), then the enveloping surface representing pressure-head would have some such form as is depicted in Fig. 130. Because of the type of forced vortex motion impressed on the liquid, the mean pressure-head rises from h_2 at the inner radius to h_1 at the outer radius, equation (8-4); but superposed upon this pattern are the changes resulting from tangential acceleration. At each blade the pressure-head suddenly jumps by the amount $h_d = p_d/w$ associated with equation (8-7), above; thereafter, as we follow a circumferential path, the pressure-head steadily declines. It is instructive to compare this idealised diagram with similar diagrams based upon actual measurements, Fig. 384, § 336.

(*Note.* A further comparison may be made between the two rotors shown in Fig. 127 and Fig. 129. Whereas in the one, the sides are flat and parallel, the other rotor has a curved or dished lower plate. By this means the radial velocity of flow, Fig. 129 (*II*), can be kept at a uniform value Y, as explained at the end of § 138.

147. Three-dimensional Flow. The types of liquid motion so far studied in this chapter have all had one distinctive characteristic, viz. that the liquid elements have all remained within a single plane normal to the axis of the apparatus. In a general sense, the motion has been two-dimensional. More complex conditions arise when there is an additional velocity component *parallel* with the axis, and these conditions will now be reviewed.

(i) *Radial flow.* Still keeping under review the apparatus shown in Fig. 124 (*a*), § 138, it is to be noted that only a part of the liquid path was examined—the part between points (1) and (2). But the arrows make it clear that the liquid, after traversing the annular space between the flat discs, can only escape by turning through a right angle. While making this turn the liquid elements manifestly travel in curved paths. Such paths are shown in a more general form in Fig. 131 (*a*), where the liquid passes between solid surfaces each consisting of a surface of revolution. In plotting the tracks of individual liquid elements, the conception of the flow-net, § 38, is still useful; but the procedure must naturally be modified to take into account the third dimension we have added. Thus, the stream surfaces will now be concentric surfaces of revolution, nested one within the other like flower-pots of assorted sizes. Since the elementary discharge in each (annular) stream-tube, dq, is constant, and since $dq = 2\pi r . dl . Y_m$ (Fig. 131 (*a*)), it is evident that the meshes of the flow-net must fulfil the condition :—

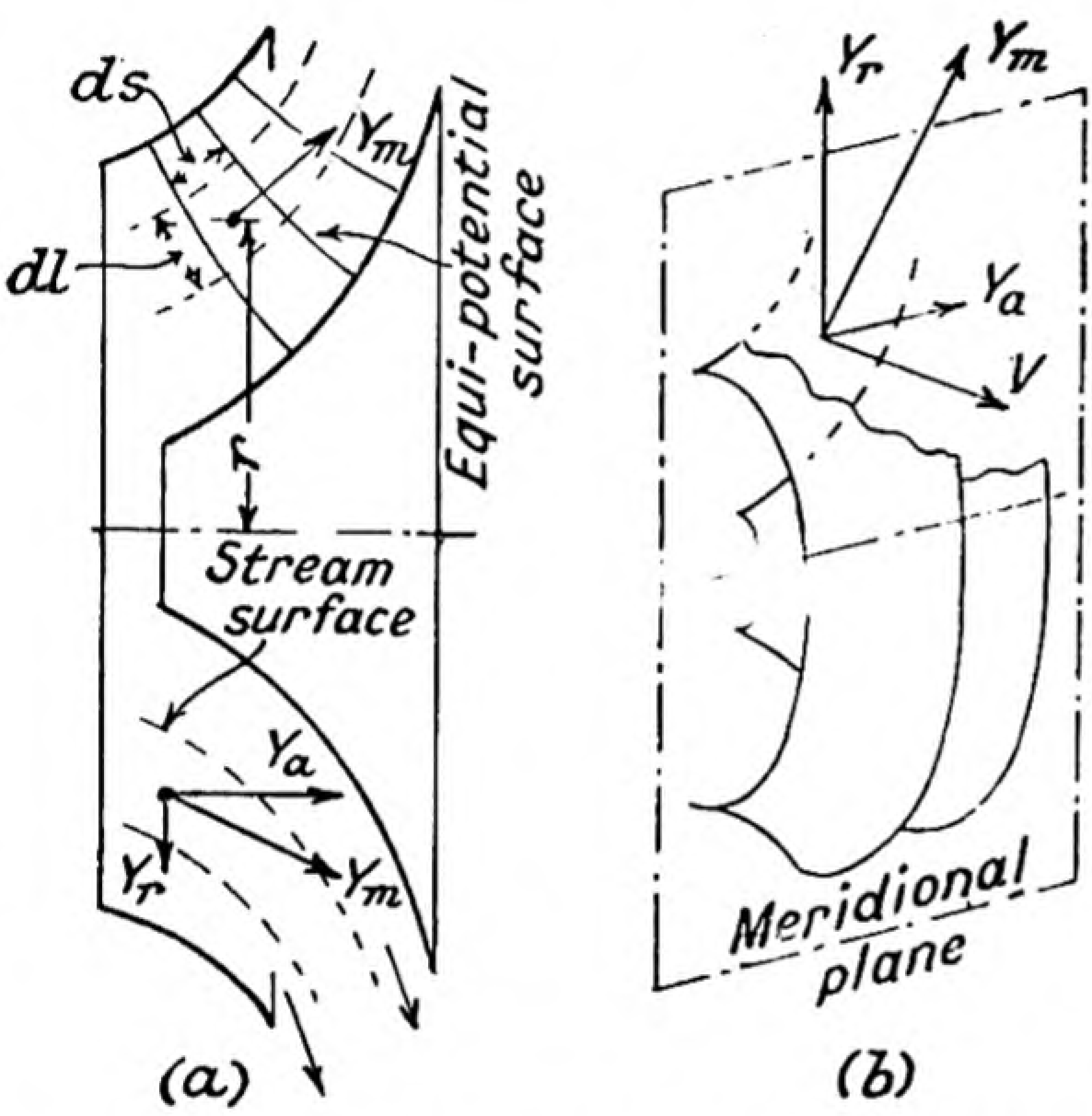

FIG. 131.—Three-dimensional flow in rotor.

$$ds/(r . dl) = \text{constant}.$$

The meshes, that is to say, are no longer in the shape of uniform squares, as they were assumed to be in § 36.

After the process has been correctly completed, and the equi-potential surfaces—also surfaces of revolution—have been added, it may be found that higher velocities prevail near the outer side of the passage, and lower velocities near the inner side, as indicated in the diagram.

Although the passage that guides the liquid is a three-dimensional one, yet each liquid element still keeps within its own plane: but this plane is now a diametral one instead of a transverse one. For this reason, by analogy with the diametral planes that are imagined to pass through the earth's axis, the plane is sometimes termed the *meridional* plane; it is the plane that contains the paper or diagram, Fig. 131 (*b*). The velocity of flow Y_m with which the liquid moves in this plane is likewise termed the *meridional velocity*; it can be resolved into two components, (i) a radial component Y_r normal to the axis, (ii) an axial component Y_a parallel with the axis.

(ii) *Combined flow.* If to these velocity components we now add another one—a tangential component or *velocity of whirl*, V, § 139—the resulting group of vectors can best be illustrated by a perspective diagram, Fig. 131 (*b*). The pressure-and-velocity-distribution within the passage will then depend upon whether the whirl components are related to free vortex flow, § 140, or to forced vortex flow, § 142; but in any event a provisional assumption is justified, viz. that the concentric stream surfaces still keep the form developed in Fig. 131 (*a*).

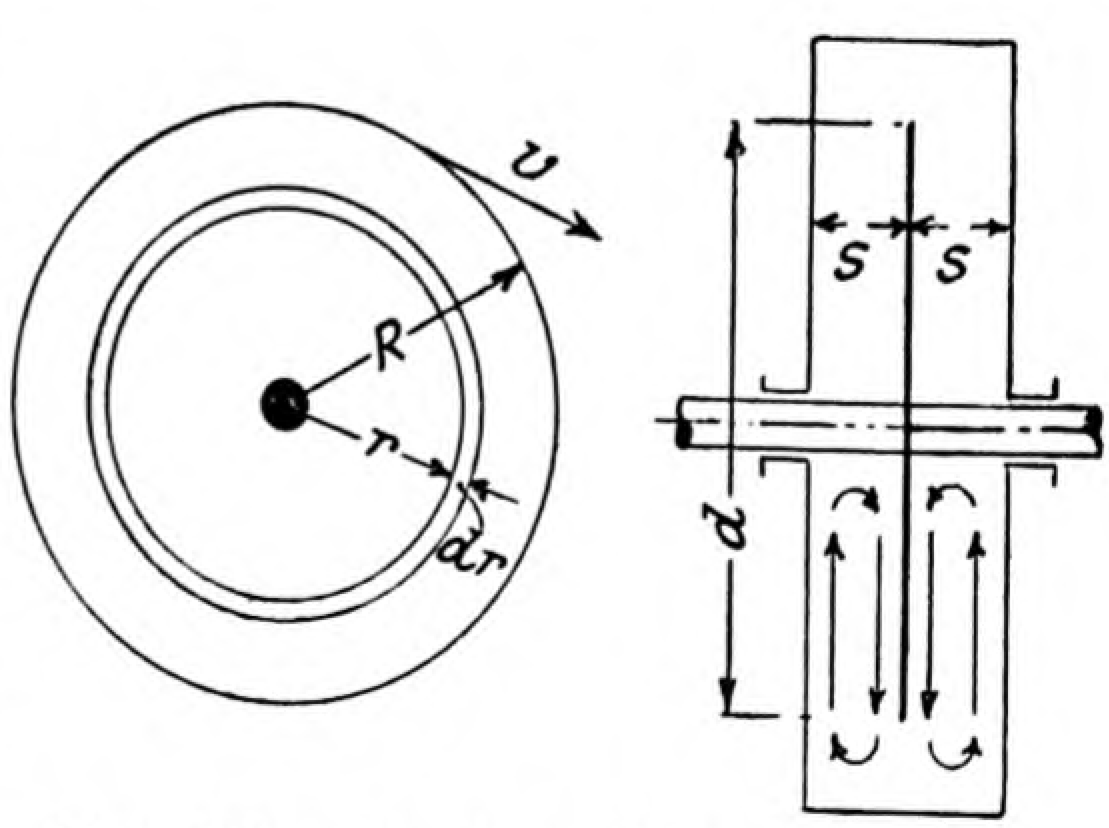

FIG. 132.—Revolving disc in cylindrical casing.

148. Surface Friction on Revolving Discs. A disc revolving in a stationary mass of liquid will be subjected to a frictional drag of the nature indicated in §§ 67, 127. Let F be the coefficient of surface friction, R the outer radius of the disc, and v its peripheral velocity (Fig. 132).

Considering an annulus or ring of radius r and width dr,

the area of the ring (on one face of the disc) is $2\pi r dr$,

" velocity of the ring is $\frac{vr}{R}$,

" surface frictional resistance on the ring is

$$F \,.\, 2\pi r \,.\, dr \,.\, \left(\frac{vr}{R}\right)^n,$$

and the energy expended per second in overcoming the frictional resistance is $F \,.\, 2\pi r \,.\, dr\left(\frac{vr}{R}\right)^{n+1}$.

Consequently the total energy per second expended in overcoming the resistance on the whole area of both sides of the disc is

$$F \,.\, v^{n+1} \,.\, \frac{4\pi}{R^{n+1}}\int_0^R r^{n+2}dr$$

$$= F \,.\, v^{n+1} \,.\, \frac{4\pi}{R^{n+1}} \,.\, \frac{R^{n+3}}{n+3}$$

$$= F \,.\, \frac{v^{n+1}}{n+3} \,.\, 4\pi R^2 \qquad . \quad . \quad . \quad (8\text{-}8)$$

Assuming that $n = 2$, as in § 68 (i), formula 8-8 reduces to

$$\text{Total energy loss per second} = \tfrac{4}{5} \,.\, F\pi v^3R^2.$$

Owing to the fact that the liquid in contact with the disc does not remain stationary, but is dragged round with the disc, the value of the friction coefficient F depends on the manner in which the disc is mounted as well as on its roughness, etc. An average value for F is 0·003 lb. per sq. ft. at 1 ft./sec., n varying from 1·85 for polished discs to 2·00 for very rough cast-iron ones.[66] These figures relate to water at atmospheric temperature only.

A general expression for the total energy loss per second would probably be of the form

$$K_{df} \,.\, w \,.\, (R_n)^{-m} \,.\, v^3R^2.$$

Such a formula is analogous with those that express the flow through smooth pipes (§ 69), and over smooth immersed surfaces (§ 127).

Experimental values for the empirical constants K_{df} and m are available in particular conditions, e.g. when the rotating smooth disc is mounted in a fixed housing with parallel flat sides, as in Fig. 132. Using the symbols :—

d = diameter of disc in inches

N = speed of rotation in r.p.m.

s = axial clearance between disc and face of housing (inches)

δ = ratio (s/d)

w = specific weight of liquid (lb./cu. ft.)

R_n = Reynolds number (dimensionless) $= \left(\frac{vR}{\nu}\right)$,

then the general expression can be transformed into the more convenient form :—

Horse-power loss on both sides of smooth disc =

$$0{\cdot}01 \,.\, \delta^{0\cdot11} \,.\, (R_n)^{-0\cdot065} \,.\, w \,.\left(\frac{d}{10}\right)^5\left(\frac{N}{1000}\right)^3 \quad . \quad \textbf{(8-9)}$$

The constants in this equation have been verified[(67)] for a range of kinematic viscosities from $\nu = 0{\cdot}004$ stokes to $\nu = 0{\cdot}2$ stokes. One reason for uncertainty in the numerical values is suggested in Fig. 132, where a type of secondary circulation is shown within the cylindrical casing. Liquid elements dragged round by the disc are influenced by centrifugal force : consequently they move outwards. An inward motion near the fixed walls of the casing completes the circulatory pattern.

PART II

PRACTICAL APPLICATIONS

CHAPTER IX

PIPES AND PIPE SYSTEMS

149. Choice between Closed and Open Conduits. When planning a conduit to convey liquid from one point to another, the first step is to decide between a closed and an open passage. More often than not a deliberate choice is entirely unnecessary : the engineer need hardly spend a long time wondering whether a pipe would be better than a channel for conducting feed-water to a high-pressure boiler or for connecting the fuel-pump to the injection-nozzle of a compression-ignition engine. But if conditions demand a formal comparison, the factors to be examined may be summarised thus :—

(i) If suitable precautions are observed, § 173, a pipe may be carried across country with little regard to gradients, Fig. 133 (i) ; it may follow the natural slopes of the ground. An open channel, on the other hand, must be laid to grade ; the bed and the water surface must remain more or less parallel,

and must slope continuously downwards, diagram (ii). If the channel cannot be aligned along or near a contour, a viaduct may be built to carry it across a valley and a tunnel or a cutting excavated to lead it through intervening high ground.

(ii) Since the cross-section of a closed passage at a given point remains unalterable, the only way of varying the rate of flow is to alter the virtual slope by throttling or the like (§ 92). By dissipating in the outlet valve, Fig. 133 (i), the surplus head, the virtual slope may be reduced from H/l to h/l, and the discharge controlled as desired. In a canal, diagram (ii), the rate of discharge may be varied by modifying the water depth, e.g. from d_2 to d_1 (§§ 101, 183).

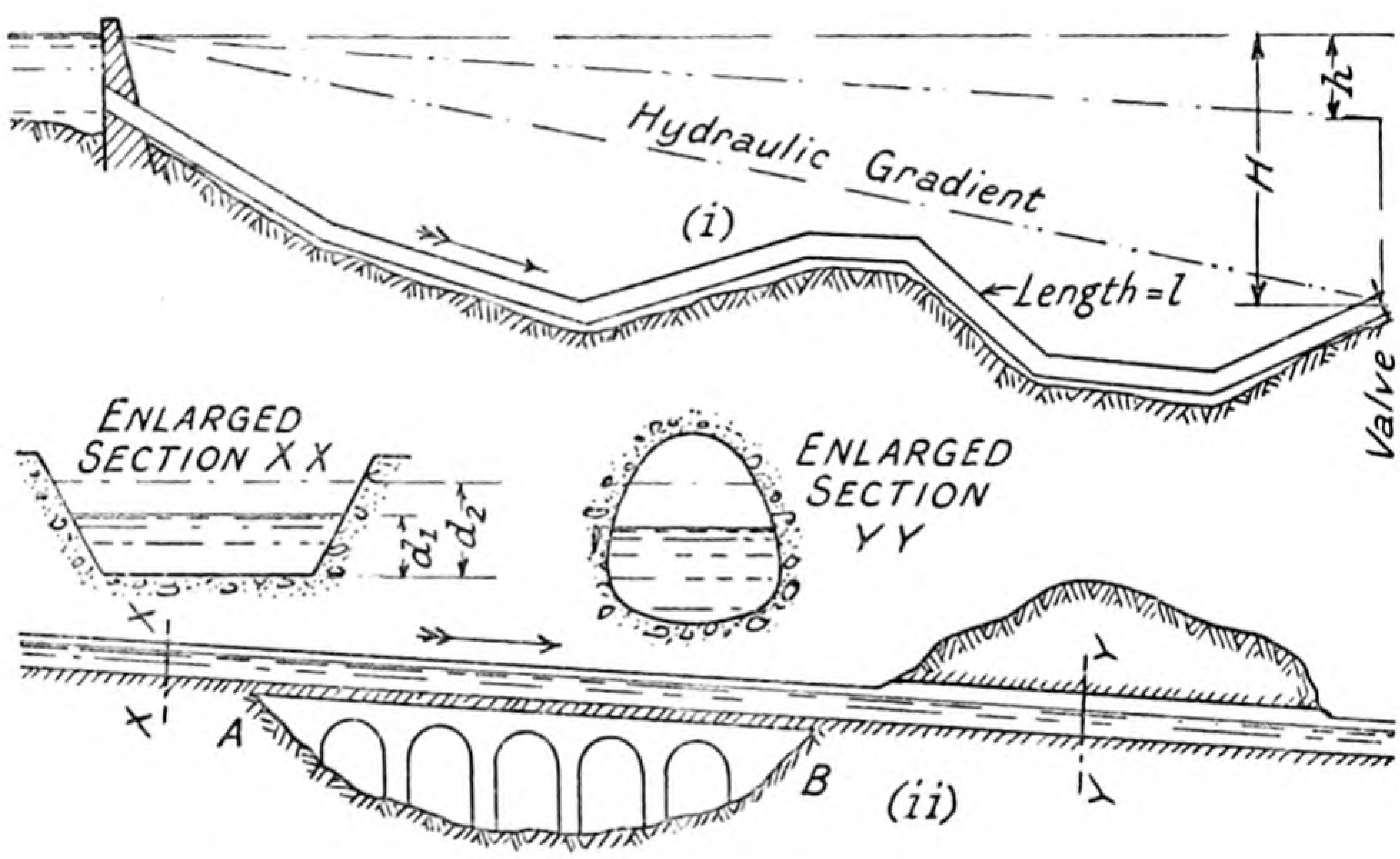

FIG. 133.—Comparison between pipe and open channel.

(iii) For reasons of strength and convenience of manufacture and installation, pipes are almost invariably of circular cross-section. There is much greater latitude when selecting the shape of a channel cross-section.

(iv) The limiting velocity in pipes rarely depends upon the danger of eroding the walls of the passage, as it does in channels. On the other hand, the ever-present threat of damage resulting from inertia shocks in pipes (§ 115) is virtually absent when channels are concerned.

When the final choice is governed by financial considerations, it will be found that the greater the volume of water to be conveyed, the more likely it is that a canal will be preferable.

In an aqueduct extending over many miles, a composite construction has advantages, lengths of pipe alternating with lengths of channel according to the local characteristics of the country.[68] Thus, for crossing the valley shown in Fig. 133 (ii), a pipe or *inverted siphon* (§ 166) from A to B might be a good deal cheaper than a channel carried on arches. **(Example 84).**

Problems of channel design are examined in Chapter X; various aspects of pipe design form the subject of the present chapter.

150. General Considerations. (i) *Mechanical strength.* This is the primary attribute we demand of a pipe. The pipe must not burst, break, or leak. The wall thickness must therefore be sufficient to enable the material to withstand:

—Tangential wall stresses due to internal pressure (equation 2-4, § 21). This is usually the predominant—or at least the most easily calculated—stress.

—Tangential stresses due to excessive *external* pressure, such as would arise if ever there were a negative pressure inside the pipe. A thin-walled pipe might then be squeezed nearly flat by the external pressure of the atmosphere.

—Longitudinal stresses resulting from the frictional drag of the liquid on the internal surface (§ 67). It is paradoxical that although nearly all formulæ for hydraulic flow are based on a study of this longitudinal force, the force itself is never directly calculated when designing a pipe.

—Resultant static and dynamic thrusts at bends and changes of direction (§§ 21, 119).

—Stresses—often indeterminate—resulting from: (*a*) Thermal expansion and contraction[69]; (*b*) The weight of the pipe itself when laid on steeply sloping ground; (*c*) Rough treatment during transport to site; (*d*) Crushing and bending loads imposed by heavy traffic on a pipe buried beneath a street or highway, or resulting from earth movements, etc.

(ii) *Resistance to corrosion, etc.* If the metal forming the pipe wall is eaten away by chemical corrosion or electrolytic action (§ 11), or destroyed locally by cavitation (§ 134), the effect will be as disastrous as if the walls were initially too thin.

To diminish or delay corrosion, therefore, iron and steel pipes are almost invariably protected by a coating of either bitumen, asphaltic mixtures of various kinds, cement, or zinc. When the pipe is run through salty ground, such protection is almost more important on the outside than on the inside surface.

(iii) *Hydraulic resistance.* The hydraulic resistance a pipe offers to the flow of the liquid is expressed in terms of the head loss.

Very often the value of the frictional loss of head is fixed beyond dispute, as for example when water flows under gravity from a low level storage reservoir to the distributing point of a town's water supply a vertical distance H below it, Fig. 133 (i). Here the energy corresponding with H must in any event be destroyed, consequently the "gravitational main" may be designed so that the frictional loss as the stipulated discharge flows through it is exactly equal to H. If a high-level reservoir were concerned such a procedure might involve an inconveniently high pipe velocity, and it would then be necessary to destroy the surplus energy by throttling through a valve.

On the other hand, if the water must be pumped up into a reservoir through a long *rising main*, Fig. 150, the friction loss is a matter of judgment that must be arbitrarily settled, largely on economic grounds. Depending upon the length of pipe and the general conditions, the frictional head h_f may range from 2 per cent. to 50 per cent. or more of the static lift. Similarly, in high-head hydro-electric installations, it is necessary to arrive at a reasonable compromise between excessive capital outlay on the pipe line and undue waste of energy due to pipe friction. In short pipes the frictional head will sometimes not exceed 1 per cent. of the static head, and even in pipes several miles in length it rarely exceeds 10 per cent., § 252 (i). (**Example 77.**)

There must consequently be a good deal of preliminary estimation and readjustment, in the light of the information detailed in various paragraphs throughout this chapter, before final answers can be given to the questions: what diameter of pipe,[70] what class of pipe, and what thickness of pipe must be chosen to convey a given quantity of liquid with a specified frictional loss.

151. Range of Materials. *Cast iron.* This is perhaps the most widely-used metal. *Centrifugally-cast* or *centrifugally-spun* iron pipes, in which the individual lengths are formed by pouring the metal into revolving moulds, are smoother and more resistant to shocks than sand-cast pipes. Although the mechanical strength is naturally less than that of wrought iron or steel pipes, the resistance to corrosion is usually greater.

Wrought iron. This metal is still in great demand for relatively small screwed-and-socketed pipes from $\frac{1}{4}$ inch to 6 inch or so in diameter.

Mild steel. For high pressures, mild-steel pipes must invariably be used. In any event, such pipes are lighter and more easily transported than cast-iron pipes. Various systems are available for rolling them from steel plate and for welding the seams.

Non-ferrous metals. Copper is replacing lead for the small-bore distribution pipes used in households. Copper and brass will resist the action of sea-water better than iron, and lead may be used for conveying concentrated acids.

Wood. Staves of wood, clamped by circumferential iron bands, form the most economical kind of large-diameter low-pressure pipe in remote districts where timber is plentiful and transport costs are high.

Cement. The great advantage of cement is its immunity from rusting. It is used in the form of plain concrete, reinforced concrete with steel reinforcing bars—sometimes pre-stressed,[(71)] —or concrete reinforced with textile or other material. *Asbestos-cement* pipes, in which asbestos fibres form the binding medium, are now frequently preferred to steel or cast iron. Naturally they will not withstand the severe treatment that the relatively heavier and more expensive metal pipes are expected to do.

Stoneware. The pipes of vitrified clay so frequently used for small sewers may occasionally have to act as pressure pipes.

Porcelain, celluloid, india-rubber, etc. Chemical processes may sometimes call for special materials such as these. There is obviously a great demand for india-rubber hoses, either with or without canvas and wire reinforcement, for conveying water for a variety of duties.

Pressure tunnels. Tunnels driven through solid rock for distances of several miles often serve as the upper part of

the closed conduits that feed hydro-electric plants, § 252 (i). Hydraulically they are classed as pipes, being in this respect quite different from the roofed open channels shown in Figs. 133 (ii), 169 and 198. The walls of the pressure tunnel may be left either rough-hewn, they may be given a lining of smooth cement, or they may have a steel-plate lining.

152. Types of Joints. Pipes are manufactured in lengths of perhaps 5 to 40 feet. The system of joining together these individual sections into a continuous line has an important bearing not only on the cost of manufacturing, laying, and

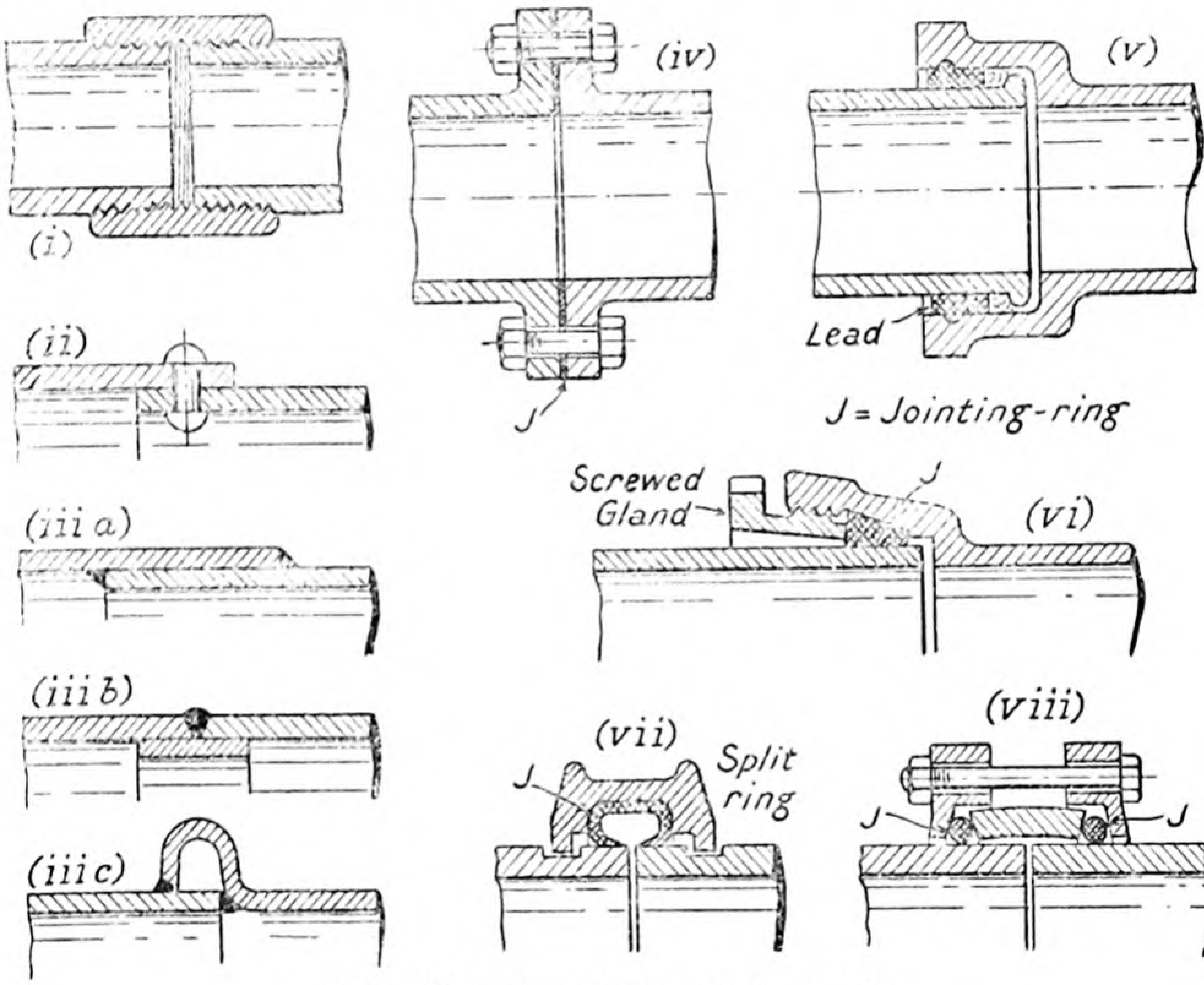

FIG. 134.—Some types of pipe joints.

maintaining the pipe, but also on its hydraulic resistance and on its water-tightness.[72], [73] Diagrams of some of the best-known types of joints are collected in Fig. 134, to which the following comments refer :—

(i) *Screwed and socketed.* The invariable method for small wrought-iron pipes.

(ii) *Riveted.* The lap joint illustrated is only one of various types available for steel pipes up to the largest sizes.

(iii) *Welded.* Lap-welded, (*a*), and butt-welded, (*b*), joints for steel pipes are here shown. The butt-welded type is by

far the most common, and modern technique enables the joints to be made without the need for the internal sleeve shown in the sketch (iii) (*b*). The hydraulic resistance is thereby greatly reduced. The circumferential chamber that distinguishes the proprietary joint (iii) (*c*) enables the seams to be tested for water-tightness without the necessity for filling the whole pipe; the test-pressure need be applied to the chamber only. Welding is a useful additional safeguard for screwed and socketed joints, especially if the line is to carry paraffin (kerosene) or similar liquids.

(iv) *Flanged joints.* In the diagram the mating flanges are cast integrally with the pipe sections; but wrought-iron and steel sections may have the flanges welded or screwed on. A rubber-insertion or similar joint-washer ensures tightness against leakage. The advantage of flanged joints is that they may very readily be broken and re-made.

(v) *Spigot and socket.* Until recently the universal choice for cast-iron water mains of all sizes, this joint depends for its tightness upon a jointing-ring of lead, either cast in place after the pipe sections are laid together, or in the form of lead-wool driven into position. The ring is finally caulked. The system is equally suitable for steel pipes.

(vi), (vii), and (viii) *Proprietary flexible joints.* With the object of facilitating pipe-laying and of giving the completed main a slight degree of flexibility, various types of joints have been developed which use india-rubber joint-rings of special form. Diagram (vi) shows a screwed gland which is used to force home into a conical socket a composite ring of lead and rubber. The *Victaulic* joint, (vii), depends upon no mechanical tightening device; the outer split cast-iron ring or sleeve serves only to locate and support the flexible moulded jointing ring J, whose tapered lips are forced firmly against the pipe extremities by the water-pressure itself. In the muff-coupling, (viii), which is specially suited to plain-ended steel and asbestos-cement pipes, tightening of the bolts squeezes the twin rubber rings J, J, hard against the loose flanges, the loose sleeve, and pipe exterior.[74]

It is to be noted that the two categories of couplings (i) to (iv) and (v) to (viii) behave differently in the following respects: A system of screwed, welded, or flanged piping constitutes a

self-sustaining unit which can usually resist both tangential (bursting) and longitudinal stresses. But because of its rigidity it can only meet temperature and similar changes by elastic deformation. Although flexible joints (v to viii) allow the pipe to be carried round gentle curves and to adapt itself to earth movements, temperature variations, and so on, yet the joints cannot be depended upon to resist a longitudinal pull. Bends, tee-pieces and the like must therefore be supported by anchor blocks fixed in the ground, otherwise the resultant thrusts generated by the static and dynamic pressures, §§ 21, 119, 150, may tear open the joints. **(Example 85.)**

(ix) *Special joints for high-pressure hydraulic transmission systems* are mentioned in § 358.

153. Hydraulic Calculations for Laminar Flow. Having made a provisional choice of a suitable material for the pipe, and knowing the physical characteristics of the liquid to be conveyed through it, we can begin actual hydraulic calculations by first finding out whether the flow is likely to be *laminar* or *turbulent*.

Although it is extremely rare to find water in ordinary pipe lines under conditions of steady, viscous, or stream-line flow (§§ 64, 65), it is not at all unlikely that the velocity of oil or similar thick liquids will be below the critical velocity.[75] Since the value of the Reynolds number, and therefore of the critical velocity, cannot be known until the velocity v and pipe diameter d are known, it is necessary first of all to estimate whether the flow is more likely to be laminar or turbulent, work out values of v, d, and R_n accordingly, and make a fresh calculation if the original assumption is found to be wrong.

If it is finally established that the flow is laminar, i.e. that $R_n = \dfrac{vd}{\nu}$ is less than 2000, then the required pipe diameter d can be calculated from formula 5-3, § 65, viz. $Q = \dfrac{\pi d^4}{128\mu} \cdot \dfrac{p_1 - p_2}{l}$, which may be written in the modified form

$$q = \frac{3{\cdot}53 d^4}{\mu} \cdot \frac{p_1 - p_2}{l} \quad . \quad . \quad . \quad (9\text{-}1)$$

in which q is the discharge in cusecs, d the pipe diameter in feet, $(p_1 - p_2)$ is the pressure drop in lb./sq. in. in l feet of

pipe, and μ is the viscosity of the liquid in $\dfrac{\text{lb. sec.}}{\text{sq. ft.}}$. (§§ 8, 371.)
(If q is in lit./sec., d in cms., $(p_1 - p_2)$ in kg./sq. cm., l in metres and μ in poises, then

$$q = \frac{0{\cdot}240d^4}{\mu} \cdot \frac{p_1 - p_2}{l}. \qquad \textbf{(Example 78.)}$$

154. Darcy Formula for Turbulent Flow. If the value of $R_n = \dfrac{vd}{\nu}$ is greater than 2800, which almost invariably happens when water flows through pipes under engineering conditions, then the motion will be turbulent and the formulæ quoted in this and in succeeding paragraphs will be applicable. Formula 5-7, § 68, $h = \dfrac{4fl}{d} \cdot \dfrac{v^2}{2g}$, can be put in the form

$$h = \frac{flq^2}{10d^5} \quad . \quad . \quad . \quad . \quad (9\text{-}2)$$

where q = discharge in cusecs.
v = mean velocity in ft./sec.
h = head lost in friction (feet).
l = length of pipe in feet.
d = diameter of pipe in feet.
f = a coefficient depending on diameter, velocity, etc.

If q is in cub. m./sec., l, d, and h in metres, then

$$h = 0{\cdot}33f\frac{lq^2}{d^5}.$$

If q is in lit./sec., h and l in metres, d in cms., then

$$h = 3305f\frac{lq^2}{d^5}. \qquad \textbf{(Example 77.)}$$

In using any of these formulæ it is necessary first to choose with the help of the following information a likely value of f, calculate provisional values of v and d, adjust the value of f if required, and thus arrive at the final pipe diameter. Note that f is a pure number, having the same value under given conditions *for all systems of units.*

For *smooth* pipes the value of the coefficient f depends directly upon the Reynolds number R_n; the relationship between the two is expressed by the curve (Fig. 135), which

is valid for *any* system of units and for *any* liquid—water, oil, spirit, etc.

Surfaces which can be regarded as hydraulically smooth are

Glass.
Lead.
Drawn brass and copper.
Cement
Asbestos cement } only in the most favourable possible conditions.
Varnished planed wood.

But the surface of natural (unpainted) wood, no matter how carefully finished, is never quite smooth in the hydraulic sense.

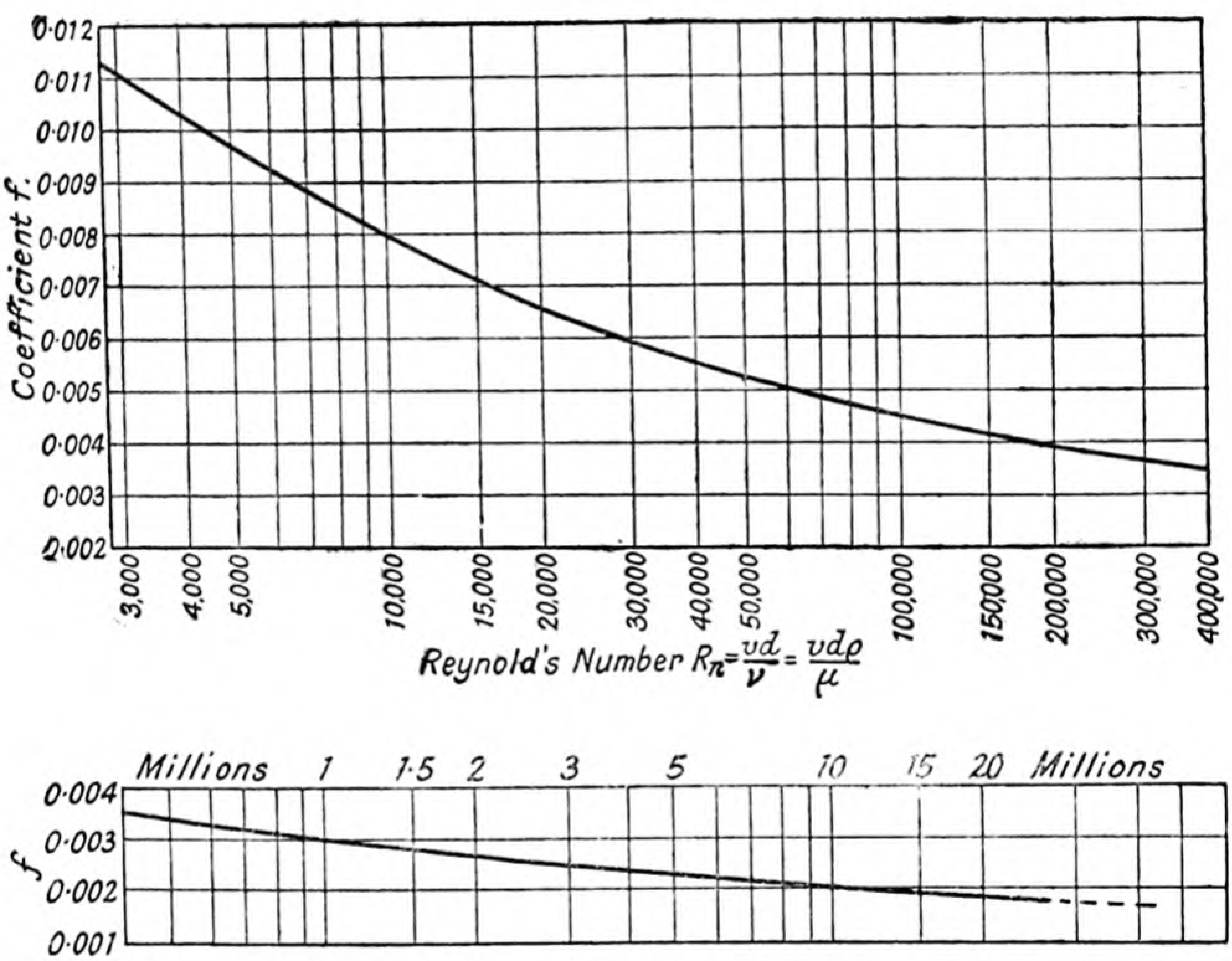

FIG. 135.—Chart for determining coefficient f for smooth pipes.

For *rough* pipes, such as the iron and steel pipes used in ordinary engineering practice, the value of f is nearly always greater than the value for an equivalent smooth pipe, nor is it now directly linked with the value of R_n. Fig. 136 shows how the pipe coefficient is influenced by the nature and the diameter of the pipe, and by the mean velocity of the water flowing in it. The graphs show :—

(i) For a given mean velocity, the coefficient invariably grows *larger* as the pipe becomes smaller. (ii) Evidently the old cast-iron pipes have so great a relative roughness (§ 80) that the flow nearly obeys the rough-law regime corresponding to a value of exponent $n = 2{\cdot}0$. (iii) On the other

hand, the 12-inch new wrought-iron pipe has such a small relative roughness that its graph approaches close to the equivalent smooth-pipe graph (broken line) transferred from Fig. 135.

Because of the practical convenience of the Darcy formula, it is useful to know how to evaluate the pipe coefficient f even

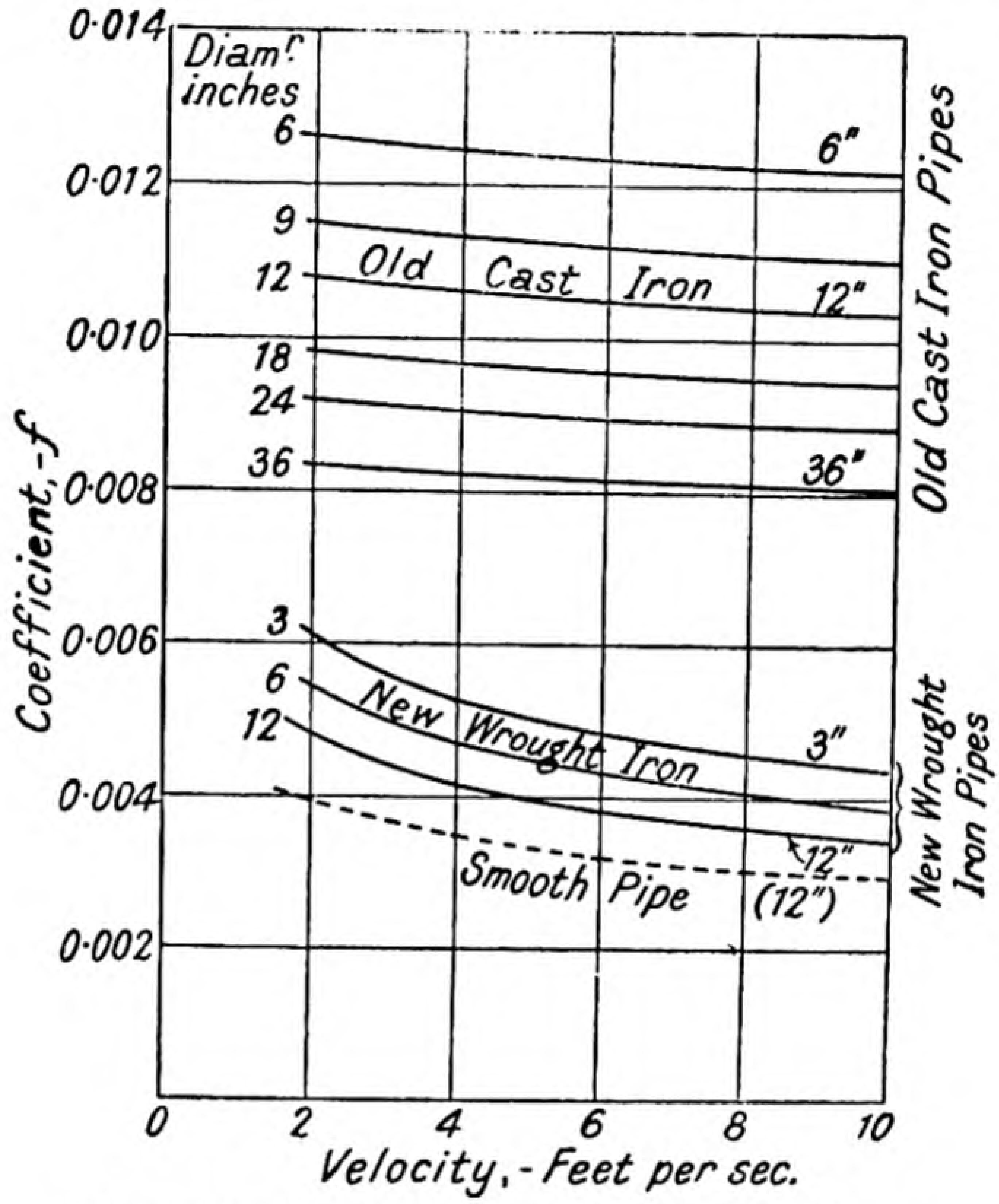

FIG. 136.—Coefficients for commercial pipes.

if the pipe surface is described by numerical values suited to other types of flow formulæ. Appropriate conversion expressions are :—

Laminar flow (§ 153) . . . . $f = \dfrac{16}{R_n}$.

Chezy formula (§ 156) . . . . $f = \dfrac{2g}{C^2}$.

Manning formula (§ 158) . . $f = \dfrac{29{\cdot}1\ N^2}{\sqrt[3]{m}}$ (m in feet).

Do. . . $f = \dfrac{19{\cdot}6\ N^2}{\sqrt[3]{m}}$ (m in metres).

(*Note.* Although in this book the pipe coefficient "f" invariably has the value $(2gdh)/(4lv^2)$, yet other authorities prefer the form $(2\ gdh)/(lv^2)$ (§ 68).

In case of doubt, it is worth remembering that the first system gives values of "*f*" within the range 0·003–0·01, while in the second system the values may be of the order 0·01–0·05.)

155. Universal Charts for Rough-Pipe Coefficients. Approximate or provisional values for rough - pipe coefficients[76], [77] may be obtained from generalised charts such as Fig. 137. The system of plotting—pipe coefficient "*f*" against

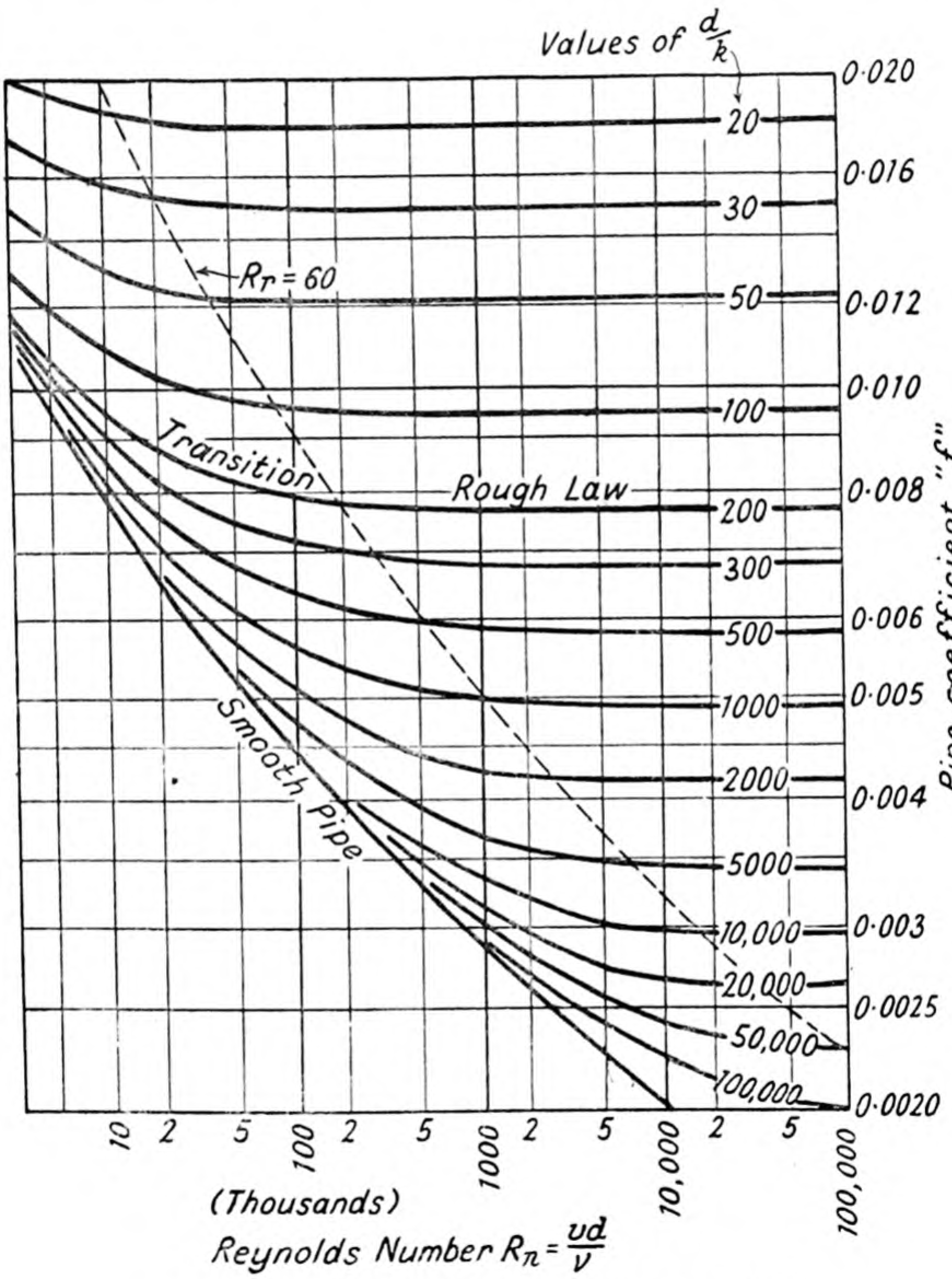

FIG. 137.—Unversal chart for pipe coefficients.

Reynolds number R_n—is the same as in Fig. 135; but now there must be a separate graph for each value of the *relative roughness* (§ 80). For convenience, it is the reciprocal of the relative roughness, d/k, that is marked on each graph.

The diagram is used as follows :—

(i) The *absolute roughness* of the pipe surface, k, is estimated from the Table below :—

Type of pipe.	"k" in inches.
Asbestos cement	0·0005
New wrought iron	0·0017
New steel	0·002–0·005
New asphalted cast iron	0·005
New uncoated cast iron	0·010
Concrete	0·01–0·20

(ii) From the pipe diameter, d (inches), and the absolute roughness, the value of d/k is computed.

(iii) The nearest appropriate curve in Fig. 137 is then selected, and, from the known value of the Reynolds number, vd/ν, the desired value of the pipe coefficient "f" is read off.

Although in principle the diagram is applicable to any liquid, yet the reasoning of § 83 makes it clear that the information given should be treated with reserve. The utility of Fig. 137 may also be assessed by comparing it with Figs. 52 and 53, § 70.

156. Chezy Formula. In this formula (formula 5-8, § 68 (ii)),

$$v = C\sqrt{mi},$$

the mean velocity in the pipe, v, is expressed in terms of a coefficient C, the hydraulic mean depth $m = \frac{d}{4}$, and the virtual slope $i = \frac{h}{l}$. If m is in feet, v is in ft./sec. ; if m is in metres, v is in m./sec.

The value of the coefficient C for water is sometimes calculated from *Kutter and Ganguillet's* formula :—

$$C \text{ in foot units} = \frac{41{\cdot}6 + \dfrac{0{\cdot}0028}{i} + \dfrac{1{\cdot}81}{N}}{1 + \dfrac{N}{\sqrt{m}}\left(41{\cdot}6 + \dfrac{0{\cdot}0028}{i}\right)}.$$

$$C \text{ in metric units} = \frac{23 + \dfrac{0{\cdot}00155}{i} + \dfrac{1}{N}}{1 + \dfrac{N}{\sqrt{m}}\left(23 + \dfrac{0{\cdot}00155}{i}\right)}.$$

(Note that the relation between the two values is : C in metric units $= \dfrac{C \text{ in foot units}}{1{\cdot}81}$.)

In these formulæ the term N is a *coefficient of roughness* or *coefficient of rugosity* which is a *pure number, independent* of the pipe diameter or the water velocity. Commonly accepted values of "Kutter's N" are :—

For Smooth cement or planed wood . . .	0·010
New wrought iron	0·011
Concrete	0·012
New cast iron : earthenware	0·013
Riveted steel	0·014
Old cast iron	0·017 to 0·019
Unlined pressure tunnels in rock . . .	0·020 or more

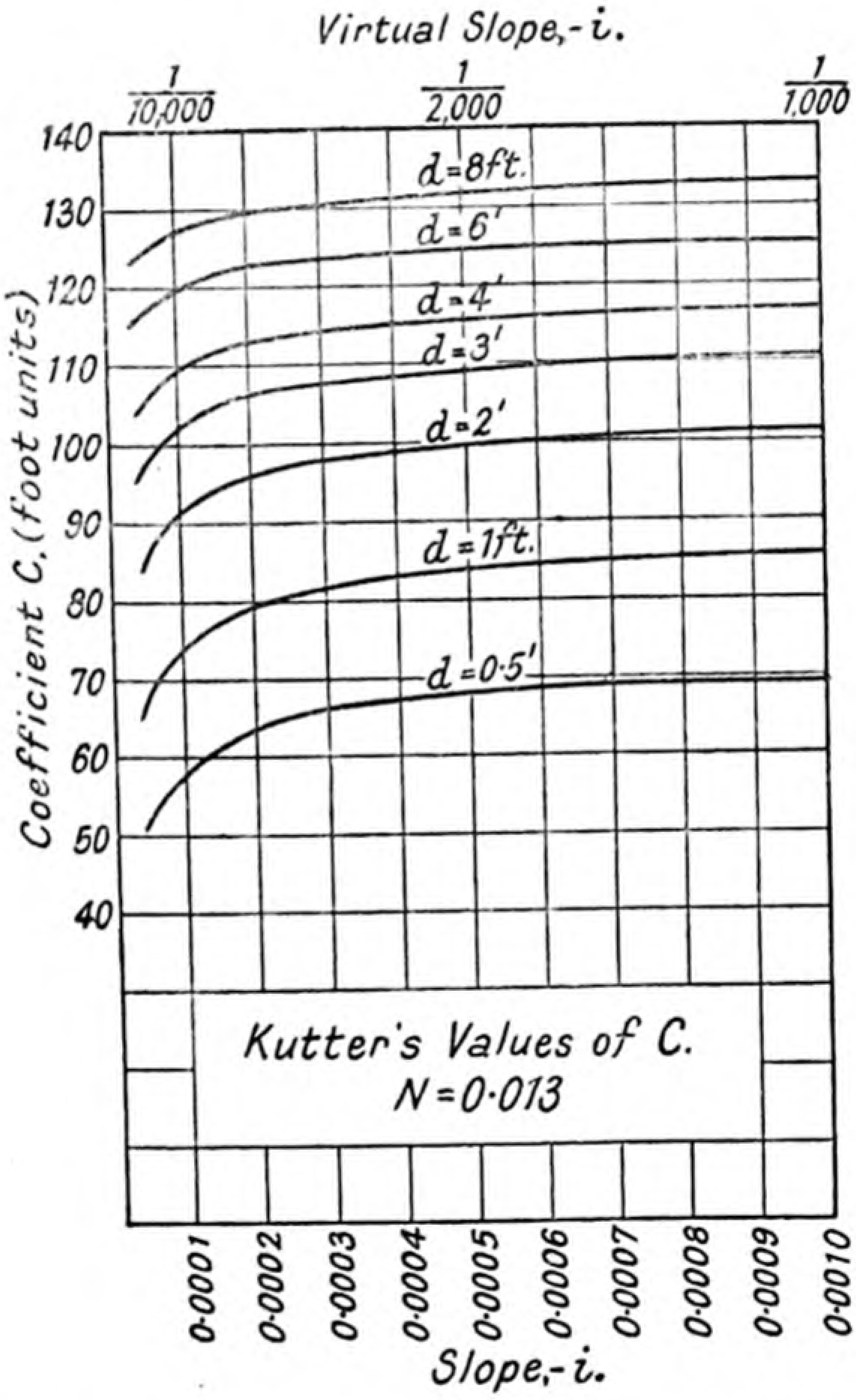

FIG. 138.—Kutter's coefficients for new cast-iron pipes.

Some values of C in foot units calculated for Kutter's $N = 0·013$ are plotted for different sizes of pipes in Fig. 138. It will be noticed that the increase of C with d or with i agrees as it should do with the diminution of f as d or v increases.

(*Note.* The connection between the Kutter's roughness number N and the absolute roughness k, § 155, is examined in § 159.)

157. Exponential or Logarithmic Formulæ. The fundamental exponential formula 5-9, § 68 (iii),

$$h = \frac{f_1 l v^n}{d^x}$$

may readily be transformed into the formula

$$v = f_2 \, m^{\frac{x}{n}} \, i^{\frac{1}{n}} \quad . \quad . \quad . \quad (9\text{-}3)$$

or into

$$q = f_3 \, d^{\frac{x}{n}+2} \, i^{\frac{1}{n}} \quad . \quad . \quad . \quad (9\text{-}4)$$

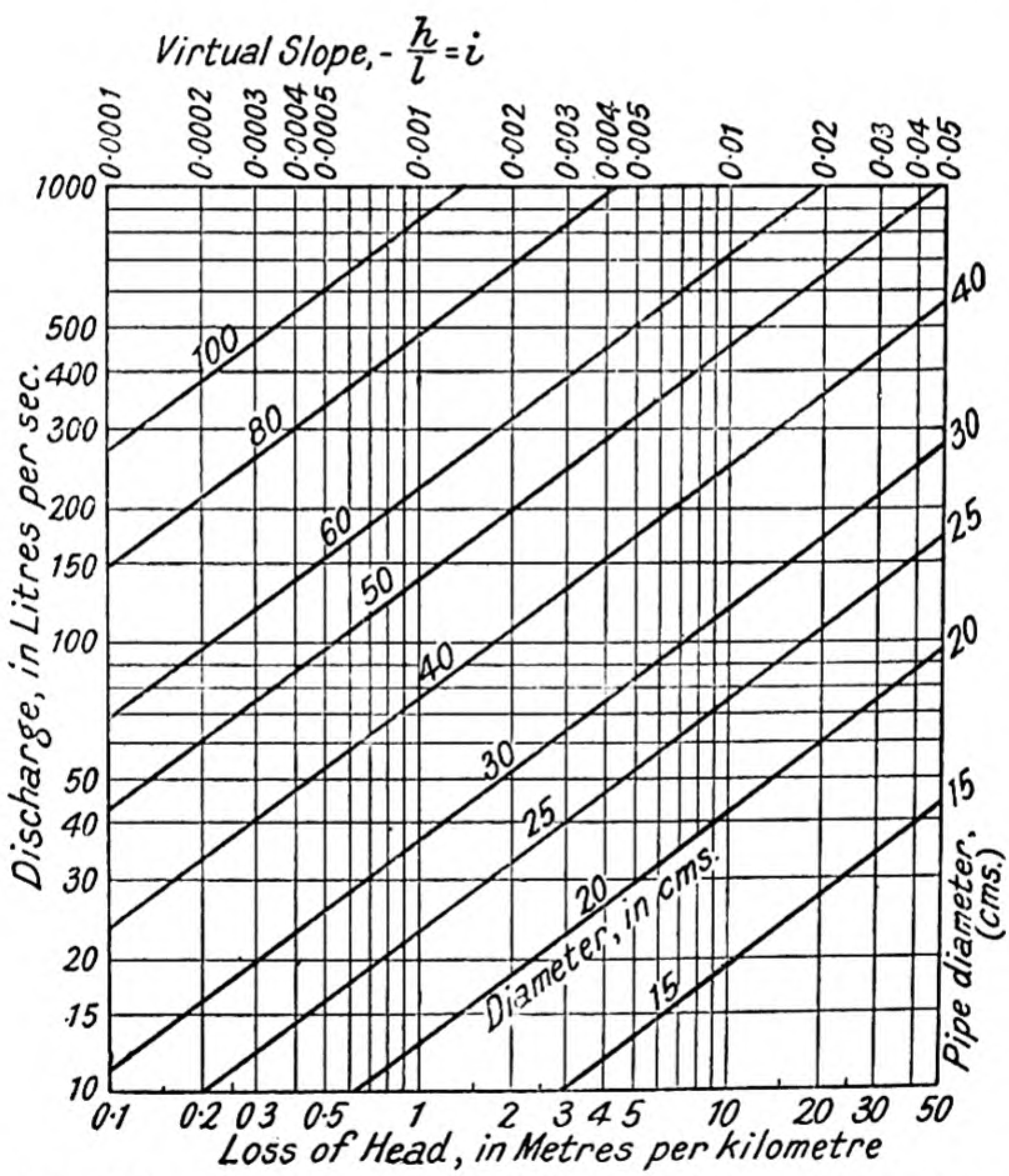

FIG. 139.—Discharge chart for new uncoated cast-iron pipes.

For a given pipe material and a given system of units, the coefficients f_1, f_2 and f_3 and the indices n and x are *invariable* for any size of pipe or any water velocity.

From the values put forward by various authorities, those of Mr. A. A. Barnes have been chosen for citation here.[78]

Type of Pipe.	f_1.	f_2.	f_3.	n	x
New asphalted cast iron . .	0·000436	174·1	47·09	1·891	1·454
New uncoated cast iron . .	0·000343	136·6	46·70	1·953	1·172
New asphalted, single riveted iron or steel	0·000386	171·4	49·41	1·898	1·372

(Foot units throughout.)

From other sources the following additional figures have been compiled :—

Type of pipe.	f_2 (v in ft./sec., m in ft.).	n.	x.
Galvanised iron . .	173	1·90	1·29
Asbestos cement . .	240	1·79	1·22
Wood stave . . .	203	1·80	1·26
Unlined canvas fire-hose .	126	1·85	1·30

Logarithmic formulæ are particularly adapted for plotting in forms suitable for ready reference, because of the fact that if the co-ordinate axes are graduated logarithmically the resulting graphs are *straight lines.* In this way Fig. 139 has been prepared from the formula 9-4 above, modified for use with metric units, viz.: Discharge through *new uncoated cast-iron pipes* in litres/sec., $q = 0{\cdot}1826\ d^{2{\cdot}60}\ i^{0{\cdot}512}$ (d in cms.). **(Example 79).**

Another chart, Fig. 140, is suitable for *bitumen-coated (asphalted) steel pipes,*[79] in which the flow of water is represented by the equation :—

$$q = 28{\cdot}6\ d^{2{\cdot}68} i^{0{\cdot}54},$$

where q is expressed in gallons per minute and d is expressed in inches. From the broken lines in this chart, mean velocities in ft./sec. may be read.

Alternatively, logarithmic formulæ may be represented graphically in the form of abacs, nomograms, or alignment charts of the kind plotted in Fig. 141; this chart permits the discharge in new asphalted cast-iron pipes to be read off. Here the Barnes formula q (cusecs) $= 47{\cdot}09\ d^{2{\cdot}769}\ i^{0{\cdot}529}$ is used, an advantage of the abac being that the axes may be graduated

both in foot and in metric units. From line *aa* we find (for example) that a 1 ft. diameter pipe could convey 7 cusecs of water with a loss of head of 2·7 ft. per 100 ft. of pipe. Line *bb*

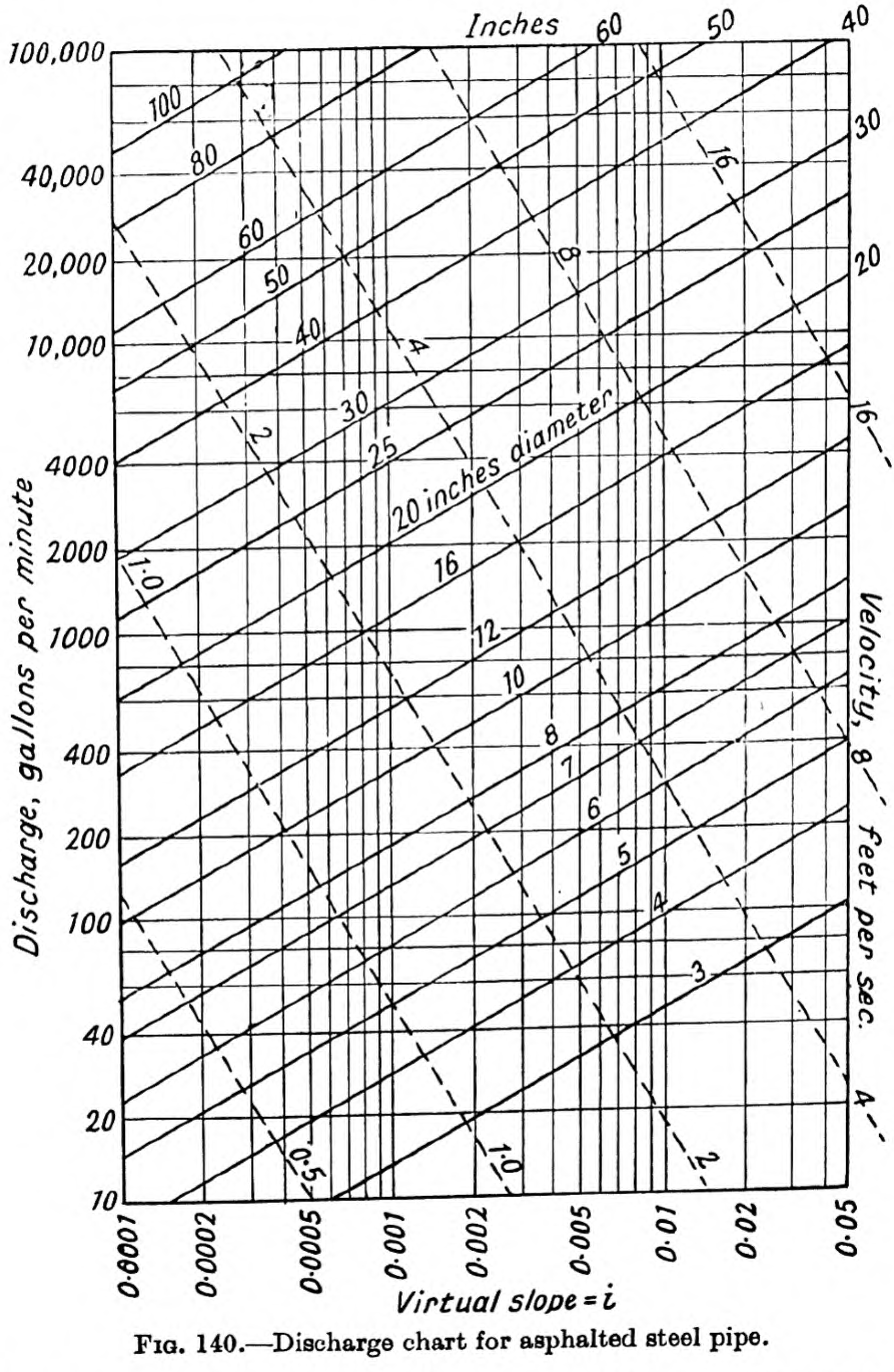

FIG. 140.—Discharge chart for asphalted steel pipe.

shows that with a virtual slope of 0·0015, the diameter of pipe required to convey a discharge of 2000 lit./sec. is 121 cms.

In the *Williams-Hazen* formula, widely used in America,

invariable *average* values of the exponents x/n and $1/n$ are selected, leaving roughness variations to be cared for solely by changes in the coefficient f_2; this variable is itself put in the form $f_2 = 1{\cdot}32\ c$, where c ranges in value between

150 (in foot units) for very smooth surfaces,

and

60 (in foot units) for very rough surfaces.

The value of c may also be slightly influenced by the size of the pipe.

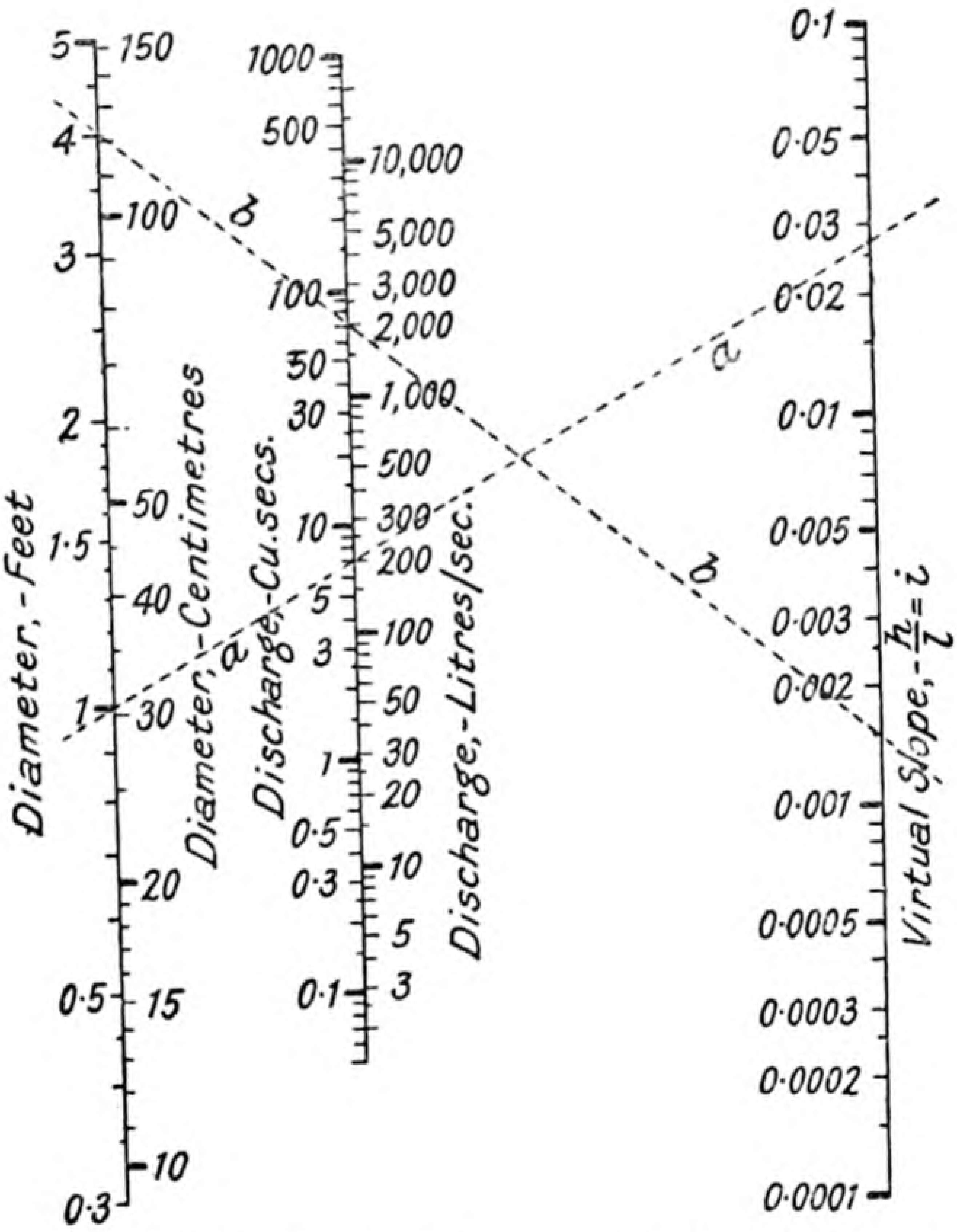

FIG. 141.—Discharge chart for new asphalted cast-iron pipes. (Barnes' formula.)

For use with foot units, the complete Williams-Hazen formula therefore reads

$$v = 1{\cdot}32\ c\ m^{0{\cdot}63}\ i^{0{\cdot}54} \quad . \quad . \quad . \quad (9\text{-}5)$$

158. Manning Type of Formula. A trifling further manipulation of the exponents x/n and $1/n$ brings a disproportionately great reward. If they are given the invariable values $x/n = \frac{2}{3}$, and $1/n = \frac{1}{2}$, then formula 9-3 will read

$$v = f_4 m^{\frac{2}{3}} i^{\frac{1}{2}} \quad . \quad . \quad . \quad . \quad (9\text{-}6)$$

In this form it is associated with the names Bruges, Santo Crimp, Strickler and Manning. Suitable values for the coefficient f_4 are given below :—

Type of Pipe.	f_4 (v in ft./sec., m in ft.).	f_4 (v in m./sec., m in metres).
New cast iron . . .	140	94
Badly corroded cast iron .	80	54
New asphalted pipes . .	170	114
Old asphalted pipes . .	140	94
Riveted pipes . . .	120	81
Cement-lined pipes . .	136	91

There is still another way of evaluating the coefficient f_4 ; it consists in using the values of *Kutter's rugosity coefficient* N, thus (§ 156) :—

$$f_4 \text{ (foot units)} = \frac{1{\cdot}486}{N}.$$

$$f_4 \text{ (metric units)} = \frac{1}{N}.$$

The corresponding forms of equation 9-6 then become

$$\left.\begin{aligned} v &= \frac{1{\cdot}486}{N}\,.m^{2/3}.i^{1/2} \; (m \text{ in feet}); \\ v &= \frac{1}{N}\, m^{2/3}\, i^{1/2} \; (m \text{ in metres}). \end{aligned}\right\} \quad . \quad . \quad (9\text{-}7)$$

This is the formula which is usually known as *Manning's formula*, although perhaps it should more strictly be called Manning's derived formula. Like all similar expressions, it confers the advantage that all calculations can be worked out *directly on the slide-rule*, without the need for logarithms. By writing $v = f_4 m^{1/6}\sqrt{mi}$, we observe that the term $f_4 m^{1/6}$ is identical with the Chezy coefficient C (§ 156).

It should again be pointed out that all formulæ of the Chezy, Kutter or Manning type are valid for water *only*.

159. Selection of a Flow Formula. An enquirer who only wants to know how big to make a pipe may reasonably feel discouraged and bewildered when confronted with such a

profusion of information as has just been offered. For his particular needs, only one formula may be right, so all the others will probably be wrong. Moreover, the formulæ quoted in §§ 154-158 have been selected from a much greater number. Yet when the complexities of the problem are realistically studied it must be admitted that a single clear-cut solution is an unattainable ideal.[80] In addition to weighing the uncertainties that pipe roughness imports into any question of pipe resistance, the designer of a pipe-line has also to try to take into account (i) the number and character of the joints, (ii) the skill with which the pipe is laid, (iii) the effect of years of service on the pipe walls (§ 161), (iv) the disturbing effect of bends, fittings, and the like. He ought, therefore, to look upon a flow formula not as a machine which will automatically turn out an answer when fed with the proper data, but as a witness whose evidence, when scrutinised in the light of his own knowledge and experience, will help him to arrive at a reasonable estimate of the pipe dimensions.

In choosing between one formula and another,[81], [82], [83], [84] the following comments may be useful :—

(i) *Ease of manipulation.* When a long and (nominally) straight pipe of uniform bore is in question, the logarithmic formulæ, § 157, have the advantage inasmuch as the desired information can be read directly from charts such as Figs. 139, 140, and 141. But if pipe friction losses account for only part of the total head available, or if the head loss or gain in turbines or pumps is involved, then the Darcy or quadratic formulæ are preferable, §§ 154, 155. The reason is that all the items that make up the total head can then be expressed in terms of velocity heads, and can thus be added one to the other, §§ 162-167.

(ii) *Size of pipe.* For the reason explained below, the Manning type of formula, § 158, is more likely to be suitable for very large pipes than the logarithmic type, § 157.

(iii) *Relative accuracy.* As logarithmic or exponential formulæ are in general purely empirical, based on observations made on pipes actually in service, they can be applied with considerable confidence to projected pipe-lines *of the same type and size* as those which provided the data.

Comparing the exponential type of formula, § 157, with the Manning type, § 158, in the light of the analysis of flow given in §§ 81, 82, we quickly observe that the Manning formula describes a *rough-law* type of flow in which the head-loss depends upon the square of the mean velocity. On the other hand, exponential formulæ having an exponent n noticeably less than 2·0, can apply only to *transition-law* flow. A single glance at Fig. 63 suggests then, that the Manning formula is more likely to be right for large rough pipes and for high velocities, while exponential types appear to be more applicable to relatively smaller pipes. It is also a fair deduction that an exponential formula can only relate to a limited range of flow conditions, having regard to the trend of the graphs reproduced in Fig. 52.

If the assumptions that led to the tracing of the curves II and III in Fig. 63, § 82, are held to be justifiable, they will be found equally profitable here. Let us then assume that the Manning formula represents a regime of flow in which the pipe coefficient f depends *only* upon the relative wall roughness

$$k/d = \frac{\text{diameter of imaginary sand grains, } k}{\text{diameter of pipe, } d}.$$

Putting aside the possibility that the *type* of roughness, i.e. whether the roughness projections are sharp and angular, or smooth and rounded (§ 79), might affect the relationship, we intend to calculate the diameter of uniform sand grains sticking to the internal pipe surface that would create the same hydraulic resistance that is found in practice. There is now no need to be bound by the Nikuradse law: the Manning equation, together with the

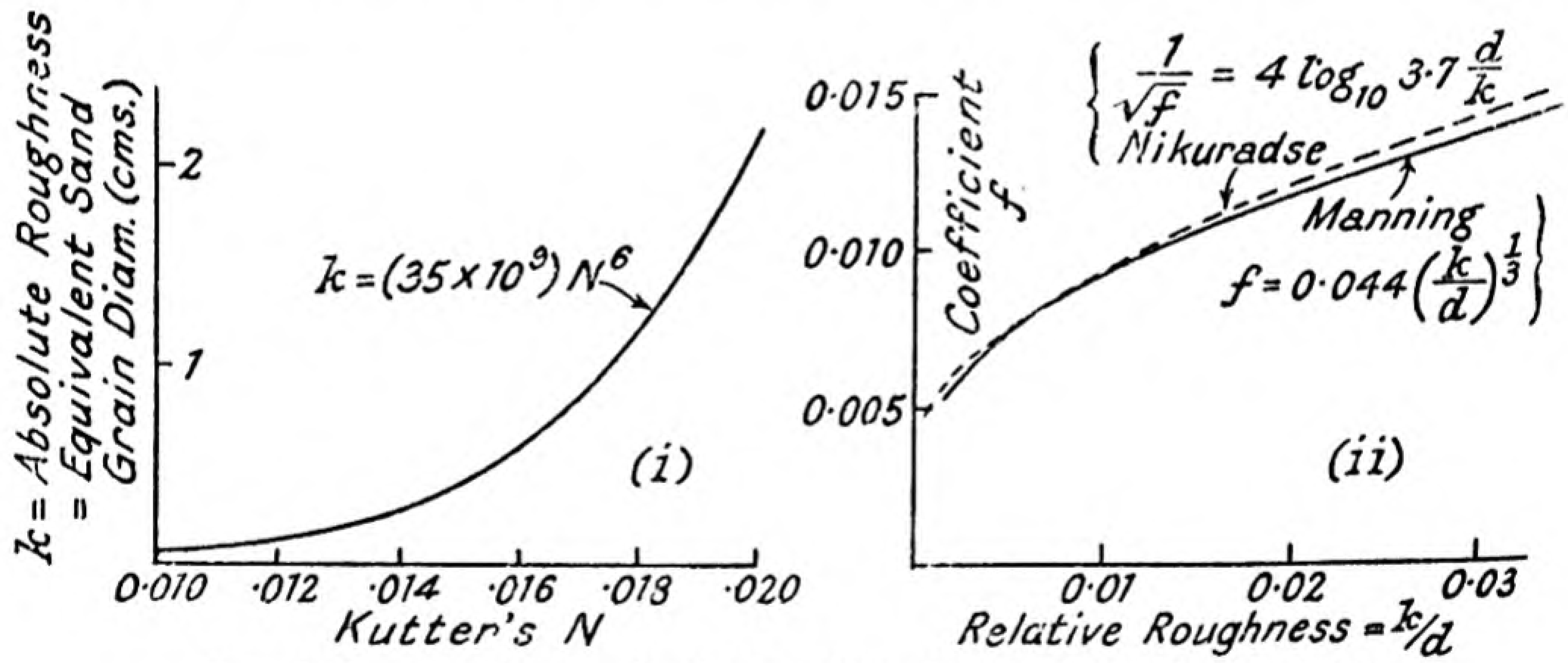

FIG. 142.—Conjectural relationships between N, k, d, and f.

Darcy equation 5-7, provides a new law that has the support of full-scale engineering practice. It is derived as follows :—

$$\text{Since } f \propto \frac{N^2}{m^{\frac{1}{3}}} \text{ (§§ 154, 158), then } f \propto \frac{N^2}{d^{\frac{1}{3}}}, \text{ or } f \propto \frac{N^2}{k^{\frac{1}{3}}}\cdot\frac{k^{\frac{1}{3}}}{d^{\frac{1}{3}}}.$$

Remembering that f is to depend only on the value of the relative roughness k/d, it is evident that (i) $\frac{N^2}{k^{\frac{1}{3}}}$ has an invariable value, (ii) the pipe coefficient f varies as the cube root of the relative roughness. By inserting suitable numerical constants, it finally appears that

$$k = \text{equivalent sand-grain diameter (cms.)} = (35 \times 10^9)N^6,$$

$$f = 0{\cdot}044\left(\frac{k}{d}\right)^{\frac{1}{3}}.$$

These relationships are plotted in Fig. 142 (i) and (ii). For comparison, the experimental values of f relating to artificially-roughened pipes are reproduced from Fig. 62. The agreement is instructive, and the actual coalescence of the two curves over a certain range shows that the numerical constants have been judiciously chosen.

Apart from the significance invested in the general shape and trend of these graphs, they have the virtue of providing a ready means of calculating the Reynolds roughness number $R_r = \frac{v_r k}{\nu}$ (§ 80). Its numerical value offers *statistical* support for the choice of one or other of the two competing types of flow formula. Guided by the tendencies revealed in Fig. 63, we can say with some degree of confidence that if R_r is *greater than* 60, then the *Manning* expression is applicable, while if R_r is *less* than 60, then an *exponential* formula may be preferable.

One must be particularly careful not to endow this number with any talismanic qualities that will magically solve all difficulties. The value 60 probably has no higher exactitude than the number 21 applied to the age of a man. Just as it is purely a legal convention to say that the transition stage between boyhood and manhood is completed at the age of 21, so it is a mathematical convenience to say that the boundary between transition-law flow and rough-law flow in full-scale engineering conditions is marked by the Reynolds roughness number 60.

160. Corrections for Variations of Liquid Characteristics. The Darcy quadratic formula when applied to hydraulically smooth surfaces, § 154, automatically takes into consideration the properties of the liquid concerned; for the appropriate value of the pipe coefficient f is read off from the graph, Fig. 135, whose abscissæ are directly related to the liquid density and viscosity. The curves in Fig. 137 are equally general. On the other hand, the coefficients tabulated for use in other conditions, and plotted in graphs such as Figs. 136, 138, 139, 140, 141, refer exclusively to moderately pure *water* at atmospheric temperature. What corrections must be applied if this stipulation cannot be satisfied ?

(i) *Temperature.* If the change is only in the temperature of the flowing water, it is to be remembered that the accompanying variations in density are hardly likely to be serious *for present purposes*, while changes in viscosity might be quite important (§ 9). Thus, for a specified discharge, pipe surface and diameter, a rise in water temperature from 32° F. to 212° F. will increase the Reynolds number by more than six times. As just explained, it is easy to assess quite accurately what effect this will have on the resistance of a *smooth* pipe. If, for instance, the original Reynolds number is 10,000, then the temperature rise will reduce the resistance by 37 per cent.;

and even if the original number is 1,000,000 there will be a reduction of about 27 per cent. in the head loss. For *rough* pipes the limiting value of 60 for the Reynolds roughness number R_r, § 159, will again be helpful. If the actual value of R_r is found to be greater than 60, then temperature effects *cannot have any appreciable effect on the flow.* If R_r is less than 60, then the probability is that the lower its value and the smoother the pipe, the more the effect of temperature is likely to approximate to what it would be on the flow through an equivalent hydraulically smooth pipe.

(ii) *Viscosity.* Although it is its influence on viscosity that chiefly empowers temperature to control hydraulic flow, yet an independent study of viscosity may create a sharper picture of the conditions arising when the pipe has to convey liquids other than water—liquids such as oils that common usage would designate as viscous.[85] Remembering that the relative viscosity of these organic compounds is very much more sensitive to temperature variations even than water is (§ 9), we may pass on to ask how to deal with the conditions most likely to arise, viz. flow along rough pipes at velocities not much above the critical velocity (§ 64). Perhaps the best guidance available at the present time is to be found in the universal chart, Fig. 137, § 155. As further evidence accumulates, as a result of full-scale tests, the margin of error inherent in such charts may be narrowed. **(Example 80.)**

(iii) *Solids in suspension.* When the liquid flowing along the pipe carries solids in suspension, its behaviour can be summarised as follows: considering a uniform horizontal pipe, it may be found that at very high velocities—say 10 or 20 ft./sec.—the head loss for the liquid-solid mixture is only slightly higher than it would be for clear water. As the pipe velocity declines, the discrepancy becomes greater, until there comes a stage at which the friction loss is nearly independent of the velocity. Beyond this point, the head loss does not fall as it does in Fig. 48 (i), for example; on the contrary, as the pipe velocity steadily diminishes, the head loss remains unaltered or it may even begin to rise. This means, of course, that meanwhile the pipe coefficient has been rapidly *rising*, until it may attain a value 10 or 20 times as great as the corresponding value for clear water.

If the pipe walls were transparent, it would be easy to see why these variations arose. At high velocities, the whole of the solid particles—sand grains or the like—are visibly swept along with the water, and the pipe is filled with a relatively homogeneous mixture. At low velocities, some of the solids settle to the bottom of the pipe, thereby partially blocking the waterway, reducing the cross-sectional area available for flow, and imposing on the fluid a much greater *real* velocity than the nominal velocity based

on the full pipe area. It is largely this increased real velocity that accounts for such an increase in the nominal pipe coefficient.

Because of the complex influences that control the transport of solids (§§ 111-113, 200), it is not possible as yet to offer simple relationships which will describe the flow of these liquid-solid mixtures; but progress is being made in evolving basic laws.[86], [87], [88]

161. Influence of Age on Pipe Performance. Returning now to the general case of flow of water at atmospheric temperature, e.g. water destined for domestic consumption, the highly important question of the *ageing* of pipes remains to be investigated. In the Tables of Coefficients given in §§ 154-158, the terms " new pipes," " old pipes " are repeatedly used. How long does it take for a new pipe to become an old pipe? And why does the pipe performance deteriorate in this way? In general terms the second question can readily be answered: the pipe grows rusty; the surface roughens; incrustations form. Thus there are at least two separate reasons for the reduction in pipe capacity: the incrustation may actually reduce the cross-sectional area available for flow, and it will certainly increase the value of the coefficient f. The scale, rust, or deposit forming in a small pipe may in course of years completely choke it.

In the same way that the conception of a standardised artificial roughness made the whole problem of pipe resistance more tractable, § 81, so the formulation of conventionalised laws of roughness *growth* may be helpful now. According to the character of the water and of the pipe wall, the pipe performance may suffer because of (*a*) the formation of projecting nodules or tubercles, (*b*) the deposition of slime or of vegetable growths, (*c*) the deposition of silt, mud, or sand, released from suspension. But for known local conditions, the combined effect of all these might conceivably be represented by conventional roughnesses growing at a uniform annual rate. If, therefore, the original projection size can be estimated from Fig. 142, and the rate of growth is known, then a forecast can be drawn up of the size of projections, and thus of the pipe performance, at any future time. Depending upon the aggressiveness of the water and the resistance of the pipe material, this growth-rate might be of the order 0·01 to 0·13 inches per year. The rate almost certainly is influenced by the pH value (hydrogen-ion concentration) of the water, and it has consequently been suggested that a

possible correlation is $2 \log_{10} \alpha = 3{\cdot}8 - p\text{H}$, where α is the increase in height of the projections in inches per year. The application of some such rules will at any rate disclose trends that are in agreement with observed facts, viz.: that the pipe performance at first falls off seriously, while later on the decline is less marked.[89]

Another method of presenting available knowledge on the question is by the use of the expression $\frac{q - q_t}{q} \times 100 = ST^y$

in which q = original discharge through the new pipe,
q_t = discharge after T years of service,
S may vary from 4·5 to 13, according to kind of water and kind of pipe,
y may vary from 0·37 to 0·57, according to kind of water and kind of pipe.

To give an impression of the gravity of the problem, it may be said that after thirty years service in America, the average carrying capacity of certain tar-coated pipes fell to only one-half of its original value.

Cleaning of encrusted pipes. If the pipe-line has been suitably designed, the bulk of the incrustations can often be removed by passing along the pipe some kind of brush or scaling-apparatus; this may restore the capacity to perhaps 85 per cent. of the original discharge. But as by this time very few traces will be left of the original protective coating of bitumen or the like, the subsequent rate of decline will probably be higher than ever. Yet this is not inevitable. If conditions are favourable, it may be possible to apply an internal coating of cement to the cleaned pipe while it remains *in situ*: a travelling machine can spray cement over the internal surface as it moves through the pipe.[90]

162. Analysis of Losses in Pipe Systems. When a pipe system is relatively short it is necessary to take into account, in addition to frictional losses, the secondary losses due to change of pipe section, etc. (§§ 85, 88). In analysing the proportions in which secondary losses and friction losses absorb the total head available, it is invariably helpful to think in terms of hydraulic gradients and energy lines, and to draw or at least to sketch the hydraulic gradient as in Fig. 143 and succeeding diagrams. This procedure is indispensable if the maximum and minimum pressures in the system are to be determined (§ 168).

The energy line in Fig. 143 (I) shows how the energy h of the water in the reservoir is used up in (*a*) overcoming loss h_L at entrance to the parallel pipe, (*b*) overcoming friction loss h_f in the pipe, and (*c*) imparting velocity energy $\frac{v^2}{2g}$ to the water at outlet. In Fig. 143 (II) the pipe has a rounded entry

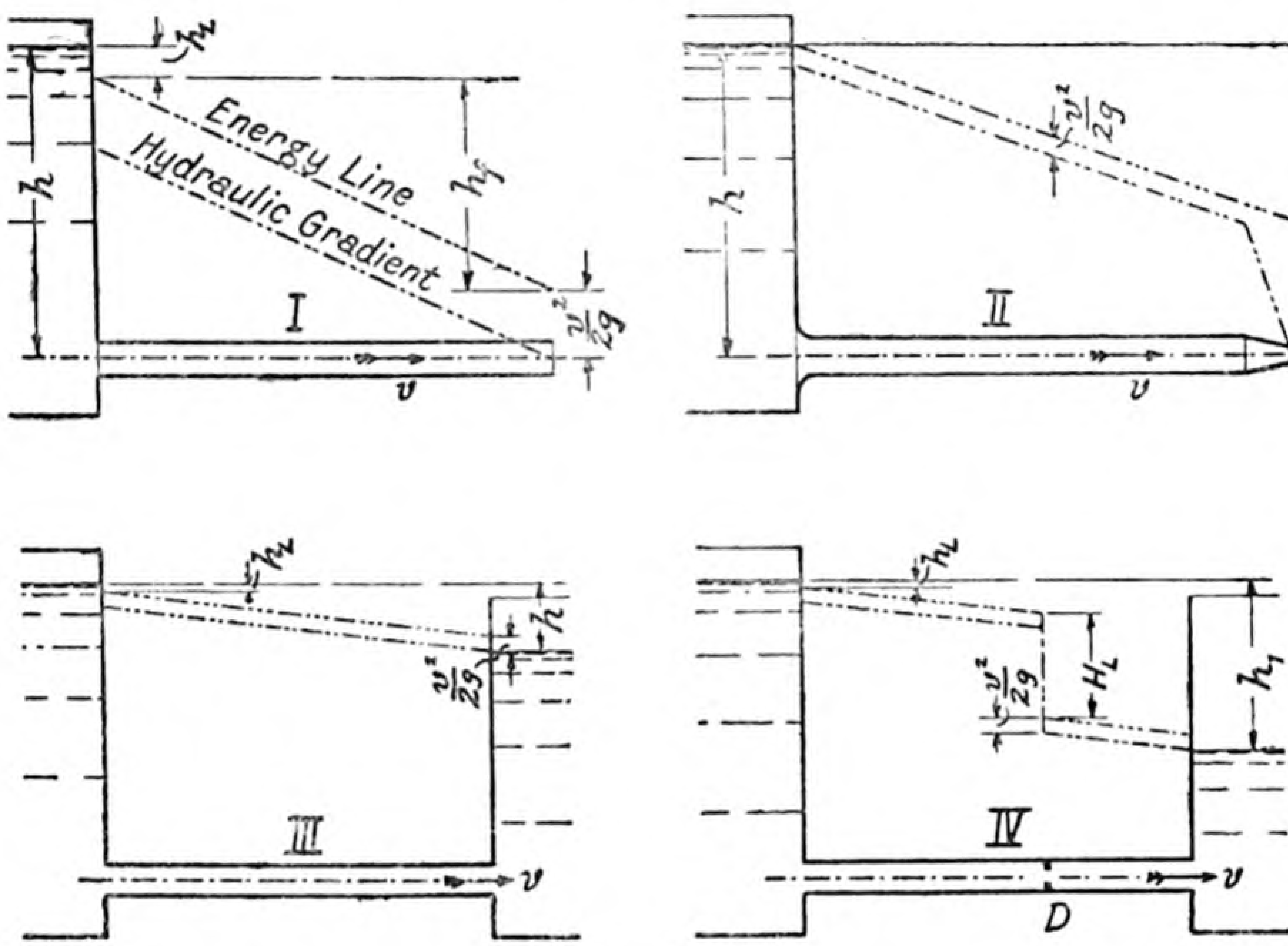

FIG. 143.—Graphical analysis of energy losses in typical systems.

imposing negligible loss, and a nozzle outlet, so that the energy h is divided between a friction loss h_f and velocity energy $\frac{V^2}{2g}$. The diminished discharge through pipe II as compared with pipe I is manifested in the flattening of the hydraulic gradient and the nearer approach of the hydraulic gradient to the energy line. These diagrams show that when we pinch the end of a rubber hose attached to a tap to induce it to project a jet further, the actual flow through the hose is *reduced ;* by thus cutting down the friction loss we have more energy to expend in producing a powerful jet.

In Fig. 143 (III) the energy h is dissipated in (*a*) loss at entry, (*b*) pipe friction, and (*c*) conversion into velocity energy, which is subsequently wasted in eddying in the downstream reservoir. To maintain the same rate of discharge from one reservoir to the other, even though the total drop in level is increased

from h to h_1, Fig. 143 (IV), an amount of energy H_L must be destroyed by means of the orifice or partly closed valve at D, § 92. The equality between the pipe velocities in III and IV is demonstrated by the agreement between the respective virtual slopes.

163. Pipes in Series. Two pipes in series, of diameter d_1 and d_2, used to convey water from one reservoir to another, will create the hydraulic conditions shown graphically in Fig. 144, in which the difference in surface levels is h.

The effect of increasing the pipe diameter from d_1 to d_2 (Fig. 144) is to flatten the hydraulic gradient and to bring the hydraulic gradient and the energy line closer together. Here

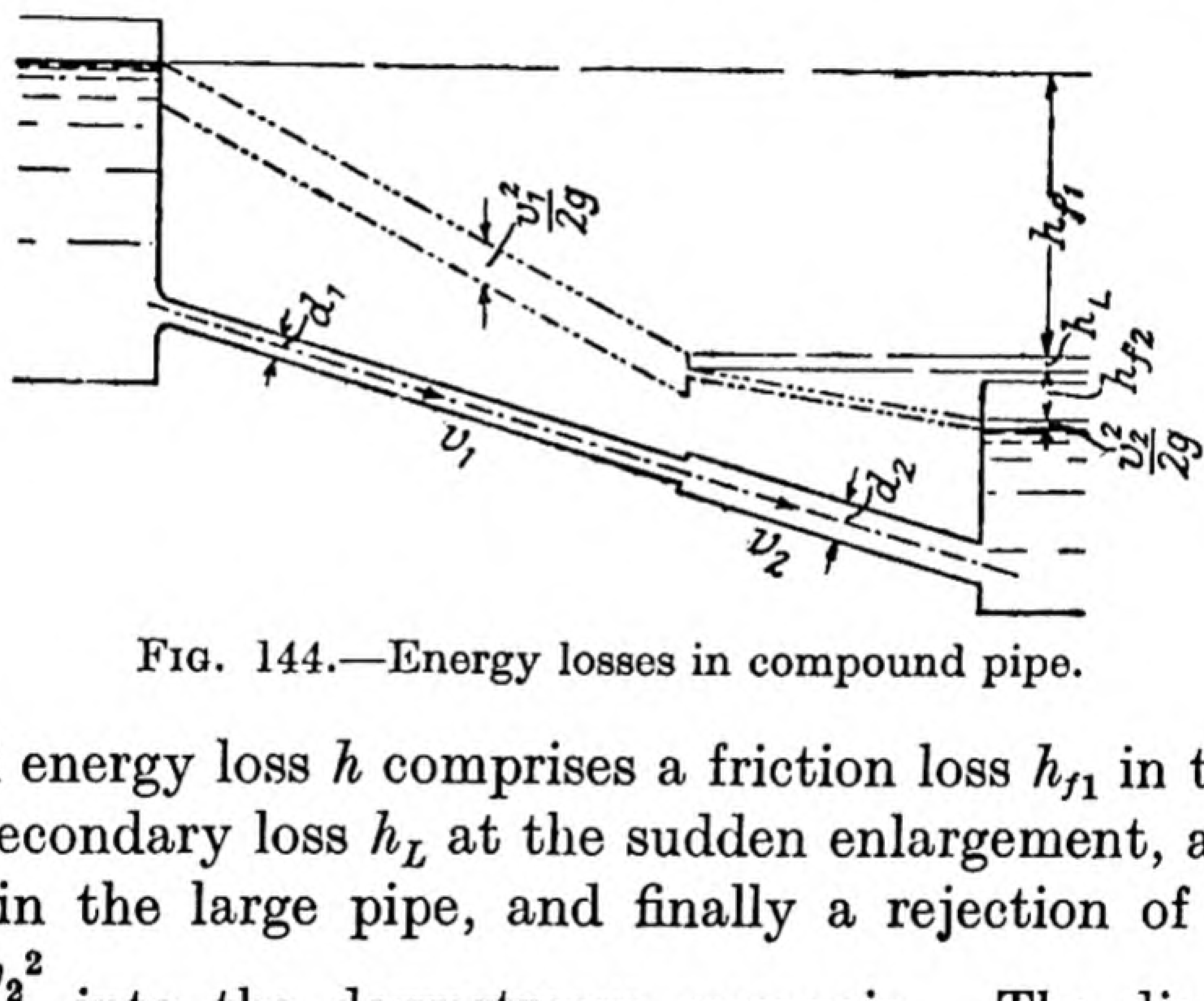

FIG. 144.—Energy losses in compound pipe.

the total energy loss h comprises a friction loss h_{f1} in the small pipe, a secondary loss h_L at the sudden enlargement, a friction loss h_{f2} in the large pipe, and finally a rejection of velocity energy $\frac{v_2^2}{2g}$ into the downstream reservoir. The discharge q through such a system can be calculated by expressing each individual loss in terms of the velocity head in *one* of the pipes—say, in terms of $\frac{v_1^2}{2g}$.

Now $$q = \frac{\pi}{4}d_1^2 v_1 = \frac{\pi}{4}d_2^2 v_2,$$

therefore $$v_2^2 = v_1^2\left(\frac{d_1}{d_2}\right)^4.$$

The general equation

$$h = \frac{4fl_1}{d_1}\cdot\frac{v_1^2}{2g} + \frac{(v_1 - v_2)^2}{2g} + \frac{4fl_2}{d_2}\cdot\frac{v_2^2}{2g} + \frac{v_2^2}{2g}$$

can thus be written

$$h = \frac{4fl_1}{d_1} \cdot \frac{v_1^2}{2g} + \frac{v_1^2}{2g}\left[1 - \left(\frac{d_1}{d_2}\right)^2\right]^2 + \frac{4fl_2}{d_2} \cdot \frac{v_1^2}{2g}\left(\frac{d_1}{d_2}\right)^4 + \frac{v_1^2}{2g}\left(\frac{d_1}{d_2}\right)^4$$

from which v_1 and therefore q can be found.

This treatment shows at the same time the advantages of the Darcy formula, as well as the need for first assuming tentative values for the pipe coefficient f which can finally be corrected when the pipe velocities are established. The coefficients of loss C_l applicable to secondary losses are similarly influenced, but to a much smaller extent, by the magnitudes of the respective velocities (§§ 93, 94). In complicated systems where bends, bifurcations, changes of section, etc., succeed one another without appreciable lengths of intervening straight pipe, the overall loss may probably be *greater* than the sum of the individual losses as calculated by the formulæ given in §§ 86-88.

164. Vertical Pipes, Draft-tubes, etc. When a pipe is vertical the conventional method of plotting hydraulic gradients breaks down, for the pressure line would invariably coincide with the pipe axis and would be meaningless. An alternative system, in which pressure heads are set off *horizontally* instead of vertically, is used in Fig. 145 to demonstrate the effect of

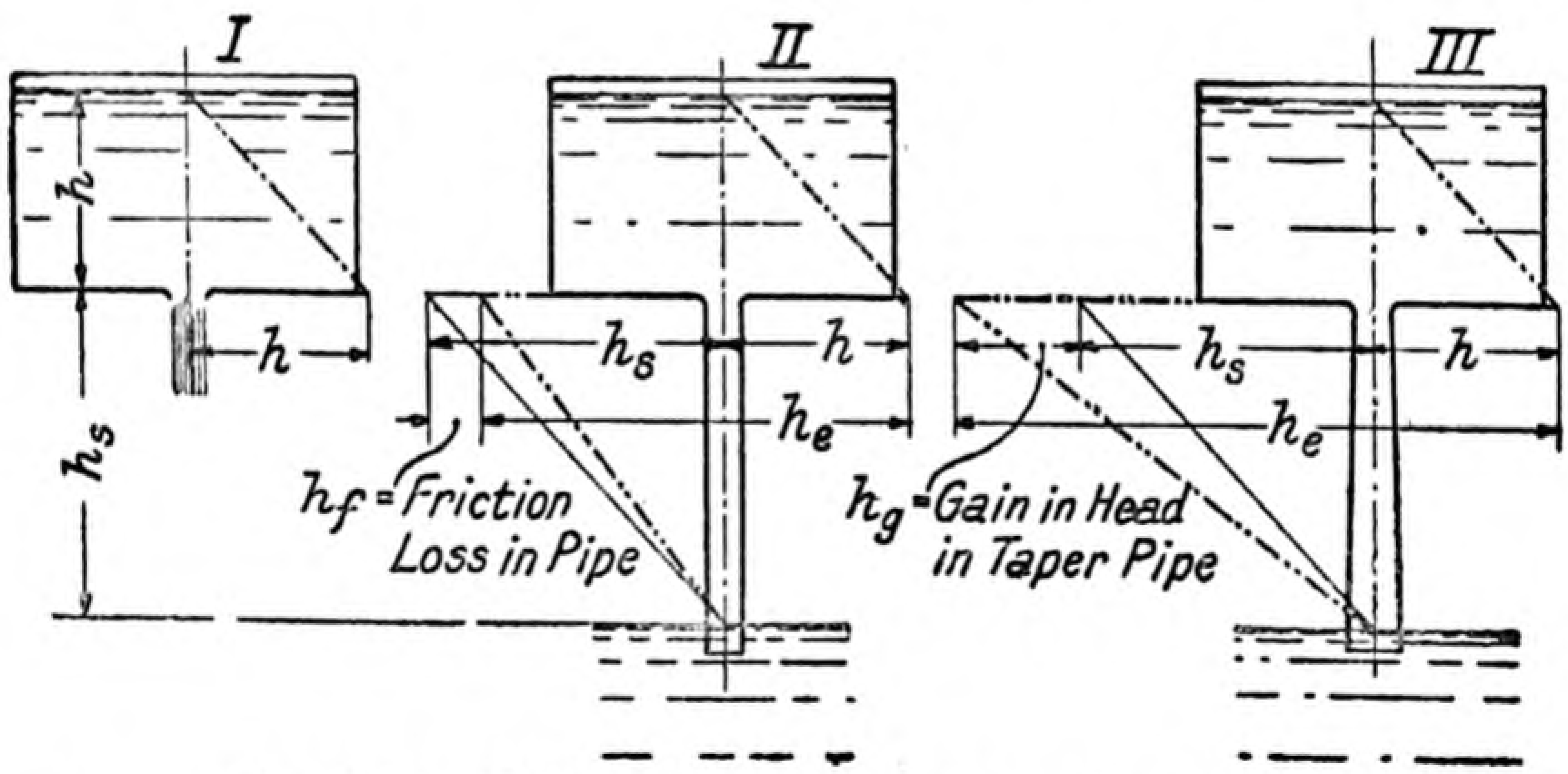

Fig. 145.—Effect of parallel and flared tail-pipes.

fitting a vertical tail-pipe to a rounded orifice in the bottom of a tank. Following the axis of the orifice downwards from the water surface, (I), we note that the increasing lengths of the offsets result in a hydraulic gradient inclined at 45° ; this inclined line corresponds exactly with those drawn in Figs. 5 and 6.

Parallel tail-pipe. The negative head generated by adding the tail-pipe is represented by offsets to the *left* of the vertical axis (Fig. 145 (II)). Allowing for a friction loss h_f in the pipe, the maximum suction head is seen to be $(h_s - h_f)$, where h_s is the static suction head ; the water is thus being "pushed" through the orifice by a positive head h, and "pulled" through the pipe by a negative head $(h_s - h_f)$. The rate of discharge is augmented accordingly, in the ratio $\sqrt{h}$ to $\sqrt{(h + h_s - h_f)}$.

Draft-tube. A flared or diverging tail-pipe (III), known as a draft-tube when forming part of a hydraulic turbine, is still more effective in improving the performance of the orifice ; this is because of the recuperation of pressure energy identical with that illustrated in Fig. 30 (*a*) or Fig. 67. If h_g represents the velocity energy effectively converted into pressure energy in the tail-pipe, then the head h_e producing flow through the orifice is $h + h_s + h_g$. This may be understood by writing the Bernoulli equation (3-1) suitably corrected, using the subscripts $_{(1)}$ and $_{(2)}$ for the upper and lower ends of the pipe respectively, and taking the lower water surface as the datum plane, § 33, thus :—

$$h_s + h_1 + \frac{v_1^{\,2}}{2g} = 0 + 0 + \frac{v_2^{\,2}}{2g} + \text{losses.}$$

The most advantageous rate of taper of the tail-pipe is about 1 in 10 (§ 87 (*b*)) ; the maximum permissible length is that at which the negative head at the upper end, $h_s + h_g$, just falls short of the limiting value $h_a - h_{ov}$ (§ 16). The pipe must be quite air-tight.

(Example 81.)

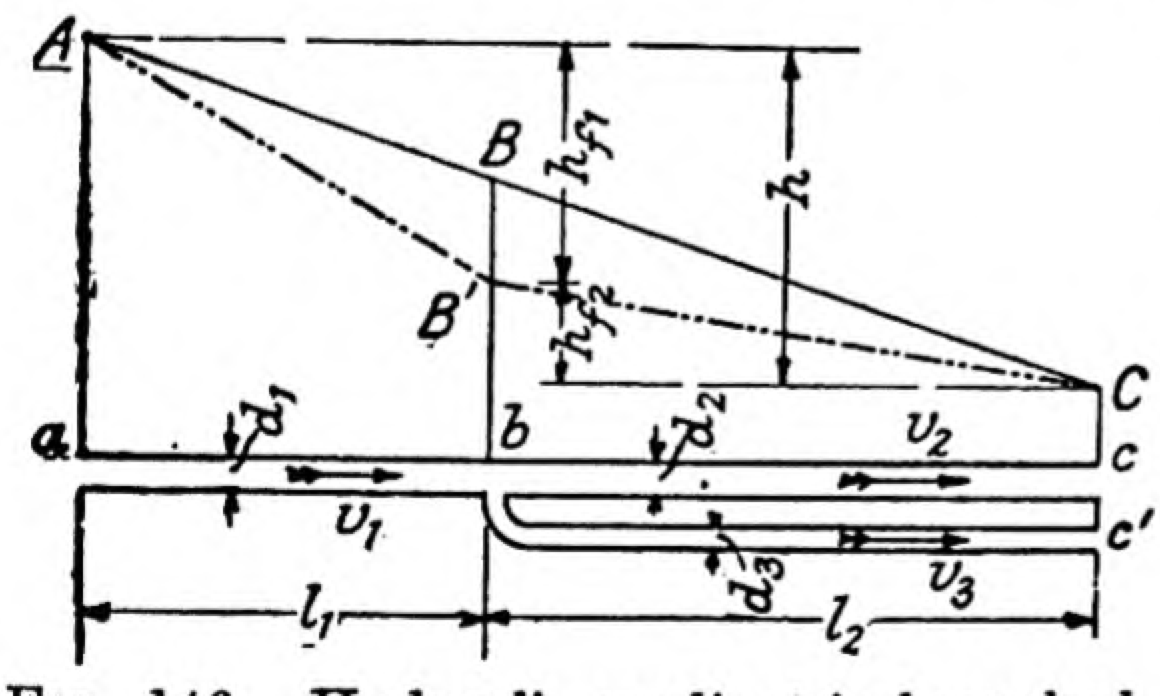

FIG. 146.—Hydraulic gradient in branched pipe.

165. Flow Through Branched Pipes. When a single pipe distributes its flow through two or more branches, the discharge may be calculated by expressing all the velocity heads in terms of the velocity head in one of the pipes, as was done in § 163. It is assumed in Fig. 146, for example, that the heads aA and cC are maintained constant, and that secondary losses are so relatively small

that they can be ignored. Before the branch bc' is connected to the main pipe abc, there is a normal hydraulic gradient ABC. After the connection is made, the diversion of some of the water into bc' relieves the main pipe bc, the virtual slope in bc is reduced from BC to $B'C$, leaving more of the total head to be expended in ab, with a consequent increase in discharge.(91)

Since both in bc and in bc' the friction loss is h_{f2} it follows that

$$h_{f2} = \frac{4fl_2}{d_2} \cdot \frac{v_2^2}{2g} = \frac{4fl_2}{d_3} \cdot \frac{v_3^2}{2g},$$

whence $$v_3 = v_2\sqrt{\frac{d_3}{d_2}}.$$

Also discharge in ab = discharge in bc + discharge in bc', viz.

$$Q = \frac{\pi}{4}d_1^2 \cdot v_1 = \frac{\pi}{4}d_2^2 v_2 + \frac{\pi}{4} \cdot d_3^2 \cdot v_3$$

or $$d_1^2 v_1 = d_2^2 v_2 + d_3^2 \cdot v_2\sqrt{\frac{d_3}{d_2}},$$

from which v_2 is obtained in terms of v_1—let us say $v_2 = kv_1$.

Finally, $$h = h_{f1} + h_{f2} = \frac{4fl_1}{d_1} \cdot \frac{v_1^2}{2g} + \frac{4fl_2}{d_2} \cdot \frac{v_2^2}{2g}$$

$$= \frac{4fl_1}{d_1} \cdot \frac{v_1^2}{2g} + \frac{4fl_2}{d_2} \cdot \frac{(kv_1)^2}{2g},$$

from which v_1 and therefore Q can be found. This solution is quite general, but in the present instance the calculation is slightly simplified because $d_1 = d_2$. **(Example 82.)**

A similar method can be applied to the discharge through two equal parallel mains ab, cd (Fig. 147), when a length l of one of them is cut out of service for repairs by the closing of the valves S, S. Here, l must be substituted for l_1, in the above equation, and $(L - l)$ for l_2; or, alternatively, since the velocity v in the single pipe is double what it is in either of the pipes that are working

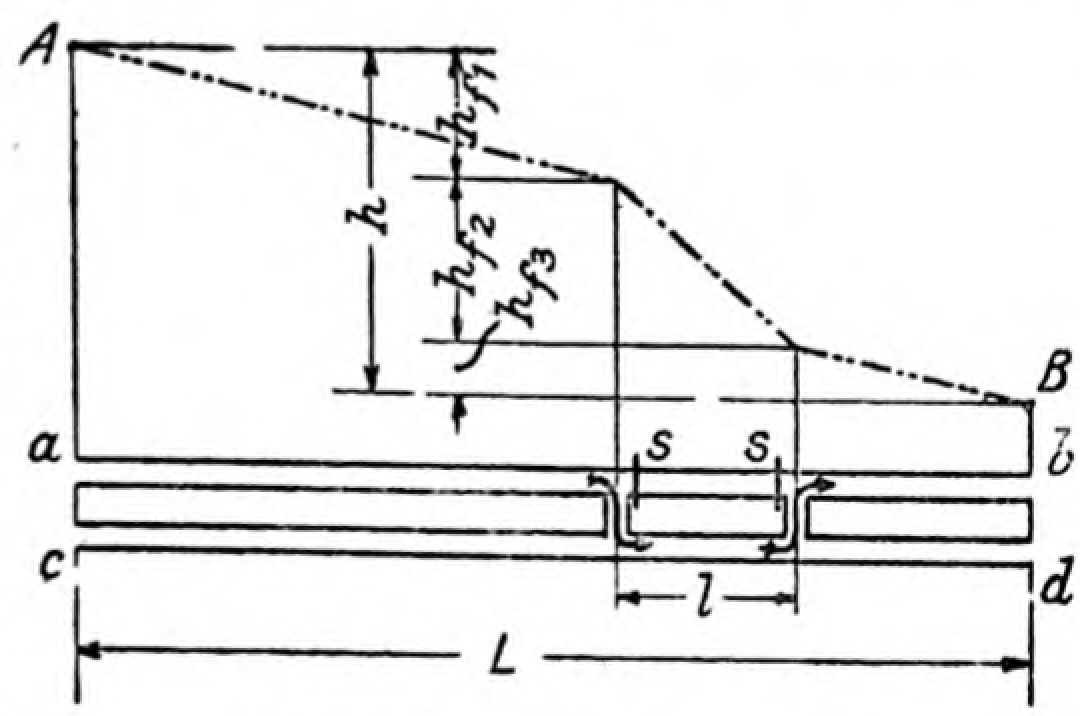

FIG. 147.—Parallel mains.

together, the virtual slope will be four times as great, and therefore

$$\frac{h_{f2}}{l} = \frac{4(h_{f1} + h_{f3})}{L - l} = \frac{4(h - h_{f2})}{L - l}.$$

This yields the value of h_{f2}, and, in turn, by writing

$$h_{f2} = \frac{4fl}{d} \cdot \frac{v^2}{2g},$$

the value of v. (Example 83).

166. Siphons and Inverted Siphons. There is no great uniformity in the use of these terms, but in this paragraph a siphon is understood to refer to a definite upward sweep of a pipe above its hydraulic gradient and below again (Fig. 148), while

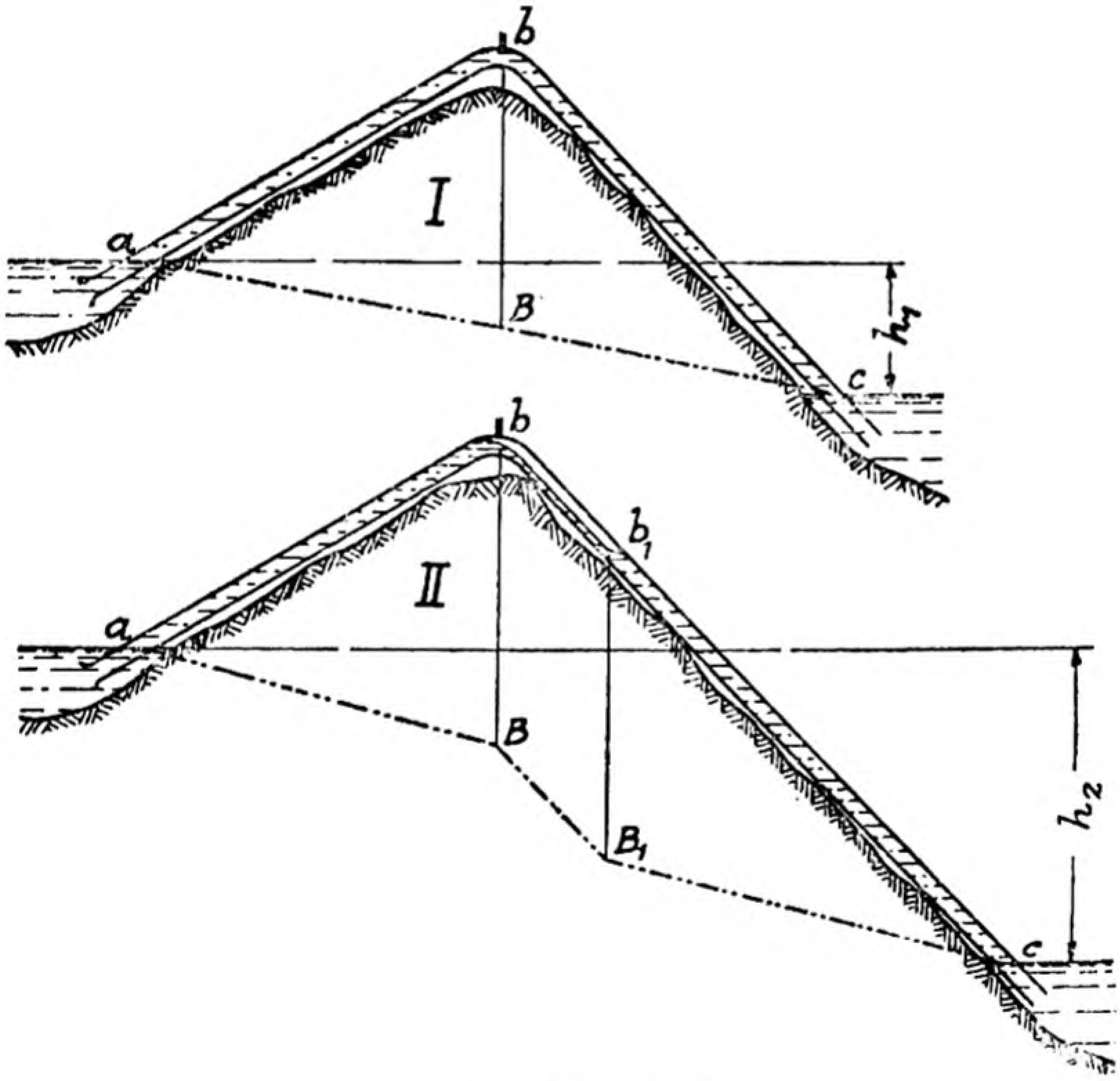

FIG. 148.—Siphon pipes.

an inverted siphon is the part of a pipe system in which the pipe sweeps down and then up again. The purpose of the siphon is to carry the pipe over an intervening bank, and of the inverted siphon to carry the pipe beneath a depression.

The limiting factor in the flow through a *siphon* is the negative head bB (Fig. 148). So long as this is not too close to the maximum possible negative head (§ 16), there will be

a normal hydraulic gradient aBc, (I), just as though the pipe had been driven straight through the bank. If now the water level in the downstream pond is progressively lowered, the discharge will increase until the limiting negative head at b is reached. Thereafter it is impossible to lower any further the position of point B, (II), or to induce any more water to flow through the siphon; continued increase in the total head drop h_2 will merely create a kink in the hydraulic gradient aBB_1c. The discharge then depends upon the slope of aB or of B_1c. In the part bb_1 of the pipe, there will be a free water surface, exposed to air or vapour at a pressure that should be equal to the vapour pressure of the water.

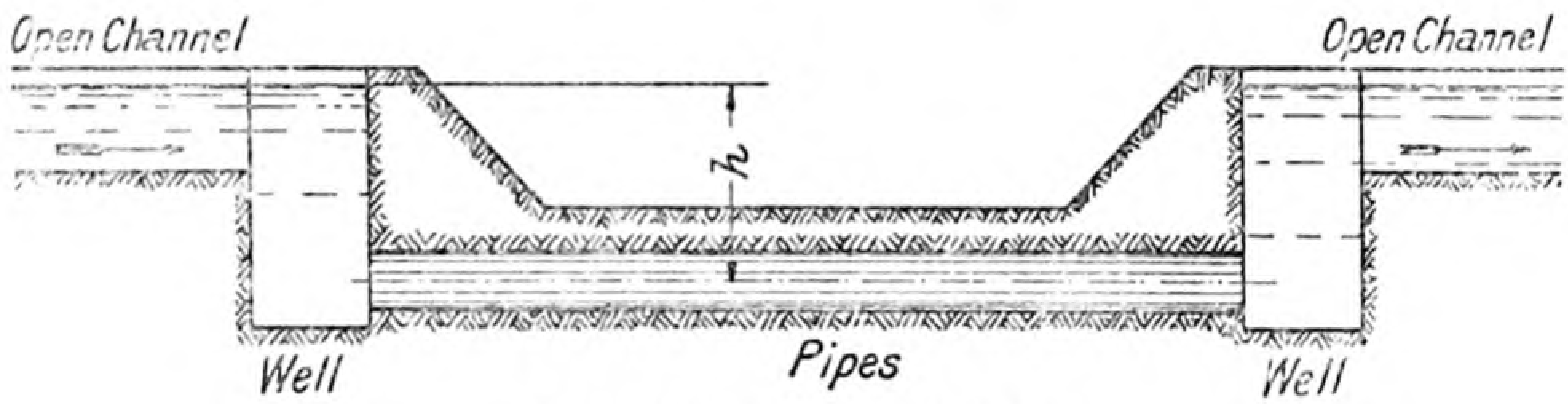

FIG. 149.—Inverted siphon.

Before water will flow through the siphon at all, the pipe must be *primed* [92] by exhausting the air from it with the aid of a vacuum pump or an ejector coupled to the highest point b. When the siphon is in operation, too, the dissolved air liberated from the water under reduced pressure, that tends to accumulate at b, must be periodically removed (§ 11). If a siphon of small diameter works under a head big enough to produce a high velocity, the air bubbles will be swept along with the water down the downstream leg and will be given no chance to collect at the top. Otherwise the following formula will give a rough guide to the quantity q of air, in cubic feet, that must be exhausted per 24 hours:

$$q = \frac{QH}{180},$$

where Q is the total volume or cubical content in cubic feet of the part of the pipe lying above the hydraulic gradient, and H is the *average* negative head in feet in this part of the pipe.

The special types of siphon known as *siphon spillways* are described in § 214.

In the *inverted siphon* (Fig. 149) the essential point is to see that the strength of the pipe is adequate to resist the maximum static pressure head h. The siphon here depicted, consisting of a number of pipes in parallel, is of a type sometimes used for conducting the water of one canal beneath the bed of another canal. The diameter of the pipes must be such that the total head loss, i.e. the difference between the water levels in the inlet well and the outlet well, is kept within prescribed limits. In a waterworks undertaking, siphons several miles long may be needed for carrying a pipe-line or aqueduct across river valleys. **(Example 84.)**

167. Effect of Pumps on the Hydraulic Gradient. A pump interposed in a pipe always produces a sudden upward jump or step in the hydraulic gradient, corresponding with the energy h_m given to the liquid by the pump. Normally

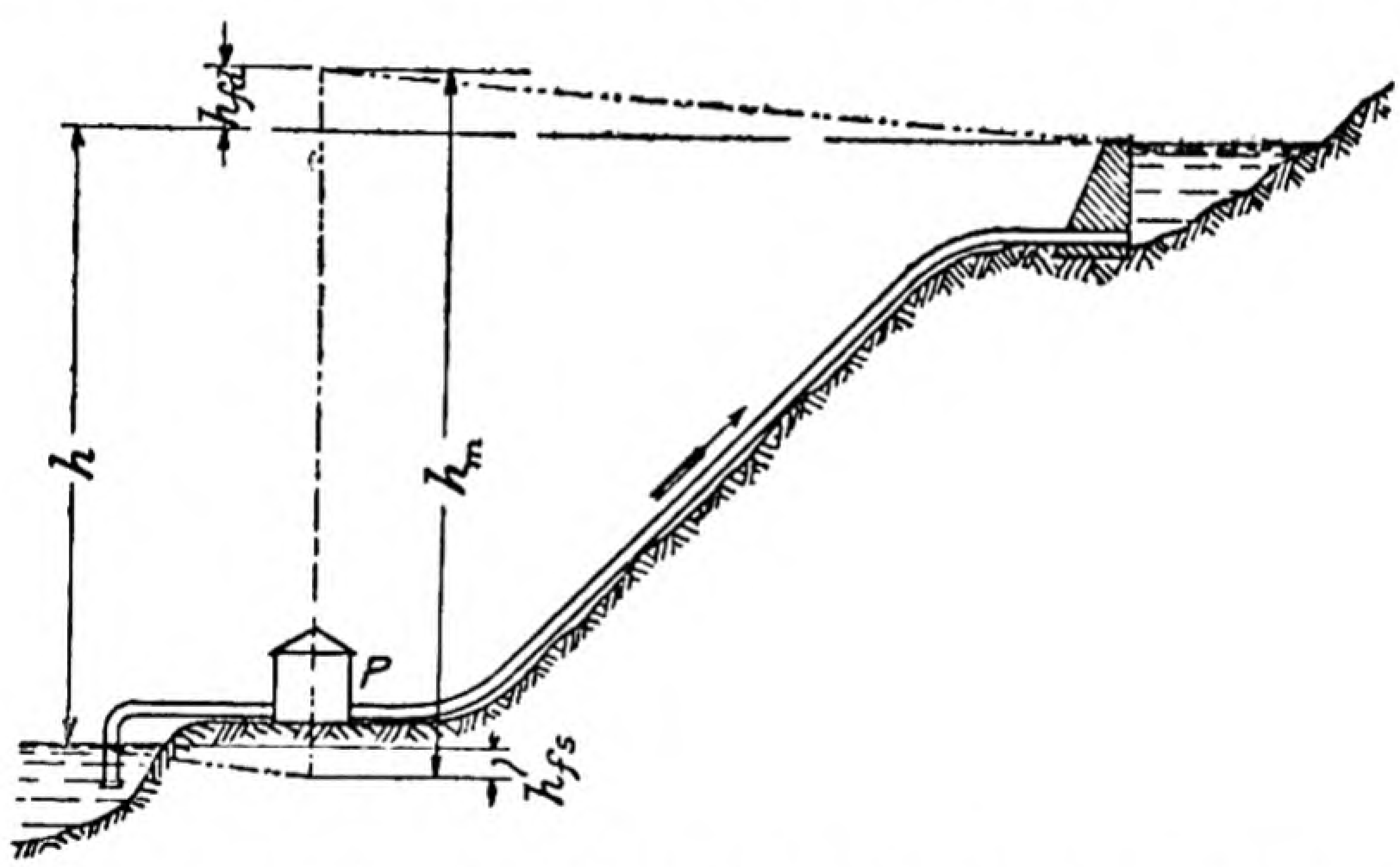

FIG. 150.—Comparison between static head and total head on pump.

h_m must be greater than the "dead" or static lift h against which the pump works, in order to overcome pipe friction. This is shown in Fig. 150, which represents a pump in the building P lifting water from a river into an elevated reservoir. Here, h_{fs} is the sum of the friction and other losses in the suction pipe, h_{fd} is the loss in the delivery pipe, and therefore $h_m = h + h_{fs} + h_{fd}$.

In a circulating-water system for a steam power station § 338 (ii), nearly the entire head h_m may be a frictional head (Fig. 151). The hydraulic gradient droops in a normal way from the water intake to the pump; it attains its maximum

level at the pump delivery flange, and thence slowly falls to the water outlet with a sharp localised drop marking the energy loss in the condenser tubes.

The effect of a *booster* pump (Fig. 152) is to increase the slope of an already existing gradient. Without the pump

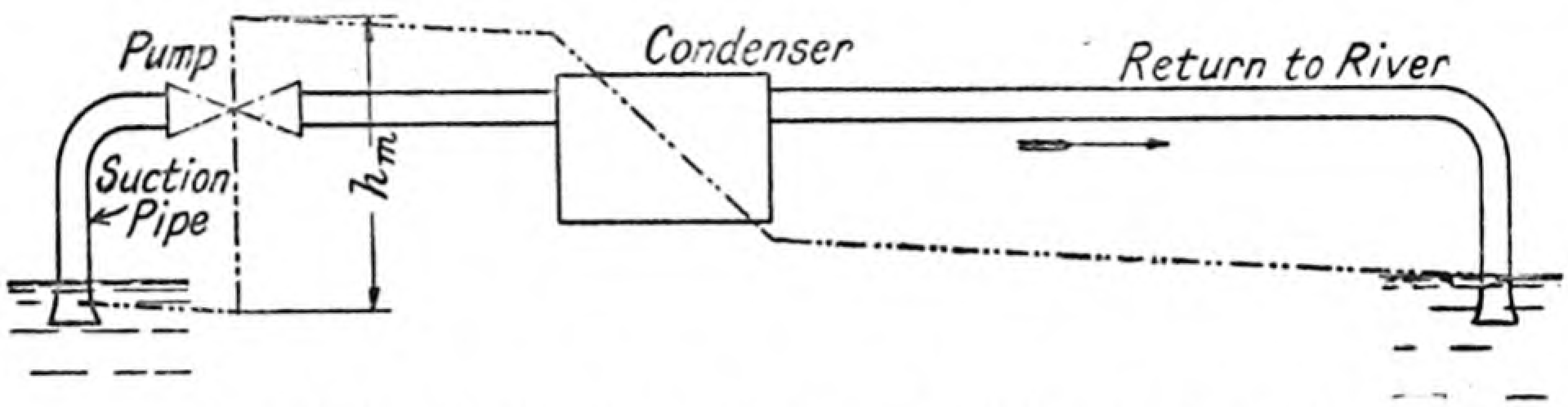

FIG. 151.—Hydraulic gradient in circulating-water system.

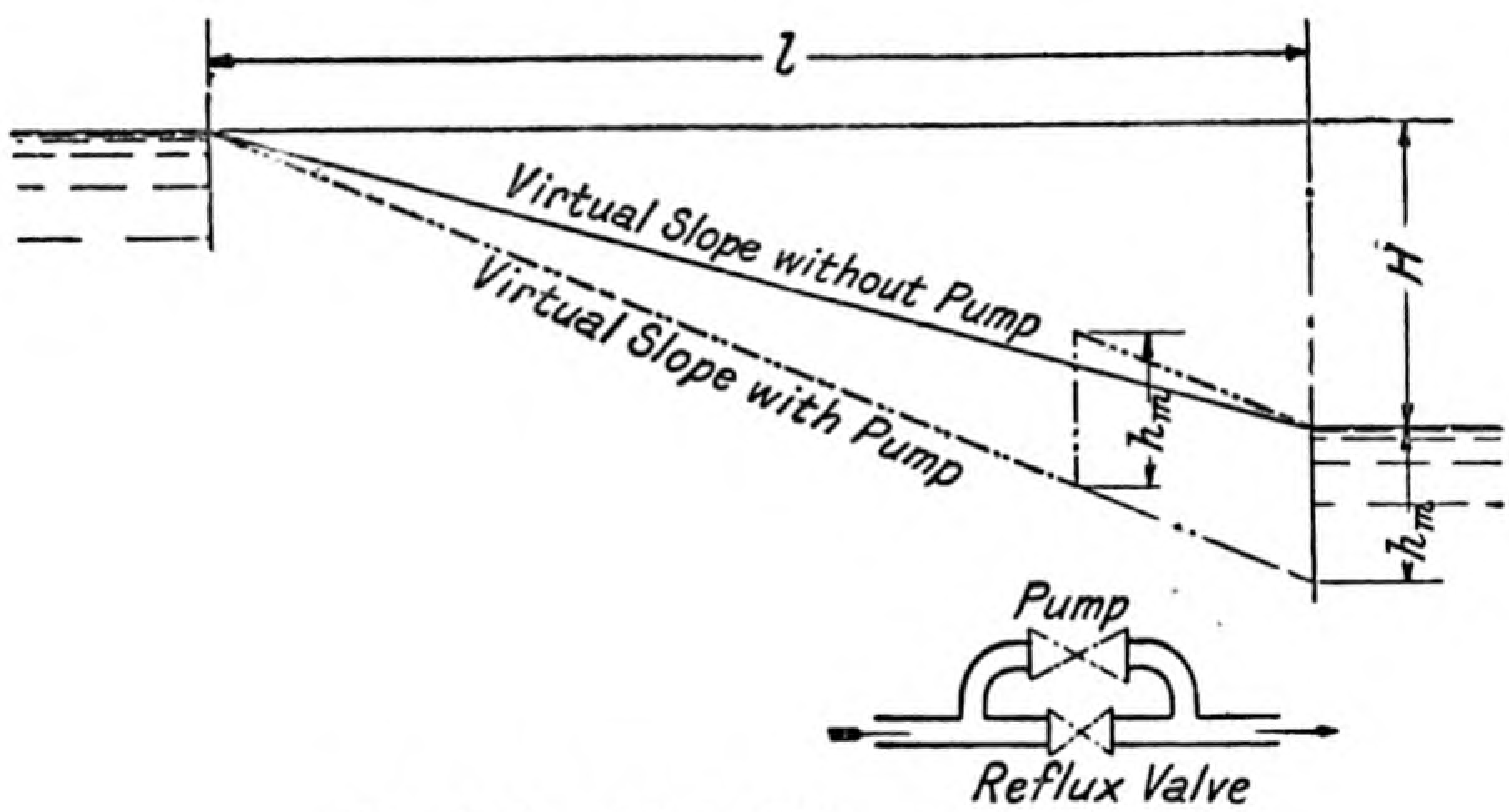

FIG. 152.—Effect of "booster" pump.

the gravitational head H produces a flow in the water main proportional to $\sqrt{\frac{H}{l}}$; with the pump in operation, generating a head h_m, the augmented flow is proportional to $\sqrt{\frac{H+h_m}{l}}$.

(Example 185).

168. Analysis of Pressures in Pipe Systems. Only when the pipe diameters at various points in the system are finally determined can the pipe thickness likewise be fixed, § 150. Even then, the maximum and minimum pressures at a specified point, which together provide the basis for estimating the wall thickness, cannot be known until the limiting types of flow have been studied. By way of example the pipe illustrated in Fig. 133 (i) may be examined—its course is

plotted to a smaller scale in Fig. 153. The minimum range of pressure will correspond with the condition of fully-open outlet valve V, and the lowest pressure at any point will be represented by the distance h_{min} at point C. The maximum pressures will occur during closure of the valve, when water-hammer pressures are superadded to static pressure (§§ 175-177); the greatest distance between the pipe axis and the hydraulic gradient is now $h_{max} = AB$, and it is accordingly at point A that we may expect the greatest pressure anywhere in the system. Apart, then, from actual fracture of the pipe, these represent the extreme range of conditions; it is specially to be noted that nowhere does the pipe axis rise *above* the hydraulic gradient, as it necessarily does in the siphon in Fig. 148, and there is thus no need to strengthen the pipe against the danger of collapse *inwards*.

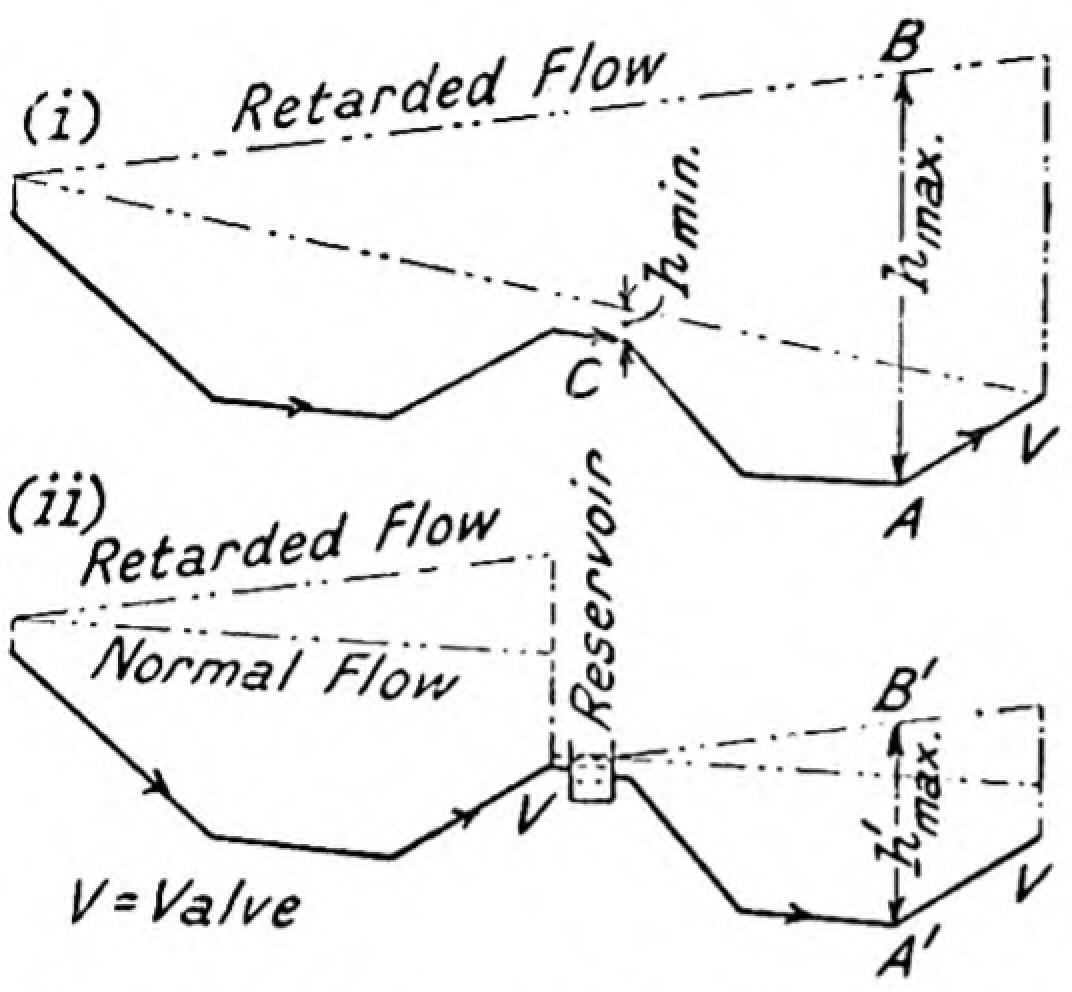

FIG. 153.—Pressure lines (i) without, (ii) with break-pressure reservoir.

With a knowledge of the maximum pressure at various points along the pipe, and of the permissible tensile strength of the chosen material, the nominal wall thickness may now be computed from formula 2-4, § 21. But to this figure must be added an allowance to cover loss of thickness due to corrosion, and a further allowance to insure against the indeterminate stresses due to ground settlement, thermal expansion, etc. From the weight of the pipe as finally designed, the size, number, and position of the anchorages can be estimated, if these are necessary. It is rarely economical to vary the thickness of small pipes to suit the pressure variations that may prevail throughout their length; but in the very costly steel pressure-pipes used for high-head hydro-electric installations (§ 253), it is essential that the wall thickness should be progressively diminished as the pressure falls off towards the head of the line.

The use of a *break-pressure reservoir* in a gravitational water main may materially lower the maximum pressure in the pipe,

and therefore the cost of the pipe. Such a reservoir is shown in Fig. 153 (ii). If the available head H in Fig. 133 (i) is excessive, and the surplus H-h would in any event have to be destroyed, then the break-pressure principle enables the dissipation to be carried out in two stages. Even during the worst conditions, during retardation of the water column, the pressure could not exceed $A'B'$, as against the corresponding value of AB without the reservoir.

The specially-constructed chambers that serve a somewhat similar purpose in a turbine pipe-line are termed *surge-tanks* (§ 254).

169. Control Valves for Pipes. Some common types of valve for controlling the flow in pipes are shown in Fig. 154.

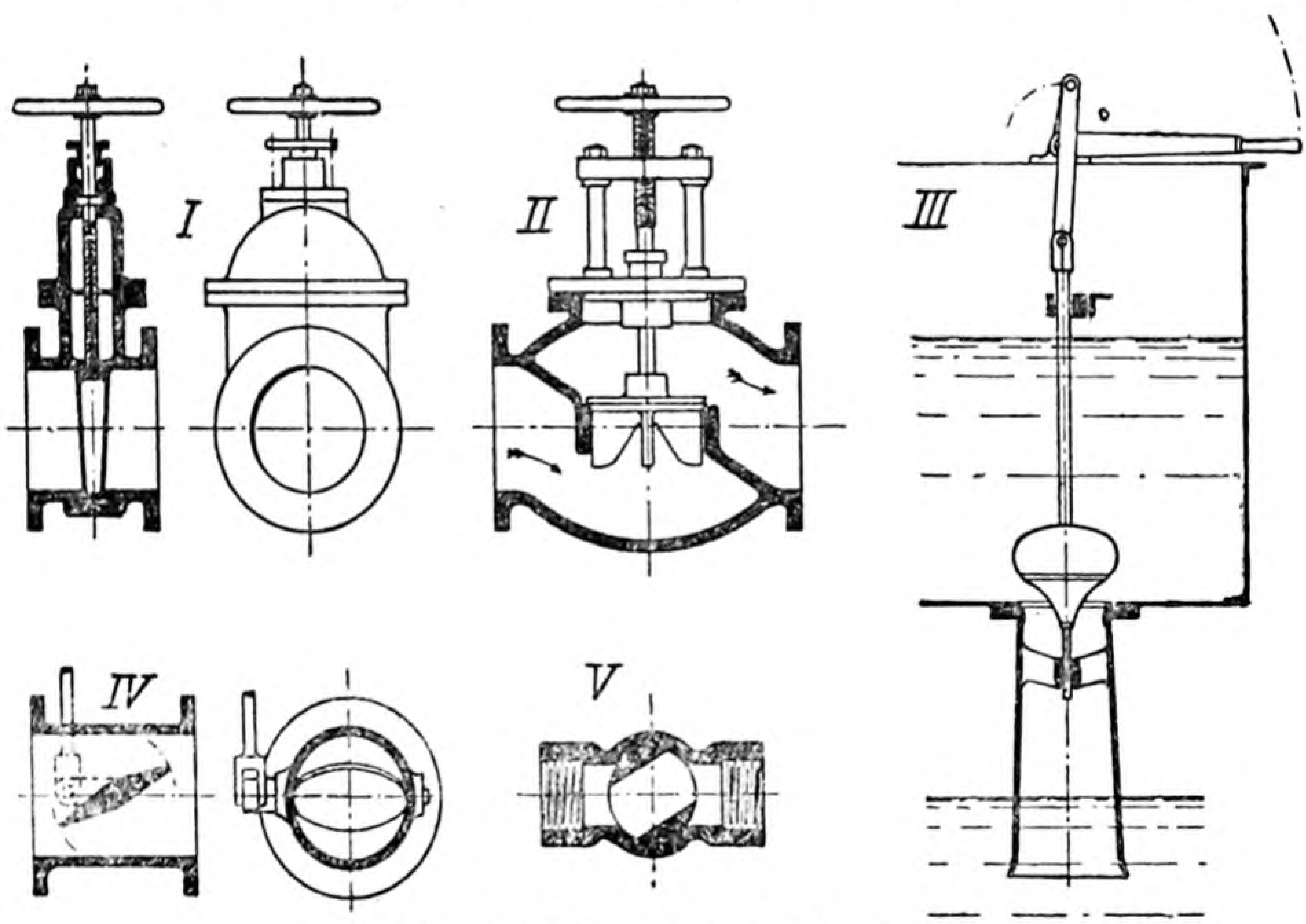

FIG. 154.—Hand-operated control valves.

For all ordinary purposes the *full-way*, *sluice*, or *gate* valve (I) is preferred: it is simple in construction, and when fully open it imposes only a small energy loss on the liquid flowing through it—about 0·1 to 0·2 times the velocity-head in the pipe. The loss in the *globe* valve (II), on the other hand, is extremely high—several times the pipe velocity-head—and so it is only small valves such as domestic water taps that are usually made thus. Both full-way and globe valves should always be arranged to close with right-handed (clockwise) rotation of the hand-wheel, and should preferably have indicators

of some sort showing at a glance whether the valve is open or shut.

The stream-lined valve (III), although belonging to the same class as the wing-guided valve used in the globe valve body (II), here offers little resistance to flow. In the figure it is shown in rapid-opening form, working in conjunction with a tail-pipe (§ 164) for the quick emptying of a measuring tank.

The special advantage of the *butterfly* valve (IV) is that it is balanced about its axis and so can be opened or closed with relatively little effort: the *plug-cock* (V), when suitably designed, offers in its fully open position no obstruction to the liquid at all.

For use in *high-pressure hydraulic transmission systems,* special valves are needed such as those mentioned in § 358.

170. Power-operated Valves. Although quite large valves can be operated by hand if the reduction-gearing between the hand-crank and the gate itself is suitably designed, yet the

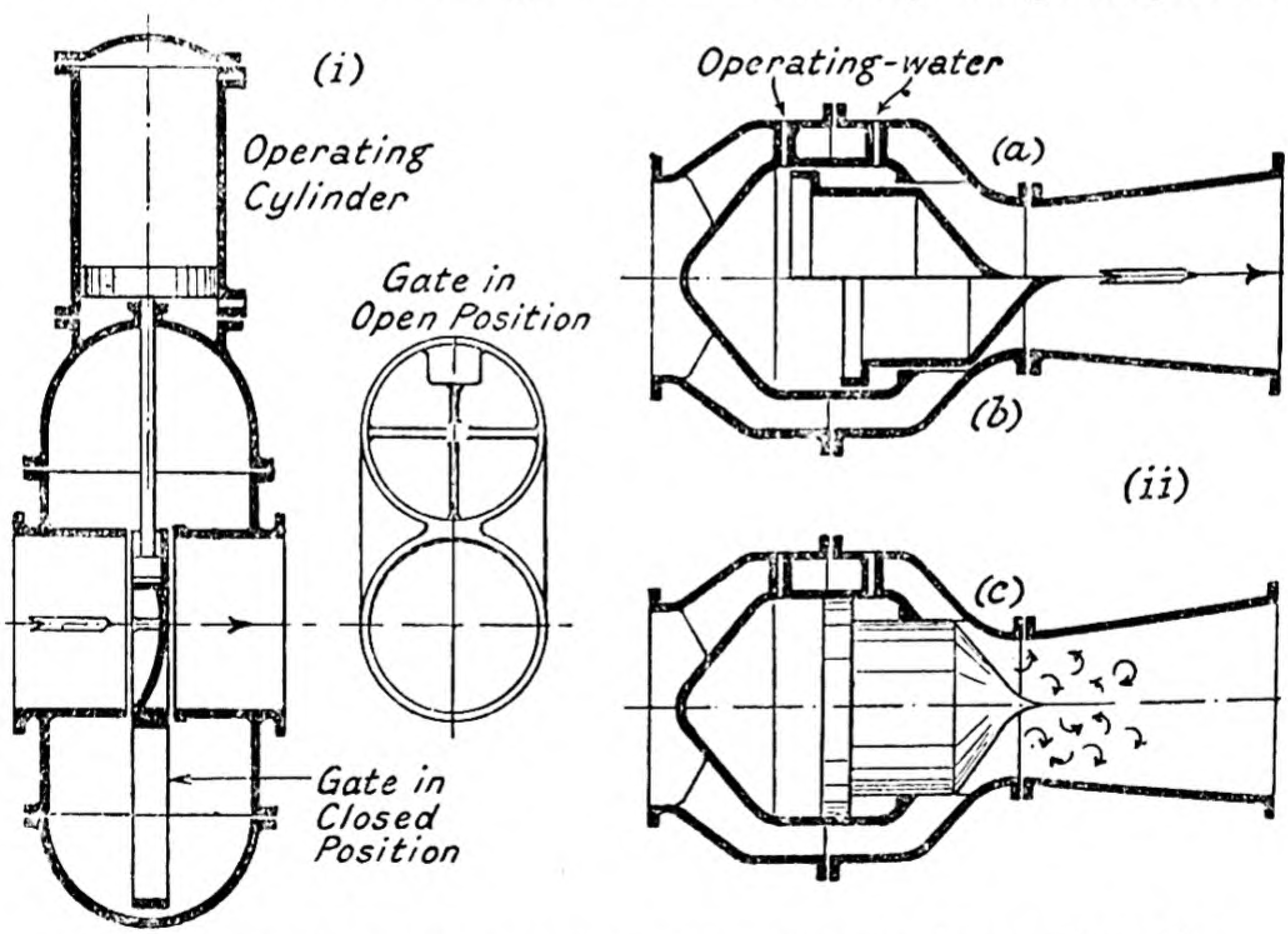

FIG. 155.—Hydraulically-operated valves: (i) spectacle-eye, (ii) needle.

time of closure—a quarter of an hour or more—may be inconveniently high for many purposes. The advantage of *electrically-operated* valves, in which a small motor fitted with limit switches is geared to the valve-spindle, is that they may be controlled

from some remote station. *Hydraulically-operated valves* can often take pressure-water from the pipe-line itself; alternatively an independent supply of high-pressure water or oil may be arranged (§ 352).

A very direct application of hydraulic power is illustrated in Fig. 155 (i), where the piston of the power cylinder is attached to the valve-spindle itself. By admitting high-pressure water to the upper or lower side of the piston, the valve is closed or opened. This *spectacle-eye* or *follower-ring* construction is very suitable for the shut-off valves in water-power installations.

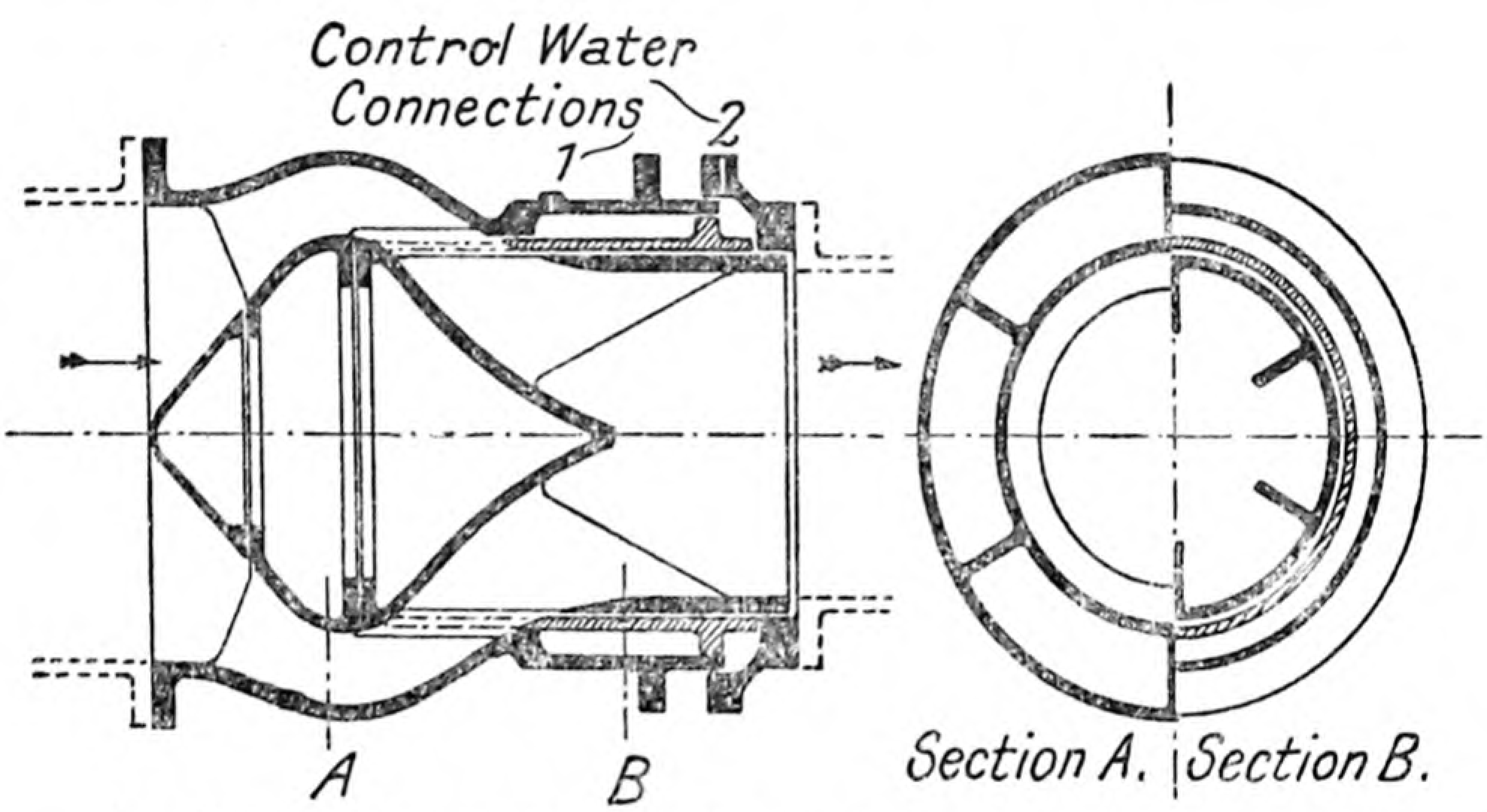

FIG. 156.—Hydraulically controlled cylindrical stream-lined valve. (Messrs. The English Electric Co., Ltd.)

The hydraulically-operated *needle-valve* in Fig. 155 (ii) is shown in three positions: (*a*) fully-open, (*b*) fully-closed, and (*c*) partly-open. Here the differential piston on which the pressure-difference is exerted is formed integrally with the conical valve itself. Another type of valve specially arranged for hydraulic control is depicted in Fig. 156. The valve itself is of cylindrical or sleeve form provided at its inner end with a flange which acts as an annular piston. In the diagram the valve (distinguished by hatching) is seen withdrawn to the inner end of its travel, allowing free passage for the water between the outer casing and the inner bulb or core. When high-pressure control water is admitted to connection 2, and connection 1 is opened to exhaust, the additional static thrust on the annular piston forces the valve slowly to the left until it bears on its seating formed on the inner core, as shown by the broken lines. In

Fig. 250 a stream-lined valve of this type is shown controlling the flow of water to a turbine.

Other mechanisms which can be built in large sizes and equipped with hydraulic control are the butterfly-valve and the plug-valve, Fig. 154 (IV) and (V).

171. Choice of Valve. Depending upon the particular service for which the valve is destined, one or other of its attributes may have to be given precedence.[93] Those of major importance are :—

The opening and closing forces should be as small as possible.
When shut the valve must be completely liquid-tight.
When fully-open it must offer the minimum hydraulic resistance to flow.
When set in the partly-open position so as to throttle the flow, the valve and adjacent piping must be able to resist the destructive action of cavitation (§ 134).

As already mentioned, the butterfly-valve, Fig. 154 (IV), has the distinction of being easily turned ; but it is not nearly so easy to keep water-tight when closed. When large power-operated plug-valves (V) are fitted with auxiliary gear for lifting the cone axially before rotation begins, then they too require a relatively small operating force. This type shares with the follower-ring design, Fig. 155 (i), the advantage of offering to the water a completely uninterrupted passage when in the open position. It will be noticed that the follower-ring acts as a short length of pipe which closes the gap in the waterway when the gate itself is withdrawn, not only virtually eliminating energy loss but minimising risk of cavitation damage. All these valves are intended for normal use only when set in the fully-open or the fully-closed positions ; it is the needle-valve, Fig. 155 (ii) (*c*), that has outstanding claims when the valve is to serve for long continuous periods as an energy-dissipator. The diagram shows how the zone of intense turbulent mixing, which is the focus of the energy loss, occupies the core of the waterway, the pipe walls themselves being relatively immune from attack.

That maid-of-all-work of regulating appliances, the sluice-valve, Fig. 154 (I), has to resist cavitation as best it can, for its users rarely give it any consideration. Sometimes the forces of destruction are too much for it ; instances are known in which, after several months working in the part-open or throttling position with particularly aggressive water, valves of

this sort have failed because the solid metal nearly an inch thick just downstream of the gate (Fig. 120, point S) has been eaten completely through. Vibration and chattering are additional causes of deterioration. From the point of view of liquid-tightness it may be noted that whereas the wedge type of gate, Fig. 154 (I), can be forced hard home into its housing, the parallel type depends upon the upstream water-pressure to hold it on its seating, Fig. 155 (i).

For reasons of economy the nominal bore of the valve may often be less than that of the pipe; the additional energy loss in the taper inlet and outlet connecting pieces is regarded as trivial.

172. Rate of Closure of a Valve. Valves controlling the flow in long pipes require careful manipulation in order to avoid excessive water-hammer or inertia pressure in the pipes (§§ 175-177). Let h be the difference in level between two reservoirs connected by a pipe of length l, diameter d, area A, and (average) pipe coefficient f; and let a be the area of opening of a valve in the pipe at the moment when the pipe velocity is v. If inertia pressure is negligible,

then $$h = \frac{4fl}{d} \cdot \frac{v^2}{2g} + \left(\frac{A}{C_c a} - 1\right)^2 \cdot \frac{v^2}{2g}, \qquad (\S\ 87\ (e))$$

and $$v = \sqrt{\frac{2gh}{\frac{4fl}{d} + \left(\frac{A}{C_c a} - 1\right)^2}}.$$

On working out various values of v so as to discover the kind of relationship between the valve opening and the pipe velocity, it is apparent that the valve can be moved some distance from its fully open position before the discharge is appreciably reduced (Fig. 157), whereas when the valve is nearing its fully closed position a very slight additional movement causes a considerable reduction in the velocity. To fulfil the condition of uniform retardation of the water column in the pipe stipulated in § 115, therefore, the valve can be closed quite quickly at first but the closing movement must be completed very slowly. In Fig. 157, for example, it is seen that the last tenth of the closing movement should occupy nearly one-half of the closing period.

An interesting automatic device for regulating the rate of closure of the stream-lined valve shown in Fig. 156 is

represented in Fig. 158. Attached to and moving with the sleeve valve itself is a small control valve having the form of a parallel spindle on which is cut a square thread of varying pitch. The operating high-pressure water on its way to the working chamber of the sleeve valve must therefore traverse

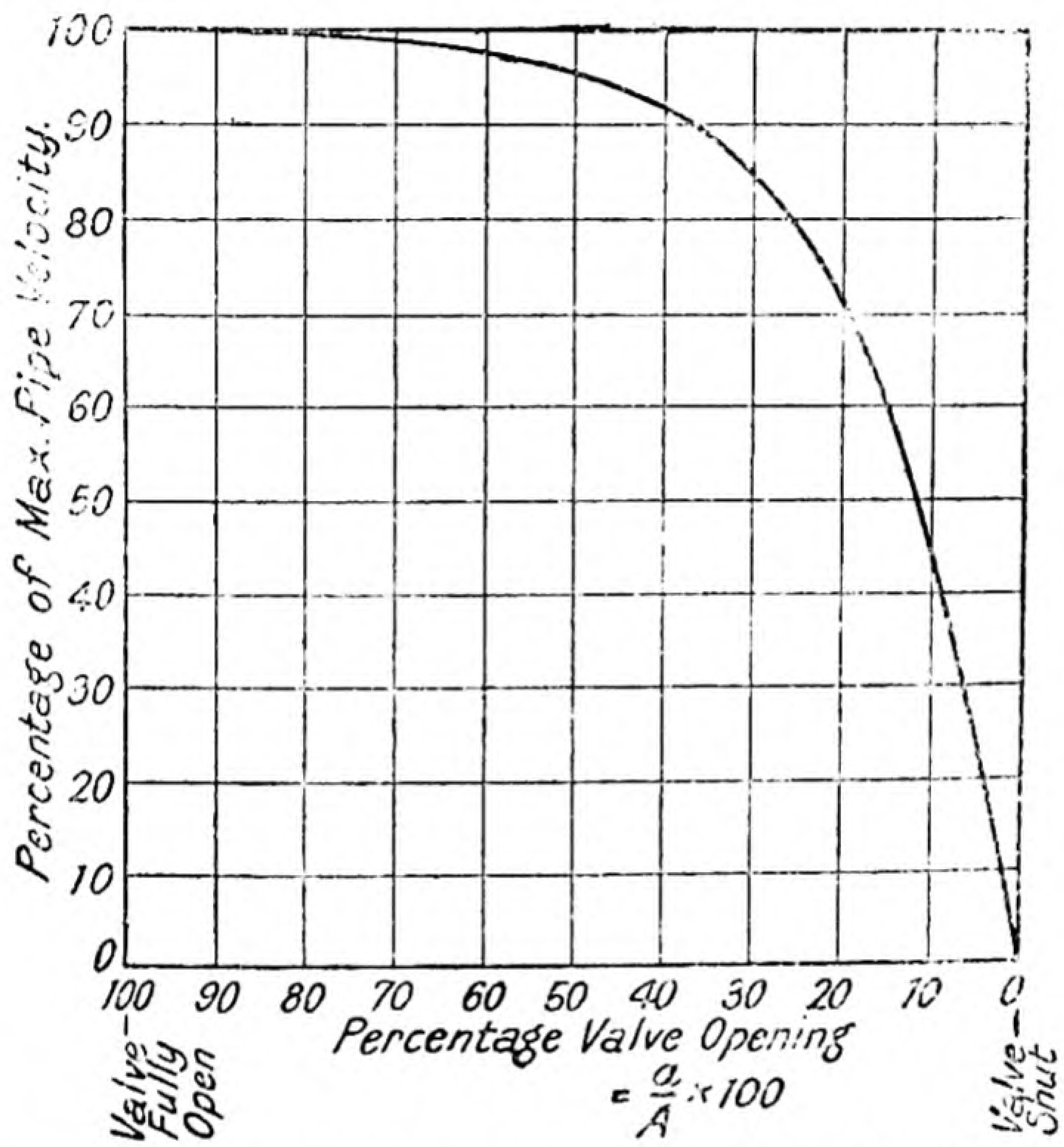

FIG. 157.—Effect of valve opening on velocity in a long pipe.

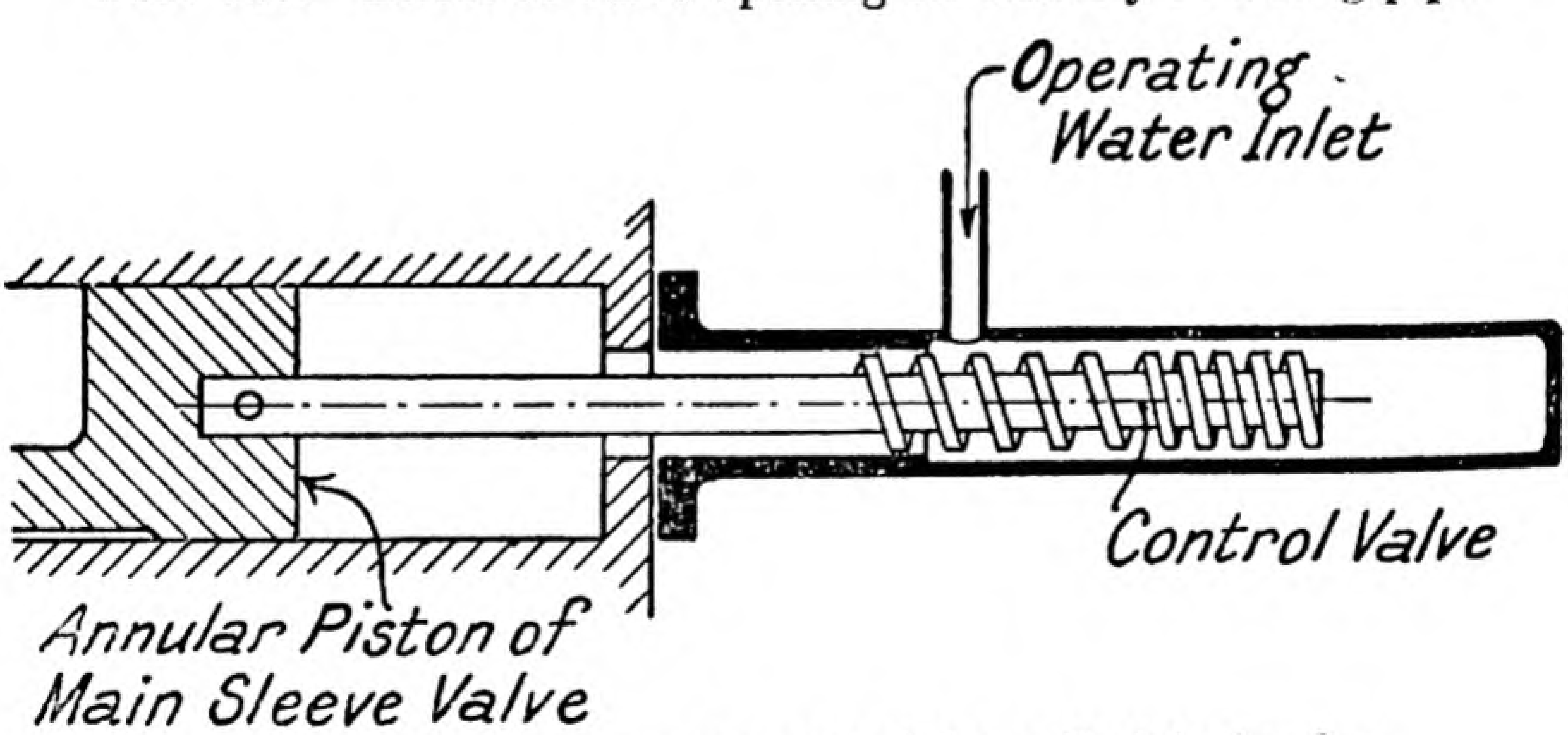

FIG. 158.—Automatic control for cylindrical value.

the resulting helical groove; as the sleeve valve approaches nearer and nearer to its fully closed position, so does the path of the operating water become longer, with the consequence that the frictional loss of head increases and the rate of movement of the sleeve valve diminishes.

Even when no question of inertia pressure is involved, it is well to remember when closing a sluice valve that the last few turns of the hand-wheel always have far more effect in checking the flow than the first few turns.

173. Auxiliary Valves. Some self-operating valves for special purposes are shown in Fig. 159. The *reflux* or *non-return* valve (I) will permit flow to take place in the direction of the arrow, but prevents flow in the reverse direction. The *air valve* (II) is fitted at each high point or summit in a long pipe line to allow any air that separates out of the water to vent itself. Normally the buoyancy of the copper float attached to the valve spindle keeps the valve up against its seating, but if sufficient air accumulates in the float chamber the float falls and allows the air to escape to the atmosphere. The size and positions of the air valves (denoted by *A.V.*) fitted to a part of a 72-in. water

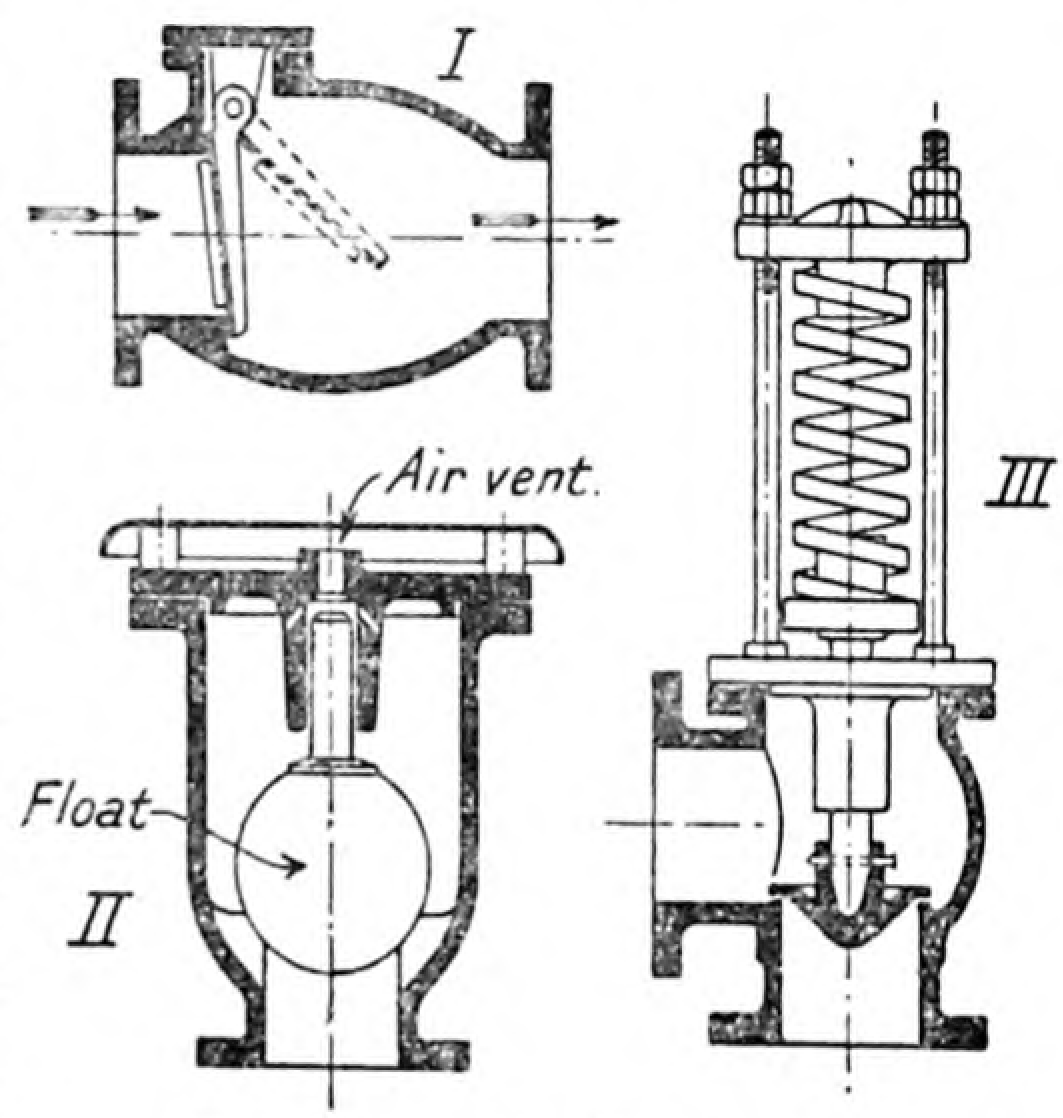

FIG. 159.—Auxiliary valves.

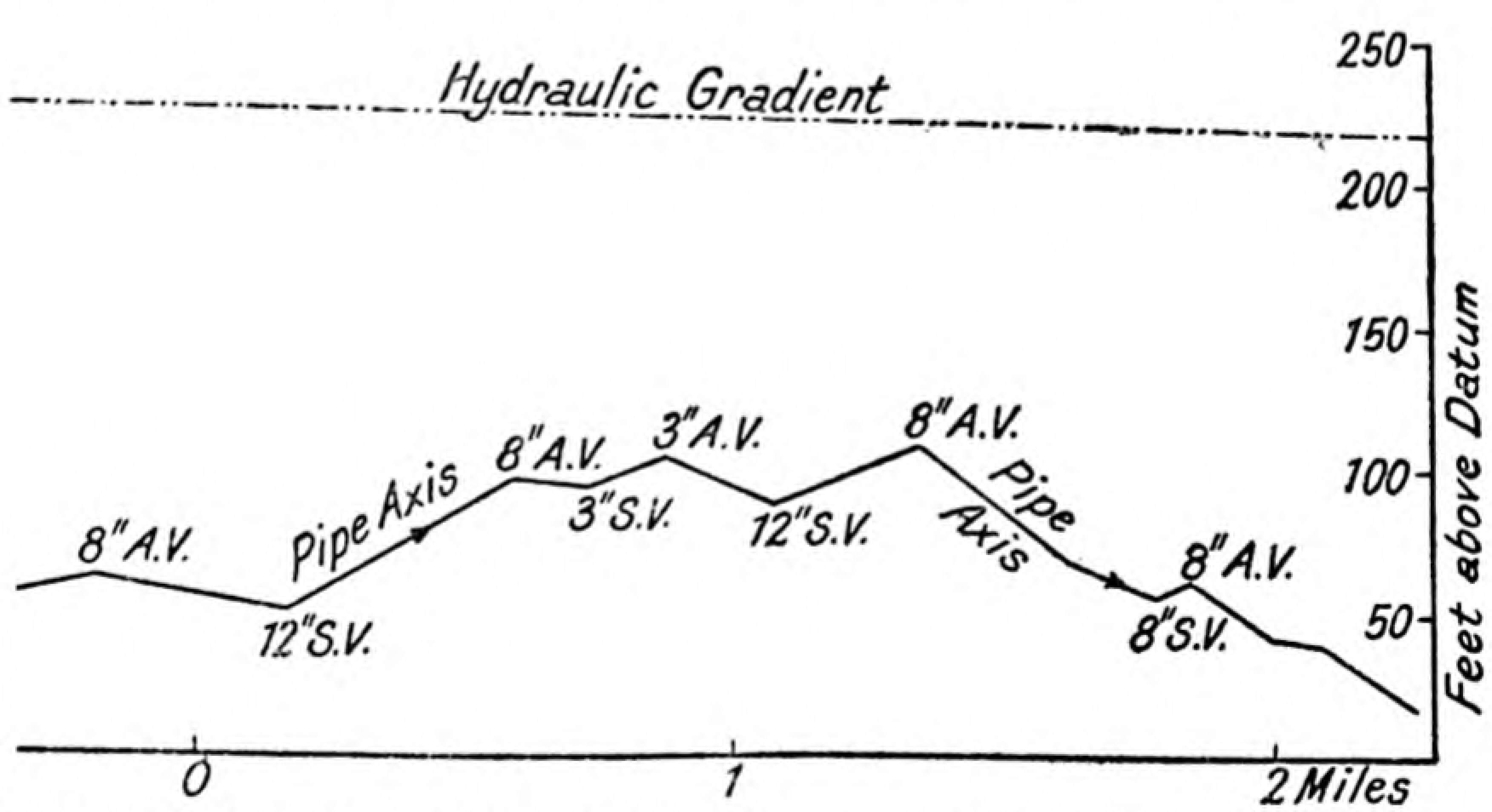

FIG. 160.—Location of air valves and scour valves on 72-in. water main.

main are indicated in Fig. 160. At the bottom of every dip in the pipe line there is a branch to which a sluice valve, marked *S.V.*, is attached for emptying purposes; when these are

opened, air valves of a larger type than those shown in Fig. 159 (II) come into operation and allow air to enter the main to replace the water that drains away. If this were not arranged for, the pipe would certainly collapse due to the unbalanced external atmospheric pressure. Such accidents are by no means unknown.

Large mechanically-operated automatic air valves are often fixed at the upper ends of high-pressure turbine pipe-lines § 252 (i), with a similar object, viz. to safeguard the pipe against collapse internally when emptied.

The spring-loaded *relief valve* (Fig. 159 (III)), protects the pipe against excessive internal pressure, *so long as* the excess pressure is not applied so suddenly that the valve has insufficient time to lift.

174. Diffusing Outlet Valves. On various occasions it has been pointed out that in order to dissipate energy in a valve, the contracted stream passing through it must be projected on the downstream side into a mass of water in which the indispensable eddying motion may be generated. If, on the other hand, surplus water is discharged into the *atmosphere* through a valve at the end of a pipe, the jet travels onwards with its energy unimpaired and may thus have a dangerously erosive effect on the rock, masonry, or even metal on which it eventually impinges. This difficulty can be overcome by the expedient of giving the water a whirl or rotational component, so that it emerges into the air with the same type of motion as that of a projectile leaving a rifled gun-barrel.

The effect is clearly visible in Fig. 161. At (I) the ordinary "solid" jet is depicted; at (II) a series of vanes corresponding to the rifling grooves of the gun-barrel have been thrust forward into the nozzle, with the result that the centrifugal force now operating on the water causes the jet to break up into a diverging cone of fine spray. The energy is now rapidly dissipated due to the eddies set up *in the air* as the drops of water move with high velocity through it.

175. Water-hammer: the General Problem. In the paragraph devoted to the analysis of pressures in pipe systems, § 168, the casual reference to inertia pressures gave a quite inadequate impression of the predominant role that these phenomena may assume. When the flow in the pipe system

I

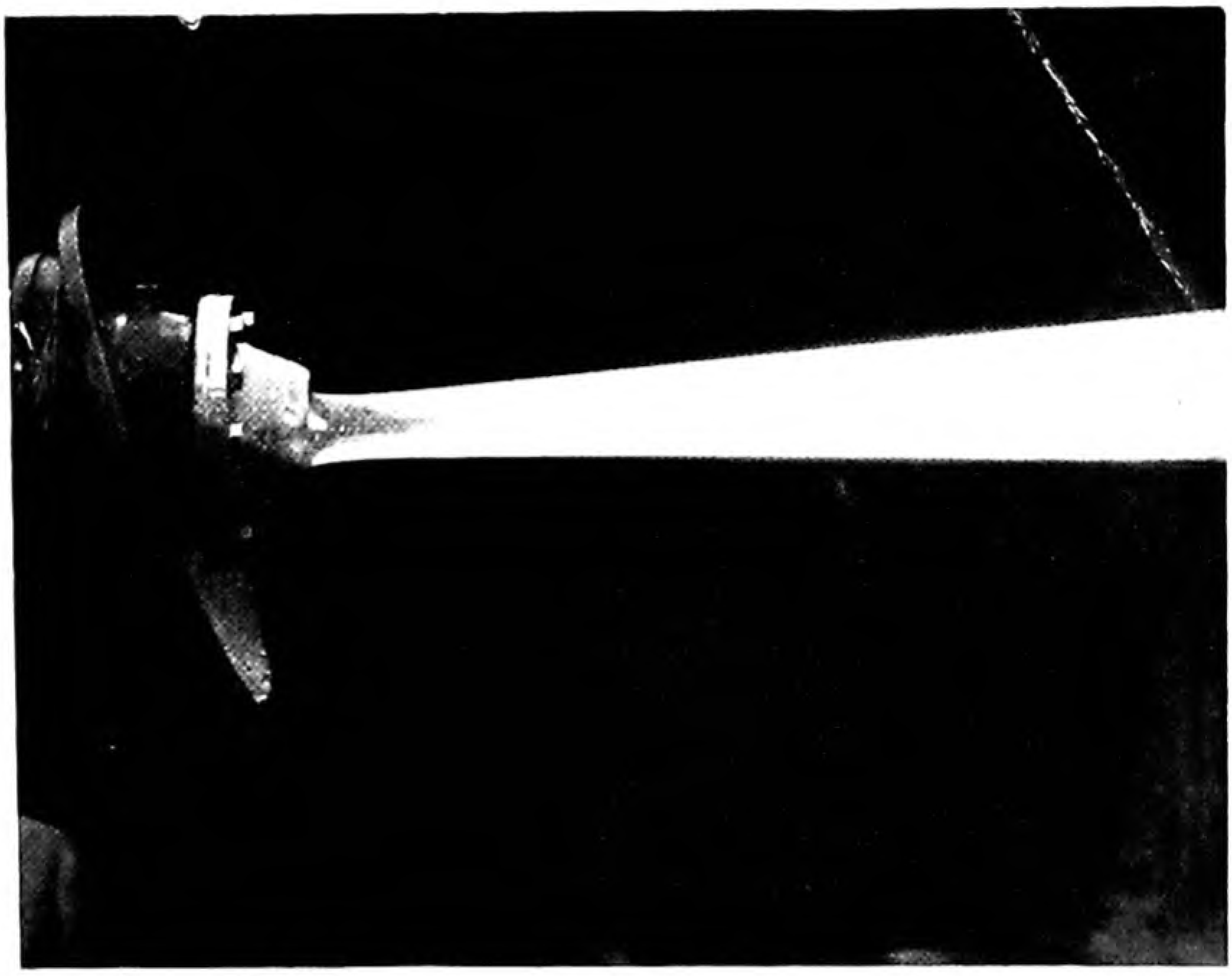

II

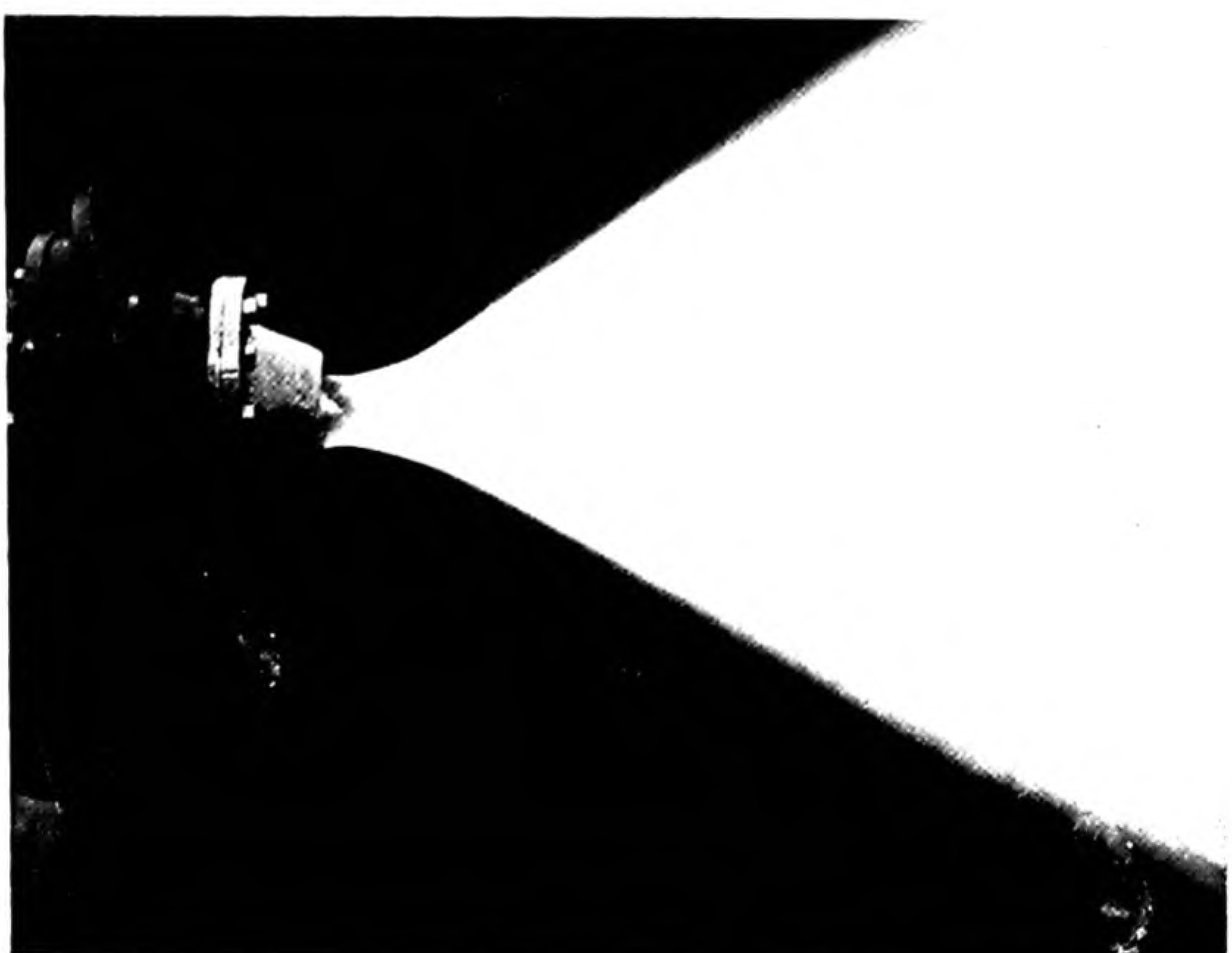

FIG. 161.—Diffusing outlet valve.

(The English Electric Co., Ltd.)

[*To face page* 246.

is controlled by a valve which can be set to give a pre-determined rate of closure and therefore possibly a known rate of retardation, § 172, there may be little difficulty in estimating the intensity of the water-hammer pressure. Here the pipe may be treated with every consideration. But very often the pipe is merely a servant of or an accessory to some more important apparatus whose own requirements must then be given precedence. Thus the starting and stopping of the pumps depicted in Figs. 150 to 152, § 167, may modify the respective hydraulic gradients in various ways that at first appear unpredictable. Similarly, the rapid changes of load [94] on a hydro-electric installation, § 253, have it in their power to inflict highly injurious pressure-changes on the water in the pipe that feeds it. **(Example 85.)** The elementary treatment of inertia pressures to be found in §§ 114-118 can therefore only be regarded as a foundation on which to base the much more involved analyses that engineering problems demand.

The first essential is to extend the treatment to all points in the pipe, and not to the single point close to the outlet valve that is the only one hitherto examined; for until this is done there can be no certainty of establishing the regions of maximum and minimum pressure, § 168. A very vivid method of presenting the problem is provided by the *stereogram* developed by Professor du Juhasz; it consists of a three-dimensional combination, Fig. 162, of the two diagrams Figs. 93 and 98. Time t, and distance x along the pipe measured from the valve B, are plotted along two horizontal axes at right-angles, while pressure p is plotted vertically. Consequently if an imaginary vertical plane parallel to AB is traversed along the t axis, its successive intersections with the stereogram will yield in turn the various hydraulic gradients plotted in Fig. 93; one of these is indicated at Fig. 162 (i). Similarly, intersections of the stereogram with a vertical plane parallel with BT will reveal the effect of the distance x upon the time-pressure wave; the wave, (iii), for instance, is noticeably different from the wave (ii) near the valve.

For instantaneous valve closure, then, we can draw a clearly-defined and comprehensive picture—though it is yet too early to say whether this is the most convenient one. For rapid but not instantaneous closure, § 118, the stereogram can be built

up by superposing a number of elementary instantaneous stereograms in the same way that time-pressure waves were constructed in Figs. 97 and 98, the process resembling the construction of "layered" topographical relief maps. The stereogram so developed in Fig. 162 (II) from Fig. 98 (IV) is highly informative; it tells us at a glance how the inertia pressure falls away continuously from a maximum near the valve to zero at the inlet end of the pipe. From a knowledge of the law connecting time with retardation of the water-column, it would ideally be possible to build stereograms to represent the most complicated types of variable flow. But it would certainly be laborious to do so—far too laborious a method for use in an engineer's office. So while accepting the stereogram as an invaluable aid to the imagination, we have recourse to other graphical devices for carrying out routine computations, being indebted for their development to exponents such as Professor R. W. Angus, and Professor Bergeron.

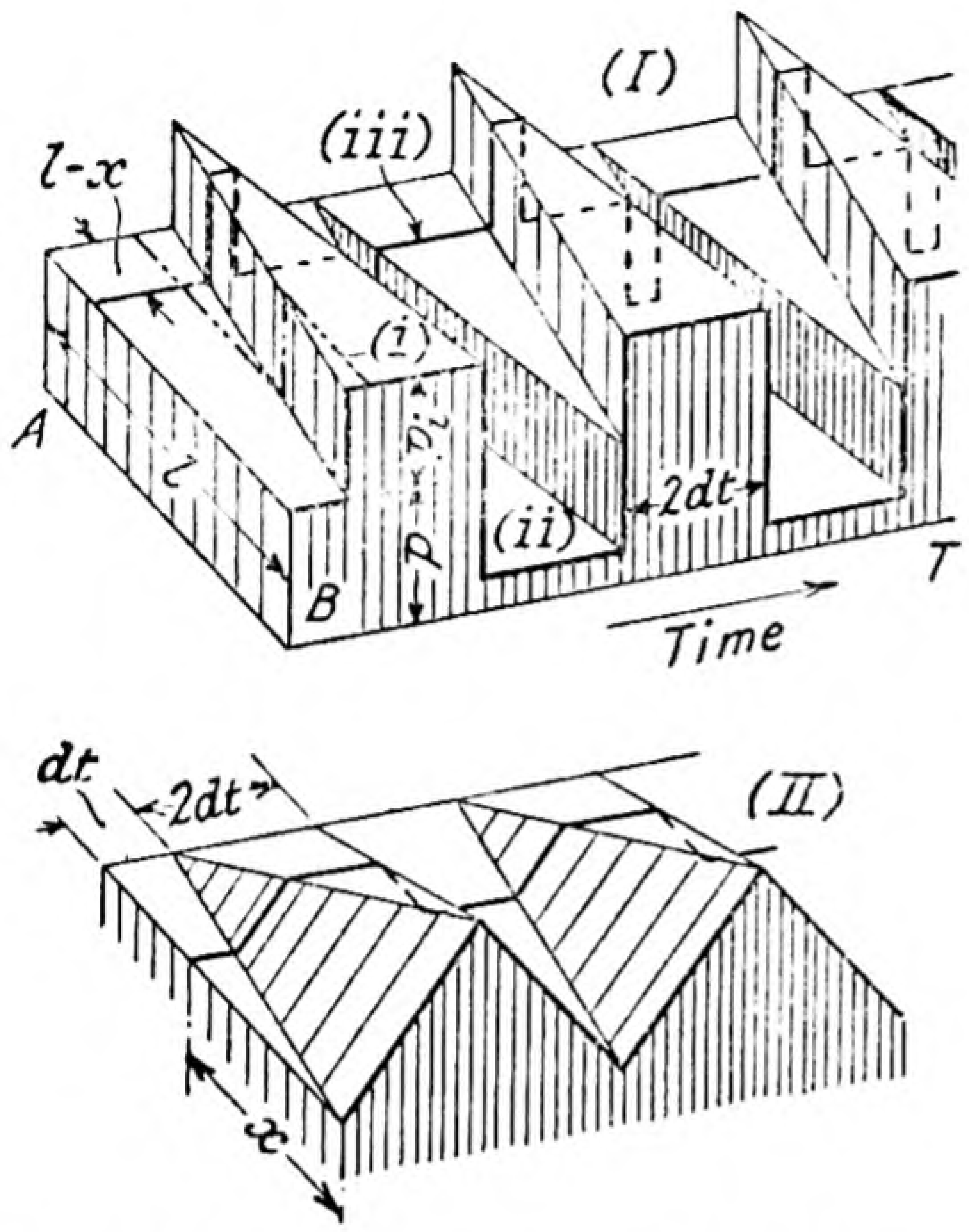

FIG. 162.—Stereograms for (I) instantaneous closure, (II) gradual closure.

176. Graphical Plotting of the Allievi Equation. If the pressure and velocity fluctuations throughout the length of the pipe, which it is our purpose to investigate, took place so slowly that they could be observed and recorded by human observers, there would be two alternative systems of collecting this information: (i) we could station an observer at each of a number of fixed points along the pipe, or (ii) we could instruct the observers to patrol the pipe, travelling continuously from end to end and back again. The first system is used in principle when making a census of road traffic; the second is preferred by the road patrols organised by British motoring associations. For present purposes the second method will be more suitable, and we are therefore going to confer on our imaginary patrolmen the means of travelling *at the speed of the compression waves* which sweep along the pipe during the retarding or accelerating period. For a specified pipe and liquid this velocity v_0 has a uniform value which can readily be calculated by the

use of the equation established in § 116—it will be of the order of 4000 ft./sec. It is the travelling observer who is going to supply the link between the stereogram and the new kind of working diagram that we intend to develop. In Fig. 163 (i) we see in plan a layered stereogram based upon pressure-changes such as were represented in Fig. 97. Deeper tints here indicate greater inertia-pressures, just as in contoured maps these darker patches indicate greater altitudes.

What would the patrolman have to record when travelling along the line PQ of the stereogram (i)? At each of a number of points he would be obliged to climb a step of height δh_i. But what the stereogram does not tell us—and in its failure to do so lies its chief defect—is that each change of pressure-head can only be brought about by a *change of velocity*. The two variables are inter-connected by the Allievi equation 7·4, § 116, which may now more conveniently be written

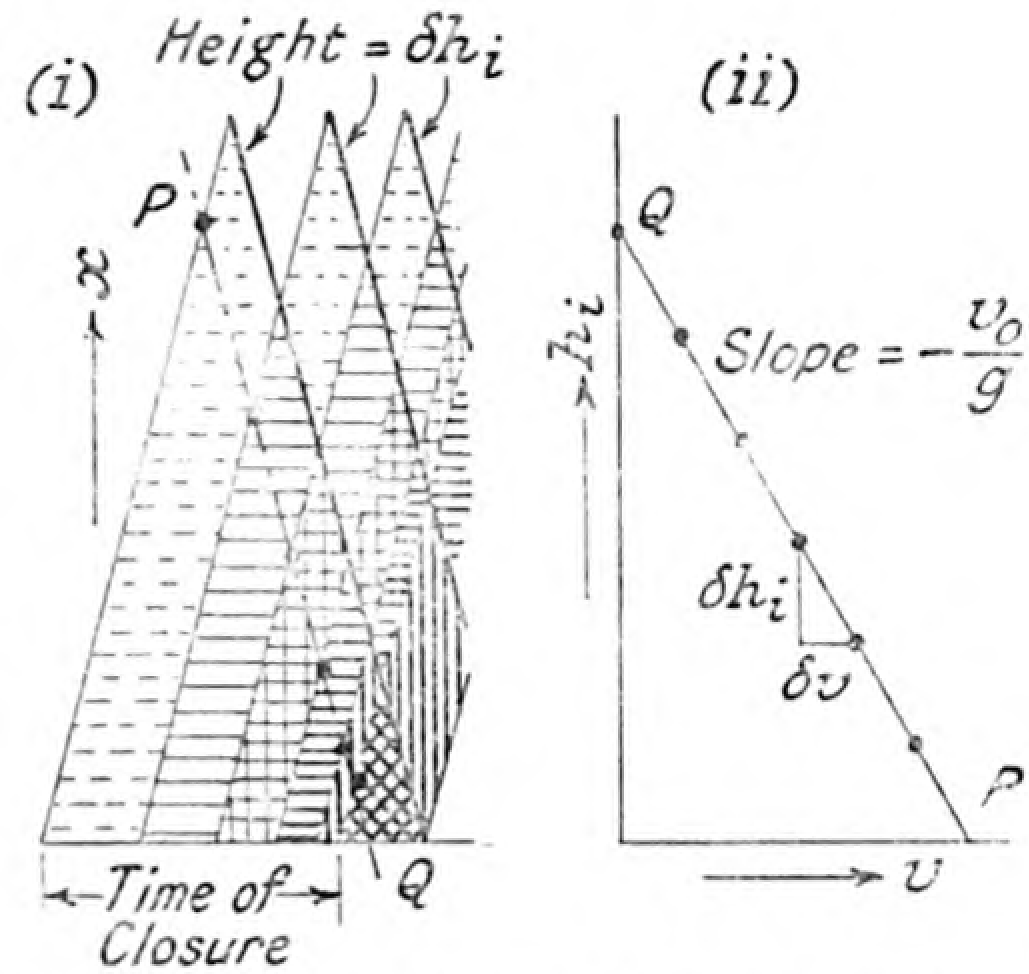

FIG. 163.—Development of velocity-head line from stereogram.

$$\delta h_i = \frac{v_o \, . \, \delta v}{g}.$$

Here is the key of this new graphical process. If successive values of pressure-head and of velocity, *as registered by the travelling observer* during his trip along the pipe, are plotted one against the other, then the resulting graph will be a straight line having a slope $\frac{v_o}{g}$. If the observer is moving *with* the original velocity, viz. towards the valve at the end of the pipe, then the sign will be negative, thus :

$$\frac{\delta h_i}{\delta v} = -\frac{v_o}{g}.$$

Such a line is plotted at PQ in Fig. 163 (ii).

If the observer is moving *against* the stream, from the valve towards the reservoir from which the liquid is issuing, then the sign will be positive, thus :

$$\frac{\delta h_i}{\delta v} = +\frac{v_o}{g}.$$

Each trip along the pipe will be represented by one such line, and the entire sequence of operations, from the initiation of the closing process to the final cessation of flow, can be displayed by a composite diagram built up from such uniformly-inclined straight lines. These $v : h$ lines are *always straight*, no matter whether the retardation is uniform or not. For example, the small time intervals between valve movements represented in Fig. 163 are purposely unequal, in agreement with an increasing rate of retardation. Such fruitful results follow from a prudent choice of variables. Four of these are involved : Time t, length x, pressure-head h, and velocity v. In Chapter VII,

either x and h or t and h were plotted one against the other; in the stereogram, all except v were represented. It is the v-h combination that is best adapted for graphical analysis.[95]

Construction of the velocity-pressure diagram. A knowledge of the law of valve closure or of retardation of the liquid column must form the foundation of the graphical method just as it was the basis of the diagrams reproduced in § 118. There is now no need to be limited to the special condition of uniform retardation; any law can be accepted. Let it be stipulated that the velocity at a point *near the valve* is related to time in the manner shown in Fig. 164 (ii). (The proviso "near the valve" is an essential one, for at a

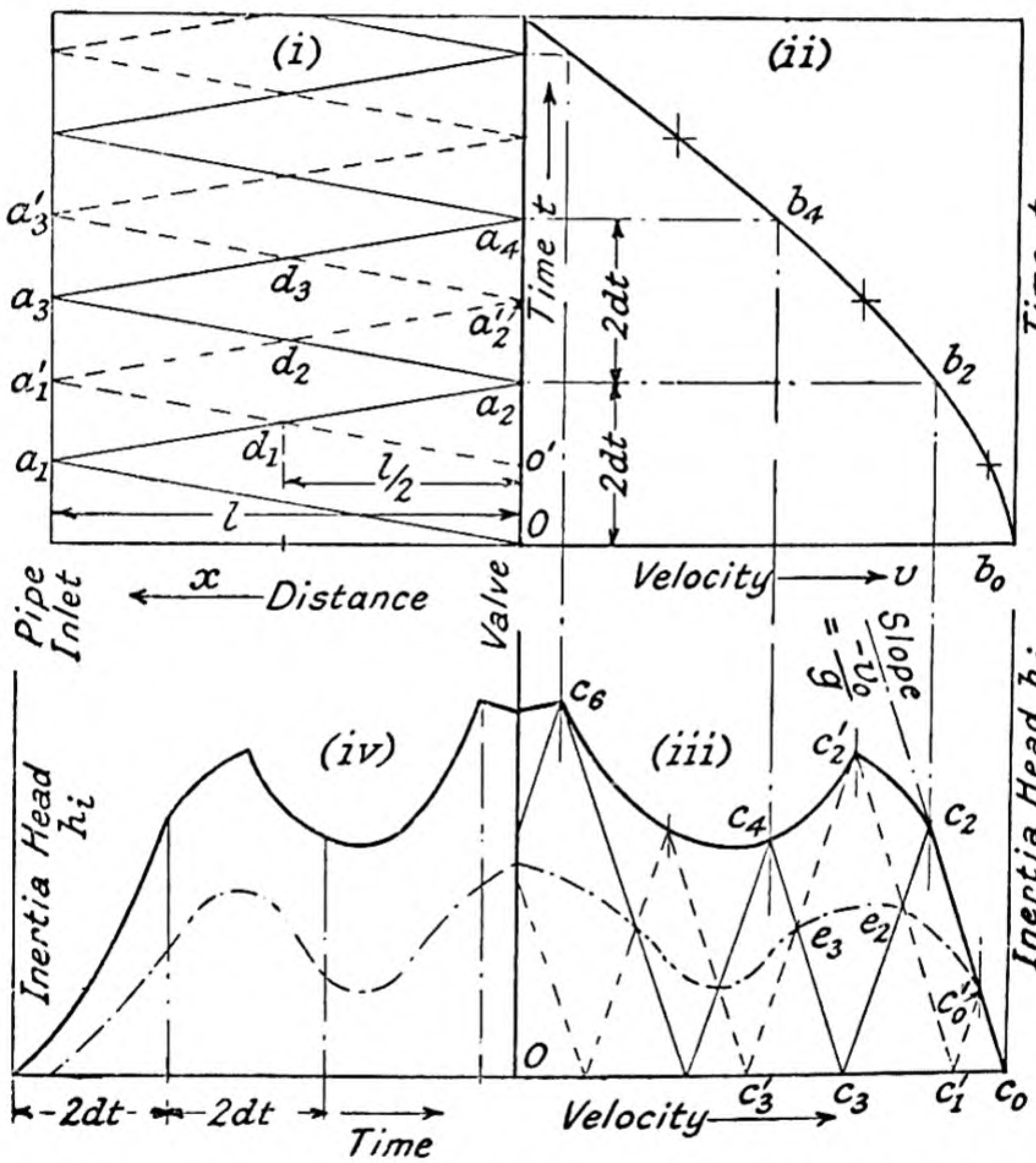

FIG. 164.—Composite plotting of distance, time, velocity and pressure-head.

given instant the velocity varies from point to point along the pipe, and it is only within our power to control the velocity of the liquid adjacent to the valve itself.) From the known length l of the pipe, and velocity v_0 of the compression wave and of the patrolmen, the time dt for the compression wave to traverse the pipe can at once be computed, enabling the track-chart of the observer to be laid out as in diagram (i), Fig. 164. Then the v and h axes are prepared, diagram (iii), ready to receive the information signalled from the observer. The successive reports will run as follows :—

1st *outward trip*, Oa_1. Nothing to report. A glance at the typical stereogram, Fig. 162 (ii), shows that no change in pressure-head or velocity can be encountered; consequently the line Oa in diagram (i) is represented by

a *point* c_0 in diagram (iii). What this means is that the observer is moving just ahead of the pressure-wave, which just fails to catch him up.

1st homeward trip, a_1a_2. The laws formulated above now become valid. As the patrolman is moving downstream, his journey will be represented on the v-h diagram by the line c_0c_2 having the negative slope $- v_0/g$. How high will the line rise ? We must refer to diagram (ii), which shows us that after a time-interval 2 dt, the velocity has fallen to a_2b_2. The graphical system of projection, $a_2 . — . b_2 . — . c_2$, is quite straightforward, while the observer's steady climb along the ridge of the stereogram is suggested in Fig. 162 (II).

2nd outward trip, a_2a_3. Already the routine is becoming familiar; the slope of the line c_2c_3 is fixed by the fundamental equation, and manifestly the position of point c_3 must correspond with zero inertia head which the observer invariably finds at the reservoir end of the pipe.

2nd return trip, a_3a_4. Again the intersection of c_3c_4 with the vertical dropped from b_4 establishes the position of c_4.

And so the process continues until the original velocity $v = Ob_0$ is exhausted.

Does the velocity-pressure diagram $c_0c_2c_3c_4c_5$ . . . give all the information we require, now that we have finished it ? What is the observer's opinion ? If his beat were between two towns, X and Y, and we asked him if he were certain he had observed everything that happened at Y, he would have to reply: "How could I possibly know what was going on at Y if at that moment I was at X ?" Exactly. The points c_0, c_2, c_4 in Fig. 164 (iii) only say what was the pressure-head near the valve at three instants of time; we know nothing whatever about the pressure-head near the valve when the observer was at points a_1 or a_3. The remedy is perfectly clear. We must send out more observers. If the second one goes on duty dt seconds after the first one, then the broken line o', a'_1, a'_2, a'_3 will represent his movements, and the information he collects will be shown by the broken line c'_0, c'_1, c'_2, c'_3 on the velocity-pressure diagram (iii). During his first outward trip he will spend part of the time traversing along a contour of the stereogram and the remainder of the time, corresponding to $c'_0c'_1$, in coasting down to zero level.

177. Interpretation of the Velocity-pressure Diagram. There should now be so closely-spaced a series of points c_0, c_2, c'_2, c_4 . . . that a fair curve can be drawn through them to serve as a record of the pressure fluctuations *near the valve.* Often the curve provides all the information needed; it shows that the maximum inertia pressure occurs at point c_6 and it is highly probably that this will also be the maximum anywhere in the pipe. If for any purpose a time-pressure diagram is desired, comparable with Fig. 98, it is easy to re-plot diagram (iii), Fig. 164, on a time base, as indicated in diagram (iv). It is hardly surprising to find that the corresponding stereogram would display none of the geometrical simplicity that characterises Fig. 162 (II).

The remaining problem is to establish for any other point in the pipe the complete velocity-pressure graph belonging to the same family as the graph c_0, c_2, c_4, c_6 already traced. Until such a record is available, there cannot be full confidence that the maximum pressure from all causes, e.g. the pressure represented by AB in Fig. 153, is known with certainty. For such intermediate points the diagram (ii) in Fig. 164 is valueless; instead, the principle of intersecting track-charts is utilised. Two observers who meet at a selected point must necessarily report identical figures at that point, and these figures

can therefore be read from the intersection of the corresponding graphs on the velocity-pressure diagram. Should a point half-way along the pipe be chosen, so that $x = l/2$, then the data relating to the intersections d_1, d_2, d_3 are given by the intersections c'_0, e_2, e_3. Transferring these points c'_0, e_2, e_3 to the time-pressure diagram (iv), we arrive ultimately at the dot-and-dash curve which is a graphical summary of events at the chosen point. As we should expect, pressures are here consistently lower than they were near the valve. It is to be noted that Fig. 164, complex though it appears to be, has only portrayed the first phase of the operations. After valve closure is finished, a regular cycle of pressure-waves will traverse the pipe of periodicity $4dt$, as indicated in Fig. 98, until friction flattens them out.

It is only when we attempt to put into practice the elegant technique just described that we encounter what seems to be a serious limitation. By what method are we going to plot the time-velocity curve, Fig. 164 (ii), that admittedly forms the foundation for the entire procedure ? The primary type of movement or of variation is the *movement of the valve* or other closing mechanism. There is no reason to doubt that the force available will suffice to shut the valve positively at any speed that may be chosen. To this arbitrarily-selected rate of closure, the cycle of pressure- and velocity-changes is wholly subservient. Remembering that even when inertia pressure is disregarded, the connection between valve opening and pipe velocity is far from simple (§ 172), it will manifestly be a great deal more complicated when the true instantaneous pressure near the valve is taken into account. Thus the curve $b_0b_2b_4$ . . . which appeared to serve as so stable a basis can itself only be determined after the pressure-changes have been plotted. It is true that from the predetermined shape of curve we could formulate the law of valve closure required to bring it into effect ; but there would be very little probability of finding any operator or any mechanism capable of maintaining so accurate a control of the valve movement.

The solution of this difficulty reveals the most advantageous aspect of the pressure-velocity diagram. By combining it with the parabolic diagram connecting pressure, velocity, and valve opening, we can plot the desired diagram c_0, c_2, c_4 without the need for the time-velocity curve, (ii) ; after a little practice it becomes possible to dispense not only with the stereogram, but with diagrams (i), (ii), and (iv) as well. If the pressure-surges consequent on the stopping of a pump are to be studied (§ 333), then the conventional pressure-velocity diagrams used for recording the performances of these pumps, § 327, may likewise be combined with the inertia-pressure diagram, Fig. 164 (iii). (Example 86.)

Before allowing the travelling observer to fade from the mind, we might remember that nowadays he is not altogether a figment of the imagination. The pilot of an aircraft flying at sonic speed is indeed travelling at the speed of pressure-waves ; but they are sound waves in air, not in water.

178. The Complete Pipe-Line. At this stage it may be assumed that most of the data are available which serve as a basis for the final lay-out of the pipe system ; the pipe diameter and wall thickness are provisionally settled, and a likely material has been chosen. Yet further decisions still remain to be made. For instance, shall the pipe be laid above ground or below ground ? Of course in an urban or any other

fully-developed area, the pipe must almost certainly be buried, for otherwise it would create an intolerable interference with communications. Considerations of safety may also favour a buried pipe, especially when the high-pressure conduit of a hydro-electric plant (§ 252 (i)) traverses mountainous country subjected to avalanches, rock-falls, and the like. Here the pipe may conveniently take the form of a pressure-tunnel driven through the rock and lined with steel plate. Public authorities who are particularly insistent on putting turbine pipe-lines out of sight are those responsible for preserving " amenities "; if they do not succeed in getting their way it may be because the cost of burying the pipe is excessive.

Coming now to conditions in which an over-ground pipe would not specifically be ruled out, e.g. a pipe carried across open country which is unlikely to be heavily populated, what would be the advantages of such a solution ? The chief one is that the pipe is always accessible : damage to the external protective coating, or leakage at the pipe-joints, can quickly be detected and remedied. In any event the outside of the pipe is likely to suffer less damage from atmospheric influences than it would be from the attacks of dissolved salts in the ground in which it might be buried. As for temperature effects, these can be countered in either of two ways. One method is to provide effective sliding expansion-joints spaced at regular intervals (see diagram in Example 85), the pipe being rigidly anchored at intermediate points. In the other method the pipe is welded into a continuous length, it is constrained by massive anchorages at all points of change of direction, and thermal effects are taken up wholly by changes in the longitudinal stress in the pipe walls. Sometimes the continuously-welded pipe is laid in zig-zag formation, thus permitting the pipe to adapt itself to temperature changes by sideways movements.(96)

In regard to the type of pipe-joint, § 152, the nature and value of the liquid cannot be ignored. Slight leakages of water from " flexible " joints might be tolerated, but these joints would not serve for costly liquids such as petroleum products. No leakage at all can here be allowed : all joints must be hermetically sealed by welding.(97)

CHAPTER X

CONTROL OF WATER IN OPEN CHANNELS

179. Types of Open Channel. After a study of the factors examined in § 149 has indicated that an open channel [98] will be preferable to a closed conduit for the specified duty, it becomes necessary to choose the most suitable *material* for the channel and the most favourable *cross-section*—for there is now no need to be restricted to circular shapes.

Natural rivers and streams. In general the engineer has here to accept the shape of waterway that nature has provided; the local improvements or corrections that lie within his power, such as dredging the bed, training, raising, or revetting the banks, or straightening tortuous reaches, may represent engineering works of the first magnitude but may nevertheless exert but a trifling influence on the average regime of the river as a whole.

Earthen canals. Large artificial canals for navigation, irrigation, drainage, and water-power developments must necessarily be cut through the local soil, the soil excavated from the bed being used if required to form the banks. As the water is thus constrained by nothing more resistant than mud, silt, or clay, velocities must be kept down to a low value—perhaps 3 ft./sec.—to minimise the risk of erosion (§ 201). Seepage, or leakage through the permeable banks and

bed, may account for the loss of immense volumes of water (§ 203).

Lined canals. Lining a large canal with impermeable and resistant material is a costly expedient, but it is being adopted with increasing willingness because (i) the smoother surface and the higher permissible water velocity together permit a smaller cross-section to be used, (ii) the loss through seepage is greatly reduced.[99] The material chosen is usually concrete, plain or lightly reinforced, either cast in place or formed into pre-cast slabs. In large projects, specially-designed travelling machines may be used: as they move slowly along the carefully-graded earthen canal, they deposit in a single operation the desired thickness of concrete lining. Brick tiles laid in cement are sometimes preferred, and clay puddle occasionally serves.

Rock-cut channels. When the channel is to be excavated in rock, only detailed analysis of costs will show the relative merits of a comparatively large rough-dressed channel and a smaller channel with smoothly-rendered walls.

Flumes. Rectangular channels of timber or concrete, or semi-circular channels of steel-plate, are convenient when relatively small amounts of water have to be carried for short distances above ground level.

Channels of closed cross-section. If the waterway has to be taken underground it must manifestly be built with some kind of roof to support the superincumbent earth or rock. Although the waterway thus resembles a closed conduit, it must not from the hydraulic standpoint be treated as such; it is nothing more than a covered-in open channel. The free water surface is throughout in contact with the atmosphere; the walls are not designed to withstand any internal pressure greater than that corresponding to the depth of water. Indeed, it is the external earth pressure that may determine the shape of the cross-section—see, for example, the typical tunnel sections shown in Figs. 133 and 198. Sewers are essentially roofed channels; they may be of concrete of circular section, or of brickwork built to circular shape, or, for small discharges, of stoneware pipes. Other types are mentioned in § 202.

180. Selection of Channel Cross-section and Slope. At least for preliminary calculations it may be assumed that

uniform flow will prevail (§ 100), that the water depth is above the critical depth, § 106, and that the treatment developed in § 101 will be applicable.

Channels that have the least cross-sectional area A for a given discharge q, surface slope i, and coefficient C are known as "best form" or "maximum discharging" channels. Examples of these are drawn to scale in Fig. 165. The semi-circular channel (I) has the least cross-section of any. The condition that trapezoidal channels should be of the best form is that both the sides and the bottom should be tangential to a semi-circle whose centre lies in the water surface. A further characteristic of semi-circular and trapezoidal best-form channels is that the hydraulic mean depth m is always one-half the water depth d, or $m = \frac{d}{2}$.

Using the area A_1 of the semi-circular channel as a standard of comparison, it is to be seen from Fig. 165 that if the side slopes of a trapezoidal channel (II) are specified to make an angle of 60° with the horizontal, the area A_2 of the best-form section is 2 per cent. greater than A_1; if the side slopes are 45° (III), then A_3 is 3 per cent. greater than A_1; while a rectangular channel (IV) equivalent to 90° side slopes, has an area A_4 5 per cent. greater than A_1. Comparing now a trapezoidal channel of the best form, having 3 : 2 side slopes (3 horizontal to 2 vertical), with a channel having the same side and bed slopes and the same discharge, but having a shallower section, $b_6 = 3d_6$ (Fig. 166), the area A_5 of the first is 6 per cent. greater than the area A_1 of the equivalent semi-circular channel, and the area A_6 of the second is 9 per cent. greater than A_1.

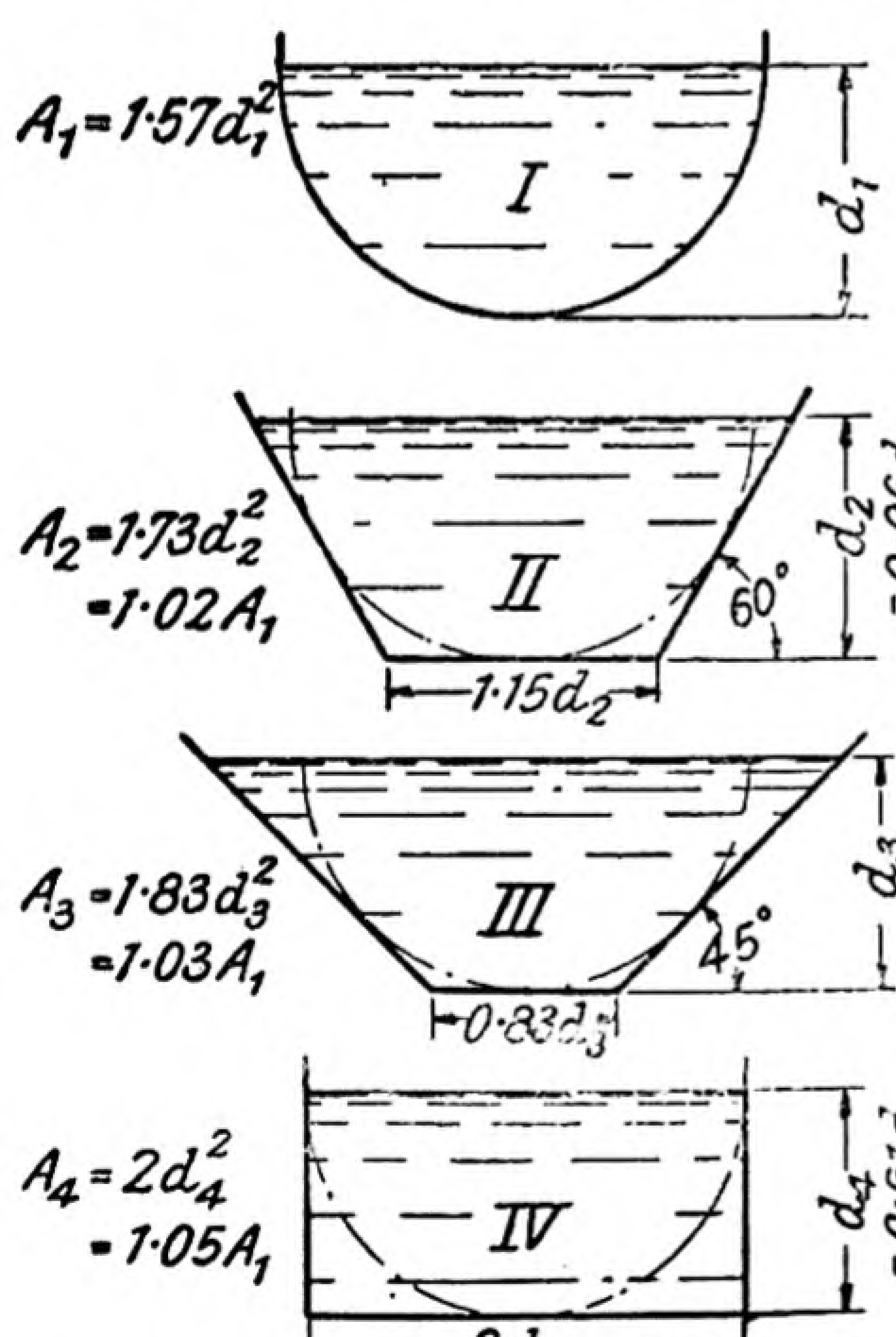

FIG. 165.—Maximum discharging channels.

On the same comparative basis, a *circular* channel *running*

full is a bad section to choose: its area is 15 per cent. in excess of the equivalent semi-circular channel, § 183.

More often than not it is neither practicable nor economical to make the cross-section of a channel of the "best form." For example, it would hardly be possible to excavate a semi-circular earthen canal—the sides would immediately cave in—and for large discharges even a "best-form" trapezoidal section with suitable side slopes would be much deeper than would for many reasons be desirable. Some of the further considerations that influence the choice of canal section are discussed in § 202.

The maximum permissible longitudinal slope of the bed of earthen canals is fixed by the water velocity that will just not cause erosion of the banks (§ 201); this slope is of the order of $\frac{1}{10000}$ to $\frac{1}{5000}$. For channels in rock, or faced with cement or brick, or for wooden or sheet metal flumes, the slope may be very much steeper than this. Since a natural river will in the course of ages continue to scour away its bed until a steady regime is reached, it follows that in their lower reaches, rivers as a rule have a longitudinal slope represented by much the same figures as those just mentioned for canals, viz. between about $\frac{1}{20000}$ and $\frac{1}{2000}$.

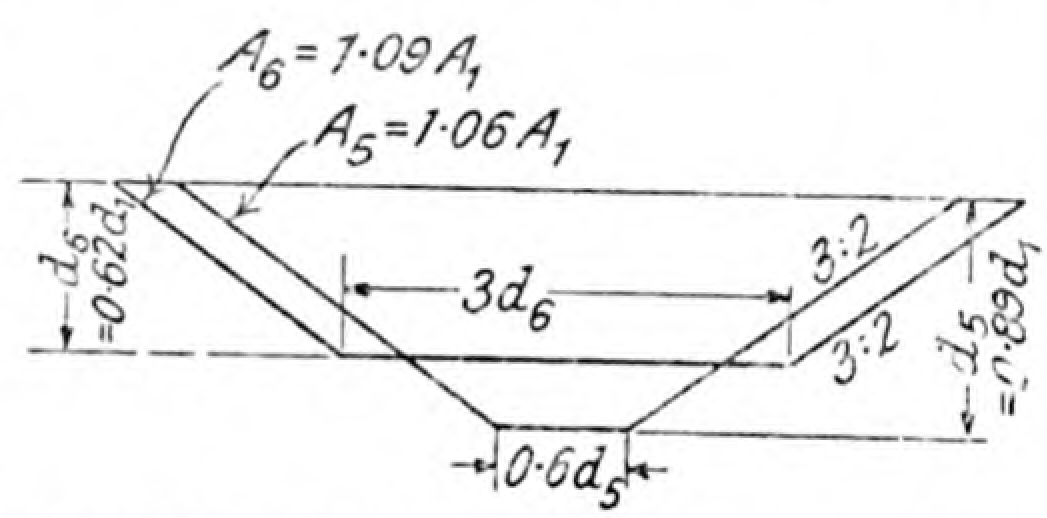

FIG. 166.—Trapezoidal channel sections.

If the natural slope of the ground is greater than the permissible slope of the artificial canal that traverses it, then the surplus head must be dissipated by *falls* spaced at intervals along the waterway. These are artificial waterfalls, comprising suitable means for protecting from erosion the downstream areas of the channel bed.

Special problems arise [100] when (i) the water flows at velocities much greater than would be associated with the above figures, (ii) the channel is not straight, but is curved in plan. Such questions lie outside the scope of this book.

181. Discharge Formulæ: (*a*) *Chezy* formula. The Chezy formula (formula 6-1, § 101),

$$v = C\sqrt{mi},$$

and the resulting formula,

$$q = AC\sqrt{mi},$$

are as much used for canal design as they are for pipe design.

Here also *Kutter and Ganguillet's* formula permits the coefficient C to be evaluated, as follows:

$$C \text{ in foot units} = \frac{41{\cdot}6 + \dfrac{0{\cdot}0028}{i} + \dfrac{1{\cdot}81}{N}}{1 + \dfrac{N}{\sqrt{m}}\left(41{\cdot}6 + \dfrac{0{\cdot}0028}{i}\right)}.$$

$$C \text{ in metric units} = \frac{23 + \dfrac{0{\cdot}00155}{i} + \dfrac{1}{N}}{1 + \dfrac{N}{\sqrt{m}}\left(23 + \dfrac{0{\cdot}00155}{i}\right)} = \frac{C \text{ in ft. units}}{1{\cdot}81}$$

In these formulæ

q = discharge in cusecs (cu. m./sec.).

v = mean velocity in ft./sec. (m./sec.).

m = hydraulic mean depth or mean hydraulic radius $= \dfrac{A}{P}$ in feet (metres).

A = area of cross-section of waterway in sq. ft. (sq. m.).

P = wetted perimeter in feet (metres).

i = longitudinal surface slope = fall in surface level per unit length.

N = Kutter's coefficient of rugosity, depending only on the nature of the sides and bed of the channel, and independent of the system of units.(101) Commonly accepted values of this coefficient are given below :—

Type of Channel.	Kutter's N.
Smooth cement or planed wood	0·010
Iron or steel plate	0·011
Unplaned wood : concrete	0·012
Earthenware : good brickwork : cast iron	0·013
Brickwork, stonework, and cast iron in bad condition	0·017
Earthen canals : good order	0·020
,, average order	0·025
,, bad order	0·030

The manner in which C varies with m and with i, for a rugosity coefficient, N, of 0·0225—a fairly safe value for

well-maintained earth canals—is illustrated by full lines in Fig. 167. (Example 96.)

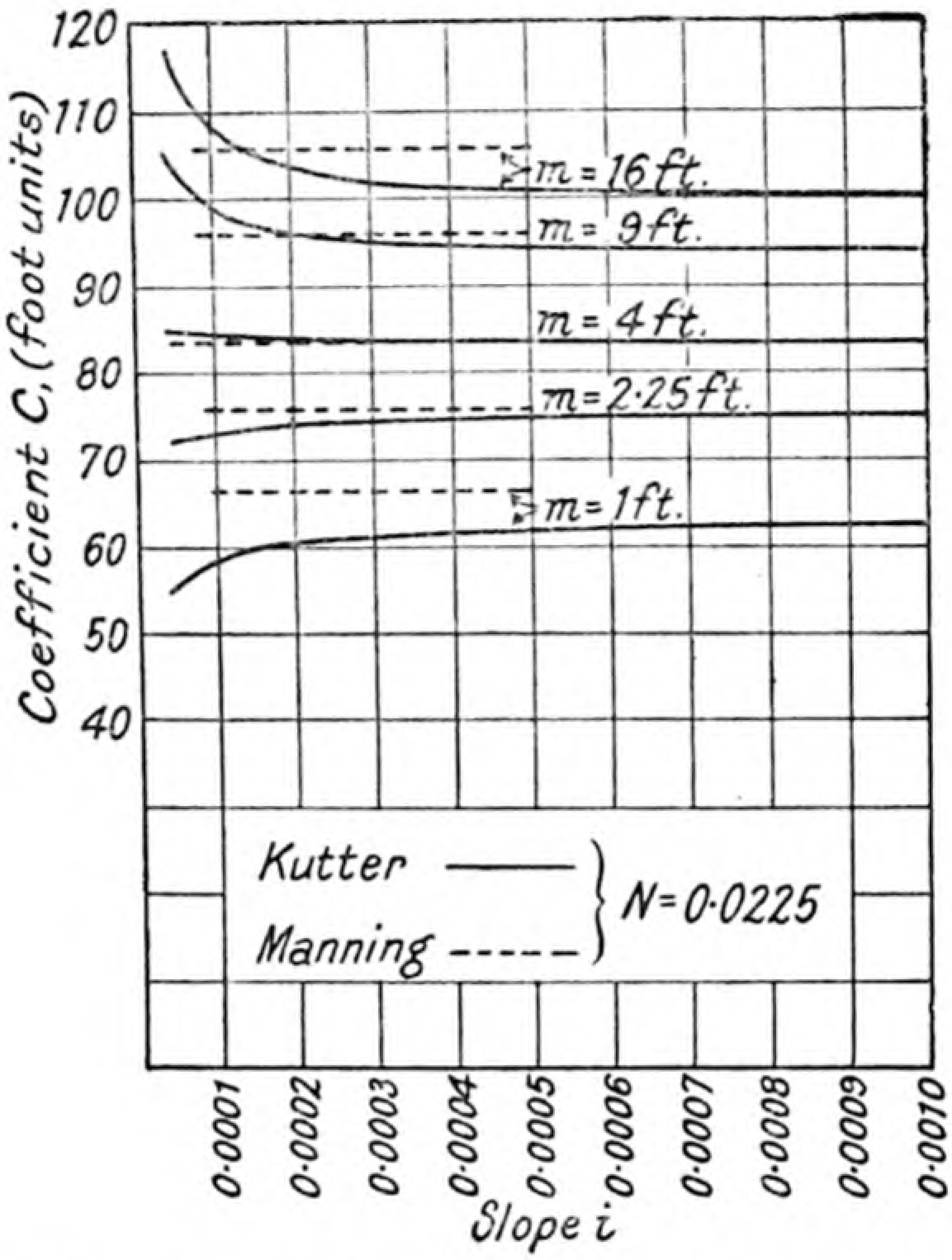

FIG. 167.—Values of coefficient C for well-maintained earthen canals.

A simpler formula for determining C is *Bazin's* formula. It is as follows :—

$$C = \frac{157 \cdot 6}{1 + \frac{\gamma}{\sqrt{m}}} \text{ (foot units),}$$

$$C = \frac{157 \cdot 6}{1 \cdot 81 + \frac{\gamma}{\sqrt{m}}} \text{ (metric units),}$$

where γ represents Bazin's rugosity coefficient, having the following values applicable to either system of units :—

Type of Channel.	Bazin's γ.
Cement: planed wood	0·109
Planks: brick, cut stone	0·290
Rubble masonry	0·833
Earthen channels: very regular or stone revetted	1·54
,, in ordinary condition	2·35
,, very rough or weed grown	3·17

182. Discharge Formulæ: (*b*) Exponential types. Using formula 9-3 (§ 157),

$$v = f_2 m^{\frac{x}{n}} \cdot i^{\frac{1}{n}},$$

Mr. A. A. Barnes [78] has established the following values for

$$f_2, \frac{x}{n}, \text{ and } \frac{1}{n},$$

these being invariable for the specified class of channel, and suitable for calculations in *foot* units :—

Type of Channel.	f_2.	$\frac{x}{n}$.	$\frac{1}{n}$.
Clean planed wood troughs	223·3	0·660	0·586
Neat cement	136·3	0·635	0·484
Clean hard brick	92·1	0·602	0·466
Clean smooth concrete	95·1	0·567	0·471
Rock-faced masonry	80·5	0·653	0·482
Earth channels in average condition	58·4	0·694	0·496

The *Manning* type of formula (9-6, § 158) can often be used for channel design. By the use of Kutter's rugosity coefficient N as tabulated in § 181, it permits the mean channel velocity to be computed thus :—

$$\left.\begin{aligned} v &= \frac{1{\cdot}486}{N} \cdot m^{\frac{2}{3}} i^{\frac{1}{2}} \text{ (foot units)} \\ v &= \frac{1}{N} m^{\frac{2}{3}} i^{\frac{1}{2}} \text{ (metric units)} \end{aligned}\right\} \quad . \quad . \quad \textbf{(10-1)}$$

As is seen by comparing the broken lines in Fig. 167, plotted by Manning's formula, with the full lines plotted from Chezy's formula using Kutter's coefficients, the agreement between the two is fairly close. **(Example 97.)**

The selection of a flow formula for a channel is hardly simpler than it is for a pipe (§ 159). For large earthen canals the Manning and the Kutter formulæ are equally authoritative; for small channels with smooth walls it may be that Bazin's coefficients are more reliable. In any event worked-out tables [102] and charts [103] are available for facilitating routine calculations. As the channel nearly always contains water at atmospheric

temperature, the complexities caused by variation of the liquid (§ 160) are generally negligible. But if the water surface is frozen over, flow conditions will be seriously disturbed.

183. Variation of Discharge with Depth. Under the conditions of uniform flow assumed in the preceding paragraphs (§ 101), it is evident from inspection of the formula $q = AC\sqrt{mi}$ that an increase of water depth in a channel of given slope i will normally result in an increased velocity v and in an increased discharge q. It is common knowledge, for instance, that a river in flood flows much faster than the same river during dry weather.

If the channel is so wide that $m = d$ approximately, then, as pointed out in § 101, q varies as $d^{\frac{3}{2}}$, where d = water depth.

If the channel is of normal trapezoidal cross-section, the relationships between d, v, q and m are of the form shown in

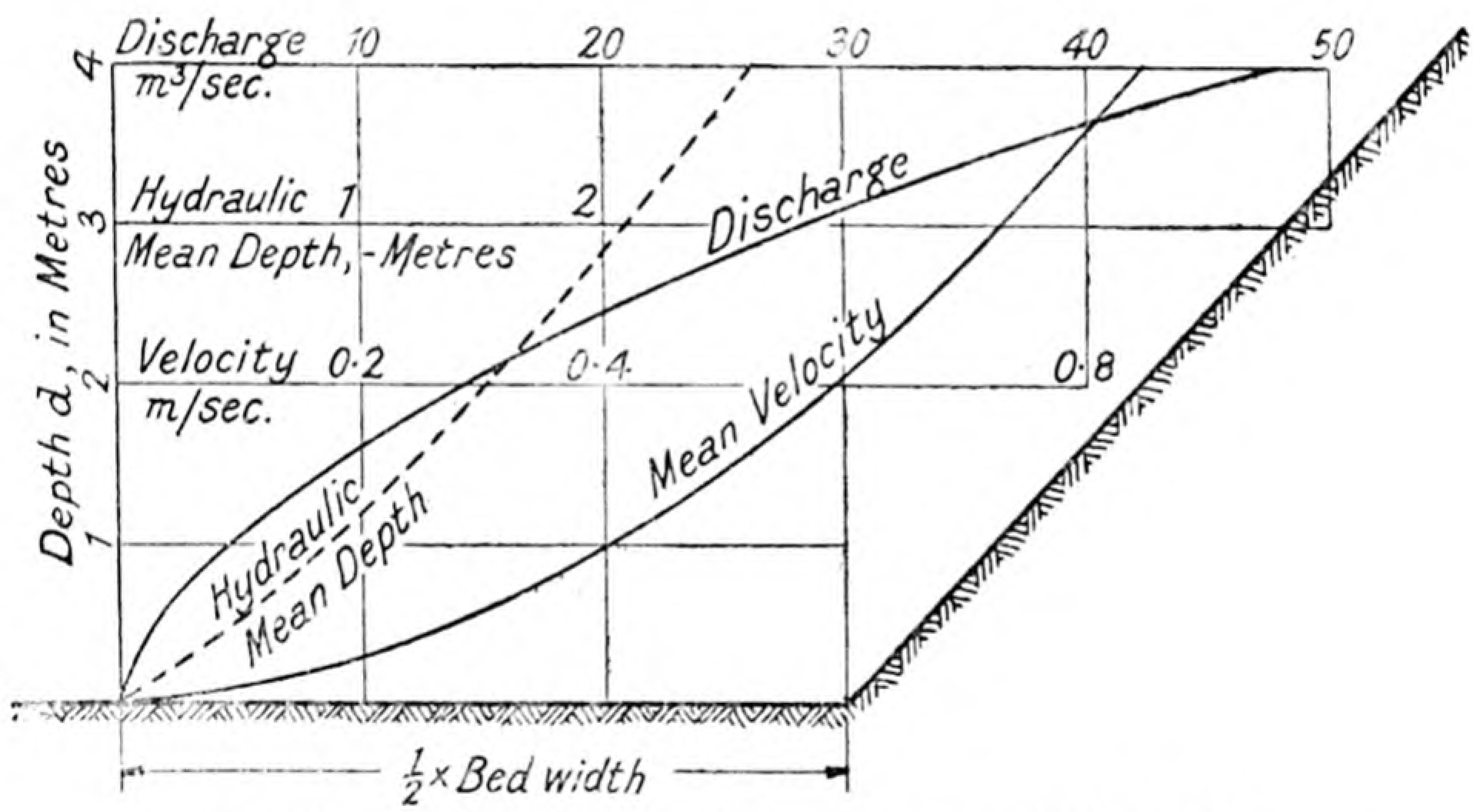

FIG. 168.—Characteristics of flow in trapezoidal channel.

Fig. 168, these graphs being plotted for the following conditions: bed-width $b = 10$ m.; maximum depth $d = 4{\cdot}0$ m.; surface slope $i = \dfrac{1}{10000}$; side slopes 1 : 1; Kutter's $N = 0{\cdot}0225$.

For a circular channel (Fig. 169) the graphs show that as the water depth becomes nearly as great as the pipe diameter, the mean velocity v and the discharge q in turn reach maximum values and then *decrease*, so that neither the velocity nor full discharge is a maximum when the channel is running the and acting as a pipe. It would not be feasible to operate

such a channel continuously at the depth corresponding to maximum discharge, for at the slightest disturbance in the flow causing a momentary increase in depth at any point, the whole waterway would at once fill, and the water would head up at the upstream end to compensate for the loss in discharging capacity.

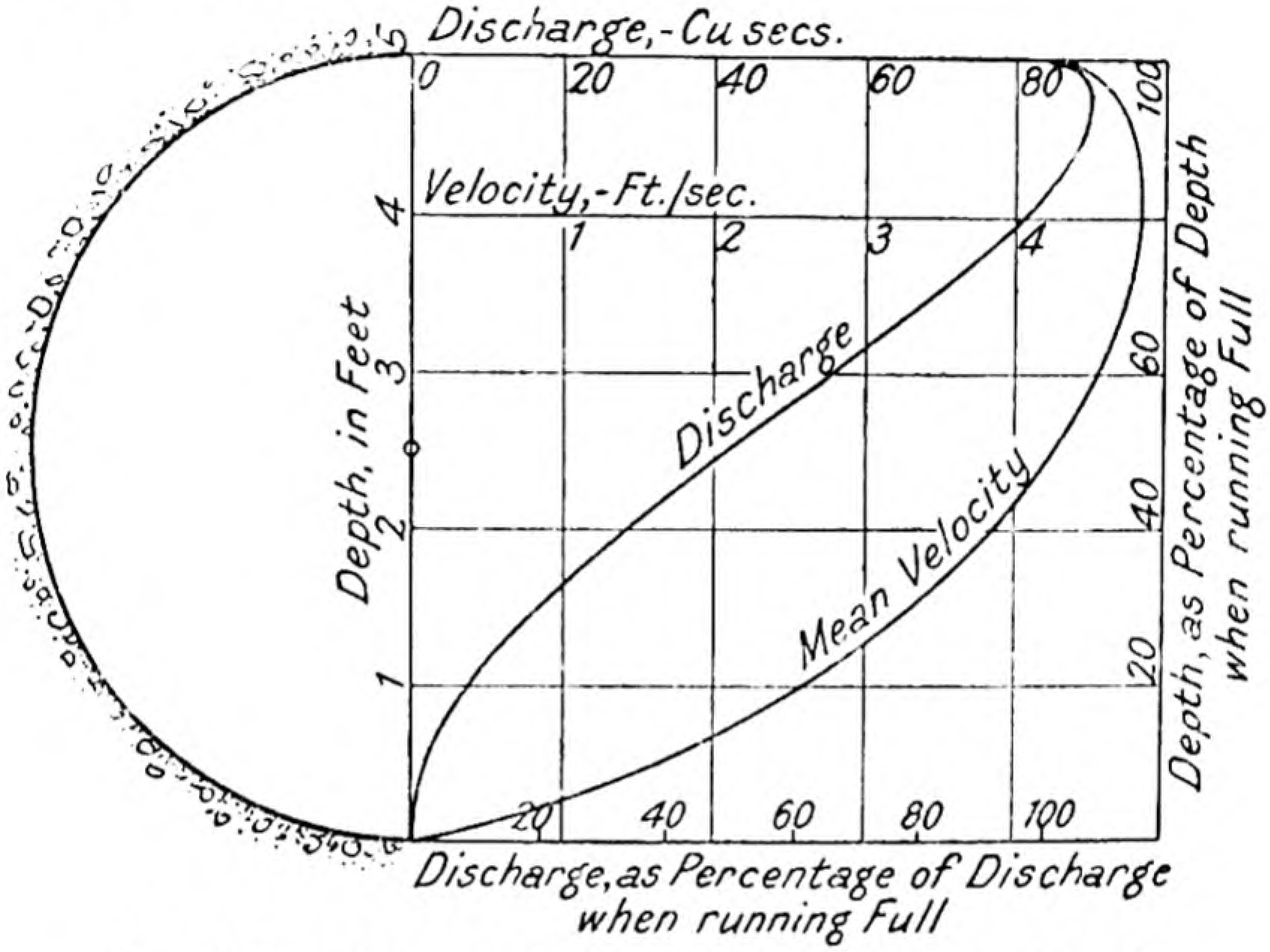

FIG. 169.—Characteristics of flow in circular channel.

Since the hydraulic mean depth m is the same, viz. $\frac{\text{diameter}}{4}$, whether the pipe is running full or running half full, the mean velocity v is the same at half depth as at full depth, and the discharge at full depth is double what it is at half depth. Fig. 169 is based on the data: diameter $= 5$ ft., slope $i = \frac{1}{1000}$, Kutter's $N = 0{\cdot}013$; but it will be found useful under other conditions for finding the proportional change in discharge in a circular channel for a given proportional change in depth.

184. Backwater Curves. As it is rare that uniform flow can be maintained throughout the whole length of a channel, the effects of local variations of depth must now be considered, on the assumption that the discharge is in no way affected, and that the original depth is above the critical depth. The causes that result in an *increase* of depth as points farther and farther downstream are compared are: (I) an obstruction

across the channel such as a weir, barrage, or similar control work, (II) the influx of a tributary stream, (III) an increase in the roughness of the channel, or a decrease in its width, and (IV) a flattening of the bed-slope. These are shown diagrammatically in Fig. 170. The water surface for some distance upstream of the point where the regime changes is now no longer plane, but curved longitudinally in a shape termed a *backwater* curve.

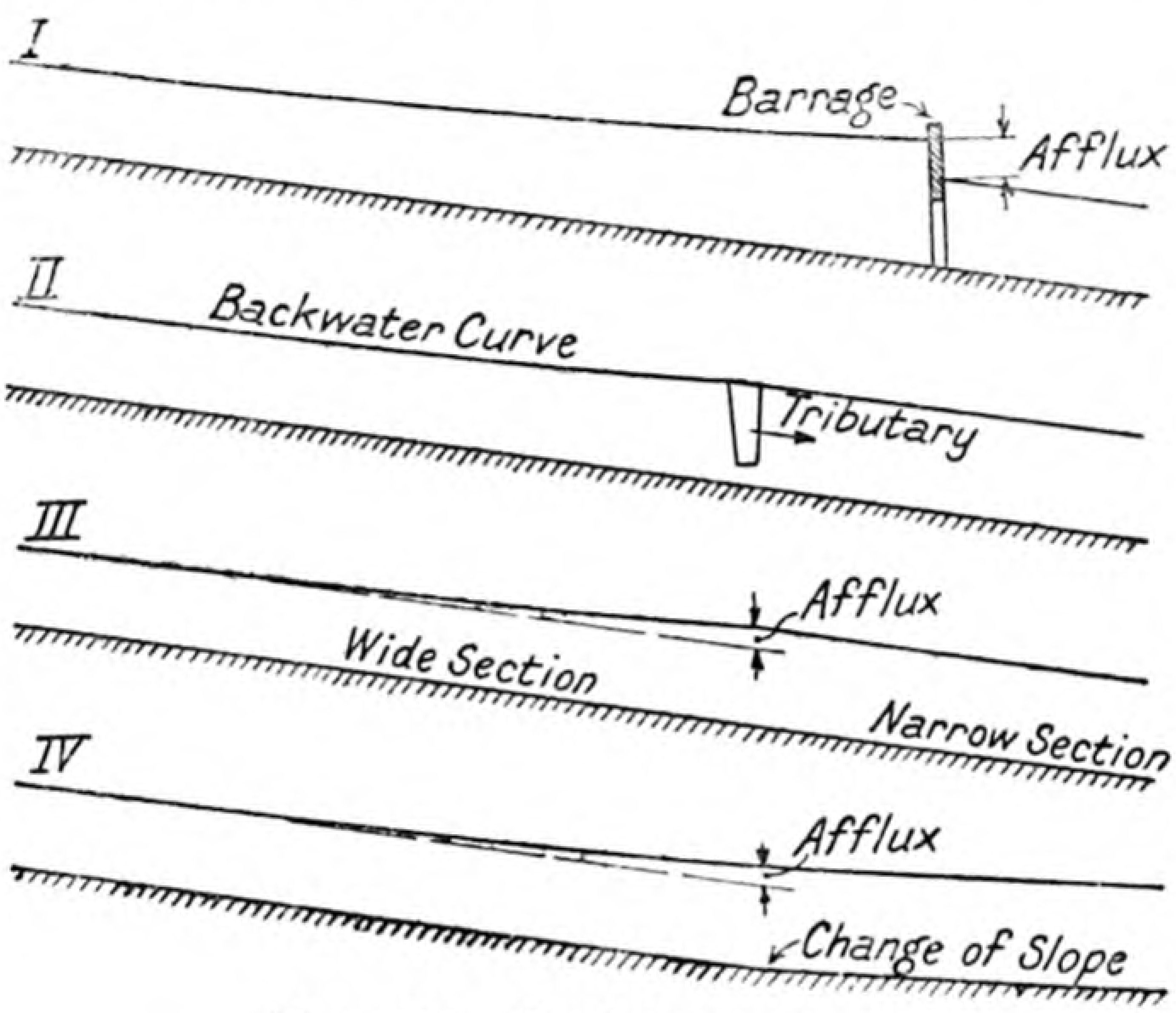

FIG. 170.—Backwater curves.

The amount by which the depth is increased or the water "headed up" by an obstruction of the nature of (I) above, is known as the *afflux*; it may be calculated by the methods given later in this chapter (§§ 188-196). Here it may be noted that under normal conditions of streaming flow the effects of such an obstruction built across a uniform channel are wholly confined to the part of the stream *upstream* of the obstruction; assuming that the discharge is unaffected, the regime downstream is in no way altered (§ 110). Under conditions II, III and IV (Fig. 170) there is no visible afflux, but the backwater curve may be treated as though caused by an afflux equal to the difference between the water depth downstream of the change point, and the water depth at a point sufficiently far upstream to be beyond the range of the backwater curve. The straight lines in Fig. 170 (IV), representing the upstream and downstream water surfaces in the regions of uniform flow, are themselves tangential to the backwater curve.

185. Methods of Calculating Length and Shape of Backwater Curves. As non-uniform flow manifestly prevails in the channel throughout the length L of the backwater curve, the fundamental formula to be used is formula 6-2 (§ 104),

$$\frac{\delta d}{\delta l} = \frac{i - \dfrac{v^2}{C^2 m}}{1 - \dfrac{v^2}{gd}}.$$

Writing this in the form $\dfrac{\delta d}{\delta l} = \dfrac{1}{S}$, we have $\delta l = \delta d(S)$, whence $L = \int \delta l = \int S \, . \, \delta d$.

In view of the difficulty of mathematically integrating this expression [104] without making unwarranted assumptions, a graphical method is usually necessary, and is carried out thus:

The afflux h is divided into a number of equal parts, ab, bc, cd, etc. (Fig. 171). Then if d_o is the original water depth

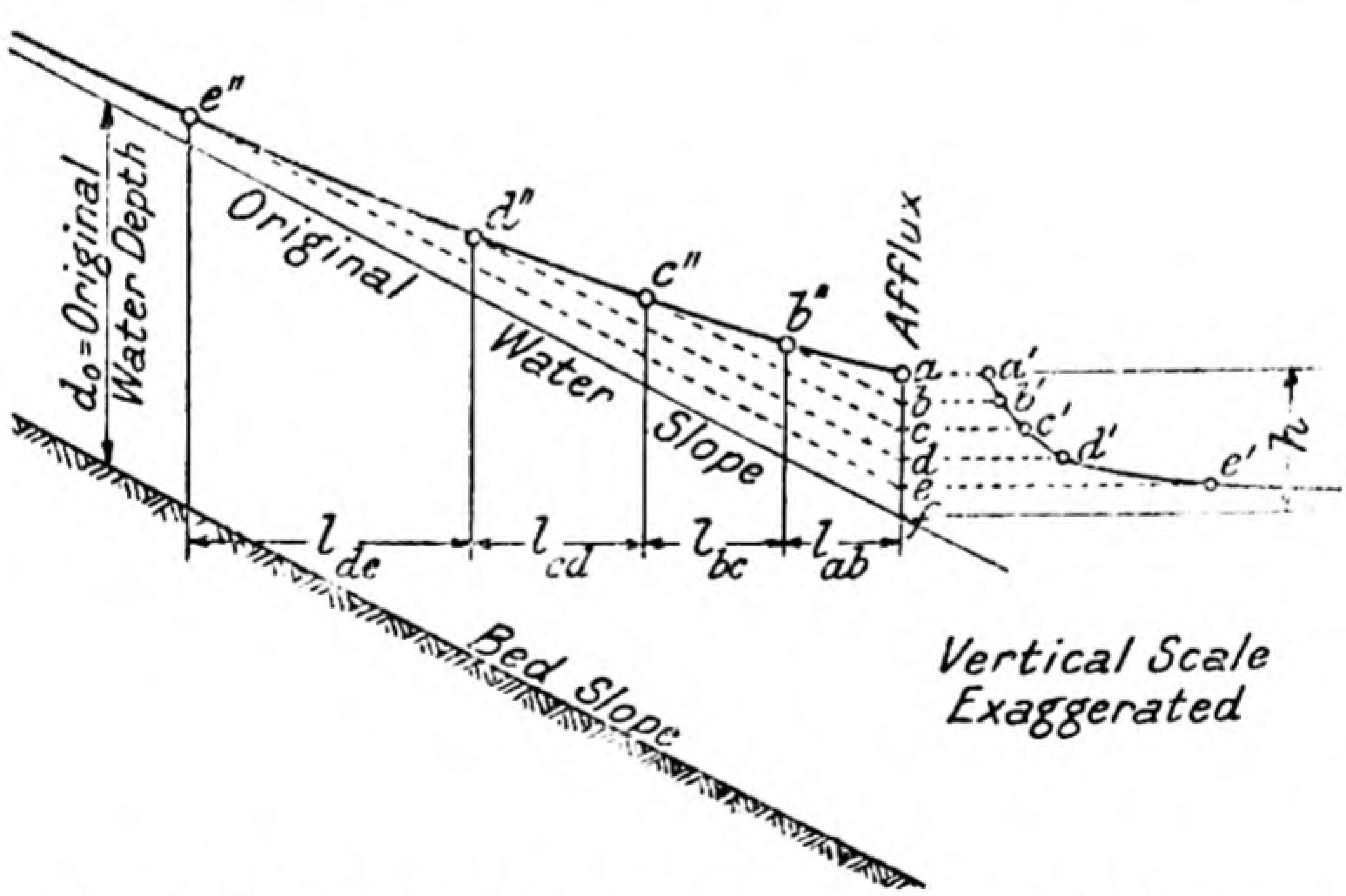

FIG. 171.—Graphical plotting of backwater curve.

under conditions of uniform flow, the water depth d_a corresponding to point a is $(d_o + fa)$; and from this, and the known discharge q and shape of the channel cross-section, the mean velocity $v = \dfrac{q}{A}$, and the hydraulic mean depth m, at point a can in turn be calculated. Inserting these values in formula 6-2, the value of S to be associated with depth $(d_o + fa)$

is determined: let this be denoted by S_a. Similarly, values of S_b, S_c, are worked out for depths $(d_o + fb)$, $(d_o + fc)$, etc., and plotted horizontally to scale as shown in the figure, where $aa' = S_a$, $bb' = S_b$, etc. Then a smooth curve is drawn through $a'b'c'$ . . . .

The area $aa'b'b$ now represents $\Sigma\delta l = \Sigma S \,.\, \delta d$ between the limits $d = (d_o + fa)$ and $d = (d_o + fb)$; that is to say, it represents to scale the length of channel associated with a part ab of the afflux, or the length of channel in which the water depth changes from $(d_o + fb)$ to $(d_o + fa)$. By setting up a vertical, distant from af by an amount $l_{ab} = \Sigma\delta l =$ area $aa'b'b$, and drawing bb'' parallel to the original water surface, we establish at the intersection b'' a point on the backwater curve. In a similar manner points c'', d'', e'', etc., are located, and finally the desired backwater curve is drawn smoothly through them.

If the actual plotting of the curve is unnecessary, and it is merely required to know at what distance upstream from a the water surface will be raised by an amount, say, fd, then the information is at once to be had by measuring the area $aa'd'd$.

A step-by-step method of plotting the curve, only slightly less laborious than the graphical integration method and not so accurate, is illustrated in Fig. 172; it depends on the

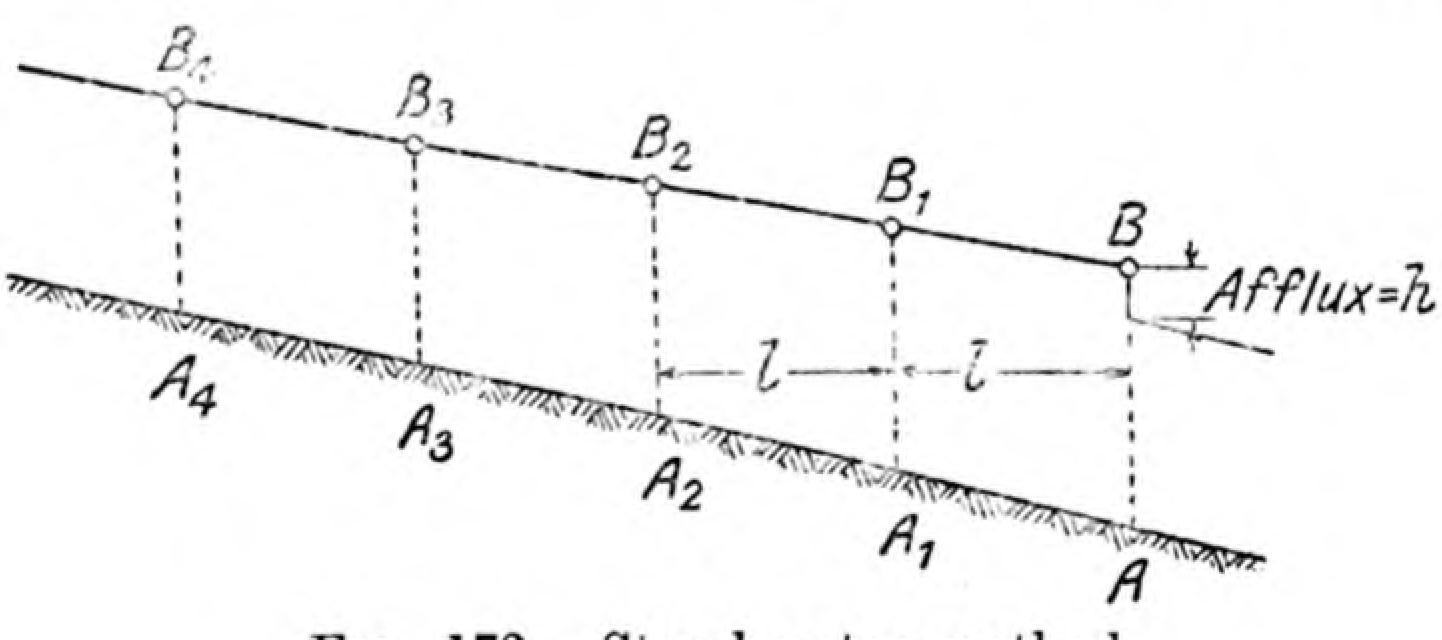

FIG. 172.—Step-by-step method.

assumption that for a distance l upstream from the afflux the surface slope remains the same as it is at A, immediately upstream. Having calculated the value of the function S_a at A as described above, the water depth A_1B_1 at a point distant l from AB will be $AB - \dfrac{l}{S_a}$. Thus the position of point B_1 on the backwater curve is established. A new value of function

S can now be worked out, based on depth AB_1, and the process is repeated until a final depth AB_n is reached that is sensibly equal to the depth for uniform flow.

Finally, a rough notion of the length of a backwater curve can be gained by assuming that the curve is an arc of a circle (Fig. 173), tangent at B to the water surface immediately upstream of the afflux, and at D to the original water surface.

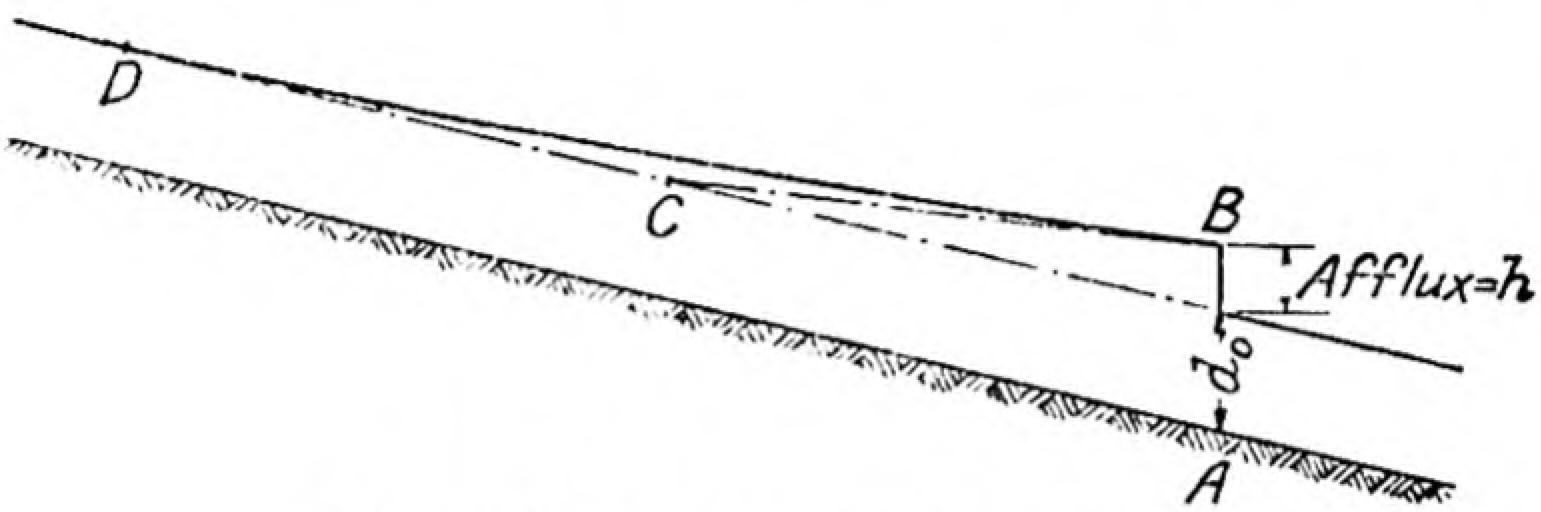

FIG. 173.—Approximate method.

Since the two tangents CB and CD are equal, the required length L of the backwater curve is $2CB = 2h \cdot \frac{\delta l}{\delta d} = 2h \cdot S$, where the values to be used in calculating function S are those prevailing at the section AB. **(Example 98.)**

For the velocities likely to occur in earthen canals, the value of $\frac{v^2}{gd}$ is so small that the term $\left(1 - \frac{v^2}{gd}\right)$ in the fundamental equation may without serious error be taken as having the value unity. In this way the work of setting out a backwater curve can be materially lightened.

186. Falling Surface or Drop-down Curves. The changes in regime that cause the water depth to become less and less as points further and further downstream are compared are of just the opposite kind to those that result in a backwater curve. Thus a *falling surface curve* (Fig. 174) may be caused by (I) a sudden drop in the channel bed, including the case of an open channel discharging freely into air (Fig. 86, § 109), (II) the diversion of water along a branch channel, (III) a decrease in the roughness of a channel or an increase in width, and (IV) an increase in the bed slope. The " drop " or difference between the original depth and the drawn-down depth may be regarded as a negative afflux, and the methods of plotting the profile of the water surface are consequently identical

with those described in the preceding paragraph, except for the change of sign.

As was pointed out in § 109, the minimum depth to which the water in a rectangular channel can by any means be drawn down is the depth d_c at which the velocity head $\frac{v^2}{2g}$ is one half of d_c.

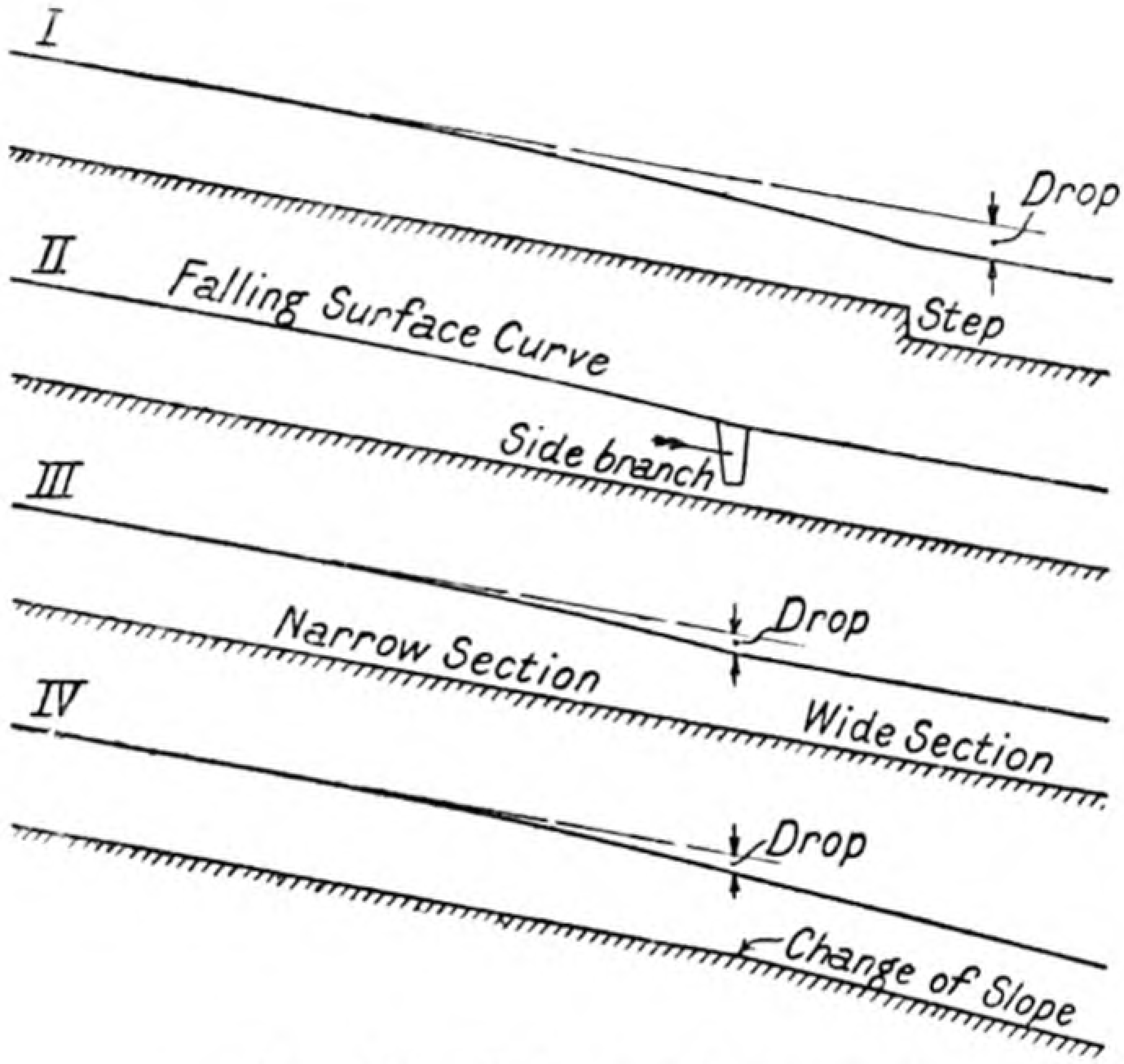

FIG. 174.—Falling surface curves.

187. Categories of Control Works. The control structures built across a natural or artificial waterway are usually intended to fulfil one or more of the following functions: (i) to impound the water, (ii) to divert the water, or (iii) to measure the water. This they achieve by altering the depth and velocity at the selected station, the flow conditions upstream being consequently modified in the manner explained in the preceding paragraphs.

Dams impose the most through-going alteration to the regime of flow, the afflux sometimes amounting to several hundreds of feet.[105] The water stored in the reservoir thus formed may be drawn off as required for domestic consumption, for irrigation, or for water-power development (§§ 204-207). When the reservoir is full and the natural flow of the river exceeds the quantity drawn off, means must be provided for disposing of the surplus water; it may be returned to the

river bed downstream of the dam by means of

— a spillway section of the dam itself (Fig. 264, § 252), which then acts as a weir (§ 188),
— a siphon spillway (§ 214),
— undersluices pierced through the dam itself (Fig. 188, § 194),
— diffusing outlet valves (§ 174),
— bell-mouthed spillways or "swallow-holes" (§ 190).

Barrages are essentially diversion works; their purpose is to divert, into a canal taking off immediately upstream, a prescribed proportion of the natural flow of the river (Fig. 194, § 197). By manipulation of the movable gates, the upstream water level can be regulated as desired.

Regulators resemble barrages in construction; but whereas a barrage controls the flow in the main river, a regulator serves to regulate the flow in an artificial canal.

Fixed weirs have no movable elements by which the water-levels may be adjusted independently of the discharge. In consequence there is usually an unvarying relationship between head and discharge which enables the weir to serve as an effective measuring device.

The main principles governing flow through or over all such control works have been explained in §§ 42-59. Other hydraulic considerations that may enter into their design are: (i) When the structure is founded on a sandy river bed, the rate of percolation beneath the foundations (§§ 96, 97, 201) must be kept within proper limits; (ii) to protect the structure itself, or the adjacent river bed, from the erosive action of the high-velocity streams issuing from the openings, it may be necessary to provide baffle-walls, stilling-basins or similar elements for dissipating the energy of the streams, § 201; (iii) the danger of cavitation erosion (§ 134) on the walls of the internal passages must never be overlooked; (iv) the static thrusts on the structure may be computed as in § 22.

188. Afflux Produced by Clear Overfall Weirs. The relation between the head h over a weir with a horizontal crest of breadth b, and the total discharge Q or the discharge q_s per unit breadth of crest, can always be put in the form

$$Q = C_W b h^{\frac{3}{2}} \quad \text{or} \quad q_s = C_W h^{\frac{3}{2}} \quad . \quad . \quad (10\text{-}2)$$

(§ 55 *et seq.*). To illustrate the way in which the coefficient C_W is influenced by the shape of the weir cross-section and by the operating head h, the diagrams (Figs. 175 and 176) are

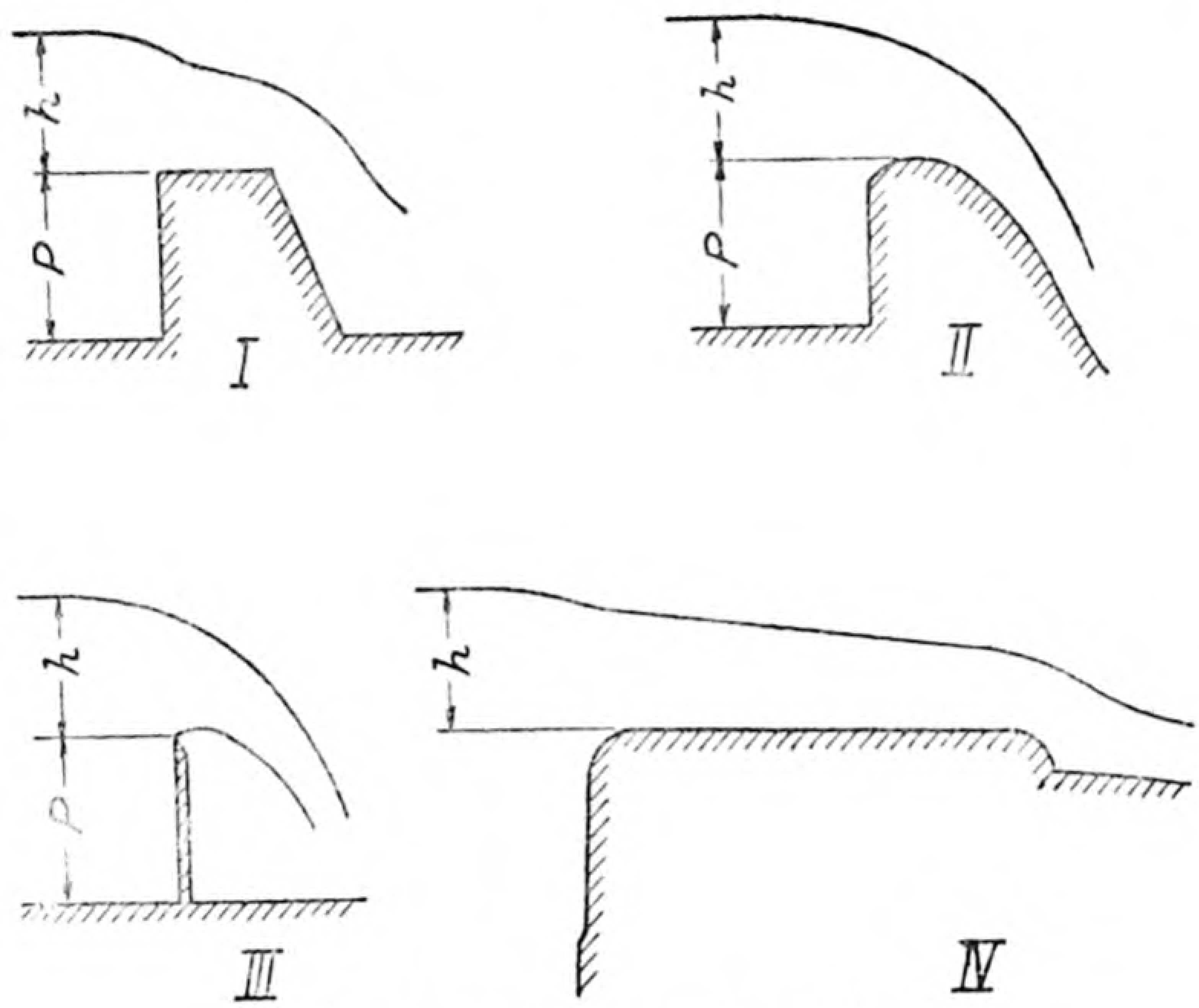

FIG. 175.—Clear overfall weirs.

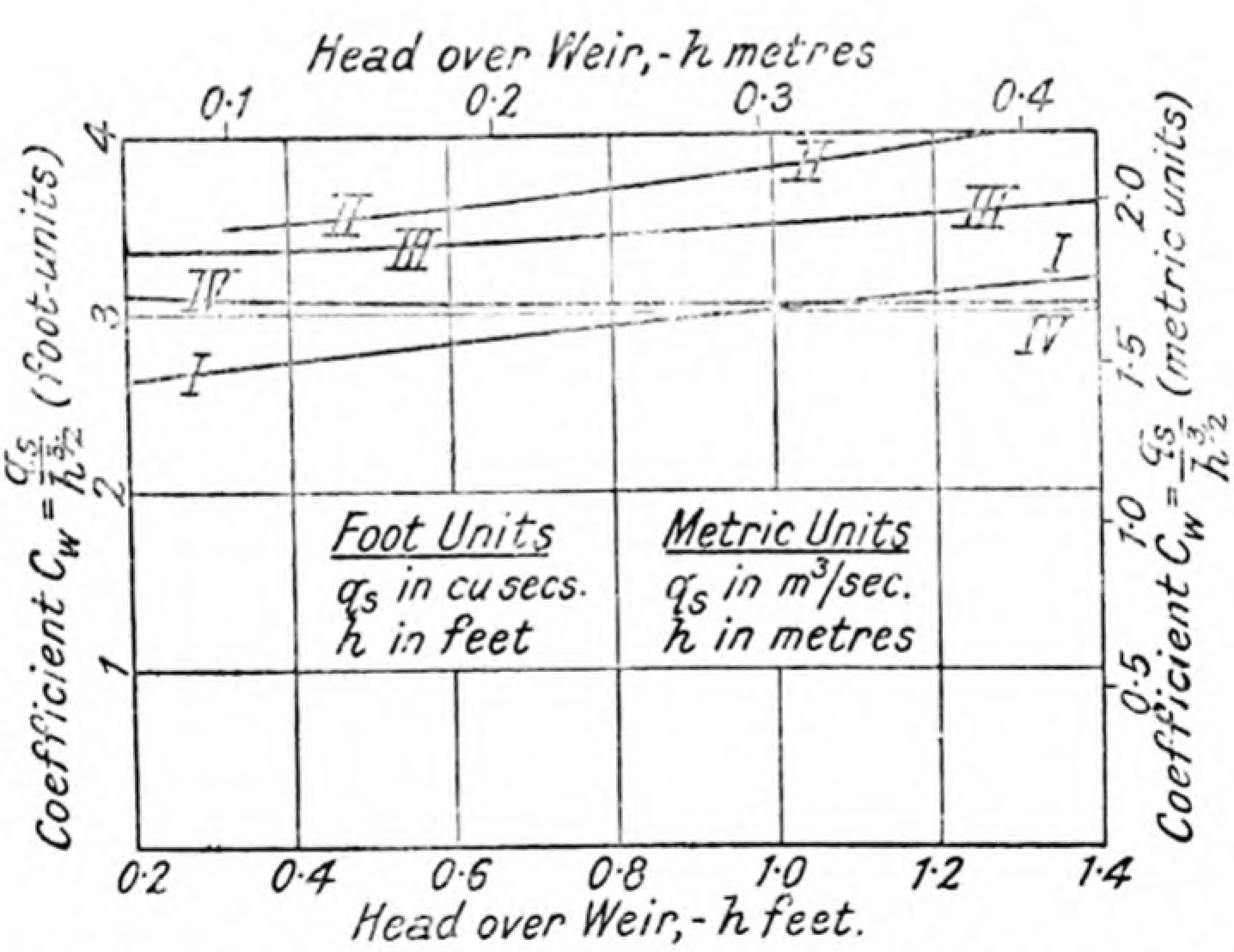

FIG. 176.—Characteristics of clear overfall weirs (height $P = 1{\cdot}64$ ft.).

submitted. Here the masonry weirs I and II are compared with a sharp-edged weir III and a wide-crested weir IV; all of them are shown discharging under a head h of 1·40 ft. (0·43 m.), and the first three have a common height P above the stream bed of 1·64 ft. (0·5 m.).

In Fig. 176 are plotted values of C_W adapted for q_s expressed both in cusecs per foot run of crest and in cu. m./sec. per metre run of crest. For each of the weirs I, II, and III, the coefficient C_W is observed to increase as the head h increases. For a given head the " ogee " weir II consistently gives the greatest discharge,(106) next in order comes the sharp-edged weir III, and lastly, with the lowest discharge of all, the type I weir.

Unless, then, a weir is of a simple, standardised form, it is difficult to make a reliable forecast concerning its coefficient ; on the other hand, weirs of types I, II, and III are very well adapted to treatment by the principle of geometrical similarity (§ 51). The coefficients relating to model weirs may lie within 1 per cent. or 2 per cent. of the coefficients relating to full-scale weirs, or in other words the *scale effect* is relatively small (§ 95). Thus the values of C_W given in Fig. 176 would be applicable with a fair degree of accuracy to any geometrically similar weirs in which the same ratio of $\frac{\text{head}}{\text{depth}}$ was maintained. **(Example 99.)**

It should be noted that since in a clear overfall weir the height of weir P is always greater than the downstream water depth d_d, the afflux produced in a uniform channel is: head over weir + height of weir − downstream depth = $h + P - d_d$.

189. Afflux Produced by Submerged Weirs.(107) There are various ways of assessing the effect of submerging or drowning a weir (§ 59). In Fig. 177 comparisons are made between the weirs I and III referred to in the preceding paragraph, and a weir V having sloping upstream and downstream faces ; they are all shown operating under a head of 1·40 ft., and they have a height P of 1·64 ft. as before. The basis of comparison is this : Suppose the upstream head h_u is to be maintained constant, what depth of submergence h_d can be allowed, or by how much may the downstream level rise above the weir crest, without reducing the discharge over the weir by more than 5 per cent. ? The figure shows that for the sharp-edged weir III, the submergence to fulfil this condition is $h_d = 0{\cdot}35\ h_u$; for the type I weir, $h_d = 0{\cdot}60\ h_u$; and for the type V weir, $h_d = 0{\cdot}90\ h_u$.

Alternatively the *affluxes* may be compared; thus for weir III, the afflux $h_L = 0{\cdot}65\ h_u$, for weir I, $h_L = 0{\cdot}40\ h_u$, and for weir V, $h_L = 0{\cdot}10\ h_u$.

Still a third method of comparison is to record the change in upstream head h_u produced by various depths of submergence h_d, with a *constant* discharge passing over the weir—say the discharge corresponding to the clear overfall head

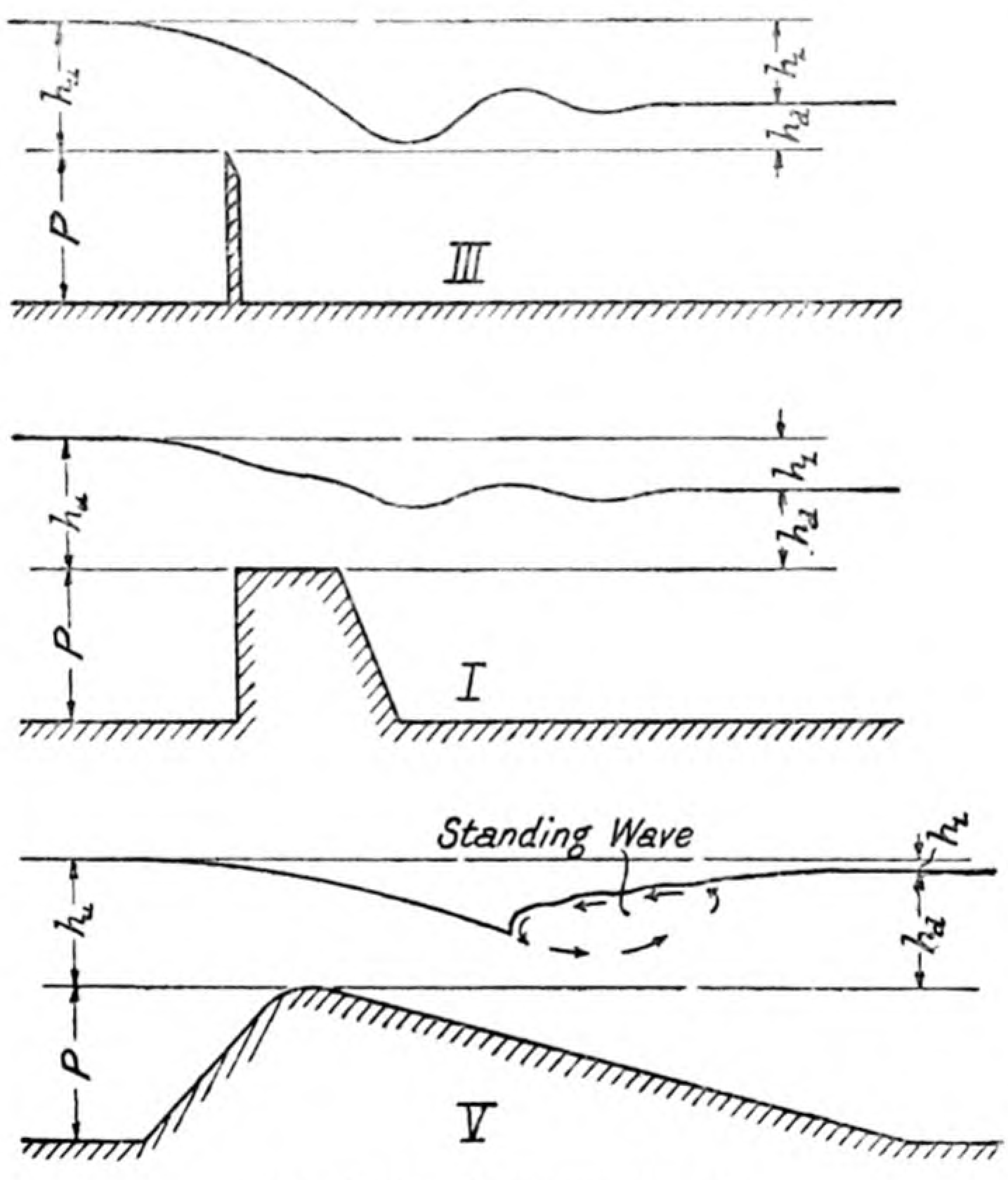

FIG. 177.—Submerged weirs.

$h = 1{\cdot}40$ ft. (Fig. 175). The resulting correlation between h_u and h_d is of the form shown in Fig. 178. As would be expected from what has already been said, the sharp-edged weir III shows itself by far the most sensitive of any to drowning; a 20 per cent. submergence suffices to affect the upstream level appreciably, and by the time the downstream level has risen to the original or clear overfall upstream level, the upstream depth has risen by 30 per cent. With the type I weir the upstream level is hardly affected until the submergence is 40 per cent. or so, while for the type V weir the corresponding figure is 70 per cent. **(Example 100.)**

The reason why the type V weir is so insensitive to submergence is that the downstream slope permits a standing wave to be formed, with the result that the water surface rises noticeably from its lowest point near the weir crest to the point at which the depth of submergence h_d is measured. The weir is therefore called a *standing wave* weir; the characteristic flat eddy or "roller" indicated by the arrows in Fig. 177 (V) is of just the same nature as is described in § 108.

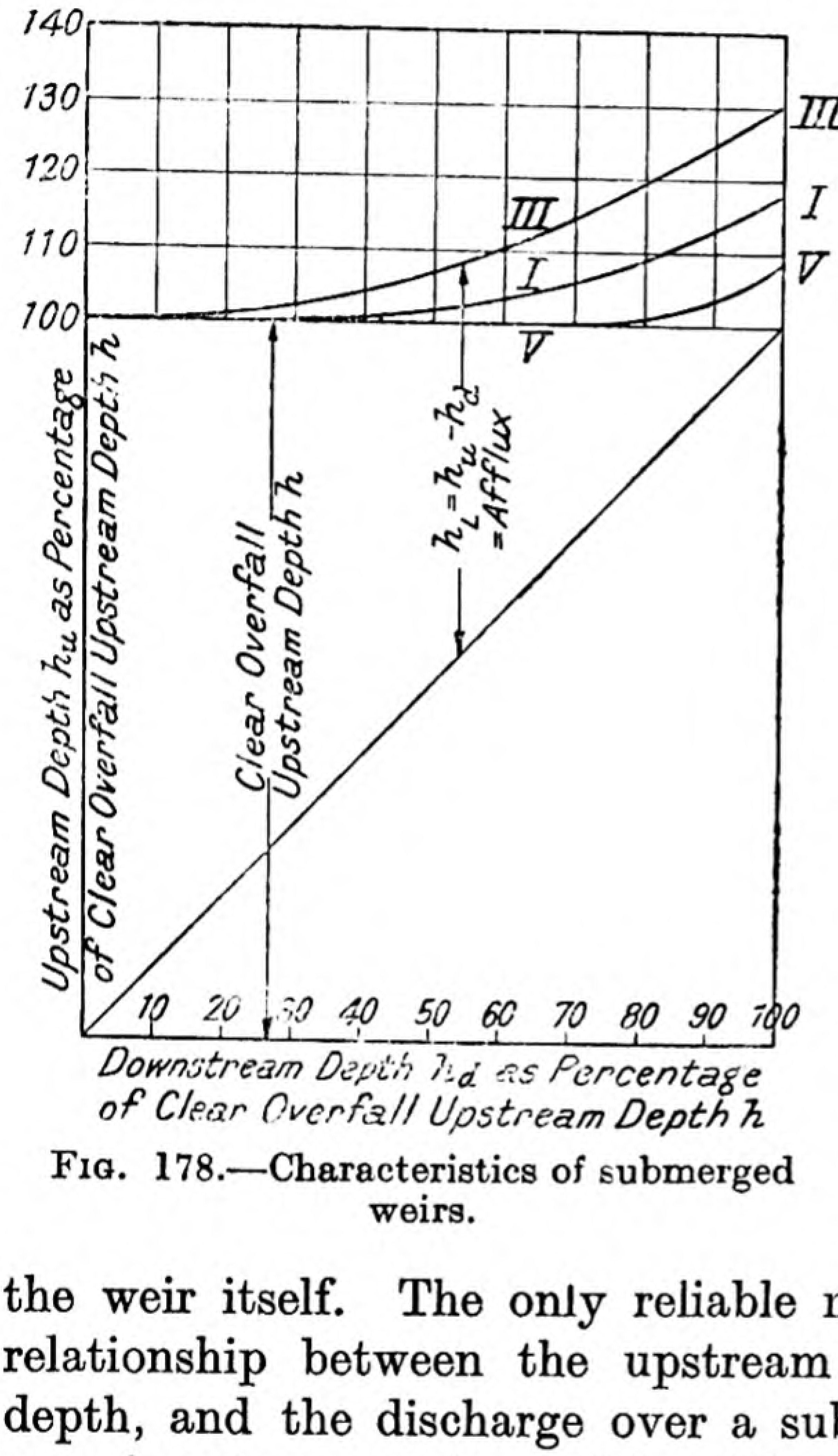

FIG. 178.—Characteristics of submerged weirs.

Although equations can be found to express approximately the shape of the curves (Fig. 178), it is to be remembered that these may be greatly influenced by the shape and width of the downstream or outlet channel, relative to the width of the weir itself. The only reliable means of establishing the relationship between the upstream depth, the downstream depth, and the discharge over a submerged weir is to make experiments on scale models. The close agreement between the results obtained from a full-size weir and the results from a model to a scale of 1 : 13·9 is shown in Fig. 179; this weir is of type I (Figs. 175 and 177).

It is to be noted that the whole of the energy represented by the afflux h_L is dissipated in turbulence: this is made manifest by the violently disturbed and undulating appearance of the water surface downstream of the weir, as suggested symbolically in Fig. 177. Consequently the downstream depth h_d must be measured at a point in the downstream channel where these disturbances have subsided and where regular channel flow has been re-established.

Automatic weirs and *siphon spillways* are described in Chapter XI.

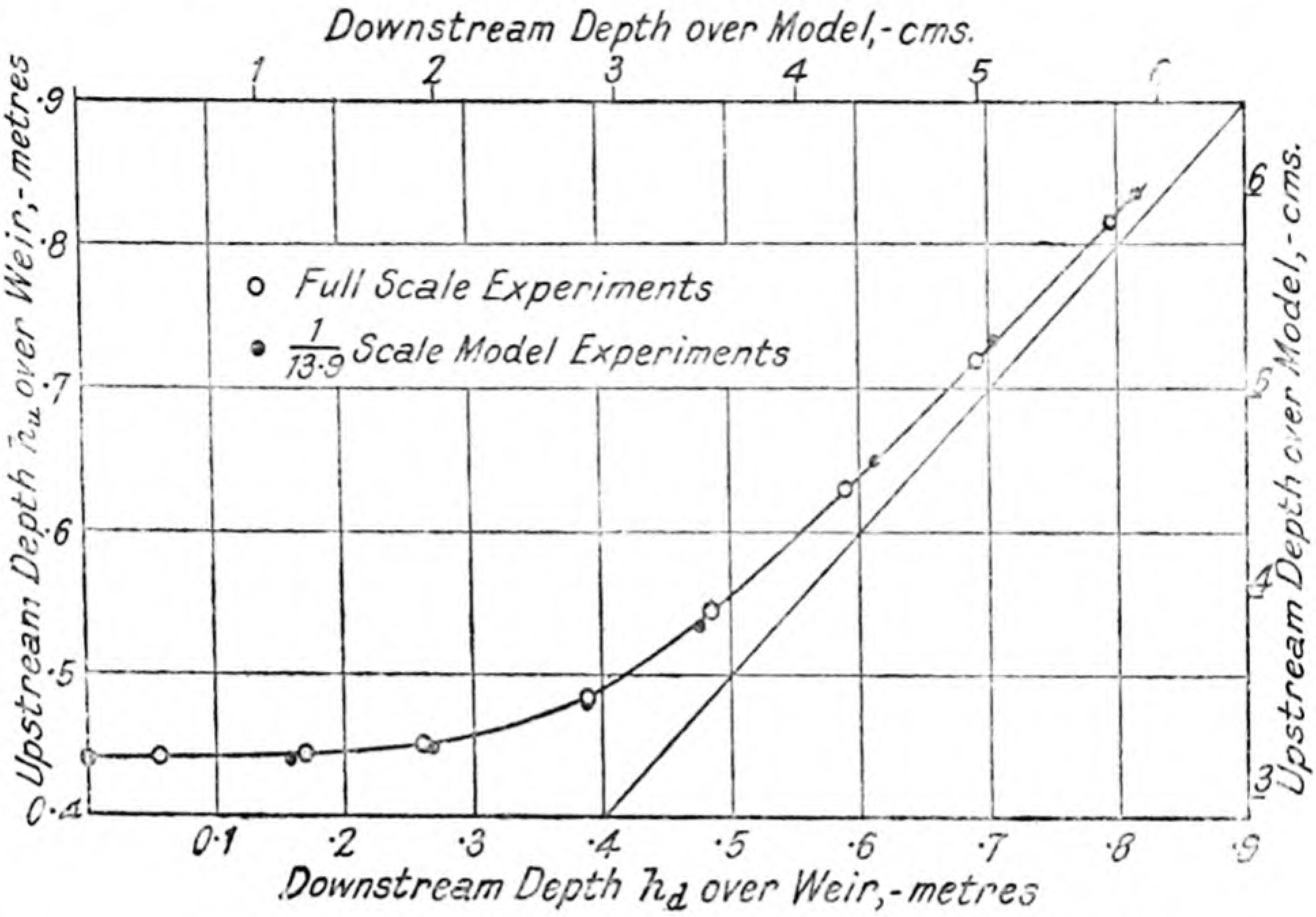

FIG. 179.—Comparison between model and full-size weirs.

190. Circular Bell-mouth Spillways. The weirs whose performance has just been described all have straight crests when viewed in plan. But even if the crest is curved, the laws of flow still hold good provided the curvature is not too sharp in relation to the head. An example of a weir with a completely

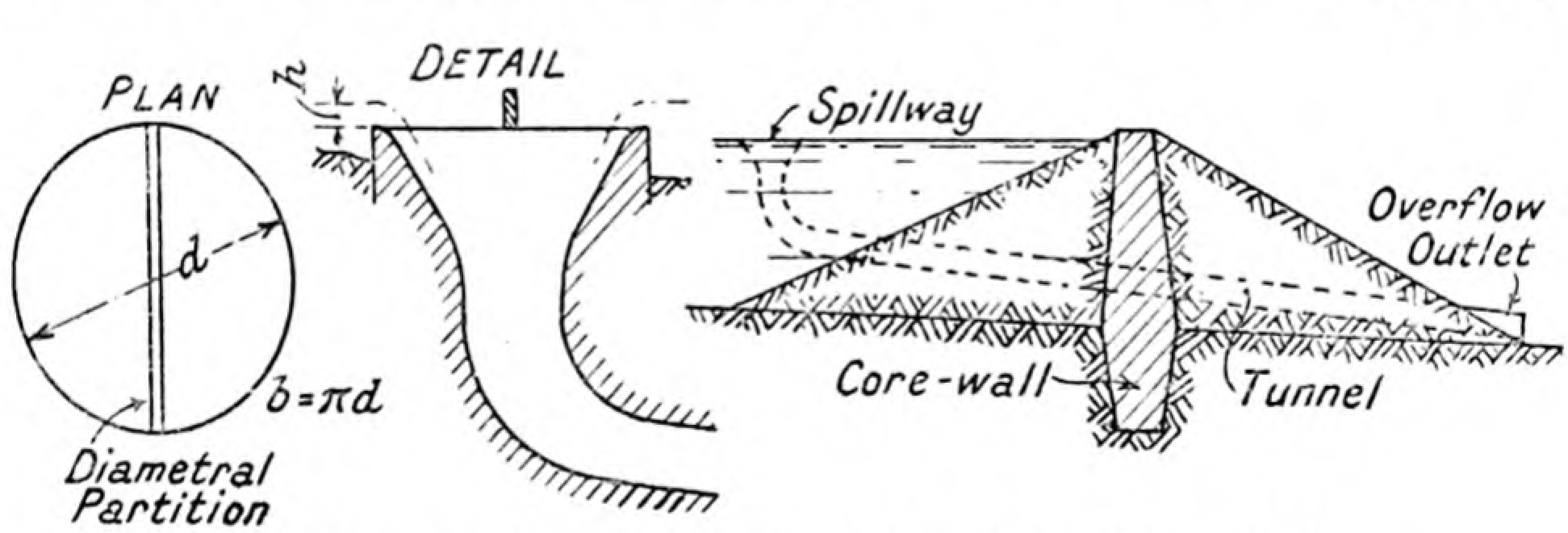

FIG. 180.—Circular spillway in conjunction with earth dam.

circular crest is illustrated in Fig. 180; described as a circular bell-mouth spillway or more colloquially as a "swallow-hole," it serves to carry off flood waters from a reservoir formed by an earthen dam. The dam itself would quickly be destroyed if water were allowed to flow over its crest. Of the two alternative disposal devices: (i) a special straight spillway section such as shown in Fig. 214 (I), formed at the side of the dam,

(ii) a bell-mouth spillway built upstream of the dam, communicating by a tunnel with the downstream river bed; it may be found that the bell-mouth spillway is considerably less expensive.[108]

For the shape indicated in Fig. 180, a value of C_w in formula 10-2, § 188, of about 2·9–3·0 may be expected so long as the head does not exceed 1/10 of the diameter. Naturally it is the circumference of the spillway which is taken as the breadth b of the weir. The performance under relatively higher heads depends a good deal upon the measures that are taken to prevent the formation of large vortices which entrain great quantities of air.[109] Radial walls or partitions are found serviceable for this purpose.

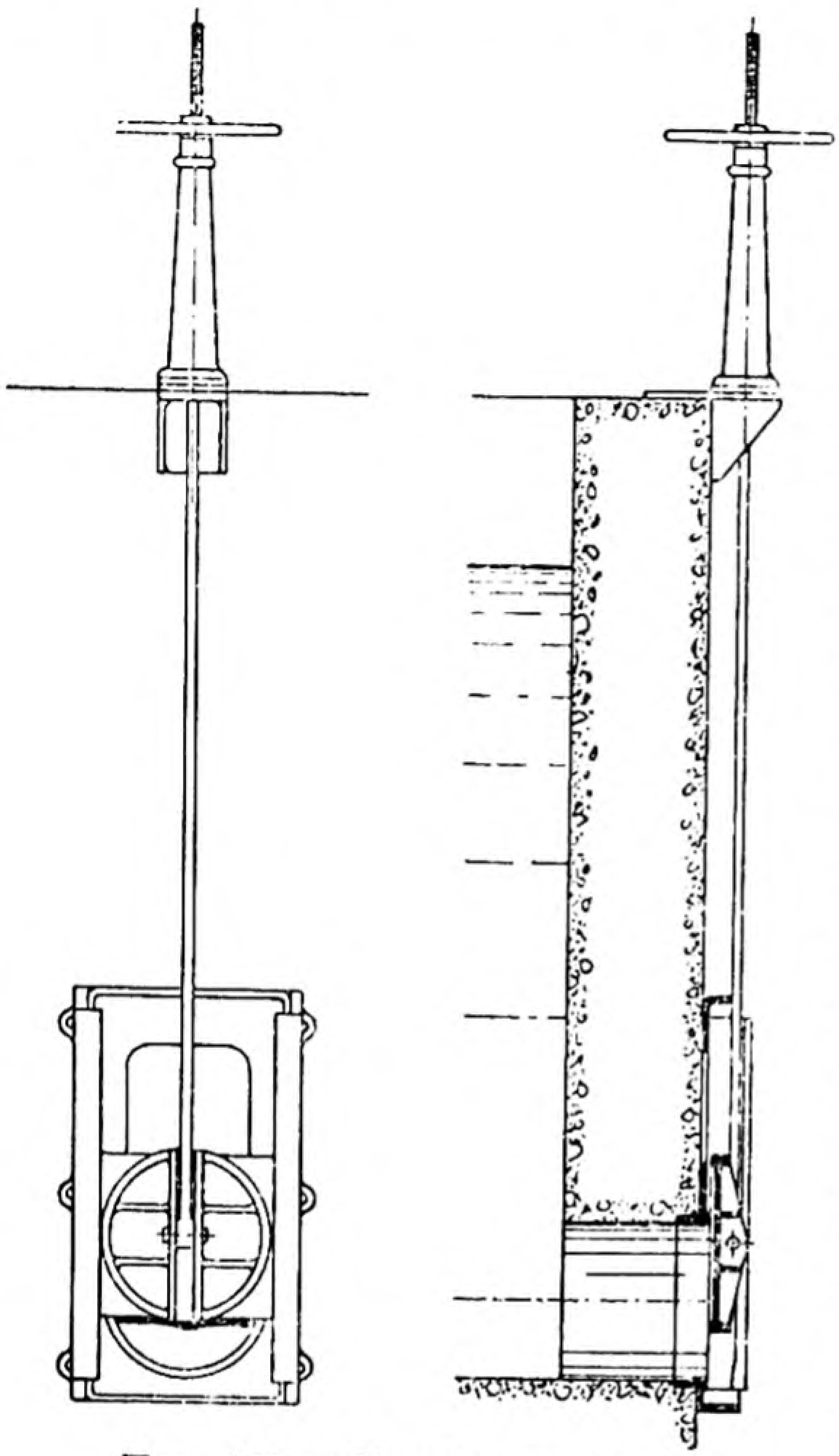

FIG. 181.—Circular penstock.

A small adjustable cylindrical spillway is shown in Fig. 212, § 212.

191. Flow Through Sluices, Regulators, etc. Single sluice gates used for the outlets of small reservoirs and the like are called (in England) penstocks; an example of a circular penstock is illustrated in Fig. 181. Barrages and canal regulators have a number of gates, usually sliding in grooves, as shown in Fig. 182; the regulator here has three openings or *vents*. By adjusting the positions of the gates, the afflux created by the regulator may be varied as desired. The construction of the gates is illustrated in Fig. 10 (iii), § 22.

The flow may be directed (*a*) between the lower gates and the floor, (*b*) between the lower gates and the upper gates, or (*c*) over the upper gates, which then act as weirs with movable crests.

192. Flow beneath Gates. (*a*) Assuming a constant discharge to be flowing down the channel, the flow *beneath* the gates may take the various forms shown in Fig. 183. If a single vent only is in operation and the water emerges into a

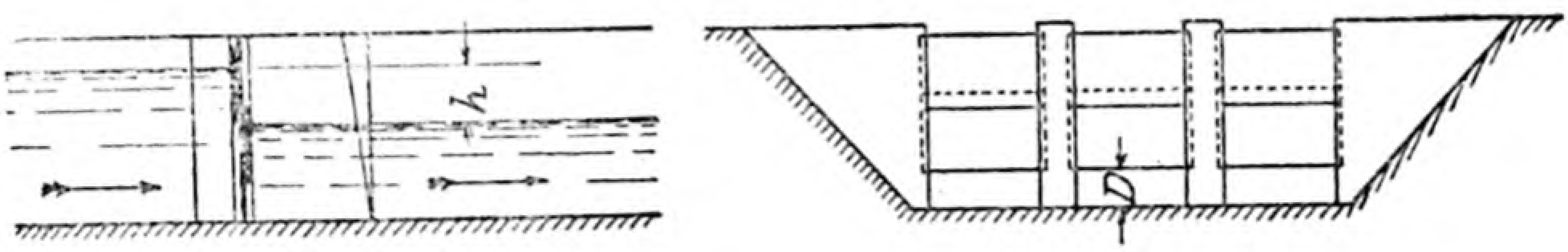

Fig. 182.—Canal regulator.

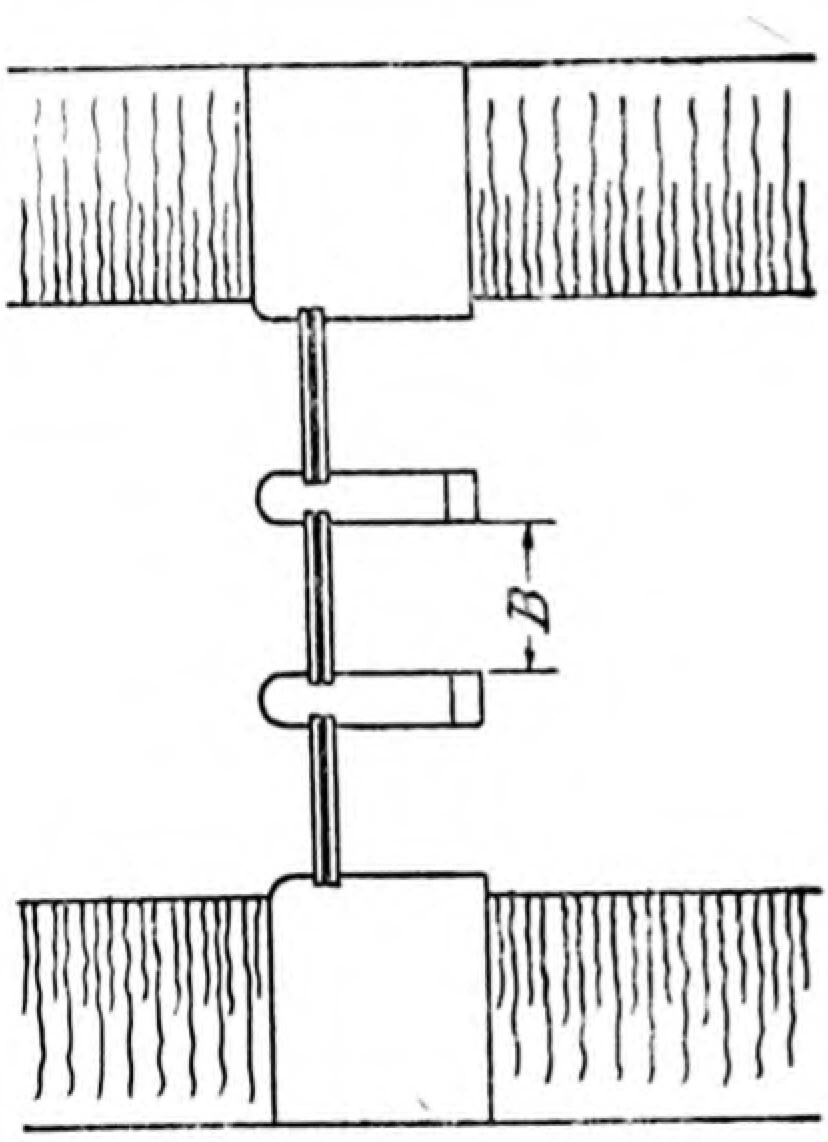

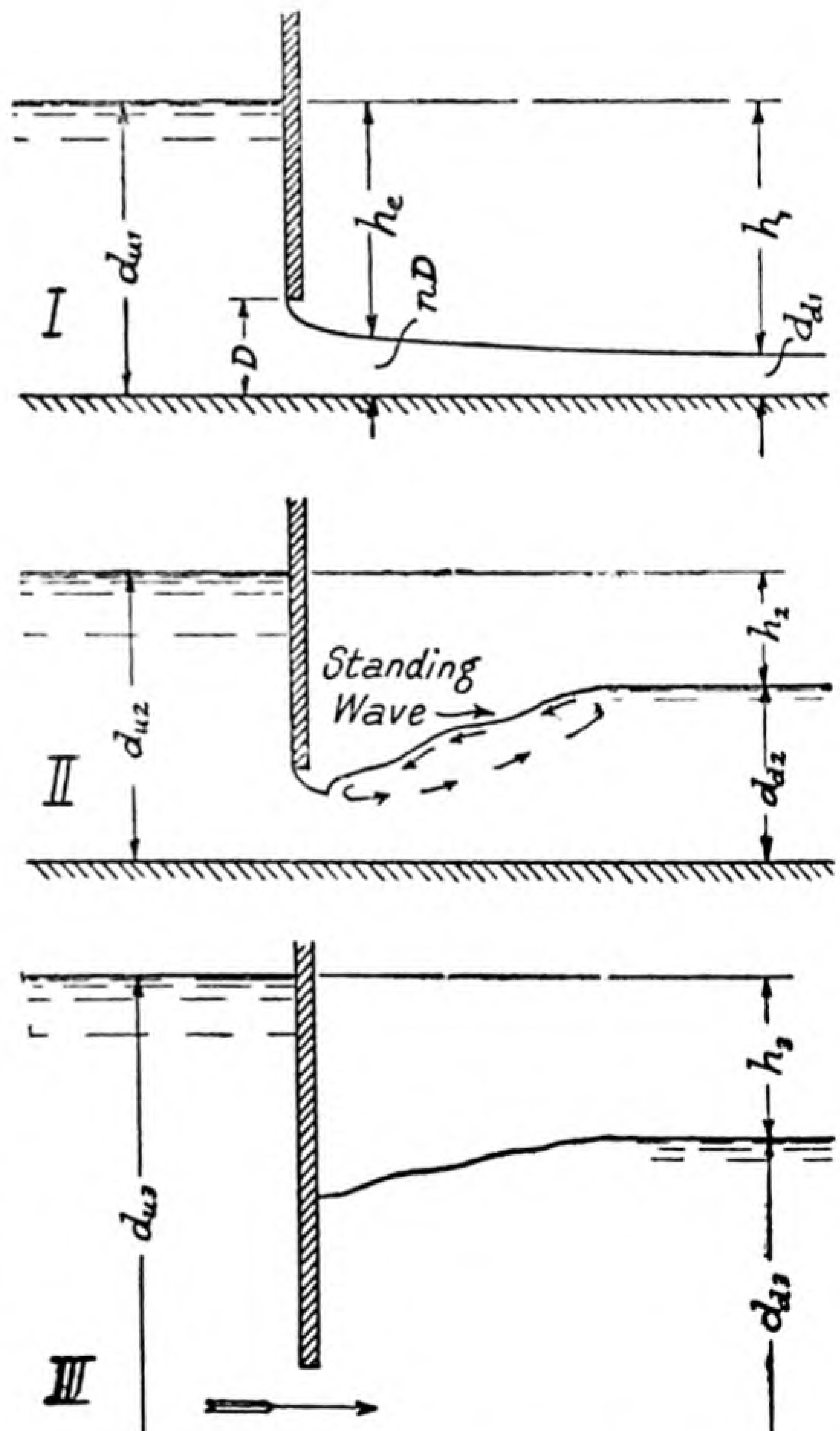

Fig. 183.—Flow beneath sluice gates.

wide, unobstructed channel as at I, the downstream depth d_{d1} may be quite small—much below the critical depth d_c—and the afflux h_1 will be considerable.(110)

If, now, because of some alteration further downstream, the downstream level begins to rise, a standing wave will be formed (§ 108), and will "walk" upstream until eventually it approaches the back of the gates, II, the downstream depth by that time having risen to d_{d2}, and the afflux having fallen to its minimum value h_2. In the meantime the upstream

depth d_{u2} has remained *unchanged.* The photograph reproduced in Fig. 184 gives an impression of the appearance of the standing wave; here the water is seen issuing from the vents, each 15 cms. wide, of a scale model regulator.

Further raising of the downstream depth to d_{d3} causes the standing wave to break down, the upstream level to rise to d_{u3}, and the afflux to increase to h_3 (Fig. 183 (III)).

These changes in the afflux h can be expressed in terms of the coefficient of discharge C_d of the sluice openings, which are here regarded as submerged orifices. If q = discharge per sluice, D = height of sluice opening, and b = width of sluice opening, then from § 45,

$$q = C_d D b \sqrt{2gh}. \quad \text{(10-3)}$$

(Example 101.)

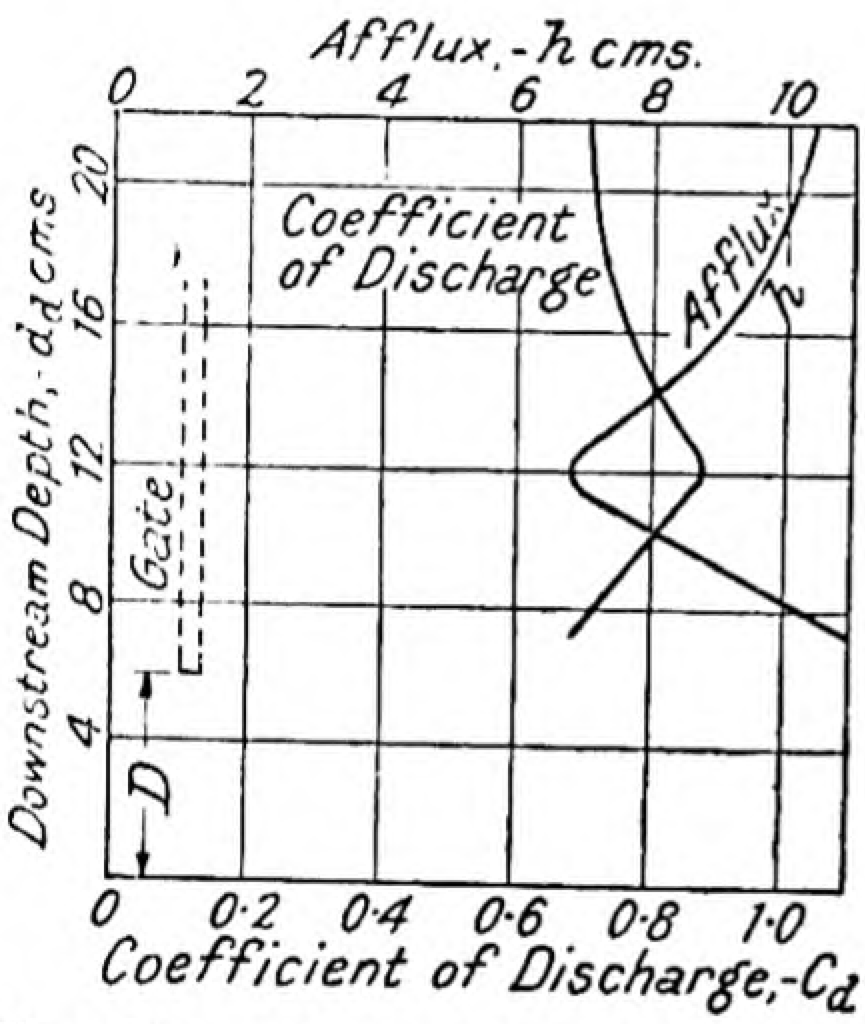

FIG. 185.—Characteristics of flow beneath model sluice gates. (q per vent = 12·4 lit./sec.).

If, for a given setting of the gate opening D, values of C_d and of h are plotted against the downstream depth d_d, then curves of the type seen in Fig. 185 will result. (These particular graphs relate to a model in which q = 12·4 lit./sec., b = 20·0 cms., D = 6·07 cms.) Characteristic features of the curves are the cusps or abrupt changes of curvature which correspond to minimum and maximum values respectively of the afflux and of the coefficient of discharge. It will be realised that these signify the breakdown of the standing wave represented in Fig. 183 (II). The observed value of d_d corresponding with the maximum height of the standing wave and with the maximum value of C_d agrees tolerably well with the height of standing wave calculated from formula 7-10 (§ 137). As the exact value of C_d for any downstream depth and rate of discharge depends so largely on the shape of the gates, piers, and downstream channel, no simple equation can be found to express it; but for regulators with flat floors of the type now being discussed,[111] the equation

$$C_d = 0{\cdot}63 + 0{\cdot}72\left(\frac{D}{d_d}\right)^2$$

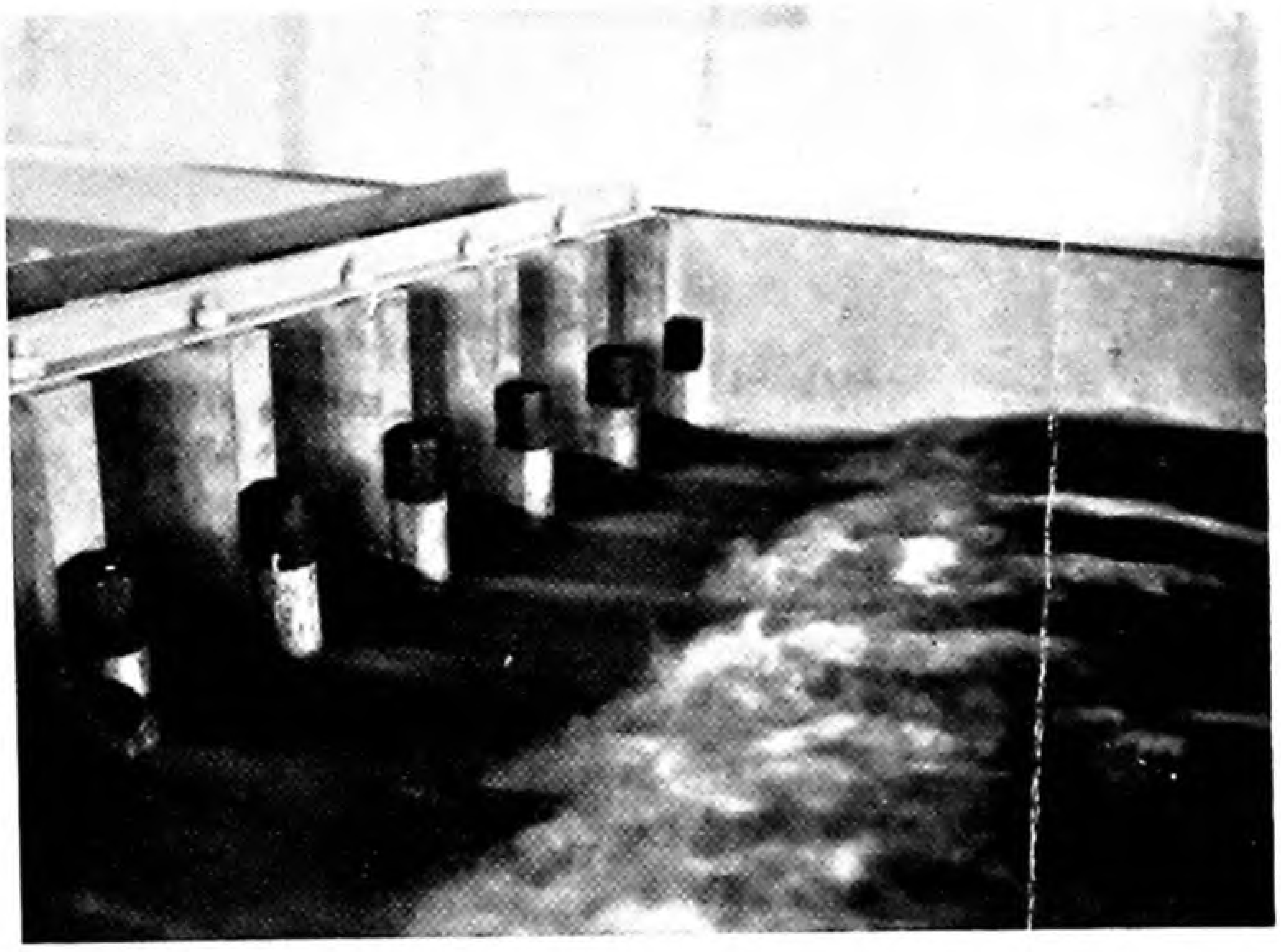

FIG. 184.—Standing wave downstream of a scale model regulator.

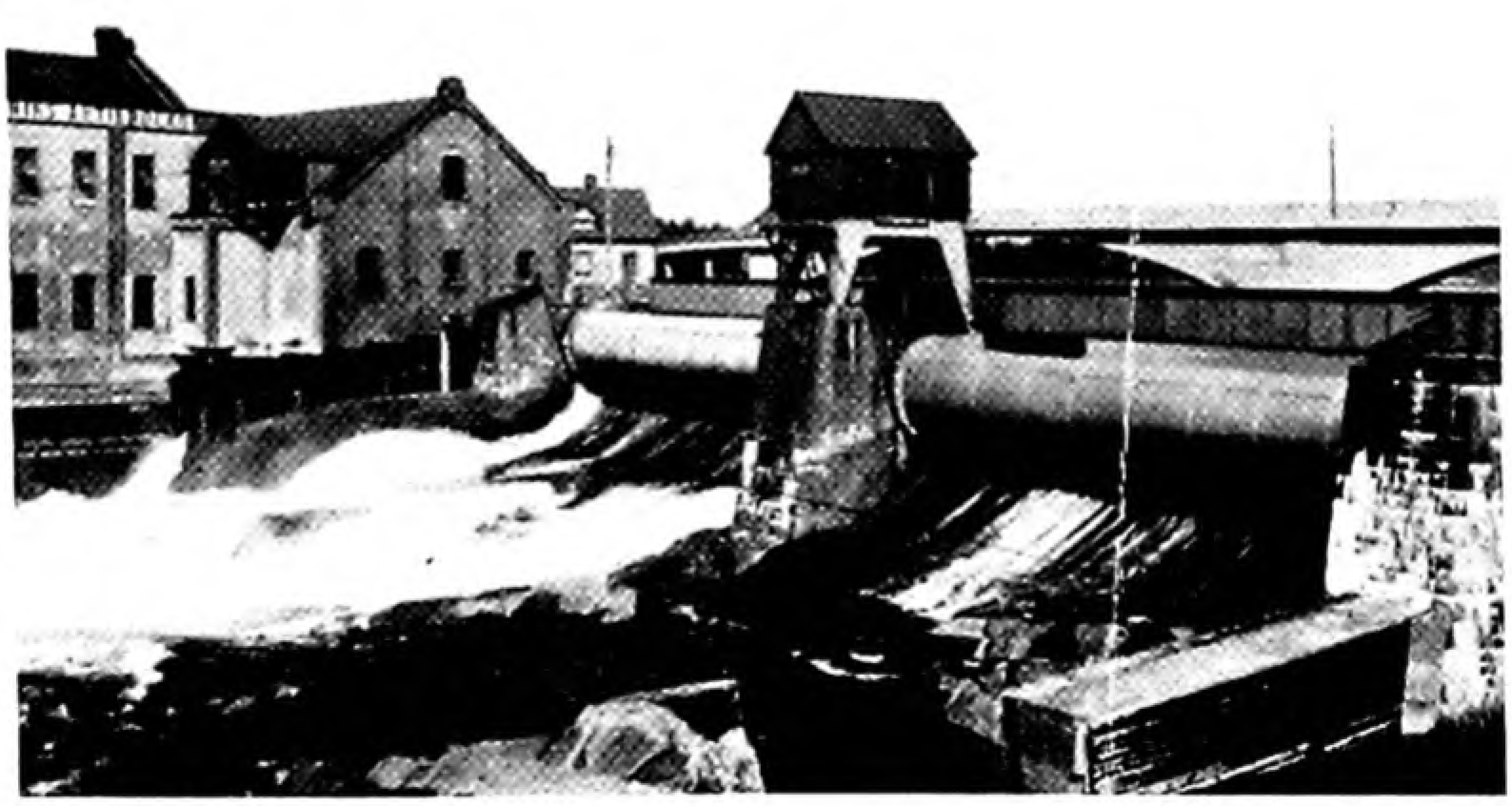

FIG. 191.—Roller gate barrage.
(See page 282.)

[*To face page* 276

gives values correct to within a few per cent. These values naturally relate to the usual operating conditions in which the downstream depth is above the point of inflection of the graphs in Fig. 185, i.e. to the conditions indicated in Fig. 183 (III).

193. Coefficients for Sluice Openings. (*b*) If the flow is directed *between* the lower and upper gates of a regulator, the variation in C_d is much less than when the flow passes beneath the lower gates. This is made clear in Fig. 186. The continuous curve I relates to flow *beneath* the gates of a model; the broken curve II to flow *between* a lower gate 6·90 cms. high and an upper gate; and the dot and dash curve III to flow between a lower gate 14·2 cms. high and an upper gate. The gate opening D is 9·00 cms., and the width of the vents 20·0 cms., in each case. When the height of the lower gate d_g was 0·345 × the width of the vents, curve II, it was found that C_d could be expressed fairly accurately by the equation

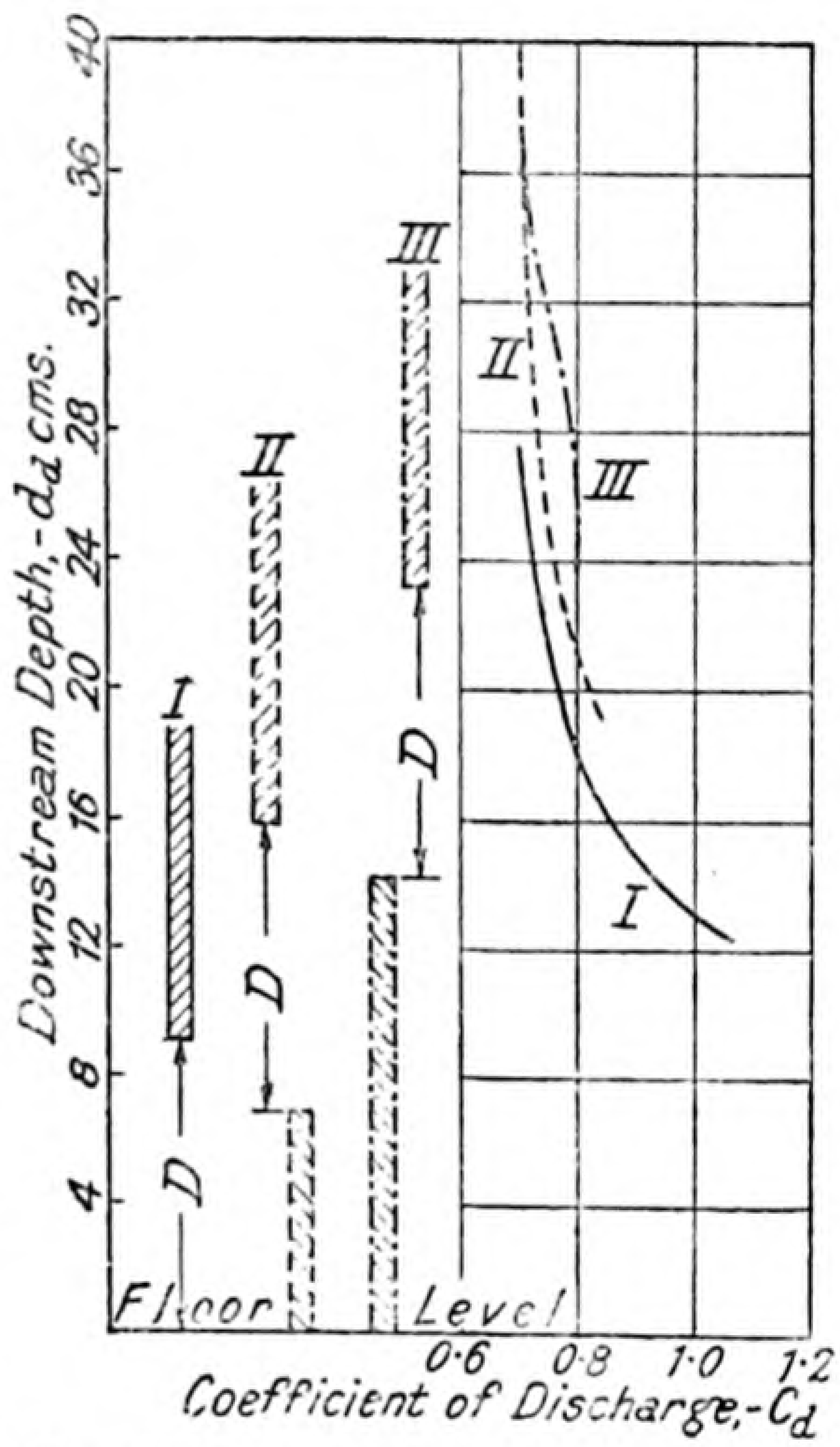

FIG. 186.—Model sluice coefficients.

$$C_d = 0{\cdot}685 + 0{\cdot}296\left(\frac{D}{d_d - d_g}\right)^2.$$

From the shape of the graphs in Figs. 185 and 186 it seems likely that with great depths of water the coefficient C_d would settle down to steady values, independent of the downstream depth d_d, the conditions then corresponding to those assumed in § 45, where the *whole* of the energy of the jet issuing through a small orifice is dissipated in eddies.

(*c*) The discharge or the afflux when the water flows *over the tops* of the gates under weir conditions may be calculated from formula 4-5 (§ 55), taking the value of C_d as 0·63 to 0·66; or Fig. 176 (III) or Fig. 178 (III) may be used. In the absence of special calibrations, great accuracy can hardly

be hoped for, but on the other hand it is rarely required, as the adjustment of the gates themselves gives the necessary control over q or h.

194. Coefficient of Discharge of Sluice Openings (*continued*). It is instructive now to treat the problem in another way: to assume that the *downstream level* instead of the discharge is kept constant, and by varying the discharge to study the correlation between upstream level and discharge. The conditions shown in Fig. 183 (I) will first be dealt with, the downstream depth being always kept *below* the value at which it could have any effect on the upstream depth. If a be the area of sluice opening, then the values of $\left(\frac{q}{a}\right)^2$ plotted against d_u are found to lie on a straight line (Fig. 187);

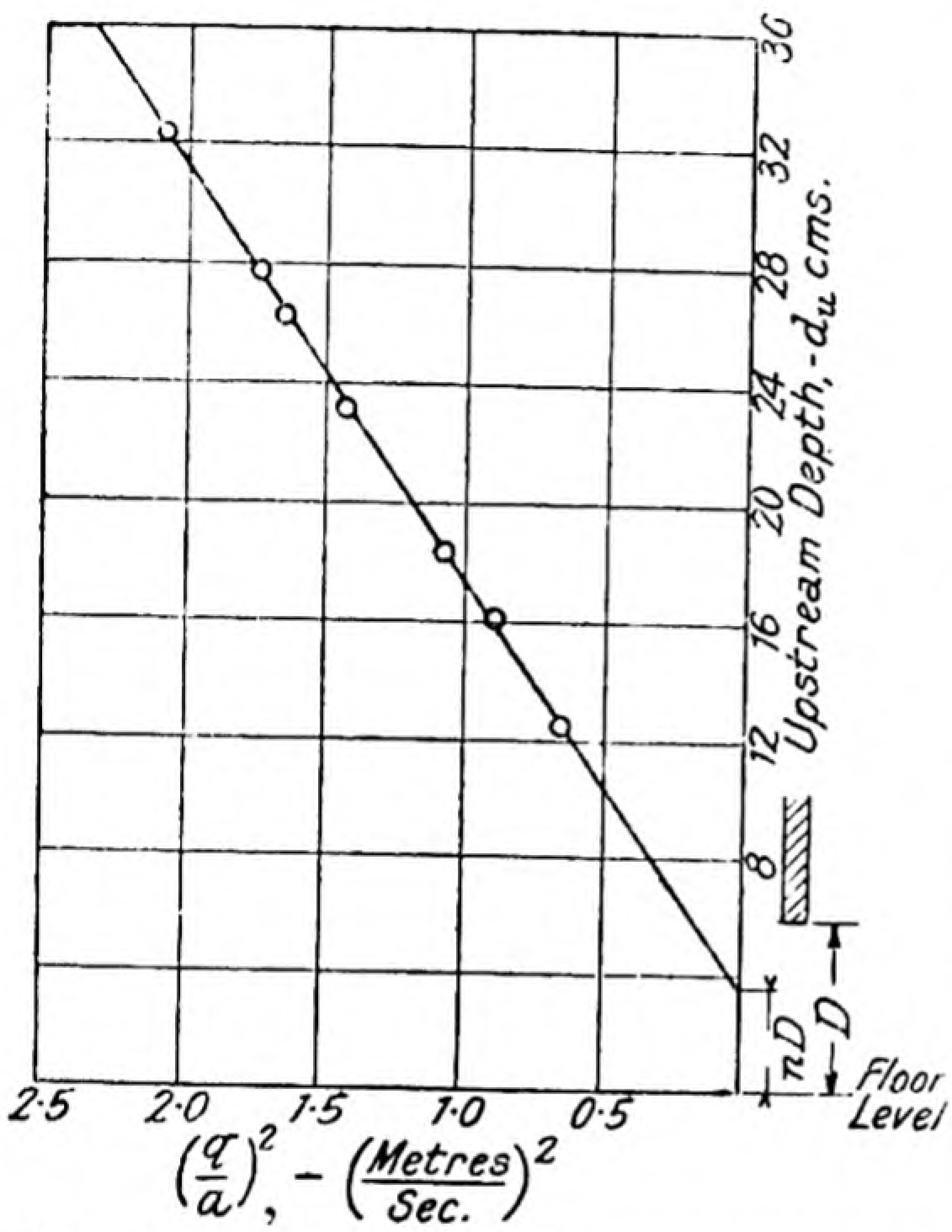

FIG. 187.—Correlation between upstream depth and discharge through a model sluice.

this line satisfies the equation

$$q = C_d a\sqrt{2g(d_u - nD)},$$

where the coefficient of discharge C_d and the ratio n are *constant* for a given gate opening. In a model having two openings 20 cms. wide and 6·0 cms. high, C_d was found to have the value 0·605, and n the value 0·600; but it can be shown by analytical reasoning that under ideal conditions both C_d and n have the value $\frac{\pi}{\pi + 2} = 0{\cdot}612$.

It is to be noted that this straight-line law is only applicable to sluices having a supported jet, i.e. to sluice openings in which the water passes between a gate and a flat floor (Fig. 183, (I)); in this figure $h_e = (d_u - nD)$ is the effective head producing flow.

To show how the values of C_d and n depend upon the shape of the sluice openings, the results of comprehensive experiments on the sluices of the Assuan Dam (112) may be quoted. These sluices (Fig. 188) are relatively deep and narrow, and the floor is not perfectly flat. Until the gate opening D is about equal to the width b, the coefficient C_d in the above formula does not vary seriously from 0·7, but for bigger openings its value mounts rapidly. The value of n remains steady at about 0·8.

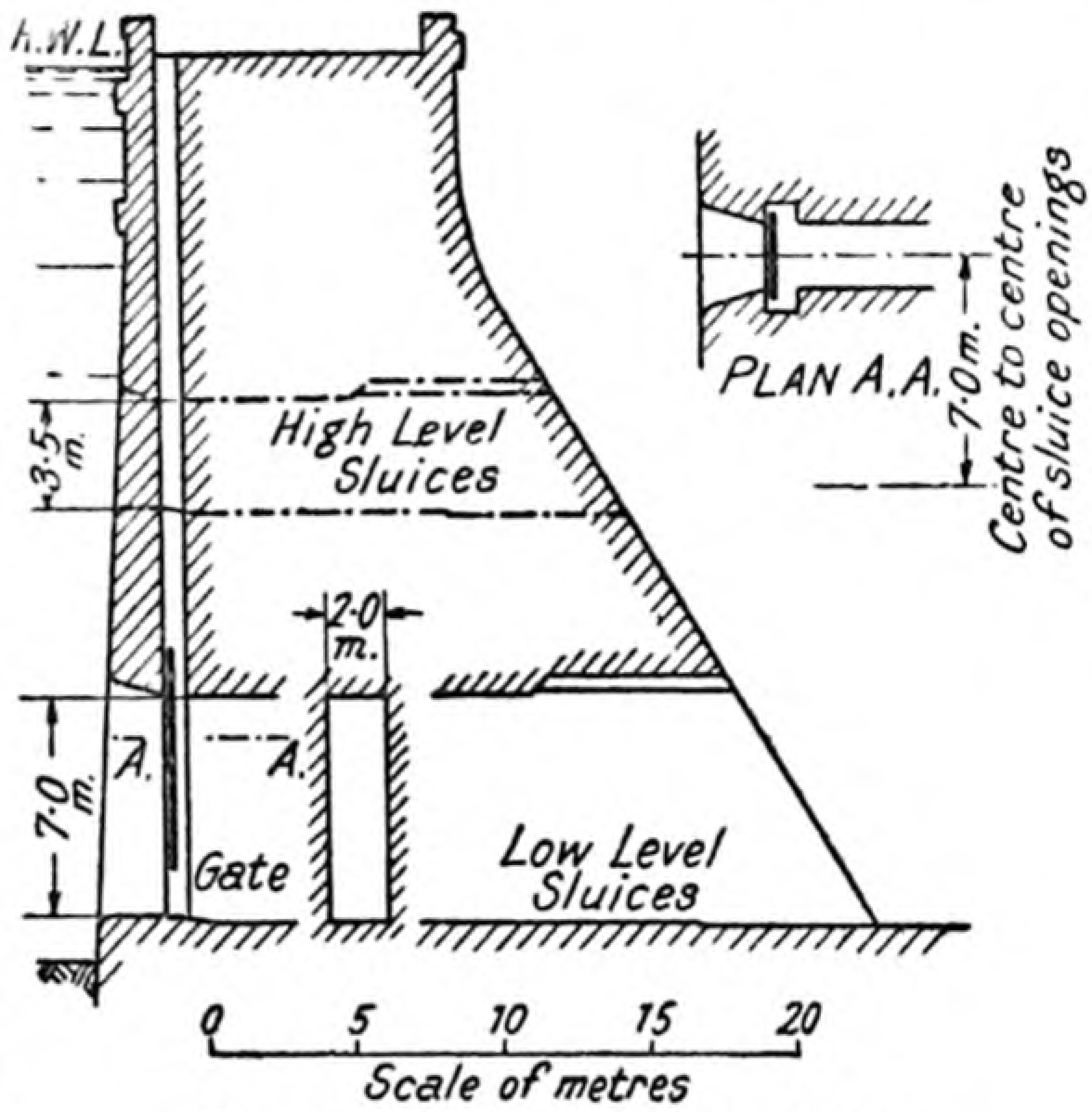

FIG. 188.—Assuan Dam sluices.

If now the downstream depth above the sluice floor, d_d, is increased and maintained at a new steady value, then a modified relationship between $(q/a)^2$ and the upstream depth d_u may be realised. Examples are plotted in Fig. 189. For free flow conditions, with the jet discharging into air, the broken line and its continuation BF form the exact counterpart of the line in Fig. 187. When the opening is submerged to a steady depth of 7·0 cms., the increasing tendency towards the formation of a standing wave in the sluice-way is manifested by the slope of the line AB. At B the process is complete; the standing wave is in operation, and thereafter, as shown by BF,

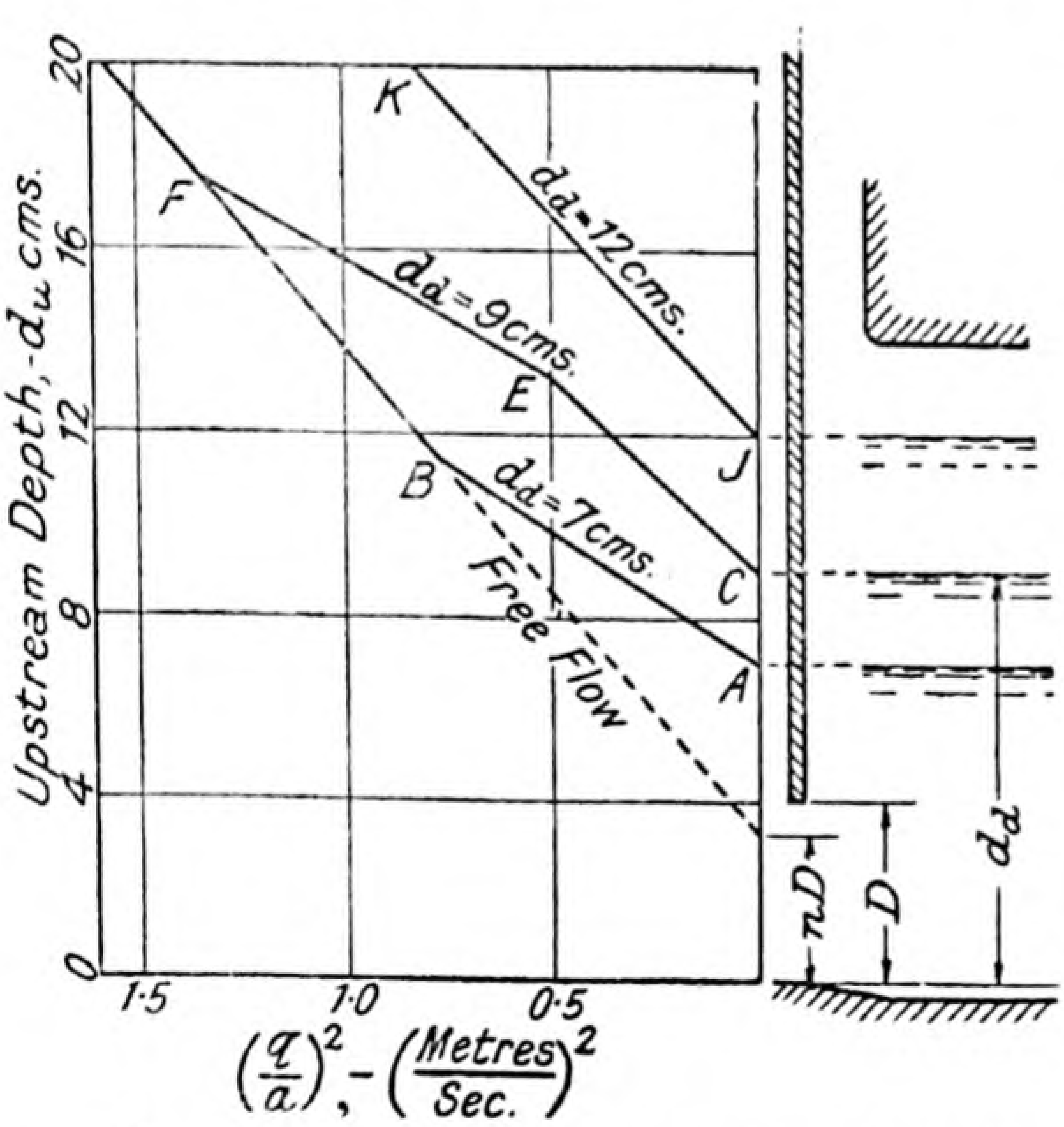

FIG. 189.—Characteristics of flow through model of Assuan Dam sluice, scale 1/50. Width b = 4 cms., opening D = 4 cms.

the sluice behaves precisely as though it were discharging into air. While the upstream depth is rising from B to F the standing wave is being pushed farther and farther down the sluice-way.

Submergence of the sluice to a steady depth d_d of 9·0 cms. naturally necessitates a higher upstream head, as shown at F, to establish the free-flow regime. The first part of the graph CE corresponds to the submerged orifice conditions described in § 45; the part EF represents the transitional stage during which the increasing strength of the jet is drawing down the water at the back of the gate preparatory to the formation at F of the complete standing wave. The line JK shows that with a submergence of 12·0 cms., the flow remains of the submerged orifice type up to the limiting upstream depth—the jet is always "smothered" by the downstream water above it, and is never able to push away this superincumbent water as it has succeeded in doing at B and at F. The discharge is therefore expressed by the equation

$$q = C_d a\sqrt{2g(d_u - d_d)},$$

which is of the same form as formula (10-3).

It will be found that if the information presented in Fig. 189 is put into the form described in § 193, the resulting curve [113] between d_d and C_d will be of much the same shape as the curve plotted in Fig. 185.

195. Rotary Gates. When the width of vertical-lift sluice gates, of the type so far considered, is great, or if the afflux is considerable, then the total horizontal static thrust that must be transmitted to the piers may be great enough to call for the interposition of anti-friction rollers or the like between the gates and the grooves in which they slide, § 22. Alternatively, the sliding type of gate is abandoned and other forms of construction may be used in which the gate has a pivoting or rotary motion.[114] Some of these are shown diagrammatically in Fig. 190.

The *Taintor gate*, (I), has a skin plate curved to a part-cylindrical shape, suitably stiffened, and the whole of the hydraulic thrust is taken by the two pivots or trunnions whose bearings are built into the walls of the piers; thus the moment of the friction when the gate is raised or lowered is very small.

(Example 7.)

The *Sector gate*, (II), in general resembles the Taintor gate, but the water flows over it instead of beneath it; moreover, as a series of pivots instead of two only may be used, the sector gate can be made in greater lengths than the Taintor gate. The *Drum gate*, (III), is formed by completely plating-in the sector gate, so that it becomes a buoyant air-tight chamber which floats on the water admitted to the recess beneath it.

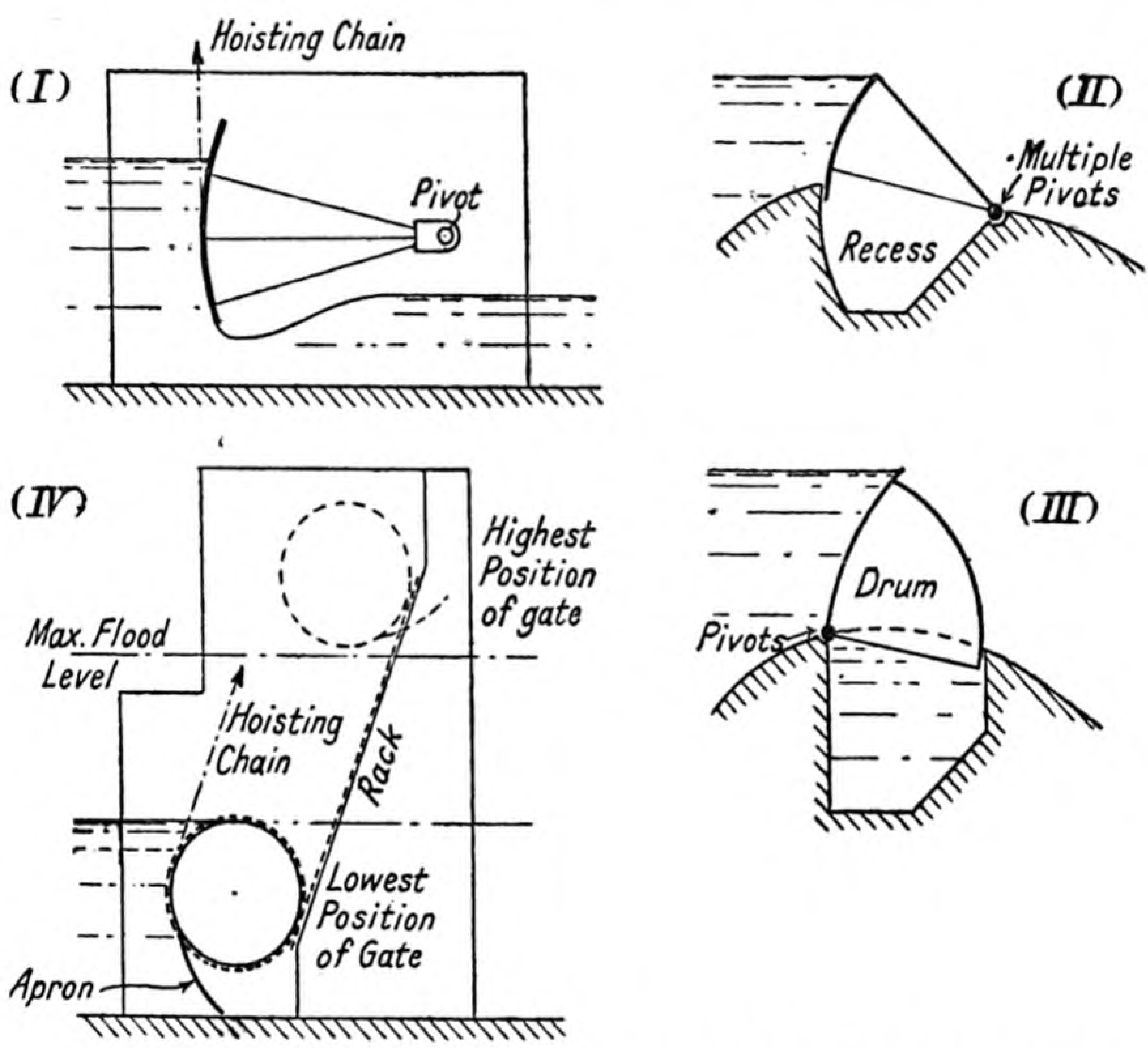

FIG. 190.—(I) Taintor gate; (II) Sector gate; (III) Drum gate; (IV) Roller gate.

No mechanical lifting gear is required, as the crest level of the gate is regulated by adjusting the quantity of water in the recess; since this may, if necessary, be automatically controlled by a system of floats so as to keep a constant water-level upstream of the gate, the gate may serve as a form of automatic weir (§ 213).

The *Roller gate* (Fig. 190 (IV)) has special advantages when the maximum width of uninterrupted waterway is called for, or when the working of the gates is likely to be hampered by ice formation; already examples 140 feet long are in operation. The gate, which is of patented design, consists of a complete water-tight platework cylinder, having spur teeth

formed round each end which engage with the teeth of two racks bolted to inclined ways formed in the sides of the piers. By means of a hoisting chain at one end or at both ends, the gate when necessary can be rolled up the ways clear of the highest flood-water level. When used normally for damming the low-stage river, flow beneath the gate is prevented by a curved apron attached to the drum and forming a seal between it and the floor of the barrage. A photograph of a roller-gate barrage, as viewed from the downstream side, is reproduced in Fig. 191 (facing page 276); the electrical hoisting gear for both gates is housed above the central pier.

Naturally the discharge coefficients [115] to be used in estimating the flow past any of these rotary gates may differ widely from those applicable to vertical-lift gates (§§ 192-194).

196. Afflux Produced by Piers in a Channel. It is convenient to treat the flow between bridge piers, or between the piers of a regulator in which the gates are lifted clear of the water, on the basis of uniform discharge and varying downstream depth. The resulting three stages, I, II, and III (Fig. 192), are then comparable with the stages shown in Fig. 183, or with those relating to a standing wave weir (Fig. 178 (V)). We have first a stage of minimum downstream depth d_{d1}, associated with a minimum upstream depth d_{u1} (Fig. 192 (I)). The change from I to II is marked by an increasing downstream depth, a diminishing afflux, a *stationary* upstream depth, and the formation of a standing wave which advances upstream and finally into the vents. Any further rise in d_d will affect d_u also; the afflux continues to diminish until in the end it has the very small value $(d_{u3} - d_{d3}) = h_3$.

The minimum upstream depth d_{u1} that will permit a discharge per opening q to pass through vents, or openings between the piers, of breadth b, can be calculated by the use of the wide-crested weir formula, 4-6 (§ 58),

$$q = C_d \,.\, 0{\cdot}385 b\sqrt{2g} \,.\, d_u^{\frac{3}{2}}.$$

C_d may have a value of 0·92 or more, depending on the shape of the piers; if the combined area of the openings is considerable in comparison with the area of the approach channel, as it usually is, a velocity of approach correction should be made (§ 56). Whether or not this minimum upstream depth d_{u1} will

be permitted to occur depends on the downstream depth d_{d1}; normally it will only occur if d_{d1} is equal to or less than $0{\cdot}67\ d_{u1}$. It was shown in § 58 that the thickness of the nappe of a wide-crested weir was $\frac{2}{3}$ of the head; or from § 109 it can be seen that the depth in the vents can never fall below the critical depth d_c, which is $\frac{2}{3}d_{u1}$. But if the shape or proportions of the downstream channel permit a recovery of head, as at II (Fig. 192), then d_{d2} may be as much as $0{\cdot}8\ d_{u2}$.

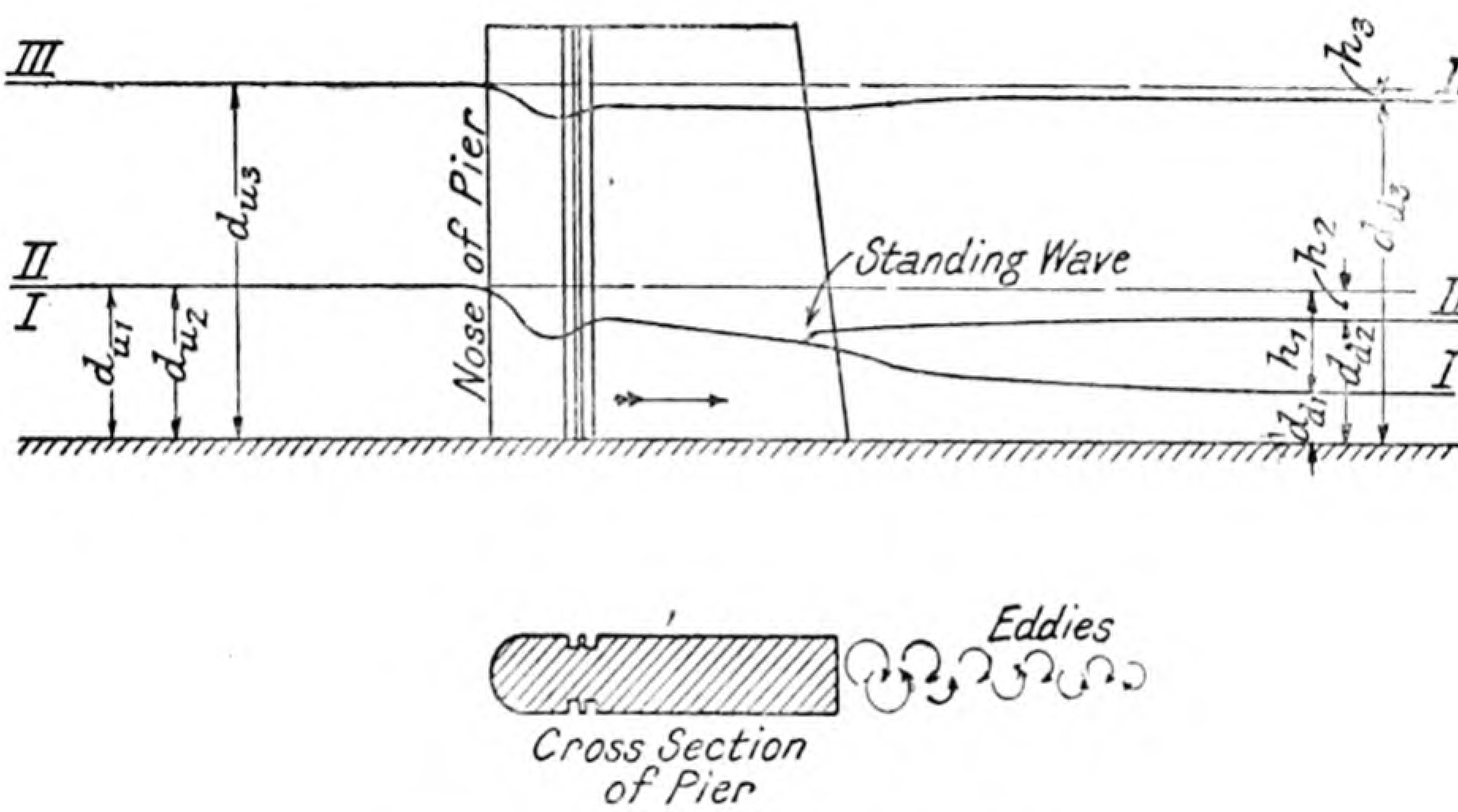

FIG. 192.—Flow between piers.

After the downstream depth has risen beyond d_{d2}, and has therefore begun to influence the upstream depth d_u, it becomes difficult to calculate the afflux until a stage is reached, III, at which the afflux h_3 is quite small compared with d_{d3}. Assuming, then, that the depth of water in the vents or between the piers was d_d, we could equate the drop in surface level h to the gain in velocity energy as the water passed from the upstream channel to the narrowed section between the piers. Alternatively, the section between the piers could be regarded as an orifice of area bd_d operating under a head h. In either case the flow may be expressed by the formula

$$q = C_d'bd_d\sqrt{2g(d_u + h_{vu} - d_d)},$$

where q is the discharge per opening, and h_{vu} is the head of approach or velocity head in the upstream channel.

It is clear from Fig. 192 (III) that actually, on account of the recovery of head in the downstream channel, the true

afflux is less than the head under which the orifice is assumed to be operating. This will manifest itself in the experimental value for C_d', which may be greater than unity. According to the author's experiments on models of openings having a combined area exceeding one half the area of the channel, C_d' has the value $\left(1{\cdot}29 - 3{\cdot}2\left(\frac{h_{vd}}{d_d}\right)\right)$, where h_{vd} is the velocity head in the *downstream* channel.[111] The piers in these experiments had rounded upstream noses and pointed downstream noses; the values of $\frac{h_{vd}}{d_d}$ did not exceed 0·05. **(Example 102.)**

Although the above treatment yields results of practical utility, it is to be noted that at stage III the afflux h_3 really represents the loss of energy due to friction as the water flows past the piers, plus the loss of energy due to eddies formed downstream of the piers, as indicated in Fig. 192.

197. Actual Operating Conditions of Weirs, Barrages, and Regulators. The conditions stipulated in the preceding paragraphs for the sake of clarifying the behaviour of the control works in question, viz. constant rate of discharge or constant downstream level, are wholly artificial and can rarely be realised

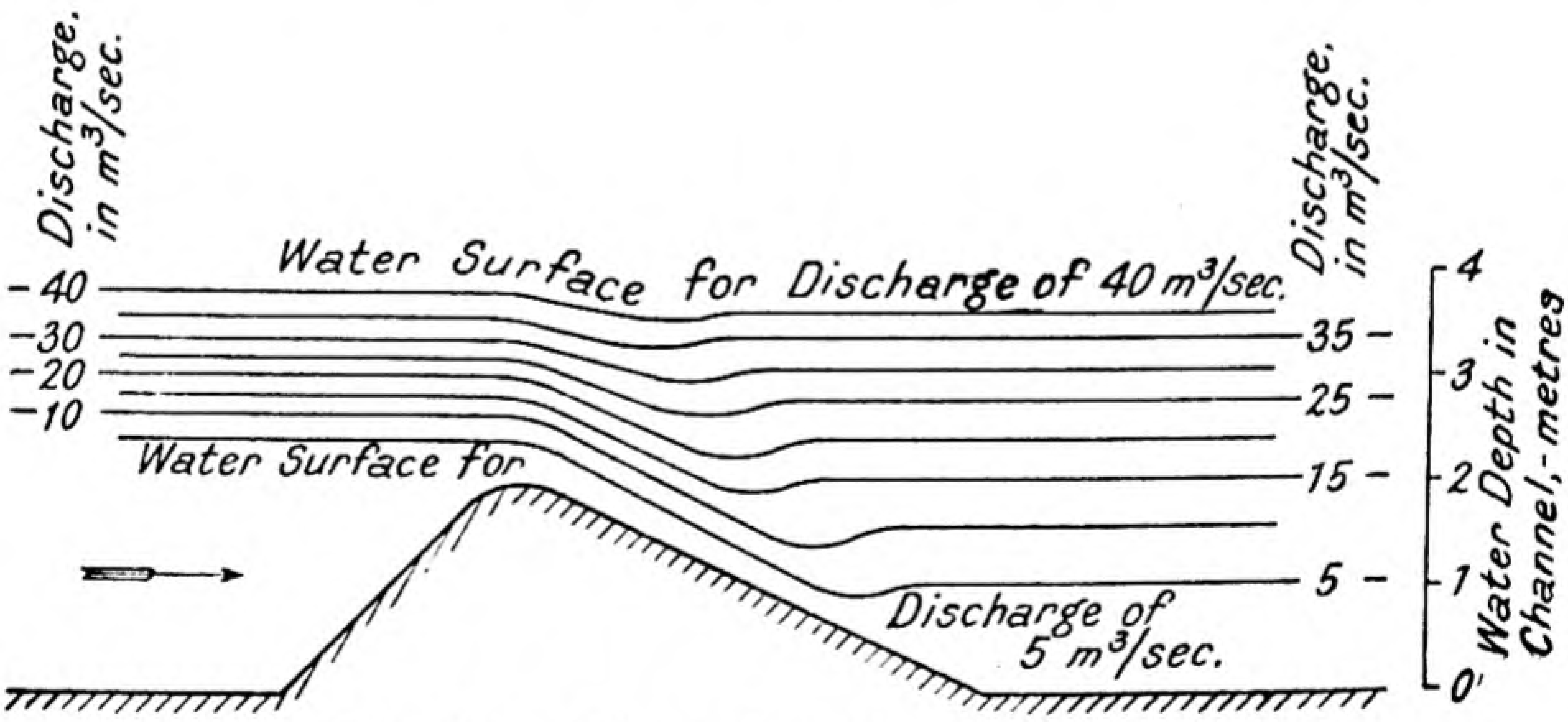

FIG. 193.—Effect of a weir on canal régime.

in practice. As a rule it is not possible to vary the discharge and the downstream depth independently; the two are linked together in the manner shown in Fig. 168, or, in other words, the downstream depth will adjust itself according to the ordinary laws of channel flow to suit the discharge, the downstream surface slope, and the area of the channel section.

With a fixed regulating work such as a weir, therefore, a given discharge can be associated only with a unique upstream depth and a unique downstream depth (assuming, of course, that the flow in the downstream channel is uniform). Thus if, for example, a standing wave weir (Fig. 177 (V)), having a height of 2·0 m., were to be built across the canal shown in Fig. 168, the water surfaces corresponding with various rates of discharge would have the forms sketched in Fig. 193. This figure illustrates very well one of the chief advantages of the standing wave weir—its ability to pass large discharges with a very small afflux.

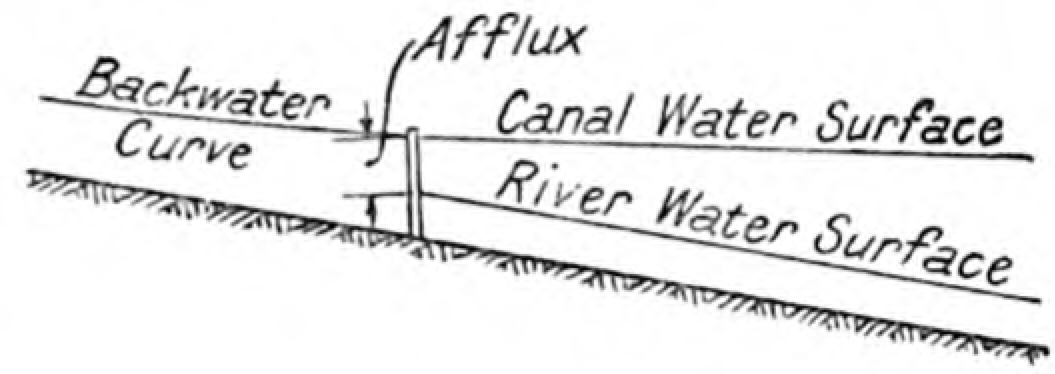

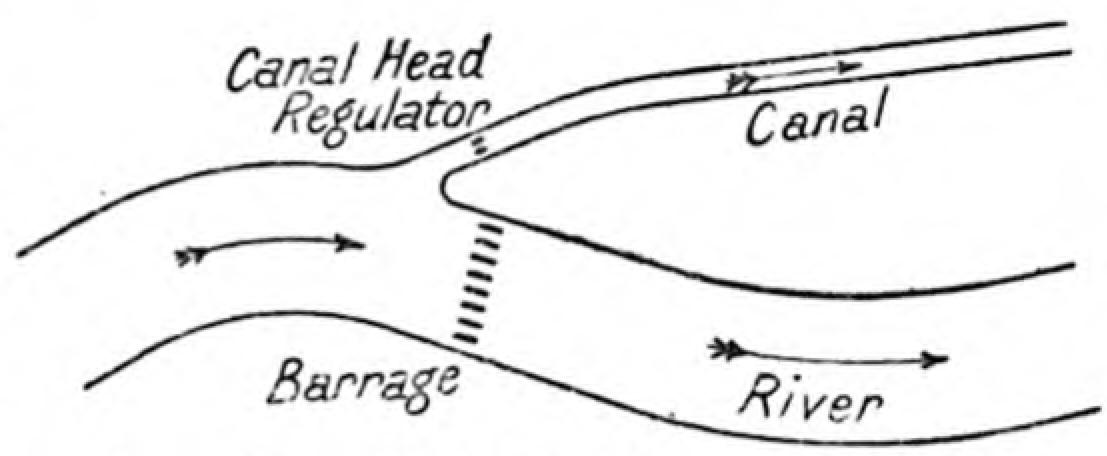

FIG. 194.—Canal head control works.

Regulators having movable gates (Fig. 182) are frequently required to maintain a constant upstream depth irrespective of the discharge; it follows that with this method of regulation the afflux *diminishes* as the discharge and the downstream depth increase. Typical conditions calling for the use of such regulators are illustrated in Fig. 194, where a barrage built across the river heads up the water sufficiently for it to enter the canal: the flow into the canal may be independently controlled by its own head regulator. By giving the canal a flatter slope than the river, the canal water surface at points some distance downstream can be brought to an appreciable height above the river surface and even above the surrounding land level, so enabling "free-flow" irrigation to be carried out at those points.[116],[117] See also Fig. 270.

198. Interference Effects in Regulators. The manner in which the total flow through a regulator is shared among the openings has a noticeable influence on their coefficients of discharge. Thus if, in a regulator having six openings, the discharge is Q when all of them are in operation, the discharge when, say, three of the openings are shut may be *less* than $\frac{1}{2}Q$, although the upstream and downstream depths are

maintained unaltered. The discrepancy between the coefficient of an opening when all the adjacent ones are working, and when it alone is working, the others being shut, may amount to as much as 10 per cent. if the flow passes between the gates and the floor.[106] This is due partly to the increased contraction at the upstream side of the openings, as a result of the transverse currents that are set up, and partly to the lessened opportunities for head recovery on the downstream side (Fig. 195).

The velocity energy that, with an equally distributed flow, is partially converted into potential head, is diverted as a consequence of unequal distribution to the formation downstream of the regulator of large and destructive eddies, vortices, or "rollers." Numerous examples have already been given of the eddying motion invariably set up when a quickly moving stream impinges on to a slowly moving stream, and of the dissipation of energy that ensues. The eddies of this nature now being discussed have the power of eroding or scouring away at a very rapid rate the earth or sand bed of the channel downstream of the regulator ; from every point of view, therefore, uniform distribution of the flow through a regulator or barrage is to be recommended.

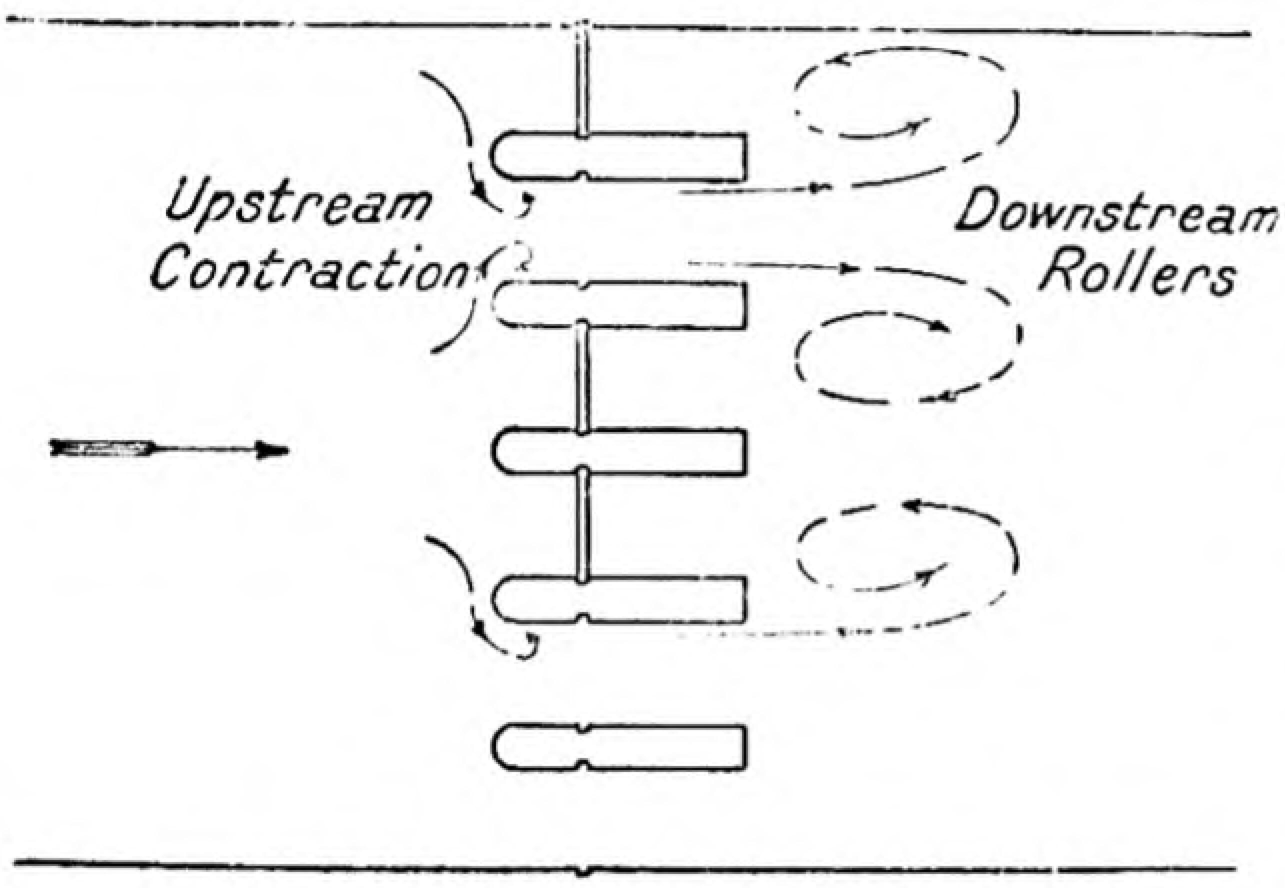

FIG. 195.—Interference effects.

199. Devices for Head Recovery in Channels. A tapered transition section in a channel permits velocity energy to be fairly efficiently converted into potential head, just as it does in a pipe.[118] In the *standing wave flume* (Fig. 196), there is a narrowed throat having (usually) a raised sill which acts as a wide-crested weir ; downstream of this there follows a flared transition section designed to restore the stream to its original breadth. The conversion of energy is carried out so effectively that the downstream depth or submergence h_d may be as much as 90 per cent. of the upstream head h_u without affecting the direct connection between h_u and Q.

If the flume has the proportions shown in the figure, and if h_d is kept below the limiting value just mentioned, then the discharge is approximately

$$Q = 3{\cdot}08\ bh_u^{\frac{3}{2}}\ \text{(foot units)};$$

viz. it is the same as for the wide-crested weir, Fig. 175 (IV).

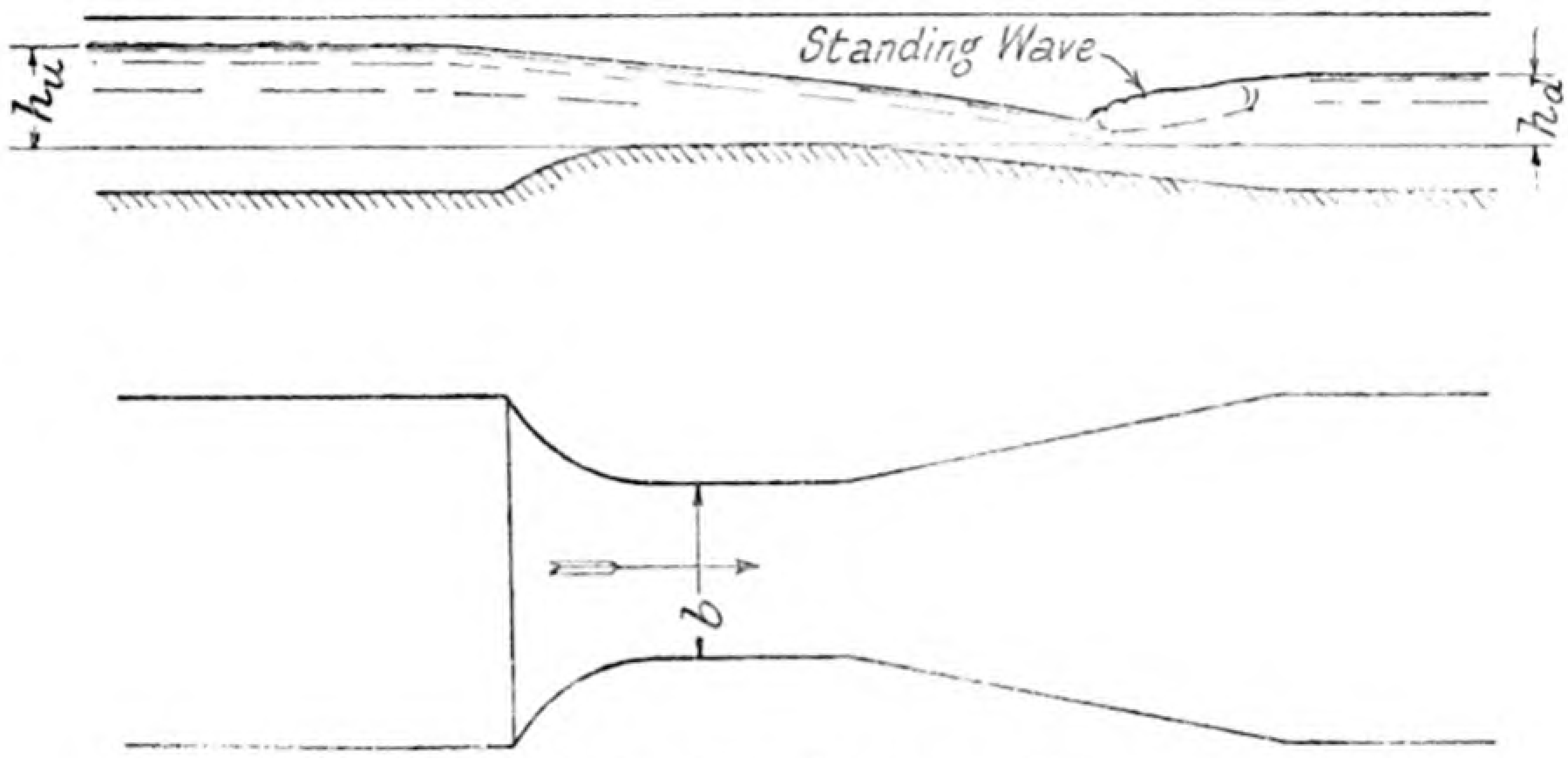

FIG. 196.—Standing wave flume.

It is this characteristic that enables the flume to serve as an effective measuring device, § 400.

Like the standing wave flume, the *standing wave regulator* (Fig. 197) has been developed by engineers in India. Although this regulator only has one opening, the loss of head as the

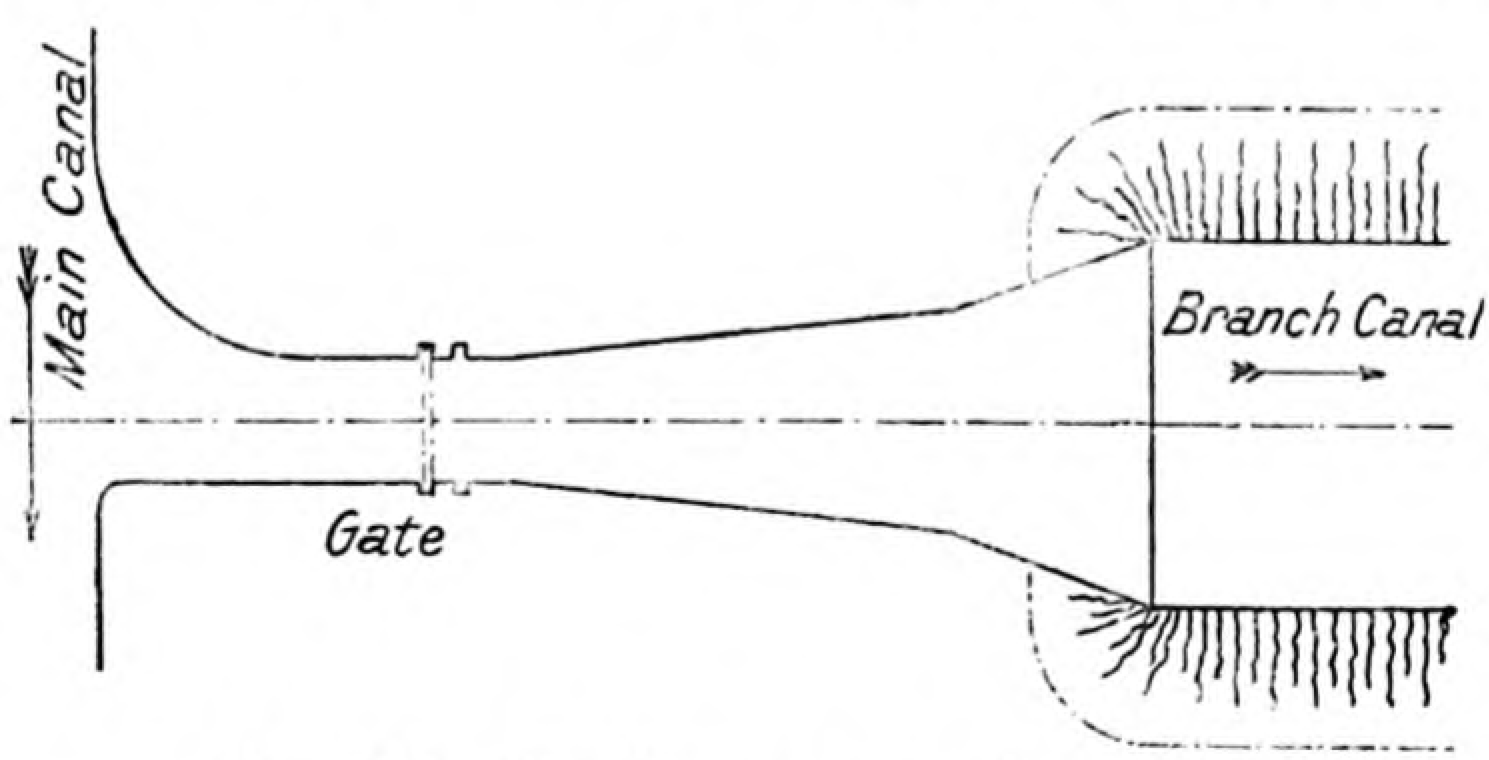

FIG. 197.—Standing wave canal regulator.

water flows through it is hardly more than it would be, under corresponding conditions, in an ordinary regulator having three openings (Fig. 182). A further advantage is that if the proportions are suitably adjusted, then the discharge into the branch canal will depend solely on the water level in the main canal, irrespective of conditions in the branch canal.

The recovery of head in such transition sections, however, is by no means conditional on the creation of a standing wave—the only object of the wave is to permit the water depth at the throat to be drawn down to the critical depth d_c, and so to ensure that the desired wide-crested weir flow is in operation. A transition section designed for velocities far below those capable of generating a standing wave is shown in Fig. 198.

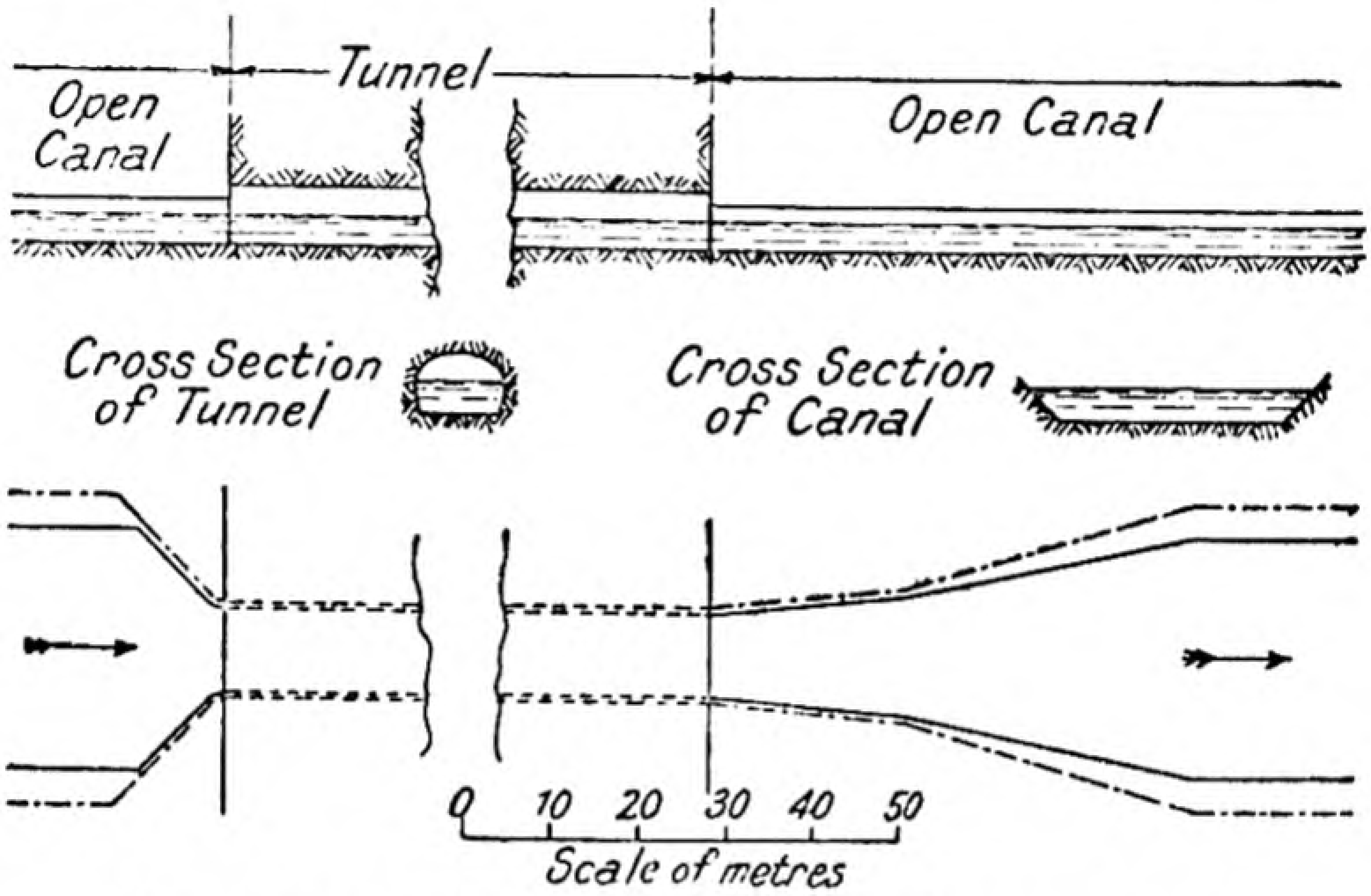

FIG. 198.—Inlet and outlet transition sections.

Here an open canal is shown passing into and out of a narrowed tunnel section. As a result of scale model experiments, a form of tunnel inlet was found that involved an energy loss equivalent to 0·05 of the velocity head in the tunnel, and a form of flared outlet that involved an energy loss of 0·15 of the velocity head in the tunnel. The outlet transition section thus had an efficiency of conversion of well over 80 per cent.

200. Movement of Solids by Flowing Streams. If it were indeed true, as the title of this chapter implies, that water only and nothing but water had to be controlled in open channels, then the work of the hydraulic engineer would be a good deal easier than it is. But in nearly all natural rivers and in most artificial canals the water carries with it solid material of various grades, e.g., finely-divided particles of clay, mud, or silt; fine sand, coarse sand; pebbles, boulders. Depending upon the relative size of the solids and the speed of the stream, the mechanism of transportation [119] may be one or other of three kinds: (i) Rolling, (ii) Saltation, (iii) Suspension.[120]

(i) *Rolling.* The laws of dynamic thrust on immersed objects (§§ 126-130) show how a horizontally-flowing stream may compel solids to roll along the bed. If the stream-bed is steeply inclined, as in a mountain torrent, then stones and boulders will have an additional incentive to roll, Fig. 199 (*a*).

(ii) *Saltation.* If the solid remains stationary on the bed, because of its own irregularities or those of the bed, then the dynamic thrust will not be parallel with the stream but will have a distinct upward component, Fig. 199 (*b*); this is a consequence of the disturbance of the flow lines around the object referred to in § 126 (iv). If now the speed of the current is increased until the object is dislodged, it will move away from the bed and will travel in

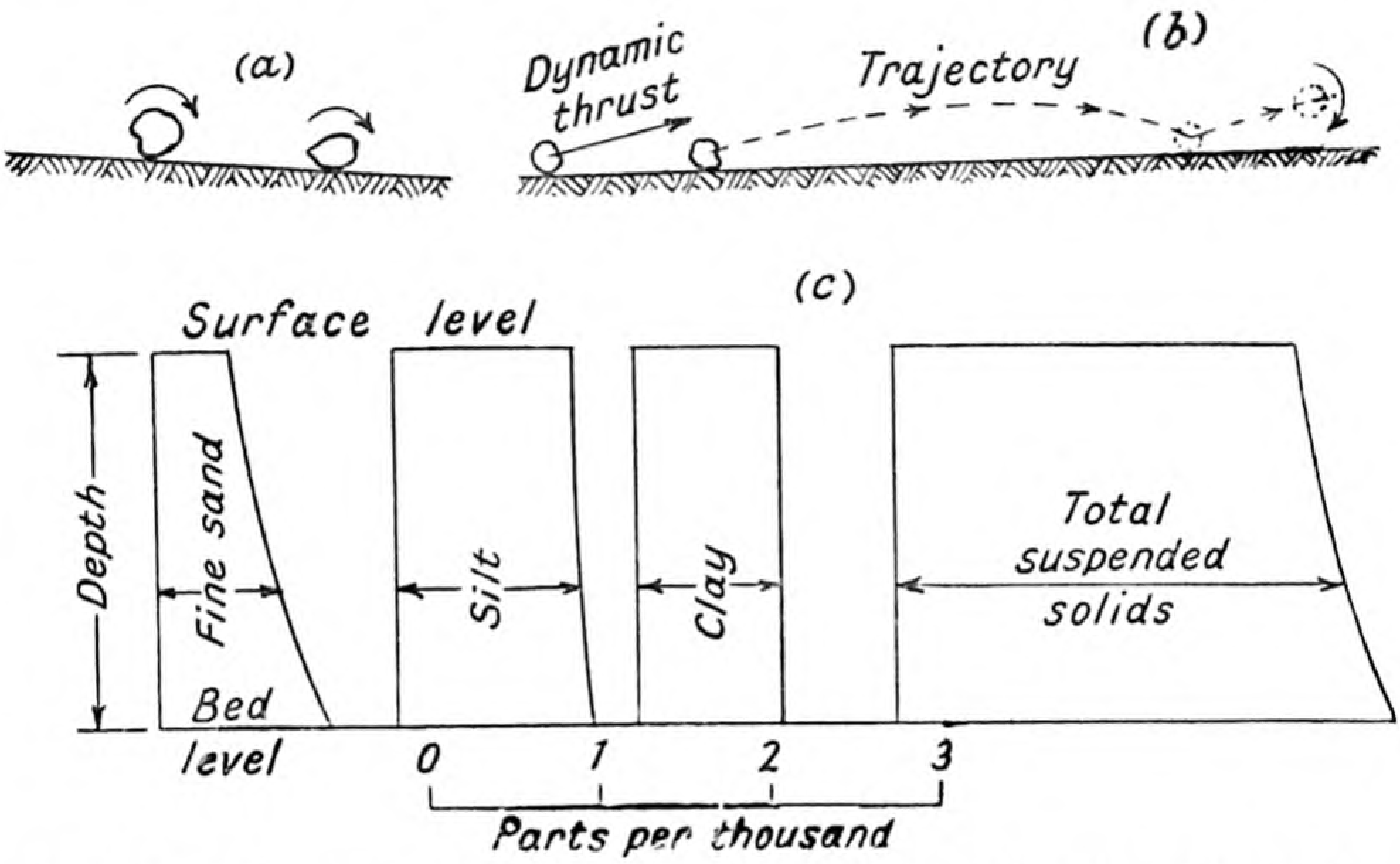

FIG. 199.—Movement of solids in flowing stream by (*a*) rolling, (*b*) saltation. (*c*) Distribution of suspended solids in river Nile in flood.

the trajectory sketched in the diagram. The reason why it descends again is that when water-borne, the solid soon acquires the velocity of the adjacent water filaments and the dynamic thrust declines. The steep velocity gradient near the bed (§ 103) assists in this type of progression which we call *saltation*, and, moreover, tends to set up a rotary motion which further encourages the downstream motion of the solid.

The behaviour of a bowler hat that the wind has blown from the head of a pedestrian accurately simulates the process of saltation. So long as the wind is moderate the hat may remain stationary on the ground for a second or two, then it may move for a few yards, and so on, thus permitting the owner to retrieve it without loss of dignity. But even in these conditions the hat may bowl along at an inconvenient speed if it lands on its rim. When the wind is strong, on the other hand, true saltation begins: the hat makes sustained flights of a dozen yards or more completely air-borne, with only momentary intervening contacts with the ground.

(iii) *Suspension.* Whereas the processes of rolling or of saltation can only influence the solids near the stream bed, the effects which bring about the suspension of solids may be felt throughout the whole depth of the waterway. In a general way, suspension is the result of turbulent mixing within the moving liquid (§§ 111-113), from which it follows that the solids will be

more closely concentrated near the stream bed than they are near the surface. By making various simplifying assumptions, we find that the curve between the concentration and depth will have the logarithmic form of Fig. 89 (b). But in natural streams—in mountain torrents, rivers flowing through alluvial plains, or tidal estuaries—the conditions are so complex that they rarely admit of mathematical treatment. The distribution of suspended material can only be established by taking samples at various depths, and by sorting out the solids into a few arbitrary grades—say, coarse sand, fine sand, and silt. A plot of such information would then probably have the form suggested in Fig. 199 (c). Each individual stream, at each particular season, would have its characteristic type of distribution of suspended solids. Examining, for instance, the hydrograph drawn in Fig. 204, § 205, we can easily believe that the peaks in the flow curve would correspond roughly with peaks in the silt concentration curve.

If the mechanism of suspension in rivers and canals cannot accurately be described in mathematical terms, still less is it possible as yet to predict analytically what will be the total transported load, viz. the sum of the bed load of moving material and of the suspended load. On the other hand, many statistics are available which show how much material various rivers do in fact carry with them: it may amount to 2 parts in 1000 parts by weight or more, viz. in 1000 pounds of very muddy river water, there may be two pounds of solid matter.

201. Erosion of Channel Bed. The material transported by a natural stream may have been eroded or scoured from the banks at some point upstream. Possible lines of approach to the essential problem of erosion are :—

(i) We may try to find, with the help of the reasoning suggested in § 200 (ii), what minimum local velocity will dislodge a particle of specified size.[121], [122] But the difficulty here is that on account of the rapid rate of velocity variation near the bed, we cannot accurately assess the speed of the filaments actually impinging on the particle. Moreover, even if we knew this local velocity it would not be easy to link it up with the mean stream velocity v. Rough figures based on nominal bottom velocities near the channel bed are :—

Class of Material.	Velocity in ft./sec. required to initiate movement.
Fine clay	0·25
Fine sand	0·70
Coarse sand	1·0
Pebbles	2·0
Large stones	5·0

(ii) We may give a fuller significance to the conception of shear stress at the channel walls; for this stress has the advantage of easy computation

by the use of the expression $\tau_0 = wmi$ (§§ 67, 101-102). Let us suppose that instead of water flowing over the sand bed of the channel we have a brush with its bristles resting on the sand. On trying to draw the brush tangentially over the sand, we shall expect that at first the sand will resist; then at a certain limiting stress the sand will yield and the bristles will tear grains away from the sand surface. In just the same way the very real tangential shearing force exerted by the water, if the velocity reaches the necessary limit, will begin to dislodge particles from the bed. For channel beds of soft earth, it has been suggested that to avoid erosion the shear stress τ_0 should not exceed

0·10 lb. per square foot.

Another factor controlling erosion is the state of the water itself—whether or not it is clear or already burdened with transported material; for like any other carrier, the water will refuse to pick up any more load if it is already carrying as much as it possibly can. This point is illustrated in Fig. 200.

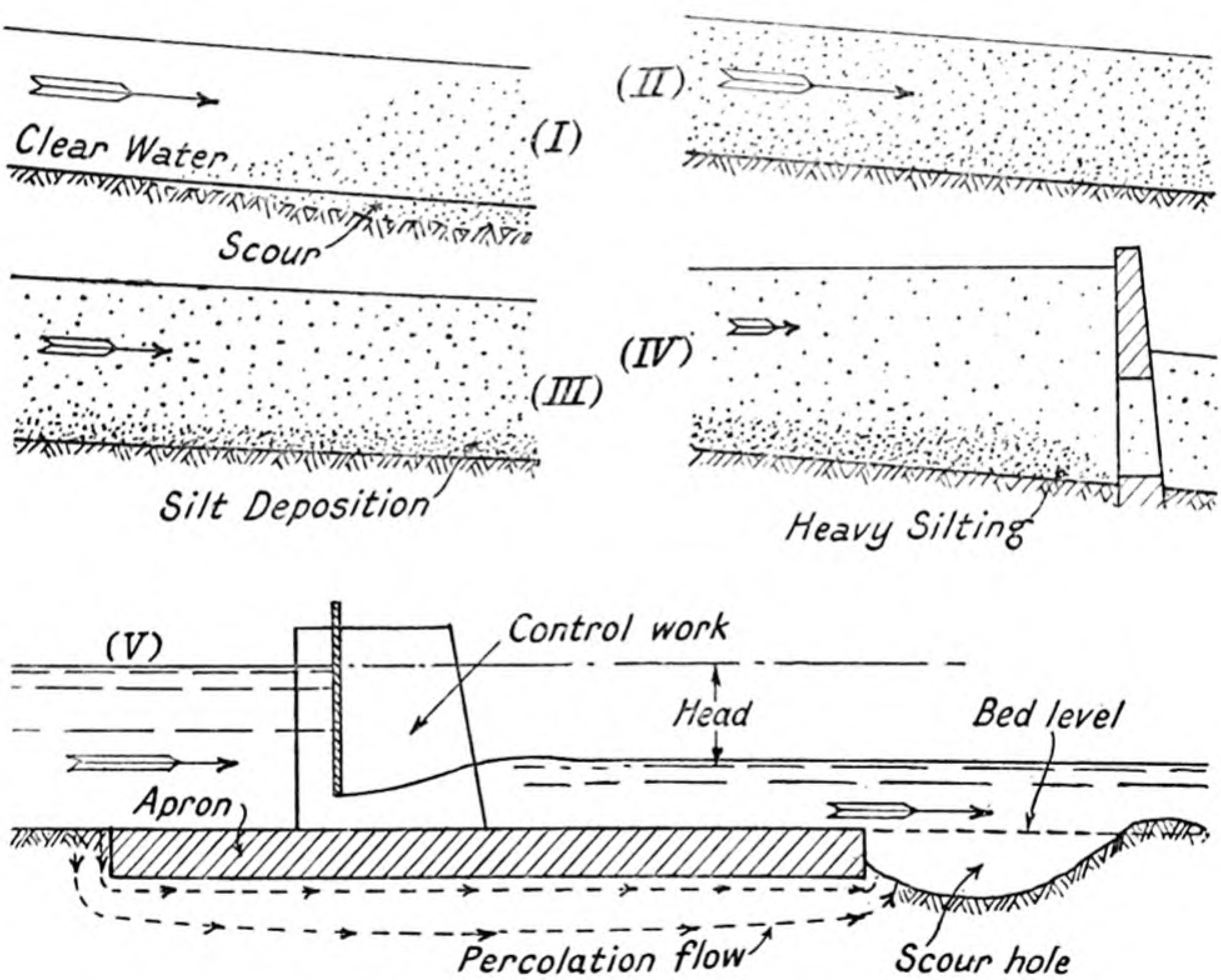

FIG. 200.—Scour, regime flow, and silting.

Clear water enters a channel at (I) at a velocity high enough to cause serious scour. Although at (II) the hydraulic conditions are in no way altered, the bed suffers no damage because by this time the water is saturated; even if it did temporarily take up a trifling additional load, it would quickly have to release it again. When a channel cut through erodible material is in this state of balance, such that deposition is exactly equal to erosion, it is said to be in regime, and is termed a *regime channel*. The alternative term, *stable* channel, is sometimes used.(123), (124) If now the regime is disturbed, e.g. by flattening the slope and reducing the velocity as at (III), then the dynamic effect generated by the turbulence of the stream will be lessened; the available forces are insufficient to sustain the suspended load, and consequently

a part of the load is thrown down. Still further reduction of the velocity, such as would occur in the reservoir formed upstream of a weir or dam, Fig. 200 (IV), would occasion still more serious deposition.[125], [126]

Local erosion downstream of control works. Many diagrams in this chapter have illustrated the exceptionally severe local turbulence liable to occur on the downstream side of barrages, weirs, etc., e.g., Figs. 177, 183, and 195. To protect the channel bed from these additional erosive influences, concrete or masonry floors or aprons may be laid down, as shown in Fig. 200 (v). But even then, scour holes might develop which, if neglected, might undermine the toe of the apron and eventually imperil the structure. Devices which arrest this tendency are protective sills or lip-walls built across the apron [127]; a similar effect may be created by depressing a part of the floor, so forming a kind of stilling-pool.

Danger may also develop if the rate of percolation *beneath* the floor is excessive, Fig. 200 (v); in that event, " piping " will occur beneath the downstream toe of the floor, the earth or sand will be washed away, and again the floor will be undermined. A usual protective device here is to drive rows of sheet-piling into the channel bed, beneath the floor. The construction of a flow-net, interpreted by the laws of percolation summarised in §§ 96-98, not only helps in estimating the velocity of percolation, but it also shows how the static pressure beneath the floor may be assessed.

202. Principles of Design of Non-depositing Channels. Consistent deposition should not be permitted in a channel that is regularly fed with water carrying suspended material, otherwise the channel will be choked and put out of service, or, alternatively, heavy expense must be incurred in periodically cleaning it out. Empirical rules that give some degree of security are :—

(i) *Irrigation canals.* In planning such a canal as is shown in Fig. 194, § 197, the first step is so to design the intake that the least possible quantity of silt is diverted from the river. So far as is practicable, then, the lower layers of river water, with their load of coarse material that creeps, jumps, or rolls along the bed, must be encouraged to continue downstream unimpeded. We do not want them in the canal. It is not easy to skim off and divert into the canal only the upper zone of water laden with fine material, but improvements are being made in selective structures—a combination of barrage and head regulator—designed with this object.[128] It may even be economically practicable to contrive sedimentation basins at the head of the canal, in which the incoming water is deliberately encouraged to throw down its heavier load. The deposits in these basins are periodically washed back into the main river.

Having drawn the finer silt into the canal, our problem is now to keep it on the move. The water velocity must be such that silt is not deposited, and yet not high enough to generate scour. This can often be arranged by maintaining a suitable relation between depth and mean velocity. A formula adapted to certain specific regions, *Kennedy's formula*, gives the relation

$$v = K_0 d^{0 \cdot 64}$$

$$\text{where } \left.\begin{aligned} K_0 &= 0 \cdot 84 \text{ (foot units)} \\ &= 0 \cdot 55 \text{ (metric units)} \end{aligned}\right\} \text{for Indian conditions,}$$

$$\left.\begin{aligned} K_0 &= 0 \cdot 56 \text{ (foot units)} \\ &= 0 \cdot 36 \text{ (metric units)} \end{aligned}\right\} \text{for Egyptian conditions.}$$

According to this empirical expression, non-silting canals are likely to be broad and shallow (Fig. 470), of quite different shape to the maximum discharging section illustrated in Fig. 165. The lower value of the factor K_0 applicable for Egyptian conditions is in compliance with the rule that the finer silt found in the Nile can be transported by a smaller velocity than is required in India.

It should be remembered that although some amount of silt deposition may occur in flood-time, the canal may be washed free again when the river runs clear (§ 201). Special outlet sluices in the canal banks are sometimes provided for the discharge of the silt thus washed out.

(ii) *Sewers.* Sewers are laid with as flat a slope as possible, not because there is much danger of erosion, but to minimise the cost of deep excavation. The minimum slope should give the necessary velocity—about 2–4 ft./sec.—to prevent deposition of mud, grit, etc., when the *least* discharge (dry weather flow) is passing. Because of the relation between depth, discharge, and velocity, § 183, it follows that the velocity when the sewer is carrying its full supply may be unnecessarily high. To some extent this tendency may be counteracted by building the sewer of the ovoid, cross-section shown in Fig. 201; although the *discharge* corresponding to the level BB is only 20 per cent. of that corresponding to level AA, yet the *velocity* corresponding to BB is 75 per cent. of that corresponding to AA. Here is another

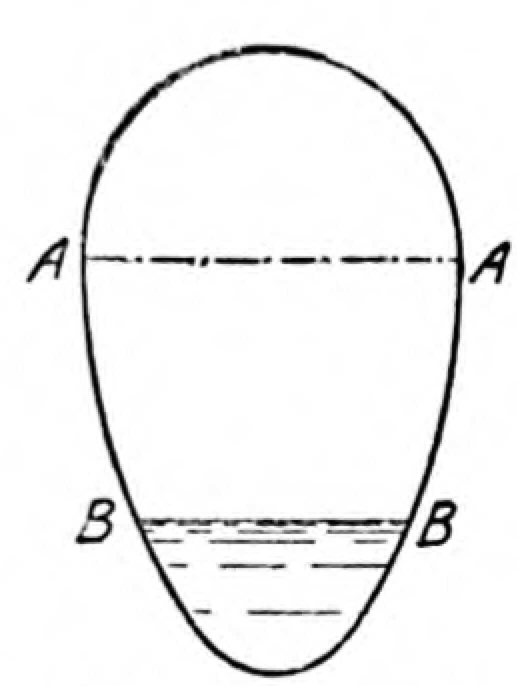

Fig. 201.—Oval sewer.

instance of controlling the transport of a suspended load by adjustments to the channel shape. The advantages of the ovoid sewer are shared, in a smaller degree but at smaller cost, by a U-shaped section, having a semi-circular bottom, vertical sides and a flat top.[129]

203. Other Factors in Channel Performance. The following notes will serve to recapitulate the factors that enter into the problem of delivering at the tail of a canal the maximum proportion of the water that flows in at the head. They clearly show the importance of intelligent maintenance.

(i) *Seepage.* In unlined earthen canals, as much as 25 to 50 per cent. of the water drawn in at the head may be lost by seepage through the banks and bed (§ 179). But it may happen that the waste may diminish with years, as the interstices through which the water leaks gradually become partially plugged by silt grains. On the other hand, the mere loss of water may be a less serious matter than the water-logging of the surrounding country into which it percolates ; this may damage the crops or promote the spread of disease—e.g. malaria—among the inhabitants.

The reverse type of flow—*from* the sub-soil *into* the channel —forms the basis of all kinds of land-drainage. Since such low-level canals or *drains* are dug for the sole purpose of carrying off surplus water, porosity of their bed and banks is in every way to be encouraged (§ 209).

(ii) *Evaporation* from the surface of water in canals rarely represents a significant proportion of the total loss. The relative loss from reservoirs is naturally much more serious (§ 10).

(iii) *Silting* of the channel will reduce its carrying capacity, and although long-continued *erosion* may increase the cross-section, yet on a smaller scale the irregularities created in the banks and bed may actually diminish the flow.

(iv) *Weeds* and other vegetable growths have the effect of increasing the effective roughness of the channel walls, and they thus spoil the channel performance. They may take root even in a lined canal, for small patches of mud and silt may give them a breeding-ground and an anchorage.

CHAPTER XI

SOME OTHER FLOW PROBLEMS

In this chapter various paragraphs are collected together which serve as appendices to the two preceding chapters; although this diversified material cannot fairly be classified directly under the headings of pipe flow or channel flow, it may have affinities with either.

The problems may be grouped into the quite independent categories of :—

(i) Storage of water in reservoirs.

(ii) Underground percolation.

(iii) Automatic control devices.

Storage of Water in Reservoirs

204. Inflow and Outflow. Earlier paragraphs (§§ 187, 195) have touched upon the spillways, sluices or other devices that control the flow from reservoirs. Now we proceed to the question of determining the necessary capacity of a reservoir to meet specified conditions. How many millions of gallons, acre-feet, or cubic metres must the reservoir contain? Beginning with the simplest case in which the natural stream has a uniform discharge q, Fig. 202, then if the outlet sluices in the dam are fully open, the outflow Q will be equal to the inflow q; the uniform water slope OA will remain virtually undisturbed. If then the outlet sluices are suitably regulated, impounding of water will begin, and in due time the water will reach its

top level, OB. Manifestly the total capacity of the reservoir will be the volume enclosed between the surfaces OA and OB; it is the volume indicated by hatching. The *rate* of impounding or the *rate* of release will depend upon the least and the greatest permissible values of the outflow Q.

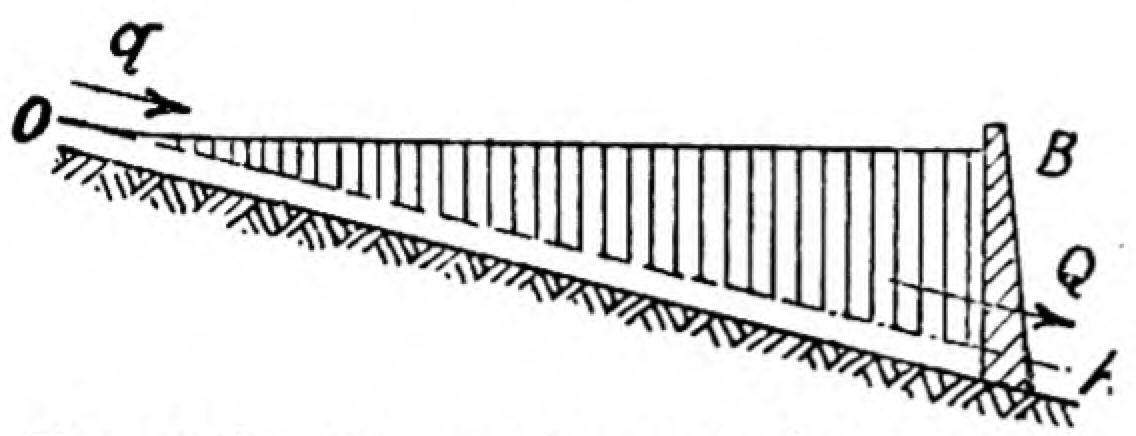

FIG. 202.—Storage capacity of reservoir.

If inflow and outflow are plotted against time, the impounding and the releasing periods are graphically shown. The idealised example in Fig. 203 (i) relates to a reservoir giving daily storage for a hydro-electric installation, § 252 (ii); it is a peak-load installation, in which the turbines operate for three hours only during each afternoon. It is during this period that the reservoir is emptied. During the remainder of the 24-hour period, the outflow passing down the river is reduced to the minimum, the difference between uniform inflow q and outflow Q being available for storage.

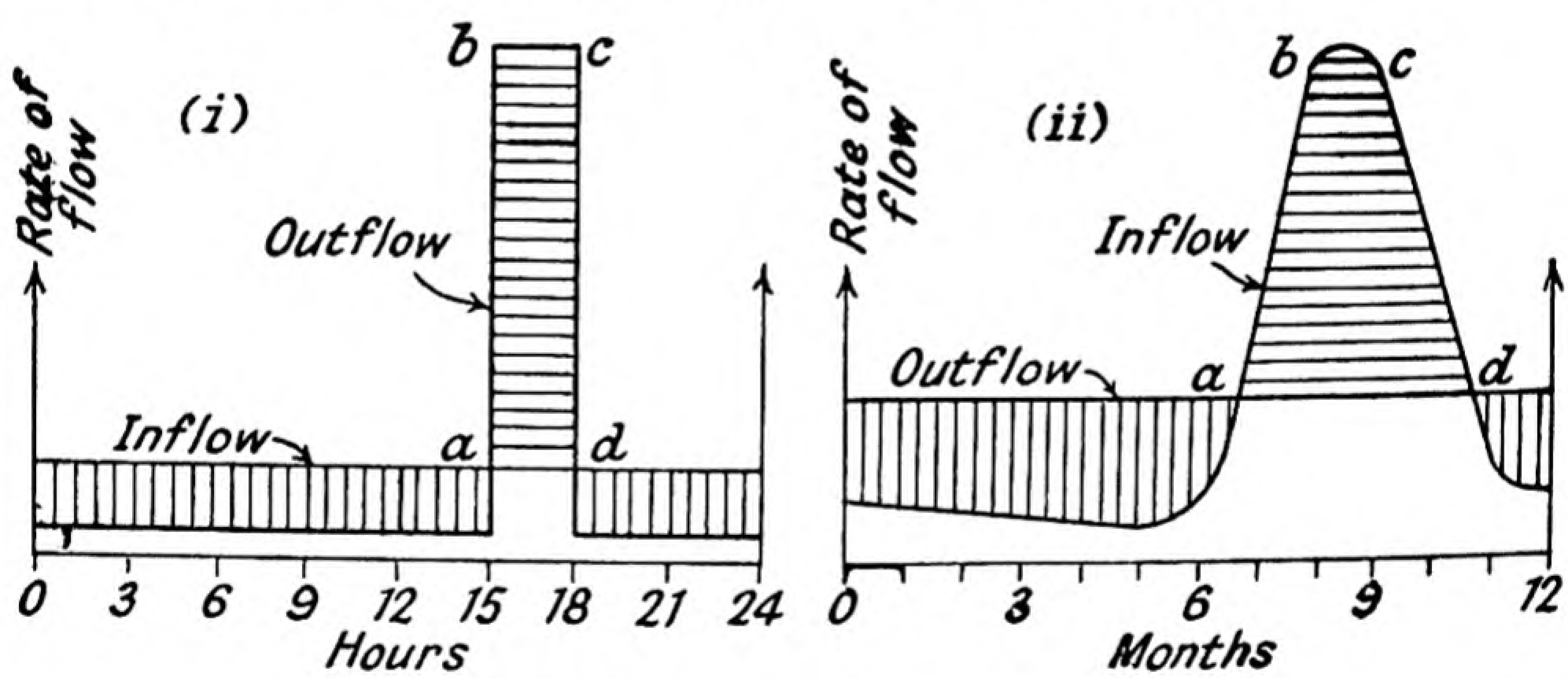

FIG. 203.—Flow into and out of reservoirs.

More frequently the purpose of the reservoir is to damp out the natural seasonal fluctuations of the stream; we want to convert the variable inflow q into a uniform outflow Q. The idealised diagram, Fig. 203 (ii) shows how the excess river water coming down during the rainy months[130] is stored in the reservoir and made available for irrigation, water-power, or domestic water-supply during the season of low river flow.

In any event the required capacity of the reservoir can be computed thus: it is directly proportional to the hatched

area *abcd* in Fig. 203. This area, to the proper scale, will be expressed by: Time × discharge

$$= Tx(L^3/T) \quad . \ . \ . \quad (\S\ 40)$$

$$= \text{Volume of reservoir.}$$

Consistent units must naturally be chosen. If discharge is quoted in terms of, e.g. cubic feet per second, then time must be expressed in seconds, and the reservoir capacity will be in terms of cubic feet.

205. Mass Curves: Construction and Use. It would be idle to expect that the flow of an actual stream would preserve, year by year, the regularity of regime depicted in Fig. 203 (ii). If a systematic series of stream-gauging records was

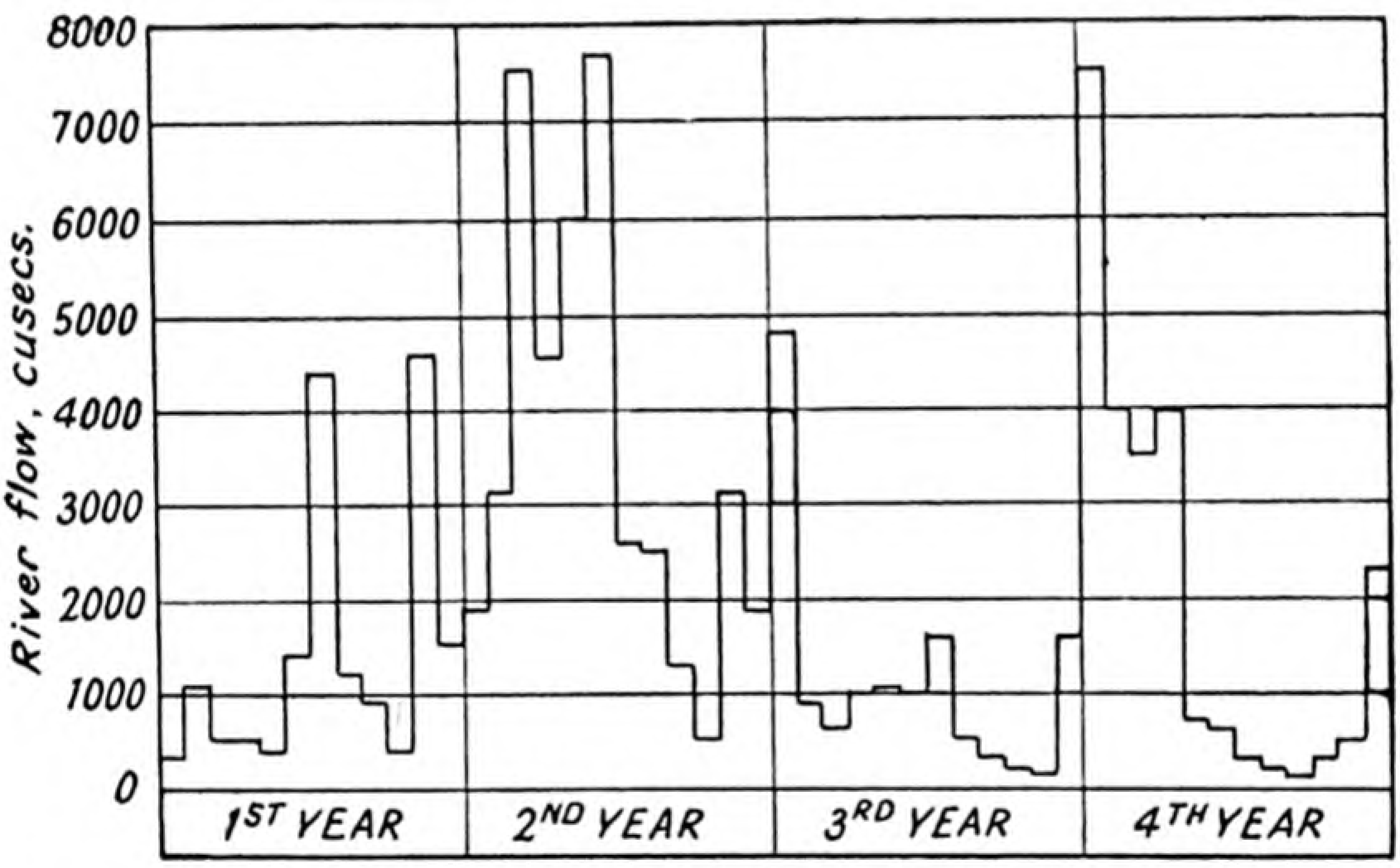

Fig. 204.—Natural stream hydrograph, showing average rate of flow in cusecs during each month.

available (§§ 397-402), these records when plotted in the form of a hydrograph might have some such appearance as Fig. 204. During the period of four years selected, great variations in monthly flow are to be observed, nor is there any close correspondence between the stream behaviour in one year and in the succeeding year. On this account the original hydrograph, Fig. 204, is not very suitable for giving information about reservoir capacity and performance; we therefore turn to a derived type of graph termed the *mass curve*. The horizontal time base is still retained; but instead of the ordinates representing *rates* of flow, they represent the *total* or cumulative

volume of water that has passed down the stream since the beginning of the stipulated period.

From the hydrograph, Fig. 204, we note that the average rate of flow during the first month, January, is 300 cusecs, and therefore the total monthly flow is

$$\frac{300 \times 3600 \times 24 \times 31}{43560} = 18500 \text{ acre-feet.}$$

This amount is set up on the mass curve, Fig. 205. Successive months are similarly treated, the total for each month being

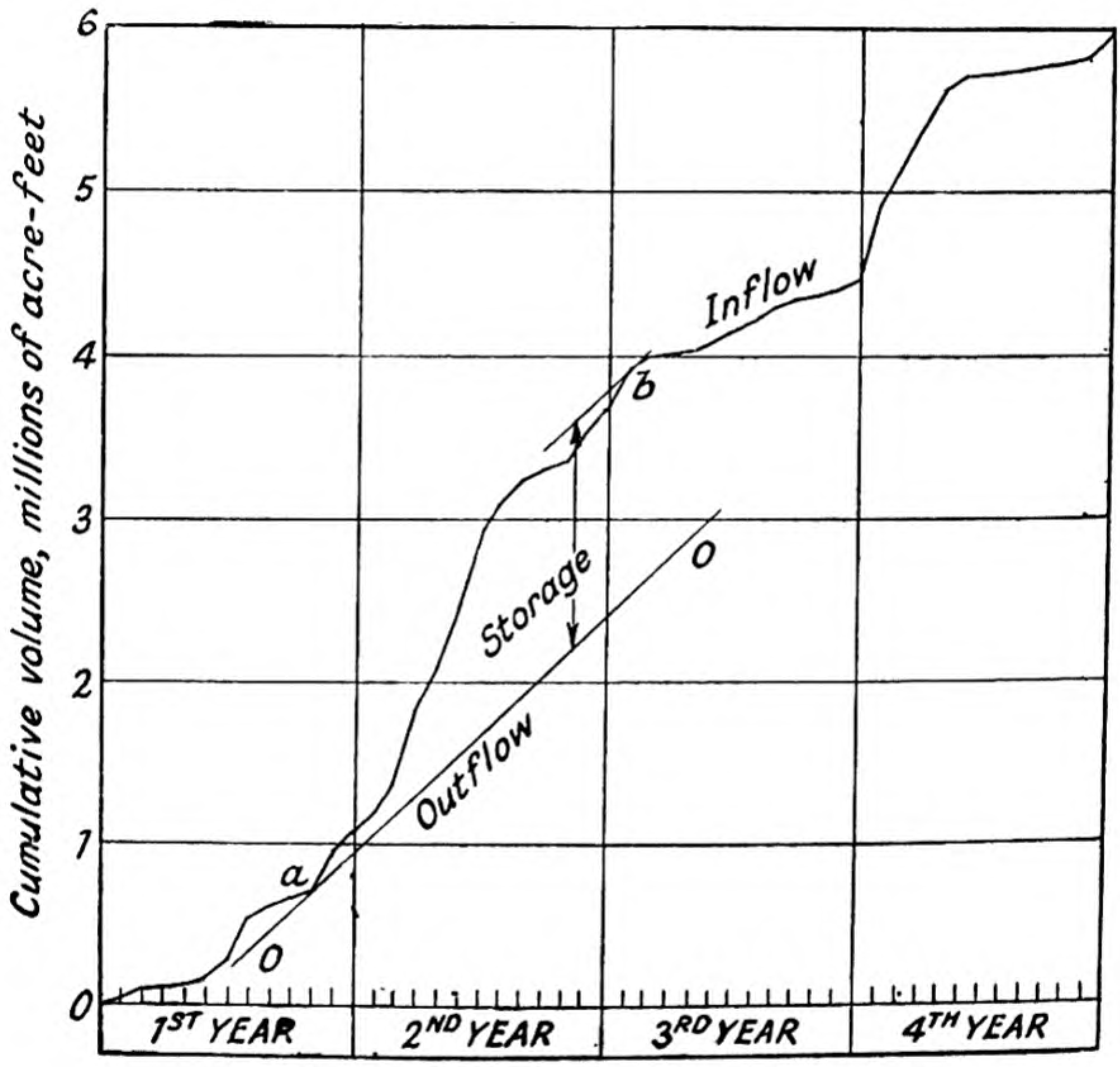

FIG. 205.—Mass curve based on Fig. 204.

added to the cumulative total of all preceding months, so yielding the completed curve seen in the diagram. If we are concerned with a reservoir to be formed in the river valley, the curve would represent the natural or unregulated mass flow into the reservoir.

The next step is to add to Fig. 205 another mass curve showing the *regulated* outflow or "draft" or draw-off Q that is to be abstracted from the reservoir. Suppose that in the present instance the draft were to be fixed at a uniform rate

of 2000 cubic feet per second, or 1,450,000 acre-feet per year; then this would be indicated in Fig. 205 by a line OO having the appropriate slope. In the diagram this line has been so located that it touches the river mass-curve at point a, clearly showing that at that point the reservoir is empty. If flow regulation begins at this stage to yield the controlled outflow of 2000 cubic feet per second, it is easy to see that thenceforward the inflow considerably exceeds the outflow; storage in the reservoir has begun. Moreover, since stored water = (total volume entering reservoir − total volume leaving reservoir), the volume contained in the reservoir at any time can be read off directly; it is the intercept between the two mass-curves. Studying the diagram we note how, month by month, the water steadily rises in the reservoir; then there are minor fluctuations, followed by a peak which indicates the maximum stored volume. This occurs at point b, where, by scaling off the intercept, we observe that the stored water has now reached its limit of 1,390,000 acre-feet. After that, the reservoir begins to empty again.

If some other value of the draft Q had been chosen, or if the draft changed from season to season, nevertheless the same method of plotting reservoir contents could be followed.

206. Method of Residuals or Departures. One disadvantage of the mass-curve system of plotting—a drawback that may become awkward when a long term of years is in question, rather than a few years only as in Fig. 204—is that the vertical scale may be inconveniently small. This objection vanishes if the method is slightly modified. In the modified type of mass-curve we plot on a time basis not the total cumulative flow, but the *residual* flow, viz. the *difference* between the observed river flow and some arbitrary fixed flow which may preferably be a little below the mean river flow. For the conditions represented in Figs. 204 and 205 a suitable value would be 2000 cusecs, and the residual flow would be computed thus:—

	Natural Inflow (cusecs)	Residual Flow (cusecs).
1st month	300	300-2000 = − 1700
2nd month	1100	1100-2000 = − 900
3rd month	500	500-2000 = − 1500

These values of " residuals " or " departures ", converted into terms of acre-feet, are then plotted *cumulatively*, taking account of sign, as in Fig. 206. Comparison between the two diagrams—Fig. 205 and Fig. 206—shows how the one is merely a magnified or exaggerated form of the other. The linear distance representing reservoir capacity is now much greater, making it easier to read off accurately the maximum stored volume, viz. 1,390,000 acre-feet.

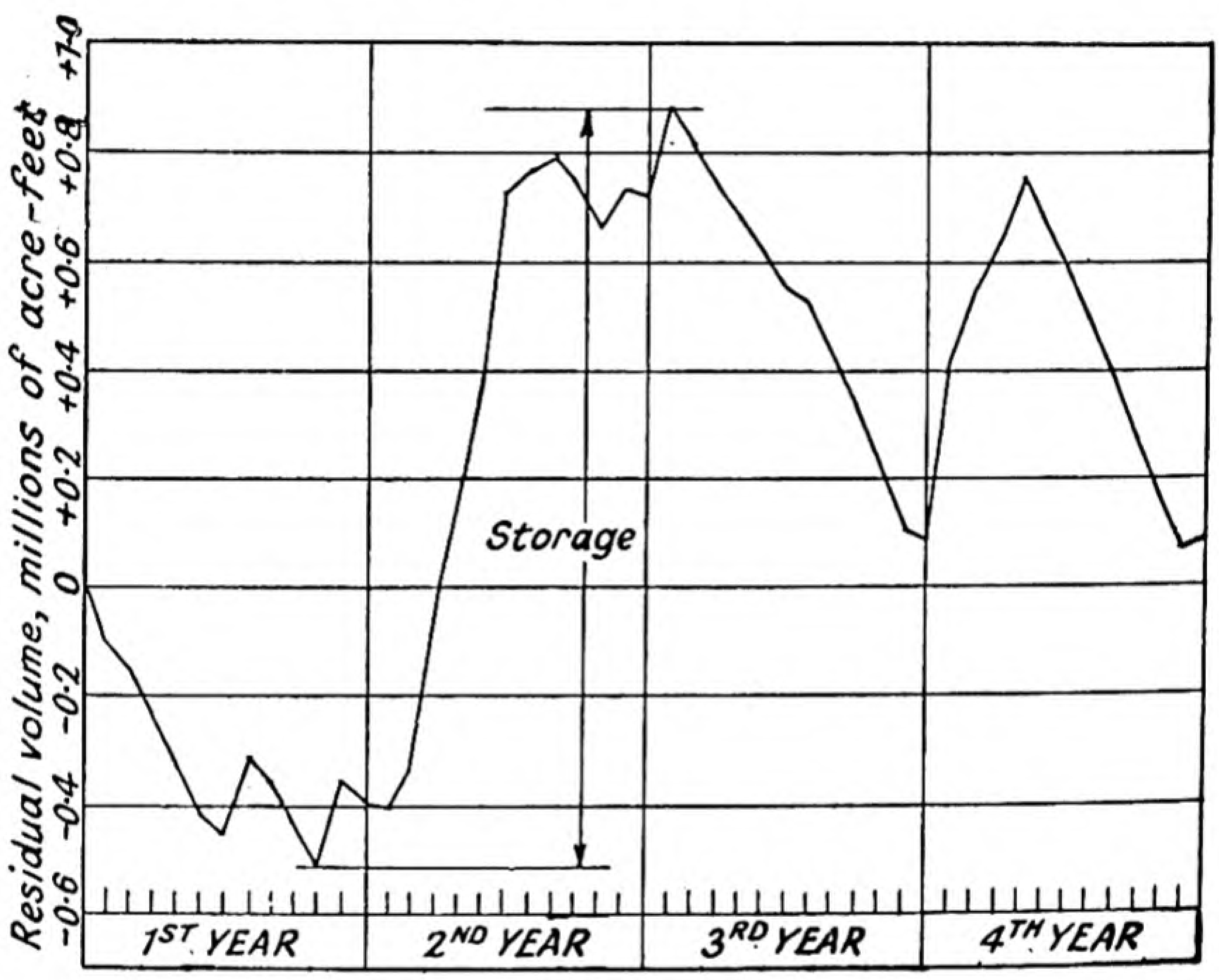

FIG. 206.—Curve of residuals based on Fig. 204.

207. Some General Considerations. Before the size—or even the site—of the reservoir can finally be fixed, additional considerations besides strictly hydraulic ones must be kept in mind. Having found a likely position in the river valley, we have to ask whether the topographical configuration is suitable for a reservoir. Can the desired quantity of water be stored without building a dam of excessive height, length, or cost? Will the geology be favourable? Are the foundations for the dam likely to be water-tight, or can they be made water-tight? Will the floor of the reservoir be impermeable?

Another question is: how will the stored water be utilised? Is the reservoir intended to be a single-purpose reservoir, i.e. will it be devoted exclusively to *either* flood protection, *or* to water-power development, *or* to irrigation? Or are the

promoters of the scheme thinking about a *multi-purpose* reservoir,[131] intended for two or more functions? The answer would have a profound effect not only upon the permissible expenditure which could economically be incurred in building the dam, but also upon the method of operating the reservoir. In certain kinds of hydro-electric installations, § 252 (ii), Fig. 267, it is advantageous to keep the reservoir level as high as possible; but if flood-protection is in question, reservoir capacity must always be kept available (at least during the flood season) to receive the flood water which would otherwise cause damage lower down the valley.

Matters more directly related to Hydraulics are:—

(*a*) *Interpretation of stream-flow records.* The irregularity of the typical hydrograph reproduced in Fig. 204 shows how imprudent it would be to base reservoir capacity upon observations during a short period of years only. How are we to estimate what abnormal droughts or floods have occurred in earlier years, or what may occur in future years? Not only, therefore, should the gauging records for the longest possible term of years be studied, but they should be interpreted by the analytical methods that are steadily being developed.[132]

(*b*) *Evaporation from reservoir water surface.* In hot, dry, sub-tropical climates, the *available* stored water may be substantially less than what is computed by means of mass-curves or the like. Such is the effect of evaporation, § 10, which may cause very serious losses of water—as much as 6 ft. depth annually.

(*c*) *Silting.* When silt-laden river water comes to rest in a storage reservoir, suspended material is inevitably thrown down (§§ 200, 201, Fig. 200 (iv)). There is no known method of economically removing these deposits; it therefore follows that in the course of years the reservoir capacity may be sensibly reduced.[121] In extreme instances the reservoir may be completely filled with solids after a life of only a dozen or a score of years: the reservoir has virtually been destroyed.

Underground Percolation

208. Collection of Water from Porous Subsoil. A major hydraulic problem has always been that of extracting from porous subsoil, for domestic or other purposes, a proportion

of the water that has fallen on the earth's surface in the form of rain. Considering an idealised section of the earth's crust consisting of a uniform thickness of sand resting on an impervious bed of clay or rock, we may expect to find that the lower layers of sand are wet and indeed completely saturated, while the upper layers are damp or almost dry. Between the two zones there will be no clearly-defined boundary. We therefore have to accept a conventional or arbitrary one: it is defined as the surface passing through the individual free-water surfaces observed in a number of wells sunk into the water-bearing medium. This imaginary surface is designated the *water-table* or the *ground-water surface.* Water can be drawn from any point below the water-table, but from no point above it.

If the underground water is at rest, the water-table may be expected to be horizontal; if rain falling uniformly on the ground above percolates downwards, it will replenish the underground supply and cause a gradual rise of the water-table. If now we begin to pump water from one of the wells, the water-table in the neighbourhood will be lowered and the resulting differential head will generate subsoil flow into the well. When the inflow from the porous strata is equal to the output of the pump, then the water-level in the well will be stabilised; the difference in level between this new water surface and the original rest level corresponding to the ideal horizontal water-table is termed the *draw-down.*(133)

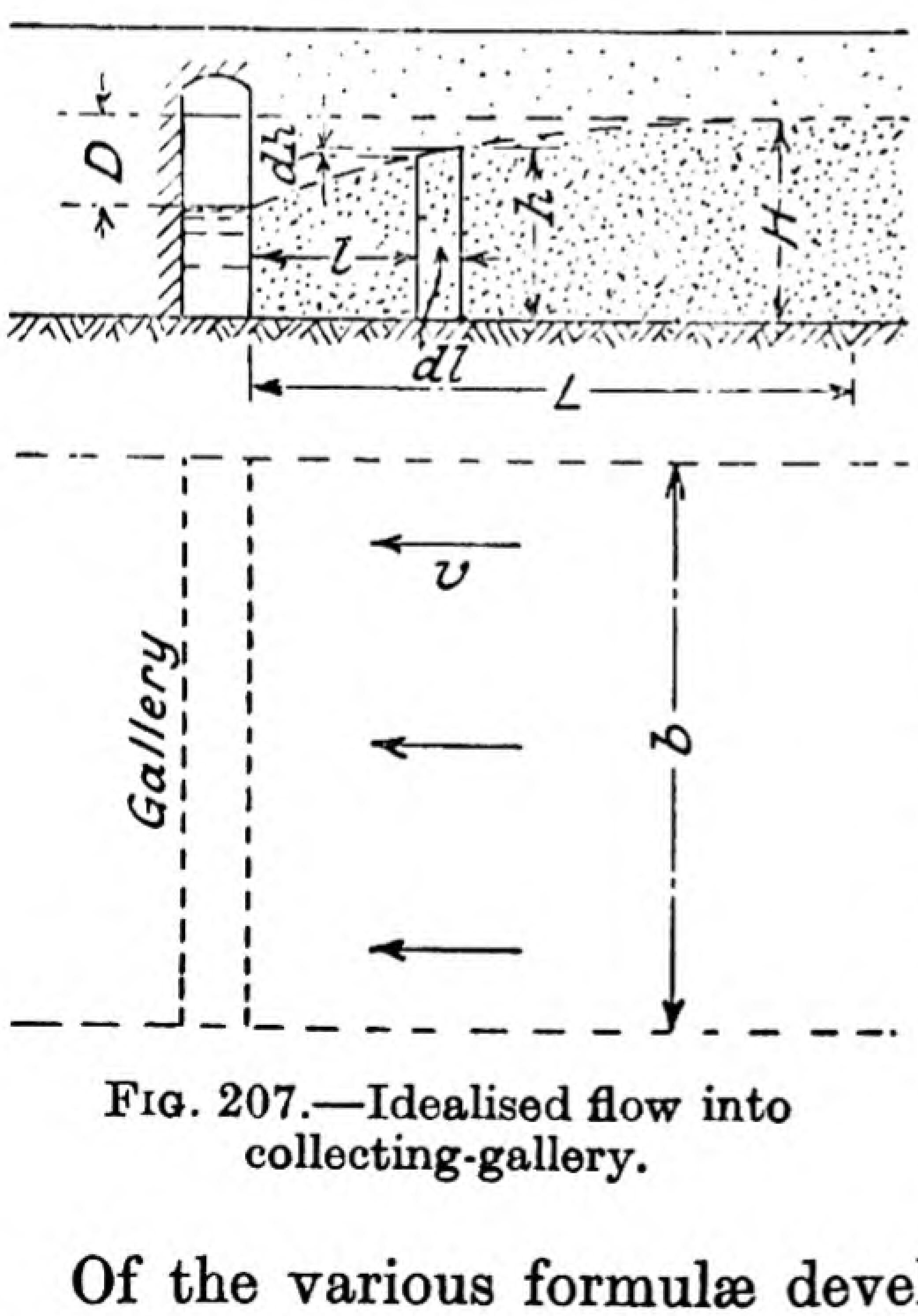

FIG. 207.—Idealised flow into collecting-gallery.

Of the various formulæ developed for expressing the rate of flow through porous material, §§ 96-98, the linear equations 5-17 and 5-18 are likely to be the most useful, for there can now be no doubt about the viscous nature of the flow. A few simplified applications will here be studied.

209. Flow into Drains and Collecting-galleries. If the water-bearing sheet is relatively wide and shallow, a long horizontal collecting-gallery will form the most suitable type of underground chamber into which the water may percolate before being drawn off by the pump.[134] Its walls may be of open-jointed masonry offering negligible resistance to the inward percolation. In the diagram, Fig. 207, it is assumed that water enters through one side only, and that the direction of flow is everywhere normal to the length of the collector. For simplicity an adjacent river may be postulated which maintains a uniform depth H of ground water at a distance L from the collector, irrespective of the rate of underground flow.

By analysis of the curved shape of the water-table it is desired to find the relationships between—

q = inflow into collector = output of pump
v = velocity of percolation (assumed horizontal)
b = length of collector
k_o = permeability of porous subsoil
D = drawdown
h = local depth of water in subsoil at a distance l from the collector.

Now the velocity of percolation through a vertical lamina of thickness dl will depend upon the local slope of the water-table, dh/dl, in this manner—

$$v = k_o \,.\, dh/dl \qquad \text{(from equation 5-17).}$$

Hence
$$q = hbv = hbk_o\frac{dh}{dl}.$$

Therefore
$$\int dl = \frac{bk_o}{q}\int hdh, \quad \text{and} \quad (L - l)\,.\,\frac{2q}{bk_o} = H^2 - h^2.$$

Whence
$$L\,.\,\frac{2q}{bk_o} = D(2H - D).$$

It will be observed that the profile of the water-table is parabolic.

This treatment is applicable also to the flow into an open drain, § 203 (i), especially when the drainage water is drawn off by pumping.

In more complex problems of this nature the construction of a type of flow-net, § 38, is often helpful.

210. Flow into Circular Well. Considering now a circular well sunk through the porous stratum down to the horizontal impermeable floor that underlies it, then the flow will be radially inwards, Fig. 208. Assuming that R is the limiting radius at which pumping from the well influences the water-table, we find that—

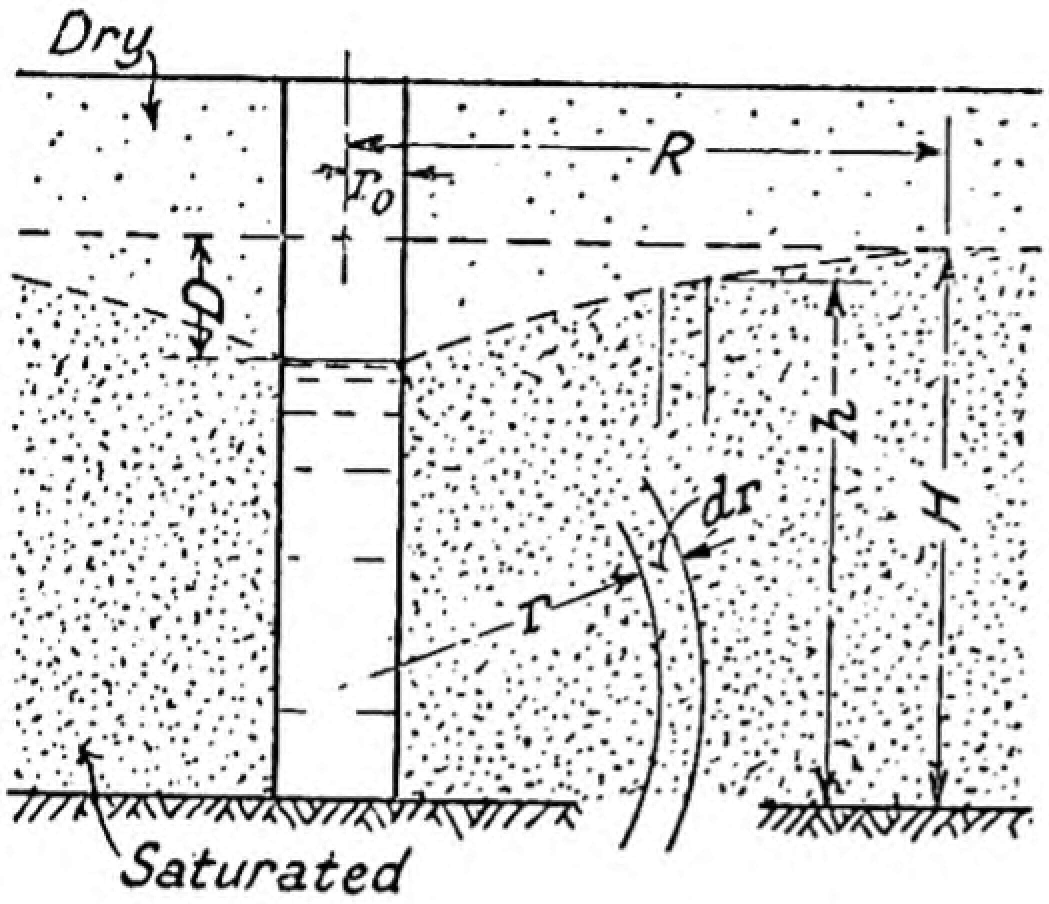

FIG. 208.—Idealised flow into circular well.

At radius r, $\quad v = k_o \cdot \dfrac{dh}{dr}.$

Therefore

$$q = h \cdot 2\pi r \cdot k_o \cdot \frac{dh}{dr},$$

and $$\frac{q}{2\pi k_o} \cdot \int \frac{dr}{r} = \int h dh.$$

Whence $$\frac{q}{\pi k_o} (\log_e R - \log_e r) = H^2 - h^2.$$

It is naturally very rare to find the geological conditions so uniform that these equations can be directly applied.[135] Especially in wells sunk into limestone the water enters through cracks and fissures rather than by direct percolation through the rock. To augment the yield of such wells, radial horizontal galleries may have to be driven which increase the area for inflow. Although in the general sense here used a well is any vertical shaft for collecting water or oil, yet in the technical sense *wells* are distinguished from *bore-holes.* Bore-holes, or drilled wells, are usually much cheaper to sink than dug wells, especially when deep-lying water is to be lifted.

AUTOMATIC CONTROL DEVICES.

211. Float Valves and Pressure-reducing Valves. The ball-cock as used in household flushing cisterns is one of the simplest devices for maintaining a fixed water level. An adaptation suitable for larger flows is shown diagrammatically in Fig. 209; it is intended to keep a steady water-level in the tank, irrespective of variations in the rate of inflow or outflow. If the float should tend to rise due to an increased

rate of inflow, it is so linked to a butterfly valve (§ 169) that this control valve tends to close; thus the water level cannot vary by more than a centimetre or two. The object of providing a separate working chamber for the float, communicating with the main tank by small openings, is to prevent "hunting" or rapid oscillations of the float.

If it is not possible to operate the valve by a float working in an open cistern it may be connected to a freely moving piston working within a vertical cylinder (Fig. 210). We then

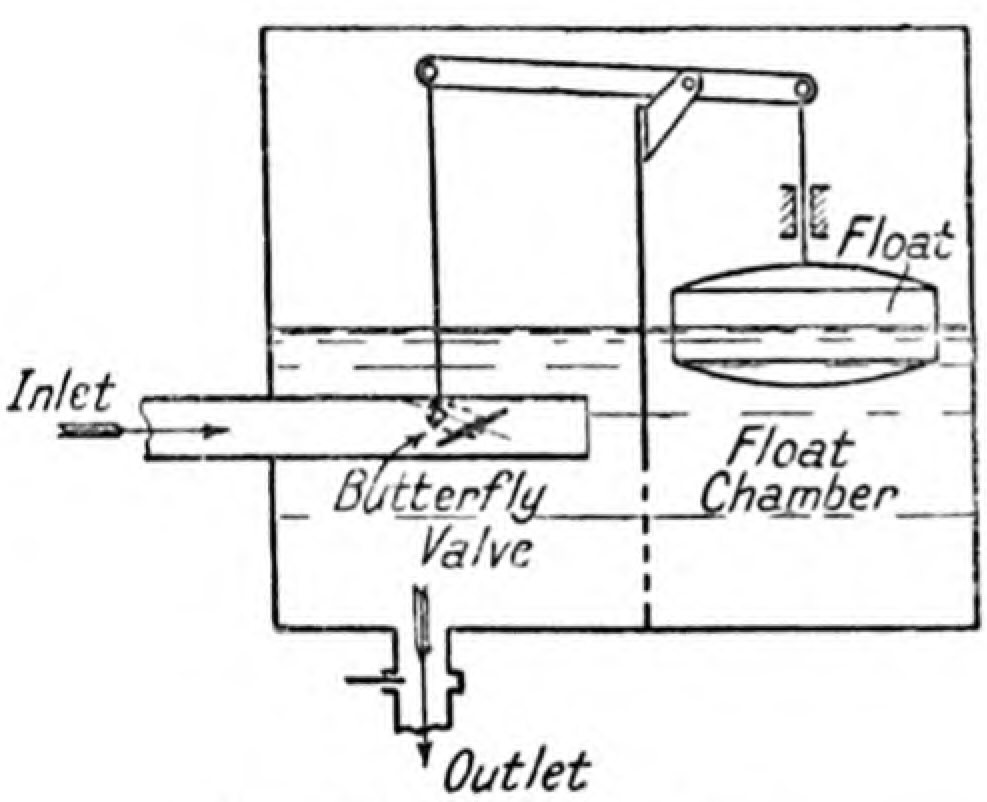

FIG. 209.—Float valve.

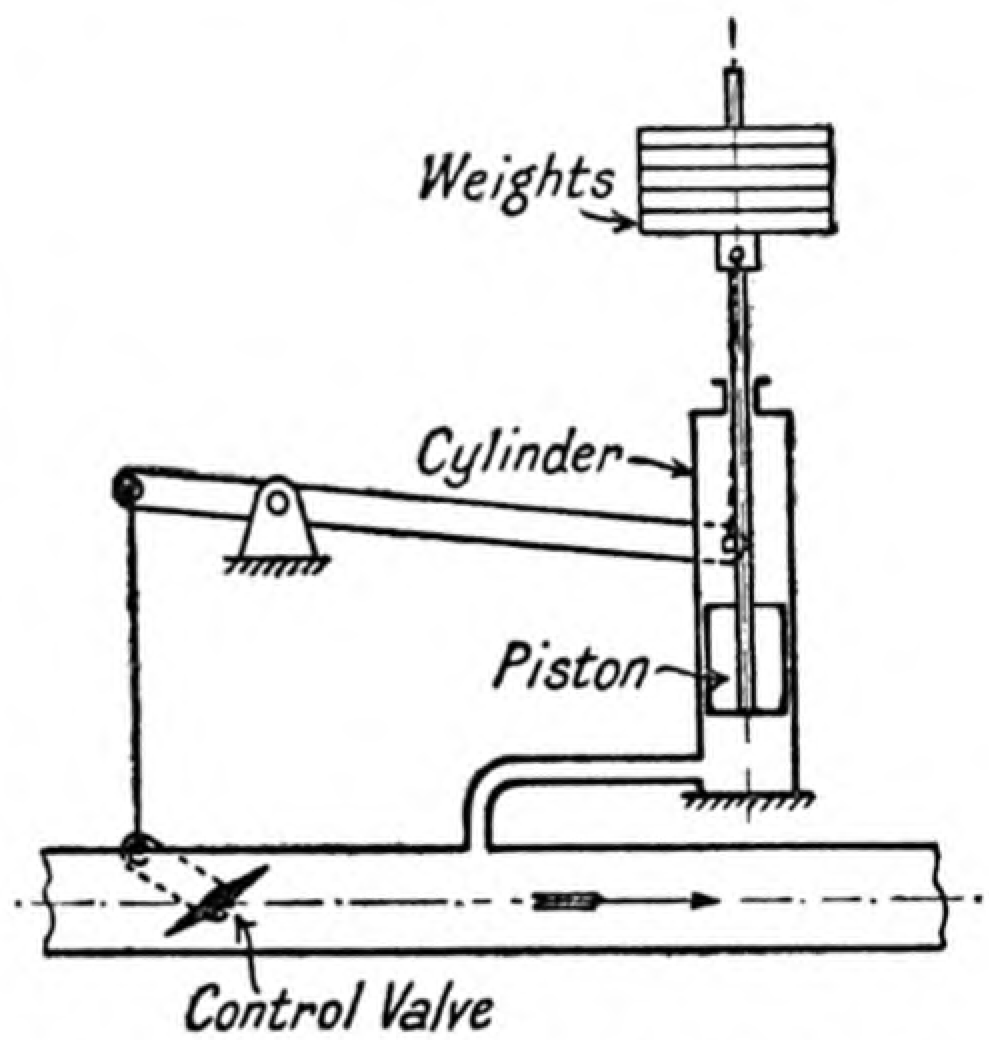

FIG. 210.—Pressure-reducing valve.

have a pressure-reducing valve. Whatever the pressure may be on the upstream side of the valve (within appropriate limits) the pressure on the downstream side will always be the same as the static pressure produced by the load on the plunger or piston; if the downstream pressure rises slightly, the piston also will rise and continue to close the valve until the necessary amount of surplus head is destroyed (§ 92). The intensity of the downstream pressure may be adjusted as desired by adding or removing weights on the piston rod.

212. Overflow Weirs. If there is no objection to spilling water to waste, a long-crested overflow weir is quite satisfactory as a means of maintaining a nearly steady water level. By providing a sufficient number of parallel troughs, the total length of spillway presented by their edges will ensure that a considerable excess of water can be disposed of without altering the water level by more than a few millimetres. Fig. 211

shows a common disposition of such constant-level tanks in a hydraulics laboratory.[136] The discharge of the centrifugal pump

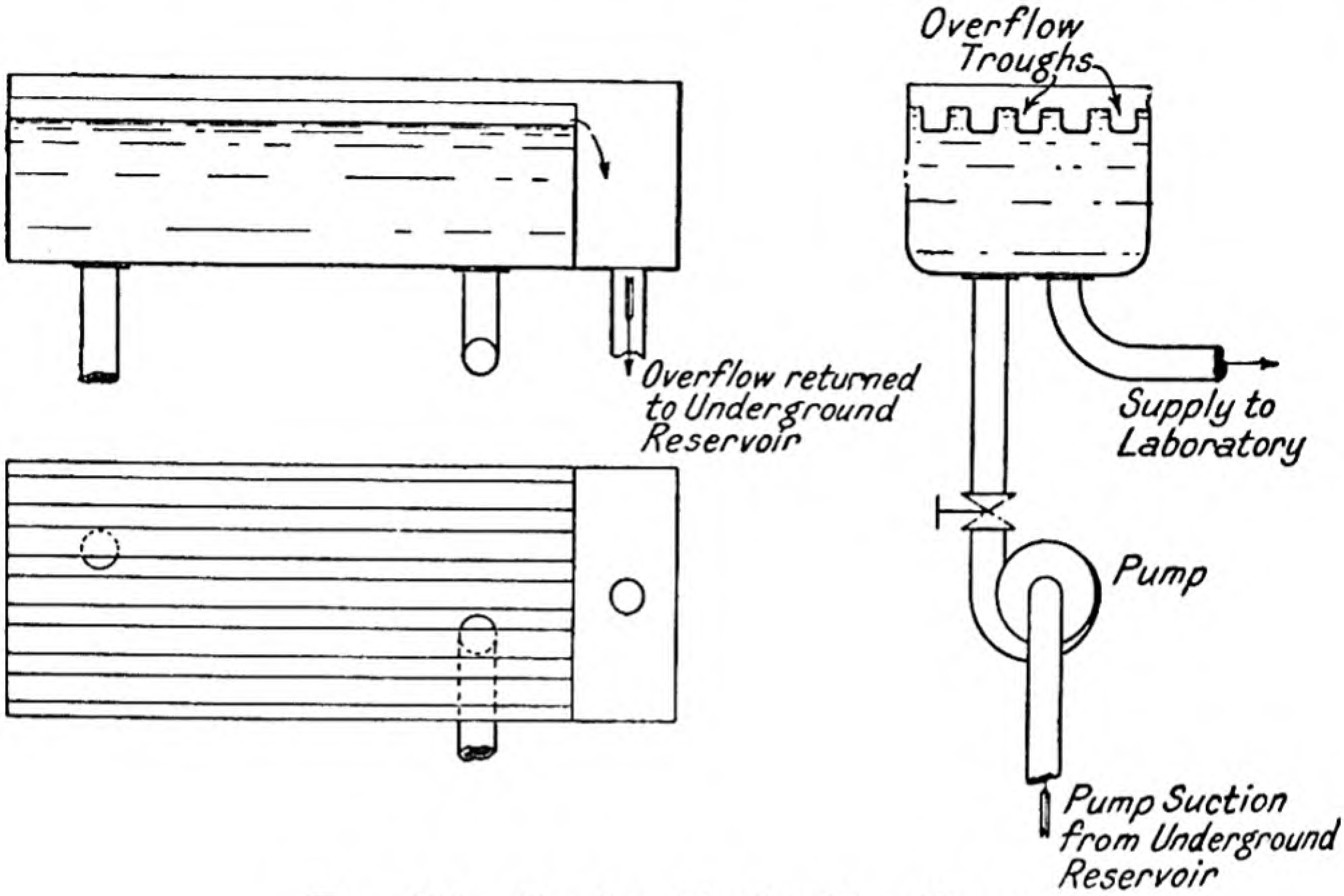

FIG. 211.—Overhead tank with spillway.

is roughly adjusted by hand to give an average rate of overflow, any subsequent changes in the demand of the individual pieces of apparatus merely altering the amount spilled to waste. As the water is continuously circulated, the only actual waste involved is represented by the trifling additional power consumption of the pump motor.

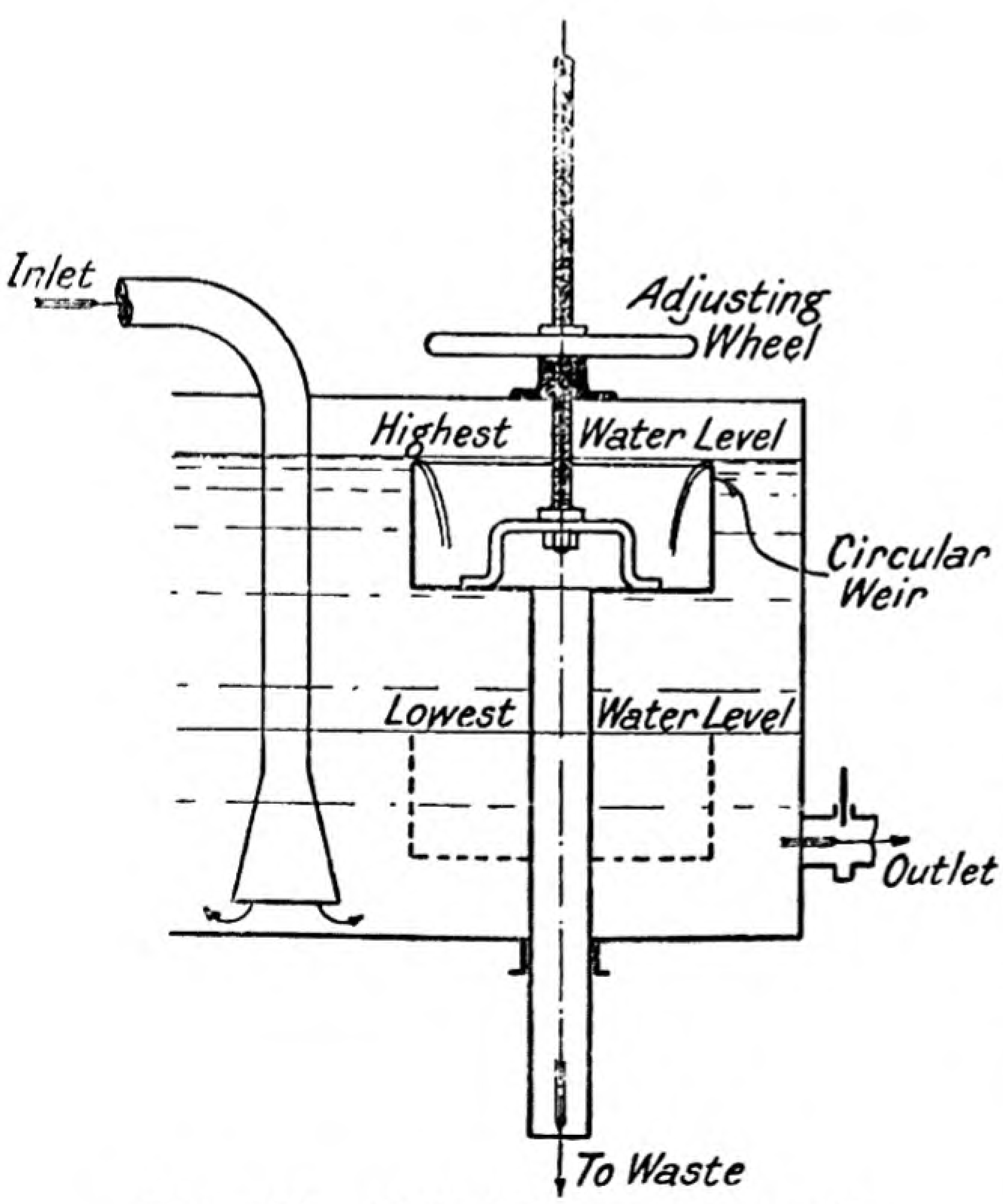

FIG. 212.—Cylindrical overflow weir.

Cylindrical overflow weirs (Fig. 212) may be made adjustable for height; here the surplus water spills over the whole

circumference of the open top cylinder and escapes down the central overflow pipe. (Example 112.)

213. Automatic Weirs. To maintain a uniform level in a canal, irrespective of the discharge, a counterbalanced pivoted weir is sometimes convenient (Fig. 213). The pulleys over which the wire ropes pass are not concentric; they are so designed that when the discharge increases, the momentary increase of static head on the pivoted gate causes it to swing downward just enough to give the required increment of head over the crest without sensibly altering the surface level. Another device serving as an automatic weir has already been described: it is the Drum gate, Fig. 190 (III), § 195.

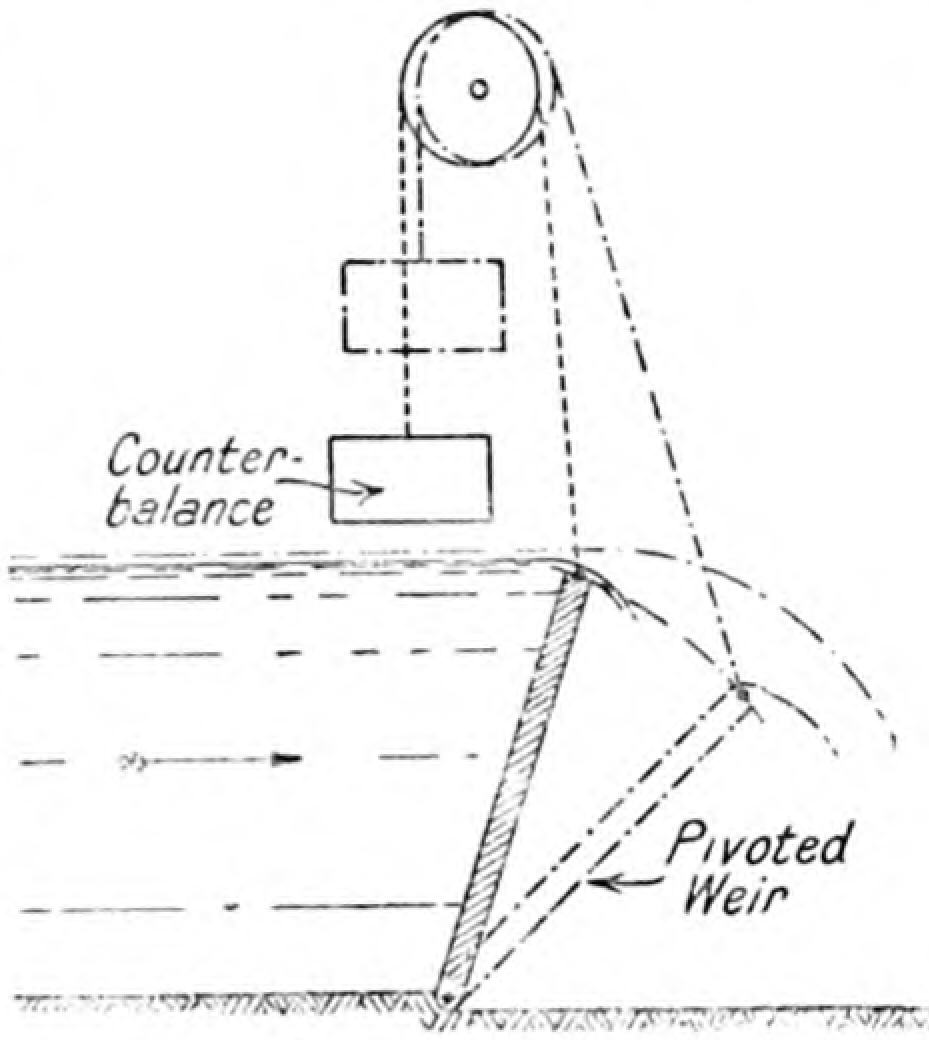

FIG. 213.—Automatic weir.

214. Automatic Siphon Spillways. A siphon spillway consists of one or more pipes, usually of rectangular section, communicating at the upper end with the upstream water

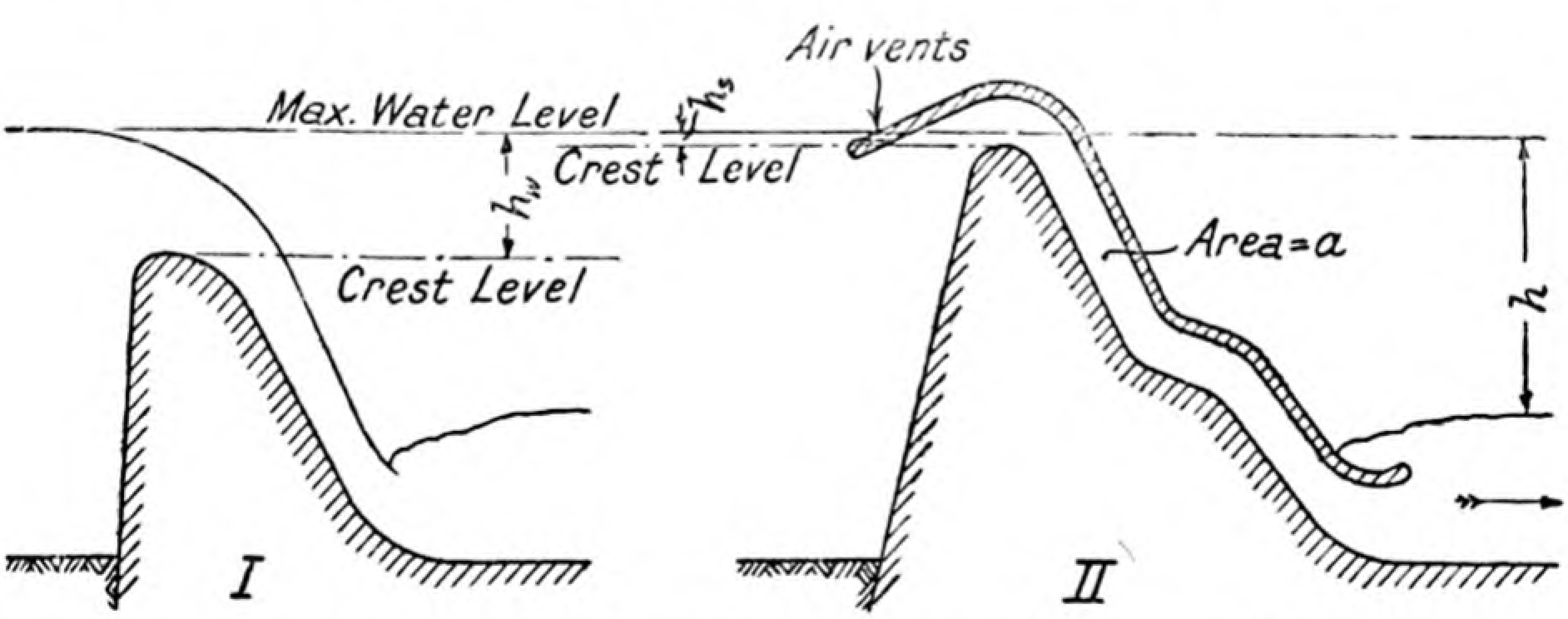

FIG. 214.—Comparison between weir and siphon spillway.

level in a canal or reservoir and at the lower end with the downstream channel (Fig. 214 (II)). It differs from the common siphon mentioned in § 166 by reason of its power of priming itself, without the use of pumps or ejectors—hence its title. The operation of priming is carried out thus: As soon as the upstream water level overtops the inner crest of the spillway, water

begins to flow over and the resulting stream is caused by the kink in the pipe to strike across the passage, so cutting off communication between the air trapped in the crown of the siphon and the atmosphere. Simultaneously, the air begins to be swept away by the stream of water; a partial vacuum is formed at the crown, which increases the rate of flow over the crest, and this augmented stream in its turn hastens the rate of evacuation of air. Quite quickly, therefore, the whole of the air has been swept out, and the siphon is discharging "full bore" under the operating head h.[137]

The purpose of the air vents shown in the diagrams is to permit the siphon to adapt its rate of discharge to the rate at which water is delivered to it by the upstream channel; this it can do either by periodically "de-priming" itself—drawing down the upstream level sufficiently to break the vacuum and throw the siphon out of action—and priming itself again, or by drawing in just enough air to maintain the desired uniform rate of discharge. In a battery of siphons working side by side, the crests and air vents may be arranged at slightly different levels, so that as the upstream level rises, the individual siphons come into action successively and not simultaneously. A much more regular effect is then secured, as most of the siphons are either running full or not working at all.

The advantage of the siphon spillway as compared with a solid weir is clearly shown by the diagrams I and II (Fig. 214). Assuming a stipulated maximum upstream level, the weir crest must be set a distance h_W below the limiting level, where h_W is the head required to carry the maximum discharge over the weir. Consequently as the discharge ranges from zero to its maximum value, the water level will vary through a distance h_W. On the other hand, the variation of level required by the siphon spillway is only h_s. Depending upon the design of the siphon, the depth over the crest h_s necessary to prime it may be no more than an inch or two, or it may be as much as one-third of the height from crest to crown. Other typical forms of siphon are shown in Fig. 215 (III) and (IV).

Regarding a siphon spillway as a curved mouthpiece, its efficiency may be expressed in terms of the coefficient of discharge C_d in the formula $q = C_d a\sqrt{2gh}$, where q is the discharge,

a the area, and h the operating head (Fig. 214 (II)). The value of C_d may range from 0·55 to 0·75 or more.

(**Example 113.**)

In computing the negative head to which the crown of the siphon is subjected,[138] the flow may be assumed—at least provisionally—to follow the laws of free vortex motion (§ 141).

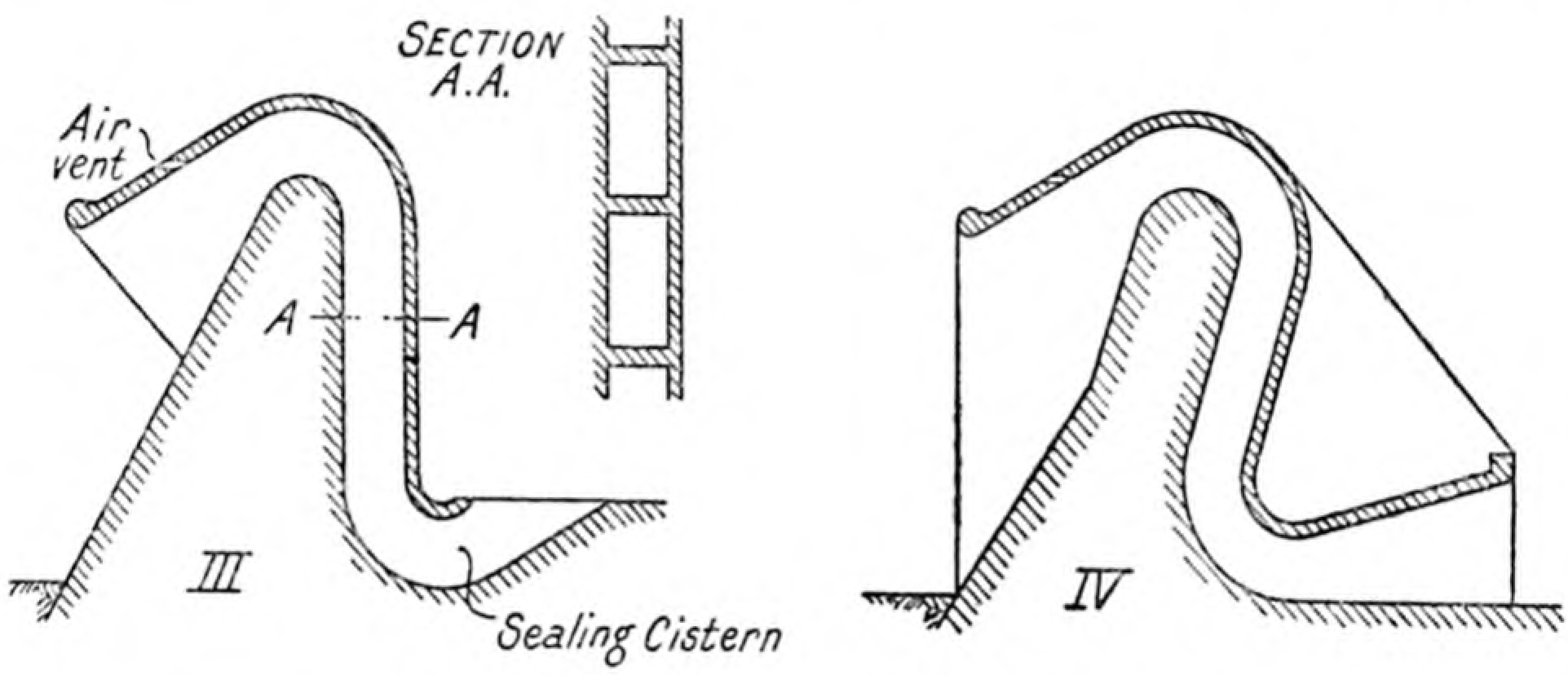

FIG. 215.—Types of siphon spillway.

215. Methods for Securing Constancy of Discharge. Any device that maintains an unvarying water level can be adapted to give a constant rate of discharge. For example, a given setting of the outlet valves in Figs. 209, 211 and 212 will ensure constant flow through them so long as the level-regulating system continues to work, and so long as the water is discharged into the atmosphere or against a uniform head. A simple apparatus that will yield a steady discharge with a *varying* water level is shown in Fig. 216 ; it is sometimes known as Mariotte's bottle. It consists of an air-tight receptacle having a calibrated orifice in its base and an adjustable air pipe projecting downwards through the top. After the vessel has been filled with liquid and the filling plug closed, the fall in surface level as the liquid escapes through the orifice will soon lower the pressure of the residual air to the point at which atmospheric air enters by the air pipe and bubbles up through the liquid.

This implies that the liquid in the plane AA passing through the lower end of the air pipe is at zero pressure above atmosphere, and thus that the orifice is discharging under a head h. So long as the air is allowed to enter freely, the operating head will remain fixed, and with it the discharge $q = C_d a\sqrt{2gh}$.

The rate of discharge can be altered as required by pulling out or pushing in the air pipe.

Both this device and the floating siphon shown in Fig. 217 are well suited for the duty of feeding small quantities of salt solution or the like at a predetermined and constant rate.

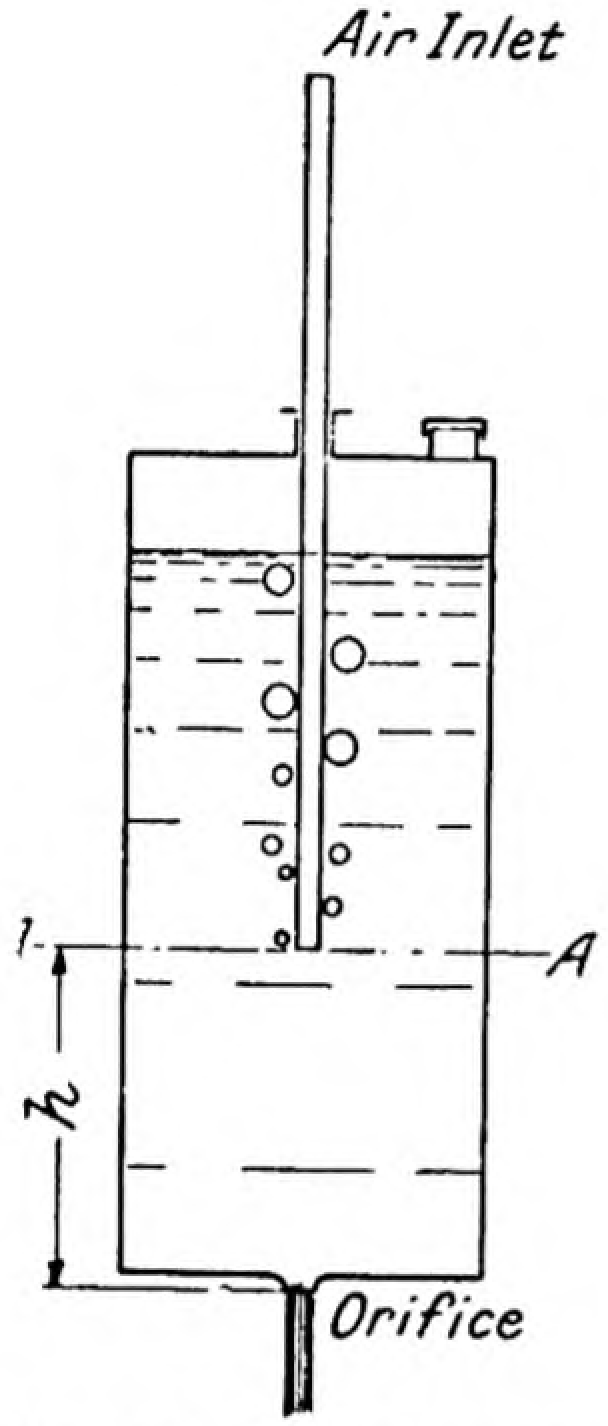

FIG. 216.—Constant discharge apparatus.

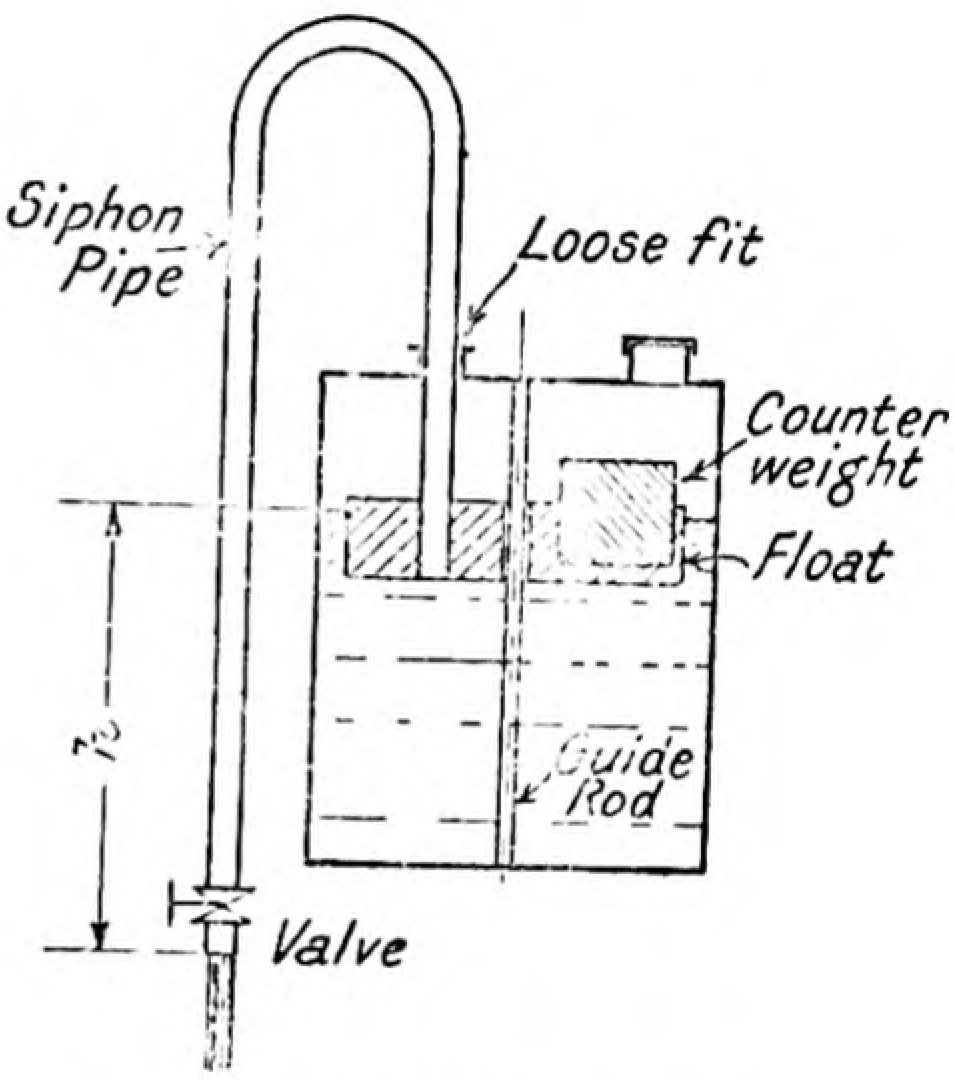

FIG. 217.—Floating siphon.

The operating head of the siphon h is not affected by the descent of the float; the discharge can be set to the desired figure by regulating the valve. This apparatus has the advantage that the reservoir can be replenished periodically without disturbing the flow.

216. Automatic Regulation of Flow in Closed Conduits. When a liquid is flowing along a closed pipe in which the *pressure* at any point may vary in an unpredictable manner, nevertheless the principle of constant area and constant head may still be utilised to ensure a constant *rate of flow*. But now it is an artificially-created *differential* head that is to be held under control. If, for instance, we insert in the pipe an orifice or pierced diaphragm as shown in Fig. 69, § 87 (d), or a Venturi tube (§ 387), and if we can contrive to keep the head loss h_L at a pre-determined figure, then the velocity v and discharge q must necessarily remain steady. As the

differential head h_L may be comparatively small, possibly it will be insufficient to operate the control valve directly, as in Fig. 210; a hydraulic servo-motor, § 356, may therefore be interposed as in Fig. 218.

Pressure-oil from a suitable source (§ 353) supplies the energy for moving the main control valve in the pipe; the differential oil-pressure acting on the servo-motor piston is itself regulated by a small escape valve A directly coupled to a pilot piston working in a small pilot cylinder. The differential pressure generated in the main pipe only has to do the work of moving the pilot piston and the oil-escape valve A. Under steady conditions of flow the load on the pilot piston is balanced by the tension of a control spring; by regulating the tension the flow can be set to the desired value.

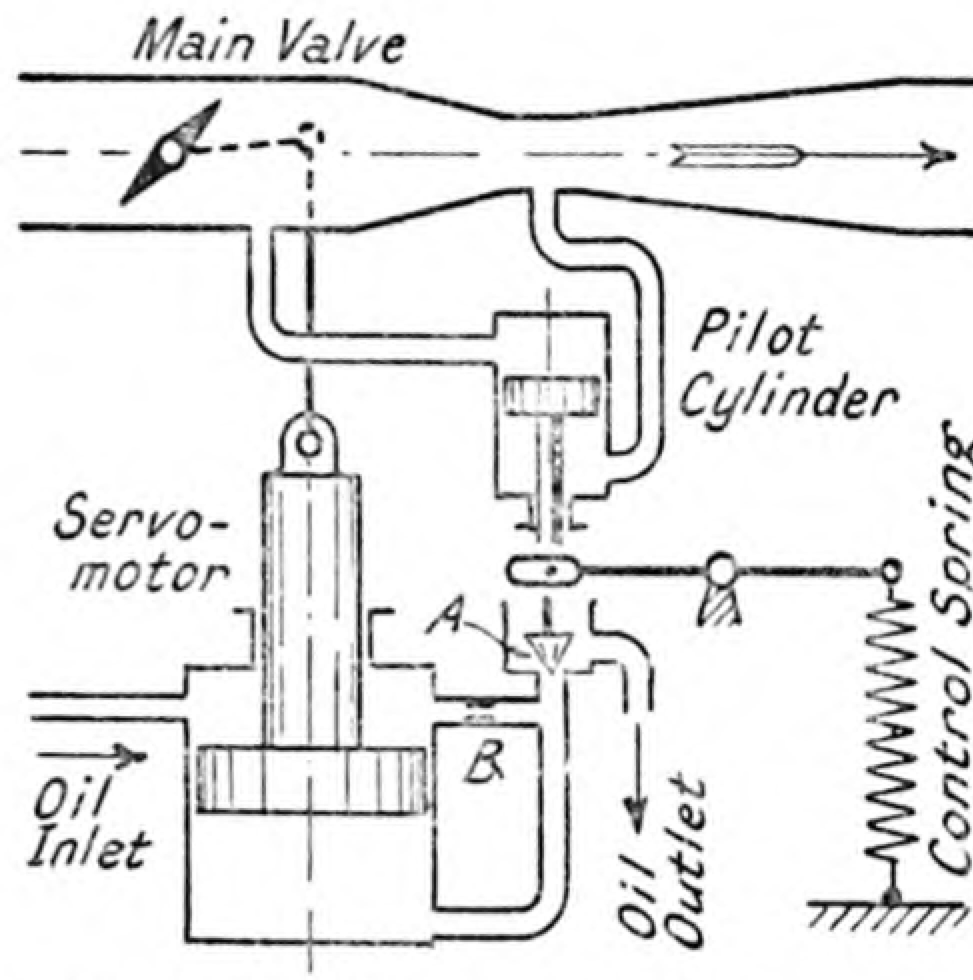

FIG. 218.—Flow-controller in pipe.

If a rise in pressure in the main pipe, upstream of the control valve, tends to increase the flow through the main valve, the augmented differential head acting on the pilot piston momentarily overpowers the spring tension. The resulting downward motion of the piston slightly closes the oil-escape valve, thereby causing the oil pressure to build up beneath the servo-motor piston, which responds by rising and reducing the opening past the main valve. A pressure drop in the pipe will initiate an opposite train of movements. The purpose of the throttling orifice B is to establish the necessary pressure-difference between the upper and lower sides of the servo-motor piston during steady conditions.

217. Modules. A module is an apparatus which maintains a uniform rate of discharge when water flows through it from one channel to another channel at a lower level, irrespective of the drop in surface level. A module using the principle of the standing wave, but necessitating a fixed upstream level, is shown in Fig. 219. It is found that if the height of gate

opening D is about 0·4 times the upstream depth d_u, then the downstream head above the bottom of the gate, $(d_d - D)$, may be as much as 60 per cent. of the operating head h before the standing wave breaks down. So long as this figure is not exceeded, the discharge will be quite independent of the downstream depth. The discharge can be varied if desired by adjusting either the upstream depth or the gate opening. In estimating the discharge from the first of the two formulæ given in § 194, the value of n for the gate with a rounded base will be 1·0, and the value of C_d will be very little short of unity.

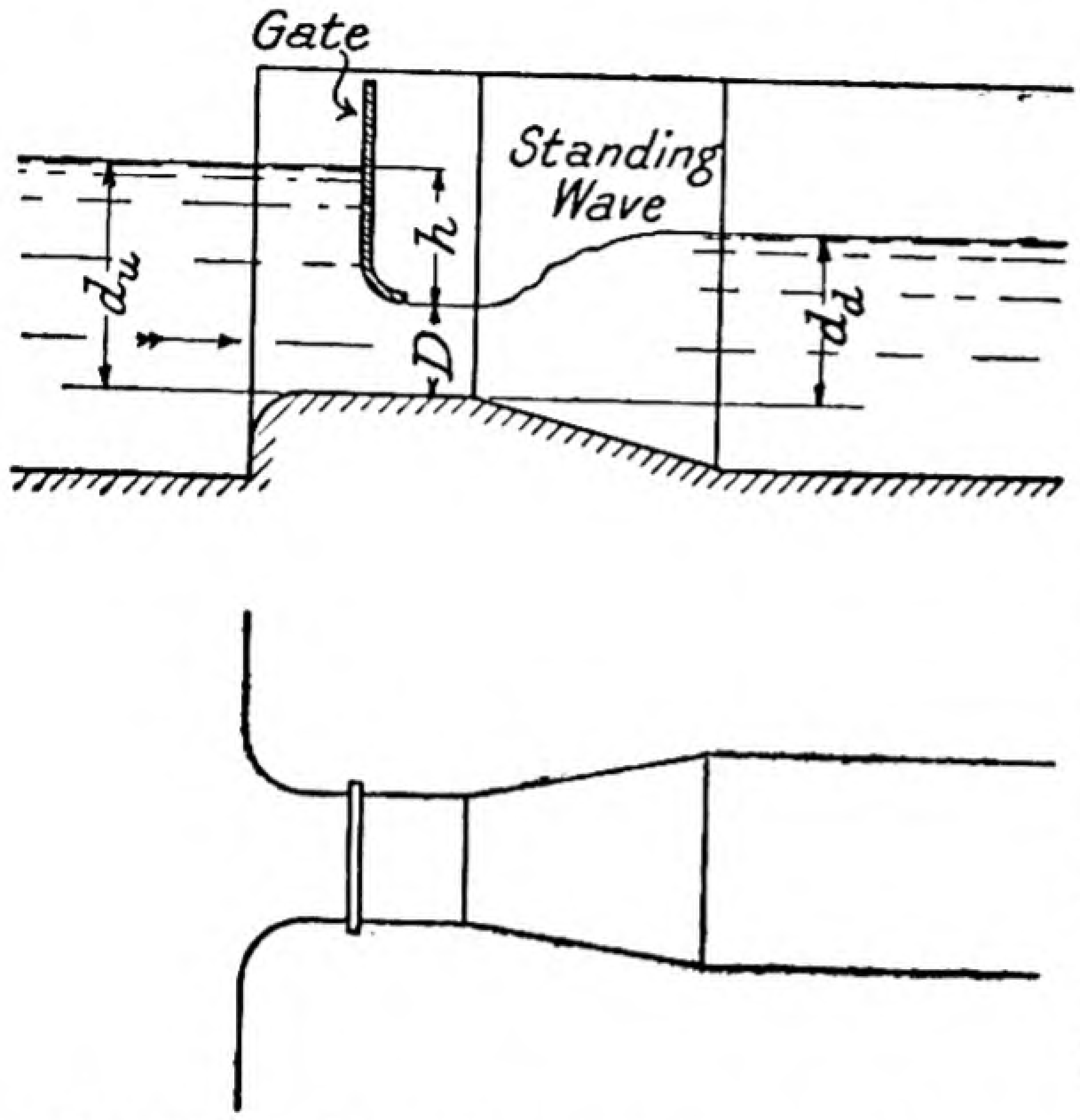

Fig. 219.—Standing wave semi-module.

For maintaining constancy of discharge with varying *upstream* levels and steady *downstream* levels, float-operated modules have been used (Fig. 220). Type I is provided with a tapered needle or plug suspended from the float, moving with the necessary clearance through an orifice plate; as the upstream level rises, the area for flow between the plug

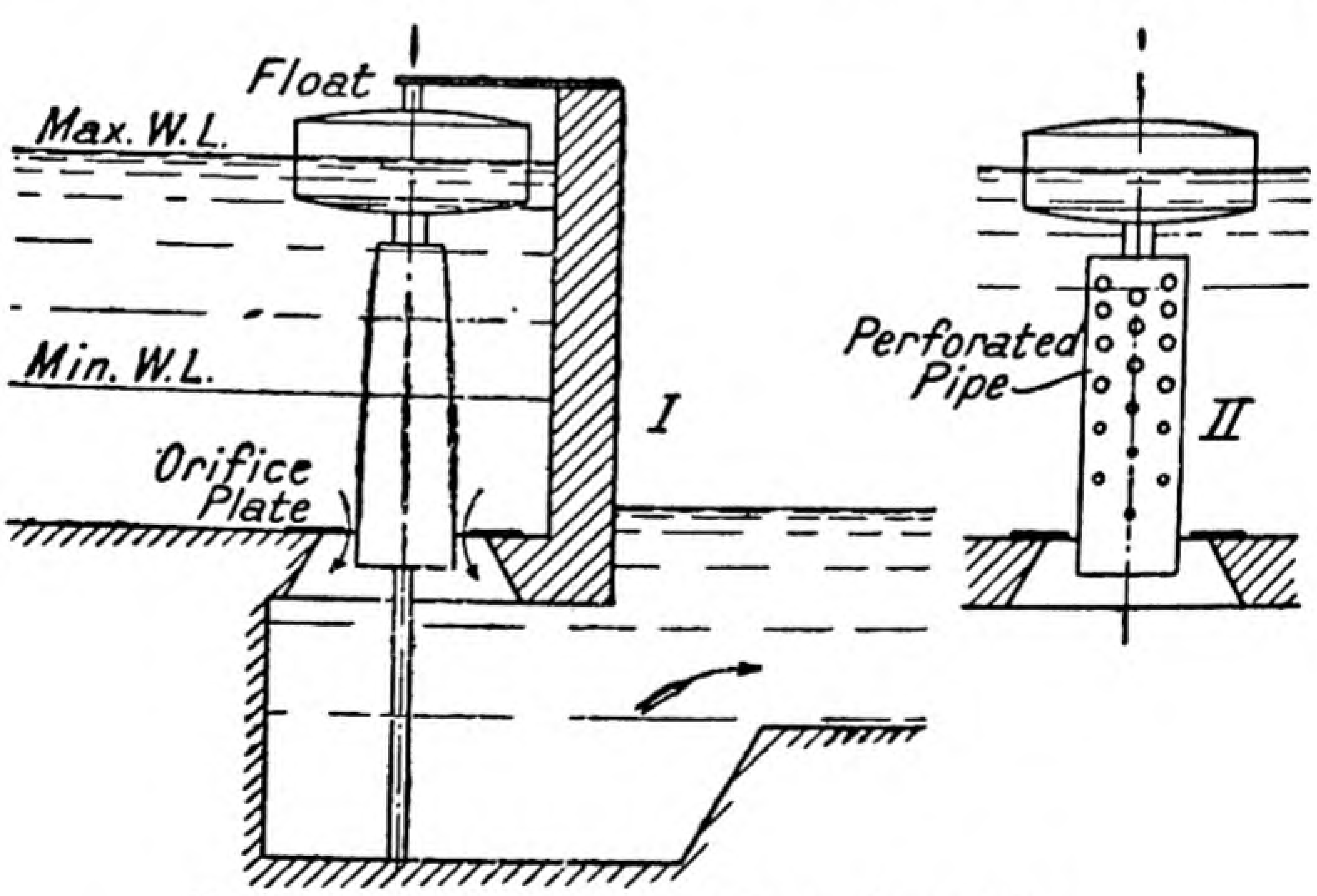

Fig. 220.—Float-operated semi-modules.

and the plate diminishes in just the right ratio to keep the discharge unaltered. Type II is cheaper to make: here the needle takes the form of a piece of parallel pipe, closed at the bottom and open at the top, having suitably spaced holes drilled through its cylindrical surface. When the float is at the top of its travel, the water can pass only through the annular space between the pipe and the main orifice. As the upstream head diminishes and the float falls, the water is now enabled to flow as well through the perforations that have passed below the plane of the orifice plate, so that again uniformity of discharge is secured.[139]

In the precise meaning of the term, none of the devices just described can claim to be called *modules*—they are really only *semi-modules*, for they can maintain constancy of flow only if the upstream *or* the downstream level is kept steady by some external means. But by combining a floating needle to take charge of variations in the upstream level, and a standing wave orifice to attend to the downstream level, a full module could be obtained, capable of controlling the discharge independently of both upstream and downstream levels. It should be explained, though, that as modules are usually required in practice to regulate the distribution of irrigation water, the conditions of service are severe, and engineers are rightly disposed to mistrust any form of apparatus for this duty that involves moving parts.

CHAPTER XII

HYDRAULIC MACHINES

218. Definitions. In the most general sense, one might expect that the term Hydraulic Machines would include any mechanical contrivance adapted to the flow of liquids. But in this book, and indeed amongst most engineers, the expression has a more restricted meaning: it is used to designate machines that serve to interchange *energy* between the moving parts of the apparatus and the liquid flowing through it. The hydraulic machine is in essence an energy converter: it converts or transforms hydraulic energy into mechanical energy, or mechanical energy into hydraulic energy.

Specific groups of hydraulic machines are named according to the direction of the energy interchange, thus :—

(i) If *hydraulic energy* is converted into *mechanical energy*, then the machines are known as

Hydraulic turbines or *hydraulic motors.*

(ii) If *mechanical energy* is converted into *hydraulic energy*, then the machines are usually known as

Pumps.

It may sometimes happen that a single machine will serve either as a motor or as a pump, depending upon the direction of flow and of rotation : but more often distinct machines are designed each for a specific purpose.

219. Hydraulic Principles Involved. Various paragraphs in Part I of this book have shown how the energy of liquids may be transferred to or from a series of revolving vanes, blades, or buckets, e.g. §§ 123-125, § 144. In all such devices the essential point of the process was the generation or absorption of torque on a revolving shaft, as a result of changes in the *angular momentum* of the liquid.

There are also other methods of energy interchange. Here it is the pressure energy of the liquid that is influenced. In the example indicated in Fig. 221, a piston or the like is shown sliding within a cylinder. If the plunger moves a distance l under a force P, then ideally the energy transferred to the liquid is $P \cdot l$, and the increment of energy *per unit weight of liquid* is p/w, where p is the increase in pressure. On a working scale the process is identical with what was described on an infinitesimal scale in §§ 25, 27.

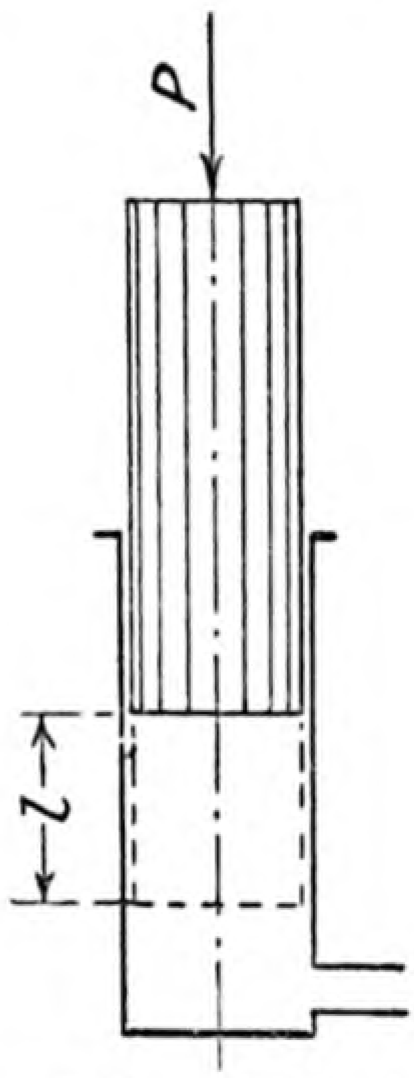

FIG. 221.—Hydrostatic machine.

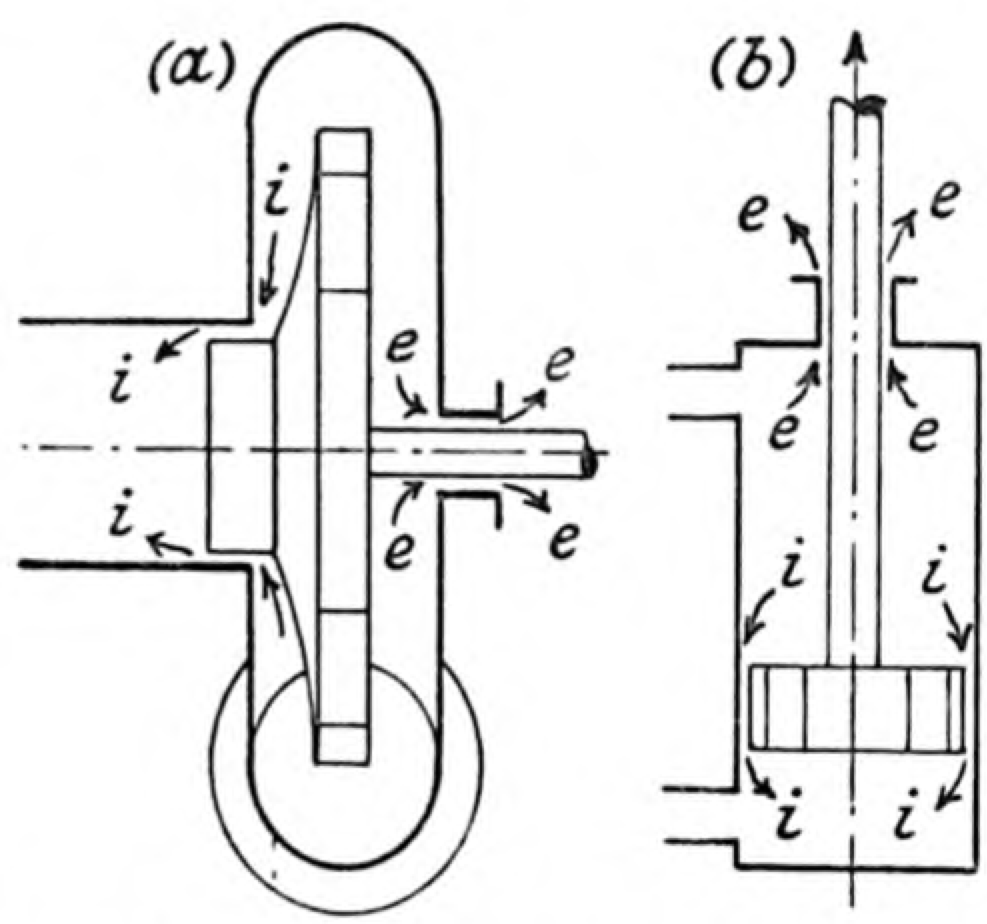

FIG. 222.—Leakage paths in (*a*) Rotodynamic machine, (*b*) Hydrostatic machine (*ii* = internal leakage, *ee* = external leakage).

Symbolically, these two main categories of hydraulic machines are depicted in Fig. 222. Those depending upon changes of angular momentum within the passages of a revolving wheel or *rotor* are known as *Rotodynamic* or *Hydrokinetic* or *Turbo* machines; [140] those that involve a direct thrust upon the liquid or displacement of the liquid are termed *positive* or *positive-displacement* or *Hydrostatic* machines. Some examples of the two types that are discussed in later chapters are :—

Rotodynamic.

Hydraulic turbines.
Centrifugal pumps.
Propeller pumps.
Hydraulic torque-transmitters and converters.

Positive-displacement.

Reciprocating pumps.
Positive rotary pumps.
Positive hydraulic motors.
Hydraulic presses, hydraulic machine-tools, etc.
Weight-loaded hydraulic accumulators.
Oil-pressure servo-motors.

These categories are not wholly comprehensive. Sometimes the engineer finds it convenient to use still other principles of energy transfer in which compressed gases may be employed, or in which energy is transferred directly from one liquid to another.

220. Basic Efficiency of Hydraulic Machines. The efficiency of any machine can be expressed in the form :—

$$\text{Efficiency} = \frac{\text{energy output}}{\text{energy input}} = \frac{\text{energy input} - \text{energy losses}}{\text{energy input}}.$$

In hydraulic machines the input and output are usually stated in terms of power or horse-power, and on this basis it is the *gross* or *overall efficiency* that concerns us. It is denoted by the symbol η_m.

The *mechanical* energy input or output will be represented by the horse-power delivered to or taken from the revolving shaft or other element of the machine.

The *hydraulic* energy input or output will have the form

$$\frac{Wh}{K_p}$$

where W denotes the weight of liquid per second flowing through the machine,

h denotes the change in total energy the liquid experiences in passing through the machine.

K_p denotes the horse-power constant, or energy per second corresponding to one horse-power.

The total energy h implies the total energy per unit weight computed as in § 33; the term relates only to the change of energy in the machine itself, which may not be the same as the overall change in the entire hydraulic system, §§ 260, 285.

Applying these general expressions to a pump, for instance, in which W is given in pounds per second and h in feet head, then $K_p = 550$ foot-lb. per sec., and

$$\eta_m = \text{Overall efficiency} = \frac{\text{Mechanical input} - \text{losses}}{\text{Mechanical input}}$$

$$= \frac{\text{Hydraulic output}}{\text{Mechanical input}} = \frac{\dfrac{Wh}{550}}{\text{Horse-power input}}.$$

The performance of *positive-displacement* machines may be also assessed in another way :—

The *volumetric efficiency* of such a machine is the ratio

$$\eta_v = \frac{\text{true or measured volume discharged per second}}{\text{swept volume or displacement volume per second}}.$$

Ideally, this ratio would have the value unity, corresponding to an efficiency of 100 per cent., if the working chambers of the machine were completely filled and emptied during each cycle, without any leakage or losses of any kind.

221. Types of Energy Loss. The highest possible efficiency of a hydraulic machine, as of any other machine, can only be realised if the energy losses are carefully analysed and reduced to their lowest limit. In a hydraulic machine the major losses can be included under the headings :—

(i) *Mechanical loss.* This includes so-called mechanical friction between fixed and moving parts, e.g. rubbing or sliding friction between a rotating shaft and its bearing.

(ii) *Disc friction.* In rotodynamic machines, energy will be dissipated by hydraulic friction between the liquid and the rotating faces of the wheel or rotor, § 148.

(iii) *Leakage loss.* If liquid escapes or leaks from a high-pressure zone of the machine to a low-pressure zone, it will carry with it energy which is subsequently wasted in eddying.

(iv) *Hydraulic losses.* While the liquid is flowing through the fixed or moving passages of the machine, it will be subject to the type of wall friction loss or eddy loss described in Chapter V. There is a possibility, too, that when the liquid leaves the machine it may take with it considerable quantities of velocity energy which cannot afterwards be recovered : this energy also is wasted.

These various types of energy dissipation will later be studied in connection with particular machines ; at this stage, leakage losses will be discussed in general terms, because of

the preponderant influence they often have on the performance of the machine. Although it is true that the distinction between the various losses is only an arbitrary one—for types (ii), (iii) and (iv) could all be classified as "hydraulic"—yet the distinction is permissible and useful.

222. Control of Leakage. On examining the disposition of the parts of typical hydraulic machines, Fig. 222, we observe that the leakage paths are of two kinds: there may be internal leakage or external leakage. In the rotodynamic machine, diagram (*a*), liquid will try to leak from the outer to the inner part of the stationary casing, and in the positive machine, diagram (*b*), the liquid will try to pass from one side of the piston or plunger to the other. Although the resultant waste of energy will be undesirable, there is no actual loss of liquid: indeed, while the machine is working there is nothing to show that leakage is occurring at all. But external leakage, e.g. past the shaft of the rotodynamic machine or the piston rod of the positive machine, is doubly troublesome, because we lose both energy and liquid. If the liquid should be valuable or noxious, the problem of recovering it or disposing of it may be quite awkward. Should the pressure inside the casing of the machine be sub-atmospheric, the resulting leakage—leakage of *air into* the casing—might still be objectionable.

For these two types of problem, two solutions are available. They may be classified as *hydraulic seals* and *contact seals*, and they represent two aspects of the compromise that always has to be resolved in such conditions.[141] The nature of the compromise is this: if we allow the smallest possible clearance between the fixed and moving parts of the machine—if we make them fit as closely as possible—then the leakage may certainly be small, but on the other hand the mechanical friction loss may be considerable. At the opposite extreme we may decide to allow no metallic contact whatever: no risk of mechanical friction will be accepted: and a small but controlled leakage flow will take place.

(i) *Hydraulic seals.* The principle of hydraulic seals—those which permit a small quantity of liquid to leak—has been explained in § 92. To minimise the flow, the clearance between the parts is kept as small as can be contrived without risk

of metallic contact, and perhaps some kind of labyrinth is arranged to give additional hydraulic resistance. Manifestly hydraulic seals are well suited for the control of internal leakage; in large rotodynamic machines no other method would be feasible.

(ii) *Contact seals.* In one type of contact seal, some kind of soft or at least flexible packing is used: in the other, contact is permitted between rigid, fixed and moving sealing surfaces.

223. Contact Seals. (*a*) *With flexible packing.* Some representative examples of packing are shown in Fig. 223.

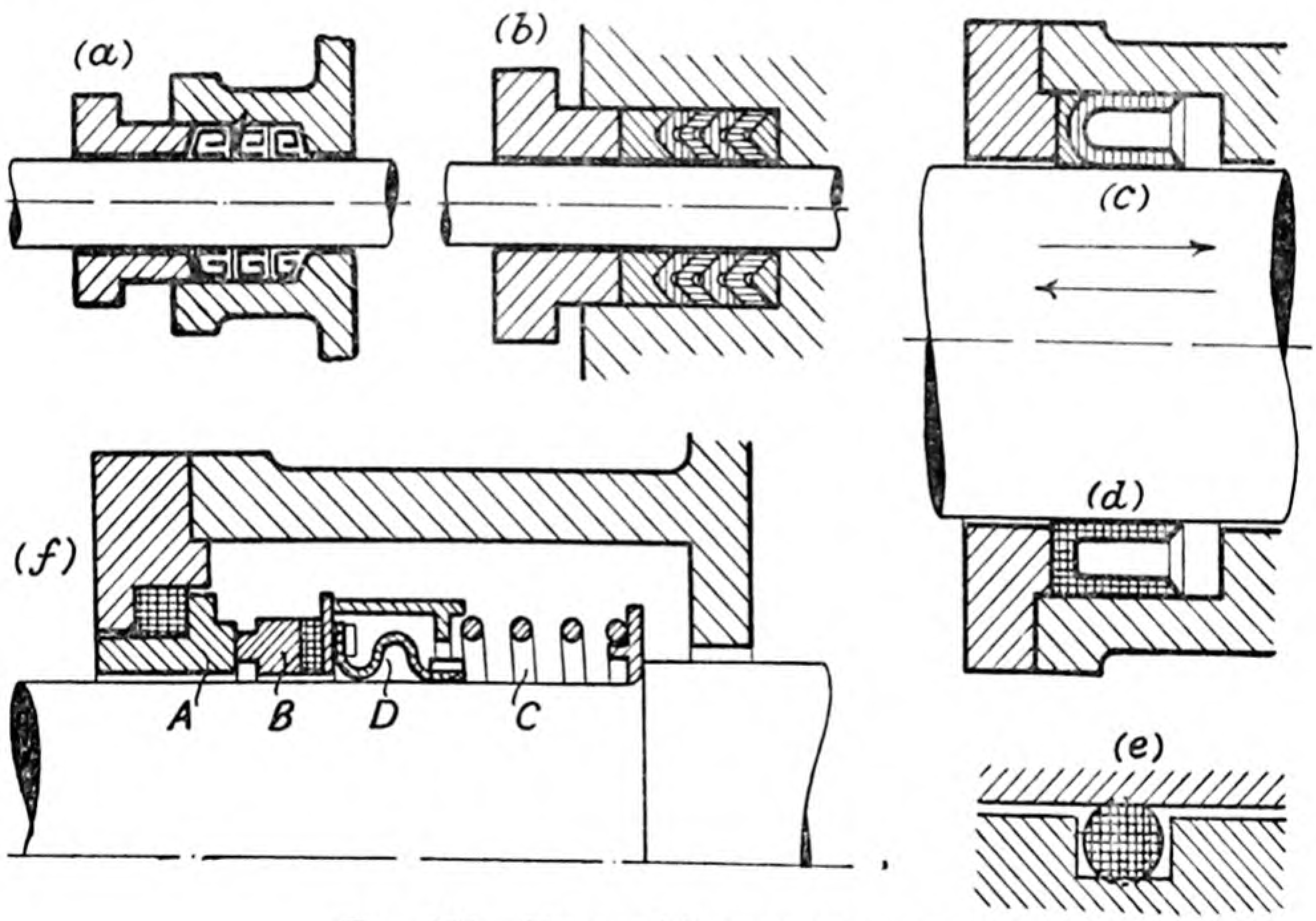

FIG. 223.—Types of " contact " seals.

Cotton or similar fibrous material is used at (*a*); it is housed within a stuffing-box and can be compressed by tightening the nuts of the gland.(142) For higher pressures, higher rubbing speeds or higher temperatures, various kinds of moulded rings are available, usually having synthetic rubber as a basis, and reinforced by asbestos, " plastic " compounds, or metal foil. In the packing shown in Fig. 223 (*b*) the rings are of " V " section, with the intention of providing a seal at each circumferential sharp edge. A packing-ring of " U "-section, as in Fig. 223 (*c*), has the advantage that it is self-tightening: the pressure of the liquid itself forces the lip of the ring into close contact with the revolving or sliding element

of the machine. When formed of leather, the "U" packing and its fellows have given excellent service for many years in various forms of high-pressure slow-speed hydraulic machinery, and a slight modification permits the principle to be adapted to the more exacting conditions of to-day. The packing-ring is bonded and moulded from reinforced rubber, preferably with a flat base as in Fig. 223 (*d*).

For small high-speed shafts, or for larger slow-speed shafts, a single moulded rubber ring may suffice, Fig. 223 (*e*), adapted to give an "interference" fit: its original internal diameter is less than the shaft diameter. Whatever form of flexible packing may be chosen, it may be necessary to adapt its composition to the character of the liquid flowing through the machine, e.g. natural rubber will serve for one kind of oil but synthetic rubber must be used for other kinds.

(*b*) "*Mechanical*" *seals.* Chosen exclusively for external sealing, these are used when the sealing device must run for very long periods without attention or adjustment, and when the loss of liquid past the seal must be brought down to its very lowest limit—which may be no more than a few grams per thousand hours of running.[143] Rigid but flexibly-mounted sealing members are relied upon, finished to the highest possible degree of accuracy. In the diagram, Fig. 223 (*f*), the stationary sealing face *A* is supported by a rubber ring; working against it is the rotating sealing ring *B* which is held up to its work by a helical spring *C*. A flexible bellows of synthetic rubber, *D*, keeps the rotating assembly liquid-tight. Depending upon the character of the liquid flowing through the hydraulic machine, the two sealing elements may be respectively of cast-iron and carbon, or steel and bronze.

In all types of so-called "contact" seals, the word is used in a descriptive sense only: they can only give continuous service if the rubbing faces are lubricated in some way or other, either by the liquid of the machine itself, or by a special supply.

224. Some General Constructional Problems. The casing or stationary element of the hydraulic machine as a whole should manifestly have the necessary mechanical strength to enable it to resist the internal pressure of the liquid, § 21. If the pressure is high, additional stiffness as

well as strength may be required, otherwise the elastic deformation of the metal may impair the fine clearances that internal "hydraulic" seals demand, § 222 (*i*). This might result either in excessive leakage, or in metallic contact, and rapid wear. In such conditions, likewise, the revolving shaft and the bearings should be of unusual stiffness to guard against inadmissible deflection. "Contact" seals, too, can only remain serviceable if the rubbing surfaces are given the highest quality of surface finish and if they move truly and without vibration. As for the hydraulic energy losses that the main flow of liquid may suffer, especially in rotodynamic machines, these can be kept within bounds by careful design of the passages of the fixed and rotating elements of the machine.

Another series of problems is linked with the effect of the liquid upon the internal components of the machine. If only clear, cold water flowed through the machine, inexpensive materials such as cast iron might be perfectly suitable; but if the liquid were hot oil, or corrosive acid, or water heavily charged with sand or gritty solids in suspension, § 11, much more resistant metals will be demanded. Nor are these chemical or mechanical attacks the only ones that the internal parts of the machine may be called upon to resist: there may be the risk—sometimes a quite serious risk—of cavitation erosion, § 134.

Manufacturing technique is therefore stretched to its widest limits in dealing with the immense diversity of engineering equipment that falls within the description of hydraulic machine. In regard to weight and bulk and the control of very great forces, the upper limit is found in hydraulic turbine units of 150,000 h.p., and in rotodynamic pumps of 65,000 h.p. At the moment, it is not economically practicable to construct machines of greater sizes than these. At the opposite extreme we encounter the problem of devising routine workshop procedure which will guarantee the working clearances of 0·00005 inch that form the "hydraulic" seals of small, high-speed hydraulic pumps and motors. Still more exacting control is needed to produce the working surfaces of mechanical seals, § 223 (*b*) which must be optically flat within a few micro-inches.

CHAPTER XIII

HYDRAULIC TURBINES: (I) CONSTRUCTION

225. Hydraulic Motors and Hydraulic Prime Movers. These are machines for converting the energy of liquids into mechanical energy (§ 218). If the liquid has acquired its energy by natural means, e.g. by reason of its geodetic elevation above the machine, then the machine will be a true prime mover. Since in general the hydraulic energy may exist in the form of potential energy, pressure energy, or velocity energy (§ 33), or of any combination of these, then the machines may be classified according to the preponderating type of energy that they utilise, thus :—

(i) *Gravity machines.* Here it is position or potential energy that is extracted from the water; the liquid undergoes only minor changes in pressure or velocity. In the *overshot water-wheel*, Fig. 224, the weight of the water contained in the *buckets* exerts a torque and thus enables power to be continuously delivered from the shaft. As the effective fall is h, the maximum proportion of the total available energy H can only be converted if the wheel diameter is as nearly as possible

equal to this gross fall H. This restriction limits the output of such machines to a few score horse-power, and consequently they have been almost wholly superseded by turbines.

(ii) *Pressure or hydrostatic machines.* These machines impose little change on the elevation or on the velocity of the liquid flowing through them, but there is always a drop in pressure—sometimes a drop of hundreds of atmospheres, § 219. As these machines nearly always form the receiving element of a hydraulic transmission system, they are described in the appropriate chapter of this book, Chapter XVIII.

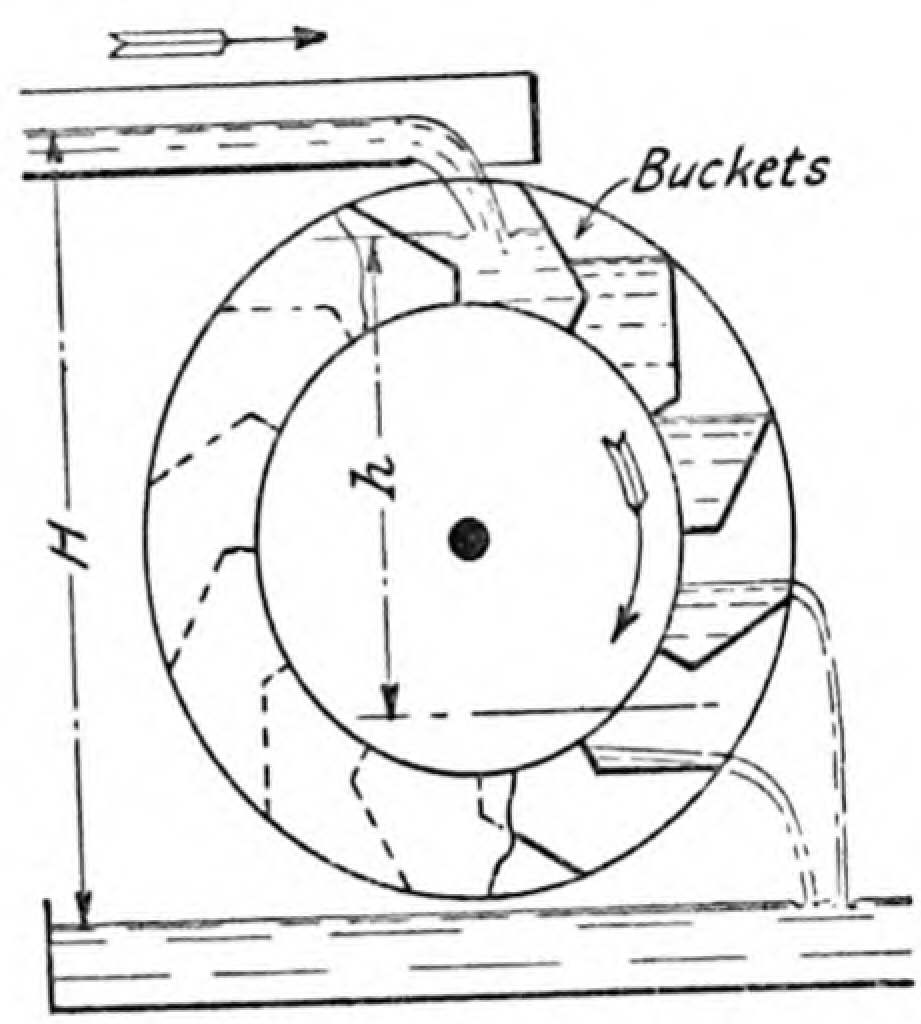

FIG. 224.—Gravity motor (overshot water-wheel).

(iii) *Velocity* machines which in some way or other abstract the velocity energy of water are known as *hydraulic turbines* and they form the subject-matter of this chapter and the following one.

The history of hydraulic prime movers probably goes back thousands of years; but it is the improvements in their design during the past 130 years, together with the contemporaneous advances in electrical engineering, that have made possible the great hydro-electric developments that have so notably assisted modern industry and transport.(144)

Note.—The term *hydraulic motor* is rarely used in the general sense attached to it in this paragraph. Usually it is reserved for pressure machines only ((ii), above).

According to English usage, a *water-wheel* is a small slow-speed machine of the type shown in Fig. 224, but in America the term water-wheel embraces all kinds of hydraulic turbine.

226. Hydraulic Turbines and their Classification. Before reaching a turbine, the water which feeds it must first pass through some kind of inlet passage in which the original store of potential energy is converted into pressure energy. In the turbine itself further transformations occur. (i) While flowing through the *guide apparatus*, the water is forced to increase its velocity and thus to acquire velocity energy at the expense

of pressure energy. (ii) The resulting quickly-moving streams of water then impinge on the vanes or blades of a revolving *wheel* or *runner*, and it is while doing so that nearly all their energy is abstracted and taken up by the wheel, for subsequent delivery at the turbine shaft. In passing through the guide-apparatus, then, the water invariably undergoes an *increase* in its tangential velocity or whirl component. In the wheel or runner, this whirl component is as nearly as possible *destroyed*, dynamic thrust being thereby generated on the blades in the manner explained in §§ 123-125, 143, 144.

Impulse or *free-jet* turbines are those in which the water leaves the guide-apparatus at atmospheric pressure ; the whole of the available pressure energy has been transformed into velocity energy, and there can thus be no further changes in pressure. The wheel revolves freely in air.

In *reaction* or *pressure* turbines, only a part of the pressure energy is converted in the guides into velocity energy ; a further drop in pressure takes place in the runner also, and there may also be re-conversions of velocity energy into pressure energy after the water leaves the runner. All the turbine passages, both fixed and moving, are completely full of water ; atmospheric air has no access to them.

The type of impulse turbine predominantly used at present is the *Pelton Wheel ;* it is suitable for a range of heads of about 500-5500 feet.

Reaction machines are represented by the *Francis* turbine, the *Propeller* turbine, and the *Kaplan* turbine, which between them cover a range of heads from about 1000 feet down to 10 feet.

The factors which influence the choice of turbine from among these types are summarised in § 283.

227. The Pelton Wheel. The guide-apparatus of this machine (Fig. 225) consists of one or more nozzles each adapted to project on to the runner a jet of circular cross-section ; the rim of the wheel is provided with ellipsoidal blades or *buckets* of the characteristic shape shown in Figs. 225, 226 and 232. After leaving the wheel, the water falls with a small residual velocity into the *tail race* or waste channel.

The general principles governing the transfer of energy from a jet to moving blades, dealt with in § 124, can be applied to the Pelton wheel as follows :—

Let H = pressure head at nozzle.
U = velocity of jet.
v = peripheral velocity of buckets.
θ = angle through which water is turned in buckets.
v_r = relative velocity of water in buckets (assumed uniform).
W = weight of water per second.

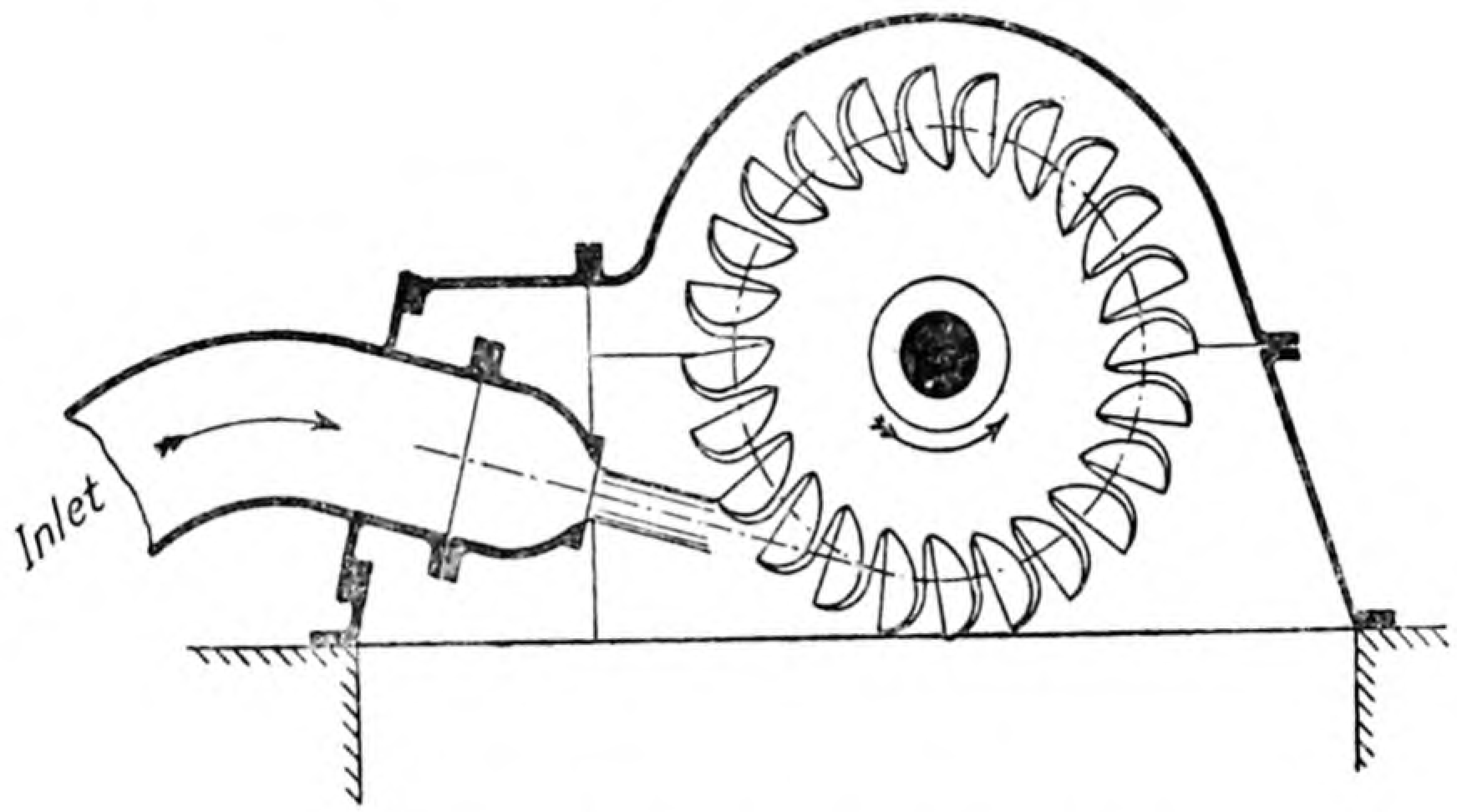

FIG. 225.—Elements of Pelton wheel.

Constructing the outlet velocity triangle (Fig. 226), we see that the absolute velocity U_1 with which the water leaves the buckets has a tangential component $V_1 = v - v_r \cos (180° - \theta)$. But clearly $v_r = U - v$, whence

$$V_1 = v + (U - v) \cos \theta.$$

Also the tangential velocity V of the water entering the wheel is in this instance represented by U; substituting, therefore, these values in the formula

$$E_o = \frac{W}{g} \cdot (V - V_1)v, \ (\S\ 124),$$

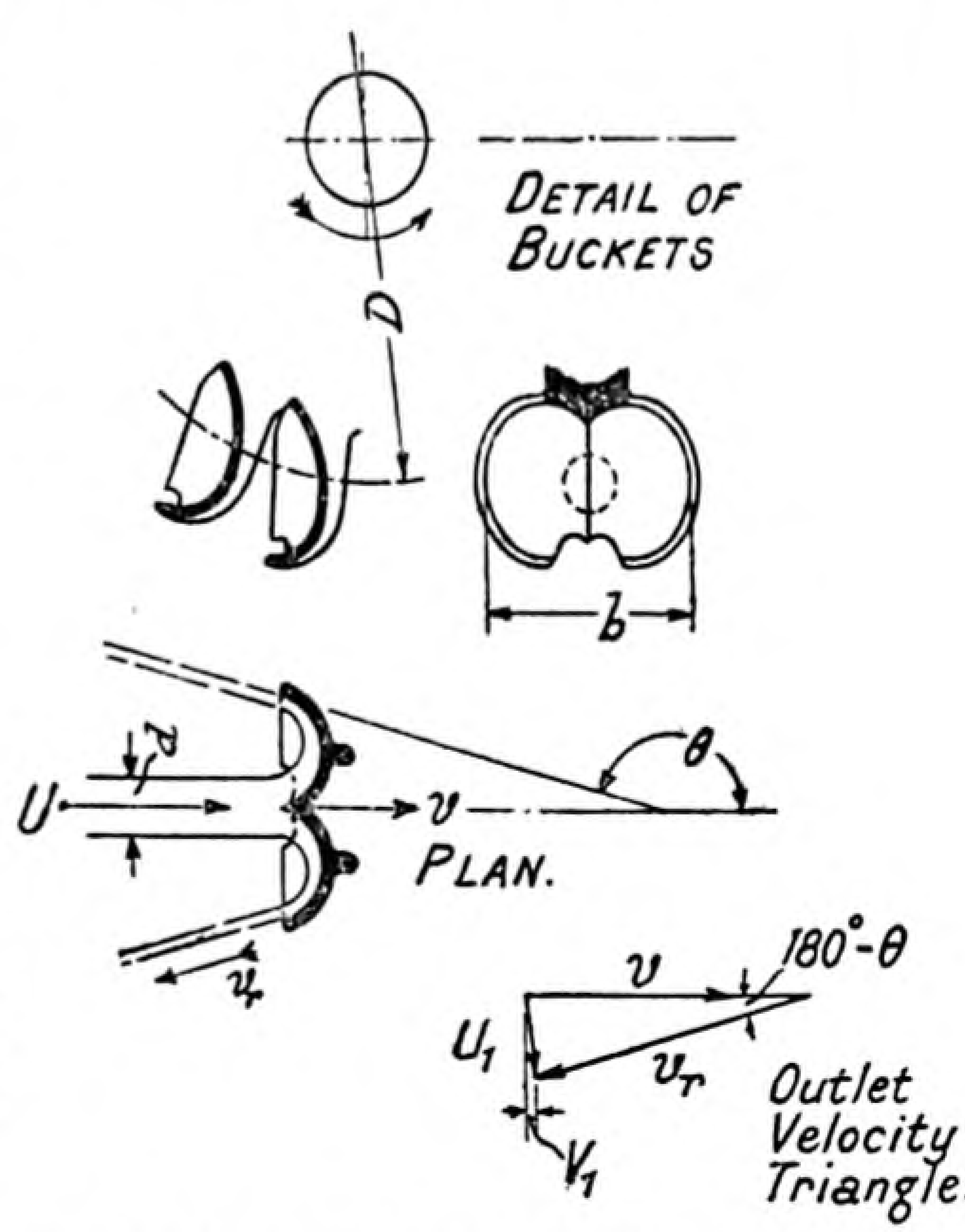

FIG. 226.—Pelton wheel buckets and velocity diagram.

we have $E_o =$ energy given to wheel per second

$$= \frac{W}{g} \cdot [U - (v + (U - v) \cos \theta)]v$$

$$= \frac{W}{g} \cdot [Uv(1 - \cos \theta) - v^2(1 - \cos \theta)].$$

This expression has the value zero when $v = 0$ or when $v = U$; it will have a maximum value at some intermediate ratio of v to U, which can be found by differentiating and equating to zero, thus

$$\frac{dE_o}{dv} = \frac{W}{g}[U(1 - \cos \theta) - 2v(1 - \cos \theta)] = 0,$$

from which $v = \frac{U}{2}$.

Under ideal conditions, then, the wheel will extract the greatest amount of energy from the jet if its pitch line velocity is one half the velocity of the jet. This maximum energy per second is represented by

$$E_o = \frac{W}{g}\left[\frac{U^2}{4}\right](1 - \cos \theta)$$

and the corresponding ideal efficiency $= \frac{\text{output}}{\text{input}}$

$$= \frac{\frac{W}{g} \cdot \frac{U^2}{4}(1 - \cos \theta)}{\frac{WU^2}{2g}}$$

$$= \tfrac{1}{2}(1 - \cos \theta),$$

which has the value *unity* if $\theta = 180°$.

228. Working Proportions of Pelton Wheels. The ratios established in the preceding paragraph require to be modified in practice to compensate for the effects of fluid friction in the nozzle and in the buckets.[145] In addition, the friction of the main bearings, and the windage loss due to the churning up of the air in the casing by the buckets, must be taken into account, § 221. Finally, it is impossible to deflect the water in the buckets through the ideal angle of 180°, for if this were done the water discharged from one bucket would foul the bucket in front of it.[146]

Empirical relationships taking these factors into account are:

(1) Velocity of jet $U = 0{\cdot}98$ to $0{\cdot}99\ \sqrt{2gH}$.

(2) Velocity of wheel at pitch diameter, $v = 0{\cdot}44$ to $0{\cdot}46$ $\sqrt{2gH}$.

(3) Angle θ through which water is deflected in buckets $= 165°$.

(4) Axial width of buckets $b = 3{\cdot}5$ to $4 \times$ diameter of jet d.

(5) Ratio of pitch diameter of wheel D to jet diameter d is normally not less than 12, but in extreme cases may be as low as 7 (see Fig. 233, § 232).

(6) Number of buckets [147] = about $\left(\dfrac{D}{2d} + 15\right)$.

(7) The axial width of the casing near the jet should not be less than fifteen times the jet diameter, otherwise the rejected water will splash back and impede the motion of the buckets.

The *gross* or *overall efficiency* of the Pelton wheel is represented by the ratio

$$\frac{\text{Brake horse-power}}{\text{Water horse-power}}, \text{ or } \frac{\text{B.H.P.}}{\text{W.H.P.}}, \quad . \quad . \quad (\S\ 220)$$

which may rise to nearly 90 per cent. in very large units, or to 85 per cent. in ordinary conditions. In calculating the gross efficiency, the water horse-power, which is represented by $\dfrac{WH}{550}$ (or $\dfrac{WH}{75}$ in metric units), is based on the net or effective head at the turbine inlet (see § 260).

In the event of a failure of the governing mechanism of a turbine, the wheel would race away under no-load conditions to a speed much in excess of its normal speed. This limiting speed—the maximum that the turbine could in any circumstances attain—is called the *runaway speed*; in a Pelton wheel it may be 80 per cent. or 90 per cent. above the normal operating speed. The wheel and the rotor of the electrical generator to which it is usually coupled are invariably designed so that they may safely withstand the augmented centrifugal stresses set up in the event, highly improbable though it may be, of the turbine running away.

The ideal velocity of the jet $\sqrt{2gH}$ is sometimes known as the *spouting velocity.* The ratio

$$\frac{\text{normal wheel velocity}}{\text{spouting velocity}} = \frac{v}{\sqrt{2gH}}$$

will be termed the *speed ratio* and denoted by the symbol ϕ.

The limiting output for a Pelton wheel unit is of the order of 68,000 horse-power, and the limiting head at the present time is 5500 ft. (say, 1700 metres).

229. Multiple-Jet Pelton Wheels. If, because of the restrictions (1), (2) and (5) above, a single jet cannot be made big enough to develop the desired power at the stipulated speed, the possible alternative arrangements of multiple jets are shown diagrammatically in Fig. 227. Either 2, 3, 4, or

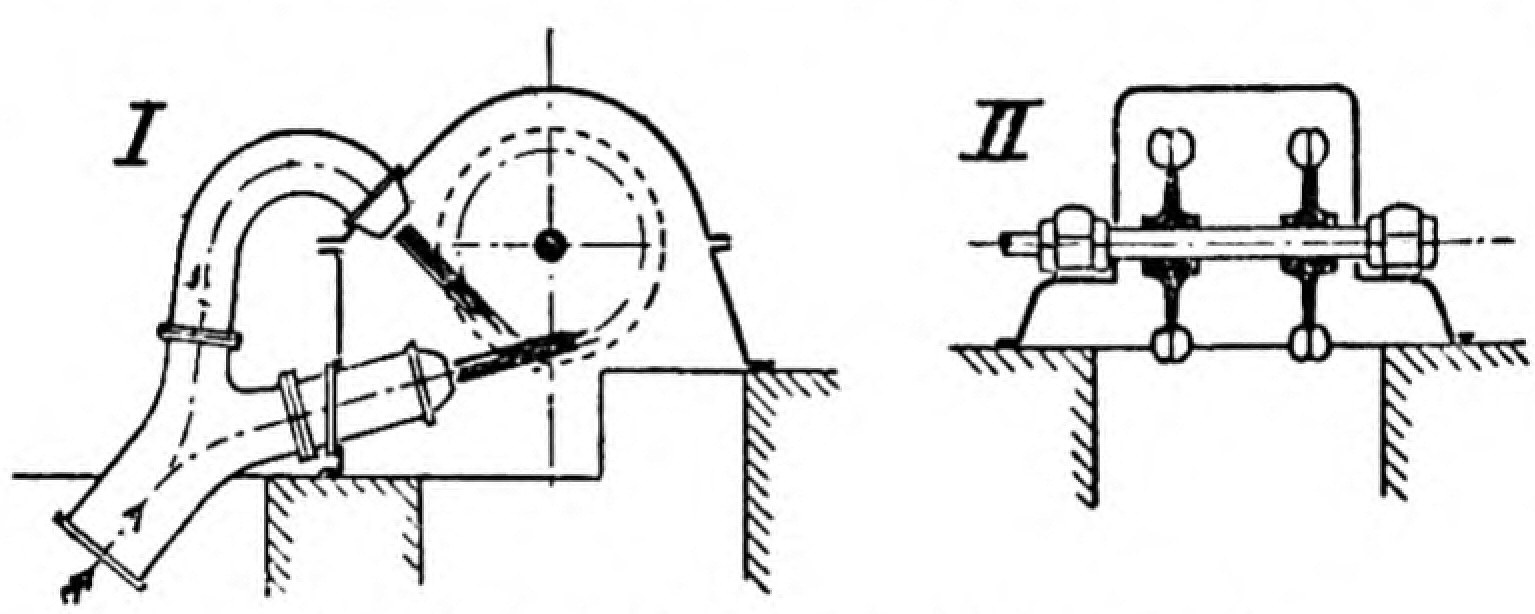

FIG. 227.—Multiple-jet Pelton wheels.

even 6 jets may be spaced round a single wheel, as at (I), or 2 or 3 wheels may be used, mounted on a common shaft (II). Sometimes a combination of the two systems is preferred, there being 2 jets to each of the wheels shown at (II). Single wheels having 3 or 4 jets are usually mounted with the shaft vertical. In any event 6 jets is the maximum allowed per turbine.[148] **(Example 119.)**

In system (I) careful design is required to ensure that the bend in the supply pipe feeding the nozzles does not disturb the flow through the nozzles and appreciably impair the efficiency. If a double-overhung disposition is chosen instead, consisting of a single wheel on either side of the electric generator,[149] then each of the two wheels has its own casing and its own single jet and supply pipe, which is kept as straight as possible. The whole revolving mass is supported by two very heavy main bearings, in-board of the turbine runners.

230. Power and Speed Regulation of Pelton Wheels. Hydraulic turbines, being usually coupled to electrical generators feeding into a supply system, are almost invariably required to run at constant speed irrespective of variations in the head and in the power output (§ 259 (ii)). Although any kind of throttle valve in the inlet pipe would serve in a crude way to adjust the supply of water to the demand, it would be quite inadmissible unless waste of water was of no account. In the first place, the essence of reducing pipe flow by throttling is the direct dissipation of energy; the valve cannot reduce discharge without simultaneously also lowering the head, § 92. In the second place, the reduced head at the nozzle would entail a smaller jet velocity, a disturbance of the speed ratio ϕ, and therefore an increase in the velocity energy thrown away into the tail race. The resulting drop in the part-load efficiency of the turbine is well shown in Fig. 291 (§ 271).

A most effective way of reducing the flow to the turbine *without* destroying energy—the standard method nowadays—is depicted in Fig. 228. Sliding axially within the nozzle

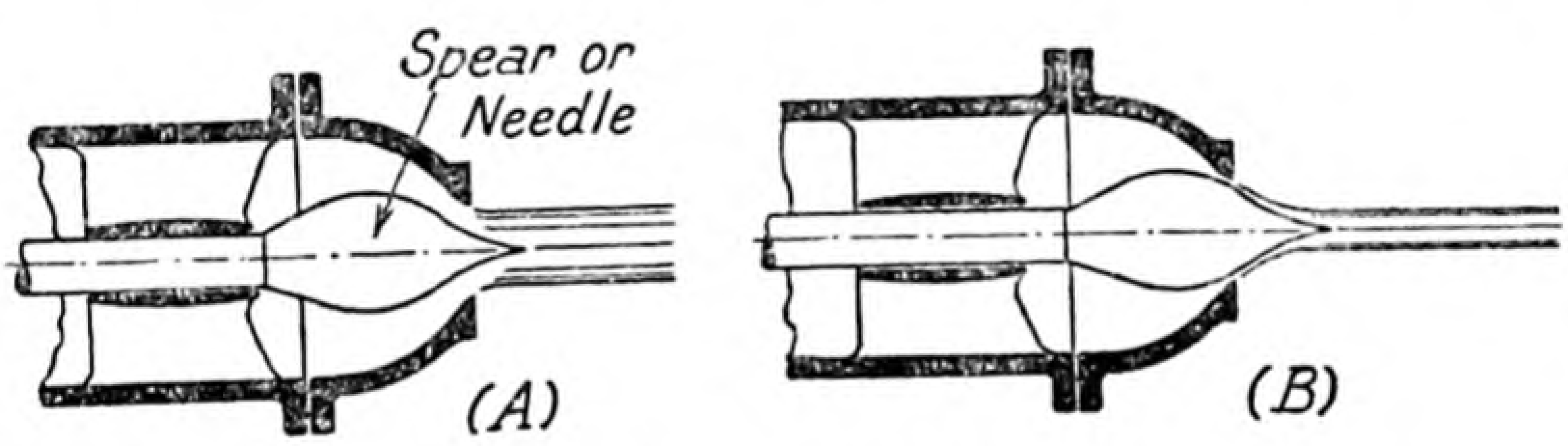

FIG. 228.—Spear or needle regulation.

is a *spear* or *needle* having a stream-lined head; as the spear is thrust further and further into the opening, from position A to position B, it leaves a diminishing annular spaec between itself and the nozzle, through which the water flows *always with the same velocity* and always coalescing into a circular jet. In effect, therefore, the device is simply one for varying the diameter of the jet.

The only drawback to the use of the spear is that it cannot be moved to close the nozzle rapidly except at the risk of generating serious dynamic or inertia pressures in the pipe line (§§ 115, 175). It must consequently be supplemented by a *deflector* (Fig. 229), which in the event of a sudden drop in the load can be moved into position B and can thus deflect

the jet partly or wholly clear of the buckets. The speed of the wheel being now well under control, the spear can be slowly moved forward, and the deflector withdrawn, until the positions of the two regulators are again stabilised with the deflector back in position *A* clear of the jet, and the spear adjusted to give the smaller flow called for by the reduced load on the

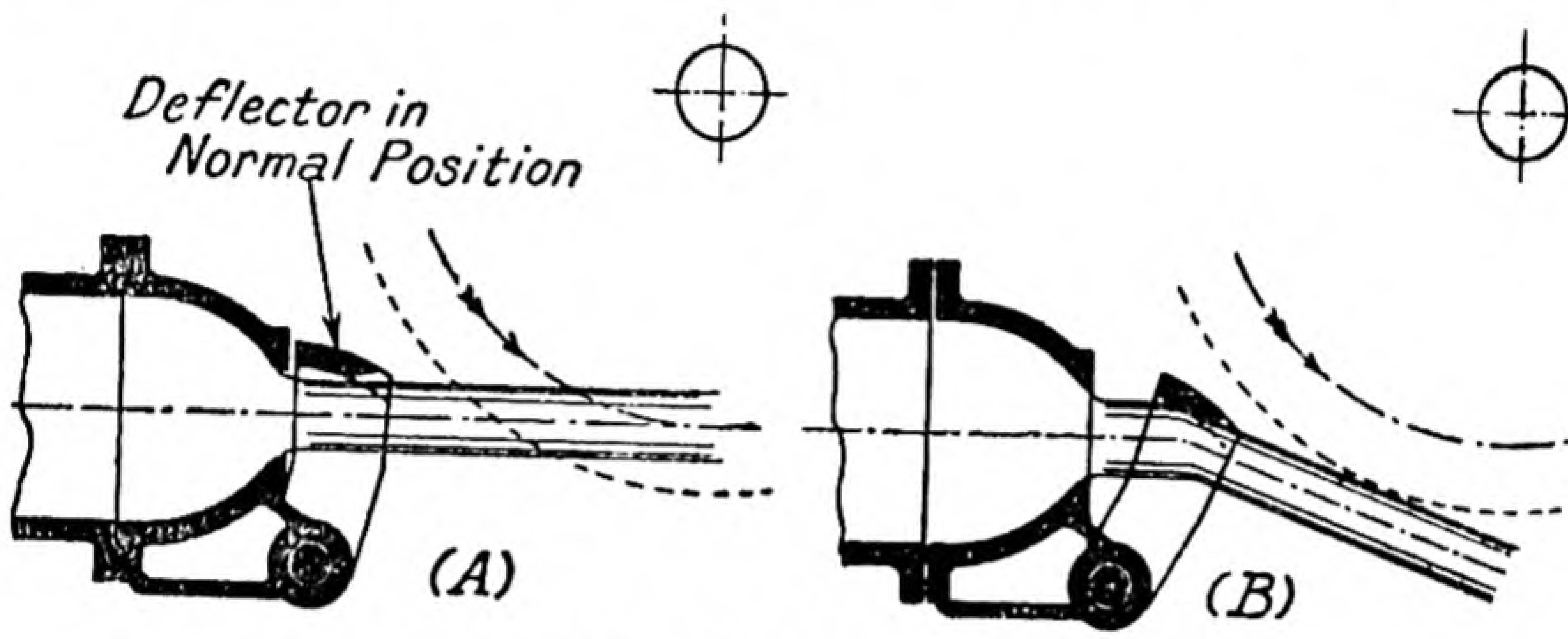

FIG. 229.—Deflector regulation.

turbine. Of course during these operations there is a slight waste of water, but this is unavoidable. The deflector may be dispensed with if the turbine nozzle is built on the principle of the diffusing outlet valve (§ 174). **(Example 120.)**

231. Servo-motor Control for Pelton Wheels. A typical system of automatic speed control for a Pelton wheel is shown schematically in Fig. 230. The apparatus which, by its

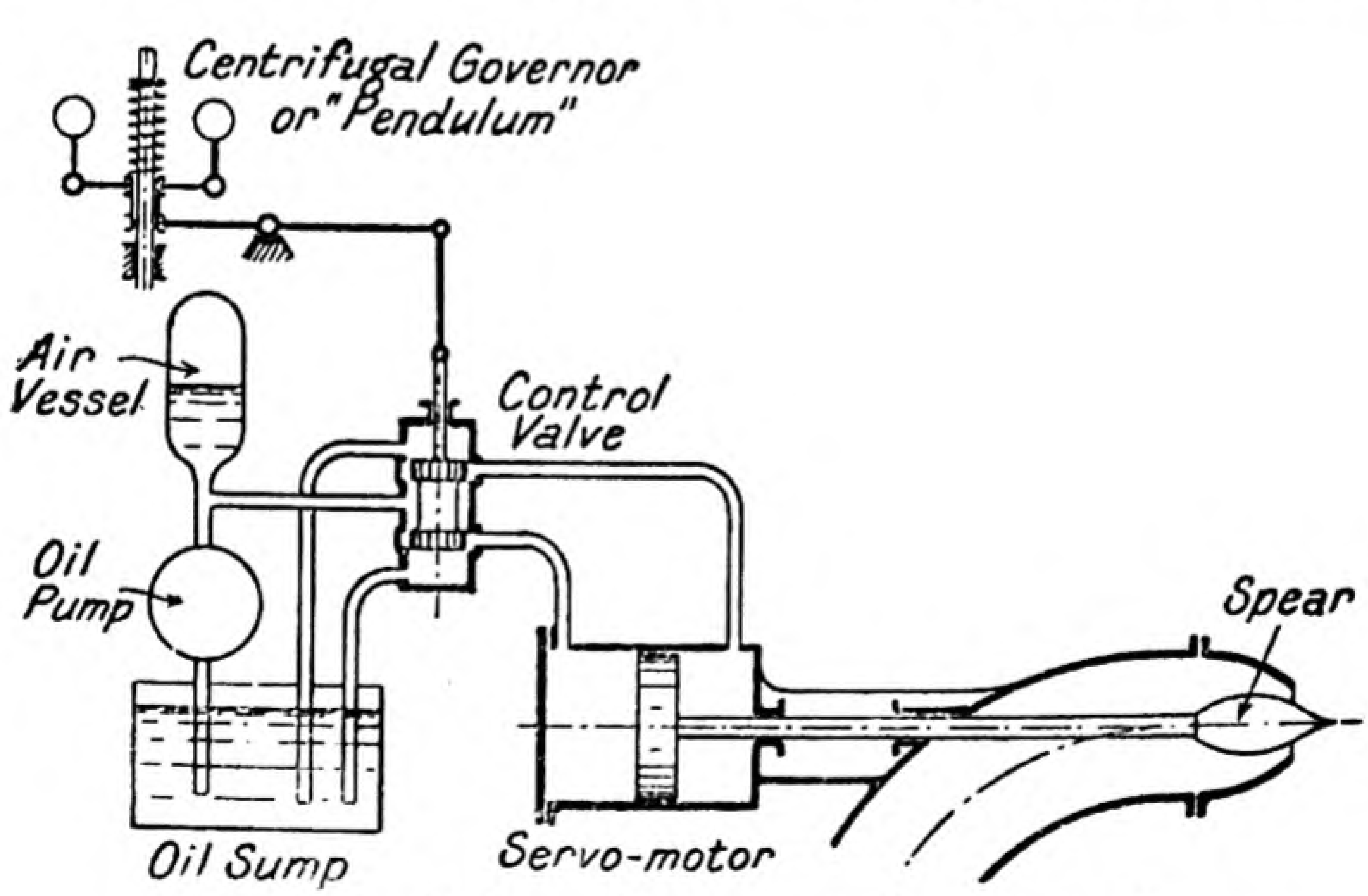

FIG. 230.—Pelton wheel governing mechanism.

sensitive response to speed fluctuations, initiates the movements described in the preceding paragraph, is a spring-loaded centrifugal governor or *pendulum*, belt- or gear-driven from

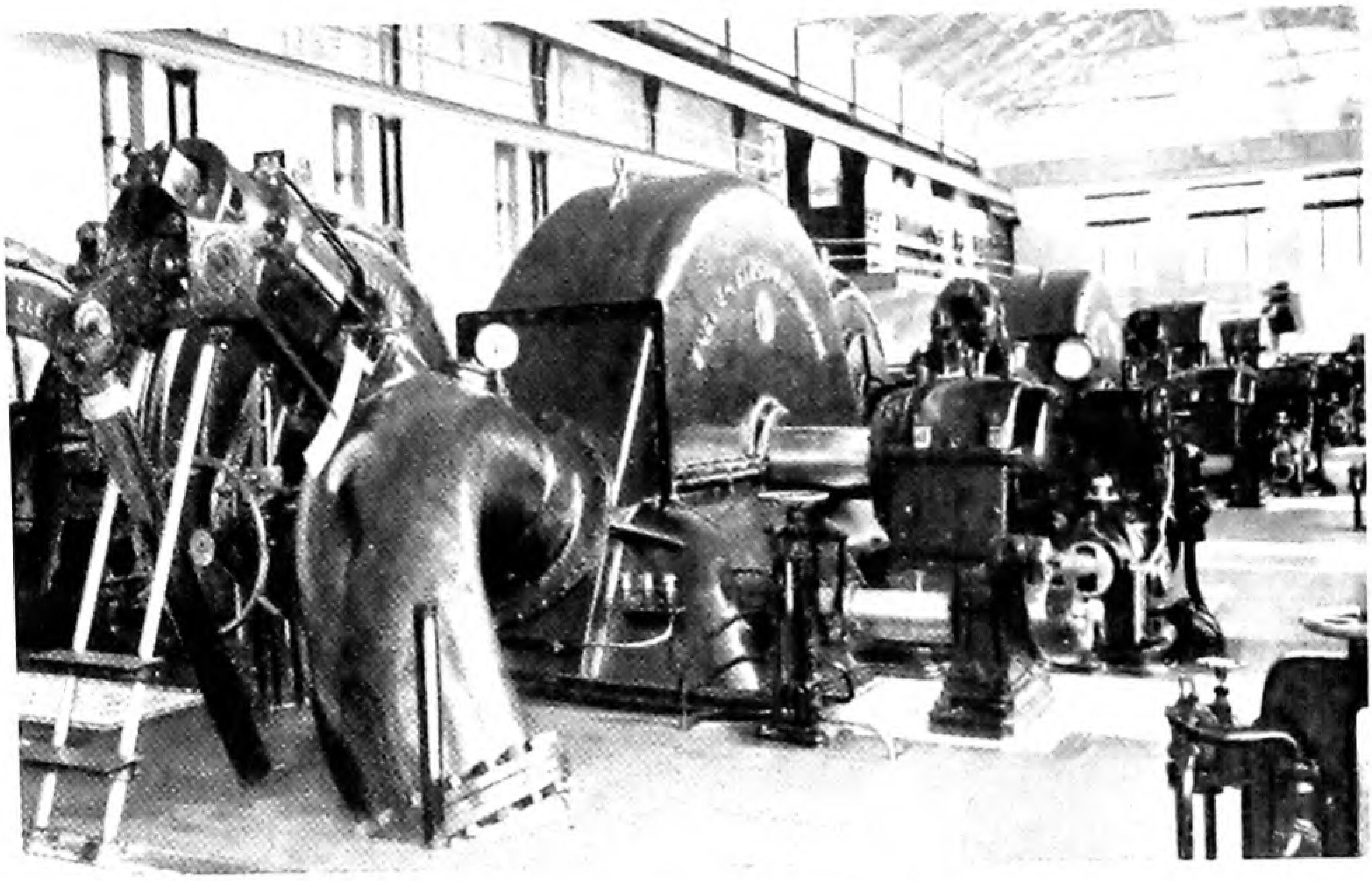

Fig. 231.—Pelton wheels in the Lochaber Power Station.
(The English Electric Co., Ltd.)

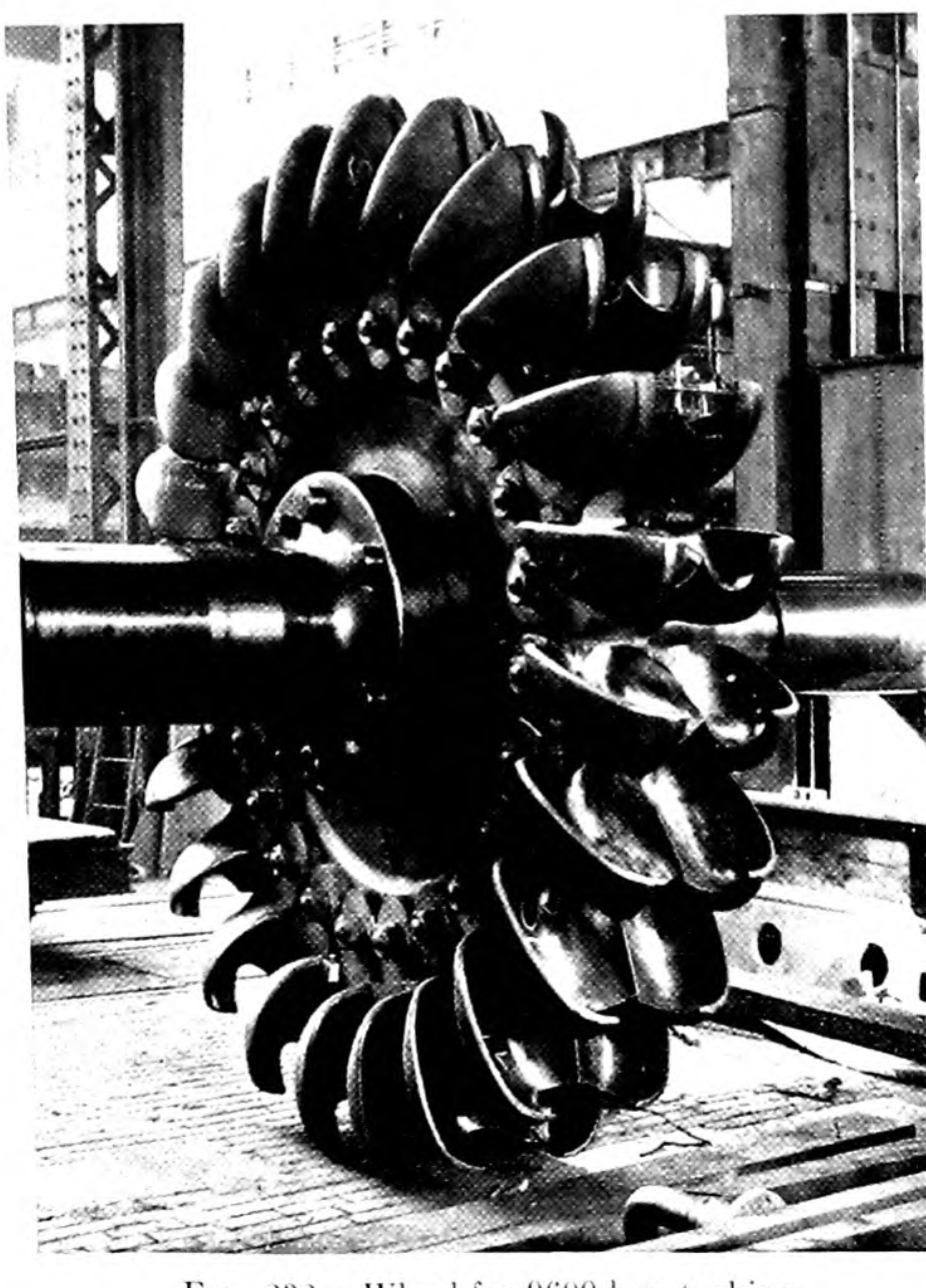

Fig. 232.—Wheel for 9600 h.p. turbine.

[To face page 330.

FIG. 233.—Integral construction of Pelton wheel runner.
(Escher Wyss Engineering Works, Ltd.)

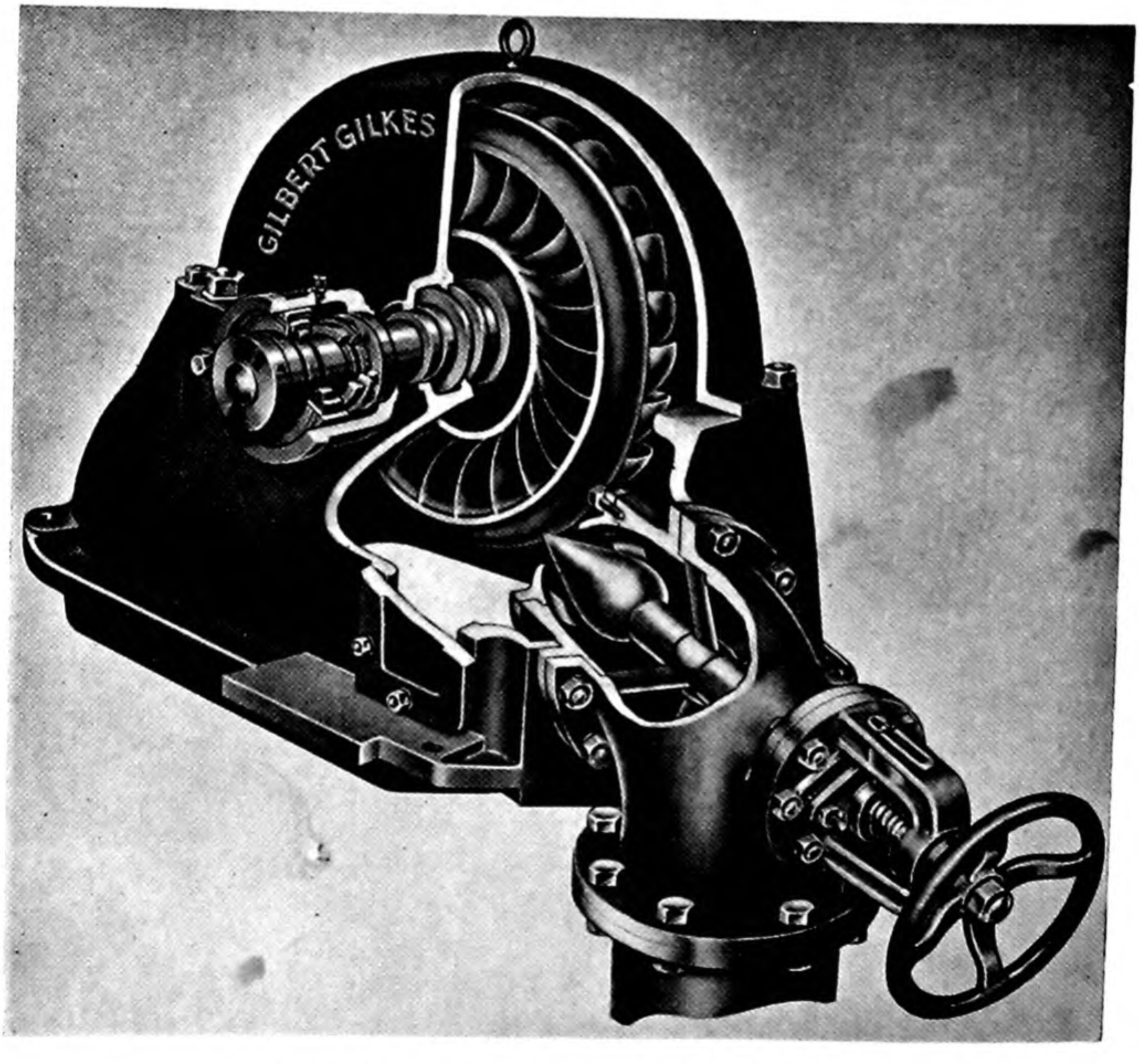

FIG. 234.—" Turgo " impulse turbine.
(Gilbert Gilkes and Gordon, Ltd.)

[*To face page* 331.

the turbine main shaft. All that the pendulum is called upon to do is to operate a small control valve of the piston type; the actual work of moving the spear or the deflector is done by an oil-pressure *servo-motor*, § 356, which consists chiefly of a main piston working in a cylinder. There are separate servo-motors for the spear and for the deflector, of which only the former is seen in the diagram, Fig. 230. The source of energy that the servo-motors draw upon is a positive rotary oil pump, working at a pressure of 15 atm. or more, driven from the turbine shaft; some amount of energy may also be stored in the air vessel above the pump (§§ 353, 354).

In the diagram the parts are shown stabilised in the positions corresponding to steady speed at about half load. An increase in the load on the turbine momentarily pulls down the speed, the pendulum fly-balls fall inwards, the control valve is raised, and pressure oil flows to the right-hand end of the servo-motor cylinder, the nozzle opening is increased and the speed restored to normal, the oil from the left-hand end of the cylinder meantime having been exhausted to the oil sump. A by-pass or relief valve must obviously be provided to permit the oil to circulate when the control valve is closed; some sort of return motion gear is also necessary, (§ 243) to prevent " hunting " of the governor. Synchronous electrical drive is sometimes preferred to mechanical drive for the centrifugal governor.

232. A Typical Pelton Wheel Installation. A large installation of Pelton wheels in the Lochaber Power Station of the British Aluminium Company is illustrated in Fig. 231. Each of the turbines develops 9600 H.P. when running at 250 revs. per min. under a head of 720 ft., each unit having one wheel and two jets. The photograph clearly shows the upper inlet bend, the needle servo-motor mounted thereon, the connecting-rod that couples the two needles together; and to the right, the deflector servo-motor and operating shaft.[150]

The wheel for one of these turbines, with its twenty-two steel buckets, is shown in Fig. 232. Here the buckets are cast separately and secured to the rim by heavy lugs and bolts. This form of construction may be contrasted with the form shown in Fig. 233, which represents a runner cast in one

piece, suitable for a Pelton wheel with an abnormally small ratio of $\frac{D}{d} = 7$. Both photographs give a good impression of the shape of the buckets, showing how the jet is split by the sharp central fin and allowed to spread in a thin sheet over the whole surface of the bucket.

233. Other Types of Impulse Turbine. Although the Pelton wheel is the type of impulse turbine that is found most suitable for large installations, it is only one among a number of designs that have been and still are used. In the machine named by its makers the " Turgo " turbine, the wheel or rotor has the appearance shown in Fig. 234. Water is projected on to it from a nozzle with needle regulator resembling a Pelton wheel nozzle ; but now the axis of the jet is disposed at an angle with the plane of the wheel, the hydraulic conditions thus resembling those seen in Fig. 108, § 124. As compared with a single-jet Pelton wheel, the " Turgo " turbine has a higher specific speed, which means that, for a stipulated head and output, its rotational speed will be higher, § 263.

234. The Francis Turbine. Because of the rigid connection between the working head and the rim velocities of Pelton wheels, and between the diameter of wheel and diameter of jet, it is readily seen that as the head diminishes, the diameter of a wheel to develop a given output grows progressively greater, and the speed of revolution progressively less. If the head falls much below 500 ft. (say 150 metres), Pelton wheels become so slow and unwieldy that they are unsuitable for ordinary use. We therefore have recourse to the relatively faster-running and more compact *Francis turbine.*

The essential parts of an inward-flow Francis turbine (Fig. 235), are (1) an outer ring of stationary guide blades forming the guide-apparatus, and (2) an inner ring of rotating blades which constitutes the wheel or runner. In this diagram these elements are seen installed in a cylindrical vessel which is a development of the one depicted in Fig. 127, § 143. Water is continuously supplied to the apparatus in order to maintain a steady head H above the turbine runner.

The changes of pressure, velocity, and energy that accompany the flow of water through the turbine are shown graphically in Fig. 235. In order to impart to the water

the velocity energy required to cause radial flow with velocity Y into the guide passages, its pressure head is diminished from an initial value H to $\left(H - \dfrac{Y^2}{2g}\right)$, and a further drop to H_0 occurs as the absolute velocity rises in the guide passages from Y to U. Under ideal conditions no energy

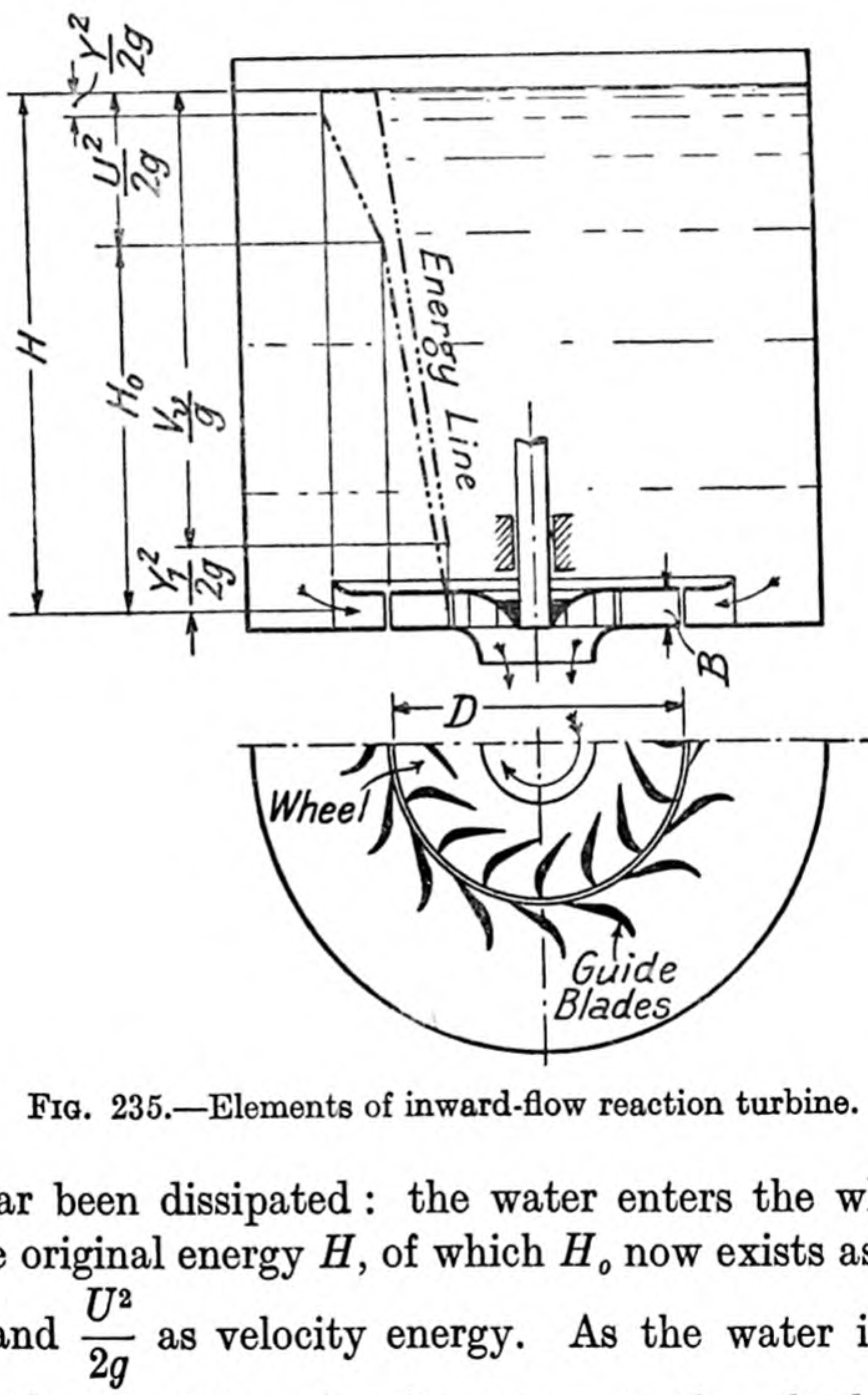

FIG. 235.—Elements of inward-flow reaction turbine.

has so far been dissipated: the water enters the wheel with its entire original energy H, of which H_0 now exists as pressure energy and $\dfrac{U^2}{2g}$ as velocity energy. As the water in passing through the wheel transfers its energy to the wheel, both its pressure and its velocity diminish; it is thus finally discharged with a very small residual velocity Y_1 and with zero pressure.

The term *Reaction turbine* applied to this machine—§ 226—can be understood by regarding the wheel passages as forming a series of rotating nozzles projecting the water backwards in a similar manner to the nozzles of a Barker's Mill, § 125. The little diagram at the end of that paragraph is a useful reminder of the basic unity of principle of all types of hydraulic turbine.

The term *Pressure turbine* implies that in passing through Francis and similar machines the water is continuously under pressure (though not necessarily a positive pressure) up to the moment when it is discharged from the runner.

235. Elements of Design of Francis Turbine Runner. Problems of turbine design are usually put in the form: What must be the size and blade angles of a runner to develop P brake horse-power when running at N revs. per min. under a head of H?

The factors involved are :—

W = weight of water per second flowing through turbine.
Q = volume „ „ „ „ „
D = diameter of runner measured over outer edges of blades (or in some other conventional manner, § 269).
B = effective width of runner at outer diameter.
v = rim velocity of outer edges of blades.
v_1 = „ „ „ inner „ „
V = velocity of whirl of water entering wheel blades.
V_1 = „ „ „ „ leaving „ „
Y = velocity of flow of water entering wheel blades.
Y_1 = „ „ „ leaving „ „
(Provisionally Y and Y_1 may be assumed equal.)
U = absolute velocity of water leaving guide passages. (Note that this is *not* the spouting velocity $\sqrt{2gH}$.)

The fundamental equation 8-5 (§ 144) shows that the work done per unit weight of water flowing through the rotating passages is

$$\frac{Vv}{g} - \frac{V_1 v_1}{g}.$$

In the Francis turbine the maximum output under specified conditions is obtained by making the velocity of whirl at exit, V_1, equal to zero, whence we may write—

Energy given to wheel per unit weight of water $= \dfrac{Vv}{g}$.

Now the energy H lost by the water in flowing through the turbine can be accounted for as follows: (*a*) $\dfrac{Vv}{g}$ is given to

the wheel, (*b*) velocity energy $\frac{Y_1^2}{2g}$ is carried away as the water leaves the wheel, and (*c*) a friction, shock, and eddy loss h_L is incurred as the water flows through the guide and wheel passages, § 221 (iv). (This loss is not shown in Fig. 235, which relates to ideal conditions only.) Equating,

$$H = \frac{Vv}{g} + \frac{Y_1^2}{2g} + h_L.$$

The ratio $\dfrac{\frac{Vv}{g}}{H}$ is termed the

hydraulic efficiency of the turbine, denoted by η_h.

Its value may range from 0·85 to 0·9 or more.

Not all of the energy per second, represented by $W \,.\, \eta_h H$ or $\frac{W \,.\, Vv}{g}$, that the wheel receives from the water appears as useful output at the turbine coupling or pulley; some of it is dissipated in disc friction acting on the outside of the runner (§ 221), and some in overcoming friction in the main bearings. To it also must be debited the power absorbed by the governor (§ 243), and the energy carried away by the water leaking past the runner.

Thus the *gross* or *overall efficiency* of the turbine $= \eta_m$

$$= \frac{\text{brake horse-power}}{\text{water horse-power}} = \frac{P}{\frac{WH}{550}} \text{ (foot units), or } = \frac{P}{\frac{WH}{75}} \text{ (metric units),}$$

is always less than the hydraulic efficiency η_h. Its value may range from 0·8 to 0·9 or more, according to the size and nature of the installation (§ 279). For methods of assessing the value of the net or effective head H to be used in all the above formulæ, see § 260.

Before beginning the design of the wheel, likely values of η_h and η_m must arbitrarily be settled upon, and a decision must also be made concerning

$$n = \text{ratio of wheel width to diameter} = \frac{B}{D},$$

and $$\psi = \text{the } \textit{flow ratio} = \frac{Y}{\sqrt{2gH}}.$$

ψ may range in value from 0·15 to 0·30 (§ 269). In these matters guidance will naturally be sought from the operating results of similar turbines already in use.

236. Details of Calculation. The routine is now as follows :—

(i) The value of W having been obtained from the relationship $P = \eta_m \frac{WH}{550}$ (or its metric equivalent), the *discharge* Q is given by $Q = \frac{W}{w}$.

(ii) Neglecting for present approximate requirements the blade thickness, the area of flow into the wheel (§ 138) is $\pi DB = \pi DnD$. Also since discharge = area × velocity,

$$Q = \pi n D^2 \times Y$$

from which the *diameter* and *width* of the wheel can be found.

(iii) To find the *rim velocity* v, the formula $v = \frac{\pi DN}{60}$ is applicable.

(iv) To find the *velocity of whirl* V at entry to the wheel, the expression $\eta_h = \frac{Vv}{gH}$ from above, is used.

(v) As seen from the inlet velocity triangle (Fig. 236), the *guide blade angle* θ must be so arranged that the water projected on to the wheel has a whirl component V and a flow component Y, hence $\theta = \tan^{-1} \frac{Y}{V}$.

(vi) In order to avoid shock losses at entry, the *inlet wheel blade angle* α must be so arranged that the first part of the wheel blade is parallel to v_r, where v_r is the relative velocity of the water, or the vector difference between the velocities U and v. It follows that

$$\alpha = \tan^{-1} \frac{Y}{V - v}.$$

(vii) In order that the water may leave the wheel without velocity of whirl, it is seen from the outlet velocity diagram that the *outlet wheel blade angle* β is $\tan^{-1} \frac{Y_1}{v_1}$. **(Example 121.)**

Two main objects in these calculations are to be observed: we desire to find out in the first place how big to make the runner so that the desired quantity of water will pass through it: then we must fit into the wheel an array of blades of such a form that they will extract from the water the stipulated energy. As for the actual shape of these runner blades, it is settled largely by a process of trial and error. The values of the angles α and β merely determine the inclination at inlet and outlet; the blades, besides fulfilling these conditions, must be so curved that the water flowing between them is smoothly accelerated from the relative velocity v_r to the relative velocity V_r with the minimum friction and eddy loss. It is important that the number of runner blades, which may be 12 or more, should not be the same as the number of guide blades, otherwise objectionable periodic impulses may be set up.

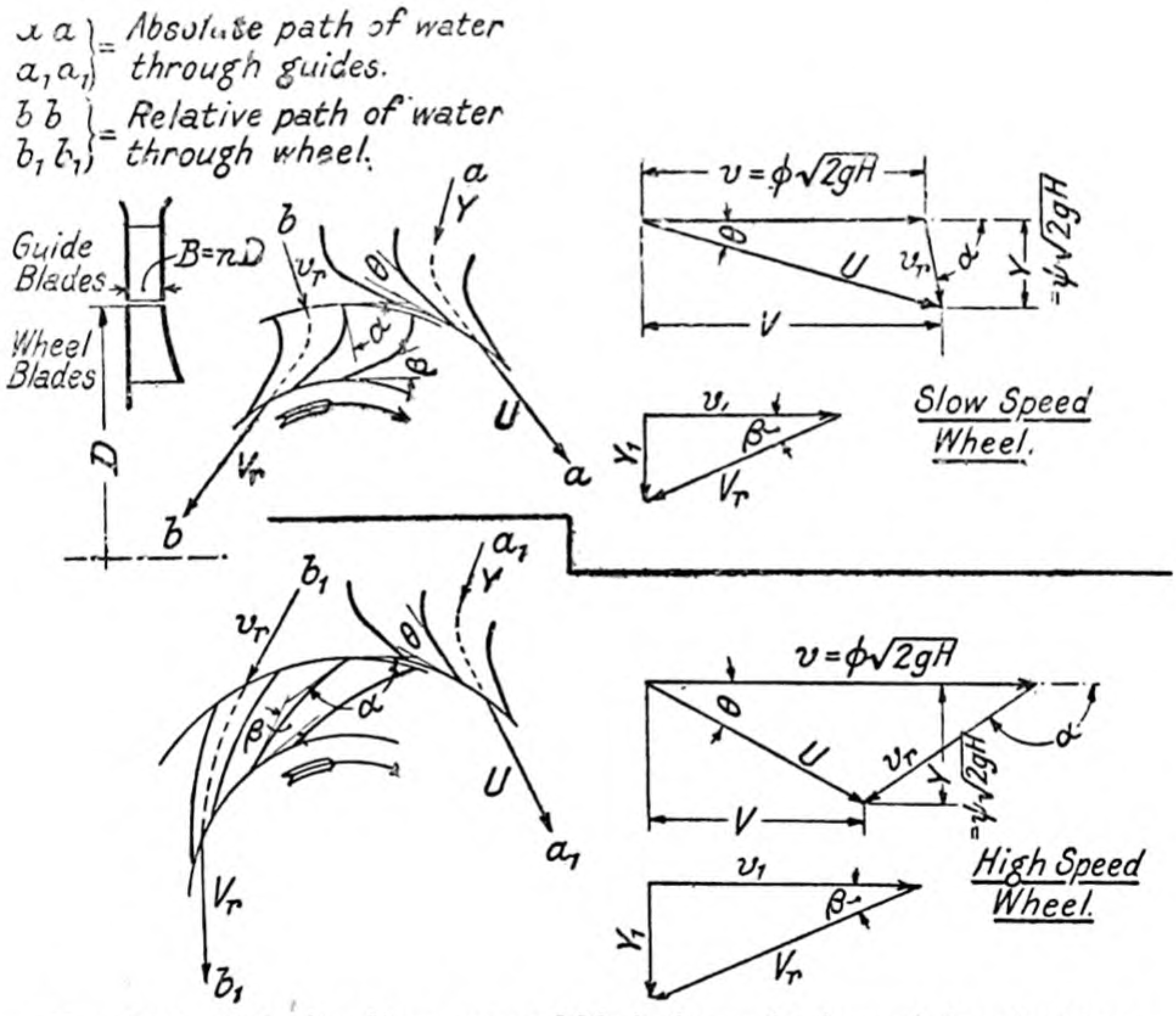

FIG. 236.—Velocity diagrams and blade forms for inward-flow turbines.

237. Speed Relationships for Francis Turbine Runners.

A comparison between §§ 228 and 235 soon shows how much greater freedom the Francis turbine offers to the designer than the Pelton wheel does. In the Francis type there is no restriction of the sort that imposes a rigid ratio $\phi = 0{\cdot}45$ between the speed of Pelton wheel buckets and the spouting velocity. Since now $v = \eta_h \frac{gH}{V}$, the velocity of the wheel v can apparently be given any value we please so long

as V is modified accordingly; though to be sure, such modifications have an important effect on the blade forms, as may clearly be seen from Fig. 236. Here two turbines are compared working under the same head; the upper diagram relates to a machine in which the speed ratio ϕ is 0·64, whereas in the lower diagram $\phi = 0{\cdot}87$. **(Example 122.)**

But when we examine the influence of large inlet blade angles on the friction loss in the wheel passages, it appears that there is, after all, a practical limit to the value of v. The higher the wheel speed, the longer and narrower do the wheel passages become, and the higher also rises the relative velocity of the water through them (Fig. 236). Beyond a certain point, therefore, the friction loss increases extremely rapidly, with the result that it is undesirable to work with a higher speed ratio than $\phi = 0{\cdot}90$, otherwise the efficiency of the turbine is seriously impaired, § 221 (iv). On the other hand, it is not possible to use a value of ϕ less than about 0·60, for below this value the turbine approaches too closely to the conditions of an impulse or free jet turbine—conditions for which it is quite unsuited. In general, then,

$$0{\cdot}90 > \frac{v}{\sqrt{2gH}} > 0{\cdot}60.$$

In regard to the rotational speed of the runner N, this can be varied, to some extent, without alteration to the water velocities or to the rim velocity or to the blade angles, by merely changing the ratio $n = \frac{B}{D}$.

238. Inward Flow and Mixed Flow Runners. With a Francis runner of given diameter, the power output for a given head can be increased either by increasing the flow ratio ψ and keeping the wheel width unaltered, or by keeping ψ unaltered and widening the wheel, viz. increasing the ratio n. Unduly high values of ψ and therefore of the flow component Y will result in excessive losses in the form of velocity energy rejected from the wheel; high values of n bring us up against one of the cardinal problems of low head turbine design—the problem of providing a big enough outlet area for the water. It is of no use to give the runner a generous inlet area if we do not allow the water to escape freely; and the only way

of escape in the pure *inward-flow* runner shown in Fig. 235 is through the orifice or "eye" which has a diameter of less than one-half of D.

The difficulty can be partially overcome by the use of the *mixed-flow* type of runner (Figs. 237 and 244), in which the direction of the water is turned from radial inward flow to axial flow while still passing through the wheel blade passages. The blades must consequently have the peculiar scoop shape indicated by the cross-sections; the outlet angle β must have the correct value both when measured in a tangential plane and in a transverse plane. The exit diameter of the runner is now nearly equal to the inlet diameter, and it may sometimes be actually greater.

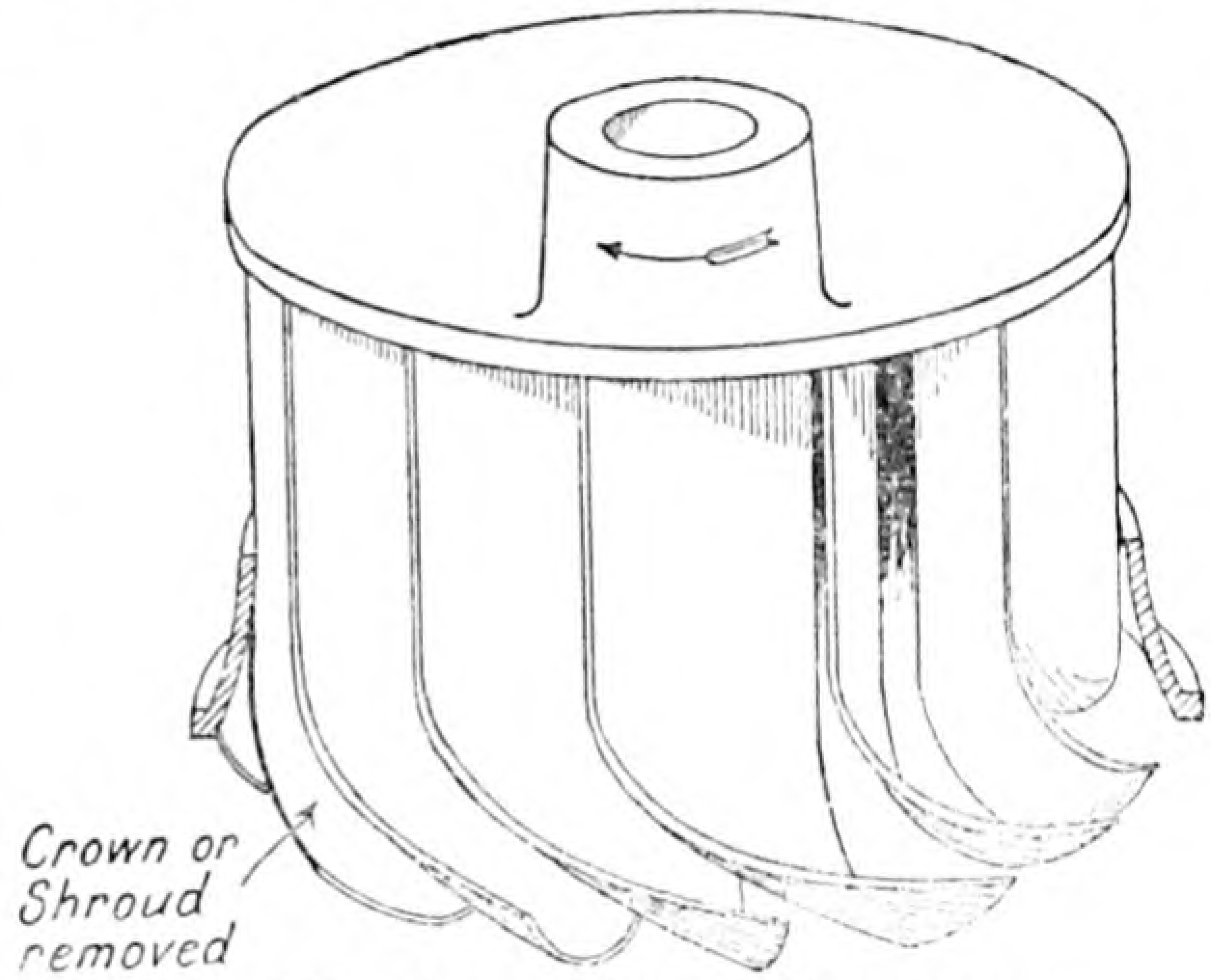

FIG. 237.—Mixed-flow turbine runner.

In extreme cases the water has attained almost pure axial flow before entering the runner (Fig. 254 (I)); here it will be observed that the blade surface is cut away considerably in order to reduce the surface friction loss noted in the preceding paragraph, experience having shown that the water is well able to find its own way across the clear space between the guides and the wheel.

Although the detailed analysis of the complex state of flow existing in these runners is a matter for the specialist in turbine design, yet a preliminary impression of design procedure may be gained from the following § 239. Alternatively, the main dimensions and characteristics of such runners may be approximately established by the methods described in the next chapter, §§ 265-269. In regard to construction, sometimes the Francis runner is a single casting in steel or stainless steel. Sometimes the individual blades may be pressed from steel plate, with boss and outer ring cast round them. Still another possibility is to fabricate the runner from steel pressings and forgings welded together.

239. Blade Form for Mixed-Flow Runner. As was pointed out in § 236, there are two distinct operations in designing any type of reaction turbine runner: first we provide the necessary passages to suit the discharge, then we insert the blades ready to accept the energy that the water brings with it. In regard to the first of these questions, the general shape of the mixed-flow runner has already been studied in § 147; moreover, Fig. 131 (*b*) gives an impression of the 3-dimensional flow that will certainly prevail when the runner gets to work. Additional simplifying assumptions are now required. Not only do we proceed as though the original concentric stream surfaces and their accompanying equi-potential surfaces will still maintain their shape unaltered, but we shall ignore the slight variations of the meridional velocity Y_m across a given equi-potential surface, § 147 (i).

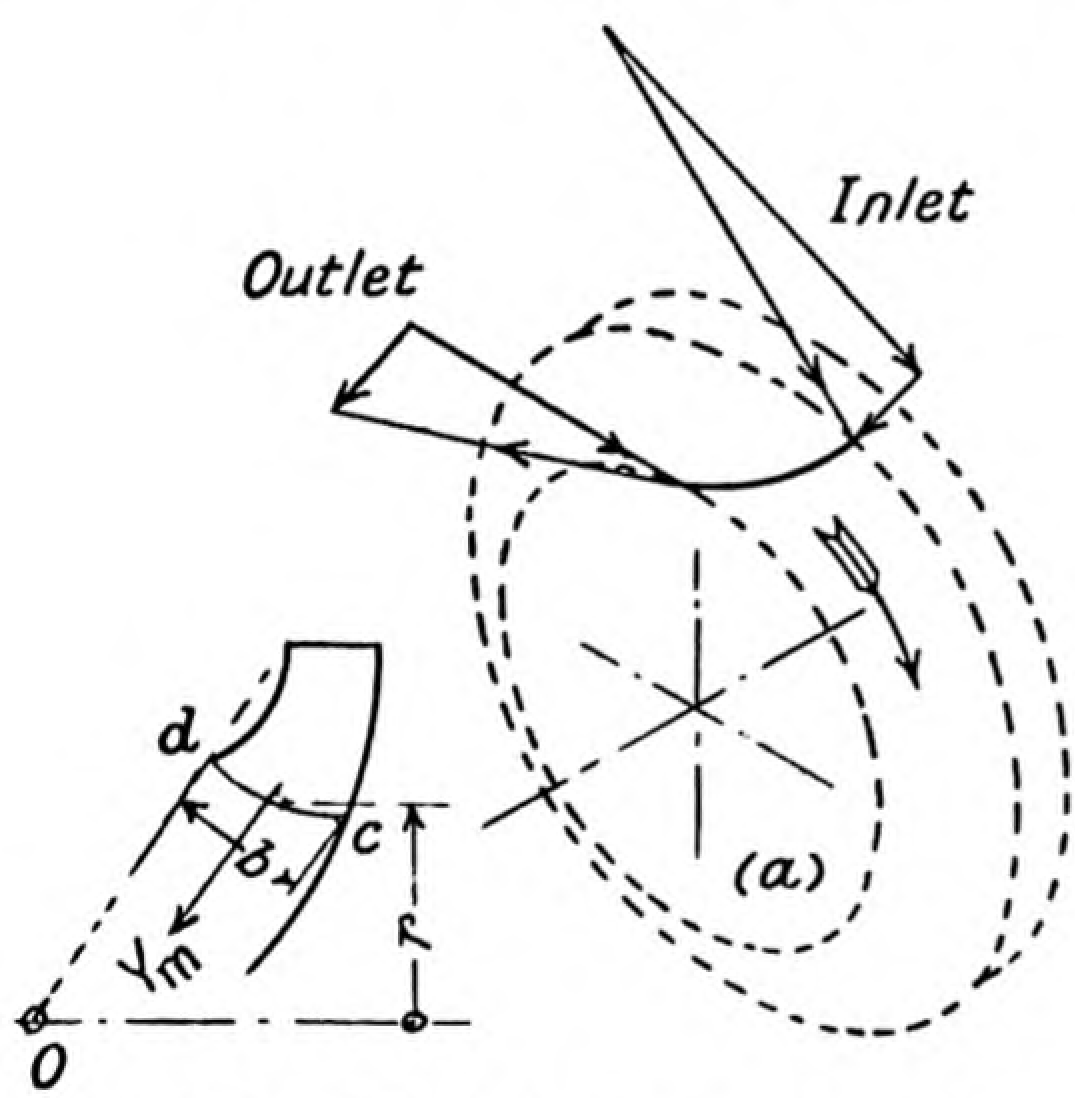

FIG. 238.—Flow through mixed-flow runner.

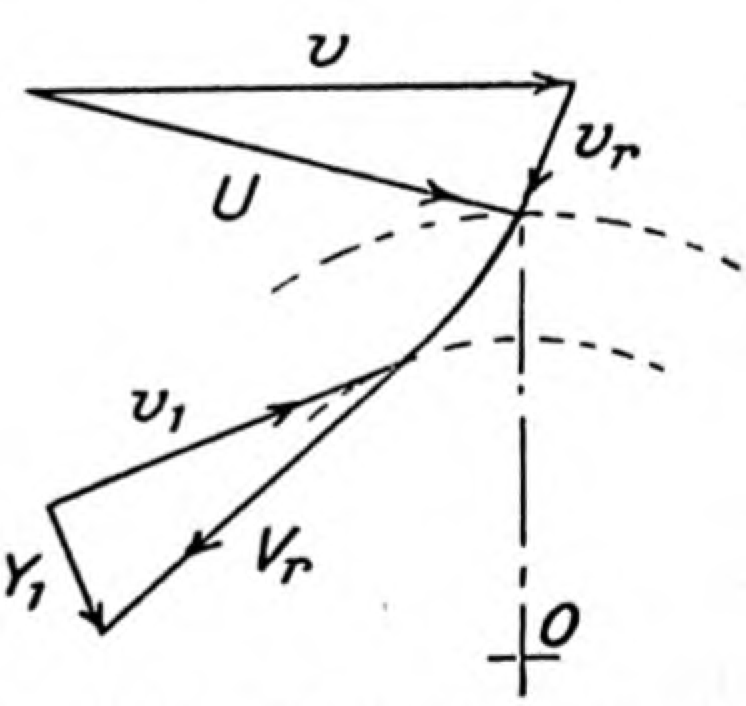

FIG. 239.—Projection of velocity diagrams on development of conical surface.

The effect is seen in Fig. 238, which represents in cross-section and in perspective a horizontal-shaft mixed-flow runner; the meridional velocity Y_m at exit, for instance, is seen to have the value

$$Y_m = Q/(2\pi rb).$$

It would not be justifiable, however, to assume that peripheral velocities are likewise uniform across the wheel passages: we know that the peripheral velocity of point *d* is greater than the corresponding velocity at *c*, nor can there be any doubt

that the whirl velocities of the water will also be dissimilar. This means that the shape of the velocity diagrams will change as we pass from one side of the passage to the other; or in other words, that each stream surface will have its own inlet and outlet velocity triangles. If the operations described in § 236 are applied to the outermost stream surface, the resulting figures would have the appearance of the perspective view, Fig. 238 (*a*). In themselves such perspective diagrams are of little use to the designer; a more effective system would be to project them on to developments of conical surfaces, Fig. 239. For the particular stream surface under consideration, the generating line of one of the cones would be tangential to the wheel surface at inlet, while the other cone would be related to the wheel surface at outlet. Alternatively, a single conical surface generated by the line *Od* might serve. By repeating the procedure for other stream surfaces, it would finally be possible to draw the shape of a complete blade.

240. Constructional Requirements. Having established the size and form of the turbine runner and of its blades, the designer next has to devise means for guiding the incoming high-pressure water into the runner, and for conducting the low-pressure water away; for the arrangement shown in Fig. 235 was intended to be diagrammatic only. A common disposition is illustrated in Fig. 240. From the inlet conduit which brings water to the turbine, the water flows into a *spiral casing* which envelops the runner; after yielding up its energy, the water escapes through an outlet passage or *draft tube*. As the diagram suggests, the spiral casing is not concentric: because of the inward flow of the water into the guide passages, the residual circumferential flow in the casing progressively declines, and the casing cross-sectional area is reduced in sympathy.

A study of Fig. 240 will show some of the points that need attention :—

(i) *Mechanical strength.* As explained in § 21, the internal water pressure is capable of setting up severe stresses in the walls of the casing. These stresses can only be kept within permissible limits by the *stay-vanes* shown in the diagram; not only do they act as stream-lined tie-bolts, but they help to give the water guidance before it comes under the influence

of the guide-blades, § 234. The material chosen for the spiral casing will depend upon the working head H. If this does not exceed about 100 feet, reinforced concrete may serve; for higher heads, riveted or welded steel plate should be used; while for the limiting head of 1000 feet or so, only cast steel will suffice.[151]

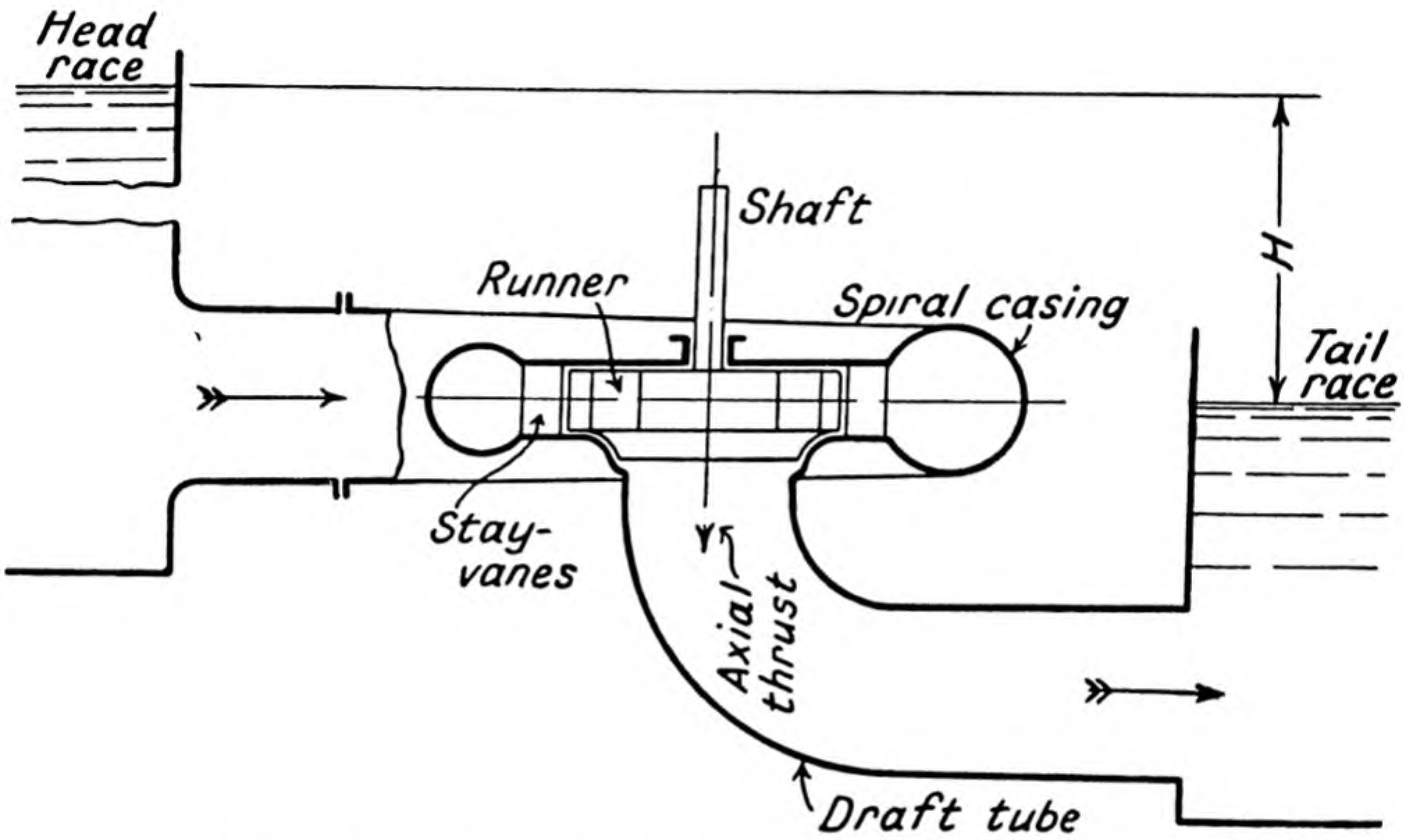

FIG. 240.—Constructional elements of Francis turbine.

(ii) *Leakage control.* From § 222, it will be evident that " contact " seals will be used for the main gland, where the turbine shaft passes through the casing, Fig. 240, and " hydraulic " seals for the runner periphery. In other words, special packings will prevent water from leaking out of the casing or air from leaking in, and fine clearances or labyrinth rings will reduce the leakage between the fixed casing and the rotating wheel.

(iii) *Axial thrust.* In addition to transmitting the torque exerted upon the runner blades, the turbine shaft may also be required to resist a considerable axial thrust. This may have two components, (*a*) in a vertical-shaft machine, as in Fig. 240, there is the weight of the runner, shaft, and other rotating elements; (*b*) there will nearly always be an unbalanced hydraulic thrust. If no suitable provision were made, this axial hydraulic thrust would be inadmissibly great. Referring to Fig. 240, it can be seen that the upper face of the runner

will be exposed to a pressure-head that is roughly equivalent to the pressure-head H_0 prevailing in the clearance space, Fig. 235. Yet over much of the lower surface of the wheel, the pressure-head more nearly approximates to the outlet head of the water as it leaves the runner (see § 321). In fact it is not difficult to contrive relieving openings, ports or passages which will modify or partially equalise these pressures, and thus bring the value of the unbalanced hydraulic thrust down to an acceptable figure.

241. The Draft Tube. This is the name given to the pipe or passage which leads the water exhausted from the runner into the tail-race or waste channel. It has two most important functions besides that of a mere water conduit: (i) it permits a negative or suction head to be established beneath the runner, so making it possible to set the turbine above tail-race level, and (ii) it acts as a recuperator of pressure energy, converting into useful pressure head a large proportion of the velocity energy rejected from the runner.

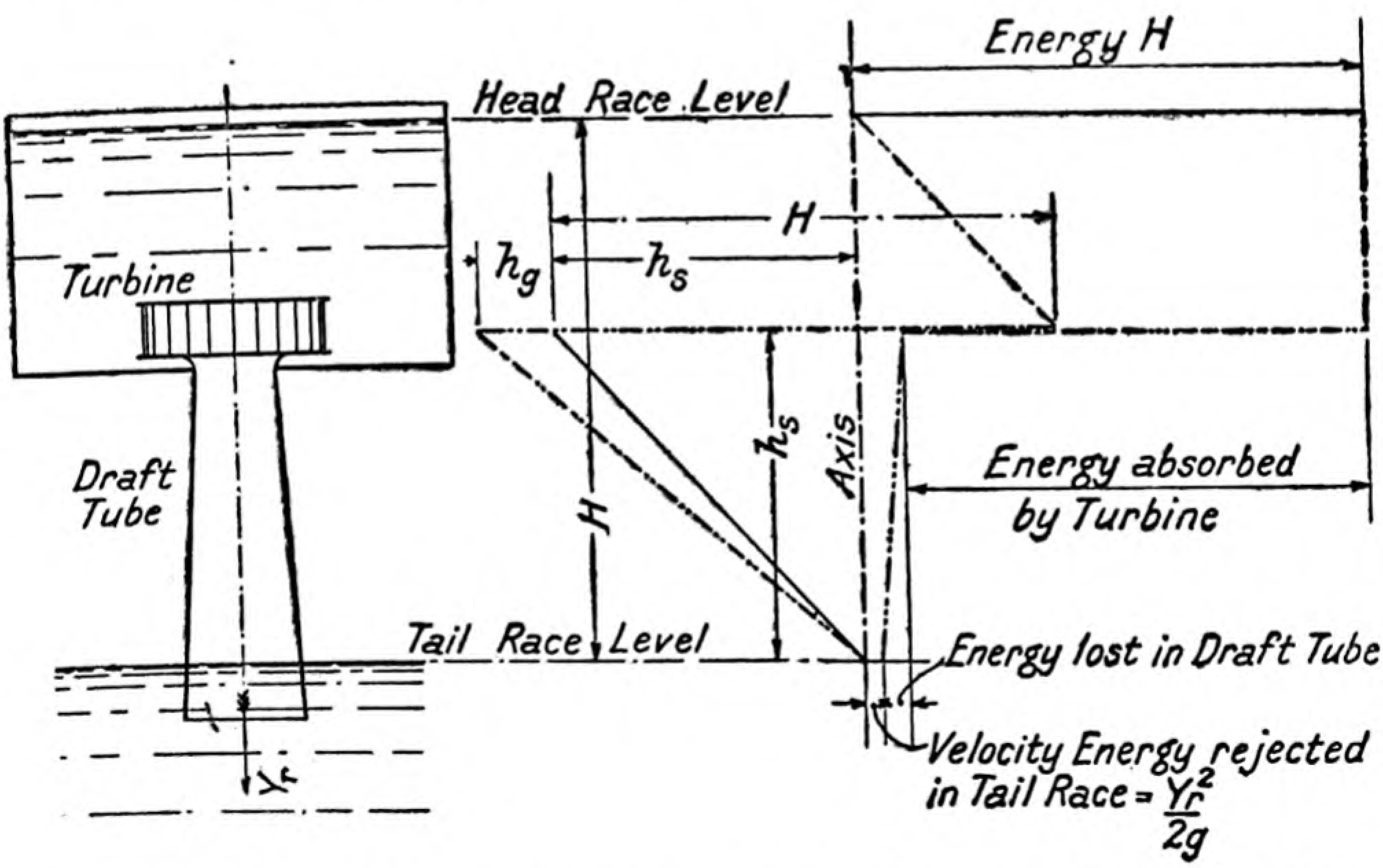

FIG. 241.—Pressure and energy changes in draft tube, as fitted to turbine shown in Fig. 235.

In a parallel draft tube, as suggested in Fig. 240, there can, of course, be no regain of head; but if the tube be "flared" or tapered (Fig. 241), there will be a reconversion of velocity head into pressure head of the sort indicated in Fig. 145 (III),

§ 164 (*b*). As a result, the drop in pressure head as the water passes through the turbine itself is now no longer H, but $H + h_g$, where h_g is the regain in head. We can now afford to be much less scrupulous about the velocity energy rejected from the runner, since the draft tube can be relied upon to convert the greater part of it into pressure energy; all that matters is the final velocity Y_r with which the water leaves the draft tube, and this can be kept as low as we like by making the outlet area big enough.

Comparing Fig. 241 and Fig. 235, we notice a most significant difference. In the elementary apparatus shown in Fig. 235, the net head was measured from the inlet water surface to the level of the turbine runner; but when a draft tube is added, as in Fig. 241, the elevation of the turbine ceases to be of importance, for the effective head H is the drop between head-race level and tail-race level. Of course occasions may arise, for example when the danger of cavitation is imminent, §§ 281, 282, in which the suction head must also be carefully controlled: this is the vertical distance h_s between the turbine and the tail-race level, Fig. 241.

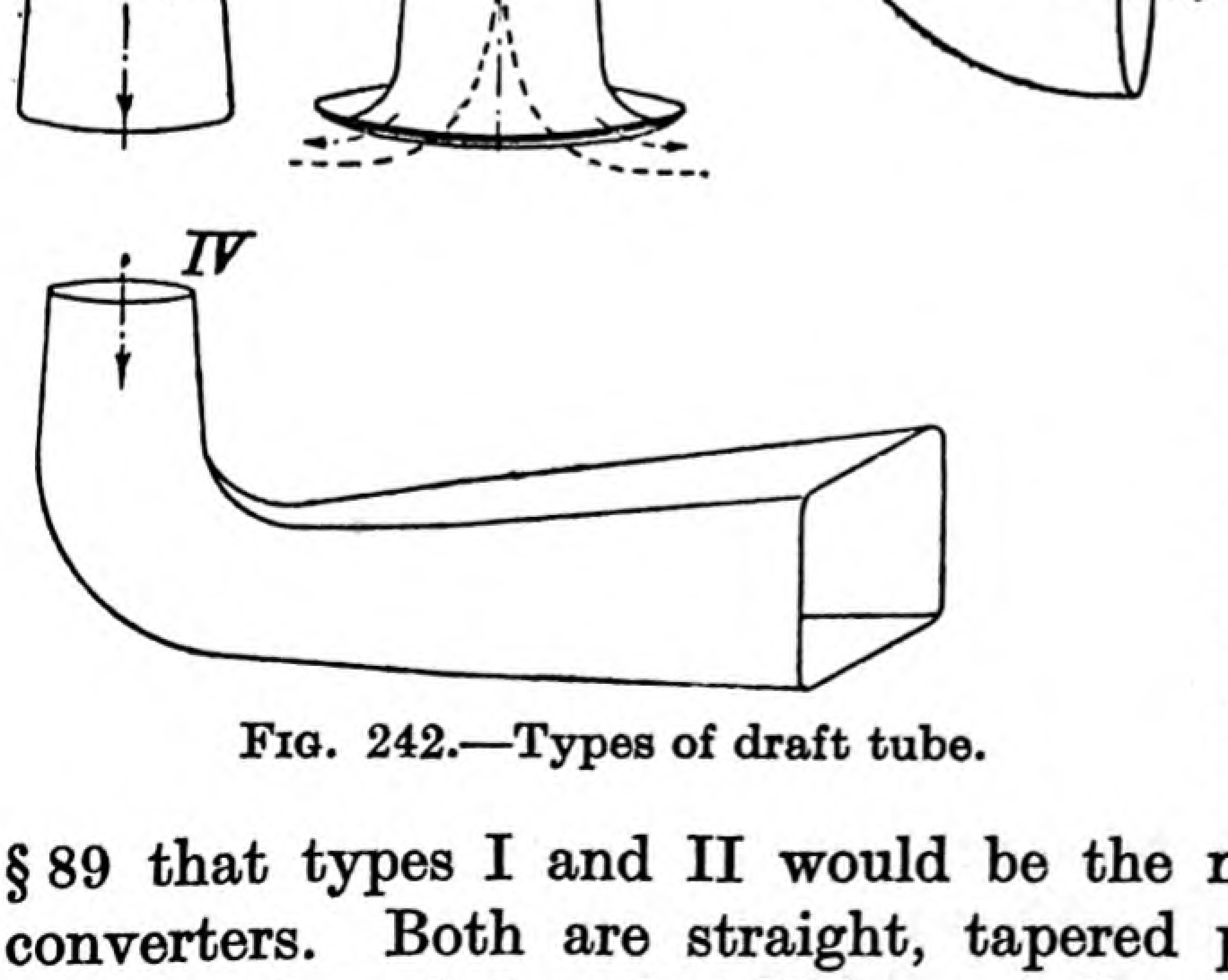

FIG. 242.—Types of draft tube.

242. Types of Draft Tube. To suit particular conditions of installation, the two basic types of draft tube discussed above can be modified in various ways, resulting in the patterns shown schematically in Fig. 242. Of these, it would naturally be expected from § 89 that types I and II would be the most efficient energy converters. Both are straight, tapered pipes, the difference between them being that II has a bell-mouthed outlet and an internal conical core. Known as the Moody "Hydraucone"

draft tube, it has the special advantage of being able to cope with helical flow, as indicated by the arrows—the flow that occurs when the water leaves the runner with a whirl component, as it may do under part load conditions (§ 273).

Unfortunately the headroom available in large low-head installations rarely permits such straight tubes to be used; although the water leaves the runner in a vertical direction, it must enter the tail-race horizontally, necessitating a 90° bend, as shown in III and IV. A loss in efficiency is bound to result.

If we take as a measure of the efficiency of a draft tube the ratio

$$\frac{\text{regain of pressure head}}{\text{velocity energy at entrance to tube}} = \frac{h_g}{\dfrac{Y^2}{2g}},$$

probable values for the types illustrated are:

Type .	I.	II.	III.	IV.
Efficiency	90%	90%	60%	80%

Other types are mentioned later in connection with the complete installations of which they form part. Especially with type IV, the precise shape that gives the highest efficiency can only be arrived at by painstaking experiments on scale models. Since the velocity energy of the water leaving the runner may amount in Francis turbines to 10 per cent. of the total head H, and in Kaplan turbines to 45 per cent. of H, the necessity for insisting on the maximum possible efficiency of regain is sufficiently plain.[152]

Just as deflecting vanes reduced the energy loss in a plain elbow, Fig. 70 (v), § 88, so also will a similar expedient improve the efficiency of a draft tube. One such deflecting vane, now termed a "splitter", can be seen in Fig. 249.

In order to show the pressure changes in the elbow draft tube, Fig. 242 (IV), an alternative treatment will offer an instructive comparison with the system preferred in Fig. 241. Let the actual draft tube, with its circular inlet and rectangular outlet, be replaced by an equivalent conical diffuser of the type seen in Fig. 67, § 87 (*b*), resulting in the system shown in Fig. 243. There has been no change in the inlet and outlet velocities; knowing these, and the draft-tube efficiency, the head regain h_g can be computed, and the hydraulic gradient

and energy line sketched just as in Fig. 67. Moreover, by scaling off the distance H_{ms}, we arrive at a highly important figure: it is the manometric suction head at the turbine exit or draft tube inlet, viz. the head that would be shown by a suction or vacuum gauge connected to this point. Its relevance is explained in §§ 281, 282, where will also be found the reason for the particular arrangement of levels seen in Fig. 243, viz. the turbine outlet being below the tail-race level.

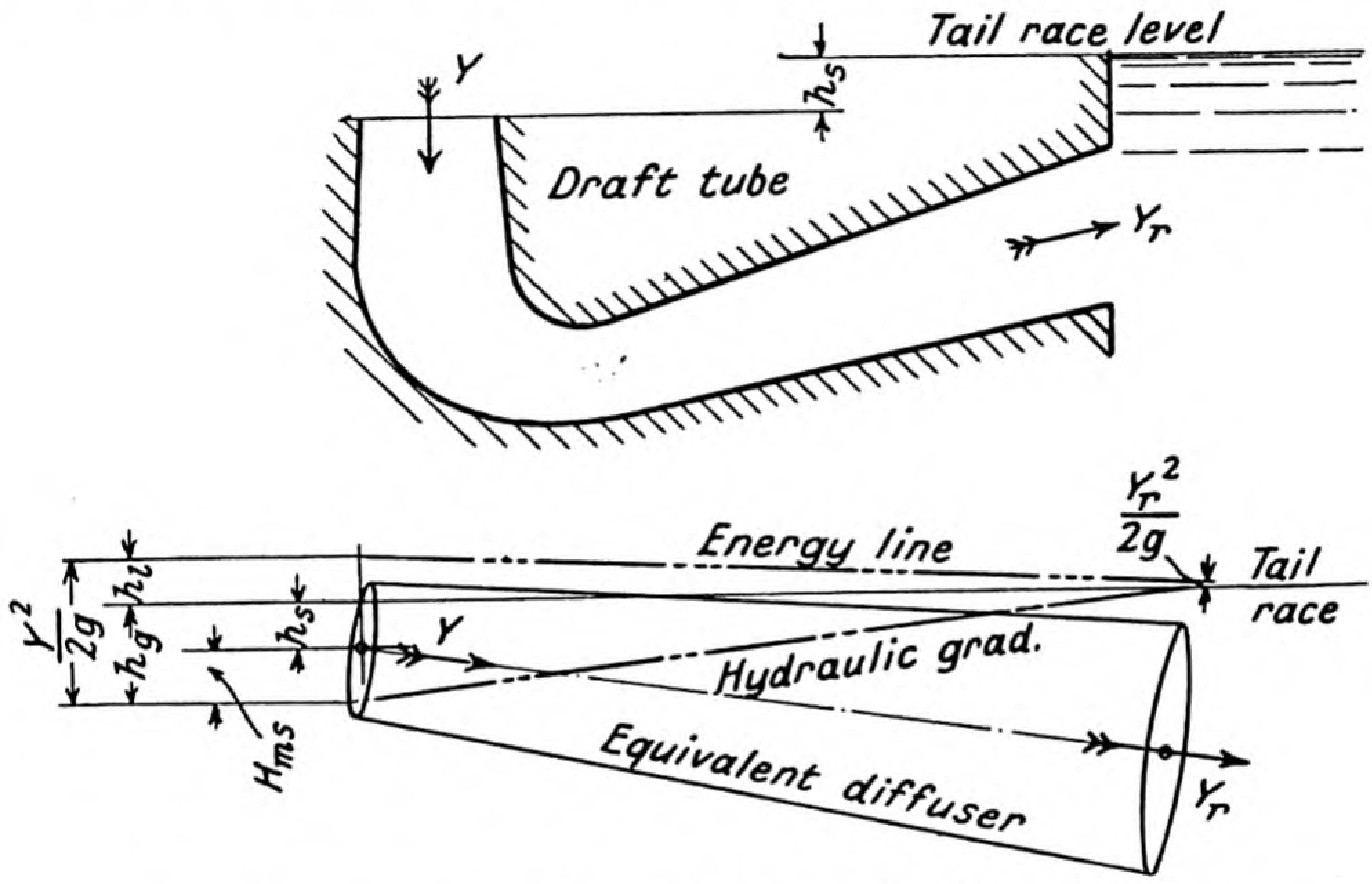

FIG. 243.—Pressure and energy changes in elbow draft tube.

243. Power and Speed Regulation of Francis Turbines. The normal method of regulating the quantity of water admitted to a Francis turbine is shown in Figs. 244, 245 and 246, and in the photographs Figs. 251 and 253. The guide blades are each pivoted about an axis parallel with the turbine axis, so that by turning them simultaneously in one direction or the other, the water passages between them may be varied in width, or completely closed. In the system of *inside regulation* adopted for relatively small low-head machines (Fig. 245), the outer end of each blade is connected by a short link to a regulating ring which can be revolved through a small angle. In the more common system of *outside regulation* (Figs. 251, 252, 253), the guide blade pivots pass through stuffing boxes in the turbine casing and carry each a small crank which in turn is linked to the outside regulating ring.

244. Reaction Turbine Governors. A typical oil-pressure servo-motor, § 356, for automatically adjusting the pivoted guides or *gates* is shown schematically in Fig. 246. It

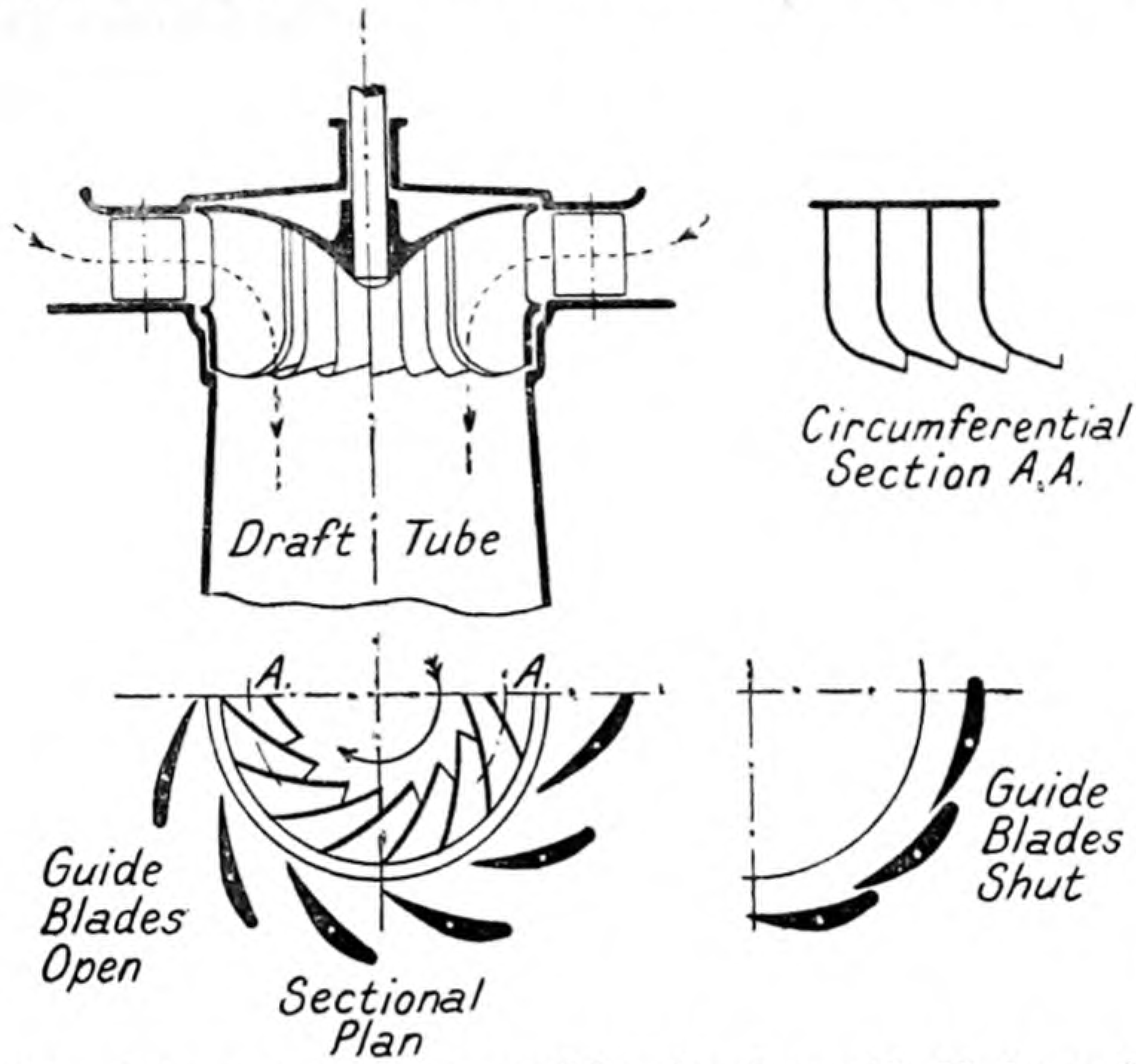

FIG. 244.—Mixed-flow reaction turbine showing guide-blade mechanism.

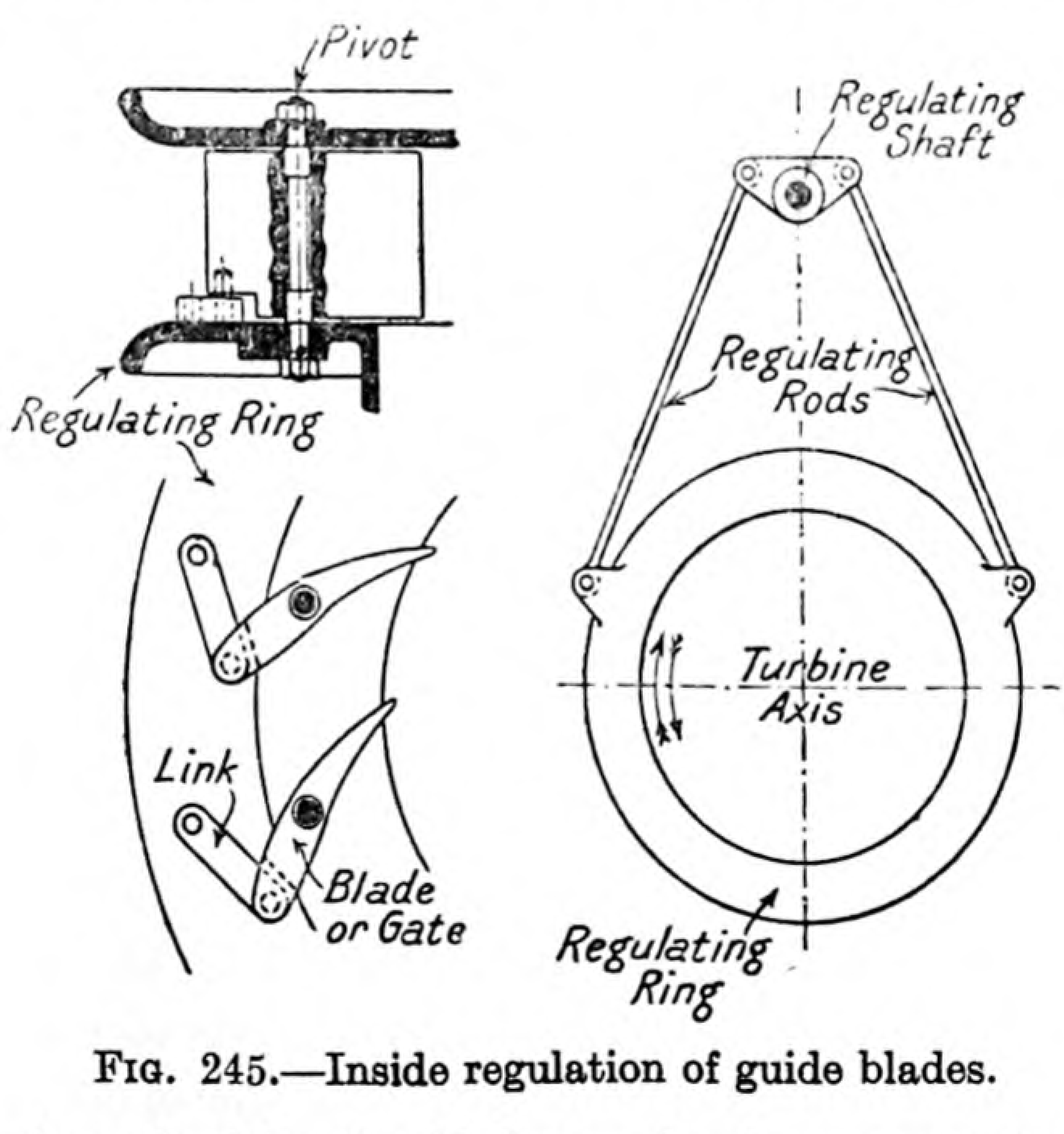

FIG. 245.—Inside regulation of guide blades.

resembles in principle the Pelton wheel servo-motor described in § 231, except that it is much more powerful because of the increased energy required to move the gates as compared with

the needle. The servo-motor piston actuates through the medium of a circular die and a short lever the regulating shaft, which is connected up to the regulating ring by a double crank and a pair of regulating rods. In the diagram the parts have taken up the position corresponding to an increase of load on the turbine: the speed has dropped slightly, the

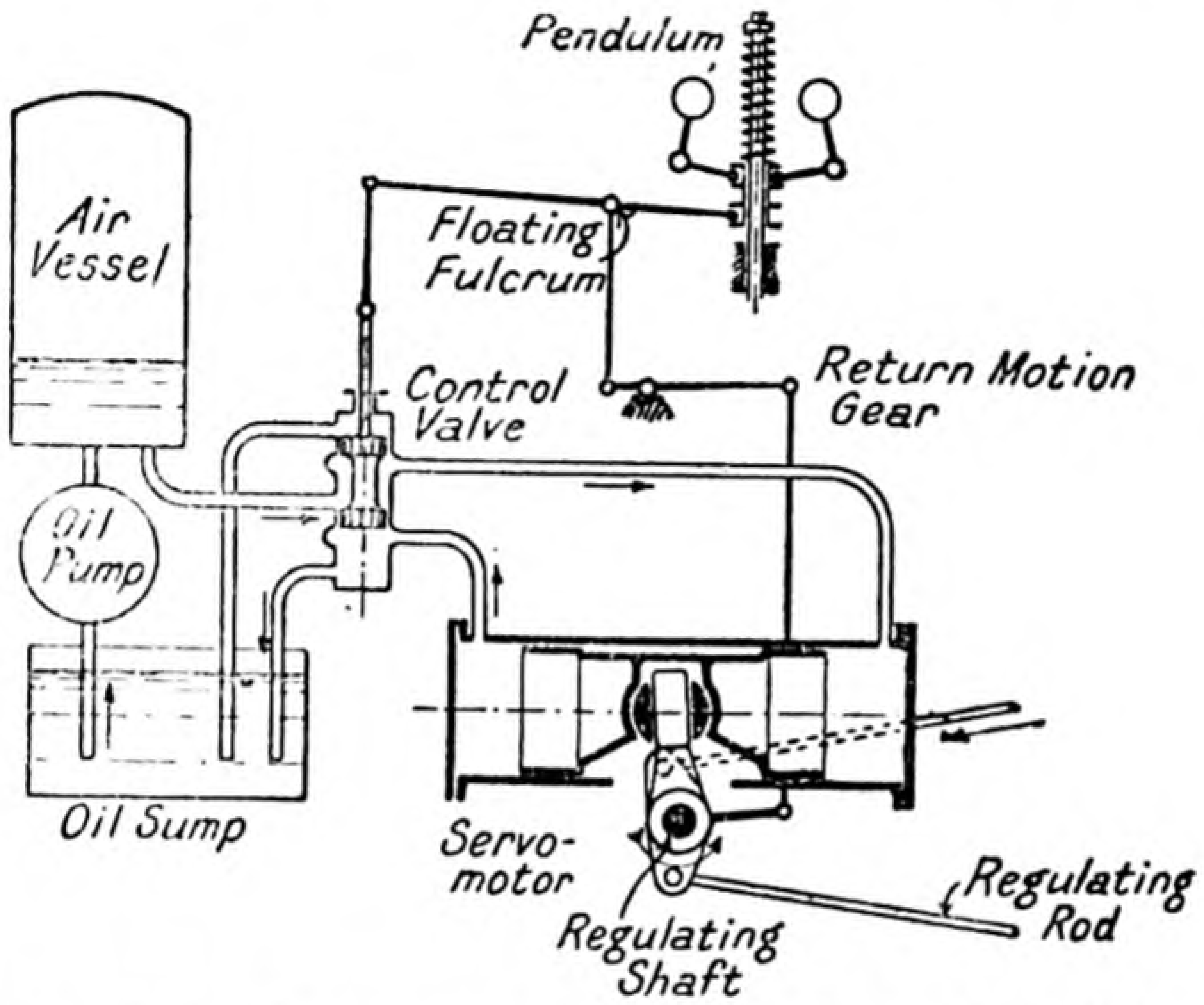

FIG. 246.—Servo-motor control for Francis turbine.

governor weights have fallen inwards, the control valve has risen, and pressure oil has been admitted to the right-hand end of the servo-motor cylinder, so moving the piston in the direction necessary to open the gates and give the turbine more water.

A difference between the governing mechanisms shown in Figs. 230 and 246 is that in the simpler one, the lever connecting the pendulum with the control valve moves about a fixed fulcrum, while in the other it has a floating fulcrum whose position is under the influence of the servo-motor piston. As the regulating shaft moves in the direction of opening the gates, the auxiliary crank on this shaft causes the floating fulcrum to move slightly downwards. Since in this way the control valve is itself under the dual control of the pendulum and of the servo-motor piston, it has a quick closing action and enables the whole mechanism to establish decisively the new position called for by a change of load, without danger of *hunting* or oscillations on either side of the desired

position.[153] The additional parts that operate the floating fulcrum constitute the *return-motion gear*; it will be evident that a further effect of this gear is to impose on the turbine a full-load speed that is slightly lower than the light-load speed.

In very large installations the servo-motor mechanism may be disposed as in Fig. 247. As twin cylinders are used, giving a balanced torque, each one can be directly coupled to the regulating-ring by a short link which is well adapted for transmitting the heavy thrusts involved.

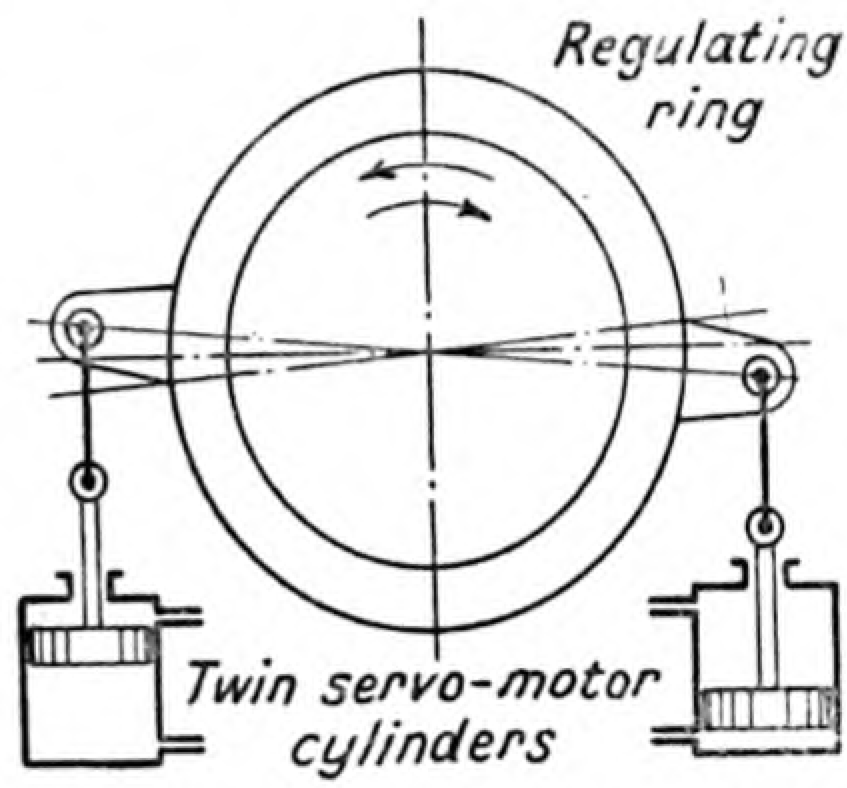

FIG. 247.—Twin servo-motors for reaction turbine control.

When the turbine is fed through a long pipe line, the governor has to undertake also the duty of opening a relief valve, which protects the pipe against the inertia effects that would otherwise accompany a sudden closure of the gates (see Figs. 250, 251). The relief valve may be regarded as the equivalent of the deflector used in a Pelton wheel.

245. Some Typical Francis Turbine Installations. In this paragraph and the next, some common methods of

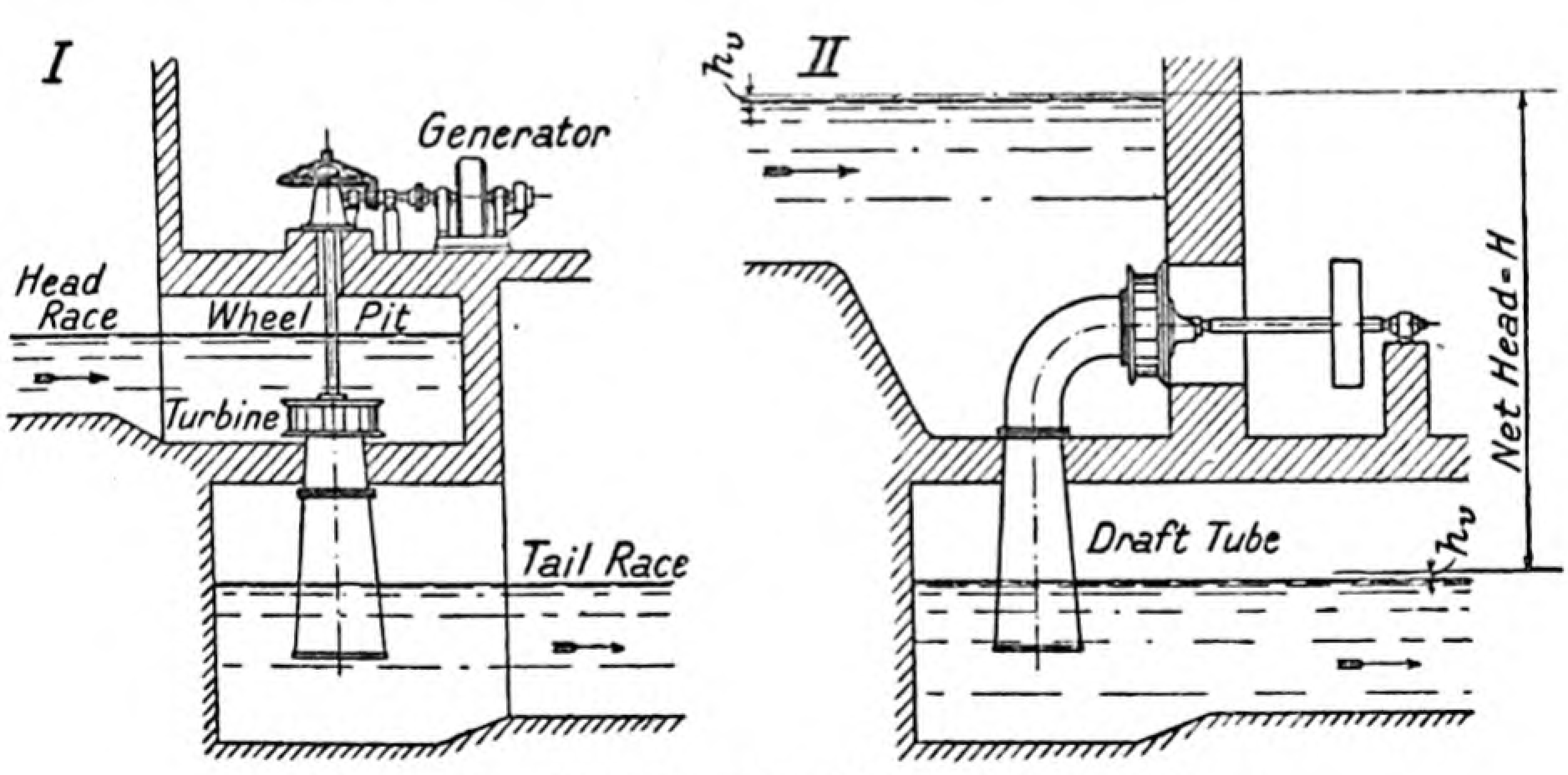

FIG. 248.—Low-head turbines in open flumes.

setting the turbine in relation to the head-race, the inlet passage, the draft tube, and the tail-race are illustrated. The diagrams are intended to be typical only.

(i) *Turbines in open wheel pits.* Fig. 248 (I) shows the best way of mounting a small, low-head machine, such as the

one depicted in Figs. 244, 245. Water flows directly from the open wheel pit or flume into the guides, and so into the tail-race *via* a straight tapered draft tube. The step-up bevel gear enables a normal horizontal high-speed electric generator to be used, in spite of the inevitably low speed of the turbine shaft. In Fig. 248 (II), a similar turbine is set horizontally, adapted for belt transmission.

(ii) *Turbine in concrete spiral casing.* This is the standard method nowadays of mounting large, low-head turbines. From the head-race canal (Fig. 249), the water flows through

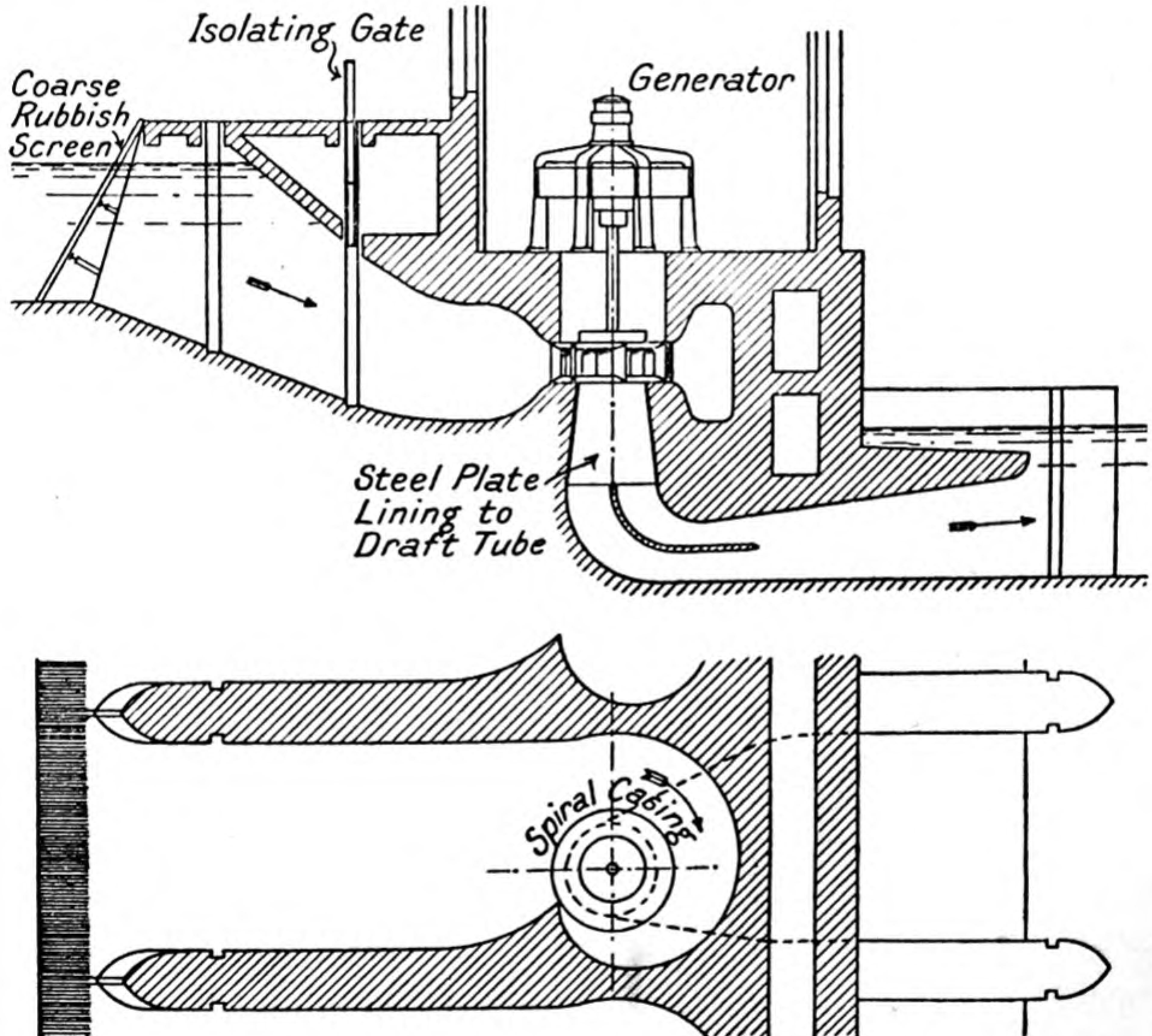

FIG. 249.—Vertical turbine in concrete casing.

a carefully-shaped inlet passage leading to the spiral casing surrounding the turbine. Due to the circumferential convergence of the walls of the casing, the water acquires a uniform whirl component which carries it smoothly into the guide passages and so to the runner. The steel plate armouring of the draft tube in the region of lowest pressure, and the curved splitter which is found to improve the efficiency of regain,

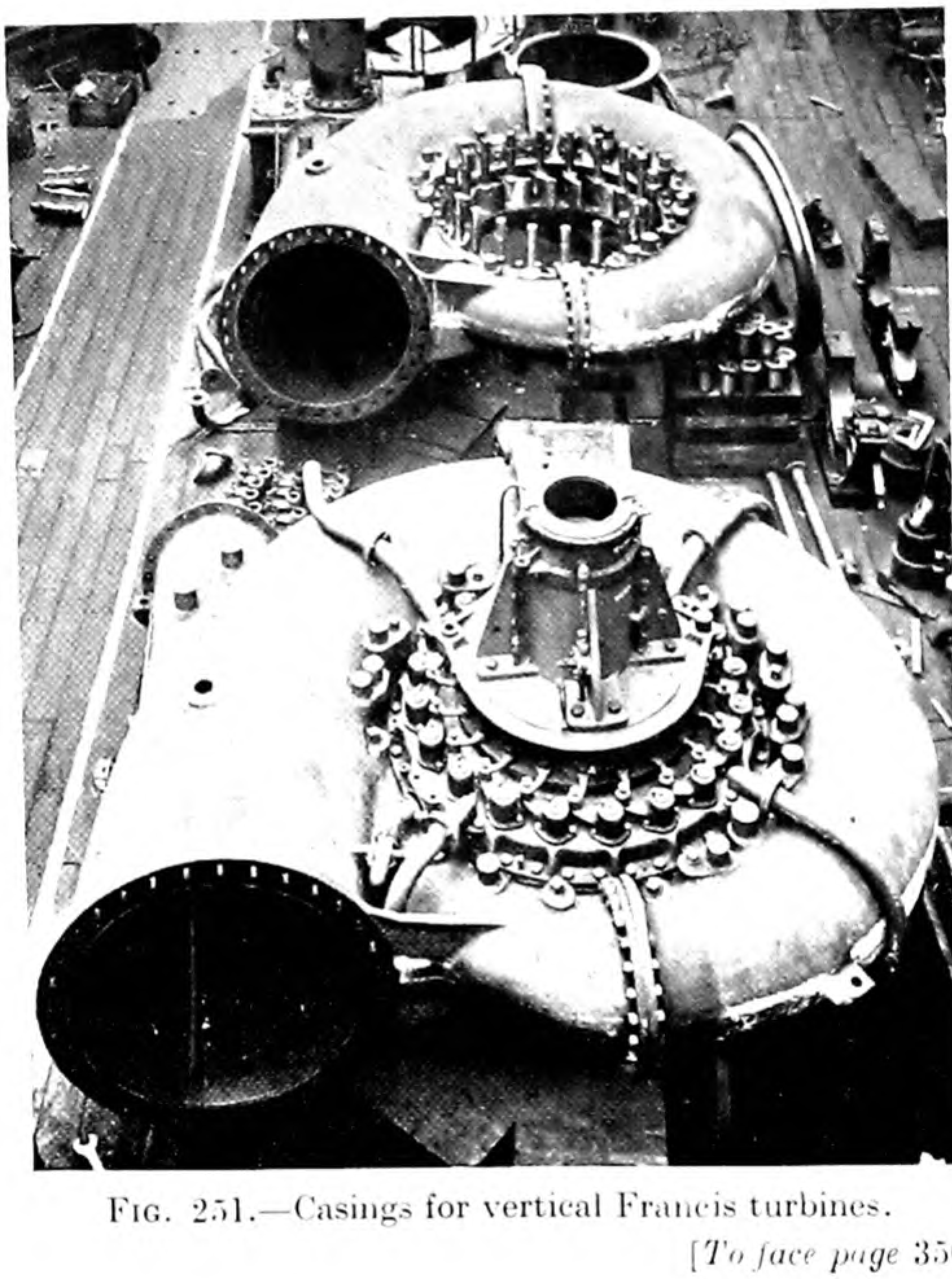

FIG. 251.—Casings for vertical Francis turbines.

[*To face page* 350.

are to be noted. From the mechanical standpoint, the vertical disposition of the units has the advantage that a single thrust bearing can support the weight of the whole of the revolving elements—turbine runner, main shaft, generator rotor, exciter armature—and in addition the hydraulic axial thrust on the runner, § 240, even though the total load may exceed 100 tons.

246. Francis Turbine Installations (contd.). (iii) *Turbines in steel casings.* Medium and high-head Francis turbines are enclosed in spiral steel casings, § 240. A large vertical shaft installation is illustrated in Fig. 250. It has a spiral

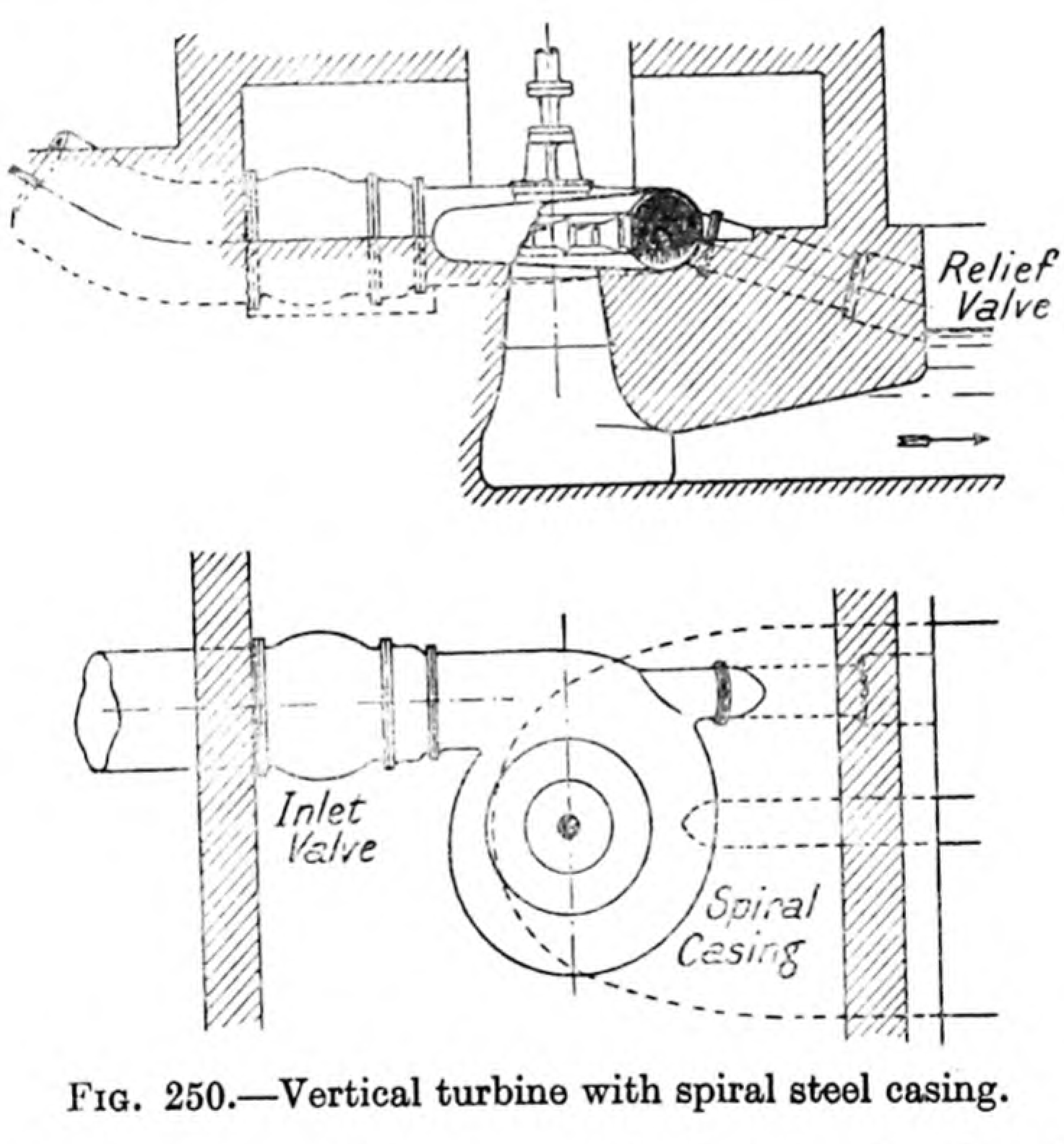

FIG. 250.—Vertical turbine with spiral steel casing.

steel casing, an interesting form of draft tube developed by the English Electric Company, a cylindrical stream-lined inlet valve of the type shown in Fig. 156, and an automatically operated relief valve for by-passing excess water direct into the tail race so as to avoid inertia pressure in the supply pipe when the turbine gates are suddenly closed.

A photograph of actual turbines of this class is reproduced in Fig. 251. The machines here shown in course of construction were supplied by Messrs. The English Electric Company for the Loch Rannoch Power Station of the Grampian

Hydro-Electric scheme; they develop 22,000 h.p. each, under a head of 515 ft.

Cross-sections through a typical horizontal-shaft spiral-cased turbine are given in Fig. 252. Attention is directed to the additional ring of fixed guide blades or *stay-vanes* cast

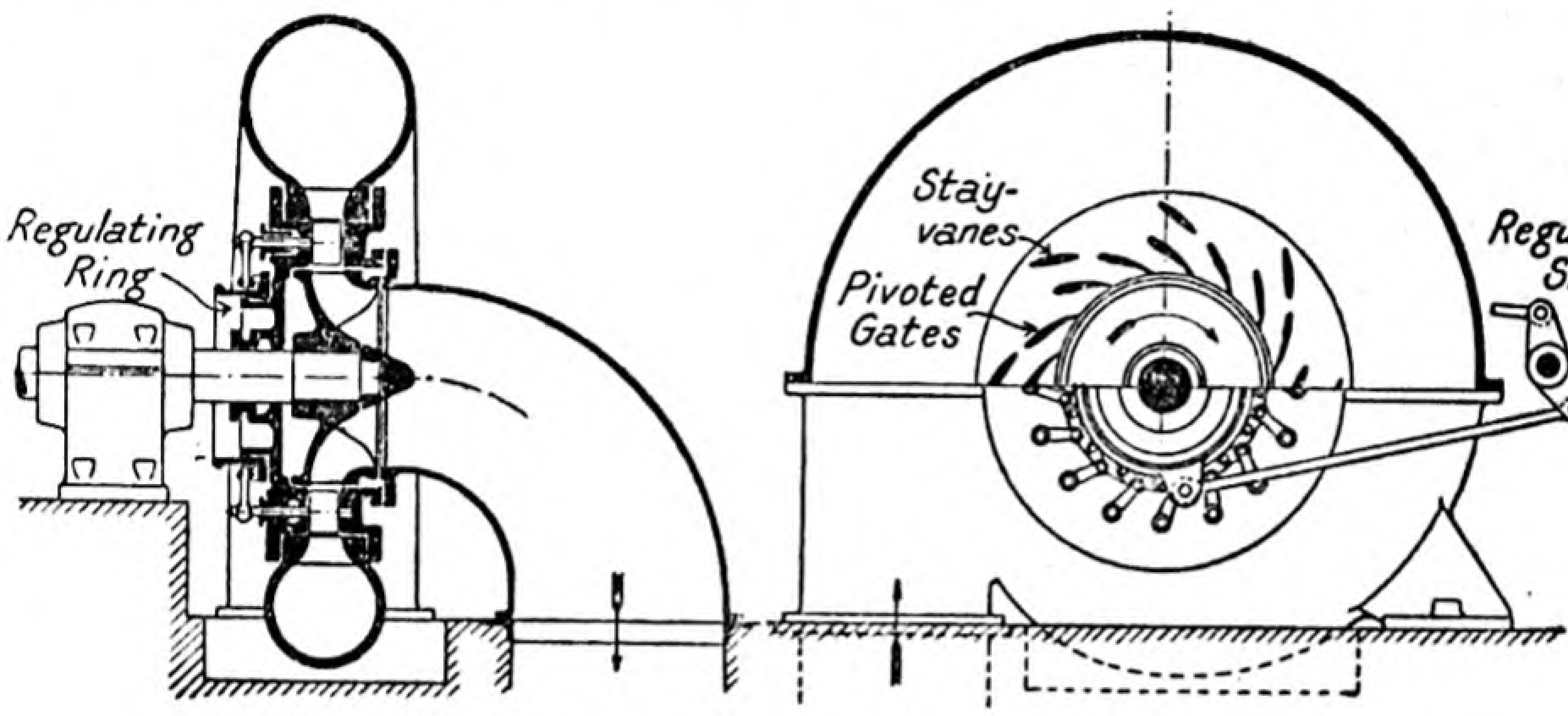

FIG. 252.—Horizontal Francis turbine in spiral casing.

in the casing outside the pivoted guides or gates, § 240. Similar *stay-vanes* are visible in Figs. 249 and 250. The photograph (Fig. 253) shows a 25,000 h.p. horizontal shaft turbine; to the right rear is the governor oil-pump with its very large air vessel or pressure receiver; to the right front is the governor and the main guide-blade servo-motor (§ 244). The runner of this machine is the central one shown in Fig. 283. The shut-off or isolating valve (not seen in Fig. 253) is of the hydraulically-operated type illustrated in Fig. 155 (i), § 170.

247. The Propeller Turbine. The development of the mixed-flow or Francis turbine into the axial-flow or propeller turbine represents the completion of the process that began when once the radial-flow or pure inward-flow runner was found inadequate. This runner had to be abandoned because its passages were too small, § 238. The demand for more water for the turbine—for more capacious passages to accommodate the water—grows more and more pressing as the available head on the turbine diminishes; because since the output power depends upon the product of head and discharge, clearly the discharge must increase as the head falls. How this demand is met is suggested in Fig. 254. Diagram (I) shows the limiting proportions of a mixed-flow turbine, where

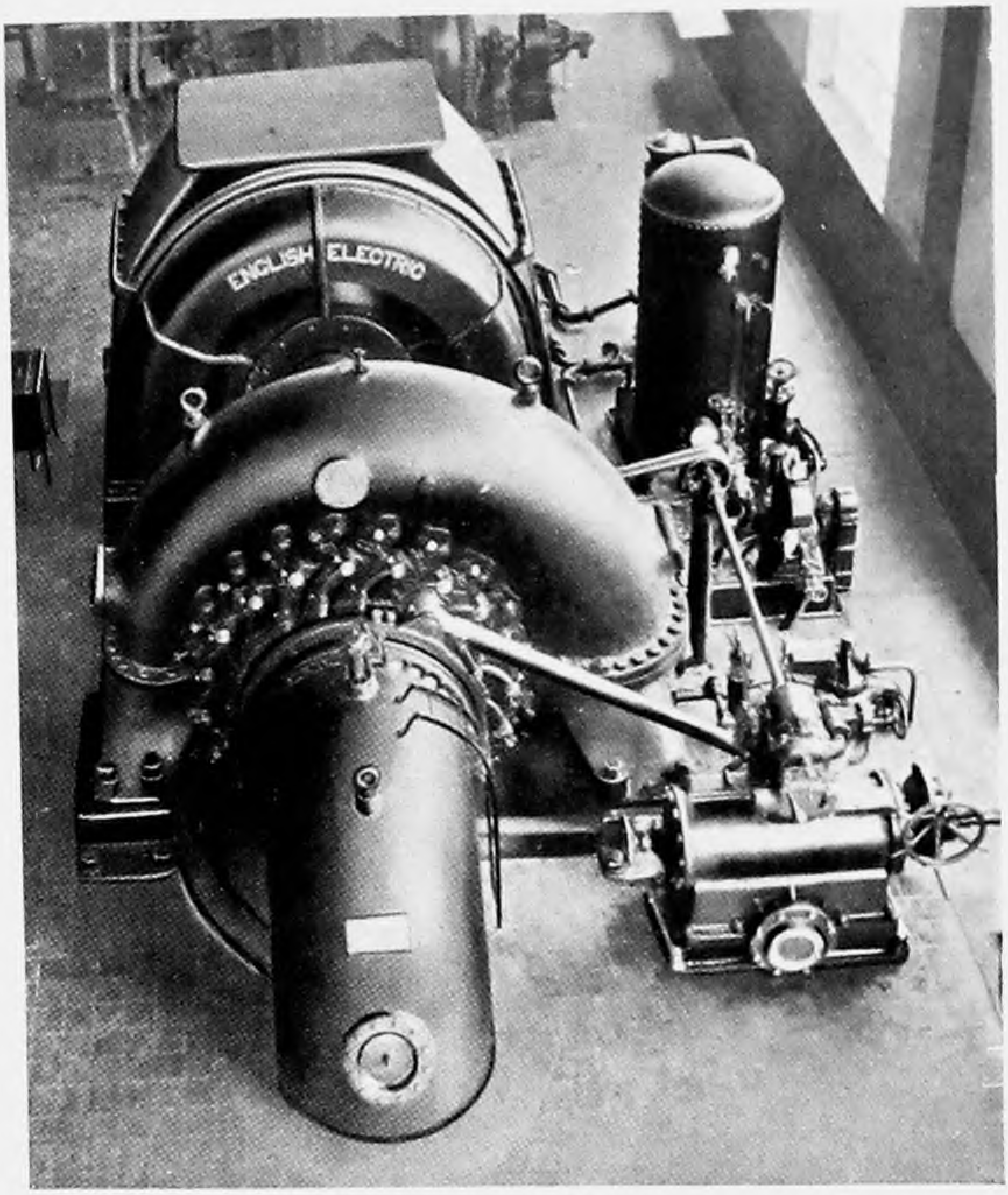

FIG. 253.—25,000 h.p. horizontal Francis turbine.
(The English Electric Co., Ltd.)

[To face page 352.

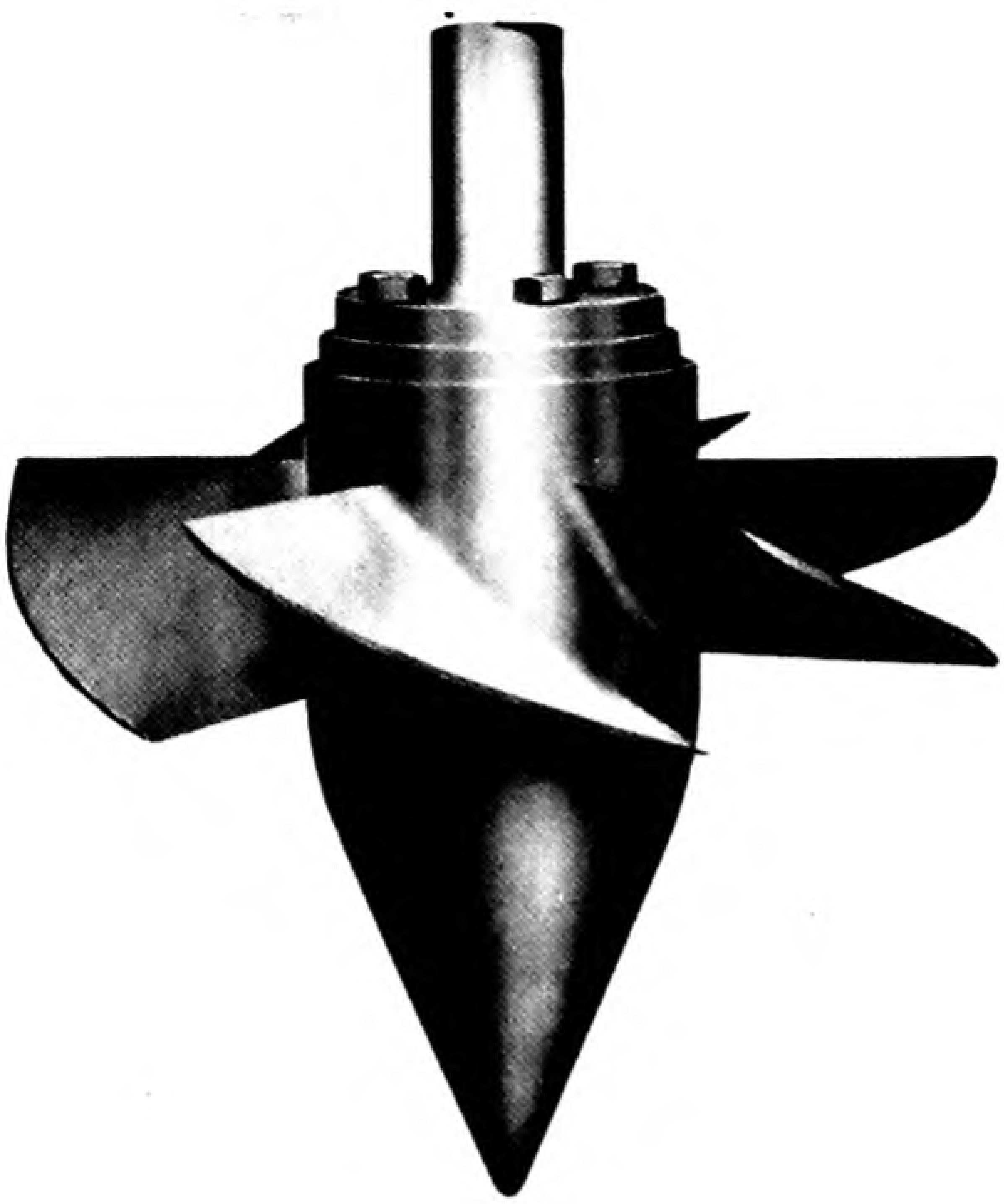

FIG. 255.—Propeller turbine runner.

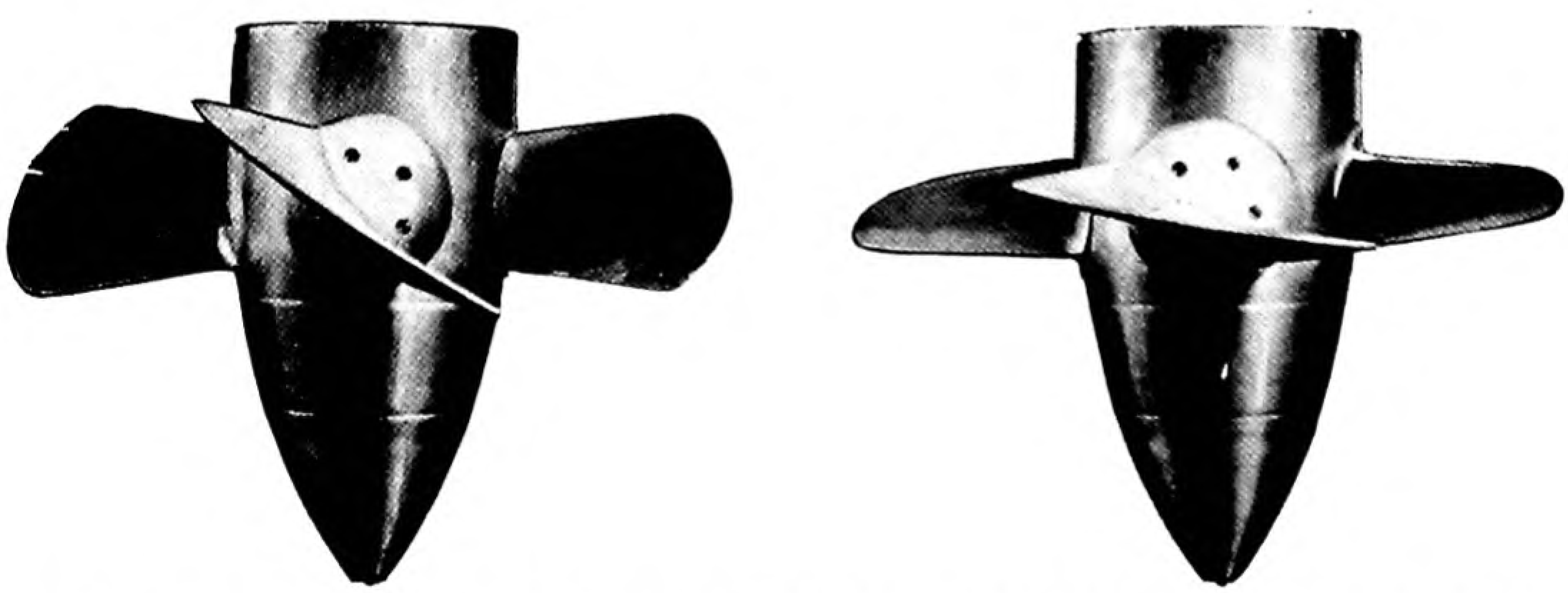

FIG. 258.—Kaplan turbine runner: (left) full-load position, (right) part-load position.

[*To face page* 353.

indeed the general direction of flow has already lost nearly all its radial or inward components. In diagram (II) these inward components have finally disappeared: by the time the water reaches the runner its flow velocity is purely axial,

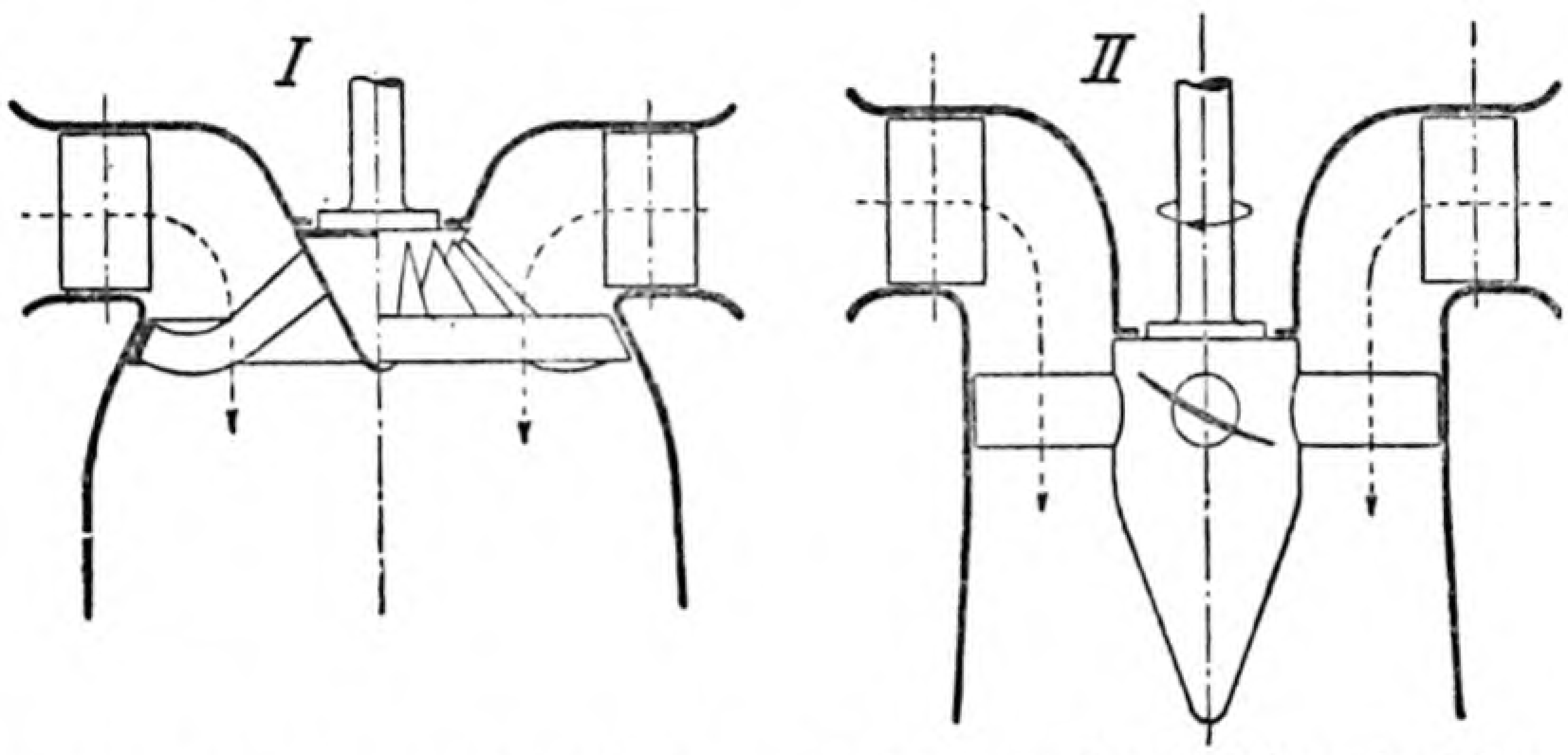

FIG. 254.—Comparison between Francis and axial-flow turbines.

or parallel with the shaft. Another change is that the number of runner blades has been reduced from 15 or more in the Francis turbine to 8 or 5 or even 3 in the axial-flow machine. What has remained virtually unchanged is the guide-apparatus or gate mechanism which controls the volume of water admitted to the runner.

In the simplest form of axial-flow runner the blades are cast integrally with the hub (as shown in Fig. 255); alternatively, the blades may be pivoted, but fitted with hand adjusting gear which can only be operated when the turbine is stopped.

In general the main dimensions of propeller turbines are established by a procedure analogous to that described for Francis machines (§§ 235, 236). The chief deviations are :—

(i) Instead of arbitrarily laying down a ratio of runner width to runner diameter, we must choose an appropriate value for the ratio $n = d/D$, where d = boss diameter and D = runner outside diameter. Remembering that the velocity of flow Y now represents the *axial* component of the absolute velocity, we can then extract the desired values of D and d from the relationship—

$$Q = \text{discharge through runner}$$

$$= \frac{\pi}{4}(D^2 - d^2)Y = \frac{\pi}{4}(D^2 - d^2)\psi\sqrt{2gH}.$$

(ii) Since the peripheral velocity v of the runner blades depends upon the radius of the selected point, the blade angles will vary continuously from the boss to the rim. At a given radius, moreover, the velocities at inlet and outlet are identical. Selecting as representative points one near the hub at radius r and one near the rim at radius R, we can proceed to study the hydraulic conditions along representative sections passing through those points, Fig. 256. Blade velocities are found as

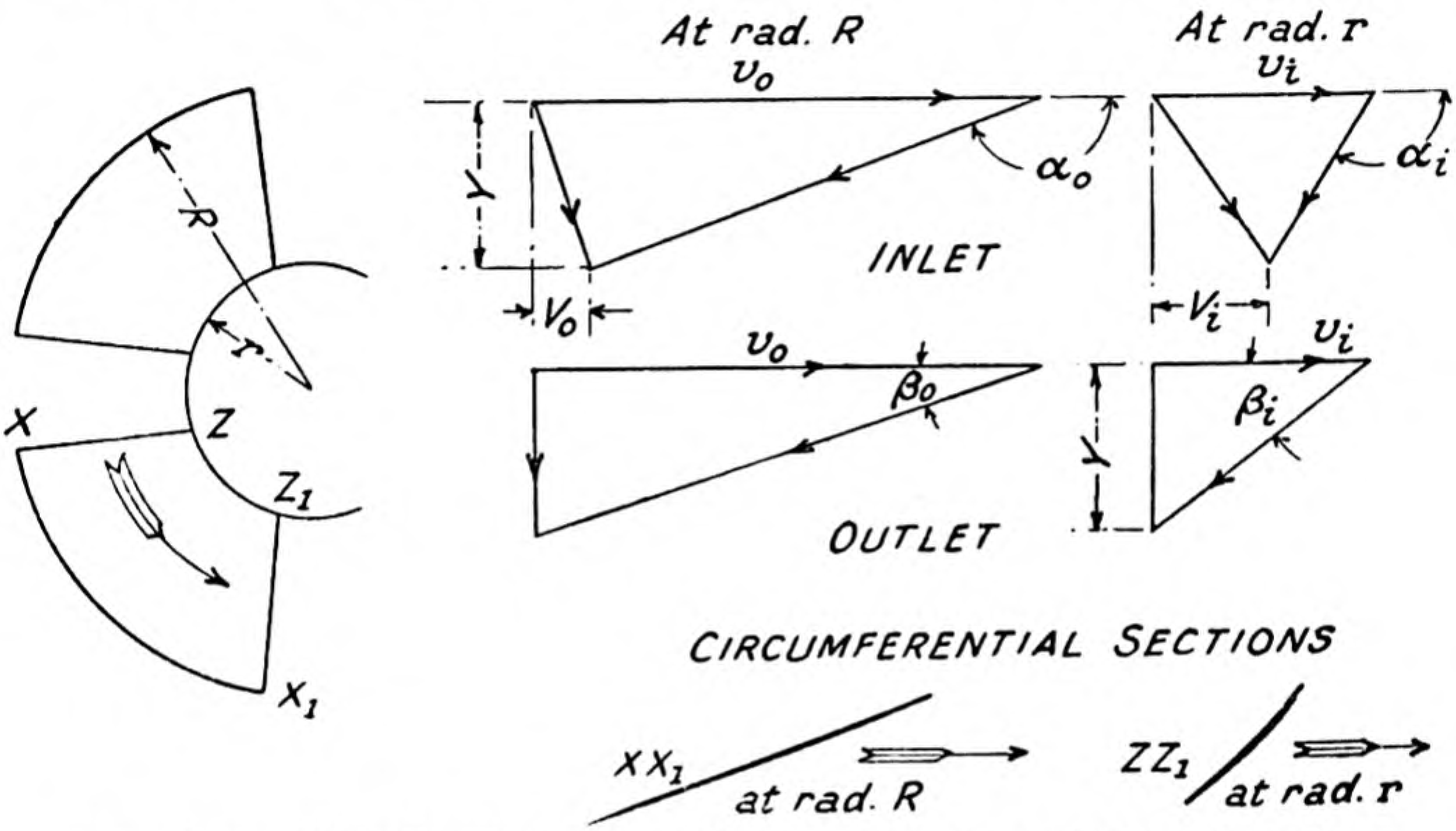

Fig. 256.—Velocity diagrams and blade forms for axial-flow turbine.

usual from the relationships $v_o = \dfrac{2\pi RN}{60}$ and $v_i = \dfrac{2\pi rN}{60}$, and corresponding whirl components of the water velocities from the general equation $\eta_h = \dfrac{V_o v_o}{gH}$, as in § 236 (iv). From the resulting velocity diagrams the blade forms can finally be sketched as in the illustration; they may profitably be compared with those shown in Figs. 255 and 258.

It is to be noted that the stipulated hydraulic conditions at inlet will only prevail if the velocity of whirl is inversely proportional to the radius, viz. if the water has free vortex motion (§ 140). But as from the moment it leaves the gates to the moment it impinges on the runner blades the water has plenty of opportunity to arrange itself according to the requirements of uniform energy distribution, it seems likely that the actual distribution will not be very different from the assumed ideal one.

248. Propeller Blades considered as Aerofoils. A curious omission may now be noted in the study of turbine design as hitherto developed. Although the whole purpose of the apparatus is to give the water the best chance of exerting a torque on the shaft or a tangential thrust on each individual blade, we have not asked what is the numerical value of this thrust in pounds or kilograms. Yet the basic process of energy transfer seemed to depend upon the dynamic thrust of liquids upon moving surfaces, §§ 123 - 125, 131. It should therefore be illuminating to return to this principle, and in fact the operation of the propeller turbine offers a convenient opportunity of doing so; its blades are so relatively few that a single one of them may be studied independently. From one such blade we select an annular strip AA shown in section and plan in Fig. 257. By the methods of § 247, the inlet and outlet velocity triangles are plotted and superposed as in Fig. 257, which at once makes it possible to evaluate the *mean relative velocity* v_r of the water flowing past the blade element.

It is at this stage that we begin to regard the blade element as an aerofoil or hydrofoil, § 131. The approach velocity which was represented by U in Fig. 116 is now represented by v_r in Fig. 257; and as the characteristics of the aerofoil are assumed to be known, there is no difficulty in computing the lift L and the drag D, and in turn the resultant thrust P. If the force P is resolved parallel to and normal to the direction of motion v of the blade element, two components finally remain: a tangential force P_t and a normal force P_n. The first tells us what contribution the blade element gives to the useful effort of making the turbine shaft revolve; the second is related to the axial thrust on the shaft, § 240 (iii). By summing together the individual thrusts on all the blade elements, the gross torque and the gross axial thrust on the rotor may be estimated.

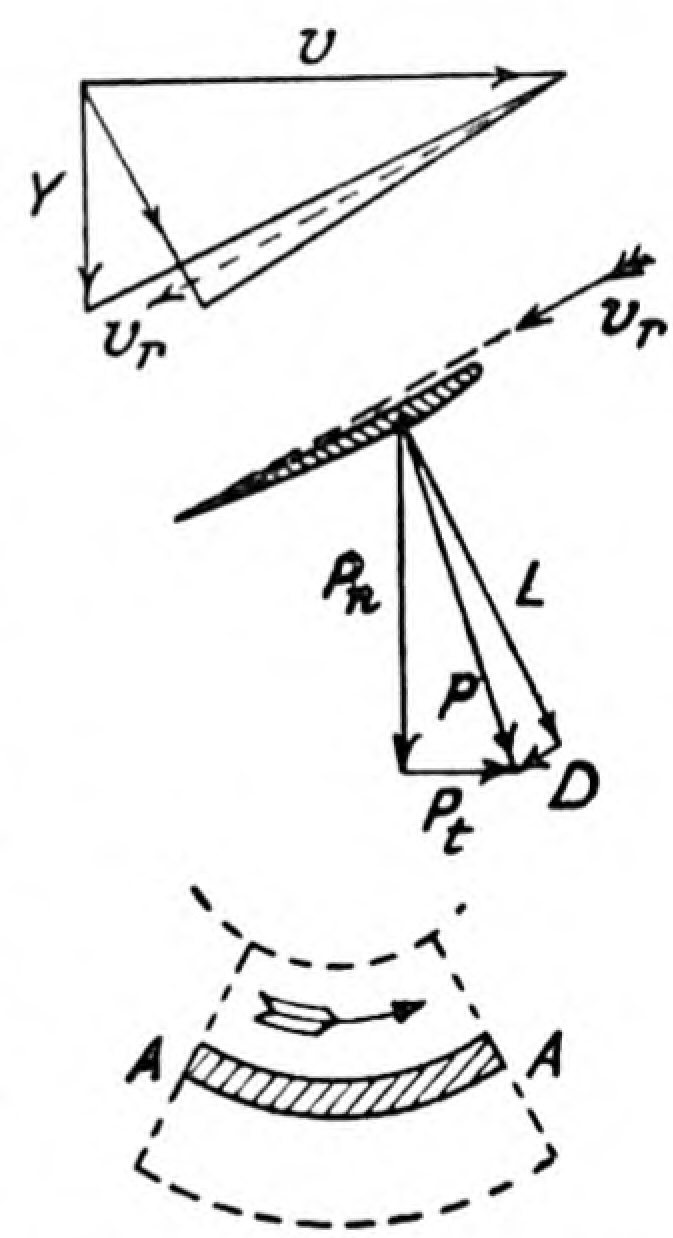

FIG. 257.—Forces on propeller-blade element.

Here it is to be noted that only in a general sense can each propeller blade element be regarded as an isolated aerofoil. What in fact happens is that each blade influences the flow past adjacent blades, and therefore the lift and drag coefficients for a single aerofoil, Fig. 117, could not be directly applied in turbine design.[154]

249. The Kaplan Turbine. Although the propeller turbine stands almost unrivalled when large energy outputs must be developed under low heads, yet in its basic form it has one quite serious disadvantage, viz. its part-load efficiency is unsatisfactory, § 276. In the Kaplan turbine this drawback is overcome by mounting the runner blades so that their angles of inclination may be adjusted while the turbine is in motion.[155] The runner thus in effect forms a variable-pitch propeller, as can clearly be seen from the photographs of a model runner (Fig. 258, facing page 353). It is for this reason that the Kaplan turbine is sometimes described as a variable-pitch propeller turbine; and indeed under full-load conditions the machine behaves in all respects like a propeller turbine.

The method of pivoting and operating the runner blades is shown schematically in Fig. 259. The stub-shaft or pivot formed integrally with each blade carries a short crank which is linked to a crosshead having as many arms as there are blades, the whole mechanism being enclosed within the central boss. Actuating the crosshead by means of a central rod passing down the hollow main turbine shaft is an oil-pressure servo-motor; its cylinder acts as the coupling between the turbine shaft and the generator shaft. Oil from the governor is admitted to the upper or under side of the servo-motor piston, so reducing or increasing the blade angle, by pipes (not shown in the diagram) passing down the generator shaft.

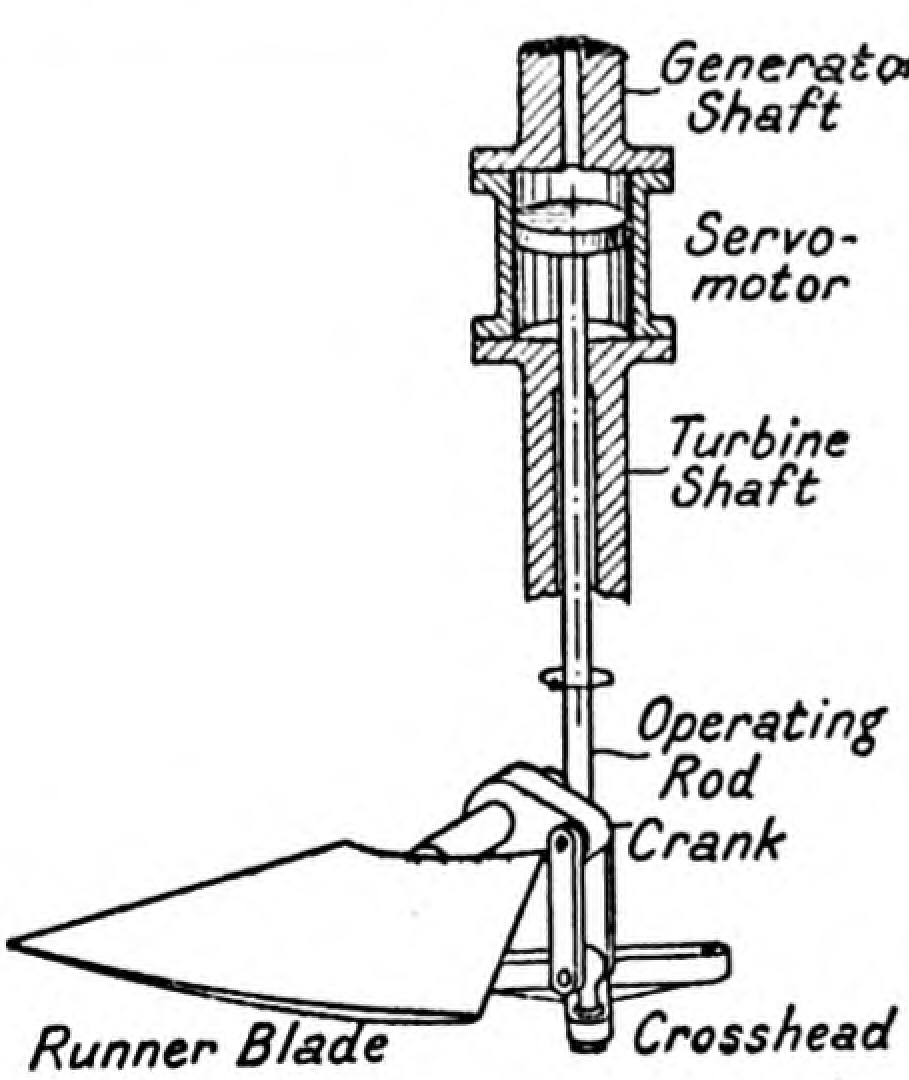

FIG. 259.—Kaplan runner blade mechanism.

The complete regulating mechanism must include not only the revolving servo-motor just described, for adjusting the runner blades, but also the normal stationary servo-motor controlling the guides or gates: the governor is required to

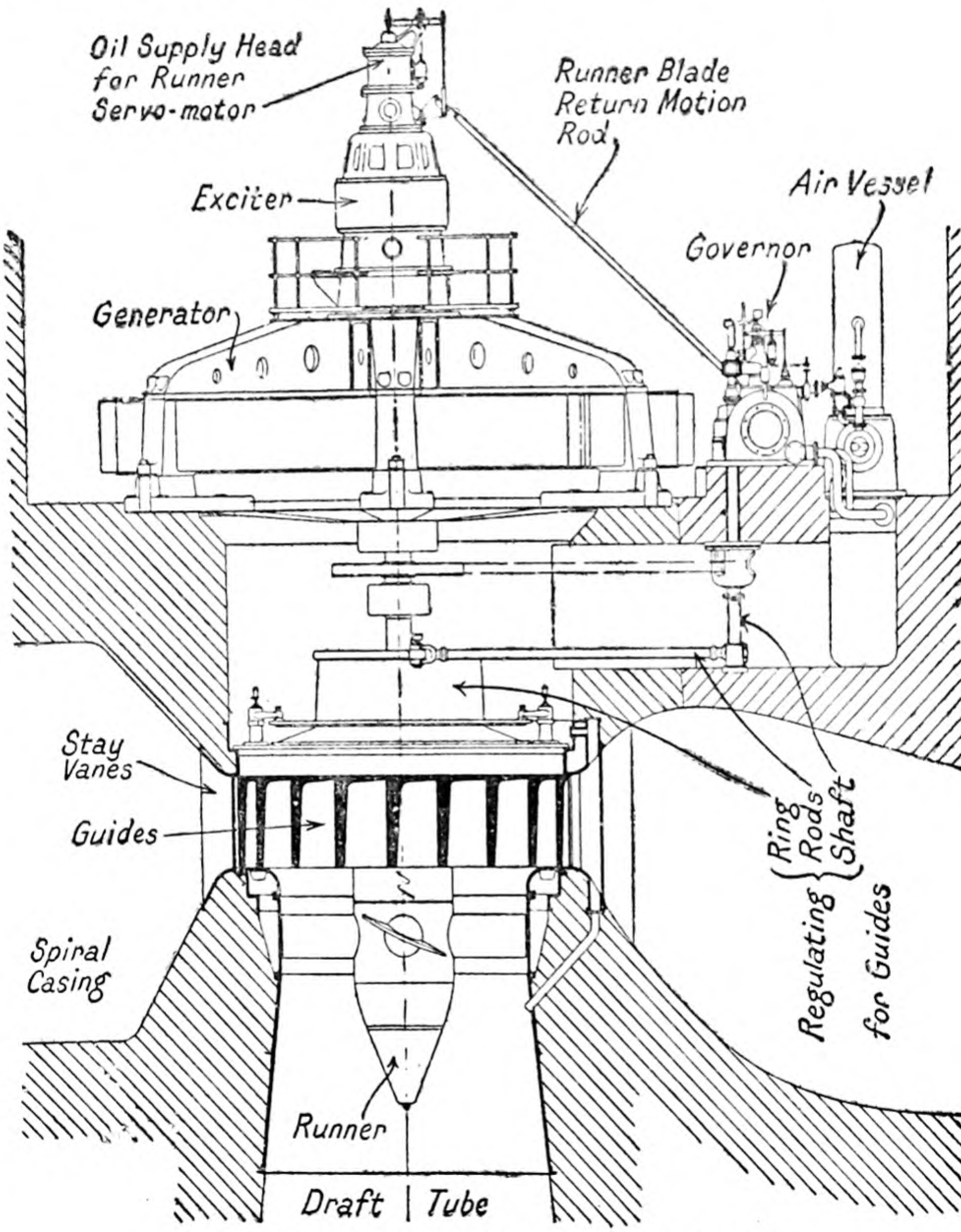

Fig. 260.—Kaplan turbine control mechanism.

actuate both sets of blades simultaneously. This arrangement is shown in Fig. 260; it does not differ materially from that described in § 244, except that the governor now also embodies a control valve for the runner blade servo-motor, the necessary correlation between the position of the valve and of the blades

being established by an independent return-motion gear. The gate servo-motor control valve and the runner servo-motor control valve are themselves inter-connected to ensure that for a given gate opening there shall be a definite runner-blade inclination.

At the present moment the limiting data controlling the design of axial-flow turbines are normally as follows :—

Head	106 ft. (say 32 m.)
Runner diameter	26 ft. (say 8·0 m.)
Flow ratio ψ	0·69
Speed ratio ϕ based on outer diameter of runner	2·09
Gross or overall efficiency	92 per cent.
Output	74,000 h.p.

250. Propeller Turbine Installations. Propeller turbines, whether with or without variable-pitch runners,[156] are usually set relatively to the intake and outlet channels in the manner shown in Fig. 249. Some interesting features of such an installation are to be observed in Fig. 261. Because in this instance the working head, 96 feet, is high for this class of machine, the spiral casing is of steel plate, of circular cross-section (§ 240 (i)). For the same reason, the runner has eight adjustable runner blades, this limiting number being necessitated by considerations of safety against cavitation, § 281. Other constructional details visible in the photograph, Fig. 261, are (i) the duplex system of gate servo-motors, Fig. 247, § 244, and (ii) the revolving runner-blade servo-motor, § 249.

As the working head on a Kaplan turbine becomes progressively lower, the considerations that control the shape of the runner, § 247, now begin to influence also the form of the spiral casing, which now has to deal with really immense volumes of water. The scale of construction can be gauged from Fig. 262 (i), which relates to a turbine developing 37,600 h.p. under a head of 11·0 metres, using 300 tons of water per second. To feed this very large flow uniformly to the runner, the walls of the spiral casing, in conjunction with the stay-vanes and the guide-blades, are no longer adequate ; they must be supplemented by the two curved guide-walls or vertical partitions. The outlet of the draft-tube, which is of the type shown in Figs. 242 (IV), 243, is similarly sub-divided ; each half is as big as a

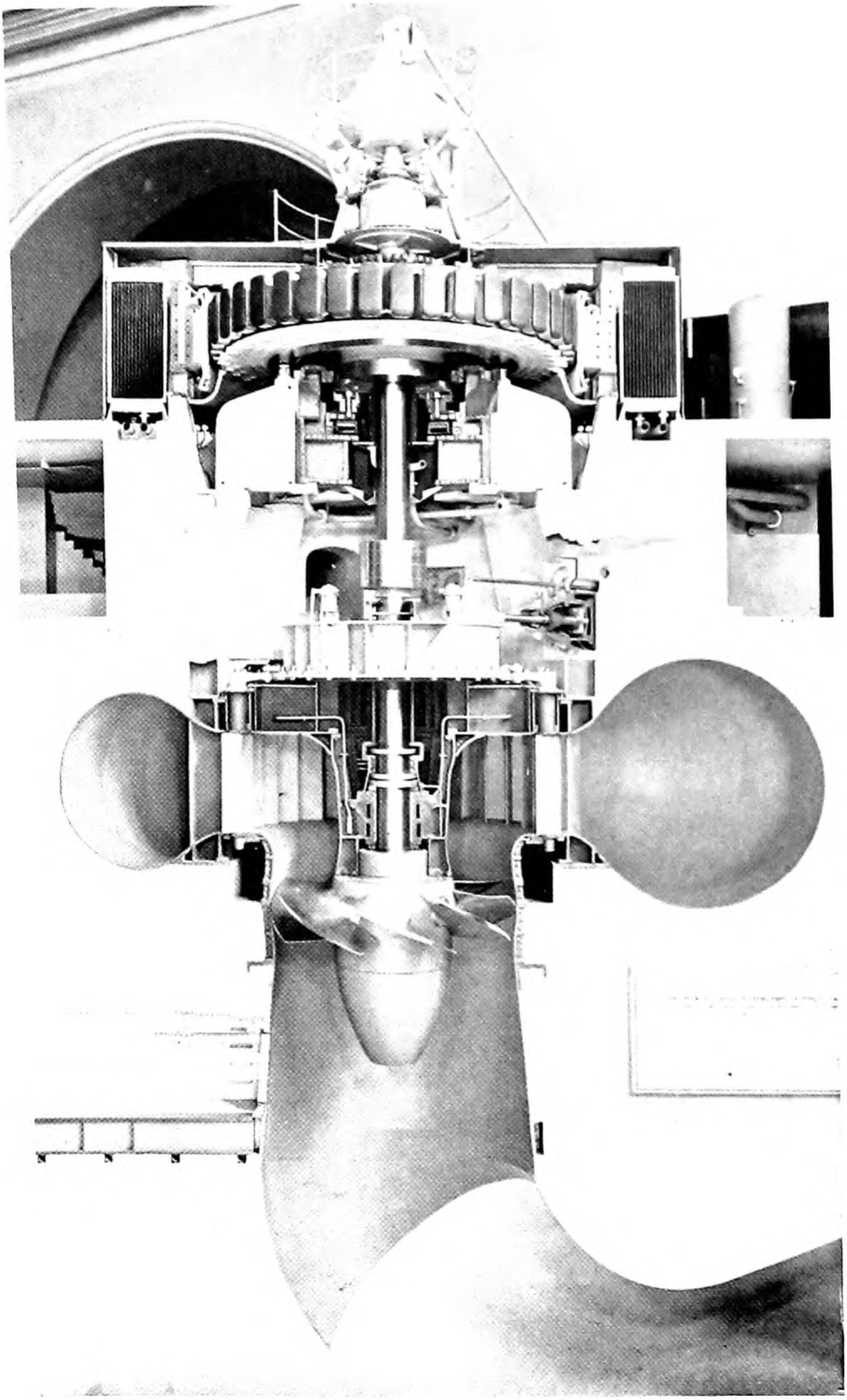

FIG. 261.—Kaplan type hydro-electric plant, 35,000 h.p.

(The English Electric Co., Ltd.)

[*To face page* 358.

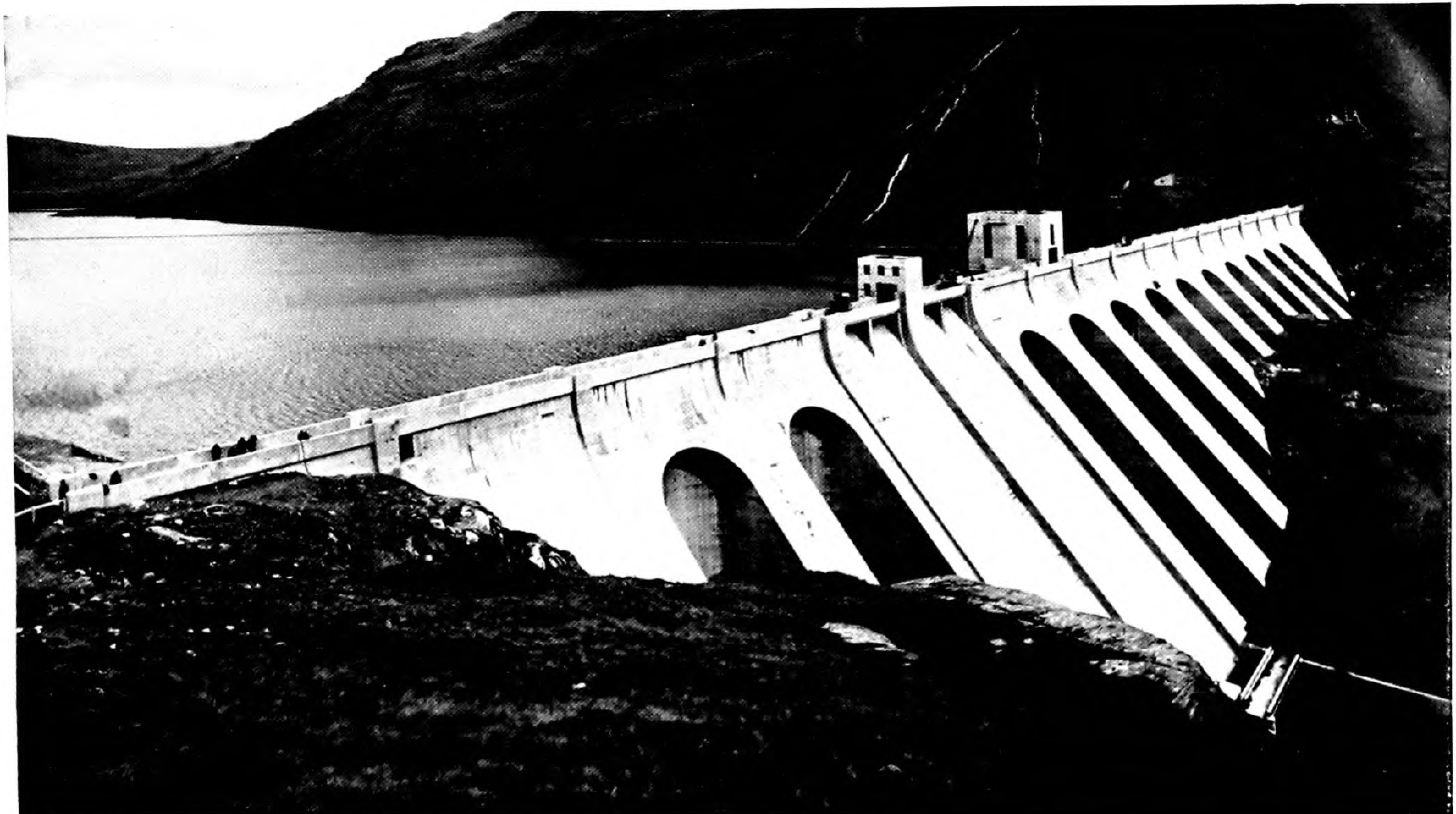

FIG. 264.—Dam and reservoir for Loch Sloy installation.

(The North of Scotland Hydro-Electric Board)

[*To face page* 359.

moderate-sized assembly hall, and considerably larger in cross-section than an underground "Tube" railway station. A schematic graph, Fig. 262 (ii), in which average absolute velocity is plotted against distance, serves as a reminder of the basic purpose of these vastly-proportioned passages: it is to accelerate the water gradually up to its maximum velocity just before it enters the runner, and then to allow the velocity to

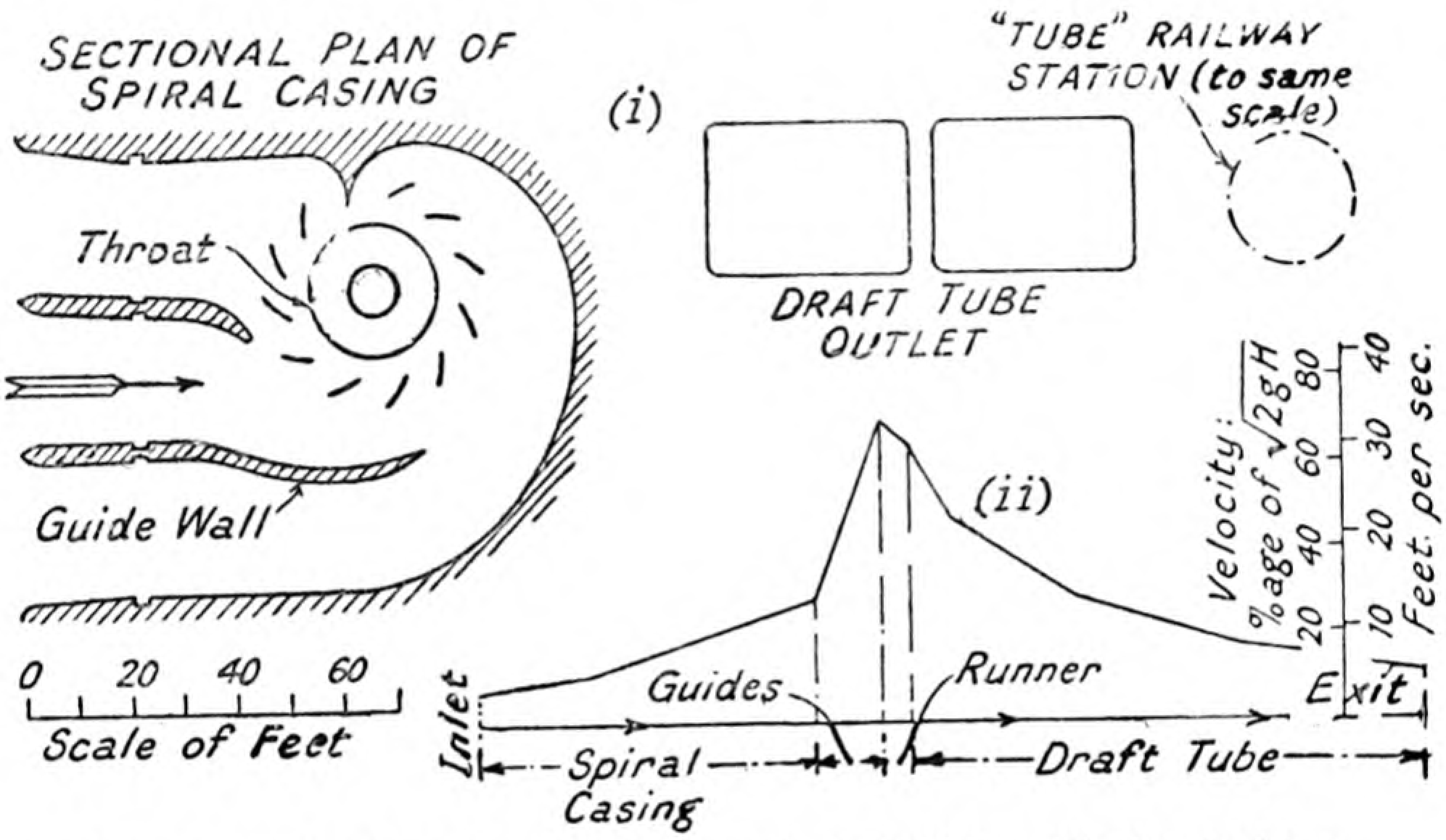

FIG. 262.—Inlet and outlet passages for 37,000 h.p. Kaplan turbine.

subside gently to a value at which it is permissible to discharge the water into the tail-race. The corresponding energy conversions will involve excessive losses unless a long enough path is provided—in this instance the distance travelled by an element of water from the spiral-casing inlet to draft-tube outlet is more than 250 ft.

251. Elements of Complete Water-power Development. In addition to the turbines themselves and the building that houses them, a water-power scheme must include the channels or conduits which lead the water to the machines and from them again, and possibly also one or more storage reservoirs.[157] Except in pumped-storage installations (§ 366), the turbines are set in an artificial "shunt" circuit in parallel with the natural water-course from which the water is abstracted. At the highest practicable point in the stream, head-works of suitable design (§ 187) divert a proportion of the natural flow into the intake channel, and after the water has

yielded up its energy to the turbines it is restored to the stream bed. The type of conduit chosen—whether open or closed, or a combination of the two, § 149—will depend upon the operating head and upon the topographical nature of the country. Although a steel pipe will probably convey all the water that is wanted for a high-head plant, yet for a low-head plant of equivalent output a canal as broad as a river may be required.

Reservoirs may provide either seasonal storage or daily storage, §§ 204-207. In either case the purpose of the stored water is to keep the turbines running during the periods when the natural stream flow is insufficient. Such periods may last for several weeks in a high-head installation, and the water drawn upon is the excess that has accumulated during the previous season of heavy rainfall or snowfall. The flow demanded by low-head plants is so relatively large that even if it is practicable to construct a reservoir at all, it will only hold a few hours' supply. But even this storage capacity may be valuable, for it will permit excess river water to accumulate during the night hours, which can later be used to supplement the natural flow during the hours of peak load during the day. Methods of disposing of surplus water are mentioned in § 187.

252. Topographical Conditions Favourable for Water Power Development.

(i) *High-head installation.* If a high head is available, a site may be chosen in which a stream descending a steep lateral valley can be dammed and a storage reservoir formed (Fig. 263); from the reservoir the water is diverted into a pressure-tunnel driven through the rock and so to the valve house at the head of the steel pipe line. Here, in addition to the main sluice valves, will be found automatic isolating valves designed to come into operation if the pipe bursts, and also the automatic air valves mentioned in § 173. As a further precaution, an open-topped *surge tank* or surge chamber is built near the mouth of the pressure tunnel (§ 254). At every point of deviation of the pipe-lines, either in the horizontal or the vertical plane, anchorages are constructed, with expansion joints provided immediately below. **(Example 85.)**

Located as close as possible to the river or lake into which the tail-race discharges, the power-house will contain either

Pelton-wheels or high-head Francis turbines. Such an installation is depicted in Figs. 264 and 265, which clearly show the reservoir, the pressure-pipes descending the mountain side, and the power-house.[158]

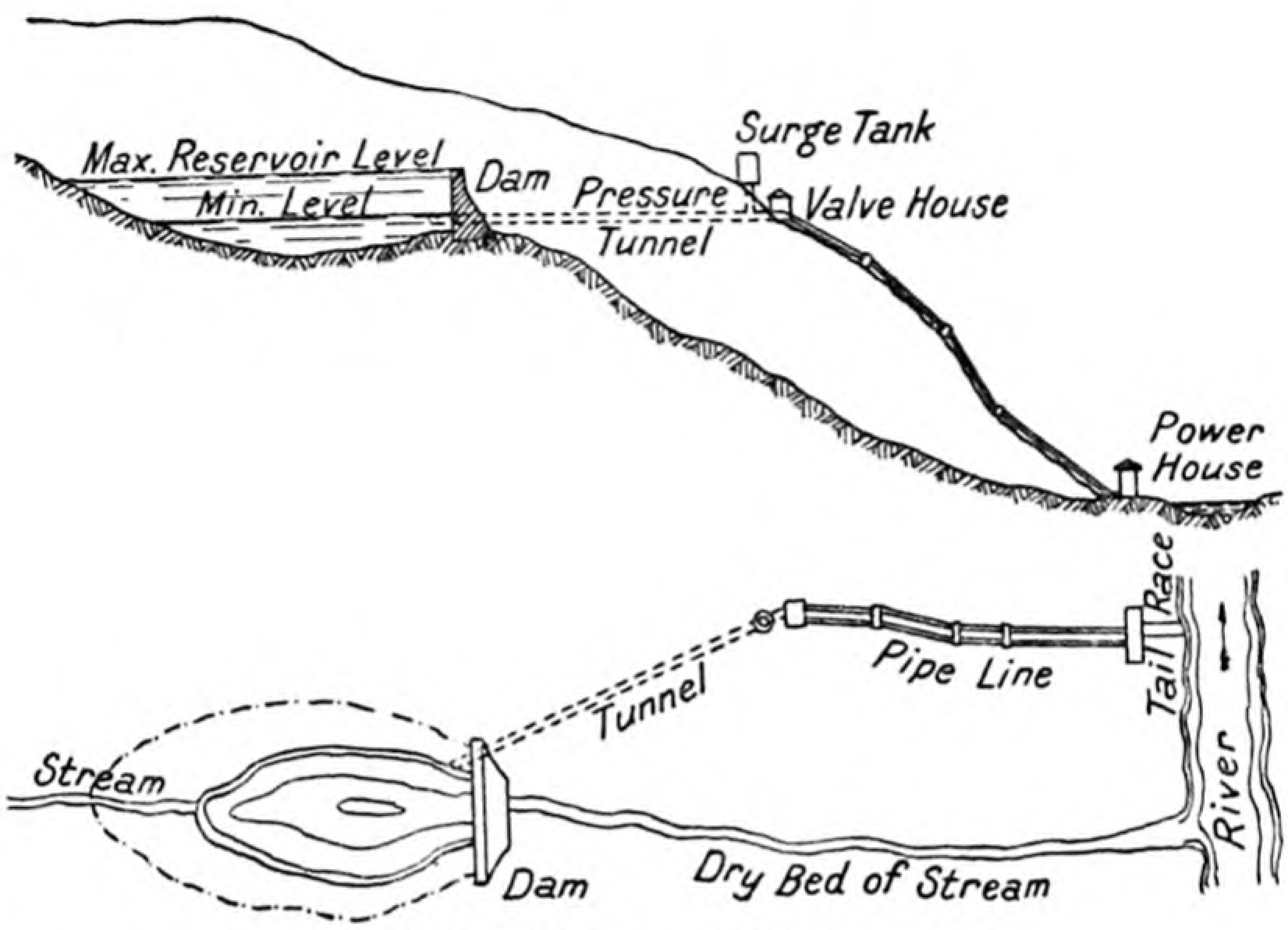

FIG. 263.—High-head development.

(ii) *Medium-head installation.* When a localised fall in the bed of a stream is to be utilised (Fig. 266), an open canal or conduit may be carried along the side of the valley as far as the power-house site. The term "penstock" applied in

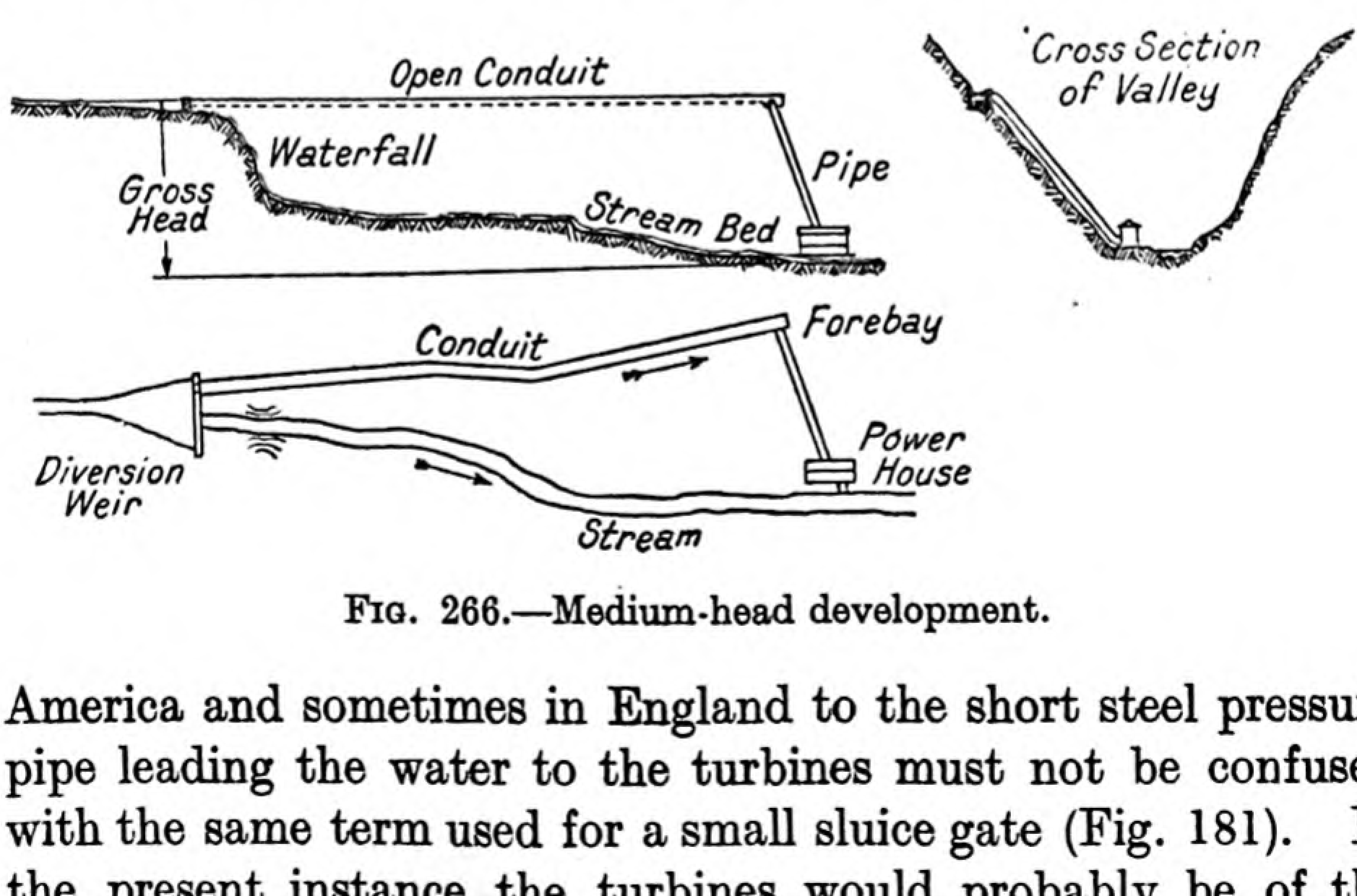

FIG. 266.—Medium-head development.

America and sometimes in England to the short steel pressure pipe leading the water to the turbines must not be confused with the same term used for a small sluice gate (Fig. 181). In the present instance the turbines would probably be of the Francis steel-encased type (§ 246).

In another class of medium-head plant, the power-house is built in the river-bed itself, adjoining the dam which at the same time forms a reservoir upstream and ensures the head-difference which the turbines are designed to exploit, Fig. 267. It is not economical to draw too heavily upon the storage volume, for as the reservoir level falls, so does the working head and therefore the energy per unit volume of water.[159]

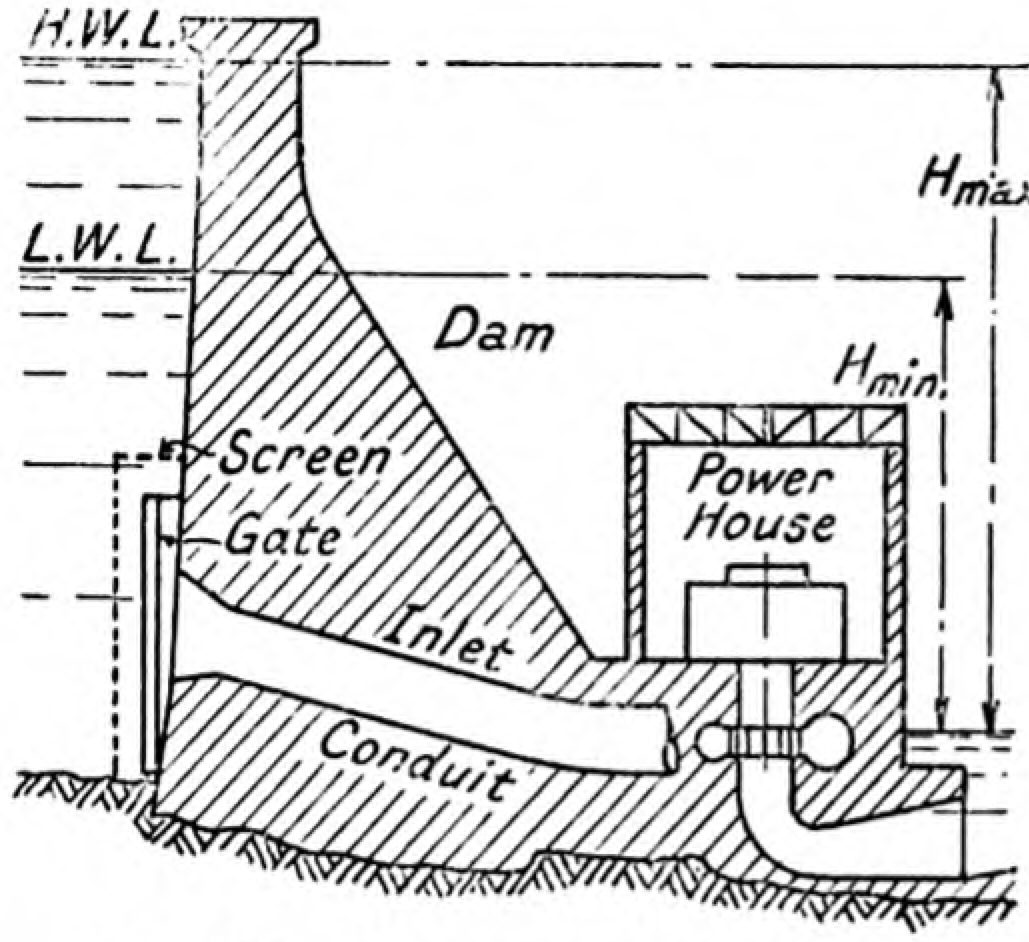

FIG. 267.—Power-house below dam.

(iii) *Low-head installations.* To produce an effective head in the river shown in Fig. 268, an afflux is created by means of a weir or barrage, § 191; frequently one-half of the barrage has regulating gates for the passage of the surplus water, while the other half constitutes the power house itself, in which two, three, or more Francis or Kaplan turbines may be disposed in the manner shown in Fig. 249. A good impression of such a project can be gained from Fig. 269. In the foreground is the power-house, spanned by an external travelling-crane; beyond is the barrage, holding up the water by an amount that is very evident in the photograph. Near the further bank of the river is the lock that permits navigation.

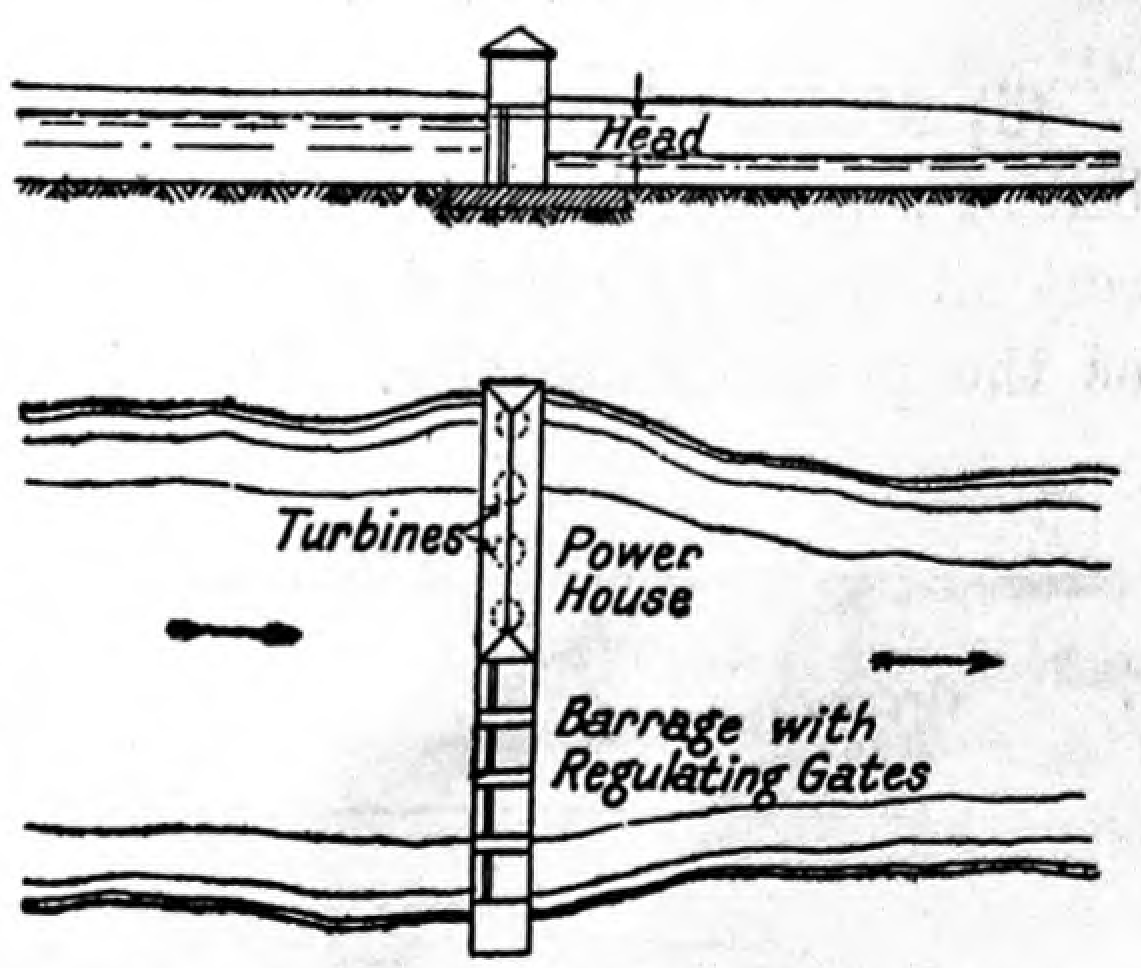

FIG. 268.—Low-head development.

Often it is impracticable, because of the lowness of the banks, to contrive a sufficient localised heading-up of the water in a river. In such circumstances the total fall over a long stretch of the waterway may be exploited, as shown in Fig.

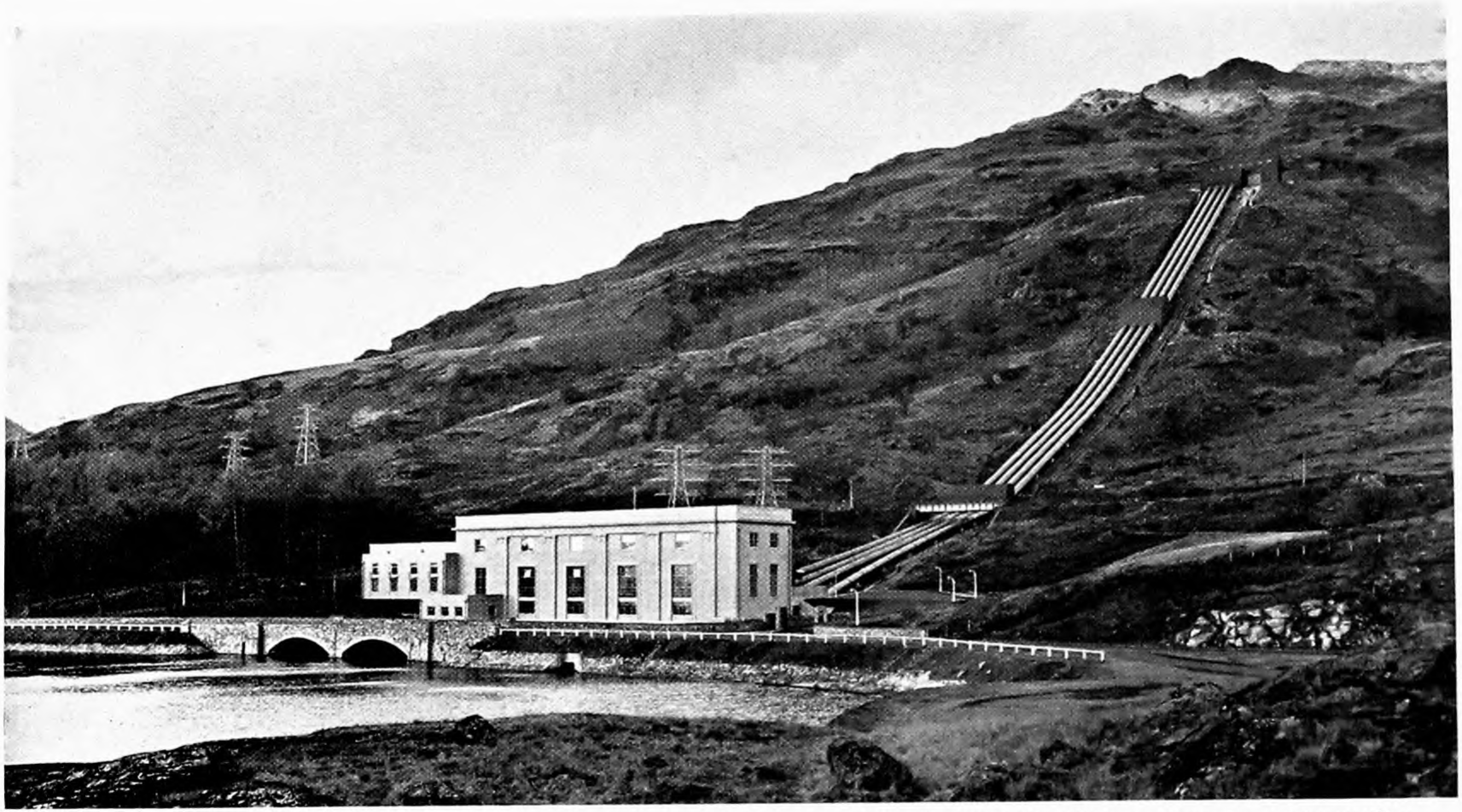

FIG. 265.—Pipe-line and power-house for Loch Sloy installation, accommodating 4 45,000 h.p. Francis turbine units.
(The North of Scotland Hydro-Electric Board)

[*To face page* 362.

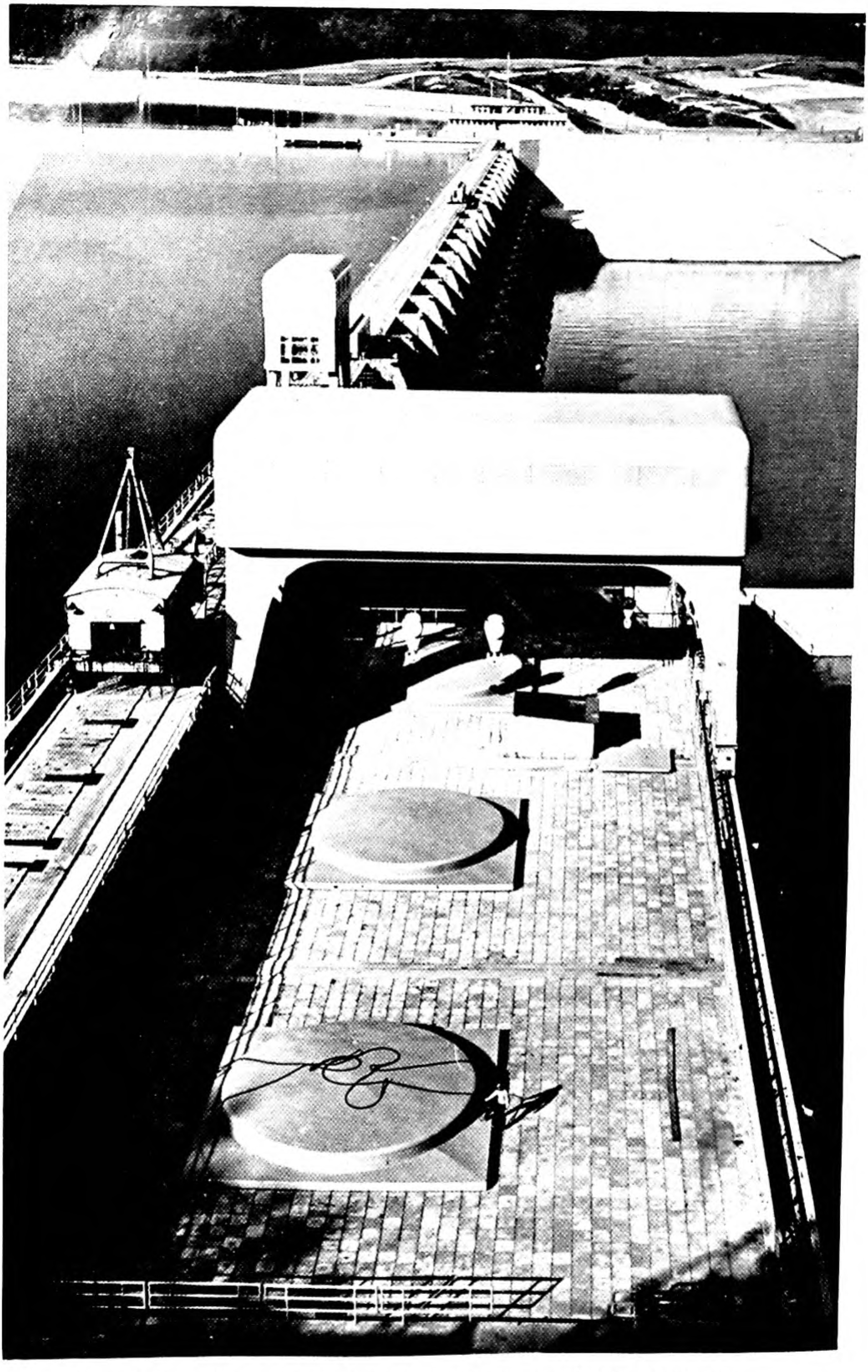

FIG. 269.—Watts Bar installation, Tennessee Valley Authority.
(U.S. Information Service)

[To face page 363.

270, by excavating head-race and tail-race canals each having a flatter slope than the river. The diversion works at the canal head would then be precisely of the form indicated in Fig. 194, § 197, and the power-house would act as a secondary barrage across the canal.

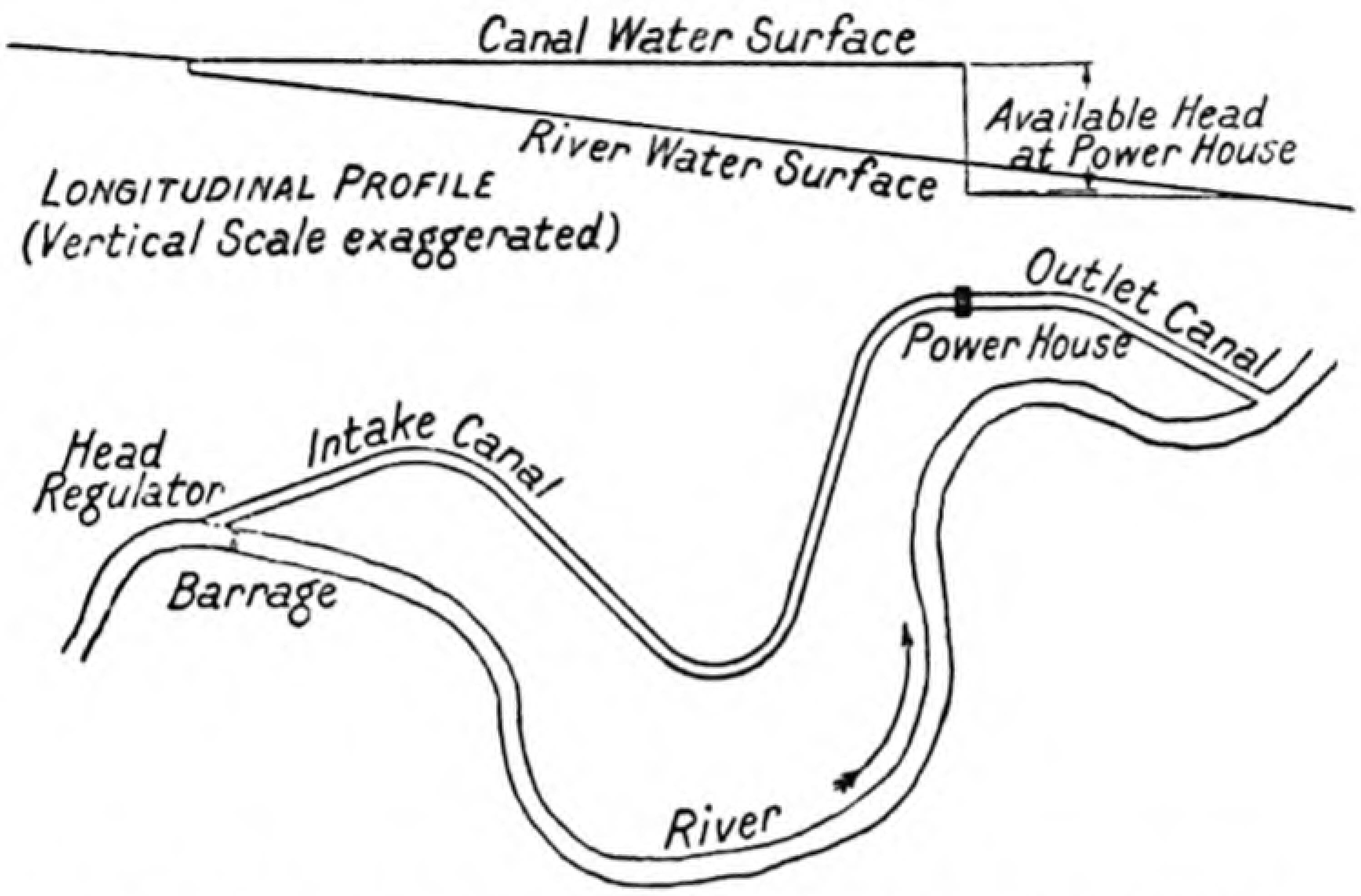

FIG. 270.—Alternative type of low-head development.

(iv) *Underground power stations.* When climatic and topographical conditions are severe, e.g. when the power house and pipe-line may be exposed to frost, snow, avalanches, falls of

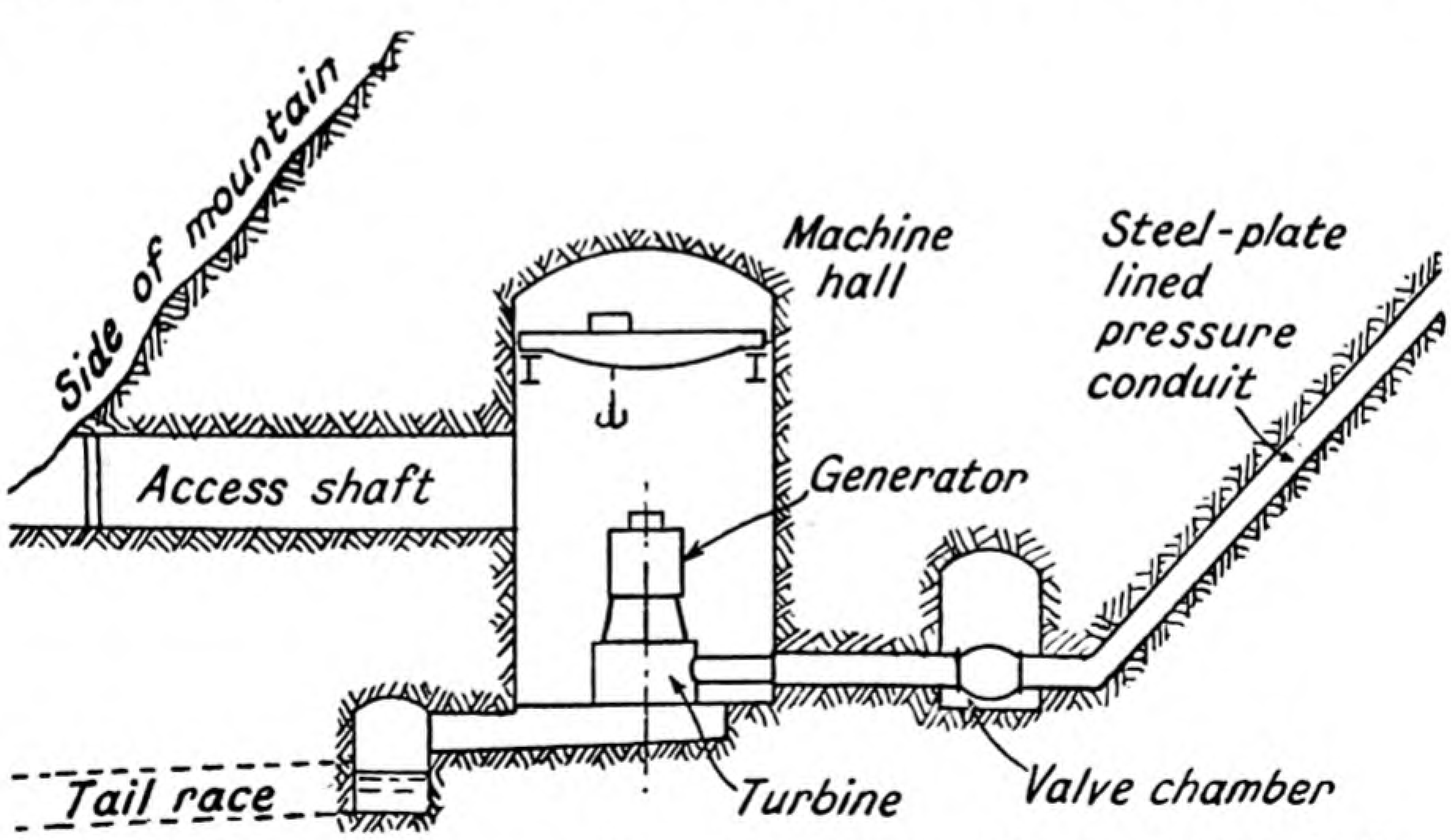

FIG. 271.—Schematic disposition of underground hydro-electric plant.

rock, and the like, then it may be worth while removing the installation altogether from these dangers.[160] This may be done by excavating, beneath the ground, a large cave or hall where the turbines can be installed in complete security; and

this advantage can likewise be shared by the pressure-pipe, which is kept wholly within the solid rock (§ 178). The resulting installation would then have the form suggested in Fig. 271. It has been found that in favourable conditions the overall cost need not greatly exceed the cost of an outdoor station comprising a conventional building—it may even be less.[161] In time of war, of course, the desirability of the underground plant is greatly enhanced.[162]

253. Pressure-surges in Turbine Pipe-lines. What make the hydraulic conditions in turbine pipe-lines unusually severe are the rapid changes in velocity necessary to comply with the varying load on the power units. If allowed to operate unchecked, these flow variations would generate serious water-hammer effects (§ 175) which reach their greatest intensity just at the point where the pipe is already most heavily stressed, that is, adjacent to the turbine inlet.[163] Here the static pressure may be of the order of 500-1000 lb./sq. in. or more, and the wall-thickness of the pipe is correspondingly great (§§ 21, 168). To reduce the weight of these lowermost pipe sections, it is customary to make the diameter rather less than it is higher up, even at the expense of increasing the local frictional loss. Especially in a high-head plant, then, we have to think of the pipe-line as one of the most costly items of the whole installation, probably a more expensive item than the turbine and generator combined. It must therefore be protected in every way, and certainly cannot be exposed to unregulated inertia effects. **(Example 86.)**

But even if it were economical or practicable to permit these inertia surges in the pipe, they would put a heavy tax on the turbine governor (§§ 231, 244). The turbine has no means of discriminating between the various pressure-changes to which it might be subjected : an increase of pressure from whatever cause will tend to augment the flow through the turbine and so to increase the speed, and it is the duty of the governor to regulate the control-mechanism accordingly. But gate closure, by setting up water-hammer in the pipe, will create the need for still further closure ; then as soon as the pipe velocity has been stabilised a re-opening movement will be demanded. This complexity is still further heightened by the periodical arrival of reflected pressure-waves (§ 118).

Two methods have already been described by which elements in the turbine control-mechanism can partially relieve these excessive pipe-line pressures: the deflector does the work for the Pelton wheel, § 230, and the automatic relief-valve for any high-head turbine, Fig. 250, § 246. But neither can give any help when load is thrown *on* and the turbine is calling for more water. The surge tank now to be described supplements these devices.

254. The Surge Tank. The principle of the surge tank, surge shaft, or surge chamber is illustrated in Fig. 272. At a point as close as possible to the turbine, a branch in the pressure-conduit communicates freely with an open-topped chamber

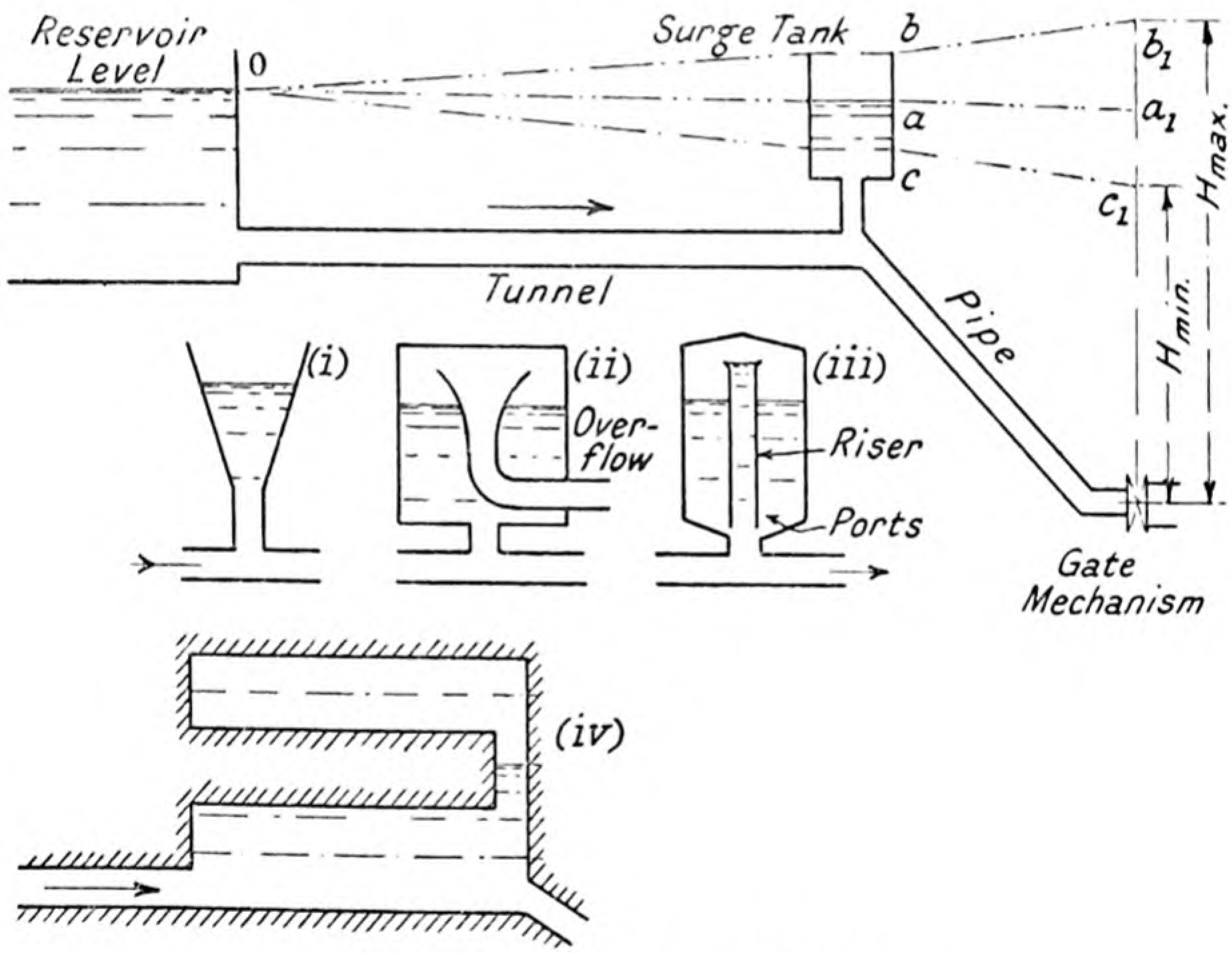

FIG. 272.—Types of surge-chamber.

whose upper lip is set a suitable distance above the maximum water level in the supply reservoir. When the turbine load is steady and there are no velocity variations in the conduit, there will be a normal pressure gradient Oaa_1, and the surge tank water surface will be lower than the reservoir surface by an amount equivalent to the frictional energy loss in the intervening conduit.[164] An increasing load which calls for more water will draw down the gradient to Occ_1, while a falling load will send up the gradient to Obb_1 (§ 115, Fig. 90). A still more

rapid gate closure would cause water to spill over the lip of the tank. Besides positively limiting in this way the pressure in the conduit upstream from it, the surge tank acts also as a small auxiliary storage reservoir. During gate closure, excess water can accumulate in the space between levels *a* and *b*, while during gate opening the volume of water between levels *a* and *c* is available for augmenting the flow down the pipe.

The ideal situation for the surge chamber is actually at the turbine inlet; but as this is rarely feasible in medium-head plants, and never in high-head plants, the usual practice is to locate it at the junction between the pressure-tunnel and the steel pipe-line, Fig. 263. Here there may be possibilities of excavating the chamber in the mountain side.

Besides the plain cylindrical tank, Fig. 263, other shapes of chamber are suited to particular conditions. Some of them are shown schematically in Fig. 272. Type (i) is conical; type (ii) has an internal bell-mouth spillway (§ 190) which permits the overflow to be easily disposed of. The advantage of the *differential* tank, type (iii), is that for the same stabilising effect its capacity may be less than that of a plain cylindrical tank. This is because the retarding head operating on the water column in the tunnel is brought to bear more promptly. Inside the tank is a riser pipe having ports at its lower end. When the pressure in the conduit increases, a small quantity of water enters the surge tank through these ports, but the bulk of the incoming water mounts to the top of the riser and there spills over into the tank. Immediately, therefore, a considerable retarding head is available, whereas in the plain tank the head only builds up gradually as the tank fills. It will be noted that no water at all is actually spilled to waste from the differential tank; this is highly advantageous so long as the protection to the pipe is adequate, for stored water is a valuable commodity which cannot carelessly be thrown away.[165]

A form of construction which has the same favourable performance as the differential tank, but which is suitable when earth or rock excavation is appropriate, is indicated in Fig. 272 (iv). Separate long, shallow galleries are provided, an upper one for storing water when the turbine load falls, and a lower one for supplying water when the load rises. The cross-section of the intervening vertical shaft is relatively small.

The basic purpose of the surge tank, then, is to permit velocity changes in the tunnel to lag behind those in the pipe. Nevertheless, the water velocity in the tunnel must eventually adapt itself to the new flow conditions demanded by the turbine, and the more quickly it can do so the better; that is why the types of tank (iii) and (iv) are preferable. It remains to be pointed out that when once spilling has begun from any type of surge-chamber, the device can do nothing further to protect the *pipe*.

255. Surge Chamber Operation. In order to follow the sequence of events in the turbine supply system, after regulation of the gates has begun, the method of Example 51, § 115, may be developed. Referring to Fig. 273, the basic factors now involved are :—

t = elapsed time in seconds, after beginning of turbine gate regulation,

z = difference in level, at time t, between reservoir water surface and surge-chamber water surface,

A = area of surge-chamber water surface (assumed uniform),

a = cross-sectional area of pressure-tunnel or conduit,

l = length of conduit,

v = mean velocity in conduit at time t.

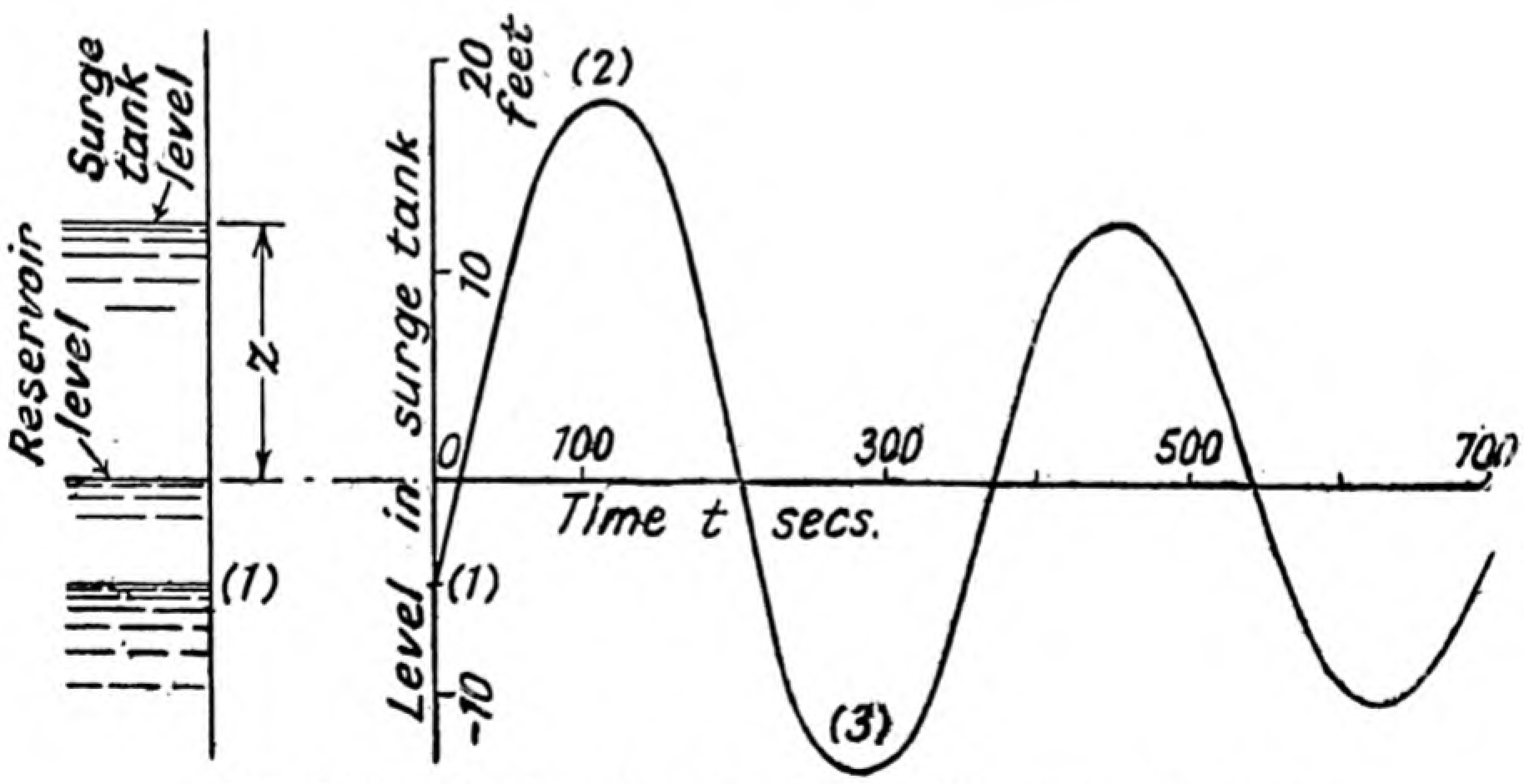

FIG. 273.—Fluctuation of water-level in surge-chamber.

The simplest conditions only will be examined here, in which the time of closure of the turbine gates is so short, in relation to the total period of pressure disturbances, that it may be assumed to be negligible. A straightforward connection

between conduit velocity v, and rate of change of level in surge tank, will therefore exist: it is

$$v = \frac{A}{a} \cdot \frac{dz}{dt}.$$

There will be a corresponding relation between the acceleration of the water in the conduit, dv/dt, and the vertical acceleration of the surge tank water surface, viz.:

$$dv/dt = \frac{A}{a} \cdot \frac{d^2z}{dt^2}.$$

Now the head-difference z is linked with the inertia head in the conduit, h_i, and the friction head h_f, by the relationship

$$\left.\begin{aligned} z &= h_i - h_f \\ \text{But} \quad h_i &= l/g \, . \, (dv/dt) = l/g \, . \, (A/a) \, . \, (d^2z/dt^2) \end{aligned}\right\} \quad . \quad (\S\ 115)$$

and $$h_f = \frac{4fl}{D} \cdot \frac{v^2}{2g} = \frac{4fl}{D} \cdot \left(\frac{dz}{dt}\right)^2 \cdot \left(\frac{A}{a}\right)^2 \Big/ 2g.$$

Hence $$z = \frac{l}{g} \cdot \frac{A}{a} \cdot \frac{d^2z}{dt^2} - \frac{4fl}{D} \cdot \frac{\left(\frac{dz}{dt}\right)^2 \cdot \left(\frac{A}{a}\right)^2}{2g}.$$

A graph of this equation, in which z was plotted against t, would show the position of the surge-tank water surface throughout the entire period up to the point of final quiescence when the water was everywhere at rest. An actual record taken from observations on a turbine installation is reproduced in Fig. 273. Point (1) represents the moment of gate closure: the whole of the head z is absorbed in friction. At point (2) the surge tank water surface has reached its highest elevation: the water column in the conduit is at rest, which means that the frictional term h_f is zero, while the rate of retardation of the column has attained its maximum value. Thereafter the excess water flows back from the surge tank *into* the reservoir, a process which only ceases at point (3), representing the minimum surge tank level. It will be noticed that if the frictional term h_f were disregarded, the water column in the conduit would oscillate under conditions of simple harmonic motion.[166] Even when in fact the effect of friction is taken into account, the oscillations may take an excessively long

time before they are finally extinguished: that is why additional damping influences, e.g. as shown in Fig. 272 (iii), are valuable.

256. Regional Hydro-Electric Developments. If it be required to exploit to the best advantage the entire water-power resources of a tract of country or a complete river basin, it is most unlikely that a single power station will serve. On the contrary, several turbine installations, or even a score or more, may be needed, each located in the most favourable position and all of them interlinked by electric transmission lines.[167] The starting-point in laying out the system will be the topography of the area, including the courses and elevations of the streams that will feed the turbines. Hydrology will follow: by means of a long series of records of stream gaugings, § 397, it should be possible to forecast the mean, the maximum and the minimum flow in each stream. If this information is lacking, estimates must be based on such rainfall records as exist. Geology will be studied next: it will indicate what kind of foundations are available for supporting power-houses, barrages or dams, and if storage reservoirs are practicable it will show whether impermeable floors can be expected.

Meantime the promoters of the scheme will have ascertained the probable character of the load in different areas. If the energy is to be transmitted to industrial cities, there will be wide variations between the day load and the night load, and between the winter demand and the summer demand. The disparity at any moment between the natural water supply available, and the electric demand, can be overcome in two ways: (i) by establishing thermal-electric stations, using steam turbines, gas turbines, or diesel engines, which can come to the help of the hydro-electric stations, (ii) by providing storage reservoirs which will compensate for fluctuations in river flow (§§ 204-207). A combination of the two methods may sometimes be demanded.

When a single river having a relatively flat longitudinal slope is to be utilised, a chain of hydro-electric power houses could be disposed as in Fig. 274; the installations would preferably be spaced so far apart that the tail-water of one station would not suffer interference from the backwater curve created by the next station downstream.[168] Installations

such as these, termed "run-of-the-river" stations because storage facilities are impracticable, inevitably generate a smaller maximum output in flood conditions than in low-stage conditions (**Example 138**). The general layout of each station would follow the lines of Figs. 268, 269.

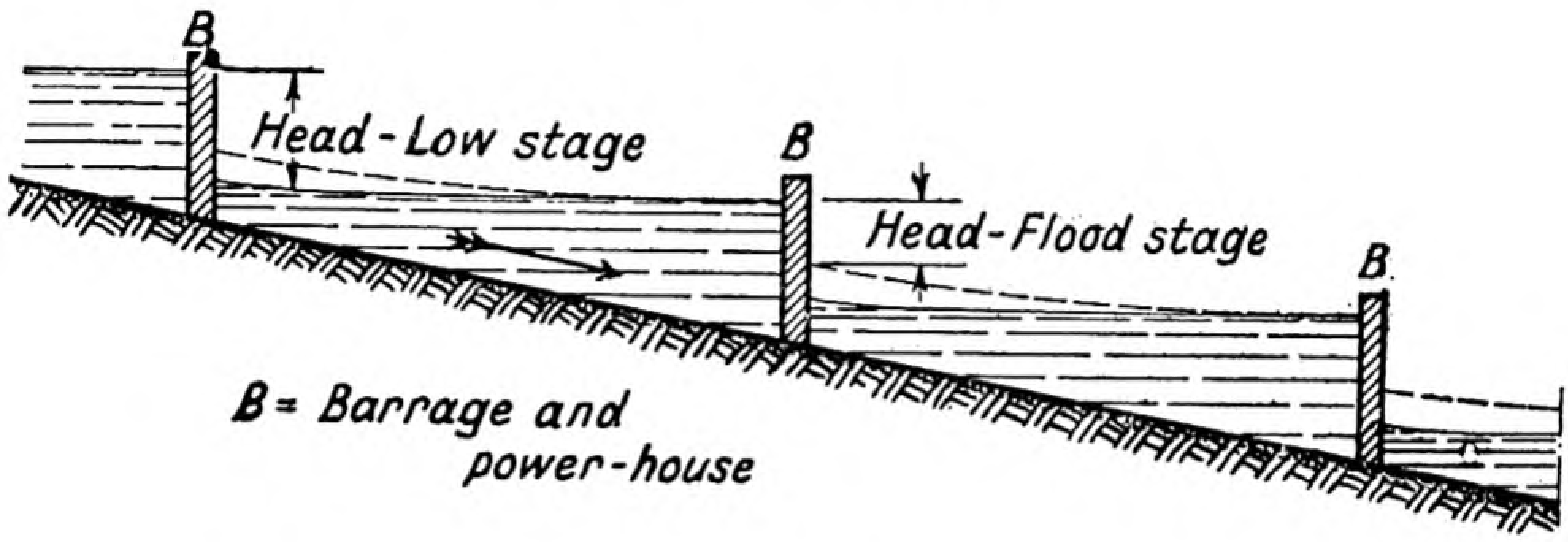

FIG. 274.—Run-of-river water-power plants.

If the river valley is narrower, steeper, and sufficiently undeveloped to permit storage reservoirs to be formed, then the installations could be located as in Fig. 275; each one might be of the type shown in Fig. 267.

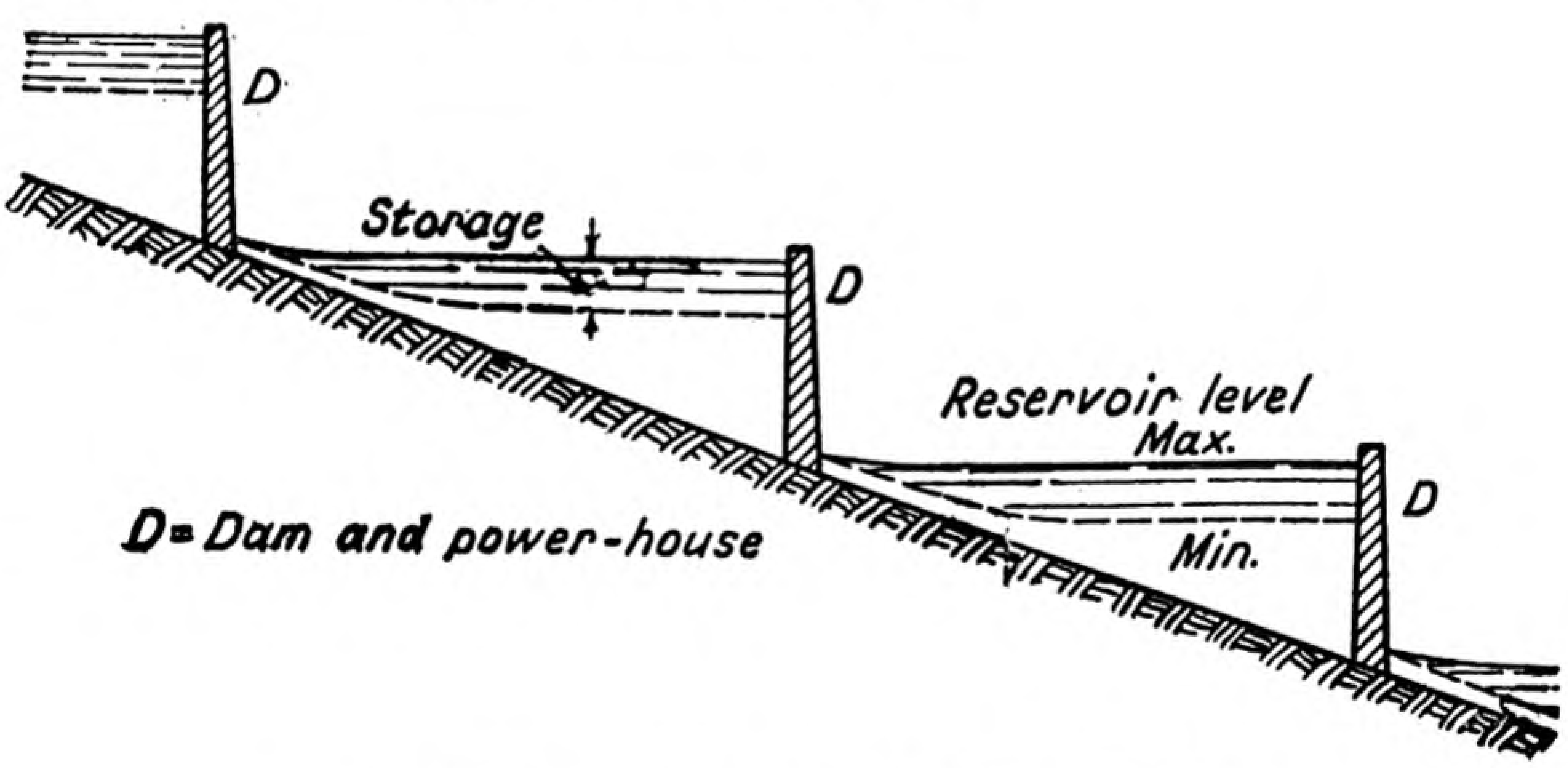

FIG. 275.—Power plants with storage reservoirs.

257. Other Arrangements. Progressing still farther upstream, we arrive at the head-waters of the catchment area, where still other possibilities of development may present themselves. High heads are likely to be available, permitting the disposition sketched in Fig. 263, § 252 (i); but the water that supplies the storage reservoir and feeds the turbines need not all come from a single stream. The flow from a number of

small streams in adjacent valleys may be diverted through tunnels into the main reservoir and thus augment the supply. It may not even be essential to locate the power house in the valley from which it derives its water. Should there be two streams in parallel valleys that afterwards unite, as in Fig. 276, and if one of them, *B*, has been eroded to a lower level than the other, *A*, then the water could be stored in the one valley and utilised in the other; the available head could be exploited more economically in this way than by the orthodox system, Fig. 263.

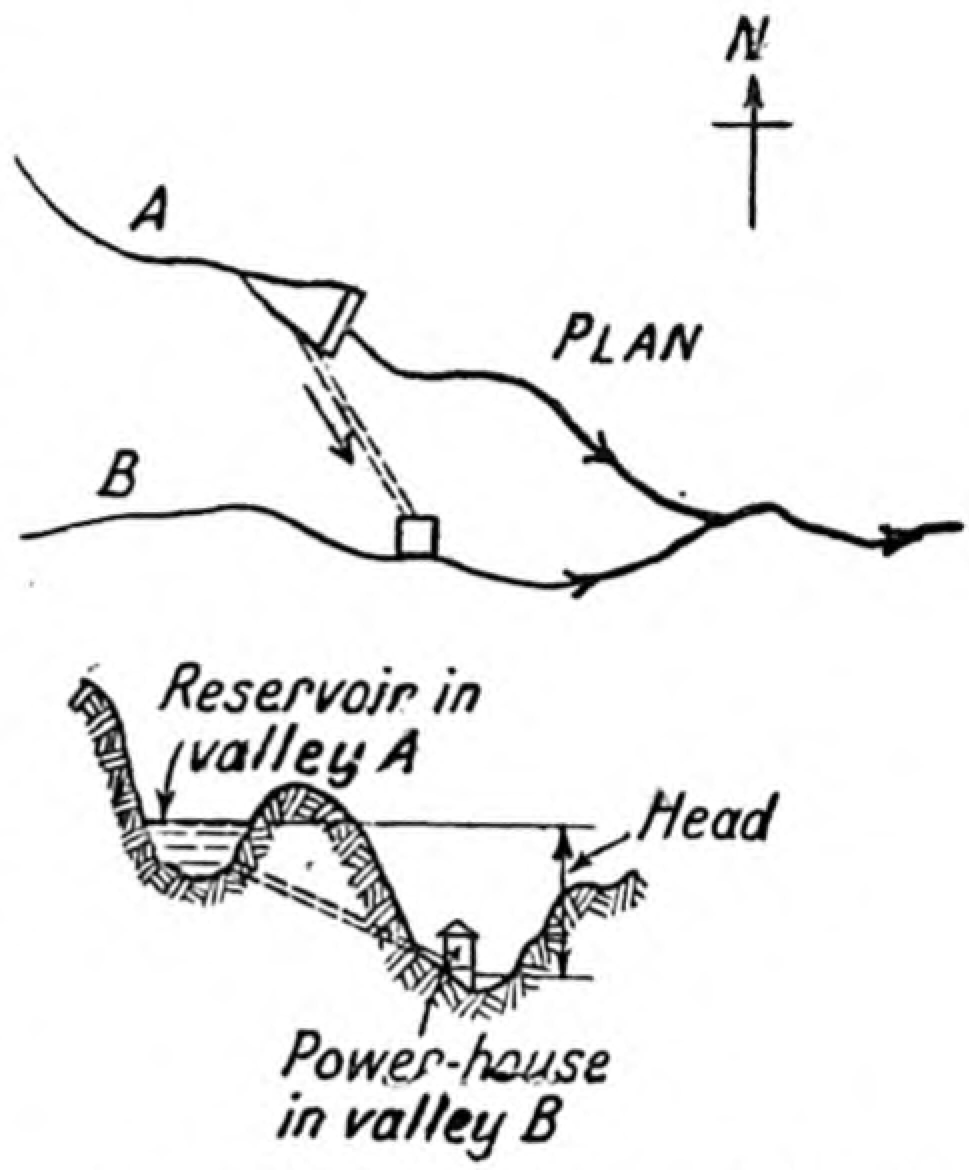

FIG. 276.—Development of flow in adjacent valleys.

Still more radical diversions are sometimes advantageous; the turbines in one catchment area may receive some of their water from quite another catchment. Such conditions are indicated in Fig. 277. By a fortunate topographical accident, it may happen that tributary *A* running into a western river basin is at a higher level than the stream *B* that flows into an eastern catchment; yet their distance apart is not excessive, which makes it feasible to divert water from stream *A* towards the east, thus augmenting the supply available for the turbines in valley *B*. Whether the inhabitants in valley *A* would be willing to concede some of their water rights is another matter: a matter that could perhaps be resolved without undue difficulty if there were some over-riding authority with powers over the whole region.

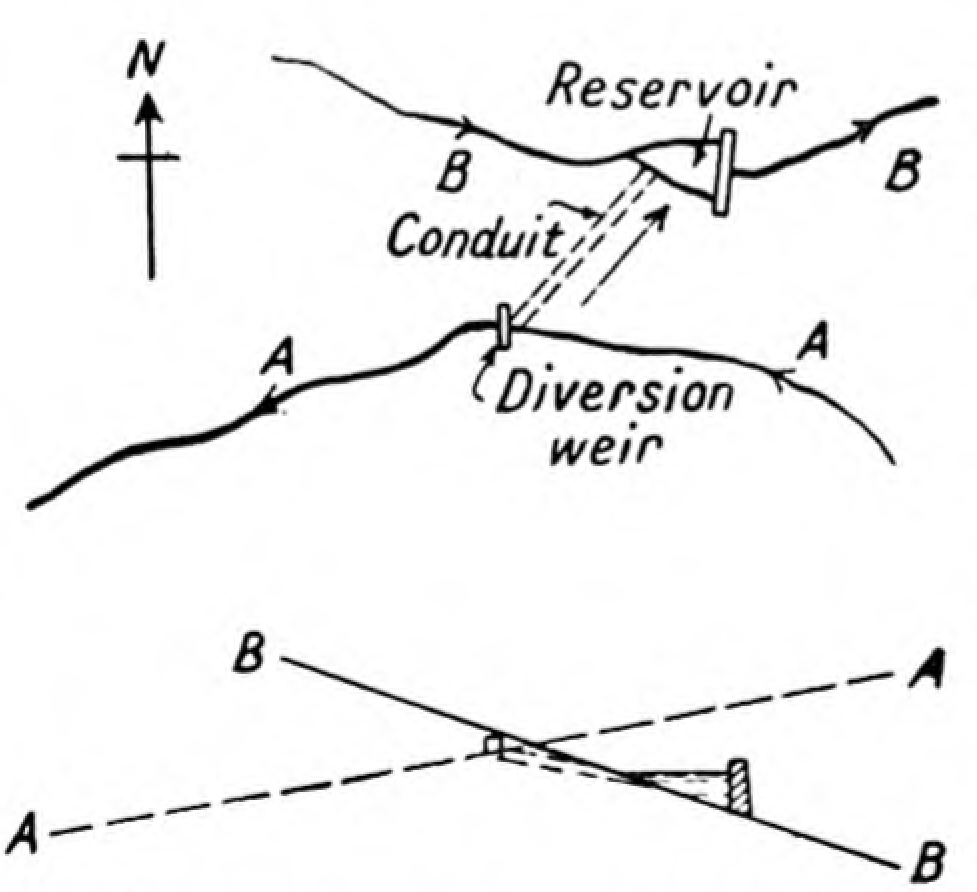

FIG. 277.—Diversion from one catchment to another.

Within recent years these administrative problems have received great attention, with the result that such organisations have been formed as the North of Scotland Hydro-Electric Board in Great Britain, the Tennessee Valley Authority in the United States,[169] and the Snowy Mountains Authority in Australia. A body on this scale might have under its control examples of all the types of interlinked installations that have just been described.

258. Tidal Power Schemes. The possibility of generating hydro-electric energy from the rise and fall of tidal waters has often been discussed.[170] Such projects usually call for the construction of a barrage across the long, narrow gulf or the tidal estuary that is to be exploited, Fig. 278; the barrage embodies sluice-gates and low-head turbines, as in Fig. 268. During the flood-tide the gates are fully open, the turbines are at rest, and the tidal water flows freely into the inlet, (i). At the top of the flood the gates are closed, and the area upstream of the barrage thus becomes a great impounding reservoir. For two or three hours of the ebb-tide this water remains quiescent; then, when the water-level on the seaward side has fallen sufficiently to create a useful head across the turbines, the turbine gates are opened, the stored water flows through the turbines on its way to the sea, and the effective or generating period of the cycle begins, Fig. 278 (ii). It continues until the arrival of the next flood-tide and the fall in upstream water level have together reduced the working head to the point at which the turbines must be shut down again.[171]

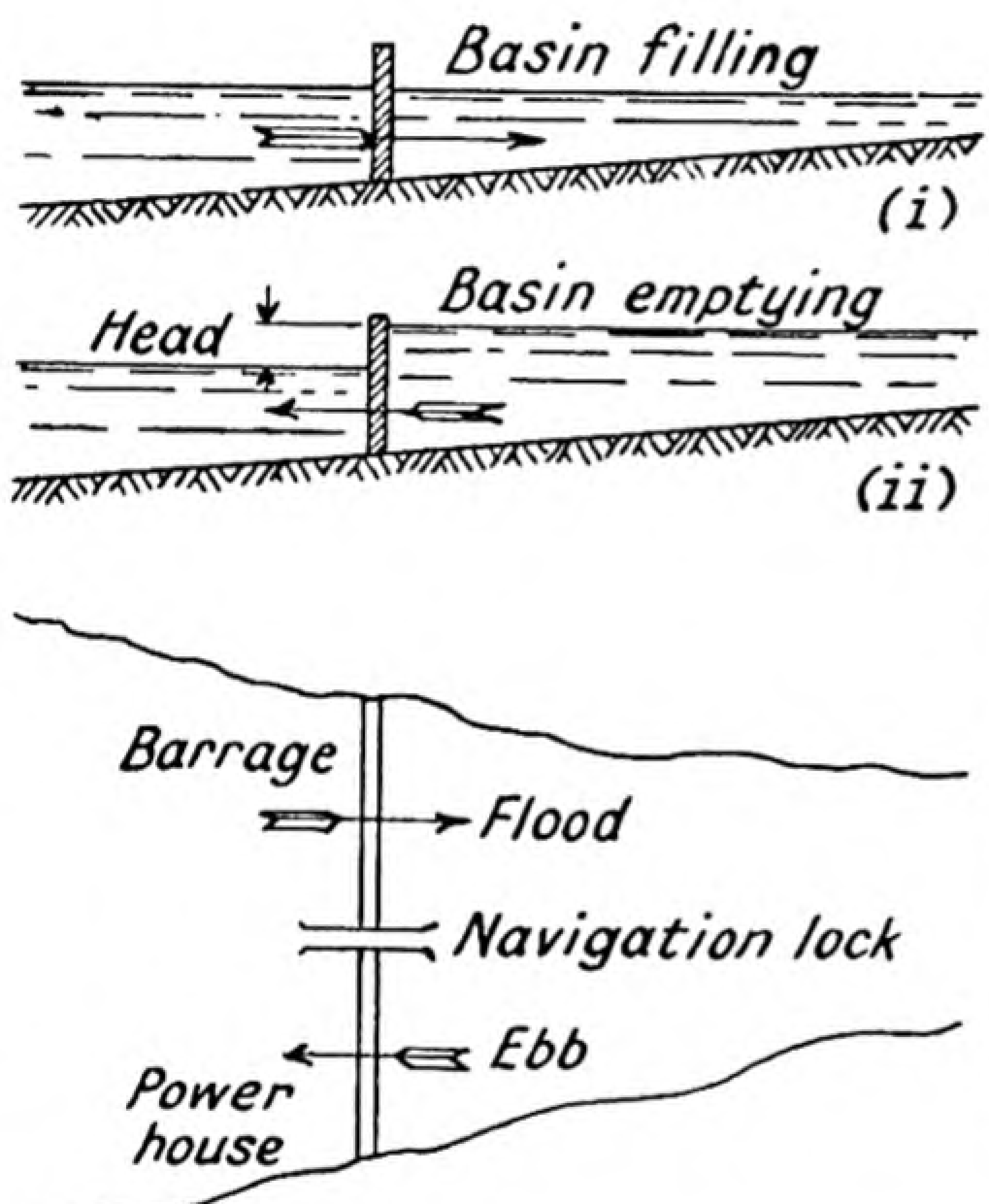

FIG. 278.—Tidal power development.

More elaborate arrangements of impounding basins may offer advantages, but these cannot wholly mask the serious drawbacks that have hitherto hampered tidal power proposals. They

are: (i) the very heavy capital cost, (ii) the daily fluctuations in the power output, which may fall to zero during two long periods every day, (iii) the additional seasonal variations as spring-tides succeed neap-tides, (iv) the risk of unfavourably altering the regime of the estuary, due to the formation of shoals or sandbanks that would impede navigation. Clearly, therefore, the only localities that offer chances of success are those with an exceptionally great tidal range, such as the Severn estuary, England.[172]

CHAPTER XIV

HYDRAULIC TURBINES: (II) PERFORMANCE

259. Conditions Influencing Turbine Performance. In the preceding chapter it was assumed that in general the turbines in question were required to work under unvarying conditions of head, speed and output. As such uniformity rarely prevails in practice, it is now necessary to review the nature of the variations that may be looked for.

(i) The head on the turbine may change, and with it the output, the speed being correspondingly adjusted so that *no sensible change* in efficiency occurs, the gate opening remaining fixed.

(ii) The head and the speed may remain steady, the output being varied by the movements of the gates or the needle. These are the normal operating conditions for most turbines.

(iii) Variations in the relationship between head and speed are common, particularly in low-head units. Although the speed is as a rule only permitted to fluctuate within very narrow limits, the head may vary through a range of 50 per cent. or more (§ 252 (iii)).

(iv) With the head and gate-opening fixed, the speed may be allowed to vary by adjusting the load. These conditions are not often found outside the laboratory and the test-plant.

260. Definition of Head. In assessing the performance of a turbine it is naturally essential to separate the energy losses occurring within the turbine from those arising in the channels and conduits leading the water into and out of the turbine. This can be done by the correct use of the term *gross head* and *net head.*

The *gross head* in a turbine installation is the difference in level between the natural water surface at the point at which the water is diverted into the head-race canal or conduit, and the water surface at the point at which the water issuing from the tail-race is returned to the stream (Fig. 266).

The *net* or *effective* head under which a *reaction* turbine operates is the difference between the total energy of the water just before it enters the turbine, and the total energy just after the water leaves the draft tube. The term *total energy* is here used in its ordinary sense, representing the sum of position head, pressure head and velocity head, § 33. In low-head installations the upstream measuring point is chosen in the head-race channel immediately in advance of the turbine, and the downstream point at the section of the tail-race near the outlet from the draft tube (Figs. 240, 248). For enclosed turbines the upstream measuring point is taken in the inlet pipe near the entrance to the turbine casing. For *Pelton wheels* the net head is the total energy of the water in the inlet pipe adjacent to the nozzle, reckoned above a datum plane passing through the lowest point of the runner pitch circle.

It is the net head H which is to be used in calculations concerning the efficiency of turbines. This is manifestly the gross head minus the energy losses of all kinds in the inlet and outlet conduits. For precise details, the relevant Standard Test Code should be consulted.

261. Turbine Performance under Unit Head. When comparing the performances of turbines of different outputs and speeds, working under different heads, it is often convenient to calculate what the outputs would be if the heads were reduced to unity—1 foot or 1 metre—the speeds being adjusted in the way referred to in § 259 (i) so that the efficiency was nominally unaffected. The primary condition for unchanged efficiency in a given turbine is that the velocity triangles under the working head and under *unit head* should be geometrically

similar. In Fig. 279, ABC represents the inlet velocity triangle for a Francis turbine, under its working head H, and abc represents the velocity triangle for the same turbine under unit head, the subscript $_u$ being used consistently to denote unit conditions.

Clearly ac must be parallel with AC, because the direction of both these vectors is definitely fixed by the guide blade

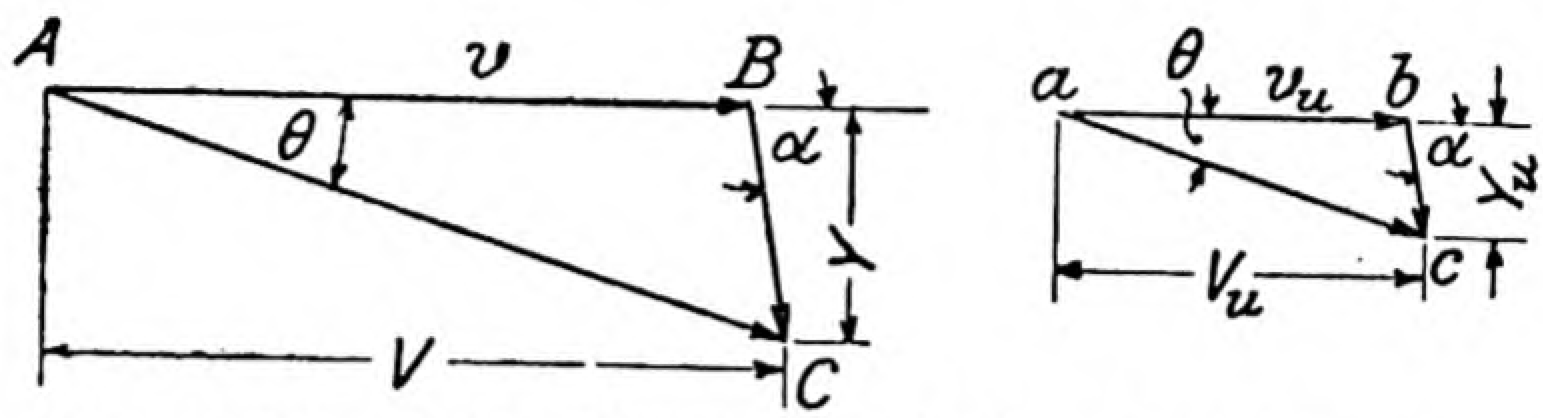

FIG. 279.—Inlet velocity diagrams for head $= H$, and head $=$ unity.

angle θ which is assumed to be constant. Also bc must be parallel with BC, because both vectors must be parallel with the first tip of the wheel blades, to avoid shock at entry. The required condition of similarity is thus fulfilled. It follows

that $$\frac{v}{V} = \frac{v_u}{V_u} \text{ and that } \frac{v}{Y} = \frac{v_u}{Y_u} \quad . \quad . \quad \text{(I)}$$

the notation of § 235 being used.

We may in turn write

$$\frac{\dfrac{Vv}{g}}{\dfrac{Y^2}{2g}} = \frac{\dfrac{V_u v_u}{g}}{\dfrac{Y_u^2}{2g}}, \quad \text{or} \quad \frac{\dfrac{Vv}{g}}{\dfrac{Y_1^2}{2g}} = \frac{\dfrac{V_u v_u}{g}}{\dfrac{Y_{u1}^2}{2g}},$$

which shows that the ratio of useful energy to wasted velocity energy is the same under unit head as it is under the working head. (The losses due to friction, etc., are here neglected.) Ideally, therefore, the stipulated condition of unchanged efficiency has been fulfilled, viz. $\eta_h = \eta_u$, and hence, from § 235.

$$\frac{Vv}{gH} = \frac{V_u v_u}{g \times 1}. \quad . \quad . \quad . \quad . \quad \text{(II)}$$

Eliminating V and V_u from equations I and II, it appears

that $$v_u = \frac{v}{\sqrt{H}}, \text{ and that } Y_u = \frac{Y}{\sqrt{H}}. \quad . \quad \text{(14-3)}$$

Since $v = \dfrac{\pi DN}{60}$, and $v_u = \dfrac{\pi DN_u}{60}$, it follows at once that

$$N_u = \frac{N}{\sqrt{H}} \quad . \quad . \quad . \quad . \quad (14\text{-}4)$$

which represents the speed of the turbine under unit head.

Again, $\phi = \dfrac{v}{\sqrt{2gH}}$, and $\phi_u = \dfrac{v_u}{\sqrt{2g\,.\,1}} = \dfrac{1}{\sqrt{2g}}\,.\,\dfrac{v}{\sqrt{H}}$,

therefore $$\phi = \phi_u.$$

Further, since $Y_u = \dfrac{Y}{\sqrt{H}}$, therefore $W_u = \dfrac{W}{\sqrt{H}}$, whence

$\dfrac{P_u}{P} = \dfrac{W_u\,.\,H_u}{W\,.\,H}$ (assuming identical gross efficiencies)

$$= \frac{\dfrac{W}{\sqrt{H}}\,.\,1}{W\,.\,H} = \frac{1}{H\sqrt{H}}, \text{ or}$$

$$P_u = \frac{P}{H\sqrt{H}}. \quad . \quad . \quad . \quad . \quad . \quad . \quad . \quad . \quad (14\text{-}5)$$

$=$ power output under unit head.

Finally, $\psi = \dfrac{Y}{\sqrt{2gH}}$, and $\psi_u = \dfrac{Y_u}{\sqrt{2g\,.\,1}} = \dfrac{1}{\sqrt{2g}}\,.\,\dfrac{Y}{\sqrt{H}}$, whence

$$\psi = \psi_u.$$

Although these identities have been deduced from the diagrams relating to a Francis turbine, they are applicable to all types of turbine, and we may therefore say in general terms :

(i) To reduce the performance of a turbine working under head H to conditions of unit head, all velocities must be reduced in the ratio $\dfrac{1}{\sqrt{H}}$.

(ii) The *unit speed* N_u of a turbine in revolutions per minute is the working speed N divided by $\sqrt{H}$.

(iii) Under unit conditions a turbine has the *same* speed ratio ϕ and the *same* flow ratio ψ as it has under its working head H.

(iv) The *unit power* P_u of a turbine, that is, its output under unit head, is found by dividing its normal output P by $H\sqrt{H}$.

25

(v) A turbine working under a fixed gate setting and fixed values of ϕ, ψ, and $\frac{N}{\sqrt{H}}$ behaves exactly like an orifice in so far as the relationship between head, velocity and discharge is concerned.

If it is a question of reducing the performance of a turbine under head H to its performance under some other head H_1,

$$\text{evidently} \qquad \frac{N_1}{N} = \frac{\sqrt{H_1}}{\sqrt{H}}, \text{ and } \frac{P_1}{P} = \frac{H_1\sqrt{H_1}}{H\sqrt{H}} \quad . \quad (14\text{–}6)$$

Some experimental observations bearing on this matter will be found plotted in Figs. 294 and 298. In § 279 it is shown that the hypothesis that efficiencies can be maintained unaltered under varying heads is not strictly valid; under unit head the measured efficiency is bound to be slightly less than under the working head.

262. Turbine Performance under Specific Conditions. Having found how a turbine will behave under unit conditions, a further step is now necessary before we can arrive at an equitable basis on which to compare turbines of different types; we must determine the characteristics of an imaginary machine identical in *shape*, geometrical proportions, blade angles, gate setting, etc., with the actual machine, but reduced to such a *size* that it will develop *one horse-power* under *unit head*. This imaginary turbine is called the *specific turbine;* the symbols expressing its performance will bear the subscript $_s$. The two runners now under comparison are shown in Fig. 280.

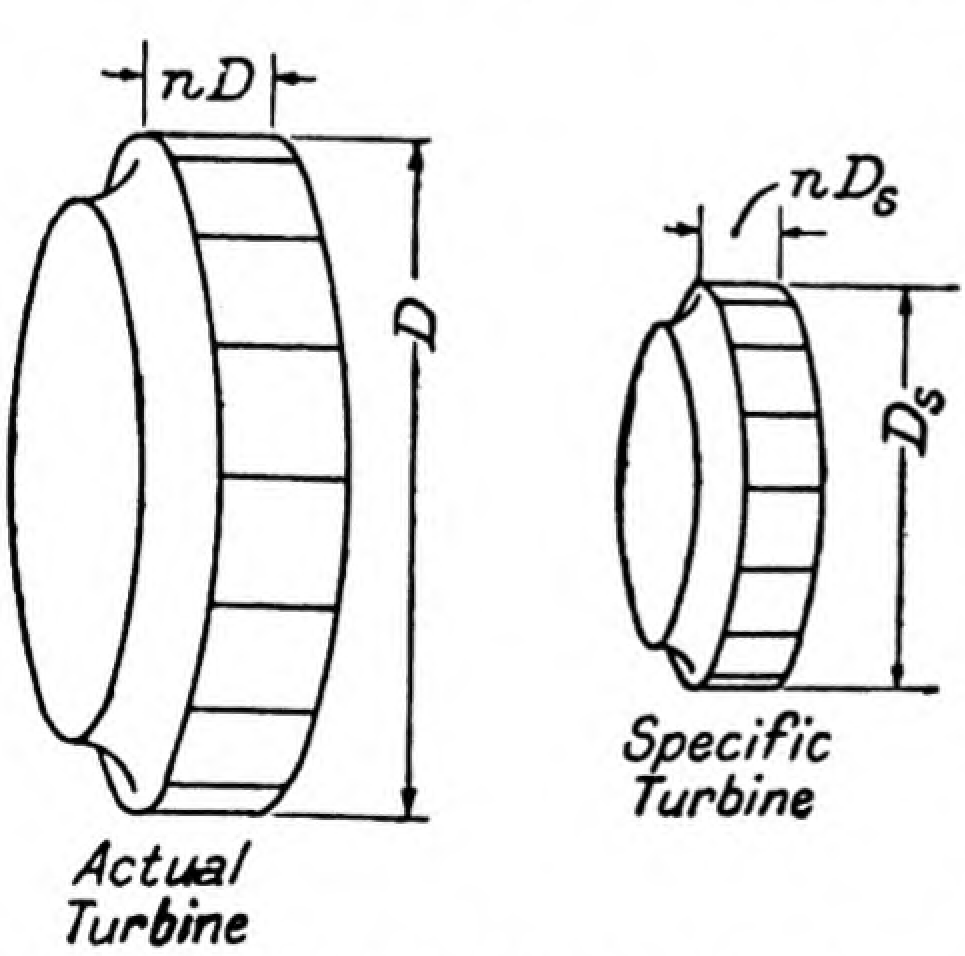

FIG. 280.—Actual and specific runners.

Remembering that the actual turbine under unit conditions and the specific turbine both work under a head of 1 foot or 1 metre, it is at once evident that corresponding velocities in the two are identical, viz. $v_s = v_u$, $Y_s' = Y_u$, etc.; for the velocity triangle *abc* (Fig 279) serves for the specific turbine as well as for the actual turbine under unit conditions.

Consequently,

$$\frac{P_u}{P_s} = \frac{\text{Power of actual turbine under unit head}}{\text{Power of specific turbine}} = \frac{W_u \,.\, H_u}{W_s \,.\, H_s}$$

$$= \frac{W_u \times 1}{W_s \times 1}.$$

But from Fig. 280,

$$W_u = w \,.\, Y_u \,.\, \pi D n D$$

and

$$W_s = w \,.\, Y_s \pi D_s n D_s,$$

$$\therefore \frac{P_u}{P_s} = \frac{D^2}{D_s^2}.$$

This shows that the power of geometrically similar turbines working under the same head varies as the square of the runner diameters. Since $P_s = 1$, we may write

$$D_s = \text{diameter of specific runner} = \frac{D}{\sqrt{P_u}}. \qquad \textbf{(14-7)}$$

From above, $v_s = v_u$, hence $\dfrac{\pi D N_u}{60} = \dfrac{\pi D_s N_s}{60}$

and therefore $N_s = N_u \dfrac{D}{D_s} = N_u \sqrt{P_u}$ (from equation 14-7).

$$= \frac{N}{\sqrt{H}} \sqrt{\frac{P}{H\sqrt{H}}} = \frac{N\sqrt{P}}{H^{\frac{5}{4}}} \qquad \textbf{(14-8)}$$

This value of N_s = speed of specific runner, is termed the *specific speed*. **(Example 135.)**

For a Pelton wheel, by putting d = diameter of jet
= $n_o \times$ diameter of wheel
= $n_o D$, . . (Fig. 281),

we obtain

$$\frac{P_u}{P_s} = \frac{\frac{\pi}{4} d^2 \,.\, U_u}{\frac{\pi}{4} d_s^2 \,.\, U_s} = \frac{(n_o D)^2}{(n_o D_s)^2} = \frac{D^2}{D_s^2},$$

from which equations 14-7 and 14-8 may be deduced.

263. Specific Speed. The significant aspect of the specific speed formula $N_s = \dfrac{N\sqrt{P}}{H^{\frac{5}{4}}}$ is that it is *independent* of the

dimensions or size both of the actual turbine and of the specific turbine ; that is to say, all turbines of the same geometrical *shape*, working under the same values of ϕ and ψ, and therefore having the same efficiency, will have the *same specific*

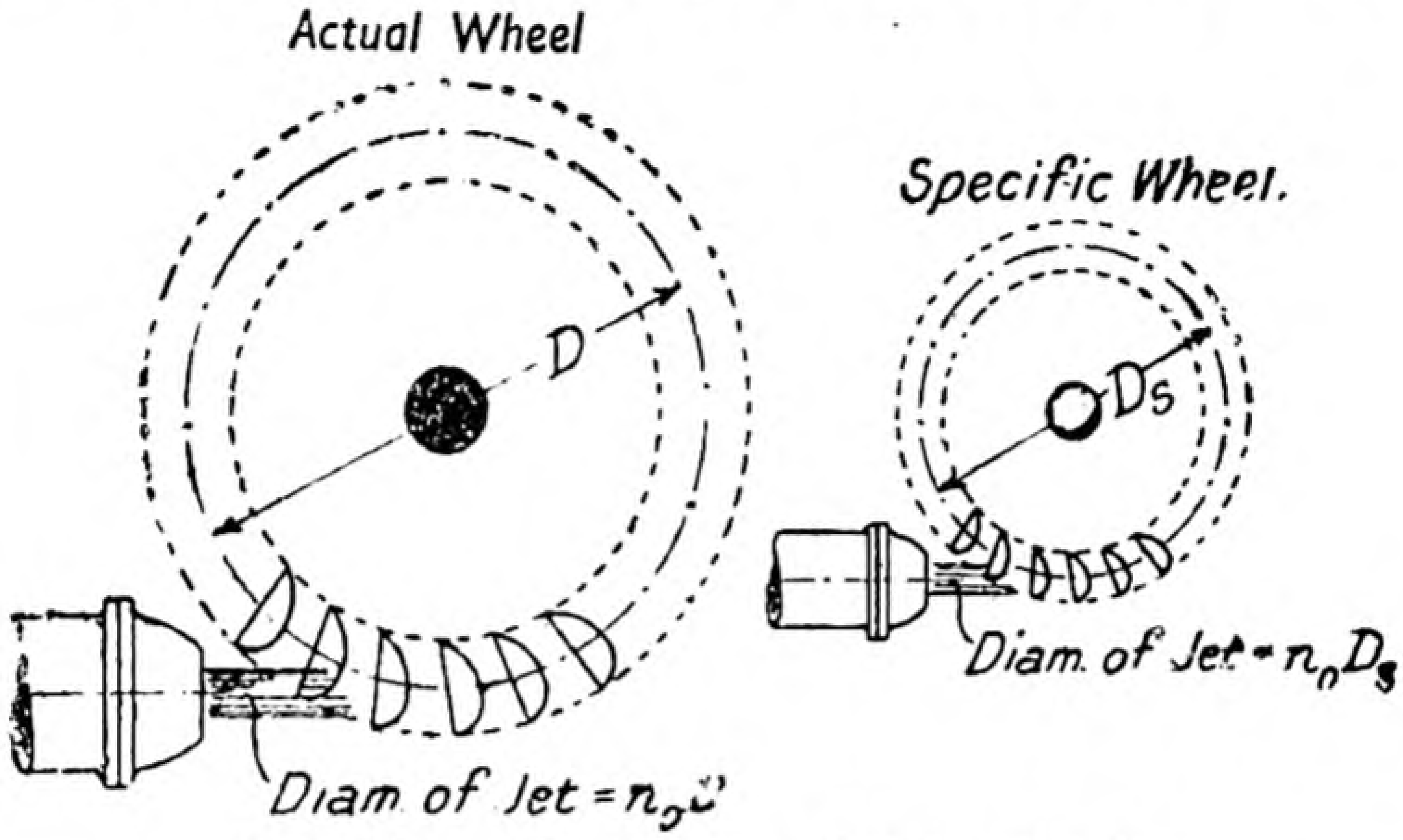

FIG. 281.—Homologous Pelton wheels.

speed. We therefore say that N_s represents the specific speed of the prototype or actual turbine, as well as of the specific turbine, and we use the term *homologous* to define such similarly-proportioned machines. Unless otherwise stated, specific speeds refer to the performance of the turbine at the value of ϕ giving maximum efficiency at normal full gate opening, § 272.

Here is a general definition : The specific speed of any turbine is the speed in revolutions per minute of a turbine geometrically similar to the actual turbine, but of such a size that under corresponding conditions it will develop 1 h.p. under unit head.

As the specific speed is not a pure number, its value depends upon the system of units employed ; thus

$$N_s \text{ in metric units} = 4{\cdot}44\, N_s \text{ in foot units.}$$
$$(H \text{ in metres.}) \qquad (H \text{ in feet.})$$
$$D_s \text{ in feet} = 8{\cdot}05\, D_s \text{ in metres.}$$

In practice the conception of specific speed is of the utmost utility—the mere knowledge of the numerical value of N_s for a given runner conveys quite a definite notion of the shape or proportions of the runner, and moreover permits its working performance to be predicted. In the following paragraphs it will be shown how information relating to specific speeds and specific runners can be used for roughly determining the main dimensions of turbines for given duties.

(A non-dimensional *shape number* n_s can readily be developed from the specific speed N_s, its value then being independent of the system of units (§ 40). This pure number is represented by

$$n_s = \frac{\frac{N}{60}\sqrt{\frac{P_o}{\rho}}}{(gH)^{\frac{5}{4}}},$$

where P_o = work done by turbine per second
= $550P$ (foot units) or $75P$ (metric units).

The specific speed and the shape number are connected thus :—

$$n_s = \frac{N_s}{273} \text{ (foot units)} : n_s = \frac{N_s}{1213} \text{ (metric units).)}$$

264. Specific Speed of Pelton Wheels. Assuming a gross efficiency of 85 per cent., and taking the ordinary limiting value of $\frac{1}{n_0} = \frac{\text{diam. of wheel}}{\text{diam. of jet}} = 12$ (§ 228), it is easy to show that all *single-jet* Pelton wheels have the *same* specific speed and the *same* diameter of specific runner. Using the notation of §§ 227 and 228, we have Q = discharge through actual nozzle

$$= \frac{\pi}{4}d^2 \times 0{\cdot}98\sqrt{2gH}$$

$$= \frac{\pi}{4}\left(\frac{D}{12}\right)^2 \times 0{\cdot}98\sqrt{2gH}$$

$$= 0{\cdot}043\ D^2\sqrt{H} \text{ (foot units).}$$

Also $$P = \frac{\eta_m WH}{550} \text{ (foot units)}$$

$$= 0{\cdot}85\frac{wQH}{550}$$

$$= \frac{0{\cdot}85 \times 62{\cdot}4 \times 0{\cdot}043D^2\sqrt{H} \times H}{550}$$

$$= 0{\cdot}00414\ D^2H\sqrt{H}.$$

From equation 14-7, D_s = diameter of specific runner $= \frac{D}{\sqrt{P_u}}$

$$= \frac{D}{\sqrt{\frac{0{\cdot}00414\ D^2H\sqrt{H}}{H\sqrt{H}}}} = 15{\cdot}6 \text{ feet.}$$

The equivalent diameter in metres = 1·94 m. (See § 263.)

(Note that in the metric system not only is the specific diameter D_s expressed by a different numeral, but the absolute diameter is only 0·408 × the diameter of the wheel in foot units—the specific wheel is definitely *smaller.*)

$$\text{Now } v_s = \frac{\pi D_s N_s}{60}, \text{ and } v_s \text{ also} = \phi\sqrt{2gH_s}$$

$$= 0{\cdot}45 \times 8{\cdot}03.$$

Substituting the above value of $D_s = 15{\cdot}6$ ft., we find

$$N_s = 4{\cdot}42 \text{ (foot units)} = \text{specific speed of Pelton wheel}$$

$$\text{or} \quad N_s = 4{\cdot}42 \times 4{\cdot}44 = 19{\cdot}6 \text{ (metric units)}.$$

For a Pelton turbine having *multiple* jets, so long as D d, N, and H remain constant, the horse-power will be directly proportional to the number of jets n_1; and since N_s then varies as $\sqrt{P}$, it will also vary as $\sqrt{n_1}$. Therefore under the stipulated ratio $\frac{D}{d} = 12$, $\quad N_s = 4{\cdot}42\sqrt{n_1}$ (foot units)

$$N_s = 19{\cdot}6\sqrt{n_1} \text{ (metric units)}.$$

The ultimate maximum value of N_s per jet, using an abnormally low ratio $\frac{D}{d} = 7$, is about 7·5 (foot units) or 33 (metric units); Fig. 233 shows such a runner. The maximum value of N_s per turbine, using 4 or 6 jets, is of the order of 12 (foot units) or 54 (metric units).

265. Specific Speed of Francis Turbines. As would be expected from § 237, a much greater range of specific speeds is available for Francis turbines than for Pelton wheels, because the value of N_s is under the control of (i) the speed ratio ϕ which itself depends on the inlet wheel blade angle α, (ii) the flow ratio ψ, and (iii) the ratio $\frac{B}{D} = n$. Alterations to any or all of these will alter the specific speed.

The general characteristics of typical runners of low, medium and high specific speeds may be seen from Fig. 282. On the left, specific runners are drawn, all to the same scale; on the right, corresponding actual runners are shown, of the size required to develop some standard output—in this instance 1000 h.p.—under the head for which each type of runner is most suited. Their speed and flow ratios are as follows:—

Runner.	Specific Speed.		Speed Ratio ϕ Based on Max. Inlet Diam.	Flow Ratio ψ Based on Runner Outlet Area.
	Metric.	Foot.		
I, I*a* .	80	18	0·69	0·14
II, II*a* .	150	33·8	0·69	0·21
III, III*a*	400	90	1·26	0·30

We observe that the increase in specific speed from 80 to 150 is obtained by increasing n and ψ, while to attain the higher value 400 it is necessary to increase simultaneously

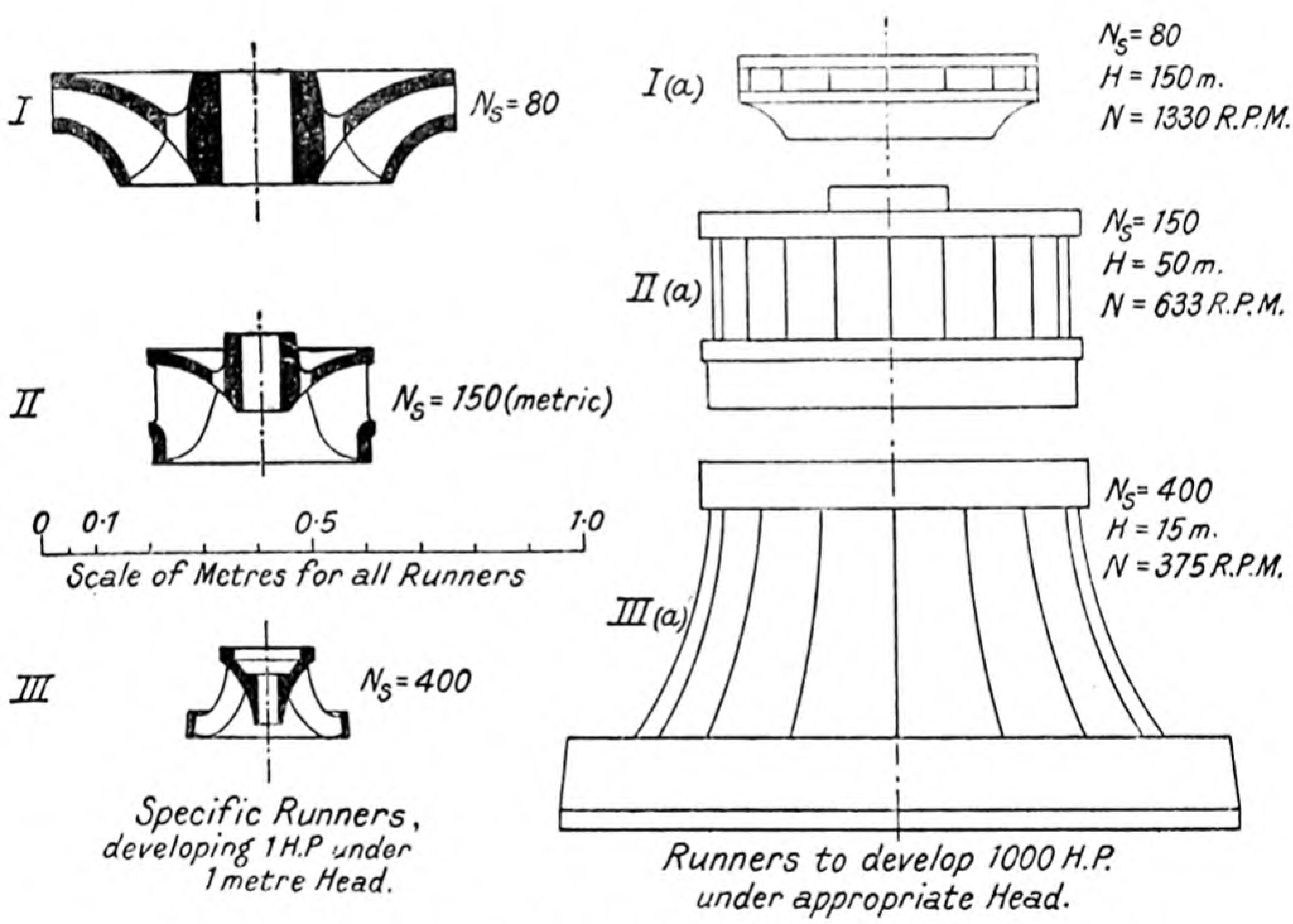

FIG. 282.—Comparison between types of Francis turbine runners.

everything that can be increased, ϕ, ψ, and n. It is also noticeable that the type of runner having the largest specific diameter and lowest specific speed has the smallest *actual* runner and highest *actual* speed.

In support of the statement in § 263 that the mere mention of a certain value of N_s can evoke a pretty accurate conception of the *shape* of the runner in question, the photographs in Fig. 283 are offered. When the eye has become accustomed

to the proportions of the runners in Fig. 282 there is no subsequent difficulty in picking out the "low speed" runner, with its narrow inlet, and in distinguishing it from the "high speed" runner characterised by its great inlet area.

Manufacturers usually find it desirable (although it is not strictly essential) to use a range of runners such that a given specific speed is associated fairly closely with a particular speed and flow ratio. This practice still further defines the inter-relation of specific speed and shape; for it implies that all runners of the same specific speed have *specific* runners of much the same shape *and* size. Fig. 284 shows the measure of agreement that may be expected. Here the full lines represent the specific runner of $N_s = 152$ (metric) corresponding to the turbines at Queenston, Niagara, built in America, which each develop 55,000 h.p. under a 93 metre head. The specific runner of $N_s = 160$ (metric) shown by the broken lines relates to a turbine of Continental manufacture having an output of 825 h.p. under 36·5 metres head.

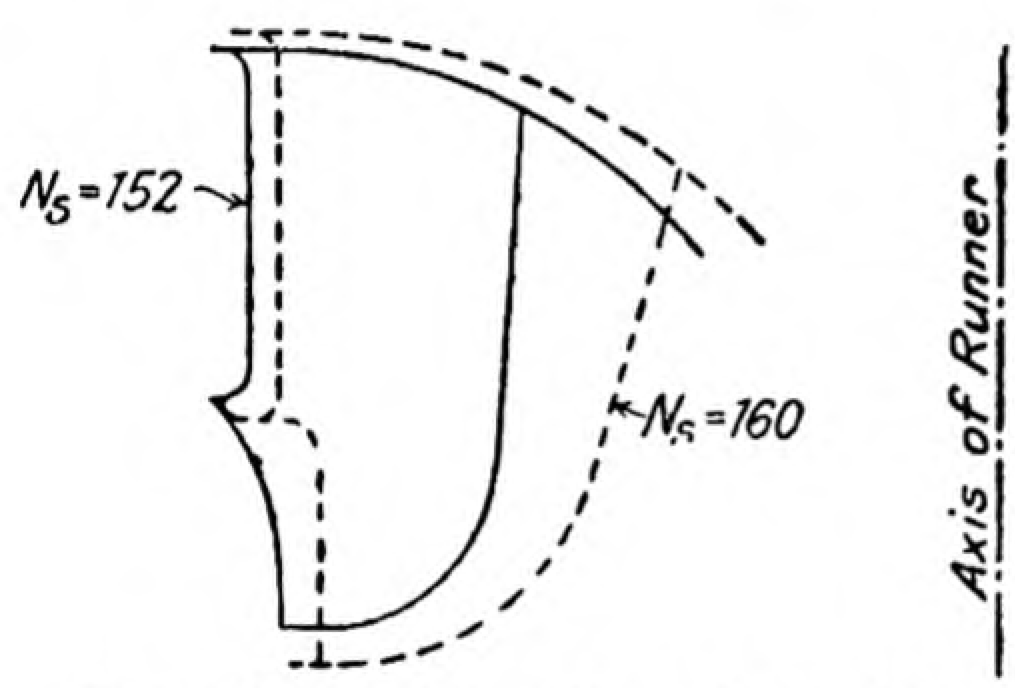

FIG. 284.—Comparison of specific runners.

266. Specific Speed of Kaplan and Propeller Turbines. The virtues of the axial-flow turbine mentioned in §§ 247, 249 can be summarised in the statement that this turbine has a very high specific speed. Values relating to the machines already described in this book are :—

	Specific speed	
	foot units	*metric units*
Fig. 255	124	550
Fig. 261	95	415
Fig. 262	180	800

The significant tendency here—that the machine working under the *highest* head has the *lowest* specific speed—will be examined in the following paragraphs. **(Example 136.)**

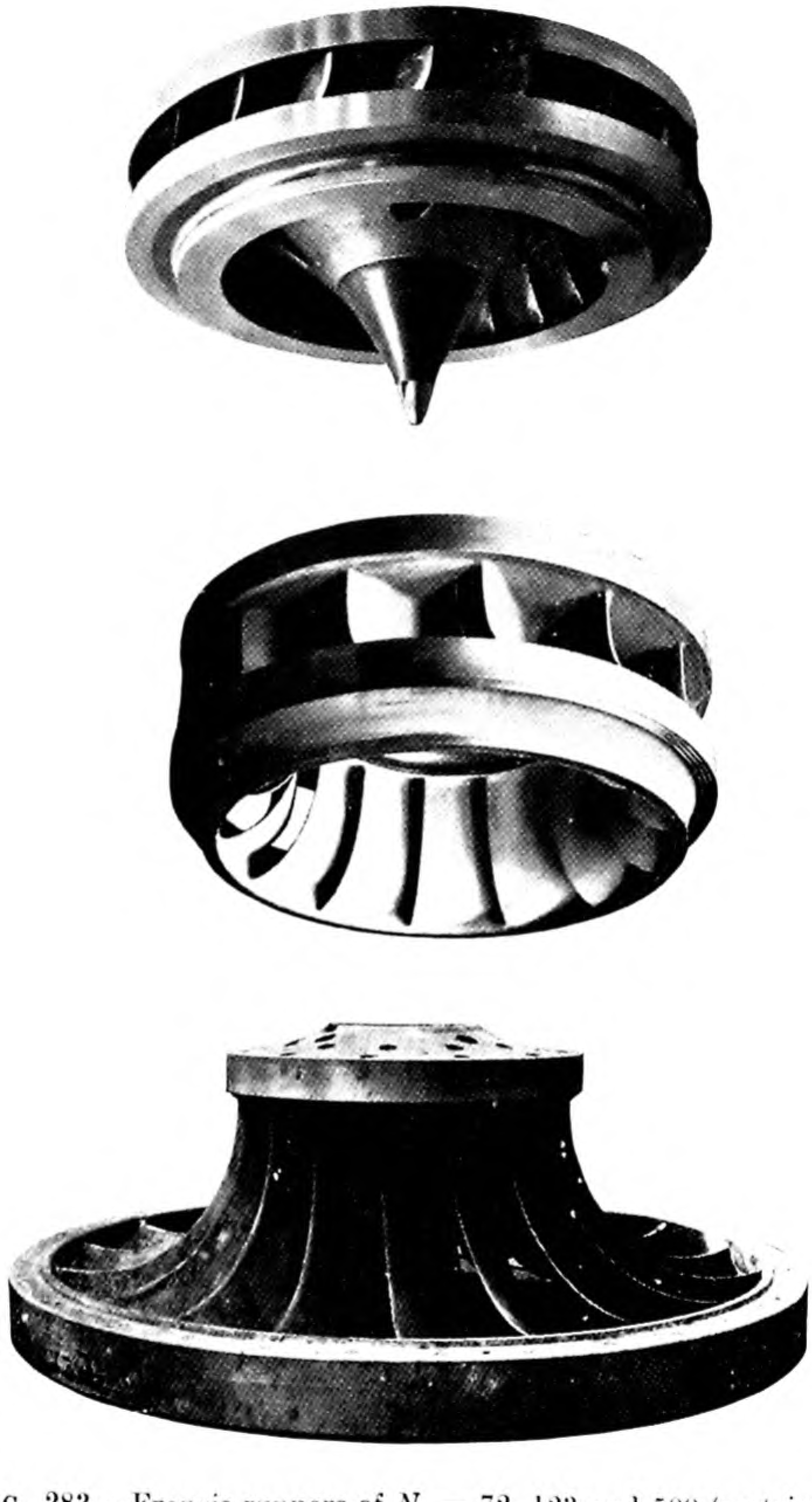

FIG. 283.—Francis runners of $N_s = 72$, 123 and 500 (metric).

[To face page 384

267. Total Available Range of Specific Speeds. A graphic illustration of the very great range of machines available at the present time is to be seen in Fig. 285, in which

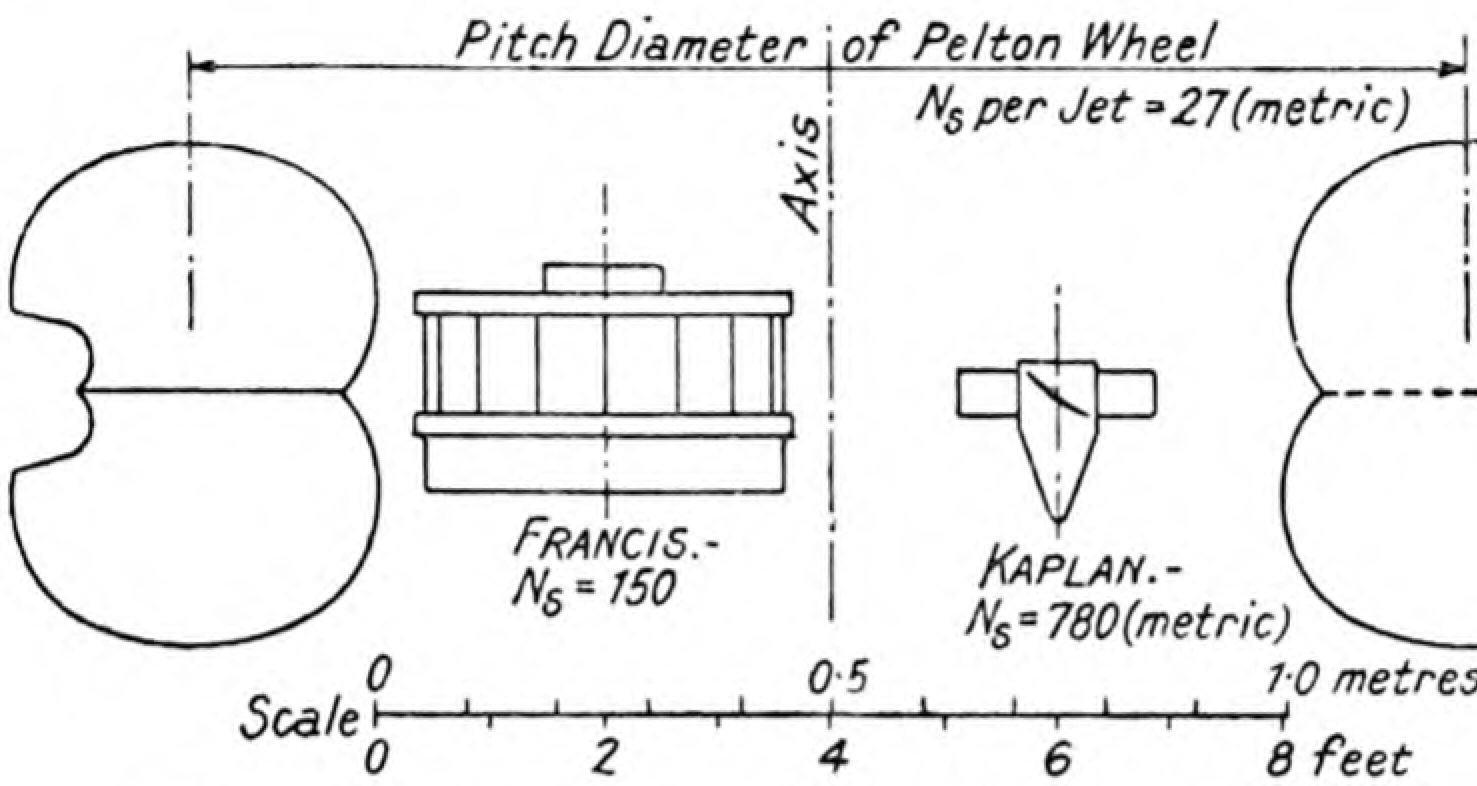

FIG. 285.—Specific runners for various types of turbine.

specific runners of the three main types of turbine are plotted to the same scale. If the runners were built to the metric dimensions, they would all develop 1 h.p. under a standard

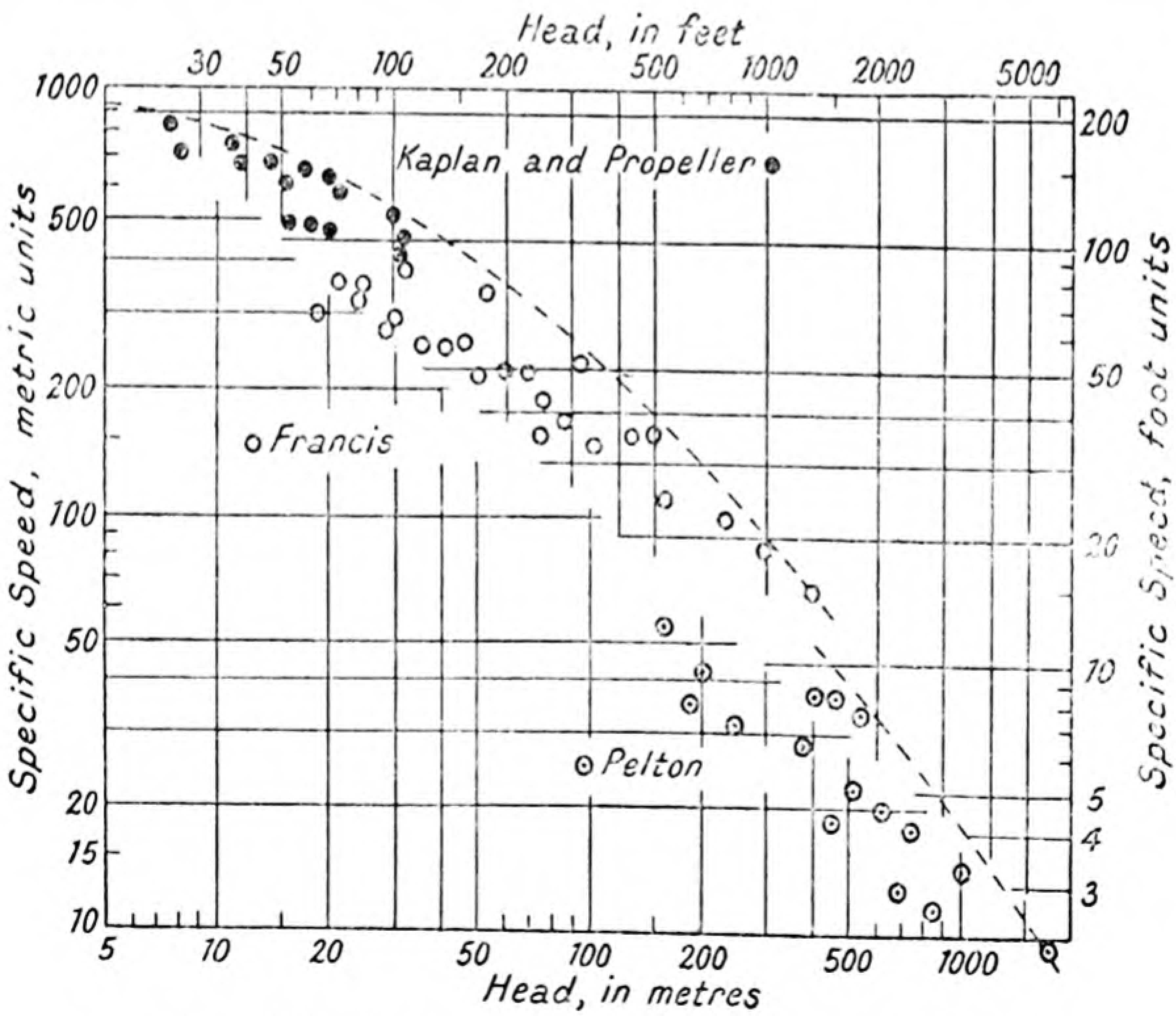

FIG. 286.—Relation between head and specific speed.

head of 1 metre, but whereas the Pelton wheel would revolve at 27 r.p.m., the Francis turbine would turn at 150 r.p.m., and the Kaplan turbine would have the very high speed of

780 r.p.m. Using the scale of feet, the equivalent speeds for runners developing 1 h.p. under 1 foot head would be 6, 34 and 176 r.p.m.

The same kind of information is conveyed in Fig. 286, but in a rather more effective form. Each point plotted in this graph represents a turbine installation either successfully at work or in course of construction ; the graph shows in the clearest possible way that it is entirely unknown in practice to find a Pelton wheel, a Francis turbine, and a Kaplan turbine all working under the same head. On the contrary, there is a fairly definite range of heads and specific speeds allocated to each kind of turbine.[173]

It is instructive to enquire why the specific speeds of (say) Francis turbines should be restricted in this way. The chief reason is, of course, that only thus can an acceptable value of the gross efficiency be ensured. If specific speed be expressed in the form (Constant $\times \phi\sqrt{n\psi}$), we may observe how inadmissible values of any of these ratios will encourage excessive energy losses of the types reviewed in § 221. For example, it was already shown in § 237 that an unduly high value of the speed ratio ϕ will involve excessive hydraulic losses in the wheel passages. There would be similar tendencies if the flow ratio ψ were too high. Although, by forcing more water through the wheel, we could raise the power output, yet the energy losses would increase at a still faster rate.

A *reductio ad absurdum* approach will show the influence of the diameter ratio $n = B/D$. Let us consider a range of inward-flow runners, all identical except for the width B. As a rough approximation, we could say that throughout this range each one of the turbines would suffer the *same* mechanical loss (§ 221 (i)), the *same* disc friction loss, (ii), and the *same* leakage loss.[177] But as the width of the wheel diminishes, so also does the output, because the discharge is declining accordingly. If, therefore, the power losses remain unchanged while the output dwindles, the gross efficiency must inevitably fall away. In the limit, when the width B has become zero, the efficiency is likewise zero.

268. Relationship between Specific Speed and Head. Although, as just implied, the curve sketched in Fig. 286 is purely an empirical one, there is no difficulty in justifying its general trend. If the head is high a relatively small volume of water will develop the necessary power ; the runner will therefore not be unduly large and its speed of rotation will be quite as high as we want. Because of the possibility of erosion of the blades, in the event of the water carrying sand or grit in suspension, we should on this ground alone prefer low speed ratios so as to ensure the lowest practicable water velocities. In every way, then, a slow-speed runner will meet requirements.

With low heads, as already pointed out, the problem is how to design water passages big enough to accommodate the very large flow that will be needed, and yet to keep the size of the machine within reasonable limits and its speed not unduly low. These conditions can only be met by adopting the highest practicable values of n, ϕ, and ψ, so that a high specific speed is inevitable.

Fig. 286 may advantageously be used as a rough check on the feasibility of projected turbine installations. If the specific speed of the proposed turbine, when plotted against head, lies within the range of values for which the particular type of turbine is suited, and below or to the left of the broken limiting curve, there is little doubt that manufacturers will be able to supply a successful plant. Each year, however, the maximum specific speed for a given head tends to increase, so that it by no means necessarily follows that makers would be unable to cope with conditions that fall within the doubtful zone of the diagram.[174]

Taking the information given in the graph in conjunction with the information given in the last sentences of § 265, it is possible to make a final rough generalisation and to say that all runners of a given type designed for the same head are likely to have much the same specific speed and much the same shape and proportions. This does not, of course, relieve the designer of the need for exercising judgment in individual cases—there is a range of high heads in which he must decide whether Pelton or Francis turbines will best meet the conditions [175] and a range of low heads where either Francis, Kaplan, or propeller turbines might be used. **(Example 137.)**

269. Summary of Design Characteristics. Some of the information offered in earlier paragraphs is here collected in tabular form for reference purposes.[176]

Type of turbine.	Range of specific speed (foot units).	Maximum head (ft.).	Maximum output (b.h.p.).	Maximum overall efficiency (per cent.).
Pelton .	4-12	5000	100,000	89
Francis .	18-90	1000	150,000	93
Propeller .	90-200	100	70,000	93

In regard to average values of the descriptive ratios ϕ, n and ψ suited for various specific speeds, they are shown by the curves in Fig. 287. As will be observed from the inset key diagram, the conventional system here used for specifying the effective diameter D of Francis runners is not the same as

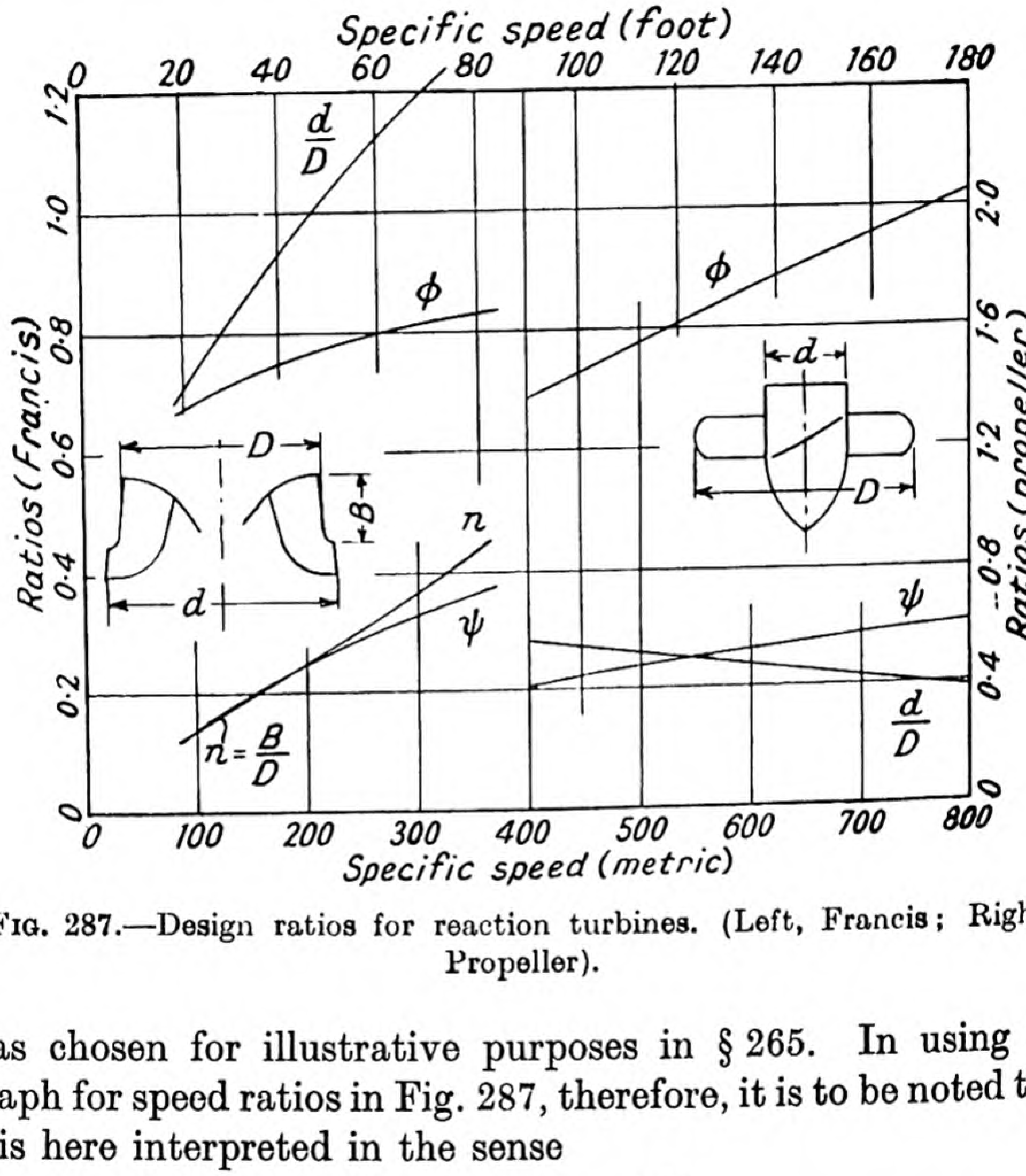

FIG. 287.—Design ratios for reaction turbines. (Left, Francis; Right, Propeller).

was chosen for illustrative purposes in § 265. In using the graph for speed ratios in Fig. 287, therefore, it is to be noted that ϕ is here interpreted in the sense

$$\phi = \frac{v}{\sqrt{2gH}} = \frac{\dfrac{\pi DN}{60}}{\sqrt{2gH}}$$

270. Characteristic Performance Curves. Here it is necessary to point out once more that the study of turbine behaviour that has been carried through the preceding §§ 261-269 has been based on one particular set of conditions—the conditions which specify that a rigid relation is maintained between head and speed (§ 259 (i)). For making general comparisons between various types and sizes of machines working

under full load, this basis is convenient and satisfactory. But the service conditions to which actual machines must conform are a good deal more complex, as may be gathered from § 259 itself. Their effect on performance can most easily be represented by the use of characteristic curves such as those that are now to be reproduced. Just as the specific speed is characteristic of the *shape* of a given class of turbine, so these performance curves are characteristic of the *behaviour* of given types of machine. This will be specially true if the graphs are plotted on a non-dimensional basis, e.g. if the speed ratio ϕ is used rather than the rotational speed N.

The general trend of some of the curves can readily be predicted. Thus the reasoning developed in §§ 123, 124 shows that, if frictional losses are disregarded, an impulse turbine running at varying speed under a steady head (§ 259 (iv)) would yield graphs such as are plotted in Fig. 288. Here the speed-torque characteristic is a straight line, and so is the speed-discharge curve. Although as the turbine construction alters, and the characteristics change their shape also, yet there may still remain a family resemblance. Thus Fig. 295 has points of similarity with Fig. 288.

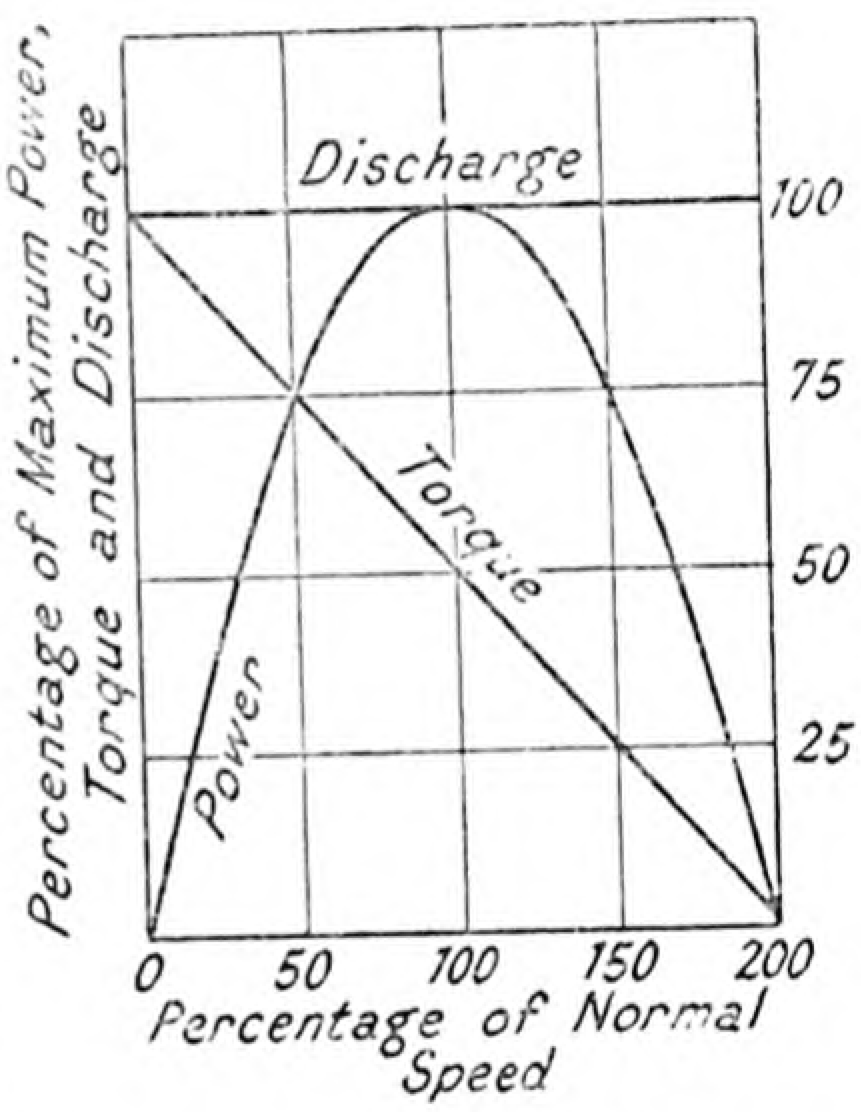

FIG. 288.—Ideal non-dimensional plot of impulse-turbine performance (H = constant.)

271. Performance of Pelton Wheels. The performance of a Pelton wheel under conditions of *uniform* head and nozzle opening, and *variable* speed, is shown by the curve in Fig. 289. Under ideal conditions this curve would have a parabolic form (§ 227), but owing to the increased windage and friction at high speeds, the maximum or runaway speed is not quite twice the working speed corresponding to maximum efficiency (§§ 228, 270). The reason why the gross efficiency falls off if the value of ϕ departs sensibly from 0·45 is that at other values of ϕ the water leaves the buckets with an undue amount of unexpended velocity energy, which is wasted in the tail-race.

Under conditions of *uniform head* and *speed*, and variable output regulated by the movements of a needle, the Pelton wheel maintains its efficiency over a wide range of output. Fig. 290

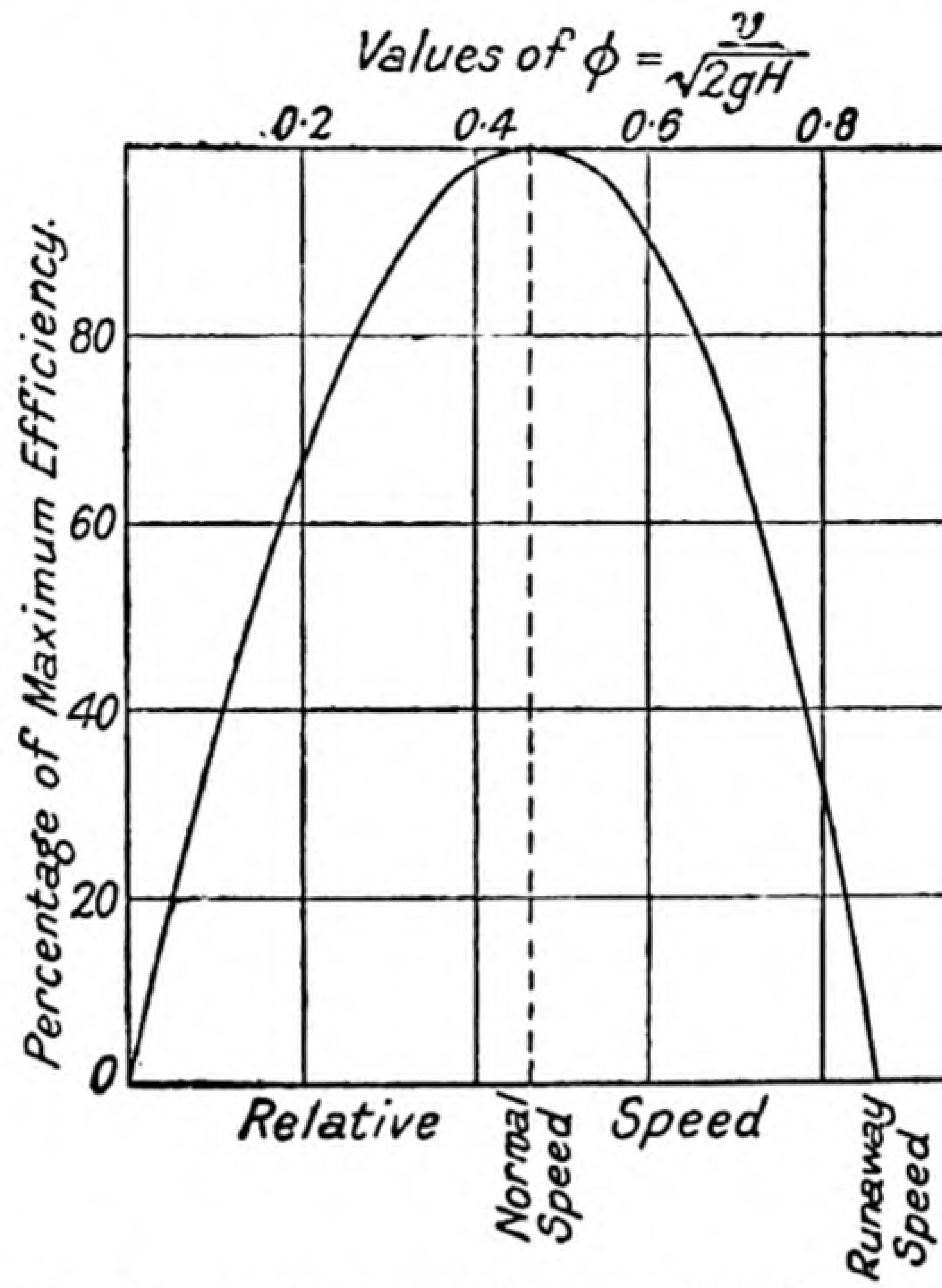

FIG. 289.—Performance of Pelton wheel (varying speed).

(I) shows the best possible results attainable with units of 10,000 h.p. and upwards, with normal values of N_s per jet, the speed corresponding with optimum values of ϕ. The abnormal curve

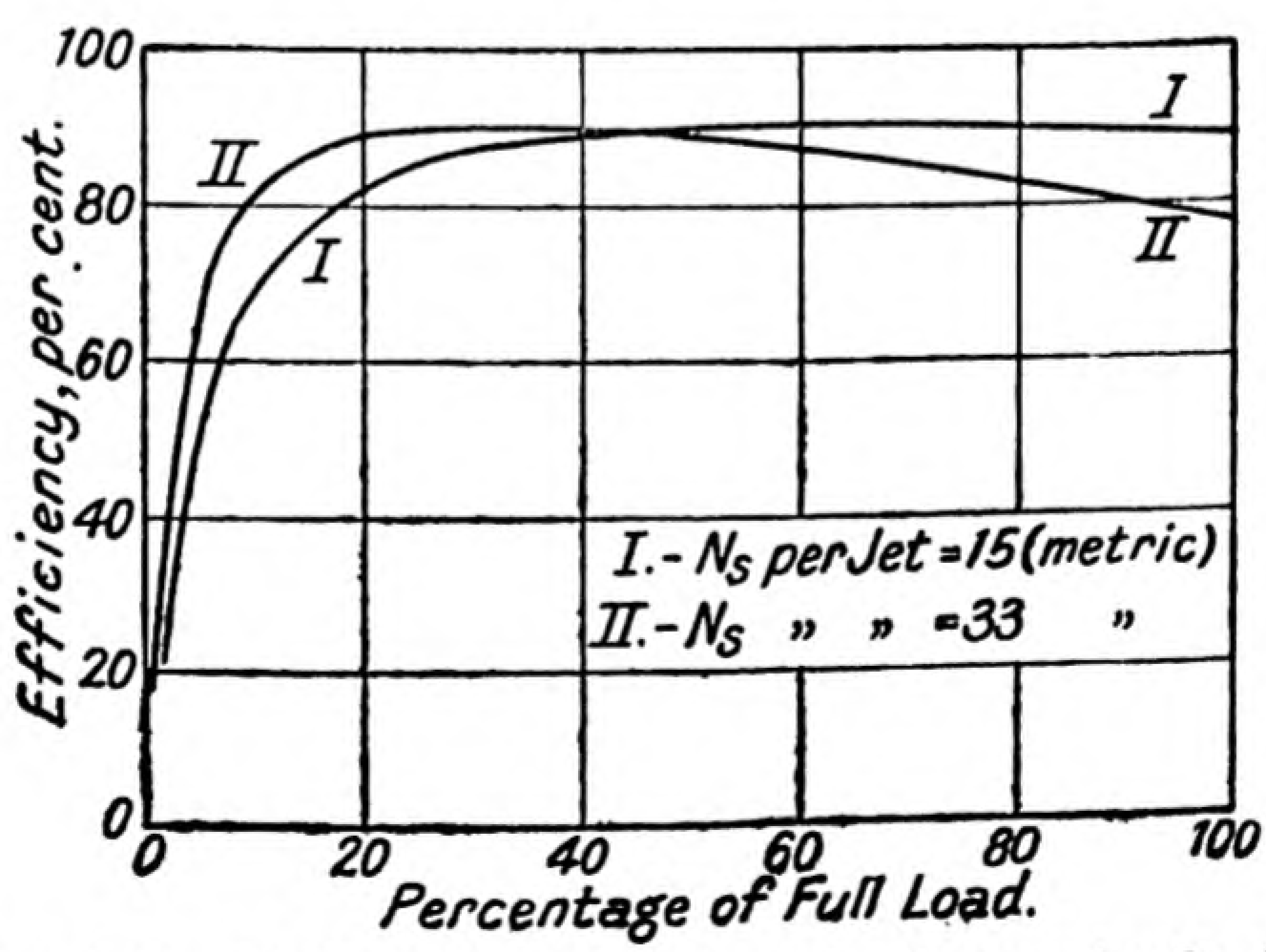

FIG. 290.—Performance of Pelton wheels (varying load).

(II) relates to the Pelton wheel having the very high N_s per jet of 33 (metric) mentioned in § 264 and illustrated in Fig. 233; this turbine is designed to give its best efficiency at the

fractional load at which it normally works. It is so rarely required to develop its full output that the corresponding poor efficiency is of little consequence; the full-load efficiency is low because the jet issuing from the fully opened nozzle is too big for the buckets.

To show how the excellence of the typical efficiency curve I (Fig. 290) depends upon the system of needle regulation, Fig. 291 is appended; it is based on the performance of a small model Pelton wheel with spear governing (I), and with throttle governing (II). (See § 230.)

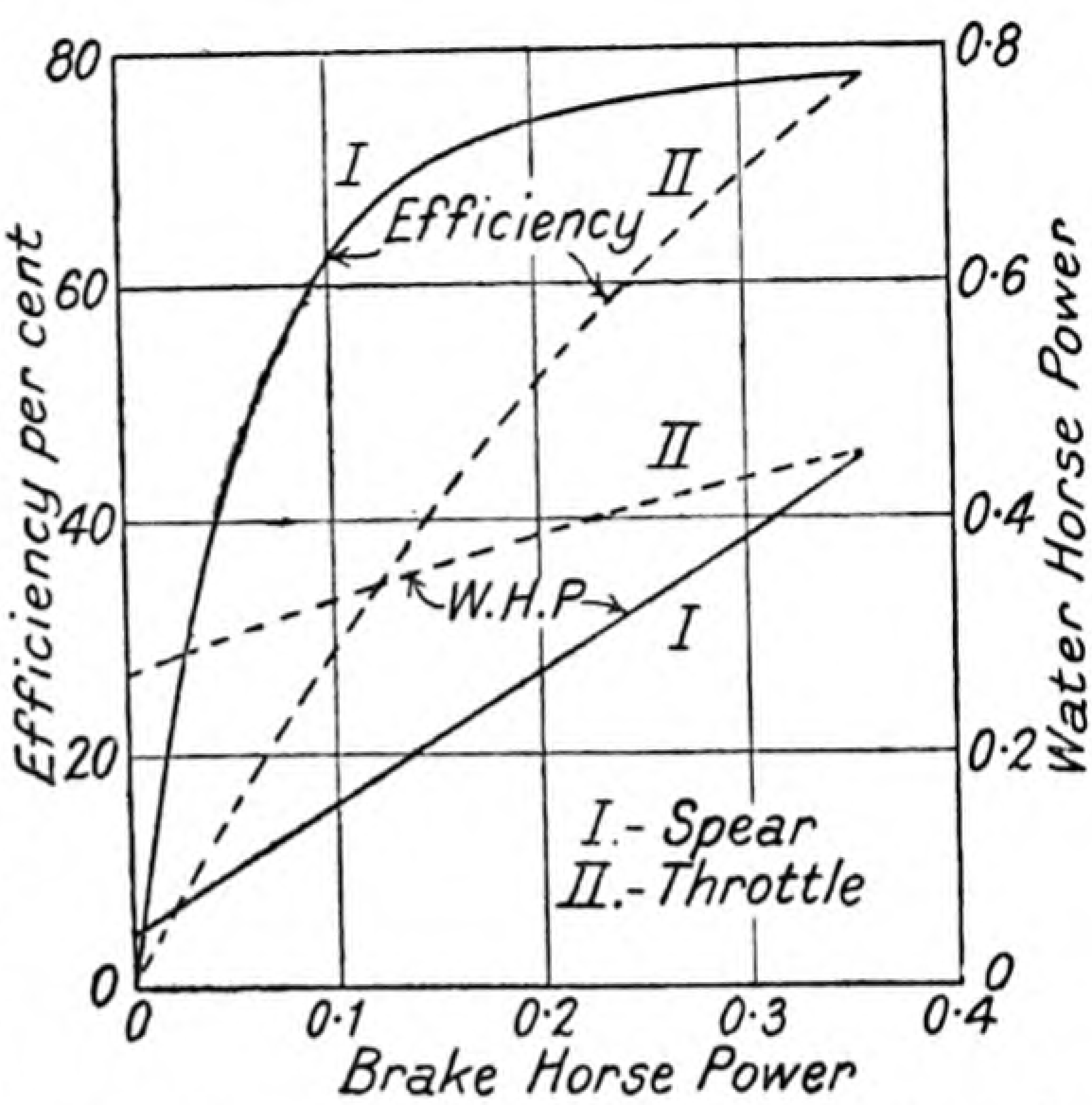

FIG. 291.—Comparison between needle and throttle regulation (H and N constant).

As for the general shape of the usual type of load-efficiency curve, this accords with what might be expected from §§ 221, 228. While the output of the wheel is being reduced under the action of the needle, the hydraulic losses are lowered in much the same proportion, and thus the gross efficiency remains unchanged. But meantime the windage and mechanical power losses have not diminished; at a later stage their relative importance increases, until ultimately they become predominant and they bring down the efficiency to zero.

272. Performance of Francis Turbines. (i) *At full gate opening and varying speed.* When a Francis turbine runs at constant head under the conditions specified in § 259 (iv), viz. with a fixed gate setting (usually full-gate opening), then the connection between speed and efficiency, output and discharge is of the form seen in Figs. 292, 293, and 294; these all relate to experiments at full-gate opening on a small inward-flow turbine having the low specific speed of 70 (metric). In Figs. 292 and 293, separate graphs show the performance at heads of 5, 6, and 7 metres respectively, while Fig. 294 shows the same results reduced to conditions of 1 metre head (§ 261); it will

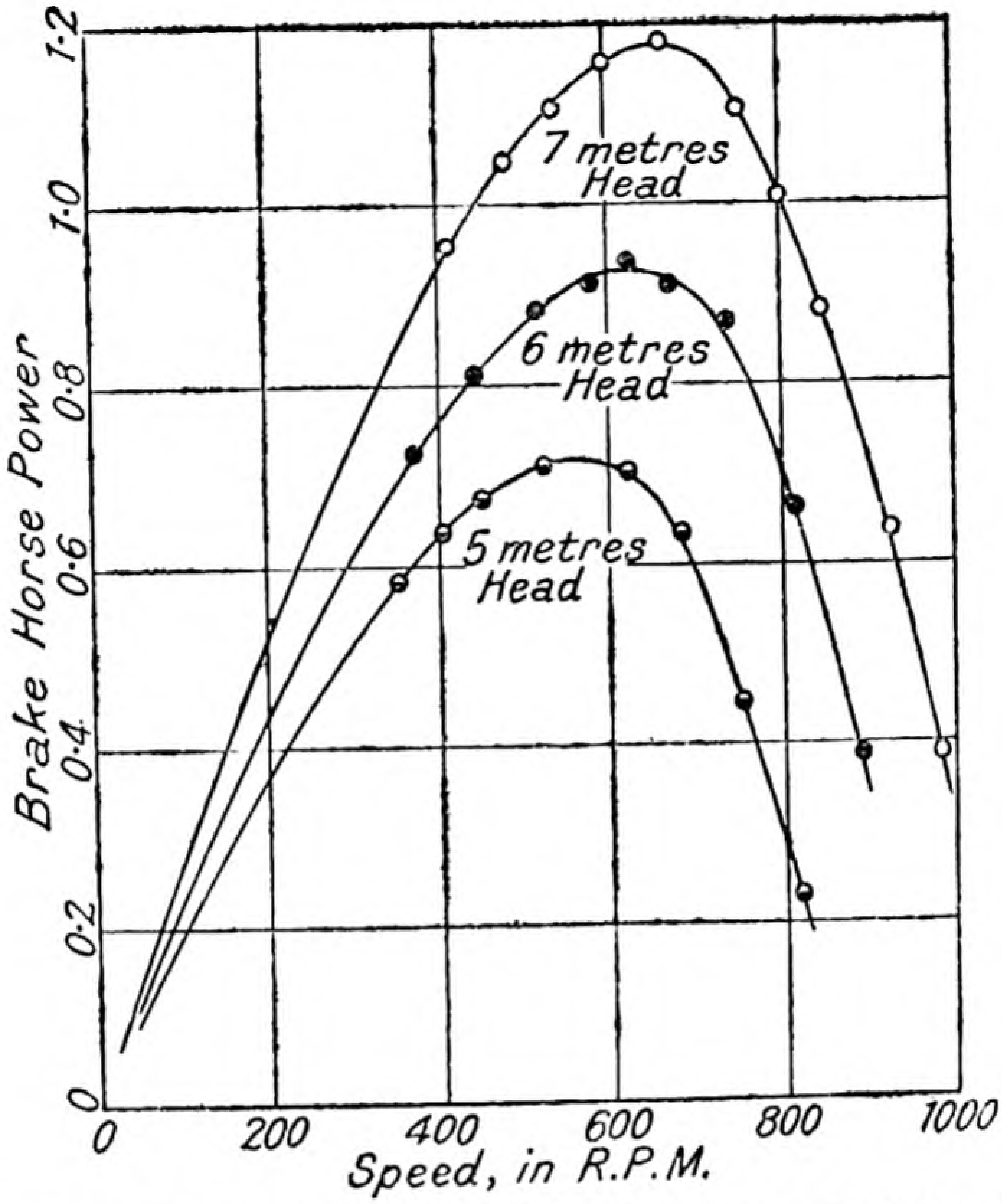

FIG. 292.—Inward-flow turbine characteristics at constant head. (N_s = 07.)

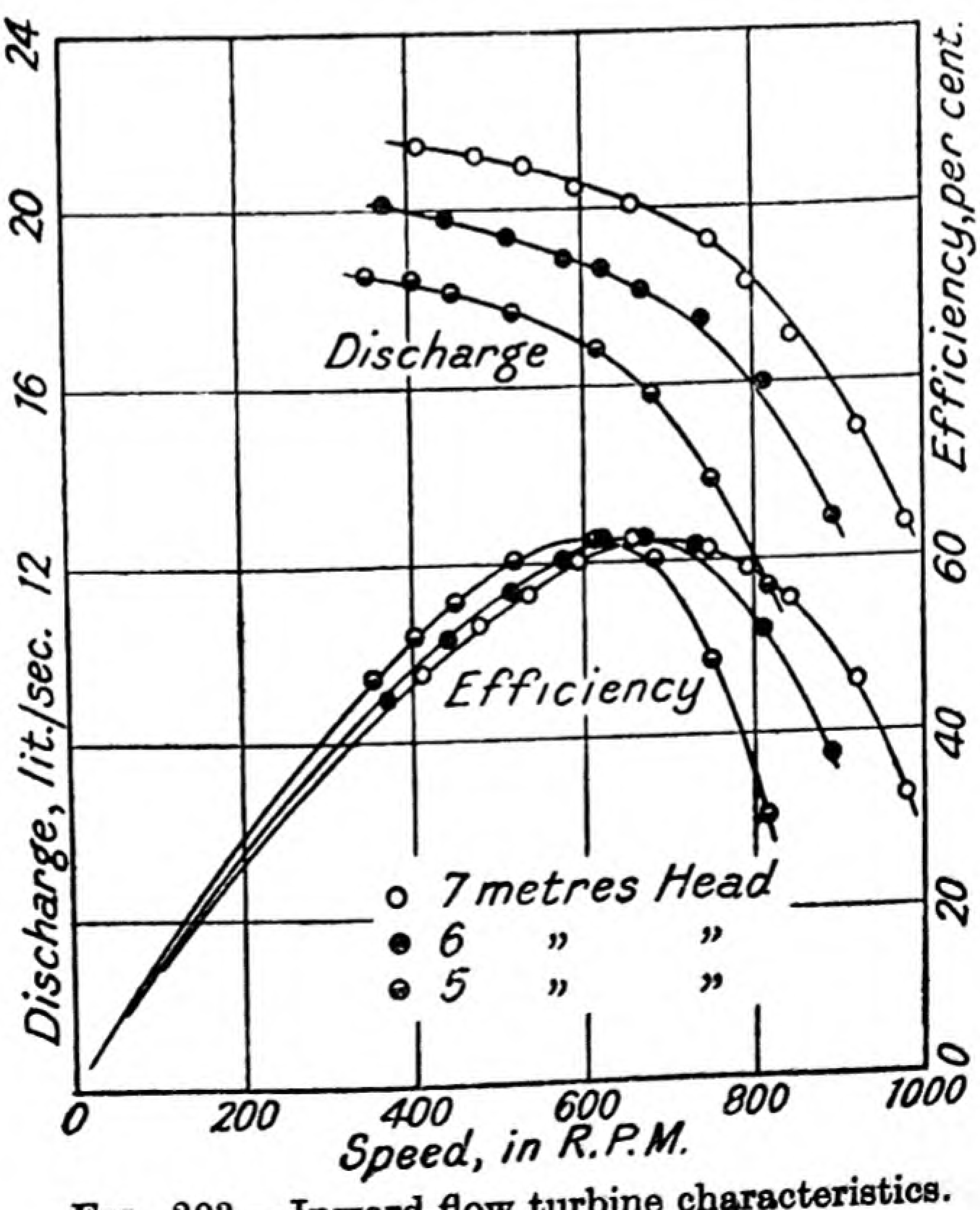

FIG. 293.—Inward-flow turbine characteristics.

be seen that under unit conditions the points corresponding to various heads lie fairly well along a single set of curves. On account of its small output and simple design, this machine yields lower gross efficiencies than would normally be expected (§ 279).

Turning now to Francis turbines of high specific speed, the performance of such a machine, of $N_s = 390$ (metric)

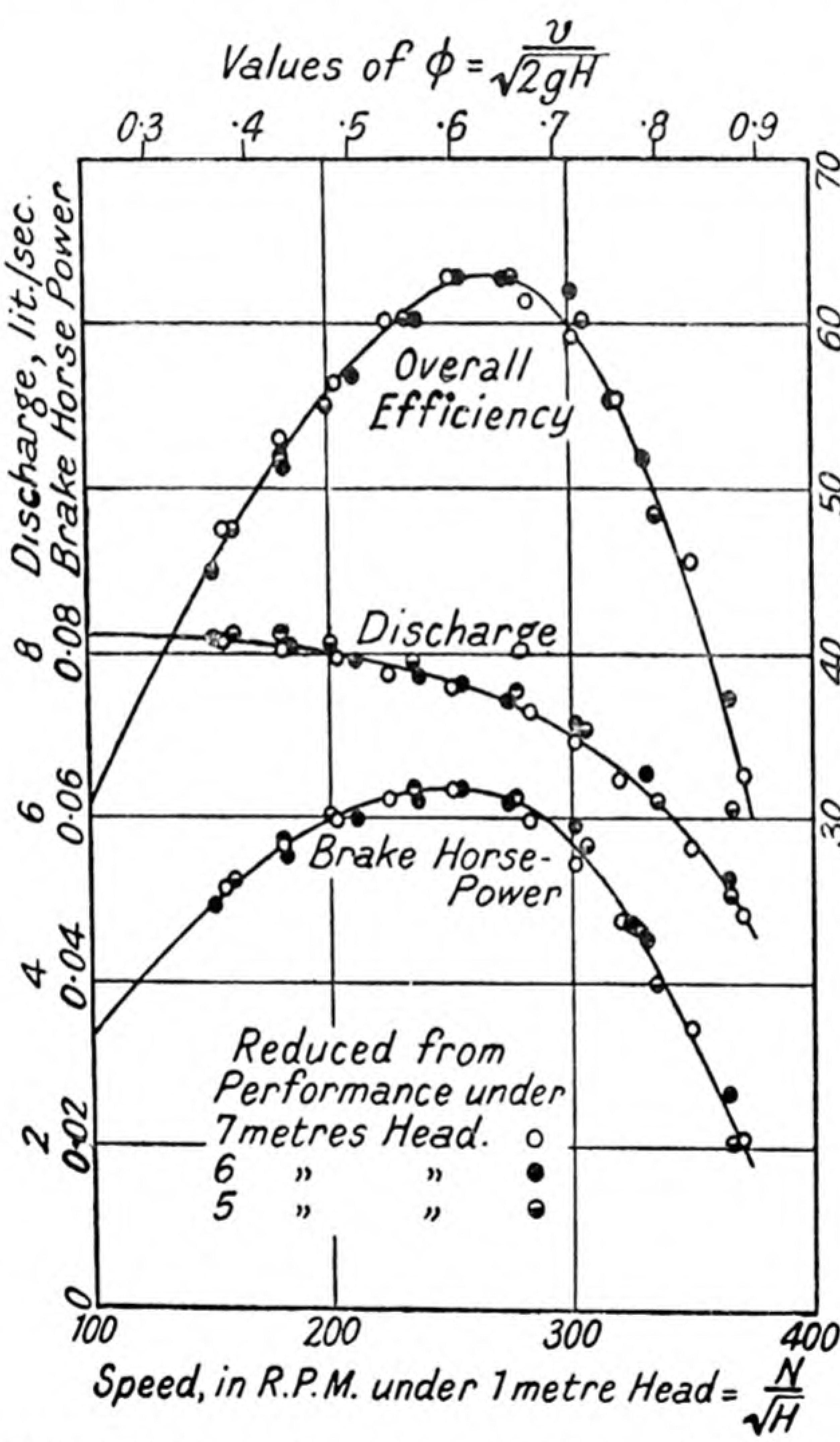

FIG. 294.—Turbine performance reduced to unit head conditions.

or 87 (foot), is expressed in Fig. 295 in terms of its performance at the normal or most favourable value of $N/\sqrt{H}$ or of ϕ. Two points of difference are to be noticed between these curves and those shown in Fig. 294: firstly, the runaway speed recorded in the former is about 95 per cent. above the normal running speed, as against 50 per cent. in the latter; secondly,

whereas the discharge through the turbine of high specific speed *increases* as the speed rises, the flow through the turbine of low specific speed *falls off* with increasing speed.

(Example 138.)

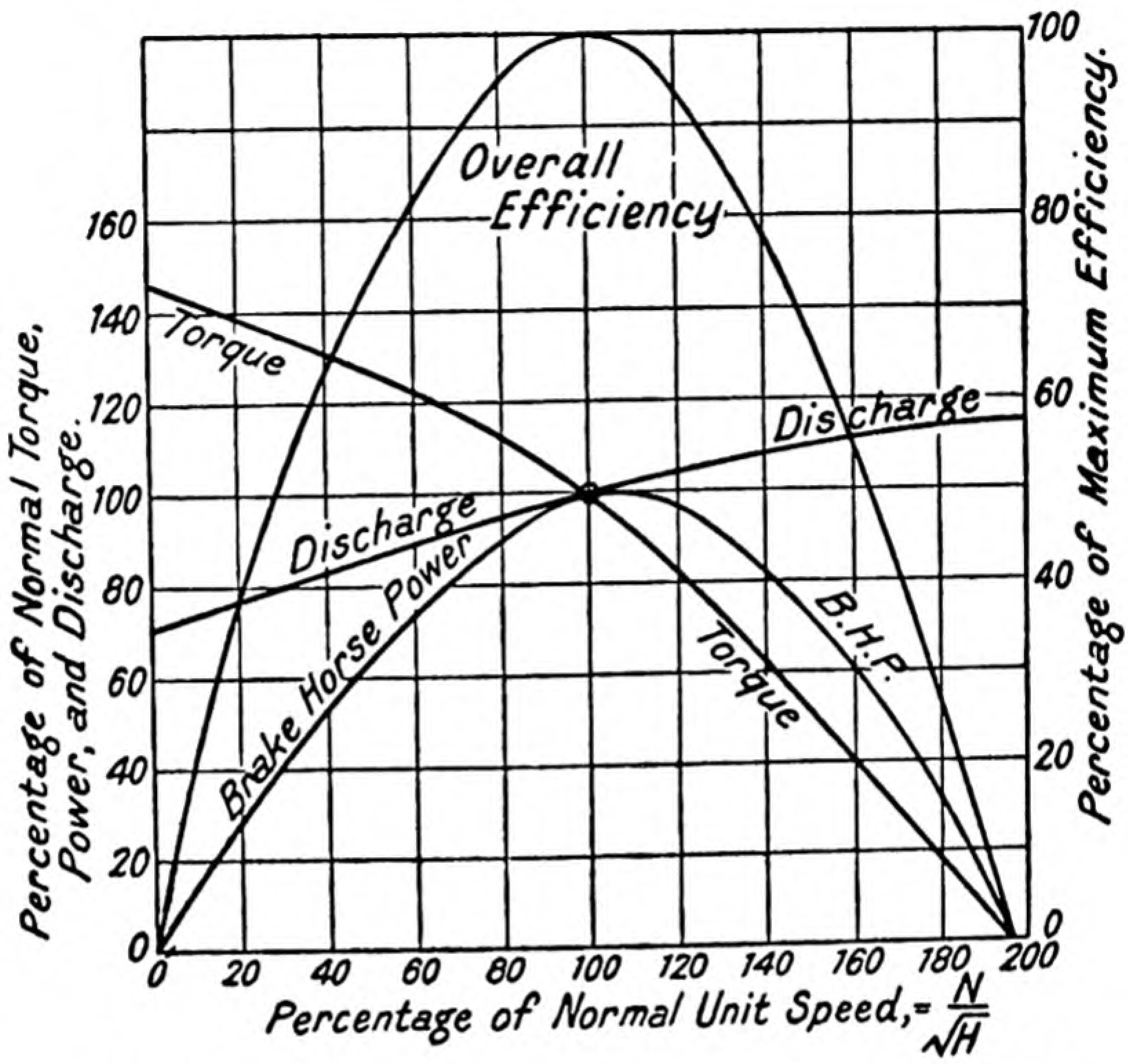

FIG. 295.—Characteristics of high specific speed turbine.

273. Explanation of Francis Turbine Characteristics. In general terms, the explanation of the drop in efficiency when the value of the speed ratio ϕ for a Francis turbine is changed from its optimum value is that the velocity diagrams no longer have the shape they were assumed to have when the turbine was designed. Evidence on this matter is given in Fig. 296; it shows the relationship between speed, discharge and head drop in the guides, under a total head of 8 metres, at full gate opening, for the small turbine whose characteristics are given in Figs. 292 to 294. This head drop in the guides is the measured difference between the pressure head at the inlet branch to the turbine casing, and the pressure head in the clearance space or region in which the water passes from the guides to the wheel; it corresponds to the distance $(H - H_o)$ in Fig. 235. In the guide passages, as in any other passage of varying cross-section, the change in pressure between inlet

and outlet ought to be proportional to the square of the discharge, and as shown in Fig. 296 it actually is so.

Remembering that in the circumstances now in question the area for flow through the guide passages and through the wheel passages remains invariable, we can at once see from the graphs that a change in rotational speed must be accompanied by a change in (i) velocity of exit from the guides U, (ii) peripheral velocity v, and (iii) relative velocities v, and V_r in the runner. Thus, in consequence of an increase in speed, the velocity diagrams, which under optimum conditions of ϕ have the shape indicated by full lines in Fig. 297, now have the distorted shape indicated by broken lines. As the first tip of the runner blades was designed to be parallel with v_r (§ 236 (vi)), it is manifestly impossible for it also to be parallel with v'_r, and therefore serious loss of energy due to shock and eddying occurs; for the relative motion of the water entering the runner is now *across* the mouths of the wheel passages instead of *into* them. Furthermore, we observe from the outlet velocity diagram that the water now leaves the wheel with a considerable velocity of whirl instead of leaving normally, as it was designed to do, this representing an additional waste of energy.

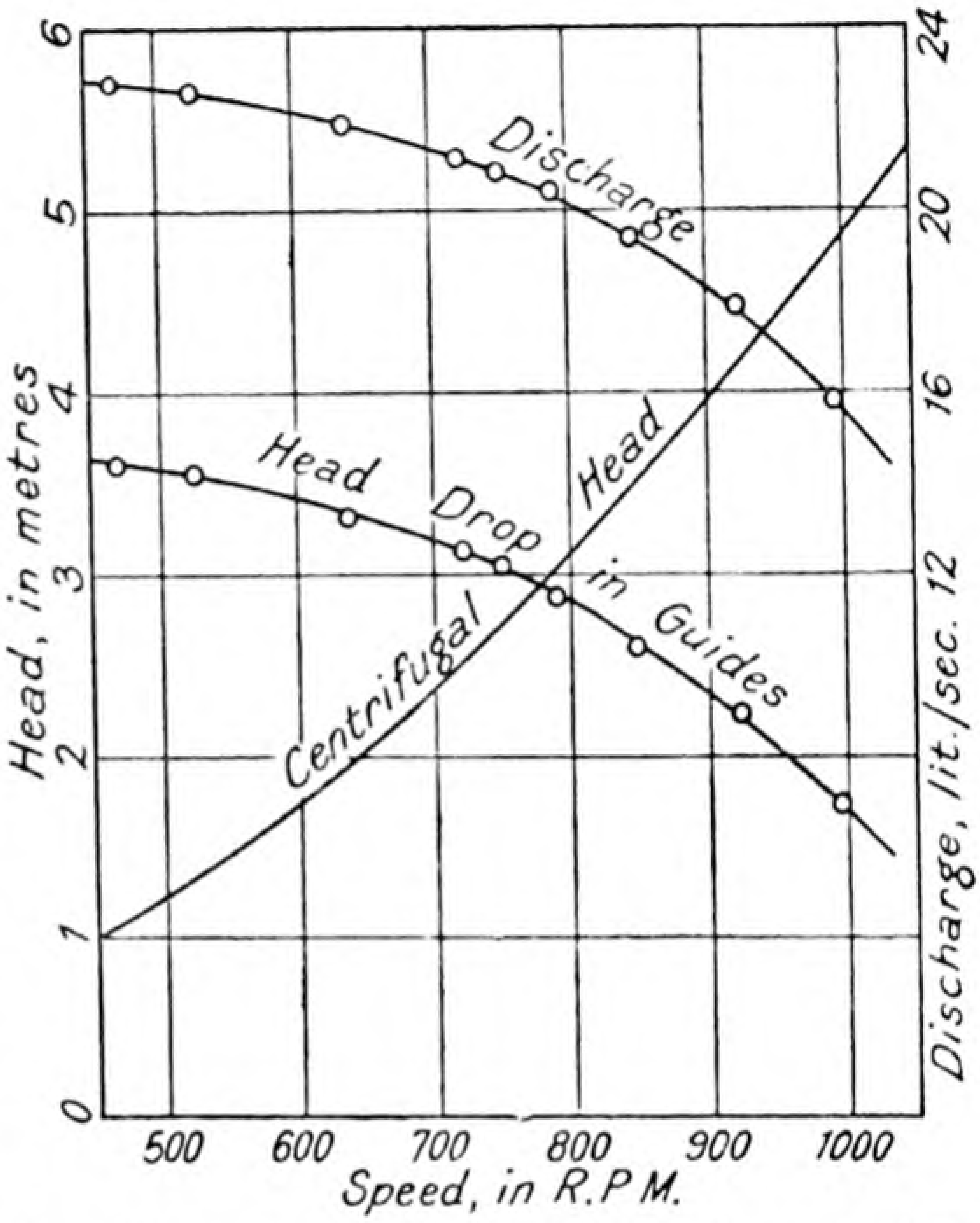

FIG. 296.—Inward-flow turbine characteristics (H = 8·0 metres).

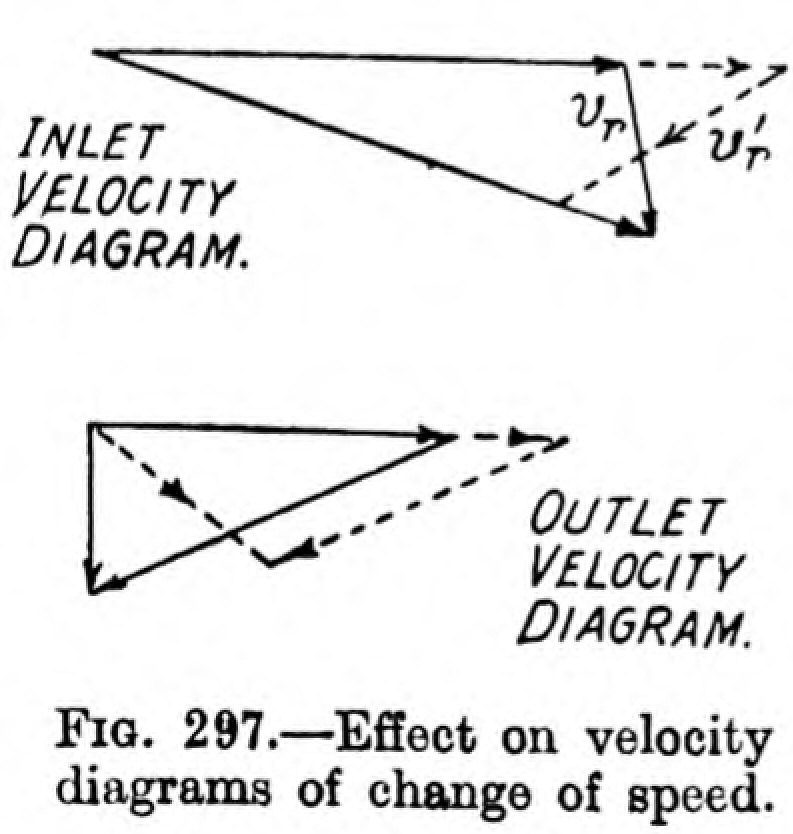

FIG. 297.—Effect on velocity diagrams of change of speed.

It remains to explain why the speed-discharge curve should droop in Figs. 294 and 296, and rise in Fig. 295. In the inward

flow turbine of low specific speed, the conditions in the runner have some resemblance to those in a forced vortex, and the resulting centrifugal head generated varies with the speed in the manner shown in Fig. 296. As this head opposes the external operating head on which the flow through the turbine depends, the discharge is bound to be less at high speeds when the centrifugal head is high than it is at low speeds when the centrifugal head is small. In turbines of high specific speed, however, the flow through the runner is so nearly axial that centrifugal head can have little effect on it.

274. Performance of Francis Turbines. (ii) *At variable gate opening.* When the operating conditions are those described in § 259 (ii), the head and speed remaining *constant*,

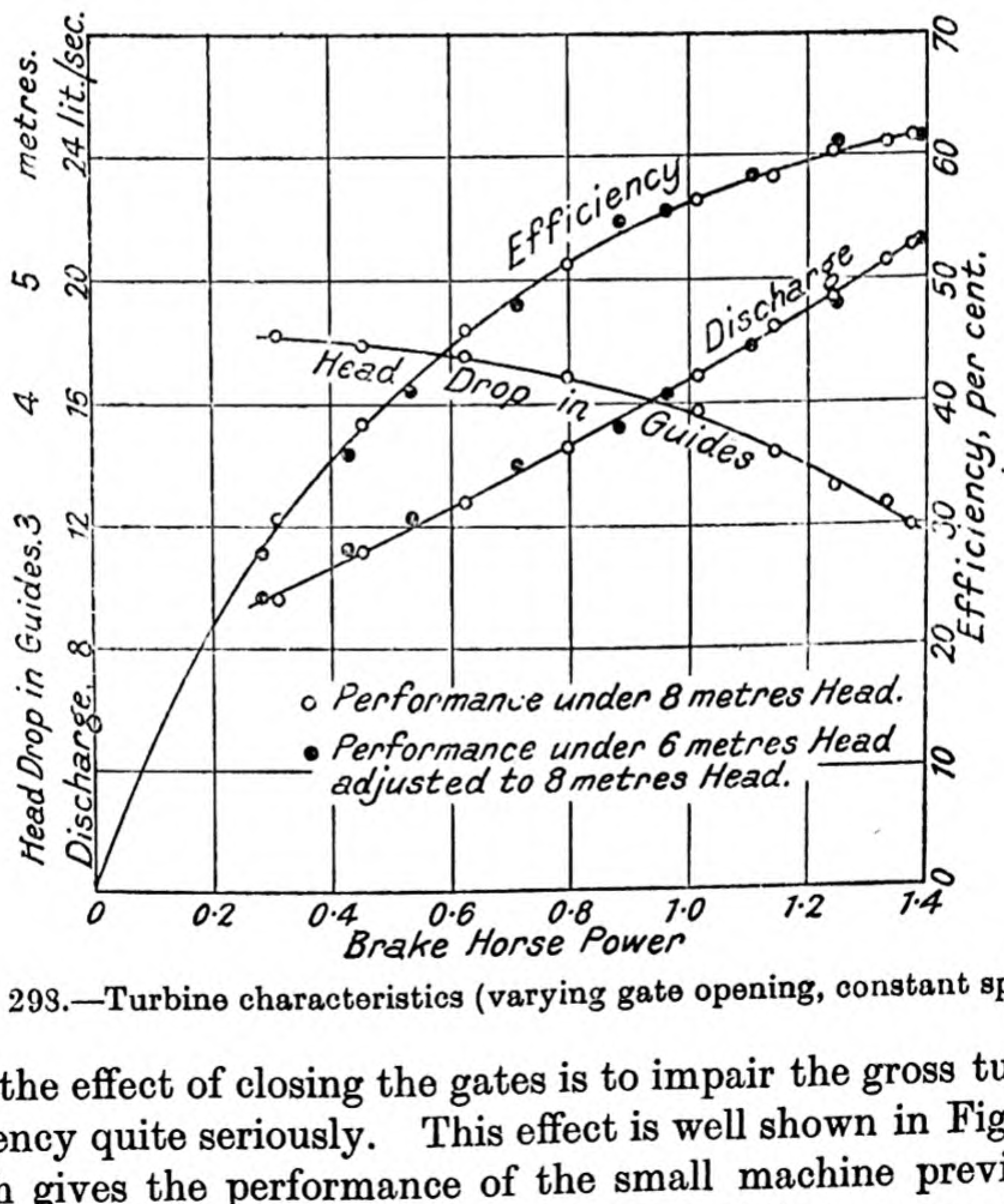

FIG. 298.—Turbine characteristics (varying gate opening, constant speed).

then the effect of closing the gates is to impair the gross turbine efficiency quite seriously. This effect is well shown in Fig. 298, which gives the performance of the small machine previously mentioned in § 272; here also there is satisfactory agreement between the points for 6 metres head and those for 8 metres head. Included in the diagram is the curve showing the head

drop in the turbine guide passages; it gives a clue to the fall in efficiency as the output is reduced under the control of the gates. The upward trend of this curve implies that the absolute outlet velocity from the guides, U, increases as the gates are closed. On the other hand, since the area of the *runner* passages remains unchanged while the flow through them declines, the relative velocity through these passages diminishes as the turbine output is reduced. Manifestly, therefore, the designed velocities can no longer be maintained. Again, there must be a distortion of the velocity diagrams; it is suggested in Fig. 299, and it is the consequent increase in eddy losses which is the predominant cause of the droop of the efficiency curve, Fig. 298.

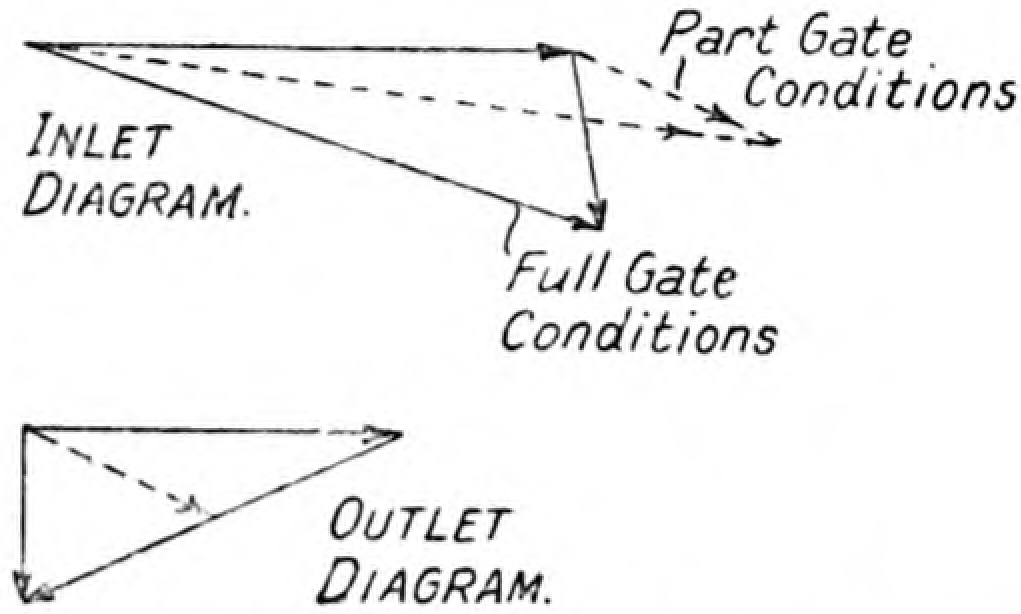

FIG. 299.—Effect on velocity diagrams of gate regulation.

Although in full-size Francis turbines developing considerable outputs, the efficiency curve under conditions of varying gate-opening are less unfavourable than Fig. 298 suggests, yet the part-load efficiency figures may weigh heavily against this type of turbine. This may be seen from the comparative curves (II) and (III) in Fig. 303.

275. Other Francis Turbine Characteristics. Low-head turbines are often required to work under conditions of *constant* speed and *varying* head (§ 259 (iii)). The performance of a Francis turbine in such circumstances, at full gate-opening, is represented by the solid-line graphs in Fig. 300; these relate to the machine of $N_s = 390$ (metric) whose performance under varying speed was illustrated in Fig. 295. It will be noticed that so long as the head does not vary by more than 20 per cent. above or below the mean, the gross efficiency is not seriously impaired. For comparison, the corresponding head-output curve broken line for the small turbine of $N_s = 70$ (metric) (Fig. 294) is added to demonstrate that a turbine of low specific speed is more susceptible to changes of head than one of high specific speed.

To record the performance of a turbine under all conditions of speed and gate setting—which none of the graphs so far

presented have done—we need to plot curves of the type of Fig. 301. These refer to a turbine of specific speed 101 (foot) or 450 (metric), operating under a net head of 4·10 metres at a normal speed of 105 r.p.m.; they show that although the turbine gives its maximum *output* at full gate opening, its maximum *efficiency* occurs at about 0·8 gate opening. The fractions indicating gate opening are to be taken as nominal values relating to the position of the gate operating mechanism, rather than to the actual effective area between the gates.

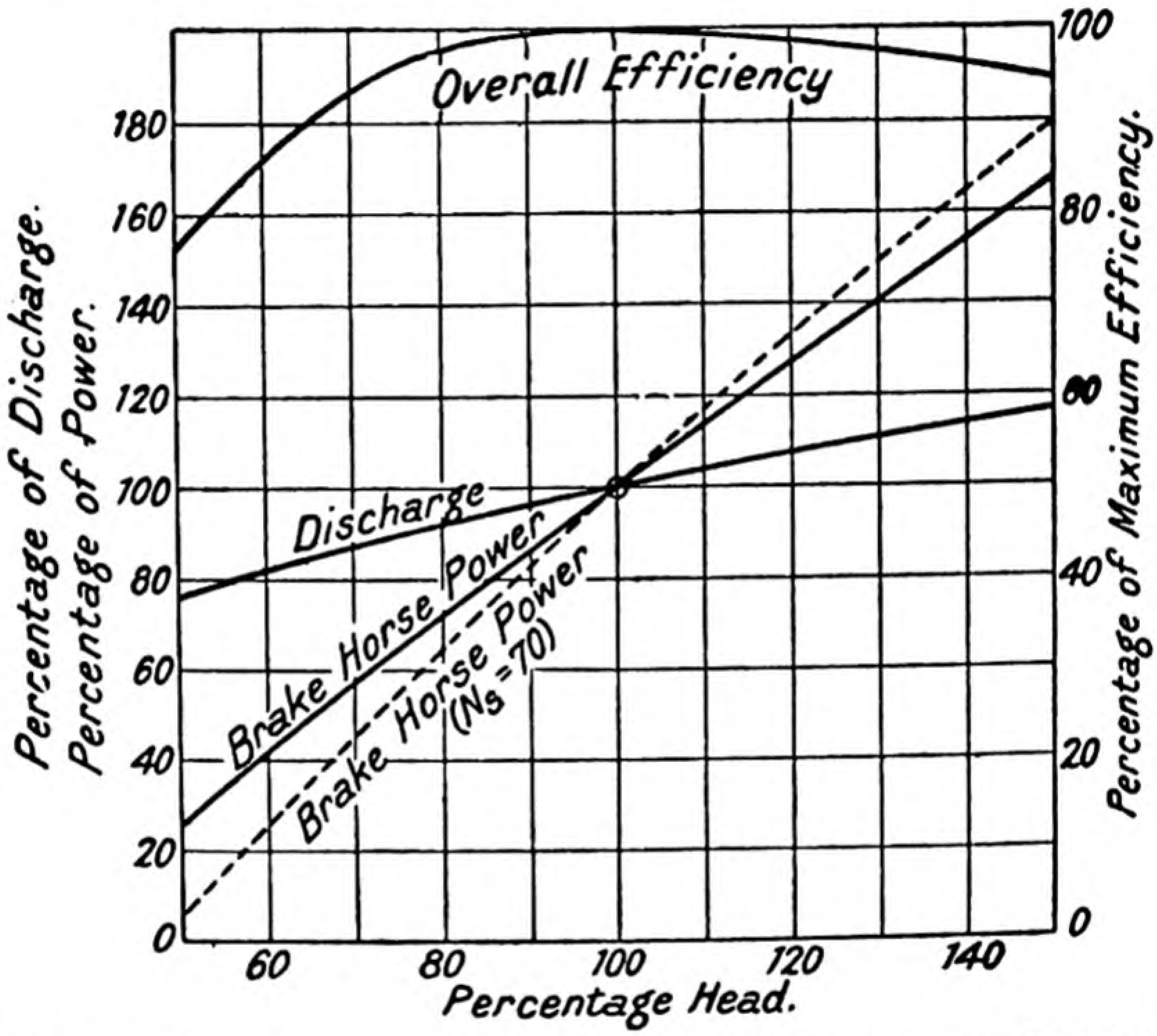

FIG. 300.—Turbine characteristics under varying head and full gate-opening ($N_s = 390$).

By suitably choosing the value of N or of $N/\sqrt{H}$, we can control to some extent the shape of the output-efficiency curve at constant speed. Suppose, for example, the speed of the turbine is to be maintained at 105 r.p.m. under all conditions; then by transferring values of output and efficiency at this speed from Fig. 301 to a new set of co-ordinates, the output efficiency curve for 4·10 m. head, shown by the full line in Fig. 302, is derived. If now the head rises from 4·10 m. to 6·10 m., the value of $N/\sqrt{H}$ falls from 52 to 42·5; we therefore take values along the appropriate vertical in Fig. 301, multiply the outputs by $6{\cdot}10^{\frac{3}{2}}/4{\cdot}10^{\frac{3}{2}}$, and so obtain the broken

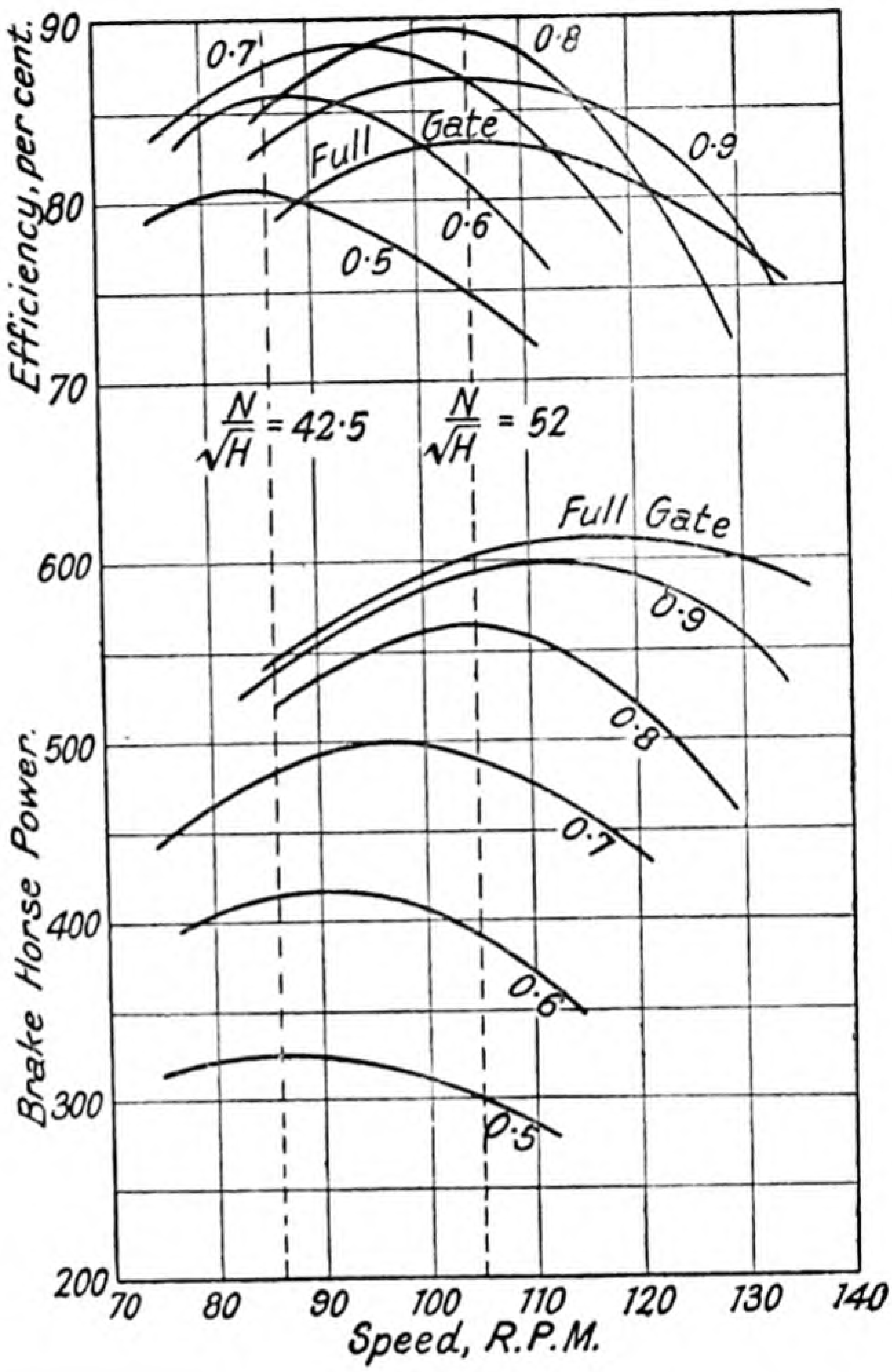

FIG. 301.—Complete turbine characteristics ($N_s = 450$).

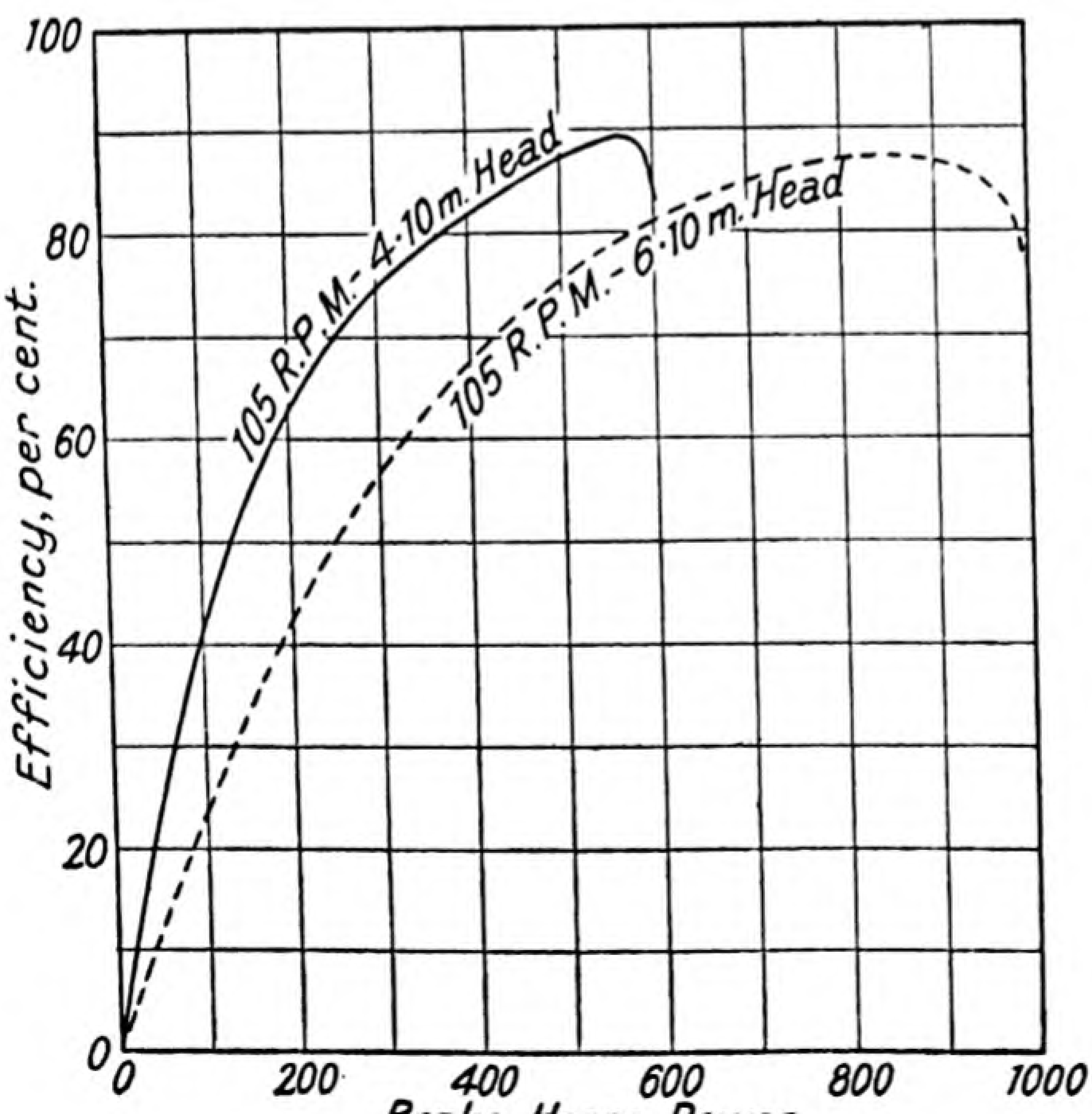

FIG. 302.—Derived characteristics (constant speed).

curve in Fig. 302. It is apparent that the constant value of $N=105$ r.p.m. has been well chosen to give the best compromise between highest possible efficiency at large gate openings at the 4·10 m. head, and high efficiency at part gate openings at the high head of 6·10. m.; for quite probably the limiting output required under any head will be 570 h.p.

276. Comparative Performance of Propeller Turbines. The characteristics of Kaplan and propeller turbines working at *constant speed* under *constant head*, at *varying gate openings*,

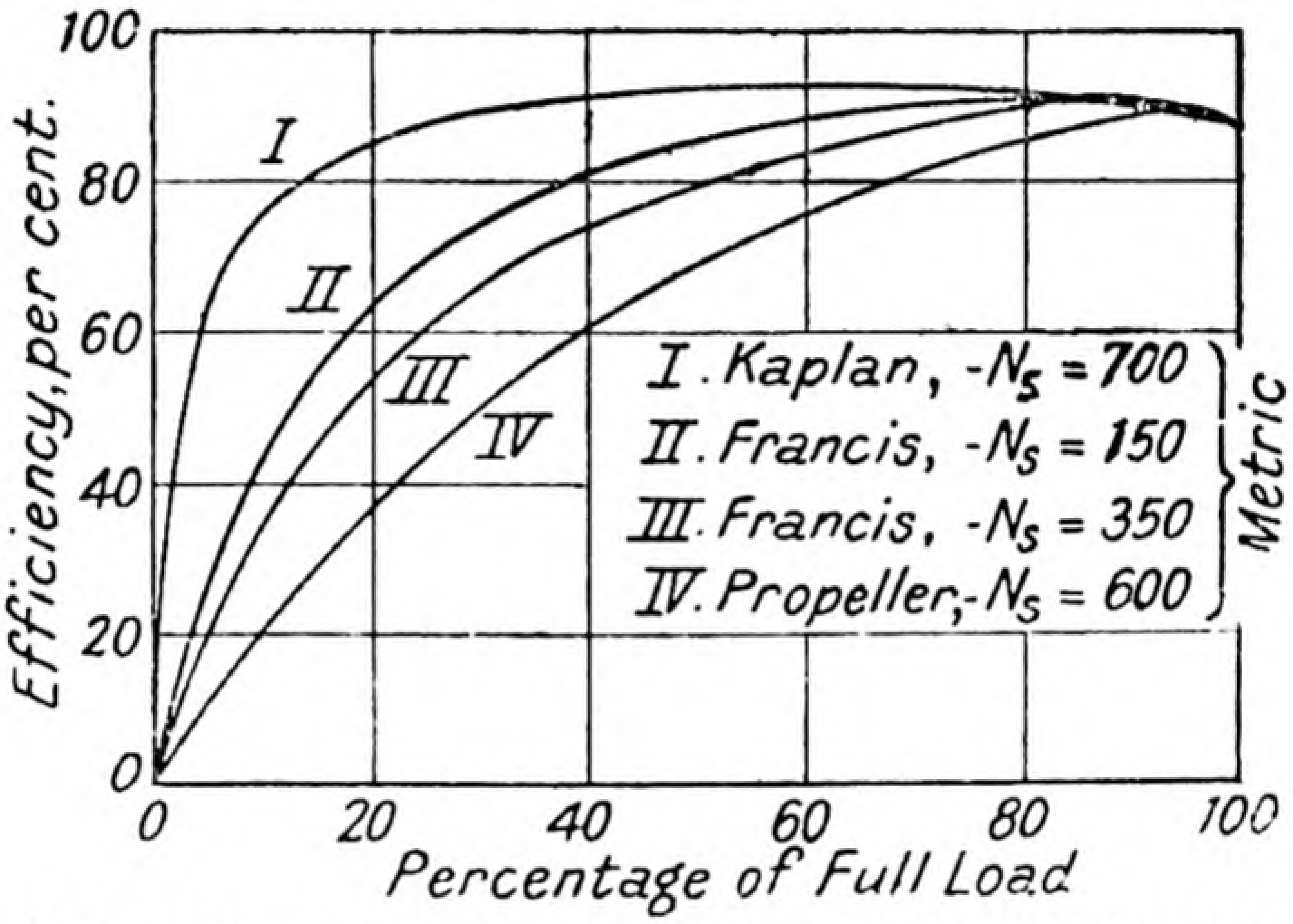

FIG. 303.—Constant-speed characteristics compared.

are represented by the curves I and IV in Fig. 303, where they may be contrasted with the corresponding curves II and III for Francis turbines. The superiority of the curve I for the Kaplan turbine, which rivals or even excels the best

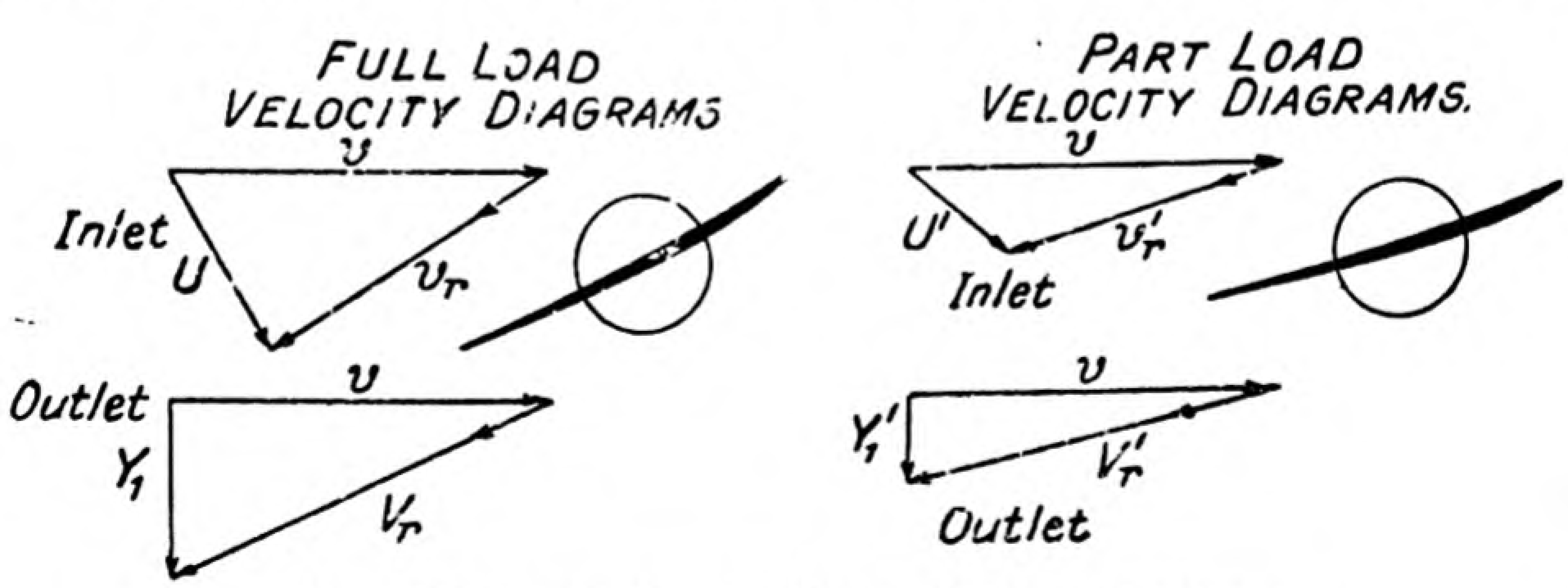

FIG. 304.—Kaplan turbine velocity diagrams.

performance of the Pelton wheel (Fig. 290 (I)), as regards sustained high efficiency even at small gate openings, may be explained with the help of Fig. 304. Here are shown inlet

and outlet velocity diagrams for a Kaplan runner working under the specified conditions at full load and at part load. Although the corresponding change in the flow through the turbine does affect the shape of the diagrams, yet as the blade angles themselves are simultaneously adjusted, the losses inevitable in a Francis turbine at part loads (§ 274) are now very largely avoided.

On the other hand, the propeller turbine at part load suffers losses due to eddying and to velocity energy rejected that are even more serious than in the Francis turbine, as is shown clearly in Fig. 303 (IV). It is thus essentially a machine for working continuously at full load. (**Example 139.**)

Performance under variable head. Under the conditions so often encountered of variable head at constant speed, the axial-flow turbine shows to particular advantage: the curve between percentage head and gross efficiency is even flatter than the one for the Francis turbine plotted in Fig. 300. Throughout a range of head of 3 to 1, the full-load gross efficiency may never fall more than 5 per cent. below its maximum value. The reason for this is linked with the exceptionally high runaway speed of the propeller turbine, which may rise to 300 per cent. of the normal working speed.

277. Parallel Operation of Turbines. The great disparity between the part-load performances of various types of machine plotted in Fig. 303 applies to single units only, and not necessarily to complete power plants. If, for instance, a

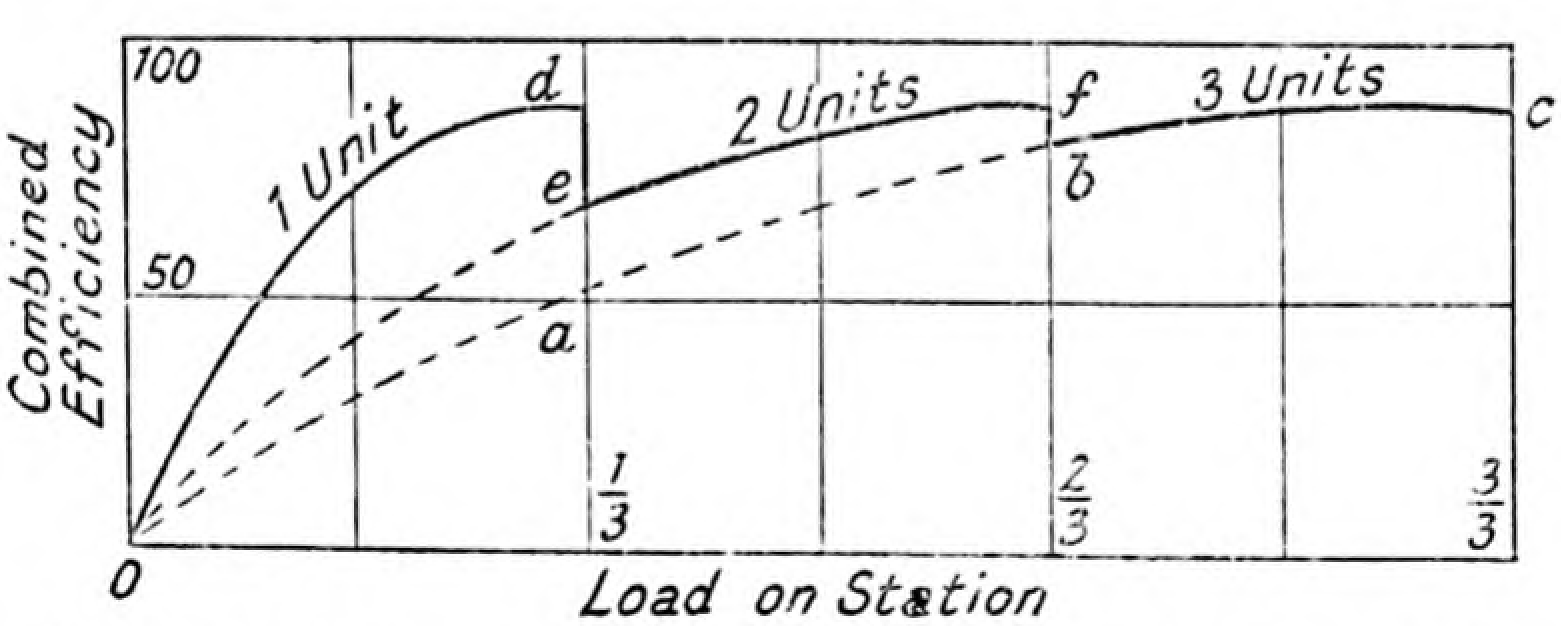

FIG. 305.—Performance of three propeller turbines in parallel.

power-house contains three propeller turbines whose individual behaviour is represented by Fig. 303 (IV), it is not to be supposed that the total station output will be regulated by closing the three sets of gates equally, so that the load is always shared

equally among the three units. This would result in the combined efficiency curve *Oabc*, Fig. 305, which is no more satisfactory than the original curve (IV). Instead, let one unit only be at work until the station output reaches one-third of its peak; with rising output this unit would quickly reach its maximum efficiency of nearly 90 per cent. at point *d*. A second turbine would be put on load as soon as the first had reached its limit, while the third would only be needed at two-thirds of the total output. The combined efficiency curve *Odefbc* is not much inferior to the curve (I), Fig. 303, relating to a Kaplan turbine. The changes in demand usually arrive at an actual station in too irregular and unpredictable a fashion for the formal curve *Odefbc* to be in fact realised, but the curve does give a good impression of the advantages of well-directed parallel operation.

Still better results could be obtained if one of the three units had variable-pitch runner-blades (Kaplan type); it could then always take charge of the variable part of the total load, leaving the non-adjustable propeller turbines to run only at their own full load.

278. Turbine Performance under Conditions of Geometrical and Dynamical Similarity. Having regard to the importance of comparative tests on scale models as a means of predicting the efficiency of turbines and of arriving at the best shape to give the blades and draft tube,[177] it is now necessary to examine more closely the assumptions made in §§ 261, 262, viz.: that homologous or geometrically similar turbines running under identical conditions of ϕ, ψ, and gate opening will have identical efficiencies. Of the total energy H that disappears as the water flows through the turbine, the greater part Vv/g is transferred to the runner, a small proportion $Y_1^2/2g$ is lost in the tail-race, and an amount h_L is wasted in friction and eddy losses in the guide and wheel passages (§ 235).

The condition that efficiency remains unaltered under change of head and change of scale is manifestly that the ratio h_L/H remains unaltered; and since it is already stipulated that all velocities must vary as $\sqrt{H}$, then the ratio $h_L\Big/\dfrac{v_r^2}{2g}$ cannot be allowed to vary. On this question the laws of dynamical similarity give clear guidance (§ 93). Regarding the runner

blade passages as geometrically-similar closed conduits in which h_L is the representative energy loss and v_r is the representative velocity, we observe from § 95 that the condition to be fulfilled can be expressed thus :—

$$\frac{h_L}{H_L} = \left(\frac{D}{d}\right)^2,$$

where the energy loss h_L and the diameter d refer to a small turbine and H_L and D refer to a large one.

The conclusion we are led to, then, is this : that under ideal conditions, in which the passages are perfectly smooth, the hydraulic efficiency $\frac{Vv}{gH}$ of a model turbine will only have the same value as that of the full scale machine if the respective heads under which they work are inversely proportional to the square of their linear dimensions. A model 1/5 the scale of the actual turbine would therefore have to work under a head twenty-five times as great.

279. Scale Effect. It is usually quite impracticable to test model turbines under the enormous heads that the foregoing analysis would dictate. Instead of attempting to do so, we use some convenient lower head and we correct the test results for the " scale effect " that is now inevitable, § 95. By observations of the head, speed, discharge, and output of the model, its gross efficiency is directly computed ; a suitable correction factor is then applied to the model efficiency, and the resulting figure should then represent the gross efficiency of the full-scale or prototype turbine. If the correction factor could be estimated with a sufficient degree of reliability, it would thereby become feasible to dispense with the costly trials or acceptance tests on the completed prototype carried out on the site, which would otherwise be essential.[178]

In establishing this highly important correlation between " model " efficiency η_m and " prototype " efficiency η_M, some of the factors involved are : (i) because dynamical similarity must now be abandoned, § 278 above, the relative hydraulic losses in the prototype should be less in the prototype machine than in the model (see Example 135) ; (ii) in regard to surface friction, although it is hardly likely that the blades of the prototype turbine could be regarded as hydraulically smooth,

yet it may not be easy to say how their relative roughness compares with that of the model blades; (iii) since gross efficiencies are now in question, the total energy losses and not merely the hydraulic losses must be taken into account, viz. those specified in § 221 and mentioned in § 235. When these are analysed, it will appear that they are relatively more serious in the model than in the prototype.

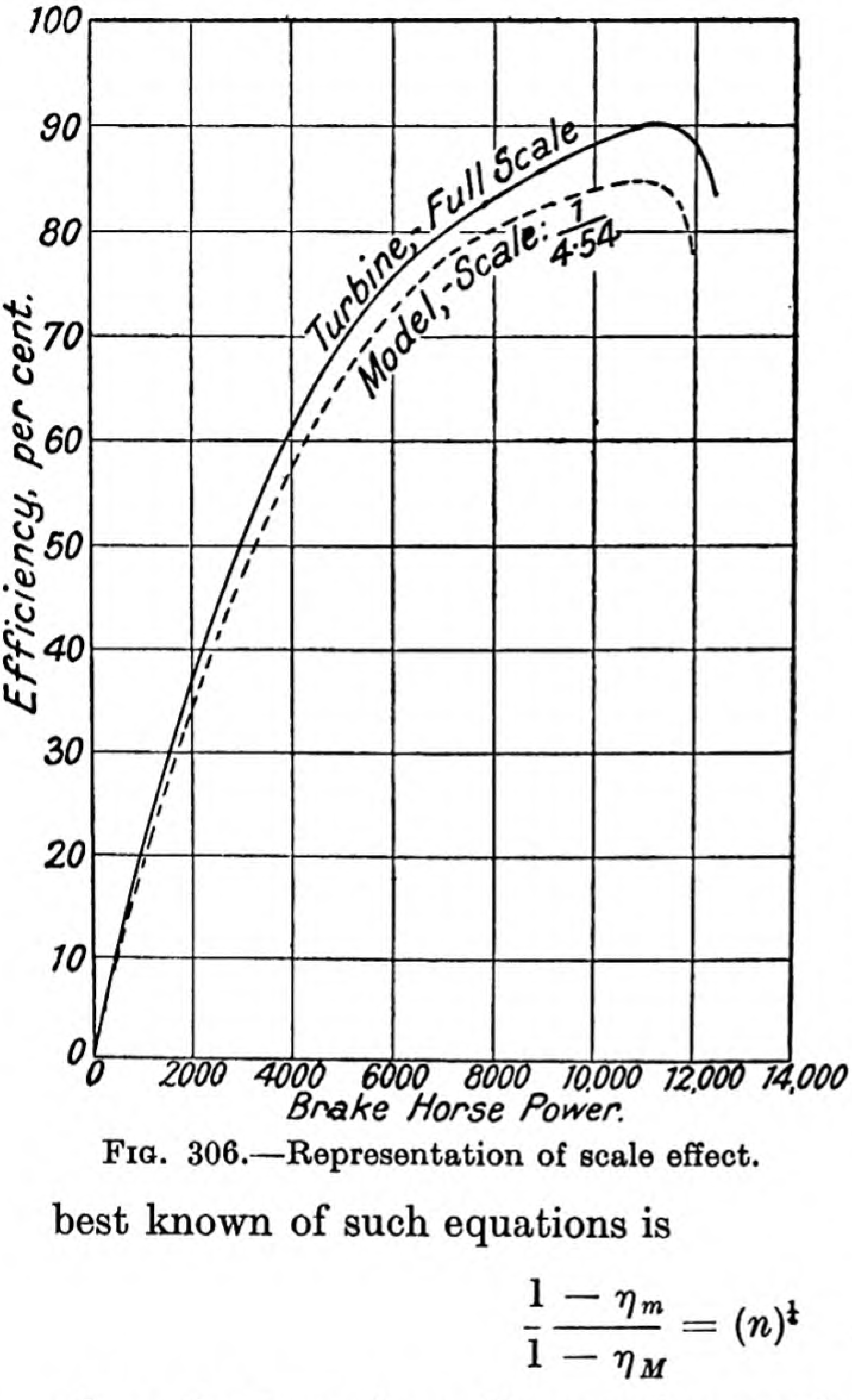

FIG. 306.—Representation of scale effect.

Complex though these inter-relations may appear,[179] yet experience has shown that their cumulative effect can be represented by a simple equation. One of the best known of such equations is

$$\frac{1-\eta_m}{1-\eta_M} = (n)^{\frac{1}{4}} \quad . \quad . \quad . \quad (14\text{-}9)$$

where the terms have the meaning previously assigned, viz. :—

η_m = measured gross efficiency of model turbine,

η_M = estimated gross efficiency of prototype turbine,

$$n = \text{scale ratio} = \frac{(\text{diameter of prototype-runner})}{(\text{diameter of model runner})}.$$

Formula 14-9 above, usually associated with the name of Dr. L. F. Moody, may be applied by way of example to the conditions shown in Fig. 306. Here are plotted on a comparative basis the measured gross efficiencies of a full-scale Francis turbine and

of a model to a scale of 1/(4·54), the operating conditions being those of § 259 (ii). The relation between the maximum model efficiency, 0·85, and the maximum prototype efficiency, 0·90, agrees very well with the relation as computed by the Moody formula. **(Example 135.)**

A note at the end of § 261 referred to the slight drop in efficiency observed when a turbine changes from its normal working head to unit head. This is a consequence of the change in the ratio $\dfrac{\text{friction loss } h_f}{\text{operating head}}$ as the water velocity falls in sympathy with the change from head H to head 1. However, it is apparent from §§ 154 and 157 that for rough surfaces, such as those presented by turbine blades after prolonged use, the coefficient f is only affected to a very small degree by changes of velocity; that is to say, the value of the exponent n in the relationship $h_f = K\ (\text{velocity})^n$ is nearly 2. Thus unless the change in head is very great, the variation in *hydraulic* efficiency is not serious. But in regard to *gross* efficiency, this is likely to decline perceptibly as the head or the output diminish.

The possibility of eliminating or reducing scale effect by using in the two systems fluids of different kinematic viscosity (end of § 95) has been successfully applied in the testing of scale models of turbines. Instead of driving the model by water, the makers drive it by *compressed air*. The kinematic viscosity of this fluid can be varied at will by altering the pressure, hence if a suitable pressure is chosen the model will simulate almost exactly the performance of its full-scale prototype. This result is attained the more easily because in air the model can be run at much higher speeds than in water. By the use of this technique the cost of carrying through a series of tests is materially reduced.

280. Pressure Distribution on Turbine Blades. Nearly at the end of two chapters wholly devoted to turbines, an enquirer might complain that nowhere has he yet found a straightforward answer to the question: "What makes the turbine go round?" Mistrustful of such concepts as energy transfer and the like, he wants to form a clear visual image of the water pushing the wheel round just as a sailor pushing on a capstan bar makes the capstan turn. In regard to impulse turbines there is not much more that can be said; the thrust exerted by the jet on the bucket is a very real thing, as anyone who has watched a fire-hose at work can testify. A method has been outlined, too, for evaluating the tangential thrust on

the blades of a propeller turbine, § 248. A more indirect approach to the problem is necessary when Francis runners are concerned: it was discussed in § 146, and depended upon the effect of tangential acceleration upon the liquid elements. Still another method of estimating the differential pressure

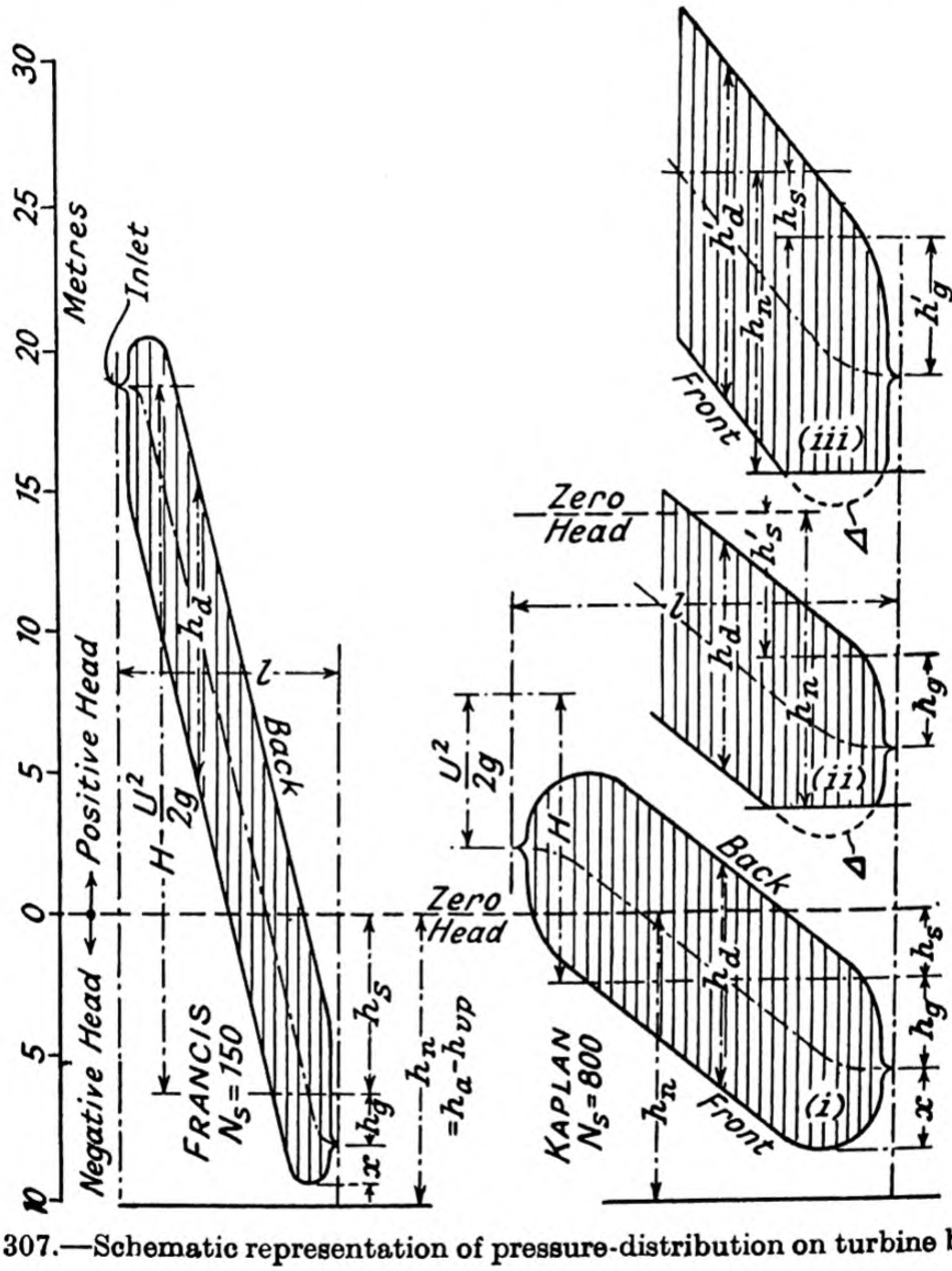

FIG. 307.—Schematic representation of pressure-distribution on turbine blades.

across a blade is this: knowing the speed and output of the runner, the torque exerted on each blade can be calculated. Then, from the projected area of the blade (projected on a plane passing through the axis, as in Figs. 282 and 284), the average differential pressure per unit area may be found. To be sure the precise manner in which the pressure is distributed will not be easy to establish, but for general purposes of

comparison we may assume it to be as shown diagrammatically in Fig. 307, the pressure difference being generally uniform but tapering off to zero at the blade tips.[180]

By the method just outlined, the diagrams have been calculated from the following data :—

	Francis.	Kaplan.
Power P . .	1000 h.p.	1000 h.p.
Specific speed N_s (metric) .	150	800
Net head H . .	50 m.	10 m.
Speed N . .	633 r.p.m.	450 r.p.m.
Number of blades .	16	5
Suction head h_s .	6·3 metres	2·3 m.

(The Francis runner is the one shown at II(a), Fig. 282.)

It is instructive to regard these pressure-diagrams as corrected forms of the hydraulic gradient plotted in Fig. 235, § 234. Evidently that elementary representation was a mean curve only, and the corresponding mean curve is still to be seen in Fig. 307. But now we have in addition the differential head h_d (§ 146). A further correction to be made to Fig. 235 must take into effect the suction head on the turbine; that is, the pressure-heads must be modified in conformity with Fig. 241, § 241. This correction has duly been carried out in the final diagrams, Fig. 307. Here the line of zero head corresponds to tail-race level: positive heads are measured above this datum, and negative heads below it.

281. Limiting Suction Head on Turbines. The areas of the pressure-distribution diagrams that most repay scrutiny are those which represent negative heads. In particular, we must verify that at no point does the computed negative head exceed the permissible limiting value $h_n = h_a - h_{vp}$ (§ 16). What is this maximum computed negative head? It is the sum of (i) the static suction head h_s on the turbine, viz. the vertical distance of the turbine above the tail-race level, (ii) the head regain in the draft tube h_g (§ 241), (iii) the depression head x, i.e. the amount by which the maximum negative head prevailing anywhere on the blade surface exceeds the negative head at the entrance to the draft tube.[181] Evidently this amount

will be related to the shape of the pressure-distribution diagrams, Fig. 307. These particular diagrams—at least for the Francis turbine and the Kaplan turbine (i)—show that safe limits have not been overstepped: the sum $h_s + h_g + x$ is less than the limit $h_n = h_a - h_{vp}$, where h_a and h_{vp} are the heads corresponding to atmospheric pressure and vapour pressure respectively.

Now let us see what happens if we gradually raise the Kaplan turbine to position (ii), the suction head increasing from $h_s = 2{\cdot}3$ m. to $h^1{}_s = 5$ m. This has the effect of lowering the pressure-distribution diagram, thus bringing part of it—the part shown by the broken line—into forbidden territory. Since there cannot be a negative head greater than the limiting one, the effective result is that part of the diagram is cut off; the total thrust on the turbine blades diminishes, so that although the speed, net head, and gate opening have *in no way altered*, yet the output has begun to decline.

The same kind of deterioration may follow an attempt to increase the net head on the turbine, while maintaining the original suction head $h_s = 2{\cdot}3$ m. In Fig. 307 (iii) the conditions are $H = 14$ m. instead of 10 m.; and remembering that the speed must increase as the square root of the head, §§ 261, 262, we deduce that the differential blade pressure must vary *directly* as the net head. Thus the value of h'_d in diagram (iii) s 1·4 times the value h_d under the original net head of 10 m. The corresponding distension of the pressure diagram has again brought part of it over the limiting-head boundary, showing that the actual performance of the turbine would fall short of expectations.

282. Effects of Cavitation on Turbine Performance. Comparison of the conditions represented in Fig. 307 (ii) and (iii) with those shown in Fig. 121 (ii), § 135, should lead us to expect similar consequences. In both instances there is a stream of water flowing rapidly over metallic surfaces in such a manner that the local absolute pressure is identical with the vapour pressure of the water. The resulting *cavitation* that occurs in the turbine not only impairs the turbine performance, but it may damage the machine itself.[182] There may be severe rattling and vibration; the threatened areas of the blade surfaces, near the tail-race or downstream edge of the front or

leading face, may become roughened, pitted, and eventually destroyed (Fig. 408). Such danger zones are indicated in Fig. 307 by the symbol Δ.

Although the method illustrated in Fig. 307 is based on the correct principles for establishing the safe limiting suction head, yet a more rapid solution is required in practice. It is provided by the use of the *Thoma cavitation factor* σ, which gives the necessary empirical relationship between the barometric head, the net head and the suction head on the turbine, thus :—

$$\sigma = \frac{h_a - h_s}{H}$$

(It is instructive to compare the cavitation *factor* with the cavitation number, § 135.) In general the turbine will be immune from cavitation if the value of the cavitation factor σ is not *less* than the minimum given in the following table :—

	Francis.			Propeller.		
Specific speed (metric)	100	250	400	400	600	800
Specific speed (foot) .	23	56	90	100	135	180
Minimum value of σ .	0·04	0·18	0·42	0·50	0·75	1·2

A graphical interpretation of the Thoma formula is offered in Fig. 308, which relates to the two machines described in § 280; this diagram uses the convention of Fig. 241 to present

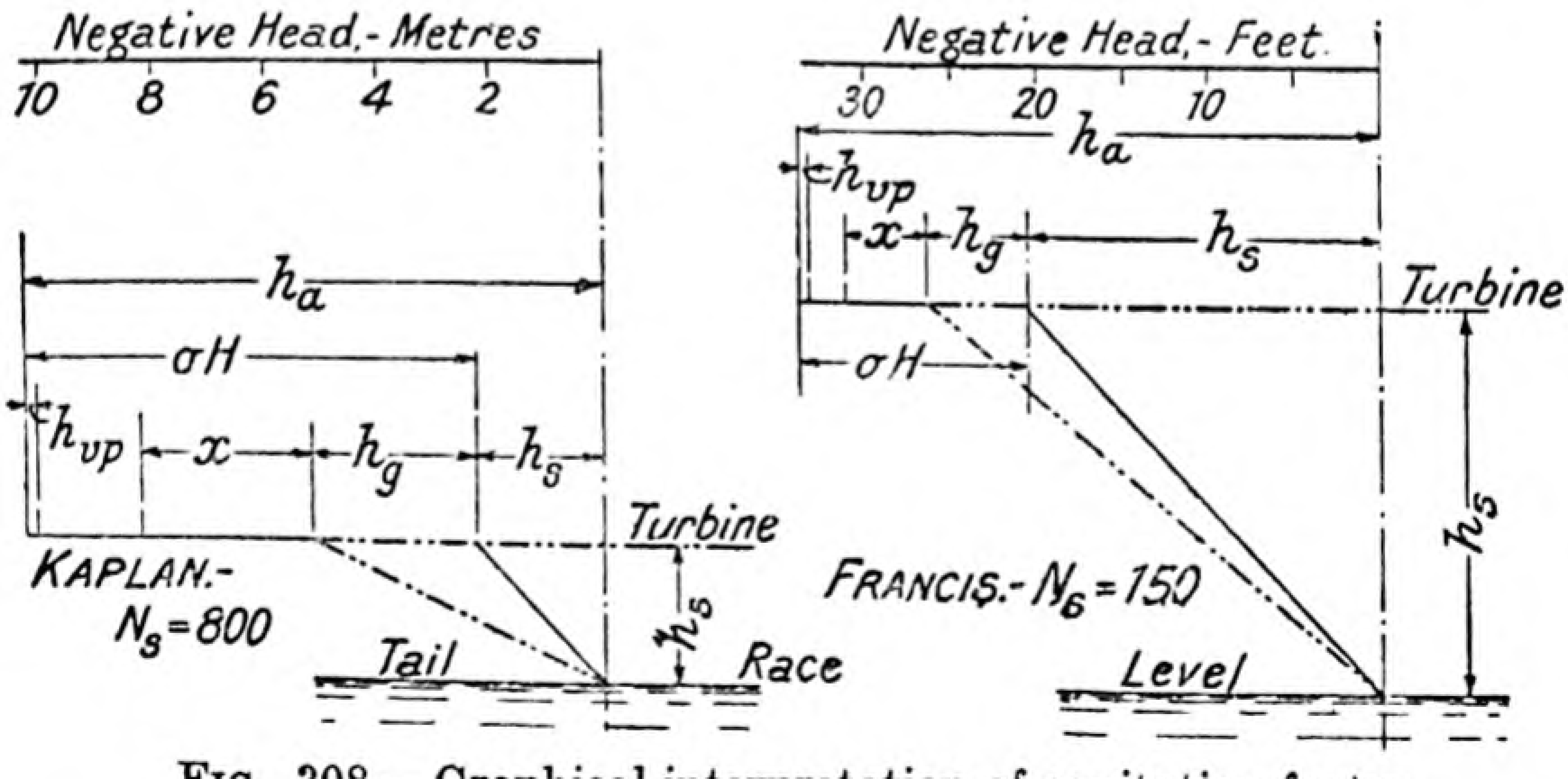

FIG. 308.—Graphical interpretation of cavitation factor.

some of the information already given in Fig. 307. It shows how either of the changes examined in § 281 will have the effect of lowering the cavitation factor below the safe limit. In

general terms the matter can be summarised thus: (i) Considering a turbine of given output P working under a given total head H, then as the specific speed increases (say by modifying the blade shape, etc.), the suction head h_s must be *reduced*—the turbine must be *lowered*. (ii) If a given turbine running at a given specific speed is set to work under an increased total head H, then here also the turbine must be lowered, i.e. the greater the total head, the less the suction head.

A method of experimentally revealing the onset of cavitation is to run a model turbine under steady conditions of speed, gate-opening, and net head, but with gradually increasing suction head h_s. If the measured output is plotted against values of σ as derived from the Thoma formula, the point at which the power begins to decline is quite sharply defined, as in Fig. 309. The bend or point of inflection in the graph is often spoken of as the *sigma-break*.

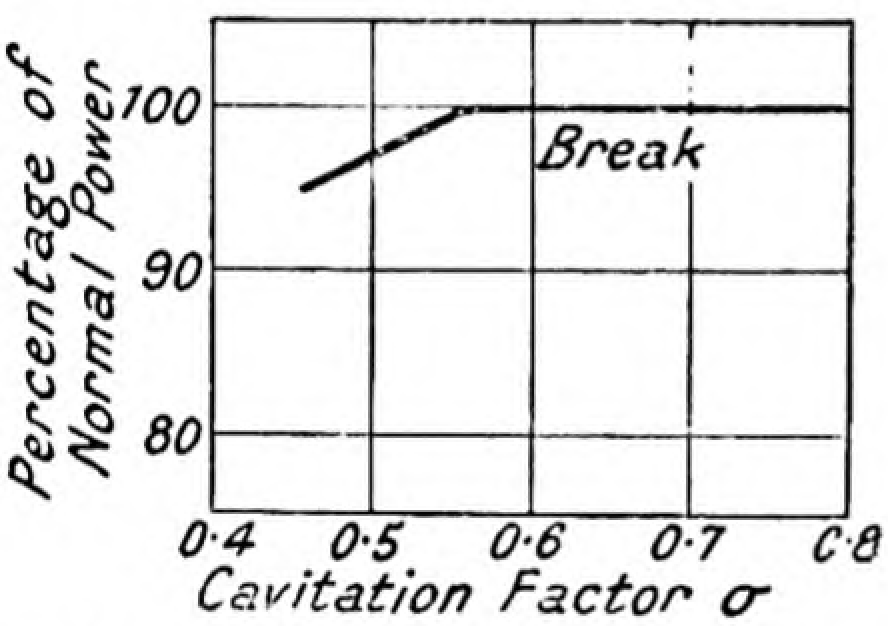

FIG. 309.—The "sigma-break."

Manifestly the surest way of preventing cavitation is to set the turbine sufficiently near the tail-race level. If for constructional reasons it becomes necessary to work at a higher suction head than would otherwise be desired, then the runner blades may be guarded against the effects of incipient cavitation by choosing specially resistant metal. Stainless steel, nickel steel, and bronze have given satisfaction; or stainless steel armouring may be welded on to the areas most subject to attack.

Pelton wheels are not immune from cavitation, although here the underlying causes are analogous to those explained in § 135. The nozzles, needles, and buckets are all liable to attack. Only experienced design and experienced choice of material will offer reasonable security against damage.

283. Final Choice of Turbine. When choosing turbines for a given duty the machines cannot be studied as isolated units. Among the various civil, mechanical and electrical engineering works that unite to form a complete water-power development (§§ 251, 252), the turbines may form a relatively

small item, whose cost might not amount to more than 10 per cent. of the total outlay.[183] They are servants, not masters. Consequently a reasonable amount of compromise is usually necessary before final details can be established. But the general rule is a simple one: the turbine having the highest permissible *specific speed* will not only be cheapest in itself, but its relatively small size and high rotational speed will ensure that the least expensive generator can be coupled to it and the least expensive building will house it. The runners, all of the same output, drawn on a comparative basis in Fig. 285, provide a graphic impression of the link between high specific speed and small dimensions. Naturally the rule is subject to limitations; one cannot raise the specific speed indefinitely. These limitations, and other factors influencing the choice of power unit, may be classified thus:—

Mechanical. The limits which practical experience has set have already been presented in Fig. 286. Considerations of blade pressure (§§ 280, 282) usually restrict the use of propeller turbines to heads below 100 feet, while considerations of mechanical strength of the spiral casing define the range of permissible heads for Francis turbines. The internal hydrostatic pressure will be excessive for a concrete casing if the head exceeds 100 feet, for a steel-plate casing if the heads exceeds perhaps 300 feet; while the absolute limit of 1000 feet head is set by the maximum attainable strength of a cast-steel casing.

Electrical. One restriction under this heading is obvious enough: the speed of a direct-coupled turbine must adapt itself to the nearest synchronous speed of the generator. Yet if desired the generator speed need not be tied to the turbine speed, at least for small low-head units. A geared hydro-electric set has already been illustrated in Fig. 248. Since step-up spur or bevel gears with efficiencies of 97 per cent. are now available, they may profitably be interposed between cased turbines of several hundred horse-power and high-speed standard generators.

Electric control methods ensure the regularity of turbine operation in various ways. Power-houses with 15,000 h.p. installed turbine capacity may be run entirely unattended, the control being automatic or under the supervision of attendants at some distant point.[184]

Civil. In large low-head installations a troublesome problem is likely to be the excavation in the river bed of the space destined for the draft-tubes. The vertical distance a, Fig. 310, cannot be brought below a fixed limit without impairing the draft-tube efficiency, and therefore the plant efficiency; yet the suction head h_s is subject to the limits set by the risk of cavitation—limits that can conveniently be expressed by the Thoma cavitation formula, § 282. If the turbine designer is prepared to make the necessary concessions, then the lower specific speed he accepts will certainly imply a rather larger and more expensive turbine, but the resulting smaller cavitation factor σ will permit the machine to be lifted higher above tail-race level. The civil engineer's exacting task in the river bed is correspondingly lightened, as Fig. 310 clearly demonstrates.

Character of load. The variability of the load may influence the choice of machine if the head lies between about 500 ft. and 1000 ft., or lies below 100 ft. For the higher range, Pelton or Francis turbines would do the duty equally well if they could always work at full load. But if the plant were destined for a traction load or conditions involving long periods of light loading, then the superior part-load efficiency of the Pelton wheel, § 271, might more than compensate for its higher first cost. Similarly the higher cost of the Kaplan turbine as compared with that of a propeller turbine is justified when light loads are predominant. The advantages in such conditions of installing in a single station the two types of machine were mentioned in § 277. The principle can be still further extended when a number of widely-separated stations feed into a common network, § 256; in the station selected as a base-load station the regulating-mechanism can be simplified because the turbines will invariably work with fully-open gates or nozzles.

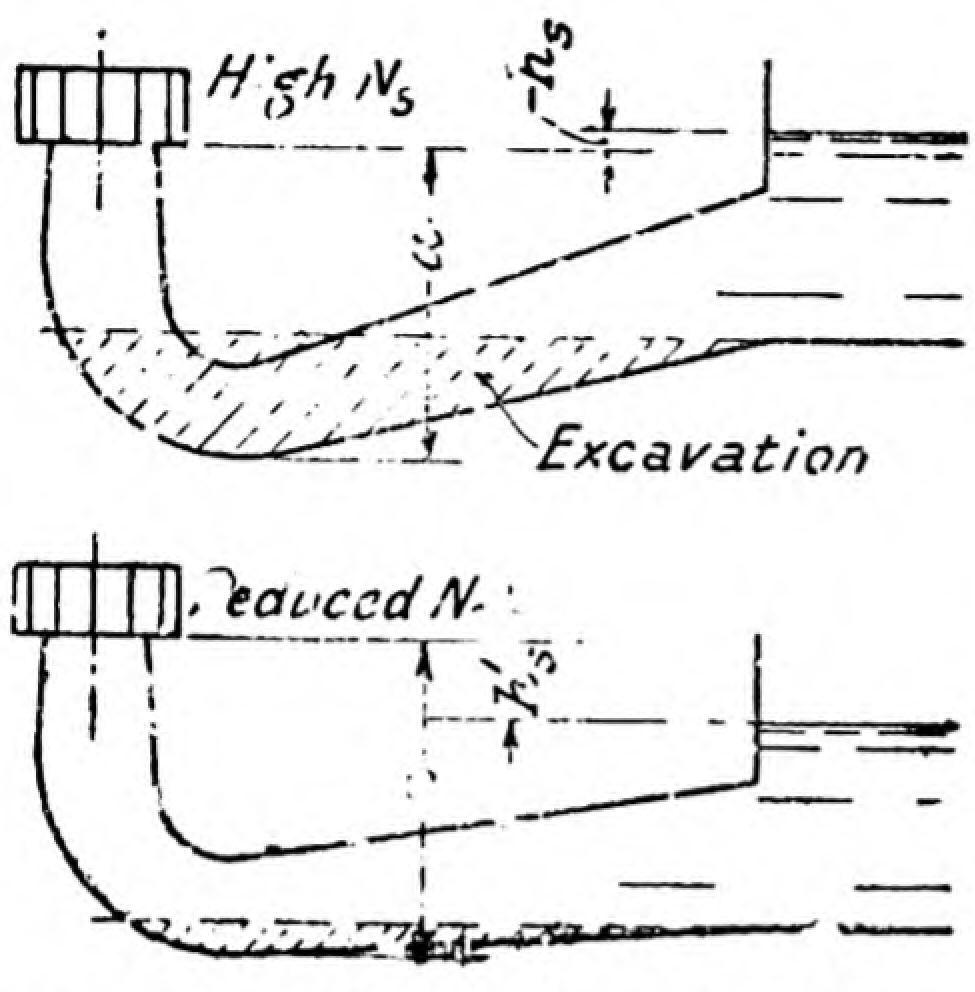

FIG. 310.—Effect of specific speed on turbine location.

The character of the load may also affect the setting of low-head units (Fig. 269). If the machines only run infrequently at full load, then on these rare occasions they may be allowed to work closer to the cavitation point than would otherwise be prudent.

Kind of water. In the 500-1000 ft. range adapted either to Pelton or Francis turbines, the presence of undue amounts of grit or sand in the water would rule out the Francis type. Its runner could not withstand the erosive action of the water. Even Pelton wheels could only be kept in service, under these difficult conditions, at the cost of periodical renewals or repairs of the needles, nozzles and buckets. It is for this reason that sand-excluding devices are sometimes installed in the turbine head-works, in the hope of keeping under control the deterioration of the turbine components.

CHAPTER XV

PUMPING MACHINERY: (I) POSITIVE PUMPS, WATER AND GAS-OPERATED DEVICES, ETC.

284. Pumps—Definition and Classification. The definition of a pump as a machine for lifting water is far too restricted for engineering purposes. Machines that are unquestionably pumps frequently do not lift liquids at all, or at any rate they do so only through an insignificant height. Such are boiler-feed pumps, forced-lubrication pumps, booster pumps, and pumps for hydraulic transmission systems. Moreover, the liquid to be pumped may not be water, but may be oil, spirit, milk, sludge, or indeed almost anything that can be made to move along a pipe.[185] A more appropriate definition would therefore be: a pump is a machine which, when interposed in a pipe, transfers energy from some external source to the liquid flowing through the pipe, § 218. That is the essential point: the *energy* of the liquid must be increased. Nearly always it is the pressure energy that is increased; but whether or not this energy is subsequently converted into potential energy—whether the liquid is actually lifted to a higher level—in no way concerns the pump.

Pumping apparatus [186] usually falls into the class of either

(i) Positive-displacement pumps, or of

(ii) Dynamic-pressure or rotodynamic pumps (Chapters XVI, XVII).

Positive pumps invariably embody one or more chambers which are alternately filled with the liquid to be pumped and then emptied again; their rate of discharge consequently depends almost wholly on the speed of rotation and hardly at all upon the working pressure.[187] These positive-displacement machines may be subdivided into

(*a*) Reciprocating pumps, and

(*b*) Rotary pumps.

Besides dealing with positive pumps, the present chapter also describes water-raising devices such as the hydraulic ram and the pneumatic ejector which are not ordinarily classed as pumps.

Comparative comments on various types of pump will be found in §§ 349, 350.

285. Efficiency of Pumping Machinery. In developing expressions for the performance of pumping and water-lifting appliances, the general treatment of § 220 may be expanded thus:—

$$\eta_m = \text{Gross or overall efficiency of pump} = \frac{\text{hydraulic energy output}}{\text{mechanical energy input}}$$

$$= \frac{\text{“ water horse-power ”}}{\text{shaft horse-power}} = \frac{\text{W.H.P.}}{\text{S.H.P.}} = \frac{\dfrac{Wh}{K_p}}{\text{S.H.P.}}.$$

(Note that this expression is the *inverse* of the corresponding one for turbine efficiency.)

Now the term h is defined as the total energy, per unit weight of liquid, received by the liquid in passing through the pump. If, therefore, the pump is used for forcing liquid through a piping system, as in Fig. 150, § 167, the *effective* energy—which we may here denote by h_m—will be greater than the dead or static lift h.

If h_v = velocity energy of liquid leaving delivery pipe,
h_{fs} = friction and secondary energy losses in suction pipe,
h_{fd} = friction and secondary energy losses in delivery pipe,
p = pressure-difference maintained between inlet and outlet of pump,
W = weight of liquid pumped per second,
q = volume pumped per second,

then $h_m = h + h_{fs} + h_{fd} + h_v = p/w$. (But see also § 325.)

The *hydraulic energy output* (*W.H.P.*) will therefore be represented by :—

$$\frac{Wh_m}{550} \quad . \ . \ . \ (W \text{ in lb./sec., } h_m \text{ in ft.}),$$

$$\frac{q \times 144p}{550} \quad . \ . \ . \ (q \text{ in cu. ft./sec., } p \text{ in lb./sq. ins.}),$$

$$\frac{Wh_m}{75} \quad . \ . \ . \ (W \text{ in kg./sec., } h_m \text{ in metres}),$$

$$\frac{qp}{7{\cdot}5} \quad . \ . \ . \ (q \text{ in lit./sec., } p \text{ in kg./sq. cm.}).$$

Specific information on pump output and efficiency in various conditions is given in §§ 304, 305.

286. Some Simple Water-lifting Devices. The simplest method of raising water, say, from a well, is to lower a bucket into the water and lift it up either hand over hand or with the help of a windlass. If the *lift*—the height through which the water is to be lifted—is relatively small, it is often more convenient to hang the bucket from one end of a light beam or rocking lever, the other end having a counterweight just heavy enough to raise of its own accord the bucket and its contents (Fig. 311). By pulling the rod and empty bucket *downwards*, leaving the counterweight to raise them on the return stroke, the labourer can use his muscles to much greater advantage than he could by trying to lift the

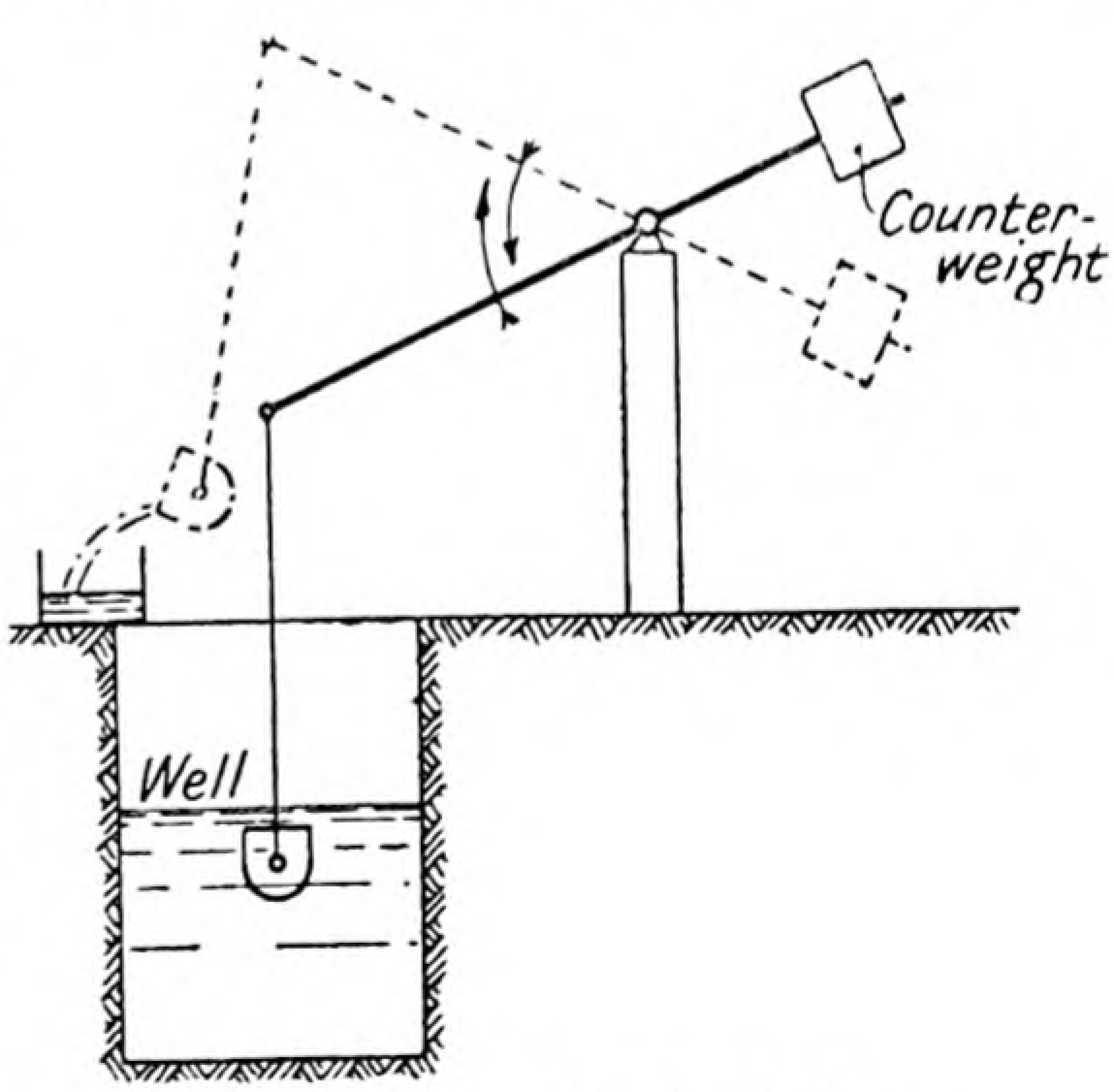

FIG. 311.—The shadoof.

laden bucket upwards. This simple and efficient machine is used in many parts of he world, especially for irrigation purposes : in Egypt it is known as the *shadoof*.

Equally widely known and used is the *Persian wheel*, (Fig. 312). Here an endless chain of buckets passes over a wheel mounted on a horizontal shaft which is driven through gearing from a vertical shaft; to the outer end of a radial arm projecting from the vertical shaft the draught animal that provides the motive power is harnessed. A device similar to the Persian wheel that can be direct-coupled to a little high-speed engine or motor, uses a loosely woven, endless, textile belt and dispenses with buckets altogether. Surface tension enables the rising side of the belt to carry up with it quite a useful quantity of water, which is flung off by centrifugal force into a suitable collector as the belt passes round the pulley. The *chaine helice* is a more durable form of the same device; it has an endless band consisting of an iron link chain surrounded by an endless coil spring, this combination giving a large surface area to which the water can cling. Under the name *Aquatole* or *water elevator*, machines of this type, with endless bands of special construction, will raise water from a depth of 100 feet or more.

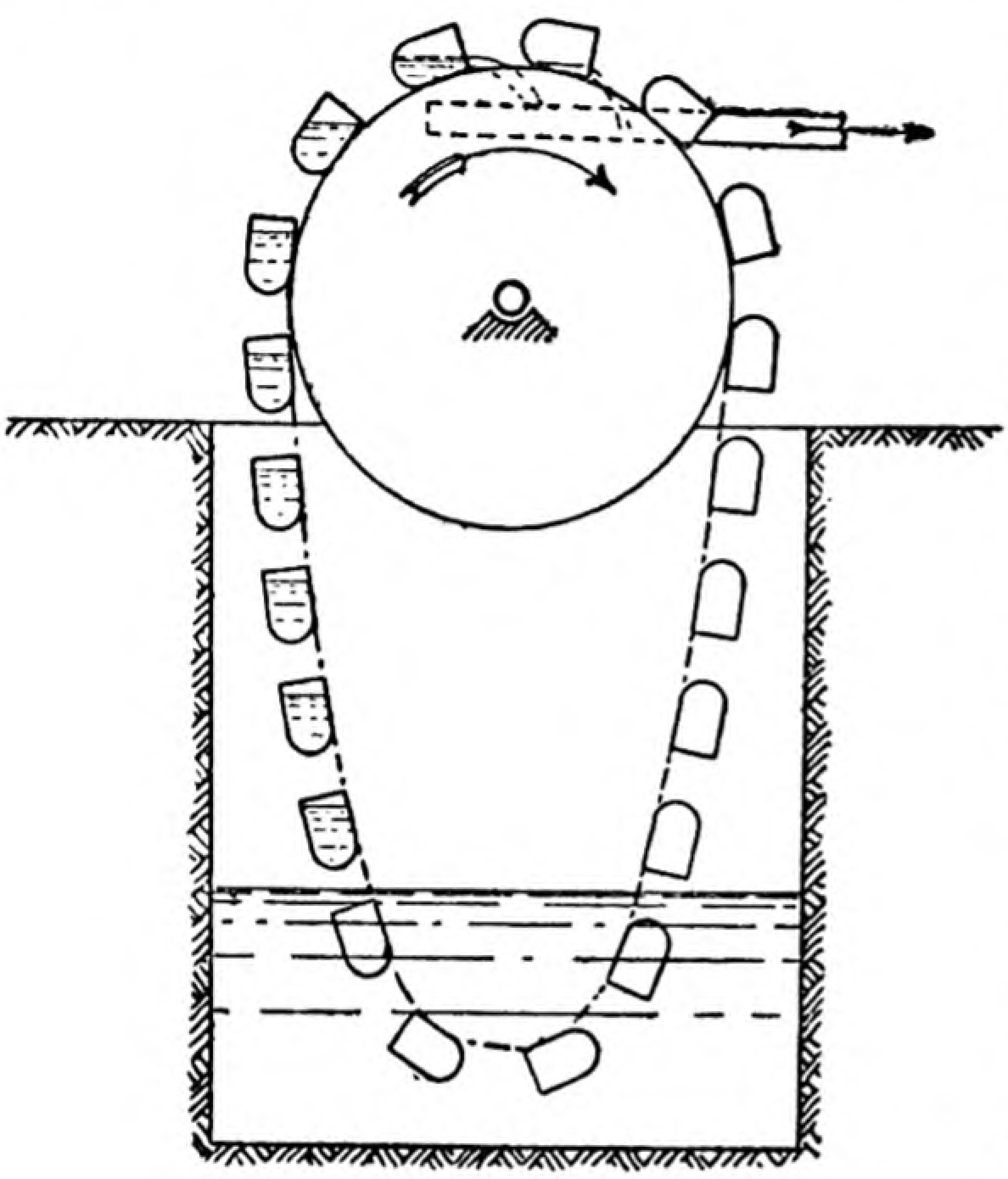

FIG. 312.—Persian wheel.

287. The Archimedean Screw. This apparatus consists in principle of a helicoid fitted within a cylinder, whose axis is inclined so that its lower end dips beneath the water to be lifted. (A helicoid is the surface generated when a line perpendicular to an axis rotates about the axis and simultaneously advances along it.) The cylinder and the helicoid together form a series of cells in which the water is lifted

when the screw is revolved, in the same way that a nut would be traversed along a quick-pitch thread. The cross-sections (Fig. 313) give an impression of the geometrical shape of the individual quantities of water that fill the cells.

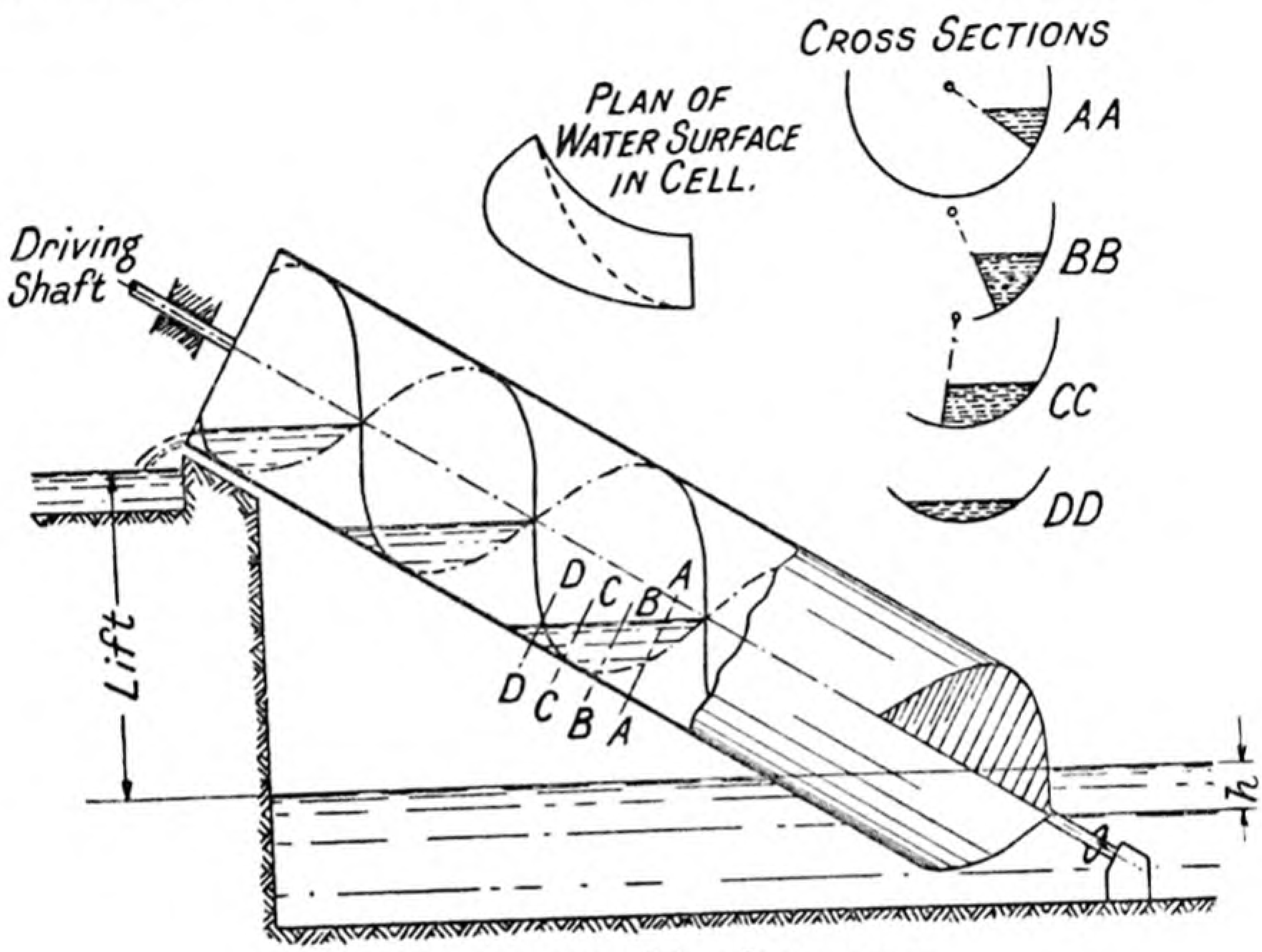

FIG. 313.—Archimedean screw.

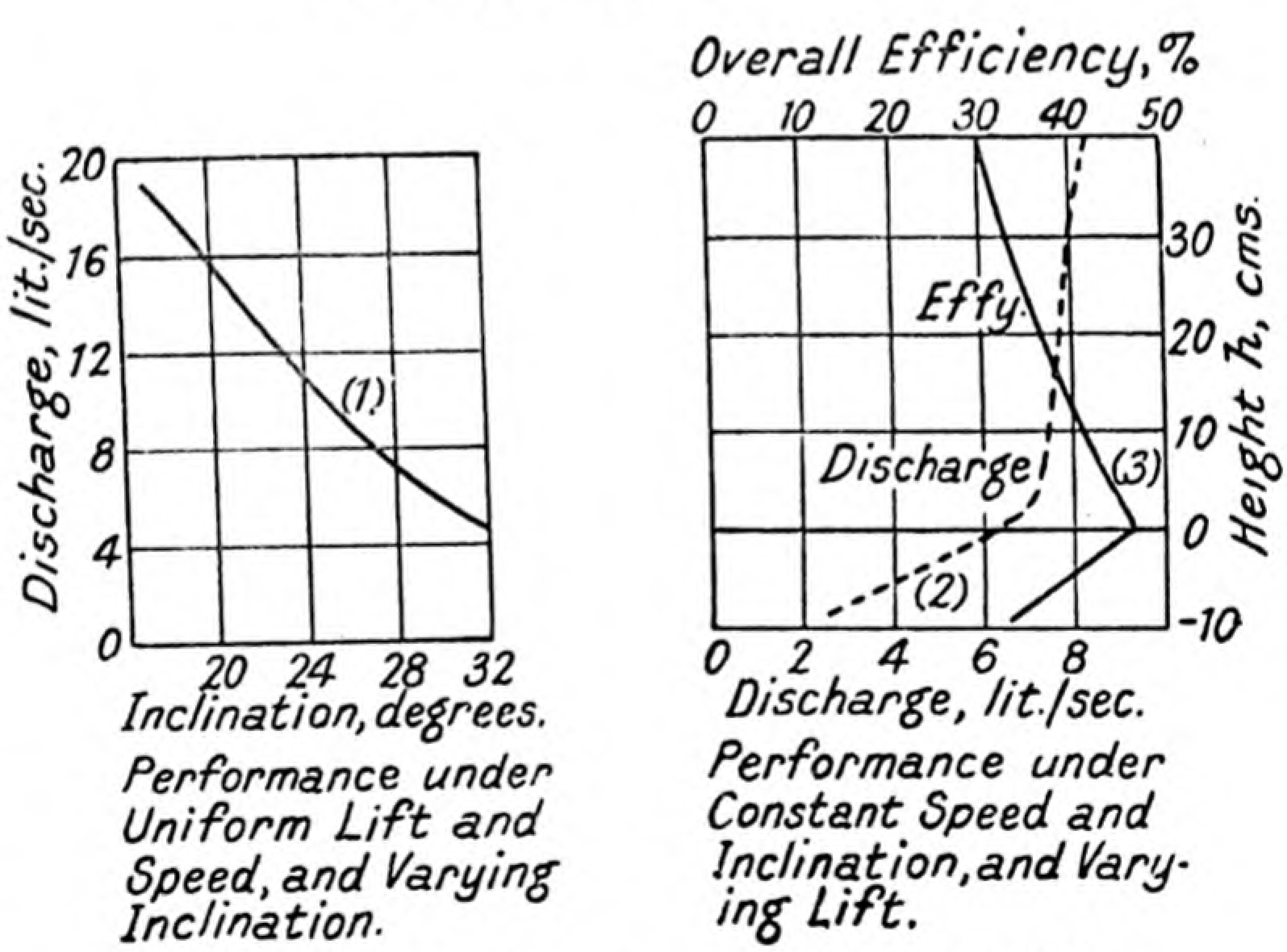

FIG. 314.—Archimedean screw characteristics.

Some experiments made by the author (188) showed that (1) the discharge of an Archimedean screw at a given speed falls off rapidly as the inclination of the axis increases; (2) the discharge at a given speed and inclination increases as the

lift diminishes; and (3) the maximum value of the overall efficiency occurs when the lower end of the cylinder is just half-immersed in the well water (Fig. 314).

As its overall efficiency, § 285, may rise to 55 per cent. or more, the Archimedean screw is fitted for certain industrial purposes, e.g. lifting corrosive liquids that would be difficult to handle by ordinary pumps.[189] Its usual duty is raising small amounts of irrigation water; but recent improvements have extended its scope. If the helicoid is of welded sheet-steel construction, working against a fixed concrete semi-cylindrical housing, then the apparatus may be on such a scale

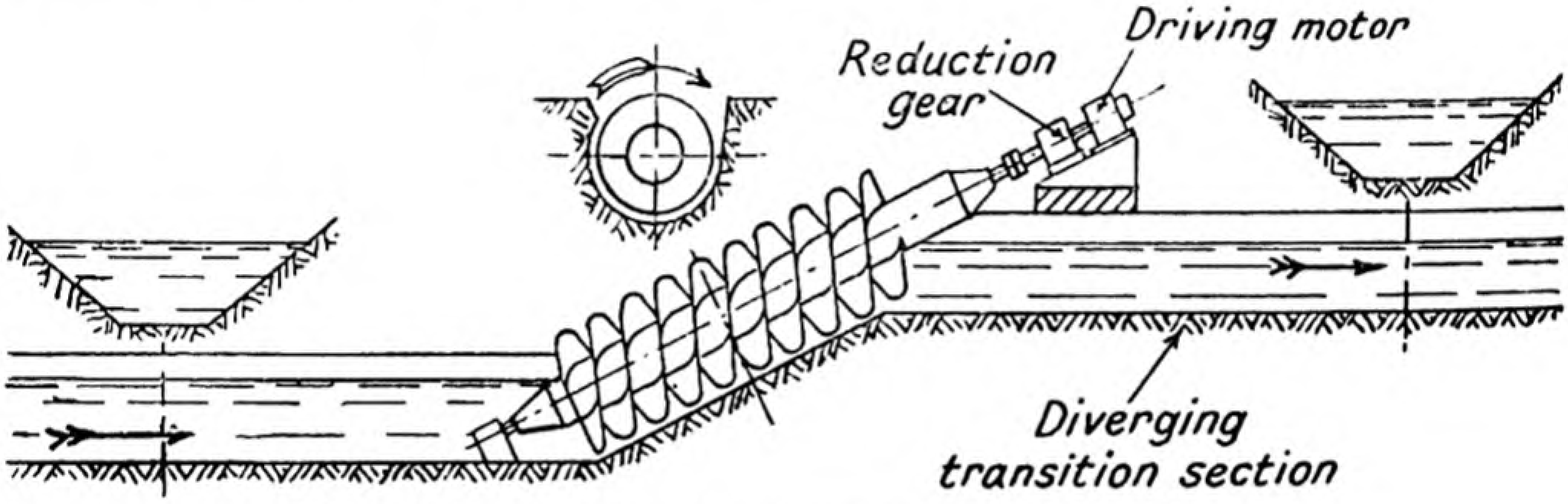

FIG. 315.—Archimedean screw in canal or drain.

that it can compete in cost and efficiency with low-lift pumping plants, § 345. An impression of such a water-raising installation is given in Fig. 315. The screw may have 2 or 3 "leads", viz. two or three intertwined helicoids: they may be as much as 5 ft. diameter and 20 ft. long, adapted for lifting a discharge of 40 tons per minute against a head of 2 to 5 ft. A geared electric motor would drive the screw.

Reciprocating Pumps.

288. Ram or Plunger Pump. The elements of a common type of reciprocating pump, the *ram, plunger* or *force* pump, are shown in Fig. 316. As the crank is rotated at uniform speed by the driving engine or motor, the cylindrical ram or plunger moves to and fro in the *pump barrel, cylinder,* or *ram case.* On the outward stroke the partial vacuum behind the ram enables the atmospheric pressure acting on the surface of the water in the well to force water up the suction pipe and past the suction valve into the pump barrel. On the inward stroke the suction valve closes, the delivery valve opens, and the

water is forced up the delivery pipe. In large pumping installations the delivery pipe is known as the *rising main.*

If D = diameter of ram or plunger,
R = crank radius or throw,
N = speed of crank-shaft in revs. per min.,

then the volume swept per stroke, or displacement $= \frac{\pi}{4}D^2 . 2R$,

and under ideal conditions the average rate of discharge per second $= Q = \frac{\pi}{4}D^2 . \frac{2RN}{60}$.

Owing to leakage past the valves and plunger, and to lag in the closure of the valves, the actual discharge Q_a is nearly always less than Q; the ratio between them is expressed either in

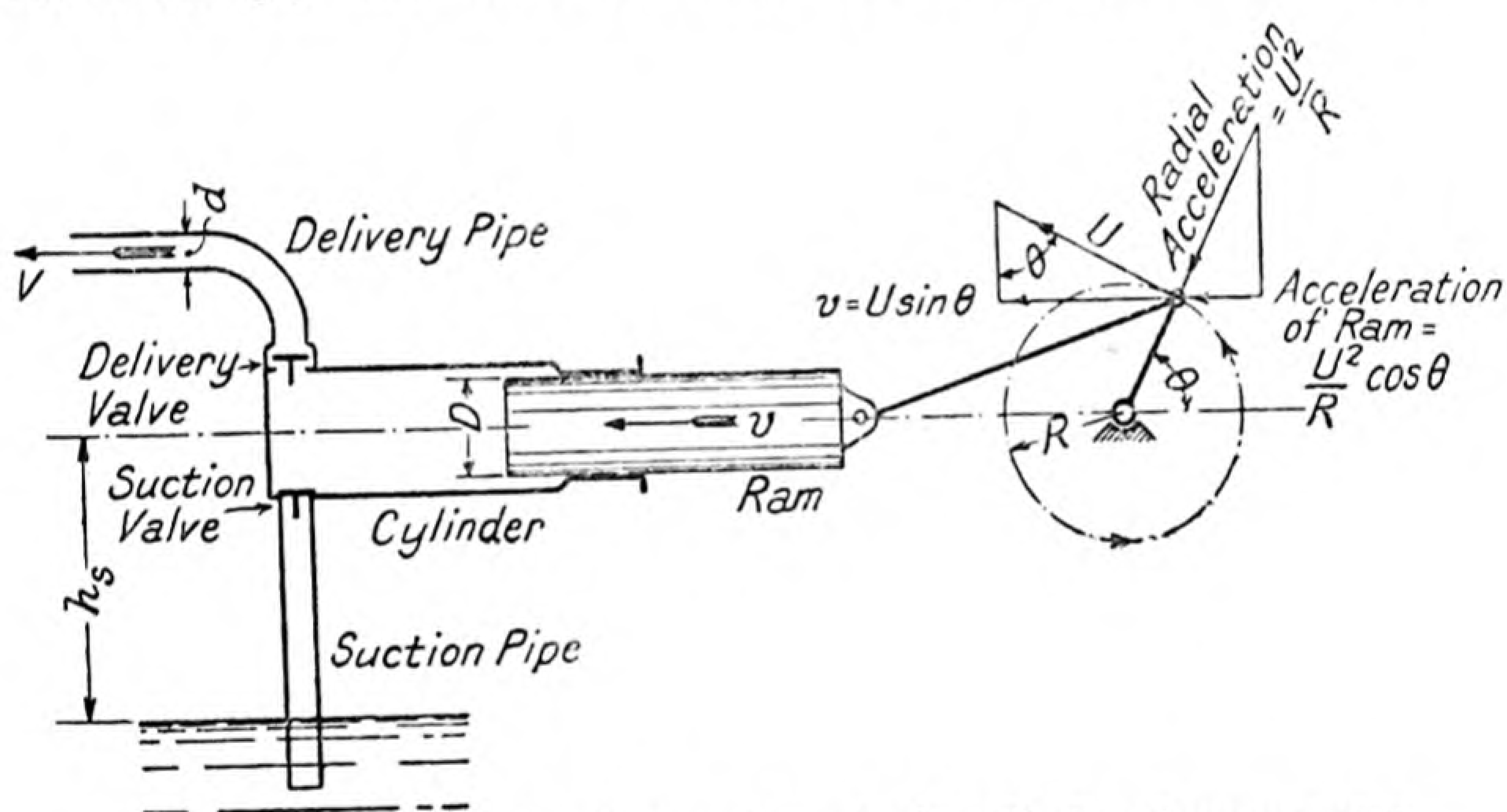

FIG. 316.—Horizontal single-acting single-cylinder plunger pump.

the form of the *volumetric efficiency*, which has the value $\frac{Q_a}{Q}$ (§ 220), or in the form of a *percentage slip*, which has the value

$$\frac{Q - Q_a}{Q} \times 100.$$

Thus

$$Q_a = \frac{\pi}{4}D^2 . \frac{2RN}{60}\left(\frac{100 - \text{slip}}{100}\right).$$

In pumps maintained in good condition the percentage slip is of the order of 2 per cent., or even less. But when the delivery pressure is high, e.g. above 1000 lb./sq. in., the compressibility of the liquid (§ 5) materially helps to increase the slip, especially if the clearance volume of the cylinder is excessive.

289. Instantaneous Rate of Discharge. The momentary rate of discharge in the delivery pipe at any instant will manifestly vary quite widely, having a value of zero during the whole of the suction stroke and rising to a maximum during the delivery stroke.

Let V = the instantaneous velocity in the delivery pipe at any instant.

v = the velocity of the ram at that instant.

θ = the angle through which the crank has turned from the outer dead centre at that instant.

U = the uniform linear speed of the crank-pin.

d = the diameter of the delivery pipe.

For the moment it will be assumed that the connecting rod is very long compared with the crank radius. From Fig. 316 we see that the velocity of the ram at any instant is identical

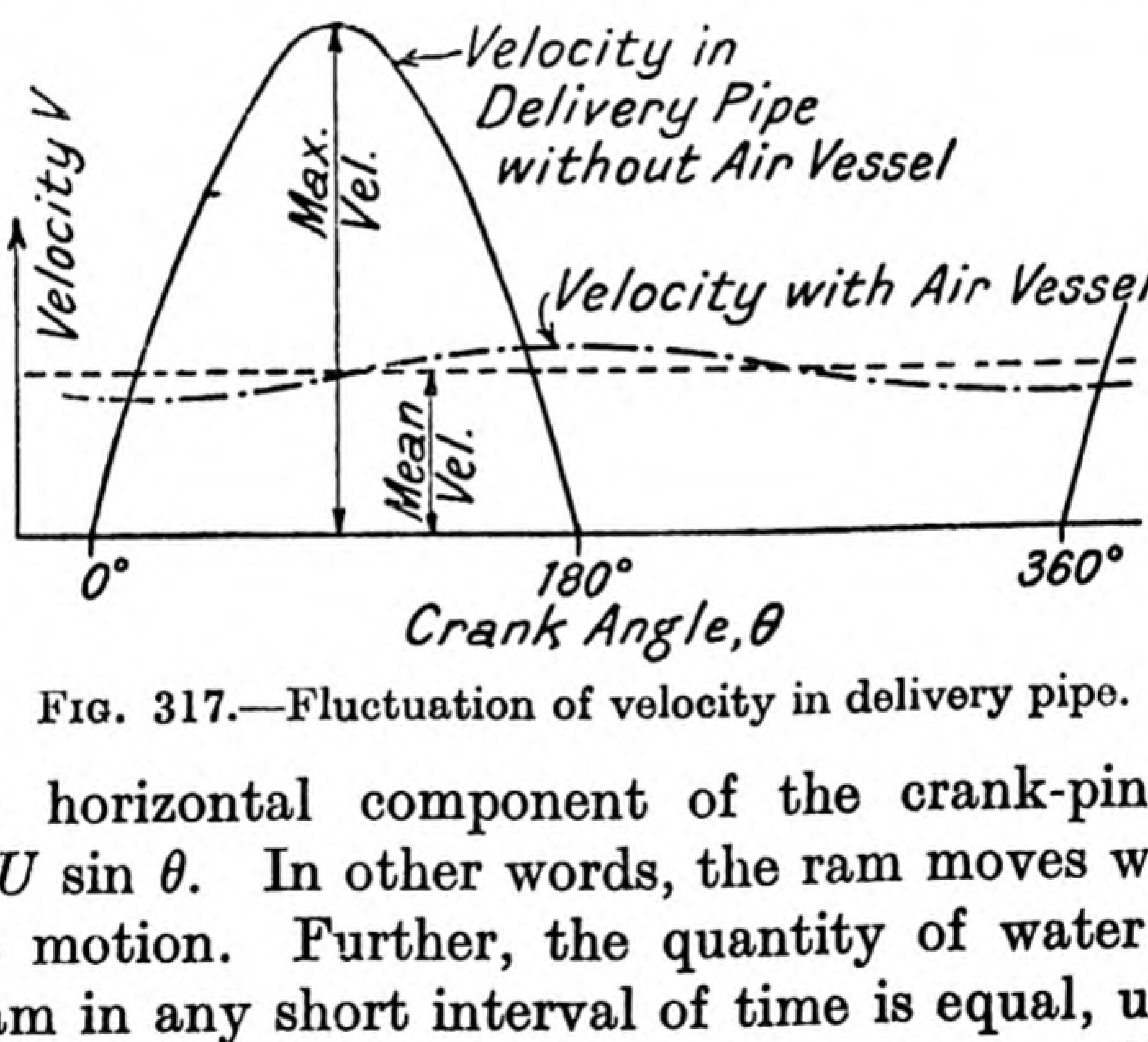

FIG. 317.—Fluctuation of velocity in delivery pipe.

with the horizontal component of the crank-pin velocity, viz. $v = U \sin \theta$. In other words, the ram moves with simple harmonic motion. Further, the quantity of water displaced by the ram in any short interval of time is equal, under ideal conditions, to the quantity flowing along the delivery pipe in that time, from which we have $\frac{\pi}{4}D^2v = \frac{\pi}{4}d^2V$, whence,

$$V = U \sin \theta \, . \frac{D^2}{d^2} = \frac{2\pi RN}{60} \, . \sin \theta \, . \frac{D^2}{d^2}.$$

The relation between θ (or time) and V can therefore be expressed by a sine curve, shown by the full line in Fig. 317. The maximum instantaneous velocity in the pipe $= \frac{2\pi RN}{60} \cdot \frac{D^2}{d^2}$

is seen to be π times the mean velocity, which is

$$\frac{Q}{\frac{\pi}{4}d^2} = \frac{2RN}{60} \cdot \frac{\frac{\pi}{4}D^2}{\frac{\pi}{4}d^2} = \frac{2RN}{60} \cdot \frac{D^2}{d^2}.$$

By using in the above expressions the diameter of the suction pipe instead of the diameter of the delivery pipe, the instantaneous velocity in the suction pipe is obtainable.

290. Inertia Pressures in Delivery and Suction Pipes. The fluctuations in the pipe velocities just referred to inevitably give rise to inertia pressures (§ 115); the intensities of these pressures can readily be calculated by finding at any moment the acceleration or retardation $\frac{dV}{dt}$ of the water in the pipe, and inserting it in the modified form of equation 7-1, § 115, $p_i = \frac{wL}{g} \cdot \frac{dV}{dt}$, where L is the pipe length.

Now $\frac{dV}{dt} = \frac{dV}{d\theta} \cdot \frac{d\theta}{dt}$, and since $V = U \sin\theta \cdot \frac{D^2}{d^2}$, then $\frac{dV}{d\theta} = U\cos\theta \cdot \frac{D^2}{d^2}$. Also $\frac{d\theta}{dt}$ = angular velocity of crank-shaft $= \frac{2\pi N}{60}$,

$$\therefore \frac{dV}{dt} = \frac{2\pi N}{60} \cdot U\cos\theta \cdot \frac{D^2}{d^2} = \frac{2\pi N}{60} \cdot \frac{2\pi RN}{60} \cdot \cos\theta \cdot \frac{D^2}{d^2}.$$

(The same result can be obtained by resolving horizontally the radial acceleration of the crank-pin as in Fig. 316.)

Substituting in the above equation, 7-1, we obtain

$$p_i = \frac{wL}{g}\left(\frac{2\pi N}{60}\right)^2 \cdot R\cos\theta \cdot \frac{D^2}{d^2}$$

which, for water at ordinary temperatures, reduces to the form

$$p_i = KLRN^2 \cos\theta \cdot \frac{D^2}{d^2} \qquad \textbf{(15-1)}$$

where $K = 0{\cdot}000147$ if L, R, D and d are in feet and p_i is in lb./sq. in.

$= 0{\cdot}000112$ if L, R, D and d are in metres and p_i is in kg./sq. cm.

The maximum and minimum values of p_i are, of course, attained at the ends of the stroke when $\cos \theta = \pm 1$.

The effect of inertia pressure on the performance of the pump [190] can conveniently be shown by plotting the ideal indicator diagram (Fig. 318). If inertia pressure could be eliminated the diagram would have the rectangular shape *abcd*; if inertia pressures are operative the delivery pressure is increased at the beginning of the stroke and diminished at the end by an amount p_i, the suction head also being greater at the beginning of the suction stroke and less at the end, the diagram having the shape *efkl*. Pipe friction is neglected. In these ideal conditions, it is to be noted that the power input to the pump remains unaltered, because area *abcd* = area *efkl*.

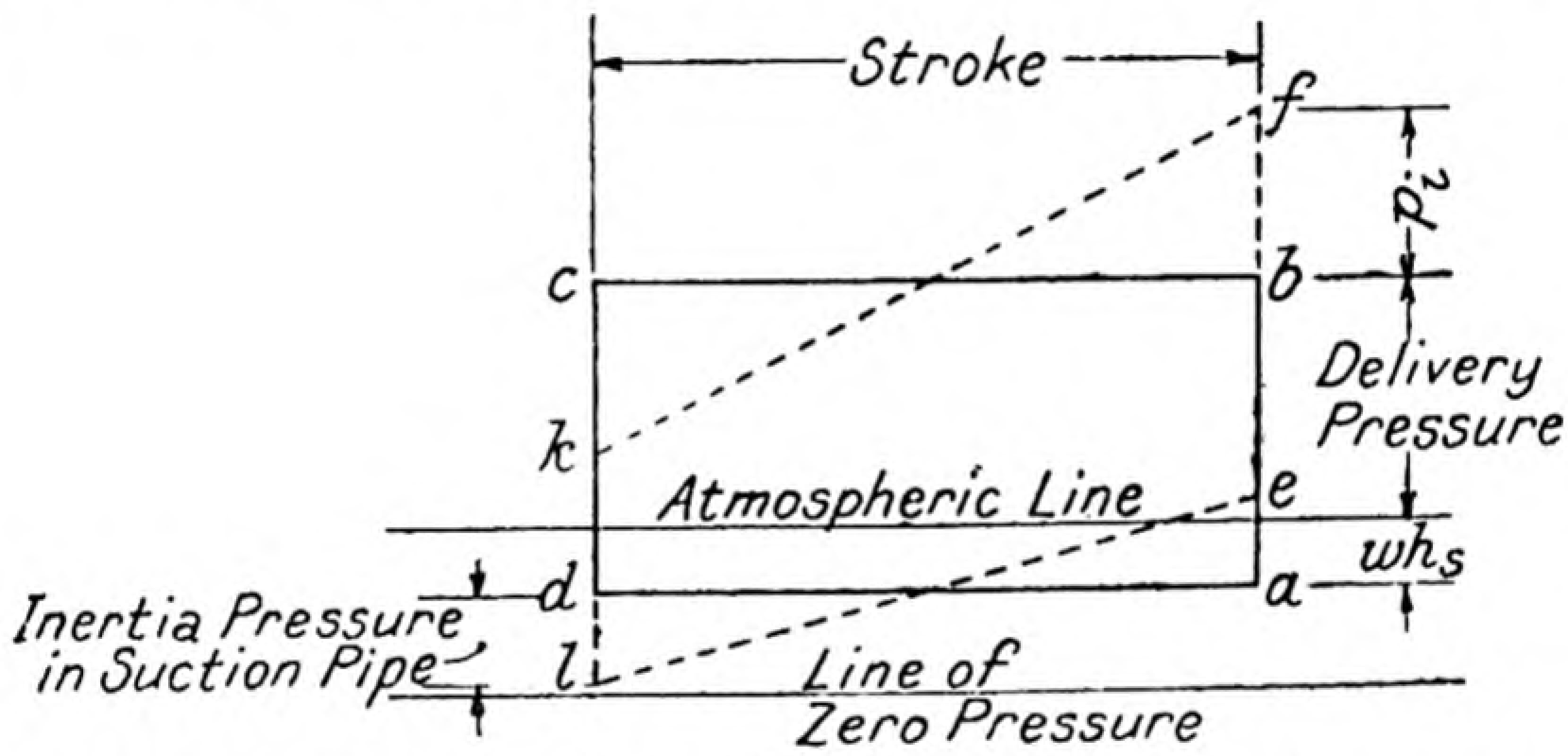

FIG. 318.—Ideal indicator diagram for reciprocating-pump.

Although the increased pressures to which the delivery side of the pump is thus subjected might be resisted by suitable strengthening of the pump parts, yet on the suction side a point may easily be reached at which the discharge begins to be affected. The only force available for accelerating the water in the suction pipe, and for raising it against the static suction lift h_s (Fig. 316), is the pressure of the atmosphere acting on the surface of the water in the suction well. Thus by no possible means can the maximum suction inertia pressure exceed the value (atmospheric pressure $- wh_s$); if the pump is driven at a speed demanding a greater rate of acceleration than this pressure can produce, the water in the suction pipe will refuse to respond—the ram will move out of the pump barrel quicker than the water can follow, and a vacuous space will be formed in the cylinder. Later in the stroke the water overtakes the ram, there being a violent hammering action

at the moment of contact. This destructive phenomenon is known as *separation* or *cavitation*. It is comparable on a large scale to the action on a microscopic scale that was described in §§ 133, 134. In order to bring under control such potentially dangerous conditions,[191] the construction of reciprocating pumps is nearly always modified in the manner explained in §§ 291-293. (Example 151.)

(*Note*.—The true values of inertia pressure are influenced by the ratio of the length of connecting rod to crank radius. If this ratio be n, then the true inertia pressure at the inner dead centre (ram fully into cylinder) is $p_i\left(1+\frac{1}{n}\right)$, and at the outer dead centre (ram fully out of cylinder) is $p_i\left(1-\frac{1}{n}\right)$, p_i being the value calculated from equation 15-1 when $\theta = 0$, or when $\theta = 180°$.)

Before assessing the maximum permissible suction lift h_s, another correction is also required. It concerns the vapour pressure p_{vp} of the liquid, §§ 16, 132, 135.

291. Use of Air Vessels. An air vessel is a closed chamber communicating with the delivery pipe at a point as close to the pump as possible, the upper part of the chamber being charged with compressed air (Fig. 319). During the delivery stroke nearly all the water that the pump delivers in excess of the mean discharge is diverted into the air vessel and there stored. During the ensuing suction stroke, the pump discharge is zero and the flow in the delivery pipe is maintained by the stored water yielded up by the air vessel. Some slight change in the air pressure must naturally take place as the water surface in the vessel rises and falls, with corresponding changes in the delivery pipe pressure and velocity; but it is only a matter of making the capacity of the air vessel great enough to bring these cyclical variations within prescribed limits. Usually it suffices to give the air vessel a volume six to nine times the pump displacement volume. Fig. 317 (broken line) gives an impression of the improvement as regards uniformity of delivery that an air vessel can produce.

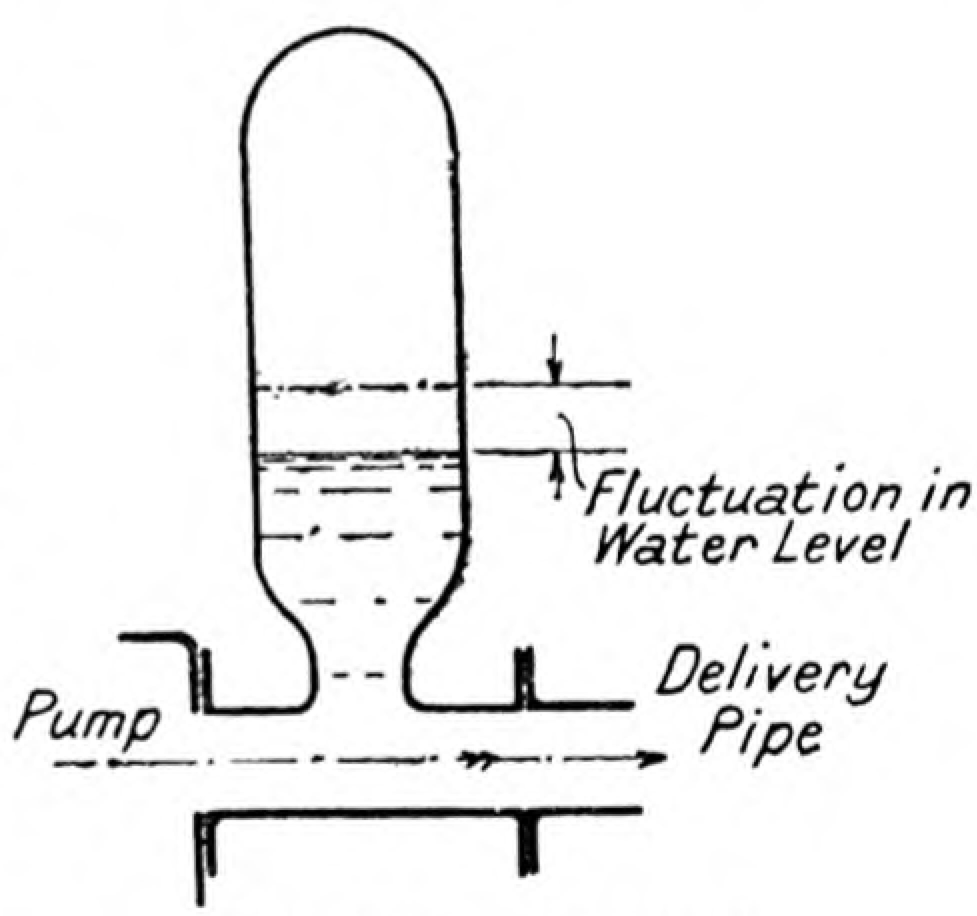

Fig. 319.—Air vessel.

Since air is slowly dissolved by water under pressure (§ 11), the air in the air vessel must periodically be renewed. This is done in large pumps by a special air compressor provided for the purpose, while in small pumps an automatic air valve—a *snifting valve*—on the pump barrel may draw in the necessary quantity of air during the suction strokes. An air vessel fitted on the suction pipe to perform exactly the same function that the air vessel does on the delivery pipe is sometimes called a *vacuum vessel.* When a number of pumps deliver into a common delivery main, an additional very capacious air vessel may serve as a junction box and so help to damp out pressure-surges liable to arise during starting and stopping of the units, §§ 175, 298 (ii).

Spring-loaded *alleviators* may replace air vessels when very high pressures are involved.

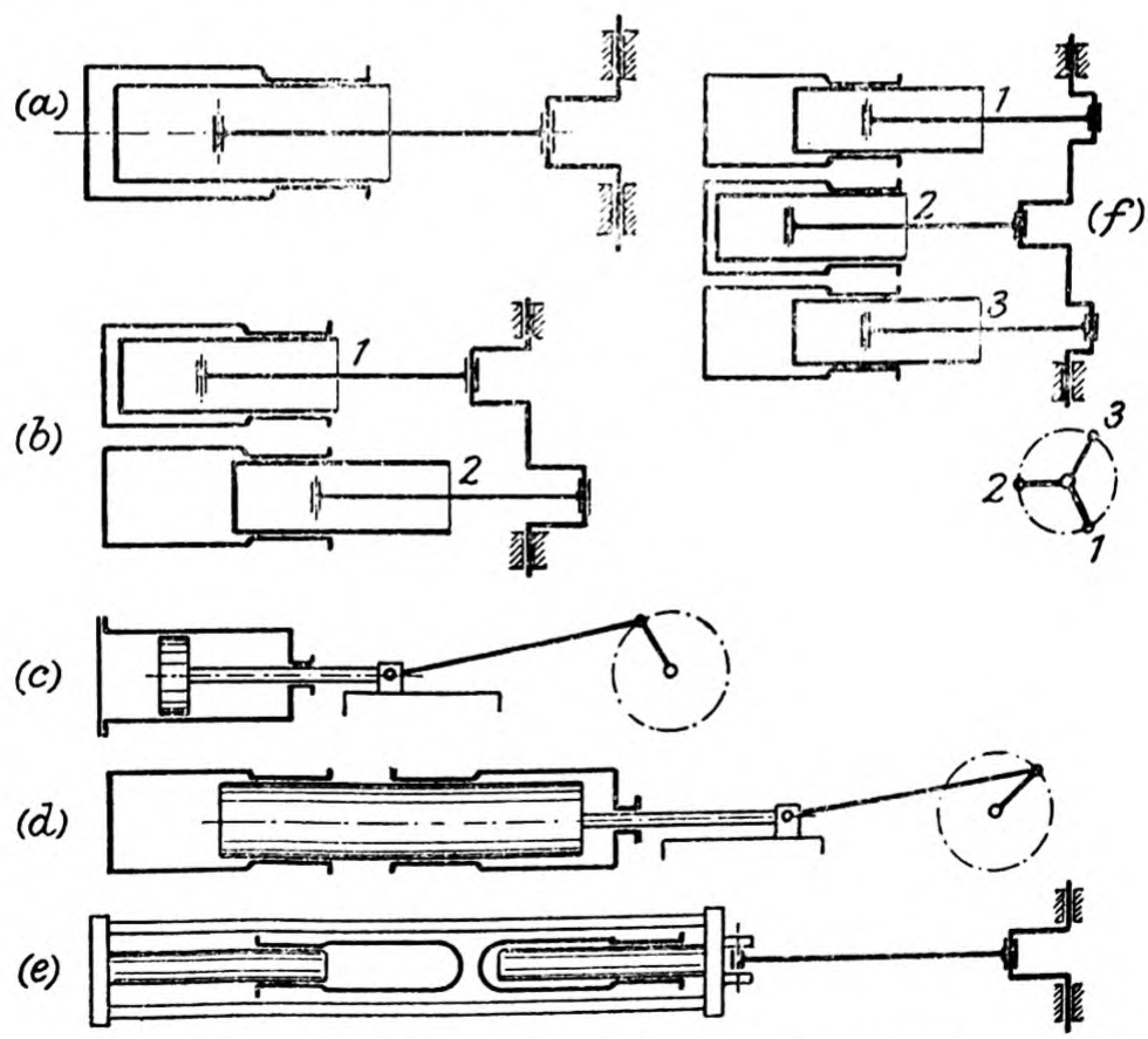

FIG. 320.—One-, two-, and three-cylinder pumps.

292. Multi-cylinder Pumps. Comparing two pumps of the same rotational speed and discharge, one with a single

large cylinder and the other with two smaller cylinders arranged to force water alternately into the delivery pipe, both without air vessels, it is evident from equation 15-1 (§ 290), that the two-cylinder pump will only generate half as great

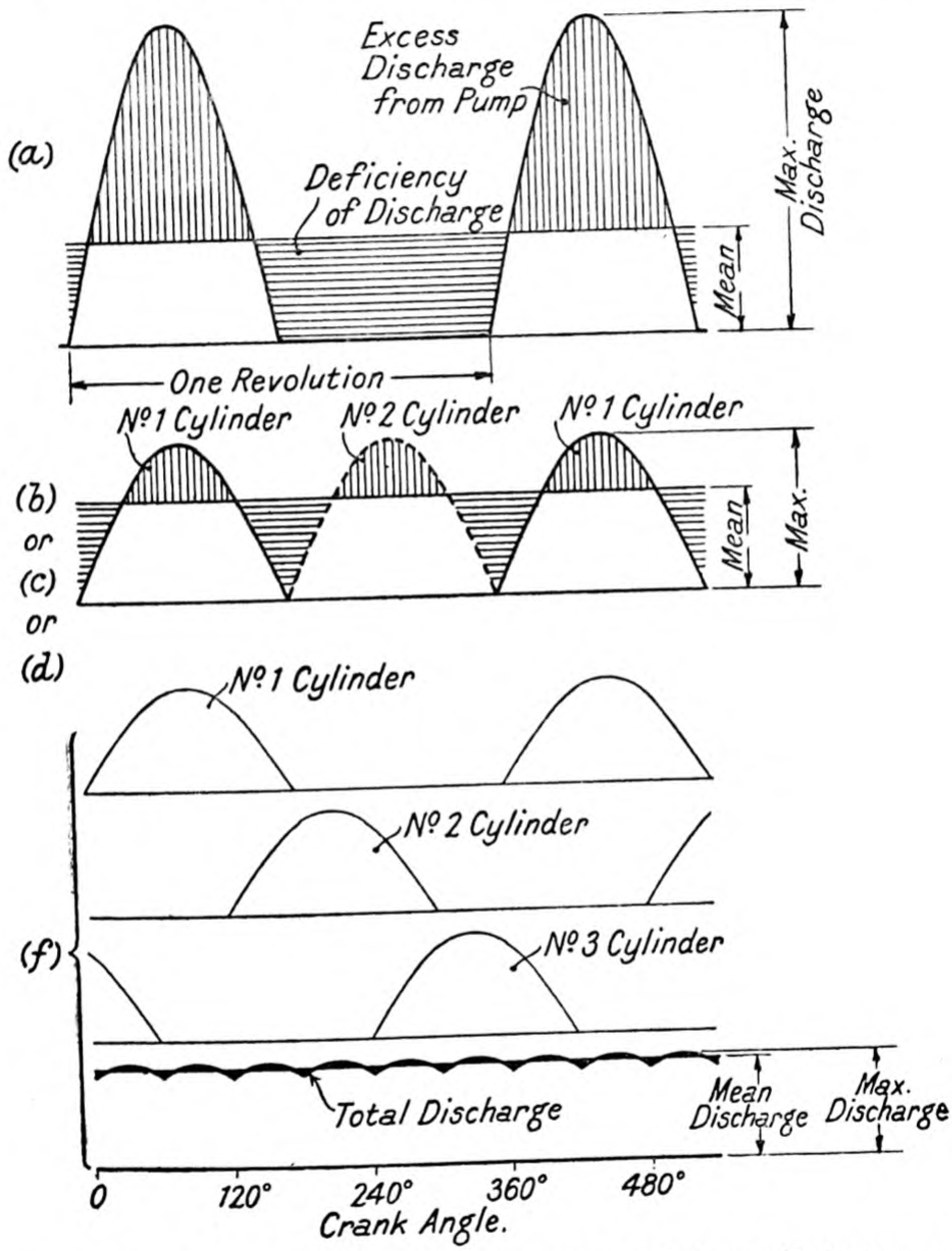

FIG. 321.—Discharge diagrams for one-, two-, and three-cylinder pumps (without air-vessels).

an inertia pressure as the single-cylinder pump. Various arrangements by which this improvement may be secured are drawn diagrammatically to the same scale in Fig. 320. The original single-acting single-cylinder pump is shown at (*a*); at (*b*) a two-throw pump with rams driven from cranks set at

180° is shown ; (*c*) represents a double-acting single-cylinder pump ; (*d*) shows a double-acting pump having two cylinders in line, driven from a single crank.

Types (*b*), (*c*) and (*d*) all yield the same gross discharge as (*a*) when driven at the same speed, but they deliver the water more uniformly. This is made clear by the diagrams in Fig. 321, in which the instantaneous discharge from each individual cylinder is compared with the mean discharge from the pump. The advantage of (*b*) and (*d*) over (*c*) is that leakage past the glands can at once be detected and remedied, whereas the double-acting pump must be dismantled before new packing rings can be inserted in the piston or *bucket*. The *outside end-packed* pump (*e*) has the further advantage over the *outside centre-packed* pump (*d*) that the piston-rod with its gland is eliminated, and this pump is therefore sometimes chosen for high-pressure hydraulic transmission systems (§ 353).

(Example 152.)

The three-throw pump (*f*) (Fig. 320), having three cranks set at 120°, represents a still further improvement. Here the maximum inertia pressures are only 1/6 as great as in the equivalent single-cylinder pump (*a*), for at several periods of the cycle two of the cylinders are delivering water simultaneously (Fig. 321). Because of its uniformity of turning moment as well as because of its uniformity of delivery, the three-throw pump is often preferred alike for small and for large installations.

A *duplex double-acting* pump is formed by combining two lines of parts such as in Fig. 320 (*c*), (*d*), or (*e*), each driven by a crank, the two cranks being set at 90°. This combination is equivalent to a four-throw pump.

A *quintuplex* or five-throw pump has five single-acting cylinders driven from a shaft having cranks set at 72°. So regular is the discharge from such a machine (as shown in the Table below) that it may be run without air vessels ; it is therefore sometimes used for high-efficiency, high-pressure boiler-feed pumping and the like duties (§ 349 (II)).

It should be remembered that the maximum values of inertia pressures, whether estimated from formula 15-1 or from the slope of the discharge curves, Fig. 321, altogether neglect the *elasticity of the liquid column* in the delivery pipe. When this is taken into account in the way described in

§ 118, it may appear that the inertia shocks are much less severe than we had imagined. The corrected figures, as set out in the Table below, serve to show in a still more favourable light the advantages of the three-throw or the five-throw pump; or in general, the superiority of an *odd* number of cylinders over an *even* number. In these calculations the delivery pipe is assumed to be very long.

Equivalent Number of Cylinders.	Angular Spacing of Cranks (Degrees).	Ratio of Maximum Inertia Pressure in Multi-cylinder Pump to Maximum Inertia Pressure in Equivalent Single-cylinder Pump, if Elasticity of Liquid Column is:—	
		Neglected.	Taken into Account.
1	360	1·000	1·000
2	180	0·500	0·500
3	120	0·167	0·044
4	90	0·250	0·103
5	72	0·100	0·016
6	60	0·167	0·044

In any event the inertia-pressure in multi-cylinder pumps may be still further mitigated by the use of air-vessels (§ 295 (ii)).

On the other hand, inertia pressures may rise above the computed values if there is resonance in the system, viz., if the natural periodicity of the pressure waves in the piping, §§ 117, 118, happens to coincide with the frequency of the cyclic impulses generated by the pump.

293. Direct-acting Steam Pump. To some extent the difficulties in regard to inertia pressures that we are trying to overcome are self-imposed. There is no natural law which says that a pump plunger *must* move with simple harmonic motion; it is we ourselves who force it to move in this way by deliberately keeping the crank-shaft speed uniform with the help of a heavy flywheel. Frequently this is unavoidable, as for example, when the pump is gear-driven from an electric motor; but there is a way of escape if steam power is available. By coupling together tandem fashion a steam cylinder and a pump cylinder (Fig. 322), rejecting completely the crank-shaft and flywheel, complete control over the maximum pressure in the delivery pipe is assured—by no means can it exceed the value: steam pressure $\times \left(\frac{\text{area of steam piston}}{\text{area of pump bucket}}\right)$.

In this direct-acting steam pump we do not arbitrarily fix a speed of revolution and with it a fixed rate of acceleration in the pipes; we allow a suitable excess of steam

pressure over and above that required to meet the static and friction heads, and let the rate of acceleration adjust itself accordingly.

This *non-rotative* machine is therefore not a true positive pump, because its output is not independent of the delivery pressure. On account of the uniformity of pressure throughout the stroke prevailing in the pump cylinder, at least when

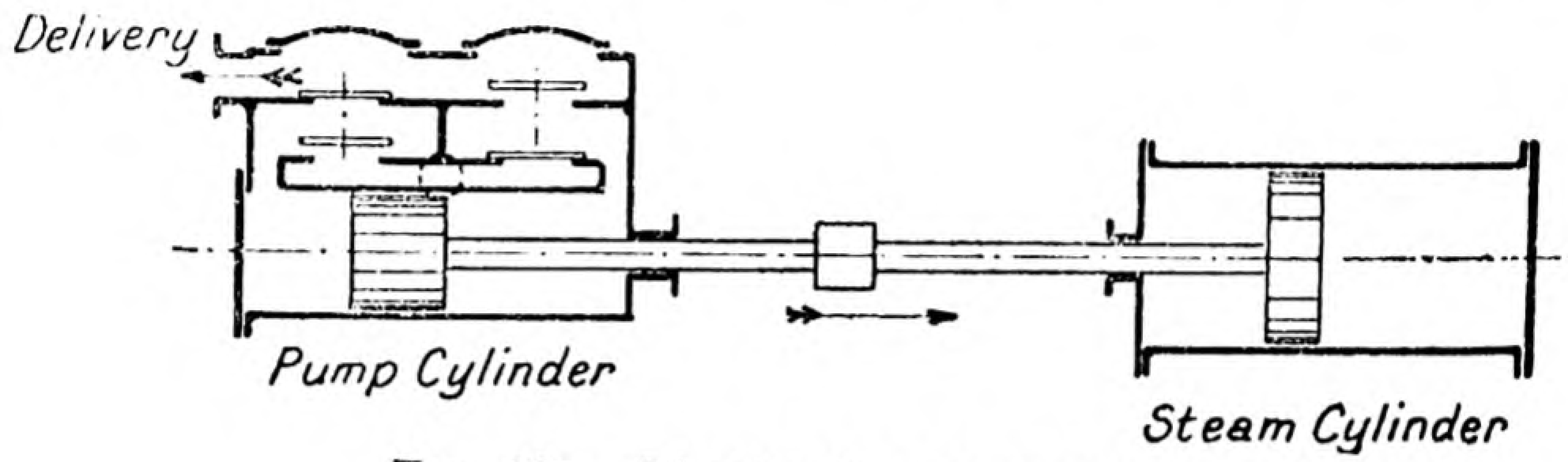

FIG. 322.—Direct-acting steam pump.

inertia effects are small (diagram *abcd*, Fig. 318), steam cannot be used expansively in the motive cylinder, which implies an unfavourable steam consumption. An improvement can be achieved either by using compound steam cylinders, § 295 (i), or by special compensating devices. A popular arrangement of these non-rotative steam pumps is the duplex double-acting system in which two sets of parts as in Fig. 322 are mounted side by side.

294. Some Examples of Reciprocating Pumps.

(i) *Small single-cylinder pump.* A cross-section through a pump having a bore of 4 ins. and a stroke of 6 ins., intended for a pressure of 50 lb./ sq. in. at 80 r.p.m., is given in Fig. 323. The automatic valves are of gun-metal, of the wing-guided type, having a large diameter and small lift so as to minimise the hammering action when they open and close. It will be noted that leakage is controlled by a simple stuffing box and soft packing (§ 223). Belt-drive is often convenient for such machines.

(ii) *High-pressure three-throw pump.* The pump shown in Fig. 324 has a duty of 200 gallons per minute (15·1 lit./sec.) against a pressure of 1500 lb./sq. in. (105 kg./sq. cm.); it is driven through gearing by a 300 h.p. electric motor. This machine is typical of those used for supplying water [192] to hydraulic power installations (§ 353). On the right is seen the

suction pipe with its branches to each of the three pump barrels; a similar manifold conducts the water to the delivery pipe. (See also § 353.)

(iii) *Totally-enclosed duplex double-acting pump.* The unit illustrated in Fig. 325 (facing p. 430), consisting virtually of two of the pumps shown in Fig. 320 (*e*), has four rams $6\frac{3}{4}$-in. diameter by 24-in. stroke; it is one of a number supplied for forcing oil, under a pressure of nearly 1000 lb./sq. in., through a

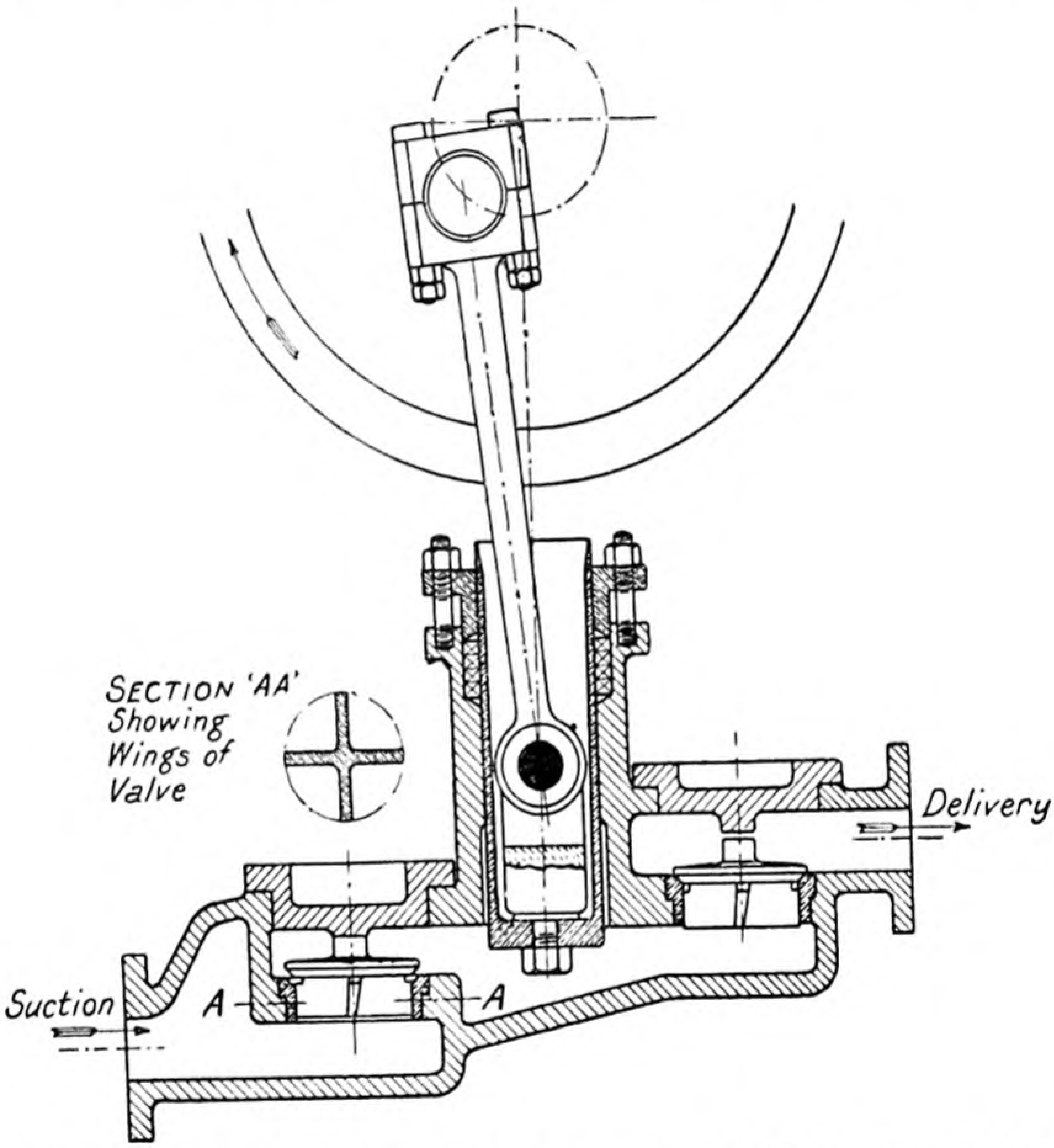

FIG. 323.—4 in. × 6 in. single-acting ram pump. (F. W. Brackett & Co., Ltd.)

pipe-line of the Iraq Petroleum Co., Ltd. All working parts are enclosed, as a protection against the severe conditions prevailing in the desert pumping stations; the pump is driven by a Diesel engine at a speed of 44 r.p.m. through double-reduction gearing.

Pumps for larger outputs have three lines of parts, each unit thus constituting in effect a double-acting three-throw pump.[193]

(Example 188.)

(iv) *High-speed high-pressure pumps.* A crank and connecting rod mechanism is not the only means of giving a reciprocating motion to the pump plunger. In the alternative arrangement shown in Fig. 326 an eccentric is used, formed solid with the rotating shaft; the outer race or roller track of the roller bearing surrounding the eccentric bears directly against the end of the plunger.[194] A spring or springs keep the plunger always in contact with the roller track. Such pumps, having two, three, or as many as six cylinders in line, are suitable for direct-coupling to electric motors running at 1470 r.p.m.; their duty would be to supply oil at a pressure of 5000 psi or more to self-contained hydraulic installations, Fig. 425, § 358. As the plungers are rarely more than an inch or so in diameter, and as the pumps run completely submerged in filtered oil, "hydraulic" sealing is quite satisfactory without the use of any kind of packing, § 222 (i).

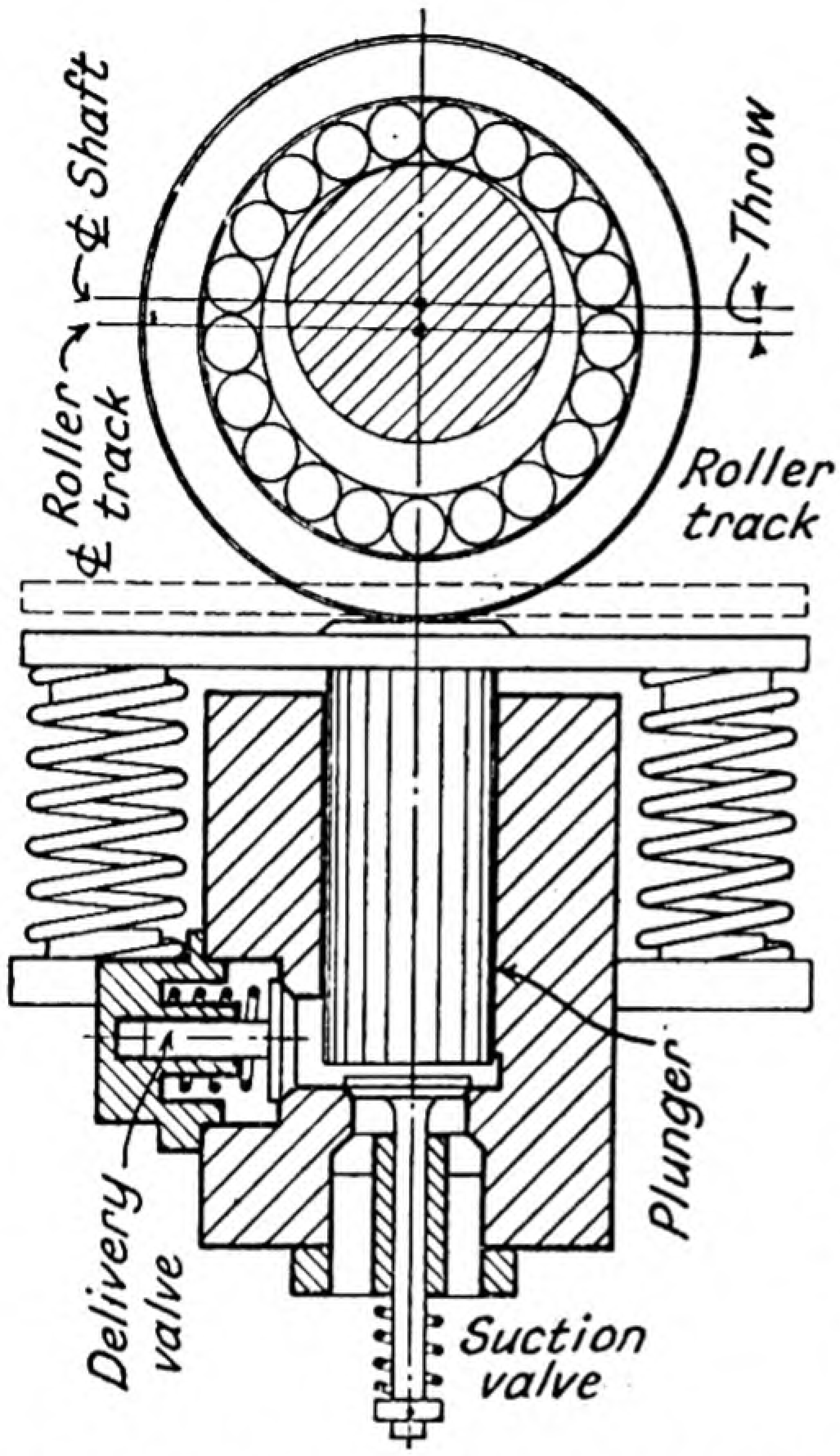

FIG. 326.—Operation of reciprocating pump by eccentric.

In other types of high-speed multiple-cylinder pumps, the plungers may be operated by a swash-plate mechanism, or the cylinders may be set radially instead of in parallel formation.

(v) *Pumps for liquid concrete.* At the other extremity of the range of reciprocating pumps now available, there are to be found machines for forcing ready-mixed concrete aggregate along pipes.[195] They have special mechanically-operated valves, in place of the poppet valves shown in Figs. 316, 323. These concrete pumps may be compared with other machines for handling solid-liquid mixtures, e.g. diaphragm pumps, § 297.

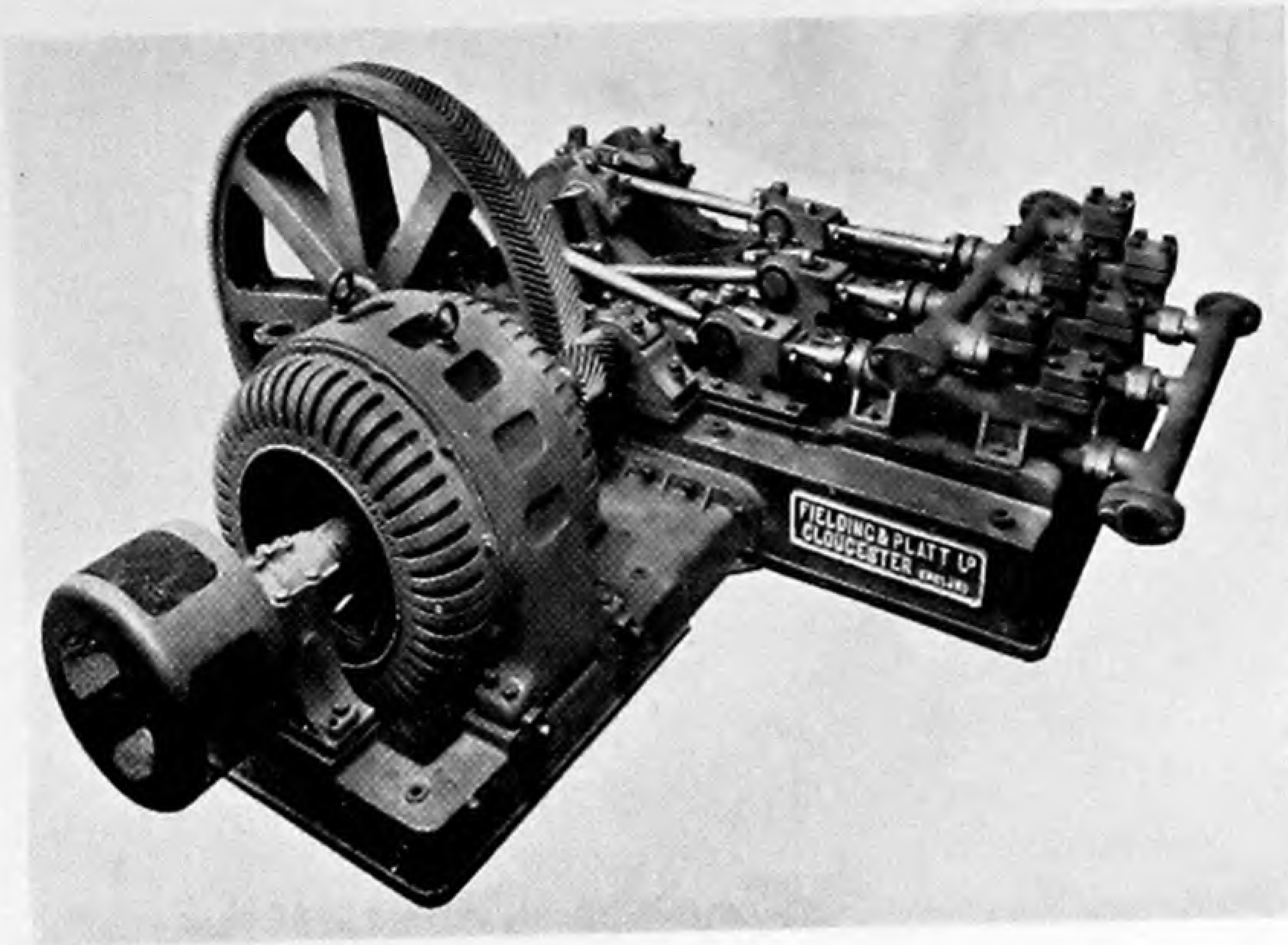

FIG. 324.—Electrically-driven three-throw pump.
(Fielding & Platt, Ltd.)

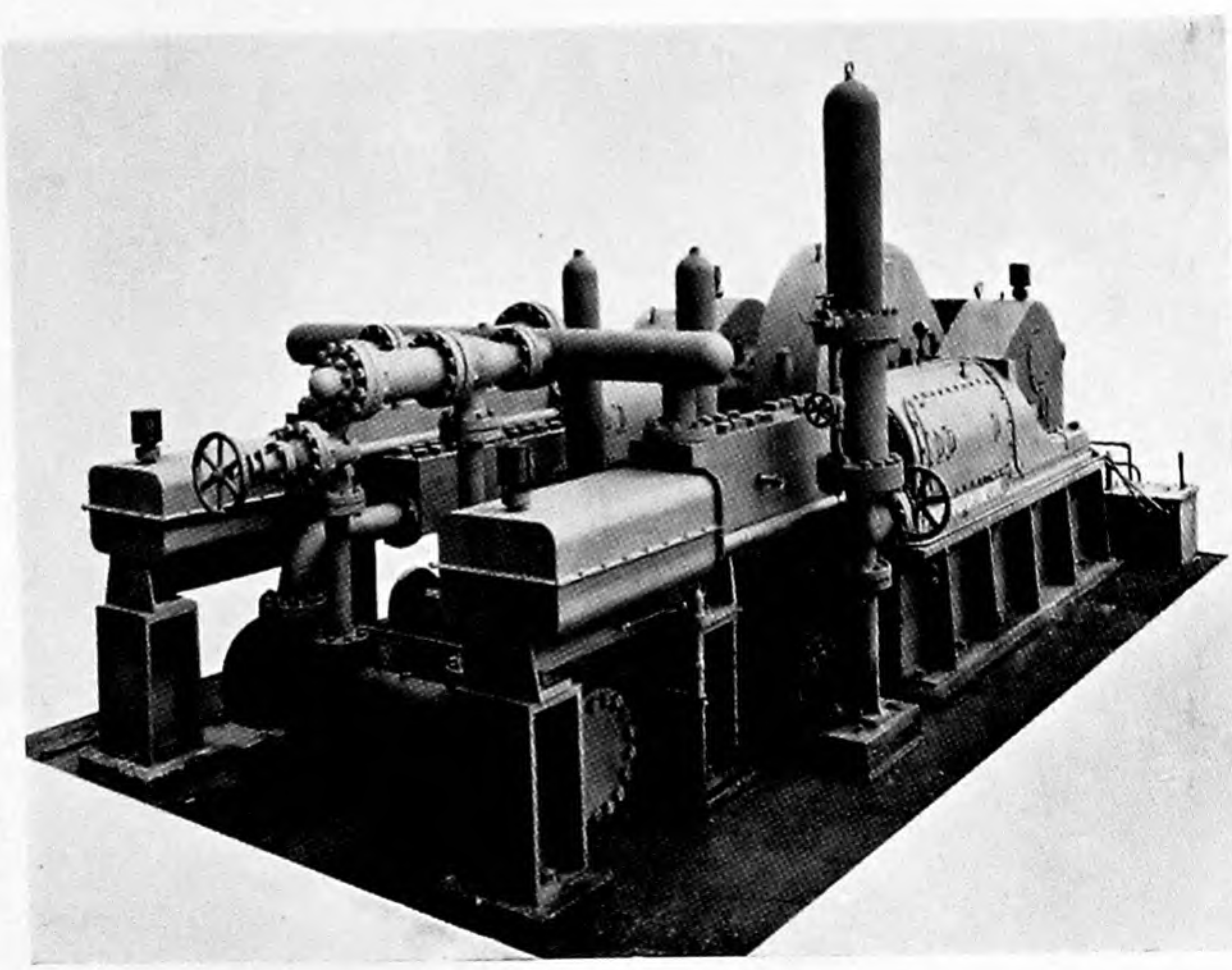

FIG. 325.—Totally-enclosed duplex double-acting oil pump.
(Worthington-Simpson, Ltd.)

[*To face page* 430.

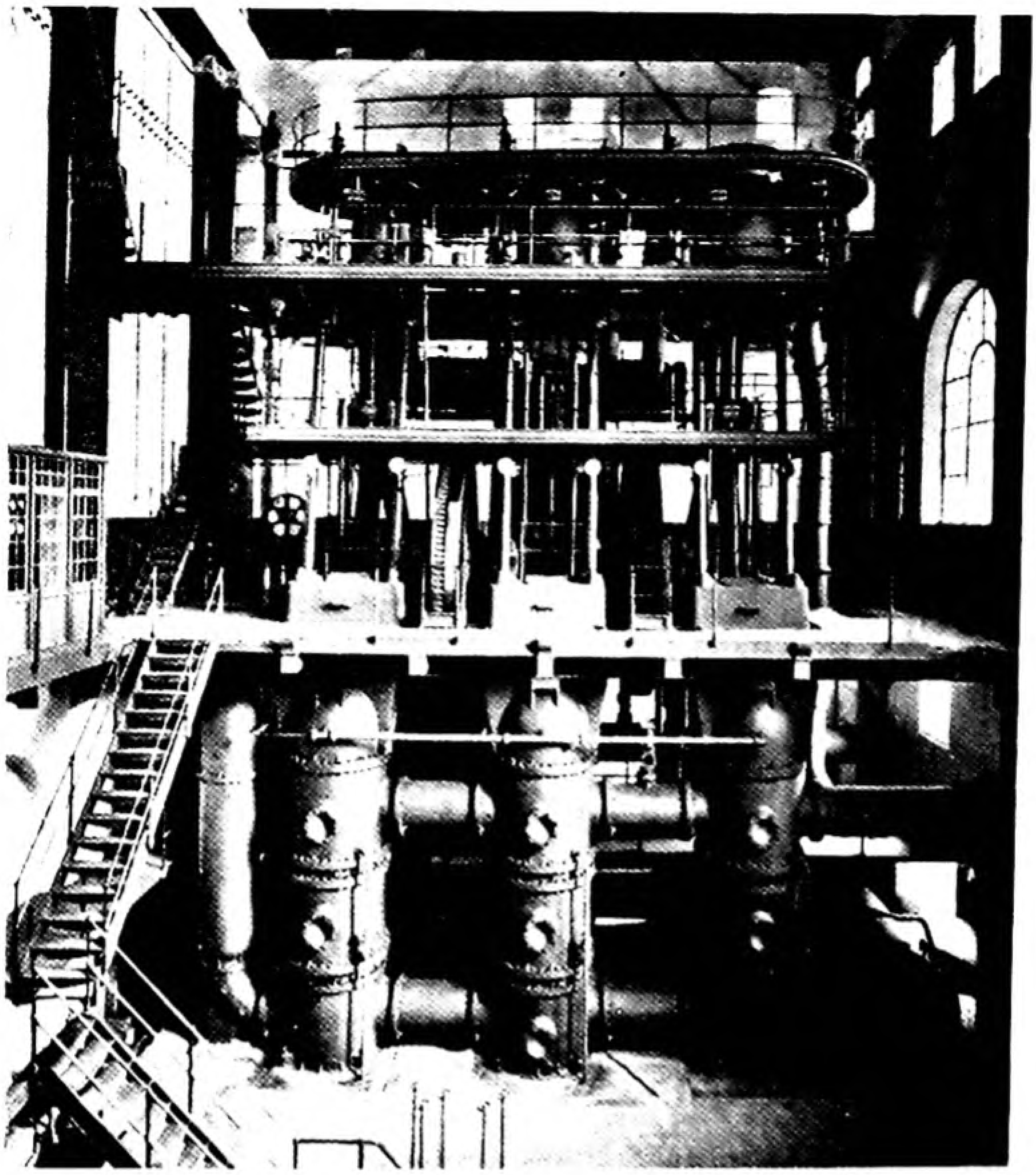

FIG. 328.—High-duty steam pumping engine.
(Hathorn, Davey & Co., Ltd.)

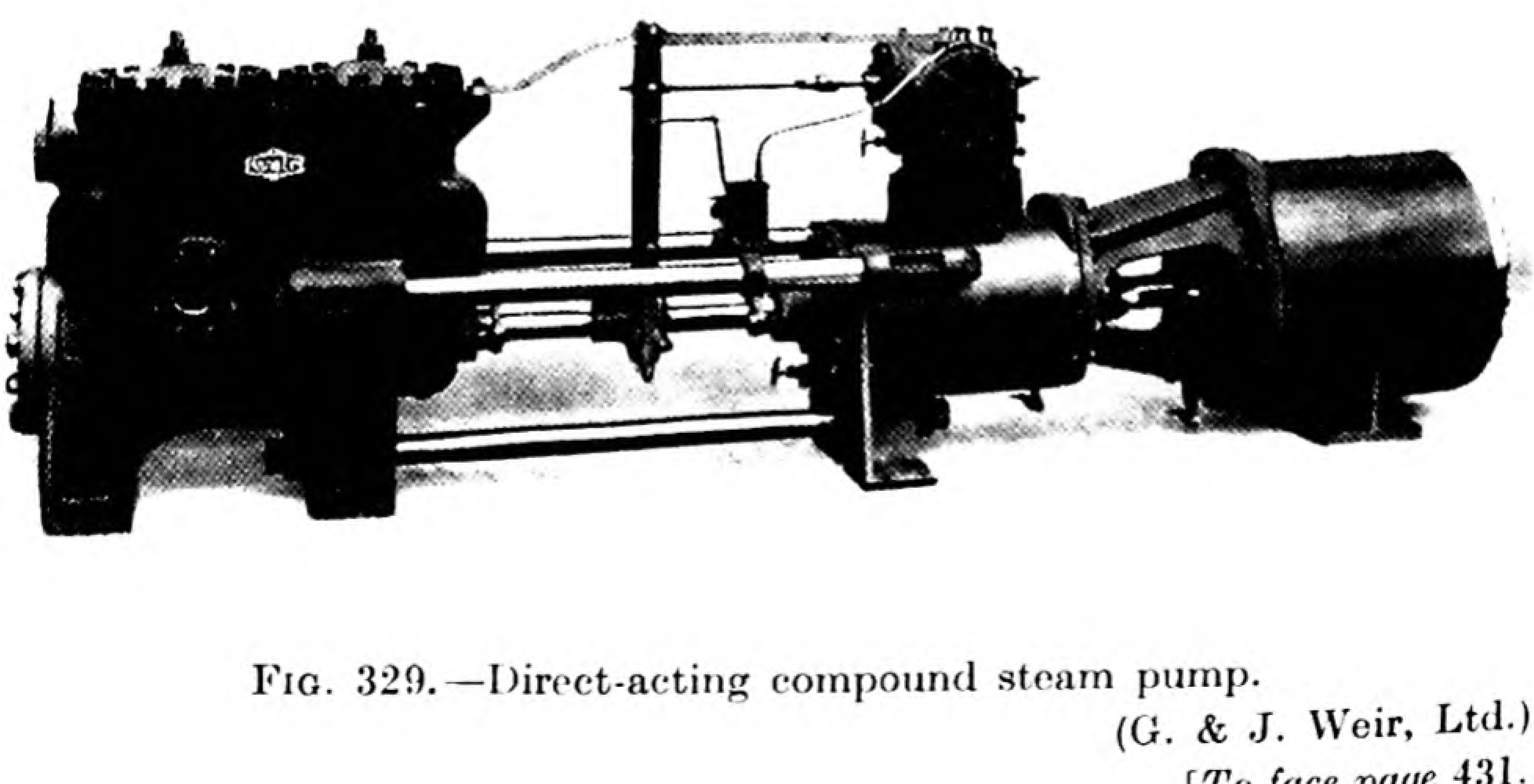

FIG. 329.—Direct-acting compound steam pump.
(G. & J. Weir, Ltd.)

[*To face page* 431.

295. Comparison between Steam Pumps. (i) *Direct-acting pump.* An example of the apparatus described in § 293 is shown in Fig. 329; it represents a compound steam pump designed to force 122 gallons of oil per minute (9·2 lit./sec.) against a pressure of 300 lb./sq. in. (21 kg./sq. cm.) when making 25 double strokes per minute. The double-acting pump cylinder, with suction and delivery valves above it, is seen to the left; above the high-pressure steam cylinder is the steam distribution valve-box, operated by a rocking lever from the main cross-head, and to the right is the low-pressure steam cylinder. For the reasons outlined in § 293, such pumps are particularly suitable for pumping oil, and also for boiler feeding.

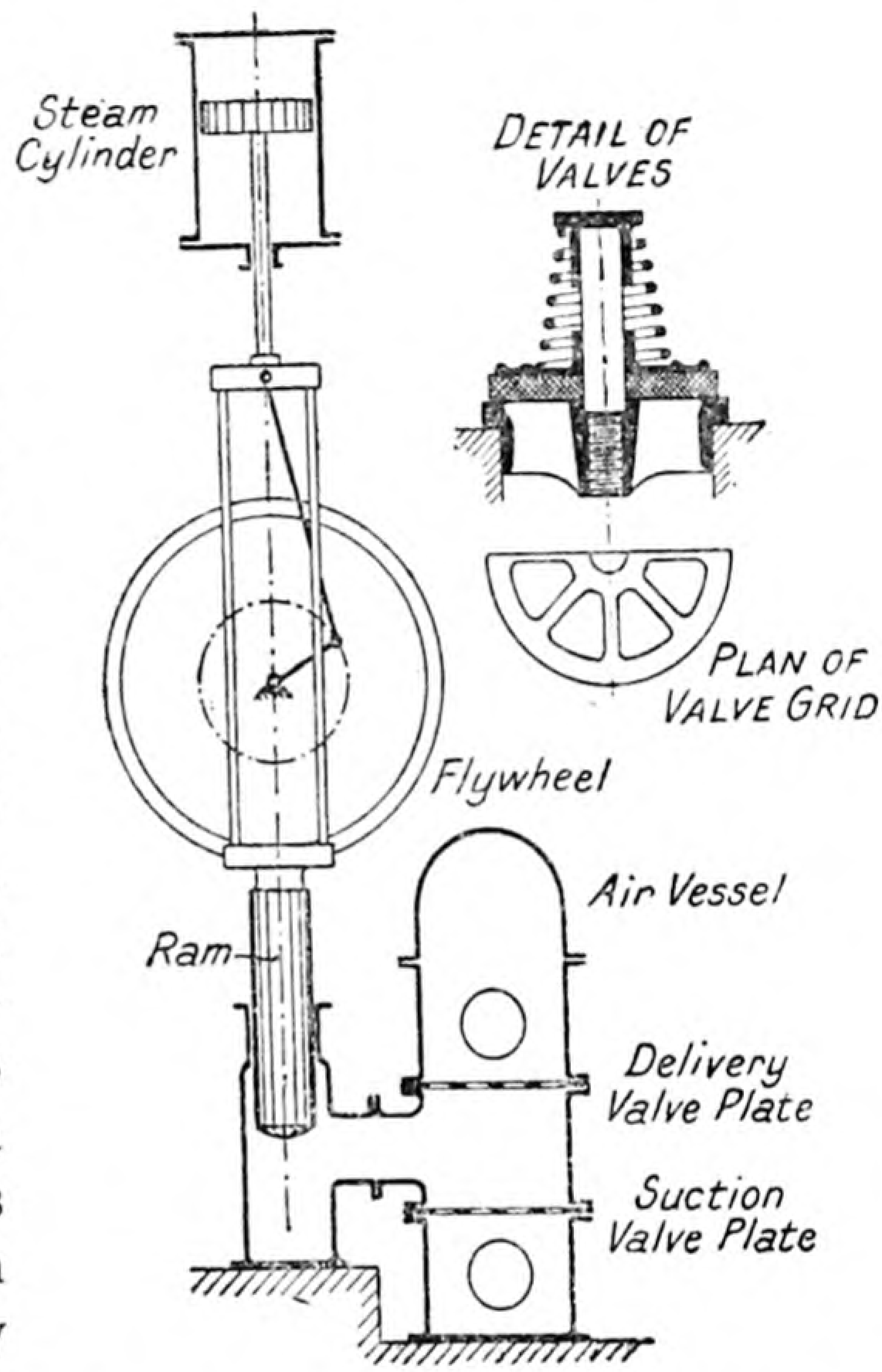

Fig. 327.—Cross-section of rotative steam pumping engine.

(ii) *Triple-expansion waterworks rotative steam pumping-engine.* A fine example of this class of machine is illustrated in the diagrammatic cross-section, Fig. 327, and in Fig. 328. Each of the three steam piston-rods is directly connected to a pump ram immediately below it, and is coupled as well by a connecting rod to the three-throw crank-shaft. Large air vessels fitted to each pump barrel reduce the risk of undue inertia pressures.

Multiple valves are used of the form shown in the diagram (Fig. 327); each consists of a spring-loaded hard rubber disc working on a bronze grid. There may be as many as eighty of these valves in each valve plate. When running at 25 r.p.m., the engine shown in the photograph will lift

16,700 gallons of water per minute (1260 lit./sec.) against a head of 140 ft. (43 m.).

Comparing these two machines, (i) and (ii), the rotative pumping engine would undoubtedly use steam more economically; being designed to run continuously during long periods, its construction would be controlled throughout by this fundamental requirement. But since it is a very costly machine and needs a large and expensive building to accommodate it, such plants are rarely installed nowadays.

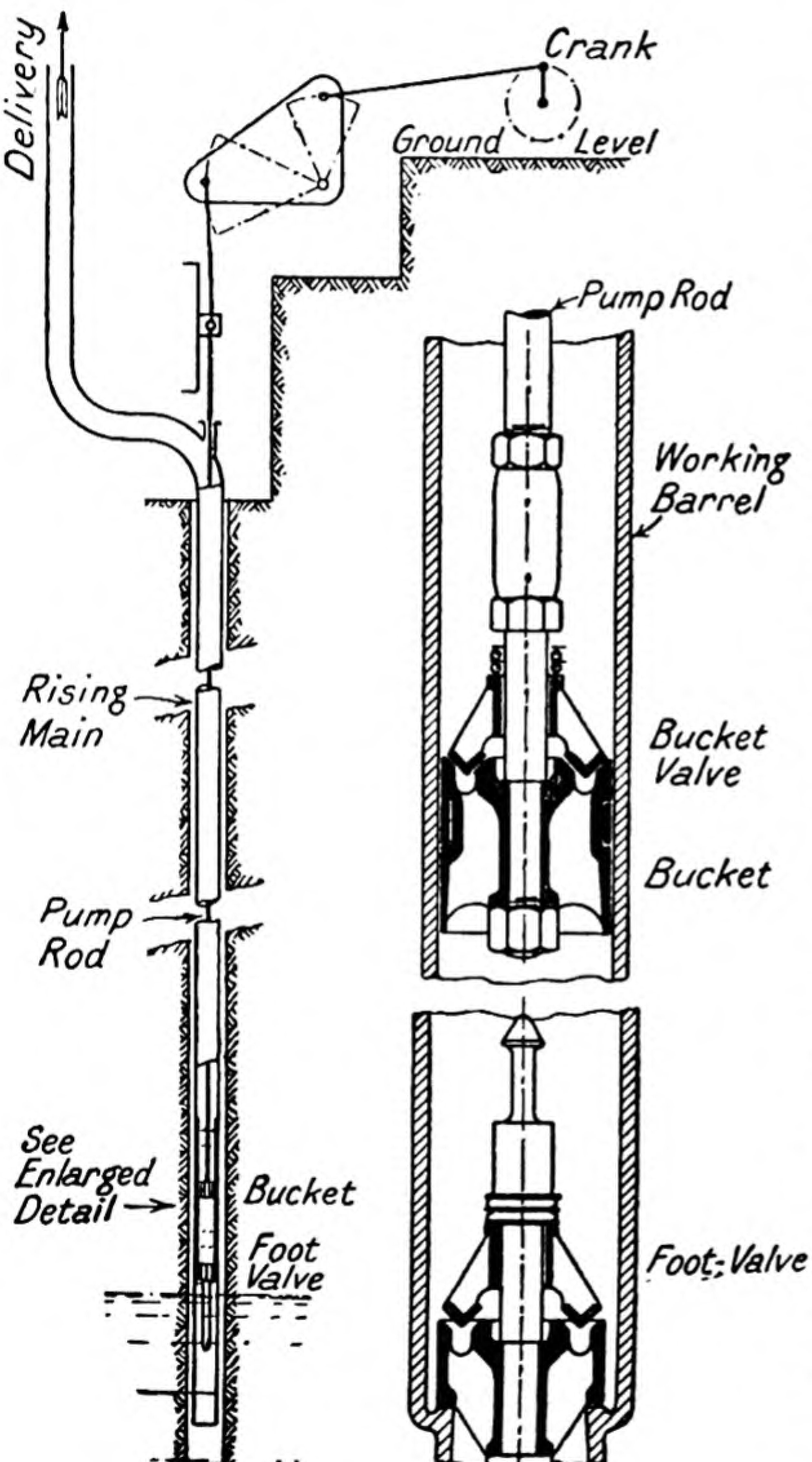

FIG. 330.—Reciprocating bore-hole pump.

296. Bore-Hole Pumps. For raising water from deep-lying underground sources, the arrangement shown diagrammatically in Fig. 330 is suitable; here a crank rotated by an engine or motor at ground level actuates through a connecting rod, quadrant, and vertical pump rod a *bucket* pump fixed at the bottom of a bore-hole. The delivery valve or *bucket valve* takes its seating directly on the piston or *bucket* itself, while the suction valve or *foot valve* rests on the bottom of the working barrel or pump barrel. As indicated in the detail view, both the valves are in this instance of the annular bevelled type, giving a large area for flow with a small lift.

As the pump rod descends, the water in the barrel merely passes from the lower to the upper side of the bucket; on the

upward stroke, the contents of the pump barrel and of the delivery pipe above it are lifted bodily, a fresh charge of water being simultaneously drawn into the barrel through the foot valve. In waterworks installations, a bore-hole pump and a ram or force pump are often used in conjunction, the one lifting the water to ground level, and the other forcing it up into the storage reservoir or into the pressure mains.

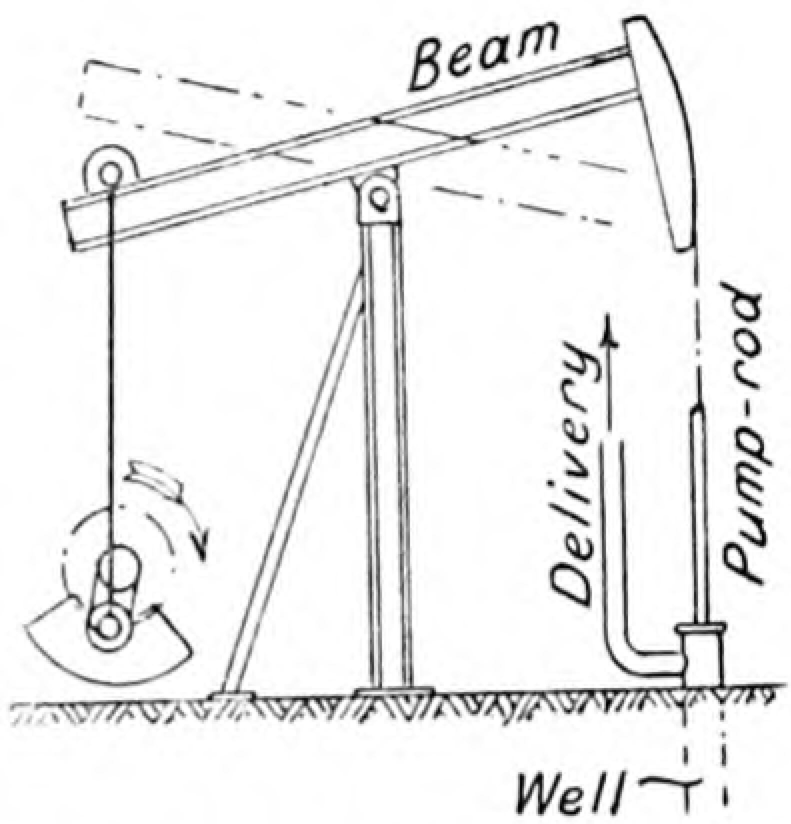

FIG. 331.—Head-gear for reciprocating oil-well pump.

When bore-hole pumps are required for raising oil from oil wells, the head-gear is usually of the type shown in Fig. 331: the rocking-beam is actuated by connecting-rods and twin cranks, driven through gearing by an oil-engine, a gas-engine, or an electric motor.[196]

297. Diaphragm Pumps. Occasionally, reciprocating pumps are provided with a reciprocating flexible diaphragm in place of a reciprocating ram or bucket, thus eliminating friction and leakage at the point where the ram passes through the

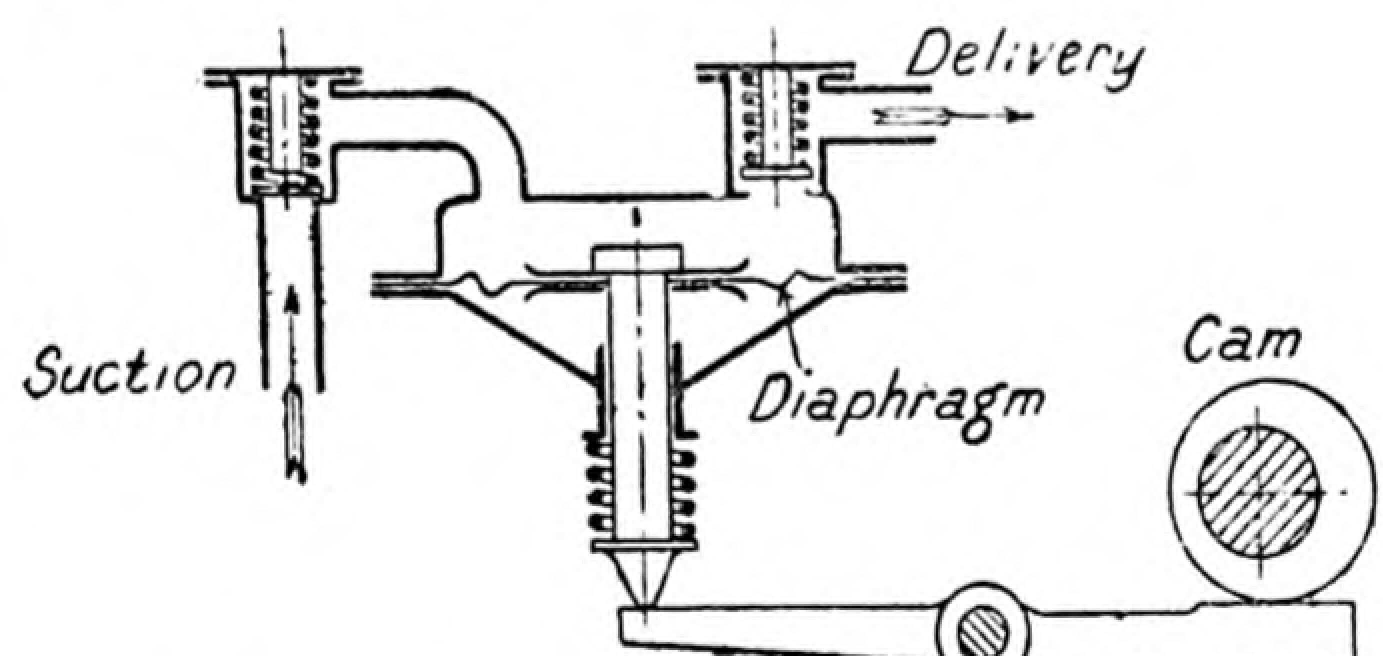

FIG. 332.—Diaphragm pump for petrol.

stuffing box. An example is illustrated in Fig. 332; here the movement of the diaphragm is obtained from an eccentric cam and a lever, the suction and delivery valves operating in the ordinary way. Such pumps are popular for lifting petrol from the rear tanks of motor cars into the carburettors.

The use of a diaphragm as an adjunct to a ram instead of as a substitute for it is exemplified in Fig. 333; like other diaphragm pumps, this pattern is particularly advantageous

for handling dirty or corrosive liquids. Although standard types of reciprocating pump might be adapted to such duties by making the working parts of porcelain, stoneware, or similar refractory material, yet it may be simpler to protect the plunger and gland from any contact whatever with the aggressive liquid. This is done by interposing between the ram and the valve-boxes a flexible india-rubber diaphragm or other type of membrane, as the illustration clearly shows. The ram and gland, working in clean water, are of normal design; the valves and casing may be made acid-resisting by coating them with lead or hard rubber. As the diaphragm is subject to no pressure-*difference*, such pumps are fitted for much higher heads than the simple type shown in Fig. 332. Ball-valves are manifestly better suited to the rough service required of them than wing-guided mitre valves (Fig. 323).

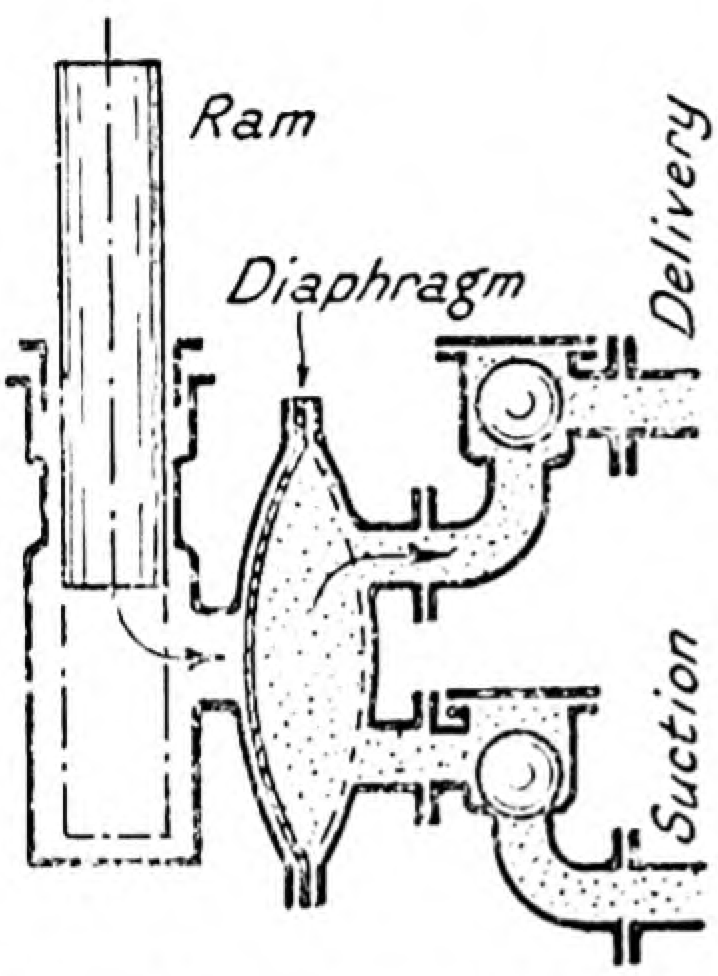

Fig. 333.—Ram-pump fitted with diaphragm.

298. Discharge-regulation of Reciprocating Pumps. The positive characteristic of the constant-speed reciprocating pump—its insistence on forcing into the delivery pipe an unvarying quantity of liquid no matter what the resistance may be—is sometimes inconveniently rigid. Of course, if the pump speed can be varied there is no difficulty whatever: the pump can be driven faster or slower to suit the demand for liquid. But electrically-driven pumps in particular must often run at constant speed. How, then, can we modify the rate of delivery as required ? [197]

(i) *Throttling : Air admission.* Any attempt to reduce the discharge by regulating a throttle-valve on the delivery side would either wreck the pump or stall the motor. Throttling the liquid on the suction side would certainly reduce the output, but the particularly gross form of cavitation set up (§ 290) might be equally disastrous. If cavitation were suppressed by admitting *air* to the pump cylinder through a snifting valve (§ 291), then throttling on the suction pipe would be quite effective. Air admission alone, without valve regulation, may lower the rate of discharge sufficiently. Whether or not the air would create trouble in the delivery system is another matter.

(ii) *Hand-operated by-pass.* The uniform flow that the constant-speed positive pump so obstinately persists in delivering need not all go into the

delivery pipe: we can divert whatever proportion we please back to the suction side again. The arrangement shown in Fig. 334 (i) is convenient when starting a positive pump against the inertia of the water column in a long delivery pipe-line. With the by-pass valve BV fully opened, the pump is run up to speed without special precautions; it circulates the liquid idly against a negligible head, the liquid column in the main pipe being meantime held back by the reflux valve NRV (§ 173). Then the by-pass valve is cautiously closed, the pump delivery pressure slowly builds up against the resistance created in the valve, until finally the pressure is high enough to force open the reflux valve and to apply an accelerating effect on the main liquid column. The isolating valve IV is closed only when the pump is taken off the line for dismantling or repair.

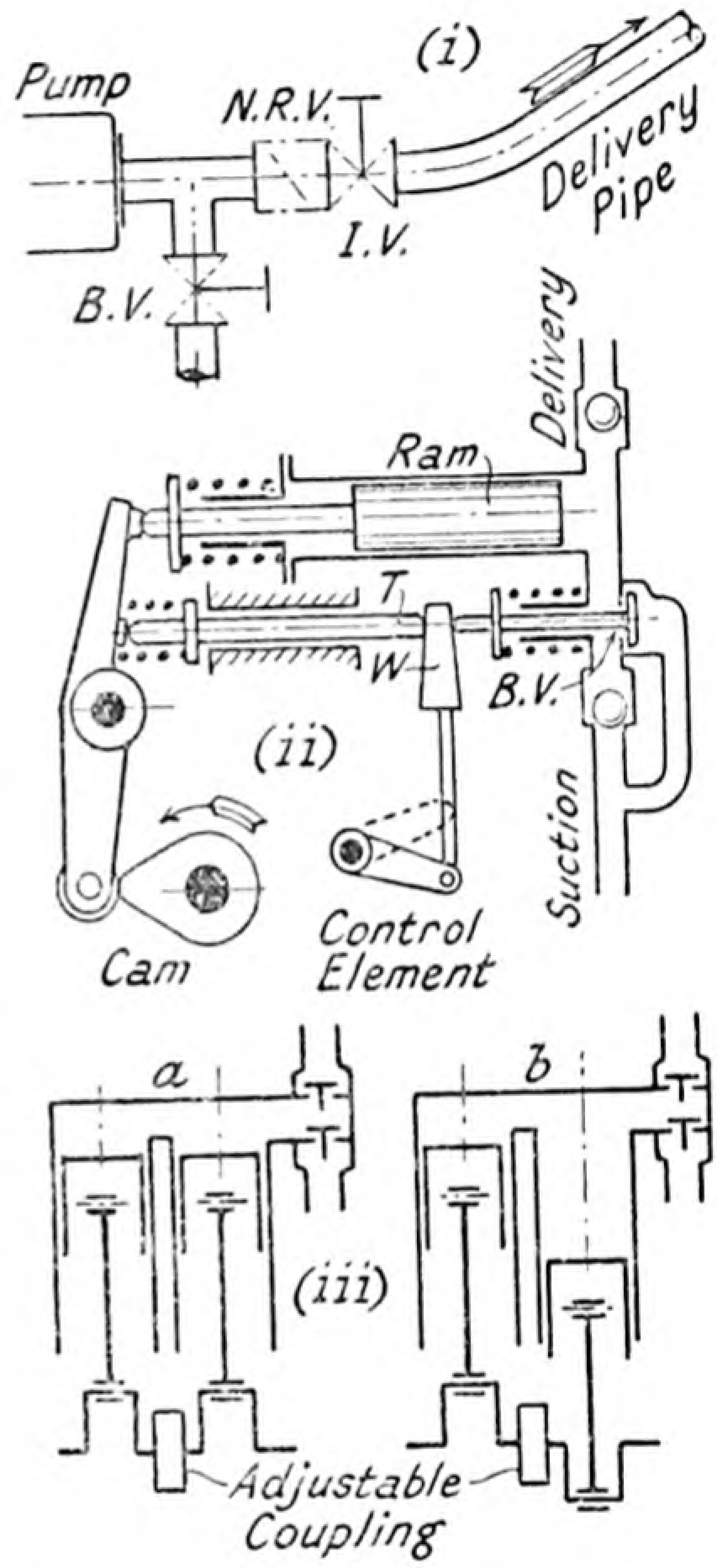

FIG. 334.—Varying the discharge of constant-speed pumps.

(iii) *Spring-loaded by-pass valve.* By substituting for the hand-operated by-pass a spring-loaded relief valve, Fig. 159 (III), then the system becomes automatic. A familiar example is found in the forced-lubrication system of motor-car and similar engines. The relief valve can be set to maintain whatever pressure is desired in the oil piping, and the excess oil beyond what is taken by the bearings is returned to the oil sump through this valve.

(iv) *Positively-controlled by-pass.* The defect of the dispositions just described is that they are almost too successful in destroying the positive character of the pump performance: they leave the rate of discharge too much at the mercy of conditions in the suction or delivery pipe. Occasions arise when we wish to regulate the output of a constant-speed pump in a *positive* manner, so that it will maintain its reduced output just as accurately as it keeps its full output. This can be done by means of a by-pass valve on each individual pump cylinder, which is mechanically opened at a pre-determined point in the delivery stroke. The pump thus measures as well as delivers the liquid fed into it, and for this reason is well adapted for injecting the charge of fuel oil into the cylinders of a compression-ignition engine. The example shown schematically in Fig. 334 (ii), cam-operated and provided with ball valves, is distinctive only because of the by-pass valve BV. This valve remains shut when the pump is giving its full output. It can be opened in varying degrees by raising the control wedge W which then permits the tappet T to come into action. The wedge is actuated either by hand or by the engine speed governor; the higher it rises, the earlier in each delivery stroke the valve BV opens and the smaller the charge of oil delivered.

(v) *Stroke-varying devices, etc.* Another way of positively regulating the discharge of reciprocating pumps running at uniform speed is to vary the stroke of the plunger or ram. It is not always easy to adjust the throw of the crank while the pump is running, but if any kind of rocking-lever or the like element be interposed between the actuating member and the plunger, as in Figs. 332 and 334 (ii), then mechanical difficulties are less serious. The problem is merely that of adjusting the position of the fulcrum of the lever or the points of application of the operating rods. Slow-running pumps can quite successfully be regulated by hand in this manner.

Progress is also being recorded with the system shown diagrammatically in Fig. 334 (iii). Two rams work in a single pump-casing having a single set of valves, each ram having its own crank and connecting-rod. The relative angular position of the two co-axial crank-shafts can be adjusted while the pump is in motion. If the two crank-pins are in line, (*a*), the effective discharge is double that of a single ram; if the cranks are set 180° apart, (*b*), the pump delivers no liquid at all. Intermediate crank-angles will ensure any desired rate of discharge between these limits.[198]

Positive Rotary Pumps.

299. Types of Rotary Pump. So multitudinous are the varieties of this great class of machine that it is difficult to arrange them in an orderly catalogue.[199] But they are usually distinguished from reciprocating pumps in the following ways:

(i) The chambers whose successive filling and emptying produces flow are not stationary; instead, they continuously revolve.

(ii) The rotation of the working chambers automatically opens and closes ports communicating with the suction and delivery pipes, thus rendering valves unnecessary.

(iii) The working chambers coming into action during each pump revolution are numerous enough to reduce inertia shocks to negligible limits (§ 292), so that air vessels are not needed.

(iv) The working chambers need not be cylindrical in shape.

For these reasons positive rotary pumps can run at much higher rotational speeds than reciprocating pumps—4000 r.p.m. is by no means the limit—and they are correspondingly lighter, cheaper, and more compact. Because flexible packing (§ 223 (*a*)) can rarely be provided to form a liquid-tight seal between rubbing surfaces, rotary pumps are more suited to handling viscous liquids such as oil rather than freely-flowing

liquids such as water or spirit. Small units are capable of developing pressures up to 3000 lb./sq. in., the demand for such machines being greatly stimulated by the development of hydraulic-transmission systems (§ 353).

It is essential to remember that the principle of operation of all such rotary machines [200] is completely different from the principle utilised in rotodynamic pumps (Chapters XVI, XVII).

Among the best-known categories of positive rotary pumps are :—

(*a*) Rotating-cylinder pumps, in which cylindrical working chambers are still retained.

(*b*) Vane-pumps.

(*c*) Gear-wheel pumps.

(*d*) Screw-pumps, which depend upon one or more revolving screws.

300. Rotating-cylinder Pumps. (i) *Radial-cylinder type.* In the mechanism illustrated in Fig. 316, § 288, the rotation of the crank makes the ram move in and out of the cylinder. But the reciprocation could be achieved equally well by holding the crank stationary and causing the frame and cylinder to revolve about it. This inversion is given practical form in the design shown in the diagram, Fig. 335. Here, seven cylinders are indicated, though three or any other *odd* number might be chosen; they are bored in a cylinder-block which revolves around a central fixed trunnion. Longitudinal holes in the trunnion constitute respectively suction and delivery ports. They communicate with grooves or slots on the circumferential surface of the trunnion which register with openings at the inner ends of the cylinders. The outer

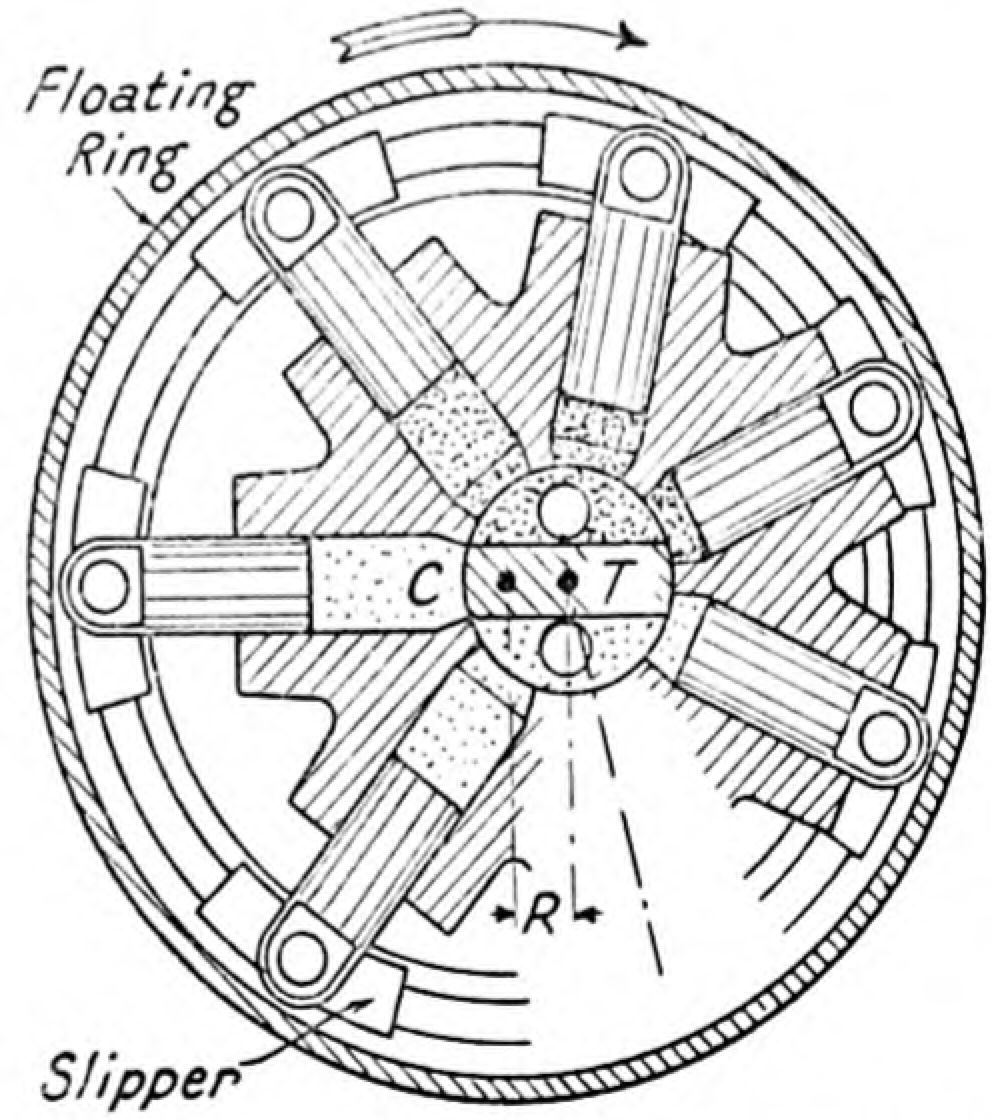

Fig. 335.—Radial-cylinder rotary pump.

ends of the plungers have pivoted slippers engaging with a circular guide-groove cut in a floating ring which freely revolves about an axis C set *eccentrically* with respect to the main trunnion axis T. The offset, eccentricity, or relative displacement of the two axes, R, Fig. 335, corresponds with the throw of the crank, R, in Fig. 316.

When the cylinder-block is driven round clockwise, the plungers that happen to lie below the centre-line are drawn out of their respective cylinders, while those above the centre-line are forced in. The result is to draw in charges of liquid during the lower half of the revolution, and to expel them during the upper half. This ensures a virtually uniform flow of liquid *in* at the suction port and *out* at the delivery port.

(ii) *Parallel-cylinder pump.* Here the multiple cylinders A have their axes parallel one with the other, and also parallel with the axis of rotation of the cylinder block (Figs. 336, 337).

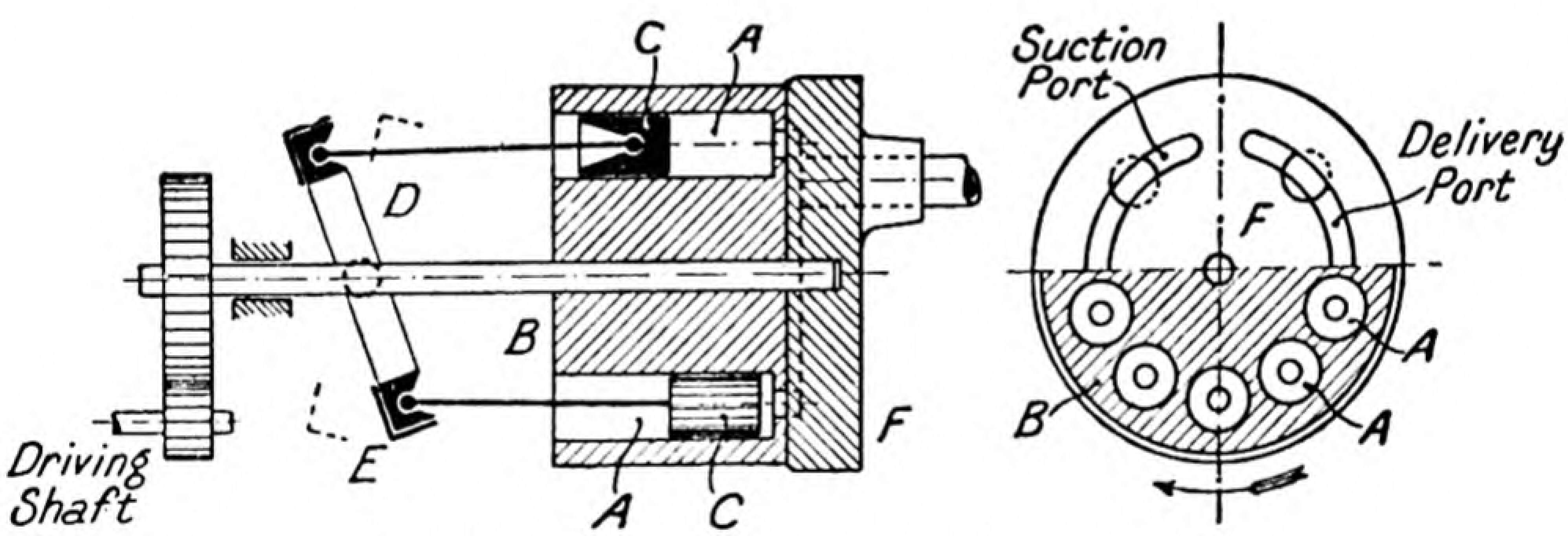

FIG. 336.—Parallel-cylinder rotary pump.

The pistons or plungers C are linked to the ring D by ball-jointed connecting-rods; the ring D revolves in a housing E at the same rotational speed as the cylinder-block B. The housing E can be tilted out of the perpendicular, and it is this angular tilt that causes the pistons to reciprocate in their respective cylinders. Manifestly the fixed plate F, with its crescent-shaped suction and delivery ports, correspond functionally with the fixed trunnion-block in Fig. 335.

These two types of rotating-cylinder pump are often distinguished by the titles (i) Hele-Shaw-Beacham (radial-cylinder), and (ii) Williams-Janney (parallel-cylinder).

301. Discharge-regulation of Rotating-cylinder Pumps. A valuable attribute of the machines just described

is that they may easily be modified so as to serve as constant-speed variable-delivery positive pumps ; [201] they offer a more elegant solution of this particular problem than is usually possible with reciprocating pumps (§ 298). Not only may the rate of discharge be varied from full-flow to zero while the pump is running steadily, irrespective of the pressure, but the direction of the flow may be reversed—liquid now enters by what was previously the delivery port. In the radial-cylinder machine, Fig. 335, these effects are achieved by mounting the bearings of the outer guide-ring in such a way that the eccentricity R can be adjusted. When this distance has been brought down to zero—when the guide-ring is concentric with the trunnion and with the cylinder block—delivery ceases altogether ; when the guide-ring bearings have been shifted still further to the right, reversal of flow begins. In the parallel-cylinder pump, Fig. 336, the angle of tilt of the housing E is adjusted by moving it about its horizontal axis which intersects at right angles the main axis of the pump. The position shown by broken lines corresponds to reversed flow.

If positive characteristics are not wanted, then the rate of flow can be put under the control of the delivery pressure; as the pressure rises the discharge declines, until at a pre-determined maximum pressure the pump merely maintains this pressure without delivering liquid. The dissected view, Fig. 337 (facing p. 442), indicates how the parallel-cylinder pump can be made to behave in this way. A small auxiliary cylinder distinguishable in the upper part of the illustration contains a piston which exerts on the tilting control-plate or housing E a thrust in opposition to the thrust of the pair of powerful helical springs seen below. As the control-cylinder is in communication with the delivery pipe the force on the piston mounts in response to the rise in pressure, and thus the tilting housing is progressively brought to the vertical or stalled position.

When pumping lubricating oil, such pumps are credited with full-load overall efficiencies up to 80 per cent., the delivery pressure being of the order of 500 lb./sq. in.

It is to be noted that rotating-cylinder pumps are reversible in another sense from that suggested above ; they belong to the class of machines mentioned in § 218 that can serve either as pumps or as hydraulic motors.

302. Vane-type Pumps. The rotating parts of these machines are designed to sweep the liquid through the passages in a nearly uniform stream. Referring to Fig. 338, a revolving element is mounted *eccentrically* within a cylindrical casing. Multiple flat radial vanes can slide freely in diametral slots formed in the rotor; each working chamber is thus formed by a pair of adjacent vanes, the flat ends of the casing and the inner and outer cylindrical surfaces. It is because of the increase in volume of each chamber as it travels round the suction side of the casing, and the subsequent reduction on the delivery side, that liquid is drawn in and then forced out again. The basic system of a plunger working to and fro in a fixed cylindrical barrel has now been finally abandoned.

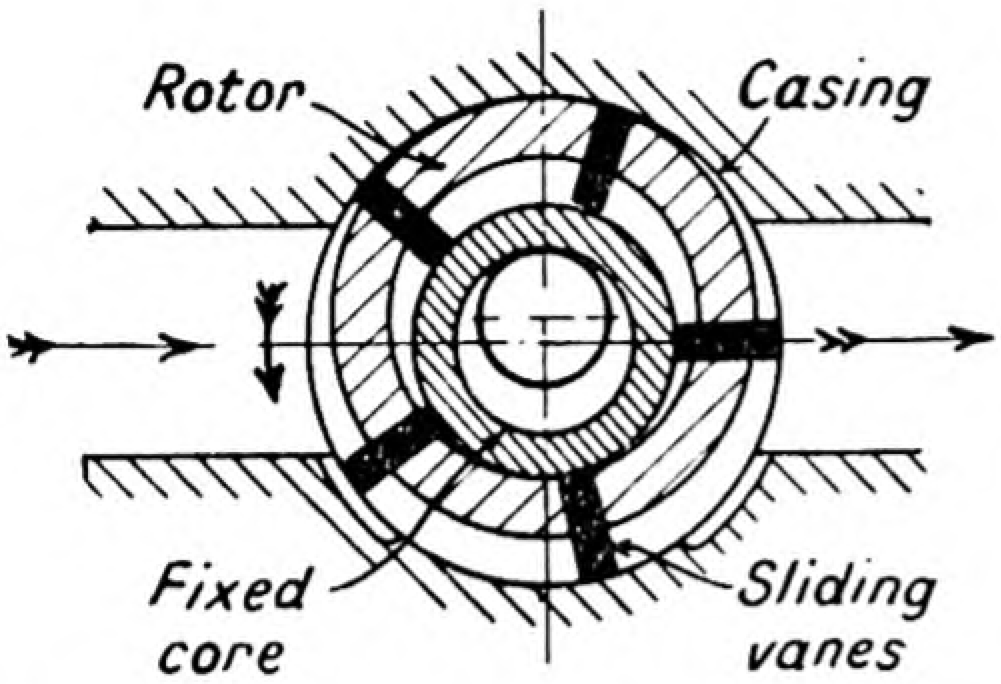

Fig. 338.—Principle of operation of Vane-type rotary pump.

A more robust type of vane-wheel pump embodies a concentrically-mounted rotor having two blades which work between the outer cylindrical casing and a central core, Fig. 339. To prevent return flow of the liquid, an additional rotating sealing member is added; it is driven by external timing gears at the same speed as the main rotor, but in the opposite direction. Recesses in the sealing member accommodate the vanes of the main rotor.

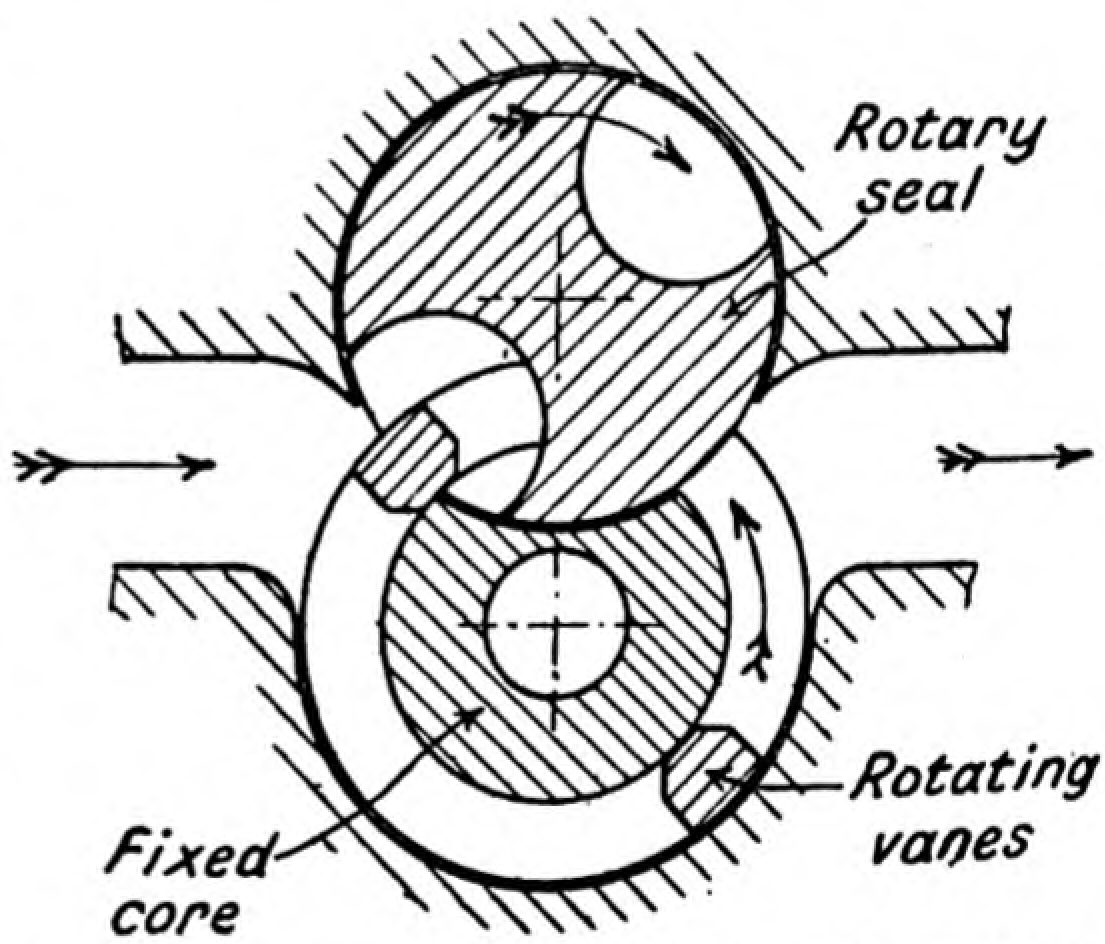

Fig. 339.—Vane-type pump with rotary sealing member.

An advantage of this arrangement is that discharge regulation at constant speed can readily be contrived. One end of the casing is adjustable axially, thus reducing the effective width of the casing and diminishing the rate of discharge proportionately.

303. Gear-wheel Pumps. A slight modification to the vane-type pump seen in Fig. 339 brings us to the gear-wheel pump, Fig. 340. It consists essentially of two identical inter-meshing spur pinions working with a fine clearance inside a suitably-shaped casing, Fig. 340. One of the pinions is keyed

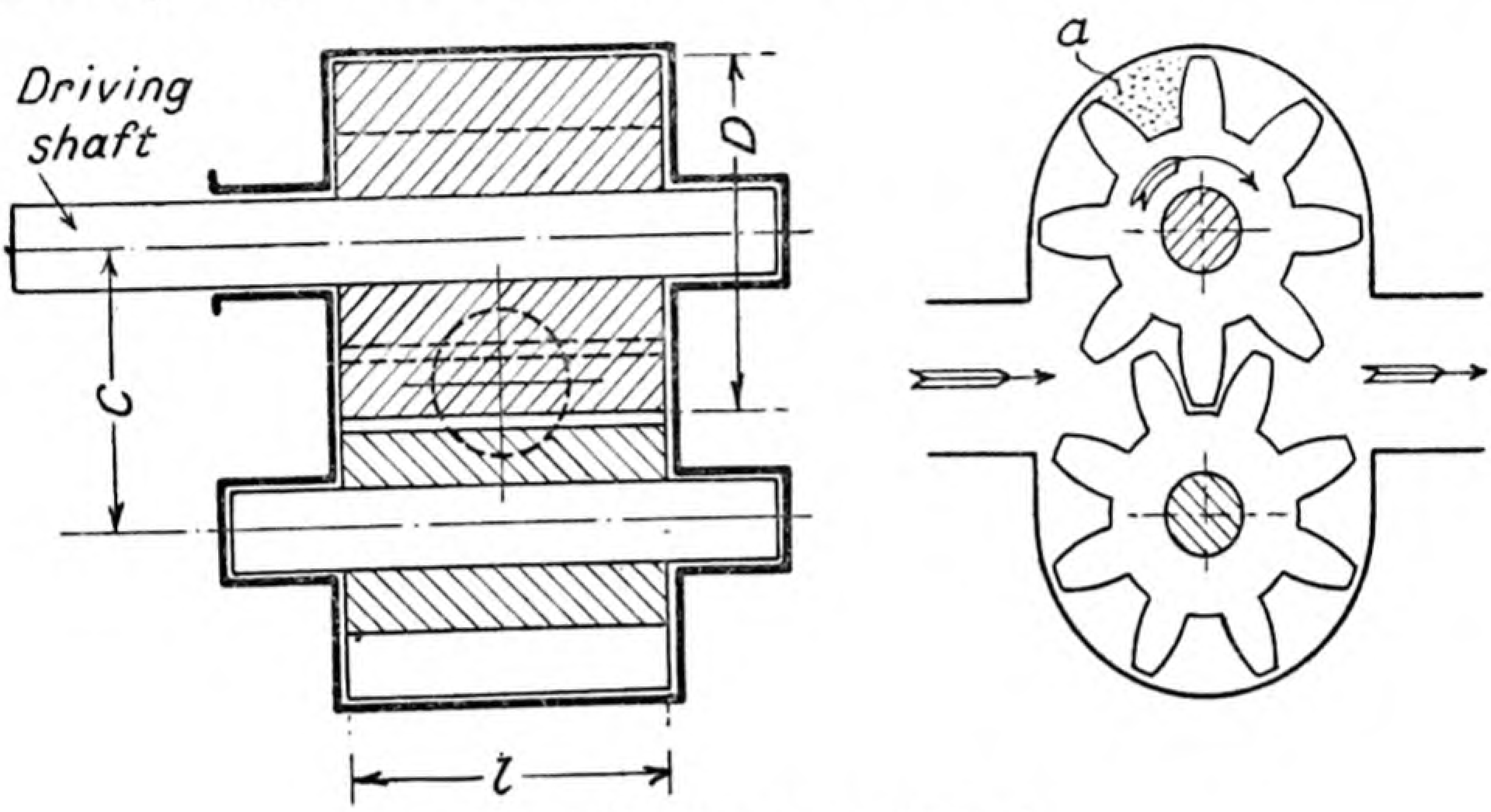

FIG. 340.—Gear-wheel pump.

to the driving shaft or is formed integrally with it, and the other pinion usually revolves idly; but in machines intended for heavy duties the two working pinions may be connected by external timing gears as in the pump shown in Fig. 339.

If a = area enclosed between any two adjacent teeth and the casing, i.e. the stippled area in the diagram,
l = axial length of teeth,
n = number of teeth in each pinion,
N = rotational speed in r.p.m.,
η_v = volumetric efficiency, §220,

then at each revolution a volume of liquid represented by $2aln$ should be carried round from the suction to the delivery side of the pump. The ideal discharge per second will be $\frac{2alnN}{60}$, and the actual discharge is $\frac{2alnN\eta_v}{60}$. This expression is not of great practical utility because of the difficulty of correctly estimating the area a; the *effective* area should take into account the liquid trapped between the inter-meshing teeth and carried back to the suction side of the pump. A more convenient way of assessing the volumetric displacement is as follows :—

If D = outside diameter of rotors,
C = centre-to-centre distance between axes of rotors,

then *volumetric displacement of pump per revolution*

$$= 0{\cdot}95\ \pi C(D - C)l \text{ (approximately)}$$

Still speaking in approximate terms, it is useful to remember that the dimensions D and C, and the number of teeth per rotor, are related in some such manner as this :—

Number of teeth .	7	10	13	18
Value of D/C .	1·28	1·21	1·16	1·12

Evidently, then, an increase in the number of rotor teeth will mean a bigger rotor outside diameter for a given displacement per unit of length of tooth. **(Example 153.)**

Small gear-wheel pumps will work against pressures of 2000 lb./sq. in. or more if specially designed for the purpose.[202] Low pressure units can be built in sizes delivering up to 1000 gals./ min. (75 lit./sec.) per pump.

Variations in construction which may be found advantageous are :—

Herring-bone teeth. Pumps with straight spur-pinions are apt to be noisy, because of the difficulty of providing a path of escape for the liquid trapped between the inter-meshing teeth. Careful design minimises the trouble, but the best way to secure quiet running is to cut the gear teeth in herring-bone or double-helical fashion.

Multi-stage pumps. For high-pressure pumps, excessive loading of the working parts can be avoided by disposing two or three units in series. As the rotors remain co-axial, and all intercommunicating passages are formed within a common casing, the machine still remains compact.

Internal gear. Here the driving pinion meshes with an internal gear-ring. In the Stone-Paramor design, Fig. 341, the pinion has four teeth and the idling gear-ring six teeth ; a fixed crescent-shaped tongue prevents return flow of liquid from delivery to suction side.

Positive Pump Characteristics.

304. Performance of Positive Pumps. The fundamental laws of positive pump performance, exposed in earlier paragraphs, can now be summarised in the graphs, Fig. 342. These

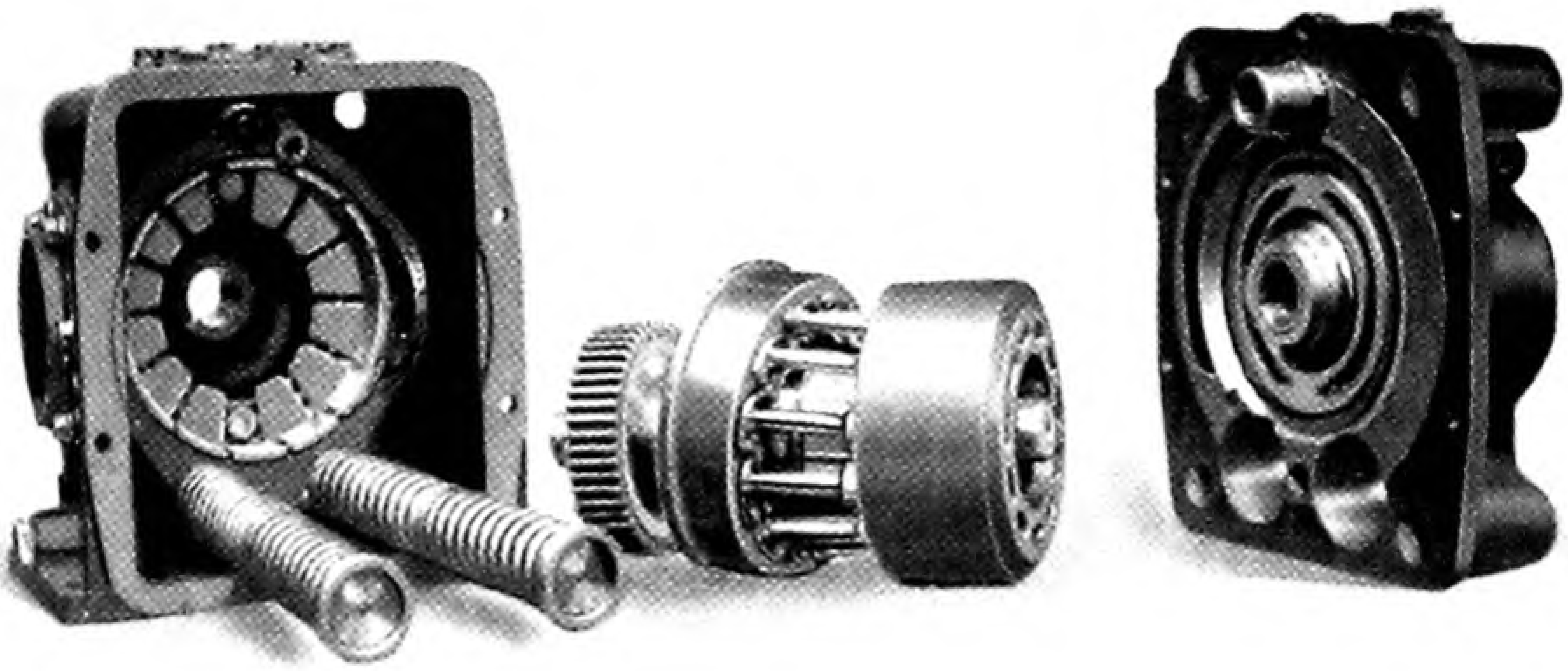

FIG. 337.—Rotary Multi-cylinder variable-delivery pump.
(See page 439.)
(The Variable Speed Gear Co., Ltd.)

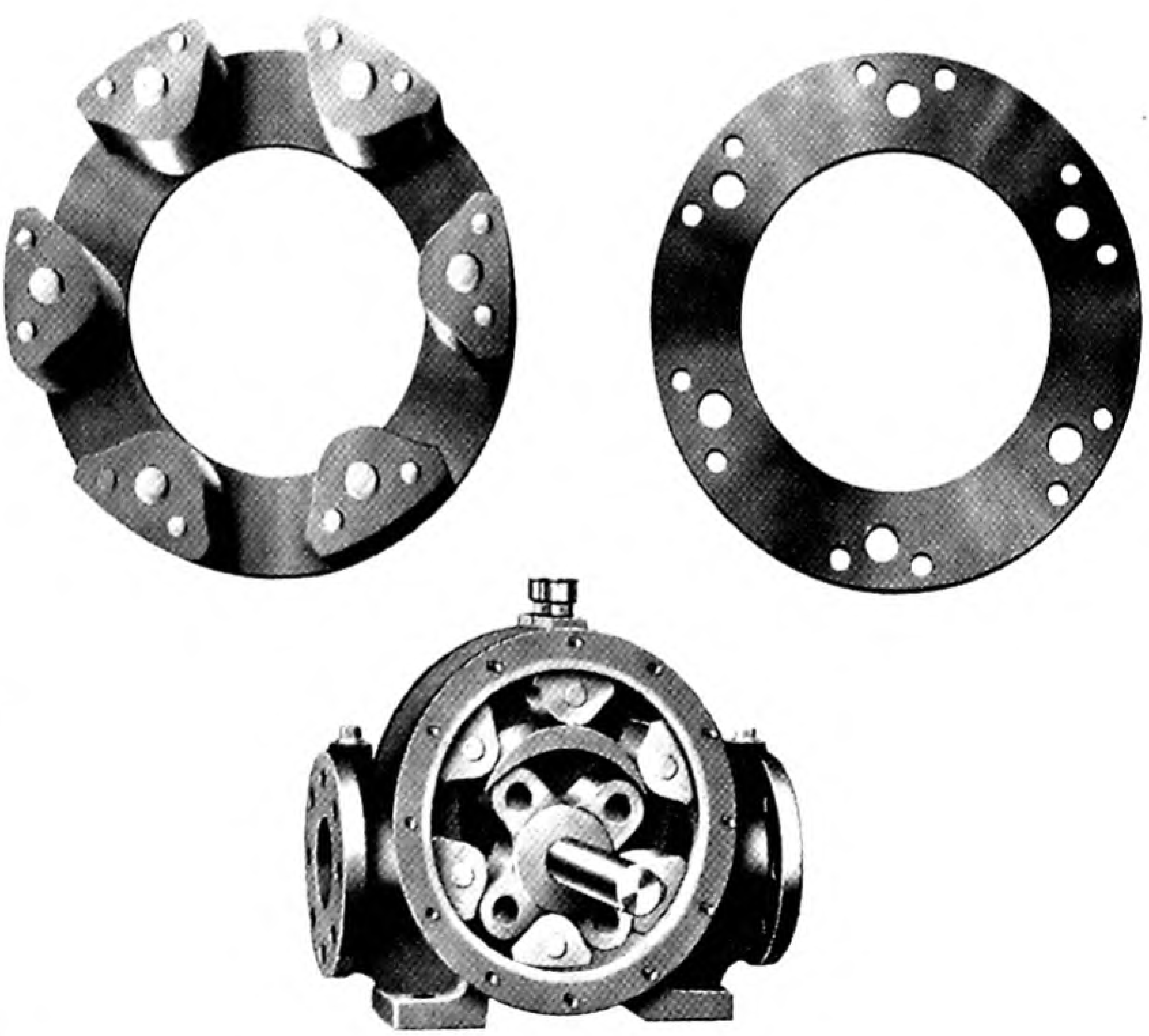

FIG. 341.—Internal-gear type of positive rotary pump.
(J. Stone & Co., Ltd.)
[*To face page* **442.**

diagrams show that under ideal conditions: (*a*) the discharge of the pump at constant speed is independent of the pressure, (*b*) the discharge varies directly as the speed, and (*c*) the input and output power at constant speed vary directly as the pressure (§§ 220, 285). As soon as the effect of slip or leakage is taken into account, § 288, the pressure-discharge curve begins to droop: it is represented by the broken line in Fig. 342 (*a*), instead of by the ideal horizontal full line.

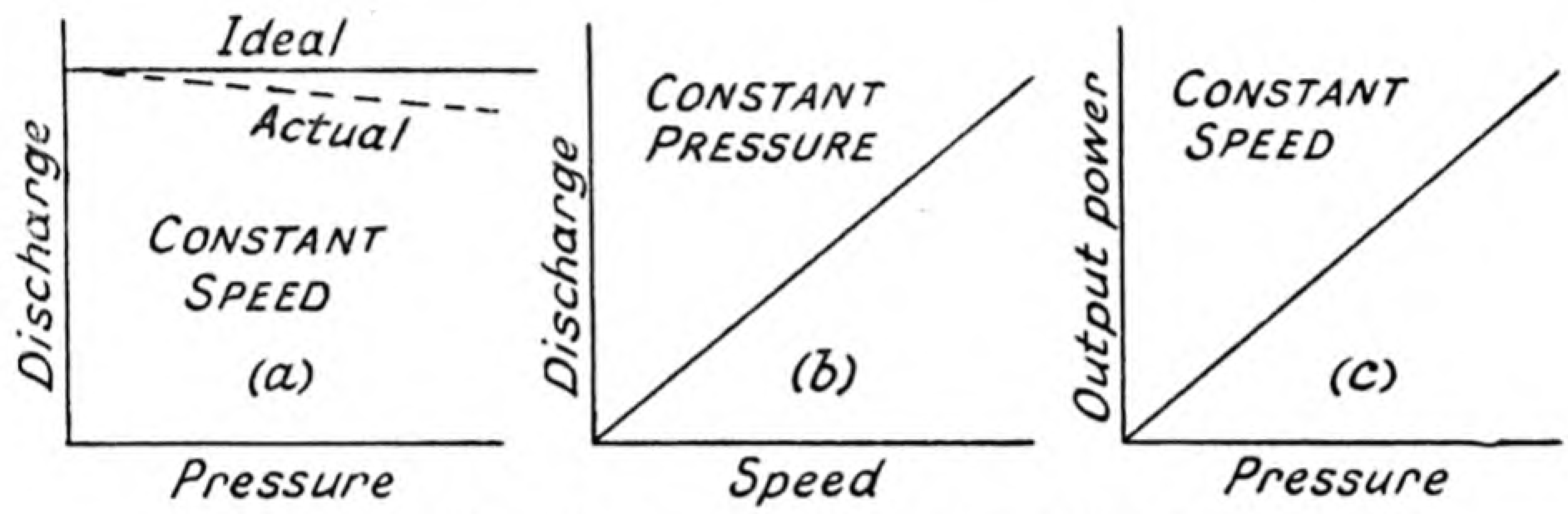

FIG. 342.—Ideal performance of positive pump.

The ratio of the actual to the ideal discharge, or the *volumetric efficiency* of the pump, § 220, may range from 0·98 in well-maintained reciprocating pumps to 0·85 in gear-wheel pumps.

In order to estimate the overall pump performance,[(191)] we refer to § 221 and find that in present conditions the energy losses to be expected comprise (i) mechanical losses, (iii) leakage losses, and (iv) hydraulic losses. (Disc friction losses, (ii), if they occur at all, can be conveniently included among hydraulic losses.) Although it is only in exceptional circumstances that these individual sources of energy dissipation can be assessed numerically, yet we can form some impression of their general trend: if the pump is run at *constant speed, varying pressure*, and (nearly) *uniform discharge*, then it is to be expected that (I) the hydraulic loss will remain substantially unchanged, (II) both the mechanical loss and the leakage loss will increase as the effective pressure-difference rises. On this basis the ideal graph, Fig. 342 (*c*), can be corrected as shown in Fig. 343 (*a*), which indicates in a conventionalised way the response of input and output power to pressure changes. The corresponding changes in overall efficiency, plotted from diagram (*a*), are given in Fig. 343 (*b*).

Turning now to results obtained from typical pumps, Fig. 344, these agree sufficiently well with the curves derived from analysis. As we should expect, a carefully-constructed reciprocating pump, (*A*), gives the highest efficiency through out the whole range of performance, and the gear-wheel pump

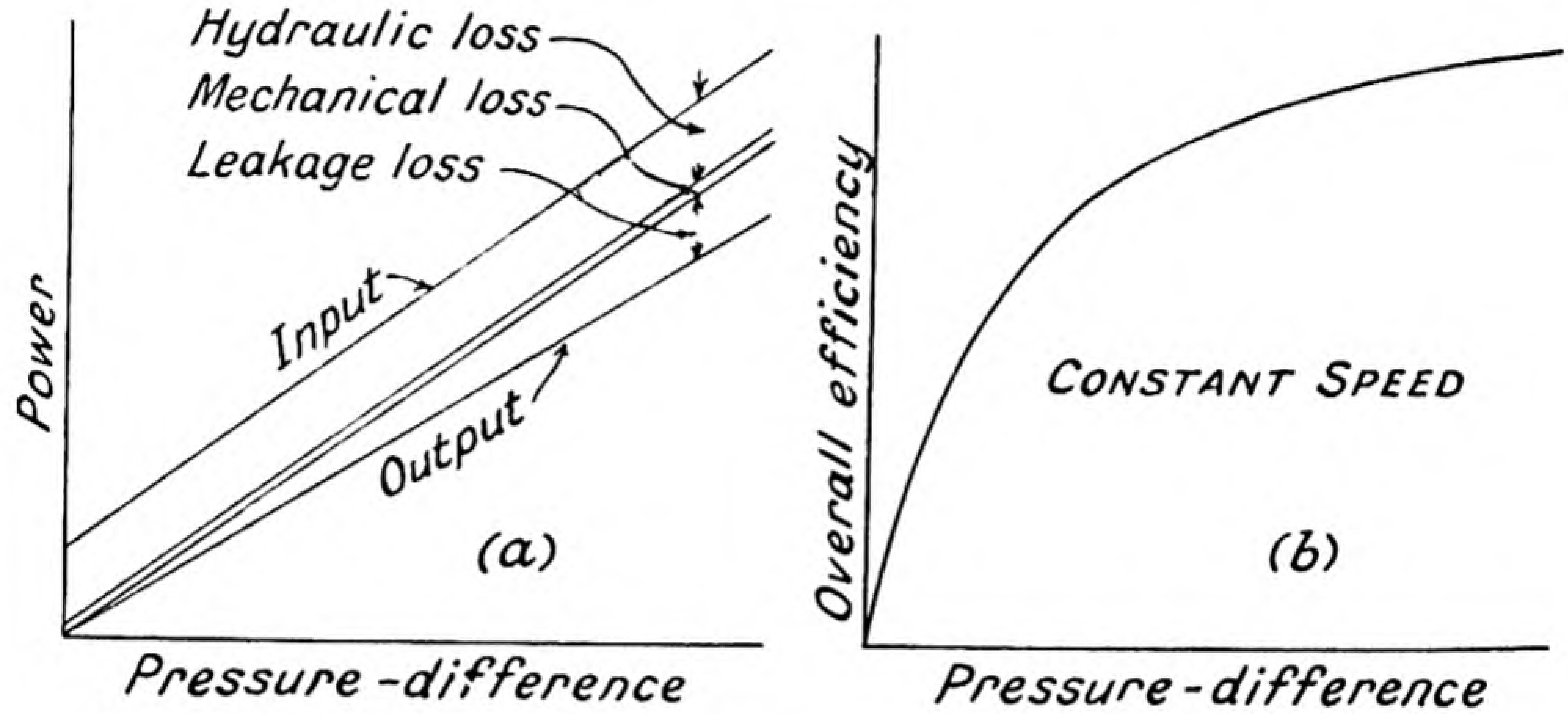

FIG. 343.—Power and efficiency of positive pump at constant speed.

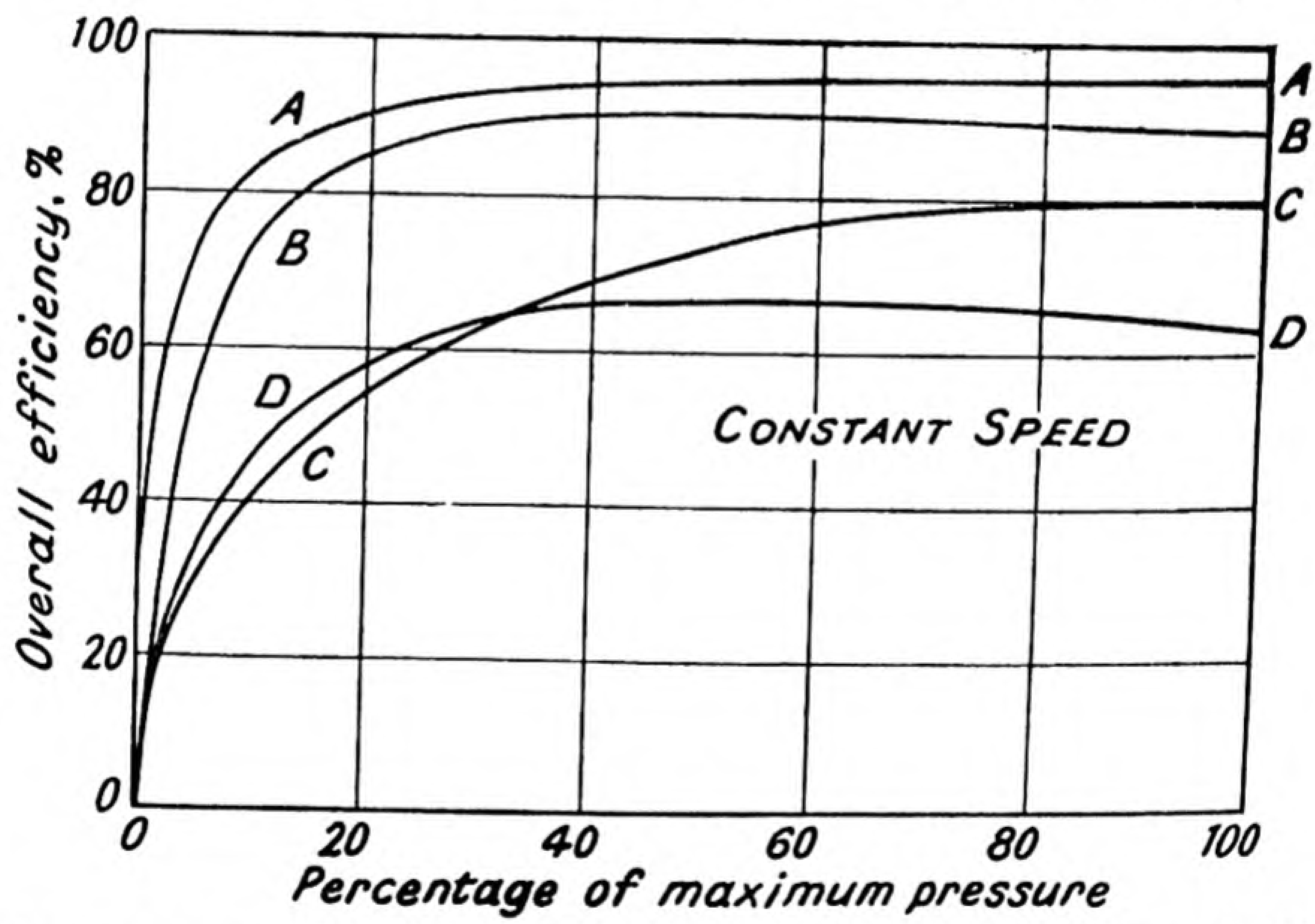

FIG. 344.—Typical performance of oil pumps: (*A*) Reciprocating; (*B*) Vane type; (*C*), (*D*), Gear-wheel.

(*C*) and (*D*), the lowest; intermediate between the two types is the vane-type of pump, (*B*), working under optimum conditions. All the curves relate to machines pumping oil; but a large 3-throw pump forcing water against a high pressure, Figs. 324 or 414, would yield an efficiency curve only slightly below curve (*A*) in Fig. 344 (see, for example, Fig. 410).

305. Effect of Speed, Viscosity, Suction Lift, etc. (i) *Speed.* Considering next a pump running at *varying* speed against a *uniform* pressure, its output power or W.H.P. is likely to be proportional to the speed. The leakage power loss may be little affected by the speed, and the mechanical loss may be expected to increase with the speed. It is the hydraulic power loss which will be most seriously altered: if the flow through the pump passages is turbulent, this loss will vary (nearly) as the *cube* of the discharge (§ 91); and even for laminar flow the loss will vary as the *square* of the speed (for discharge here depends directly upon speed, Fig. 342 (*b*)). If, then, the hydraulic energy loss is a substantial proportion of the gross energy loss in the pump, it follows that as the pump speed *increases* the overall efficiency will *drop*. This effect is very manifest in Fig. 345. Two curves are plotted to show the performance of a gearwheel pump; but no matter whether a high-viscosity oil or a low-viscosity oil is used, the overall efficiency declines quite unmistakably as the speed rises.

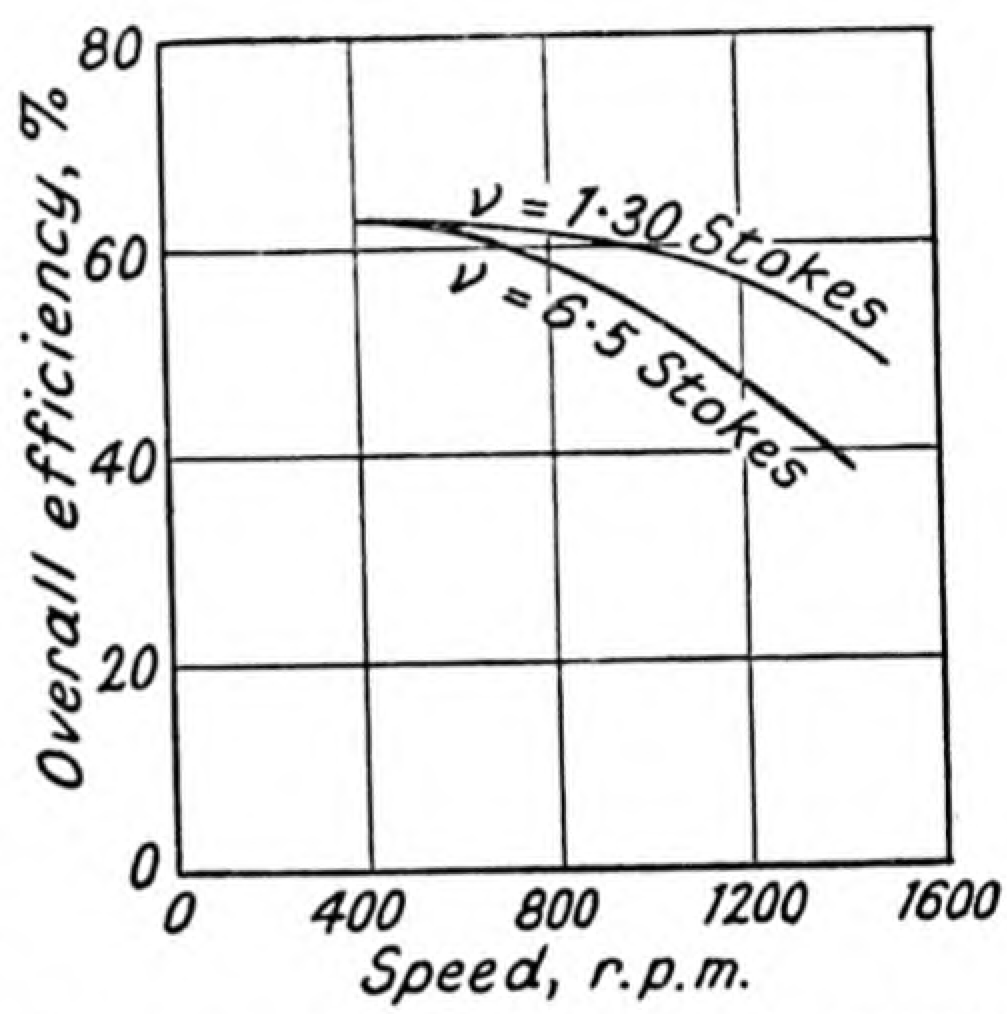

FIG. 345.—Effect of speed and viscosity on gear-wheel pump performance.

(ii) *Viscosity.* At first sight it does not seem easy to predict how a change in viscosity of the liquid will influence the pump performance. One would expect a "thickening" of the liquid to reduce the leakage loss, while on the other hand it might increase the hydraulic loss. If the latter effect preponderated, then an increase in liquid viscosity would reduce the pump efficiency. Such a correlation is certainly to be observed in the graphs reproduced in Fig. 345: for a given speed and pressure, the overall efficiency of the gearwheel pump when the liquid has a viscosity of 6·5 stokes is sensibly below the efficiency corresponding to a viscosity of 1·3 stokes.

(iii) *Complete pump characteristic.* Analysis suggests that the most effective way of treating pressure, speed and

viscosity is to examine them in conjunction instead of separately.[203]

This becomes possible if simplifying assumptions are accepted: these are, that both the main flow and the leakage flow throughout all the pump passages is laminar, and that the mechanical energy loss is negligibly small. It can then be shown that the pump gross efficiency η_m depends *only* upon the value of the non-dimensional expression or characteristic number $\dfrac{\mu n}{p}$

where μ = liquid viscosity,

n = pump speed in revs. per second,

p = effective pressure-difference.

To ensure that consistent units are chosen, § 40, it would be convenient to express viscosity in *poises*, and pressure-difference in *dynes per square centimetre.* As the pump characteristic number changes, so will the overall efficiency; and if the one is plotted against the other, the resulting characteristic curve should show how the pump will behave throughout its complete range of performance.

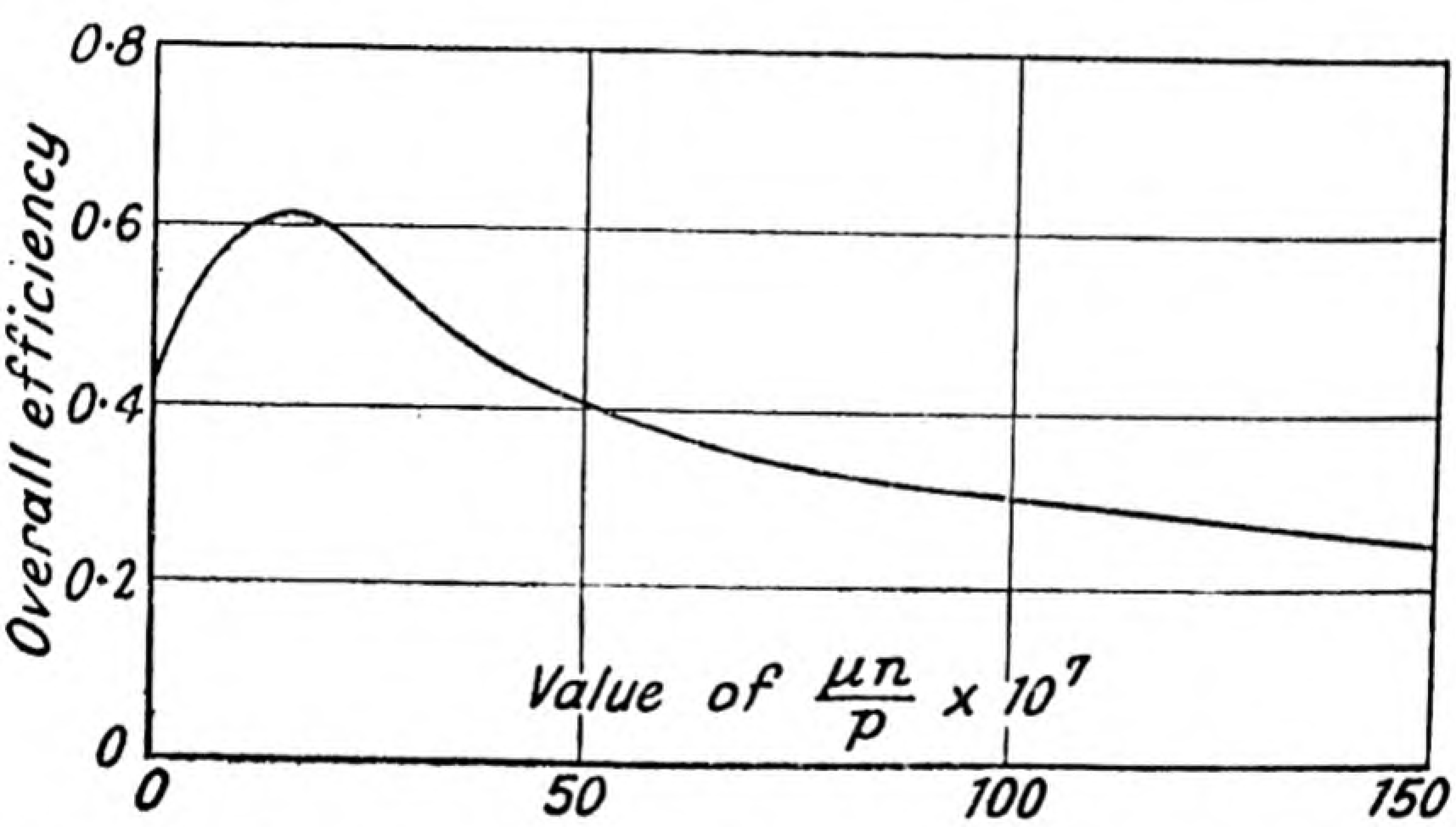

FIG. 346.—Non-dimensional plotting of gear-wheel pump performance (max. discharge = 3 lit./sec.).

An example of such a curve, based upon test results of a particular gear-wheel pump, is given in Fig. 346. Although the "scatter" of the plotted points (not shown here) is quite pronounced, yet the curve does give a fair impression of the value of the characteristic number likely to give the best pump efficiency. On the other hand, test figures from a larger gear-wheel pump, such as the one associated with Fig. 345, could not be made to fit any such general curve. Further experience is needed to show the limits of utility of this non-dimensional treatment as applied to actual positive rotary pumps.

(iv) *Suction lift.* An important aspect of pump performance is its suction capacity, viz. its ability to lift liquid up the suction pipe. A general examination of this question will be found in § 335, and one particular solution has been given

in § 290. Additional points specially applicable to positive rotary pumps are these: (a) Although the inertia effects or cyclical pressure fluctuations in these pumps may be less serious than in reciprocating pumps, § 292, yet they nearly always exist; moreover, the conditions of installation frequently prohibit the use of air vessels, § 291; (b) When positive rotary pumps are installed in, e.g. aircraft,[204] conditions are likely to be particularly severe, because the atmospheric pressure p_a (equation 16-6, § 335) is likely to be very low, while the vapour pressure of the liquid may be high. Especially in gear-wheel pumps, there is a possibility of these influences creating excessive noise and wear.

Water-Operated Lifting Appliances

306. Hydraulically-driven Reciprocating Pump. The pumps hitherto described have derived their energy from an engine, an electric motor, or a steam boiler. Occasions arise, however, when the energy available is itself in the form of hydraulic energy at a low pressure, and it is required to convert this into high-pressure hydraulic energy. This can be done by a modification of the direct-driven steam pump, Fig. 322, § 293. Instead of admitting steam to the motive cylinder, we admit low-pressure water. The resulting hydraulically-operated pump is found to work very well. Any desired ratio between the motive-water pressure and the pumped pressure is achieved by suitably proportioning the respective areas of the pistons; a mechanically-operated pilot valve controls a hydraulically-operated main valve which distributes the incoming motive water. The apparatus has been developed to the point at which one unit supplied with motive water under a head of 33 feet will pump 60 galls./min. of water against a head of 320 feet, with an overall efficiency exceeding 80 per cent.

To distinguish such direct-acting devices from others which perform similar functions, the name *hydrostat* is sometimes used. It will be observed that the motive cylinder of a hydrostat is in effect a very simple form of hydraulic motor, § 353.

307. The Hydraulic Ram: (i) Construction. The hydraulic ram is a simple and interesting device which enables the *dynamic* pressure of water flowing under a low head to

lift a proportion of this water to a higher head. It consists of a *supply pipe* or *drive pipe* AB (Fig. 347), connected at its upper end to the supply reservoir and at its lower end to a valve box E; the valve box has two automatic valves, a *waste valve* or *impulse valve* C opening downwards and a *delivery valve* G opening upwards. Above the delivery valve is an air vessel F, to the foot of which the delivery pipe D is connected.

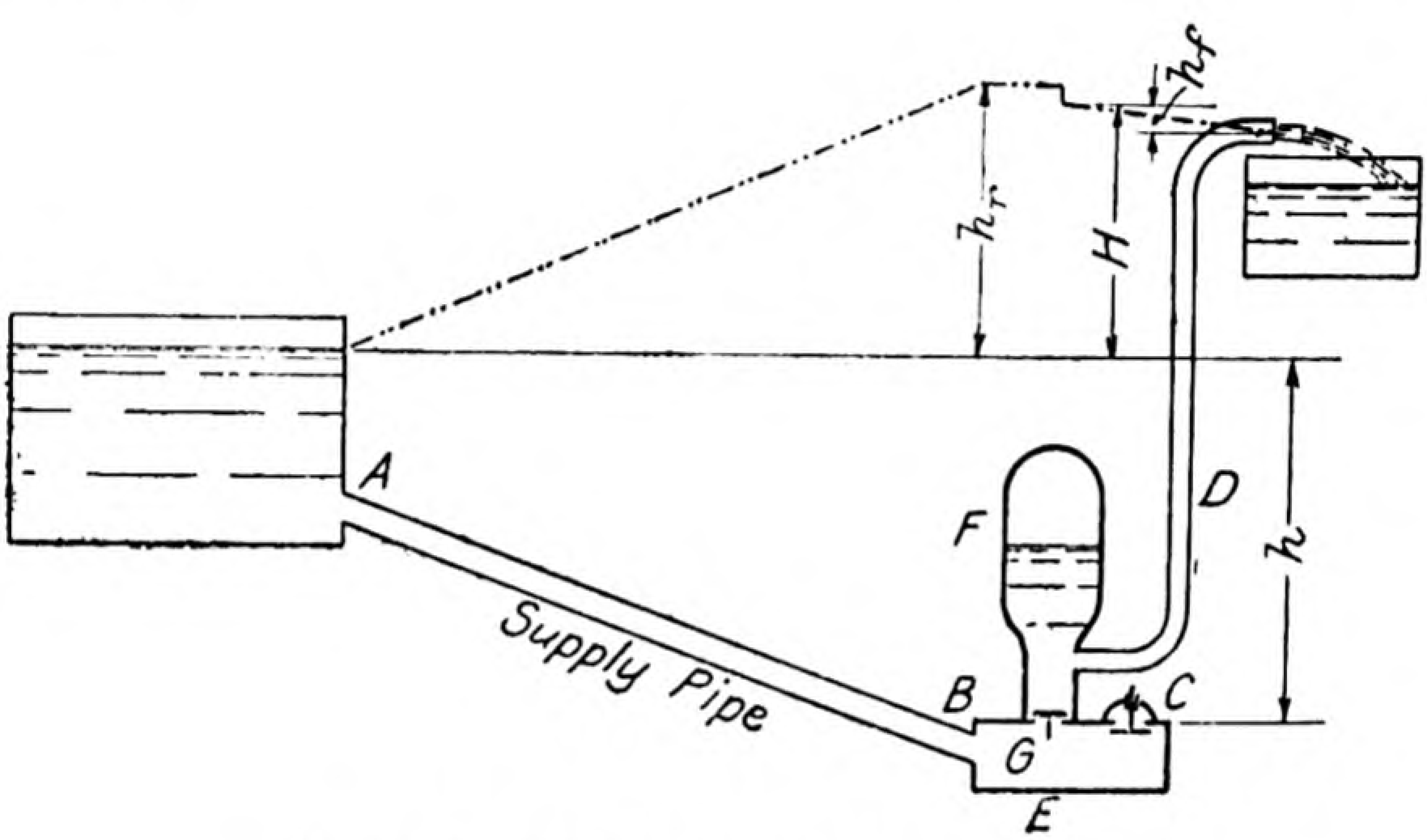

FIG. 347.—Elements of Hydraulic ram.

The principle of action of the ram is illustrated in Fig. 90 (§ 115), where it was shown that closing a valve at the end of a pipe could result in a *rising* hydraulic gradient. The supply pipe AB (Fig. 347) corresponds to the pipe AB (Fig. 90); the waste valve C (Fig. 347) corresponds to the valve at B (Fig. 90). By causing this waste valve successively to open and close, we generate in the supply pipe the dynamic pressure or inertia pressure that we rely upon to force the water up the delivery pipe.[205]

308. The Hydraulic Ram: (ii) Operation. The working cycle is represented graphically in Fig. 348, where in the upper diagram the velocity in the supply pipe, and in the lower diagram the pressure head in the valve box, are plotted against time. At point *a* the waste valve is assumed to have just been opened, either by being pushed open by hand, or automatically in the manner described later; the valve box pressure head has therefore fallen to zero, i.e. to the pressure of the atmosphere, and the column of water in the supply pipe

has just begun to move under the full accelerating head h. The delivery valve meanwhile is kept on its seat by the full delivery pressure. (See Example 51.)

Water from the supply reservoir is now running straight to waste through the waste valve. As the rate of discharge past the valve increases, due to the acceleration of the water column in the supply pipe, an appreciable head is called for

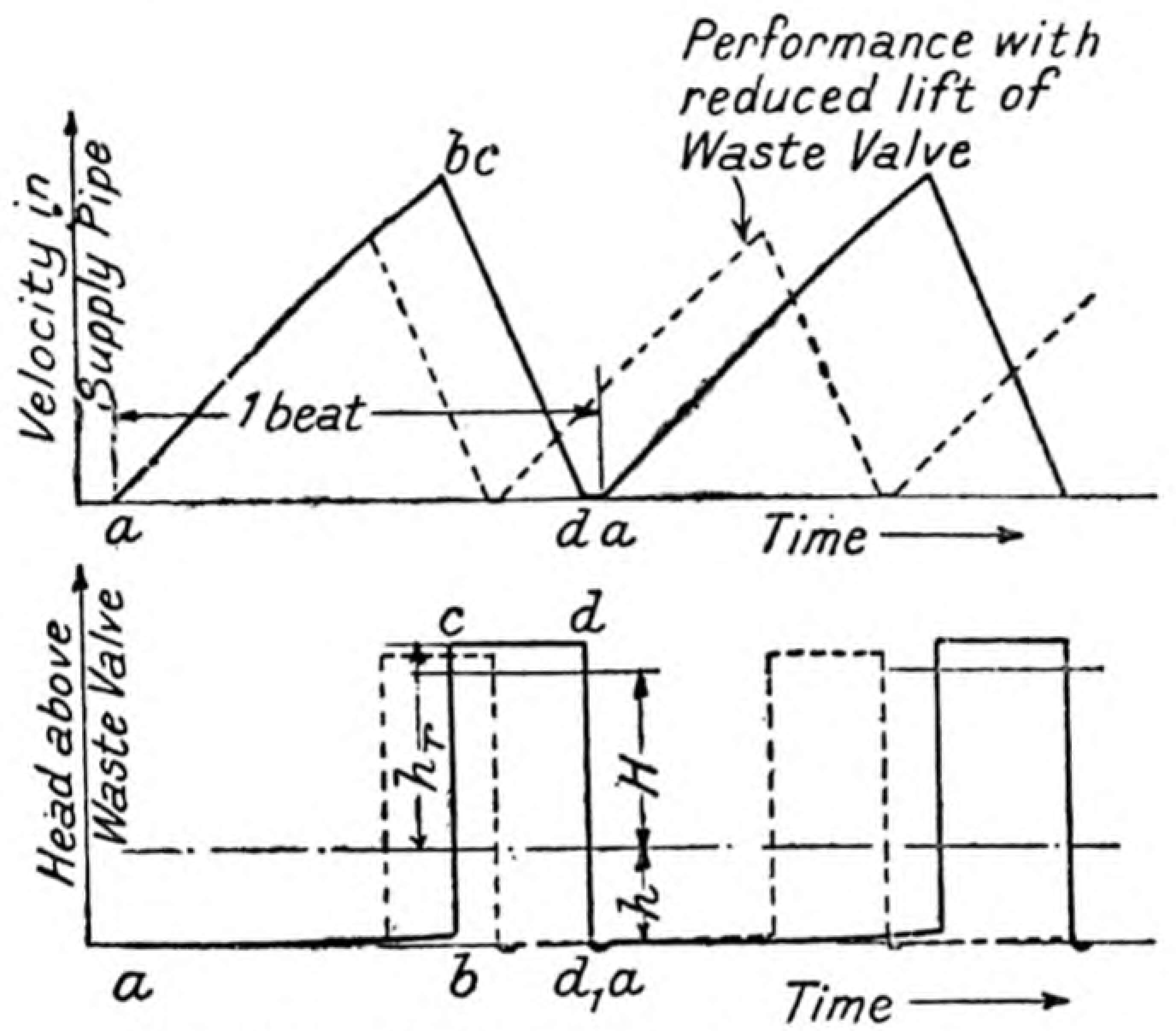

FIG. 348.—Working cycle of hydraulic ram.

to give the water the necessary velocity of efflux, with the result that the pressure head in the valve box begins to rise (ab, Fig. 348). It rapidly reaches a value at which the static thrust together with the dynamic thrust acting on the lower face of the valve is greater than the downward force due to the weight of the valve. The waste valve thereupon almost instantaneously closes. For the rest of the cycle it is held up on to its seat by the pressure in the valve box.

Although we have now succeeded in (almost) instantaneously closing a valve at the end of a pipe, the conditions of § 116 hardly apply, because the inertia pressure in the present instance cannot exceed that due to the delivery head plus valve and pipe friction. As soon as the pressure attains this value, which it does almost immediately after the closure of the waste valve, the delivery valve is forced open; water flows straight through from the supply tank into the air vessel and the delivery pipe, the flow continuing until the original kinetic

energy of the water column in the supply pipe is exhausted. It is this, the working or useful part of the cycle, which is represented by the rising hydraulic gradient in Fig. 347. In Fig. 348 the correspondence between the retarding head h_r and the steep downward slope *cd* of the velocity curve is very clear.

(Example 154.)

To understand how, at point d_1 in Fig. 348, the pressure in the valve box momentarily falls below atmospheric, so permitting the waste valve to open automatically and the cycle of operations to be repeated indefinitely, reference may be made to § 116; there it is shown how the effect of the compressibility of the water and the elasticity of the pipe, under conditions of rapid valve closure, is to produce a wave of negative pressure. Advantage is taken of this brief moment of negative pressure to draw into the valve box through a small orifice or through an automatic valve a small quantity of air which serves to keep the air vessel charged. The air vessel serves precisely the same purpose as it does in a reciprocating pump (§ 291); although water flows intermittently through the delivery valve, it passes along the delivery pipe in a nearly steady stream.

309. The Hydraulic Ram: (iii) Performance. There are two ways of assessing the gross efficiency of a hydraulic ram. In the *Rankine* system we choose as a datum level the water surface in the supply reservoir, we take the energy input to be the energy yielded up by the water that flows through the waste valve during the part *ab* (Fig. 348) of the cycle, and we base the useful output on the head H to which the water is lifted above datum level (Fig. 347) during the part *cd* of the cycle. (H should include if necessary the friction head h_f in the delivery pipe.)

If W is the weight of water per minute escaping past the waste valve under a head h, and w_o is the weight per minute forced up the delivery pipe, then

$$\eta_r = \text{Rankine efficiency} = \frac{w_o H}{Wh}.$$

Alternatively the datum plane may be taken as that passing through the waste valve. The energy per minute received by the ram must then be reckoned as the total flow down

the supply pipe $(W + w_o)$ multiplied by the supply head h, and the energy output must be based on the total head $(h + H)$ to which the water is lifted above the waste valve level. The corresponding overall efficiency

$$\eta_a = \frac{w_o(h + H)}{(w_o + W)h}$$

is known as the *D'Aubuisson* ratio ; its value is naturally higher than the Rankine efficiency.

The chief causes of energy loss which usually limit the efficiency to 75 per cent. or so, even under favourable conditions, are (i) friction and secondary losses in the supply pipe and in the valves, and (ii) velocity energy carried away by the water leaving the waste valve.[206] In a given ram working under fixed supply and delivery heads, both (i) and (ii) vary roughly as the square of the mean velocity in the supply pipe, whereas the energy input varies directly as this mean velocity ; hence it should be possible by reducing the mean velocity to improve the efficiency. This can readily be done by reducing the lift of the waste valve, a modification which, by limiting the maximum supply pipe velocity, diminishes the mean velocity as desired (compare the broken curve with the full curve, Fig. 348).

The following figures, extracted from the results of tests on a small ram, show how effective this procedure is ; the test

Supply head h = 1·58 metres. Delivery head H = 3·00 metres.

Number of Beats Per Minute.	Waste Water Per Minute W	Useful Water Per Minute w_0.	Overall Efficiency.	
			Rankine.	D'Aubuisson.
92	32·0 kg.	7·36 kg.	0·44	0·54
110	23·6	6·28	0·51	0·61
157	13·0	4·09	0·59	0·69

Performance of ram with varying waste-valve lift.

with the greatest number of " beats " or cycles per minute is naturally the one with the least valve lift, as will be apparent from the full and broken curves (Fig. 348). The figures

also demonstrate the adaptability of the ram; for normal working the lift of the waste-valve can be adjusted to yield a moderate discharge at a fair efficiency, yet if maximum efficiency is of no consequence, nearly twice the output is possible.

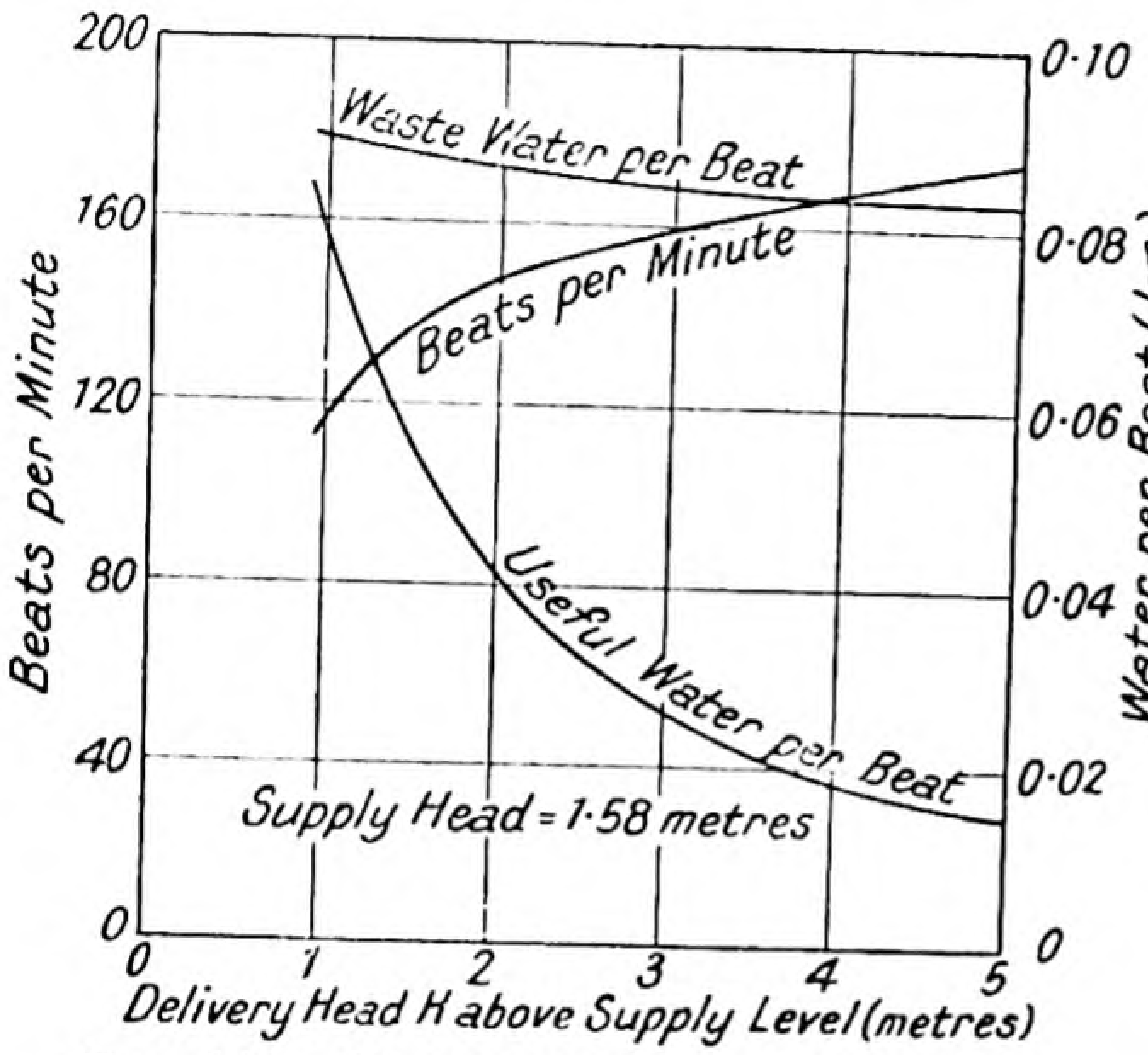

FIG. 349.—Characteristics of hydraulic ram.

The characteristic performance of a hydraulic ram, working under conditions of *constant* waste-valve lift, *constant* supply head, and *varying* delivery head, is shown in Fig. 349. It will be observed that the number of beats per minute increases as the delivery head increases; this may be explained with the help of the curves in Fig. 350, which are reproduced from autographic records or indicator diagrams of valve box pressure. Allowing for the effects due to the inertia of the valves and of the indicator parts, the shape of these graphs agrees quite well with the shape of the ideal diagram (Fig. 348). When the delivery head is increased from 1·9 metres to 4·0 metres, the more rapid retardation impressed on the water column in the supply pipe reduces the time taken to bring the column to rest from 0·21 sec. to 0·10 sec.; the accelerating period, however, is sensibly unaffected. Thus the total duration of one cycle or beat is diminished, and the beats per minute increase.

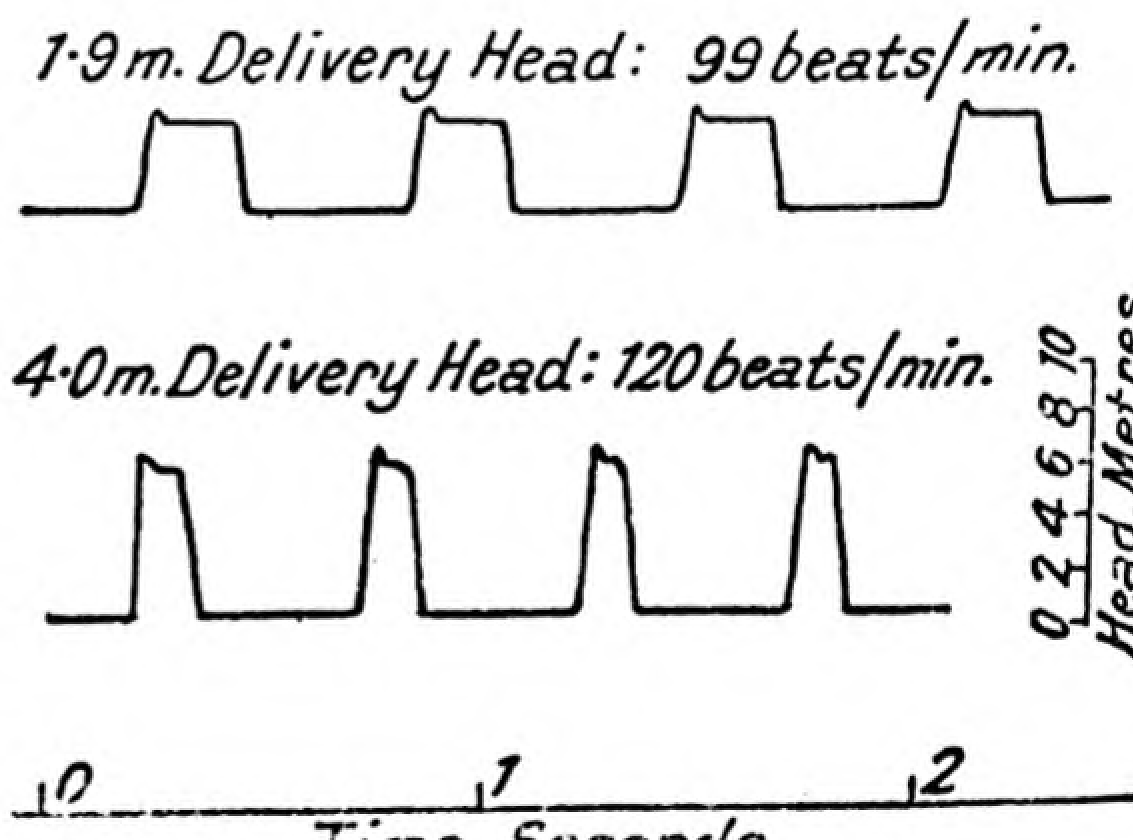

FIG. 350.—Autographic pressure records from hydraulic ram.

The hydraulic ram will work satisfactorily with much greater ratios of H to h than those just quoted, though when the extreme conditions are reached, with the delivery head twenty or more times as great as the supply head, the efficiency becomes very low.

Other limiting figures are :—

Useful water delivered	300 galls./min.
Diameter of supply pipe	12 inches.
Supply head	50 feet.
Delivery head	200 feet.

These data [207] relate to a machine of exceptional size ; rams normally in use are a good deal smaller than this, and they work under less onerous conditions.

310. The Jet Pump. Using an electrical analogy, the hydraulic ram may be regarded as a step-up transformer, con-

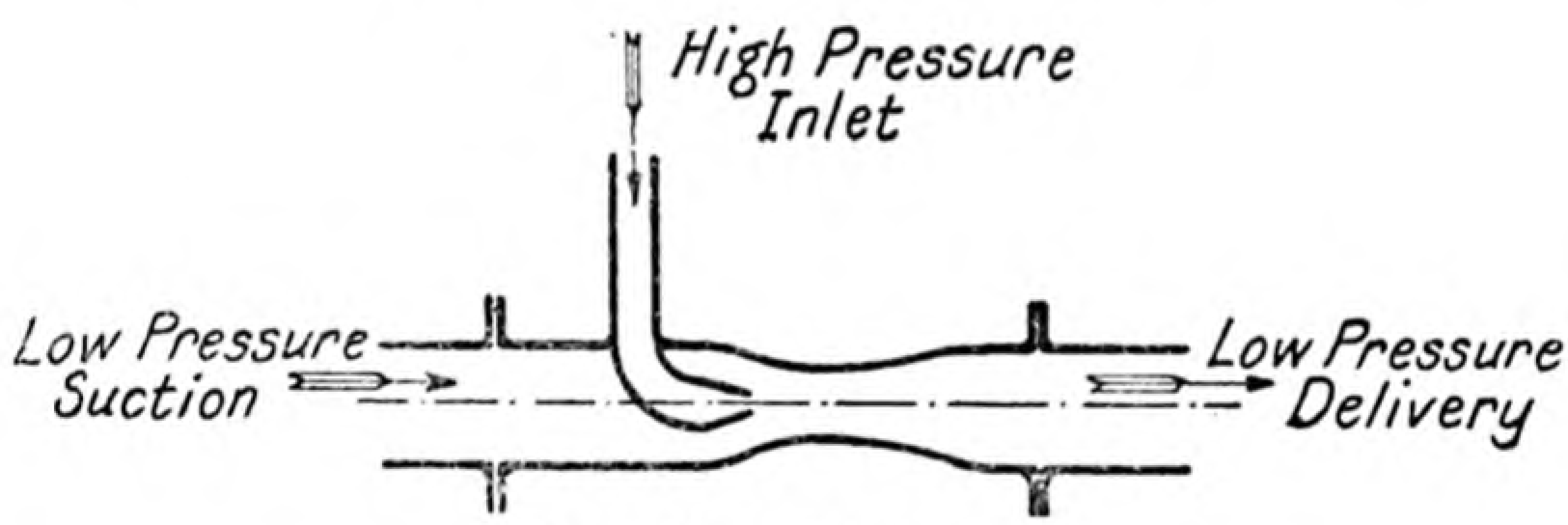

FIG. 351.—Jet pump.

verting a large flow at a small pressure into a smaller flow at a larger pressure. The jet pump (Fig. 351) is a step-down transformer : a stream of high pressure water, having had its energy converted in a nozzle into velocity energy, is enabled to impart some of this energy to the water surrounding the jet, and thus to project a relatively large stream of low-pressure water into the delivery pipe.[208] Owing to the losses entailed during the mixing of the two streams of water, the efficiency of the apparatus is rarely more than 25 per cent.

GAS-OPERATED DEVICES.

311. Displacement Principle. If a supply of a gas under pressure is available, it may be employed for lifting liquids by directly displacing them from vessels of suitable form. The principle is shown diagrammatically in Fig. 352 : the liquid gravitates into the vessel through an inlet valve,

and when the vessel is full, the gas inlet valve automatically opens and the liquid is ejected through the delivery valve.

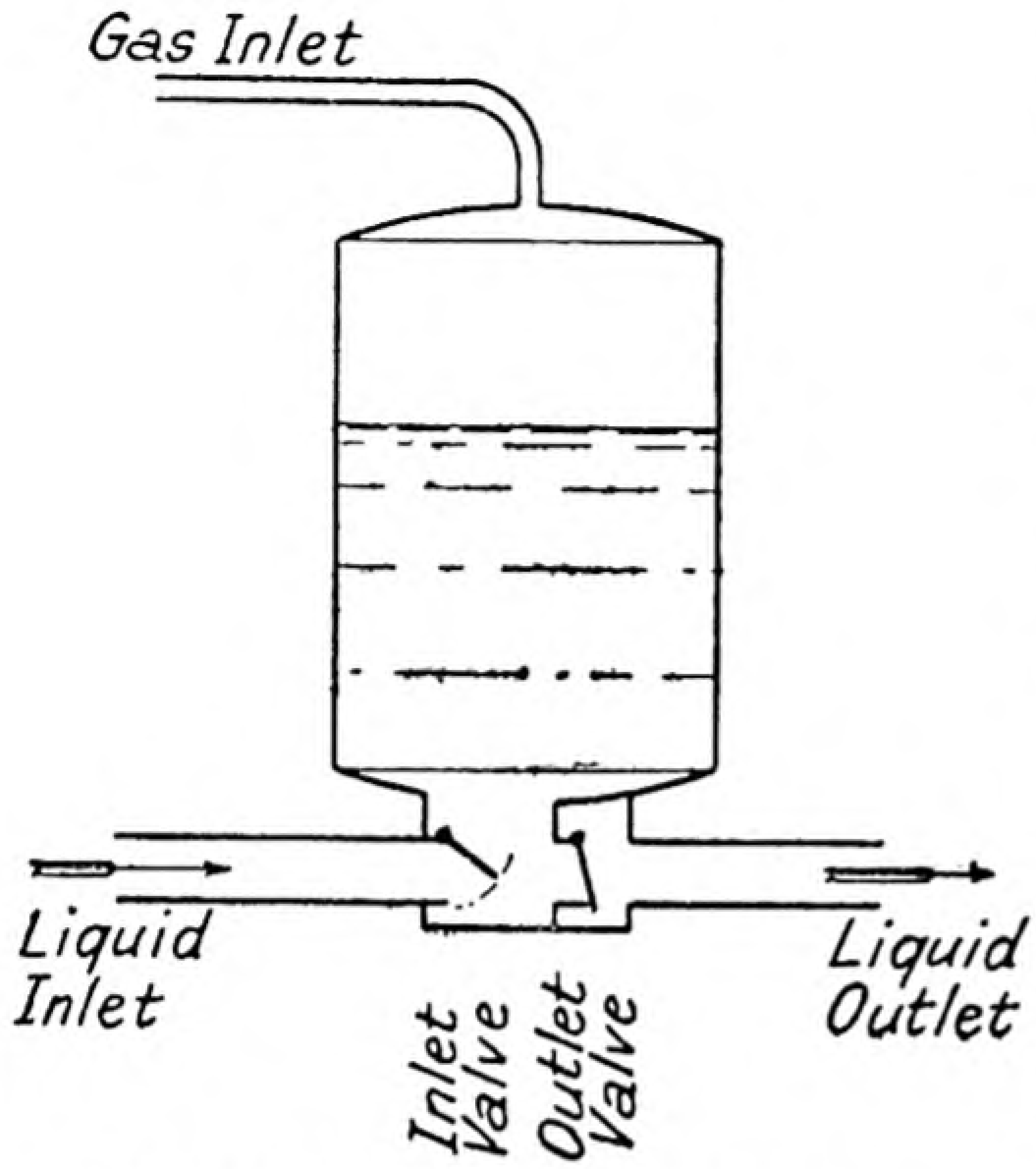

FIG. 352.—Pneumatic ejector.

(i) *The pulsometer.* This is a type of pump in which the gas used is steam. Although simple in construction, it is extremely wasteful in operation because of the very large proportion of steam which is condensed, without doing useful work, by contact with the cold liquid and with the wet walls of the chamber. Historically it is interesting on the ground that it was one of the earliest forms of steam pump.

(ii) *The pneumatic ejector.* When air is used for displacing the liquid, the apparatus is often known as a pneumatic ejector. It is well fitted for such duties as the raising of sewage, for handling corrosive liquids in chemical works, and for lifting other viscous liquids or solid-liquid mixtures.[209]

An improved type of closed-circuit sewage ejector has two chambers working in parallel, with an electrically-driven rotary air compressor mounted above.[210] As the liquid flows into one of the chambers, the displaced air is drawn into the compressor and is forced at a higher pressure into the other chamber from which liquid is being ejected. At the end of the stroke the direction of air flow is reversed. Power consumption is thus reduced, and there is no nuisance arising from the discharge to atmosphere of contaminated air.

(iii) *The Humphrey internal-combustion pump.* In this apparatus, the pressure required to expel the liquid from the working chamber is generated by the ignition, in the working chamber itself, of a combustible mixture of gas and air. The successive operations of air and gas inlet, compression, expansion, and exhaust are carried out as they are in the cylinder of a rotative four-stroke gas or oil engine, the inertia of the column of water in the delivery pipe being made

to do the duty normally done by the inertia of the engine flywheel. The internal-combustion pump is suitable for lifting large volumes of water against a low head, e.g. in irrigation schemes.[211] It is possible that the application of the two-stroke principle may widen the possibilities of this interesting apparatus.

312. The Air Lift Pump. Although the air lift pump uses compressed air just as the pneumatic ejector does, the principles of operation of the two devices are quite different. In the air lift pump, the function of the air bubbles that are caused to mix with the water is so to reduce the density of the mixture that the weight of a given column of mixture is less than the weight of a much shorter column of "solid" water § 11. The air (Fig. 353) is introduced through one or more nozzles at the bottom of the air supply pipe, into the water at the foot of the rising main fixed in a well. As soon as the column in the rising main has become impregnated with air bubbles, the pressure due to the column of length L is less than that due to the static pressure H, with the result that flow begins, and water and air issue from the top of the rising main so long as the supply of air is maintained.

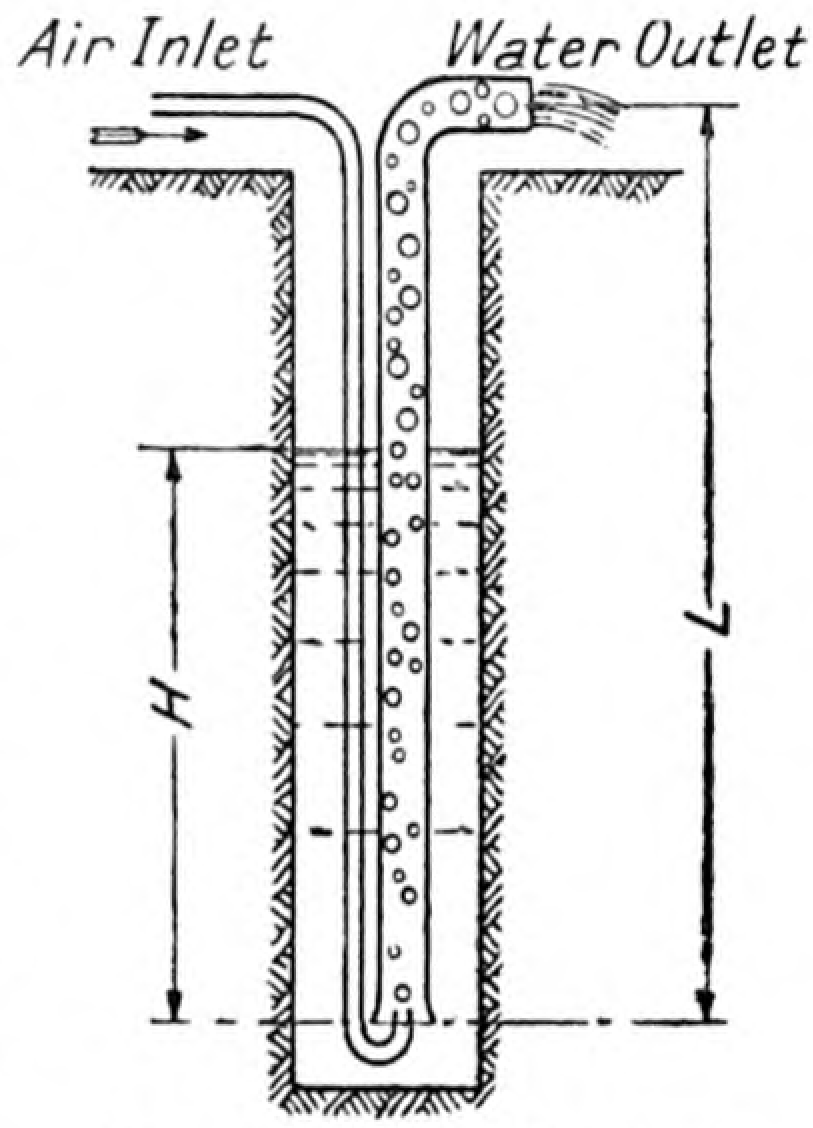

FIG. 353.—Air lift pump.

Best results are obtained if the useful lift $(L - H)$ is less than the submergence H, the ratio $\left(\frac{H}{L-H}\right)$ varying from 4 when H is 100 ft., to 1 when H is 300 ft. The advantages of the air lift pump are that it has no moving parts below water level, and therefore cannot be damaged by solids in suspension in the water; also that it can raise more water through a bore-hole of given diameter than any other form of pump. On the other hand, its efficiency is low: of the energy expended in compressing the air, only between 20 per cent. and 40 per cent. appears in the form of useful water horse-power.

CHAPTER XVI

PUMPING MACHINERY: (II) CENTRIFUGAL PUMPS

313. Dynamic-pressure Generators. The pumps now to be described are essentially machines for generating dynamic pressure. When they are interposed in a pipe-line, it is convenient to think of flow as taking place not because the water is pushed bodily along as it is by the ram of a reciprocating pump, but rather because the pressure generated modifies the hydraulic gradient in a way that makes flow inevitable (Fig. 150, § 167). The analogy with an electrical generator is quite close; such a machine produces an electrical pressure difference whether current is taken from it or not —if the external resistance is large the current will be small, but if the external resistance is small a large current will flow.

In just the same way the discharge from a dynamic-pressure pump is directly influenced by the resistance or pressure against which it works, the behaviour of the pump being therefore widely different from that of the positive pumps discussed in Chapter XV.

In construction, dynamic-pressure pumps closely resemble hydraulic turbines—they may be regarded, indeed, as reversed reaction turbines (§ 226). Whereas in the turbine, high-pressure water is fed into the casing and mechanical energy is

given out at the shaft, in the pump we feed energy into the shaft with the purpose of increasing the pressure energy of the water flowing through the pump.[212] The terms and symbols used in Chapters XIII and XIV will thus as a rule be applicable here also ; a common descriptive term, *rotodynamic*, § 219, will likewise cover the two classes of machinery.

According to the general direction taken by the liquid as it flows through the rotating wheel of the pump, dynamic-pressure machines are classified as

(i) Centrifugal pumps (Chapter XVI).
(ii) Propeller pumps
(iii) Half-axial and screw pumps } (Chapter XVII).

But as the boundary line between the classes is often very indeterminate, it is sometimes quite difficult to say whether a particular machine is, for example, a centrifugal pump or not. Although this lack of definition is apt to be inconvenient, it does serve to underline the identity of principle governing the entire range.

314. Fundamental Equations for Centrifugal Pump. The centrifugal pump is the counterpart of the inward flow turbine (Fig. 235, § 234). In its simplest form it consists of a bladed wheel, now called the *impeller* instead of the runner, revolving in a concentric casing (Fig. 354) ; owing to the type of forced vortex motion impressed by the blades on the water flowing between them, dynamic pressure is generated as explained in §§ 143 and 144. In this way, the water is lifted from the tank on the left to the tank on the right, through a vertical height H. The relationship between the head generated, the impeller speed and blade angles, and the discharge, may be established as follows :—

Let

W = weight of water per second flowing through pump.
Q = volume of water per second flowing through pump.
D = outer diameter of impeller.
B = width of impeller at outer circumference.
v = rim velocity at outer edge of blades.
v_1 = rim velocity at inner edge of blades.
V = velocity of whirl of water at outer circumference.
V_1 = velocity of whirl of water at inner circumference.
Y = radial velocity of flow of water leaving impeller.
U = absolute velocity of water leaving impeller.
V_p = velocity in pipes, assumed equal to Y.
γ = impeller blade angle at outer edge.
β = impeller blade angle at inner edge.
H = dead or static head.

In the following preliminary analysis it is assumed that (i) the blade thickness is neglected, (ii) friction losses in the pipes and pump passages are negligible, (iii) the velocity of whirl at inlet, V_1, is zero, and (iv) the inlet edges of the blades are parallel to the relative velocity V_r.

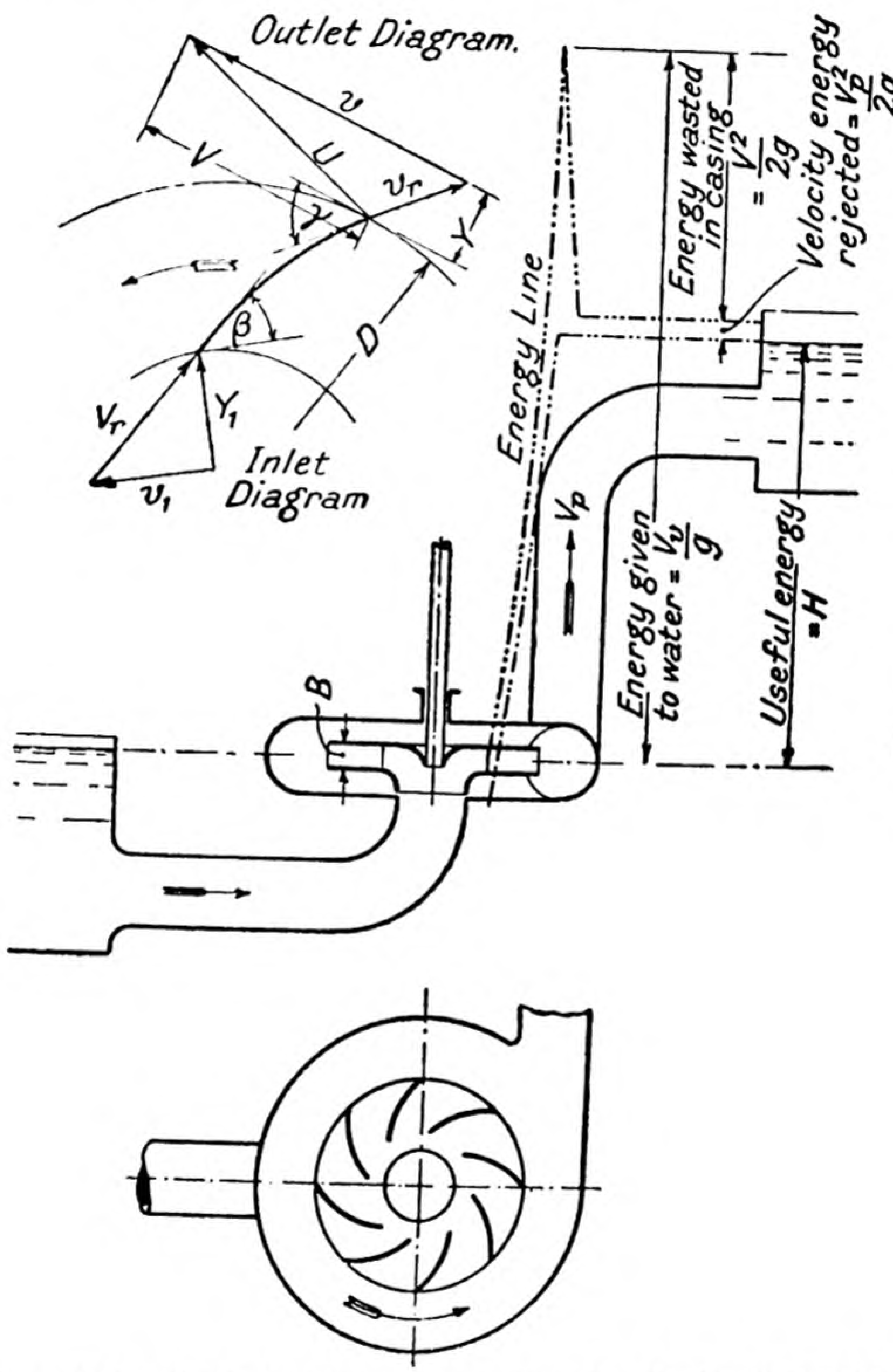

FIG. 354.—Centrifugal pump energy and velocity diagrams.

Applying formula 8-5 (§ 144), we have, under ideal conditions: Energy that must be supplied to impeller per unit weight of water $= \dfrac{Vv}{g}$. Now immediately before entering the impeller the total energy of the water, referred to a datum plane passing through the water surface in the suction well, is

zero (Fig. 354); after leaving the impeller the water has pressure energy H and velocity energy $\frac{U^2}{2g}$. Since the energy fed into the impeller shaft must be equal to the increase in energy of the water, we can write $\frac{Vv}{g} = H + \frac{U^2}{2g}$,

or
$$H = \frac{Vv}{g} - \frac{U^2}{2g} \quad . \quad . \quad . \quad (16\text{-}1)$$

Substituting in this equation the values $U^2 = (V^2 + Y^2)$ and $V = (v - Y \cot \gamma)$ obtainable from the outlet velocity diagram (Fig. 354), we derive the alternative equation

$$H = \frac{v^2 - Y^2 \operatorname{cosec}^2 \gamma}{2g} \quad . \quad . \quad (16\text{-}2)$$

Since $v = \frac{\pi DN}{60}$, and $Y = \frac{Q}{\pi DB}$, the desired connection between speed, head, and discharge is now available.

315. Ideal Efficiency of Simple Centrifugal Pump. Under the ideal conditions assumed in the preceding paragraph, the efficiency of the pump will be represented by

$$\eta_i = \frac{\text{useful output per sec.}}{\text{total input per sec.}} = \frac{WH}{W \cdot \frac{Vv}{g}} = \frac{gH}{Vv}.$$

Substituting the values of H and V obtained above, we find that

$$\eta_i = \frac{v^2 - Y^2 \operatorname{cosec}^2 \gamma}{2v\,(v - Y \cot \gamma)}. \quad . \quad . \quad (16\text{-}3)$$

To show the manner in which the efficiency is influenced by changes in the blade angle γ, the following values have been calculated from equations 16-2 and 16-3, assuming a constant value for the flow ratio $\psi = \frac{Y}{\sqrt{2gH}} = 0{\cdot}25$.

Outlet Blade Angle γ (see Fig. 355).	Speed Ratio $\phi = \frac{v}{\sqrt{2gH}}$.	Ideal Efficiency η_i.
90°	1·03	0·47
45°	1·06	0·58
20°	1·24	0·73

Remembering that the angle γ for the pump corresponds to the angle $(180° - \alpha)$ for a turbine runner, the tendencies exhibited in this table and in Fig. 355 agree precisely with those noted in § 237. In that paragraph it was shown that values of ϕ beyond a certain limit—say 0·9—were impracticable on account of the high frictional loss in the long and narrow wheel passages that would be entailed. It is equally inadmissible to have such passages in the pump impeller, hence in practice it is rare to find values of γ less than 20°. The futility of trying to obtain a high efficiency by the adoption of a very small blade angle is seen from Fig. 355, where, in addition to the three impellers referred to in the above table, a fourth impeller in the nature of a *reductio ad absurdum* is sketched.

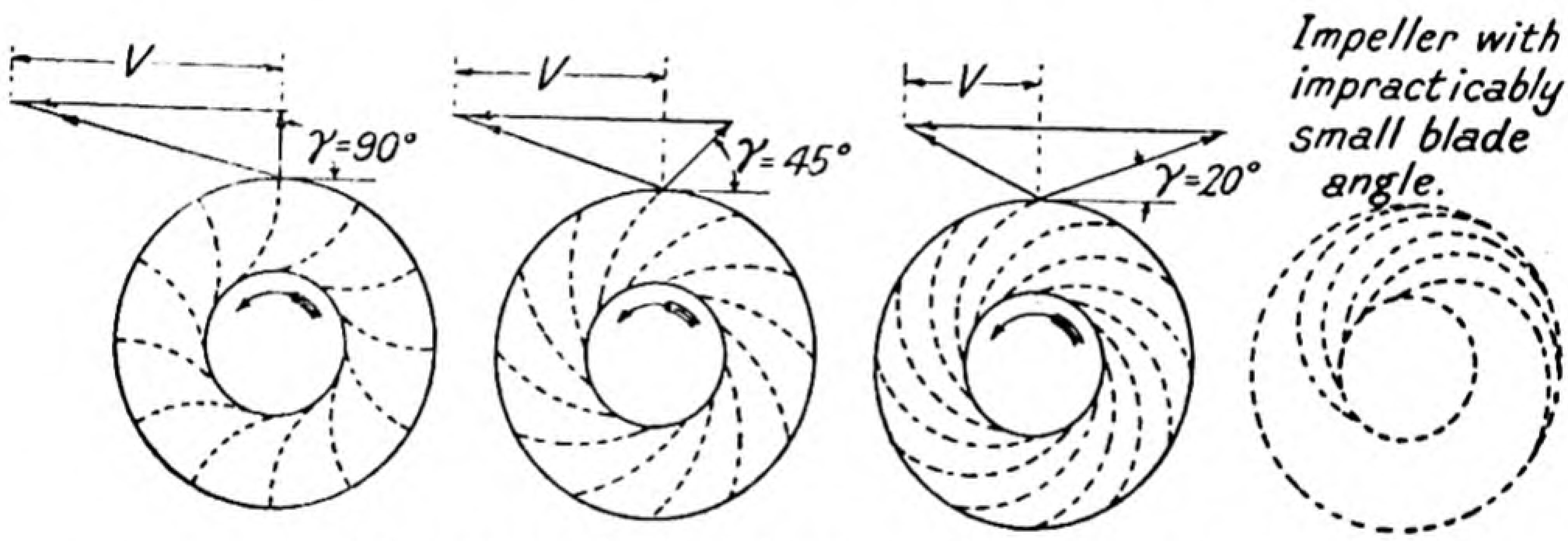

FIG. 355.—Connection between v, γ, and η_i.

If, then, we are limited to a maximum *ideal* efficiency of only 70 per cent. or so, it is useless to hope for an actual working efficiency of more than perhaps 65 per cent., which compares very unfavourably with the efficiencies of 90 per cent. realised in turbine tests. The energy line plotted in Fig. 354 gives the clue to this discrepancy; it is seen to rise high above the delivery water level, showing that much more energy is given to the water than is called for. The whole of this excess energy, which is represented by $\frac{V^2}{2g}$, is wasted in shock and eddy losses in the casing. The connection between reduced velocity of whirl and increased efficiency is demonstrated in Fig. 355, and in the Table to which it refers.

The difficulty arises in this way, that there is a direct misapplication of energy in the pump itself. What we want to extract from the pump is an amount of pressure energy H, and we accordingly put into the pump an amount of

energy $\frac{Vv}{g}$. But what, in fact, we get out of the impeller is the desired pressure energy H which we do want, and in addition velocity energy $\frac{U^2}{2g}$ which is of no use to us at all. To be sure a small loss of velocity energy $\frac{V_p^2}{2g}$ unavoidably occurs at the exit from the delivery pipe, but otherwise the creation of velocity energy seems to represent pure waste.

It is really not necessary to waste this velocity energy, though; all that is required is some device capable of converting at least part of it into useful pressure head.[213]

(**Example 166.**)

316. Pump with Guide Blades. By modifying the form of the pump casing and providing it with fixed guide blades (Fig. 356), the water leaving the impeller with velocity U is given the opportunity of flowing through a set of diverging passages which gradually reduce the velocity to U_o, with a consequent gain in pressure head (§ 87 (*b*)). The pressure rise in the pump now takes place in two stages; in the impeller there is an increase of pressure head H_o, and in the guides an increase

$$h_g = K\left(\frac{U^2 - U_o^2}{2g}\right),$$

where K is the efficiency of conversion of the diverging passages—say 70 per cent. at most.

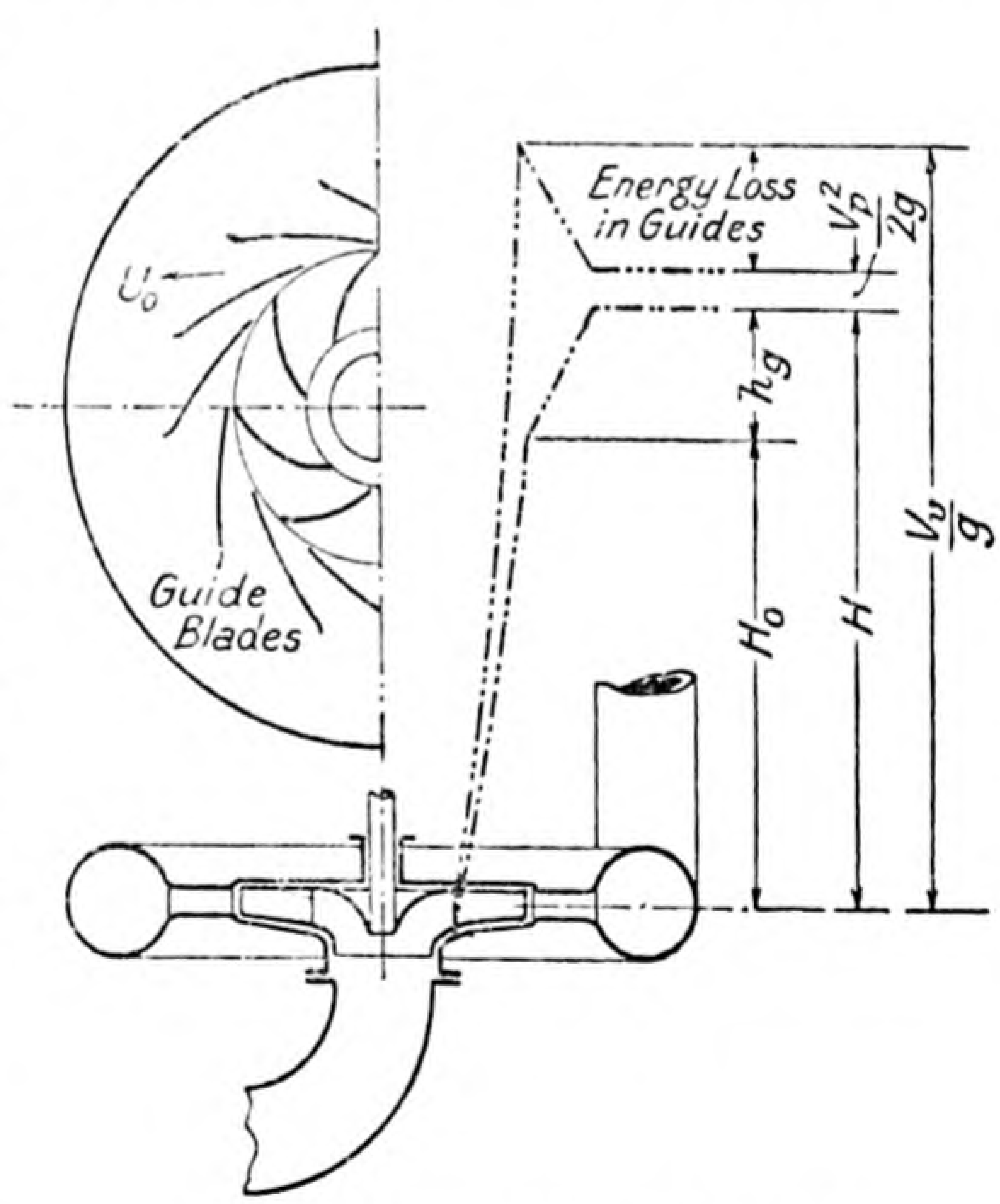

Fig. 356.—Pump with guide blades.

Comparison between the energy lines in Figs. 354 and 356 shows the improvement that the guide blades have effected. Since H_o is less than H, the total input $\frac{Vv}{g}$ has been reduced,

and therefore the efficiency is increased. The appearance of the guide blade ring or *diffuser ring* is to be seen from Fig. 364 (facing p. 470).

Another pertinent comparison may link together the hydraulic gradients in Figs. 356 and 235; in this way the basic resemblance between pumps and turbines is still more clearly revealed. Likewise the pump guide blades are seen to be, in effect, stay-vanes (Fig. 252), which add to the structural strength of the casing as well as guide the liquid.

317. Pump with Volute Casing. The volute casing (Fig. 357) is a simpler and less expensive device for the recuperation of pressure energy than the diffuser ring, and is often no less efficient; it is the counterpart of the spiral casing used in turbines, §240. In the constant-velocity form of volute, the successive cross-sections taken at different points round the circumference increase in such a way that the velocity v_w of the water circulating in the casing is uniform, having a value equal to about two-thirds of the velocity of whirl V of the water leaving the impeller. The loss of energy due to shock is thus reduced from $\frac{V^2}{2g}$ to $\frac{(V - v_w)^2}{2g}$, or even less.

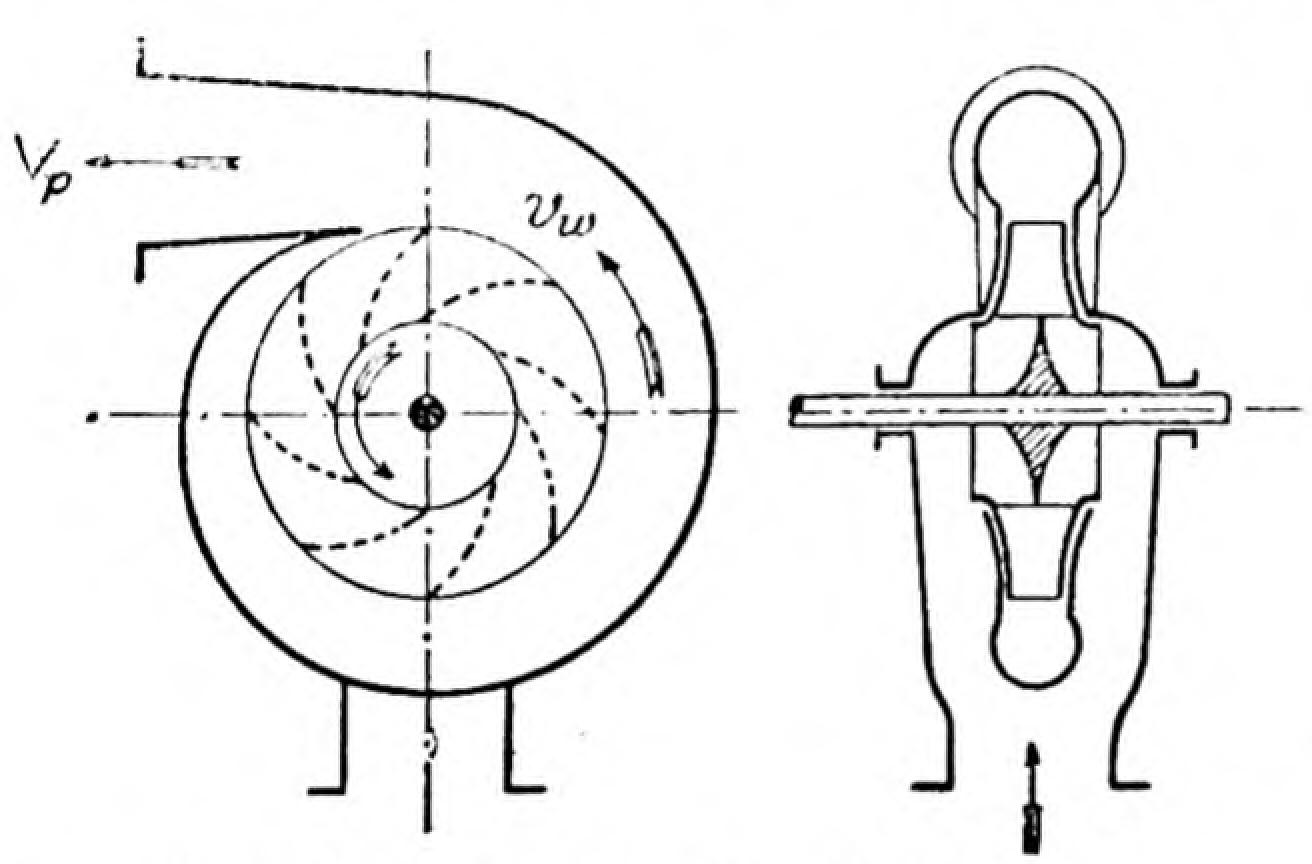

FIG. 357.—Pump with volute casing.

By adding to the volute itself a conical or tapered outlet passage (Fig. 357), it is easy to reduce the water velocity from v_w to the still lower outlet velocity V_p, with a consequent additional gain in pressure head, as in § 87 (*b*).

In the variable-velocity volute, the cross-section of the casing increases at a more rapid rate than in the constant-velocity volute, the mean velocity of the water circulating in the casing continuously diminishing from a value V at the smallest cross-section to the value V_p at the outlet flange; the casing may thus be regarded as one long diverging passage wrapped around the entire periphery of the impeller.

A photograph of a 27-in. volute pump is reproduced in Fig. 358 (facing p. 470).

In the above explanation it has been assumed that at any cross-section of the volute casing the velocity of the water will be uniform at all points. But if the casing be regarded as a curved passage, free vortex flow (§ 141) may be expected, and hence the peripheral velocity of the water at the inner radius, near the impeller outlet, will be appreciably greater than the mean velocity v_w; this will result in a reduced energy loss, and an increased efficiency of the casing, regarded as a device for transforming velocity energy into pressure energy.

318. Specific Speed of Pumps. The utility of the conception of specific speed in defining the shape and performance of the wheel is just as great when applied to pumps as it is in connection with turbines (§ 263). A slight modification to the formula $N_s = \frac{N\sqrt{P}}{H^{\frac{5}{4}}}$ is desirable, however, in order that specific speed may be expressed in terms of the three fundamental factors in pump design, viz., head in feet H, speed in r.p.m. N, and discharge in gallons per minute Q.

Now Q gals./min. $= 10 . Q$ lb./min., and $P =$ water horse-power output $= \frac{10 . Q . H}{33000}$,

whence specific speed =

$$N_s = \frac{N\sqrt{\frac{10 . Q . H}{33000}}}{H^{\frac{5}{4}}} = 0{\cdot}0174 \frac{N\sqrt{Q}}{H^{\frac{3}{4}}} \quad . \quad \textbf{(16-4)}$$

Often the numerical coefficient is omitted, and the

$$\textit{relative specific speed } N_{sr} = \frac{N\sqrt{Q}}{H^{\frac{3}{4}}}$$

is used as a description of the impeller.

In metric units, where $N =$ r.p.m., $H =$ head in metres, and $Q =$ discharge in litres/sec., the specific speed

$$N_s = \frac{N\sqrt{\frac{Q . H}{75}}}{H^{\frac{5}{4}}} = 0{\cdot}1155 \frac{N\sqrt{Q}}{H^{\frac{3}{4}}}.$$

To convert N_s (foot) to N_s (metric), multiply by 4·44. To convert relative specific speed N_{sr} (foot) to N_s (metric) multiply by 0·0774. It is, of course, essential when quoting specific speeds to state in which system they are expressed.

In general terms, the specific speed of a rotodynamic pump may be defined as the speed in revolutions per minute of a pump geometrically similar to the actual pump, but of such a size that under corresponding conditions it would generate one water horse-power when working against unit head.[214]

The non-dimensional *shape number* (§ 263) can be adapted to dynamic-pressure pumps thus :—

$$\text{Shape number } n_s = \frac{\frac{N}{60}\sqrt{q}}{(gH)^{\frac{3}{4}}}.$$

Manifestly, if H is in feet, q must be in cub. ft./sec. ;
H is in metres, q must be in cub. m./sec.

The conversion factors between specific speed and shape number, already quoted, are equally applicable here.

If the expression for shape number n_s is applied in its basic form to commercial pumps, the resulting numeral may be inconveniently small. A preferable alternative form is therefore

$$\text{Shape number } n_s = \frac{1000 \cdot \frac{N}{60}\sqrt{q}}{(gH)^{\frac{3}{4}}}.$$

A further advantage of the non-dimensional system is that it eliminates the effect of the density of the liquid. On the other hand, specific speed formulae such as equation 16·4 are strictly valid only for *water* or for liquids having the same density as water.

319. Types of Impellers. The normal range of specific speed for which centrifugal pump impellers are suited is, as would be expected, much the same as it is for Francis turbine runners, viz. from about 18 to 100 (foot), or 80 to 450 (metric). Typical low and high speed impellers are compared in Fig. 359 ; in general, impellers of low specific speed are used in conjunction with diffuser rings (§ 316), while volute pumps (§ 317) may be expected to have impellers of medium to high specific speed. Thus Fig. 359 II shows the impeller belonging to the pump illustrated in Fig. 358 ; its shape is markedly different from the shape of the low specific speed

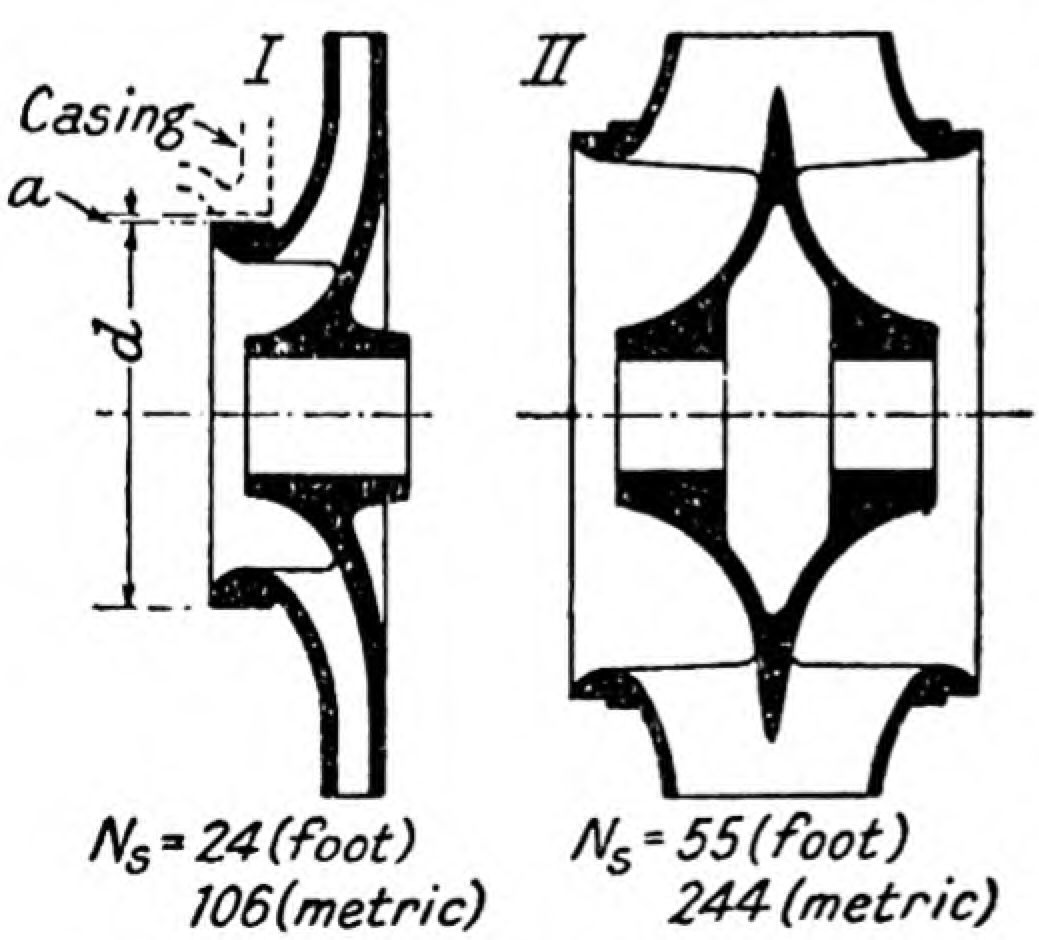

FIG. 359.—Types of impellers.

impellers seen in Figs. 364 and 369. Although there is by no means the same direct connection between the head and the specific speed of centrifugal pumps that was observed in relation to turbines (§ 268), nevertheless the same tendencies operate, so that the probability is that a high-lift pump will have a low specific speed impeller working in conjunction with guide blades, while a low-lift pump, unless of very small capacity, would be likely to have an impeller of high specific speed and a volute casting.[215]

For the reasons mentioned in § 322, the increase in head demanded from a single impeller rarely exceeds 500 ft. (say 150 metres).

The following figures show the usual range of values for the flow ratio and the speed ratio of impellers :—

	Low Specific Speed.		High Specific Speed.
Speed ratio $\phi = \dfrac{v}{\sqrt{2gH}}$	0·95	to	1·25
Flow ratio $\psi = \dfrac{Y}{\sqrt{2gH}}$	0·10	to	0·25

Apart from questions of specific speed, the *double-inlet* or *balanced-suction* type of impeller, shown at II in Fig. 359 and also in Figs. 357 and 358, has an advantage over the *side-inlet* type I in that end thrust on the shaft (§ 321) is virtually eliminated. Further, if the casing is split in a diametral plane as in Fig. 358, the shaft and impeller may be examined or removed without disturbing the pipe connections.

Sometimes *open* or *skeleton* impellers are preferred, the blades being supported by the central boss only. There are no enclosing discs or *shrouds* ; leakage past the blades is prevented as far as possible by keeping as small a clearance as is practicable between the blade edges and the inner walls of the casing.

320. Flow Conditions in Impeller Passages. Only if the impeller had very closely-spaced blades would it be justifiable to say that outlet velocity diagrams such as those in Figs. 354 and 355 truly represented the various directions of flow. But in practice it is not possible to guide the liquid so positively.

The more numerous the blades the greater is the total area obstructed by the metal of the blades themselves, and the greater the frictional loss of head. In any event the choice of wide passages makes it easier to mould and to trim the impeller casting, and it also reduces the risk of the pump becoming choked by floating rubbish.

The *minimum number of blades* consistent with an acceptable efficiency may vary from 6 to 12.

It is hardly to be expected that the change from an infinite to a finite number of blades will leave the pump performance unaltered. If we carried the process to its limit and gave the impeller only one blade, this solitary element would tend rather to churn up the liquid than to impress useful energy on it. Experiments made on impellers of identical size, speed, and blade angle, but with different numbers of blades, prove that as the blades become fewer, the head developed progressively declines.[216] The effect is just as though the outlet blade angle had been reduced, which in turn implies a diminution in the outlet whirl component.[217] Thus if in Fig. 360 (i) the full-line velocity triangle represents the ideal conditions hitherto assumed, as in Figs. 354 and 355, then the *effective* outlet angle will be γ_n instead of γ, and the whirl velocity will fall from V to V_n. The ratio V_n/V may be of the order 0·6 to 0·8. Equation 16-2 at once shows how the head generated declines in sympathy with the fall in the *effective* outlet blade angle.

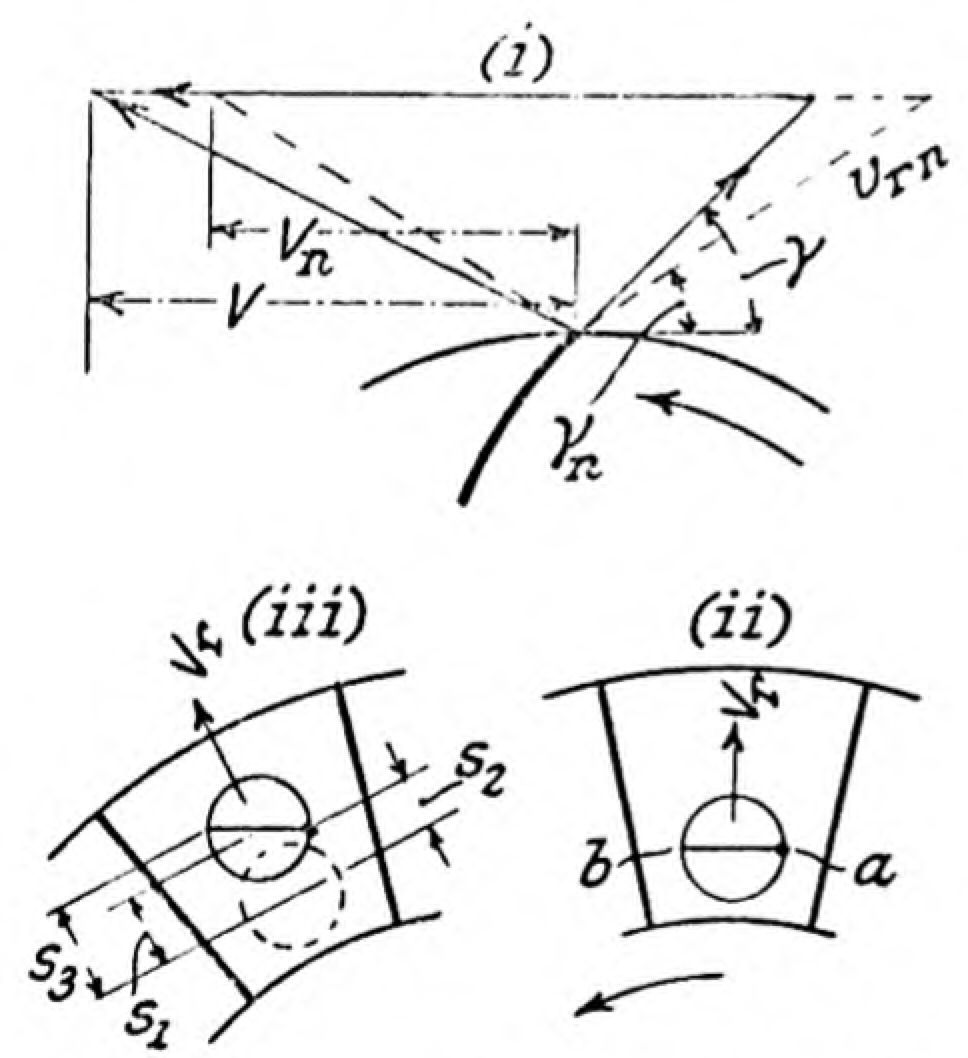

FIG. 360.—Comparison between ideal and real tangential velocity.

An explanation of the liquid's refusal to be strictly guided by the blades when leaving the impeller is suggested in Figs. 360 (ii) and (iii). Here a circular element of liquid is imagined to be flowing along an impeller passage enclosed between radial blades. Although the element is very positively being moved outwards with velocity V_r, it is under no such compulsion to revolve about its own axis. Thus while the impeller is moving

from position (ii) to position (iii), and the centre of the element has travelled a relative distance s_1, yet the orientation of the element with respect to the pump casing has not altered; that is to say, a point a on the element has moved a shorter relative distance (s_2) than point b, (s_3). With respect *to the impeller*, therefore, the element appears to be rotating in the opposite direction to the shaft.

Referring now to Fig. 361, diagram (i) gives an impression of the resulting velocity distribution in an actual impeller passage, while diagram (ii) symbolises the conditions at outlet; the clockwise rotational tendency of the elements, superimposed on the outward flow of the main streams of liquid, makes it inevitable that the outlet velocity vector v_{rn} should be deflected out of alignment with the blade tips. The velocity distribution in the blade passages suggested in Fig. 361 (i) presumably implies that the distribution of *pressure head* will be generally of the form shown in diagram (iii); for if the energy is assumed to be uniform then the highest head will be found in the region of lowest velocity.[218] At any rate it is undoubtedly true that along the leading face of the blade the pressure must be greater than along the trailing face, Fig. 130, § 146. If there were no such differential pressure, no torque need be applied to make the impeller revolve. Experimental proof of these predictions will be found in Fig. 384, § 336.

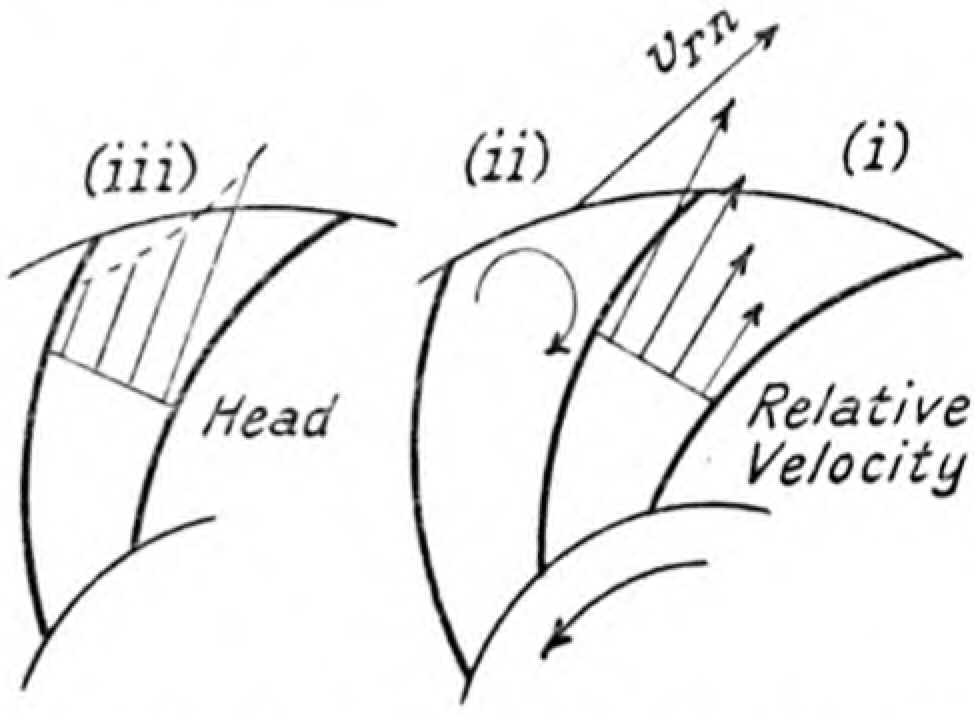

FIG. 361.—Conjectural conditions in impeller.

321. Axial Thrust: Leakage Loss. The end thrust on side-inlet impellers mentioned in § 319 originates in this way: assuming that the water in the casing on both sides of the impeller is stationary (although in fact it will tend to be carried round by the frictional drag of the impeller cheeks), its pressure will be sensibly equal to that at the impeller outlet. But whereas this pressure acts over the whole of the right-hand face of the impeller (I), Fig. 359, there will be an area of diameter d on the left-hand face which is exposed to suction pressure only. A differential static thrust acting towards the impeller inlet is thus generated, which must be resisted in some suitable manner. In small pumps a ball thrust-bearing may suffice, while for high-pressure pumps acting in series the hydraulic balancing device shown in Fig. 368 is satisfactory. Another solution is to try to equalise the opposing forces acting on the impeller, in the manner illustrated in Fig. 362;

relieving holes in the impeller disc permit the suction pressure to be established on both sides, where necessary, and a circumferential seal prevents any significant inflow of high-pressure water into the low-pressure space. Alternatively, equalising pipes may connect the two sides of the pump casing.

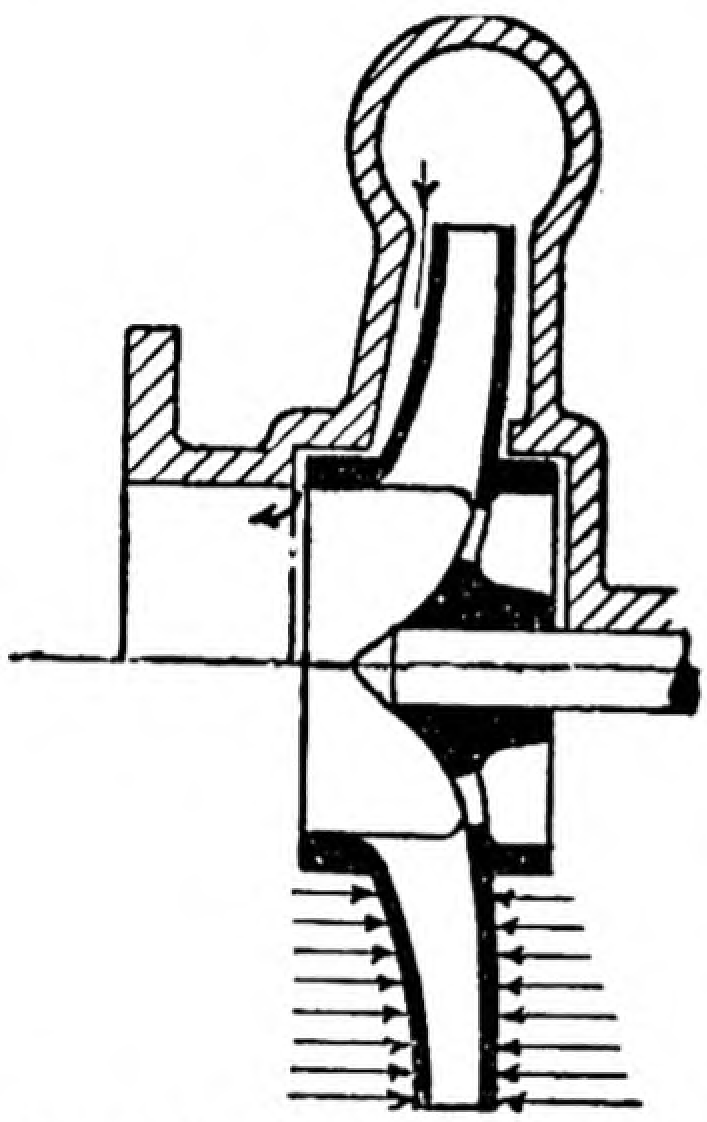

FIG. 362.—Balanced side-inlet impeller.

In centrifugal pumps as ordinarily built, it is not possible to devise a completely water-tight seal between the delivery and suction spaces, and consequently there is always a small return flow around the outside of the impeller, as suggested in Fig. 362. This leakage-, clearance-, slip-, or short-circuit loss may amount to perhaps 5 per cent. of the total discharge (§ 222), its actual value naturally depending upon the pressure difference and upon the radial width of the clearance *a*, Fig. 359 (I). Renewable bronze neck-rings permit this clearance to be brought back to normal if the leakage has become excessive owing to wear, and good results are also obtained with india-rubber neck-rings. The efficacy of such circumferential seals is materially improved if they are formed on the labyrinth principle [219] shown in Fig. 74 (v), § 92.

322. Multi-stage Pumps. For generating high heads it is in many ways advantageous to use a number of relatively slow-speed impellers arranged in series, one pumping into the other, rather than a single impeller running very fast.[220] Firstly, by this method the surface friction loss on the external surfaces of the impeller discs or shrouds (§ 148) is substantially reduced. A comparison between a single-stage pump generating a head H, and a two-stage pump having two impellers each generating a head $\left(\frac{H}{2}\right)$, may be put in tabular form as below. It is here assumed that the pumps have the same discharge and speed ratio, and that the impellers are all of the same diameter. The total disc friction loss in the two-stage pump is thus only 0·7 of the loss in the single-stage pump, although there are two impellers instead of one.

	Single-stage Pump.	Two-stage Pump.
Rim velocity of impeller .	$v = \phi\sqrt{2gH}$	$v_2 = \phi\sqrt{2g\frac{H}{2}} = \frac{v}{\sqrt{2}}$
Relative energy loss in disc friction per impeller (from equation 8-8, § 148) .	Kv^3D^2	$Kv_2{}^3D^2 = K\left(\frac{v}{\sqrt{2}}\right)^3 D^2$
Total relative disc friction loss per pump . .	Kv^3D^2	$2K\left(\frac{v}{\sqrt{2}}\right)^3 D^2 = \frac{Kv^3D^2}{\sqrt{2}}$
Relative specific speed of impeller	$\frac{N\sqrt{Q}}{H^{\frac{5}{4}}}$	$\frac{\frac{N}{\sqrt{2}}\sqrt{Q}}{\left(\frac{H}{2}\right)^{\frac{5}{4}}} = 1{\cdot}19\frac{N\sqrt{Q}}{H^{\frac{5}{4}}}$

Other advantages realised by breaking up the total pressure rise into a number of stages are :—

(i) The number of stages may so be chosen that the shaft speed of the pump is suited to the speed of revolution of the driving engine or motor.

(ii) Centrifugal stresses in the material of the impeller may be kept within desired limits.

(iii) Owing to the reduced pressure difference between the outlet and inlet of the impeller, the "slip," leakage, or return flow from delivery to suction side of the pump is diminished (§ 321).

(iv) The characteristics of the pump may be modified (§ 328) by using in the different stages impellers having different individual characteristics.

(v) By arranging side-inlet impellers in pairs, back to back, axial thrust on the shaft may be neutralised (§§ 321, 324).

(vi) The lower specific speed of the individual impellers permits the pump to work against a higher suction lift (§ 337).

The number of stages to be adopted depends on the limitations of speed of the driving agent, as pointed out in clause (i) above, and also upon the relation between discharge and total head.[116] If these factors are known, the head per stage can be fixed, subject to the restrictions suggested in § 319, viz. specific speed per impeller not to be less than about 18 (foot) or 80 (metric), with a provisional maximum limit of head per

stage of 500 ft. (160 metres). (See Example 171.) Constructional difficulties may arise if the number of stages per pump greatly exceeds 8 or 10.

323. Construction of Multi-stage Pumps. Essential components of the multi-stage pump, in addition to the impellers, are the stationary *return passages* that conduct the liquid from one impeller to the next. In the system shown diagrammatically in Fig. 363, they are formed within the pump casing. Their construction can be seen from Fig. 364; each return passage includes a set of guide-blades, § 316, for the recuperation of the velocity energy of the liquid leaving the impeller. It follows that in traversing the pump, the liquid undergoes changes such as are indicated in Fig. 365. In each impeller, the liquid absolute velocity increases: in each return passage the absolute velocity falls again; but the pressure-head continuously rises. As for the outer casing which contains the fixed and rotating elements, its design will be influenced by the maximum pressure generated; quite often, forged or welded steel must be used. A photograph of such a pump is reproduced in Fig. 366; it is a boiler-feed pump having a duty of 1360 gallons per minute of water at a temperature of 300 deg. F.,

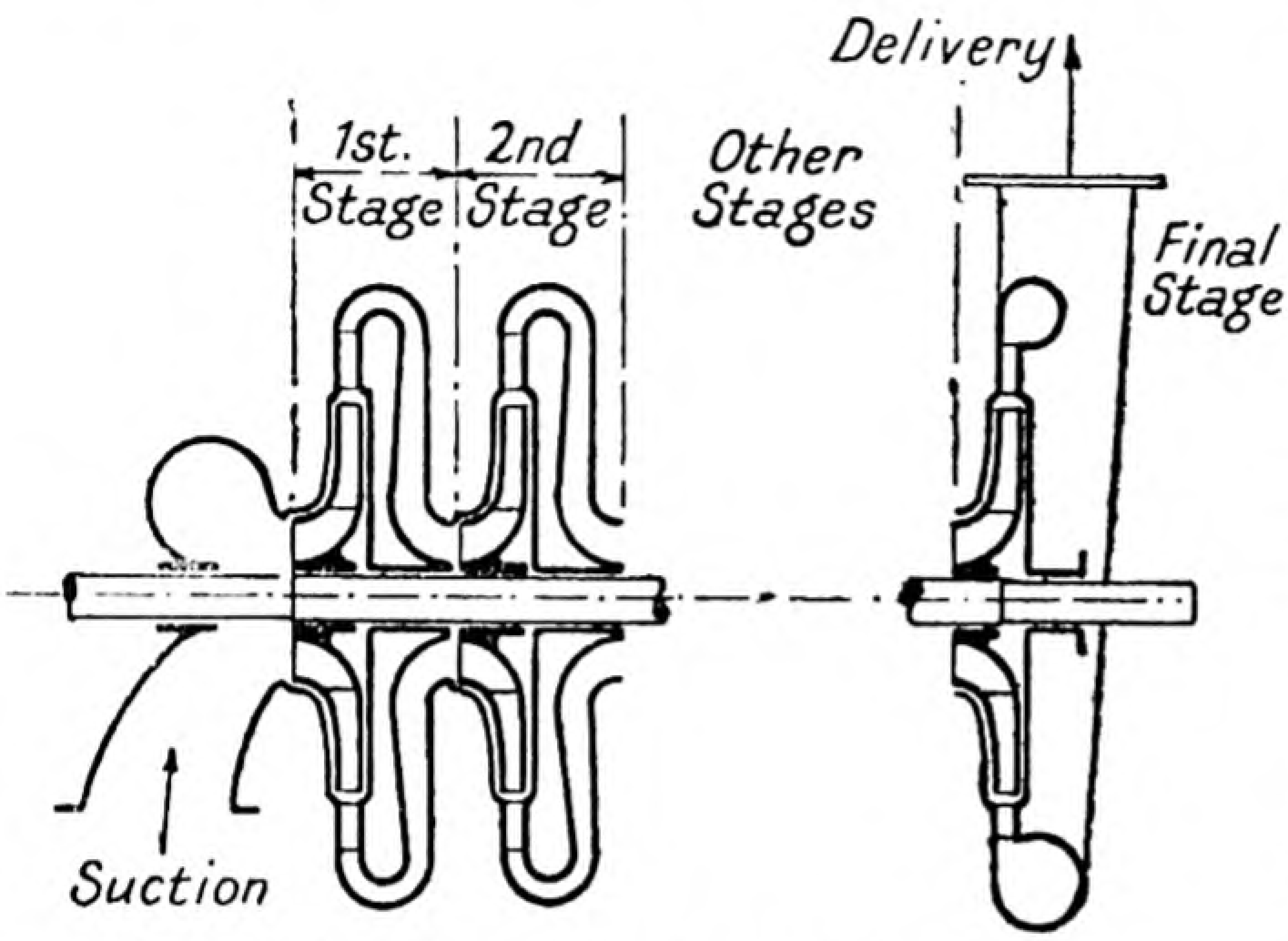

Fig. 363.—Elements of Multi-stage pump.

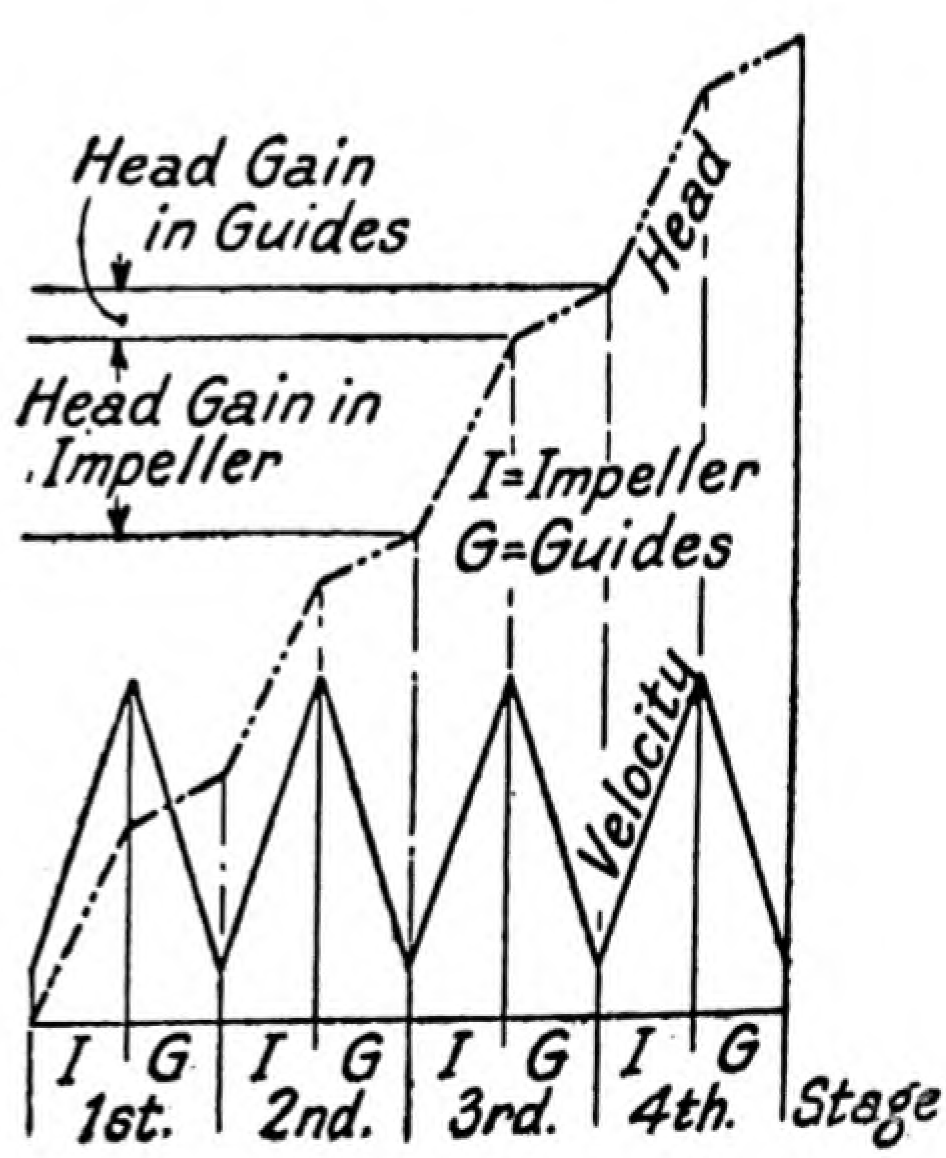

Fig. 365.—Flow through 4-stage pump.

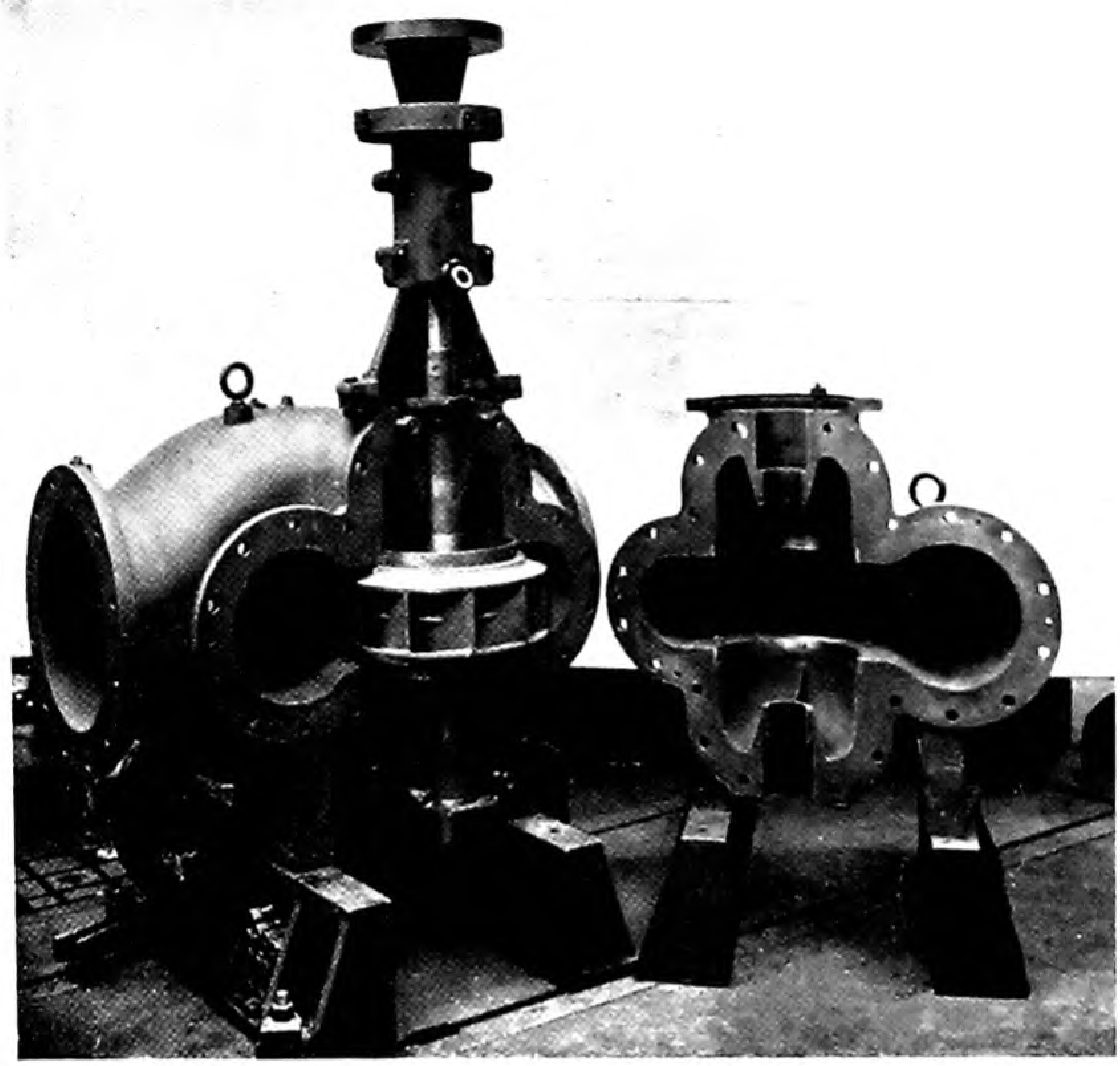

FIG. 358.—27-inch vertical-shaft centrifugal pump.
(See page 463.)
(The Mirrlees Watson Co., Ltd.)

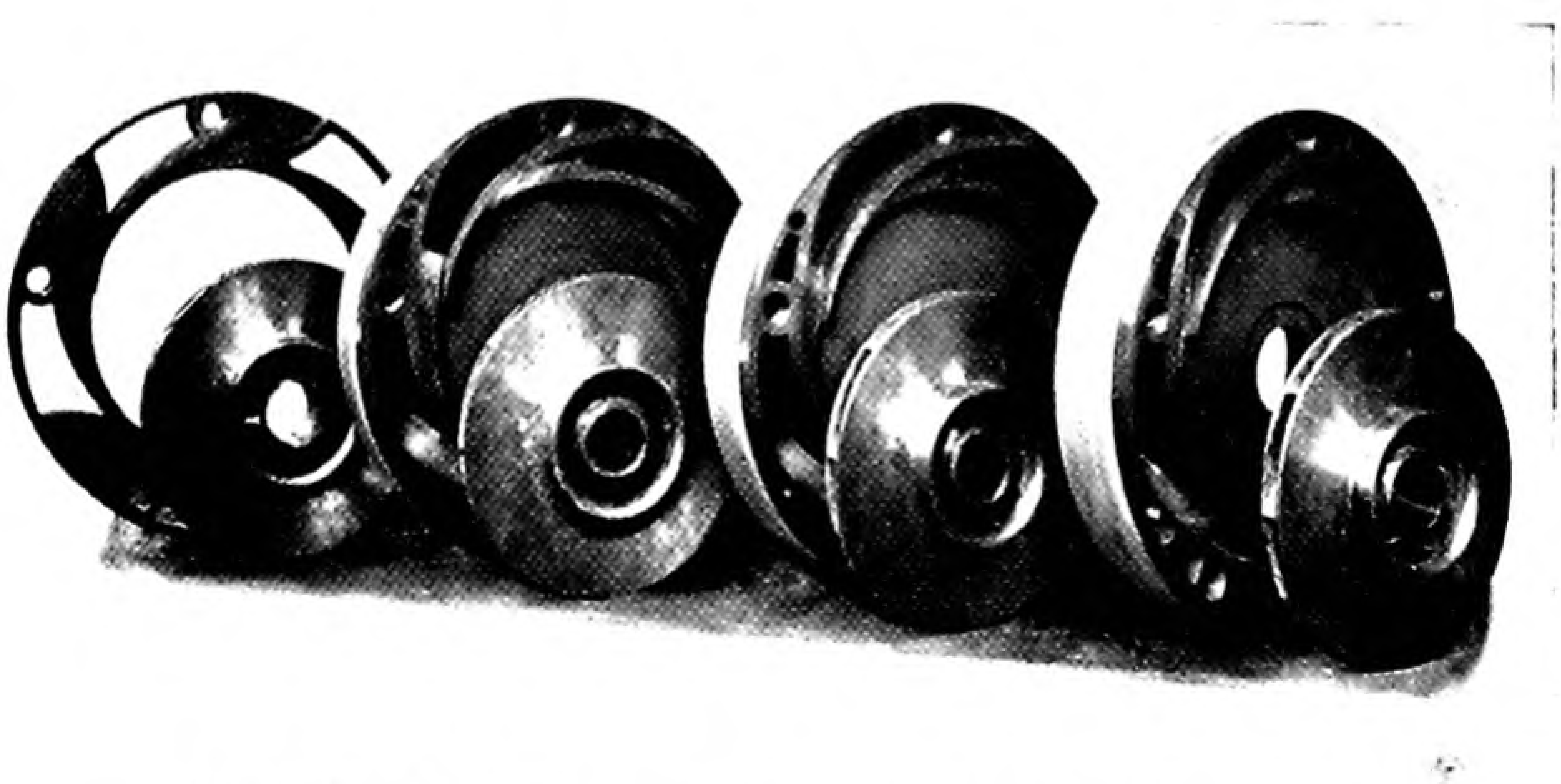

FIG. 364.—Impellers and diffuser rings for 4-stage pump.
(Sulzer Bros., Ltd.)
[*To face page* 470.

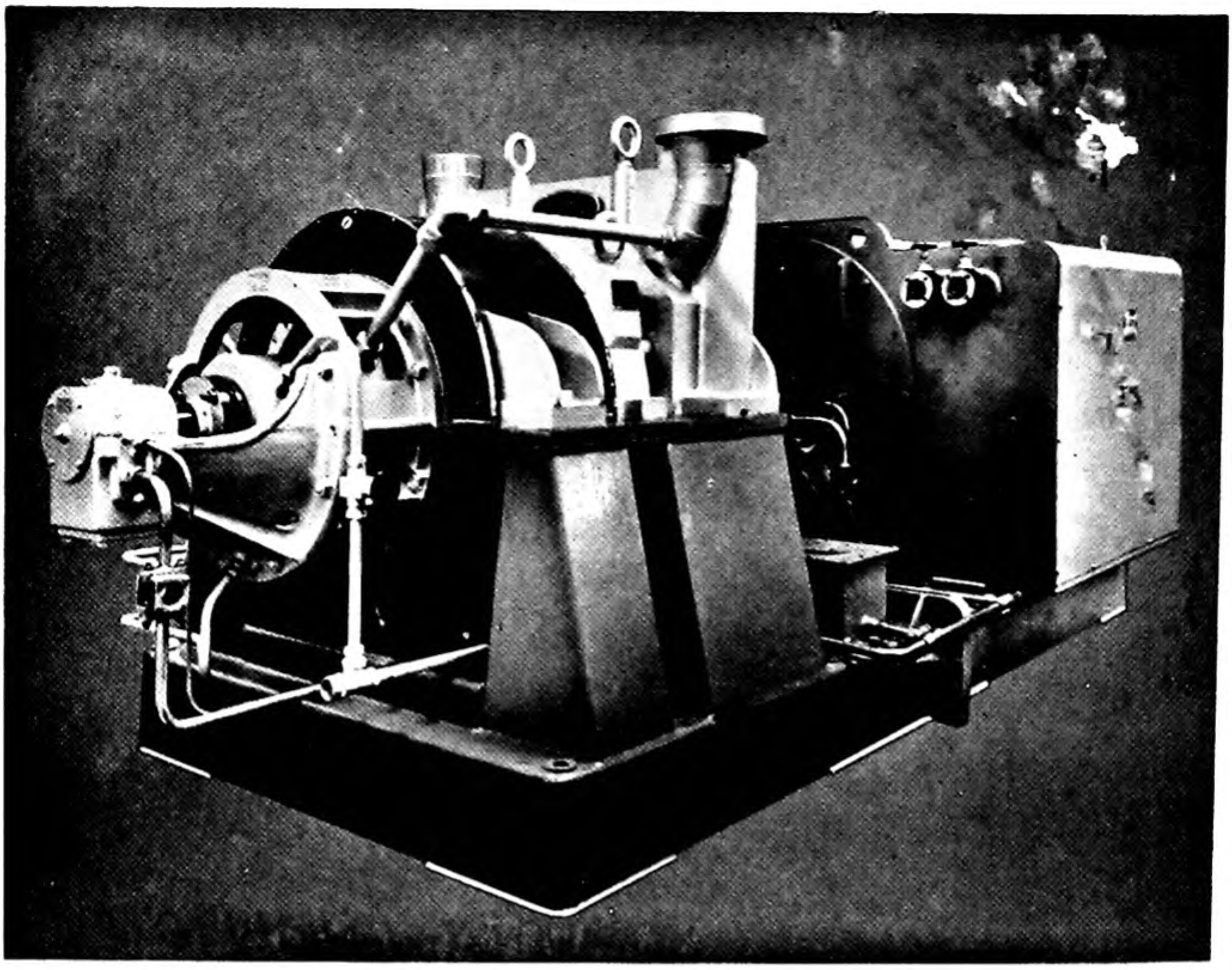

Fig. 366.—Multi-stage boiler-feed pump.
(The Harland Engineering Co., Ltd.)

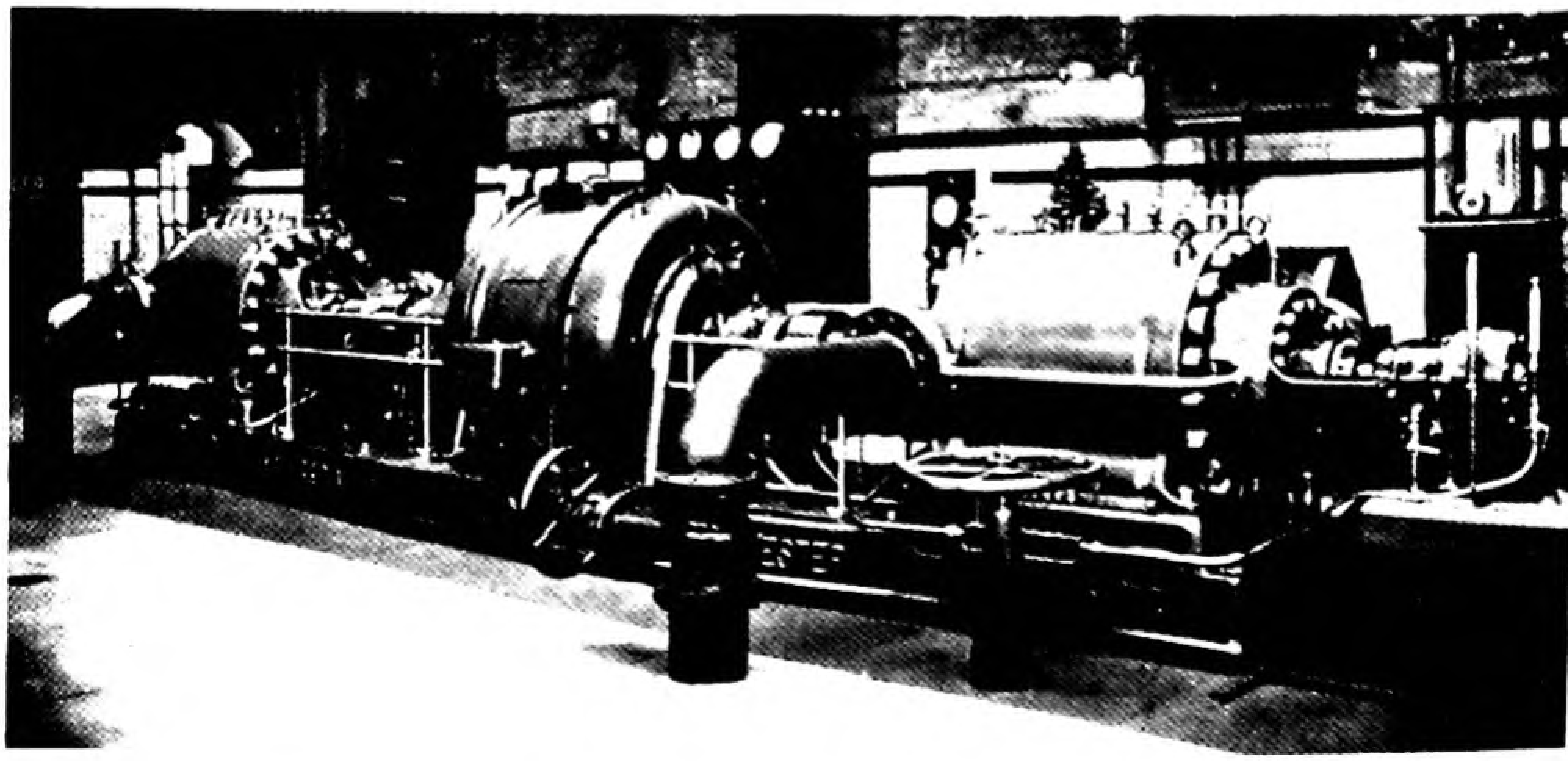

Fig. 367.—Two electrically-driven pumps in series.
(Mather & Platt, Ltd.)

[*To face page* 471.

against a total pressure of 1300 psi (3280 feet head), when running at 3570 r.p.m. The 1600 h.p. driving motor seen in the background is itself water-cooled.

In other circumstances, where high rotational speeds may be considered undesirable, high heads may nevertheless be generated by using two independent multi-stage pumps connected in series by external piping. A single electric motor may drive the pumps, as in Fig. 367.

324. Balancing the Axial Thrust. Even in single-stage pumps using side-inlet impellers, the question of the axial thrust on the impeller needs careful study (§ 321). Manifestly in multi-stage pumps the problem will be greatly accentuated, for the axial thrusts on the individual impellers will be cumulative, all acting in the same direction. It may therefore happen that the gross axial load may amount to several tons. Sometimes a heavy type of ball thrust bearing will serve to resist this load, but more often the simple hydraulic device seen in Fig. 368 is preferred. Its main element is a rotating balancing disc secured to the shaft outside the high-pressure end of the casing; it is of such a diameter that the full delivery pressure acting on the face of the disc is in excess of the combined axial thrust on all the impellers. While the pump is in operation a small flow of water is allowed to leak from the last stage through the groove *a* and between the balancing disc and the casing, finally escaping at atmospheric pressure to a drain. The rate of leakage will automatically adjust itself so that the pressure drop in the groove is such that the resulting hydraulic thrust on the balancing disc is exactly equal to the combined axial thrust, in the opposite direction, on the impellers. As the leakage water must also pass radially between the outer edge of the disc and the casing, there will always be a film of water at this point preventing metallic contact and so ensuring satisfactory lubrication.

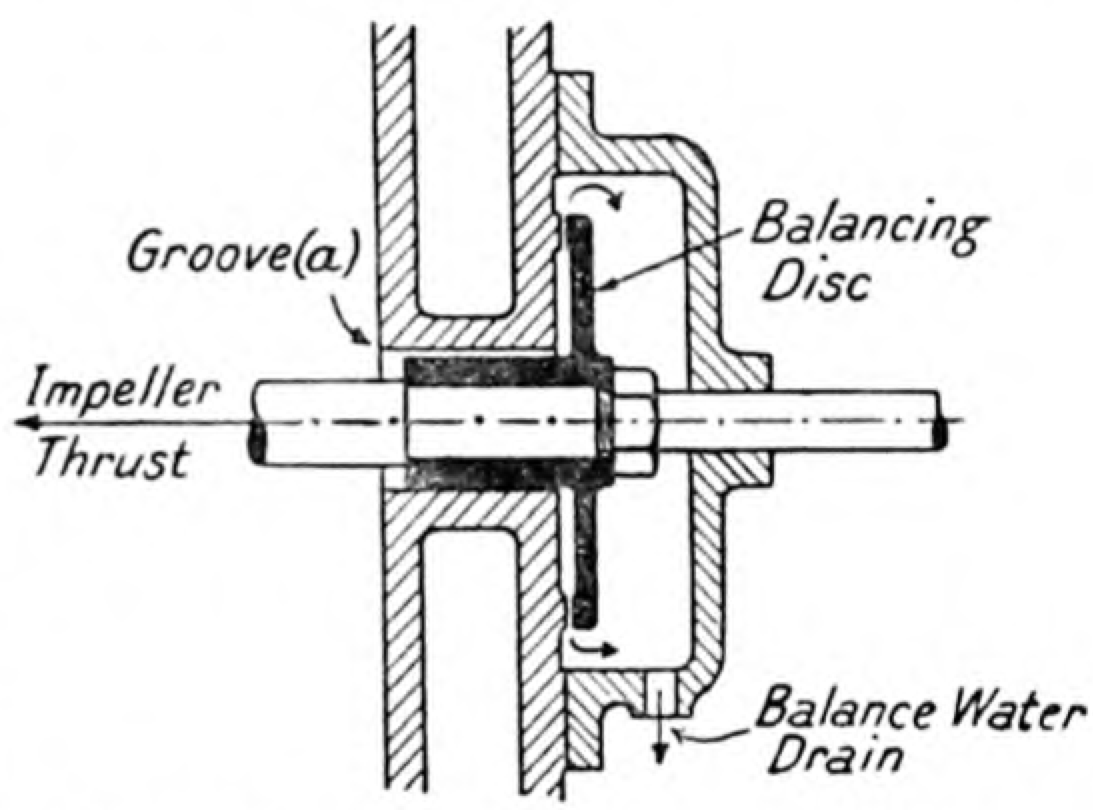

FIG. 368.—Hydraulic balancing device.

Quite another solution of the end thrust problem can be applied if the pump has only two stages: the two impellers are set back to back, so that their axial thrusts act in opposite directions and thus neutralise each other. No balance disc—no concentric return passages—are required: volute type of recuperators, § 317, now suffice, while a transfer passage cast in the pump casing serves to direct the liquid from the first stage to the second. The resulting very convenient disposition of the parts can be judged from Fig. 369; when the top half of the casing of this split-casing two-stage pump is lifted, the interior of the pump is fully exposed to view. A similar balancing principle may even be extended to 4-stage pumps, two opposed pairs of impellers being used. In the arrangement illustrated in Fig. 370, in which there are virtually four independent pumps, the underhung external transfer pipe from the 3rd stage to the 4th stage is quite prominent.

Performance of Centrifugal Pumps

325. Hydraulic Efficiency of Centrifugal Pumps. The efficiency of a pump as computed by equation 16-3, § 315, might have little relation to the actual performance of the machine, because this equation disregards both recuperation of energy and frictional losses of energy. For practical use we require relationships of the kind developed for turbines in § 235; there is no uniformity in presenting them, and so the terms and treatment now to be employed are not necessarily standard ones.[221] (i) The *manometric* or hydraulic efficiency of a rotodynamic pump gives a measure of the efficiency with which it generates pressure; it is the ratio of the total pressure head difference H_m imparted to the water in passing through the pump, to the hydraulic input $\frac{Vv}{g}$. That is, manometric efficiency

$$= \eta_h = \frac{H_m}{\frac{Vv}{g}} \quad . \quad . \quad . \quad (16\text{-}5)$$

How is this total head H_m to be evaluated? A provisional approach was indicated in Fig. 150, § 167; a corrected diagram is now offered in Fig. 371. Here the hydraulic gradient makes

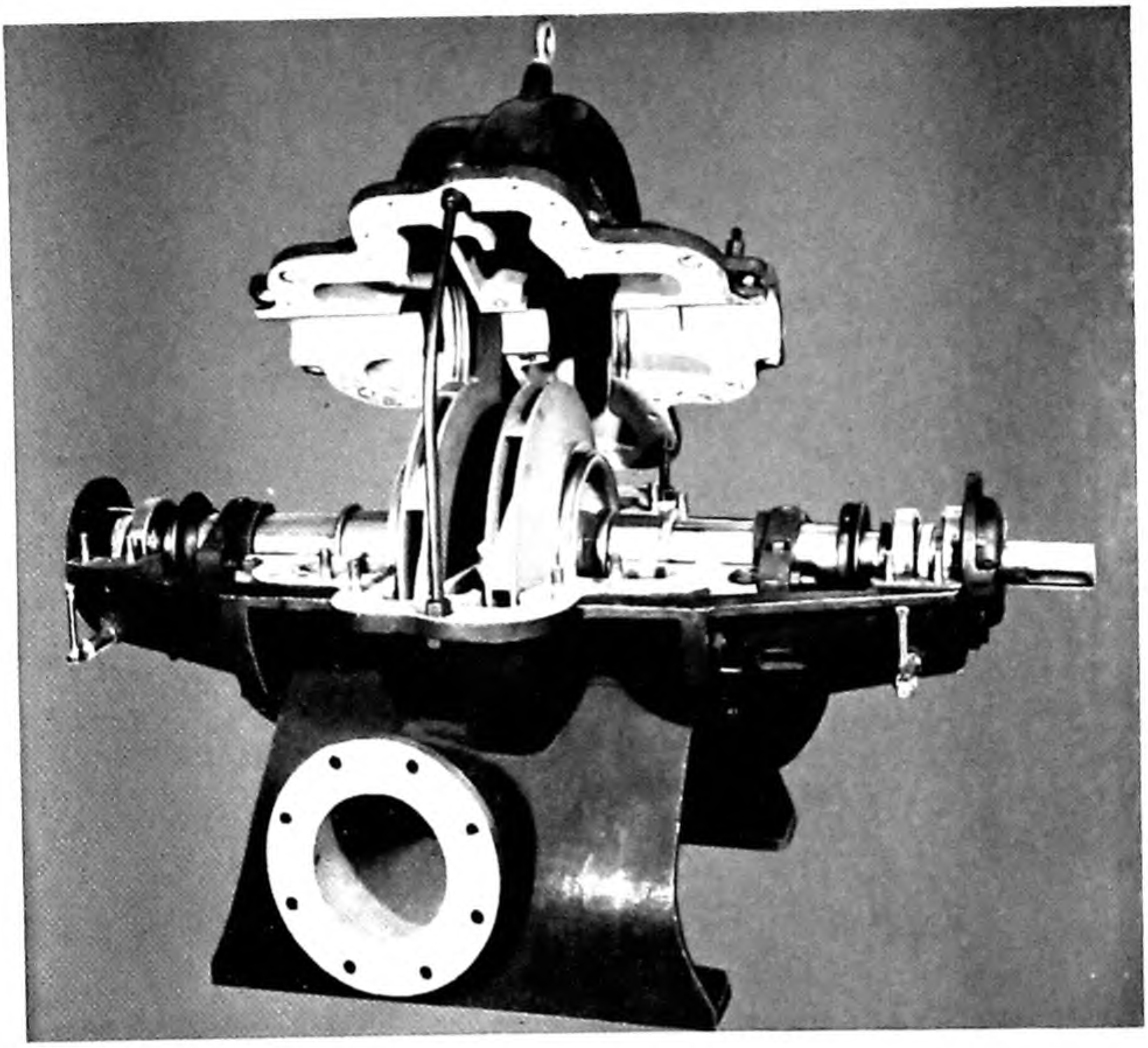

FIG. 369.—Two-stage centrifugal pump, with back-to-back impellers (Gwynnes Pumps Ltd.)

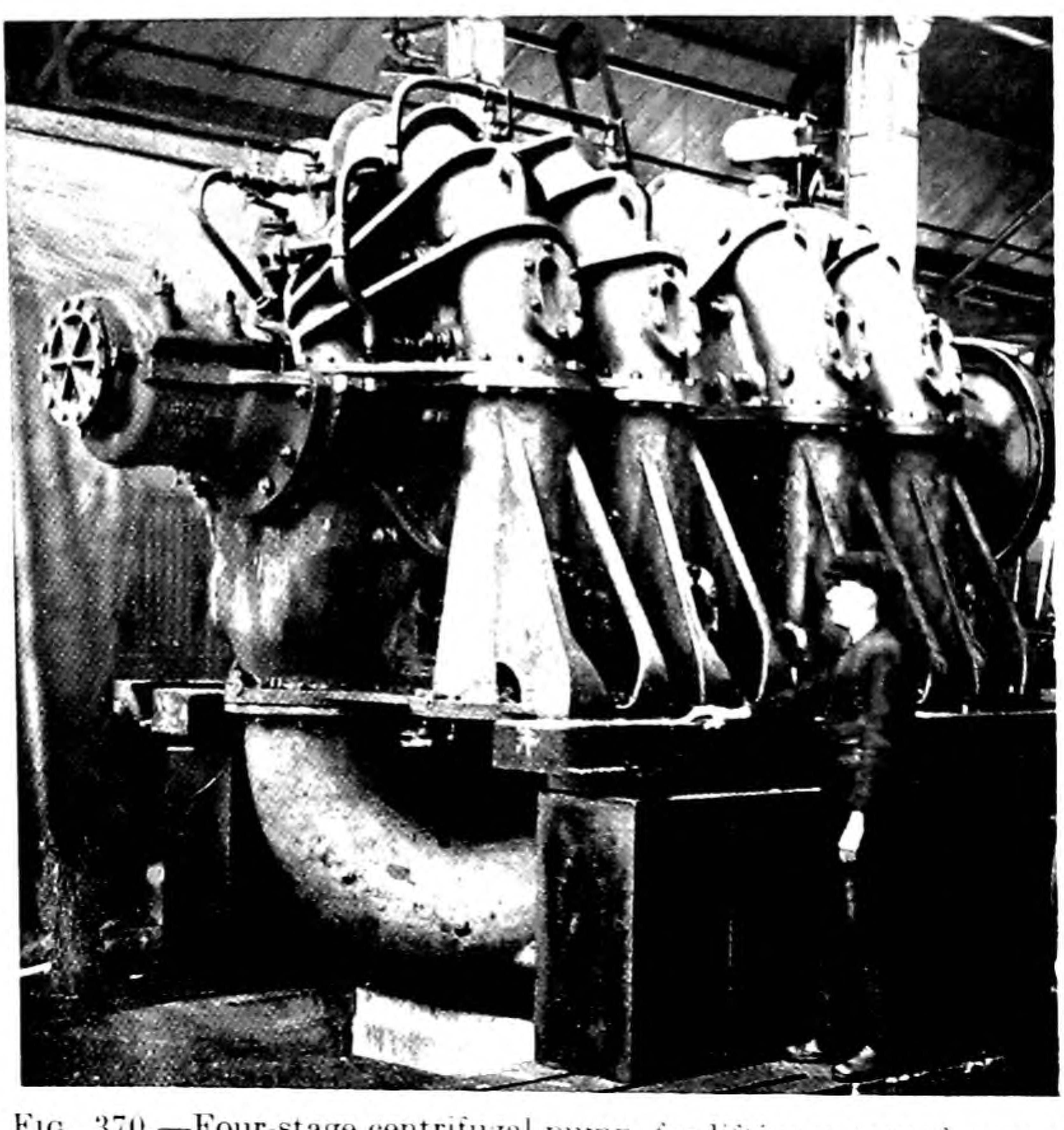

FIG. 370.—Four-stage centrifugal pump, for lifting screened sewage.

it clear that the total rise in pressure head H_m is the sum of the static lift H_s, the pipe velocity head $\frac{V_p^2}{2g}$, and the combined friction and other losses in the suction and delivery pipes, h_{fs}, and h_{fd}. The total rise is also seen to be the arithmetical sum of the reading H_{ms} of a vacuum gauge fixed on the suction

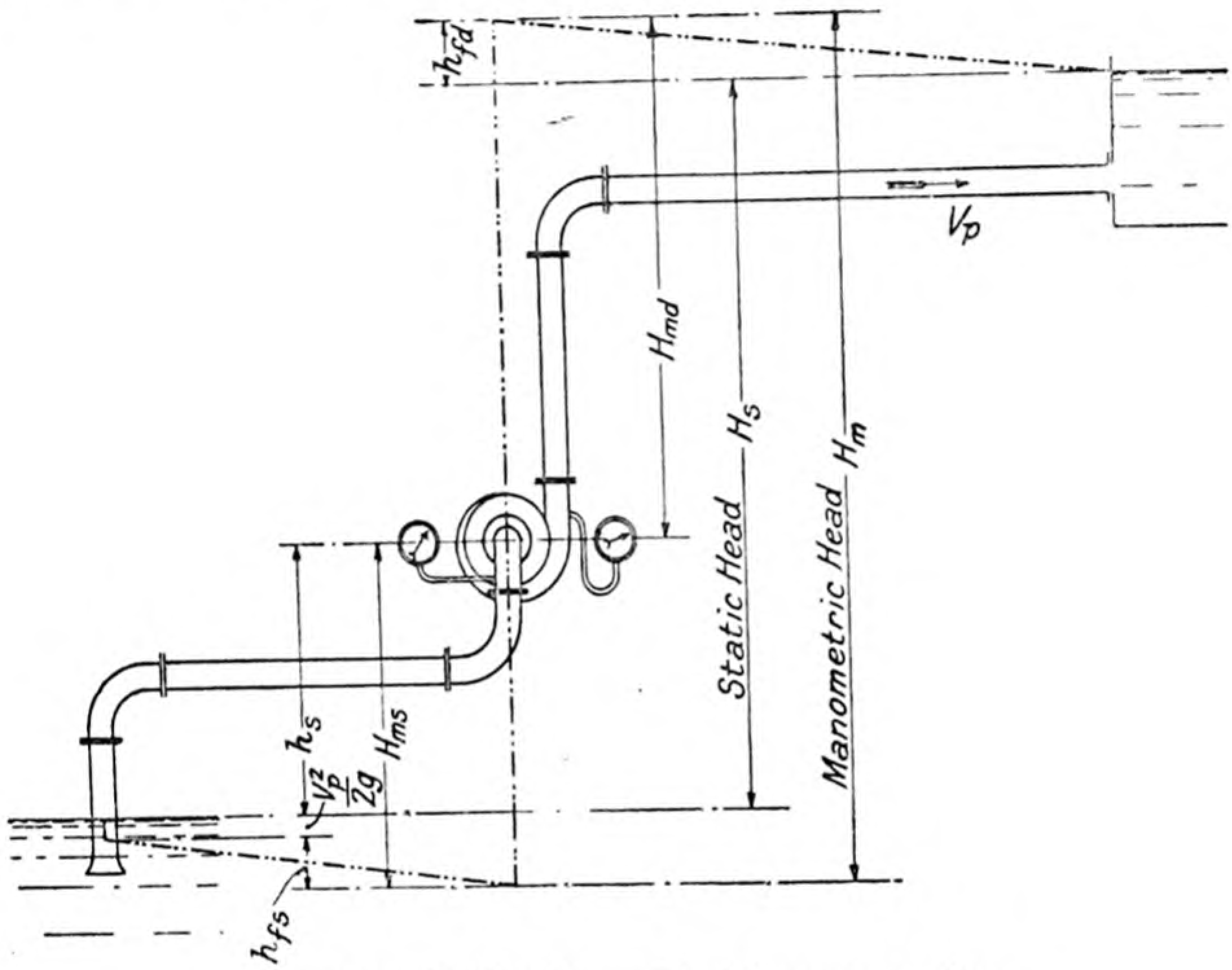

FIG. 371.—Hydraulic gradient in pump system.

pipe just before the pump, and of the reading H_{md} of a pressure gauge on the delivery pipe just after the pump. For this reason H_m is termed the *manometric head* generated by the pump, where

$$H_m = H_s + h_{fs} + h_{fd} + \frac{V_p^2}{2g} = H_{ms} + H_{md}.$$

This equation is only correct if the suction and delivery pipes are of the same size; if, however, they are of different diameters, so that the respective velocities at the gauge points are V_{ps} and V_{pd}, then $H_m = H_{ms} + H_{md} + \frac{V^2_{pd}}{2g} - \frac{V^2_{ps}}{2g}$. In general terms, H_m must always show the total increase in energy given to the water in passing through the pump. In America the term *dynamic head* is used as an equivalent of manometric head.

The general nature of the hydraulic losses sustained by the water in flowing through the pump has already been discussed (§§ 315-317). They consist of (i) the friction and eddy losses as the water flows through the impeller passages, and (ii) the friction and eddy losses in the guide passages or volute casing. The relative proportions of these losses,(222) for typical pumps of low and of medium specific speed, are plotted to scale in Fig. 372.

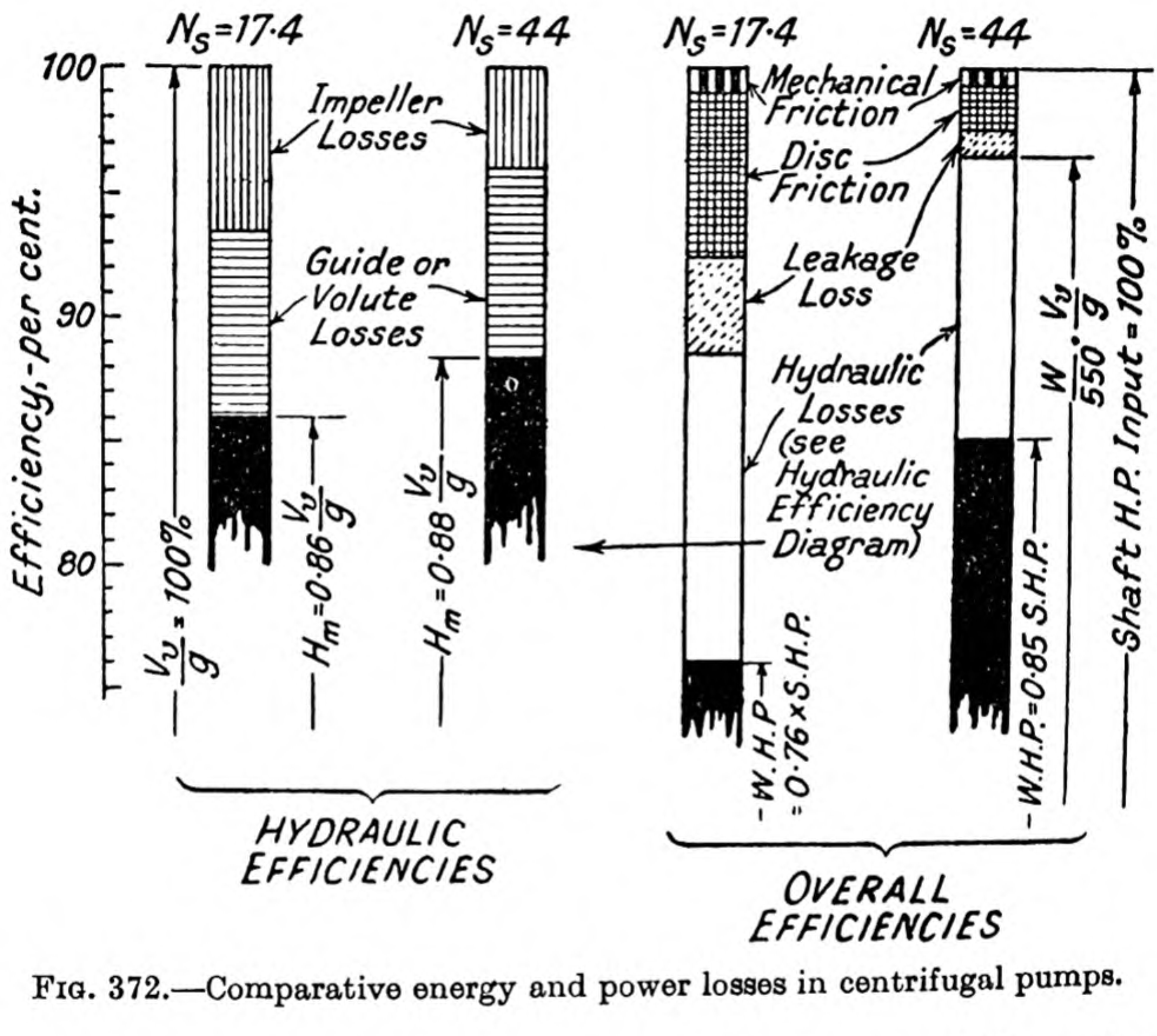

FIG. 372.—Comparative energy and power losses in centrifugal pumps.

We observe that the manometric efficiency of the volute pump of specific speed 44 (foot) is 88 per cent., as against 86 per cent. for the guide-blade pump of $N_s = 17{\cdot}4$ (foot). It is instructive to note that the losses entailed in energy recuperation by means of guide passages (§ 316), viz. 7·5 per cent. of the total input, are hardly any less than the losses involved in the use of a volute (§ 317), viz. 7·7 per cent., in spite of the apparent hydraulic advantages of the former method.

326. Overall Efficiency. The overall or gross efficiency of a pump, no matter whether it is a positive or a rotodynamic

machine (§§ 220, 285), is the ratio of the water horse-power output to the power input at the pump shaft, viz.

$$\text{gross efficiency} = \eta_m = \frac{W.H.P.}{S.H.P.}.$$

Now the shaft horse-power, *S.H.P.*, must include various items in addition to the power needed to impart an amount of energy $\frac{Vv}{g}$ to a weight of water per second W. These items (§ 221) are :—

(*a*) The power required to pump through the impeller the additional weight of water per second w_l which slips or leaks back from the pressure to the suction side of the pump, and which never passes through the delivery pipe at all (§ 321). In multi-stage pumps having the hydraulic balancing device mentioned in § 324, w_l must include also the water that leaks past the balancing disc.

(*b*) The power to overcome surface or disc friction on the external faces or shrouds of the impeller, § 148.

(*c*) The power to overcome the mechanical friction of the main bearings and glands.

It follows that the overall pump efficiency is invariably less than the hydraulic efficiency, as may be seen from Fig. 372.

As for the numerical value of the gross efficiency, this is influenced chiefly by (i) the specific speed of the pump, (ii) the size or output of the pump. One of these trends is manifest in Fig. 372 : as the specific speed rises, the efficiency is likely to increase. For an explanation of this interconnection, it is helpful to study the relative distribution of power losses in the two types of pump, and to interpret these as suggested in §§ 267, 321, 322. The question of rotor size was touched upon in § 279, and is again mentioned in § 330 : an increase in output is likely to bring about a slight increase in efficiency. In a general way, then, one might say that an overall efficiency of the order of 88 or 90 per cent. can only be approached if the pump output is at least several hundred horse-power, and if the specific speed is within the range 30-45 (foot-units). At the other extreme, a user of a multi-stage pump of low specific speed might be well content with a pump gross efficiency of 70 per cent. **(Examples 167, 168.)**

Occasionally, in connection with low lift pumps, the term *static efficiency* is used: it is based on a value of the water horse-power output that takes into account *only* the static lift and not friction or velocity heads as well. Thus if H_s is the static head through which the water is raised, the static efficiency is represented by

$$\frac{\frac{WH_s}{550}}{S.H.P.\text{ input}} \quad \left(\text{or} \quad \frac{\frac{WH_s}{75}}{S.H.P.\text{ input}} \text{ in metric units}\right).$$

Its value must thus inevitably be less than the gross efficiency based on the manometric head. The utility of this conception of efficiency is that it gives credit to the efforts made by the designer to secure a satisfactory regain of head by means of diverging outlet pipes or passages.

327. Centrifugal Pump Performance. Up to this point we have assumed that the pump is working consistently at its *design point*, viz. that its speed, head and discharge have the fixed values specified in the original design. But now we desire more extensive information: we want to know how the pump will behave if any or all of the conditions are modified, e.g. if the speed is increased or the head is lowered. These changes can best be recorded and studied by the use of characteristic curves of the sort plotted in Figs. 373, 374, and 375. Each curve represents the behaviour of the pump at one particular speed, the head being varied—usually by adjusting a throttle valve on the discharge pipe—and the observations made from which discharge and shaft horse-power input may

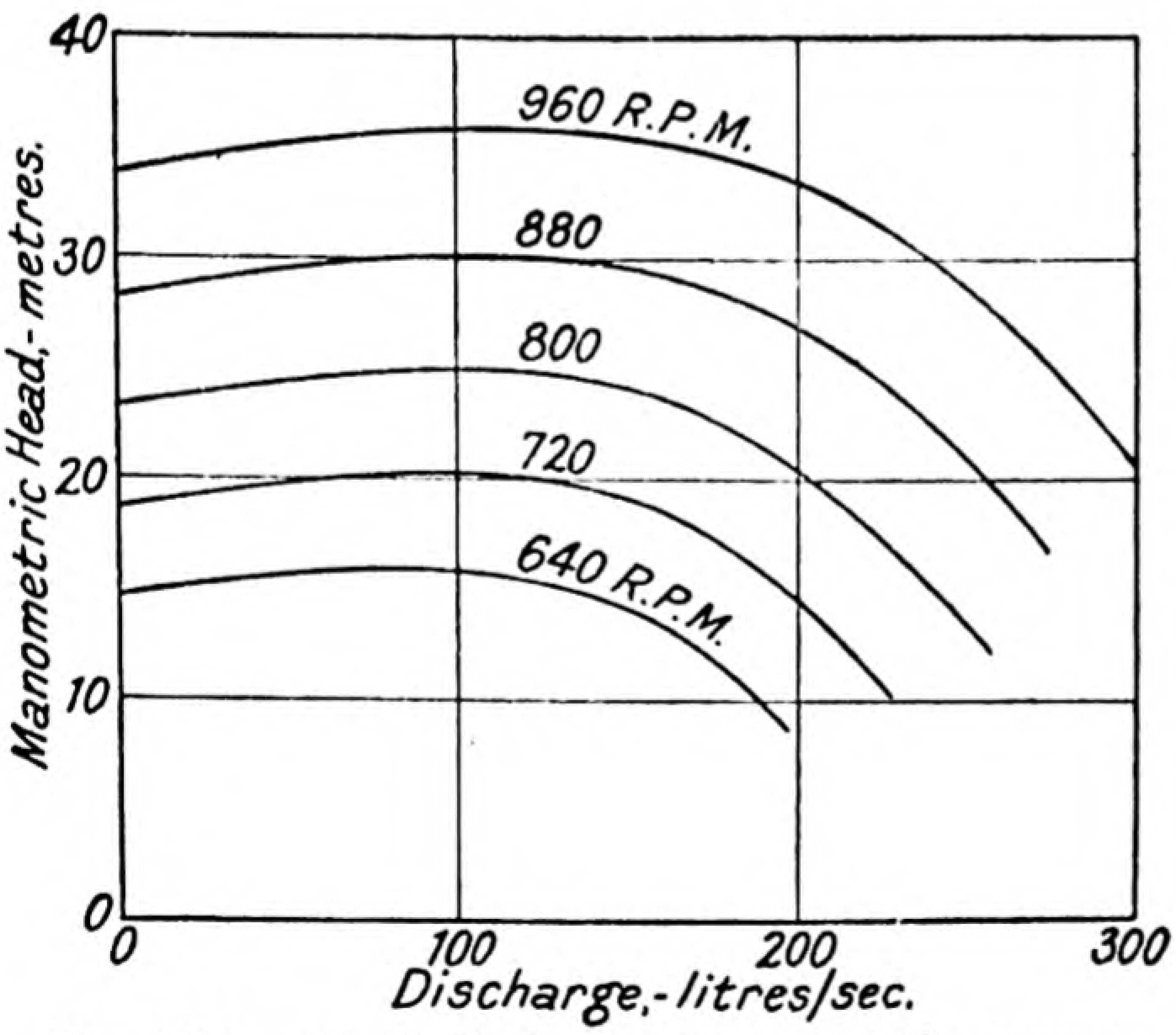

FIG. 373.—Head-discharge characteristic curves.

be computed. In every case, discharge is plotted horizontally while the ordinates represent respectively (i) head, (ii) input, (iii) overall efficiency.

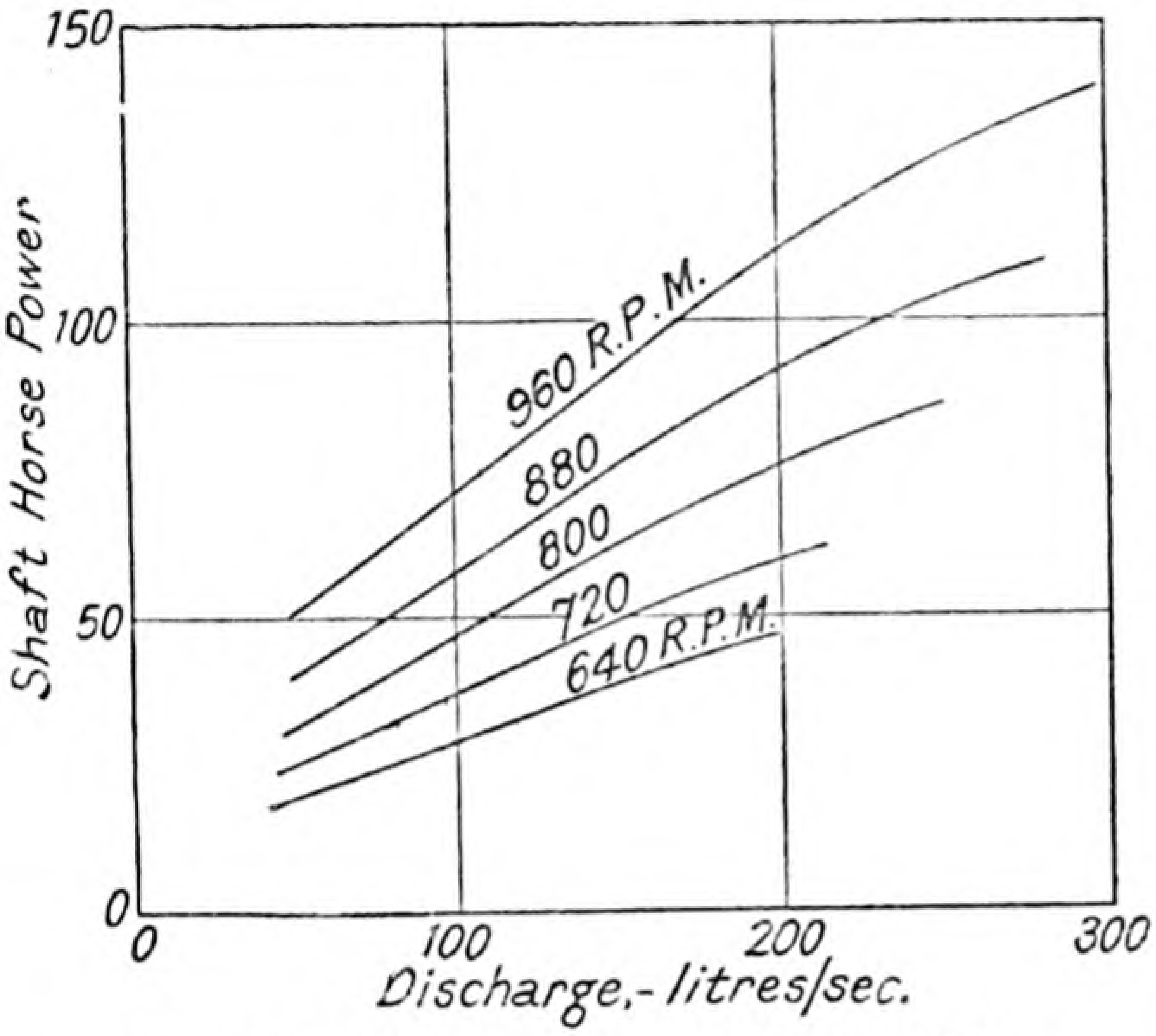

FIG. 374.—Power-discharge characteristics.

The information included in Figs. 373 and 375 may be combined in a single set of graphs (Fig. 376) by plotting a series of *iso-efficiency* curves. Drawing across Fig. 375 a horizontal representing (say) efficiency = 60 per cent., we note the rates of discharge at which this line cuts the efficiency curves at various speeds, and we transfer the resulting values to the corresponding head-discharge curves (Fig. 373). A smooth curve drawn through the points then gives the 60 per cent. iso-efficiency line. Repeating for other efficiencies, the complete series is obtained (Fig. 376).

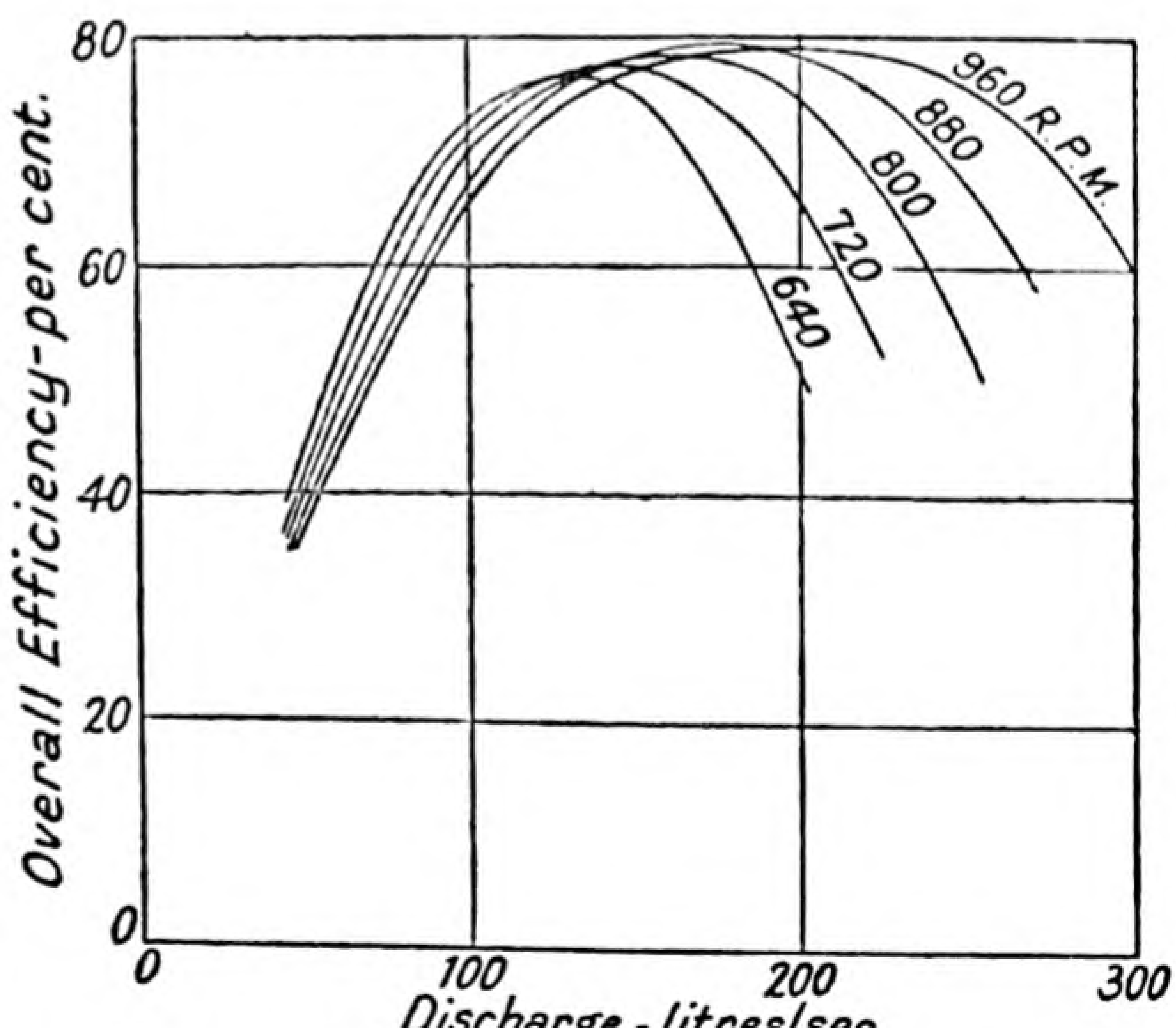

FIG. 375.—Efficiency-discharge characteristics.

A single point on Fig. 376 gives all necessary information concerning the speed, head, discharge, and power of the pump. For example, if a discharge of 220 lit./sec. at a head of 25 metres is called for, the required speed is found by interpolation to be 875 r.p.m.,

and since the overall efficiency is 76 per cent. the shaft horse-power is $\dfrac{220 \times 25}{75 \times 76} = 97.$ **(Example 169.)**

328. Types of Pump Characteristics. For purposes of comparison, another type of characteristic is reproduced in Fig. 377. Denoting the pump concerned as type *B*, and the pump which yielded the curves in Fig. 376 as type *A*, the following differences are to be observed :—

(i) The head-discharge characteristic *A* (Fig. 376) rises gently to a maximum and then falls again, so that at a given speed the head corresponding to zero discharge is substantially the same as it is at the discharge corresponding to maximum efficiency. On the other hand, the type *B* characteristic, after indicating a maximum head at a point quite near the zero discharge point, descends steadily, the head generated when the efficiency is a maximum being only 73 per cent. of the head corresponding to zero discharge.

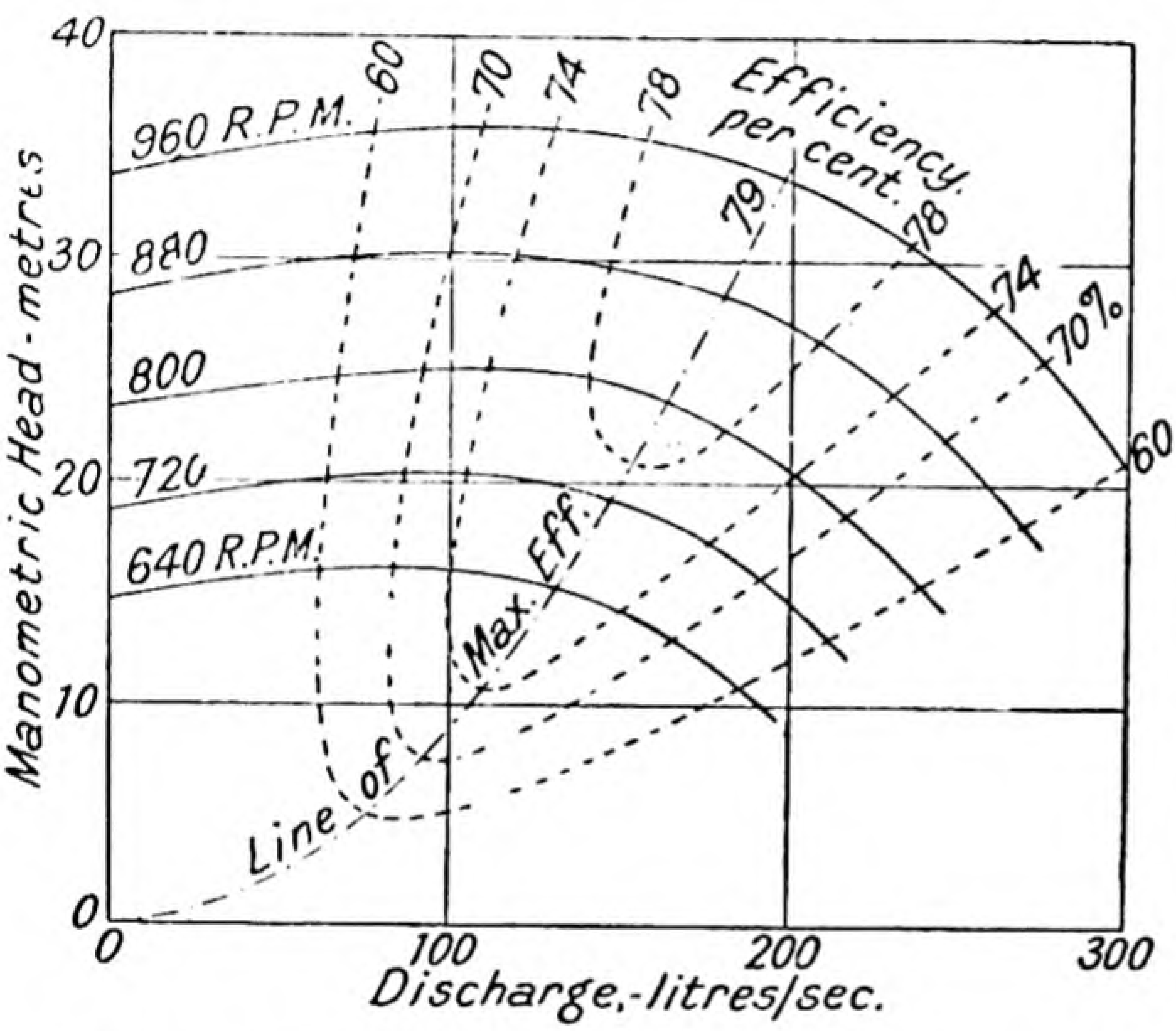

FIG. 376.—Characteristics with iso-efficiency curves (pump *A*).

(ii) The horse-power characteristic *A* (Fig. 374) rises continuously, whereas characteristic *B* indicates a maximum horse-power at the discharge corresponding to maximum efficiency, and a smaller power for discharges greater or less than this.

These differences clearly show how the performance of a pump is under the control of the designer, who by suitably modifying the impeller or casing can give the pump the characteristics he desires. Because in pump *B* there is only one rate of discharge (at a given speed) corresponding to a given head, it is said to have a *stable* head-discharge characteristic. Pump *A* has an *unstable* characteristic, for at each speed there

is a range within which a given head may be associated with two rates of discharge; thus at a speed of 960 r.p.m. and a manometric head of 35 metres, the discharge may be either 45 or 165 lit./sec. The sensitiveness of the pump in these regions of its performance is very marked, e.g. a 70 per cent. increase in discharge (from 120 to 205 lit./sec.) will result either from a $4\frac{1}{2}$ per cent. increase in speed (920 to 960 r.p.m.) at a constant head of 33 metres, or from a 9 per cent. reduction in head (36 m. to 33 m.) at a constant speed of 960 r.p.m.

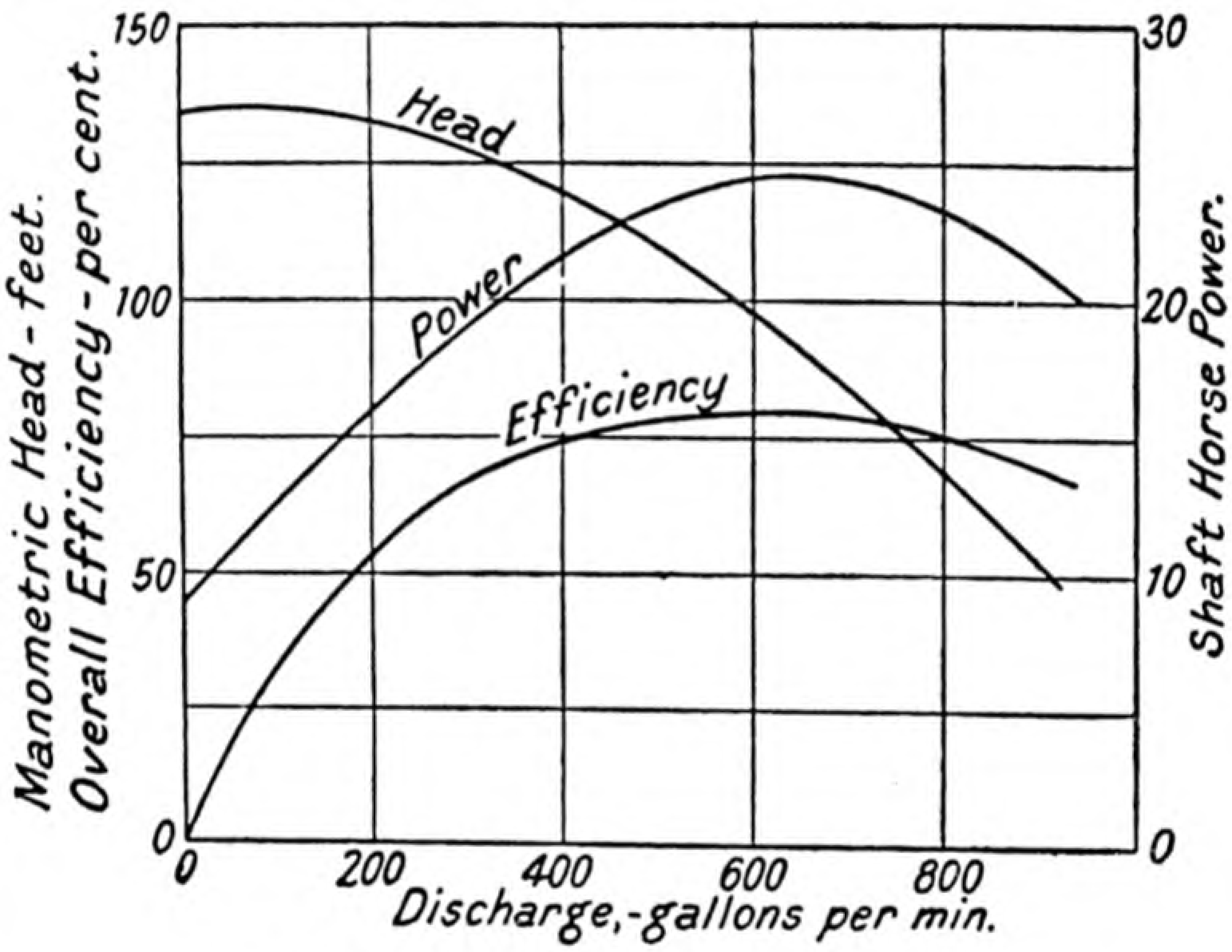

FIG. 377.—Characteristics of pump B.

The difference between the horse-power characteristics, paragraph (ii) above, is expressed by saying that pump B has a *self-regulating* or *non-overloading* characteristic; for at the designed speed no possible alteration of the hydraulic conditions can impose a load on the driving engine or motor greater than the maximum power shown by the curve. But supposing pump A to run normally under the conditions ensuring maximum efficiency, it would be desirable for the driving motor to have a rating 20 per cent. or so in excess of its working load, as a safeguard against the additional load that would inevitably come upon it if for any reason the head fell away.

In weighing the relative advantages of the two types of characteristics, it should be remembered that the external

manometric head H_m against which the pump has to work is itself very often linked up with the rate of discharge; for example, when a pump is required to force water through a long delivery main. The apparent instability of pump A now disappears, for except at low rates of discharge the external head curve cuts each of the characteristic curves at one point only. But if two identical pumps with unstable characteristics deliver in parallel against an unvarying head, then they may behave very unaccountably. Instead of sharing the water equally, one or the other in turn may try to take it nearly all, resulting in a violent surging action which may reach a dangerous intensity. **(Example 170.)**

329. Analysis of Characteristic Curves. From equation 16-2 (§ 314), it is readily seen that the lift H generated under ideal conditions by a centrifugal pump impeller may be expressed by the equation $H = CN^2 - KQ^2$, the corresponding ideal head-discharge curve being of the form I (Fig. 378). The disparity between this ideal parabolic curve and an actual characteristic as shown by the broken curve may be explained as follows: at low rates of discharge the head recovered in the guide passages or in the volute, which is ignored in equation 16-2, causes the actual head to rise above the ideal head; but later on, especially when the discharge is in excess of that for which the guide passages were designed, the friction, eddy, and shock losses in impeller and casing are greater than the regain in head, and the actual curve then falls below the ideal one. The eddy and shock losses are of the same general nature as those illustrated in Figs. 297, 299; as the blades are adapted to one set of conditions only, they cannot be wholly suitable for other conditions. *See also* § 344.

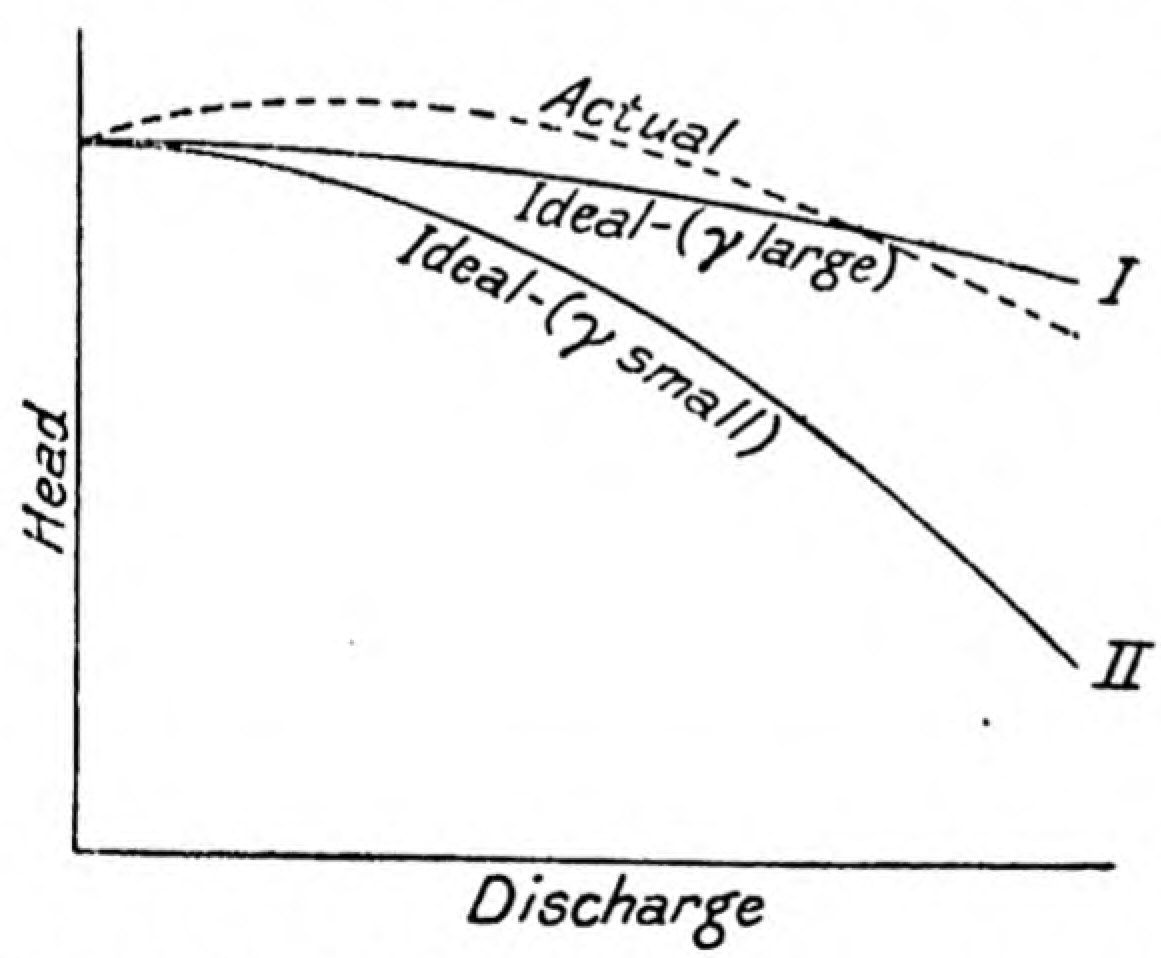

FIG. 378.—Ideal and actual characteristics.

Since the factor K in the equation $H = CN^2 - KQ^2$ depends upon the value of $\operatorname{cosec}^2 \gamma$ (equation 16-2), the effect

of diminishing the blade angle γ will be to cause the ideal characteristic to fall more sharply. Thus curve I (Fig. 378) is typical of an impeller having a large angle γ and curve II relates to an impeller with a small angle. It is to be noted that both of these ideal characteristics are inherently stable.

330. General Relationships between Speed, Head, Power, and Discharge. It was shown in §§ 261 and 262 that similar turbines should have identical efficiencies so long as the velocity diagrams remain geometrically similar. Applying the same reasoning to the pump velocity diagrams (Fig. 354, § 314), we find that the conditions for maintaining unchanged the shape or proportions of the velocity diagrams under changing heads or speeds are:

(i) The ratio $\frac{v}{Y}$ must be kept constant, from which it follows that $\frac{N}{Q}$ must be invariable, or that N must vary directly as Q.

(ii) If the ratio $\frac{v}{Y}$ is invariable, it is evident from equation 16-2 that $H = \text{constant} \times Y^2$, or that H must vary directly as Q^2 or as N^2.

(iii) Since the horse-power varies as QH, it follows from (i) and (ii) that the power varies as Q^3 or as N^3.

On any iso-efficiency curve, therefore, such as those plotted in Fig. 376, the following relationships or affinity laws should hold[223] :—

$$\begin{aligned} \text{The discharge} &\propto \text{speed}, \\ \text{head} &\propto (\text{speed})^2, \\ \text{power} &\propto (\text{speed})^3. \end{aligned}$$

According to this analysis all iso-efficiency curves should be parabolas passing through the origin, and it will be noticed that the points of maximum efficiency at each speed in Fig. 376 do in fact lie on a parabola. The reason for the slight departure of the other curves from the ideal law has been touched upon in § 278: it may here be restated in this way—the actual efficiency would only remain the same under the specified conditions if the power *wasted* as well as the *useful* water horse-power varied as (speed)³. Now §§ 148 and 91 show that neither disc-friction power loss nor pipe-friction power loss

obeys the cubic law unless the exponent n is exactly 2. As in fact its value is found to be slightly less than 2, there must necessarily be a small increase in efficiency as the pump speed or discharge increases, in accordance with the stipulated affinity laws.

Apart from this disturbing influence, it could be said that if, instead of plotting values of H_m, Q, and P for various speeds, we were to plot values of $\frac{Q}{N}$, $\frac{H_m}{N^2}$, and $\frac{P}{N^3}$, then all the points would fall on a single set of curves representing the performance of the pump at a speed of 1 r.p.m. But as the numerical values

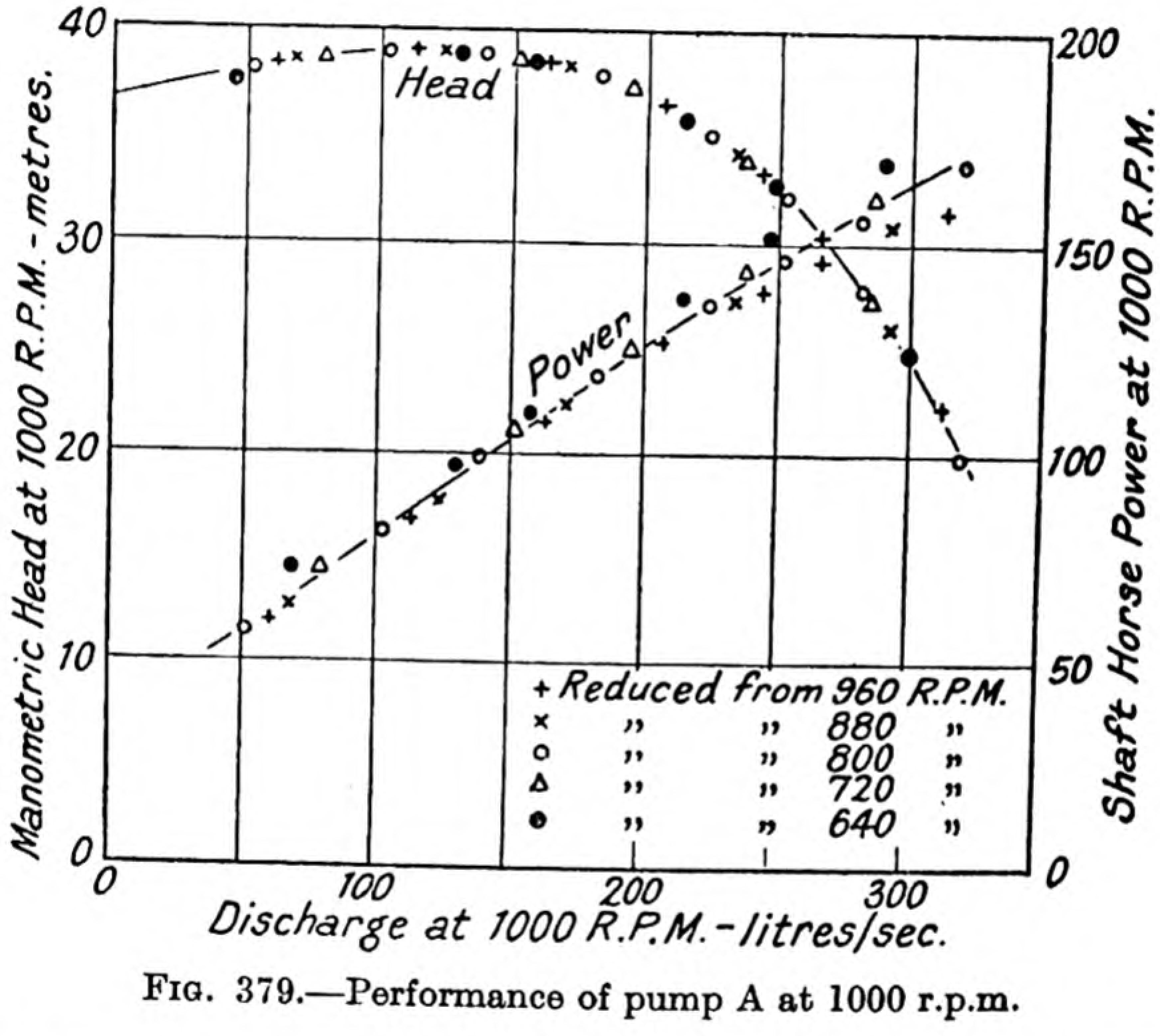

FIG. 379.—Performance of pump A at 1000 r.p.m.

involved would be inconveniently small, it would be of greater practical utility to plot instead curves relating to the performance of the pump at some higher standard speed—say, at 1000 r.p.m. This has been done in Fig. 379. Having chosen a number of points on the curves in Figs. 373 and 374, the respective values of discharge are divided by $\frac{N}{1000}$, of head by $\left(\frac{N}{1000}\right)^2$ and of power by $\left(\frac{N}{1000}\right)^3$. These reduced values lie sufficiently fairly on the mean curves to permit Fig. 379

to serve as a summary of the whole of the information presented in Figs. 373 to 376.

331. Characteristics reduced to Standard Conditions. A final generalisation is reached by plotting from the observed data of a pump's behaviour a head-discharge characteristic curve showing the performance of a geometrically similar pump having an impeller of *standard diameter*—say 1 ft.—running at *standard speed*—say 1000 r.p.m. This relationship between $\frac{H_m}{D^2}\left(\frac{1000}{N}\right)^2$ and $\frac{Q}{D^3}\left(\frac{1000}{N}\right)$ is of great utility in comparing pumps of different sizes, speeds, and specific speeds.[224] In Fig. 380, for instance, the performances

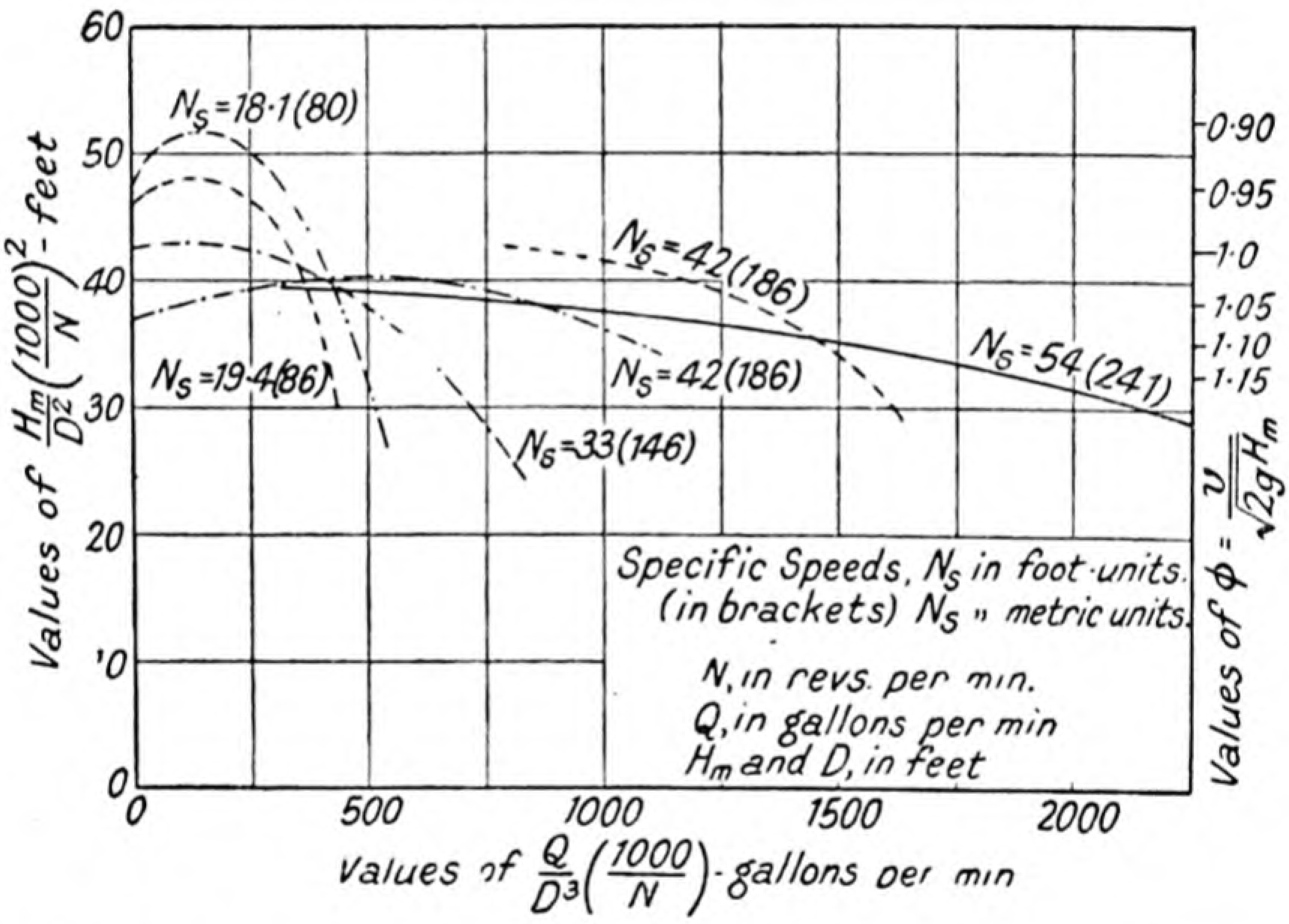

FIG. 380.—Performance of pumps with impellers 1 ft. diam. running at 1000 r.p.m.

of a variety of pumps by different makers are shown reduced to these standard conditions; the figure shows that whereas low specific speed pumps rarely yield a " reduced " discharge exceeding 500 gallons per minute, the " reduced " discharge of high specific speed pumps may rise to 2000 gallons per minute or more. In short, the " reduced " characteristic curve describes the pump's performance just as conveniently as the specific speed describes the pump's shape. **(Example 171.)**

The derivation of the " reduced " pump characteristic is as follows: By reducing the diameter of the impeller from D feet to 1 foot, keeping the

speed at 1000 r.p.m., the area for flow is diminished in the ratio $\frac{1}{D^2}$, and both the rim velocity and the velocity of flow are diminished in the ratio $\frac{1}{D}$. Consequently if the discharge passing through the impeller of diameter D at 1000 r.p.m. is $Q \times \left(\frac{1000}{N}\right)$, then the reduced discharge passing through the impeller of diameter 1 foot will be $Q \times \frac{1000}{N} \times \frac{1}{D} \times \frac{1}{D^2} = \frac{Q}{D^3}\left(\frac{1000}{N}\right)$.

Similarly, since manometric head $\propto$ (rim velocity)^2, the head at 1000 r.p.m. will be reduced from the value $H_m\left(\frac{1000}{N}\right)^2$ when the impeller is D feet diameter to the value $\frac{H_m}{D^2}\left(\frac{1000}{N}\right)^2$ when the impeller is 1 foot diameter.

By a slight rearrangement, the values used in Fig. 380 can be put into *non-dimensional* forms in harmony with the non-dimensional shape number developed in § 318. Suitable expressions are :—

$$h_c = \text{characteristic head number} = \frac{gH_m}{n^2D^2},$$

$$q_c = \text{characteristic discharge number} = \frac{Q}{nD^3}.$$

As in all such expressions, § 40, the units must be consistently chosen, e.g.

g = acceleration of gravity in foot units.
H_m = manometric head in feet,
n = revolution per second,
D = diameter in feet,
Q = discharge in cubic feet per second.

(Example 187.)

332. Influence of Physical Properties of Liquid Pumped.

332. Influence of Physical Properties of Liquid Pumped. (*a*) *Temperature.* It has been assumed in the preceding paragraphs that the liquid passing through the pump is pure water at atmospheric temperature. Changes in the density of the liquid will not affect the head-discharge characteristics, but they will affect the *pressure* generated, because pressure = head × density. If, therefore, a pump develops a pressure p and requires a horse-power input *S.H.P.* when dealing with water, the pressure and power when dealing with a liquid of specific gravity S.G., under identical conditions of head, speed, and discharge, will be p. (S.G.) and *S.H.P.* × (S.G.) respectively (§ 285).

In this connection the effect of temperature on the density even of water should not be overlooked. It was pointed out in § 5 that the density of water at 400° F. is only 87 per cent. of its density at normal atmospheric temperature; and in steam power stations centrifugal pumps may have to handle water at higher temperatures than this. Since the feed-pump

is required to deliver a specified *weight* of water per hour against a stipulated boiler pressure, the power input to the pump *increases* as the temperature rises, thus : *S.H.P.* varies as *W.H.*, i.e. as $\frac{W \cdot p}{w}$. For this reason it is more economical to place the feed-heaters on the delivery rather than on the suction side of the feed-pump. The appearance of a high-pressure, high-temperature boiler feed pump has been illustrated in Fig. 366.

(*b*) *Viscosity.* The effect on the head-discharge curve of using liquids more viscous than water is inappreciable, so long as the kinematic viscosity is not more than about thirty times that of water. An increase in the viscosity does, however, increase the power required to drive the pump under given conditions of speed, head and output. For viscosities much greater than those mentioned, the head generated at a given speed and discharge declines seriously.[(225)]

The laws of dynamical similarity are as valuable in this connection as they were when applied to turbines (§ 278). By making tests on scale models of pumps using *compressed air* as a working fluid instead of water, the performance of full-scale machines may be predicted fairly accurately and at small cost.[(226)]

333. Piping and Accessories for Centrifugal Pumps. The successful working of a centrifugal pump depends to quite a large extent on the correct layout of the piping to which it is connected—particularly of the suction piping. The precautions that must be observed are nearly all concerned with the removal of air from the suction pipe and with preventing the ingress of air. Before the pump can generate pressure at all it must be *primed*—§ 334—and during the operation of the pump the air liberated from the water in the suction pipe, under the influence of the negative head (§ 11), must continually be disposed of. Whenever a centrifugal pump runs badly or irregularly or ceases to deliver altogether, the trouble more often than not will be found to be caused by excessive amounts of air in the pipe or the pump.

A typical small pumping plant is shown diagrammatically in Fig. 381. The water from the well first passes through a strainer on the end of the suction pipe, designed to keep

out floating rubbish from the pump, and then through a *foot-valve*, which is a form of reflux or non-return valve (§ 173) opening upwards. The suction pipe should rise all the way to the pump, without any loops such as those shown by the broken lines, in which air could collect and spoil the performance of the pump by forming an *air lock*. Scrupulous care is needed to see that all joints in the pipe are perfectly

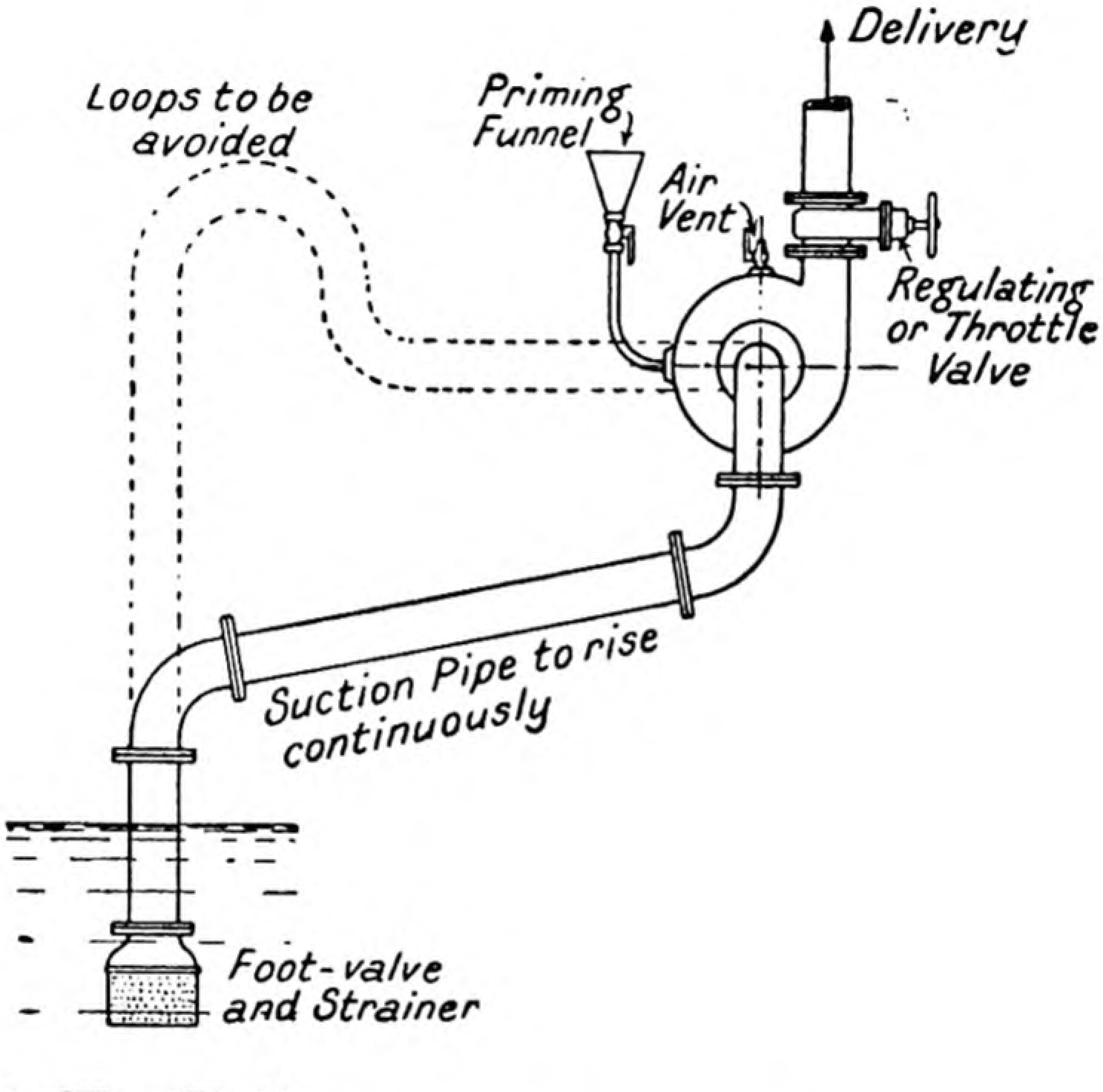

FIG. 381.—Piping layout for small pump.

airtight. In brief, the shorter and straighter the suction pipe, and the nearer the pump is to the well water surface, the less will be the likelihood of difficulties in working. The maximum permissible suction lift may be estimated in the manner suggested in §§ 335, 337, 348.

The screw-down or sluice-valve on the delivery pipe is useful for regulating the output of the pump. It should be left closed while the pump is being primed and run up to speed, and should be closed again before the pump is stopped, otherwise the full delivery pressure will be transmitted to the suction pipe, with the possibility of an added inertia pressure when the water column begins to flow backwards and is suddenly checked by the closing of the foot-valve.[227]

With electrically-driven pumps there is often a danger that a failure of the power supply may bring about such a stoppage of the pump, with open delivery valve; an impression of the violence of the pressure surges that may follow is given by Fig. 382, which is a reproduction of an actual time-pressure record in these conditions. (See also §§ 117 and 118.) Excessive

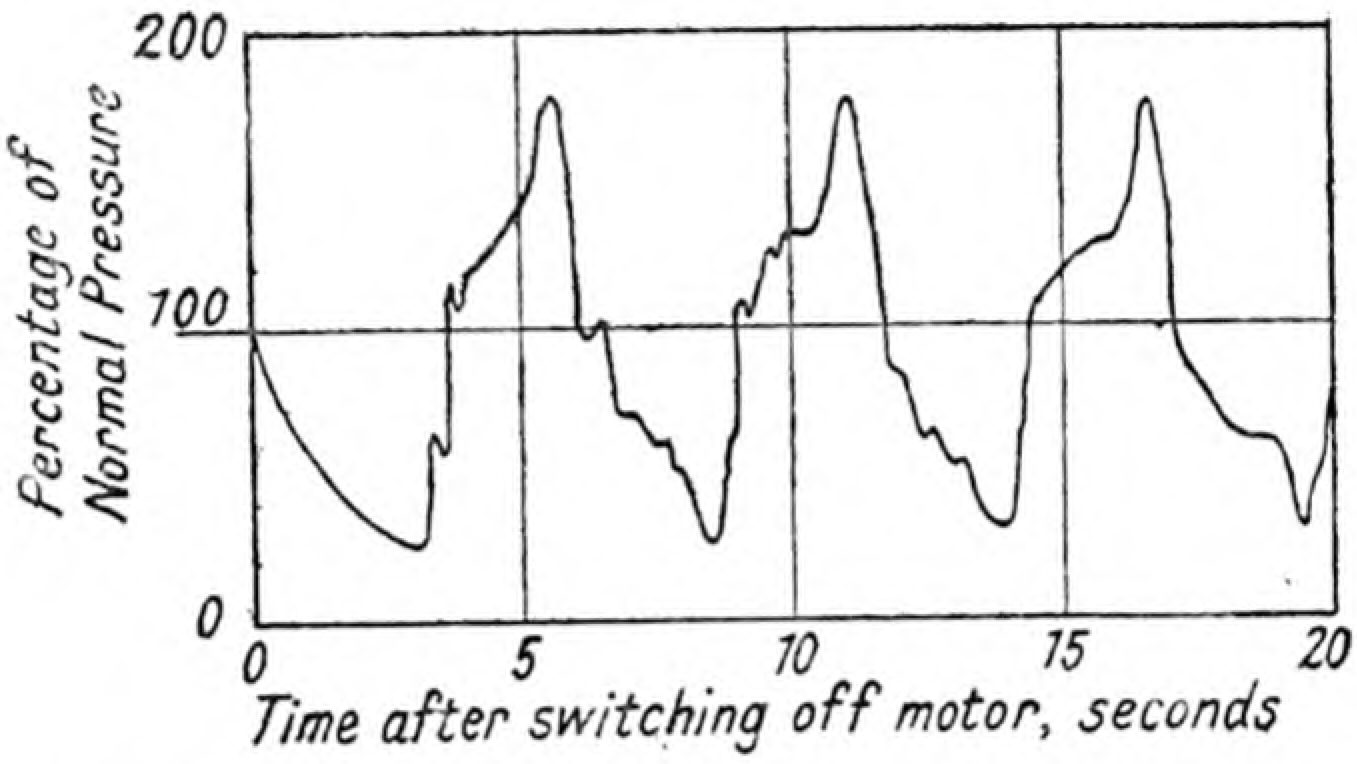

FIG. 382.—Pressure surges in delivery pipe.

pressures of this sort may be guarded against by (i) putting a large-capacity air-vessel in communication with the delivery pipe, near the pump;[228] (ii) increasing the inertia of the revolving parts of the pump and motor, so that they will only gradually slow down when the motor trips out;[229] or (iii) interpolating in the delivery pipe an automatic valve which will open when the motor stops, so allowing the pressure surge to dissipate itself through a side branch open to atmosphere.[230]

In regard to the sizes of suction and delivery pipes, these should preferably be chosen to give a pipe velocity within the range 5 to 9 ft./sec. (say 1·5 to 3 m./sec.); sometimes the suction pipe is given a rather larger diameter than the delivery pipe.

Engineers find it useful to keep in mind some rough notion of the probable output of pumps of various sizes, for example:

A 6-in.	pump	will discharge	about	700	gallons	per minute.
,, 12-in.	,,	,,	,,	3000	,,	,,
,, 24-in.	,,	,,	,,	11,000	,,	,,
,, 36-in.	,,	,,	,,	25,000	,,	,,

The dimension in each case represents the diameter of the suction and delivery branches. If, as may frequently happen, the diameter of the pump branch is less than that of the pipe, a tapered connecting-piece may be inserted: examples are to be seen in Fig. 388, § 338 (i).

334. Priming Devices. Since the pressure generated in a centrifugal pump impeller is proportional to the density

of the fluid that fills the passages, an impeller running in air would produce only a negligible pressure: that is why the pump must be primed, by first filling it with the proper working medium. In the arrangement shown in Fig. 381, water is poured into the priming funnel from some external source, and the air vent above the casing is opened. When all the air has been displaced from the suction pipe and the pump casing, and the system is filled throughout with water, the cocks may be closed and the pump started.

Larger pumps are primed, not by pouring water into them from above, but by evacuating the casing and suction pipe with the aid of an air pump (Fig. 388) or a steam ejector (Fig. 392 (i)); water is thus drawn up the suction pipe from the well.

By interposing in the suction pipe a special reservoir containing a supply of water, it becomes possible for the pump to prime the pipe and casing automatically. Specially designed *self-priming* pumps are described in § 340.

335. Limits of Suction Lift. A pump of any kind is enabled to lift liquid from an open well or reservoir only because of the atmospheric pressure p_a acting on the free liquid surface in the well. When we speak of the pump "lifting," "drawing," or "sucking" liquid, what really happens is that the pump relieves the pressure in the casing to such an extent that the atmospheric pressure forces the liquid up the suction pipe. Since it is impossible by any means to create in the pump an absolute pressure lower than the vapour pressure p_{vp} of the liquid (§ 16), the limiting available pressure difference is $p_a - p_{vp}$. This is all we have to depend upon to perform the following duties:—

(i) Raising the liquid through a vertical height h_s, where h_s is the *static suction lift* or difference in level between the well water surface and the pump centre-line (Fig. 371).

(ii) Overcoming energy losses of all kinds, h_{fs}, in the suction pipe and foot-valve.

(iii) Imparting velocity energy h_v to the liquid in the suction pipe.

(iv) Overcoming pressure-losses h_{lp} in the pump itself.

If w is the density of the liquid under the working conditions of temperature, etc., then

$$\frac{p_a - p_{vp}}{w} \text{ must not be less than } h_s + h_{fs} + h_v + h_{lp}.$$

The limiting suction lift [231] is therefore

$$h_s = \frac{p_a - p_{vp}}{w} - h_{fs} - h_v - h_{lp} \quad . \quad (16\text{-}6)$$

It can only be surpassed if we are prepared to accept the risk of *cavitation* (§ 134).

336. Pressure Changes within the Pump. It is convenient to separate the pressure changes in the suction pipe from those occurring in the pump itself. Referring to § 325, we note that $h_s + h_{fs} + h_v$ can be represented by the reading H_{ms} of a vacuum gauge connected to the suction pipe; as regards the term h_{lp}, some insight into its nature is afforded by Fig. 383. This diagram gives an impression of the pressure-distribution on a blade of a centrifugal pump impeller, and it thus supplies for the pump the kind of information that Fig. 307, § 280, supplies for turbines. The method of presentation, though, is rather different; it is a modification of the method used in Fig. 118, § 131, for plotting the pressure distribution on an aerofoil. But whereas in Fig. 118 the dynamic pressure fades away to zero at the trailing tip of the aerofoil, in Fig. 383 the total blade-pressure tends to increase because of the head impressed on the liquid as it flows outward through the impeller. It is the inlet relative velocity V_r which corresponds to the velocity U in Fig. 118. An instructive comparison may also be made between Fig. 383 and Fig. 361.

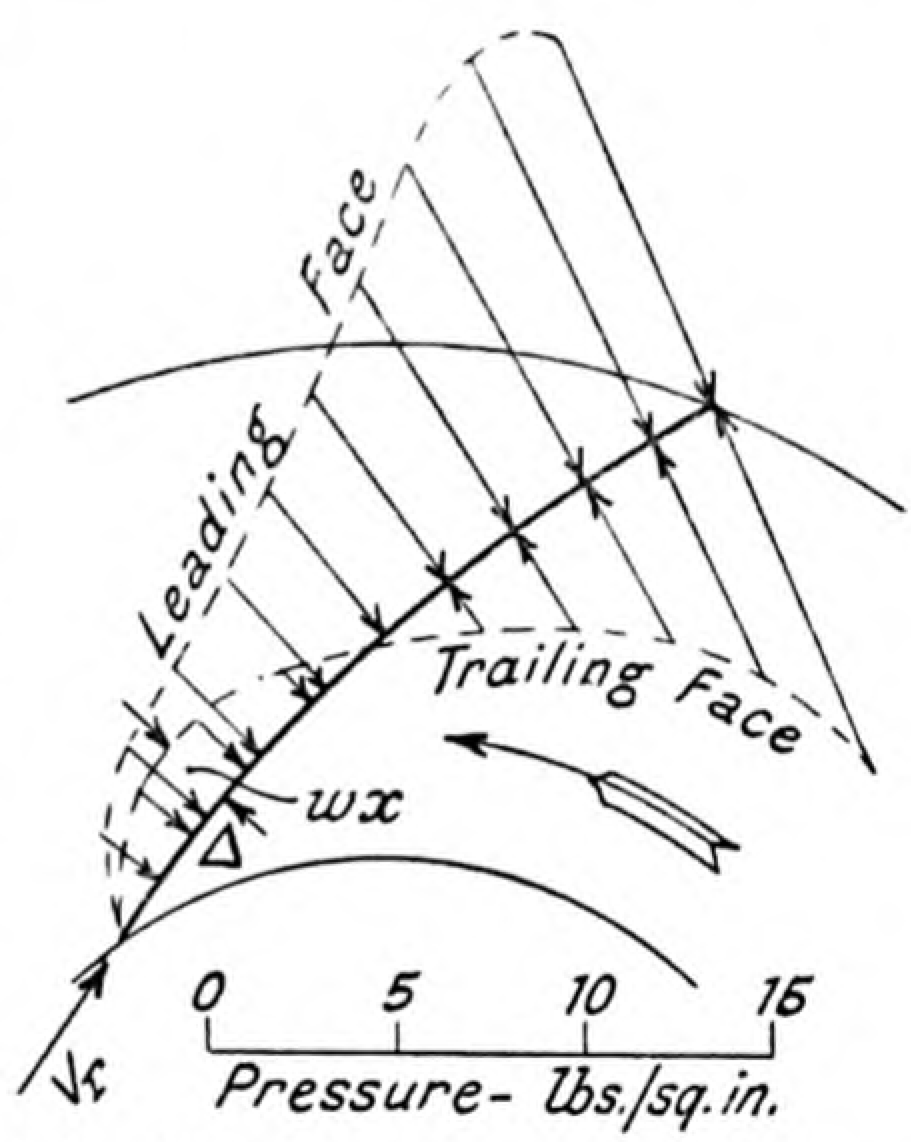

FIG. 383.—Pressure-distribution on impeller blade (total head about 23 feet).

We are now particularly concerned with the negative dynamic pressure, or pressure-head deficiency, x, sometimes

termed the *depression head*. By analogy with Fig. 118, we may fairly assume that this can be put in the form $x\alpha V_r^2/2g$. Moreover, the term h_{lp} above, or the head difference between the vacuum gauge tapping in Fig. 371 and the point of minimum absolute pressure Δ, Fig. 383, may be written $h_{lp} = h_{lc} + x$, where h_{lc} is the energy loss in the inlet part of the pump casing. The gist of the whole argument is, then, that h_f, h_v and h_{lp} will all *increase* as the rate of flow increases (other things being equal), from which it follows that the limiting suction head h_s *diminishes* as the discharge increases.(232)

All these considerations—and indeed most aspects of pump performance—are graphically summarised in the photographs reproduced in Fig. 384. They are photographs of cardboard models: their object is to indicate on a true vertical scale the experimentally-observed pressure-head at different points within the passages of rotating impellers.(233) In effect, the diagrams are corrected versions of the original simplified three-dimensional diagram which, in Fig. 130, § 146, was derived only by analysis. The data plotted in Fig. 384 relate to vertical-shaft impellers revolving at a speed of 430 r.p.m. in a counter-clockwise direction when viewed from above. Discharges are expressed as a percentage of the designed discharge, viz. the discharge Q corresponding to maximum gross efficiency, § 327. Other conditions controlling the experiments were:

Fig. (*a*) Impeller with 6 radial blades (shown in black).
Discharge = 25 per cent. of Q.

(*b*) Impeller with radial blades as in (*a*).
Discharge = 125 per cent. of Q.

(*c*) Impeller with customary form of backward-curved blades.
Discharge = 50 per cent. of Q.

As a datum for plotting the pressure-heads, the pressure-head at impeller inlet is accepted: this is taken as zero head. Negative heads, or the regions of negative heads, are distinguished by vertical hatching.

With these conventions in mind, let us now examine, say, Fig. 384 (*a*). Looking first at the nearer side of the model, viz. the side which represents the distribution of pressure-head along the *back* or trailing face of a blade, we are at once struck by the pronounced dip or droop in the hydraulic gradient. Evidently the depression head suggested in Fig. 383 is no mere mathematical abstraction: by scaling off the maximum negative head plotted in Fig. 384 (*a*), we find that its value is about 18 per cent. of the head generated in the impeller. On passing to the next diagram (*b*), we observe a much augmented value of the depression head: the value of x, corresponding to the increased discharge of 125 per cent. of Q, is now about 40 per cent. of the generated head H. Noting next the run of the lines denoting pressure-changes along a *circumferential* path, these likewise bear out an earlier forecast: not only is there a rise in pressure-head between the trailing face of one blade and the leading face of the following blade (Fig. 361 (iii), § 320), but the gradient steepens as the discharge increases (Fig. 384, (*a*) and (*b*)). Another kind of comparison between diagrams (*a*) and (*b*) can be linked up with the shape of the head-discharge characteristic of a pump, Fig. 373, § 327. Although

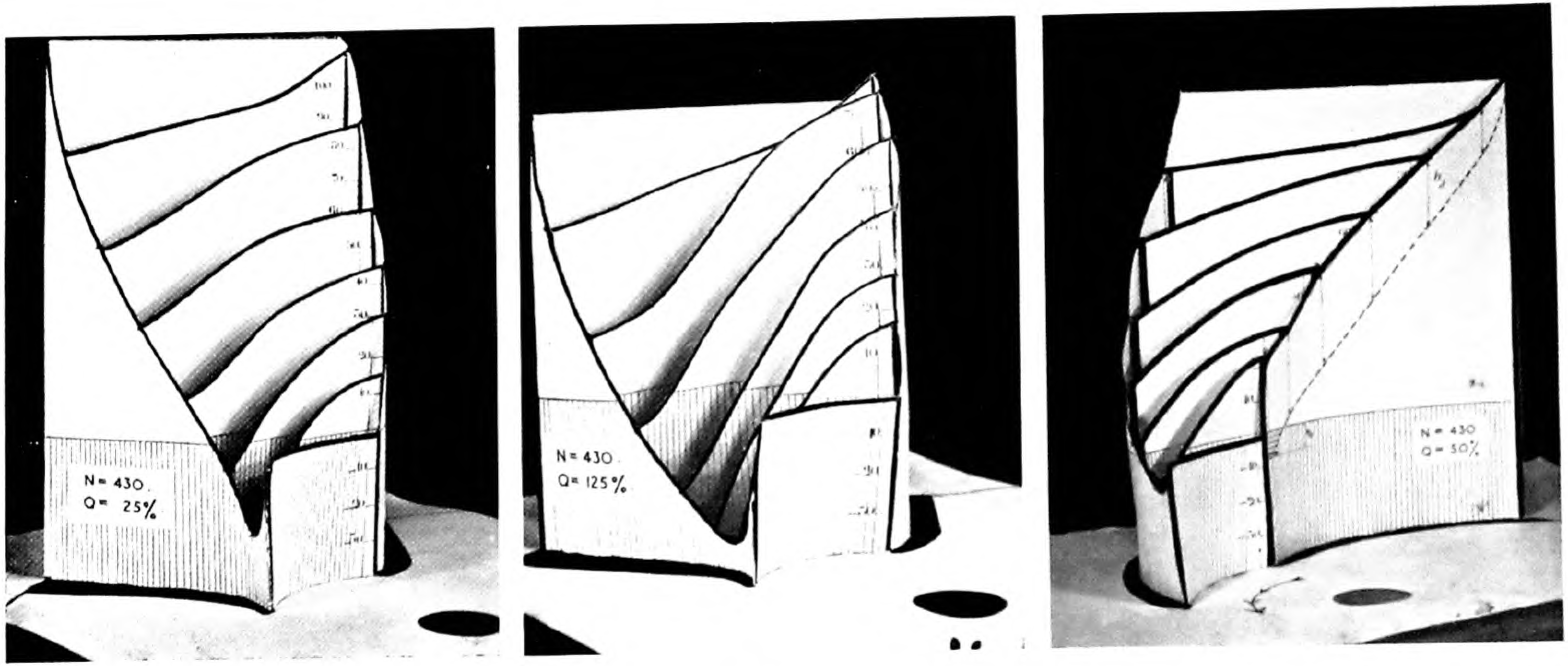

(a) (b) (c)

FIG. 384.—Models showing distribution of pressure-head in rotating impellers.

(Mr. Said Abdallah.)

[To face page 490.

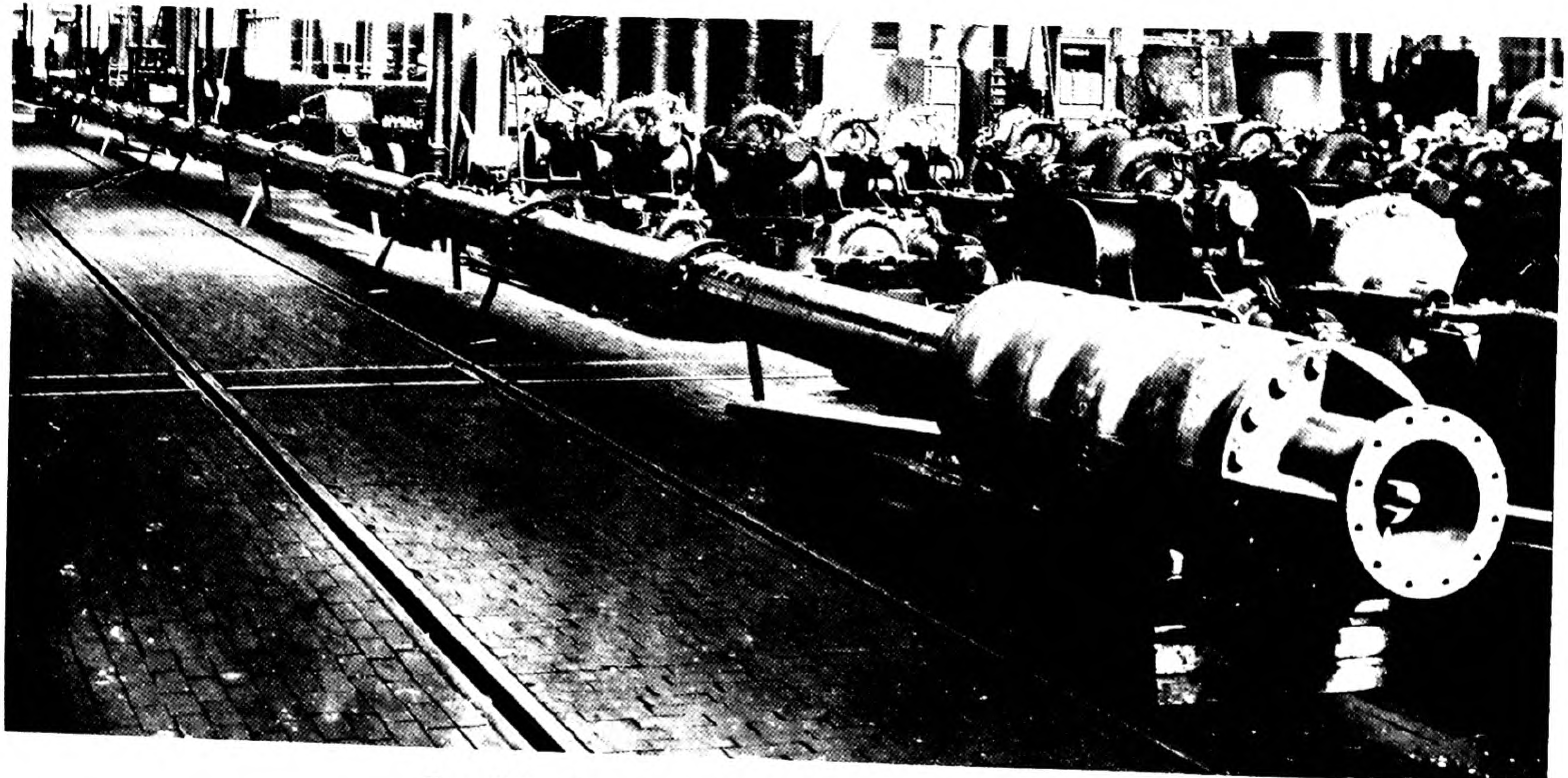

FIG. 391.—Four-stage bore-hole pump and rising main.
(See page 496.)

(Mather & Platt, Ltd.)

[*To face page* 491.

it is true that in the one case we are concerned only with the head generated in the impeller, and in the other with the total manometric head, yet the two are sufficiently closely related to supply mutual confirmation. The essential point is that as the discharge goes up the generated head goes down.

Arriving finally at diagram (c), Fig. 384, we have now left the exaggerated conditions associated with radial blades, and we are concerned with the behaviour of impellers as ordinarily used in centrifugal pumps. Although the observed depression head is less pronounced than it was in diagrams (a) and (b), it is still there. A new and most instructive feature of diagram (c) is that it reveals the face of the model linked with the *leading* face of the impeller blade. On the model the hydraulic gradient along the trailing face has been transferred and indicated by the broken line: the differential head h_d across the blade is thus clearly defined, the resulting closed figure thereby presenting itself for comparison with the diagrams derived by analysis in Fig. 307, § 280.

From this accumulation of evidence alone, can we compute in numerical terms what suction head a particular pump will sustain? At least we can say this: if the pump is put on test, its behaviour does agree with what we have been led to expect. A record of such a test is plotted in Fig. 385. The pump here is the one whose characteristics were given in Fig. 377, nor can there be any doubt about the decline in suction lift as the discharge increases.

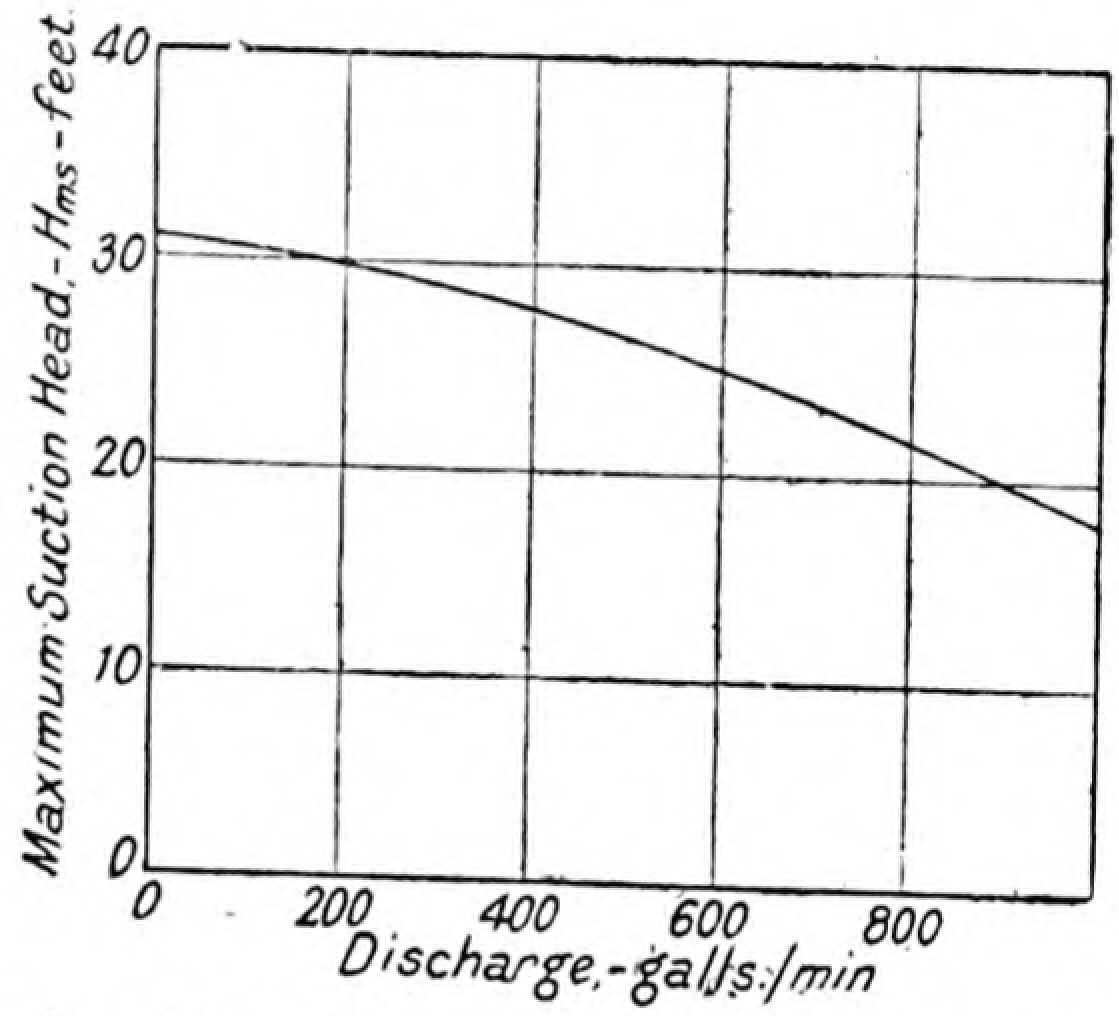

FIG. 385.—Variation of suction lift with discharge.

337. Considerations Affecting Suction Lift. If a pumping installation is to be so designed that the pump is set as high as is practicable above the water-level in the suction well, then each of the terms h_{fs}, h_v, h_{lc}, and x must be as small as possible. To this end some of the following measures may be suitable :—

(i) *Suction line.* A short, straight, wide suction pipe will ensure the least values of h_{fs} and h_v. But unless the foot-valve and strainer, Fig. 381, are very carefully designed, the energy loss in these elements may be as much as $4h_v$. A clogged or choked strainer will still further increase the loss.

(ii) *Pump casing.* A form of pump casing designed to impose minimum loss h_{lc} on the incoming liquid is illustrated in Fig. 386; the inlet is volute-shaped, of generous cross-section. A device which ensures that the high vacuum created

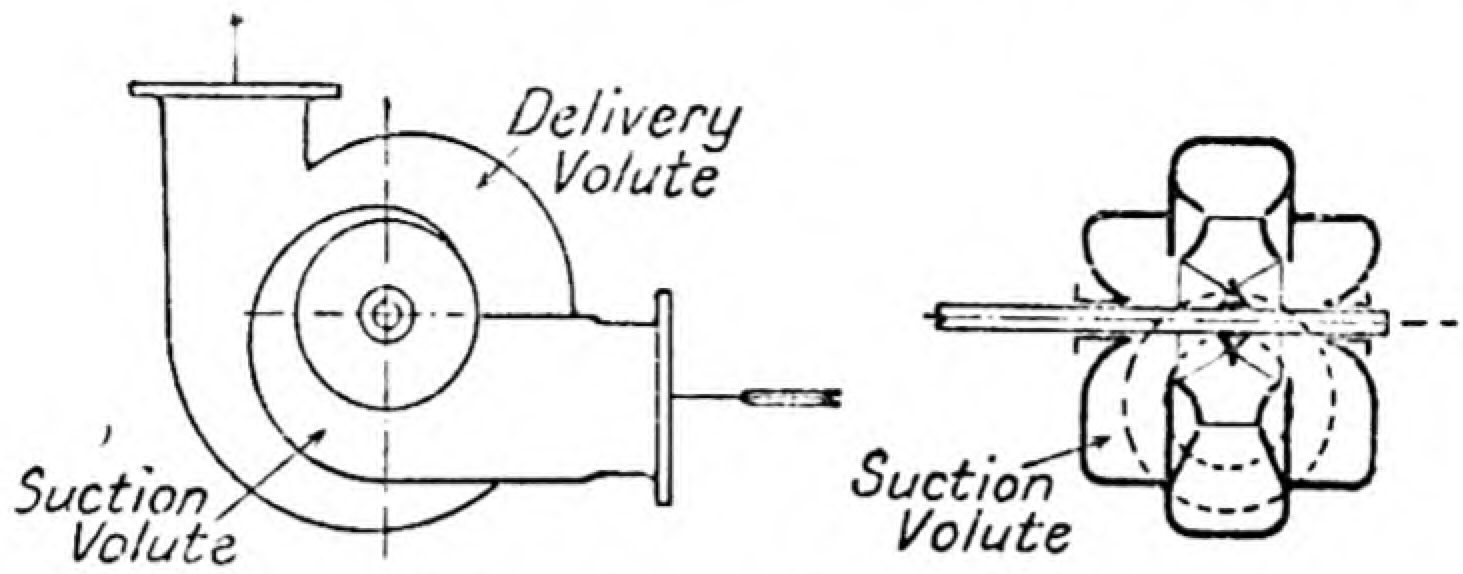

FIG. 386.—Pump with inlet volute.

by the impeller shall not be spoiled by the ingress of air is shown in Fig. 387. It is a *liquid-sealed gland*, so called because sealing liquid from the pump volute is fed to the lantern-ring enclosed within the stuffing-box. If leakage occurs at all, it will be a leakage of high-pressure liquid past the main gland into the atmosphere or back into the pump casing; but air cannot possibly find its way along the shaft into the casing.

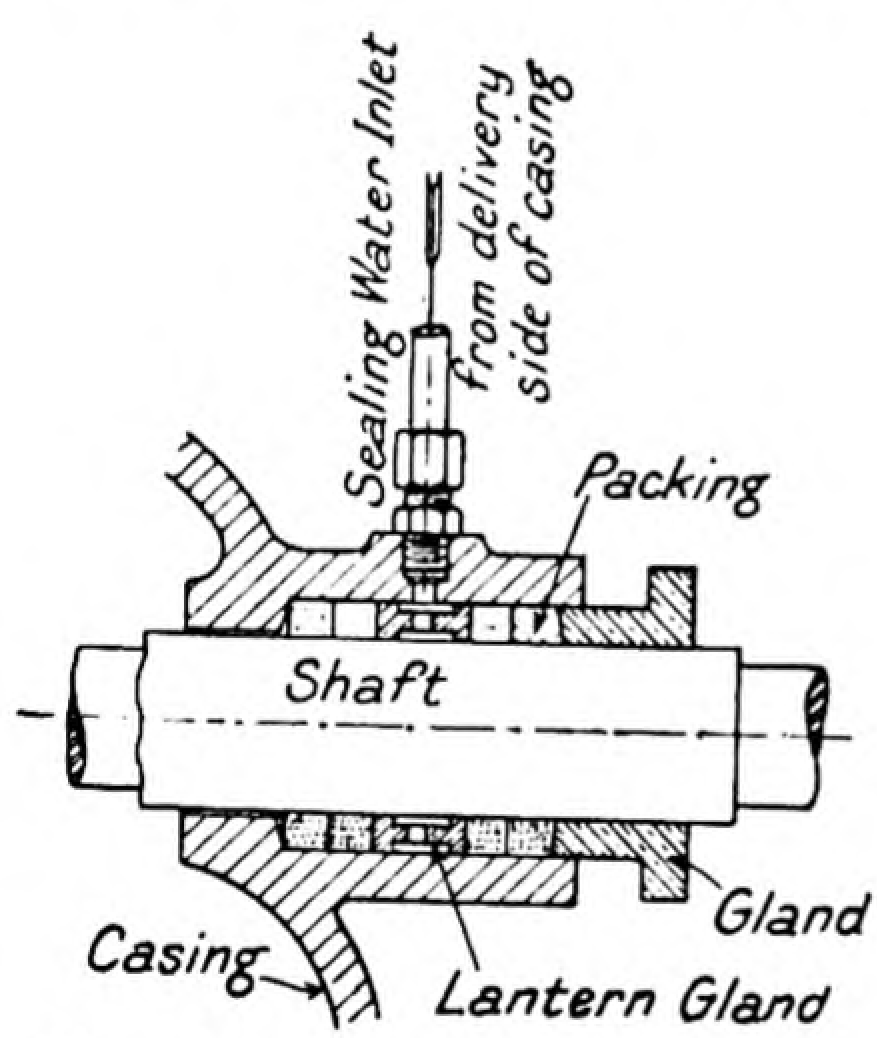

FIG. 387.—Water-sealed gland.

(iii) *Impeller.* Since the head deficiency x varies as V_r, it is roughly true to say that x also varies as v_1, where v_1 is the peripheral velocity of the inner rim of the impeller. On the other hand, the total manometric head generated, H_m, depends upon the velocity v of the *outer* rim of the impeller. It is quite possible to vary v_1 independently of v by varying the ratio of the inner to the outer impeller diameter. Thus for a given manometric head H_m and outer rim velocity v, the desired low values of v_1, V_r, and x could be secured by giving the impeller a small-diameter eye; that is to say, of the two impellers shown in Fig. 359, § 319, type I would be more suitable for high suction lifts than type II. In general, the *lower the specific speed*, the more successful the pump is likely to be in

creating a high vacuum.[234] It is for this reason that multistage working might be advisable if a high suction lift is required in conjunction with a high total head (§ 322 (vi)). In brief, the inlet edge of the impeller blades must move as slowly as possible.

Although all needful steps may have been taken to guard against the risk of cavitation at normal outputs, it does not follow that damage will not occur at part loads. The altered flow conditions may then resemble those of a stalled aerofoil, Fig. 116 (B), which afford greatly increased opportunities of destruction. Nor is it only the blade surfaces that may be attacked; the impeller shrouds or even the fixed diffuser blades may be eaten away in quite unpredictable areas. Fortunately the technique of building up the metal again by welding makes such occurrences much less disastrous than they used to be.

Evidently any simple formula for computing suction lift that purported to take into account all these various tendencies would only have a very rough validity. One of the most useful expressions, the Thoma formula, is explained in §§ 348, 349 (III).

Pumping Plants

338. Some Typical Pumping Installations.

(i) *Irrigation plant.*—Fig. 388 shows schematically a low-lift plant intended for pumping water from a river into an irrigation canal. The pump is of the double-inlet type, having two separate suction pipes; these are provided with air vessels in which liberated air may accumulate instead of being carried into the pump. At intervals the air is evacuated by the vacuum pump which serves also for priming the main pump. No foot valves are fitted. If the range of river water level between low water and flood conditions is considerable, limitations of suction lift may necessitate the pump being set below flood level. To guard against the accidental immersion of the driving engine—say, a Diesel unit—some engineers would prefer to set it above highest possible flood level, coupling it to the pump by belt.

Similar types of pump of high specific speed yet generating a low head, are likewise adapted to land drainage and similar duties.[235]

(ii) *Circulating-water pumping plant.* A very common lay-out for the pumps supplying cooling water to the condensers of large steam power stations is illustrated in Fig. 389. A vertical-shaft motor drives the pump, and a non-return

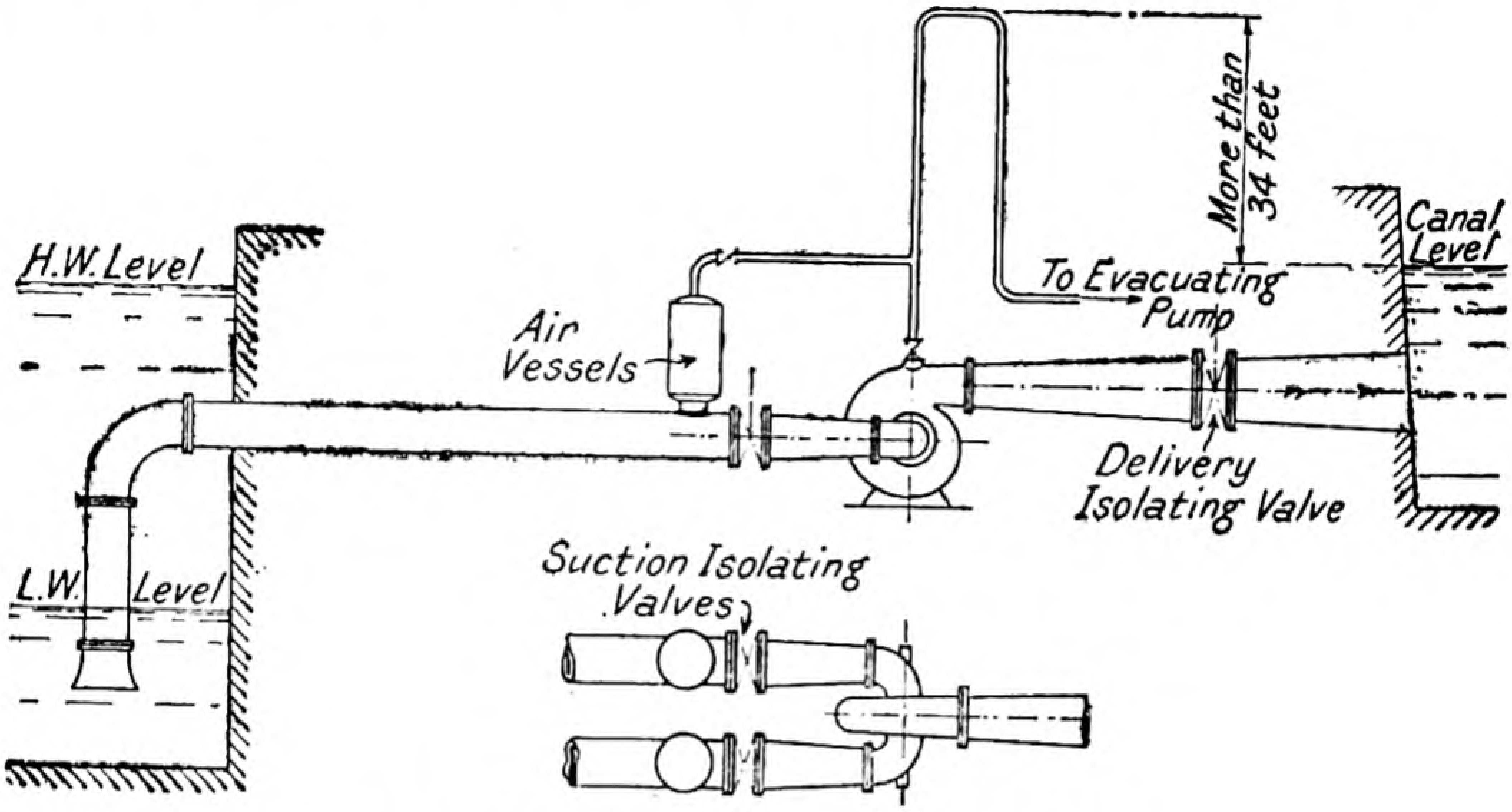

FIG. 388.—Irrigation pumping plant.

valve prevents return flow of water when the pump is stopped.[236] Fig. 358 shows a pump designed for a duty of this sort; Fig. 151, § 167, shows the hydraulic gradient in the piping system to which it is connected.

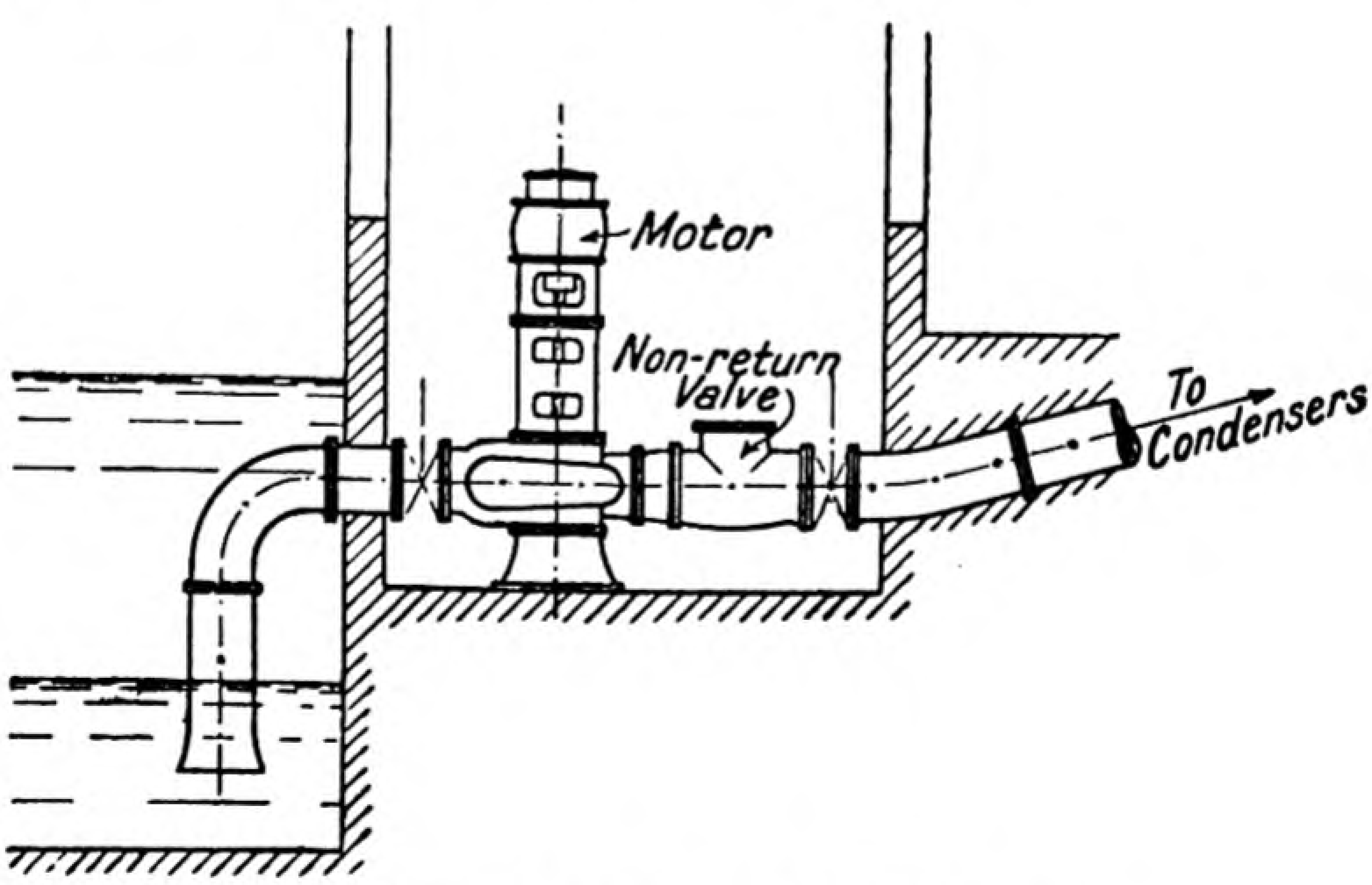

FIG. 389.—Circulating-water pump.

(iii) *Pumps for solid-liquid mixtures.* For handling liquids heavily charged with solids, e.g. crude sewage, special " choke-less " pumps are available; the impeller is of simplified form

having only two or three blades, so spaced that any object that can pass through the suction pipe can also pass through the impeller.[237] The efficiency is relatively low, but this can be tolerated so long as the construction is robust enough to give reliable service. If the solids are abrasive, upkeep costs can be reduced by fitting renewable internal parts of hard steel or of indiarubber.

On the other hand, if screened sewage is to be handled, then a special design of pump may hardly be necessary. See, for instance, Fig. 370.

(iv) *Boosting installations.* For use in pipe systems where pressure-boosting is required, § 167, standard types of centrifugal pumps are generally acceptable. Here the particular problem is how to control the discharge and the boosting head to suit the varying demand in the system. Variable-speed drive is often obligatory, and in large installations there may be multiple pumps disposed either in series or in parallel.[238] In smaller and simpler plants, constant-speed pumping sets may run intermittently. Boosting stations using propeller pumps are described in § 345.

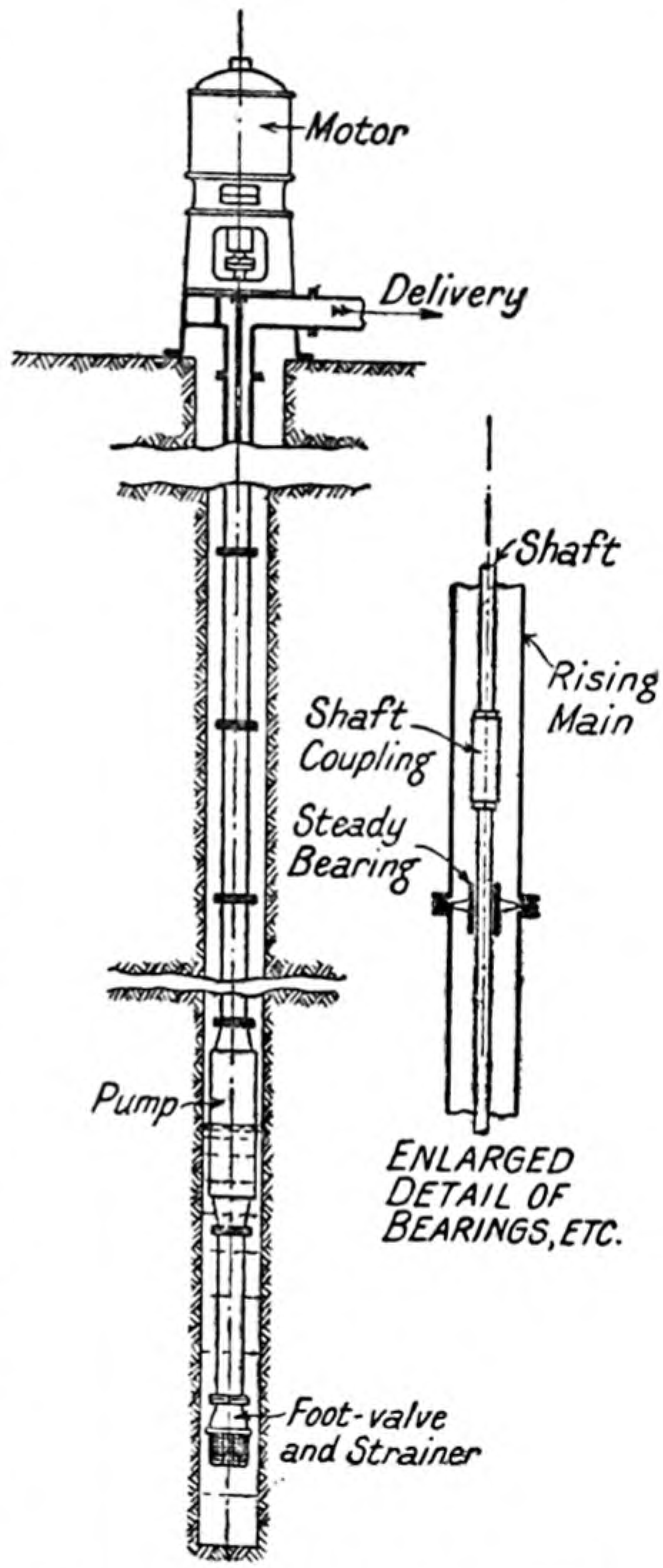

FIG. 390.—Centrifugal bore-hole pump.

339. Centrifugal Bore-hole Pumps. Vertical-spindle multi-stage pumps are used extensively to-day for raising water from bore-holes (Fig. 390). An engine or motor at ground level transmits power down a vertical shaft, co-axial with the rising main or delivery pipe, to the pump suspended from the bottom of the pipe. Static lifts, from water surface to ground level, of 500 ft. (say 150 metres) are within the capacity of such

installations, with an efficiency $\frac{\text{W.H.P.}}{\text{motor B.H.P.}}$ of 70 per cent. Yields of 300 gals. per min. from a 12-in. bore-hole, 1000 gals. per min. from a 21-in. bore-hole, up to 2500 gals. per min. from a 30-in. bore-hole, are feasible.[239]

A photograph of a 4-stage bore-hole pump, assembled in the makers' works, together with its rising main or vertical delivery pipe, is reproduced in Fig. 391 (facing p. 491).

The disadvantages of the long shaft connecting motor and pump, with its numerous bearings, may be overcome by the use of special motors designed to work below water level; the complete unit, consisting of a submersible motor direct-coupled to the pump, is lowered down the bore-hole or well. In one arrangement the motor is housed in a kind of diving-bell, kept charged by a compressor at ground level with compressed air at a pressure high enough to exclude water. In another system the stator coils of the motor are contained within a water-tight sheath, and the rotor revolves in a casing containing pure water.[240]

340. Self-priming Pumps. Of the various special types of centrifugal pump available, the self-priming machine is one of the most useful. In a large well-staffed pumping installation planned for nearly continuous working, it involves no great hardship for the attendants to manipulate the evacuating pump or ejector now and again (§ 334). But if a small portable unit must quickly be set to work by unskilled hands, additional parts to be operated and kept in order would constitute a serious drawback. The user wants to drop the suction hose into the well or sump and begin pumping straight away.

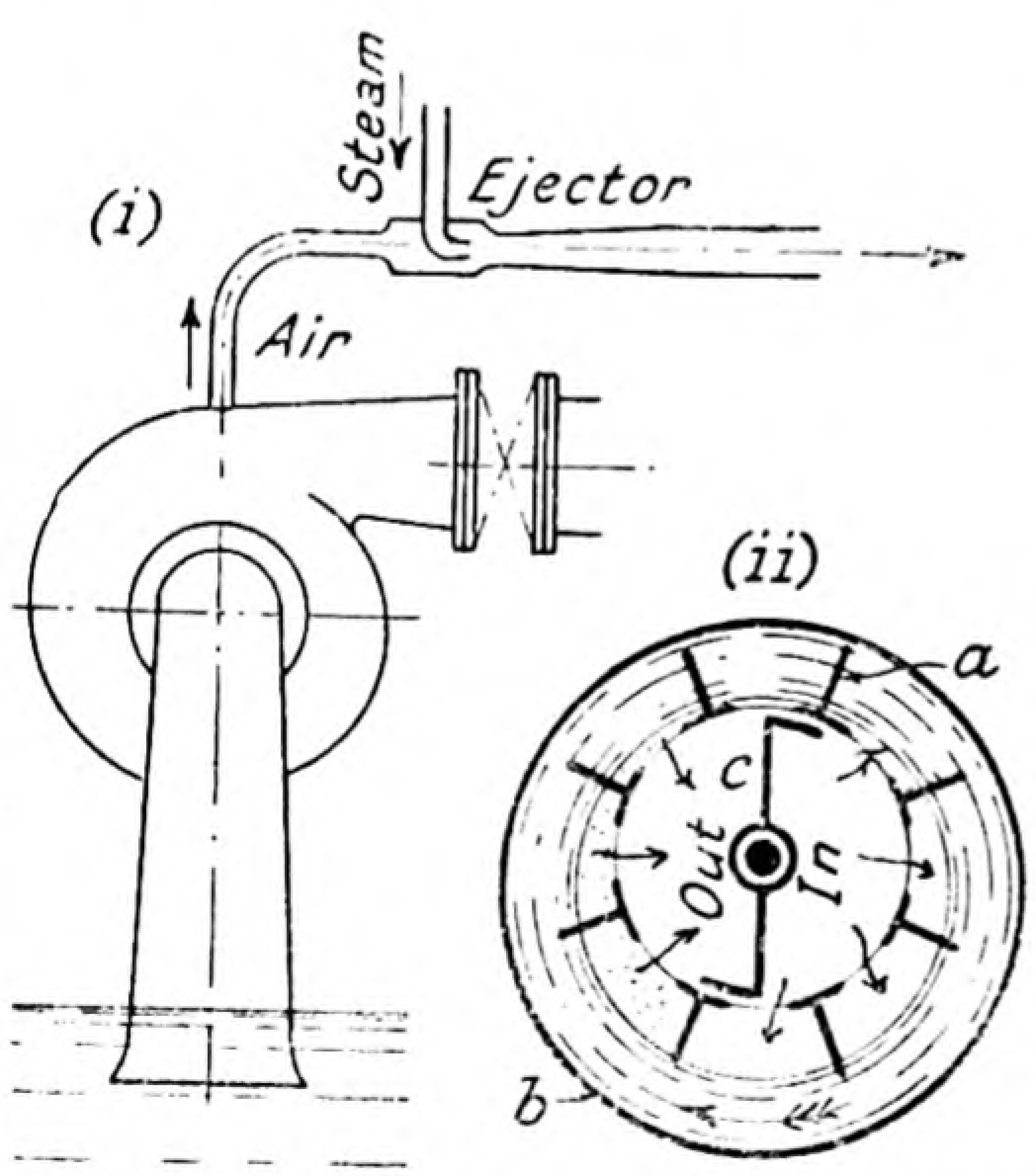

FIG. 392.—(i) Priming by steam ejector; (ii) water-ring pump.

The elements of the problem are re-stated in Fig. 392 (i). Somehow or other the air in the casing and suction pipe must be got rid of: so what equivalent can we embody in the pump itself, that will automatically come into action when the

pump starts, as a substitute for the ejector shown in the diagram? Of the varied solutions now available,[241] two will here be described:—

Water-ring pump. In this machine a more or less standard centrifugal pump is provided with a water-ring evacuating pump mounted co-axially in a common casing. The radial-bladed water-ring rotor *a*, Fig. 392 (ii), is set eccentrically with respect to the fixed circular casing *b*. A fixed partition *c* separates the inlet port from the outlet port; air or water from the centrifugal pump casing can flow through the inlet port, and the fluid is discharged through the outlet port to the main delivery pipe. When the pump is started, the water remaining in the water-ring casing *a* is compelled by the rotor blades to revolve also, and because of centrifugal force it is flung against the circumferential wall of the casing *b*; it is this rotating ring of water that gives the evacuating pump its title. Each space bounded by the inner surface of this ring, by the inner rim of the rotor, and by a pair of adjacent rotor blades constitutes a compartment or cell of variable capacity. As the blades descend (Fig. 392 (ii)), the enclosed volume of the cell increases; as the cell ascends during the remaining half of a revolution, the volume diminishes. Each cell therefore draws from the inlet port a definite volume of fluid and then discharges it through the outlet port.

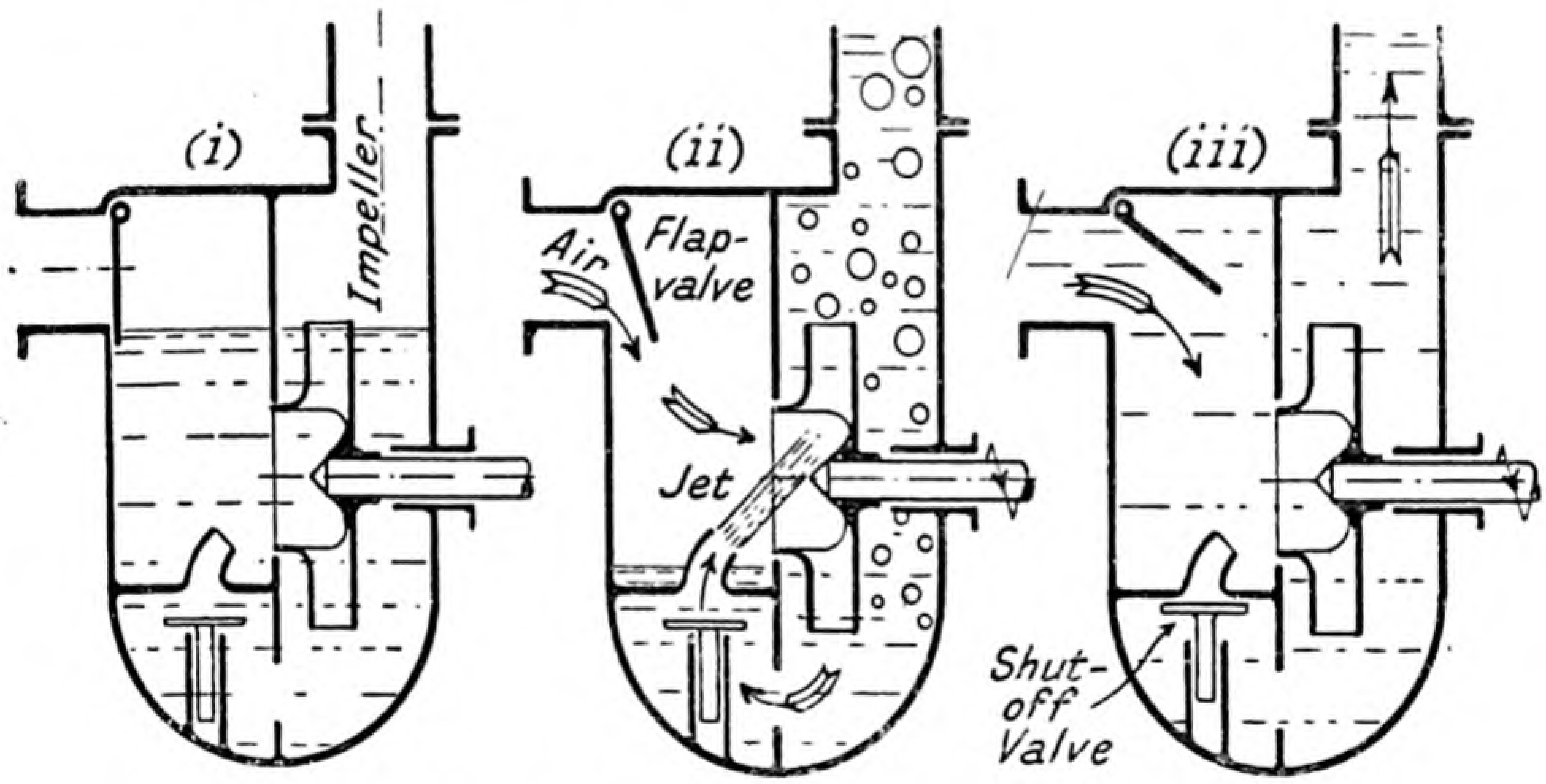

FIG. 393.—Water-jet type of self-priming pump.

Beginning, then, with the entire apparatus dry except for the essential residual water in the water-ring pump casing, the sequence of events is as follows:—

(i) Main shaft started. Pump impeller revolves idly in air. Evacuating rotor begins to draw air from suction pipe.

(ii) Evacuation continues. Suction pipe full of water. Centrifugal pump casing partly evacuated, but impeller still not operative.

(iii) Impeller begins to discharge as soon as evacuation complete. Flow begins through suction pipe and delivery pipe.

(iv) Normal pump operation, the water-ring pump now delivering a small quantity of water and working in parallel with the main pump.

Water-jet pump. This machine embodies a water-jet as the evacuating element; it is projected directly into the eye of the impeller, Fig. 393. The nozzle is located in the lower part of the suction chamber, the suction pipe being connected to the upper part of this chamber. Consequently when the pump stops, sufficient water remains to keep the impeller submerged. The following comments relate to the three diagrams in Fig. 393 :—

(i) Conditions when pump stopped.

(ii) Pump impeller running at normal speed. Its rotation has drawn water from the suction chamber and raised it in the delivery chamber which forms the pump casing. The resulting head-difference creates flow through the nozzle into the impeller, and thus a continuous circulation of water is maintained. The jet entrains with it air from the suction casing; then the flap-valve opens and air is progressively evacuated from the suction pipe. As the vacuum increases, so does the pressure-difference producing flow through the nozzle; the strength of the jet grows accordingly. The impeller continues to deliver a mixture of air and water—the water is re-circulated and the air passes into the delivery pipe.

(iii) Normal operation. When water has been drawn sufficiently high up the suction pipe, it enters the suction chamber and the pump thereafter delivers "solid" water. As the impeller is now generating its full pressure-difference, the current approaching the nozzle from below is so powerful that it lifts the shut-off valve and cuts the nozzle out of action. From this moment the shut-off valve is held up on its seat, and the flow through suction pipe, impeller, and delivery pipe is in every way normal.

The price paid for the modifications that make a centrifugal pump self-priming is a sensible lowering of the efficiency; this will be evident from the diagrams. Naturally the initial cost of the pump is higher, too, but in many instances the additional outlay is well justified.

CHAPTER XVII

PUMPING MACHINERY: (III) PROPELLER AND SCREW PUMPS

341. Axial-Flow or Propeller Pumps. These machines have a family resemblance to Kaplan and propeller turbines (§§ 247 to 249), and they have the same advantages, viz. compact construction and high specific speed.[242] There are usually three sets of blades in a propeller pump (Fig. 394), (i) a set of inlet guide blades, (ii) the rotating propeller or rotor blades, and (iii) the outlet guide blades. The purpose of the inlet blades is to guide the incoming water axially into the wheel, so that it enters without velocity of whirl; the wheel blades impart a whirl component to the water, and the outlet blades take the whirl out again, allowing the water to flow axially along the discharge pipe. This routine of imparting and then removing the whirl component corresponds exactly with what is done in the centrifugal pump (§ 316); there is no other way of generating dynamic pressure in a rotodynamic pump.

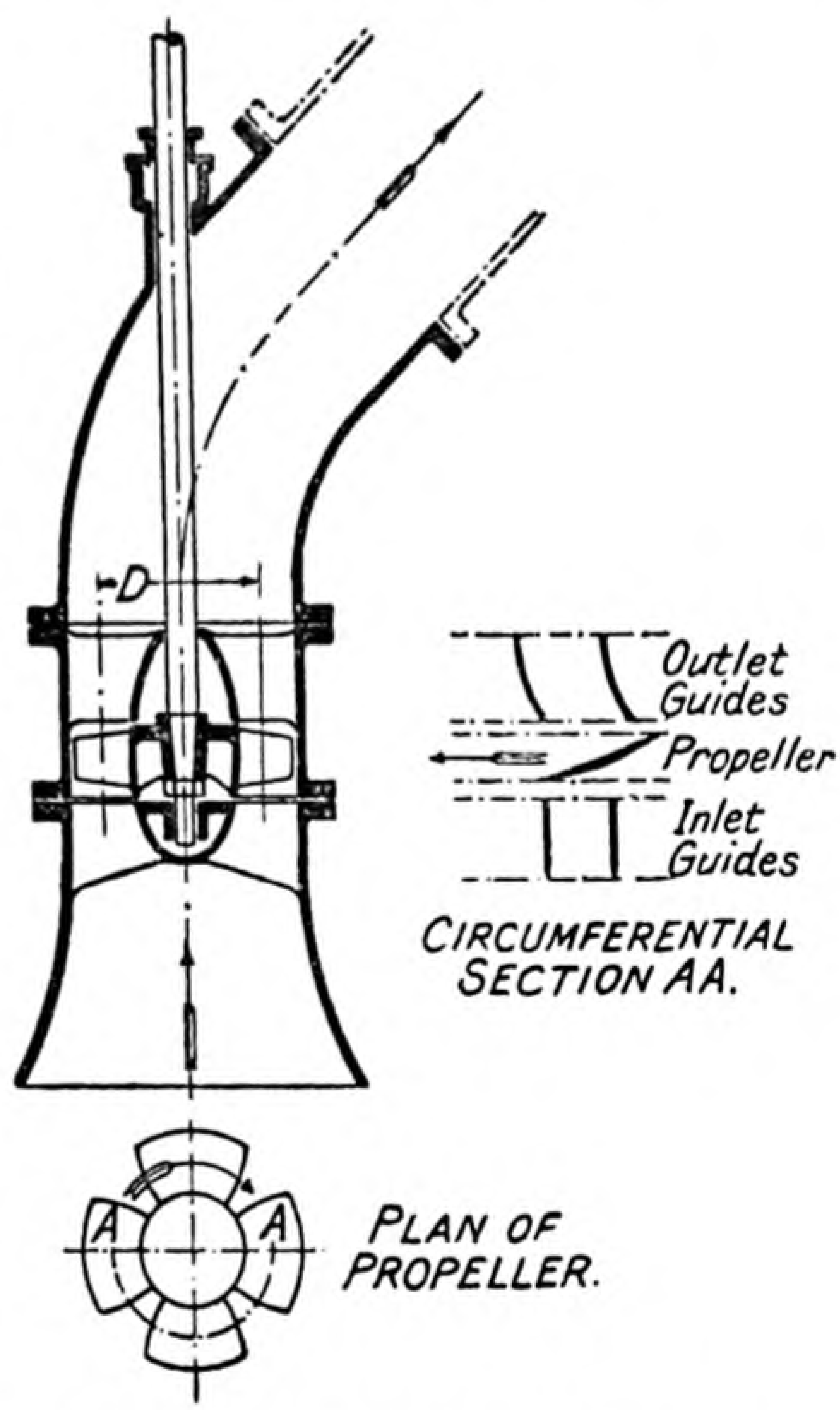

FIG. 394.—Elements of propeller pump.

Because of the variations in the velocity of the blades at different radii, the hydraulic conditions alter as points further and further from the axis are considered (§ 247); but for simplicity the conditions prevailing at the mean diameter D will here be discussed. Comparing the propeller pump velocity diagrams, (Fig. 395) with the centrifugal pump diagrams (Fig. 354), we notice that the whirl component V bears a smaller ratio to v than it formerly did, while the flow component Y bears a larger ratio to $\frac{Vv}{g}$.

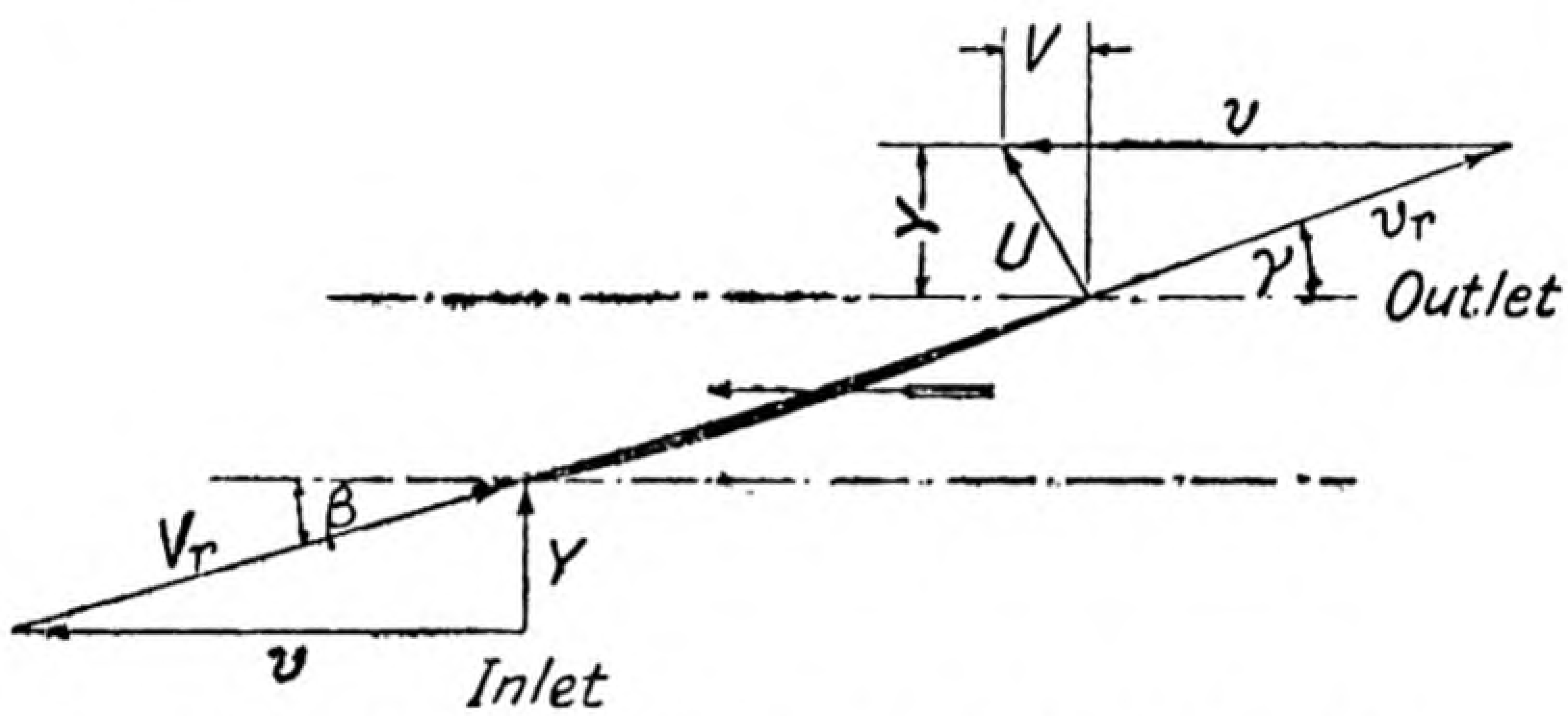

FIG. 395.—Propeller pump velocity diagrams.

Since equation 16-2, § 314, $H = \dfrac{v^2 - Y^2 \operatorname{cosec}^2 \gamma}{2g}$, is applicable to both types of machine, it follows that both the speed ratio ϕ and the flow ratio ψ will have bigger values in the axial-flow pump than they have in the centrifugal pump. Further, specific speed depends upon $\phi\sqrt{\psi}$, hence N_s will be higher.

Limiting values commonly accepted in practice are—

Speed ratio ϕ for propeller pumps (based on mean diameter of propeller)	$= \dfrac{v}{\sqrt{2gH}} = 1{\cdot}60.$
Speed ratio ϕ for propeller pumps (based on outside diameter)	$= 2{\cdot}1.$
Flow ratio ψ	$= \dfrac{Y}{\sqrt{2gH}} = 0{\cdot}45.$
Specific speed N_s	up to $\begin{cases} 180 \text{ (foot)} \\ 800 \text{ (metric)} \end{cases}$
Relative specific speed N_{sr}	10,000 (foot).

The duty imposed upon the outlet guides of changing an absolute velocity U to a smaller velocity Y is not very onerous,

and even if the ideal regain of head $\dfrac{U^2}{2g} - \dfrac{Y^2}{2g}$ is by no means realised, the total loss of energy here cannot be very great. Consequently the gross efficiency of propeller pumps, based on the manometric head (§ 325), is reasonably good—75 to 80 per cent. or even more.

342. Aerofoil Theory of Propeller-pump Design. In this paragraph and the next one, the principle of design studied in § 248 is now applied to axial-flow pumps and developed in greater detail.[243]

Remembering that any propeller blade forms one of a ring or series of blades, we must first enquire into the behaviour of a fixed aerofoil, Fig. 116, when it is not solitary but is itself set in a group—a *grid* or *cascade*—of identical blades. In Fig. 396 the original single aerofoil is shown at (i) and the family of aerofoils set at the same angle is shown at (ii). Experiments reveal the following effects of companionship :—

(1) The single blade has no ultimate influence on the direction of the liquid stream flowing past it. At a sufficiently great distance behind the blade, the velocity U of the liquid is in no way different from what it was originally, (i). The cascade of aerofoils, (ii), on the other hand, does permanently deflect the entire liquid stream through an angle δ.

(2) Whereas the angle of attack α, and therefore the lift and drag of a single aerofoil are related wholly to the magnitude and direction of the approach velocity U, the corresponding values for the cascade are more nearly dependent upon the velocity U_m which is the vectorial mean of the approach velocity U and the leaving velocity U_l. Although, therefore, the blades at (i) and (ii), Fig. 396, have exactly the same inclination to an arbitrary datum line, yet the *effective* angle of attack has been reduced from α to α_e.

(3) The lift and drag of the aerofoils in cascade must now be regarded as the components of the total dynamic thrust normal and parallel to the *effective* or mean velocity U_m. Almost certainly the lift and drag coefficients will no longer have the values they had originally ; but if the " cascade " values are lacking, then the single-aerofoil figures may provisionally be accepted in conjunction with the effective angle of attack α_e.

(4) The pressure-distribution over the element of the cascade will no longer conform to what was shown in Fig. 118, although it will remain of the same general type.

343. Application of Theory. Having established the main dimensions of the rotor by the method outlined in § 247 (which serves as well for pumps as for turbines), we may concentrate attention on the narrow annular strip of a blade distinguished by hatching in Fig. 396 (iii). *It is this strip which is to serve as our aerofoil.* A developed side view of it, in company with its fellows which together make up the complete rotor or propeller, is to be seen at (iv). The velocity diagrams plotted in Fig. 395 are still applicable, and they are re-plotted at (v) in Fig. 396. The mean radius R and the radial width b of the elements have already been chosen, (iii) ; their peripheral velocity

$v = 2\pi RN/60$ can quickly be computed; a suitable number of blades, n, can be fixed upon; so that the outstanding points to be settled are—

The inclination of the blades which will ensure that the stipulated whirl component V is imparted to the water.

The chord length c which will enable each element to deliver to the water the stipulated energy.

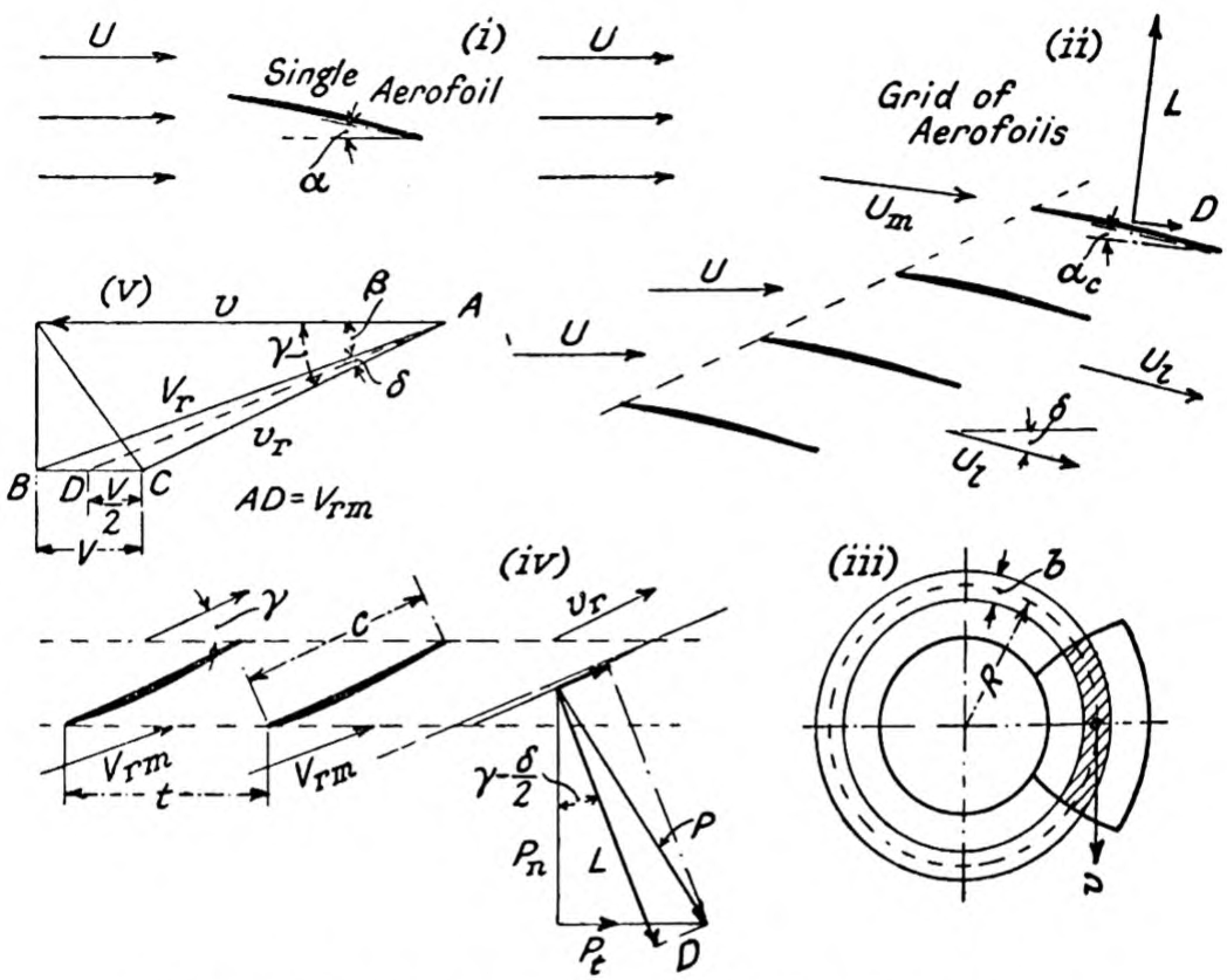

FIG. 396.—Propeller-pump blades considered as aerofoils.

Blade inclination. The essential condition to be fulfilled is that the water approaches with a relative velocity V_r, and leaves with a relative velocity v_r. By turning and reversing the grid of aerofoils (ii), they can quickly be brought into the positions shown at (iv), the corresponding data being

$$V_r = U \qquad v_r = U_l \qquad V_{rm} = U_m \qquad \gamma - \beta = \delta$$

A sufficiently accurate way of finding the vectorial mean velocity V_{rm} is indicated at (v), where BD is set off $= V/2$, and $V_{rm} = DA$. Requirements will be satisfied, then, if the aerofoil elements are so set that they deflect the relative streams through an angle of $\delta = \gamma - \beta$.

Chord length. We must now ascertain what will be the characteristics of our chosen type of aerofoil, Fig. 396 (ii), when set so that the angle of deflection δ is $\gamma - \beta$ and the pitch t is $2\pi R/n$. Suppose that the corresponding angle of attack (in relation to U_m), lift coefficient, and drag coefficient, are α_c, C_L, and C_D; then for each propeller-blade element we may write

$$\text{Lift } L = C_L \,.\, bc \,.\, \frac{wV_{rm}^2}{2g}. \qquad \text{Drag } D = C_D \,.\, bc \,.\, \frac{wV_{rm}^2}{2g}.$$

By plotting to some arbitrary scale the values of L and D, perpendicular and parallel respectively *to the mean vector* V_{rm}, as at (iv), the tangential component P_t of the total resultant dynamic thrust can be expressed thus :—

$$P_t = \frac{P_t}{L} \cdot C_L bc \cdot \frac{wV_{rm}^2}{2g}. \qquad \text{(I)}$$

The desired but still unknown chord length c can finally be extracted by making an alternative estimate of the tangential component P_t, thus :—

Weight of water per second acted upon by each blade element

$$= w \cdot \frac{2\pi Rb}{n} \cdot \psi\sqrt{2gH_m} \ \ldots \text{ (from diagram (iii)).}$$

Energy imparted per unit weight, $\frac{Vv}{g} = H_m/\eta_h$ . . . (§ 325).

$\therefore E$ = energy per second per blade $= w \cdot \frac{2\pi Rb}{n} \cdot \frac{Vv}{g} \cdot \psi\sqrt{2gH_m}$. But, on the other hand, E = the work done per second in driving round the blade element with velocity v against the resistance of the tangential component $= P_t v = P_t \cdot \frac{2\pi RN}{60}$, from which

$$P_t = E \Big/ \frac{2\pi RN}{60} \qquad \text{(II)}$$

Equating expressions (I) and (II), and extracting the desired value of the chord length c, completes the process, which is then repeated for other blade elements at other radii.

Although a good deal of experience is required in actually modifying, interpreting, and applying to practical problems of design the simplified principles just laid down, yet the treatment itself is highly instructive. Thus :

(i) A study of the force diagram, Fig. 396 (iv), makes it clear that the most favourable blade form is the one which gives the least value of drag D. The expression $(P_t v - DV_{rm})/P_t v$ serves as a measure of the efficiency of the blade element—although this must necessarily be higher than the hydraulic efficiency $= \eta_h = gH_m/Vv$ of the complete pump (§ 325).

(ii) From the measured values of the normal or axial component P_n of the total dynamic thrust (Fig. 396 (iv)), the total axial thrust on the propeller shaft can be estimated, and a suitable thrust-bearing designed.

(iii) If the pressure distribution over the blade surfaces can be established, then the relationship between total head and permissible suction lift can be more clearly visualised (§ 336).

344. Characteristics of Propeller Pumps. A comparison between the characteristics of a propeller pump at constant speed (Fig. 397) and those of a centrifugal pump (Figs. 373 to 377) reveals these notable differences :—

(i) The head-discharge curve for the propeller pump falls very steeply, the working head corresponding to maximum

overall efficiency being hardly more than one-third of the head corresponding to zero discharge. **(Example 186.)**

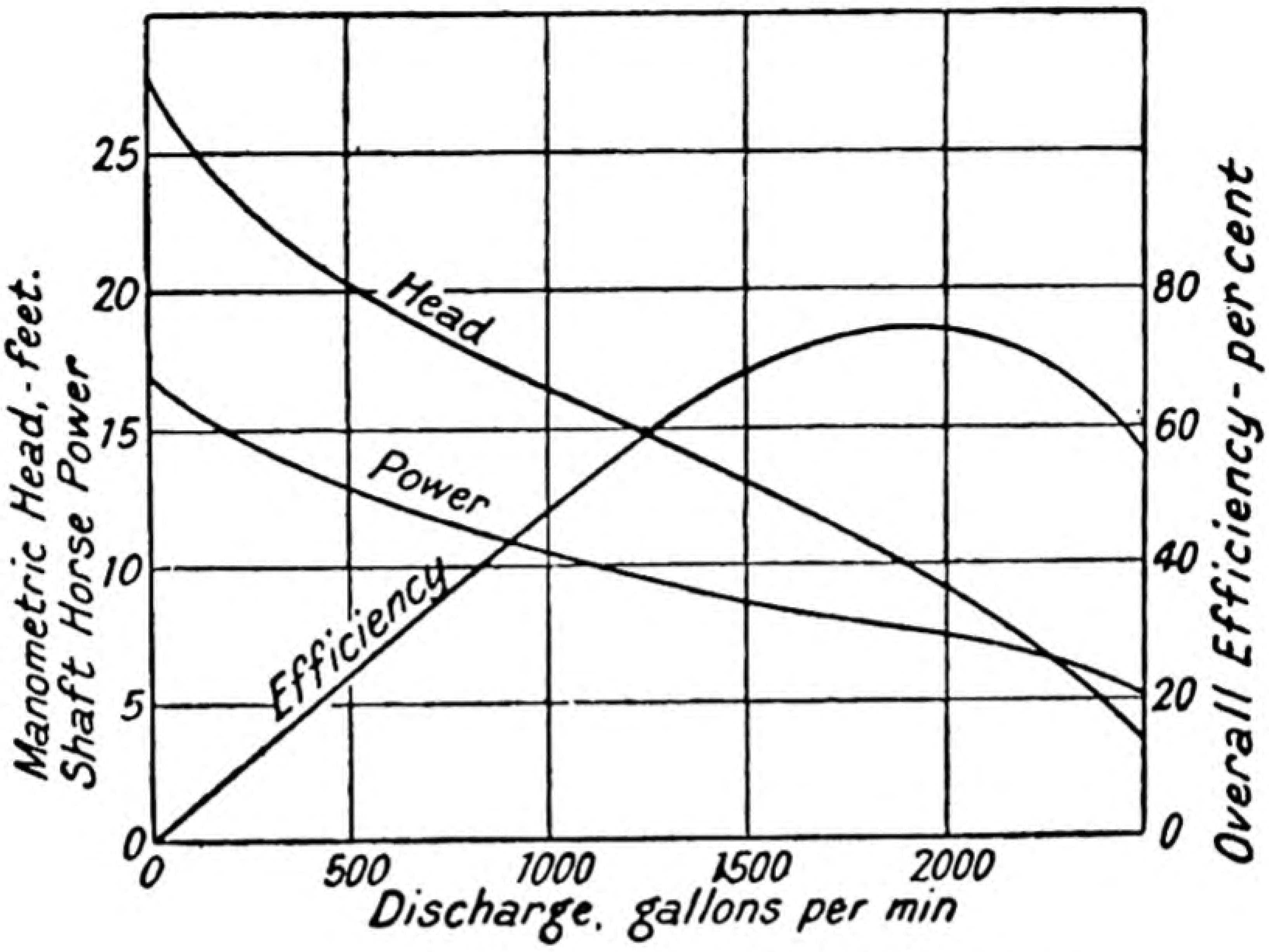

FIG. 397.—Characteristics of propeller pump.

(ii) The power required by a propeller pump continuously *diminishes* as the discharge increases, whereas a centrifugal pump usually takes most power at maximum discharge.

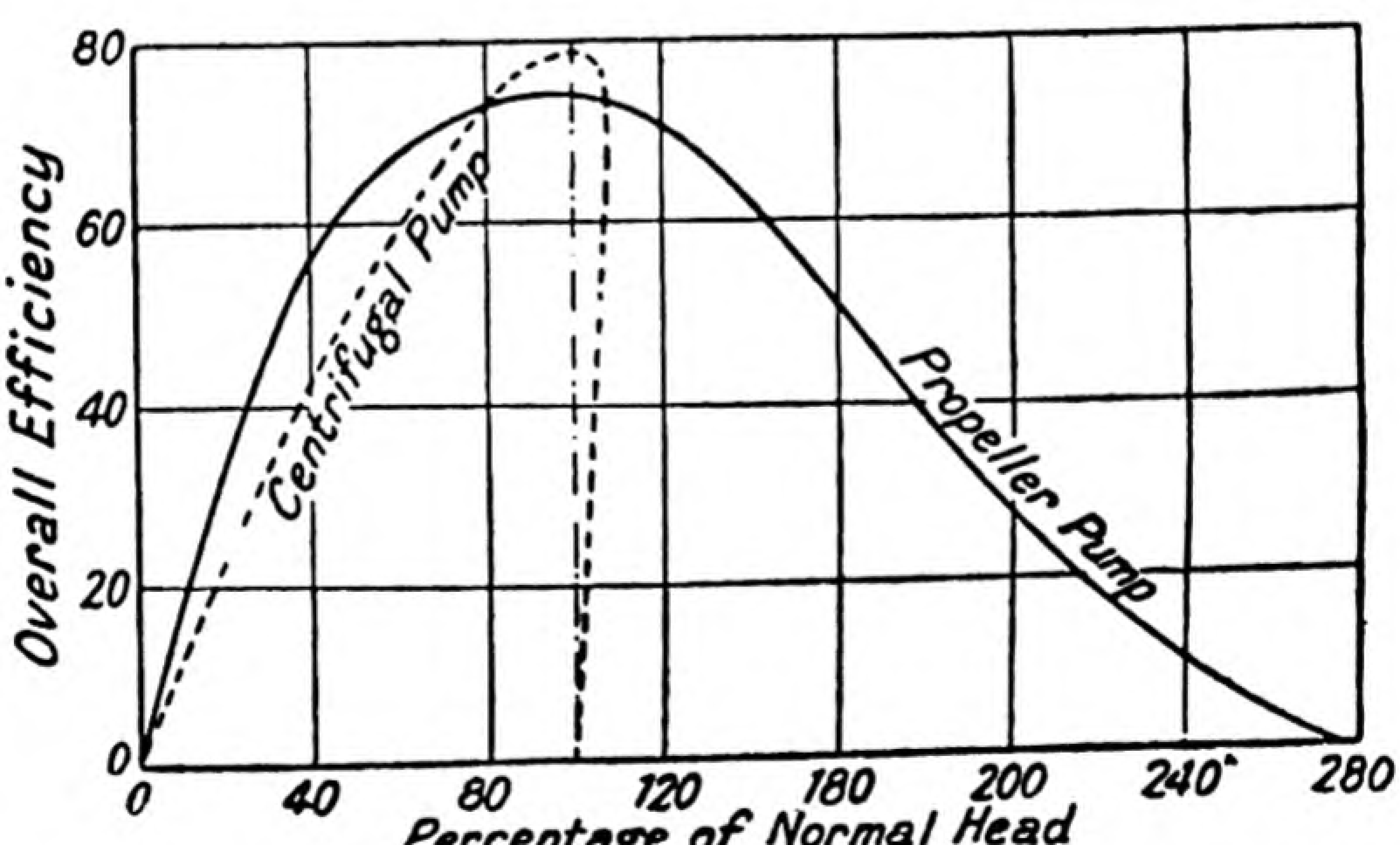

FIG. 398.—Derived characteristics for pumps at constant speed.

Another instructive kind of comparison is plotted in Fig. 398—here efficiency per cent. is plotted against head at constant speed; a stated variation in head evidently has far less effect on the efficiency of the propeller pump than it has on the efficiency of the centrifugal pump. An equivalent ten-

dency in the performance of propeller turbines has already been mentioned, § 276.

The aerofoil theory outlined in §§ 342, 343 is particularly helpful in explaining the part-load performance of propeller pumps. When velocity and force diagrams are plotted both for normal discharge (i) and reduced discharge (ii), Fig. 399, it is clearly to be seen that reducing the flow is equivalent to bringing the aerofoil element into the stalled position, Fig. 116 (B). As a consequence, the tangential component of the total dynamic thrust on the element increases from P_t to P_t', which helps to account for the trend of the power characteristic in Fig. 397. At the same time the outlet whirl component has risen from V to V', and the resulting increase in the product Vv/g is sufficient to explain the shape of the head characteristic. The canted blade-element shown in broken lines gives a clue to the method of overcoming these undesirable tendencies—we must use a variable-pitch propeller (§§ 276, 346).

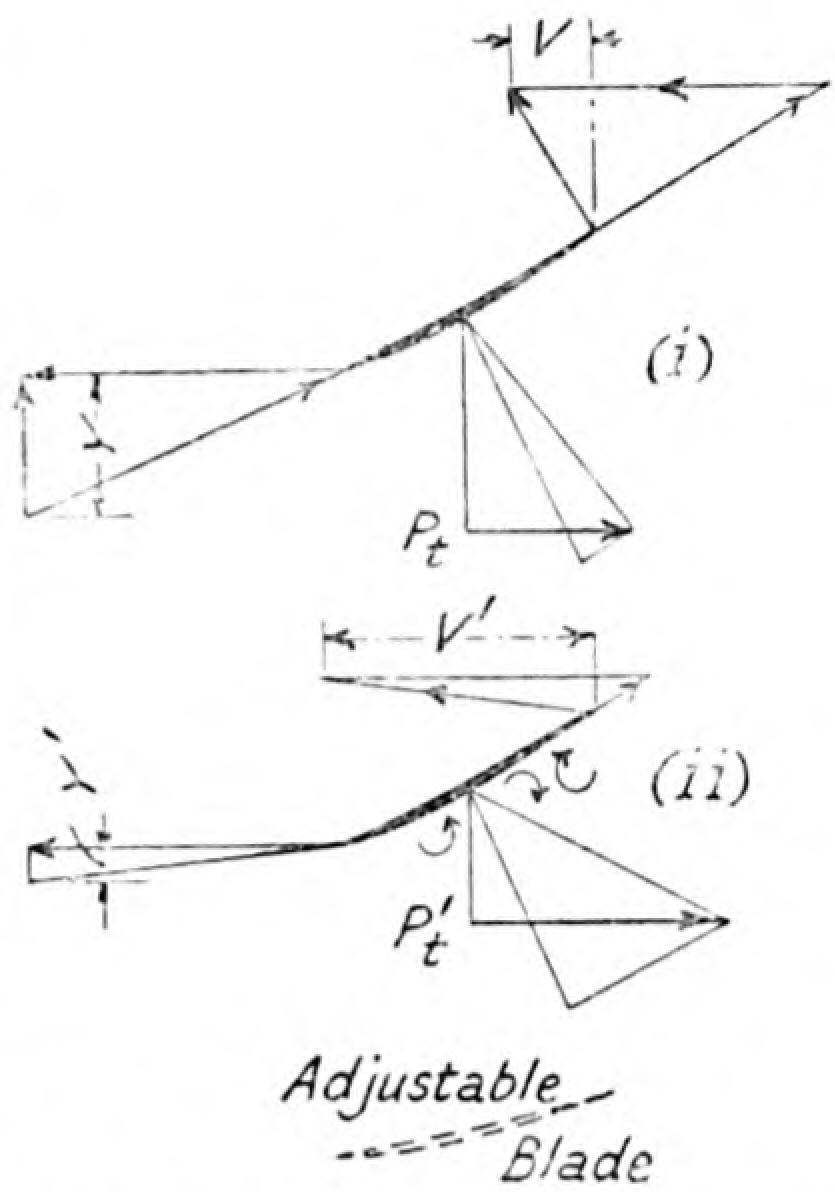

FIG. 399.—Velocity diagrams for (i) full-flow, (ii) part-flow conditions, in axial-flow pump.

345. Applications of Propeller Pumps. Whenever large quantities of liquid have to be moved against a low head, there is a possibility that a propeller pump can be successfully applied; if the percentage head variation is considerable, such a pump will have definite advantages over a centrifugal pump, and in any event it will be smaller, lighter, and capable of being driven by a smaller and faster-running motor. In effect, the pump is a part of the pipe system, nor need its diameter be any greater than that of the pipe. This was made clear in Fig. 394. As such a vertical-shaft pump would usually be set below the water level in the suction chamber from which it draws, its rotor would be permanently submerged and therefore no priming would be necessary, § 334.

As for the horizontal installation depicted in Fig. 400 (I), it can be claimed for it that no valves at all are needed in the pipe system; not even the non-return flap valves seen in diagram II. In order to prevent siphonic return flow from outlet to inlet channel when the pump stops, a vacuum-breaker is essential; it admits air to the pump casing, and is operated either by hand or automatically whenever the electric

power supply is interrupted. Without this safeguard there would be a danger of the motor being driven backwards way at a speed much beyond its designed speed, the pump then acting as a propeller turbine. Like all siphonic systems (§ 166), the one shown in Fig. 400 (I) must be primed before the pump will work. This disadvantage cannot be charged against the inclined pump, Fig. 400 (II), for its rotor is set below water-level, ready to run at any time. On the other hand, the non-return flap valves, which correspond with the foot-valve of the centrifugal pumping plant, Fig. 381, may be heavy and costly.

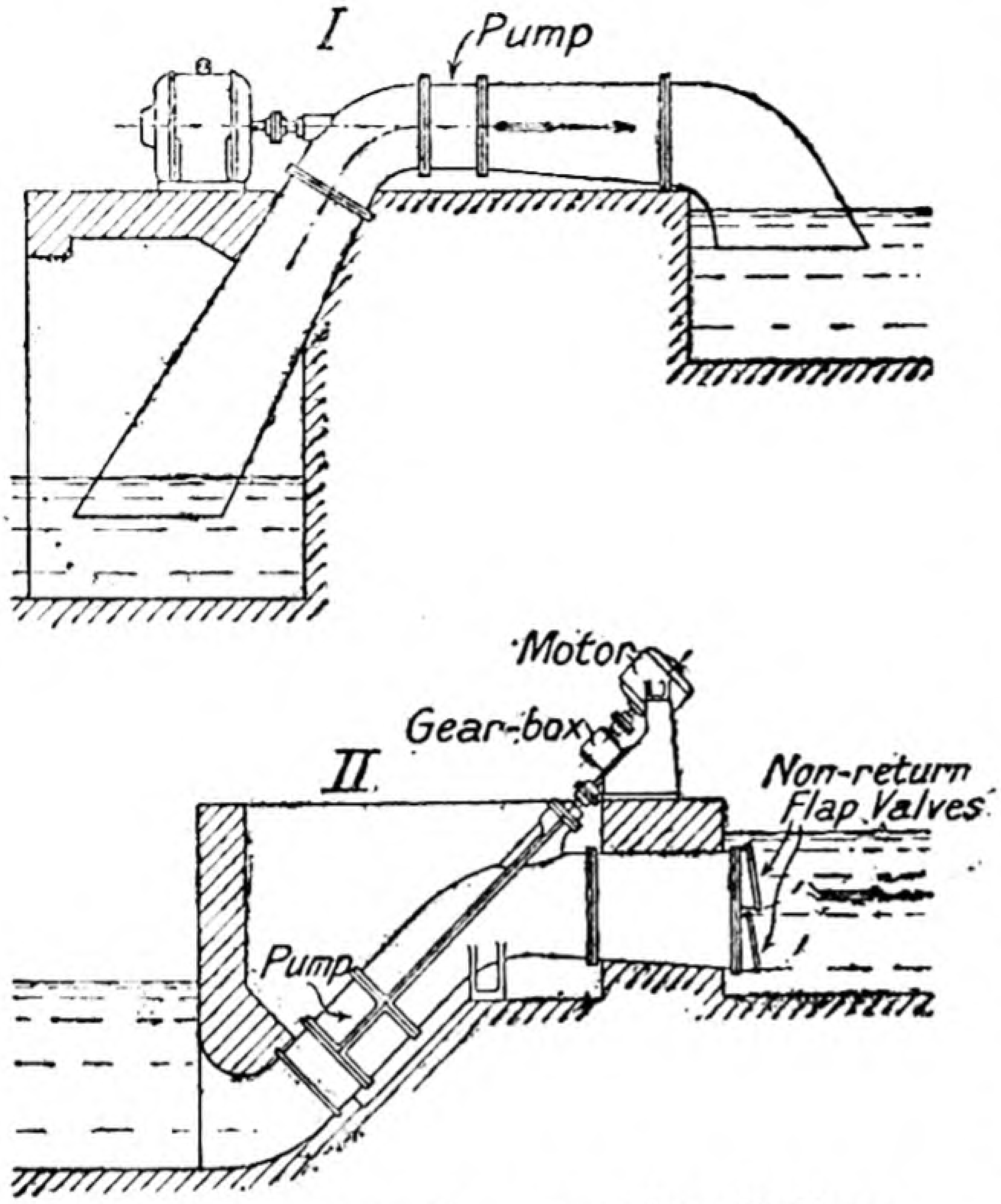

FIG. 400.—Propeller pump installations.

Another example of an inclined axial-flow pump is illustrated in Fig. 401: it is one of a series of boosting installations spaced along the Thirlmere aqueduct which supplies water to the city of Manchester (England). With normal rate of flow, the gravitational discharge is controlled by the natural slope of the hydraulic gradient. If more water is required, the booster pumps are set to work, thus increasing the virtual slope, § 167. By means of a two-

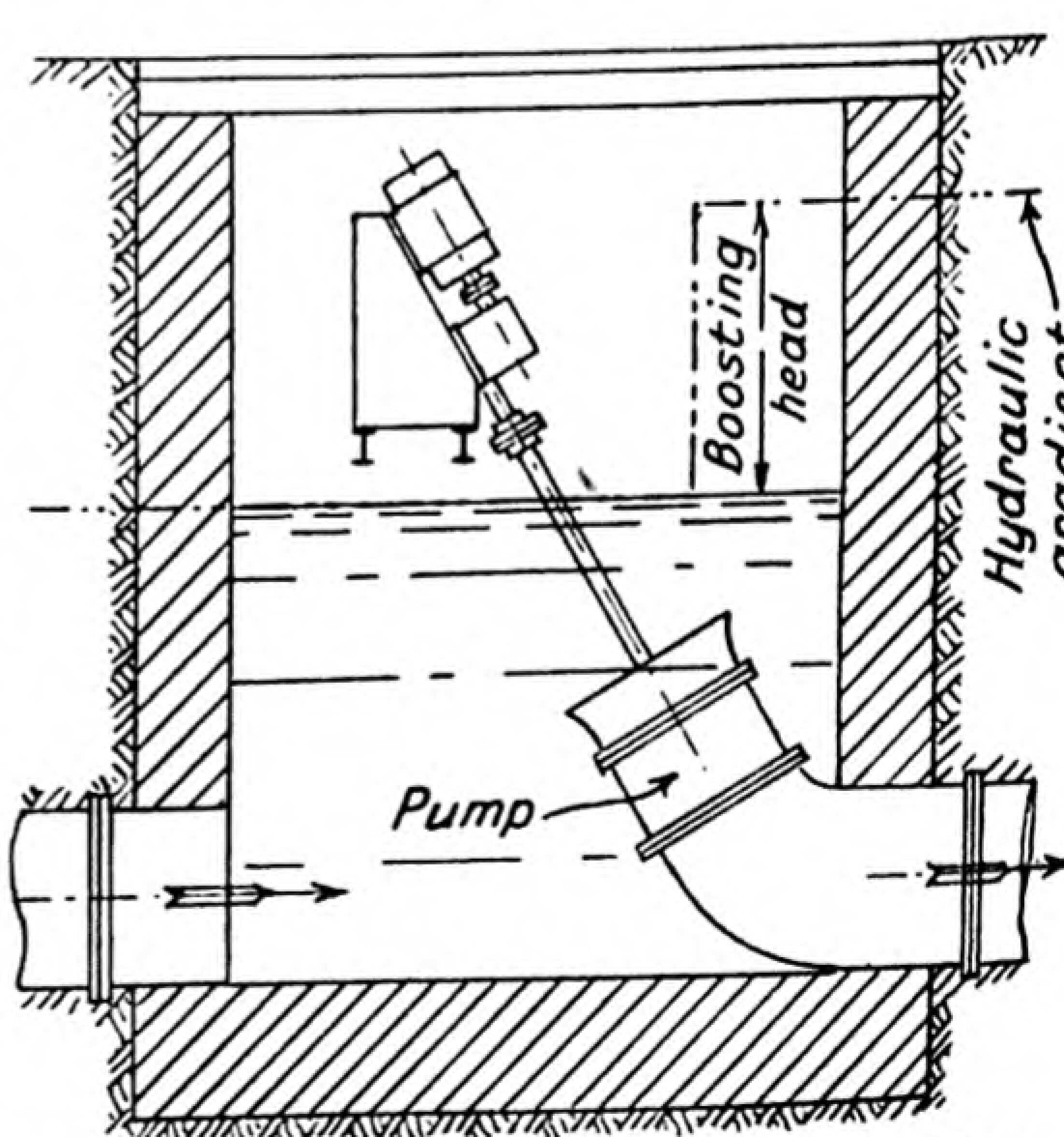

FIG. 401.—Booster pump installation.

speed gear-box between the electric motor and the pump, either a small or a large "boosting" head may be generated. The essential simplicity of the installation is specially to be noted: the complete pump is housed within the elbow which guides the water into the pipe. It is significant that the gear-boxes seen in Fig. 400 (II) and in Fig. 401 are both speed-*reduction* devices; for although the pump rotors have a high *specific* speed, yet their rotational speed is low because of their large diameter in relation to the small working head. **(Example 185.)**

Although single-stage propeller-pumps are not often chosen for heads above 40 ft. or so (12 metres), multi-stage pumps have a much greater range. Bore-hole propeller-pumps having as many as 7 stages will lift more water from a given bore than an equivalent centrifugal bore-hole pump, § 339.

346. Variable-Pitch Propeller Pumps. The excessive pressure and power consumption associated with the working of a propeller pump at constant speed and small discharges (Fig. 397) are serious disadvantages; but they may be eliminated by providing the pump with adjustable propeller blades whose inclination can be suited to the discharge just as those of a Kaplan turbine can be (§ 249). Such pumps are especially suitable when it is required to raise large but variable volumes of water against a constant but low head at uniform shaft speed with minimum power consumption—conditions often found in electrically-driven drainage stations.

Considering the propeller blades to be temporarily fixed at each of (say) six different positions, then for each position a head-discharge and an efficiency characteristic identical with those of a propeller pump could be obtained, yielding the six sets of curves plotted in Fig. 402. But at the working head—in this instance 5 metres—the pump is seen always to be running nearly at the peak of the efficiency curves; consequently during normal operation, when the discharge is controlled by hand regulation of the blades, the discharge-efficiency curve would be one enveloping the individual efficiency curves. A higher efficiency at part discharge is thus possible than with any other type of rotodynamic pump. This favourable feature of the variable-pitch propeller pump is also indicated in Fig. 402 by the steady fall of the power curve as the discharge declines; an explanation is to be found in Figs. 304 and 399.

Even although the expense of a pump with fully adjustable propeller blades may not be justified, it is frequently advantageous to have the blades of a propeller pump arranged so that

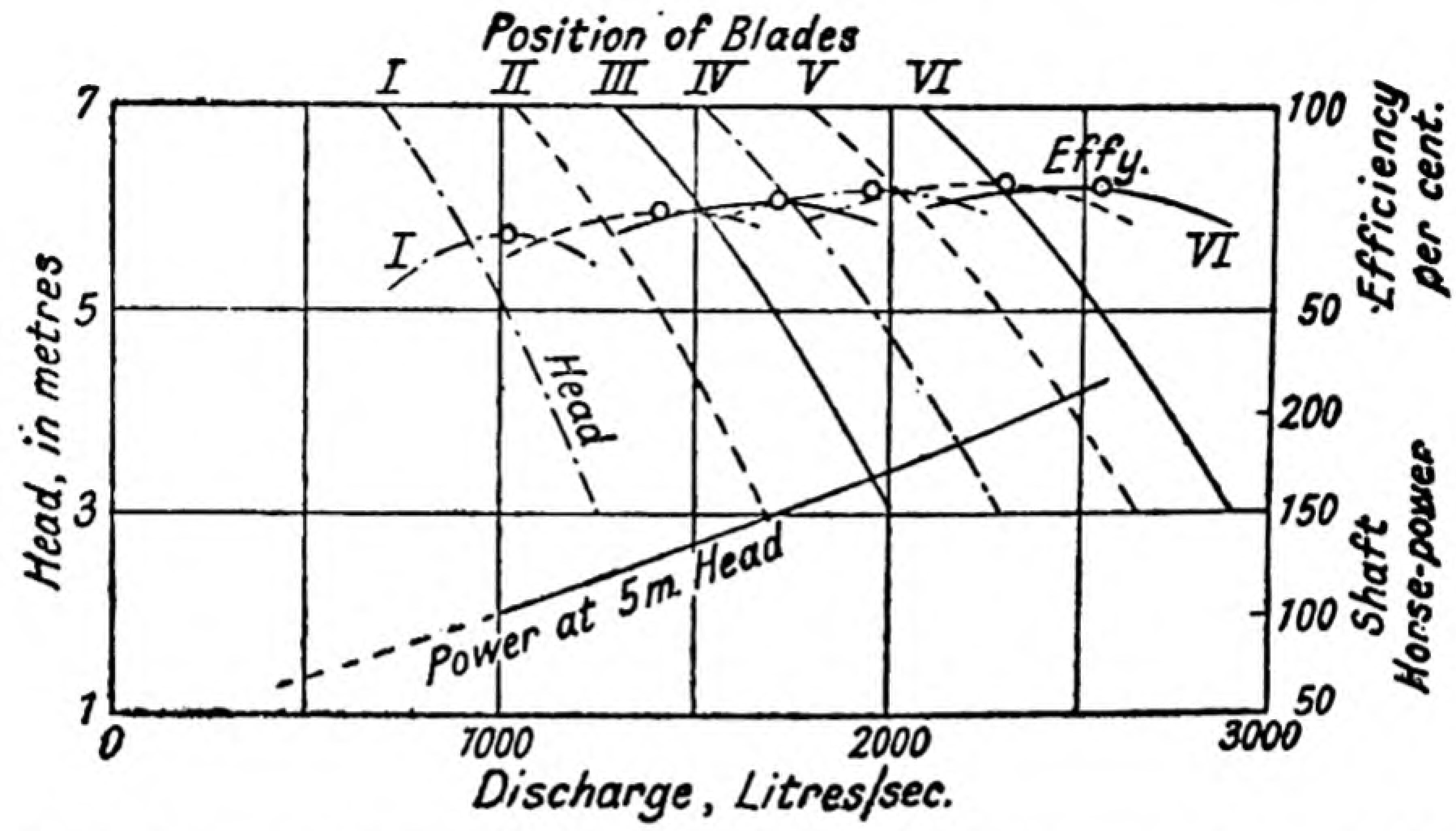

FIG. 402.—Characteristics of variable-pitch propeller pump at constant speed.

when the unit is stopped and drained, small adjustments of the blade angles may be made, in order to obtain the most favourable efficiency.

When a group of axial-flow pumps is in question, rather than a single unit, then the advantages of the variable-pitch principle are less important (see § 277).

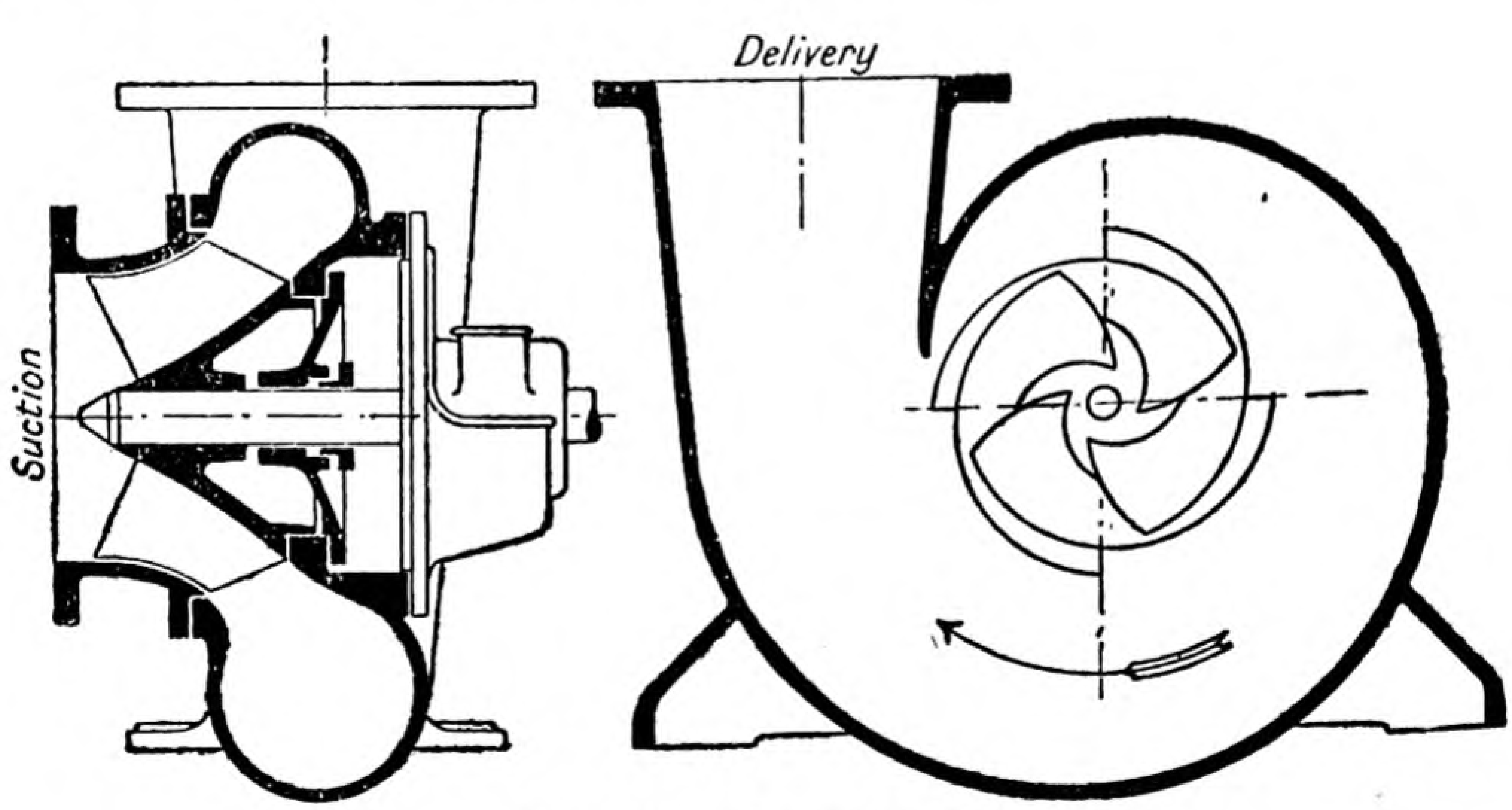

FIG. 403.—Screw pump.

347. Screw Pumps. Screw pumps or half-axial pumps are intermediate, both in construction and in performance,

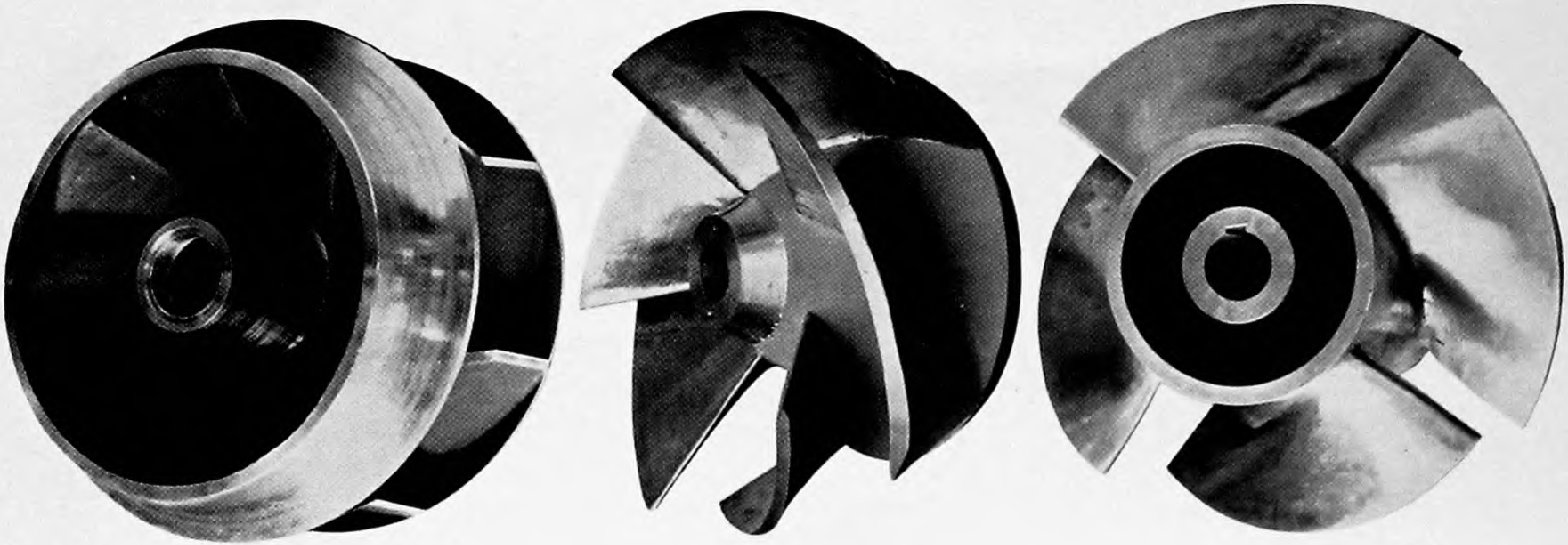

(I) (II) (III)

FIG. 404.—Typical forms of rotodynamic pump rotor.

(I) Centrifugal pump. $N_s = 66$ (foot units).

(II) Screw pump. $N_s = 89$ (foot units).

(III) Propeller pump. $N_s = 115$ (foot units).

(Gwynnes Pumps, Ltd.)

[*To face page* 508.

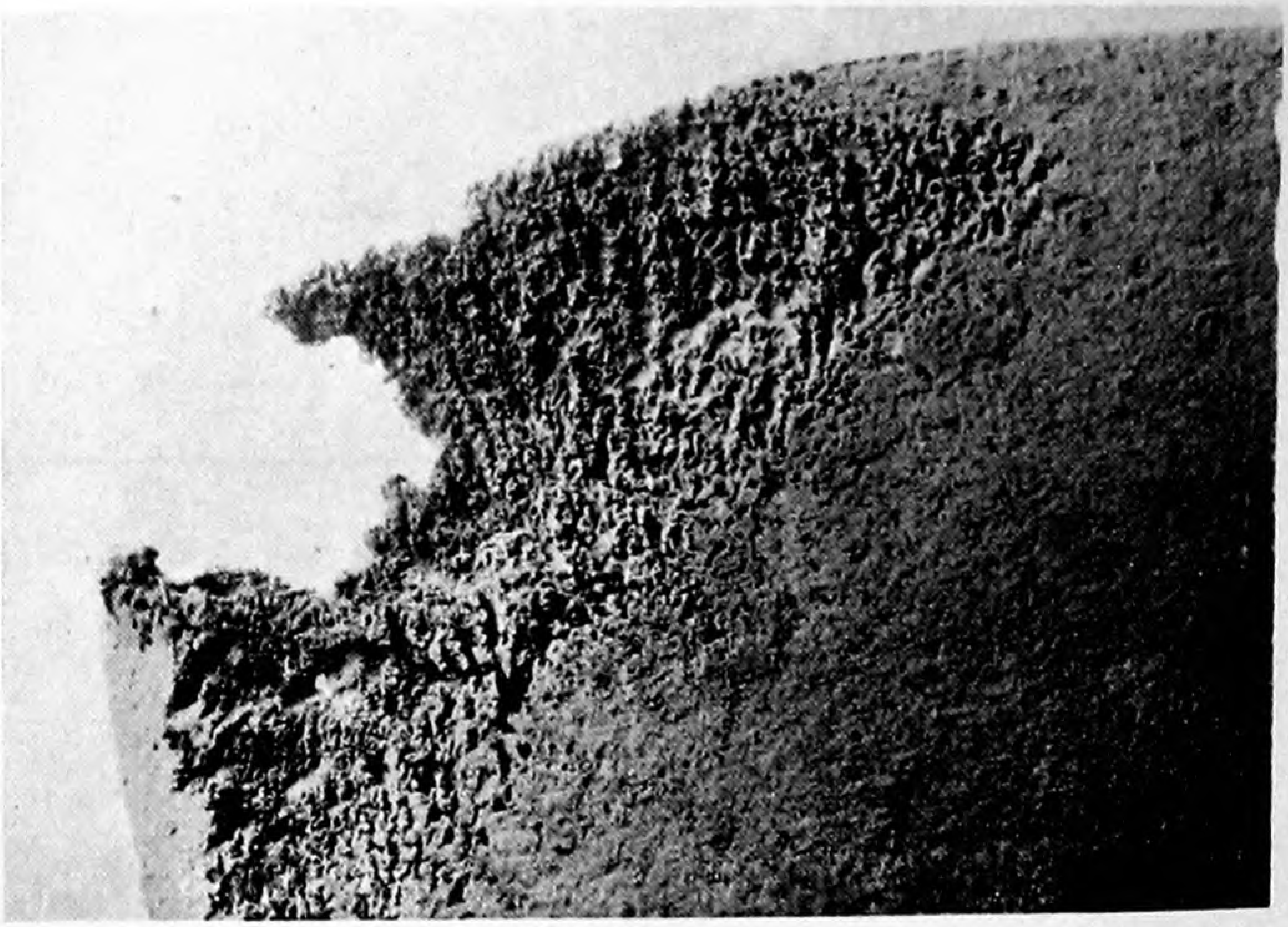

Fig. 408.—Damage caused by cavitation to propeller-pump blade.
(*Scale about one-third natural size.*)

[*To face page* 509.

between centrifugal pumps and propeller pumps.[244] Fig. 403 shows a typical screw pump, and a photograph of the screw rotor of such a unit is reproduced in Fig. 404 (II). The photograph is a composite one, showing on a comparative basis the rotors of (I) a centrifugal pump, (II) a screw pump, and (III), an axial-flow pump. It is evident that the inlet edges of the screw rotor resemble those of a propeller pump rotor, but the outlet edges and the volute casing into which the water is discharged, are more reminiscent of a centrifugal pump. The head-discharge characteristic of the screw pump (Fig. 405) is quite like that of a centrifugal pump, and its power characteristic, being nearly horizontal, is free

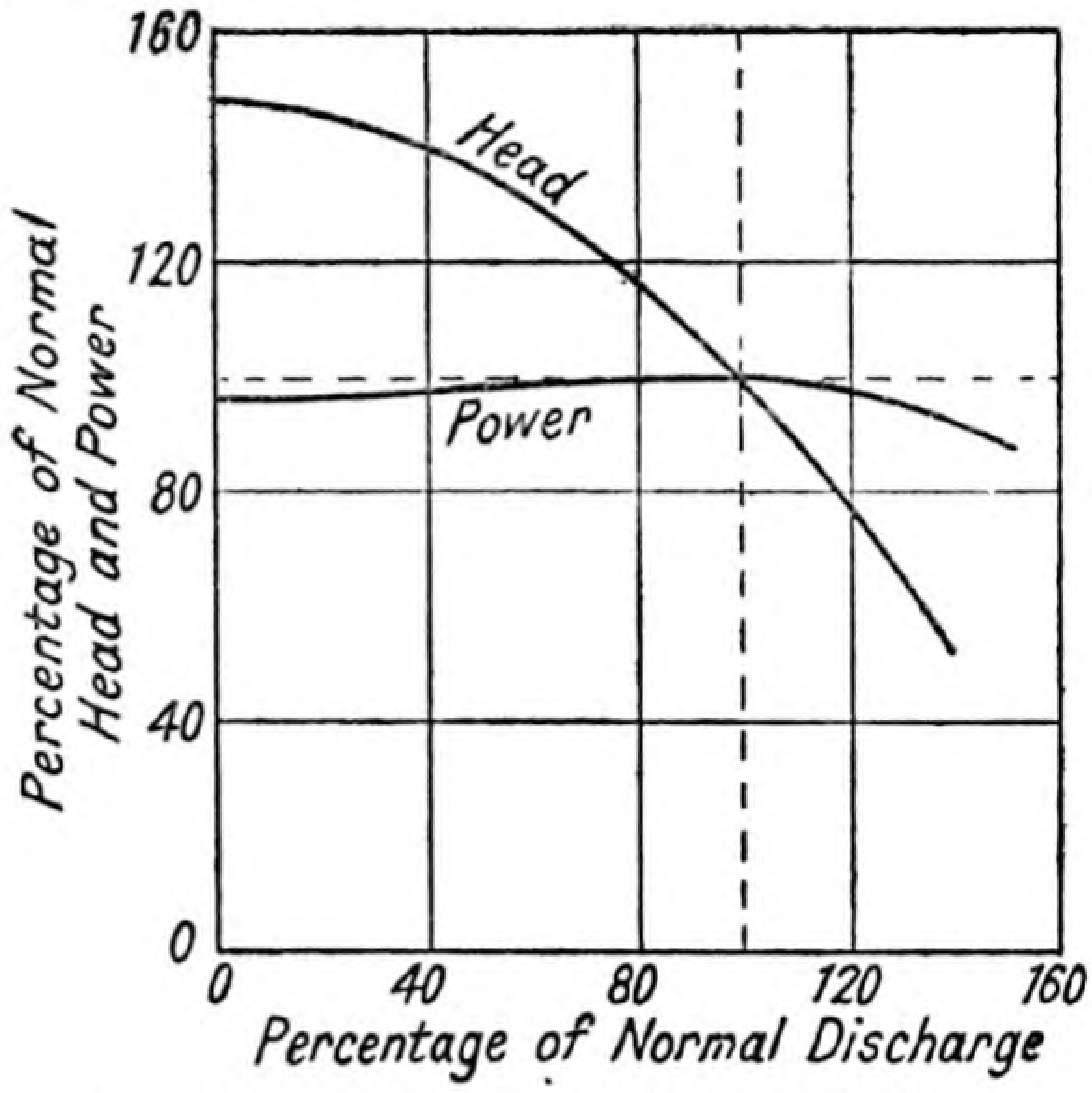

FIG. 405.—Characteristics of screw pump.

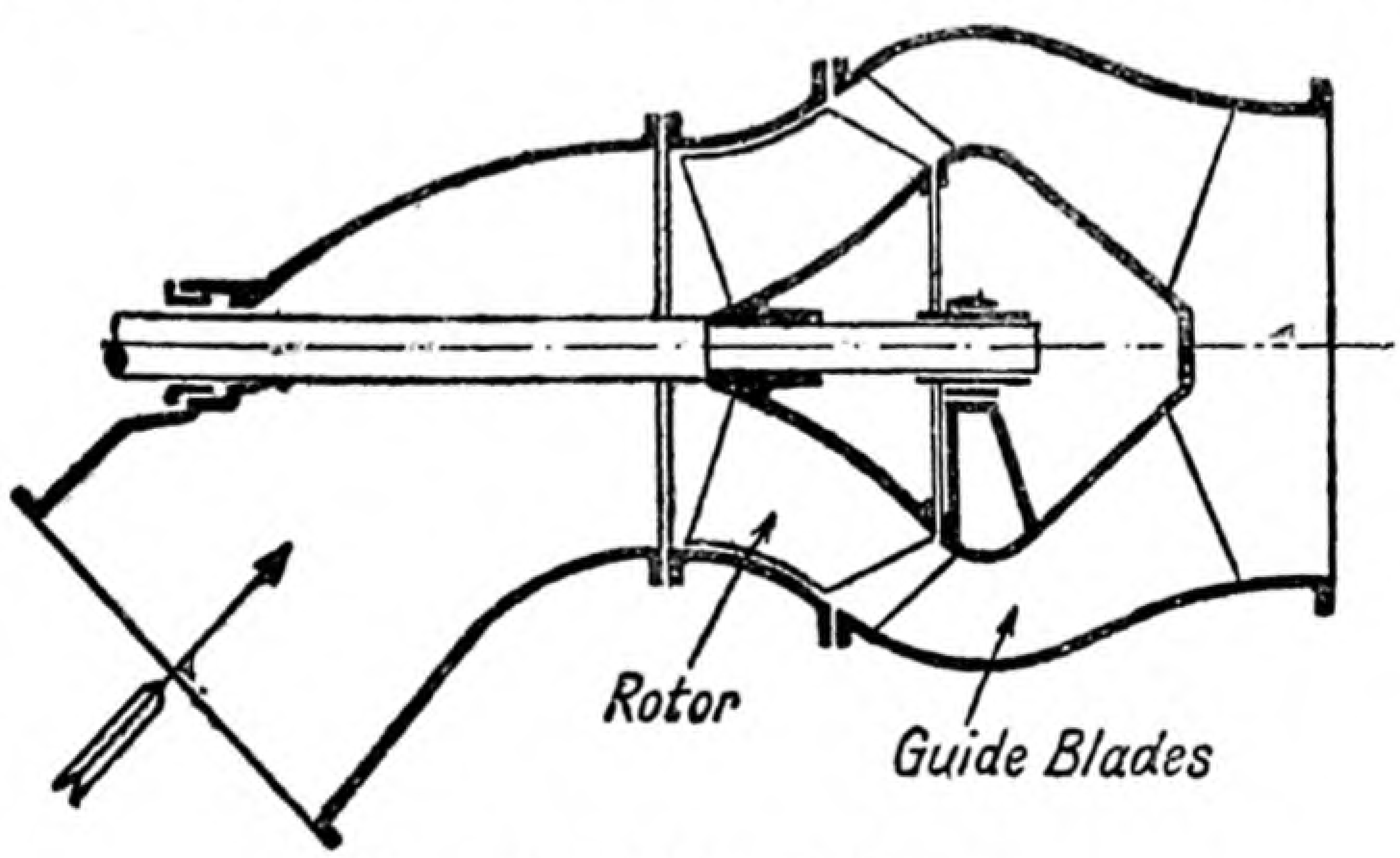

FIG. 406.—Half-axial pump.

from the unfavourable features of the propeller pump power curve. Overall efficiencies of 85 per cent. have been claimed for screw pumps working at specific speeds of 400-450 (metric).

The difference between the pump illustrated in Fig. 403, and the one shown in Fig. 406, is that in the latter the conversion of velocity head into pressure head is carried out by

means of outlet guide blades instead of by a volute casing. In other respects the construction and performance of the two types are nearly identical. For purposes of identification the guide-blade pump is sometimes called a *half-axial* pump.

Multi-stage half-axial bore-hole pumps are as successful in their own field as are multi-stage centrifugal pumps (§ 339) and multi-stage propeller pumps (§ 345) in theirs.

348. Suction Lift, Cavitation, etc.: A General Survey. It is easy to see that in an axial-flow pump the question of limitation of suction lift is of even greater moment than it is in a centrifugal pump. That is because the depression head within the pump is likely to be relatively greater. According to the reasoning of § 336, the depression head is linked with the relative velocity of the liquid over the rotor blades; and it is evident from § 341 that in a propeller pump this relative velocity, expressed in terms of the spouting velocity $\sqrt{2gH_m}$, is higher than in any other type of rotodynamic pump. These trends or tendencies must now be put into precise numerical form: we want to be able to estimate the numerical value of the suction lift in specified conditions. It is the Thoma type of expression that will help us, § 282; if it was found so useful for turbine installations, it should, when suitably modified, give equally valuable guidance when applied to pumps.

If, in equation 16-6, § 335, we write $H_{ms} = h_s + h_{fs} + h_v$, and if the term $\sigma' H_m$ is accepted as generally representative of the head deficiency x or of h_{lp}, then it is permissible to say that

$$H_{ms} = \frac{p_a - p_{vp}}{w} - \sigma' H_m \quad . \quad . \quad (17\text{-}1)$$

where H_{ms} is the manometric suction head on the pump, § 325, and σ' is the Thoma cavitation factor. Here, as in § 282, the fundamental assumption is accepted that the depression head varies directly as the total manometric head H_m. But it would not be safe to use the actual values of σ suggested in § 282, for the following reason:—The leading edge of the turbine blade, where the greatest negative *dynamic* pressures may be expected to occur, occupies a position some distance removed from the point in the machine where the lowest average absolute pressure prevails, viz. the entrance to the

draft tube; but the leading edge of the pump blade (Figs. 383, 396) is moving in a zone where already the average absolute pressure is at its lowest.[245] In consequence the values of σ' applicable to pumps are *higher* for comparable specific speeds than the values of σ for turbines; suitable values of σ' are plotted in Fig. 407.

So far as any such relationships can be universal (§ 337), the graph is applicable to *all kinds of rotodynamic pump*—centrifugal, propeller, and screw. Yet the limitations of Fig. 407 should be clearly realised. Only in a general sense is it true to say that pumps of the same specific speed have the same geometrical shape: for instance, a single-inlet impeller having the same specific speed as a double-inlet impeller, Fig. 359, would nevertheless have different proportions. Other kinds of variation were pointed out in § 337 (ii). What we do learn clearly enough from formula 17-1 and its accompanying Fig. 407 is this: that as the *total* head on a pump goes up, the *suction* head must come down. Thus, with a propeller pump of specific speed 600 (metric) running always at its design point, the static suction head can be 3·7 metres if the total manometric head is 5 metres, but must be reduced to only 1·2 metres if the total head is raised to 7 metres.

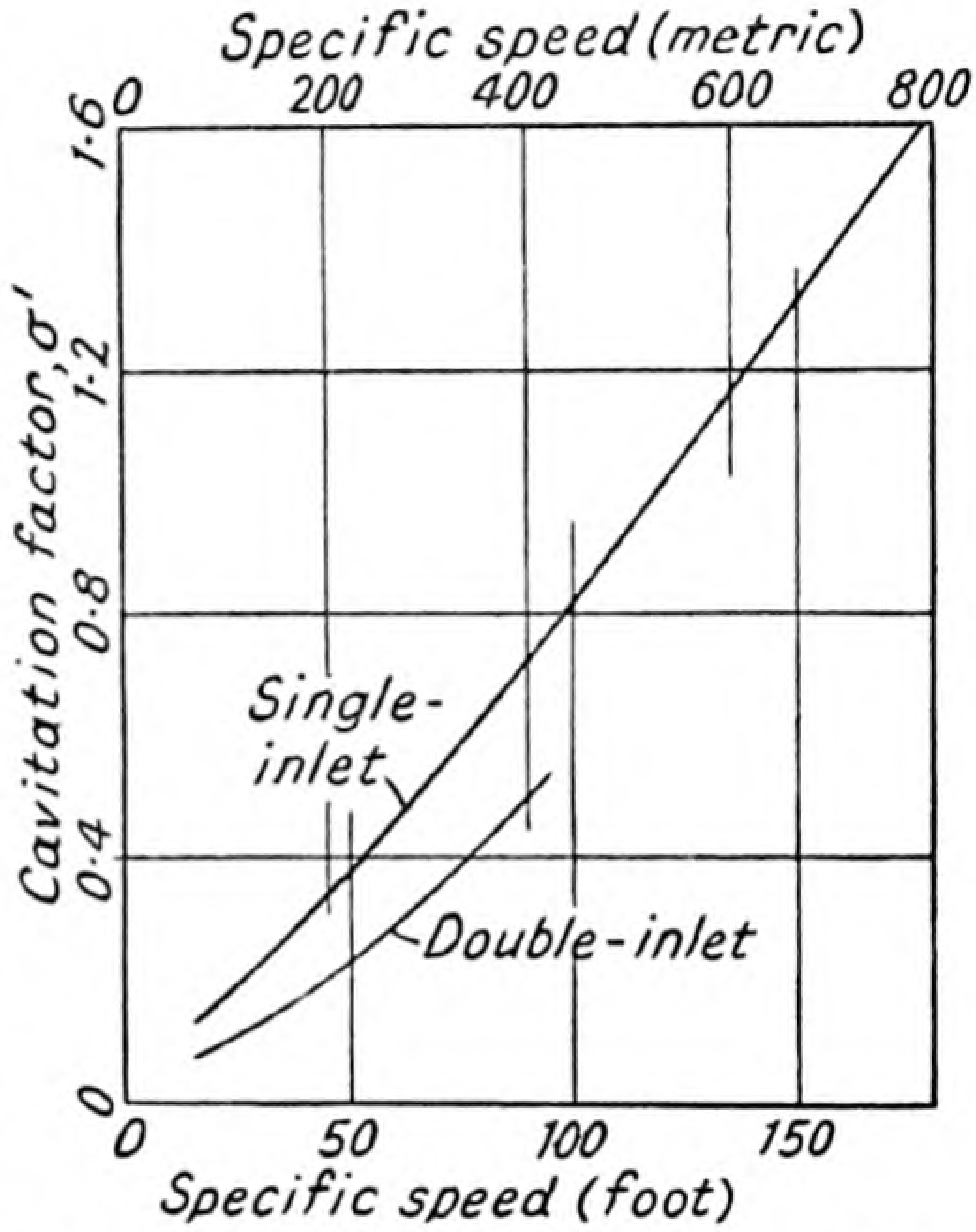

FIG. 407.—Values of cavitation factor σ' for rotodynamic pumps.

The consequences of running a propeller pump under an excessive suction head are vividly pictured in Fig. 408 (facing p. 509); cavitation has not only attacked and partly destroyed a part of the under surface of the blade, but has eroded the outer circumferential edge.[246] The action in this instance has been unusually severe because of the high proportion of dissolved salts in the drainage water the pump has been handling.

Clearance cavitation is the name given to the particular action that damages the outer edge of the blades of axial and half-axial machines. Leakage is constantly taking place through the circumferential clearance between these edges and the fixed housing of the pump, and the resulting eddy-formation generated in a region where the suction head is already high is very favourable to vaporisation of the water. Erosion of the blade edges naturally increases the leakage and impairs the pump efficiency.

349. General Comparisons between Main Types of Pump. In the three chapters devoted to pumping machinery a fair notion has been given of the range of duties for which each class of machine is suitable. This paragraph will present a few pictorial comparisons and will examine a few outstanding points.[247]

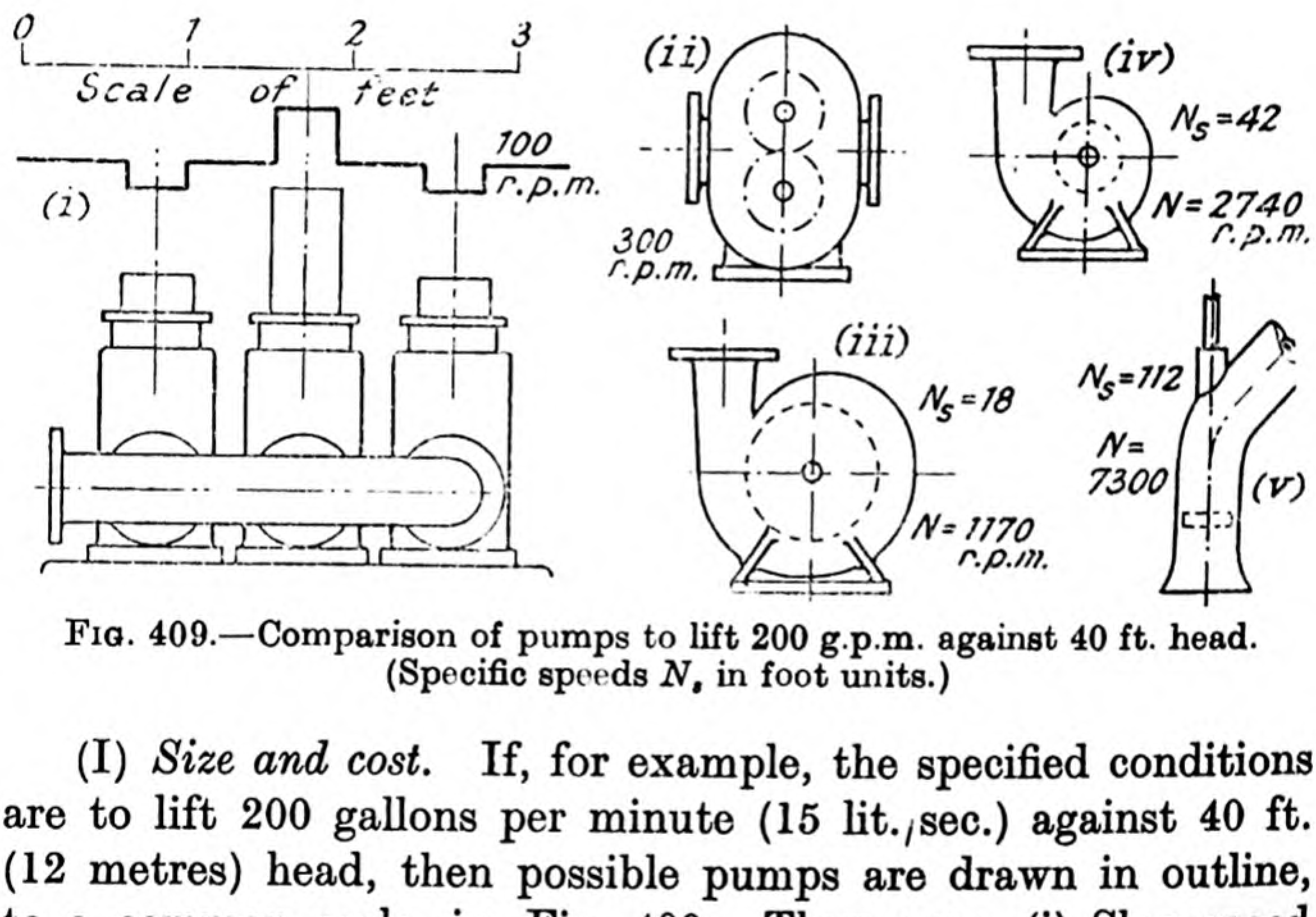

FIG. 409.—Comparison of pumps to lift 200 g.p.m. against 40 ft. head. (Specific speeds N_s in foot units.)

(I) *Size and cost.* If, for example, the specified conditions are to lift 200 gallons per minute (15 lit./sec.) against 40 ft. (12 metres) head, then possible pumps are drawn in outline, to a common scale, in Fig. 409. They are: (i) Slow-speed 3-throw ram pump; (ii) Gear-wheel pump; (iii) Slow-speed centrifugal pump; (iv) High-speed centrifugal pump; (v) Propeller pump. Here is manifestly an instance in which the reciprocating pump is ruled out by reason of its bulk, weight, and cost; it would probably require, also, single- or double-reduction gearing for coupling it to its driving motor or engine. On the other hand, the little propeller pump would have to be driven at a fantastically high speed. The effective choice is thus narrowed to the gear-wheel pump and the centrifugal pump: in the end it might be decided by the nature of the liquid. **(Example 188.)**

(II) *Efficiency at varying outputs.* When a variable discharge has to be forced against a high and uniform pressure, then a *variable-speed reciprocating pump* will always have the highest average efficiency. The representative graphs in Fig. 410 relate to boiler-feed pumps working in parallel; each pumps water at a temperature of 375° F. from a suction pressure

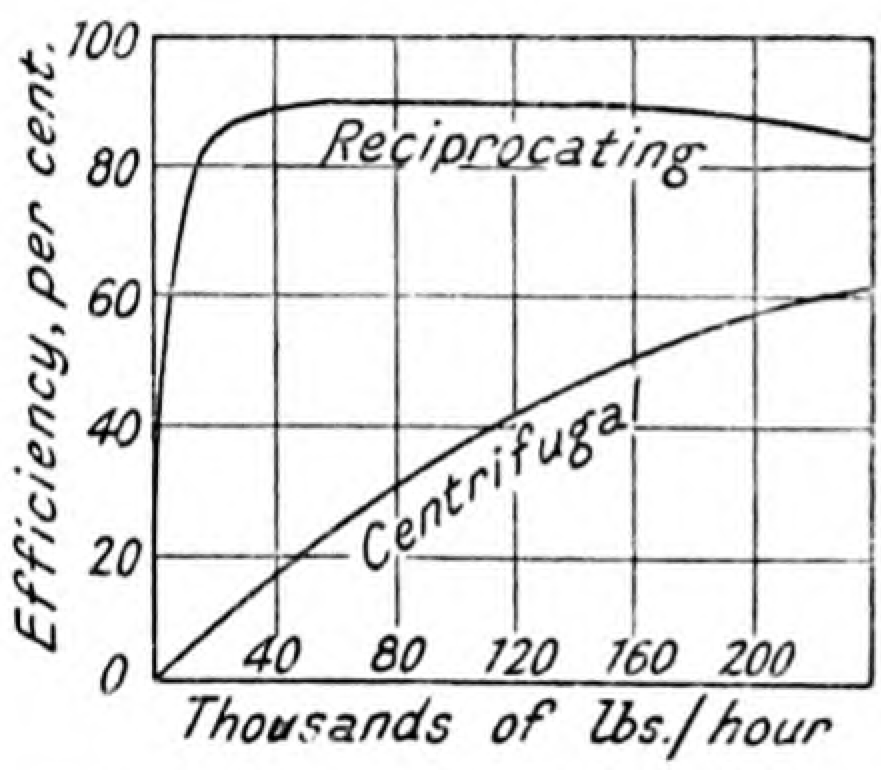

FIG. 410.—Comparison of boiler-feed pumps.

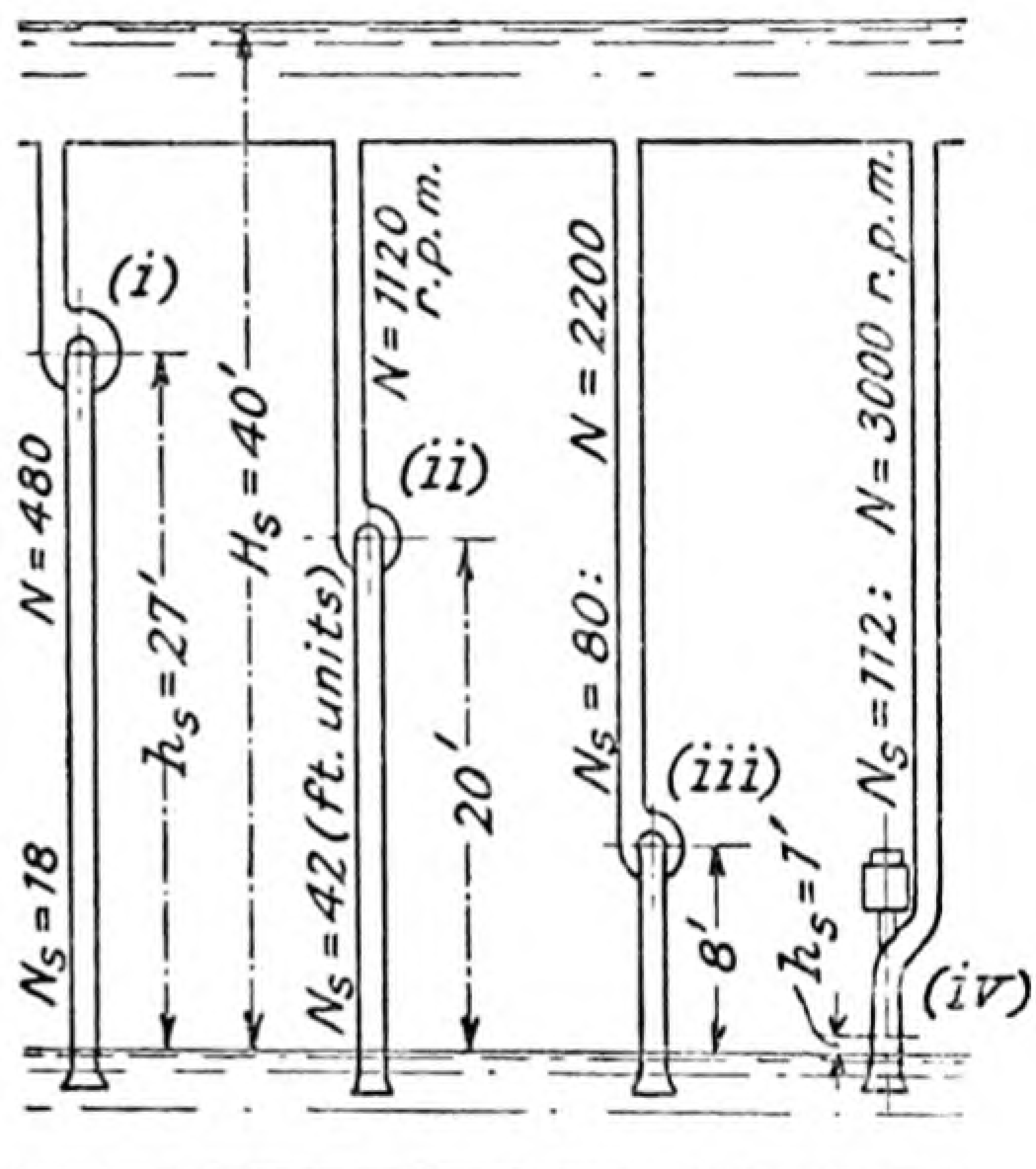

FIG. 411.—Pumps lifting 1150 g.p.m. against 40 ft. head.

of 305 lb./sq. in. to a delivery pressure of 2300 lb./sq. in. Not only has the reciprocating pump by far the better performance at part-loads, § 305 (1), but it is much superior to the centrifugal pump at full-load also. It is of the 5-throw type (§ 292), totally enclosed, forced lubricated, driven through single-reduction gearing from a 800 h.p. variable-speed D.C. electric motor at a maximum crankshaft speed of 100 r.p.m. The reason for preferring such a machine is clear, and it applies to all high-pressure, high-duty installations.[248] The annual cost of the power absorbed by the pump is so high in relation to the first cost of the pump that a very expensive machine will in the end be the most profitable one if it is built with the single end in view of securing the highest possible efficiency and the greatest durability.

In general, the *higher the head* and the *smaller* the discharge, the more likely is it that a positive-displacement pump will be preferable to a rotodynamic pump.

(III) *Suction lift.* The arguments developed in §§ 335-337, 348 are summarised in Fig. 411. Together with a screw pump, three rotodynamic pumps having specific speeds identical with those in Fig. 409 are represented, working as before against a head of 40 ft., but now each delivers 1150 g.p.m. They are installed at the limiting height above the suction well as indicated by the Thoma formula. The diagram gives a clear impression of how the necessities of suction lift may govern the choice of pump, viz. :—

Static Head (feet).	Discharge (g.p.m.).	Ref., Fig. 411.	Static Suction Lift (feet).	Type of Pump.	Specific Speed (foot).	Speed r.p.m.
40	1150	(i)	27	Slow-speed centrifugal	18	480
		(ii)	20	High-speed centrifugal	42	1120
		(iii)	8	Screw - - -	80	2200
		(iv)	1	Propeller - - -	112	3000

(IV) *Starting conditions.* When the pump discharges into a long rising main, the inertia pressure required to set the liquid column in motion cannot altogether be disregarded, § 115. Only the centrifugal pump is able to look after itself in such conditions; it can be run up to speed without any special precautions, generating maximum head when the liquid column is at rest and absorbing minimum power (Fig. 377). The half-axial pump, Fig. 405, is nearly as good, except that the driving motor must develop its full output as soon as it has reached full speed. On the other hand, if a propeller pump had a driving motor designed only for normal duty, then the motor might be seriously overloaded at the beginning of the accelerating period (Fig. 397). There is a choice of two safeguards: (*a*) the motor may have special starting-gear [249] designed to bring it up to speed quite slowly, (*b*) a branch on the delivery pipe close to the pump may allow water to escape from a vertical open topped stand-pipe when the delivery head rises above pre-determined limits. This escape-pipe serves the same purpose as the hand- or spring-controlled by-pass that is indispensable for positive pumps, § 298 (ii), (iii).

(V) *Positive action.* So-called positive pumps are not the only ones that manifest a positive tendency. There are

occasions when a rotodynamic pump can be just as obstinate —just as insistent on having its own way. If such a pump is set to deliver a stated discharge at a specified speed, it will insist on generating a certain head which is fixed by its particular characteristic. Whether we want so much head or not, we cannot prevent the pump from creating it. If the head is more than we require, the surplus must be dissipated in a throttle-valve or similar device. A reciprocating pump, on the other hand, will generate a pressure just sufficient to overcome external resistances. A constant-speed centrifugal boiler-feed pump is thus relatively at a disadvantage, inasmuch as at low rates of flow a good deal of energy must be wasted at the check-valve.

(VI) *Kind of liquid.* Positive pumps are much more fastidious about the kind of liquid they will accept than rotodynamic pumps are. Positive rotary pumps insist on completely clean (grit-free) liquids ; reciprocating pumps much prefer clean liquids, but centrifugal and propeller pumps will often tolerate silt, floating debris and even sand in the water, without complaint.

(VII) *Performance characteristics.* Basic performance characteristics at constant speed are summarised in Fig. 412. The discharge of the reciprocating pump —here represented by a plunger pump —is virtually insensitive to variations in head. An opposite tendency controls the centrifugal pump: over a fairly wide range of discharge, the head may remain nearly constant. Intermediate in behaviour is the propeller pump: any alteration in discharge at once provokes a substantial change in head.

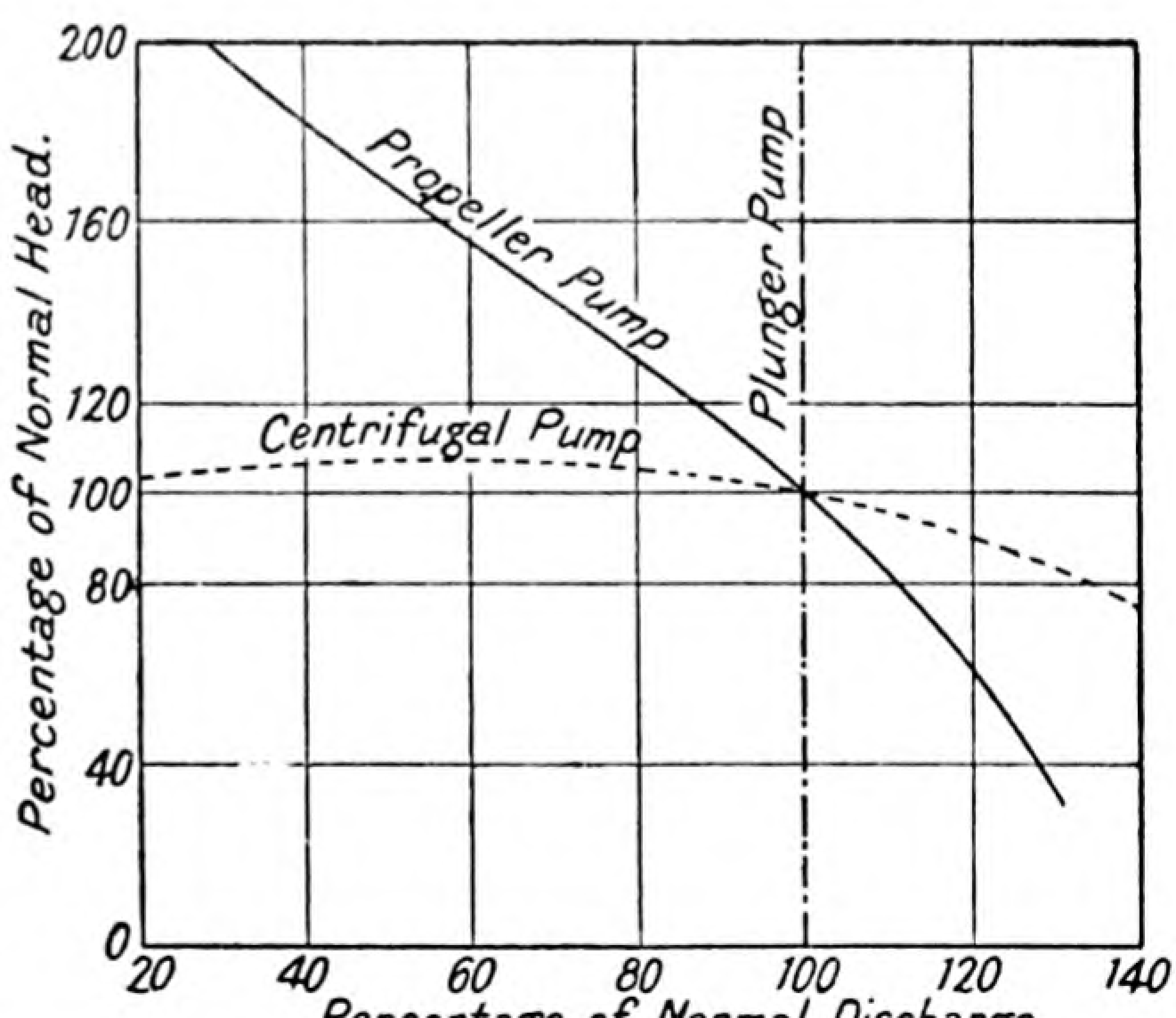

FIG. 412.—Comparison of pump characteristics at constant speed.

350. Final Choice of Pumping Plant. Since a pump is basically an energy converter, and since the overall cost of pumping will depend upon the cost of the energy supplied to the pump, no general comparison between pumping plants is valid unless it takes these energy costs into account.[250] A

Duty.	Type of Pump.	Type of Motive Unit.
Waterworks: raising water from below ground, from streams, etc.	(Reciprocating well-pump: reciprocating bore-hole pump) Centrifugal well-pump: centrifugal bore-hole pump	(Steam engine). Electric motor. Oil-engine.
Waterworks: forcing water into pipe systems, reservoirs, etc.	(Reciprocating pump) Single-stage or multi-stage centrifugal	(Steam engine). Electric motor. Oil engine. Steam turbine. Gas turbine.
Irrigation and land drainage	Centrifugal Screw Propeller	Electric motor. Oil engine.
Pumping sewage (including other liquids containing solids in suspension)	(Reciprocating) Special centrifugal Pneumatic ejector	(Steam engine). Electric motor. Oil engine. Compressed air.
Auxiliary services in steam power stations (land and marine): Circulating water pumps	Centrifugal Propeller	Electric motor.
Feed pumps	Centrifugal	Electric motor. Steam turbine.
	Reciprocating	Electric motor. (Steam engine).
Pumping oil	Reciprocating Positive rotary Centrifugal	Steam engine. Electric motor. Oil engine.
Hydraulic transmission	Reciprocating Positive rotary	Electric motor, or main motive unit.

comprehensive survey of such questions lies far outside the scope of this book, yet it is possible to suggest what a variety of factors require consideration. We want to know: (i) how much the pump will cost, (ii) how much the motive unit will cost, viz. the engine or motor that drives the pump, (iii) what will be the annual cost of fuel or electrical energy, (iv) what other expenditure will be incurred, e.g. cost of land, cost of buildings, administrative costs, maintenance charges, etc. The relative proportions of those items will vary in different parts of the world and in different installations, and even in the same pumping plant they will be influenced by fluctuations in price levels.[251]

The above Table, therefore, is hardly more than a reminder of what multitudinous possibilities there are. At least it recognises a distinction between the numerous plants still in operation, based on the knowledge of earlier days, and those that would probably be installed today.[252] The former, which although not in the popular sense up-to-date, are still giving good service are indicated by brackets ( ).

CHAPTER XVIII

HYDRAULIC TRANSMISSION AND STORAGE OF ENERGY

351. Hydraulic Transmission and its Competitors. A great diversity of methods is available for transmitting energy from an engine or other prime mover to a neighbouring or a distant point. According to the intervening distance, the engineer may choose (i) belt, (ii) chain, (iii) shaft, (iv) gear, (v) compressed air, (vi) electricity. Nevertheless still another system, employing liquid under pressure, continues to make headway in face of this varied competition.

Why is hydraulic transmission able to extend its scope in this manner? One reason is that it prefers to co-operate rather than to compete. Co-operation with electric transmission is especially fruitful, and it is an alliance of long standing. Immense reserves of water-power in some inaccessible gorge would have had little importance if electric power lines had not been available to conduct the energy to centres of industry. The energy may go into a hydro-electric station through a pipe several feet in diameter: it comes out along an overhead conductor less than an inch in diameter. There would consequently be no advantage in trying to conduct water power, actually in the form of hydraulic energy, over long distances, when electrical methods can do the duty so much more economically. An electric motor, too, is so simple

and so highly developed a machine for running continuously at high rotational speeds, that few hydraulic motors could hope to surpass it. Yet even on this basis of equal speeds and outputs, the hydraulic machine may be more compact and much lighter than the electrical one.

Hydraulic transmission is pre-eminent when the work to be done requires a slow, steady *thrust*, that can if necessary be indefinitely maintained. When extremely heavy thrusts have to be developed, of the order of 5000 or 10,000 tons, nothing else but hydraulic pressure will serve. But no matter whether a force of this magnitude is required in a hydraulic press, or whether a thrust of a few pounds on the brake-shoes of an automobile will suffice, the system will possess the basic advantages of silence, simplicity, smoothness of operation, and ease and positiveness of control. Sometimes, too, the overall efficiency may rise as high as 75 or 80 per cent.

352. Elements of a Hydraulic System. In principle the elements of a liquid transmission system may be expected to be—

(i) a hydraulic generator for converting the mechanical energy of the prime mover into hydraulic energy (§ 218).

(ii) a pipe which will serve as a transmission line (§ 91),

(iii) a hydraulic motor for re-converting the energy into mechanical energy.

Various dispositions of these elements are shown schematically in Fig. 413. In the simplest one, diagram (i), identical units embodying a cylinder and piston act either as generator or as motor; thus the motor piston reproduces exactly the motion of the pump piston—or it would do if leakage could be eliminated and if the pipe and liquid were inelastic.[253] A coil-spring supplies energy during the idle return stroke. If an enlarged motor cylinder is preferred, as at (ii), then the stroke of the motor piston is reduced *but the thrust is magnified;* the complete installation then fulfils the same purpose as a lever, worm-gear, screw and nut, or other mechanism for giving a mechanical advantage.

For providing a continuous flow of energy the arrangement (iii), Fig. 413, is more suitable. The power given out by the

engine A is converted by the pump or generator B, and is carried along the pipe D to the hydraulic motor E. After the liquid has delivered up its energy it is run to waste, consequently the liquid must be water.

A system particularly convenient when electrical energy is to be converted is illustrated at (iv). In accordance with the principles suggested in § 351, the electric leads are run as close as possible to the point E where the mechanical energy is finally to be delivered. A very short, closed hydraulic circuit connects the pump B to the hydraulic motor E, and as the same liquid

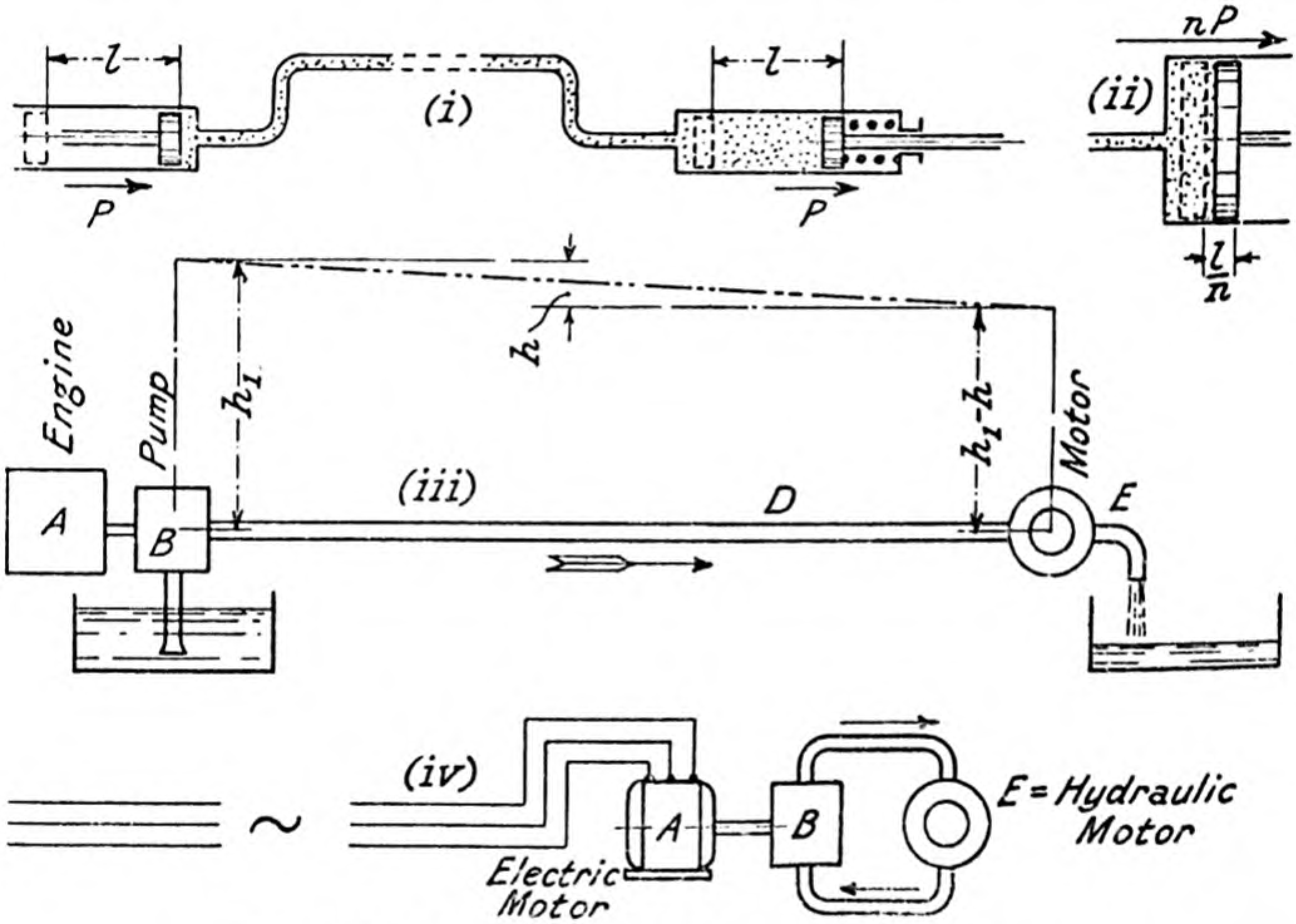

FIG. 413.—Typical hydraulic transmission systems.

is circulated continuously we can well afford to use oil instead of water.[254] The purpose of interposing the hydraulic gear between the electric motor A and the shaft of the hydraulic motor E is to increase the torque, to convert rotary motion into reciprocating motion, or to effect transformations of a similar nature (§ 356).

Another classification of hydraulic transmission systems would follow the lines proposed in § 219. On the one hand, we might use (i) *Rotodynamic* or *Hydrokinetic* systems, or on the other hand, (ii) *Positive* or *Positive-displacement* or *Hydrostatic* systems. Examples of the first kind will be examined

in §§ 360-365, while §§ 354-359 will be devoted to the more frequently used positive systems.

353. Choice of Hydraulic Generators and Motors. From the great variety of pumps described in Chapters XV, XVI, and XVII, and from the hydraulic motors mentioned in § 225, we are free to choose whichever combination best suits the specified conditions.(255) The *working pressure* will manifestly have a weighty influence, but this also is under our control. From § 91, and from Fig. 413 (iii), it appears that for a given frictional loss h the efficiency of transmission $(h_1 - h)/h_1$ will progressively rise as the inlet pressure-head h_1 increases. For a stipulated power "through-put," again, the quantity of liquid pumped per second, W, will diminish as the pressure-head h_1 increases. It follows that the highest possible working pressure should be chosen which just does not involve constructional difficulties or excessive maintenance charges, for in this way the pump, pipe, and motor will be relatively small and compact. The usual range of pressures found suitable is 200-3000 lb./sq. in. (13 to 200 atm.), but much higher pressures are sometimes preferred.

Pumps. The considerations set out in § 349 suggest that a reciprocating-pump will form the most suitable hydraulic generator, and for large installations it stands unrivalled. Almost invariably it will be driven through gearing by an electric motor. The illustration of such a pump reproduced in Fig. 324 was chosen so as to show the details of construction. The external appearance of a very large unit can be gathered from Fig. 414 (facing p. 527); it is totally enclosed, and the working parts have forced lubrication. The motor coupled to the input shaft of the reduction-gear is rated at 1100 h.p. Units of more usual size will transmit 200 h.p. at a pressure of 3000 lb./sq. in., the 3-throw crankshaft running at 160 r.p.m. The ram-cases and valve-boxes will probably be machined from solid steel forgings, and rams and valves will be of alloy steel. The glands may have moulded packing of the type shown in Fig. 223 (*d*).

For stand-by units designed for intermittent service only, such an expensive construction would hardly be economical; a multi-stage centrifugal pump, as illustrated in Fig. 367, would be suitable here, its lower efficiency being accepted

because of its lower first cost. Moreover, as this machine generates a nearly constant pressure irrespective of the output, it can deliver direct into the piping system without the intervention of an accumulator, § 354.

Closed-circuit systems, Fig. 413 (iv), using lubricating-oil or a specially-prepared liquid as a working medium, can profitably be fed by multi-cylinder positive pumps, either with fixed cylinders, § 294 (iv), or with rotating cylinders, §§ 300, 301. When the duty is relatively small, then the vane-type or gear-wheel pump is suitable, §§ 302, 303.

Motors. Hydraulic turbines (Chap. XIII) are rarely used at the receiving end of a hydraulic system; they cannot compete on comparable terms with electric motors. But occasionally small Pelton wheels are installed for light duties. The basic type of hydraulic motor, as the output element of a transmission system, is a ram or piston working in a cylinder (Fig. 413 (i)); the reciprocating motion so developed can be reduced, amplified, or transformed according to particular needs (§ 355).

If a continuous rotary motion is wanted [256], the choice lies between :—

(i) reversed rotating-cylinder pumps, § 300,

(ii) reversed vane-type or gear-wheel pumps, §§ 302, 303,

(iii) motors with multiple fixed cylinders and mechanically-operated valves.[257]

It will be apparent from § 304 that the overall efficiency of a given machine, acting as a motor, is likely to be slightly lower than when it is running as a pump; nevertheless, because of advances in manufacturing technique, hydraulic motor efficiencies approaching 80 per cent. may be realised in favourable conditions.

354. The Hydraulic Accumulator. In any of the systems illustrated in Fig. 413, the supply of liquid delivered by the pump must exactly keep pace with the demand of the motor. It follows that if the pump were a positive one and the speed of the hydraulic motor were constantly varying, the pump speed would also have to be regulated. This would be highly inconvenient in conditions such as are shown in Fig. 415, where a number of motors E, E, E, draw from a common supply pipe D fed by the pump B; the pump is driven by the

engine or motive unit *A*. The answer to this problem is the hydraulic accumulator, which can be interposed in the supply pipe as at *C*; it serves as a storage apparatus for excess water.[258]

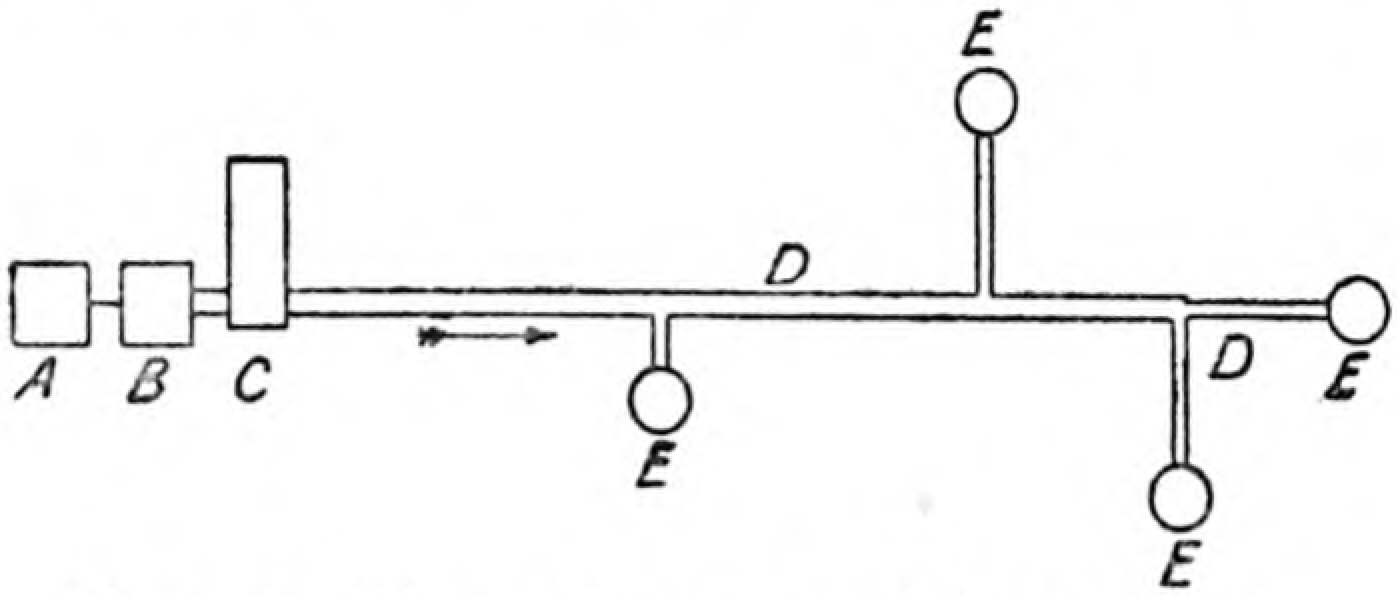

Fig. 415.—Distributing system with accumulator.

(i) *Weight-loaded type.* As shown diagrammatically in Fig. 416, this apparatus consists of a cylinder and ram loaded with ballast—scrap iron or any cheap and heavy material—contained within a plate-work shell. When the pump discharges more water than the hydraulic motors can utilise, the surplus water makes room for itself by raising the load; when the demand for water is heavy, the supply from the accumulator supplements that from the pump. Automatic tripping devices stop the pump or by-pass the water when the accumulator is full. The stuffing box with its "U" leather packing should be noted—it has been described in § 223 (*a*).

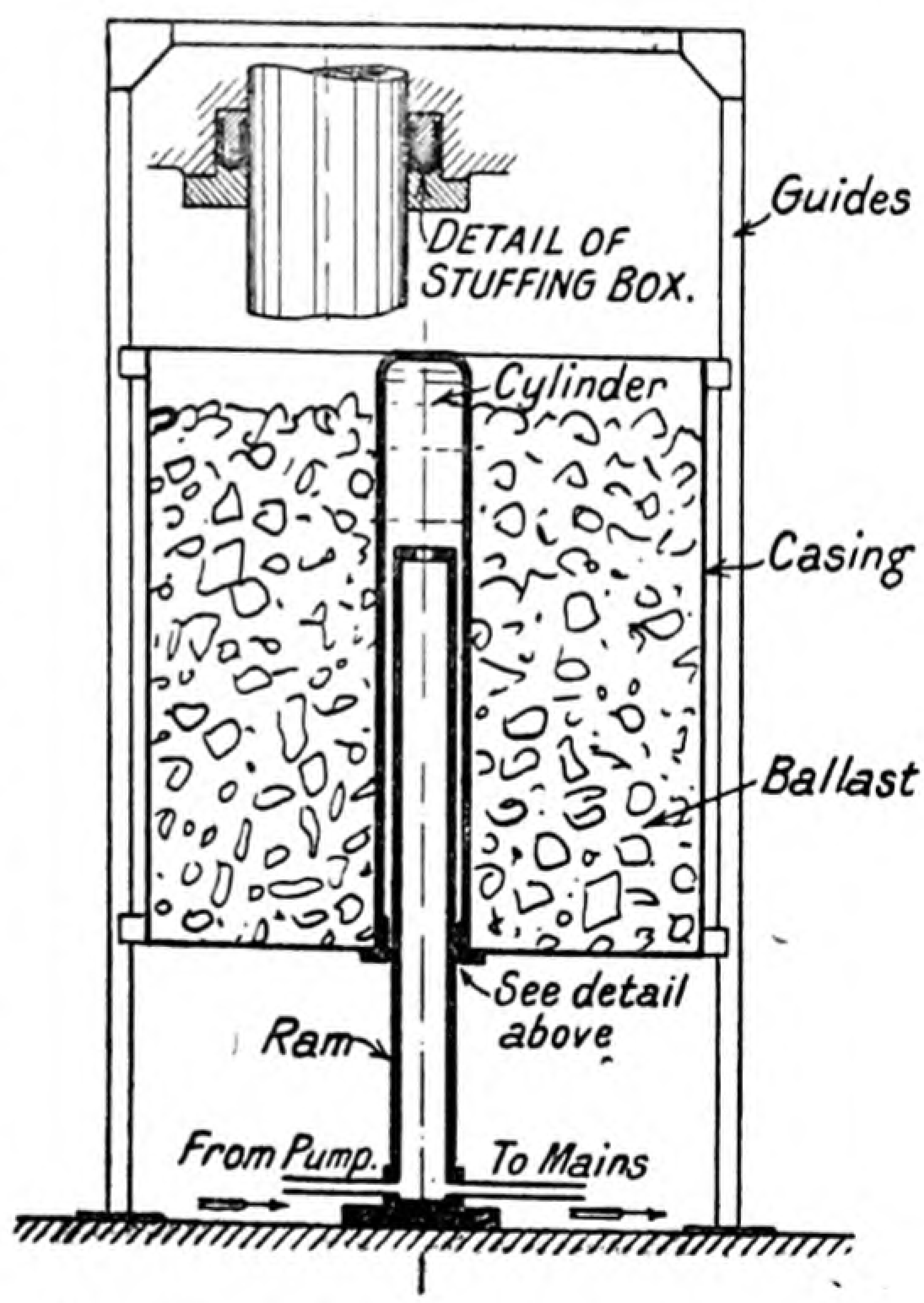

Fig. 416.—Weight-loaded accumulator.

(Example 196.)

(ii) *Steam-loaded type.* On ship-board, where hydraulically-operated auxiliary machinery is often used, the heavy moving mass needed by the weight-loaded accumulator would be out of place. The needful steady thrust on the accumulator ram

is therefore supplied by steam-pressure acting on a large piston. The upper part of the steam cylinder is kept at boiler-pressure, and the lower part communicates with the condenser (Fig. 417 (i)).

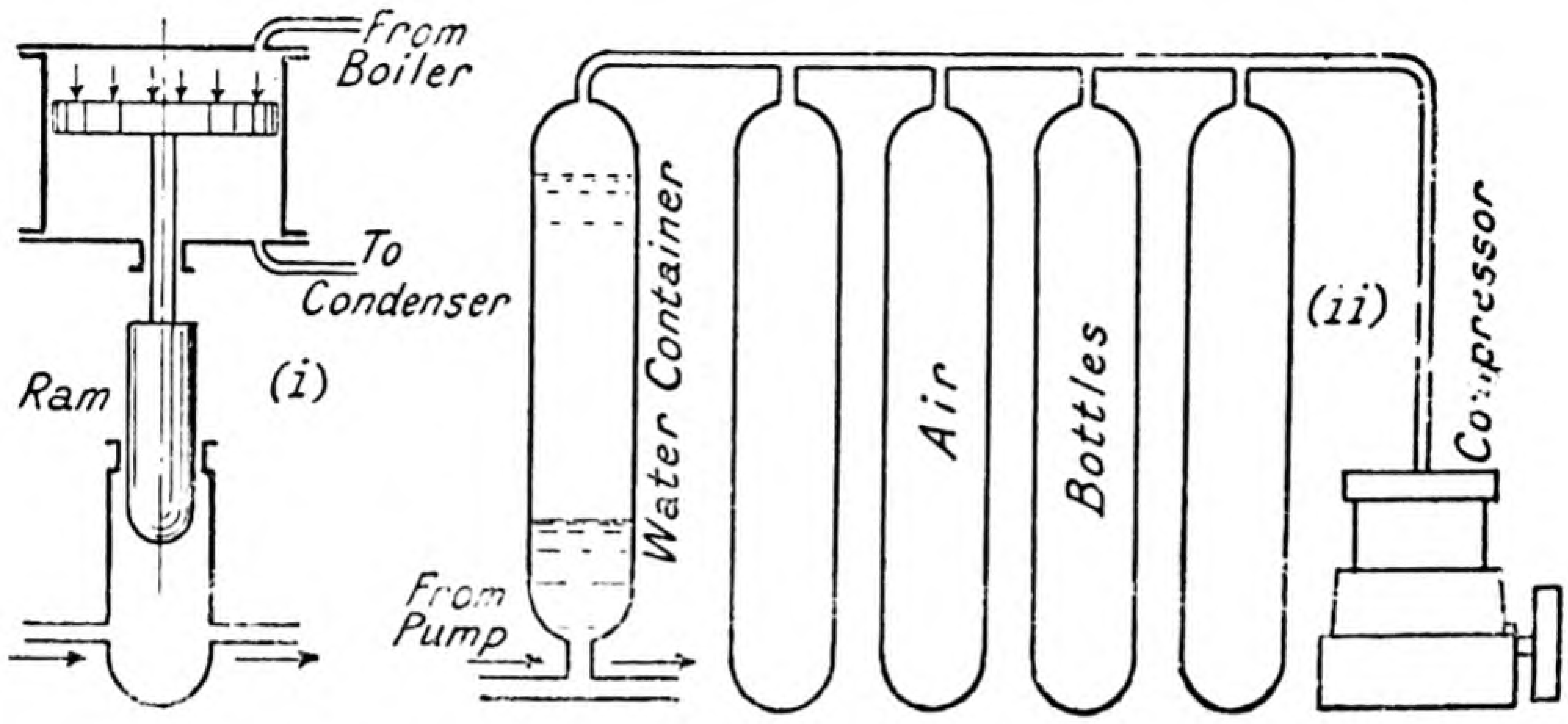

FIG. 417.—(i) Steam-loaded, and (ii) air-loaded accumulator.

(iii) *Air-loaded type.* Here there are no moving parts (Fig. 417 (ii)). Air contained in a battery of tall air vessels is maintained at the average pressure in the hydraulic system; as the surface level in the water-container rises or falls, there are corresponding slight variations in the air pressure, but these are usually unobjectionable. A power-driven compressor forces the initial charge of air into the bottles and replenishes it from time to time. Moving in sympathy with the surface level in the water-container is an external mercury column which operates electrical contacts and so controls the starting and stopping of the main pump when the accumulator approaches the empty or full condition.

355. Some Typical Hydraulic Machines. The hydraulic *lift* or *hoist* (Fig. 418 (I)) is a good example of the class of work that hydraulic power appears to be well fitted for; when high-pressure water is admitted to the cylinder, then the ram, the platform, and the goods mounted on it, are forced upwards; when the outlet valve is opened, the lift descends. But in fact it is only rarely that hydraulic drive can successfully compete with electric drive in this particular field. A *hydraulic jack* consists in effect of a portable short-stroke lift fed from a hand-pump formed integrally in the casing. When the load on a hydraulic hoist is to be lifted through a height greater than

the stroke of the ram, a *multiplying gear* is useful; it is a system of sheaves and wire-rope or chain resembling a block and tackle. In Fig. 418 (II) it is adapted to a hydraulic crane.

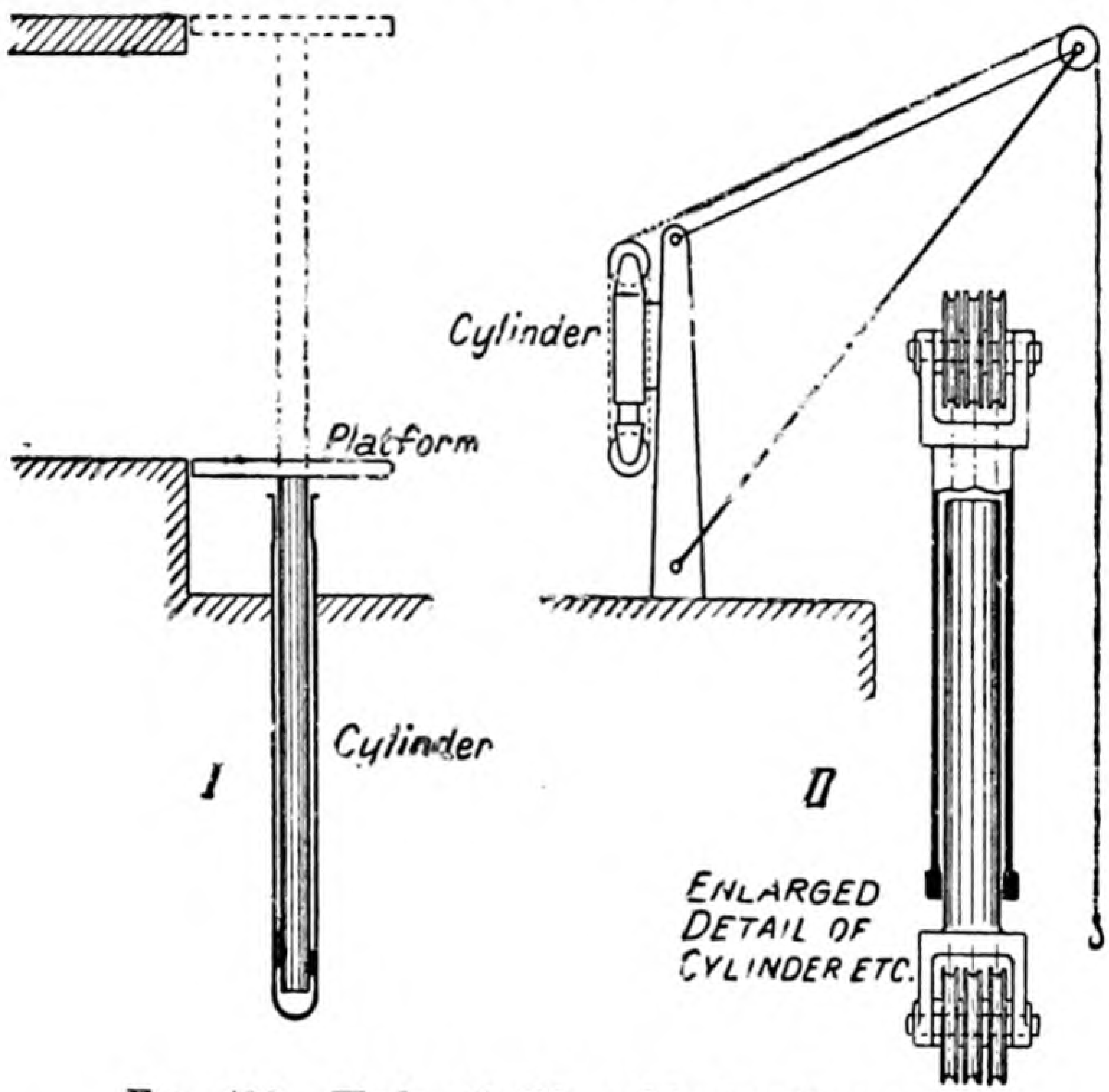

FIG. 418.—Hydraulic lift and hydraulic crane.

The *press* (Fig. 419)—a development of the apparatus originally invented by Ernest Bramah—is a type of machine for which hydraulic power has unique advantages.[259] This particular example can exert a total thrust of 450 tons on the material placed between the fixed upper table and the moving lower table. Multiple rams are provided, and can be seen in the illustratiou; one or more of them are brought into operation according to the thrust required. If a single ram only were used, the machine would be most wasteful at low loads, for just as much high-pressure water would be needed for a thrust of 1 ton as for 400 tons, the excess energy being destroyed in the control valve. Still further economy can be realised by providing a separate supply of low-pressure water for bringing the table up to its work before the main operating thrust is applied.

The hydraulic *riveter* shown in Fig. 420 can exert a thrust of 50 tons on the rivet brought between the fixed and moving *snaps*. The thin copper pipe that suffices to conduct the

water to the cylinder is to be noted; above the cylinder is the operating valve and control lever (§ 358).

The *hydraulic intensifier* is a boosting device used when the normal pressure of water is insufficient. It embodies two rams coupled axially together, a small one and a large one, each working in its own cylinder; thus when relatively low-pressure liquid is admitted to the large cylinder, high-pressure liquid may be drawn from the small cylinder. Fig. 417 (i) represents the principle, except that water instead of steam acts upon the upper piston.

The *winch* or *capstan* is typical of the slow-speed rotary hydraulic machine that is driven by a radial-cylinder motor (§ 353). It may serve for hauling or warping, on ship-board or on quays, or may actuate lift-bridges, dock-gates, and the like.

356. Closed-Circuit Hydraulic Systems and Servo-Mechanisms. When a system is to consist of a pump and one hydraulic motor only, not too far away, it is often convenient to form the piping in a closed system, the low-pressure oil exhausted from the motor being returned to the pump.[260]

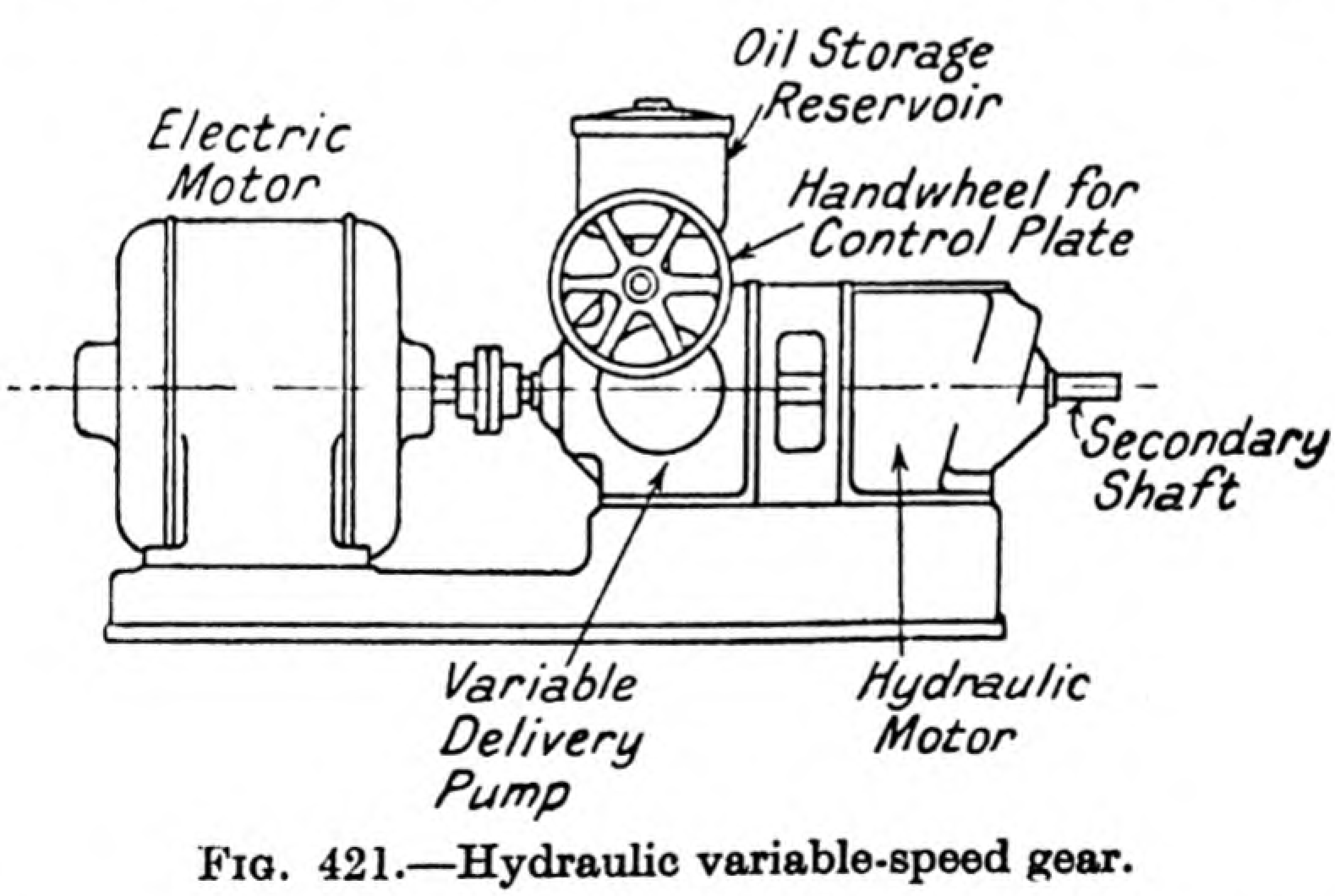

FIG. 421.—Hydraulic variable-speed gear.

Comparing the basic diagram, Fig. 413 (iv), with the equipment illustrated in Fig. 421, it will be observed that the input hydraulic element B now takes the form of a variable-delivery rotating-cylinder pump, § 301, while the output element E or hydraulic motor is an identical machine with fixed control plate. The combination thus serves as a variable-speed reduction gear.

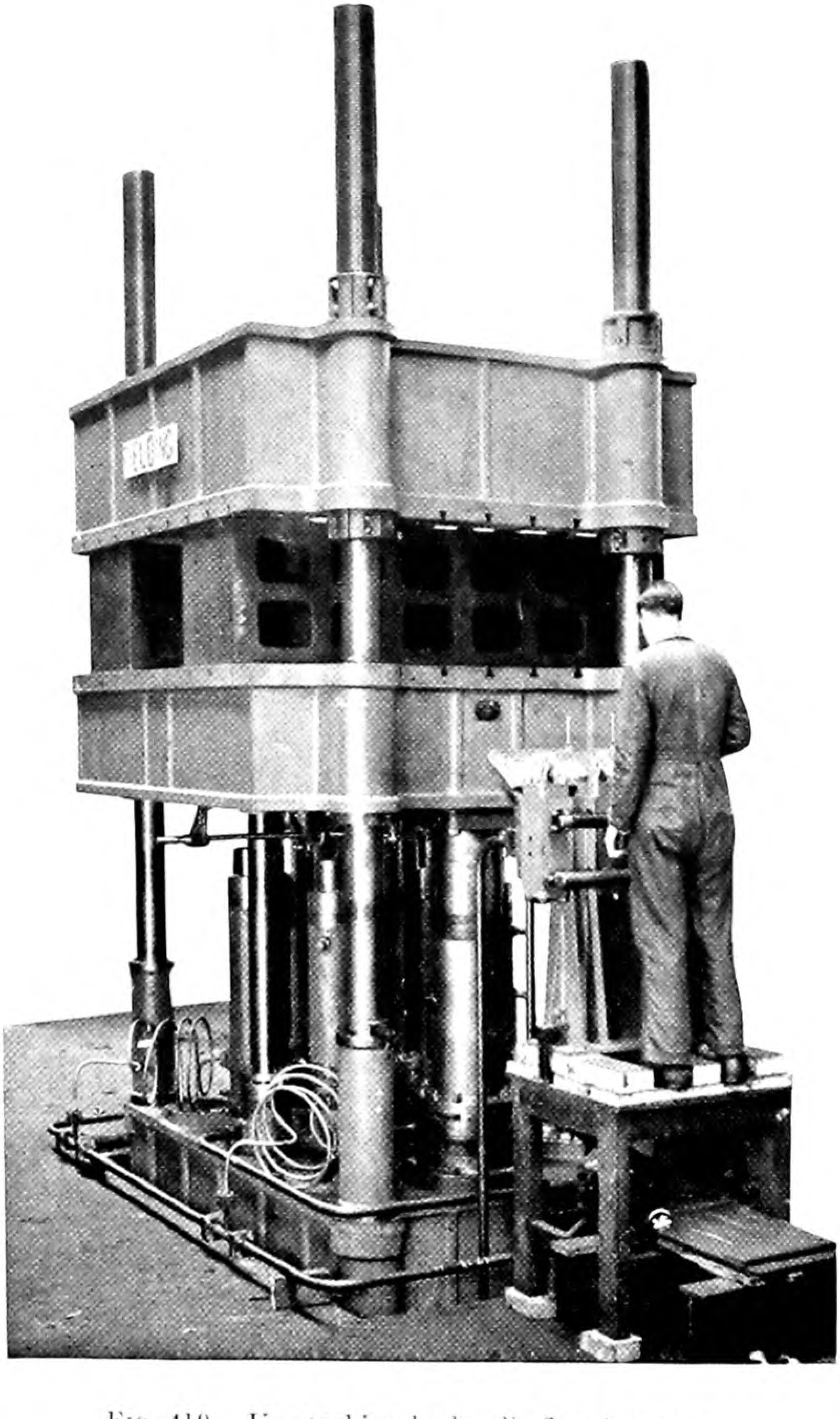

FIG. 419.—Up-stroking hydraulic flanging press.
(Fielding & Platt, Ltd.)

[*To face page* 526.

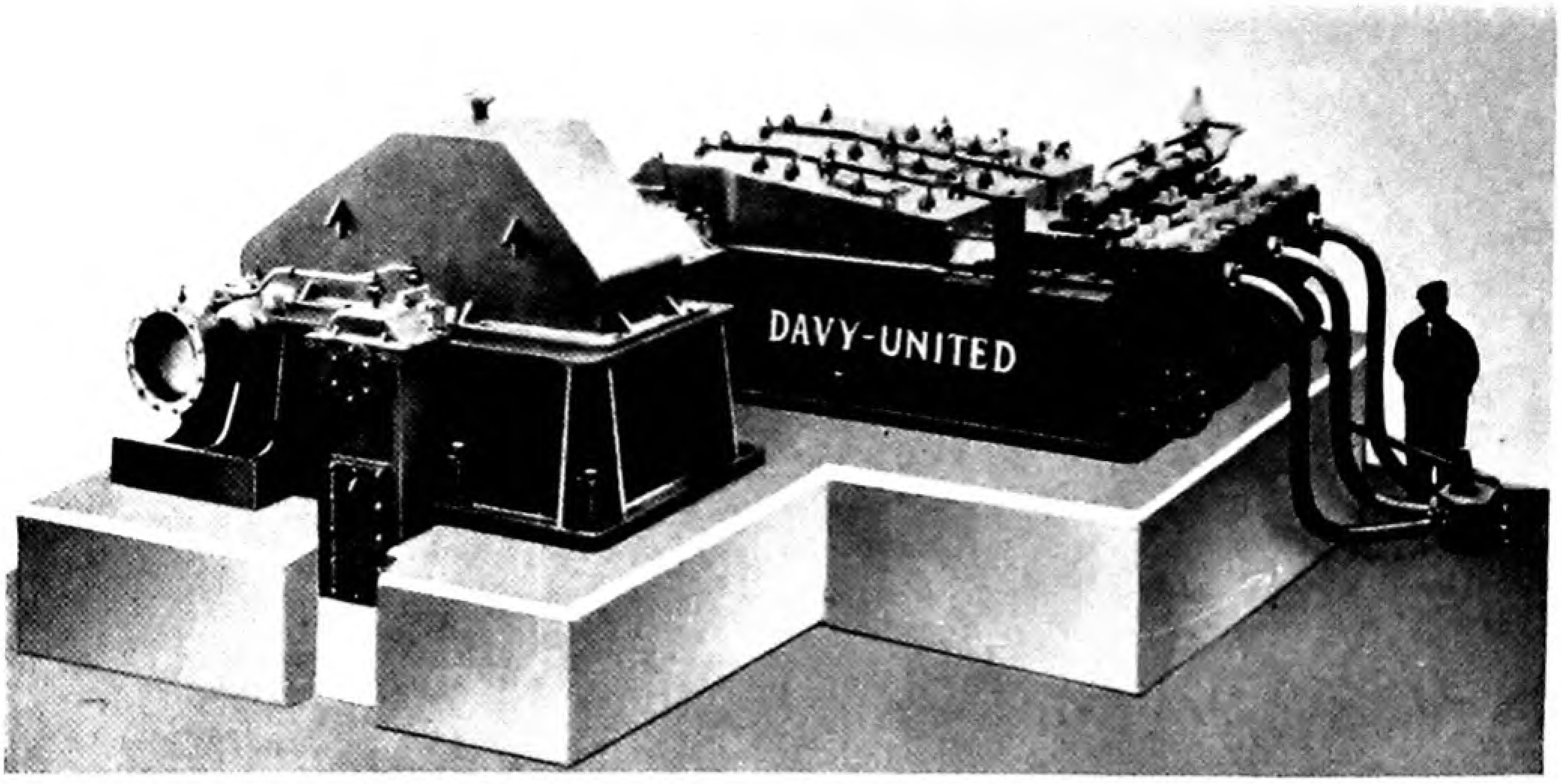

FIG. 414.—Totally enclosed three-throw pump for transmitting 1100 h.p.
(Davy-United Ltd.)
(See page 521.)

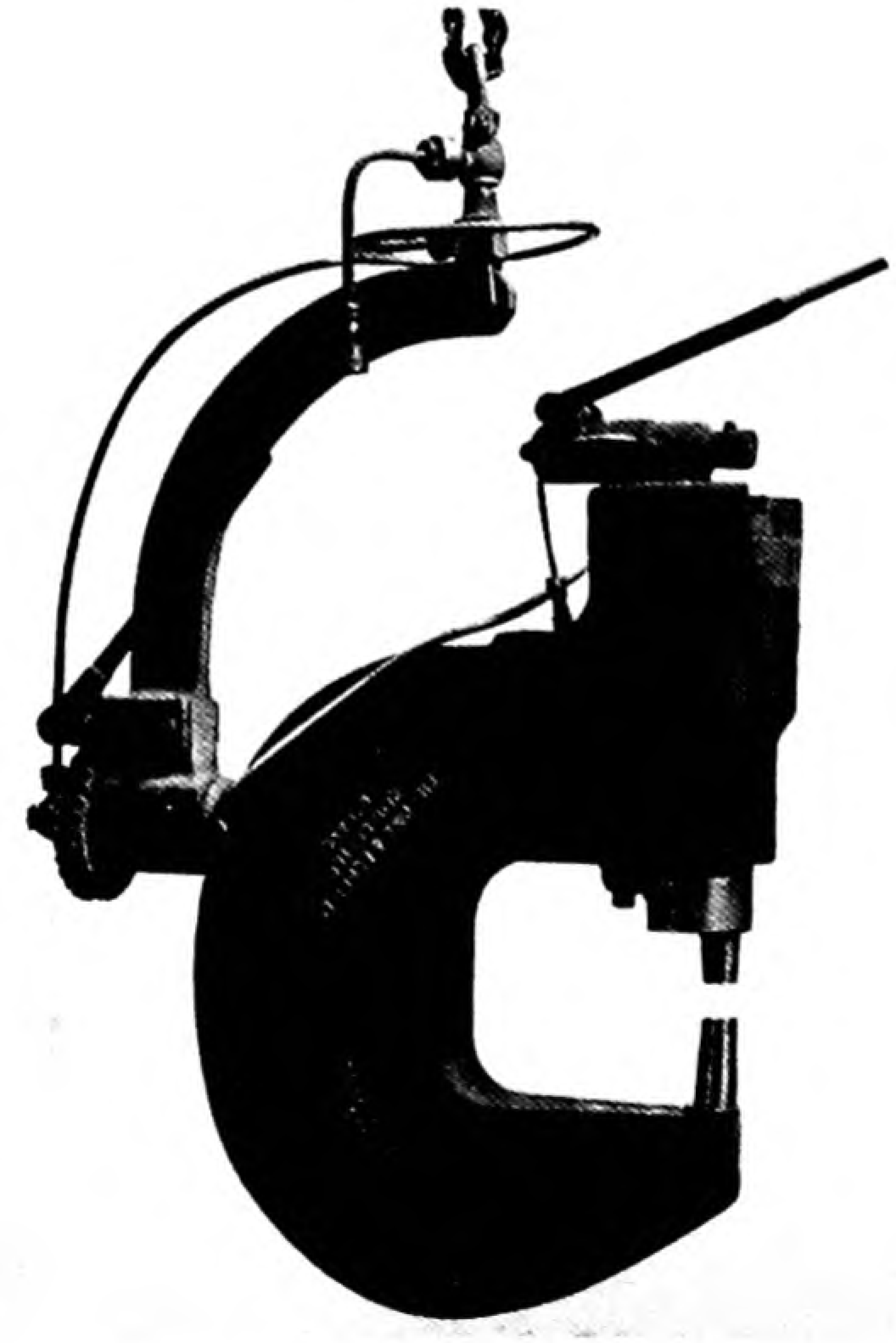

FIG. 420.—Hydraulic riveter.
(Fielding & Platt, Ltd.)
[*To face page* 527.

When the pump control-plate (Fig. 336) is in its neutral position the speed reduction ratio is infinity, from N pump speed to zero hydraulic-motor speed; as the control plate is brought over, the discharge of the pump increases and the reduction ratio falls until eventually it becomes unity. If the automatic gear shown in Fig. 337 is in operation, the reduction ratio will automatically adjust itself to suit the torque demanded from the hydraulic motor. As the torque increases, the pressure in the system will build up, the auxiliary cylinder on the pump pushes over the control-plate, the pump discharge falls off, and the secondary shaft slows down. A constant speed, constant output, electric motor can thus drive the pump without danger of overloading.

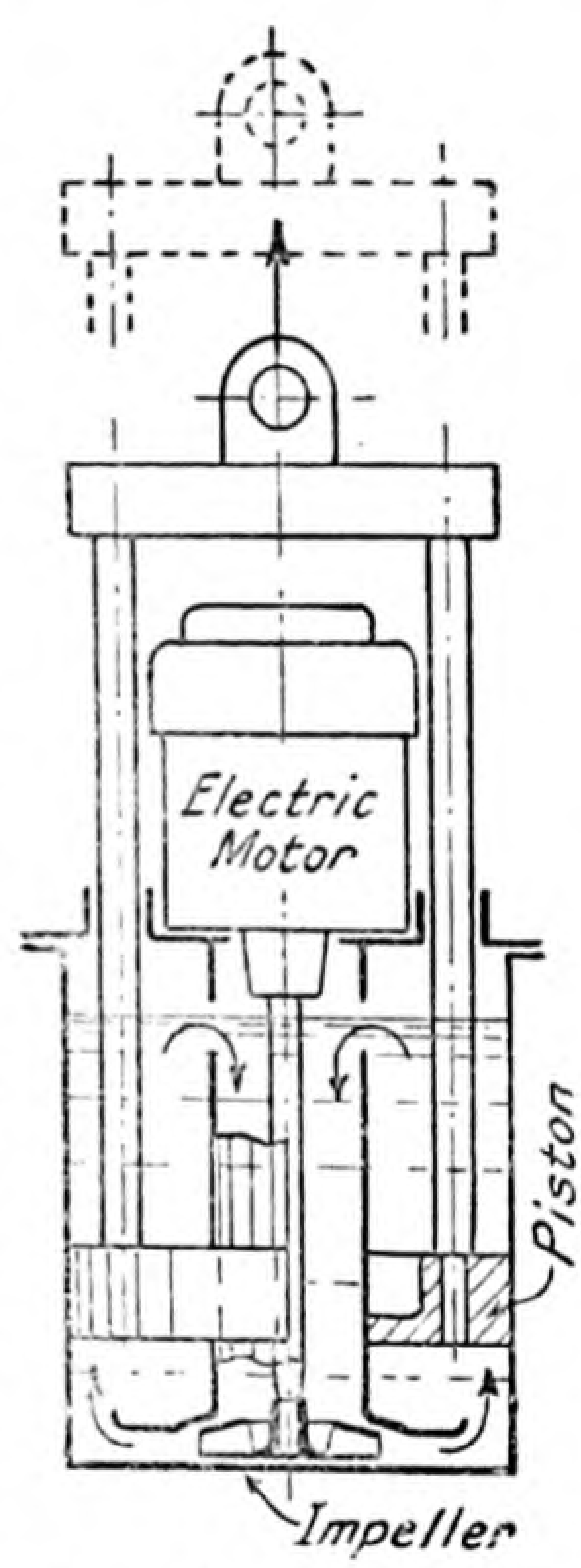

FIG. 422.—Thrustor.

The electro-hydraulic *thrustor*, Fig. 422, represents a particularly intimate assembly of electric motor, pump, and hydraulic motor. It is used for actuating valves, levers, brakes, and the like, and in general for replacing manual effort by a controlled mechanical thrust. The little electric motor directly drives the impeller of a centrifugal pump which can draw its oil from the upper side of the hydraulic-motor piston and deliver it to the under side. As soon as the current is switched on, the annular piston rises at a rate determined by the resistance it encounters, and it continues to exert a steady thrust until the motor is switched off again; then it sinks back to its original position. The characteristics of the pump ensure that the apparatus cannot be over-loaded.

Hydraulic Servo-mechanisms. These are systems devised for the specific purpose of amplifying or intensifying a signal or movement received from some external agency.[261] An elementary example is depicted in Fig. 423 (i): it consists basically of an "output" cylinder, and an "input" element in the form of a spindle and control valve. As the left-hand end of the servo-motor piston rod is anchored to a fixed

support, a pressure-difference applied to the piston will cause the whole assembly to move axially. Flexible pipes connect the cylinder to the pressure-oil pump.

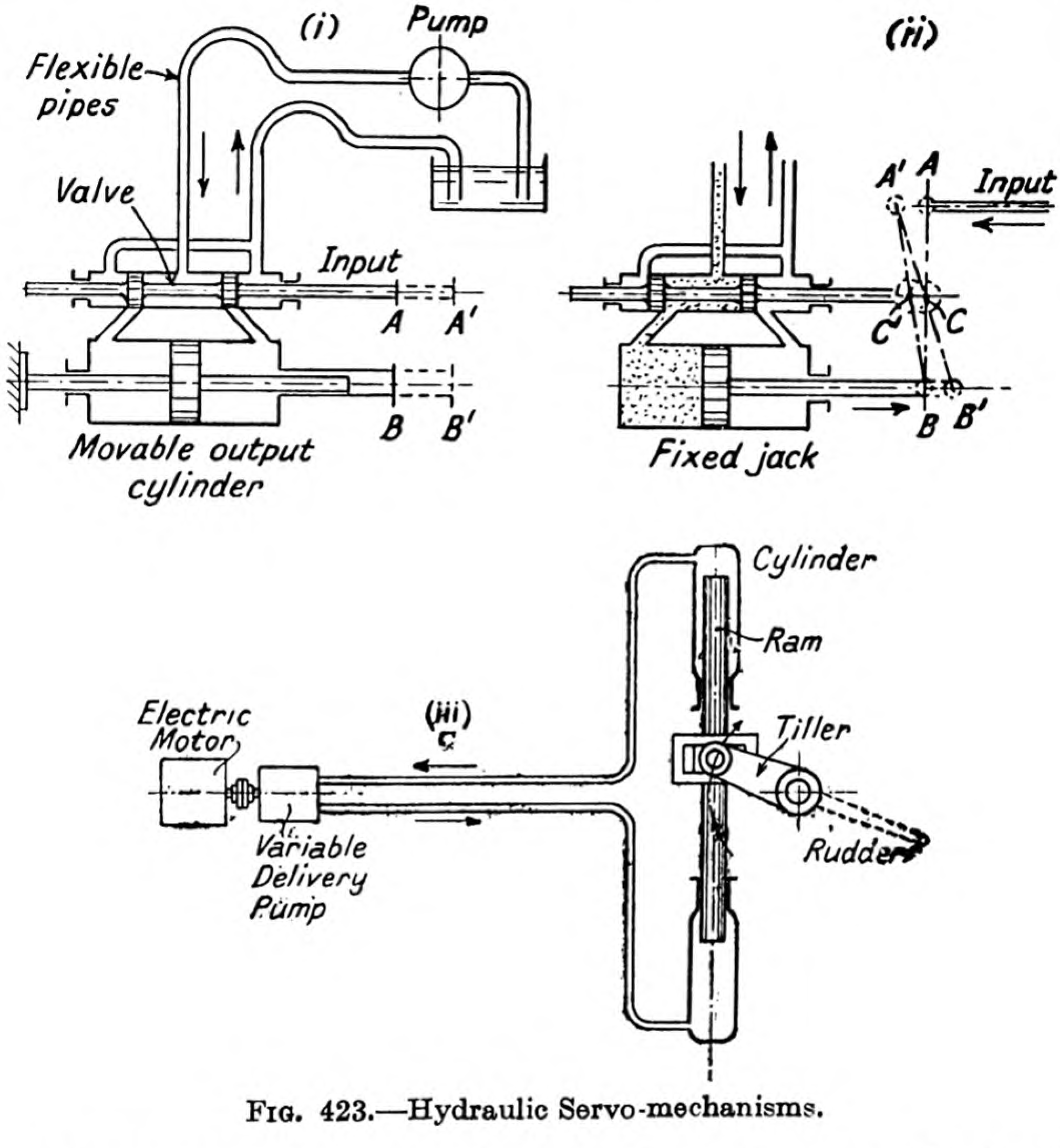

FIG. 423.—Hydraulic Servo-mechanisms.

Suppose now that, from its original position at A, the input spindle is moved slowly by hand to a new position at A′. At the slightest relative displacement of the control valve, pressure-oil will enter the right-hand end of the servo-motor cylinder, which will thereupon also begin to move to the right. In effect, any movement of the " input " element will be faithfully reproduced by the " output " element: the displacement *BB′* will be equal to the displacement *AA′*, but the force exerted will be magnified many times. Depending upon the diameter of the servo-cylinder and the pressure maintained by the oil pump, the thrust developed by the output cylinder

may be 1000 or more times greater than the originating force on the input spindle. In general, the servo or *slave* cylinder or jack obediently carries out any orders it receives.

If a fixed output cylinder should be preferred, this can easily be contrived by using lever ACB, as in Fig. 423 (ii), interconnecting the input element, the control valve, and the servo-piston-rod. An input displacement from A to A' has moved the valve through a distance CC', thereby admitting oil to the left-hand end of the servo cylinder. The resulting effect or working stroke of the servo-piston rod, from B to B', has had the additional result of returning the valve spindle to its original position at C: it is this self-cancelling property, by which the mechanism becomes stabilised in its new position, that characterises all true servo-mechanisms.[262] Many variants of systems such as these are embodied in aircraft control mechanisms, e.g., wing-flaps, rudders, etc.[263]

A servo-apparatus adapted to a ship's steering-gear is illustrated in Fig. 423 (iii). Here the signal received from the ship's navigating-bridge is applied not to a control-valve spindle as in diagrams (i) and (ii), but to the control-plate of a variable-delivery pump, § 301. This movement has directed pressure-oil to the cylinder on the port side of the vessel, forcing over the tiller and rudder in the desired direction: the movement of the rams, transmitted back to the oil-pump, cancels the originating signal and leaves the pump control-plate in its neutral position.[264]

Examples of servo-mechanisms used for controlling hydraulic turbines have been described in §§ 231, 244 and 249: in every instance the input signal is automatically originated by the centrifugal governor of the turbine.

357. Hydraulically-operated Machine Tools. In nearly all machine tools, such as lathes, drilling-machines, shaping-machines, and the like, there are to be found sliding elements that must be forced or fed along guides at a controlled rate; and as such rectilinear motion is of just the kind that invites the application of hydraulic power, we can observe continuous development in this field.[265] A representative example of such a specialised closed-circuit system—in this instance a shaping-machine—is shown schematically in Fig. 424. The essential component here is the ram-head A which

carries the cutting-tool. By means of the motive cylinder *B* and piston *C*, it is forced forward in its guides at a suitably low speed during the cutting stroke, and withdrawn at a faster speed during the return stroke.

Electrical energy received from the supply-mains is converted by the constant-speed electric motor *E* and positive rotary pump *D* into hydraulic energy; the pressure oil is directed by a control valve *J* to one end or the other of the motive cylinder *B*. The control valve is actuated through suitable mechanism by tappets on the ram-head. In the diagram the arrows show the direction of oil flow during the cutting stroke: from the reservoir *G* the oil passes through the strainer *F* and up the pump suction pipe on its way to the motive cylinder. Meantime low-pressure oil is returned through the control valve back to the reservoir.

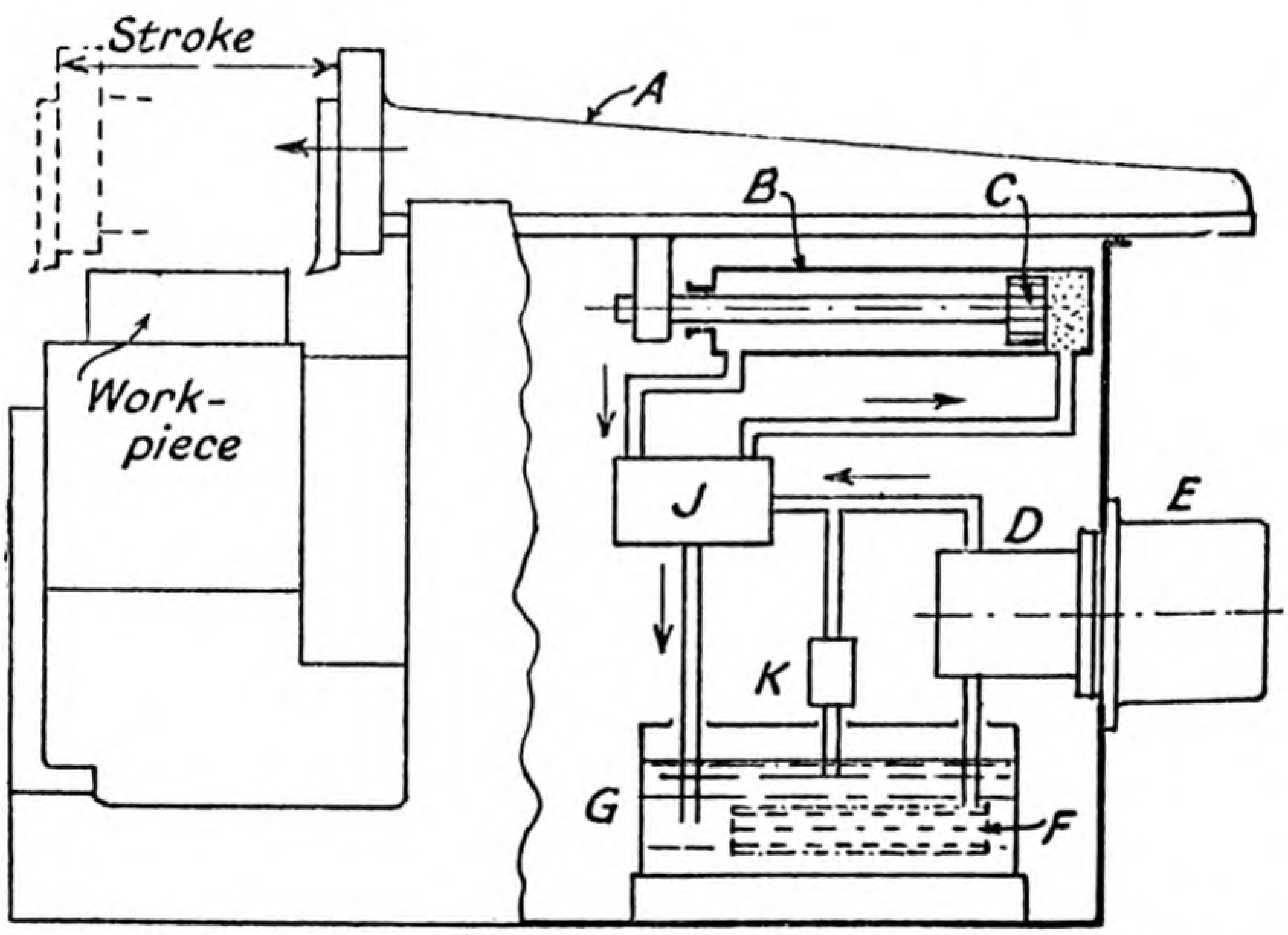

FIG. 424.—Schematic view of hydraulic shaping-machine.

The advantages of the self-contained system are here very manifest.[266] During the cutting stroke the pressure in the pump will build up only to the intensity needed to force the cutting-tool past the work-piece; on the return stroke a much lower pressure will be called for, with a corresponding reduction in the electrical input to the motor. No damage can occur if the machine should accidentally be overloaded, e.g. by an attempt to take too heavy a cut; for in such an eventuality

the moving parts will stall and the pressure-oil will be discharged harmlessly through the relief-valve *K* back to the reservoir.

358. Choice of Liquid, Piping, Control-Valves, etc. In order to meet the severe conditions of high pressure and possibly vibration that will occur in a closed-circuit hydraulic system, modifications may be needed to the pipes and valves described in Chapter IX before they will be acceptable.

Liquid. The liquid medium which itself transmits the hydraulic energy may—and indeed must—be chosen to suit the characteristics of the pump and the hydraulic motor.(267) Some of the requirements to be met are: (i) Since external leakage will be prevented by "contact" seals embodying flexible packing, § 223 (*a*), the liquid which will have access to the packing must not dissolve or otherwise damage it; (ii) to avoid excessive friction losses in the piping and pump passages, etc., the liquid viscosity should not be too high; (iii) the viscosity should not be unduly influenced by temperature changes, § 9, because variations of viscosity may affect pump and hydraulic motor performance, § 305; (iv) as the internal working parts of the pump, motor and control organs have no other lubricant than the liquid flowing throughout the system, this liquid must have adequate lubricating properties.(268)

For many land installations, i.e. those described in the preceding paragraphs, a light mineral (petroleum) oil is likely to be suitable, provided always that the seals in the glands are of synthetic rubber and *not* of natural rubber. The oil viscosity should preferably be adapted to the type of pump in some such manner as the following:—

	Kinematic Viscosity in Stokes at 70° F.
Gear-pumps, § 303, slow speed positive pumps . .	1·0 – 2·0
High-speed vane type pumps, § 302	0·4 – 0·8
High-speed reciprocating pumps, § 294 (iv) . .	0·2

For more specialised duties it may be necessary to use vegetable oils (castor-oil base), because they do not attack natural rubber seals; or else the synthetic liquids known as "silicones", which require quite special seals.

Piping and Joints. Seamless steel pipe will nearly always be demanded. If this is of small bore—say ½ in. or so—the

joints may be made by proprietary fittings which ensure a quite oil-tight metal to metal connection. Flanged joints will probably be better for pipes of 1 in. diameter and over. Only for low pressures will the screwed connections shown in Fig. 134 (i) be acceptable; for the higher range of pressures the flanges may be brazed or welded to the pipes and the joint rings may be of copper or synthetic rubber.[269]

Control valves. The duties to be performed by an elementary type of control organ can be seen from Fig. 425. In this

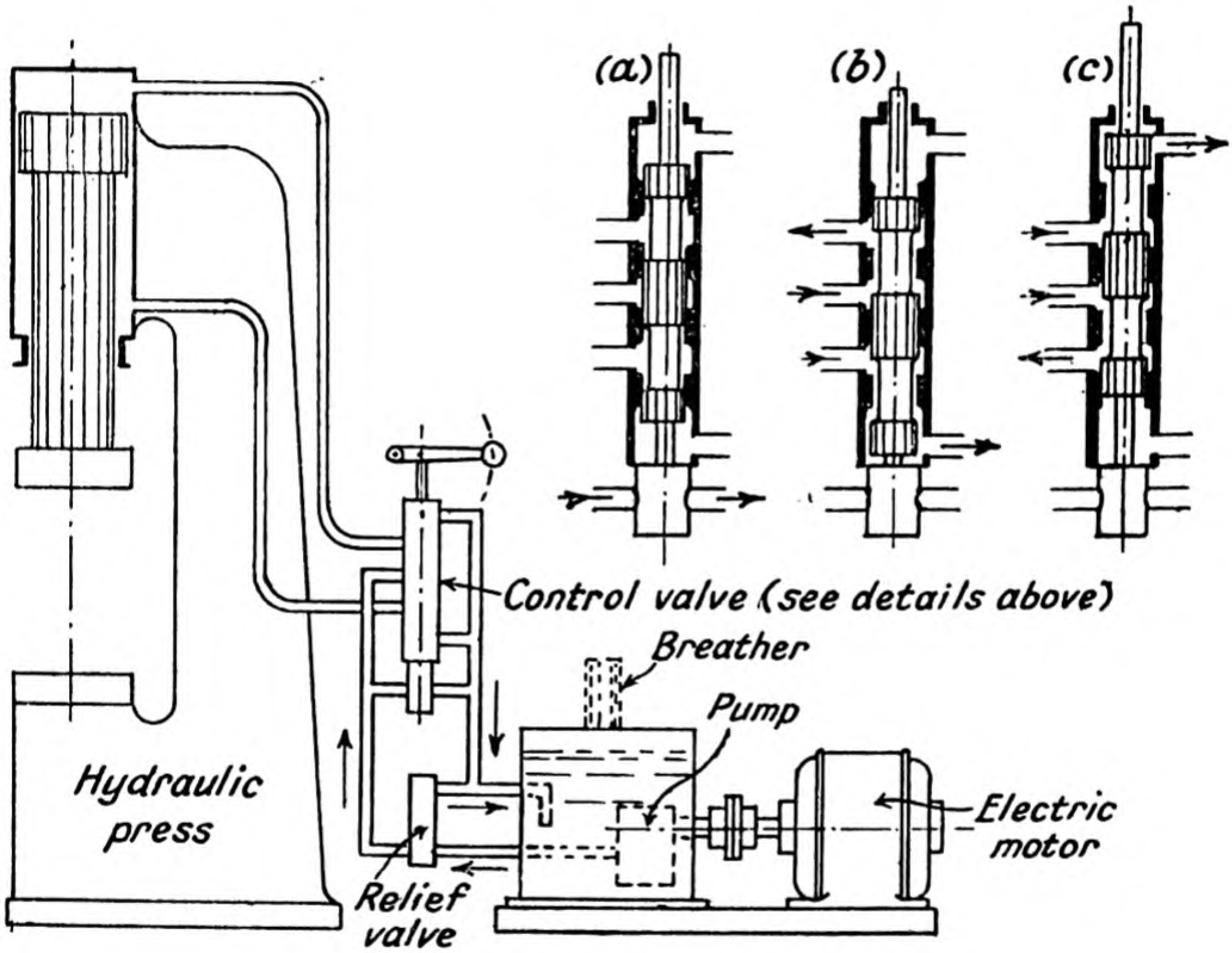

FIG. 425.—Self-contained hydraulic system.

system the purpose of the valve is to direct the pressure-oil from the pump to the "down-stroking" hydraulic press. Of the balanced-piston type, working axially within a multi-ported housing, the valve can be set by means of a hand lever into any one of three positions. Position (*a*) is neutral: oil passes freely from the pump back to the oil reservoir, the main ports being closed and the press ram being "locked" at a chosen part of its stroke. When the control valve is lowered to position (*b*) the pressure-oil immediately has access to the upper part of the press cylinder and the working stroke begins.

The return or upward stroke is effected by putting the control valve in its uppermost position (*c*).

In regard to other parts of the system illustrated in Fig. 425, the pump is of the high-speed multi-cylinder type, § 294 (iv), wholly immersed in the oil contained in the reservoir; the "breather" ensures that the pressure in the reservoir cannot rise above atmospheric, while yet excluding dust. The position for the oil-reservoir adopted in Figs. 424 and 425 may be contrasted with the elevated position preferred in the equipment shown in Fig. 421.

Further development of the hand-operated valve described above[270] will result in the much more complex automatic control valves as used, for instance, in the hydraulic shaping-machine, § 357. Should the installation comprise a number of adjacent hydraulic systems, the control-valves may be mounted in a single control panel.

359. Comparisons between Transmission Systems. When an installation includes more than one hydraulic motor, a choice may be required between (i) an accumulator system in which a central pumping station *AB* delivers water into a common pipe system supplying all the hydraulic motors, Fig. 415, and (ii) a number of self-contained and independent assemblies, each having its own pump and hydraulic motor, § 356 and Figs. 421-425. In summarising the arguments on either side, it may be added that the trend of technical opinion more and more favours the independent system.[271]

(*a*) The outstanding attraction of the accumulator is that its storage capacity enables the size of the pump to be greatly reduced. The most powerful hydraulic machines, viz. hydraulic presses, § 355, usually make a very intermittent demand on the water supply; although the working stroke may only occupy a fraction of a minute, the idle time during which the work is being adjusted in the press may be of several minutes' duration. So long, then, as the accumulator is big enough to deliver energy at the necessary rapid rate, the pump which charges it continuously may be relatively small.

(*b*) The limiting pressure established by the accumulator is often advantageous; it gives a guarantee that the thrust on the ram of, e.g. a hydraulic riveter will not exceed a stipulated amount, and consequently the pressure may be left on indefinitely. Nevertheless, the weight-loaded accumulator may momentarily deliver a pressure greater than that developed *by its pump*. When there is a heavy draw on the supply main, the speed of descent of the accumulator ram and its load may cause the equivalent kinetic energy to rise quite high. Then when this movement is checked by the closure of the hydraulic motor control-valve, or by the increased resistance the hydraulic motor encounters, a very sensible water-hammer effect may be generated.

(c) The pumps in a central station are likely to have a higher average efficiency than those in independent systems. Firstly, they are larger; and secondly, they always work either at full load or at no load, but never at part load. Besides, they will probably be of a type that is inherently more efficient than the pumps chosen for independent installations.

(d) As a virtually constant pressure prevails in the supply mains of an accumulator system, the water is bound to be used ineffectively when the hydraulic motors are working at part load, even if complicated installations of multiple rams, high- and low-pressure supply systems, and so on, are provided (§ 355).

(e) In a self-contained system without accumulator or air vessel, the pressure generated by the pump is only as high as is called for by the resistance encountered by the hydraulic motor. Moreover, the rate of movement of the motor ram is very nearly proportional to the speed of the positive pump, which is advantageous when the feed systems of machine tools are to be hydraulically operated.

(f) Independent installations using electrically-driven pumps give many opportunities for simplified control by means of push-buttons, etc. A combination of a high-capacity low-pressure pump, and a smaller high-pressure pump reduces the time for carrying through repetition processes. If they feed a press, the first pump is used to bring the ram rapidly up to its work, while the second completes the power stroke. An automatically controlled variable delivery pump, § 301, has the same advantages. In any event an assemblage of units can be supplied with power more easily through a network of electric wiring than through a system of high-pressure piping.

(g) Hardly any choice is left when the high-pressure hydraulic system operates auxiliary equipment on vehicles of various kinds, e.g., tipping-trucks, fork-lift trucks, and aircraft. The self-contained, closed-circuit disposition is here almost obligatory.

On the whole, then, it seems likely that the smaller the units, the more suitable the self-contained system becomes.

Rotodynamic Devices.

360. Dynamic-pressure Transmission Systems. When power has to be transmitted from one high-speed revolving shaft to another co-axial and adjacent shaft, then the objections to using the principle of the hydraulic turbine disappear; for such duties, on the contrary, a combination of a transmitting element in the nature of a centrifugal pump impeller, and a receiving element resembling a turbine runner, is highly satisfactory. As ordinarily used, these devices perform the functions of a friction clutch; they are then known as *hydraulic couplings*.[272]

The driving and driven elements of a hydraulic coupling are identical in appearance—each consists of an annular

chamber of "D" section, subdivided by radial blades (Figs. 426 and 427 *). They are enclosed in or they together form a casing completely filled with oil or other suitable liquid. Supposing the driven shaft *B* to be at rest, and the driving shaft *A* to be revolved slowly, a forced vortex will be generated in the impeller *A*, and in consequence oil will be forced outwards and projected with a definite whirl component on to the stationary blades of the runner *B*. Due to the destruction of the angular momentum corresponding to this velocity of whirl, a tangential force or torque is exerted on the runner blades. Meantime, there being no centrifugal head to resist it, the oil can make its way freely to the inner eye of the runner, and across to the impeller again, so circulating continuously.

If the speed of *A* is now increased, the torque imposed on *B* may rise sufficiently to overcome the resistance which has hitherto held it at rest; further increase in the impeller speed will cause the runner speed to increase at a still faster rate, until at designed full load and speed the driven member *B* only lags behind the driving member *A* by about 2 per cent.—for practical purposes the two shafts may be considered as directly coupled. Yet the transmission, so far from being rigid, has a beneficial cushioning effect: it damps out any torsional inequalities that the driving shaft might tend to deliver.

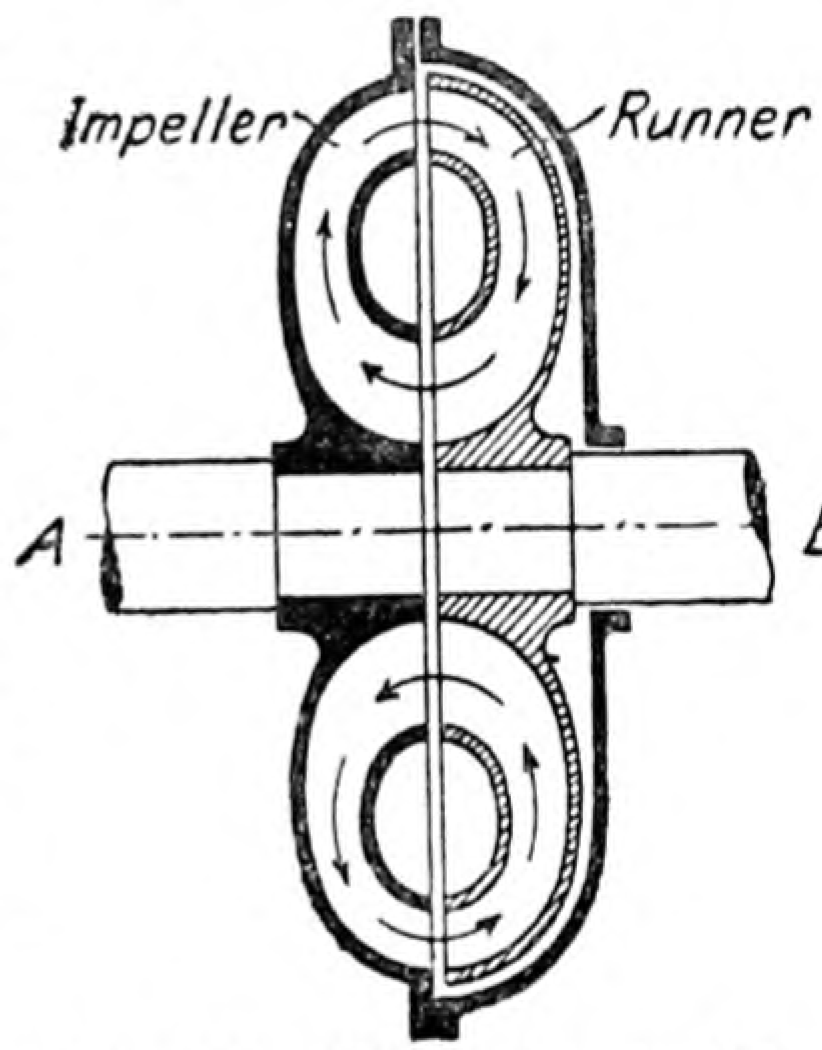

FIG. 426.—Hydraulic coupling.

Although under running conditions there is a forced vortex both in *A* and in *B*, the slight lag of the one behind the other always ensures the necessary excess of centrifugal head in the impeller to maintain a continuous flow of liquid from the outer edges of the impeller blades to the outer edges of the runner blades.

361. Control Devices for Hydraulic Couplings. The coupling shown in Fig. 426 is only suitable for conditions,

* Facing page 542.

as for example in a motor-car transmission, where the driving member A can receive its energy from an engine which has a sufficiently low *idling* speed to prevent undue torque being generated when the road wheels and therefore driven member B are at rest. Because when so used the impeller is formed within the engine flywheel, the coupling is known to motorists as a *fluid flywheel.*

For ordinary engineering services, however, the driving shaft A is required to run at constant speed, and we desire the coupling to start the driven shaft B from rest and to bring it up to sensibly the same speed as A. There are two ways of doing this. In one method pipes are provided for draining the oil out of the casing and feeding it in again as required. With the casing empty, no torque can be transmitted from A to B; as oil is gradually fed in, the shaft B begins to revolve and finally takes up its full load and speed when the casing is full. To "declutch," the oil is drained away.

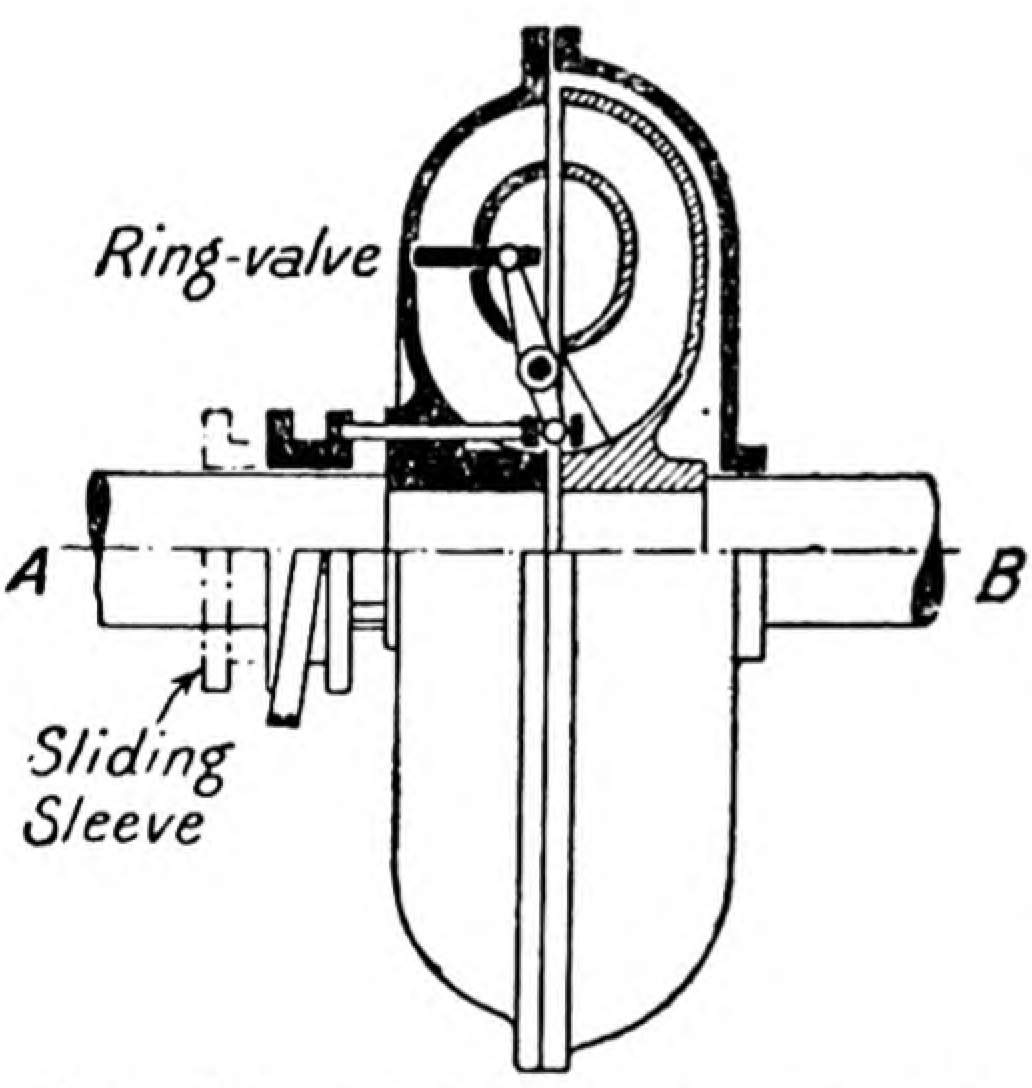

FIG. 428.—Hydraulic coupling with ring-valve.

In the second method, a cylindrical shutter or *ring-valve* regulates the circulation of oil (Fig. 428). When the shutter is withdrawn, the oil circulates normally and the coupling transmits its full power; to stop the driven member B, the ring-valve is slid along axially and so interrupts the flow from the impeller to the runner. Couplings controlled by either of these methods can successfully be used for transmitting power from Diesel engines to the track-wheels of rail-cars and shunting locomotives, and to excavators and similar machinery. Very large ones have been installed in Diesel engine-driven warships and in other types of ships.

362. Performance of Hydraulic Couplings.

(i) Since its tangential momentum due to velocity of whirl suffers no change as the oil passes from the impeller blades to the runner blades, and as it returns from the runner blades

to the impeller blades, it follows that the torque transmitted to the driven shaft B must be identical with that imparted to the driving shaft (§ 144). Thus, apart perhaps from a slight frictional drag if any non-rotating elements are used, the coupling always *transmits torque without change*, no matter what the actual or relative speeds of the two members may be.

(ii) Since the power transmitted by a rotating element is proportional to torque × rotational speed, and since, as just stated, the torque output from the coupling is equal to the torque input, it follows that $\frac{\text{power output}}{\text{power input}} = \frac{\text{runner speed}}{\text{impeller speed}}$. This ratio also represents the *efficiency* of the coupling. With the normal lag or slip of 2 per cent., the efficiency is thus 98 per cent.

The difference between power input and power output is wasted in shock, eddying and fluid friction, and is wholly converted into heat.

(iii) Considering the driving shaft A to be running at constant speed, and the coupling to be transmitting no load, there will be no slip and the efficiency will be 100 per cent. If now the driven shaft be lightly loaded, it will slow down, and at once the circulation of oil from one member to the other will begin. If the load be increased, the only way of increasing the torque accordingly is to increase the quantity of oil per second impinging on the runner blades; this can only be done by reducing the centrifugal head in the runner that opposes the centrifugal head in the impeller, for the rate of circulation of oil depends on the *difference* of these centrifugal heads.

In brief, the runner must slow down still further. We therefore see that as the torque *increases*, the slip *increases* and the efficiency *decreases*.

An interesting analogy can be worked out between the behaviour of the hydraulic coupling under these conditions of constant impeller speed, and the behaviour of a shunt-wound direct-current electric motor. The back pressure or centrifugal head generated in the runner exactly corresponds to the back E.M.F. in the armature; as the load pulls the speed down, this opposing pressure is reduced, so increasing the flow of current—of oil or of electricity—on which the development of torque depends.

(iv) Since the power required by a centrifugal pump at a given efficiency varies as the cube of the speed (§ 330), the power transmitted by a hydraulic coupling at a given slip ratio will also vary as the *cube* of the speed. **(Example 197.)**

(v) Comparing *geometrically similar couplings running at the same rotational speed and slip ratio*, then the power transmitted will vary as the *fifth* power of the diameter.

(vi) In general, then, if D represents the diameter of a coupling of a given geometrical shape, and N the rotational speed :—

$$\text{Torque transmitted} \propto N^2D^5.$$

$$\text{Power transmitted} \propto N^3D^5.$$

363. Characteristics of Hydraulic Couplings.

(i) *Stalled torque conditions.* The characteristics plotted in Fig. 429 relate to a coupling running at varying *input* speed N, and working against a load that keeps the output shaft B always *stalled* or stationary. One of the curves shows the performance when the coupling is filled with oil, and the other shows the effect of partially draining away the oil, § 361 (a); in either case the stalling torque varies very nearly as the *square* of the input speed.

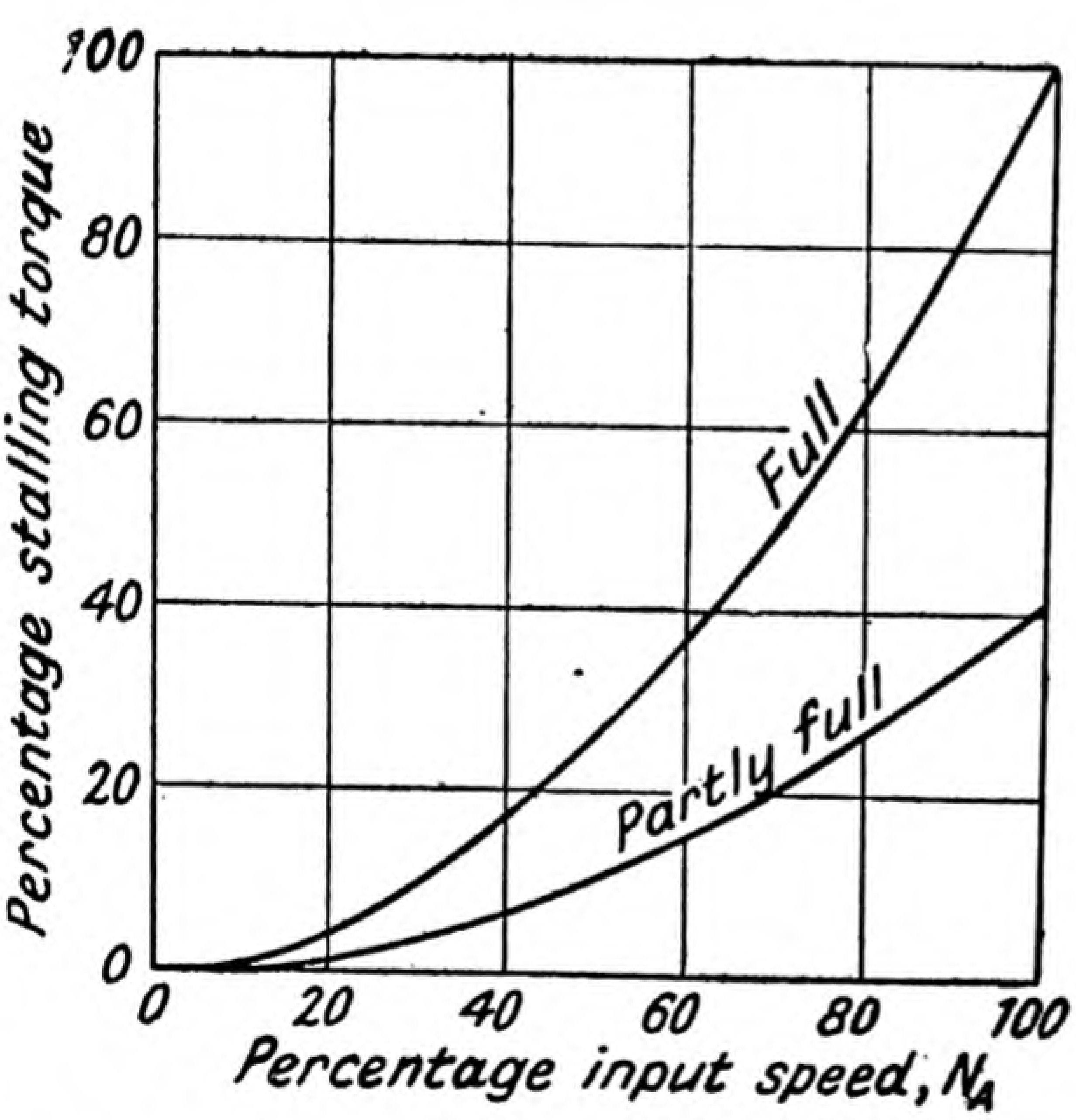

FIG. 429.—Performance of stalled hydraulic coupling.

(ii) *Constant input speed and varying output speed.* Turning now to the conditions of § 362 (iii), we observe from Fig. 430 (a) that the *effective* range of the characteristics is quite a small part of the total range. As soon as the load on the driven or output shaft B has raised the slip by more than a few per cent., the torque and the power transmitted rise high above their normal values ; if the equipment could withstand such heavy

overloads, the input power might exceed three times the normal or designed full-load input. These excessive values could be avoided by running the coupling only partly full of oil, Fig. 430 (b).

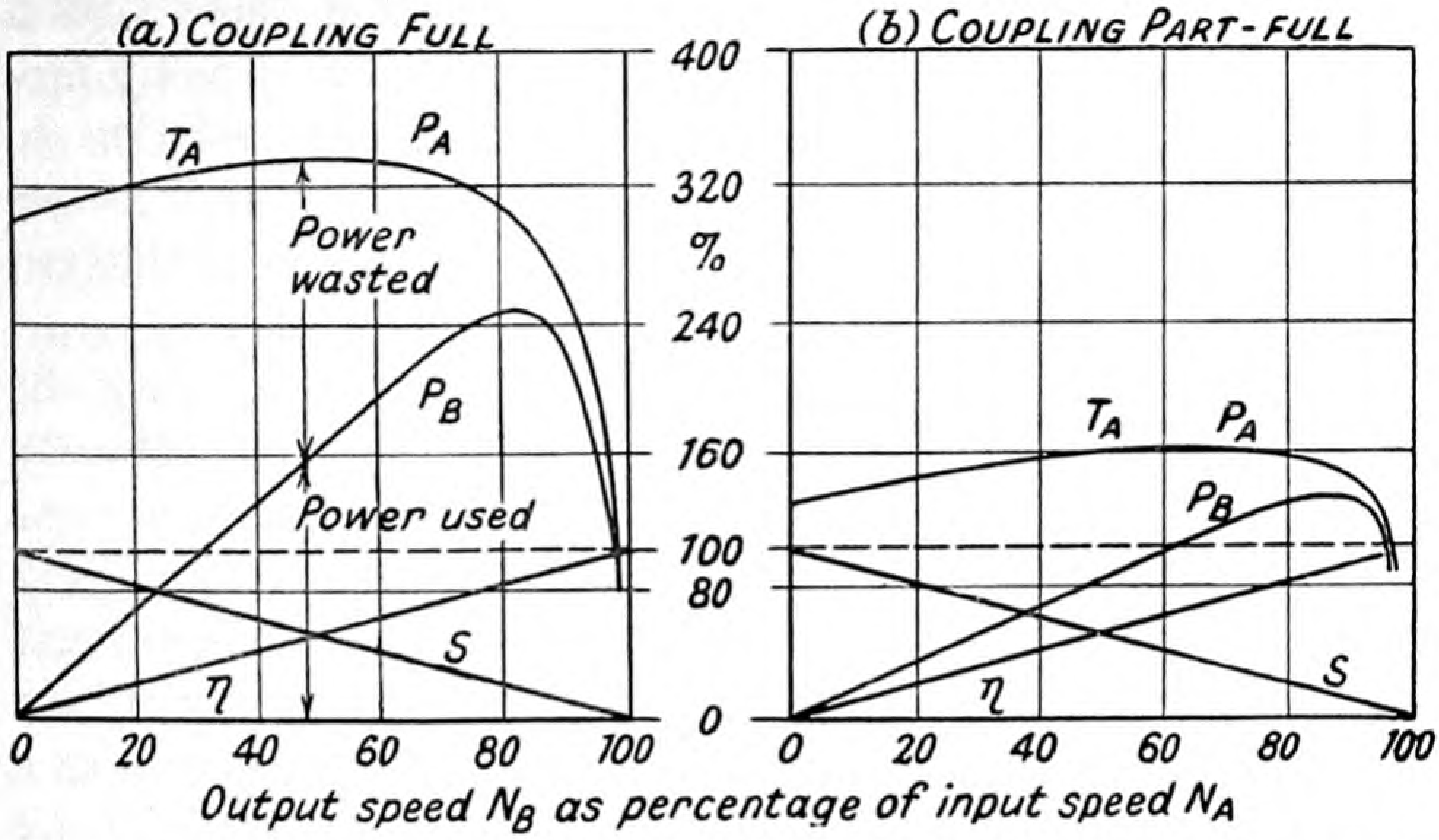

FIG. 430.—Effect of output shaft speed, etc., on performance of hydraulic coupling running at constant input shaft speed N_A.

T_A = input and output torque, P_A = input power, P_B = output power — all expressed as a percentage of normal full-load performance.

S = percentage slip : η = percentage efficiency.

Taken in conjunction, the characteristics plotted in Figs. 429 and 430 show the adaptability of the hydraulic coupling when used for services such as power-driven excavators. By suitably matching the speed of the driving engine and the size and filling of the coupling, it is possible to ensure that the shovel will stall at a predetermined load, thus positively limiting the maximum forces on the main components.

364. The Hydraulic Torque-converter. (i) *Fixed speed ratio.* By suitably controlling the quantity of oil in a normal coupling, § 361, any desired speed reduction between the driving and the driven shafts may be realised. Indeed, so long as the stipulated speed variation is not excessive, then the principle can very conveniently be applied to variable-speed centrifugal pumps and fans driven by constant-speed electric motors. But if the slip normally exceeds 10 or 20 per cent., the power loss grows excessive (§ 362 (ii)), and the problem of

heat dissipation becomes prominent. To establish a permanent and considerable reduction in speeds, then, the coupling must be modified by adding to it a new element—the fixed *reaction member* shown at *C* in Fig. 431. It has guide-blades resembling those of a centrifugal pump diffuser ring, Fig. 364; and if this ring is correctly proportioned in relation to the impeller and runner (which are now of different diameters) then a gear-ratio of 5 : 1 may be realised with an efficiency of nearly 90 per cent. As the torque output may now be four times as great as the torque input, the mechanism is known as a hydraulic or hydro-kinetic torque converter.[273]

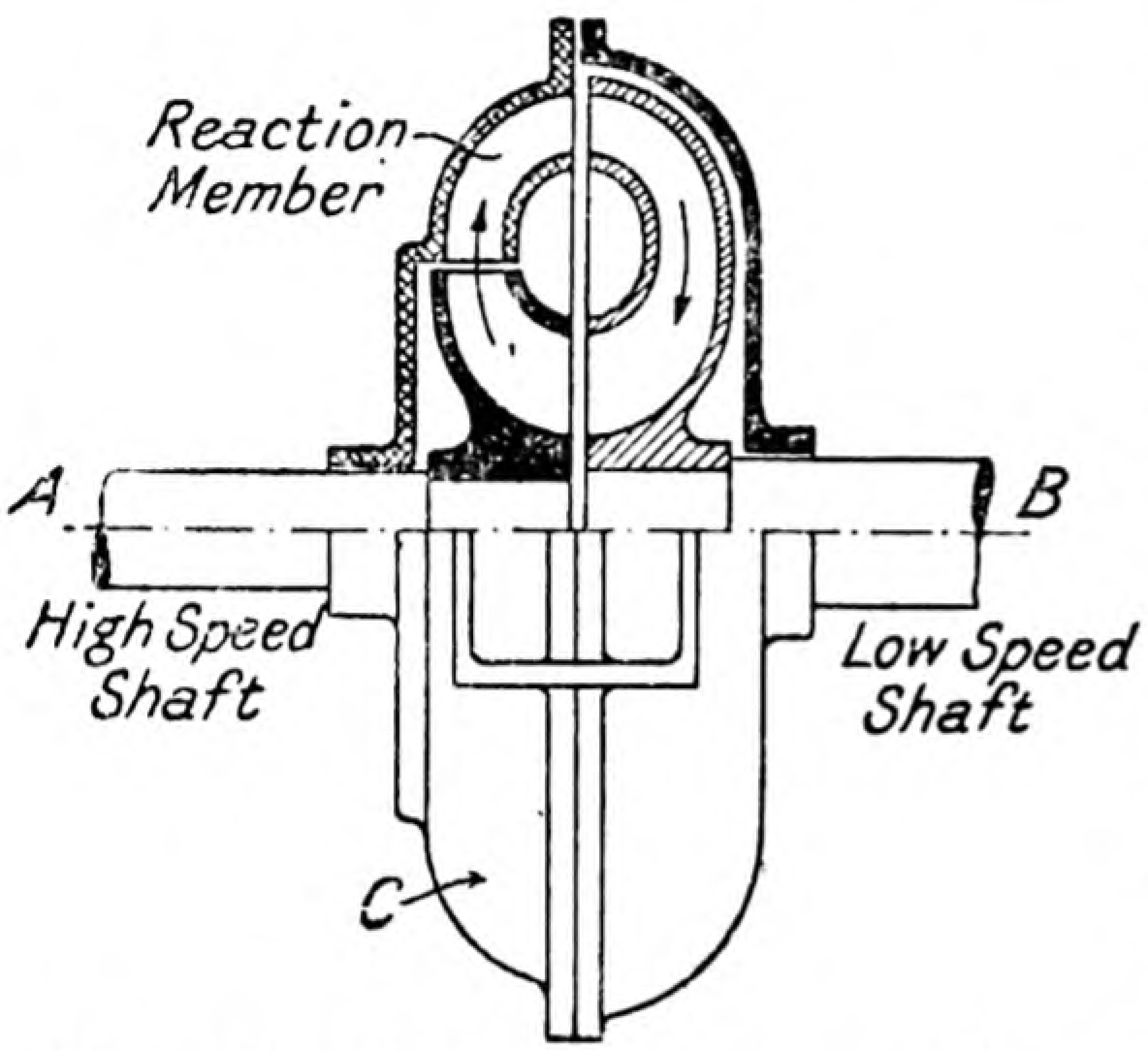

FIG. 431.—Hydraulic torque-converter.

This is the device originally invented by Dr. Föttinger for coupling high-speed marine steam-turbines to slow-speed propeller shafts; when it was superseded for this duty by the more efficient mechanical gearing, it was developed on the one hand into the Vulcan-Sinclair torque transmitter or hydraulic coupling, §§ 360-363, and on the other into the variable-speed torque-converter.

(ii) *Variable speed-ratio.* Any departure from designed conditions will impair the efficiency of a standard torque-converter, Fig. 431, just as it spoils the performance of any other rotodynamic pump or turbine. Yet the utility of the mechanism would be much enhanced if the gear-ratio were free to adjust itself to the load, without too serious a loss of power. In the *Vickers-Coats* variable speed-converter this is achieved by freely pivoting the blades of the reaction member. In the *Lysholm-Smith* design a multi-stage principle is adopted; there are three concentric rings of runner blades E_1, E_2, E_3, revolving as a single element, two sets of stationary reaction blading, C_1, C_2, and one impeller D, Fig. 432. As the inlet edges of the blades are of bulbous form, the eddy loss occasioned by changes of load or speed are much less than with normal

turbine blading, Figs. 297, 299 ; in consequence a fairly high overall efficiency can be maintained throughout a considerable range of speed reduction and torque variation, as Fig. 432 clearly shows. The performance curves are plotted for conditions of uniform (relative) input torque T_1. When fitted

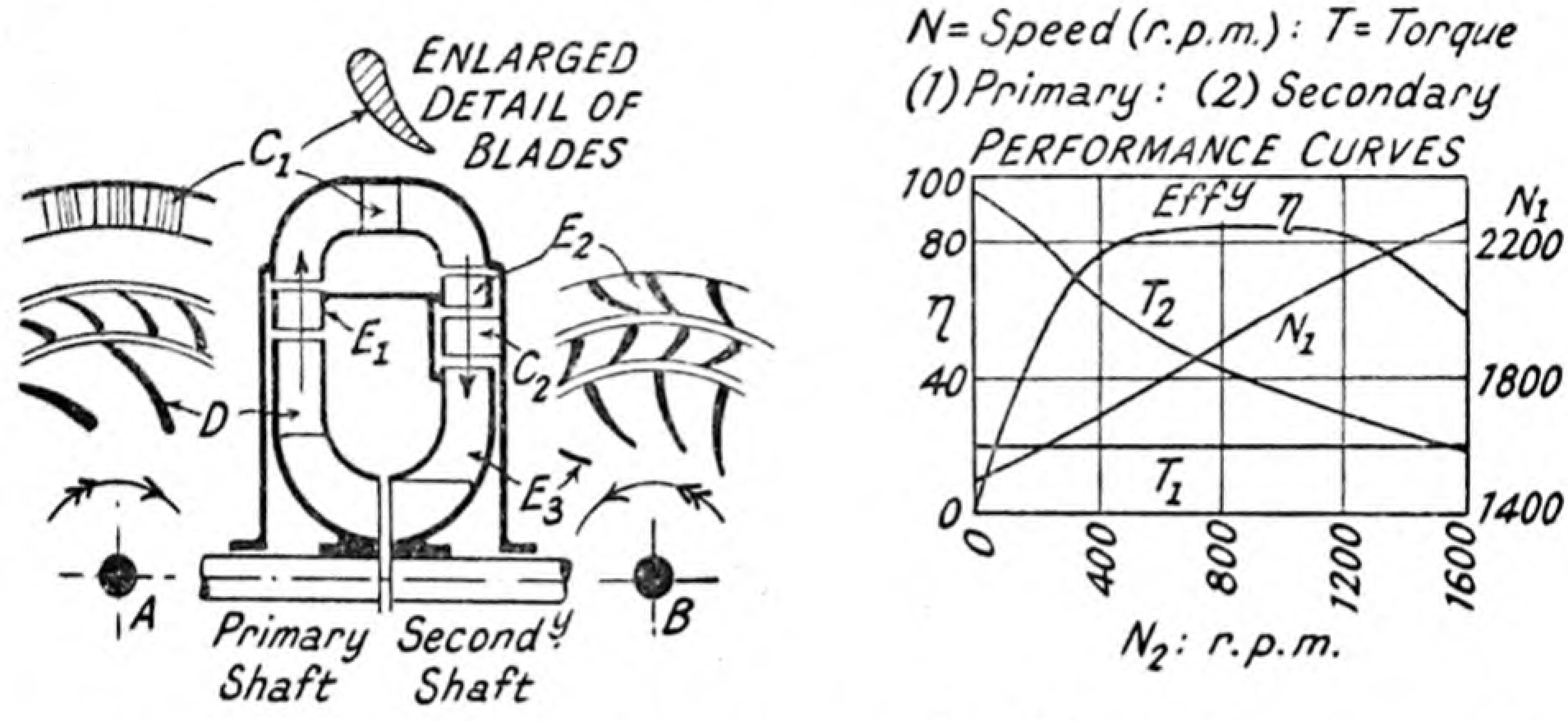

FIG. 432.—Construction and performance of multi-stage torque-converter.

to public road and rail vehicles driven by internal combustion engines, these converters act as infinitely variable gear-boxes.[274] No gear-changing is necessary ; the vehicle moves off smoothly when the throttle is opened, and thereafter the gear-ratio accommodates itself automatically to the load, gradient, and throttle-opening. For normal running after the vehicle has accelerated sufficiently, the torque-converter is cut out of action and a direct drive substituted. This may be done either by means of a two-way friction clutch or an auxiliary torque transmitter (§§ 360, 362). Continued development of the multi-stage principle has made variable-speed torque converters widely acceptable for private motor-cars.[275]

365. Other Rotary Transmission Systems. (i) *Hydro-mechanical couplings.* Although the 2 per cent. loss of power in the normal coupling (§ 360) is not a serious matter in a motor-car transmission, it is more than can be tolerated in the very large couplings now used in pumped storage plants (§ 368). In the Escher Wyss-Föttinger hydro-mechanical coupling, the difficulty is overcome by the use of a reaction member as in Fig. 431, in conjunction with revolving members so designed that at a predetermined load the runner has exactly the same speed as the impeller. When synchronism

between the shafts has been attained, they are mechanically locked by a type of sliding claw clutch.

(ii) *The Froude hydraulic brake.* This apparatus, which is used for measuring the test-bed output of engines, electric motors, etc., differs considerably in detail from the couplings described above, but can fairly be said to resemble in principle the arrangement mentioned in § 361 in which the amount of liquid in the casing of a coupling can be varied. The driving element of the Froude brake is directly connected to the shaft of the engine under test; the driven element is not allowed to rotate, but its tendency to rotate, or its torque, is measured by a system of levers and weights. By correctly adjusting the quantity of water flowing through the apparatus, the torque and therefore the output of the machine under test can be varied as desired.(276) Manifestly the characteristics of the system resemble those plotted in Fig. 429, § 363 (i).

LARGE-SCALE HYDRAULIC STORAGE.

366. Gravitational Hydraulic Storage Systems. Three methods have already been mentioned for storing pressure-energy during periods of low demand and yielding it up when the supply is deficient. A plunger-pump air vessel (§ 291) stores perhaps a cubic foot of water for a second or less; the air vessel of a turbine governor (§§ 231 and 243) may store a larger volume of oil for a longer period; while in the cylinder of a weight-loaded accumulator (§ 354) still greater amounts of energy may be stored. We speak indifferently of oil or water or energy, because in a hydraulic transmission system we know that so long as we are storing liquid under pressure we are storing energy too.

But such devices are quite inadequate when energy on a large scale has to be stored for hours or days or months; the only feasible scheme in such conditions is to store water in natural or artificial high-level reservoirs, the energy then, of course, being in the form of potential or position energy. When excess energy is available, it is utilised to drive centrifugal pumps which in due time fill the reservoir; when the reservoir is required to yield up its energy, the water is drawn off through hydraulic turbines.(277)

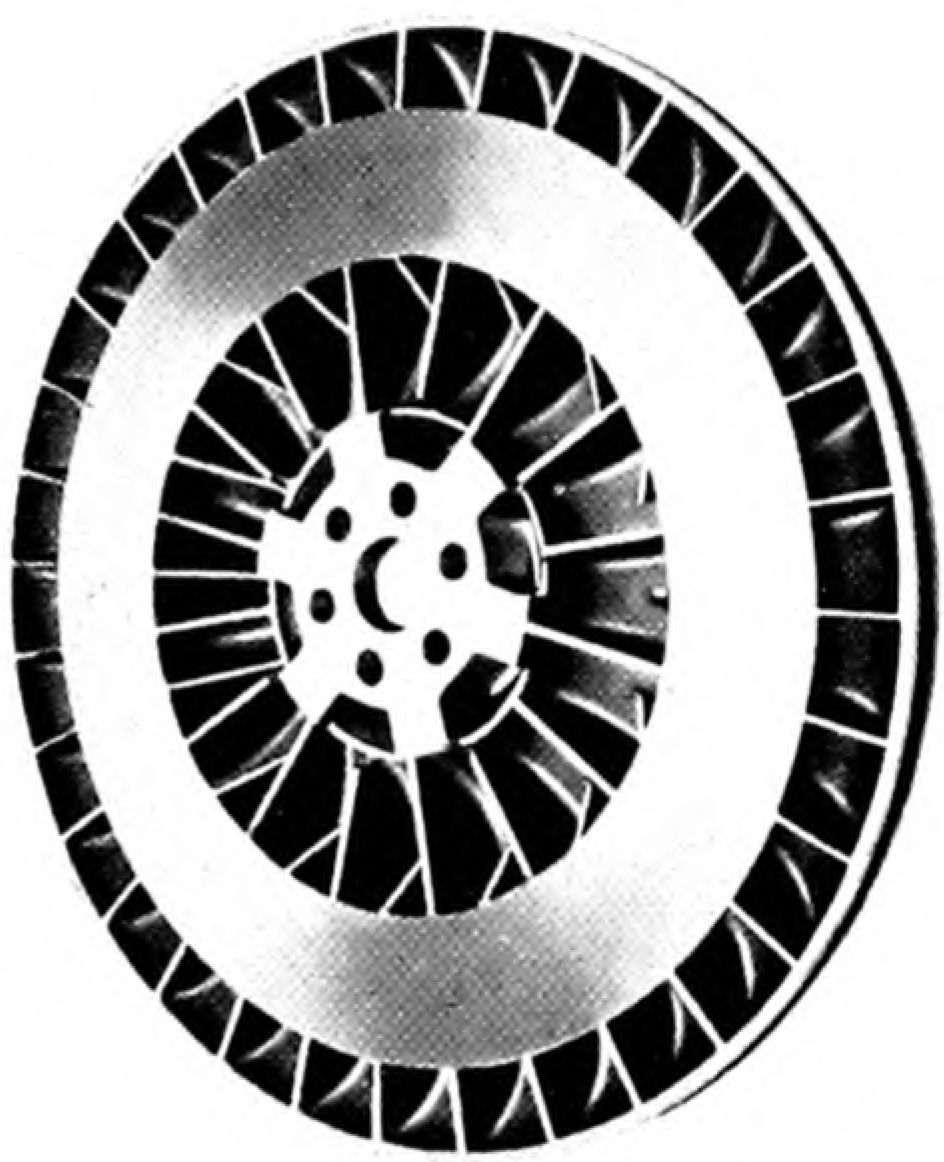

Fig. 427.—Element of hydraulic coupling.
(See page 535).
(Metropolitan-Vickers Electrical Co., Ltd.)
[*To face page* 542.

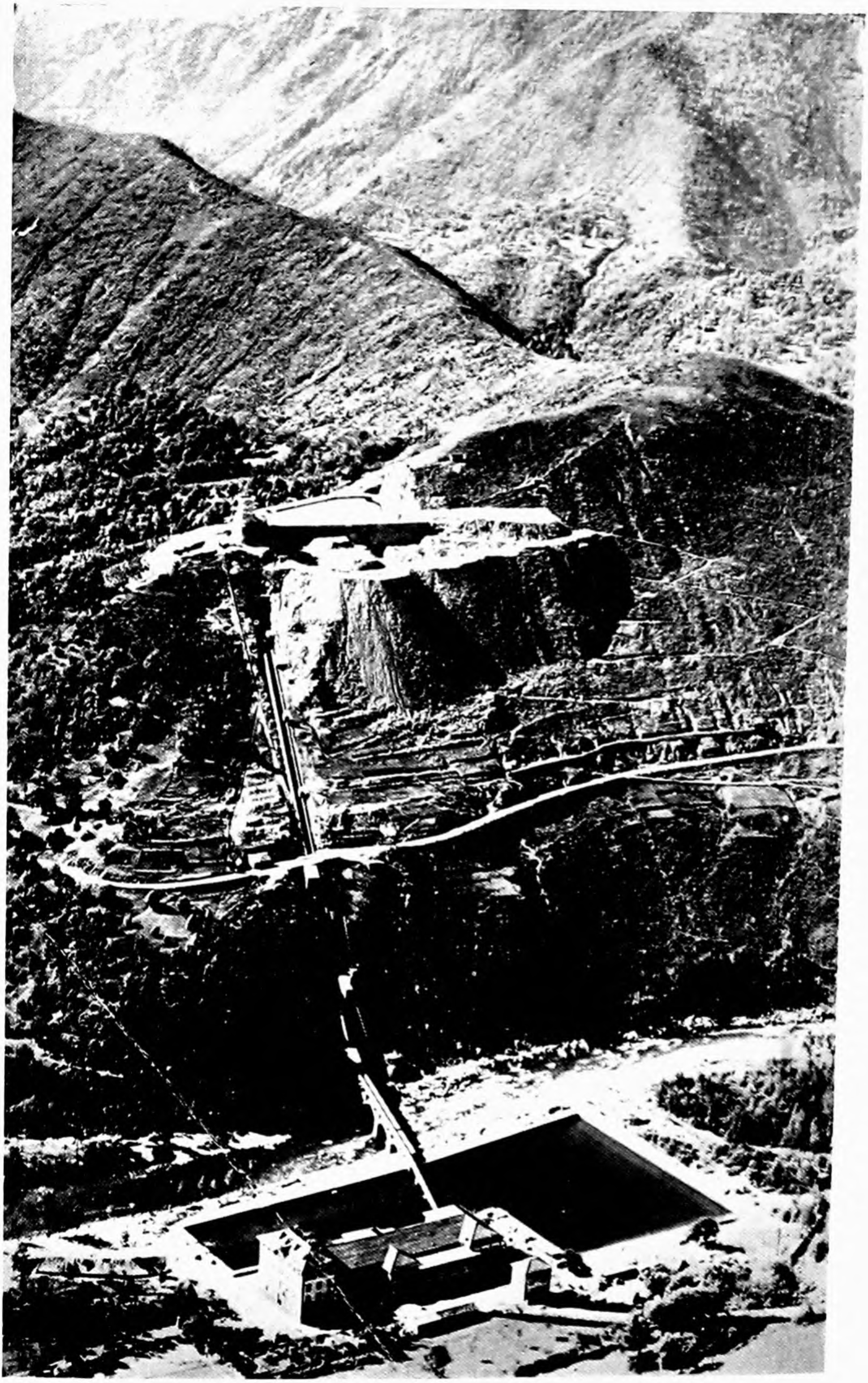

Fig. 433.—Hydraulic-pumped storage installation.
(Sulzer Bros., Ltd.)

[To face page 543.

Fig. 433 gives a good impression of a relatively small pumped storage installation. The upper and lower reservoirs each have a capacity of 1,750,000 cu. ft., and the average difference of water level is 500 ft. The pressure pipe, 5 ft. 9 ins. diameter, leading from one to the other, is clearly distinguishable; pumps of 4000 h.p. are installed in the machine house seen at the bottom of the illustration.

367. Conditions Favourable to Pumped Storage Schemes. In large electrical distribution systems there is invariably a large disparity between the minimum demand in the early hours of the morning and the peak demand just after nightfall. On the other hand, the power plant in steam generating stations is tending more and more to a type which can maintain its high thermal efficiency only when operating under steady full-load.

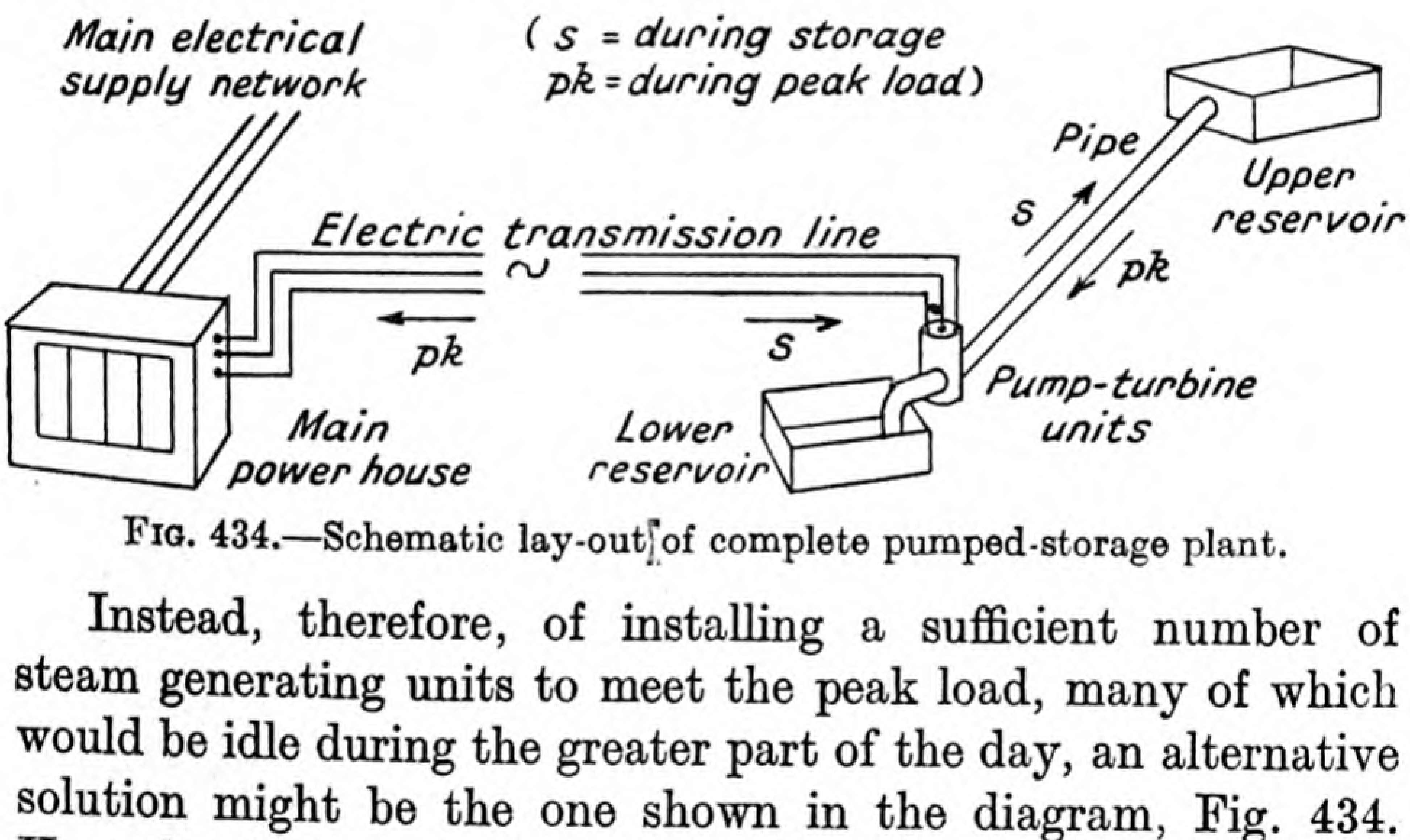

FIG. 434.—Schematic lay-out of complete pumped-storage plant.

Instead, therefore, of installing a sufficient number of steam generating units to meet the peak load, many of which would be idle during the greater part of the day, an alternative solution might be the one shown in the diagram, Fig. 434. Here the main power house has a smaller installed capacity, but the units are intended to work continuously under a high load factor. When these machines can no longer meet the peak demand from the external supply network, auxiliary energy is derived from the hydraulic turbines and transmitted electrically to the main station. During the succeeding period of low demand, excess electrical energy flows in the reverse direction, and permits the centrifugal pumps to lift water back again from the lower to the upper reservoir. If topographical conditions permit, and especially if peak load current can be sold at a specially high tariff, the scheme may be

economically feasible, in spite of the conversion losses in the pumps, the pipe line, and the turbines.

Should the source of energy be itself a water-power station, an auxiliary storage installation may be not only desirable but essential. This would be the case if the discharge in the river which fed the main low-head turbines was insufficient to meet the peak load; here the only way of generating the desired maximum output would be to supplement the output of the low-head machines by that of the high-head turbines utilising stored water. **(Example 198.)**

Although hydraulic storage stations are usually built to equalise daily changes in demand, they can deal with seasonal variations if the reservoirs are of large enough capacity, storing water in the summer and giving it out again in the winter, or *vice versa.*

368. Equipment of Hydraulic Storage Plants. The three main elements to be combined in each of the units accommodated in the machine house of a pumped storage scheme are (i) a hydraulic turbine through which the stored

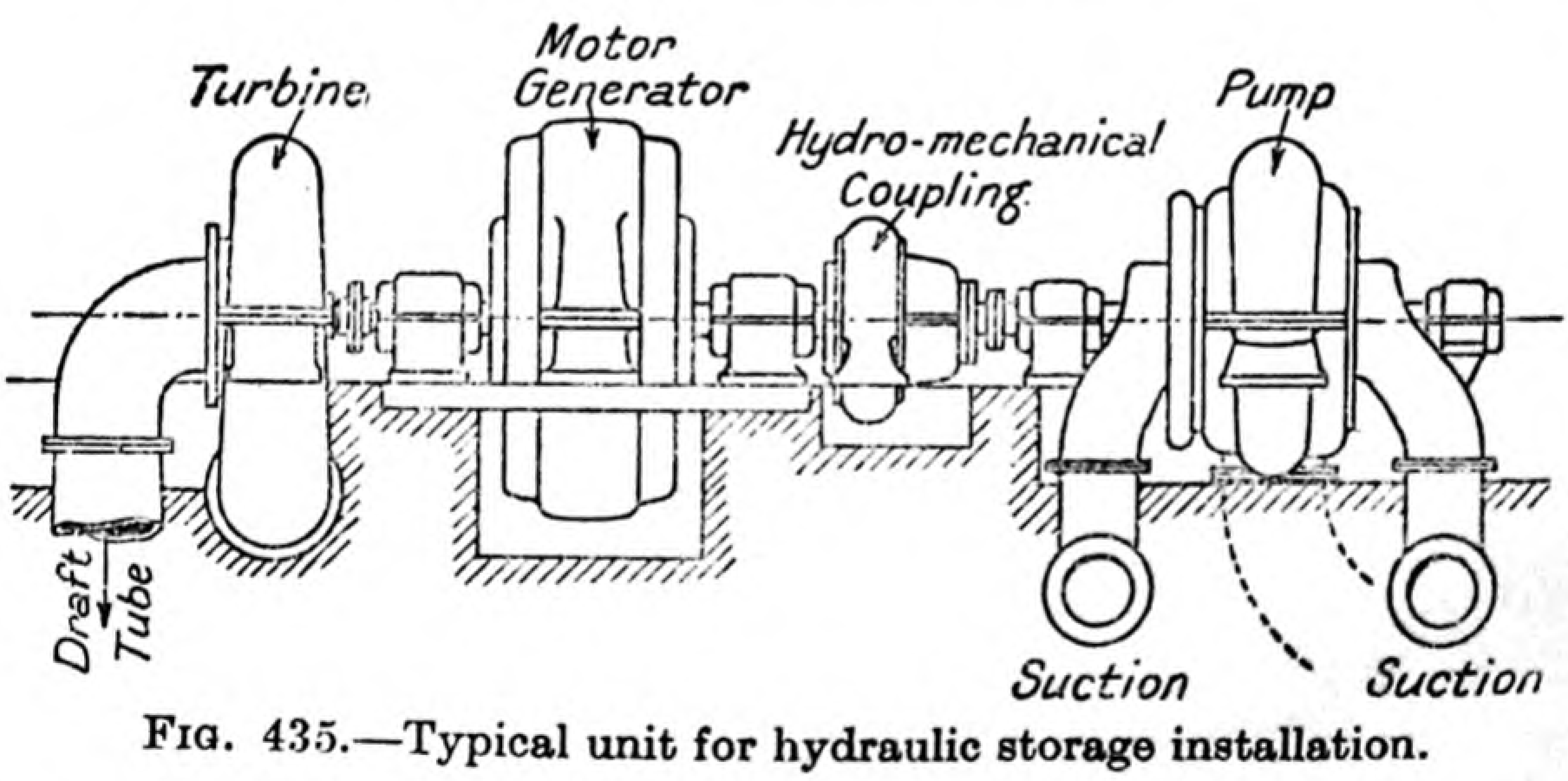

FIG. 435.—Typical unit for hydraulic storage installation.

water flows from the upper to the lower reservoir, (ii) an electrical unit acting as a generator when the turbine is working and as a motor when the pump is working, and (iii) a centrifugal pump which when driven by the motor lifts water from the lower to the upper reservoir.[278]

A typical arrangement is shown diagrammatically in Fig. 435; the three units are mounted co-axially, the electrical component being permanently coupled to the turbine, but having a hydro-mechanical coupling (§ 365 (i)), so that it can be connected

to or disconnected from the 2-stage pump. During power generation, the pump is uncoupled and remains at rest; during storage, the turbine runner revolves idly, eddy losses being avoided by emptying the turbine casing. Such well-contrived automatic control devices are installed for reversing the flow of water in the pipe-line, and the flow of electrical energy in the transmission line, that the change-over from "generating" to "pumping" can be completed in less than two minutes.

Vertical-shaft units may sometimes be preferred, each embodying perhaps a Pelton wheel and a 4- or 5-stage centrifugal pump.[279] In Continental Europe, where conditions chiefly favour such installations, the energy transmitted by each set—horizontal or vertical—may exceed 20,000 or even 50,000 horse-power.

A question that may now very reasonably be asked is this: if a single electrical machine can act either as a motor or as a generator, why cannot a single hydraulic machine likewise serve either as a turbine or as a pump? The answer is to be found in §§ 235, 315: if the hydraulic rotor always ran at the same speed, the head generated during pumping would be less than the head supplied to the turbine when the direction of rotation was reversed. It is for this reason that the set depicted in Fig. 435 comprises a single-stage turbine but a two-stage pump. Now if this condition of invariable speed—a condition imposed solely by the electrical element—can be relaxed, then the whole pumped-storage installation can be simplified. Such plants have been designed in the United States: variation in the speed of the electrical unit is contrived by changing the number of stator poles in circuit. In one such set the speed is 300 r.p.m. during pumping, and 257 r.p.m. during generating; the reversible, 11,000 h.p. hydraulic unit, resembling a conventional vertical Francis turbine, requires no pivoted gates because it is intended to work always at full-load, either as pump or turbine.[280]

369. Other Pumped Storage Systems. In the installations described in §§ 366-367, a fixed quantity of water circulates between the upper and the lower basins, the system being hydraulically isolated from any other hydraulic machines. But these conditions are not essential: there are other ways

in which pumps and turbines may help one another.[281] In the example illustrated in Fig. 436, a natural lake forms the storage basin for a high-head hydro-electric plant, much as it does in Fig. 263, § 252 (i). The storage capacity between levels A and B can be made available by building a dam or barrage at the outlet of the lake; but the valuable additional storage between levels B and C cannot be drawn upon by any free-flow system—for it is here assumed that an outlet tunnel would be uneconomical or otherwise impracticable. Motor-driven pumps are accordingly installed as indicated in the diagram, Fig. 436: they take their power supply from the main electrical network, they lift water from the lake into the outlet channel, and thus ensure that virtually the full capacity of the lake is utilised.[282] Since the head on the pumps is quite small in relation to the head on the turbines, the diminution in the net power output is inconsiderable.

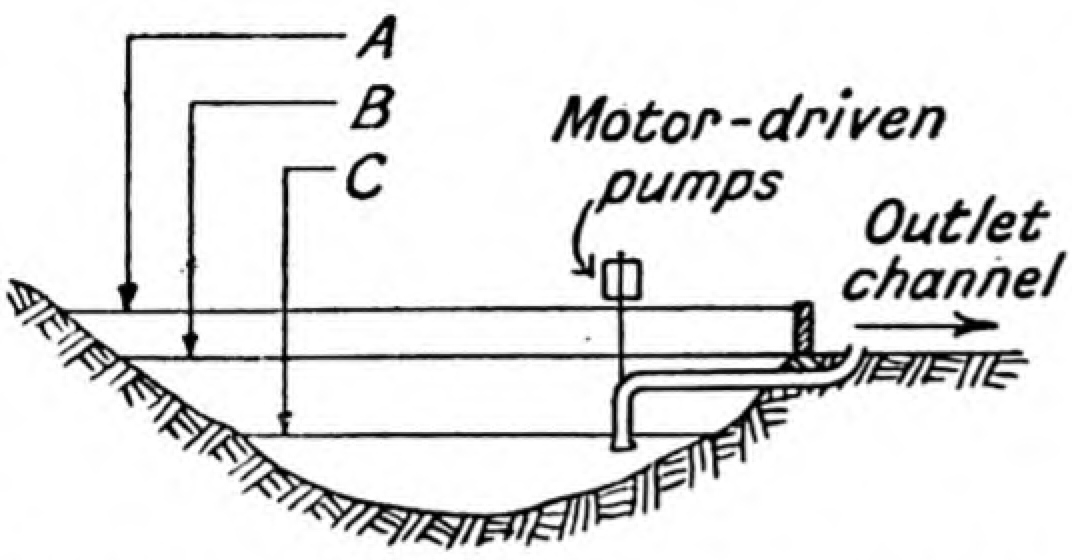

FIG. 436.—Natural lake used as storage reservoir.

An alternative arrangement of auxiliary pumps, adapted to the layout shown in Fig. 266, § 252 (ii), ensures short periods of emergency peak-load operation for the main water turbines. As seen in Fig. 437, the duty of these pumps is to lift water from the supply canal into a small auxiliary storage reservoir near the head of the pipe-line leading down to the main turbines; as the reservoir would be filled during the night, or during other periods of low demand, there would be plenty of surplus energy to drive the pumps. During peak-load periods the discharge of the supply canal might be insufficient to feed

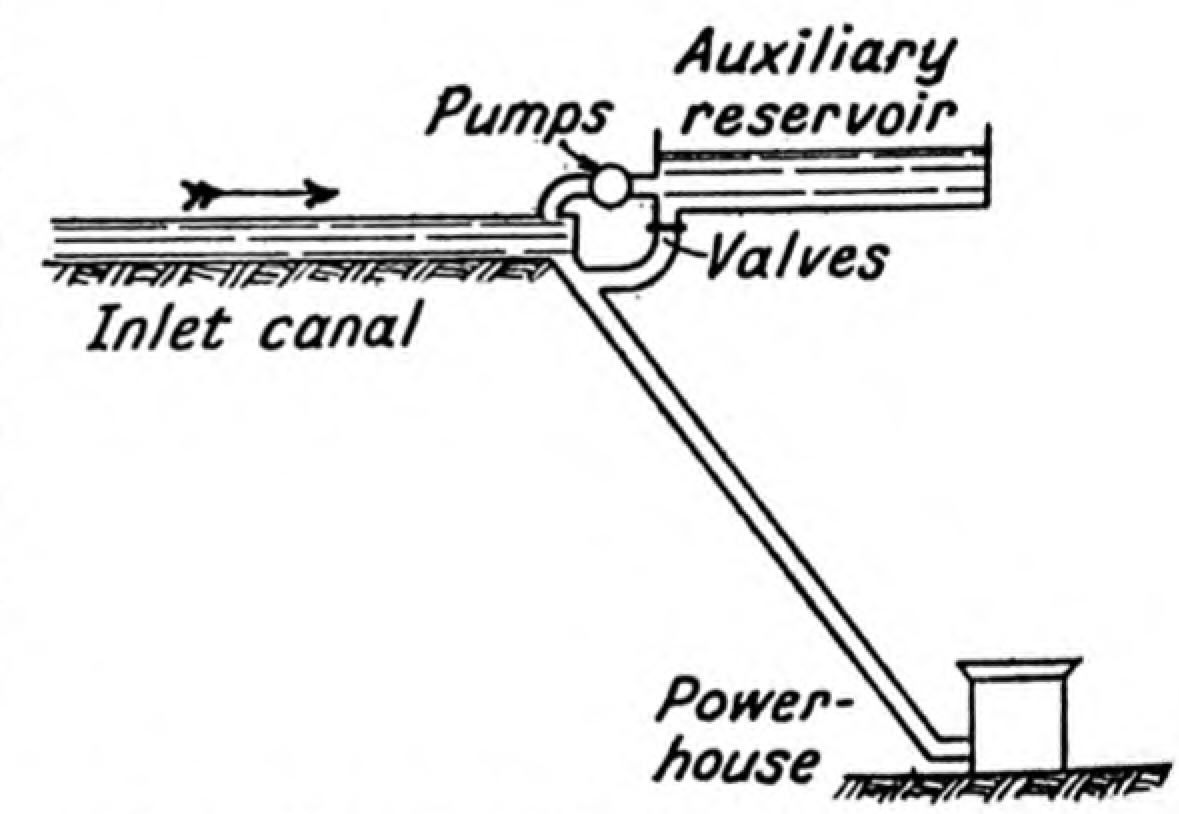

FIG. 437.—Auxiliary pumped-storage reservoir for turbine installation.

the turbines: the pumps would then be stopped, the stored water in the reservoir would be released into the pipe-line, and the combined flow—canal plus reservoir—would then allow the turbines to develop the additional output required of them.

Still other possibilities might occur in conditions resembling those of Fig. 277, § 257. If the westward-flowing stream there described were at too low a level to permit its waters to drain by gravity into the reservoir on the main stream *B*, nevertheless they could still be utilised if an electrically-driven pumping plant were installed. The pumps, running either continuously or intermittently, would force water through the conduit from stream *A* into stream *B*, and in due course this water would feed the main hydraulic turbines, situated at a much lower level in valley *B*.

CHAPTER XIX

HYDRAULIC MEASUREMENTS

For convenience of reference, notes on carrying out the measurements usually necessary in hydraulic operations are here collected together in the final chapter of the book.[283]

370. Measurement of Viscosity. (*a*) *Absolute methods.* By using the principles outlined in this paragraph, the viscosity of liquids in absolute units (§ 8) can be determined from direct observations.[284]

(i) *Capillary tube.* In this apparatus, Fig. 438 (i), the liquid under test is allowed to flow through a capillary tube of measured diameter d and length l. Having observed the pressure-drop $(p_1 - p_2)$, and the rate of flow Q, the experimenter can then extract the desired value of the viscosity μ from equation (5-3), § 65. But this would only be an approximate figure: to obtain a precise value it would be necessary to apply a correction taking into account the velocity of efflux of the liquid leaving the capillary tube.

(ii) *Falling sphere.* The type of laminar flow to be exploited here is to be found when a small spherical solid attains its *terminal velocity* when descending through the liquid to be tested, § 129. The sphere may be a polished steel ball as used

in ball bearings: it is dropped through an opening into the sample of liquid in a glass tube, Fig. 438 (ii). The observer notes the time t seconds for the ball to fall a distance l cms.

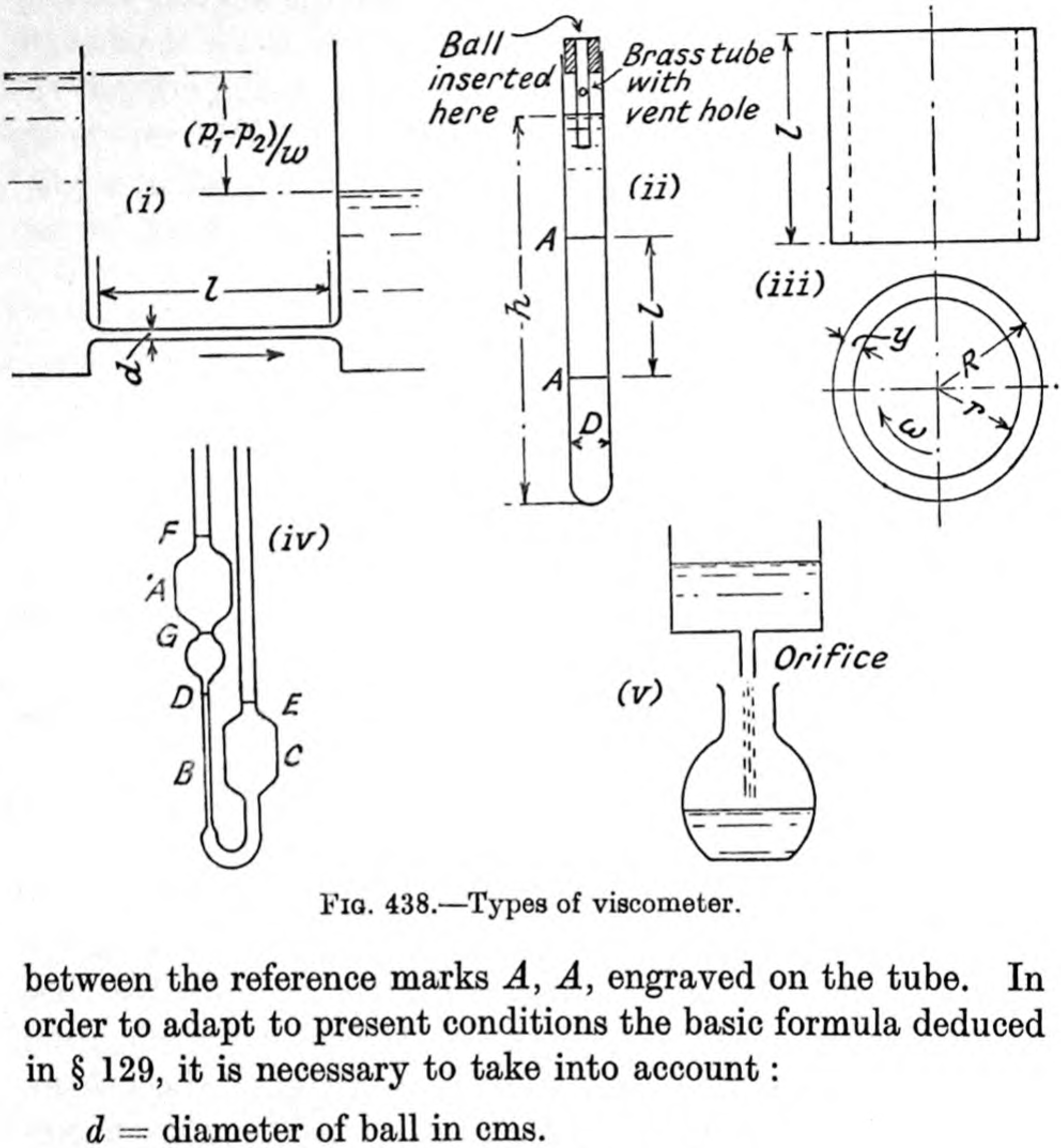

FIG. 438.—Types of viscometer.

between the reference marks A, A, engraved on the tube. In order to adapt to present conditions the basic formula deduced in § 129, it is necessary to take into account:

d = diameter of ball in cms.

σ = specific mass of steel ball in gm./cu. cm.

ρ = specific mass of liquid in gm./cu. cm.

D = diameter of glass tube in cms.

h = height of column of liquid in tube in cms.

g = acceleration of gravity in cms./sec./sec. = 981.

The desired value of the viscosity μ in poises is then derived from the formula:—

$$\mu = \frac{td^2(\sigma - \rho)g}{18\, l\left(1 + \frac{2{\cdot}4d}{D}\right)\left(1 + \frac{5d}{3h}\right)}.$$

(iii) *Rotating cylinder method.* Here the liquid under test is contained within the annular space between two concentric cylinders, Fig. 438 (iii). If the outer cylinder is held stationary, and the inner cylinder is rotated with uniform angular velocity ω, then the conditions can be likened to those depicted in Fig. 2, § 7 ; the only essential change is that the original flat plates are now rolled up into cylindrical form. Assuming first that the radial thickness of the film of liquid, y, is very small in relation to the radius R of the outer cylinder, we can adapt formula 1-1 thus :—

$$A = \text{area} = 2\pi Rl.$$

$$P = \text{tangential force} = \mu \,.\, 2\pi Rl \,.\, \frac{\omega R}{y}.$$

$$T = \text{torque} = PR = \mu \,.\, 2\pi R^3 l \,.\, \frac{\omega}{y}.$$

If the measured value of the torque T is known, the desired value of the viscosity μ can at once be computed.

A corrected expression for the torque T, if the film thickness $y = (R - r)$ is appreciable, can be written

$$T = \mu \,.\, 4\pi l \,.\, \left(\frac{R^2 r^2}{R^2 - r^2}\right) . \,\omega.$$

371. Measurement of Viscosity. (*b*) *Relative or Industrial methods.* Instruments based strictly upon fundamental principles are often not very well suited for routine industrial measurements, either because of the refinements of construction they demand, the skill required in operation, or uncertainty about small corrections to be applied to the results they yield. Simpler instruments will often suffice, which will give a relative value of viscosity or a value expressed in arbitrary units.[285] Such instruments may on occasion be adapted to non-Newtonian liquids, § 11, as well as to liquids whose behaviour follows the normal laws of laminar flow. Of the many types of viscometer now available, two will be described.

(iv) *U-tube Viscometer.* This instrument, Fig. 438 (iv), embodies a capillary tube as in § 370 (i) ; but now the capillary B forms part of a glass U-tube of special shape ; enlargements or bulbs at A and C serve as containers for the sample of

liquid under test. The measured specific mass of the liquid is ρ. In use, the viscometer is first filled with the liquid up to the level of the engraved marks D, E; then the liquid is blown or sucked up into bulb A until it rises a little higher than mark F. To make a test, the liquid is now released: it is allowed to flow freely through the capillary tube B into bulb C, the observer noting the time t in seconds for the level to fall from mark F to mark G.

The whole test is now repeated with a standard liquid of known viscosity, e.g. distilled water or sugar solution of stipulated strength, whose viscosity is μ_1 and specific mass ρ_1. If the observed time of descent is t_1 seconds, then the desired value of the viscosity of the sample liquid is $\mu = \mu_1 \dfrac{t\rho}{t_1\rho_1}$. To adapt the procedure to a wide range of viscosities, a set of 4 or more U-tubes would be available, having graded sizes of capillaries.[286]

(v) *Orifice type of viscometer.* In these very popular instruments, the sample of liquid is allowed to flow through a short tube or orifice of standard dimensions, Fig. 438 (v). One observation only is required: it is the time in seconds, t_o, required for a stipulated volume of liquid to flow from the upper vessel or cup into the measuring vessel below. This numeral alone is accepted as an indication of the liquid's viscosity; the true viscosity in poises can only be obtained by the use of conversion factors or conversion tables.

The viscometer most widely used in Great Britain is the *Redwood No. 1 instrument*, and its conversion equation is:

$$\mu \text{ in poises} = \left(0{\cdot}0026\, t_0 - \frac{1{\cdot}72}{t_0}\right) \times \text{S.G. of liquid},$$

where t_o is the observed time of flow. Thus a liquid described in industrial circles as having a viscosity of "Redwood 150 seconds" and S.G. 0·95 would have an absolute viscosity of 0·37 poises.

Corresponding instruments in America are the Saybolt Universal viscometer, and on the continent of Europe, the Engler; but each has its own arbitrary conversion equation or conversion chart.

With any instrument *temperature control* of the sample under test is of the highest importance, because of the sensitivity of viscosity to temperature changes, § 9. By means of stirring devices, liquid baths surrounding the sample, or other methods, the test liquid must be kept at a uniform and accurately measured temperature.

Range of utility. Figures suitable for general guidance are as follows; they show how the type of instrument should be adapted to the probable viscosity of the sample.

U-tube viscometer	from about 0·01 to 15 poises.
Falling sphere viscometer . . .	from about 10 to 250 poises.
Redwood No. 1 viscometer . .	below 5 poises.
Redwood No. 2 viscometer . .	above 5 poises.

Measurement of Pressure and Pressure Head.

372. Glass-tube Gauges.

(i) *Piezometer tube.* A piezometer tube is a vertical glass tube with its upper end (usually) open to the atmosphere and

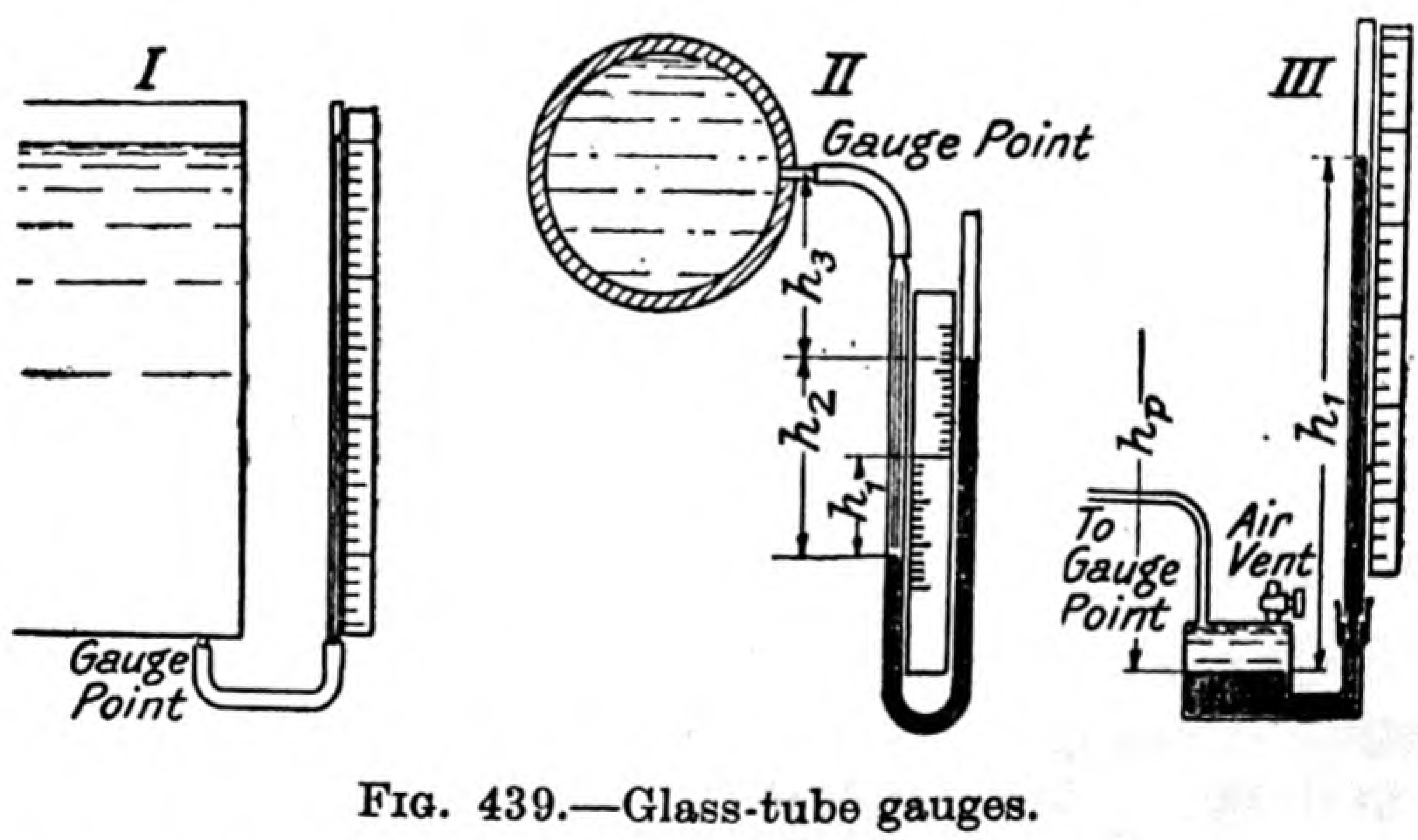

Fig. 439.—Glass-tube gauges.

its lower end connected to the point at which it is desired to measure the pressure head. The pressure head is read off directly from a scale (Fig. 439 (I)). Owing to the effect of surface tension (§ 6), the liquid in the tube stands at a slightly higher level than it does in the vessel to which it is connected; the difference in level for water in a tube $\frac{1}{4}$ in. diameter is 0·18 in., but is inappreciable for tubes of $\frac{1}{2}$ in. diameter and over.

(ii) *Double column mercury manometer.* If the variations of pressure head are beyond the range of a simple piezometer tube, a glass U-tube containing mercury may be used (Fig. 439 (II)). The column of mercury of height h_2 is balanced by a column of water of height $h_2 + h_3$, plus a water column equivalent to the head h at the gauge point. Hence

$$13{\cdot}6\, h_2 = h_2 + h_3 + h.$$

Since $h_1 = \frac{1}{2}h_2$ (assuming the gauge tubes to be of equal diameter), we have

$$13{\cdot}6h_2 = 0{\cdot}5\, h_2 + h_1 + h_3 + h,$$

or

$$h = \text{head at gauge point}$$
$$= 13{\cdot}1\, h_2 - h_0,$$

where $h_0 = \mathrm{h}_1 + h_3 =$ vertical distance between gauge point and zero of scale; and $13{\cdot}6 =$ specific gravity of mercury.

In general, putting (S.G.) for the specific gravity of the liquid whose pressure head is being measured, and $(\text{S.G.})_1$ for the specific gravity of the liquid in the U-tube,

$$h = h_2\left(\frac{S.G._1}{S.G.} - 0{\cdot}5\right) - h_0.$$

(iii) *Single column mercury manometer.* In this instrument (Fig. 439 (III)), one of the mercury columns is held in a shallow, wide, iron container, observations being made only of the level of the other column which is contained in a glass gauge tube. Letting a represent the area of the glass tube, and A the area of the container, an *increase* of head h at the gauge point will raise the indicating mercury column by h_2 and lower the mercury surface in the container by $h_2 \cdot \dfrac{a}{A}$.

Before the additional head h is applied, the column of mercury of height h_1 will balance a column of water of height $h_p = 13{\cdot}6\, h_1$. After the additional head is applied, the height of the mercury column is $h_1 + h_2 + h_2 \cdot \dfrac{a}{A}$, and the height of the equivalent water column is $h_p + h_2 \cdot \dfrac{a}{A} + h$, that is

$$h_p + h_2 \cdot \frac{a}{A} + h = 13{\cdot}6\left(h_1 + h_2 + h_2 \cdot \frac{a}{A}\right).$$

Hence, by subtraction,

$$h + h_2 \cdot \frac{a}{A} = 13{\cdot}6\left(h_2 + h_2 \cdot \frac{a}{A}\right),$$

or

$$h = h_2\left(13{\cdot}6 + 12{\cdot}6\,\frac{a}{A}\right),$$

which permits the scale behind the indicating column to be directly calibrated.

Observe that both in this instrument and in the manometer (ii) above, the connecting pipe between the gauge point and the manometer must be kept full of water (or of the metered liquid).

(Example 208.)

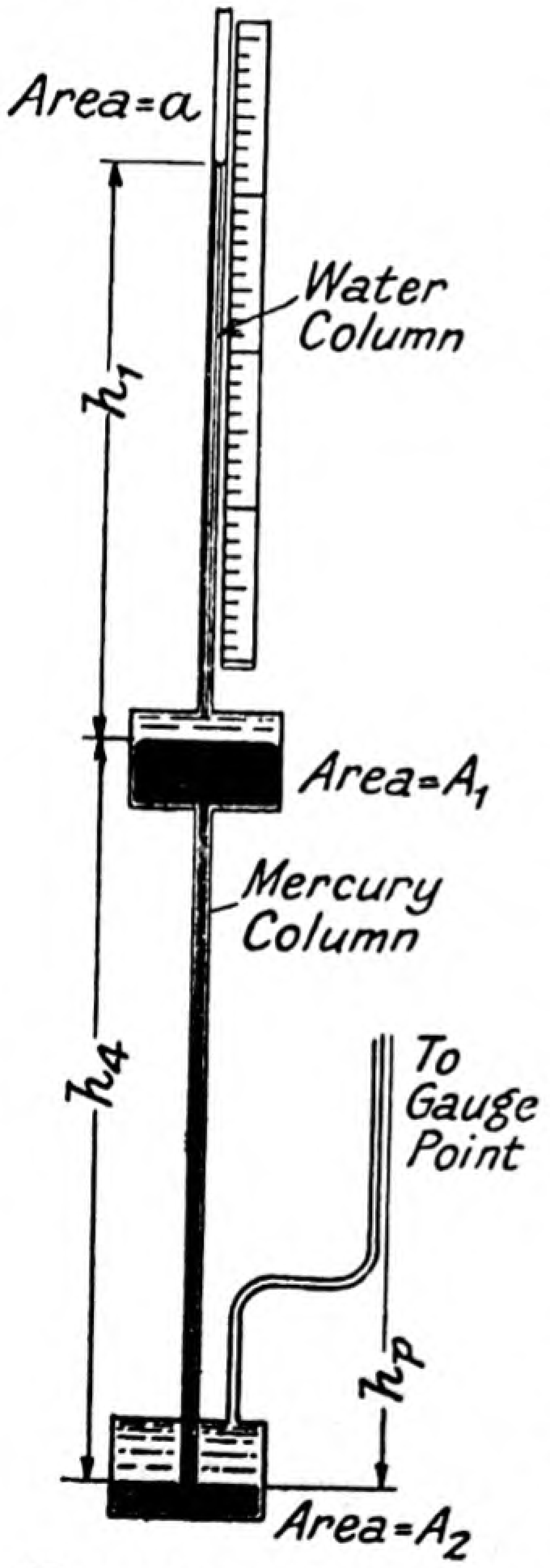

Fig. 440.—Compound manometer.

(iv) *Compound manometer.* This apparatus can be recommended when the total pressure head is relatively large, but suffers small variations; here a mercury column serves merely to balance the constant part of the head, the actual indications being read from a water column (Fig. 440). At a given moment let h_1 be the height of the water column, h_4 the height of the mercury column, and h_p the height of the equivalent water column. Then

$$h_p = h_1 + 13{\cdot}6\,h_4.$$

Now suppose the water in the indicating gauge tube to fall by h_2, the area of this tube being a. The mercury in the upper container, of area A_1, will thereupon fall by $h_2 \cdot \frac{a}{A_1}$, and the mercury in the lower container, of area A_2, must rise by an amount $h_2 \cdot \frac{a}{A_2}$. The height of the equivalent water column will now be

$$h_p' = \left(h_1 - h_2 + h_2 \cdot \frac{a}{A_1}\right) + 13{\cdot}6\left(h_4 - h_2 \cdot \frac{a}{A_1} - h_2 \cdot \frac{a}{A_2}\right),$$

and the *diminution* of pressure head H at the gauge point

corresponding to a fall of the water indicating column of h_2 is seen to be

$$H = h_p - h_p' - h_2 \cdot \frac{a}{A_2} = h_2\left(1 + 12{\cdot}6 \cdot \frac{a}{A_1} + 12{\cdot}6\,\frac{a}{A_2}\right).$$

The scale from which readings are taken can be calibrated accordingly.

373. Differential Gauges. These are used for measuring differences of pressure head; in Fig. 441 (I), and (II), two types are illustrated adapted for indicating the frictional loss h in pipes. Type (I) consists of two piezometer tubes side by

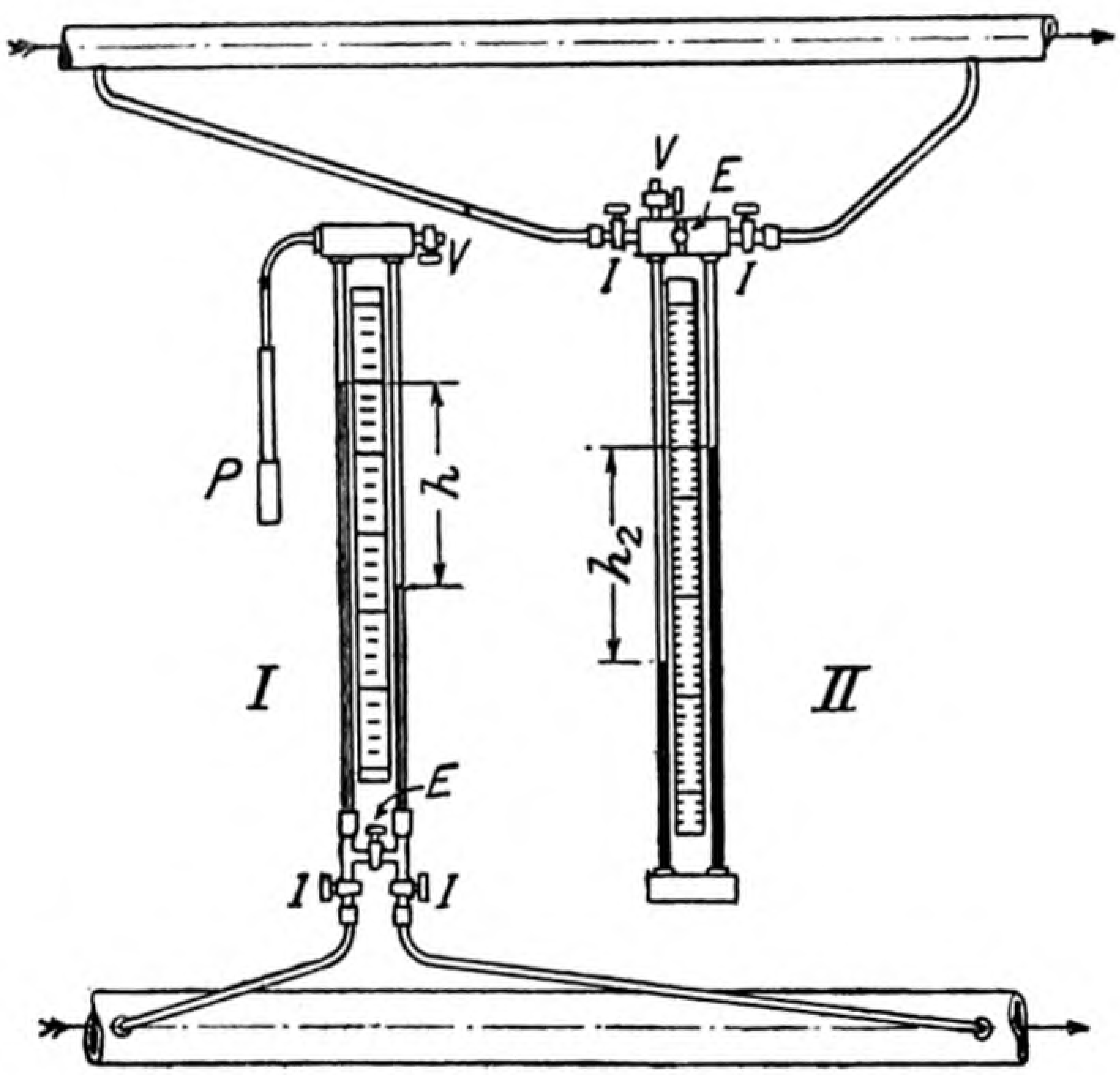

FIG. 441.—Differential gauges.

side, their upper ends having a connection to which an air pump P may be screwed—a bicycle tyre pump answers very well. By working the pump, or opening the air vent V, the water in the glass tubes may be brought to the desired part of the scale irrespective of the pressure in the main pipe. If this pressure is less than atmospheric, a suction pump must be used to draw the water columns up into the gauge tubes; but this arrangement should be avoided if at all possible, on account of the danger of troublesome air leaks into the connecting pipes.

In the differential U-tube manometer (Fig. 441 (II)), mercury of S.G. 13·6 may be used if the pressure difference h

is large, and carbon tetrachloride of S.G. 1·60, if the pressure difference h to be measured is small. Using the symbols of § 372 (ii),

$$h = h_2\left(\frac{S.G._1}{S.G.} - 1\right).$$

A differential *micromanometer* for measuring very small pressure differences is shown diagrammatically in Fig. 442; here the U-tube is opened out until the indicating leg is nearly horizontal, and it is mounted on a pivoted frame actuated by a micrometer screw. After the pressure difference has been applied, the screw is rotated until the indicating column is brought back to its original position; from the readings of the micrometer head of the screw, the desired pressure difference may be calculated.

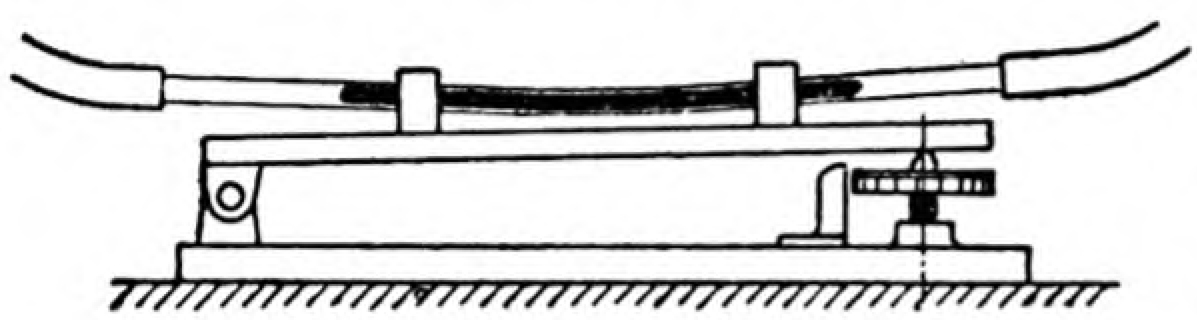

FIG. 442.—Differential micromanometer.

The *mercury balance* illustrated in Fig. 443 has the advantage that changes in the specific gravity of the indicating liquid need not be taken into account, and that fragile glass

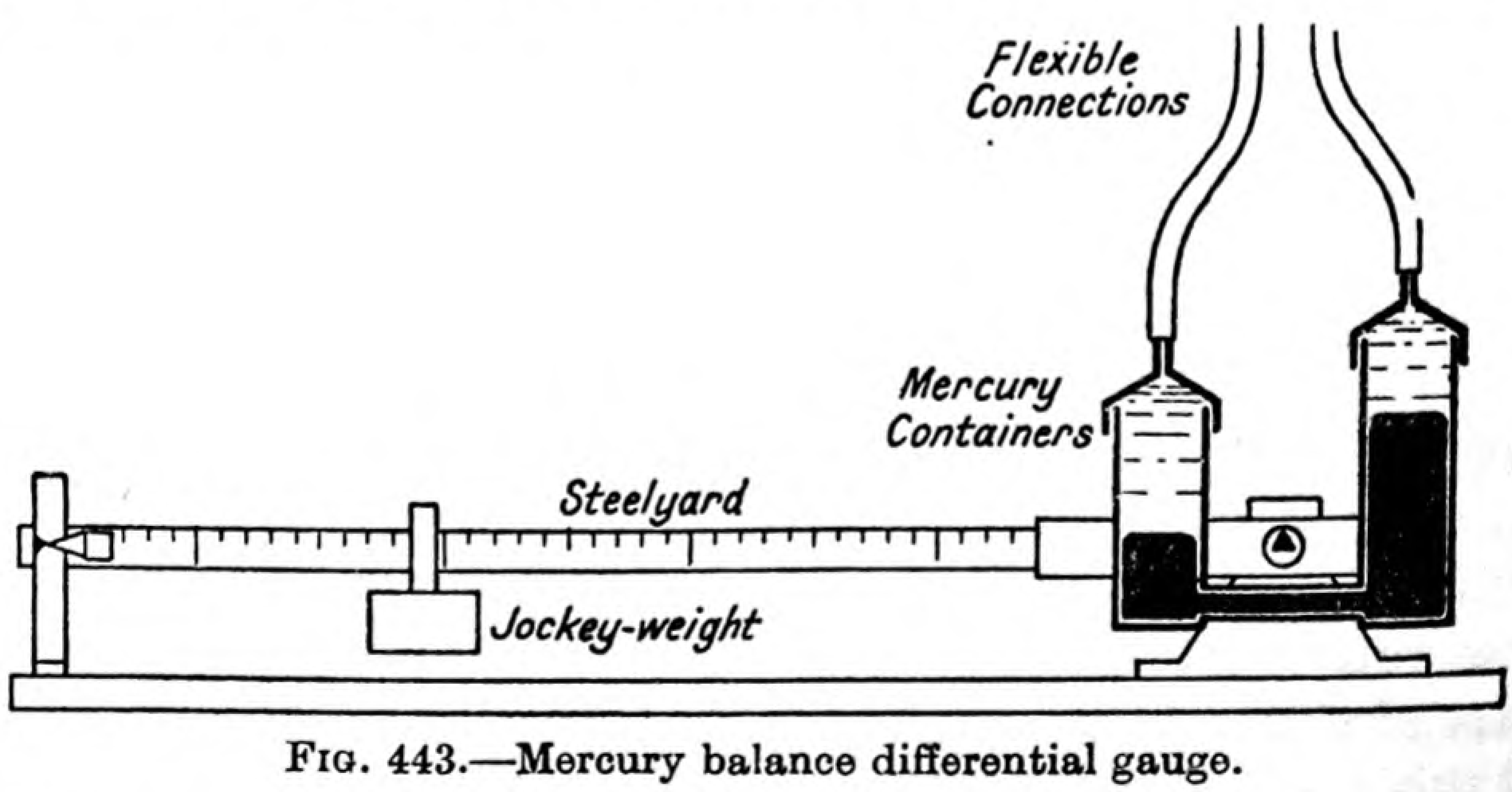

FIG. 443.—Mercury balance differential gauge.

tubes are not required; for very high pressures the flexible connections as well as the mercury containers may be of metal. The two interconnected containers form a double-column mercury manometer which is mounted on knife-edges; an applied differential head of water destroys the equilibrium of the system, which is restored by moving the jockey weight

along the steelyard. Thus the position of the jockey weight serves as a measure of the differential head. In another form of the instrument known as the *ring balance*, more suitable for gases than for liquids, the U-tube is bent into a circle or ring, whose angular deflection indicates the differential head.

374. Dial Gauges. The dial type of pressure or vacuum gauge, in which an elastic metallic curved tube or an elastic metallic diaphragm operates a pointer moving over a scale,

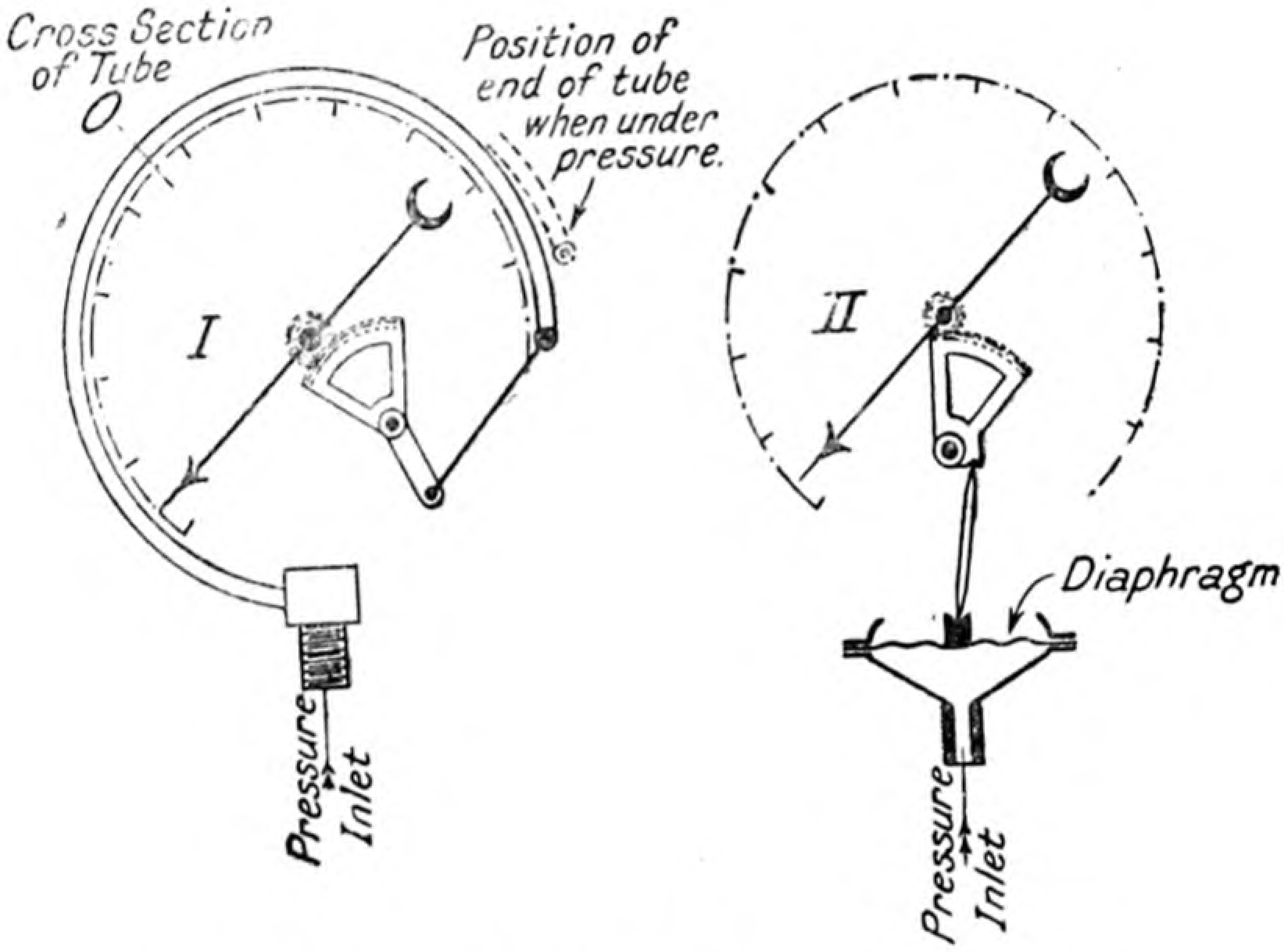

FIG. 444.—Bourdon and diaphragm dial gauges.

is very well adapted for the measurement of liquid pressures, and for high pressures is usually the only practicable kind (Fig. 444 (I) and (II)). The movement of a flexible metallic bellows may also be used to actuate the indicating pointer. Such gauges should periodically be checked against a gauge testing apparatus; in use they should be protected by a cock or fine adjustment needle valve against the heavy inertia shocks to which water piping systems are liable.

375. Pneumatic Manometer. This device (Fig. 445) is most serviceable when the indicating scale must be fixed at some distance from the gauge point; it works satisfactorily even if the distance is 1000 ft. An air bell is fixed near the bottom of the tank in which we wish to measure the pressure, and a supply of compressed air is led into the bell at such a rate that there is a small leakage beneath its lower

edge, the air bubbling up through the surrounding liquid. The air pressure thus automatically adjusts itself to the pressure due to the head h of liquid; it may thus be measured by any convenient type of manome ter.

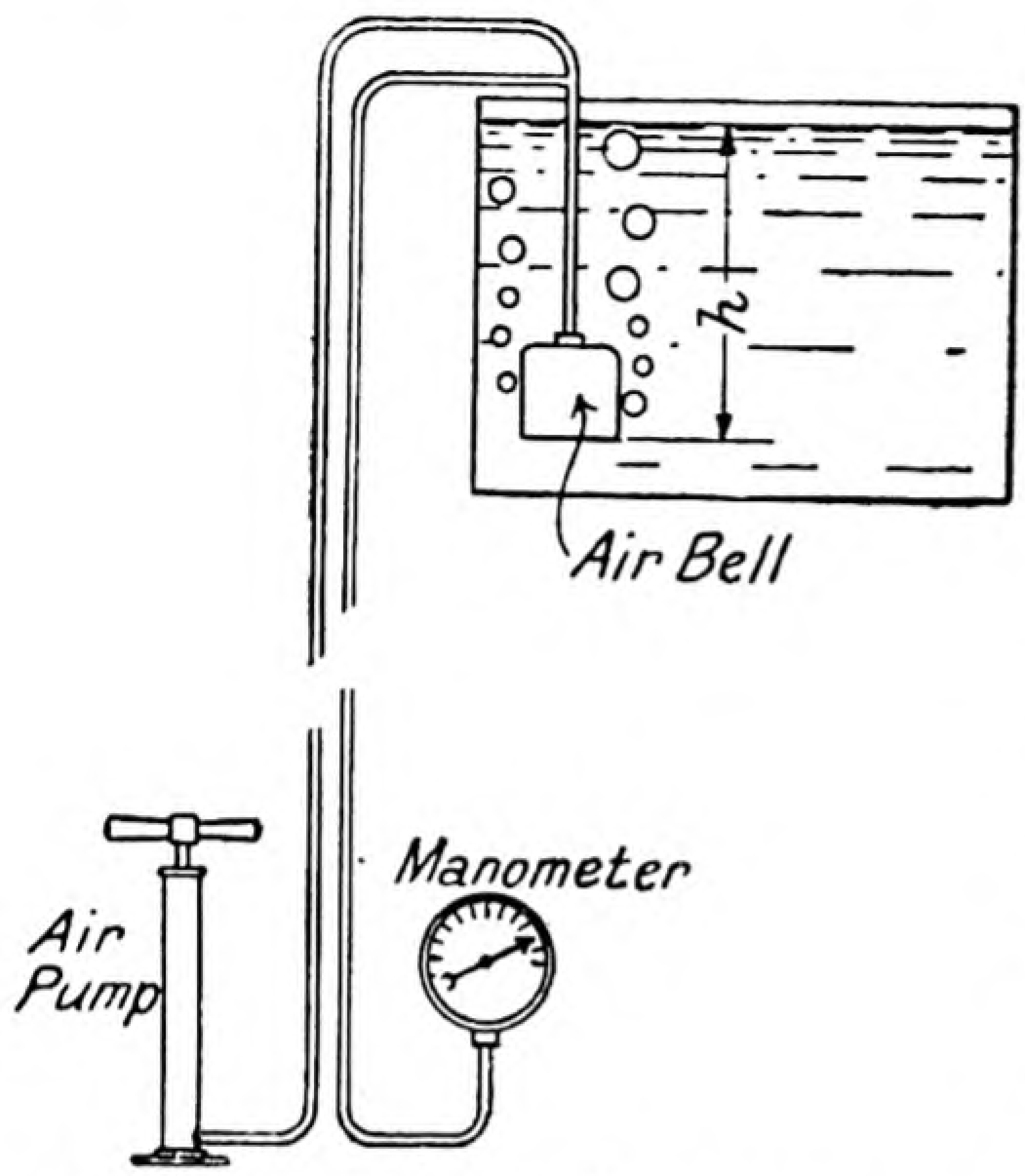

FIG. 445.—Pneumatic manometer.

For intermittent use a hand air pump is provided, which is operated each time before the gauge is read.

376. Hook and Point Gauges. These are the simplest and most reliable gauges for measuring the relative levels of free water surfaces with a probable error of $\frac{1}{1500}$ ft. (0·2 mm.). A hook gauge consists of the graduated stem A to which the hook is attached (Fig. 446),* the clamping screw B for coarse adjustments, the slow-motion screw C for bringing the point of the hook exactly into the water surface, and the vernier D from which readings are taken. The vernier is attached to a fixed housing within which the stem can be traversed vertically. A suitable method of mounting and using the gauge is illustrated in Fig. 456, § 385.

Point gauges are specially adapted for determining the levels of the free surfaces of rapidly moving streams—they resemble hook gauges except that the point projects straight downwards, and is lowered on to the surface of the water from above.

377. Float Gauges. These are commonly used for indicating the depth of water in reservoirs or in overhead tanks; but when properly built they are quite suited for precise measurements.[287] The diagram (Fig. 447) shows a pair of precision float gauges adapted for differential readings. The floats may be of copper or zinc, loaded with water ballast; they move within float chambers connected by piping and valves I, I, to the main tanks or channels where water levels are to be observed. The overhead pulleys should be of aluminium,

* Facing page 562.

accurately balanced and mounted on ball bearings. Sometimes it is preferable to substitute a graduated flexible flat steel tape for the stranded wire and straight brass scale which connect the float to the counter-weight. The probable error when using such gauges need hardly be greater than with hook gauges.

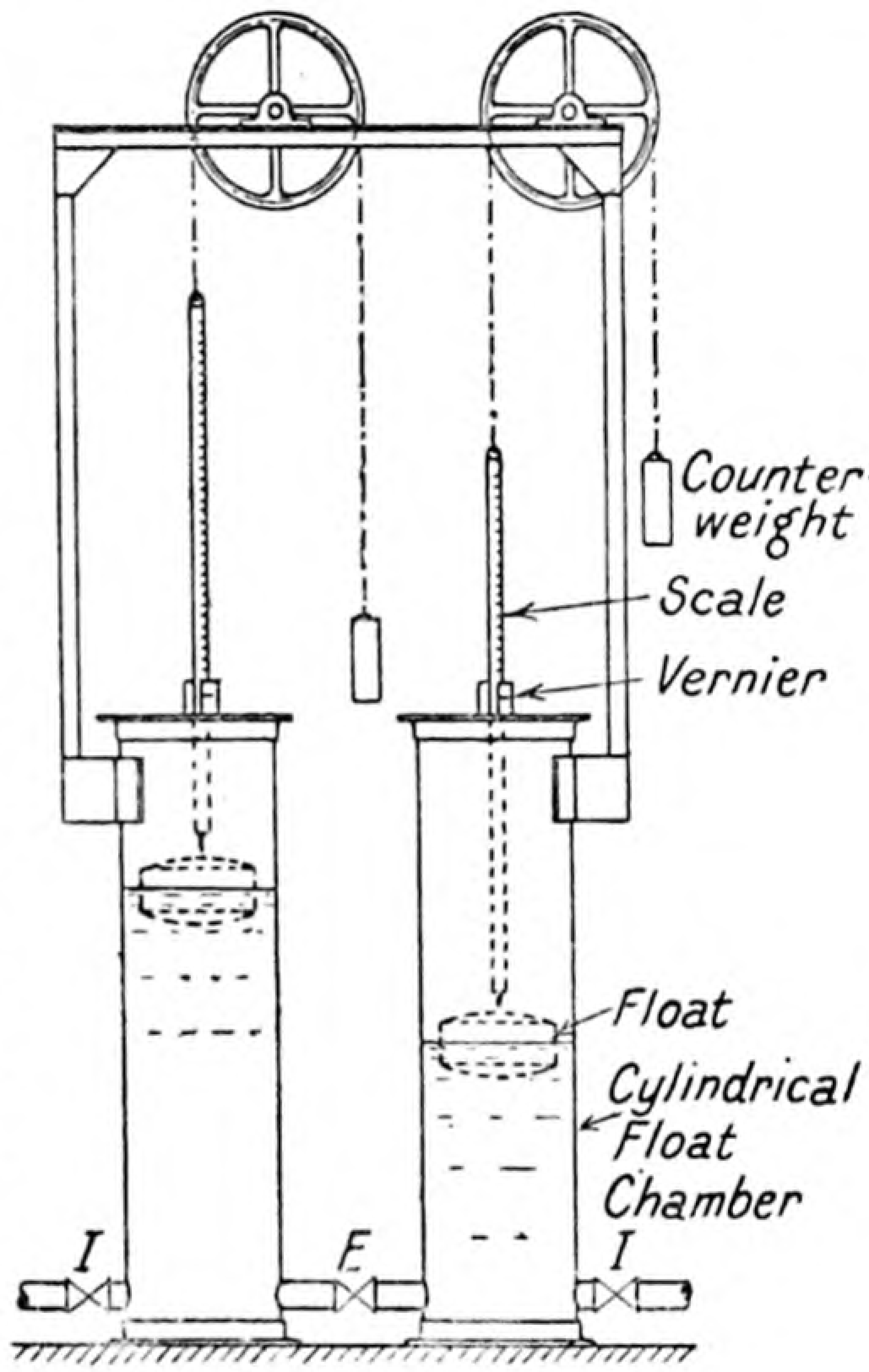

FIG. 447.—Float gauges.

Some observers like to read the scales from a distance with the help of a surveyor's level; sometimes a pointer moving over a circumferential scale is attached to the spindle of the pulley. By the addition of suitable electrical transmitting and receiving apparatus, float gauges may be made to operate indicating dials at distances up to 20 miles or more. In one system, the movement of the pulley actuates a contact moving over a close-coiled resistance, and so varies the current flowing in the line wires, the position of the needle of the electrical indicator at the receiving end being altered accordingly. Alternatively, a step-by-step system may be used, the movement of the float and of the pulley causing a succession of impulses to be transmitted which, with the aid of a relay, enables the indicating pointer at the receiving end to be positively controlled.

378. General Comments on Gauges, Manometers, etc.

(i) The scales or dials of pressure gauges can be graduated to read either in terms of head or of pressure by the use of the expression $p = wh$ (§ 12).

(ii) The connecting pipes between the gauge points and the gauge wells, when hook or float gauges are used, should be of generous diameter, any necessary damping effect being obtained by interposing a short length of small-bore tubing in each line.

The resulting capillary or viscous damping is preferable to throttling by partially-closed cocks or valves. During the intervals between gauge readings, these constrictions may be short-circuited, so that the new water levels in the gauge-wells may quickly stabilise themselves.

(iii) To avoid air locks in the connecting pipes, i.e. to ensure that the pipes are always completely filled with indicating liquid, the pipes must be properly graded as in Fig. 441. Suitably-located vent-cocks V can discharge air forced out of solution (§ 11) or that has leaked into the system.

(iv) Equalising cocks E (Figs. 441 and 447) are useful for permitting a flush of water straight through the system and thus blowing air bubbles away; when these are left open, and the isolating cocks I are closed, the zero reading of the gauge may be checked.

Measurement of Volume, Weight, and Velocity.

379. Measurement of Volume. The estimation of the volume of liquid in reservoirs, cisterns, tanks, etc., depends on measurements of the liquid surface level, in conjunction with a knowledge of the cross-sectional area of the vessel in a number of horizontal planes. Thus any convenient depth-measuring device may be used, with its scale directly calibrated in units of volume. The pneumatic gauge (§ 375) is particularly adaptable for this purpose—it serves equally well for indicating the quantity of liquid in a tank on the roof of a building, as for showing the quantity in the oil fuel tanks of a motor ship.

If the weight of liquid is required, a collecting-tank may be mounted on a platform weighing-machine.

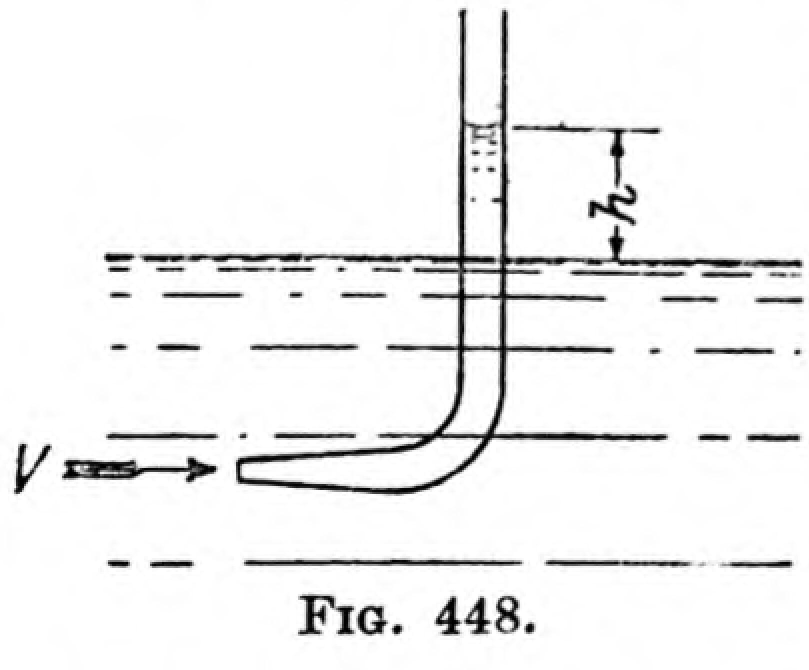

Fig. 448.

380. Measurement of the Velocity at a Point in a Liquid. (i) *Pitot tube.* The principle of this instrument is shown diagrammatically in Fig. 448, where a bent tube drawn out into a nozzle is seen immersed in a flowing stream with the nozzle pointing upstream. Due to the dynamic pressure exerted on the stationary liquid in the mouth of the tube, the water in the vertical limb rises above the surface of the stream by an

amount h which is very nearly proportional to the square of the velocity V; thus by observing h the desired velocity V may be calculated (§ 120).

For commercial measurements an adaptation named the "Pitometer" is often used; it has two nozzles, one pointing upstream and the other downstream, these being enclosed within a sheath so that they can be folded together and the instrument passed through the wall of the pipe in which the liquid is flowing (Fig. 449). A plug-cock having a suitably large opening permits this to be done while the pipe is under pressure.[288]

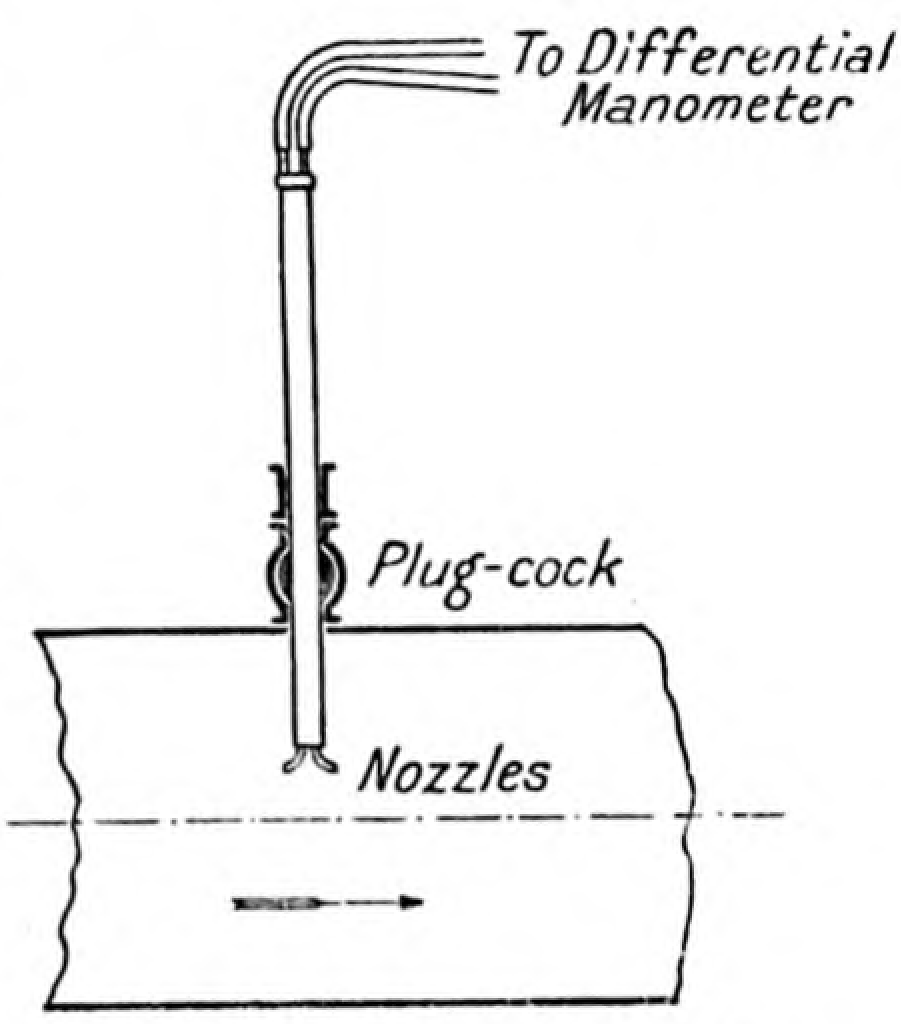

FIG. 449.—The Pitometer.

The differential pressure generated at the mouths of the two nozzles is read from a U-tube differential manometer (Fig. 441 (II)); this reading having been converted into terms of head of water h, the required velocity at the point is obtained from the equation $V = C\sqrt{2gh}$. The value of the coefficient C is read off from a calibration curve, of which a specimen is reproduced in Fig. 450. This curve reveals the advantage of using an

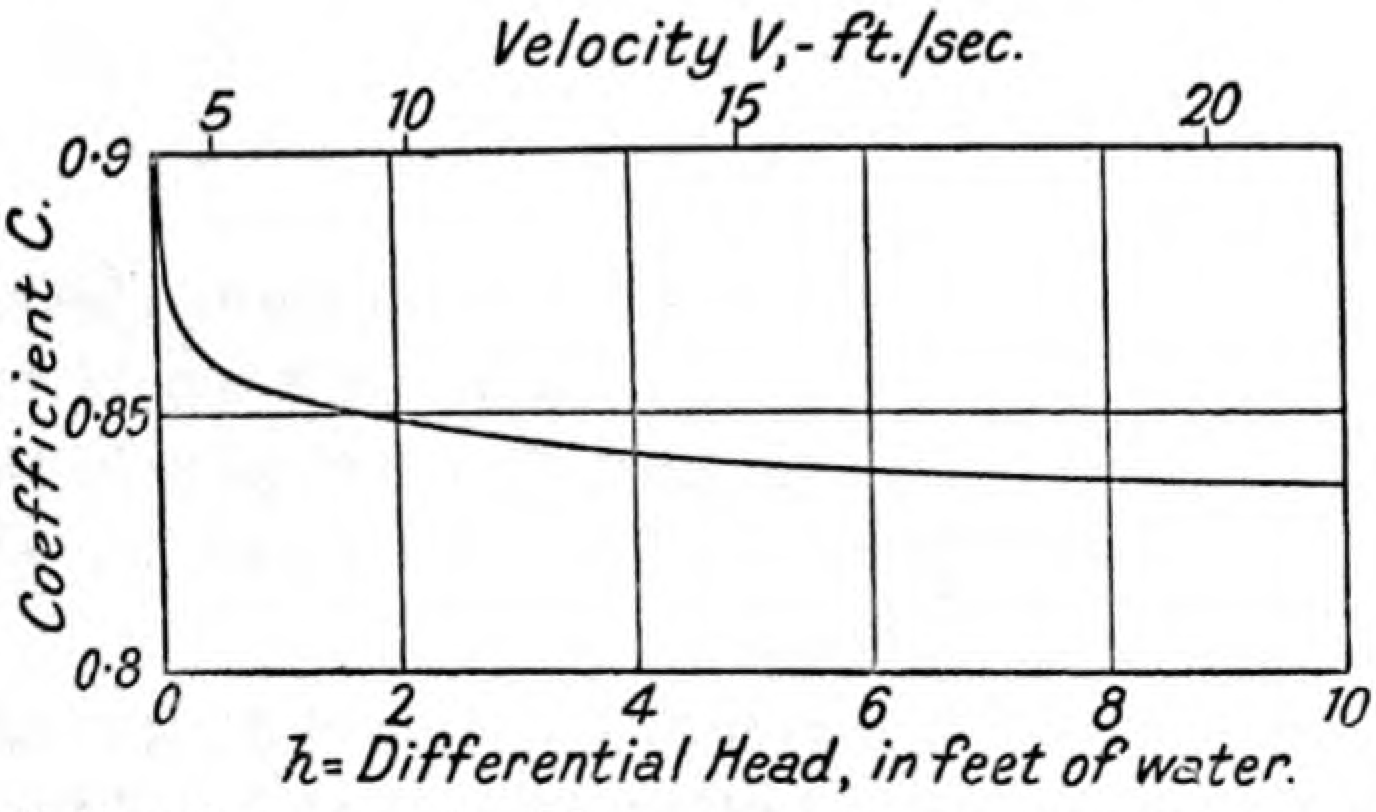

FIG. 450.—Calibration curve for Pitometer. (The British Pitometer Co., Ltd.)

upstream and a downstream orifice—the differential head for a given velocity is greater, and may therefore be read with a smaller proportional error, than when a single orifice is used.

If the mean velocity across the whole cross-section of the flowing stream is required, and hence the rate of discharge, the results of a number of velocity observations at different points must be integrated, as explained in § 391.

It is to be noted that in its usual form, the Pitot tube can measure the magnitude of liquid velocities, but not their direction: that is to say, before using the instrument we must know what is the direction of the liquid stream. If we do not know it, nevertheless adaptations of the Pitot tube are available for first of all determining the velocity direction, and then measuring the magnitude of the velocity. For two-dimensional flow, the *Pitot cylinder* is available; for three-dimensional flow, the *Pitot sphere* can be used.[289]

381. Velocity Measurements. (ii) *The current meter.* There are two general types of current meter. The *Price* meter (Fig. 451) has a ring of conical cups or buckets fixed to a vertical spindle mounted in a frame which is lowered into the open stream to the point at which the velocity is to be measured.

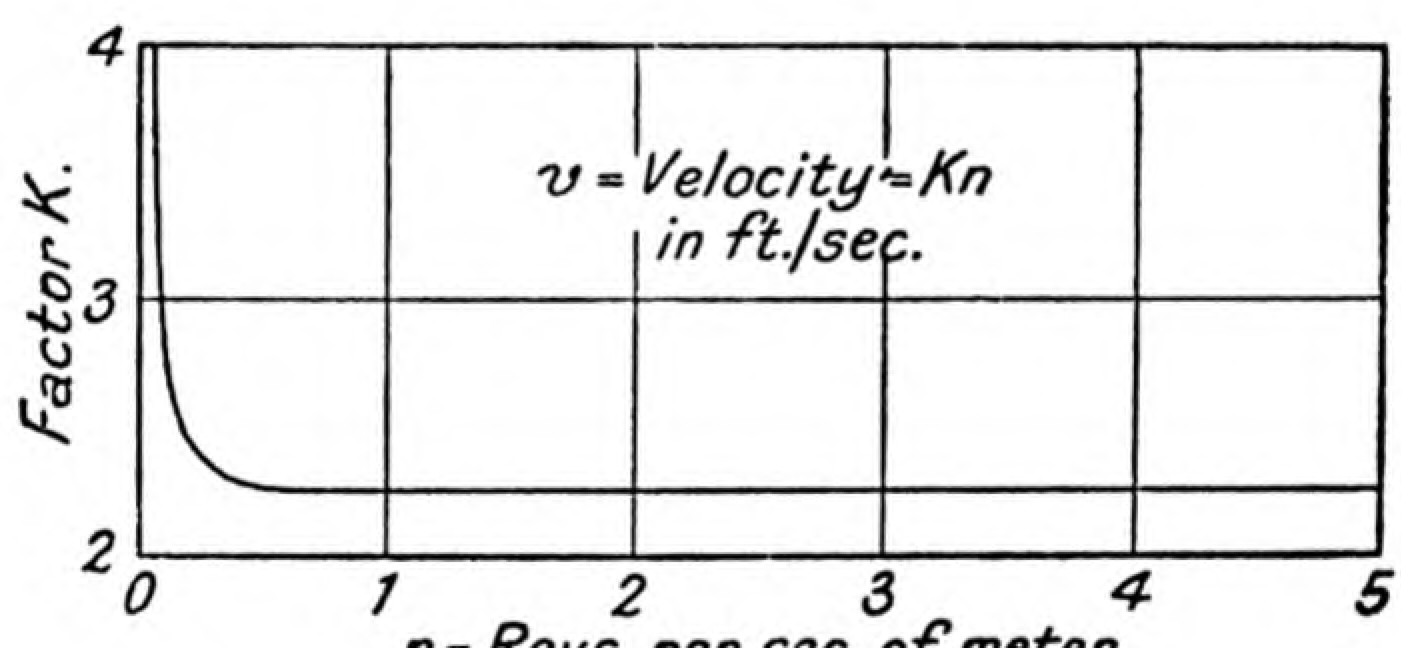

FIG. 453.—Rating curve for Price meter.

If the buckets were stationary, the dynamic thrust of the moving stream on the buckets concave to it would be greater than on those convex to it (§ 121 (*c*)), consequently they begin to revolve, and finally reach a steady speed at which the thrusts are equalised.

The indication of the speed of rotation is carried out by an electrical contact, closed at every revolution of the spindle, which operates, by means of a small battery and flexible leads, a bell, buzzer, or other signalling device in a suitable position above water-level. These signals are noted by an observer provided with a stop-watch. The stream velocity corresponding

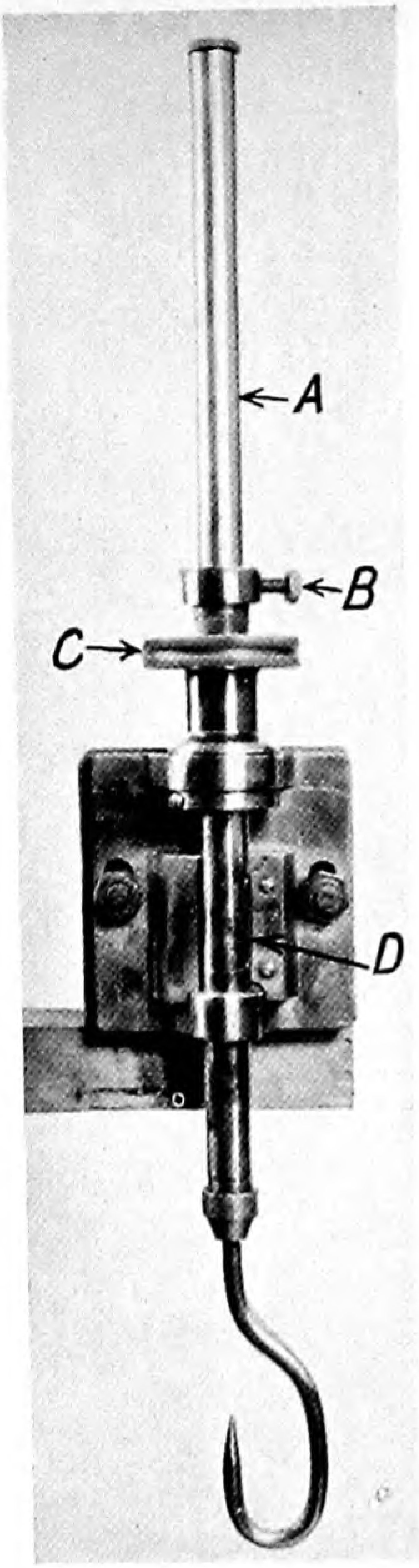

FIG. 446.—Hook gauge.
(See page 558.)

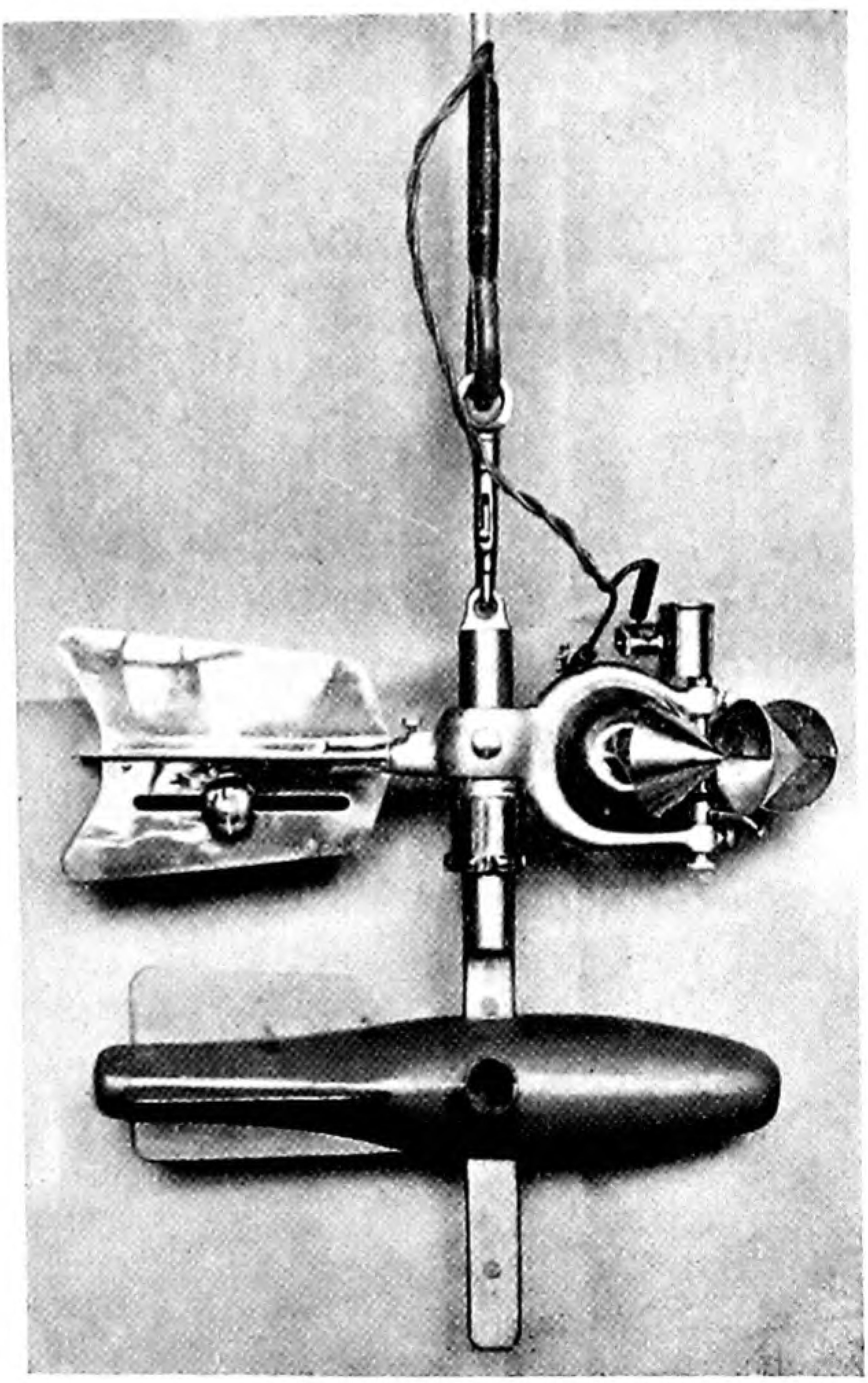

FIG 451.—Price current meter.
(E. R. Watts & Co., Ltd.)

[*To face page* 562.

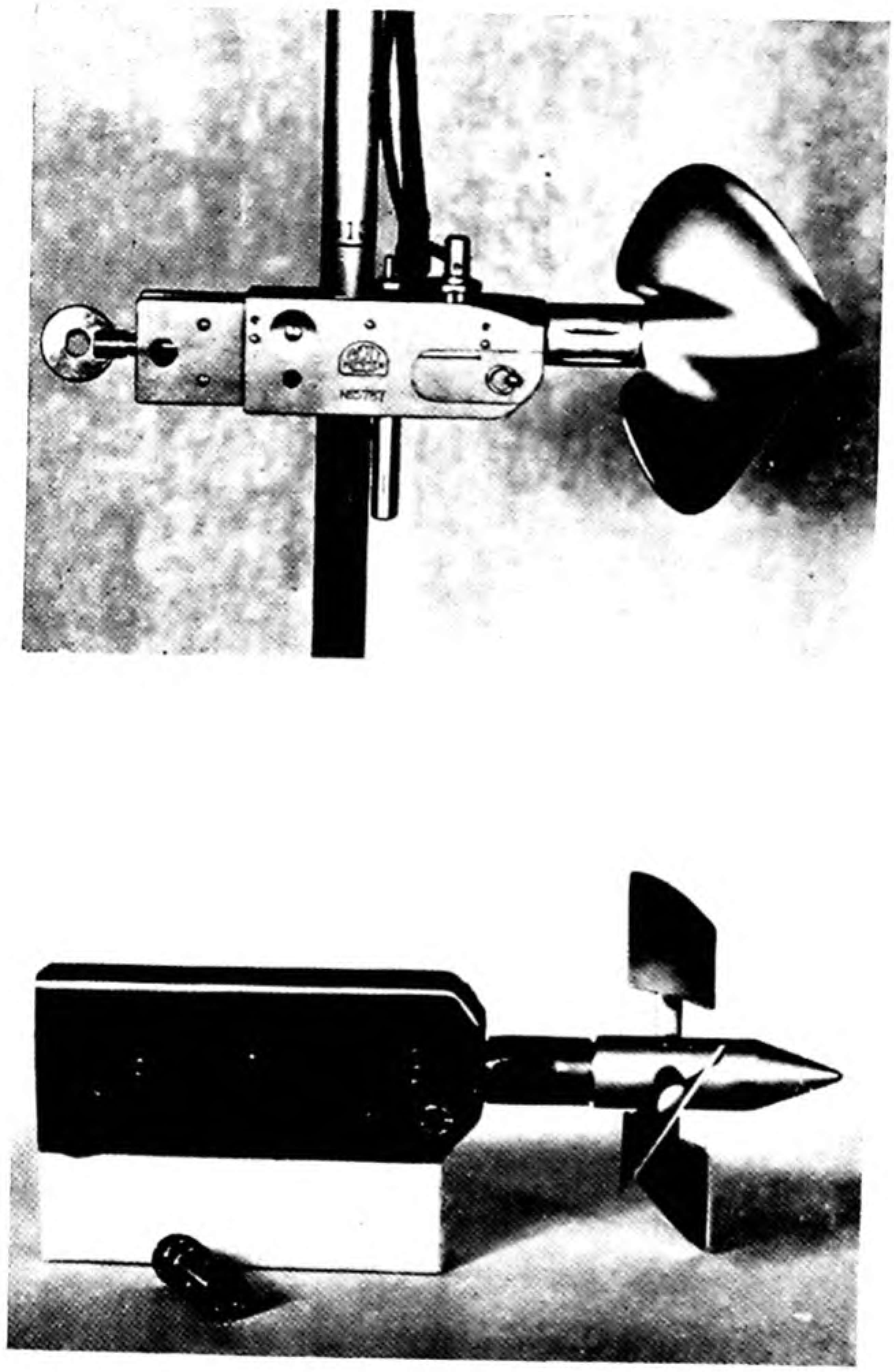

FIG. 452.—Propeller type current meters. (Dr. A. Ott.)
(above: screw-type: . . . below: spoked-type)

[*To face page* 563.

with the observed speed of the current meter is read off from a calibration chart or table (Fig. 453).

The *propeller* type of current meter (Fig. 452) is set with the axis of its 2- or 3-bladed propeller parallel with the direction of flow of the stream. A worm formed on the propeller spindle engages with a wormwheel which actuates a contact and so delivers audible signals in a similar manner to that described above. Alternatively the impulses may be automatically recorded on a tape chronograph.

An advantage of the propeller type of meter is that its registrations are less affected by turbulence than are those of the Price meter. If the Price meter[290] is used in greatly disturbed water, it always indicates a velocity greater than the true mean velocity at the point; the propeller meter, and especially the 3-bladed form shown in Fig. 452 (lower), registers only velocity components parallel to its axis.

The calibration or "rating" curve required with all types of current meter is constructed empirically from the results of rating tests made on the individual instruments, the meter being towed through still water at known speeds. The rating curve for a Price meter, reproduced in Fig. 453, shows how nearly the relation between speed of meter and velocity of water is a linear one, even down to very low velocities.

Measurement of Rate of Discharge.

When a liquid is flowing along a parallel waterway of known cross-sectional area, the rate of discharge may be obtained either by passing the whole flow into or through some suitable measuring device, or by measuring the velocity at a number of points in the cross-section of the conduit. The methods to be described first are those likely to be found convenient in hydraulic laboratories, works testing plants, etc., where it is usually quite practicable to divert the flow into special measuring appliances.

382. Absolute Methods. The fundamental method of discharge measurement, and the method against which all others should whenever possible be checked, is to collect and measure in a calibrated tank or reservoir the quantity of liquid q flowing in time t. The mean rate of discharge Q is then $\frac{q}{t}$. For small

discharges a tank mounted on a weighing machine serves very well; larger flows must necessarily be collected in tanks calibrated in units of volume (§ 379). Gauge tubes or float gauges are suitable for measuring the change of surface level in the tank during the test.

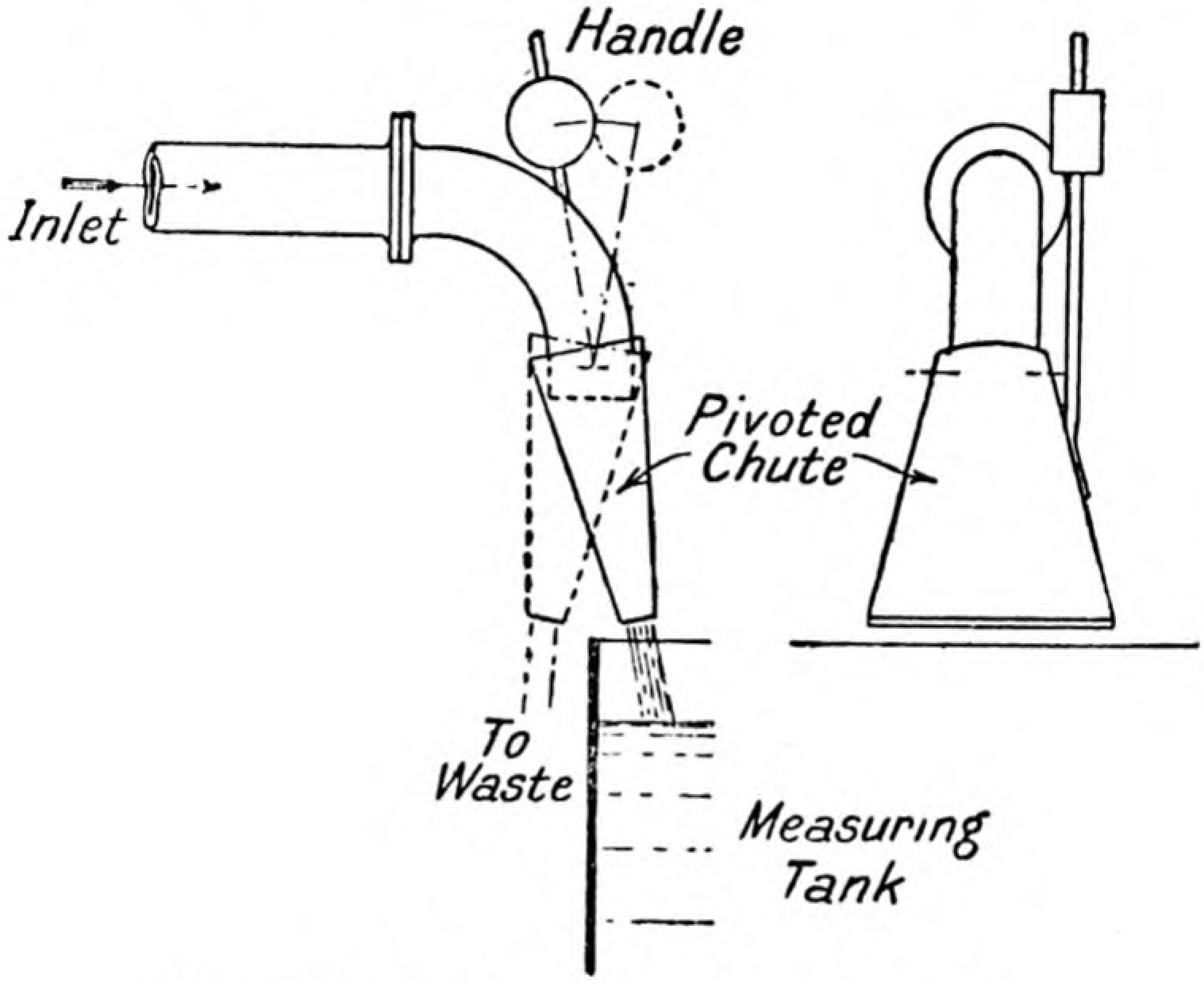

FIG. 454.—Inlet gear for measuring tank.

Among the precautions to be observed are:—

(i) The tank must be big enough to permit a duration of test t of at least 100 secs., and longer if possible.

(ii) A correction must be made for leakage, if measurable, through the walls of the tank or reservoir and past the outlet valve.

(iii) A quick operating gear for switching the liquid into the tank or to waste at the beginning and end of the test is essential; a suggestion is given in Fig. 454. A useful type of emptying valve is shown in Fig. 154 (III).

(Example 209.)

383. Travelling Screen Method. In principle this also is an absolute method, but instead of letting the water level rise in the measuring tank, we make one end of the tank movable and deduce the rate of discharge from the speed at which the incoming water pushes the movable end along. The tank takes the form of a long cement-lined channel whose bed is truly level and whose walls are truly plumb and parallel.

On the top of the walls a pair of accurately levelled rails are laid, forming a track for a light trolley with ball-bearing axles. The travelling screen which constitutes the movable end of the tank is hung from the trolley so that it may either be drawn up clear of the water or lowered so that it fits vertically with very small clearances across the channel.

When conditions of flow in the channel are stabilised, the trolley is taken to the upstream end, the screen is lowered, and the whole contrivance soon attains a uniform speed; the speed over a measured length of track is then recorded by an electric chronograph, and the required mean velocity of the water is obtained by adding to the speed of the trolley a small correction to allow for friction and leakage.

Evidently so costly an installation can only be considered at all when a long series of high-precision gaugings is in question.

384. Orifice Method. In this simple method, which enables small discharges to be measured with an error that ought

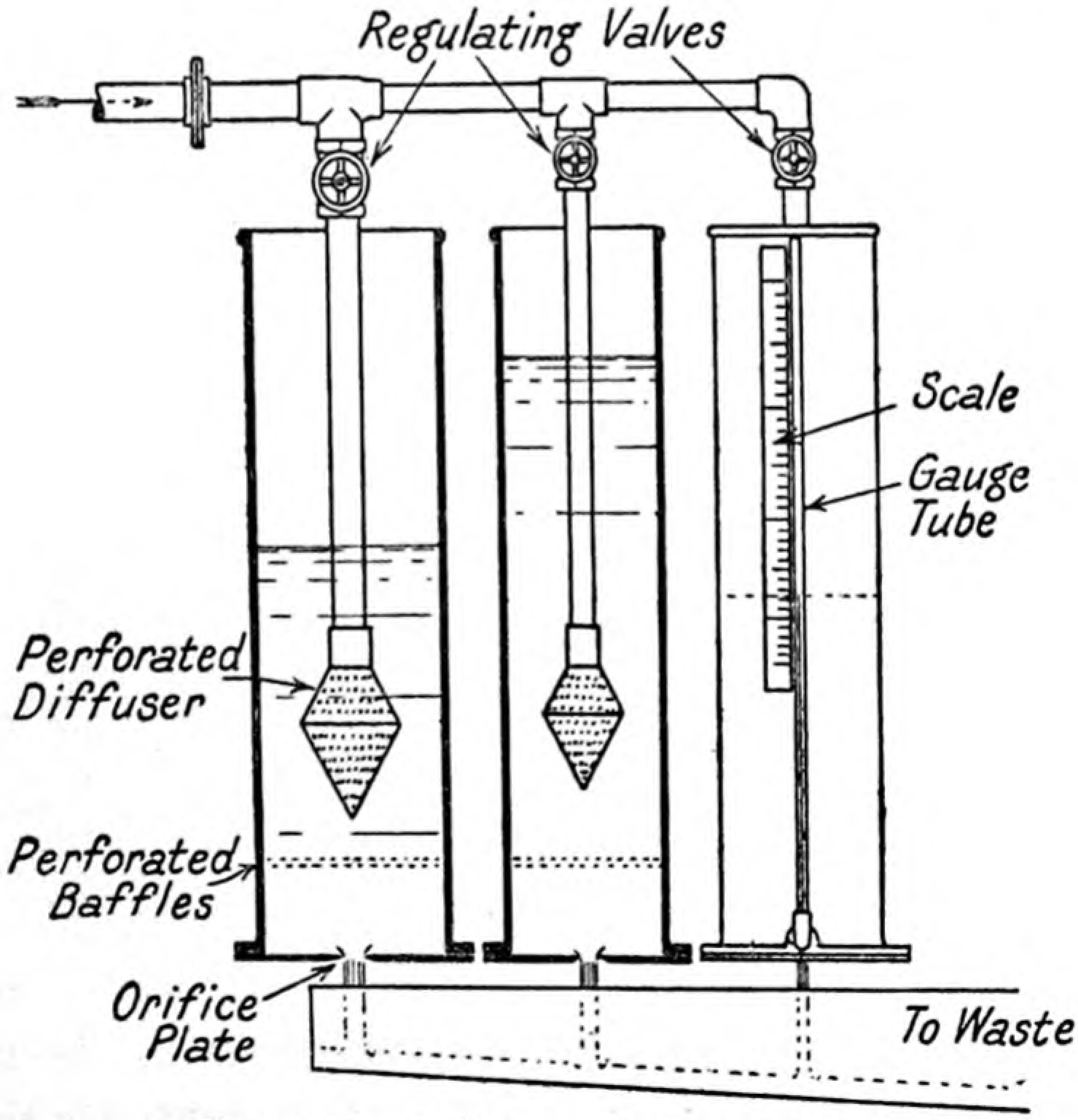

FIG. 455.—Orifice gauging apparatus.

not to exceed 1 per cent. or 2 per cent., the liquid is diverted through one or more orifices or nozzles and the head over the orifice is read from a glass gauge tube. Since this head varies

approximately as the square of the discharge, its range will be inconveniently great if the flow is very variable, and it is therefore advantageous in such cases to have a number of gauging tanks mounted side by side (Fig. 455), the orifices being of different sizes—having areas, say, in the ratio 1 : 2 : 6.

By suitably regulating the inlet valves, the liquid can be measured in whichever combination of tanks gives the greatest head, and thus all discharges over a range of 1 : 20 can be gauged with nearly uniform accuracy. If the scales on the gauge tubes cannot be directly calibrated with reference to a standard measuring tank (§ 382), then formula 4-2 (§ 43) may be used for sharp-edged orifices. In any event the graduations permit the flow to be read off at once in terms of lit./sec., gallons per minute, etc., as desired.

385. Gauging by Sharp-edged Weirs. For the range of discharges met with in works and laboratories, the 90° *V*-notch and the rectangular weir with suppressed end contractions

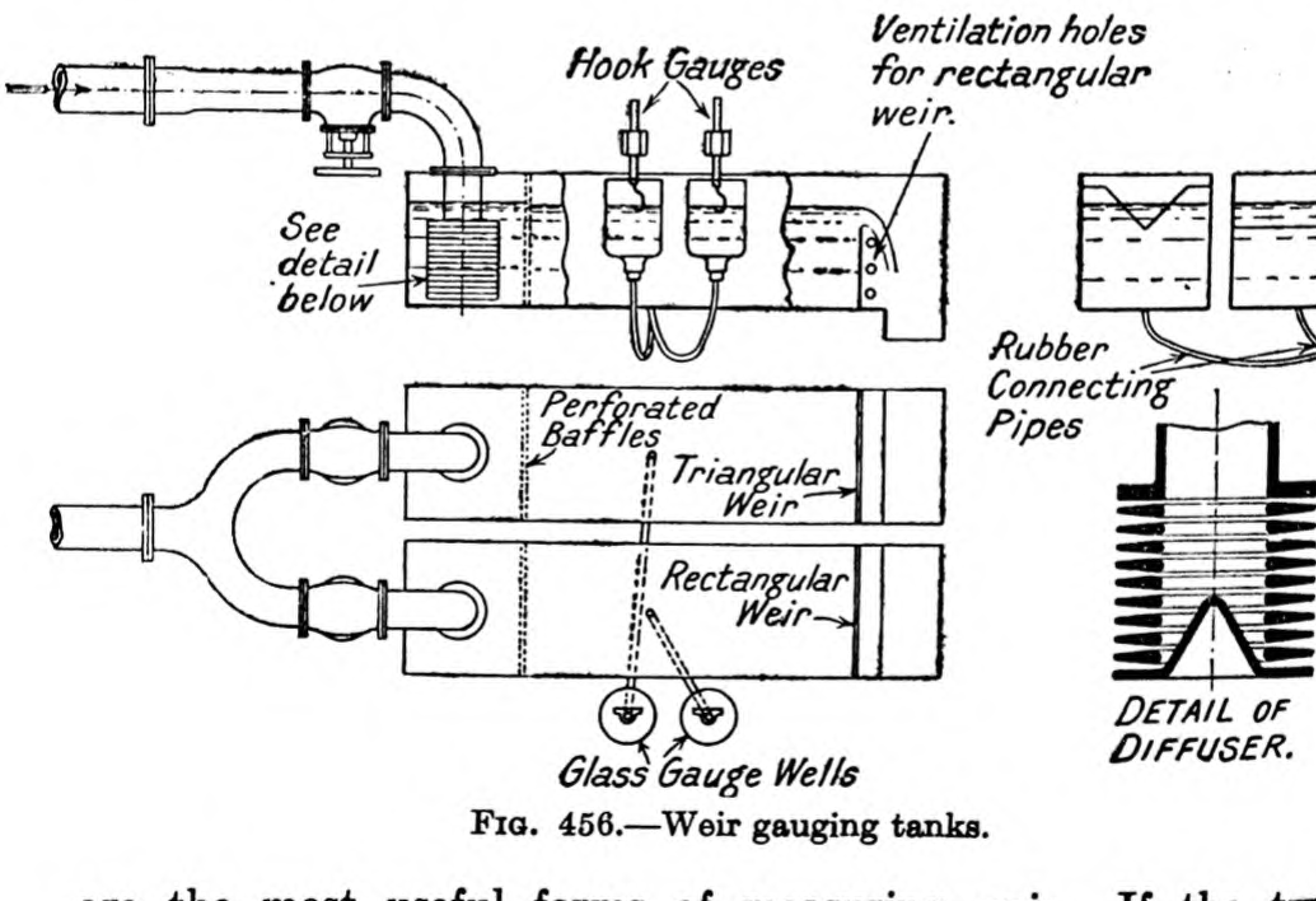

FIG. 456.—Weir gauging tanks.

are the most useful forms of measuring weir. If the two are arranged in parallel, as in Fig. 456, a considerable range of flows may be dealt with in the one apparatus. The incoming water should be led into the gauging tank below the surface level, so as to avoid splashing and air bubbles: the simple type of diffuser shown in the diagram, consisting

of cast-iron taper flanges threaded together, is most effective in damping out major eddies before the water reaches the perforated baffles.

If the tanks are set at about eye level, the hook gauges, mounted each in a glass gauge well, can be adjusted either by looking down at the points or by looking upwards at their reflections in the water surface; when the point appears to meet its reflection, the adjustment is correct. Fixed point gauges, set exactly in the plane of the weir crests by means of a spirit level and straight-edge, serve as reference points for establishing the zero readings of the hook gauges. This zero reading or still water reading is substracted from the hook-gauge reading taken when water is flowing: the difference represents the desired weir head H.

For the triangular notch, the discharge formulæ at the end of § 54 are recommended;[291] the Rehbock formula (§ 57) is suitable for the rectangular weir. In neither case is any velocity of approach correction necessary, provided that the mean velocity in the V-notch gauging tank does not exceed 0·5 ft./sec. (0·15 m./sec.).

Occasionally it is advantageous to use a weir of such a shape that the head over the weir crest is directly proportional to the discharge. This requires an opening in the weir plate taking the form of a vertical slot, wider at the bottom than at the top; the device is then termed a *proportional weir* or a *Sutro weir*.[292]

Measurement of Rate of Discharge in Closed Conduits.

386. Classification of Flow-meters. Meters are industrial instruments designed to give direct information about the quantity of liquid flowing under pressure along a pipe-line.[293] As a rule no calculation or manipulative skill of any kind is required, the quantity or the rate of flow being indicated by pointers or recorded on charts.

Rate-of-flow meters measure the instantaneous rate of discharge along the conduit, the units here being gallons per minute, cubic feet per second, or in general, volume in unit time. These devices usually comprise two separate elements,

(i) a primary element through which the liquid flows, thereby generating a differential head, and (ii) a secondary element which responds to the differential head and perhaps translates it into terms of rate of flow, §§ 387-389. But sometimes the two elements are combined, and a movable component directly indicates the rate of flow. Such an instrument is the *Rotameter*.

Quantity, *total-flow*, or *volume* meters (§§ 393, 394) are those which show the total quantity of liquid, in gallons, cubic feet, or other units of volume, that has passed through the pipe during the interval between two successive readings.

By suitable modification or computation, either class of meter can be made to give the information that the other class is primarily intended to yield. Thus the mean rate of flow passing through a quantity meter is found by dividing the total flow by the elapsed time, while the total volume flowing through a rate-of-flow meter may be obtained by a process of graphical or mechanical integration (§ 390).

Quantity meters are subdivided into

(i) *Inferential* meters, in which the revolutions of a rotating element acted upon by the flowing liquid are counted, § 393.

(ii) *Positive* or *displacement* meters, in which the record of total flow is based upon counting the number of times that measuring-chambers of known volume are successively filled and emptied.

387. The Venturi Meter. In the Venturi meter the desired differential head is generated by causing the water to flow through a narrowed throat (Fig. 457), the water then passing into a diverging taper section in which a proportion of the velocity energy is reconverted into pressure head.[294] To ensure that mean pressure heads are registered at the up-stream gauge point and at the throat, a ring of small radial holes at each of these positions communicates with a circumferential belt to which the actual pressure connections are made.

Differential mercury or water gauges (§ 373), float gauges (§ 377), or the single column mercury gauge (§ 372 (iii)), are suitable for indicating the differential head, according to the range of flow and the static pressure in the pipe. The last-named is often the most convenient form of instrument; the

upstream gauge point of the meter is connected to the mercury container of the gauge (Fig. 439 (III)), and the throat of the meter to the top of the indicating column. (Note that the formula in § 372 (iii) is now no longer applicable.) The scale may be calibrated directly in units of discharge, so that the rate of flow is read off at once from the position of the mercury column. If the mercury column is short and wide, the motion of an iron float riding on its surface can be made to actuate a pointer travelling over a circumferential dial scale graduated in lit./sec., gals./min., etc. (Fig. 462).

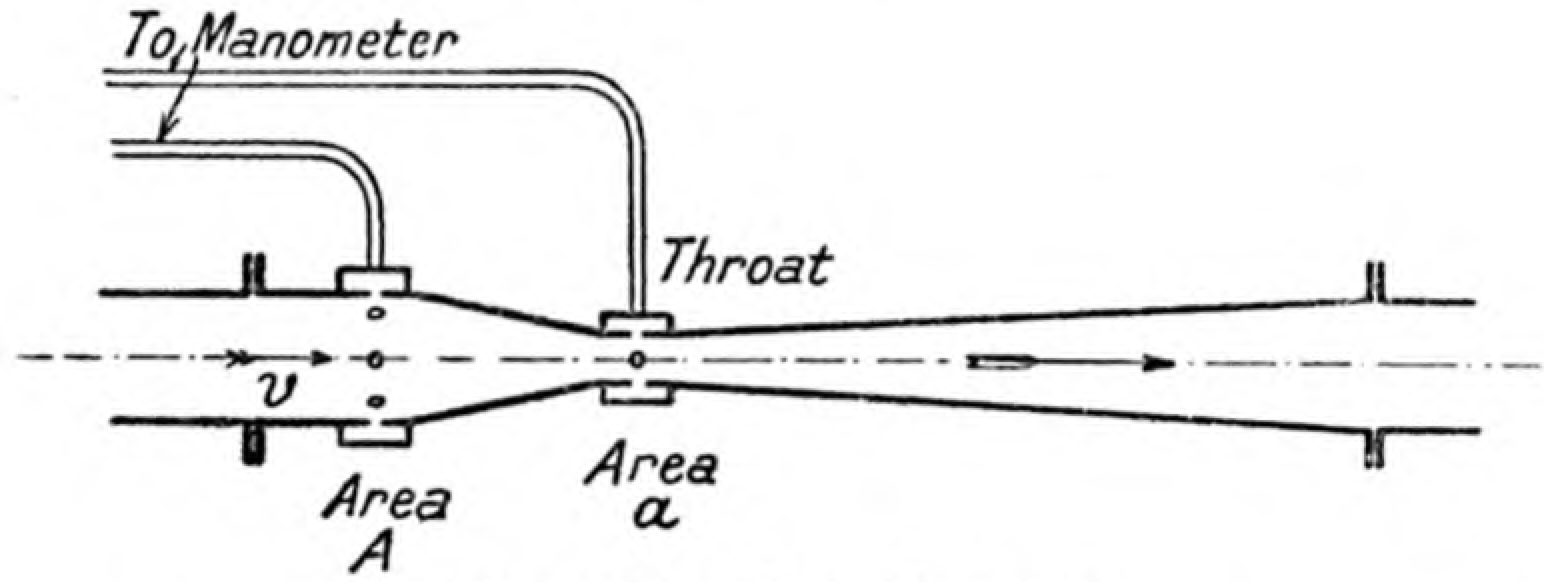

FIG. 457.—Venturi meter.

The relation between differential head, in terms of head of liquid being measured, h, and the discharge Q, is established as follows :—

By Bernoulli's theorem (§ 33), loss of pressure energy h can be equated to gain in velocity energy, viz.,

$$h = \frac{\left(v \cdot \frac{A}{a}\right)^2 - v^2}{2g},$$

where v = velocity in pipe at upstream connection,

A = area of pipe,

a = area of throat.

Therefore
$$v = \sqrt{\frac{2gh}{\left(\frac{A}{a}\right)^2 - 1}}.$$

To allow for friction and imperfect energy conversion, a coefficient of discharge must now be introduced, viz.

$$Q = C_d A v = C_d A \sqrt{\frac{2gh}{\left(\frac{A}{a}\right)^2 - 1}}.$$

The value of C_d may provisionally be taken as 0·975 ; but it will be evident from § 93 that with small pipes or low rates of flow, lower values may be expected.(295)

The Venturi meter is a simple and reliable instrument, suitable for a great range of pipe sizes—say from 2 inches to 20 feet diameter. **(Example 210.)**

388. Orifice Meters. These meters utilise the pressure drop sustained when water flows through a pierced diaphragm or orifice in a pipe (§ 87 (*d*)) ; they differ from the Venturi meter only in the sense that no provision is made for recovering head, viz. for reconverting velocity head into pressure head.(296) Thus, whereas in the Venturi meter the overall loss of energy need not exceed 15 per cent. of the differential or measuring

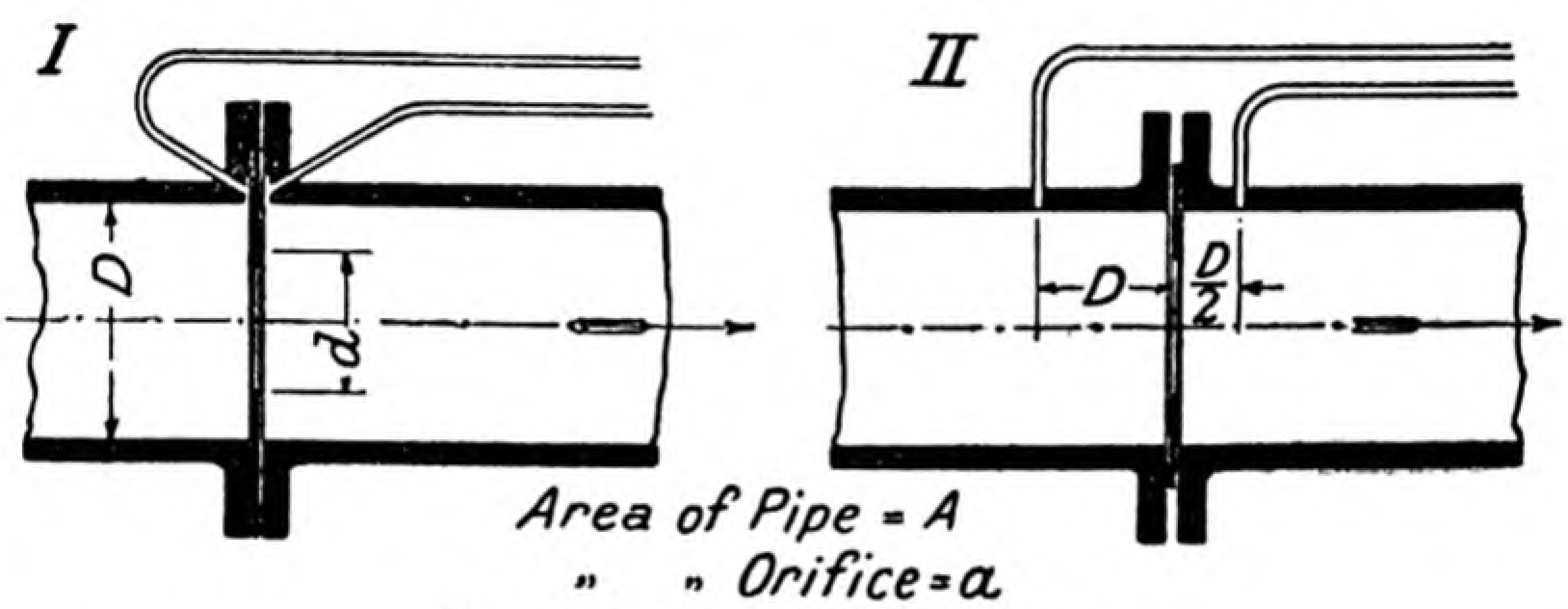

FIG. 458.—Orifice meters.

head, in the orifice meter this loss may be 50 per cent. or even 80 per cent. of the differential head.(297) In both meters there is the same relationship between the differential head h and the discharge Q, viz.

$$Q = C_d' \cdot A \sqrt{\frac{2gh}{\left(\frac{A}{a}\right)^2 - 1}} \quad \text{or} \quad Q = C_d' a \sqrt{\frac{2gh}{1 - \left(\frac{a}{A}\right)^2}}.$$

The most consistent values of the coefficient C_d' prevail when the connections are made actually in the plane of the orifice plate (Fig. 458 (I)) ; here the plate is simply a flat ring of sheet brass or monel metal, about 1 mm. thick, having a plain parallel hole (not bevelled), clamped between adjacent flanges in the pipe-line. The graph (Fig. 459) (full lines) indicates the relationship between the orifice ratio $\frac{a}{A}$, the nominal Reynolds number $R_n = \frac{\frac{Q}{a} \cdot d}{\nu}$, (§ 64) and the coefficient C_d'. The broken

line shows the value of the corresponding coefficient C_d'' for Reynolds numbers from 400,000 to 800,000, if the pressure connections are made at a distance D upstream and $\frac{D}{2}$ downstream from the orifice plate (Fig. 458 (II)).

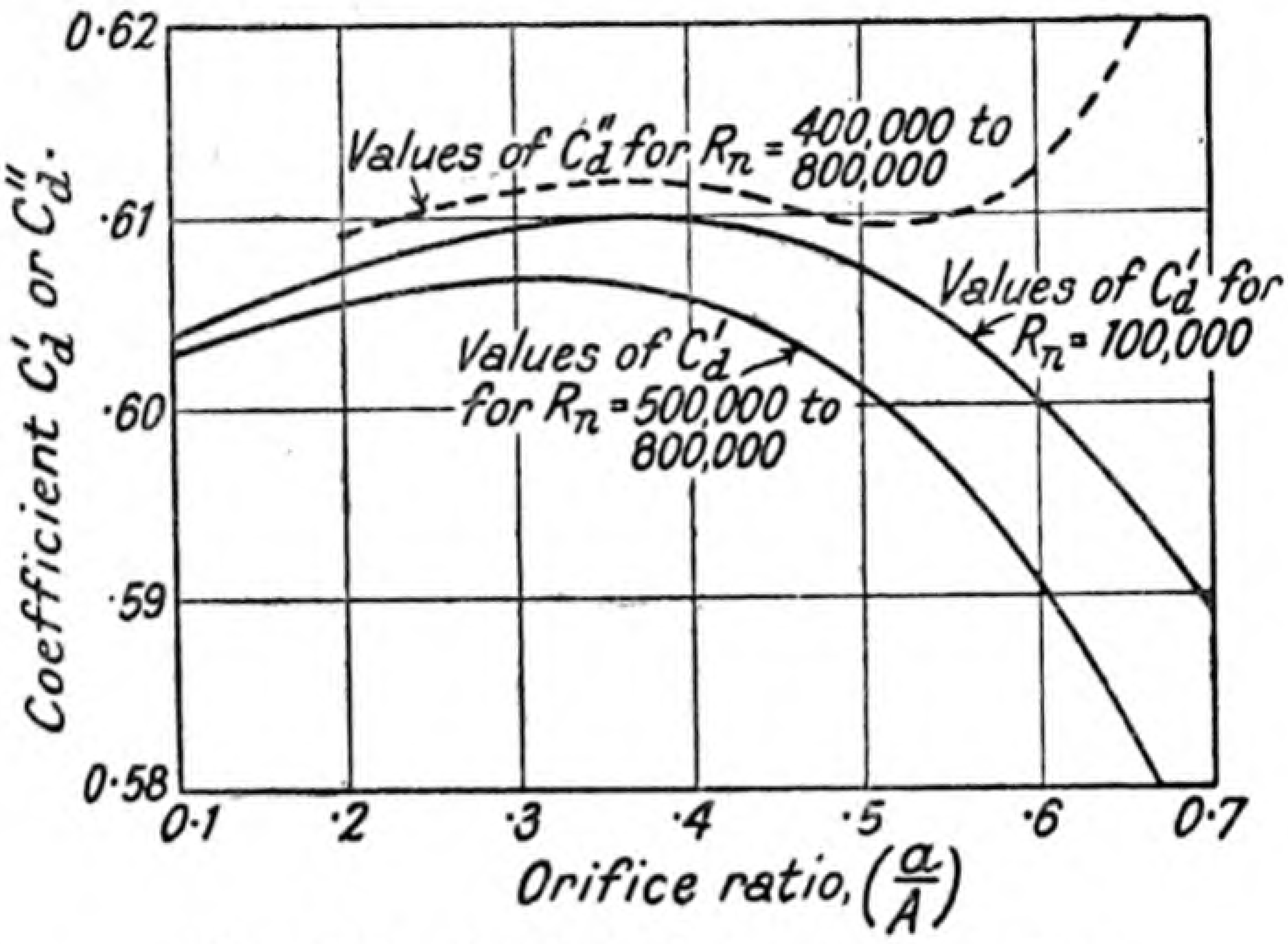

FIG. 459.—Coefficients for orifice meter.

Any of the gauges or "secondary elements" mentioned in the preceding paragraph for measuring the differential head in a Venturi meter is equally suitable for the orifice meter. An interesting type of single-column mercury manometer designed

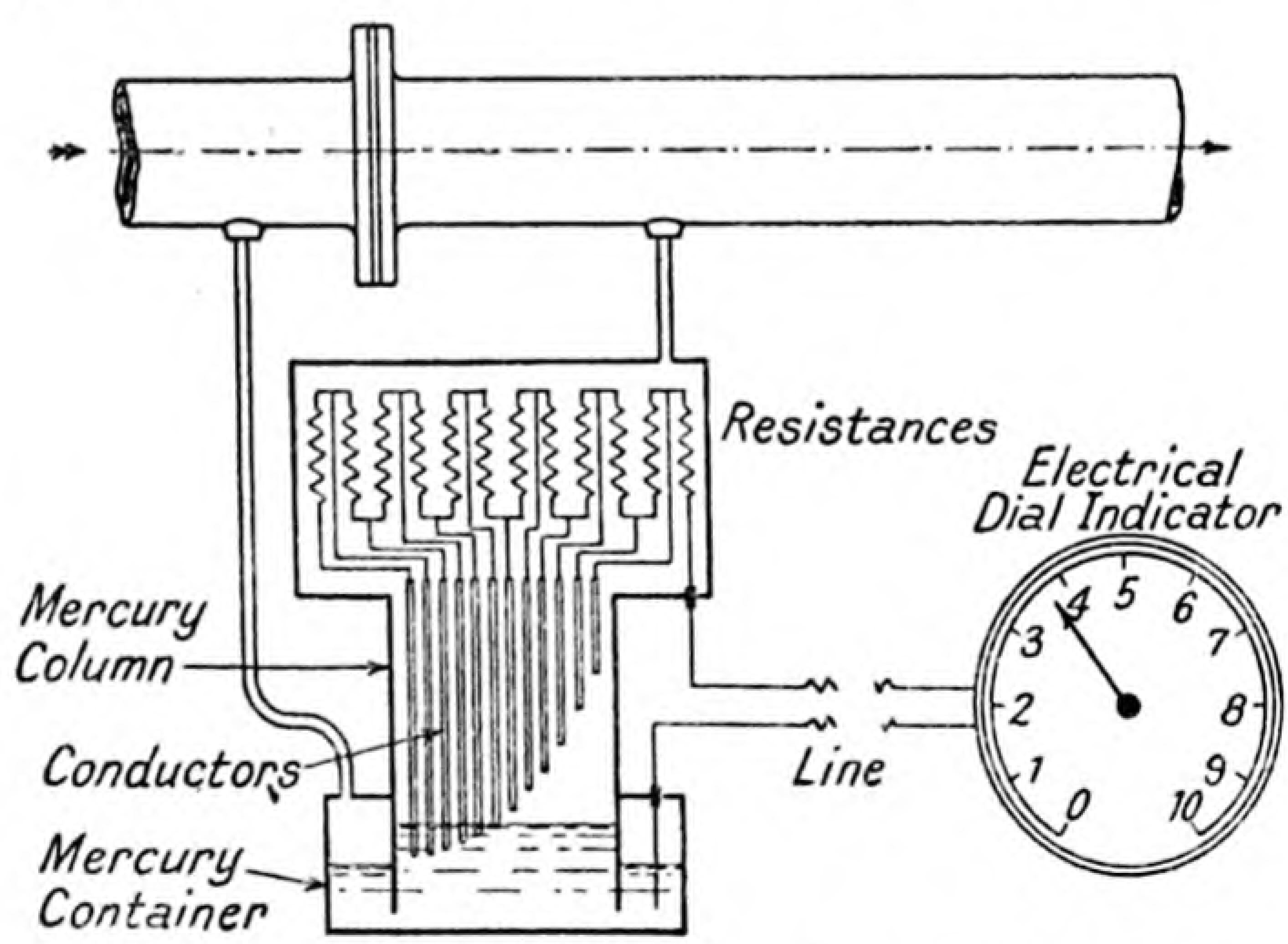

FIG. 460.—Principle of distant-reading orifice meter.

to transmit readings electrically to distant dial gauges has been developed by Messrs. Electroflo Meters, Ltd. (Fig. 460). Conductors of graduated lengths project vertically downwards above the short, wide mercury column; as the mercury

surface in the column rises due to an increase in differential head, it makes contact in turn with more and more of the conductors, so cutting out of circuit the electrical resistances interconnecting the upper ends of the conductors. The current flowing through the electrical circuit can thus be made exactly proportional to the water flow in the pipe, and the distant indicators from which readings are taken may consist simply of an ammeter and a watt-hour meter, the one graduated in units of *rate* of discharge and the other in units of *total* discharge.

Venturi and orifice meters should if possible be set in such a position that the liquid immediately before reaching them traverses a reasonable length of straight pipe ; also the pressure at the throat or downstream connection should preferably not be less than atmospheric, because of the risk of air entering the connecting pipe and vitiating the readings. Especially with hot liquids, there is also the risk of vaporisation and consequent *cavitation* (§ 133) if the throat pressure is too low.

389. Pipe Bends used as Meters. The differential head generated when water flows round a pipe bend under approximately free vortex conditions (Fig. 461) can sometimes be used as a measure of the discharge.[298] The ideal relationship between q and h was established in § 141, and reference may now be made to the results of experiments which enable the actual flow q_a tobe roughly assessed. Writing $q_a = C_d\, q$, it has been found that for 90-deg. bends in circular iron and steel pipes the value of the coefficient of discharge C_d depends chiefly upon the ratio R/c (where R is the radius of the axis of the bend and c is the radius of the pipe). This coefficient ranges in value from about 1·02 when $R/c = 6$ to about 1·25 when $R/c = 2$. So long as the main velocity in the pipe does not fall below about 4 feet/sec., the value of the coefficient is little affected either by velocity changes or by turbulent conditions upstream of the bend. For making rough comparative measurements the bend meter has the unique advantage that it entails no additions or alterations to an existing pipe system, except for

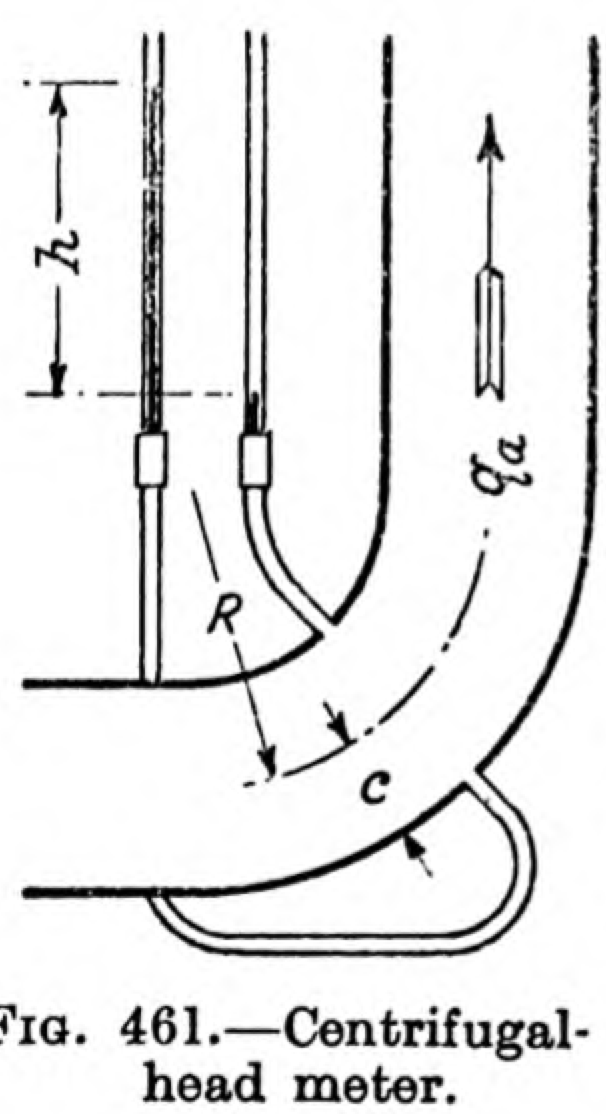

FIG. 461.—Centrifugal-head meter.

the drilling of the pressure orifices. If suitably calibrated, on the other hand, the meter may be used for precision measurements.

390. Flow Indicators, Recorders, and Integrators. (i) *Indicators.* The utility of flow-meters would be very restricted if the desired rate of discharge could only be known by making calculations of the sort explained in §§ 387 and 388. The modifications which permit direct readings to be made were briefly mentioned in § 387, and they are illustrated in Fig. 462. It will be noticed that the graduations are not uniform, but are more open at the upper range of flows ; this is a consequence of the quadratic relationship between discharge and differential head.

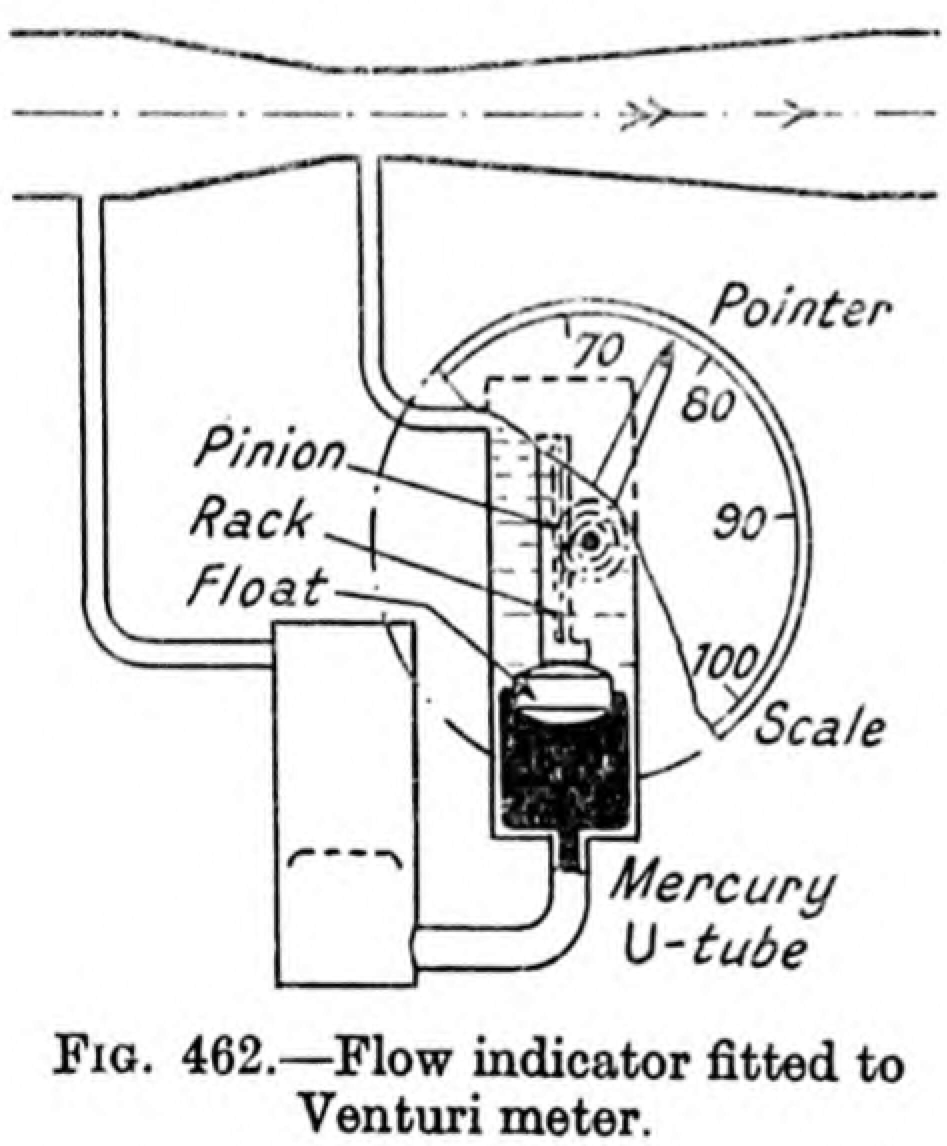

FIG. 462.—Flow indicator fitted to Venturi meter.

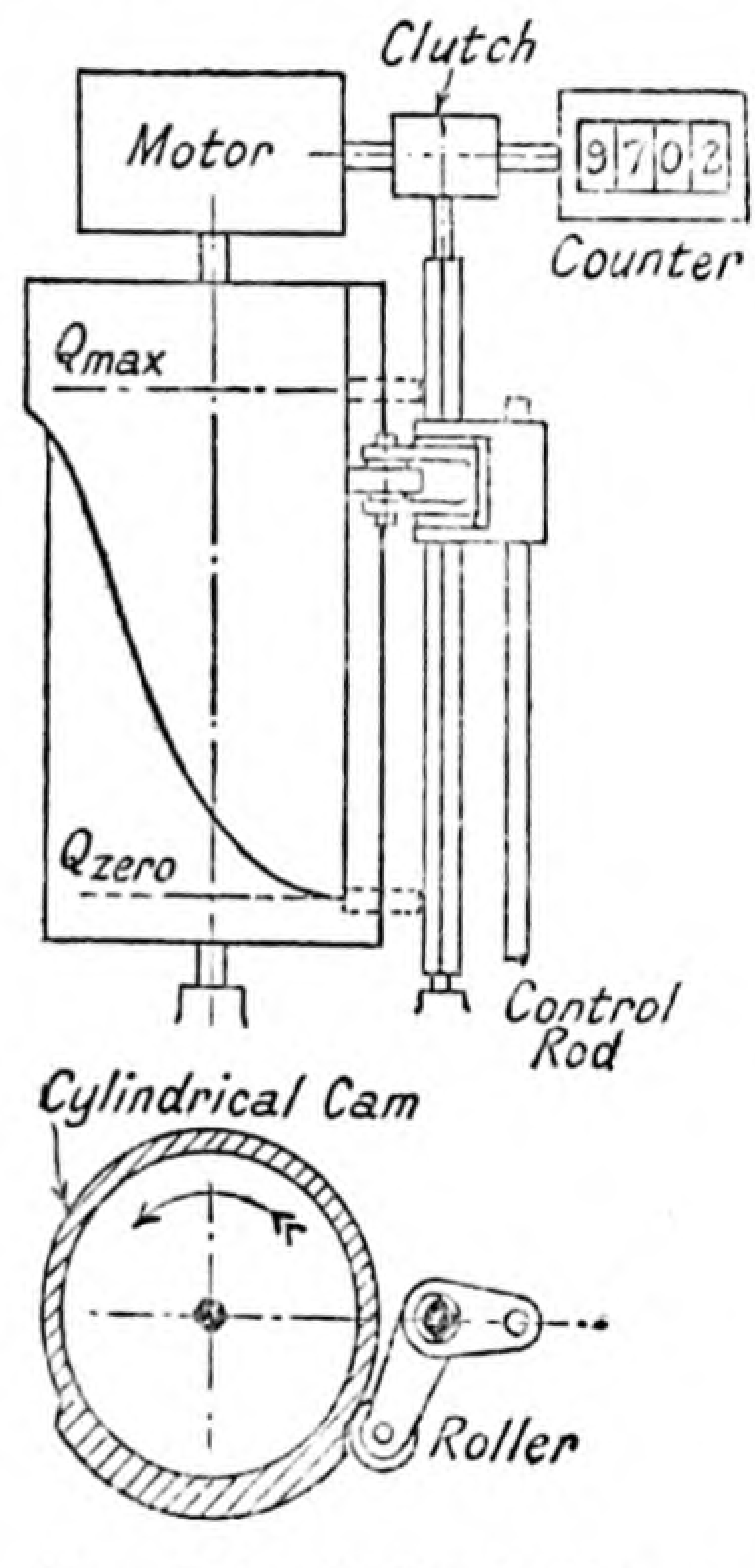

FIG. 463.—Cylindrical cam flow integrator.

(ii) *Recorders.* Having given the mercury column the means of actuating an external pointer, it is not a very difficult further step to provide a pen which will leave a trace on a chart moved by clockwork. When the chart is removed from the recorder at the end of the day or week, it represents a graph between time and rate of flow.

(iii) *Integrators.* The addition of an integrating device enables a rate-of-flow meter to register also the total volume of liquid that has flowed during a given period. This information can be read from a counter such as is shown in Fig. 463 ;

the counter is intermittently coupled to a constant-speed motor whose motive power may be clockwork or electricity. This motor also drives at constant speed a cylindrical cam whose surface is cut away as indicated in the diagram, the shape of the raised edge being such that when developed it would be a parabolic curve. The cam-roller can be traversed vertically by a control-rod coupled to the float of the mercury U-tube which forms the secondary element of thc flow-meter; the roller bracket is so mounted on a squared shaft that whenever the roller rides up on to the raised surface of the cam, the counter is clutched in to the motor, and the counter begins to register. As soon as the slow revolution of the cam has allowed the roller to drop back again, the counter is de-clutched and temporarily ceases to register.

Evidently, then, when there is no flow and no differential head is being generated, the control-rod and cam-roller will be in their lowest position and the counter will not register. When flow begins and the mercury surfaces in the U-tube are displaced, the figures of the counter will be advanced to a greater or less extent for each turn of the cam; and the parabolic edge of the cam ensures that the total registration is proportional to the total flow and not to the displacement of the control rod.

An electrical method of integration was illustrated in Fig. 460.

391. Pitot Tube. In using the Pitot tube (§ 380) to measure pipe flow, the mouths of the orifices are traversed in turn across two diameters of the pipe at right angles, so yielding two sets of velocity observations at a number of points —say 10 or 20—in each diameter. Plotting velocity against diameter, velocity distribution curves of the sort reproduced in Fig. 464 are obtained. The mean velocity over the whole cross-section is now computed as follows:—

The pipe cross-section is first divided into a number of rings of equal area, and each ring sub-divided into two equal areas by the broken circles seen in the figure. Considering the ring distinguished by hatching, we erect ordinates from the points at which it is intersected by the two diameters, and scale off from the velocity curves the actual velocities at these four points; the mean of these velocities gives the mean velocity over the ring. Repeating for the other rings,

the mean of the mean ring velocities will represent the desired mean velocity in the pipe. Multiplying this by the pipe area, we finally obtain the discharge.

The observations plotted in Fig. 464 were taken in an 8-in. pipe at a section where the flow was still much disturbed just after passing a bend and a T-piece in the pipe. If there are no such disturbances, if, that is, the flow is measured at the end of a long, straight length of pipe, then the relationships given in § 71 may be helpful. In such conditions

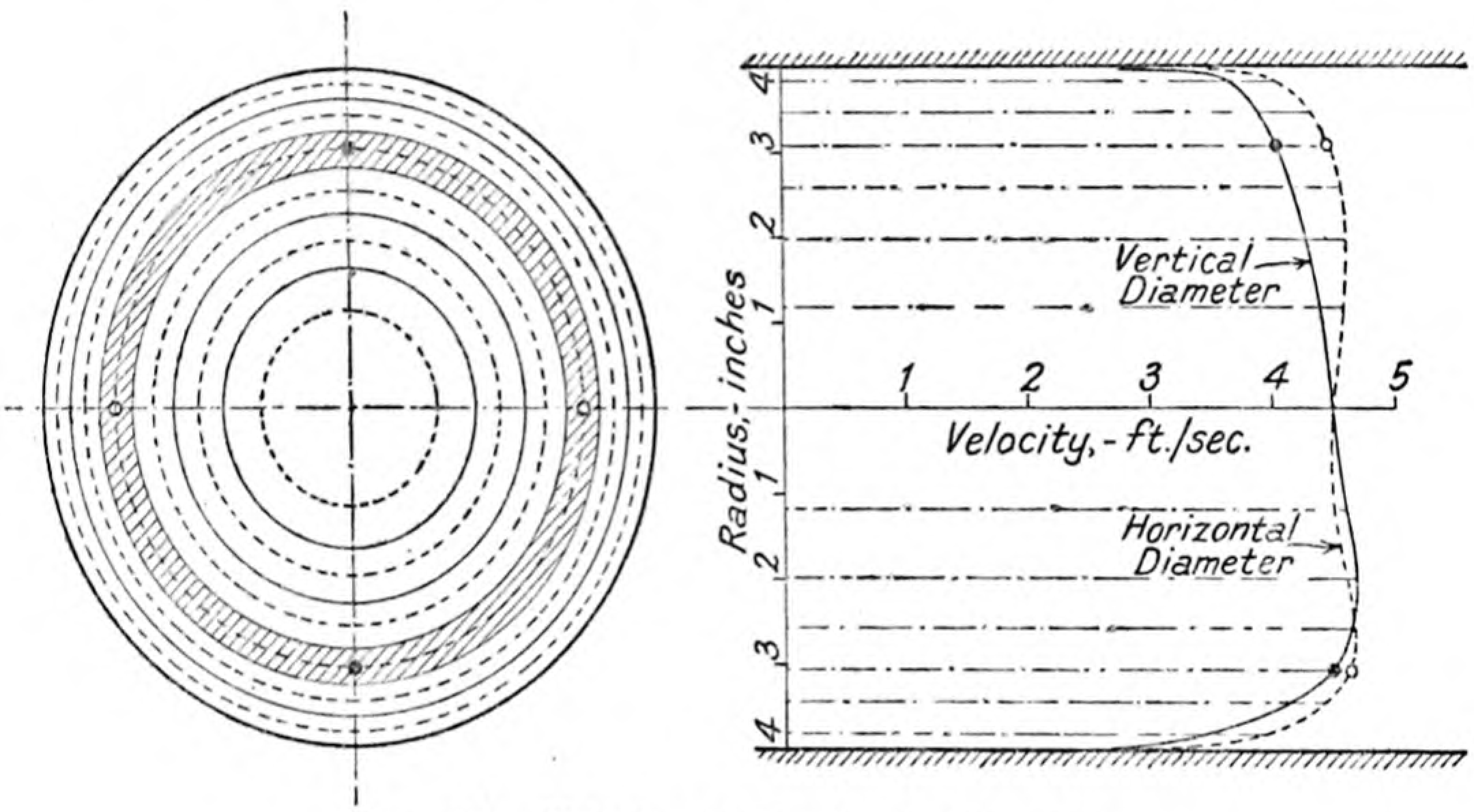

FIG. 464.—Velocity distribution in 8-in. pipe.

the local velocity u at a radius of $r = (\frac{3}{4} \times \text{pipe radius } R)$ is very nearly identical with the mean velocity v. Thus a single Pitot-tube measurement taken at this radius will enable a very close estimate of the discharge to be made. **(Example 211.)**

392. The Current Meter. The propeller type of current meter (§ 381 (ii)) can be used for measuring the flow in large pipes and conduits; it is secured to the end of a rod projecting into the pipe and traversed across two diameters in the same way as the orifices of a Pitot tube. The method of computing the discharge follows the same lines as those just explained.

To reduce the duration of the observations, two or more instruments may be mounted on the same rod; on the other hand, if means for calibrating it are available, a single meter may be permanently fixed at the pipe axis.

393. Rotary Meters. A type of current meter specially suited for pipes of 2 in. to 18 in. diameter is represented in Fig. 465. Here the propeller is of nearly the same diameter as the pipe; it operates through a train of non-corrodible gears a dial or counter mechanism which registers the total flow in gallons, litres, etc. The graphs (Fig. 466) show that the helical meter remains sufficiently accurate for commercial purposes over a wide range of flow, and that the loss of head suffered by the water passing through it is relatively small.

The flow in smaller pipes, down to $\frac{1}{4}$ in. diameter, can be measured by the vane-wheel meter, of which a sectional view is given in Fig. 467. The little celluloid or vulcanite wheel is rotated by the flow of water in the manner of a turbine runner; the total revolutions, converted into terms of water volume, are indicated on the dials.[299]

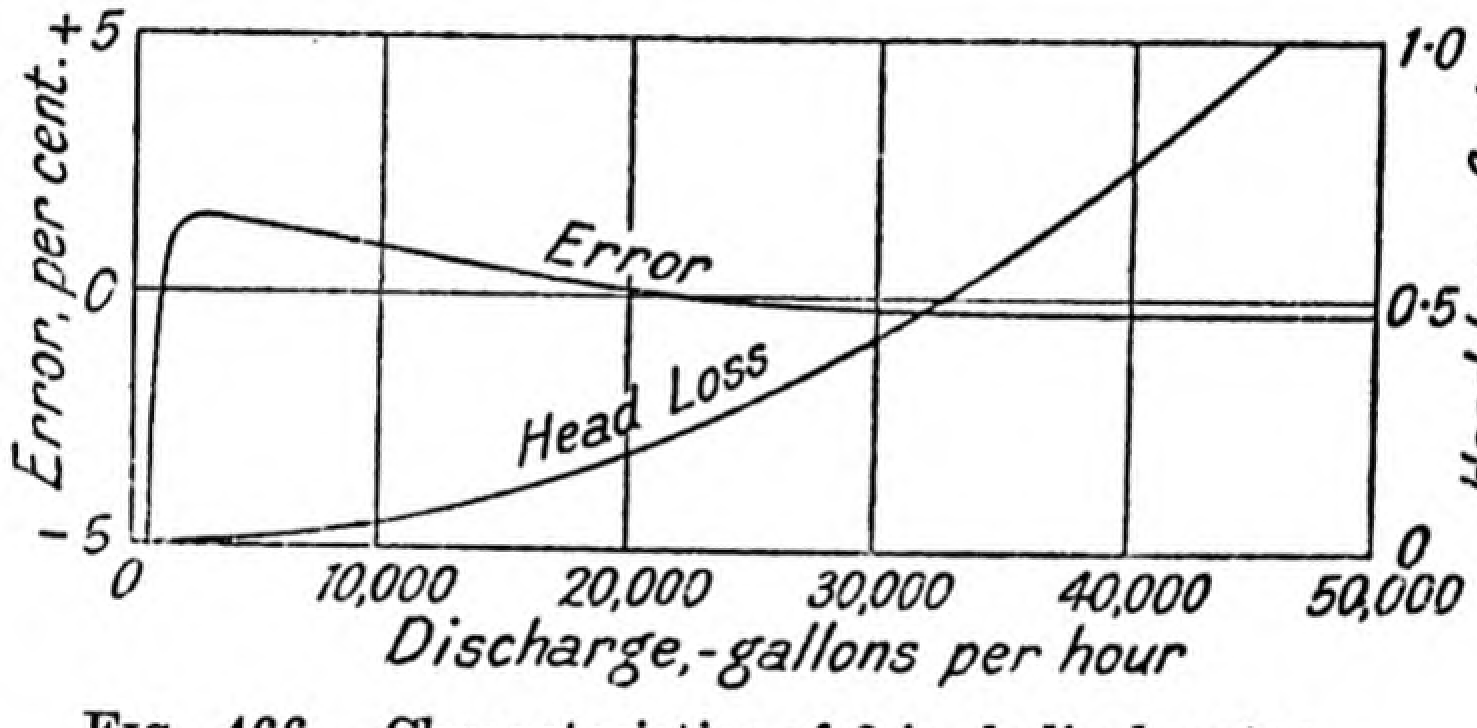

FIG. 466.—Characteristics of 6 in. helical meter.

The particular advantages of these meters are (i) the ratio between minimum and maximum registered flow can be far greater than in any apparatus depending upon differential head; (ii) the total volume flowing through the meter is directly recorded, without the need for integrating mechanisms; this information is often more useful than the instantaneous rate of discharge, especially when water is being delivered to consumers who pay by the gallon or the cubic metre.

Rotary meters, unlike differential head meters, §§ 387-389, are not unduly sensitive to the conditions in the pipe system in which they are installed. Yet if the liquid is allowed to approach the meter in a state of excessive turbulence, or if other gross irregularities of flow are permitted, the meter readings may be seriously falsified.[300]

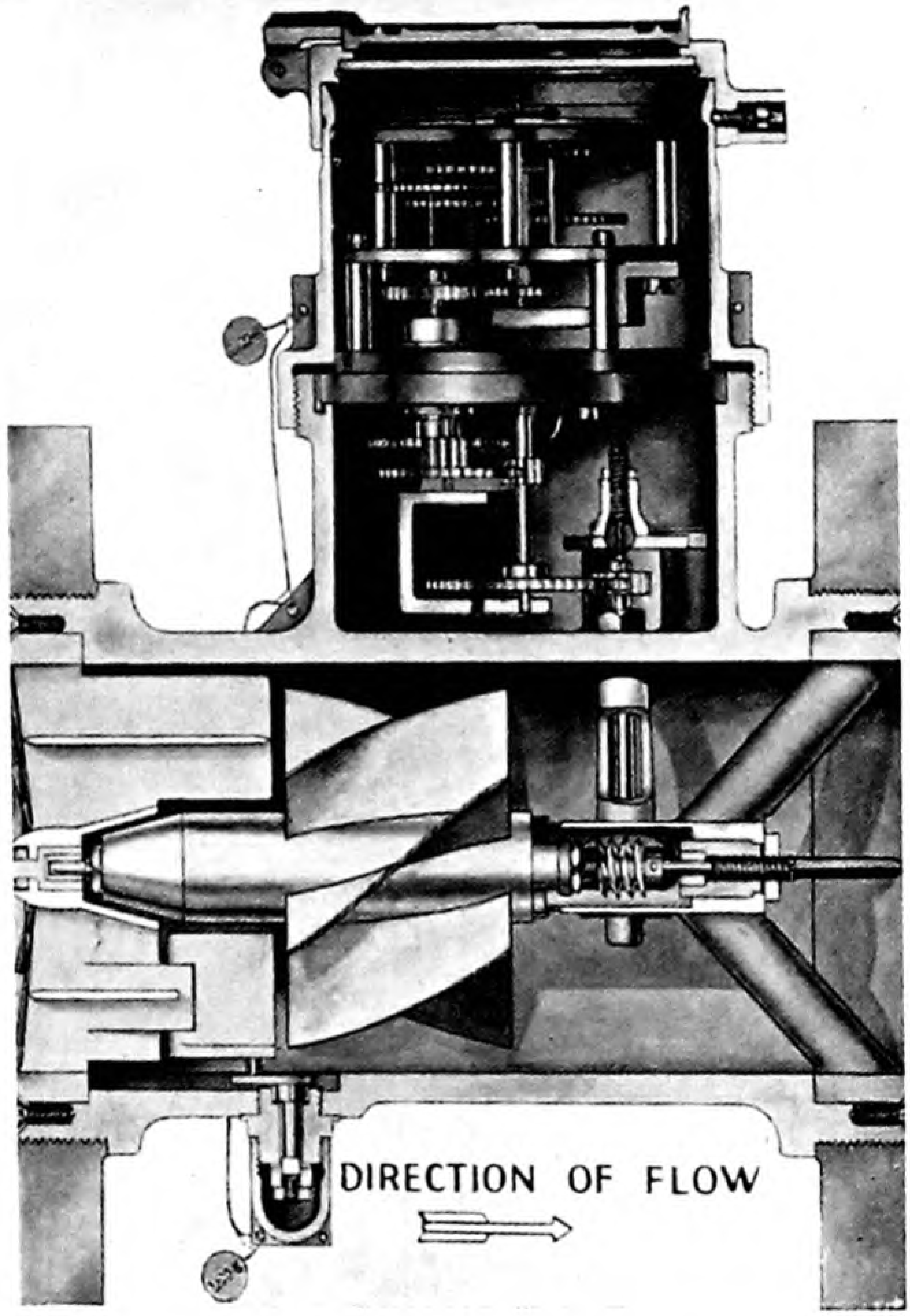

FIG. 465.—6-in. "Helix" meter.
(The Leeds Meter Co.)
[To face page 576.

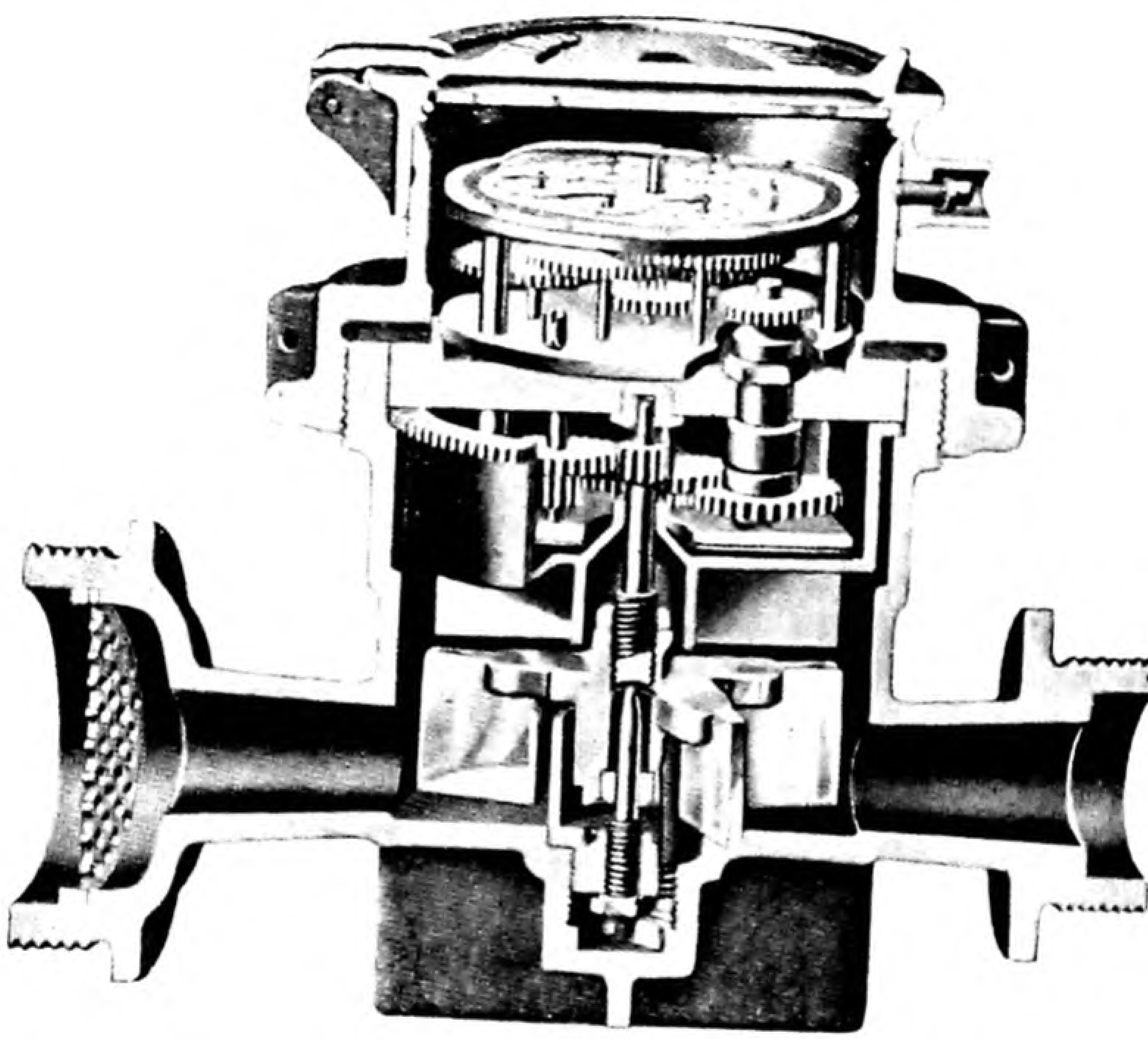

FIG. 467.—Vane-wheel meter.

[*To face page 577.*

394. Positive Meters. These instruments fulfil a similar purpose to the *inferential* rotary meters just described; both of them are designed to register the total volume of liquid that has passed through them, rather than the rate of flow. Positive or displacement meters might be described as reversed positive pumps (Chap. XV) or as hydrostatic hydraulic motors running under no load. Since it is the primary attribute of such machines that the rate of discharge is proportional to the rate of revolution, evidently the total number of revolutions will give a measure of the total flow.

The fundamental element of the positive meter is the measuring chamber which is alternately filled and emptied; it corresponds to the cylinder of a reciprocating pump. Sometimes a single cylindrical chamber is used; multiple cylindrical chambers are also popular, and these are frequently disposed in the manner of the cylinders of a rotating-cylinder pump, in conjunction with a swash-plate or wobble-plate. Because of the relative ease with which cylindrical chambers can be machined to fine limits, and because of the possibility of providing some form of seal or packing between the piston and the cylinder walls, such chambers are to be found in the most accurate types of meter. Nevertheless a great variety of non-cylindrical measuring chambers is successfully used.

As compared with the helical type of inferential meter, § 393, the positive meter

- is suited for a lower range of flows, not exceeding perhaps 200 gallons per minute;
- can deal only with clean liquids, and not with unfiltered liquids;
- is likely to be more accurate, especially at very low rates of flow;
- imposes a much greater loss of head on the liquid flowing through it.

Familiar examples of positive meters are those which measure the fuel delivered to the tank of an automobile at a filling-station.

395. The Allen Salt-velocity Method. In this interesting method, devised by Professor C. M. Allen, of Worcester, U.S.A., the speed of an injected quantity of salt solution passing down the pipe is measured.[301] The saturated solution

of common salt is stored in a container A (Fig. 468), subjected to compressed air pressure, such that when the quick-acting gate valve B is opened, a " dose " of salt solution will be forced into the main pipe through the spring-loaded valve C. The dose will now be carried along the pipe with a velocity equal to the mean water velocity, but it will rapidly become more dilute, and diffused throughout a greater and greater axial length, (§§ 75,84) because of the variations in the water velocity at different points of the cross-section.[302]

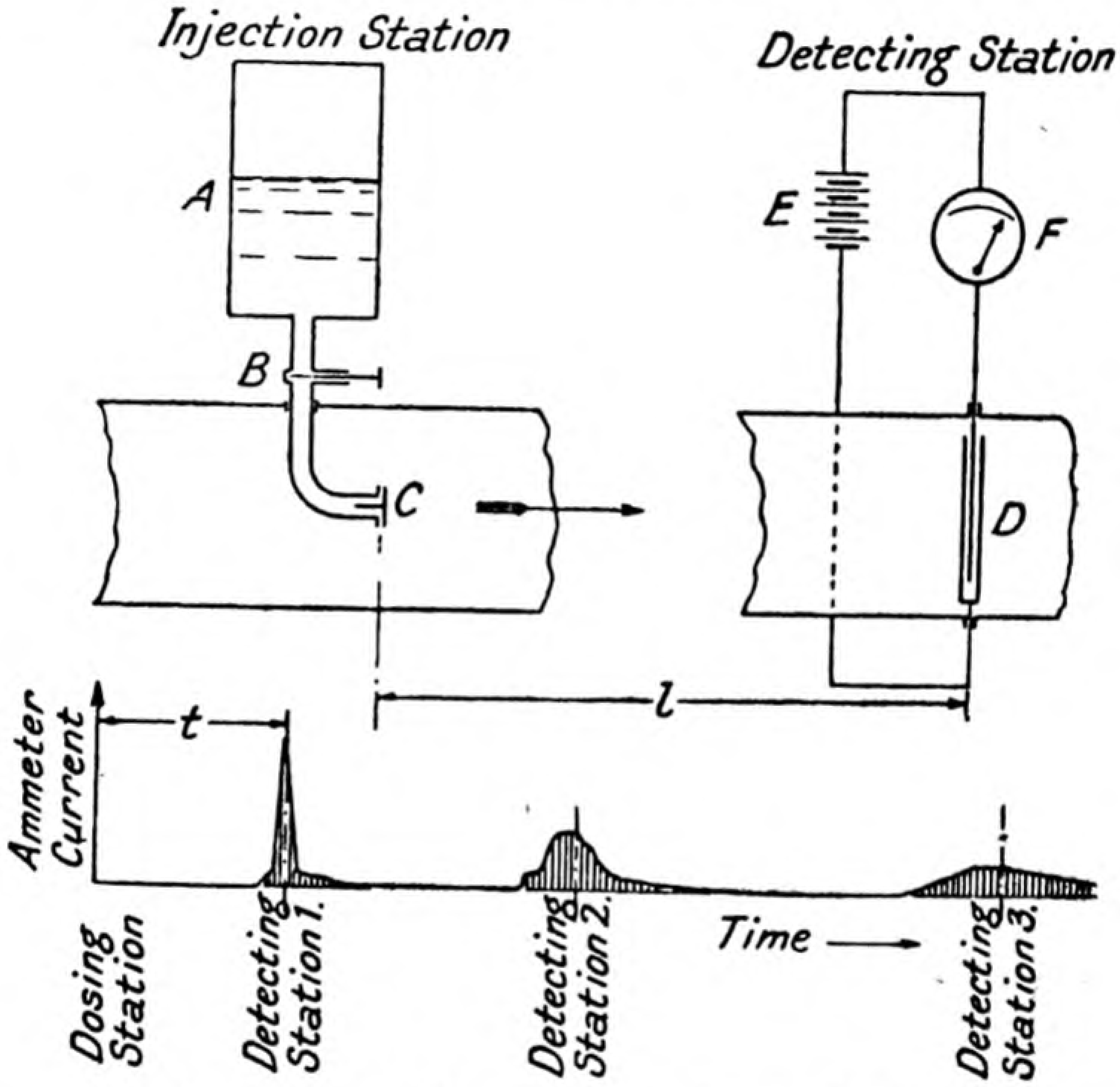

FIG. 468.—Allen salt-velocity method.

To detect the transit of the dose past a station at a known distance downstream from the injection station, electrodes D are arranged within the pipe, in circuit with a battery E and a recording ammeter F. The conductivity of the water normally passing the detecting station is too low for any appreciable electric current to be shown by the ammeter; but as the conductivity of salt water is much higher, the presence of the dose is immediately registered by the ammeter. Similar detecting stations may be arranged still further downstream.

A typical autographic ammeter record for such a series of stations, current being plotted against time, is reproduced in Fig. 468. The points on the time scale corresponding to

the centre of gravity of the hatched areas are taken as the instants at which the dose reaches the respective stations. Dividing distance l by time t, the required mean velocity is obtained. In spite of the flatter "hump" on the autographic record relating to the more distant detecting stations, and the consequent greater difficulty in accurately determining the position of the centre of gravity, it is found that the velocities computed from these results are less liable to serious error than are those from the upstream detecting stations.[283]

396. The Gibson Inertia-pressure Method. Mr. N. R. Gibson, of the Niagara Falls Power Company, has developed a method of velocity measurement based on the inertia pressure generated when a valve at the end of a pipe is closed. Referring to formula 7-1 (§ 115), it will be seen that if the length, diameter, inertia pressure, and time of closure are known, the original velocity can be calculated.

The method is particularly applicable to the measurement of the discharge in turbine supply pipes, and comparative tests show that it gives reliable results.[303] A disadvantage that it shares with the Allen method (above) is that unless the pipe is known to be of exactly uniform cross-section, careful measurements of diameter throughout its whole length must be made.

Measurement of the Rate of Discharge in Open Streams.

397. Current Meter Gaugings. The chief practical questions to be settled when using the current meter (§ 381) for stream gauging are (*a*) the selection of the points in the cross section at which the observations are to be taken, and (*b*) the method of supporting the instrument at the chosen positions.[304]

On the first point information will be found in § 103. If the meter is held midway between the water surface and the channel bed, the measured velocity multiplied by 0·96 will give, with sufficient accuracy for routine gaugings, the mean velocity over the whole vertical. Alternatively, if observations are made in one vertical at 0·2 and at 0·8 of the depth, the mean of these will represent the mean velocity over the vertical.

For use in shallow streams, the meter may be clamped at the appropriate height to a graduated rod standing in the

bed (Fig. 452), the observer wading from point to point. If a bridge crosses the stream without obstructing it or disturbing the flow, the meter may be lowered into the water from the bridge. In the absence of any such fixture, the meter may be hung from a wire rope fixed across the channel, a system of light control cords operated from the bank permitting the meter to be brought in succession to the desired points in the channel cross-section.[305] In gauging large canals and rivers, it is usually necessary to use a boat, which accommodates the

TABLE OF CURRENT METER OBSERVATIONS.

(Instrument—Price Meter.)

(A) Distance from Bank (measured at water surface) (metres).	(B) Mean Distance between Soundings (metres).	(C) Sounding (metres).	(D) Area of Section =B × C (sq. m.).	(E) Revolutions of Current Meter in One Minute at Half Depth.			(F) Mean r.p.m. of Meter at Half Depth.	(G) Corresponding mean Velocity at Half Depth (from rating curve) (metres/sec.).	(H) Mean Velocity over Section = 0·96 × G (met./sec.).	(K) Discharge in Section = D × H (cub. m. per sec.).
				1	2	3				
0	—	—	—	—	—	—	—	—	—	—
4	4·0	1·90	7·6	38	39	39	38·7	0·439	0·421	3·20
8	6·0	3·40	20·4	47	48	45	46·7	0·528	0·507	10·35
16	8·0	4·10	32·8	56	58	57	57·0	0·644	0·618	20·28
24	8·0	4·00	32·0	56	54	55	55·0	0·621	0·596	19·08
32	8·0	4·10	32·8	61	60	63	61·3	0·691	0·664	21·78
40	8·0	3·90	31·2	61	59	62	60·7	0·684	0·656	20·46
48	8·0	4·00	32·0	56	57	58	57·0	0·644	0·619	19·80
56	6·0	4·50	27·0	58	55	56	56·3	0·635	0·610	16·48
60	4·0	3·50	14·0	42	43	43	42·7	0·484	0·465	6·51
64	4·0	1·70	6·8	35	35	33	34·3	0·390	0·375	2·55
68	—	—	—	—	—	—	—	—	Total	140·49

Canal Discharge = 140·5 cubic metres per second.

observers and carries the tackle for raising and lowering the meter (Fig. 469); the boat is moored to a wire rope stretched taut across the canal. At each of a suitable number of points across the breadth of the channel the depth is measured with

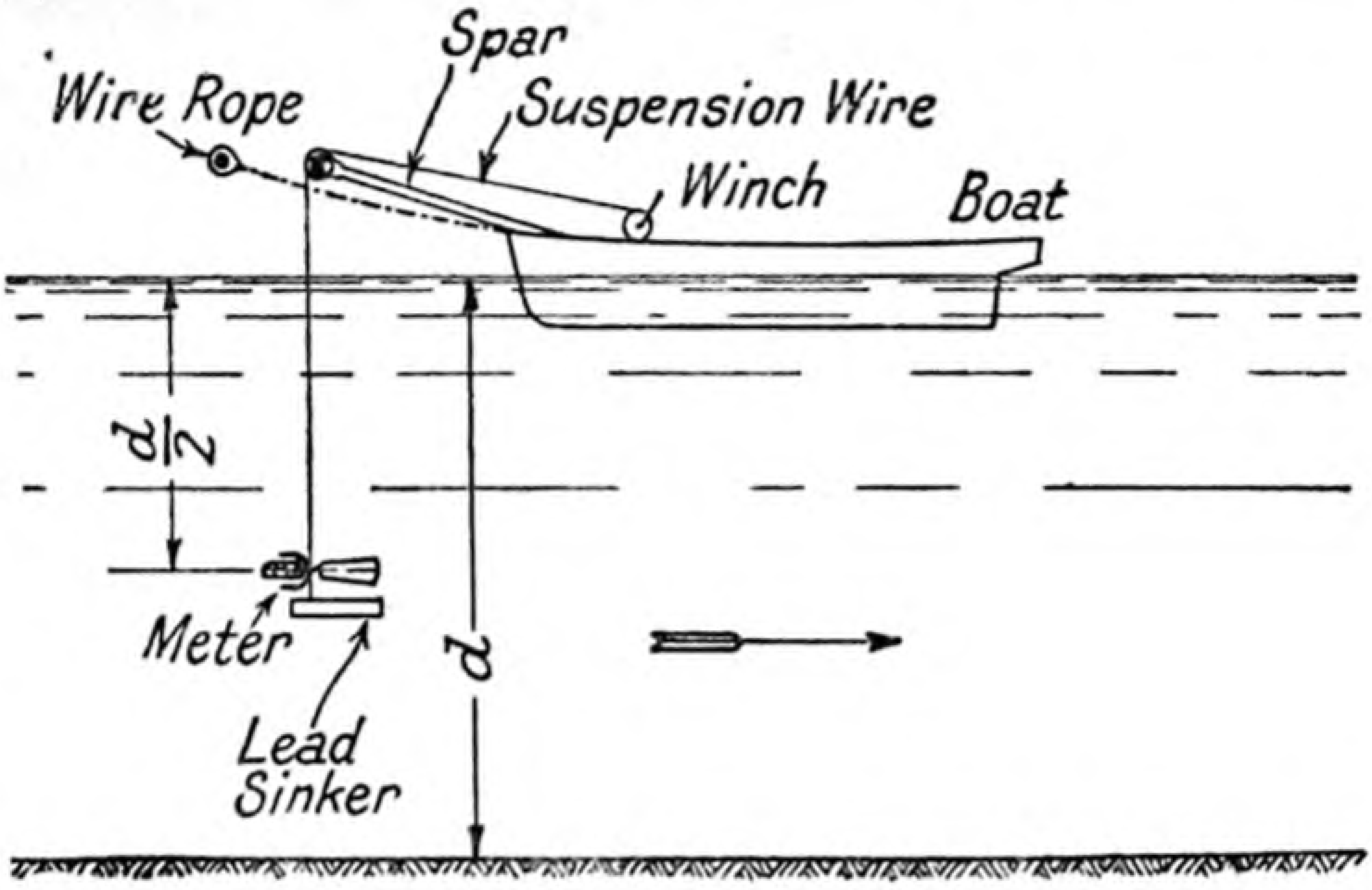

FIG. 469.—Current meter gauging in river.

a sounding-rod, the meter is lowered to one-half of this depth, and the rate of revolution recorded. If it is impracticable to use the wire rope as a means of locating the boat, then it must be anchored and its position determined by sextant observations.

The table (above) indicates how the observations taken during the gauging of a canal by the method illustrated in

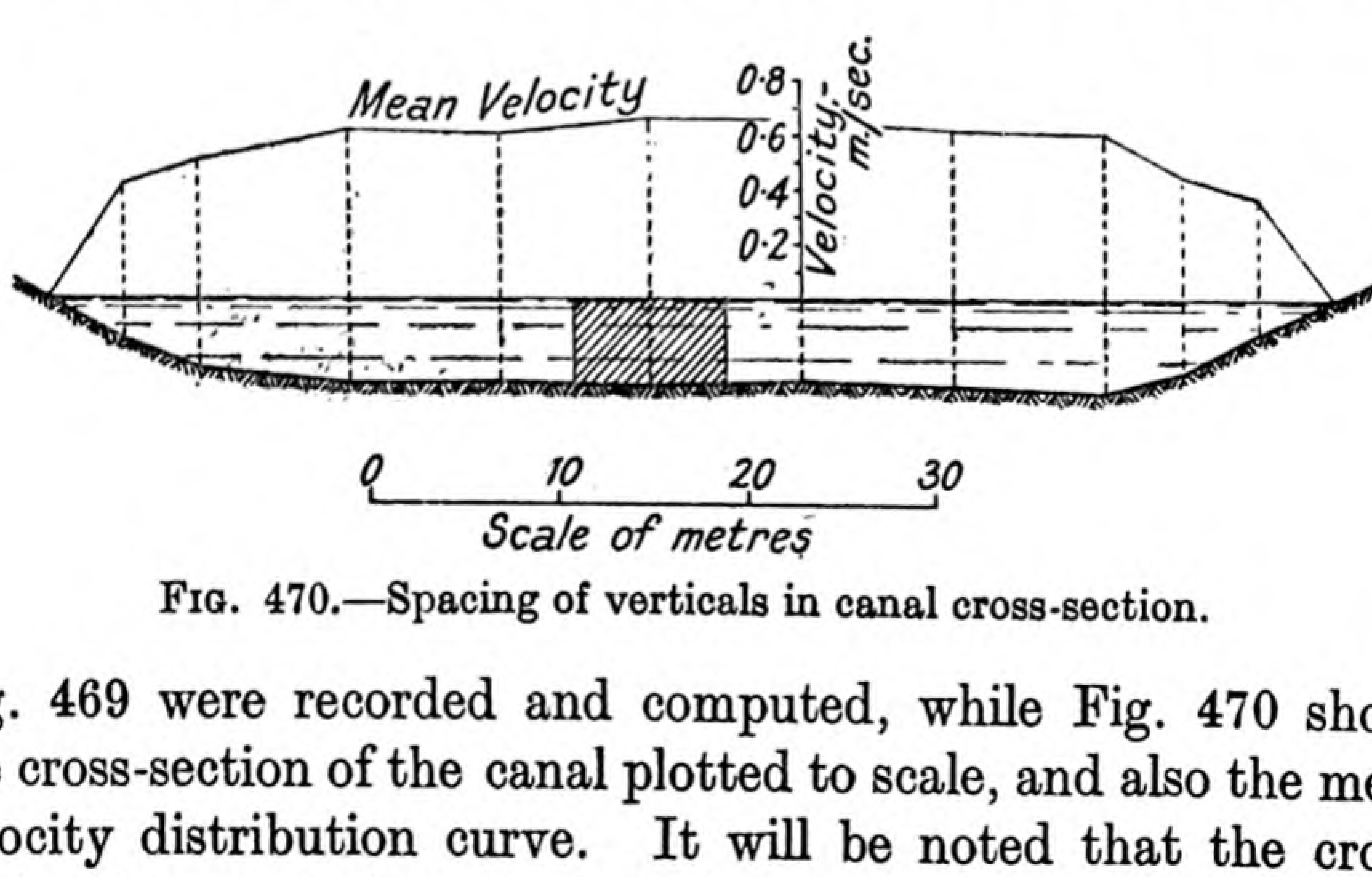

FIG. 470.—Spacing of verticals in canal cross-section.

Fig. 469 were recorded and computed, while Fig. 470 shows the cross-section of the canal plotted to scale, and also the mean velocity distribution curve. It will be noted that the cross-section is assumed to be divided into a number of rectangles such as the hatched one in the figure; the area of the rectangle multiplied by the mean velocity at its axis represents the

discharge to be credited to it. The sum of the individual discharges gives the total canal discharge.

The table of observations reveals a fairly common characteristic of stream flow in large channels; during successive intervals of 1 minute, the rate of revolution of the current meter at a given position is sometimes seen to vary, showing that the motion of the water is not perfectly uniform but is subject to slight pulsations or surgings.

In the example just quoted, only one current meter observation was made for every 24 sq. metres of canal cross-section. So wide a spacing between the observation points is only admissible if the regime in the stream is unusually steady, if the section is symmetrical, and if the gauging station is at the downstream end of a long, uniform straight stretch of waterway. In less favourable conditions a relatively greater number of observations must be made, even as many as one per square metre (say 10 sq. ft.) of cross-section.

The length of time required for a single discharge measurement involving perhaps 150 separate meter observations might be impracticably great if a single instrument only were available, hence a technique has been developed for using multiple meters simultaneously. The principle is seen in Fig. 471.

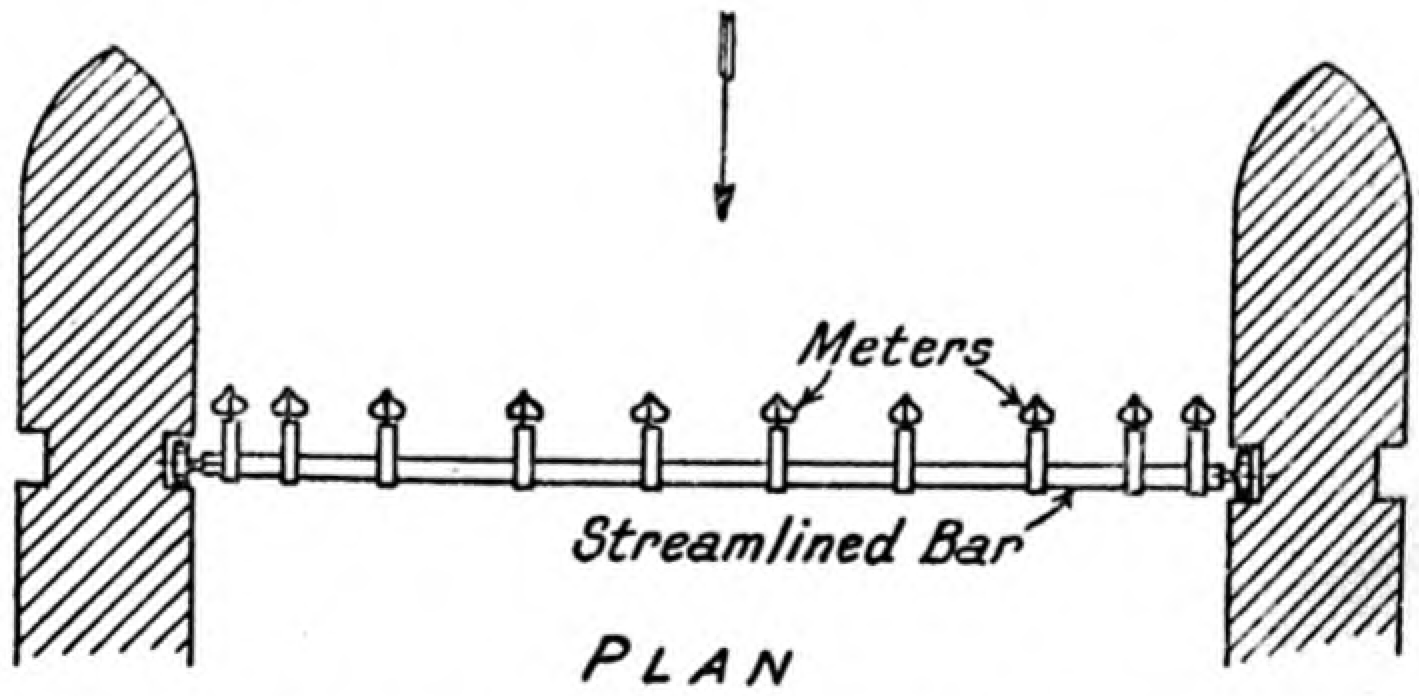

FIG. 471.—Multiple meters for gauging flow through turbines.

The meters are attached to a horizontal bar fitted at its ends with rollers so that it may slide vertically in the grooves of a low-head turbine inlet structure (see Fig. 249). By bringing the frame successively to various levels, the whole area between the piers may be rapidly explored, and the discharge through the turbine calculated. Chronographic recording of the speed of the meters is, of course, essential.

398. Floats. The time taken for a floating object to traverse a known distance will give an approximate indication of the velocity of a stream.[306] Three types of floats are illustrated in Fig. 472. The *surface* float I may consist of a bottle ballasted so that only its neck projects above the water; the *sub-surface* float II is formed of a weighted canister attached to a small indicating float, the connecting cord being adjusted

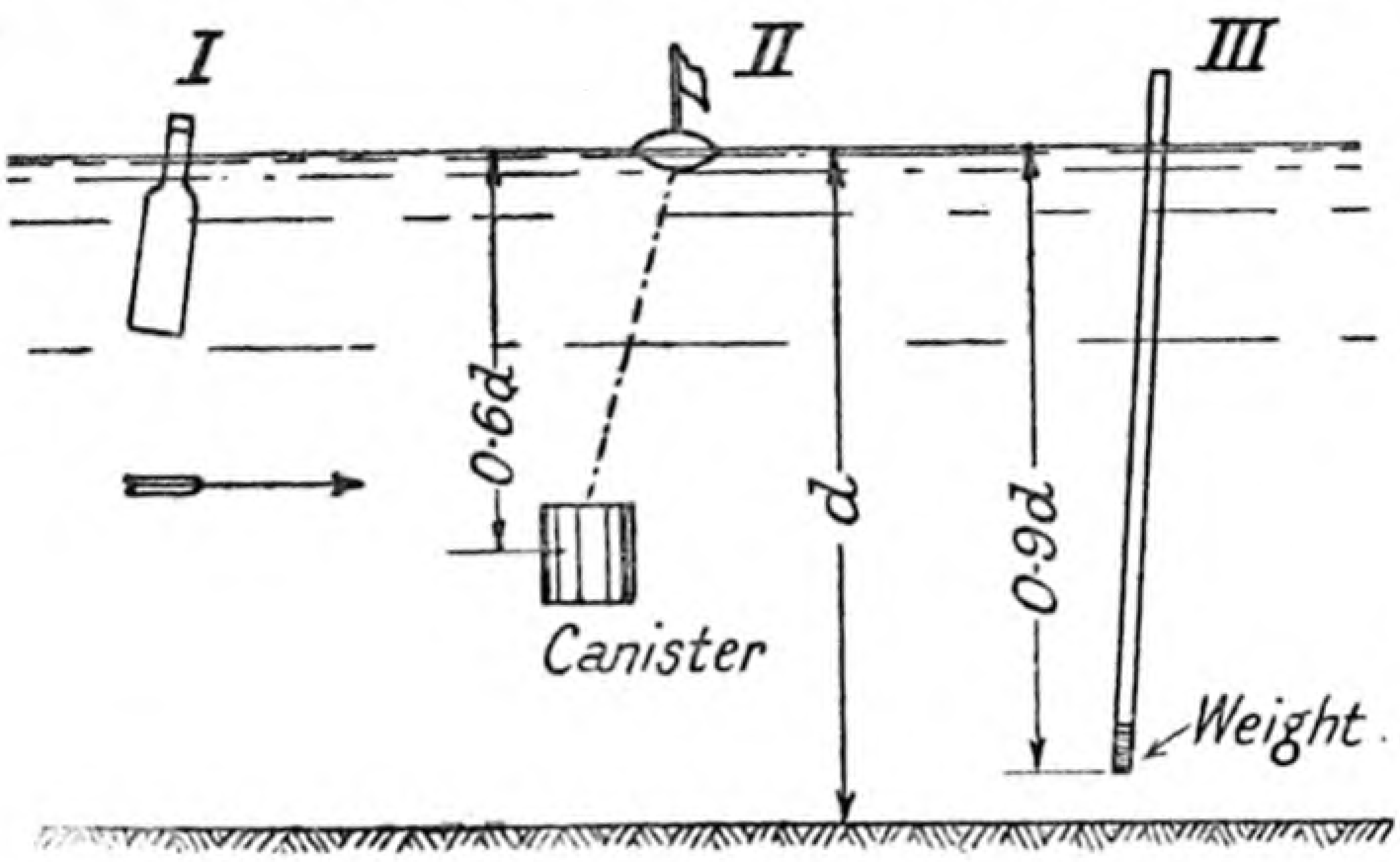

FIG. 472.—Float gauging.

so that the canister travels at 0·6 of the stream depth; the *rod* float III consists of a weighted tube or rod, of which the depth of the immersed part is 0·9 of the stream depth.

The mean velocity of the stream, in the vertical plane along which the float travels, is taken as about 0·85 of the measured speed of type I, and as being identical with the speed of types II and III (§ 103). Because of the many possible sources of error involved in their use, e.g. the direction of the wind, and the inequalities of the bed of the stream, floats are rarely used nowadays for precise discharge measurements.

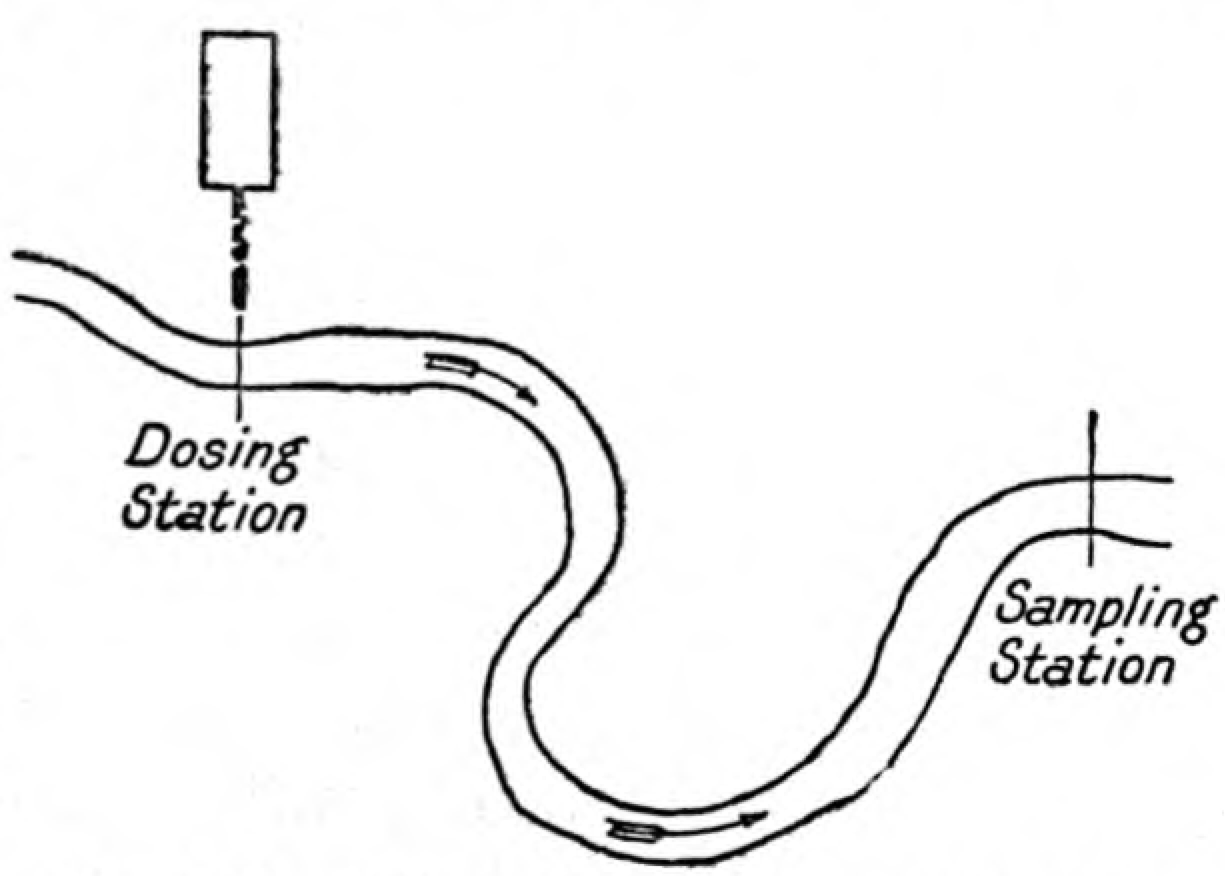

FIG. 473.—Stream gauging by salt-titration.

399. Salt-titration Method. The principle of the salt titration or salt-solution method is entirely different from that used in the salt-velocity method (§ 395). Two stations

are chosen a suitable distance apart, an upstream dosing station and a downstream sampling station (Fig. 473). At the dosing station, a strong solution of common salt is fed continuously into the stream at a uniform rate. At the sampling station samples of "dosed" water are taken from the stream, and samples of "undosed" or natural water are also collected just upstream of the dosing station. By means of Mohr's titration method, using solutions of silver nitrate and potassium chromate, the concentration of salt in the various samples is then accurately determined.

Let k_0 = weight of salt in unit volume of undosed water.
k_1 = ,, ,, ,, ,, salt solution.
k_2 = ,, ,, ,, ,, dosed water.
q = rate of discharge of salt solution.
Q = ,, ,, stream.

Since the total weight of salt leaving the dosing station in unit time must be the same as the weight arriving at the sampling station in unit time, we may write

$$Qk_0 + qk_1 = (Q + q)k_2,$$

whence $Q = q\left(\frac{k_1 - k_2}{k_2 - k_0}\right)$, which gives the desired information.

In applying this technique, attention must be given to the following points :—

(i) The stream itself must be naturally or artificially turbulent, to ensure thorough admixture of the added salt solution. This condition is fulfilled if the water passes over a weir or through a turbine in its passage from the dosing station to the sampling station.

(ii) The salt solution must be well distributed over the cross-section of the stream at the dosing station, and at the sampling station the samples must be taken at points uniformly distributed over the cross-section.

(iii) The concentration of the salt solution should be about 1 part by weight of salt to 4 parts by weight of water. § 215 contains suggestions for feeding the solution into the stream at the necessary uniform, measured rate. Preferably the rate of flow should be such that at the sampling station there will be not less than 1 part of salt in 30,000 parts of water.

400. Calibrated Sluices, Weirs, etc., and Other Gauging Methods. If the flow of a stream can be diverted over a sharp-edged weir, which will as a rule only be practicable for relatively small discharges, the formulæ of §§ 55 to 57 are applicable.[307] Masonry weirs (§ 188) will give accurate results provided they are calibrated by means of scale model experiments or by current meter observations.[308] With the same proviso—careful calibration—sluice gates and regulators (§§ 191 to 194), will yield quite reliable discharge figures. One of the chief objections to the use of measuring weirs, the afflux or loss of head they entail, can be greatly minimised by choosing the standing wave type (Fig. 177 (V)), or the *standing wave flume* (§ 199).[309] Throated flumes of the sort shown in Fig. 196 are often described as *Venturi flumes* ; in various forms they can successfully be used for stream-gauging in small or in large channels.[310]

The *Pitot tube* (§ 380) is suitable for measuring the flow in rapid streams only. The usual range of river and canal velocities generates too small a differential head for it to be accurately measured.

The *salt velocity method* (§ 395) has been used for the gauging of open streams, but the computation of the mean cross-section of the waterway throughout the whole distance from the injection station to the detection station is apt to be very toilsome.

401. Stage Discharge Curves. The results of a series of gaugings at a given point in a stream can very conveniently be recorded in a *stage discharge curve ;* this is a graph plotted between depth and discharge similar to Fig. 168, § 183, but with the important difference that instead of being constructed from computation it is drawn through the points that represent observed depths and discharges. Consequently at any later date a fairly good estimate of the discharge can be arrived at by merely noting the depth of the stream and reading off the desired rate of flow from the chart. Fig. 474 represents the stage-discharge relationship for the Nile at Nag Hammadi.

Naturally the section under consideration must be beyond the range of any downstream regulating work which, by variations in the backwater it produces, might affect the depth gauge ; also the stage discharge curve must periodically be

checked in order to detect any changes in the regime of the river due to the formation of sandbanks, or to erosion of the bed and banks.

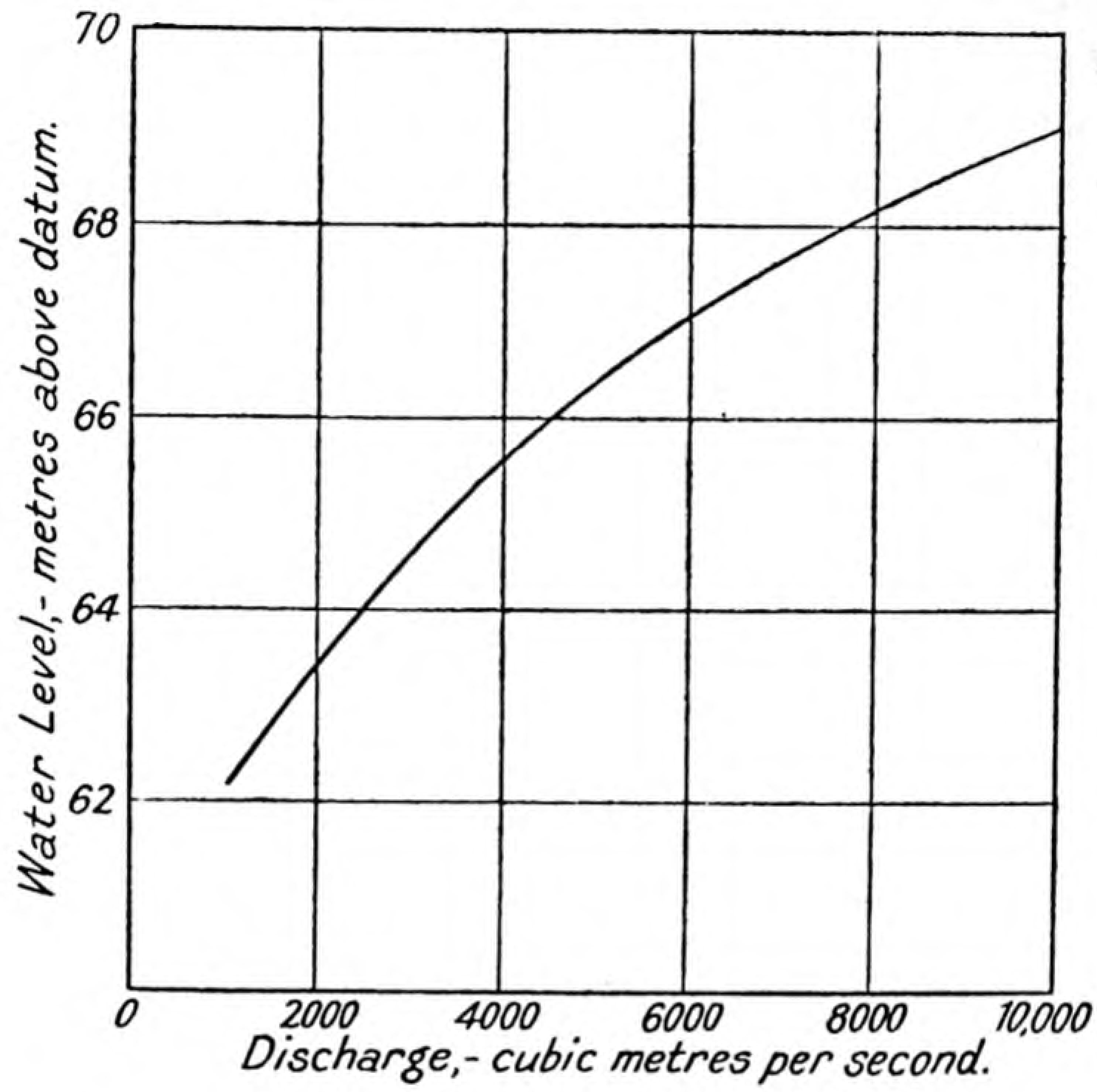

FIG. 474.—Stage discharge curve.

402. Comparison of Gauging Methods. As a result of various comparative tests,[311] the opinion is gaining ground that in the absence of weirs or sluices calibrated against absolute standards, the current meter affords the most reliable means of gauging steadily flowing streams, and that the salt titration method is the best for small turbulent streams. With carefully-made observations neither of these methods should be in error by much more than 1 per cent. or 2 per cent.

(*Note.*—The terms "steadily flowing" and "turbulent" in this and the preceding paragraphs are here used in their ordinary significance, and not as distinguishing between velocities below and above the critical velocity. See § 29 (iv).)

In regard to flow measurements that depend upon observations of head or of differential head, it is useful to classify these according to the correlation between observed head h and computed discharge Q.

For orifices,
the Venturi meter,
the Pitot tube,
sluice openings
} the relation is approximately $h \propto Q^2$.

For rectangular weirs,
masonry weirs, standing wave flumes
} the relation is approximately $h \propto Q^{\frac{2}{3}}$,

For the triangular weir or V-notch } ,, ,, ,, $h \propto Q^{\frac{2}{5}}$.

These relationships are shown graphically in Fig. 475, which makes it clear that when variable flows are concerned weirs have an advantage over orifices. For example, if the flow over a triangular weir falls from the maximum discharge (100 per cent.) to half discharge (50 per cent.), Fig. 475 shows that the corresponding head falls only from 100 per cent. to 76 per cent.; but if the water flows through an orifice or Venturi meter, a similar reduction of the discharge by 50 per cent. entails a drop in measuring head from 100 per cent. to 25 per cent. In the second case there is thus an increased possibility of error at low discharges.

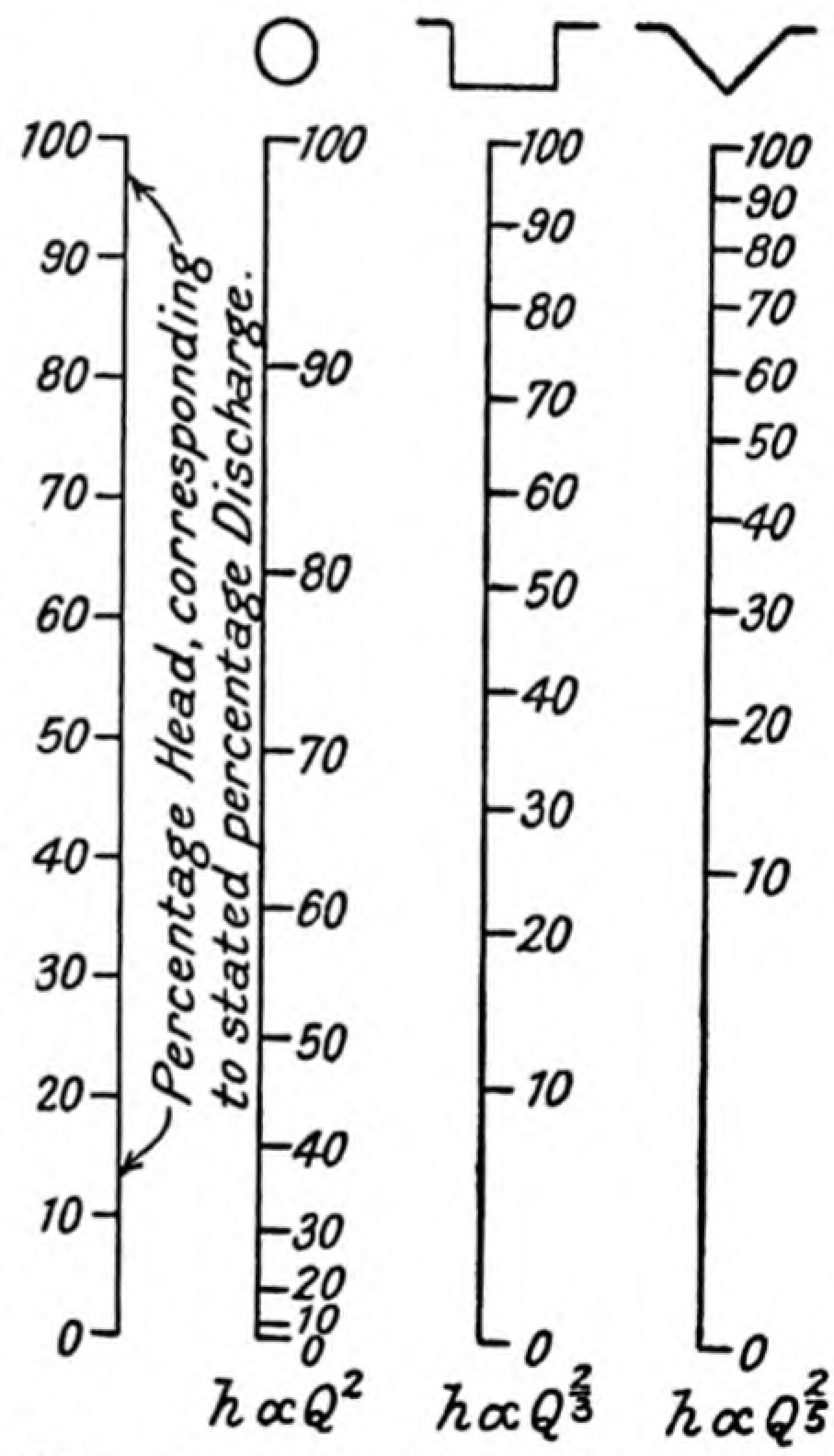

FIG. 475.—Graphical comparison of gauging methods.

EXAMPLES

PART I

CHAPTER I

EXAMPLE 1.

A piston 11·96 cms. diameter and 14·00 cms. long works in a cylinder 12·00 cms. diameter. If the lubricating oil which fills the space between them has a viscosity of 0·65 poises, calculate the speed with which the piston will move through the cylinder when an axial load of 0·86 kg. is applied. Neglect the inertia of the piston.

Solution :—

In the formula $P = \mu \,.\, A \,.\, \frac{v}{y}$, we have

$$P = 0{\cdot}86 \times 1000 \times 981 = 844{,}000 \text{ dynes},$$

$$\mu = 0{\cdot}65 \text{ poises},$$

$$A = 12{\cdot}00 \times 3{\cdot}14 \times 14 = 528 \text{ sq. cms. (approx.)},$$

$$y = \frac{12{\cdot}00 - 11{\cdot}96}{2} = 0{\cdot}02 \text{ cms.},$$

$$\therefore\ v = \text{velocity of piston} = \frac{Py}{A\mu} = \frac{844{,}000 \times 0{\cdot}02}{528 \times 0{\cdot}65}$$

$$= \mathit{49{\cdot}3\ cms./sec.}$$

EXAMPLES *for Solution :—*

2. The space between two square flat parallel plates is filled with oil; each side of the plates measures 2 ft., and the thickness of the oil film is 0·004 in. When the plates are inclined at 20° with the horizontal (the lower plate being fixed), it is found that the upper plate, which weighs 7·2 lb., slides over the lower plate at a maximum speed of 0·3 ft./sec. What would be the viscosity of the oil ?
Ans. 0·00067 lb. sec./sq. ft. = 0·32 poises.

3. The lower end of a vertical shaft rests in a footstep bearing; the shaft is 10 cms. diameter and it is separated from the bearing by an oil film 0·1 mm. thick, the viscosity of the oil being 1·5 poises. Both the lower end of the shaft, and the surface of the bearing, are flat. What would be the power absorbed by the bearing when the shaft was rotated at a speed of 750 r.p.m. ? Ans. 0·123 h.p.

4. A lubricating oil has the following properties at atmospheric pressure :—

At temperature 60° F., density = 0·915 gm./ml.

kinematic viscosity = 200 centistokes.

At temperature 180° F., kinematic viscosity = 8 centistokes.

Estimate what would be the density and the kinematic viscosity of the oil, at a temperature of 180° F., and a pressure of 5500 psi.

Ans. About 0·90 gm./ml. : about 20 cs.

CHAPTER II.

EXAMPLE 5.

Calculate the maximum height of water column at a temperature of 140° F. that could be maintained by a vacuum pump when the true atmospheric pressure was 14·5 lb./sq. in.

Solution :—

From Fig. 1, the vapour pressure of water at 140° F. is 0·205 kg./sq. cm. = 0·205 × 14·22 lb./sq. in.

$= 2{\cdot}92$ lb./sq. in.

The pressure available for sustaining the water column

$$= p = \text{atmospheric pressure} - \text{vapour pressure}$$
$$= 14{\cdot}50 - 2{\cdot}92 = 11{\cdot}58 \text{ lb./sq. in.}$$
$$= 11{\cdot}58 \times 144 \text{ lb./sq. ft.}$$
$$= 1666 \text{ lb. /sq. ft.}$$

Now the relative density of water at 140° F. = 0·98 from) Fig. 1),

$$\therefore w = \text{weight per unit volume}$$
$$= 62{\cdot}4 \times 0{\cdot}98 = 61{\cdot}1 \text{ lb./cu. ft.}$$

Hence *height of water column* $h = \frac{p}{w} = \frac{1666}{61{\cdot}1}$

$$= \mathit{27{\cdot}3\ ft.}$$

EXAMPLE 6.

Calculate the forces acting at the two hinges and at the clamp of the rectangular door shown in the sketch, if the level of the sea water (S.G. 1·03) outside the door is 10·0 ft. above the top of the door, which is itself vertical.

Solution :—

The depth $\bar{h}$, below the free surface, of the C.G. of the area is $10{\cdot}0 + \frac{8{\cdot}6}{2} = 14{\cdot}3$ ft.

The area A exposed to the hydrostatic pressure is

$$8{\cdot}6 \times 5{\cdot}2 = 44{\cdot}7 \text{ sq. ft.}$$

The weight per unit volume w of the liquid is

$$62{\cdot}4 \times 1{\cdot}03 = 64{\cdot}2 \text{ lb./cu. ft.}$$

Therefore

$$\begin{aligned} P = \text{static thrust} &= wA\bar{h} \\ &= 64{\cdot}2 \times 44{\cdot}7 \times 14{\cdot}3 = 41{,}000 \text{ lb.} \\ &= 41{,}000/2240 = 18{\cdot}3 \text{ tons.} \end{aligned}$$

The moment of inertia of a rectangular area about its C.G. is given by

$$\frac{bh^3}{12}, \quad \therefore I_G \text{ for door} = \frac{5{\cdot}2 \times 8{\cdot}6^3}{12} = 276 \text{ ft.}^4$$

The depth h_p of the centre of pressure $= \dfrac{I_G + A\bar{h}^2}{A\bar{h}}$ (formula 2-3)

$$= \frac{276 + 44{\cdot}7 \times 14{\cdot}3^2}{44{\cdot}7 \times 14{\cdot}3} = \mathit{14{\cdot}73\ ft.}$$

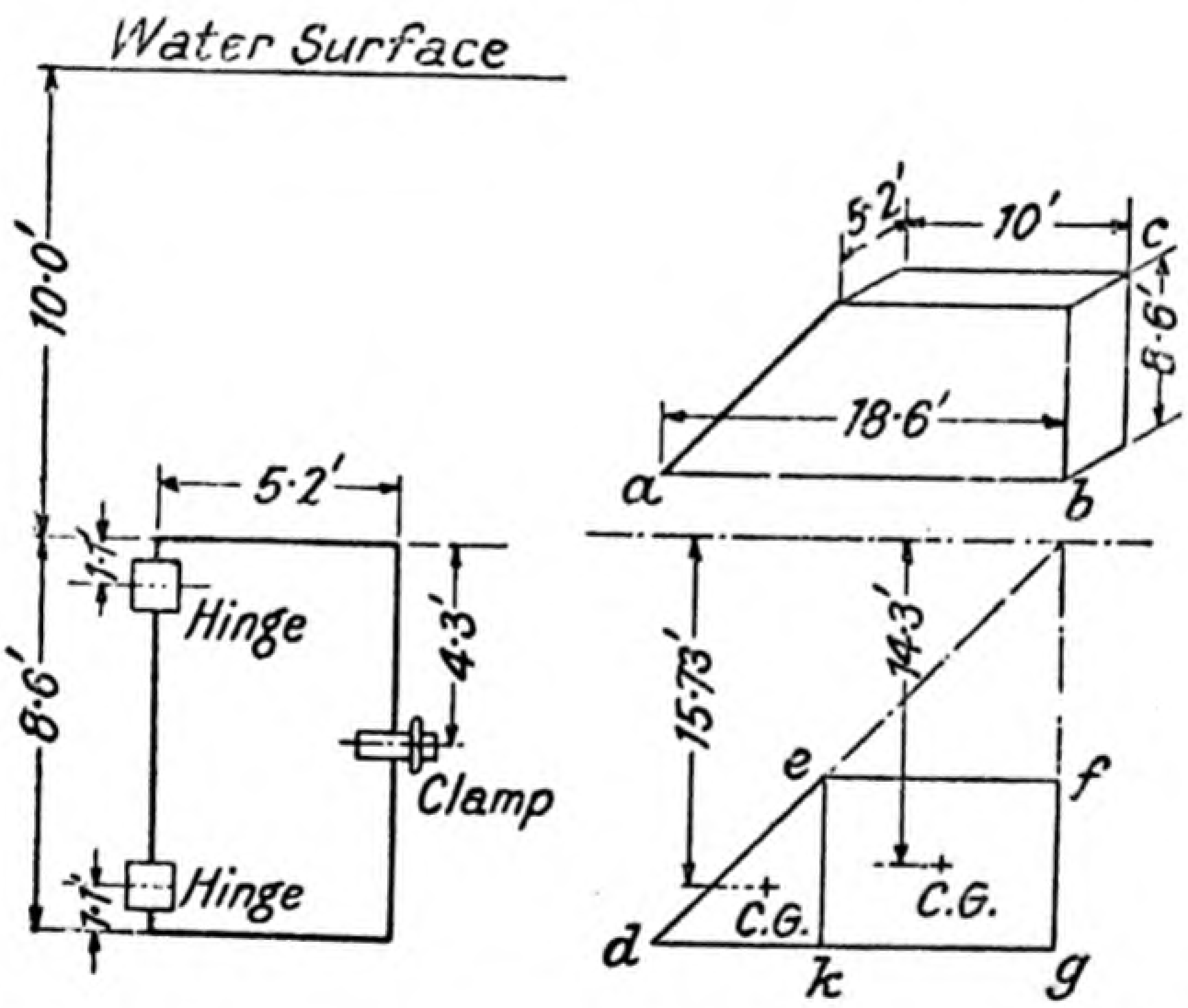

The centre of pressure thus lies $14{\cdot}73 - 14{\cdot}30 = 0{\cdot}43$ ft. vertically below the centre of gravity of the area.

Let P_b = force on clamp,
P_c = force on upper hinge,
P_d = force on lower hinge.

Taking moments about a vertical axis through the hinges, we have

$$P \times 2{\cdot}6 = P_b \times 5{\cdot}2,$$

whence

$$P_b = \textit{force on clamp} = P \times \frac{2{\cdot}6}{5{\cdot}2} = \frac{18{\cdot}3}{2} = \mathit{9{\cdot}15\ tons.}$$

Taking moments about a horizontal axis through the lower hinge, we have

$$(P_c \times 6{\cdot}4) + (P_b \times 3{\cdot}2) = P \times (3{\cdot}20 - 0{\cdot}43),$$

whence P_c = *force on upper hinge = 3·33 tons.*

Finally P_d = force on lower hinge $= P - P_b - P_c$

$$= 18{\cdot}3 - 9{\cdot}15 - 3{\cdot}33$$

$$= \mathit{5{\cdot}82\ tons}.$$

Alternative method of finding position of centre of pressure :—

The volume of the prism *abc* (see sketch)

$$= 8{\cdot}6 \times 5{\cdot}2\left(\frac{10{\cdot}0 + 18{\cdot}6}{2}\right) = 640 \text{ cu. ft.}$$

Total static thrust

$$P = \text{weight of liquid in prism}$$
$$= 640 \times 1{\cdot}03 \times 62{\cdot}4 = 41{,}000 \text{ lb.}$$

Moment of area *efkg* about water surface $= 10{\cdot}0 \times 8{\cdot}6 \times 14{\cdot}3$
$= 1230$ ft.^{3}

Moment of area *ekd* about water surface $= \dfrac{(8{\cdot}6)^2}{2} \times 15{\cdot}73$
$= 581$ ft.^{3},

$\therefore$ Moment of total area *defgk* $= 1230 + 581$.

But moment of total area also = area $\times h_p = 8{\cdot}6 \times 14{\cdot}3 \times h_p$,

whence h_p = depth of centre of pressure
= depth of C.G. of prism below water surface

$$= \frac{1230 + 581}{123} = \mathit{14{\cdot}73\ ft.}$$

Example 7.

A Taintor gate (§ 195, Fig. 190 (I)) is 30 feet wide; it is curved to a radius of 18 feet, and its pivots are 14 feet above the floor of the sluice-way. The gate is closed, having a depth of 12 feet of water on its upstream side, but no water on the downstream side.

What would be the total resultant hydraulic thrust on the gate? (see diagram overleaf.)

Solution :—

Dividing the immersed length of the gate profile into a number of equal elements—say 6—each of length Δl, we draw horizontals through the mid-point of each element, and obtain a series of intercepts such as *ab*, cut off by the triangle ABC, which are proportional to the static pressures. Transferring these lengths to

the gate itself, as at $a'b'$, the actual pressure distribution over the gate is obtained, and the resultant thrust is found by constructing the polygon as shown below (viz.: $a''b''$ equal and parallel to $a'b'$, etc.) and measuring the closing length, which is found to be 38·5 feet.

Now since the length Δl of each element is 2·34 feet, and the horizontal width of the gate is 30 feet, then the total thrust on the element under a head h will be

$$2{\cdot}34 \times 30 \times 62{\cdot}4h = 4380h \text{ lb.},$$

and consequently the total resultant thrust on the gate will be

$$\frac{4380 \times 38{\cdot}5}{2240} = 75{\cdot}4 \text{ tons.}$$

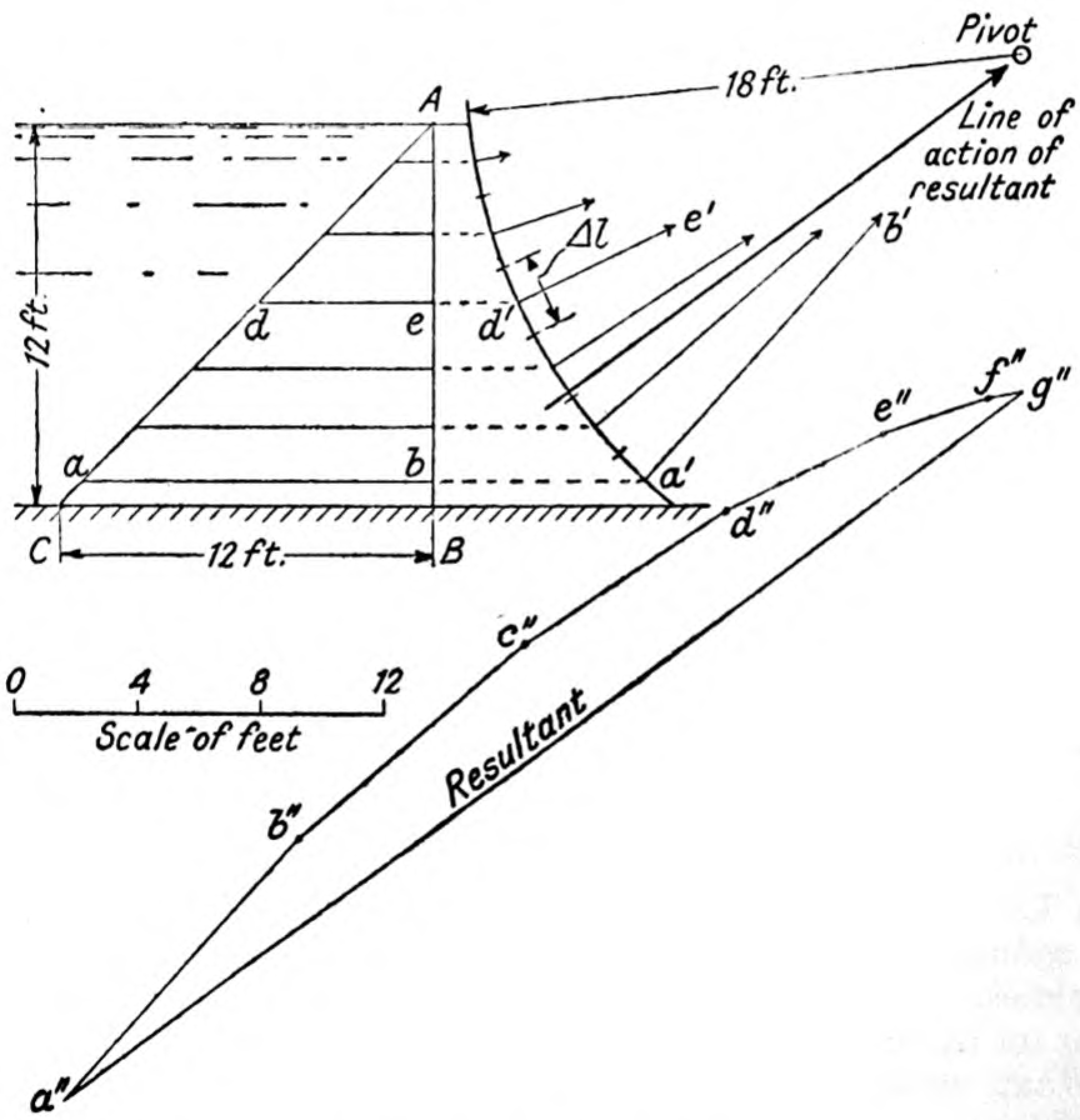

This thrust will be equally divided between the two pivots; its line of action will pass through the pivots, in a direction paralle to the closing line $a''g''$ of the polygon.

(*Note.*—The above solution is only approximate, because it has been assumed that the centre of pressure of each element coincides with its centre of gravity. But by taking a sufficiently great number of elements, the error can be reduced to negligible limits.)

EXAMPLE 8.

A long pipe-line is to be tested hydraulically to a pressure of 40 kg./sq. cm. The pipe is first filled with water at atmospheric pressure (the ends being closed), and then more water is forced in by means of a pump until the necessary test pressure is reached. Assuming that there is no longitudinal extension of the pipe, calculate the weight of this additional water to be handled by the pump. The data are: Length of pipe = 2154 metres; internal diameter of pipe = 55 cms.; thickness of pipe walls = 14 mm.; bulk modulus of water = K = 21,000 kg./sq. cm.; Young's modulus for pipe walls = E = 2,100,000 kg./sq. cm.

Solution:—

$$f_t = \text{tangential stress in pipe wall} = \frac{pd}{2t} = \frac{40 \times 55}{2 \times 1{\cdot}4} \quad (\S\ 21)$$
$$= 785 \text{ kg./sq. cm.}$$

$$\text{Increase in pipe diameter when pressure is applied} = \frac{df_t}{E}$$
$$= \frac{55 \times 785}{2{,}100{,}000} = 0{\cdot}0206 \text{ cm.}$$

$$\text{Increase in volume of pipe} = \frac{0{\cdot}0206}{2} \times \pi \times 55 \times 215{,}400$$
$$= 384{,}000 \text{ c.c.} = 0{\cdot}384 \text{ cub. metre.}$$

$$\text{Diminution in volume of water} = \text{initial volume} \times \frac{p}{K} \quad (\S\ 5)$$
$$= \frac{\pi}{4} \cdot (0{\cdot}55)^2 \times 2154 \times \frac{40}{21{,}000} = 0{\cdot}975 \text{ cub. m.}$$

$$\text{Compressed volume of water forced in by pump} = 0{\cdot}384 + 0{\cdot}975$$
$$= 1{\cdot}359 \text{ cub. m.}$$

$$\textit{Weight of water handled by pump} = 1359\left(1 + \frac{40}{21{,}000}\right)$$
$$= \text{about } \mathit{1363\ kg.}$$

EXAMPLES *for Solution:—*

9. Compute the static thrust on each end of a cylindrical tank 20 ft. long and 4 ft. diameter, set with its axis horizontal. Spirit of S.G. 0.76 completely fills the tank, and rises as well up a vertical vent pipe communicating with the uppermost part of the tank. The vertical distance between the liquid level in the vent pipe, and the axis of the tank, is 6·5 feet. Ans. 3870 lb.

10. A rectangular pontoon 70 ft. long, 24 ft. wide, and 8 ft. deep weighs 140 tons; it carries on its upper deck a load of 100 tons. The centre of gravity of the pontoon is 4 ft. below the upper deck, and the centre of gravity of the load is 8 ft. above the deck. Both centres of gravity lie on the vertical centre line of the pontoon. Find the metacentric height when the pontoon floats in sea-water weighing 64 lb./cub. ft. Ans. 3·1 ft.

11. A dock gate 45 ft. high and 20 ft. wide is hinged horizontally at the bottom and maintained in a vertical position by horizontal chains at the top. On one side of the gate sea-water stands at a depth of 32 ft., and on the other at a depth of 20 ft. What would be the total tension in the chains ? Ans. 52·5 tons.

CHAPTER III.

EXAMPLE 12.

A pipe of varying section has areas of 9·2, 25·8, and 6·5 square centimetres respectively at the points 1, 2, and 3. The heights of these points respectively above a datum plane 00 are 92, 65, and 21 cms. The pipe is connected at its upper end to a tank in which the free water surface is 2 metres above the datum plane. Neglecting all losses, calculate (i) the discharge through the system, (ii) the velocity energy and the pressure energy at each of the three points.

Solution :—

Inserting in equation 3-1, § 33, the values $z = 200$ cms., $z_3 = 21$ cms., we have

$$200 = 21 + \frac{v_3^2}{1960},$$

from which $v_3 = 591$ cms./sec. and

Discharge $= a_3 v_3 = 6{\cdot}5 \times 591 = 3850$ c.c./sec. $=$ *3·85 lit./sec.*

Also $v_1 = q/a_1 = 3850/9{\cdot}2 = 418$ cm./sec.,

and $v_1^2/2g =$ *velocity energy* at (1) $=$ *89·2 cms.*

Pressure energy at (1) $= 200 - 92 - 89{\cdot}2 =$ *18·8 cms.*

Similarly, velocity energy at (2) $=$ 11·3 cms.

Pressure energy at (2) $=$ 123·7 cms.

EXAMPLE 13.

A horizontal closed passage is shaped so as to impart uniform acceleration to the liquid flowing through it. At point *A* the mean velocity is 5·0 ft./sec., and the pressure-head is 4·9 ft. ; the slope of the hydraulic gradient is 1/10. What would be the mean velocity, and the pressure-head, at point *B*, distant 3·8 ft. from *A* ? Show that the result is consistent with Bernoulli's theorem.

Solution :—

From equation (3-2), acceleration $= \frac{dv}{dt} = g \cdot \frac{dh}{dl}$

$= 32{\cdot}2 \times \frac{1}{10} = 3{\cdot}22$ ft./sec.^{2}

According to Newton's law, $v_B^2 - v_A^2 = 2 \,.\, a \,.\, s,$

or $v_B^2 - (5{\cdot}0)^2 = 2 \times 3{\cdot}22 \times 3{\cdot}8$

whence $v_B = \text{velocity at } B = 7{\cdot}04 \text{ ft./sec.}$

also $h_B = \text{head at } B = 4{\cdot}9 - \dfrac{3{\cdot}8}{10} = 4{\cdot}52 \text{ ft.}$

By Bernoulli's theorem,

$$h_A - h_B = \frac{v_B^2 - v_A^2}{2g} = \frac{(7{\cdot}04)^2 - (5{\cdot}0)^2}{64{\cdot}4}$$

$$= 0{\cdot}38 \text{ ft., which agrees with previous result.}$$

Example *for solution :—*

14. In the closed passage shown in Fig. 22, the conditions at transverse plane 00 are : Width of passage = 3 ins. ; velocity of water = 38 ft./sec. ; absolute pressure of water = 6·2 psi. What would be the velocity, and the absolute pressure, at a point X in the horizontal axis of the passage, distant 6-ins. to the left of plane 00 ?

Ans. About 9·5 ft./sec. : 15·3 psi.

CHAPTER IV.

Example 15.

The jet condenser of a marine engine is situated 9 ft. below the water line, and the vacuum in the condenser is shown by a gauge to be 27·2 ins. of mercury. Calculate the rate of discharge through the nozzle, which has a diameter of $1\frac{1}{8}$ inch and a coefficient of discharge of 0·96.

Solution :—

Positive pressure head at entrance to nozzle = 9 ft.

Negative pressure head in condenser $= \dfrac{27{\cdot}2}{12} \times 13{\cdot}6$

$= 30{\cdot}85$ ft. of water.

h = total difference of head producing flow $= 9 - (-\,30{\cdot}85)$

$= 39{\cdot}85$ ft.,

$$\therefore\ q = \textit{discharge through nozzle} = C_d a\sqrt{2gh}$$

$$= 0{\cdot}96 \times \frac{\pi}{4}\left(\frac{1{\cdot}125}{12}\right)^2\sqrt{64{\cdot}4 \times 39{\cdot}85}$$

$$= \mathit{0{\cdot}336\ cu.\ ft./sec.}$$

Example 16.

Water issuing from a sharp-edged orifice 0·86 in. in diameter under a head of 2·45 ft. is collected in a rectangular tank 3·62 ft. wide and 5·99 ft. long. In 511 secs. the water level in the tank is

found to rise 0·723 ft. Calculate the coefficient of discharge of the orifice.

Solution :—

Volume of water collected in 511 secs. $= 5{\cdot}99 \times 3{\cdot}62 \times 0{\cdot}723$
$= 15{\cdot}69$ cu. ft.,

$$q = \text{mean rate of discharge} = \frac{\text{volume}}{\text{time}} = \frac{15{\cdot}69}{511} = 0{\cdot}0307 \text{ cusecs},$$

$$a = \text{area of orifice}$$

$$= \left(\frac{0{\cdot}86}{12}\right)^2 \cdot \frac{\pi}{4} = 0{\cdot}00403 \text{ sq. ft.},$$

$$C_d = \textit{coefficient of discharge} = \frac{q}{a\sqrt{2gh}}$$

$$= \frac{0{\cdot}0307}{0{\cdot}00403 \times \sqrt{64{\cdot}4 \times 2{\cdot}45}} = \mathit{0{\cdot}605}.$$

EXAMPLE 17.

A right-angled triangular notch, and a sharp-edged rectangular weir 28 cms. broad, are to be used alternatively for gauging a discharge estimated to be about 15 lit./sec. Find in each case the percentage error in computing the discharge that would be introduced by an error of 1 mm. in observing the head over the weir.

Solutions :—

For the *V*-notch, $Q = \frac{8}{15} C_d \sqrt{2g} \, . \, H^{\frac{5}{2}}.$

Inserting the values $Q = 15{,}000$ cu. cm./sec.,
$C_d = 0{\cdot}593,$
$g = 981$ cm./sec./sec.,

we find $H = \mathit{16{\cdot}30}$ *cms.*

Writing now $Q = KH^{\frac{5}{2}}$, and differentiating,

we have $$\frac{dQ}{dH} = \frac{5}{2} \, . \, KH^{\frac{3}{2}},$$

whence $$\frac{dQ}{Q} = 2{\cdot}5 \, \frac{dH}{H}.$$

Substituting $dH = 0{\cdot}1$ cm., and $H = 16{\cdot}30$ cms.,

$$\frac{dQ}{Q} = 2{\cdot}5 \, . \, \frac{0{\cdot}1}{16{\cdot}3} = 0{\cdot}015,$$ or *percentage error = 1·5 per cent.*

For the rectangular weir, $Q = \frac{2}{3} C_d b \sqrt{2g} \, . \, H^{\frac{3}{2}}$,
from which $H = \mathit{9{\cdot}49}$ *cms.* (assuming $C_d = 0{\cdot}623$).

Writing $Q = K_1H^{\frac{3}{2}}$, and differentiating, we find $\dfrac{dQ}{Q} = 1{\cdot}5\,\dfrac{dH}{H}$.

Substituting $dH = 0{\cdot}1$ cm., and $H = 9{\cdot}49$ cms.,

$$\frac{dQ}{Q} = 1{\cdot}5\,.\,\frac{0{\cdot}1}{9{\cdot}49} = 0{\cdot}016, \text{ or } \textit{percentage error} = \textit{1·6 per cent.}$$

(*Note.*—Although the head to be measured is so much greater for the *V*-notch than for the rectangular weir, yet the percentage error resulting from a given error in observation is in this case very nearly the same.)

EXAMPLE 18.

Water flows along a rectangular channel 20 ins. wide and 15·4 ins. deep, and then over a sharp-edged Cippoletti weir of 1·00 ft. crest length. If the water level in the channel is 0·609 ft. above the weir crest, calculate the discharge over the weir.

Solution :—

Approximate discharge, neglecting velocity of approach,

$$= Q = \tfrac{2}{3}C_d b\sqrt{2g}\,.\,H^{\frac{3}{2}}$$

$$= \tfrac{2}{3} \times 0{\cdot}632 \times 1{\cdot}00 \times \sqrt{64{\cdot}4} \times (0{\cdot}609)^{\frac{3}{2}} = \textit{1·61 cusecs.}$$

Now area of approach channel $= \dfrac{20}{12} \times \dfrac{15{\cdot}4}{12} = 2{\cdot}14$ sq. ft.,

$$\therefore\ v_a = \text{velocity of approach} = \frac{1{\cdot}61}{2{\cdot}14} = 0{\cdot}75 \text{ ft./sec.,}$$

$$\therefore\ \frac{v_a^{\,2}}{2g} = \frac{(0{\cdot}75)^2}{64{\cdot}4} = 0{\cdot}0087 \text{ ft. (approx.).}$$

Substituting this value in the formula

$$Q = \tfrac{2}{3}C_d b\sqrt{2g}\left[\left(0{\cdot}609 + \frac{v_a^{\,2}}{2g}\right)^{\frac{3}{2}} - \left(\frac{v_a^{\,2}}{2g}\right)^{\frac{3}{2}}\right],$$

we find : *true discharge = 1·64 cu. ft./sec.*

(*Note.*—Evidently the true velocity of approach will be slightly greater than the approximate value 0·75 ft./sec. first obtained, but the difference between the two values is far too small to have any sensible effect on the computed value of the discharge.)

EXAMPLE 19.

Calculate the time required to empty a cylindrical horizontal tank, 14 ft. diameter, and 14 ft. long, through a circular orifice 2 inches diameter pierced in the lowest point of the shell. The tank is originally half full of water ; the mean coefficient of discharge of the orifice is 0·62.

Solution :—

When the head over the orifice is h, the area A of the water surface is $14 \times 2\sqrt{7^2 - (7-h)^2} = 14 \times 2\sqrt{h(14-h)}$.

Using the equation $q \,.\, dt = A \,.\, dh$,

we have $$C_d a\sqrt{2gh} \,.\, dt = 28\sqrt{h(14-h)} \,.\, dh.$$

Now $$a = \text{area of orifice} = \frac{\pi}{4}\left(\frac{2}{12}\right)^2 = 0{\cdot}0218 \text{ sq. ft.},$$

$$\therefore\ dt = \frac{28(14-h)^{\frac{1}{2}}}{0{\cdot}62 \times 0{\cdot}0218 \times 8{\cdot}03} \,.\, dh = 257{\cdot}5\ (14-h)^{\frac{1}{2}}\, dh,$$

$$\therefore\ T = \int dt = -\ 257{\cdot}5\left[\frac{(14-h)^{\frac{3}{2}}}{\frac{3}{2}}\right]_{h=0}^{h=7}$$

$= 5800$ secs. $=$ *about 97 minutes* $=$ *time to empty tank.*

(*Note.*—The actual time required to empty the tank would probably be greater than this, due to the formation of a free vortex when the head over the orifice became very small, § 140.)

EXAMPLES *for Solution :—*

20. Water under a head of 1670 ft. flows through a nozzle 6 ins. diameter which has a coefficient of discharge of 0·985. What would be the water horse-power of the jet ? Ans. 11,650 h.p.

21. A bell-mouthed orifice having a diameter of 2·5 cms. and a coefficient of discharge of 0·97 works under a head of 0·86 metre of water. What percentage increase of discharge would be produced by adding to it a horizontal diverging mouthpiece having an outlet diameter of 3·4 cms. ?

When the diverging mouthpiece is in use, calculate :—

(i) The coefficient of discharge based on the orifice area.

(ii) The coefficient of discharge based on the outlet area.

(iii) The negative head at the junction between the orifice and the mouthpiece.

As ume that 20 per cent. of the working head is lost in friction, etc., in the orifice and mouthpiece. Ans. 71 per cent.
1·66
0·89
164 cms.

22. A sharp-edged circular orifice 1·506 ins. diameter projects a jet horizontally under a head of 6·72 ft. The measured diameter of the jet at the *vena contracta* is 1·186 ins. A point in the axis of the jet is found to be distant 4·46 ft. horizontally from the orifice and 9·37 ins. vertically below it. Calculate the coefficients of velocity, contraction, and discharge for the orifice.
Ans. 0·973 ; 0·621 ; 0·605.

23. In an ornamental fountain there are 12 nozzles, each 3 cms. diameter, all inclined upwards at an angle of 45° with the horizontal. The jet issuing from each nozzle is required to fall into a basin at a point distant 1·4 metres vertically beneath the nozzle, and 4·6 metres horizontally from it. The coefficient of velocity for the nozzles may be taken as 0·97, and air friction may be neglected. What would be the pressure head on the nozzles, and the total quantity of water required ? Ans. 1·86 metres.
50 lit./sec.

24. It is required to estimate the discharge, under a head of 7·65 ft., over a spillway weir 164 ft. long. A model is made reresenting the cross-section to a scale of 1/10, but only 3 ft. long. Under what head should it be tested ? If under the correct head this model gives a discharge of 7·09 cub. ft./sec., what would you expect the discharge over the full-scale spillway to be ?

Ans. Head = 0·765 ft. ; q = about 12,300 cu. ft./sec.

25. A sharp-edged rectangular gauging weir with suppressed end contractions was found to give a hook-gauge reading of 16·63 cms. when a discharge q was flowing over it. When the ventilation holes under the nappe were closed, the hook-gauge reading fell to 16·53 cms. for the same discharge q. The hook-gauge zero reading (§§ 376, 385) was 10·18 cms. What percentage error in estimating the discharge would result from inadvertently leaving the ventilating holes closed ? Ans. 2·4 per cent.

26. A reservoir having a surface area of 2410 sq. ft. is to be emptied over a rectangular weir having a crest length of 11·0 ins. and a mean coefficient of discharge of 0·65. How long will it take to lower the head over the weir from 7·32 ins. to 2·68 ins. ?

Ans. 21 mins.

CHAPTER V.

EXAMPLE 27.

Calculate the flow through a capillary tube 10 cms. long and 0·12 cm. diameter, if the viscosity of the liquid is 0·25 poises and the pressure difference at the two ends of the tube is 0·08 kg./sq. cm.

Solution :—

The values to be substituted in the formula $q = \frac{\pi d^4}{128\mu} \cdot \frac{(p_1 - p_2)}{l}$

are : d = diameter in cms. = 0·12,
μ = viscosity in poises = 0·25,
$p_1 - p_2$ = pressure drop in dynes/sq. cm.
$= 0{\cdot}08 \times 1000 \times 981$
$= 78{,}500$
l = 10 cms.

whence q = *discharge in cu. cm./sec. = 0·160.*

(*Note.*—As a check, to make certain that the velocity is in fact below the critical velocity, we calculate $v = \frac{q}{a} = 14{\cdot}1$ cm./sec., therefore Reynolds number

$$R_n = \frac{vd}{\nu}$$

$$= \frac{14{\cdot}1 \times 0{\cdot}12}{0{\cdot}25}$$

(assuming that $\rho = 1$) $= 6{\cdot}77$

which is very much below 2000).

EXAMPLE 28.

Water at a temperature of 20° C. flows through a smooth brass pipe 2·5 cms. diameter at mean velocities ranging from 16 cms./sec. to 16 metres/sec. Plot curves between (i) mean velocity and coefficient f, and (ii) mean velocity and true exponent n, for the full range of velocities.

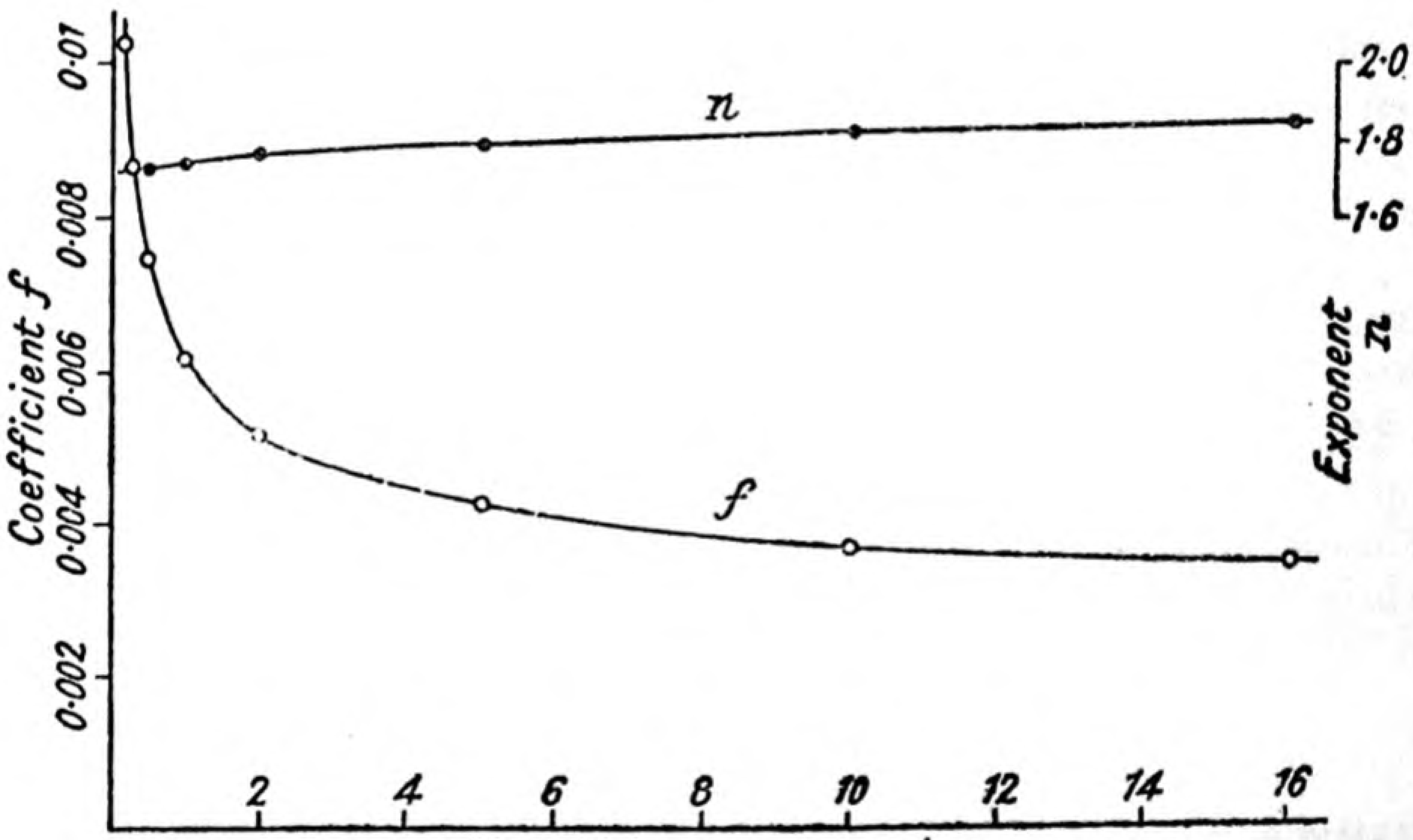

Solution :—

(i) At a temperature of 20° C. the viscosity of water is 0·0101 poises (§ 9), and consequently for a pipe diameter $d = 2{\cdot}5$ cms. the relationship between Reynolds number R_n and mean velocity v is

$$R_n = \frac{v \times 2{\cdot}5}{0{\cdot}0101}.$$

Inserting now various values of v, corresponding values of R can at once be obtained, and the required values of f can be read off directly from Fig. 51, thus permitting the curve between v and f to be plotted as shown.

(ii) For a given pipe, equation 5-9 may be written in the form $h = Kv^n$, and equation 5-7 may be put in the form $h = K_1 f v^2$,

where K and K_1 are constants. Consequently $Kv^n = K_1 f v^2$, from which

$$f = (K/K_1)v^{n-2},$$

and therefore $\log f = (n - 2) \log v + \log (K/K_1)$.

A curve between $\log f$ and $\log v$ must now be plotted, and by measuring at various points the slope of the curve, which is equal to $n - 2$

$$\left(\text{or} \quad \frac{\log (f + \delta f) - \log f}{\log (v + \delta v) - \log v} = n - 2\right),$$

the desired values of n are obtained, and plotted as shown.

(*Note* (i).—Since in the present diagram, values of v are plotted to a *linear* scale instead of to a logarithmic scale, as in Fig. 51, the very rapid diminution in the value of f as the Reynolds number increases from a value of about 4000 is very clearly seen.

Note (ii).—When the range of velocities considered is sufficiently great, the value of n is not quite constant, but increases slightly as the velocity increases (§ 159).)

EXAMPLE 29.

The following observations were made during the flow of water through a straight pipe 3·15 cms. diameter, q being the discharge in litres per second, and h the loss of head, in cms. of water, in a length of 3·00 metres of pipe :—

q	0·585	0·837	1·188	1·540	1·905	2·322	2·740
h	5·9	12·2	21·2	35·0	53·0	74·2	104·3

Find the value of n in the equation $h = Kv^n$, and also find the value of the pipe coefficient f when the velocity is 2·00 m./sec.

Solution :—

Area of pipe $= \frac{\pi}{4} \times 3{\cdot}15^2 = 7{\cdot}80$ sq. cms.

$$v = \text{velocity in cms./sec.} = \frac{q \times 1000}{7{\cdot}80}.$$

Having in this way calculated the velocity corresponding to each rate of discharge, values of $\log v$ and of $\log h$ may be taken out and plotted as shown in the figure.

Now since $h = Kv^n$, $\log h = \log K + n \log v$

and $\log h_1 = \log K + n \log v_1$,

whence $n = \dfrac{\log h - \log h_1}{\log v - \log v_1}$ = slope of line = (by measurement) *1·84.*

Also when $v = 200$ cms./sec., log $v = 2{\cdot}301$, and, from the graph, log $h = 1{\cdot}550$, whence $h = 35{\cdot}5$ cms.

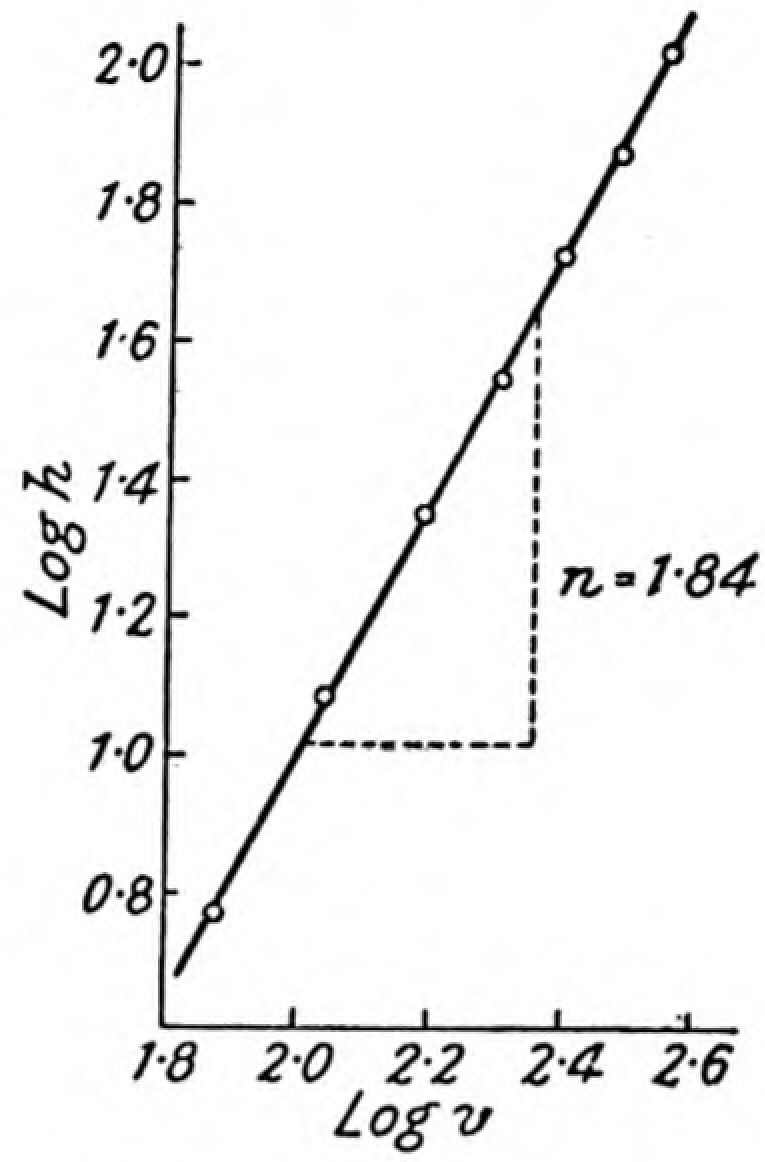

Inserting known values in the formula

$$h = \frac{4fl}{d} \cdot \frac{v^2}{2g}, \text{ we have } 35{\cdot}5 = \frac{4f \times 300}{3{\cdot}15} \cdot \frac{(200)^2}{2 \times 981},$$

whence *pipe coefficient* $f = 0{\cdot}0046$.

(*Note.*—In this example the range of velocities is sufficiently small for the variation in the value of n, noted in Example 28, to be inappreciable.)

EXAMPLE 30.

A pipe *ABCD* of uniform diameter is made up of three straight lengths of which *AB* measures 202 ft., *BC* 800 ft., and *CD* 92 ft. The levels above datum are : $A = 782{\cdot}3$ ft., $B = 764{\cdot}0$ ft., $C = 620{\cdot}9$ ft., and $D = 614{\cdot}8$ ft. A gauge at A shows a pressure of 17 lb./sq. in., and a gauge at D shows 96 lb./sq. in.

State the direction of flow along the pipe, and the water pressure in the pipe at a point E which is 700 ft. above datum.

Solution :—

$$h_a = \text{pressure head at } A = p/w = 17 \times \frac{144}{62{\cdot}4} = 39{\cdot}3 \text{ ft.}$$

$$h_d = \text{pressure head at } D \qquad = 96 \times \frac{144}{62{\cdot}4} = 221{\cdot}5 \text{ ft.}$$

Pressure head + position head at $A = 39{\cdot}3 + 782{\cdot}3 = 821{\cdot}6$ ft.
Pressure head + position head at $D = 221{\cdot}5 + 614{\cdot}8 = 836{\cdot}3$ ft.

Since velocity head at A = velocity head at D, difference in total energy of water at A and at $D = 836{\cdot}3 - 821{\cdot}6 = 14{\cdot}7$ ft. The water is therefore *flowing from D to A*, and loses 14·7 ft. lb.

of energy per lb. *en route*. Neglecting secondary losses, the whole of this energy is absorbed in overcoming surface friction. Total length of pipe $= 202 + 800 + 92 = 1094$ ft., therefore i = virtual slope = loss of head per foot of pipe $= \frac{h}{l}$

$$= \frac{14 \cdot 7}{1094} = 0 \cdot 01345.$$

Consequently loss of head from D to $C = 0\cdot01345 \times 92 = 1\cdot24$ ft.
C to $B = 0\cdot01345 \times 800 = 10\cdot76$ ft.
B to $A = 0\cdot01345 \times 202 = 2\cdot72$ ft.

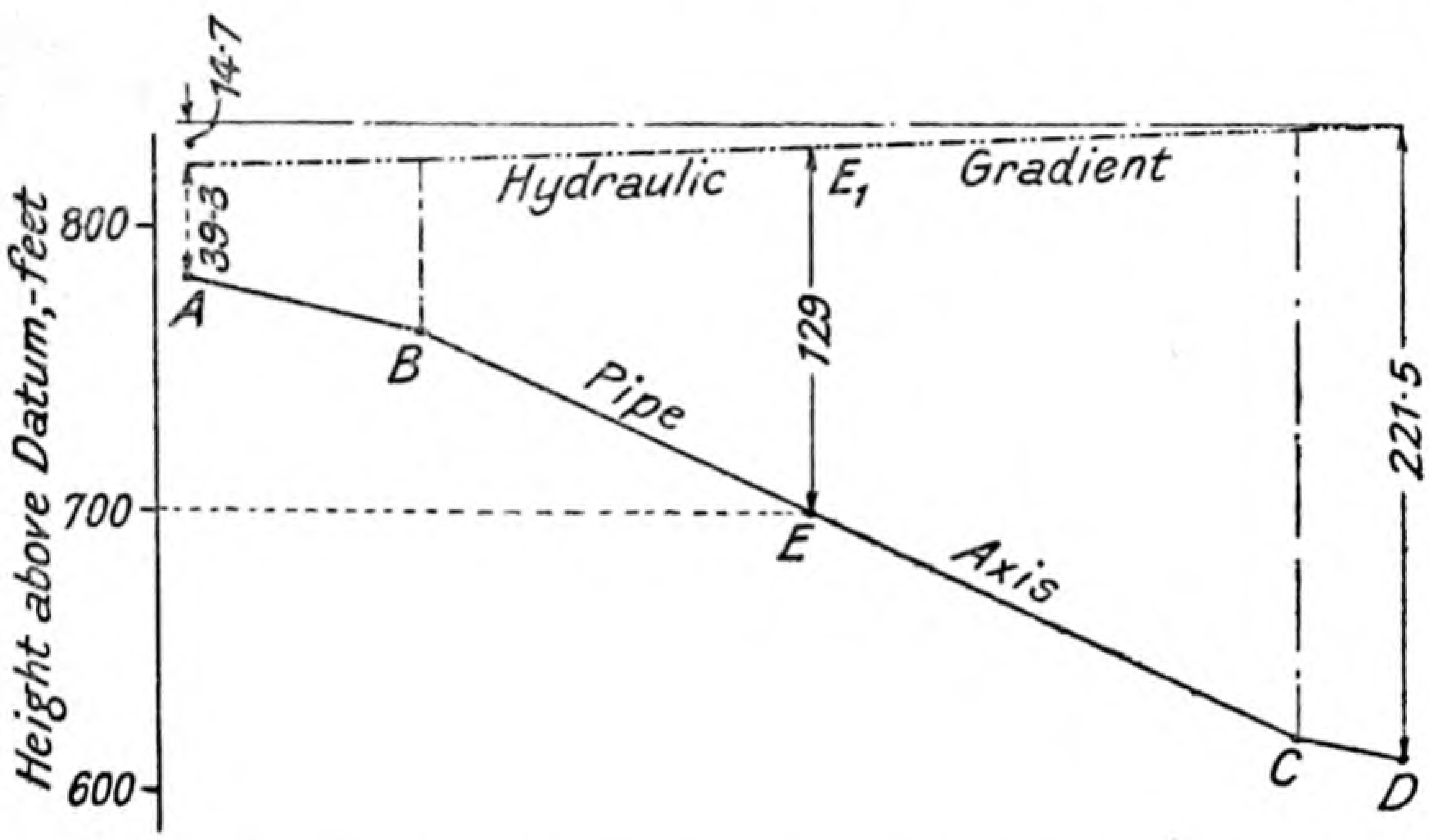

By plotting to scale the pipe axis and the hydraulic gradient, as in the figure (or by arithmetic), the distance EE_1, representing the pressure head at E, is found to be 129 ft., whence

$$\textit{pressure at } E = 129 \times \frac{62\cdot4}{144} = 56 \textit{ lb./sq. in.}$$

(*Note* (i).—There is no essential connection between the slope of the pipe axis and the slope of the hydraulic gradient.

Note (ii).—The exaggerated vertical scale used for clearness in the figure makes it impossible for *horizontal* distances to be set off truly to scale.

Note (iii).—The conditions in this example may be compared with those in Fig. 150.)

EXAMPLE 31.

Two pipes each have a length L; one of them has a diameter D, and the other a diameter d. If the pipes are arranged in parallel the loss of head when a total quantity of water Q flows through them is h; if the pipes are arranged in series and the same quantity Q flows through them, the loss of head is H. If $d = \frac{1}{2}D$, find the ratio of H to h, neglecting secondary losses and assuming the pipe coefficient f has a constant value.

Solution :—

When the pipes are laid in parallel, the friction loss h is the same no matter whether the water flows through the large pipe or through the small one.

Therefore $\qquad h = \dfrac{4fL}{D} \cdot \dfrac{V^2}{2g}, \quad$ or $\quad h = \dfrac{4fL}{d} \cdot \dfrac{v^2}{2g},$

whence $\qquad \dfrac{V^2}{D} = \dfrac{v^2}{d} = \dfrac{2}{D} \cdot v^2, \quad \therefore\ v = \dfrac{V}{\sqrt{2}},$

$\therefore$ discharge Q_o in large pipe $= \dfrac{\pi}{4}D^2 \cdot V$, and

discharge q_o in small pipe $= \dfrac{\pi}{4}d^2 \cdot v = \dfrac{\pi}{4} \cdot \dfrac{D^2}{4} \cdot \dfrac{V}{\sqrt{2}} = 0{\cdot}177\ Q_o.$

Now $\qquad Q = Q_o + q_o = Q_o + 0{\cdot}177\ Q_o, \quad \therefore\ Q_o = 0{\cdot}85\ Q,$
and $q_o = 0{\cdot}15\ Q.$

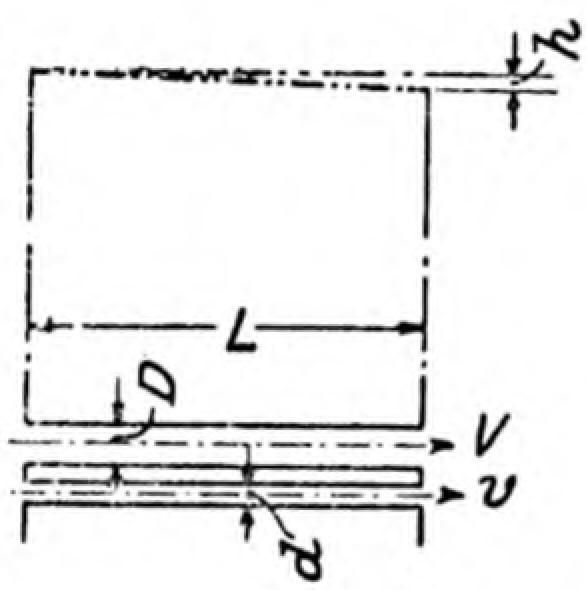

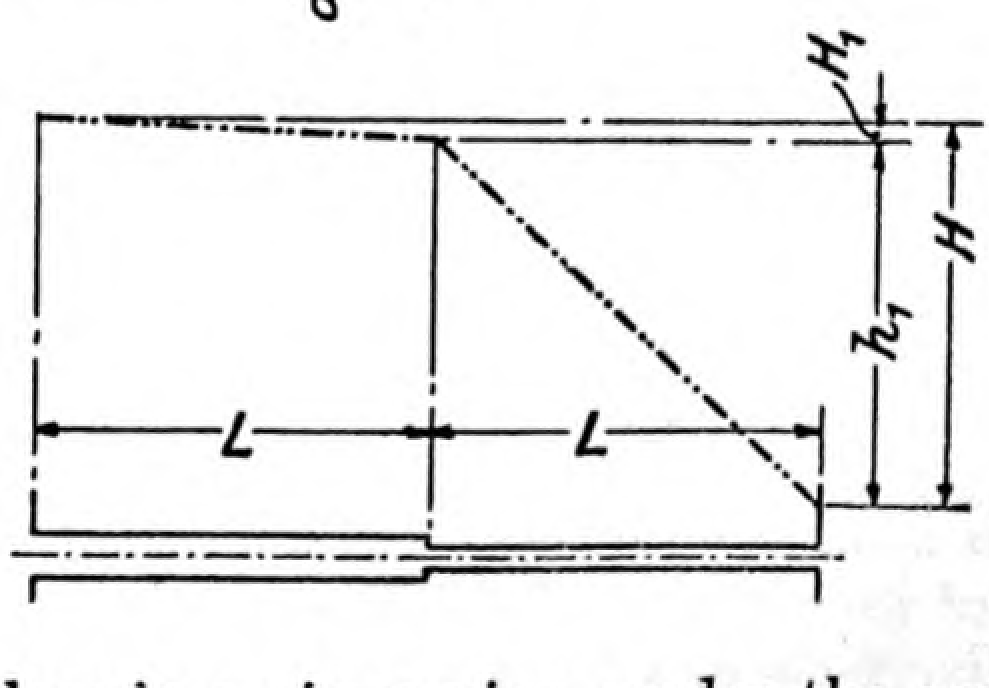

Since friction loss in a given pipe, under the assumed conditions, varies as (velocity)^2, i.e. varies as (discharge)^2, the loss H_1 in large pipe when pipes are in series $= h \times \left(\dfrac{Q}{Q_o}\right)^2$

$$= 1{\cdot}38\ h,$$

and the loss h_1 in small pipe when pipes are in series

$$= h \times \left(\frac{Q}{q_o}\right)^2 = h \times \left(\frac{Q}{0{\cdot}15\ Q}\right)^2$$

$$= 44{\cdot}4h,$$

$\therefore$ *Total loss* $H = 1{\cdot}38h + 44{\cdot}4h = 45{\cdot}8h$ (see figure).

(*Note.*—This example illustrates the following approximate relationships :—

(i) In a given pipe the virtual slope h/l varies as the *square* of the velocity or of the discharge.

(ii) For a given discharge the virtual slope varies inversely as the *fifth* power of the diameter, viz. $\frac{h}{l}$ varies as $\frac{1}{D^5}$.)

EXAMPLE 32.

Water at a temperature of 22° C. flows through a smooth straight pipe A, 4 cms. diameter, at a mean velocity of 42 cms./sec. Oil of density 0·94 gm./c.c. and viscosity 0·28 poises flows through a smooth pipe B, 12 cms. diameter, at such a velocity that dynamical similarity exists between the two systems.

Examine the conditions at two corresponding points, distant 0·15 × radius from the pipe wall, and show that the two values of the ratio

$$\frac{\text{eddy shear stress}}{\text{viscous shear stress}}$$

are identical.

Solution :—

Pipe A :—R_n = Reynolds number $= \dfrac{42 \times 4 \times 0{\cdot}998}{0{\cdot}0095} = 17{,}600.$

From Fig. 51, corresponding value of pipe coefficient $f = 0{\cdot}0068$.
Specified distance $y = 0{\cdot}15R = 0{\cdot}3$ cm.

From the modified form of equation 5-10, § 71, the velocity gradient at this point

$$= \frac{du}{dy} = \frac{2{\cdot}5 \times 42}{0{\cdot}3}\sqrt{\frac{0{\cdot}0068}{2}} = 20{\cdot}4 \text{ secs.}^{-1}.$$

From § 67, total shear stress at pipe wall

$$= \rho \,.\, f \,.\, \frac{v^2}{2} = 0{\cdot}998 \times 0{\cdot}0068 \times \frac{(42)^2}{2} = 5{\cdot}98 \text{ dynes/sq. cm.}$$

Since total shear stress depends upon r/R, then shear stress at radius 1·7 cms.

$$= 5{\cdot}98 \times \frac{1{\cdot}7}{2} = \mathit{5{\cdot}10\ dynes/sq.\ cm.}$$

Now viscous shear stress at radius 1·7 cms.

$$= \mu \,.\, \frac{du}{dy} = 0{\cdot}0095 \times 20{\cdot}4 = 0{\cdot}194 \text{ dynes/sq. cm.}$$

Therefore *eddy shear stress*

$$\tau_r = \tau_t - \tau = 5{\cdot}10 - 0{\cdot}19$$
$$= 4{\cdot}91 \text{ dynes/sq. cm.}$$

Finally, ratio

$$\frac{\text{eddy shear stress}}{\text{viscous shear stress}} = \frac{4{\cdot}91}{0{\cdot}194} = \mathit{25{\cdot}4}.$$

Pipe B :—To achieve dynamical similarity,

$$R_n \text{ for pipe } B = 17{,}600 = \frac{V \times 12 \times 0{\cdot}94}{0{\cdot}28},$$

from which V = mean velocity in pipe B = 436 cms./sec.

Applying the methods already used, we find that—

Velocity gradient at rad. 5·1 cms.	= 70·5 secs.$^{-1}$.
Total shear stress ,, ,,	= 516 dynes/sq. cm.
Viscous shear stress ,, ,,	= 19·7 dynes/sq. cm.
Eddy shear stress ,, ,,	= 496 dynes/sq. cm.

Ratio $$\frac{\text{eddy shear stress}}{\text{viscous shear stress}} = 25{\cdot}3.$$

At the two selected points, therefore, we do in fact find that the ratio of acceleration force to viscous force is the same.

(These calculations show what a very real thing the shear stress or drag at the pipe wall actually is. In the two pipes the respective values are 0·012 and 1·27 lb./sq. ft.)

EXAMPLE 33.

Using the following values for the smooth pipes shown in Fig. 77, find the discrepancy between the true value of $\left(\frac{Q}{q}\right)$ and the value calculated directly from the principle of geometrical similarity. $H = 1{\cdot}85$ m., $L = 3{\cdot}00$ m., $D = 6{\cdot}0$ cms., D_n = diameter of nozzle = 4·0 cms.

The small pipe is made to one-third the scale of the large pipe.

Solution :—

Total energy loss H = friction loss in pipe + velocity head of water leaving nozzle.

If V_p = velocity in large pipe, then

$$H = \frac{4fL}{D} \cdot \frac{V_p^2}{2g} + \frac{V^2}{2g}$$

(neglecting small losses at pipe entry and in nozzle itself).

$$\text{Also } Q = \frac{\pi}{4} D^2 V_p = \frac{\pi}{4} D_n^2 V, \quad \therefore\ V = V_p\left(\frac{6{\cdot}0}{4{\cdot}0}\right)^2 = 2{\cdot}25 V_p.$$

For a first trial, assume $f = 0{\cdot}005$. Substituting known values in the energy equation, we have

$$185 = \frac{4 \times 0{\cdot}005 \times 300}{6} \cdot \frac{V_p^2}{1962} + \frac{V_p^2\,(2{\cdot}25)^2}{1962},$$

from which $V_p = 245$ *cms./sec.*

$$\text{Now Reynolds number } R_n = \frac{V_p D}{\nu} = \frac{245 \times 6}{0{\cdot}01} \text{ (approx.)}$$

$$= 147{,}000.$$

From Fig. 51 it is seen that the true value of f corresponding to $R_n = 147{,}000$ is 0·0042. Inserting this value of $f = 0{\cdot}0042$ in the energy equation, we find that

$$V_p = \text{true velocity in pipe} = 247 \text{ cms./sec.},$$

$$\therefore\ Q = \frac{\pi}{4} . 6^2 \times 247 = \mathit{6980\ cu.\ cm./sec.}$$

In a similar manner it is found that for the small pipe the corresponding values are

$$R_n = 28{,}200 \text{ (approx.)},$$
$$f_o = 0{\cdot}0060,$$
$$v_p = 139 \text{ cms./sec.}, \quad \therefore\ q = \mathit{436\ cu.\ cm./sec.}$$

Hence true value of $\dfrac{Q}{q} = \dfrac{6980}{436} = \mathit{16{\cdot}00}$, but value derived from principle of geometrical similarity $= (\text{scale})^{\frac{5}{2}} = 3^{\frac{5}{2}}$

$$= \mathit{15{\cdot}60}.$$

Therefore *discrepancy* $= \dfrac{16{\cdot}00 - 15{\cdot}60}{16{\cdot}00} = \mathit{0{\cdot}025\ or\ 2{\cdot}5\ per\ cent.}$

Inserting known values, we now find :—

Coefficient of discharge of large nozzle (based on total head) $= \dfrac{Q}{\frac{\pi}{4} D_n{}^2\sqrt{2gH}}$

$$= \mathit{0{\cdot}922}.$$

Coefficient of discharge of small nozzle (based on total head) $= \dfrac{q}{\frac{\pi}{4} d_n{}^2\sqrt{2gh}}$

$$= \mathit{0{\cdot}900}.$$

EXAMPLES *for Solution* :—

34. What diameter of pipe would be required to convey 940 lit./sec. of water through a distance of 1240 m., with a loss of head of 18 m.? Take Chezy's $C = 55$ (metric). Ans. 67 cms.

35. Calculate the power that can be transmitted with an efficiency of 95 per cent. through a pipe $4\frac{1}{2}$ ins. diameter and 9060 ft. long. The initial pressure in the pipe is 853 lb./sq. in., and the pipe coefficient f is 0·006.

What quantity of water would be required per second?

Ans. 77·5 h.p.
0·365 cusecs.

36. A curved smooth pipe of special shape has an outlet diameter d, and when water flows through it under a head H its coefficient of dischage is found to be C_d.

If now a geometrically similar smooth pipe three times the diameter of the first one is to be tested under a geometrically similar head, what must be the kinematic viscosity of the liquid used, in order that the coefficient of discharge may have the same value, C_d, as before ?

Take the kinematic viscosity of water = 0·01 stokes.

Ans. 0·052

37. A sluice valve in an 8-in. pipe carrying 4 cusecs is to be partially closed in order to dissipate 55 horse-power by throttling, the discharge remaining unaltered. Estimate the area of the valve opening (assuming a coefficient of contraction C_c of 0·65), and state also the pressure drop in the valve. Ans. 0·0615 sq. ft.
52·5 lb./sq. in.

38. What would be the rate of flow of water through a brass pipe 1·8 cms. diameter and 5 metres long, if the loss of head were 5·2 cms. of water ? Give two solutions, (i) assuming a water temperature of 5° C., (ii) assuming a temperature of 95° C. State the value of the Chezy coefficient for both conditions.

Ans. 74·0 cu. cm./sec., 96·6 cu. cm./sec.
$C = 42{\cdot}8$ and 55·8 (metric units).

39. An inclined pipe has a diameter of 5 ins. at a point A which is 4·2 ft. above datum, and a diameter of 3 ins. at a point B which is 5·4 ft. above datum ; there is a sudden contraction between the two points. A discharge of 276 imperial gallons per min. of spirit, of S.G. 0·85, flows through the system. The pressures at the two points are 3·78 and 1·58 lb./sq. in. Neglecting friction, what would be the coefficient of loss C_l in the sudden contraction ?

Ans. 0·50.

40. Show that if the coefficient f for a smooth pipe has the approximate value $0{\cdot}08\ R_n^{-0{\cdot}25}$, then for a liquid of given viscosity the values of n and x in the equation $h = \dfrac{f_1 l v^n}{d^x}$ are 1·75 and 1·25 respectively.

41. Estimate the thickness of the laminar boundary layer in the two pipes described in Example 32. What would be, in each pipe, the ratio : $\dfrac{\text{laminar boundary layer thickness}}{\text{pipe diameter}}$?

Ans. 0·045 cm. ; 0·136 cm. ; $\frac{1}{88}$.

42. A pipe 5540 ft. long and 12 ins. diameter conducts water from a reservoir. The outlet valve at the end of the pipe is 115 ft. below reservoir level, and it is adjusted to give an outflow of 3 cu. ft./sec. At a point A, 2400 ft. from the reservoir and 98 ft. below it, there is another valve on a short branch connected with the pipe, from which 2 cu. ft./sec. are drawn. The pipe coefficient is 0·006. Estimate the approximate pressure at point A and at the main outlet. Ans. 27 lb./sq. in. ; 29 lb./sq. in.

43. A sand filter is 6 metres diameter and the sand bed is 2 metres deep. The sand grains have a mean diameter of 1·2 mm.; the porosity may be taken as 0·39. What would be the loss of head when water at a temperature of 10° C. flows downwards through the filter at the rate of 2250 cubic metres per day? Assume that the grains are (i) spherical, (ii) angular.

Ans. (i) 21 cm., (ii) about 39 cm.

CHAPTER VI.

EXAMPLE 44.

Calculate the discharge in a channel of semi-circular cross-section 3 ft. wide, in which the longitudinal slope is 1 in 4500. Assume uniform flow, and take $C = 80$. What would be the average shear stress at the channel walls?

Solution :—

$$\text{Area of waterway} = A = \frac{1}{2}\left(\frac{\pi}{4}D^2\right) = \frac{1}{2}\left(\frac{\pi}{4} \times 3^2\right) = 3{\cdot}53 \text{ sq. ft.}$$

$$\text{Wetted perimeter} = P = \tfrac{1}{2}\pi D = \tfrac{1}{2}\pi \times 3 = 4{\cdot}71 \text{ ft.}$$

$$\text{Hydraulic mean depth} = m = \frac{A}{P} = \frac{3{\cdot}53}{4{\cdot}71} = 0{\cdot}75 \text{ ft.}$$

$$\text{Mean velocity} = v = C\sqrt{mi} = 80\sqrt{0{\cdot}75 \times \frac{1}{4500}} = 1{\cdot}03 \text{ ft./sec.}$$

$$\textit{Discharge} = Q = Av = 3{\cdot}53 \times 1{\cdot}03 = \mathit{3{\cdot}64 \ cusecs.}$$

$$\textit{Shear stress} = \tau_0 = wmi = 62{\cdot}4 \times 0{\cdot}75 \times \frac{1}{4500} = \mathit{0{\cdot}0104 \ lb./sq.ft.}$$

EXAMPLE 45.

What will be the approximate water surface slope in centimetres per kilometre at a point in a rectangular channel at which the discharge is 28 cu. metres/sec., the bed width is 15·2 m., the depth is 3·1 m., the bed slope is 15 cms. per km., and C has the value 62 (metric)?

Solution :—

$$\text{Area of waterway} = A = 15{\cdot}2 \times 3{\cdot}1 = 47{\cdot}1 \text{ sq. met.}$$

$$\text{Mean velocity} = v = \frac{Q}{A} = \frac{28}{47{\cdot}1} = 0{\cdot}594 \text{ m./sec.}$$

$$\text{Hydraulic mean depth} = m = \frac{47{\cdot}1}{15{\cdot}2 + 2 \times 3{\cdot}1} = 2{\cdot}20 \text{ m.}$$

$$\text{Bed slope} = i = \frac{15}{1000 \times 100} = 0{\cdot}00015.$$

Inserting these values in formula 6-2, $\dfrac{\delta d}{\delta l} = \dfrac{i - \dfrac{v^2}{C^2 m}}{1 - \dfrac{v^2}{gd}}$,

we find that $\dfrac{\delta d}{\delta l} = 0{\cdot}000109$.

Since this has a positive sign, it is evident that the water depth *increases* in a downstream direction, and that the water surface slope at the given point is *less* than the bed slope by an amount 0·000109, i.e.

$$\textit{Water surface slope} = 0{\cdot}00015 - 0{\cdot}000109 = 0{\cdot}000041$$
$$= \mathit{4{\cdot}1\ cms./km.}$$

(*Note* that in the Chezy equation $v = C\sqrt{mi}$, the symbol i refers to the water surface slope, but in the non-uniform flow equation used above, the symbol i refers to the bed slope.)

Example 46.

A channel 16 ft. deep has a bed slope of 1/15,000 and a Chezy coefficient of 90 (foot units). The water is charged with suspended silt consisting of grains 0·05 millimetre diameter. At a level 4 ft. above the bed level, the silt concentration is 0·022 lb./cu.ft. What would be the concentration gradient at this level ?

Solution :—

Two-dimensional flow will be assumed, which implies that the channel is so wide that the hydraulic mean depth m is equal to the depth d. The assumption makes it permissible, too, to accept for channel flow the law of velocity distribution expressed in equation (5-10), § 71. On this basis we write :—

$$\tau_0 = \text{shear stress at channel bed} = wmi \ldots \qquad (\S\ 102)$$
$$= 62{\cdot}4 \times 16 \times \frac{1}{15{,}000}.$$
$$= 0{\cdot}0665 \text{ lb./sq. ft.}$$

Also τ = shear stress at depth 12 ft. below water surface

$$= 0{\cdot}0665 \times \frac{12}{16} = 0{\cdot}050 \text{ lb./sq. ft.}$$

Velocity gradient at level 4 ft. above bed

$$= \frac{du}{dy} = \frac{2{\cdot}5}{4}\sqrt{\frac{0{\cdot}0665}{1{\cdot}94}} \text{ (from eqn. (5-10))}$$
$$= 0{\cdot}115 \text{ sec}^{-1}.$$

From § 76, shear stress = eddy viscosity × velocity gradient (neglecting absolute viscosity).

$$\therefore\ 0{\cdot}050 = \eta \times 0{\cdot}115$$

or η = eddy viscosity = 0·435 lb. sec./sq. ft.

$$\therefore \epsilon = \text{kinematic eddy viscosity} = \eta/\rho = \frac{0{\cdot}435}{1{\cdot}94}$$

$$= 0{\cdot}224 \text{ sq. ft./sec.}$$

Now U = terminal velocity of descent of spherical silt grains (in c.g.s. units)

$$= \frac{981\,(0{\cdot}005)^2\,.\,(2{\cdot}6 - 1{\cdot}0)}{18 \times 0{\cdot}01} \quad . \quad . \quad . \quad \text{from § 129}$$

$$= 0{\cdot}218 \text{ cms./sec.} = 0{\cdot}0071 \text{ ft./sec.}$$

Applying finally equation (6-3), we have

$$0{\cdot}0071 \times 0{\cdot}022 = 0{\cdot}224\ .\ \frac{\delta n}{\delta d},$$

from which *concentration gradient* $= \dfrac{\delta n}{\delta d} = 0{\cdot}0007$ lb./ft.^{4}

(It will be understood that the above solution is only intended to give a general notion of the various factors involved, and of the magnitude of the numerical values. But the result is plausible—it shows that as the concentration gradient is so small, the silt would be fairly evenly distributed. As for the terminal velocity U, reference to § 129 shows that it lies within the range which permits the use of Stokes' law.)

Examples *for Solution:—*

47. In a laboratory a model rectangular channel is made of varnished planed wood, of dimensions 3″ × 1½″. What surface slope would be required to give a water velocity of 1·4 ft./sec.? The specified surface ranks as hydraulically smooth, and the water temperature is 68° F. Ans. About 1 in 350.

48. It is required to compare the cross-sectional area of four open rectangular channels, all having the same discharge q, the same slope i, and the same Chezy coefficient C; but the shape ratio = bed-width/depth is to have the values respectively of 1, 2, 3, and 4. Draw the sections to scale; and also plot a graph between shape ratio and cross-section of channel, from which you can choose the ratio which gives minimum cross-sectional area of waterway.

49. A strip of metal of length l and width b is rolled so as to form a channel of semi-cylindrical cross-section. When water flows along this channel with a slope i, the discharge is found to be q.

If now an identical strip of metal were bent so as to form a channel of triangular cross-section, having a 60° included angle, what would then be the discharge, in terms of q, with the same slope i? Assume C remains unchanged. Ans. 0·56 q.

50. A discharge of 3·8 cu. m./sec. flows along a rectangular channel 2 m. wide. Calculate the total energy per unit weight for various depths, plot a curve between depth and total energy, and find from the curve the critical depth. Ans. $d_c = 0{\cdot}72$ m.

CHAPTER VII.

EXAMPLE 51.

A pipe 3260 ft. long and 10 ins. diameter, whose outlet is closed by a valve, communicates with a reservoir in which the water surface is maintained at a height of 51 ft. above the outlet. If the valve is suddenly opened, plot a curve between time after opening and velocity in pipe. Take a mean value of $f = 0{\cdot}006$, and neglect secondary pressure oscillations.

Solution :—

Neglecting the resistance of the valve and the elasticity of the pipe and of the water, the total head $h = 51$ ft. is available for (i) overcoming pipe friction, (ii) imparting velocity head to the water, and (iii) accelerating the water column. Thus

$$h = \frac{4fl}{d} \cdot \frac{v^2}{2g} + \frac{v^2}{2g} + \frac{l}{g} \cdot \frac{dv}{dt},$$

and therefore $$\frac{dv}{dt} = \left[h - \frac{v^2}{2g}\left(\frac{4fl}{d} + 1\right)\right]\frac{g}{l}.$$

Writing $J = \left(\frac{4fl}{d} + 1\right)$, we have $\frac{dv}{dt} = \left[\frac{2gh}{J} - v^2\right]\frac{J}{2l}$,

and thus $$dt = \frac{\frac{2l}{J} \cdot dv}{\left[\left(\sqrt{\frac{2gh}{J}}\right)^2 - v^2\right]}.$$

Integrating,

$$t = \int dt = \frac{2l}{J} \cdot \frac{1}{2\sqrt{\frac{2gh}{J}}} \cdot \log_e \left[\frac{\sqrt{\frac{2gh}{J}} + v}{\sqrt{\frac{2gh}{J}} - v}\right]$$

$$= \frac{2{\cdot}3026(l)}{\sqrt{2gh} \cdot \sqrt{J}} \cdot \log_{10} \left[\frac{\sqrt{\frac{2gh}{J}} + v}{\sqrt{\frac{2gh}{J}} - v}\right],$$

where t is the time in seconds for the column to attain a velocity v ft./sec.

Inserting in this equation values such as $v = 1$, $v = 2$, etc., corresponding values of t are calculated, viz. 2·02 secs., 4·13 secs., etc., so permitting the required graph to be drawn.

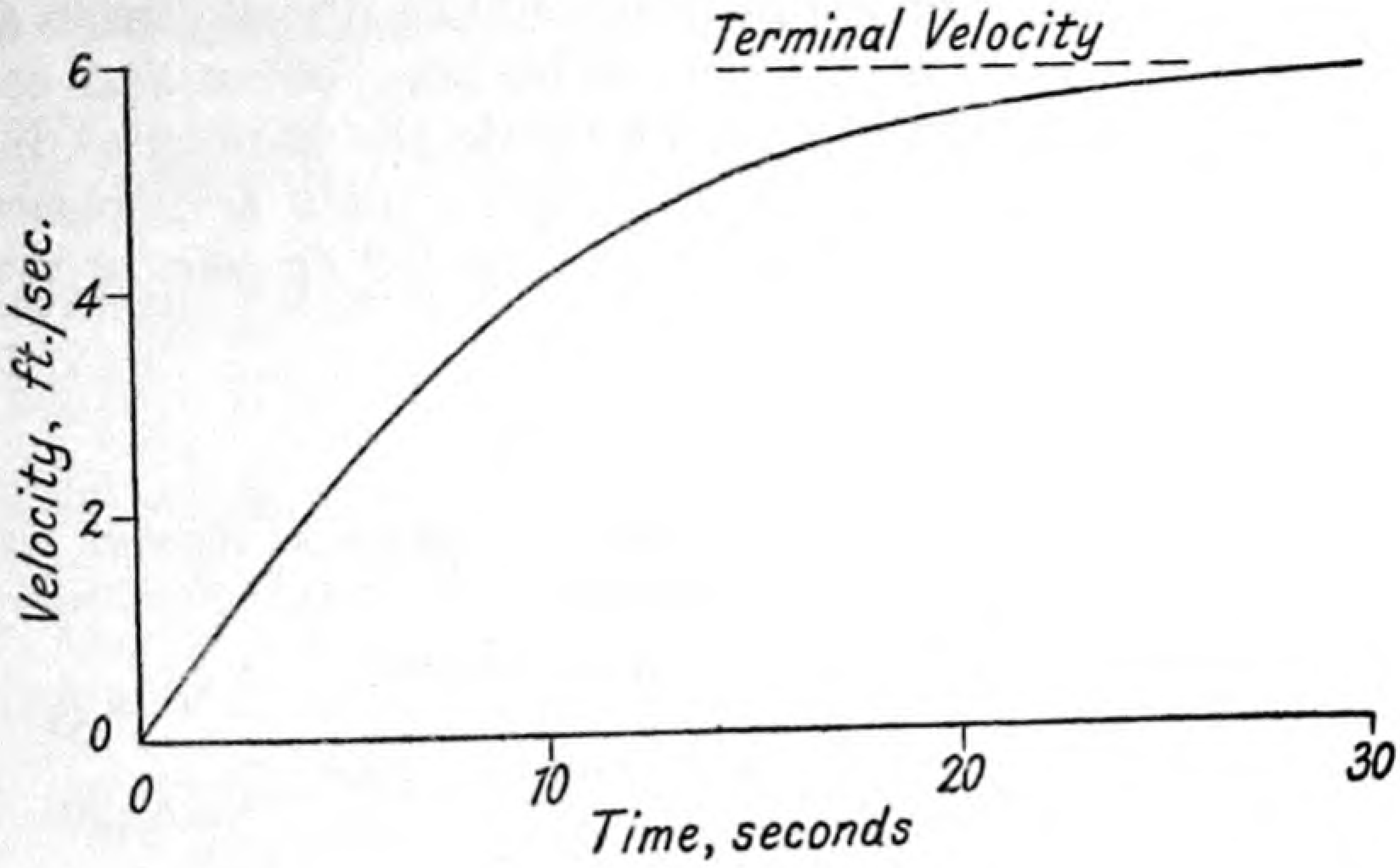

EXAMPLE 52.

Water is flowing along a cast-iron pipe 4 ins. diameter and $\frac{1}{2}$ in. thick, when a valve at the end of the pipe is suddenly closed. Calculate the maximum permissible discharge in the pipe, before the valve is closed, in order that the pressure rise may not exceed 240 lb./sq. in. Take the Modulus of Elasticity of cast iron as 17,000,000 lb./sq. in.

Solution :—

Taking pounds and inches as the units, we have

$$p_i = \frac{v}{\sqrt{\frac{g}{w}\left(\frac{1}{K} + \frac{D}{TE}\right)}}$$

$$= \frac{v}{\sqrt{\frac{32\cdot2 \times 12 \times 1728}{62\cdot4}\left(\frac{1}{300000} + \frac{4}{0\cdot5 \times 17000000}\right)}}$$

$$= \frac{v}{\sqrt{0\cdot0407}}.$$

Since p_i is given as 240 lb./sq. in., $v = 48\cdot4$ ins./sec.
$= 4\cdot03$ ft./sec.

and *permissible discharge* $= Av = \frac{\pi}{4}\left(\frac{1}{3}\right)^2 . 4\cdot03$
$= 0\cdot352$ *cusecs.*

If the term $\frac{D}{TE}$ is neglected, $v = 3\cdot78$ ft./sec.,
and discharge $= 0\cdot330$ cusecs.

It will be observed that the resulting error is on the safe side.

EXAMPLE 53.

A uniform flat plate 80 cms. square, weighing 45 kg., is pivoted freely about its upper horizontal edge, so that it hangs vertically downwards. A horizontal jet of water is then directed from a fixed nozzle on to the plate, at a distance 65 cms. below and at right angles to the axis of suspension. Calculate the horizontal distance through which the centre of gravity of the plate is displaced due to the pressure of the jet, if the jet delivers 8·5 kg./sec. of water at a velocity of 12 m./sec.

Solution :—

Let α be the angle through which the plate is moved, and let l be the required displacement of the C.G.
Taking moments about the axis of suspension,

$$\text{Weight of plate} \times l = \text{normal dynamic thrust} \times \frac{65}{\sin(90-\alpha)},$$

$$\therefore 45 \times l = \frac{W}{g} \cdot U \frac{\sin(90-\alpha)\, 65}{\sin(90-\alpha)} = \frac{8{\cdot}5 \times 12 \times 65}{9{\cdot}8},$$

whence l = *15·0 cms. = displacement of* C.G.

(Note that a coefficient of impact of 1·0 has been assumed.)

EXAMPLE 54.

Calculate the horse-power generated by a hydraulic machine having blades shaped as shown in the sketch. Velocity of jet = 22 m./sec. ; velocity of blades = 12·7 m./sec. ; discharge of jet = 35 kg./sec. Assume ideal conditions.

Also plot to scale the absolute path of the water, taking the transverse width of the moving blades as 20 cm.

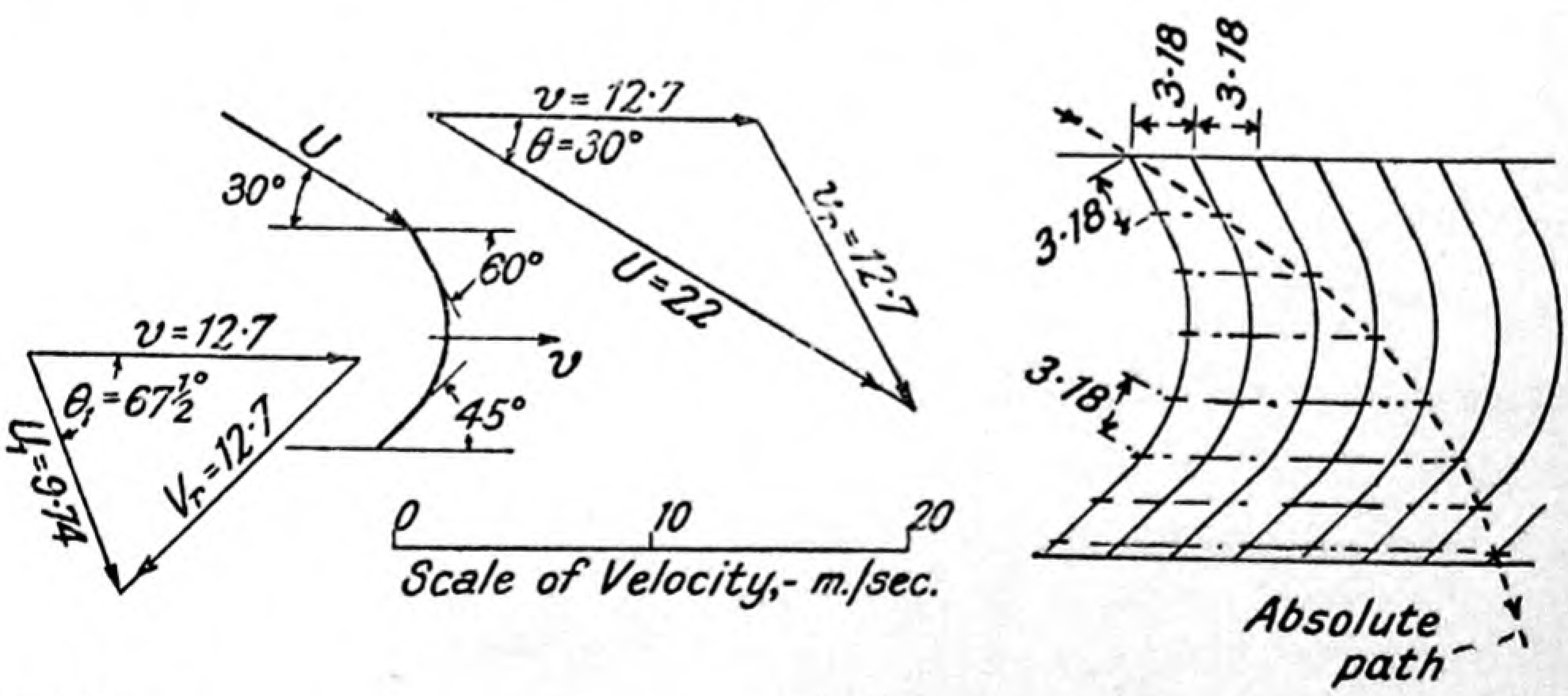

Solution :—

By graphical construction or by analytic methods, the velocity diagrams are found to have the shapes here indicated. The absolute

velocity of the water is thus changed while passing through the wheel from 22·0 to 9·74 m./sec. Therefore

$$\text{Efficiency of machine} = \frac{U^2 - U_1^2}{U^2} = \frac{22^2 - 9{\cdot}74^2}{22^2} = 0{\cdot}805.$$

$$\text{Water horse-power} = \frac{WU^2}{2g} \cdot \frac{1}{75} = \frac{35 \times 484}{19{\cdot}62 \times 75} = 11{\cdot}50.$$

$$\textit{Useful horse-power} = \text{Efficiency} \times \text{water horse-power}$$
$$= 0{\cdot}805 \times 11{\cdot}50 = \mathit{9{\cdot}27}.$$

Alternative solution :—

Tangential thrust on blades $= P =$ change of momentum/sec. in direction of $P = \frac{W}{g} . U \cos \theta - \frac{W}{g} . U_1 \cos \theta_1$

$$= \frac{35}{9{\cdot}81} (22 \times 0{\cdot}866 - 9{\cdot}74 \times 0{\cdot}383) = 54{\cdot}8 \text{ kg.}$$

$$\textit{Useful horse-power} = \frac{\text{work done/sec.}}{75} = \frac{Pv}{75}$$

$$= \frac{54{\cdot}8 \times 12{\cdot}7}{75} = \mathit{9{\cdot}27}.$$

Absolute path of water :—

Successive positions of the moving blade can be drawn at intervals of, say, 1/400 sec. In this interval of time, a blade will move a linear distance of $12{\cdot}7 \times 100 \times 1/400 = 3{\cdot}18$ cms. ; and since the relative velocity along the blade, v_r, happens to be also 12·7 m./sec., an element of water will travel a distance of 3·18 cms. along the blade during the interval of 1/400 sec. As seen in the diagram, the absolute path traced out by the liquid element will be the resultant of these two motions.

EXAMPLE 55.

A smooth, flat plate of 50 cm. side is exposed to a current of water at a temperature of 20° C., having a velocity of 4·2 metres/sec. What will be the total drag on the plate if it is set with two of its sides vertical (i) when the plate is parallel with the stream, (ii) when the plate is normal to the stream, the drag coefficient here being 1·20 ?

Solution :—

(i) From § 127, $R_n = \frac{420 \times 50}{0{\cdot}01} = 2{,}100{,}000,$

$$\therefore f_d = 0{\cdot}074\ (2{,}100{,}000)^{-0{\cdot}2} = 0{\cdot}00402.$$

$$\text{Shear stress} = \tau_0 = 0{\cdot}00402 \times 1{\cdot}0 \times \frac{(420)^2}{2} = 355 \text{ dynes/sq. cm.}$$

Total surface drag (on both sides of plate)

$$= \frac{2 \times 50 \times 50 \times 355}{981 \times 1000} = \mathit{1{\cdot}81\ kg.}$$

(ii) Taking specific weight of water as 1·0 kg. per litre (cubic decimetre), then

$$\text{Form drag} = 1{\cdot}2 \times 5 \times 5 \times 1 \times \frac{(42)^2}{196} \quad \text{(dimensions in decimetres)}$$

$$= \mathit{270\ kg.}$$

EXAMPLE 56.

A horizontal tapered pipe of the sort shown in Fig. 67 is connected at its larger or downstream end to a tank in which the water surface is 5·8 ft. above the pipe axis. The diameter d_1 is 4 ins. and the diameter d_2 is 7 ins. The water temperature is 122° F., and the atmospheric pressure is 14·4 lb./sq. in. Estimate the maximum discharge that could flow through the pipe into the tank before fully-developed cavitation occurred.

Solution :—

h_a = head corresponding to atmospheric pressure $= \frac{14{\cdot}4}{61{\cdot}8} \times 144$

$= 33{\cdot}5$ ft.

h_{vp} = head corresponding to vapour pressure $= \frac{1{\cdot}85}{61{\cdot}8} \times 144 = 4{\cdot}3$ ft.

h_n = limiting negative head $= h_a - h_{vp} = 29{\cdot}2$ ft.

h_l = energy loss in tapered pipe (assumed) $= 0{\cdot}14\ \frac{(v_1 - v_2)^2}{2g}$.

But

$$v_2 = v_1 \times (4/7)^2 = 0{\cdot}325\, v_1,$$

and

$$h_l = 0{\cdot}14 \frac{(0{\cdot}675 v_1)^2}{2g}.$$

Referred to a datum plane coincident with the pipe axis, we can write the energy equation

$$h_1 + \frac{v_1^2}{2g} = h_2 + \frac{v_2^2}{2g} + h_l,$$

or

$$-29{\cdot}2 + \frac{v_1^2}{64{\cdot}4} = 5{\cdot}8 + \frac{(0{\cdot}325 v_1)^2}{64{\cdot}4} + \frac{0{\cdot}14(0{\cdot}675 v_1)^2}{64{\cdot}4},$$

from which $v_1 = 52{\cdot}1$ ft./sec., and

$q = a \,.\, v$ = *limiting discharge = 4·55 cu. ft./sec.*

EXAMPLE 57.

A pipe of fixed diameter d is suddenly enlarged to a diameter D. Find the ratio between D and d in order that the rise in pressure when a given discharge flows past the enlargement shall be a maximum.

Solution :—

From § 136, dynamic pressure $= p_i = \frac{w}{g} \cdot v_2(v_1 - v_2)$.

Differentiating, and equating to zero,

$$\frac{dp_i}{dv_2} = \frac{w}{g} \cdot (v_1 - 2v_2) = 0,$$

whence $v_1 = 2v_2$, or $a_2 = 2a_1$, or $\frac{D}{d} = \sqrt{2}$.

(Note that corresponding maximum increase in head $= \frac{v_2(v_1 - v_2)}{g}$

$$= \frac{\frac{1}{2}v_1(v_1 - \frac{1}{2}v_1)}{g} = \frac{\frac{1}{4}v_1^2}{g} = \frac{1}{2} \cdot \frac{v_1^2}{2g}$$

= one-half of the velocity head in the small pipe.)

EXAMPLE 58.

A discharge of 35 cusecs flows along a rectangular channel 5 ft. wide. What would be the critical depth in the channel ? If a standing wave were formed at a point where the upstream depth was 0·6 ft., what would be the rise in water level produced by the standing wave ?

Solution :—

$$d_c = \text{critical depth} = \frac{v_1^2}{g} = \frac{\left(\frac{Q}{bd_c}\right)^2}{g} = \frac{\left(\frac{35}{5 \times d_c}\right)^2}{32{\cdot}2},$$

from which $d_c = \sqrt[3]{1{\cdot}521} = \mathit{1{\cdot}15\ ft.}$

Depth downstream of standing wave $= d_2$

$$= -\frac{d_1}{2} + \sqrt{\frac{2v_1^2 d_1}{g} + \frac{d_1^2}{4}}$$

$$= -\frac{0{\cdot}6}{2} + \sqrt{\frac{2 \times \left(\frac{35}{5 \times 0{\cdot}6}\right)^2 \times 0{\cdot}6}{32{\cdot}2} + \frac{(0{\cdot}6)^2}{4}}$$

$= 1{\cdot}97$ ft.

Therefore, *rise in water level* $= 1{\cdot}97 - 0{\cdot}6 = \mathit{1{\cdot}37\ ft.}$

EXAMPLES *for Solution :—*

59. A rectangular tank, 12 ft. long and 5 ft. wide and 5 ft. deep, is mounted lengthwise on a lorry ; it contains 3·5 tons of oil of S.G. 0·79. If the lorry, when travelling along a straight level road,

slows down with a negative acceleration of 8 ft./sec./sec., what would be the depth of oil at the two ends of the tank, and what would be the net forward thrust of the liquid on the tank ?

Ans. 4·15 ft. : 1·17 ft. : 1945 lb.

60. A pipe leading from a reservoir is 12,600 ft. long and its outlet end is 485 ft. below the reservoir level. The initial velocity in the pipe, before the outlet valve is closed, is 3·1 ft./sec. ; the velocity of the compression waves through the water is 4200 ft./sec. Neglecting friction and other damping effects, plot to scale a graph between time in seconds, and pressure near the outlet valve, if the valve is closed (i) instantaneously, (ii) in such a way as to bring the water column to rest with uniform retardation in 14 secs.

61. Water under a static head of 30 metres is discharged through a pipe 15 cms. diameter and 40 metres long and then through a nozzle whose area is 1/10 the area of the pipe. Calculate the dynamic thrust on a plate held perpendicularly in front of the jet, taking f for the pipe $= 0{\cdot}008$, C_d for the nozzle $= 0{\cdot}98$, and coefficient of impact $= 0{\cdot}95$.

Ans. 90 kg.

62. A water-wheel having flat radial blades is 7 ft. mean diameter, and water impinges tangentially on to it under a head of 18 ft. through a nozzle 3 ins. diameter. The coefficient of velocity for the nozzle is 0·97. Plot a curve between speed of wheel in r.p.m., and (i) torque, (ii) power developed (neglecting friction), for the full range of possible speeds.

Ans. Max. torque = 362 ft. lb.
Max. h.p. = 1·55.

63. A Barker's Mill has its nozzles set at a radius of 85 cms. ; and it is found that when the mill is held stationary, it exerts a torque of 2 kg. m. and uses 3·4 lit./sec. of water. What will be the discharge, the torque and the power generated (the supply head remaining unaltered) if the mill is allowed to revolve at 180 r.p.m. ? Neglect friction losses.

Ans. 8·66 lit./sec.
1·03 kg. m.
0·260 h.p.

64. A sphere of aluminium of diameter 4·7 in. and S.G. 2·63, is suspended from a thin wire 4·9 ft. long. The sphere is immersed in a flowing stream of water moving with velocity 2·0 ft./sec. How far would the sphere be swept down-stream, viz. what would be the horizontal distance between the point of suspension of the wire and the C.G. of the sphere ?

Ans. 0·36 ft.

65. A cylinder 16 cms. diameter extends horizontally, at right angles, completely across a channel 150 cms. wide in which the water velocity (assumed uniform) is 2·82 m./sec. The axis of the cylinder is 1·47 m. below the free water surface, and the drag coefficient is 1·20. The barometric pressure is 762 mm. mercury. What would be the horizontal dynamic thrust on the cylinder, and the maximum absolute pressure on its surface?

Ans. 117 kg., 1·227 kg./sq. cm.

66. For a solid object of the sort shown in Fig. 121(I), the minimum permissible value of the cavitation number is 0·8. What should be the maximum velocity of the water approaching the object if the water temperature is 140° F. and the absolute pressure before the water reaches the solid is 28·3 psi.? Ans. 21·9 ft./sec.

67. Calculate the power wasted in the standing wave referred to in Example 58. Ans. 2·14 h.p.

CHAPTER VIII.

EXAMPLE 68.

Outward radial flow takes place between two parallel circular plates 0·9 m. diameter and 7·5 cms. apart. Water enters through an orifice 30 cms. diameter in the centre of each plate, and at outlet it discharges freely into the atmosphere. Neglecting all energy losses, calculate the negative head at the inner edges of the plates, and state what would be the axial thrust forcing the plates together. The rate of discharge is 280 litres/sec.

Solution :—

(Dimensions in decimetres.)

$$Y_1 = \text{velocity of flow at outer periphery} = \frac{280}{3{\cdot}14 \times 9 \times 0{\cdot}75}$$

$$= 13{\cdot}25 \text{ dm./sec.}$$

Y_2 = velocity of flow at inner periphery = 39·8 dm./sec.

$$\text{Velocity of flow at any radius } r = Y = Y_1 \times \frac{4{\cdot}5}{r}.$$

$$h = \text{negative head at any radius } r = \frac{\left(Y_1 \cdot \frac{4{\cdot}5}{r}\right)^2 - Y_1^2}{196}$$

$$= 0{\cdot}895\left(\frac{20{\cdot}2}{r^2} - 1\right).$$

Substituting $r = 1{\cdot}5$ dm.,

then *head at inner edge* = 7·15 dm.

= *0·71* metres of water.

Thrust on elementary ring of radius r and radial width δr

$$= w \,.\, h \,.\, 2\pi r \,.\, \delta r.$$

$$\textit{Total thrust on whole surface} = \int_{r=4\cdot5}^{r=1\cdot5} 1 \times 2\pi r \,.\, \delta r \times 0{\cdot}895\left(\frac{20{\cdot}2}{r^2} - 1\right)$$

$$= \left[113 \log_e r - \frac{5{\cdot}62 r^2}{2}\right]_{r=4\cdot5}^{r=1\cdot5}$$

$$= \textit{74 kg.}$$

EXAMPLE 69.

A cylindrical vessel 2 ft. diameter and 3 ft. 9 ins. deep, open at the top, is rotated about its vertical axis at a speed of 105 revs. per min. If the vessel when at rest was full of water, how much water will remain when the vessel has reached its full speed ?

Solution :—

$$\text{Angular velocity} = \omega = \frac{2\pi N}{60} = \frac{6\cdot28 \times 105}{60} = 11\cdot0.$$

Centrifugal head = distance, below rim of vessel, of lowest water

$$\text{level} \qquad = \frac{\omega^2}{2g}r^2 = \frac{11\cdot0^2}{64\cdot4} \, . \, 1^2 = 1.88 \text{ ft.}$$

Volume of water thrown out of vessel by centrifugal action
= volume of paraboloid of revolution
= $\frac{1}{2}$ × volume of enveloping cylinder = $\frac{1}{2}(3\cdot14 \times 1^2 \times 1\cdot88)$
= 2·95 cu. ft.

Original capacity of vessel = $3\cdot14 \times 1^2 \times 3\cdot75 = 11\cdot78$ cu. ft.
Thus *volume of water remaining in vessel* = 11·78 − 2·95
= *8·83 cu. ft.*

EXAMPLE 70.

The water contained in an annular space of outer radius 48 cms. and inner radius 25 cms. is rotated so as to form a vortex. At the inner periphery the velocity of whirl is 8·2 m./sec., and the pressure is 2·44 kg./sq. cm. What will be the pressure at the outer periphery if (i) a free vortex is formed, (ii) a forced vortex is formed ?

Solution :—

Under free vortex conditions, velocity of whirl V_1 at outer

$$\text{periphery} \qquad = V_2 \, . \, \frac{r_2}{r_1} = 8\cdot2 \times \frac{0\cdot25}{0\cdot48} = 4\cdot27 \text{ m./sec.}$$

$$\text{Therefore centrifugal head} = \frac{V_1^2}{2g}\left[\left(\frac{r_1}{r_2}\right)^2 - 1\right]$$

$$= \frac{4\cdot27^2}{19\cdot62}\left[\left(\frac{0\cdot48}{0\cdot25}\right)^2 - 1\right] = 2\cdot50 \text{ m.}$$

$$\text{Corresponding pressure rise} = \frac{2\cdot50 \times 1000}{10000} = 0\cdot25 \text{ kg./sq. cm.}$$

Total *pressure at outer periphery* = 2·44 + 0·25 = *2·69 kg./sq. cm.*

Under forced vortex conditions, velocity of whirl V_1 at outer

$$\text{periphery} \quad = V_2 \, . \, \frac{r_1}{r_2} = 8\cdot2 \times \frac{0\cdot48}{0\cdot25} = 15\cdot75 \text{ m./sec.}$$

$$\text{Centrifugal head} = \frac{V_1^2}{2g} - \frac{V_2^2}{2g} = \frac{15{\cdot}75^2}{19{\cdot}62} - \frac{8{\cdot}20^2}{19{\cdot}62}$$

$$= 9{\cdot}22 \text{ m.}$$

Corresponding pressure rise $= 0{\cdot}1 \times 9{\cdot}22 = 0{\cdot}92$ kg./sq. cm.
Total *pressure at outer periphery* $= 2{\cdot}44 + 0{\cdot}92 = $ *3·36 kg./sq. cm.*

EXAMPLE 71.

A rotating wheel has an outer diameter of 2 ft. and an inner diameter of 1 ft. It is so shaped that the oil flowing through it, of S.G. 0·81, has a uniform radial flow component of 8 ft./sec., corresponding to a discharge of 5 cu. ft./sec. Its speed of revolution is 700 r.p.m. The wheel has 12 radial blades; the liquid enters at the outer periphery with a tangential velocity equal to the rim velocity.

Use two alternative methods to compute the ideal torque on each blade: also estimate the pressure difference across a blade, at a radius of 0·75 ft.

Solution:—

$$\text{Weight of liquid flowing per second} = W = 5 \times 62{\cdot}4 \times 0{\cdot}81$$
$$= 252 \text{ lb./sec.}$$

$$\text{Tangential velocity at entry} = V_1 = v_1$$
$$= \frac{\pi DN}{60} = 73{\cdot}2 \text{ ft./sec.}$$

$$\text{Tangential velocity at exit} = 36{\cdot}6 \text{ ft./sec.}$$

$$\text{Torque per blade} = \frac{\text{Torque on wheel}}{12} = \frac{W}{12g}(V_1r_1 - V_2r_2)$$

from § 144.

$$= \frac{252}{12 \times 32{\cdot}2} \cdot (73{\cdot}2 \times 1{\cdot}0 - 36{\cdot}6 \times 0{\cdot}5)$$

$$= 35{\cdot}7 \textit{ ft. lb.}$$

Alternative solution:—

$T =$ Torque exerted on one blade by liquid element at radius r, of thickness dr and width b.

$$= p_d \,.\, dr \,.\, b \,.\, r.$$

Now $p_d =$ pressure difference $= (wl)/g \times \alpha$ . . . eqn. (8-7)

$$= \left[62{\cdot}4 \times 0{\cdot}81 \times \frac{2\pi r}{12} \Big/ 32{\cdot}2\right] \times 2 \times 8 \times \frac{2\pi \times 700}{60}.$$

Also $\qquad b \,.\, r = \dfrac{Q}{2\pi Y}$ (§ 138) $= \dfrac{5}{2\pi \times 8} = 0{\cdot}099.$

Inserting these values, we find

$$\text{Torque per blade} = \int_{r=0\cdot5}^{r=1} 0\cdot82 \times 1170 \times 0\cdot099 \, . \, r \, . \, dr$$

$$= 35\cdot7 \; ft. \; lb.$$

Pressure-difference across blade at radius 0·75 ft. $= p_d$

$$= \frac{62\cdot4 \times 0\cdot81 \times 3\cdot14 \times 0\cdot75}{6 \times 32\cdot2} \, . \, 1170 = 720 \text{ lb./sq. ft.} = 5\cdot0 \text{ psi.}$$

(The most significant figure in this example is the value of the Coriolis acceleration, 1170 ft./sec./sec. It is 36 times as great as the acceleration of gravity, g.)

EXAMPLES *for Solution:—*

72. A 90° bend in a pipe is of square section, 12 × 12 cms.; the inner radius of the bend is 20 cms. and the outer radius is 32 cms. If the differential head between the outer and inner faces is 19·1 cms. of water, what would you expect the discharge through the bend to be? Ans. 28 lit./sec.

73. A wheel having radial blades is rotated about a vertical axis so as to impart forced vortex motion to the water contained within it; the outer diameter is 22 ins. and the inner diameter is 11 ins., the speed is 435 r.p.m., and the pressure at the inner radius is 6·4 lb./sq. ins. Plot to scale a graph between radius and (i) pressure energy, (ii) total energy, or sum of pressure energy and velocity energy.

74. A closed cylindrical vessel 65 cms. diameter is half-filled with water and then rotated with its axis horizontal at a speed of 600 r.p.m. If the water rotates as a forced vortex at the same angular velocity as the vessel, what would be the total axial thrust tending to burst the flat ends? Ans. 879 kg.

75. Calculate the power given from the water to a wheel 4·6 ft. external diameter, 3·0 ft. internal diameter, and 3 ins. wide, when 6 cusecs are flowing through it. The wheel has radial blades, it revolves at 325 r.p.m., and the water enters at the outer circumference with a velocity of whirl equal to the peripheral velocity of the wheel. What is the velocity of flow at the outer and at the inner rim of the wheel? Ans. 74·2 h.p.
1·66 ft./sec.
2·55 ,,

76. What would be the power wasted in disc friction on the two outer faces of the wheel referred to in Example 75? Ans. 30·7 h.p.

PART II.

Although Part II of the book relates to practical applications of the basic material studied in Part I, it is not to be expected that the following Examples will always offer complete solutions to the problems propounded. For the sake of clarity, simplifying assumptions are frequently made that would not be permissible in an engineer's office. In particular, economic questions can rarely be taken into account.

CHAPTER IX.

EXAMPLE 77.

Calculate the minimum diameter of pipe required to supply a water turbine developing 500 h.p. under the following conditions: Efficiency of turbine = 82 per cent.; static head = 430 ft.; length of pipe = 2330 ft.; pipe coefficient $f = 0{\cdot}006$.

Solution :—

It is shown in § 91 that if H is the static head, and h the friction loss in a pipe, water horse-power delivered is equal to

$$P = \frac{W(H-h)}{550} = \frac{W}{550}\left(H - \frac{4fl}{d}\cdot\frac{v^2}{2g}\right) \quad \text{(foot-units)}$$

$= K \,.\, W\,(H - K_1 \,.\, W^2)$, where K and K_1 are constants for a given pipe. Differentiating and equating to zero, we have

$$\frac{dP}{dW} = K(H - 3K_1W^2) = 0, \quad \text{or} \quad H = 3K_1W^2 = 3h,$$

showing that a given pipe will transmit maximum power for a given initial head when the friction loss is one-third of the initial head. Similarly, the smallest pipe that will transmit a given power will be the one in which the friction loss $= \frac{1}{3}H$.

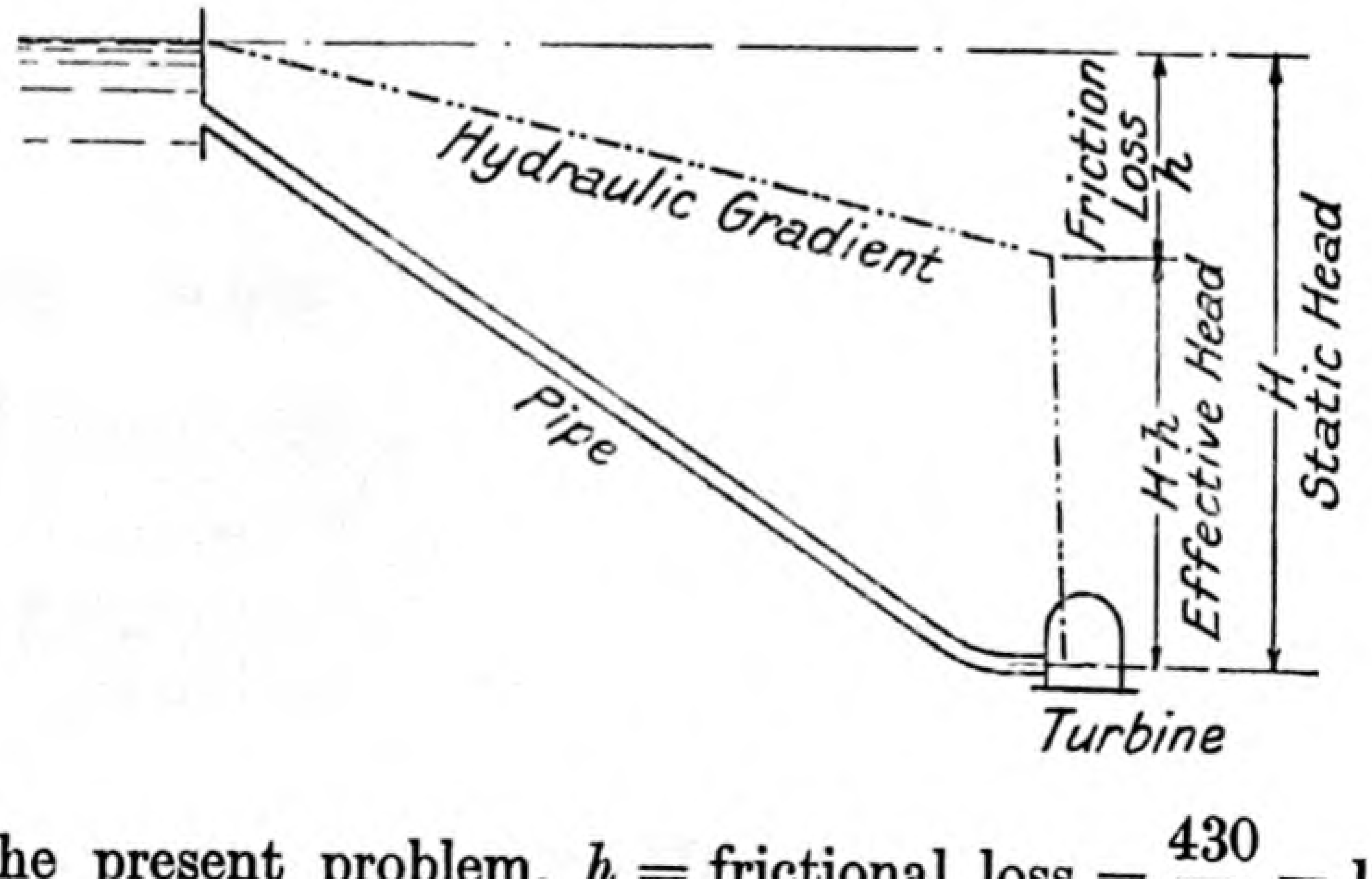

In the present problem, h = frictional loss $= \frac{430}{3} = 143{\cdot}3$ ft., and the available or effective head at the turbine $= 430 - 143{\cdot}3$
$= 286{\cdot}7$ ft. (see diagram).

Since efficiency of turbine $= \dfrac{\text{useful horse-power}}{\text{water horse-power}}$, . . (§ 235)

$$\text{W.H.P.} = \frac{500}{0 \cdot 82} = 610 \text{ ; but also W.H.P.} = \frac{W(H-h)}{550}$$

$$= \frac{W}{550}(286 \cdot 7),$$

whence $W = 1170$ lb./sec., and $Q = \text{discharge} = \dfrac{1170}{62 \cdot 4} = 18 \cdot 77$ cusecs.

To find the diameter of pipe required to transmit 18·77 cusecs with a friction loss of 143·3 ft., the appropriate values are inserted in formula 9-2, viz.

$$h = \frac{flq^2}{10d^5}, \text{ or } 143 \cdot 3 = \frac{0 \cdot 006 \times 2330 \times 18 \cdot 77^2}{10 \times d^5},$$

from which $d = 1 \cdot 28$ *ft.*

(*Note.*—In practice the pipe would hardly ever be made of this minimum diameter, for the following reasons: (i) it would rarely be permissible to waste one-third of the energy of the water in pipe friction, (ii) the reduced head at the turbine necessitates a larger and more costly machine than would otherwise suffice, and (iii) there would be difficulties in regulating the speed of the turbine.)

EXAMPLE 78.

What pressure would be required to force 24 litres per second of oil of viscosity 3520 Redwood and S.G. 0·95 through 1260 metres of 18 cm. diameter piping ?

Solution :—

$$\text{Velocity of oil} = v = \frac{q}{a} = \frac{24000}{\frac{\pi}{4} \cdot 18^2} = 94 \cdot 3 \text{ cms./sec.}$$

From § 371, a viscosity of 3520 Redwood is found to be equivalent to 8·70 poises,

$$\therefore \text{ Reynolds number } R_n = \frac{vd\rho}{\mu} = \frac{94 \cdot 3 \times 18 \times 0 \cdot 95}{8 \cdot 7} = 185.$$

As this value is far below the critical value of 2000, the flow in the pipe will be viscous, hence formula 9-1 is applicable. Inserting known values, we have

$$24 = 0 \cdot 24 \cdot \frac{18^4}{8 \cdot 7} \cdot \frac{(p_1 - p_2)}{1260},$$

from which $(p_1 - p_2)$ = *pressure drop in pipe* = *10·4 kg./sq. cm.*

EXAMPLE 79.

A pump is to lift 485 lit./sec. of water against a static head of 12·6 m., through an uncoated cast-iron pipe 282 m. long which has one 90° bend and a bell-mouthed entry. Estimate the diameter of pipe required, if it be stipulated that pipe losses of all kinds must not exceed 20 per cent. of the dead head.

Solution :—

For a first trial, secondary losses may be neglected.

Accordingly, friction loss $h = 0{\cdot}2 \times 12{\cdot}6 = 2{\cdot}52$ m.

$$\text{Virtual slope } i = \frac{h}{l} = \frac{2{\cdot}52}{282} = 0{\cdot}00894.$$

From inspection of Fig. 139, which relates to the flow through uncoated cast-iron pipes, it is found that the intersection of $q = 485$ and $i = 0{\cdot}00894$ lies between the lines representing 50-cm. and 60-cm. diameter pipes. Say $d = 52$ cms. or 0·52 m. In a 0·52 m. diameter pipe the velocity

$$v = \frac{q}{a} = \frac{0{\cdot}485}{\frac{\pi}{4} \times 0{\cdot}52^2} = 2{\cdot}28 \text{ m./sec.}$$

Secondary losses = velocity head + loss in bend (the loss at inlet may be neglected)

$$= \frac{v^2}{2g} + 0{\cdot}3\,\frac{v^2}{2g}$$

$$= 1{\cdot}3 \times \frac{2{\cdot}28^2}{19{\cdot}6} = 0{\cdot}35 \text{ m.}$$

The ratio $\dfrac{\text{friction loss}}{\text{total loss}}$ is therefore represented by $\dfrac{2{\cdot}52}{2{\cdot}52 + 0{\cdot}35}$ $= 0{\cdot}88$, and the true permissible friction loss is thus $0{\cdot}88 \times 2{\cdot}52 = 2{\cdot}21$ m. Using the corrected value of $i = \dfrac{2{\cdot}21}{282} = 0{\cdot}00784$, we now find from Fig. 139 that *required pipe diameter = 54 cms. or 0·54 m.*

As a check, the corrected value of the secondary losses is calculated, and is found to be 0·30 m. The total losses are thus $2{\cdot}21 + 0{\cdot}30 = 2{\cdot}51$ m., which is within the limit of 20 per cent. of the dead head.

(*Note.*—In practice it might be wise to base the calculations on a discharge 30 per cent. or more in excess of the stipulated discharge, to compensate for the inevitable falling off in the carrying capacity of the pipe as the walls in course of time become pitted or fouled. (See § 161).)

EXAMPLE 80.

A pipe-line is to carry a discharge of 200,000 barrels of oil per day. The oil has a kinematic viscosity of 0·50 stokes and a S.G. of 0·89 ; in a length of 110 miles of pipe, the permissible pressure-drop is 800 psi. What diameter of steel pipe would be required?

Solution :—

Converting the data into suitable units, it is found that :

$$q = \text{discharge} = 13{\cdot}0 \text{ cusecs},$$
$$h = \text{head loss} = 2070 \text{ ft.},$$
$$l = \text{length} = 580{,}000 \text{ ft.}$$

Assuming provisionally a value for the pipe coefficient f of 0·005, and inserting above values in equation (9-2), § 154, it appears that

$$2070 = \frac{0{\cdot}005 \times 580{,}000 \times 13^2}{10 \times d^5},$$

from which d = pipe diameter = 1·88 ft.

and v = mean velocity = q/a = 4·7 ft./sec.

Therefore R_n = Reynolds number $= \dfrac{4{\cdot}7 \times 1{\cdot}88 \times 929}{0{\cdot}50} = 16{,}400.$

From § 155, a suitable figure for the absolute roughness k of steel is 0·005 in., whence $d/k = (1{\cdot}88 \times 12)/0{\cdot}005 = 4500$.

Referring now to Fig. 137, we find that the value of f corresponding to $R_n = 16{,}400$ and $d/k = 4500$ is 0·0070.

Evidently the original value selected was too low. When the corrected value of f is inserted in eqn. (9-2), as above, the corrected value of d is found to be 2·01 ft. On checking the value of f, the chart Fig. 137 shows that the value 0·0070 is still acceptable, and thus the value of the pipe diameter, d, will be slightly over 2 feet ; the nearest value to satisfy manufacturing needs can be taken.

(*Note.*—Evidently within the limits of accuracy here attainable, it would be permissible to treat the pipe as having a hydraulically smooth surface, for which the values of the pipe coefficient plotted in Fig. 135 would serve.)

EXAMPLE 81.

An overhead rectangular tank, 21 ft. long, 10 ft. 6 ins. wide, and 5 ft. 3 ins. deep, is to be emptied by a vertical pipe 5 ins. diameter fixed in the bottom of the tank. The pipe is 14 ft. long, and at its lower end it dips into a drain or sump in which the water level is kept constant, 10 ft. 3 ins. below the bottom of the tank. Assume pipe coefficient $f = 0{\cdot}007$. If the tank is originally quite full, calculate how much water will escape in the first two minutes after emptying begins.

Solution :—

When the water surface in the tank is at a height h above the water surface in the drain, the head h is accounted for as follows :—

(i) Loss of energy at entrance to pipe $= 0{\cdot}5 \,.\, \left(\frac{v^2}{2g}\right)$.

(ii) Friction loss in pipe $= \frac{4fl}{d} \,.\, \frac{v^2}{2g}$.

(iii) Velocity energy at outlet $= \frac{v^2}{2g}$.

Equating, $h = 0{\cdot}5 \,.\, \frac{v^2}{2g} + \frac{4 \times 0{\cdot}007 \times 14}{0{\cdot}42} \,.\, \frac{v^2}{2g} + \frac{v^2}{2g}$,

from which $v = 5{\cdot}14 \sqrt{h}$. Using now the method of § 61, and writing $q \,.\, dt = A \,.\, dh$, we have

$$\frac{\pi}{4} \,.\, (0{\cdot}42)^2 \,.\, v \,.\, dt = 21 \times 10{\cdot}5 \,.\, dh.$$

Substituting the above value of v in this equation gives us

$$dt = \frac{21 \times 10{\cdot}5}{0{\cdot}136 \times 5{\cdot}14\sqrt{h}} \,.\, dh.$$

Integrating, $T = 316 \times 2\, [h_1^{\frac{1}{2}} - h_2^{\frac{1}{2}}]$.

Now T is given as 2 mins. = 120 secs., and h_1 = original total head $= 10{\cdot}25 + 5{\cdot}25 = 15{\cdot}5$ ft. Inserting these values, we find that h_2 = head at end of interval $= 14{\cdot}05$ ft.

Consequently, fall in water surface in tank $= 1{\cdot}45$ ft., and *quantity of water* escaping from tank $= 1{\cdot}45 \times 21 \times 10{\cdot}5 =$ *320 cu. ft.*

(*Note.*—(i) As it is now possible to find the average velocity v in the pipe, the value of the coefficient f may be checked with the help of Fig. 136, and corrected if necessary.

(ii) If the tail-pipe were removed, and the water allowed to flow through the plain hole in the bottom of the tank, it would be found by the method of § 61 that nearly double the time would be needed to discharge the same quantity of water.)

Example 82.

A steam pumping-plant forces water through a 24-in. diameter main, the static lift being 178 ft. and the friction head being 130 ft. It is found that 3200 tons of coal per year are required to drive the pumps. In order to reduce the coal consumption, a 27-in. diameter main is laid, of the same length as the first main, the two working in parallel. Calculate the annual saving in coal, assuming that the discharge and efficiency of the pumps, and the pipe coefficients, remain unaltered.

Solution :—

Let v = original velocity in 24-in. main,
v_1 = reduced velocity in 24-in. main,
v_2 = velocity in 27-in. main,
h = original friction head,
h_1 = reduced friction head.

Now $h = \frac{4fl}{d} \cdot \frac{v^2}{2g}$; also $h_1 = \frac{4fl}{d} \cdot \frac{v_1^2}{2g}$ in 24-in. main

and $h_1 = \frac{4fl}{d_2} \cdot \frac{v_2^2}{2g}$ in 27-in. main.

Therefore $$\frac{v_1^2}{d} = \frac{v_2^2}{d_2} \quad . \quad . \quad . \quad . \quad . \quad . \quad (I)$$

and $$\frac{h_1}{h} = \frac{v_1^2}{v^2} \quad . \quad . \quad . \quad . \quad . \quad . \quad (II)$$

From (I) we see that $v_2^2 = v_1^2 \cdot \frac{d_2}{d} = v_1^2 \cdot \frac{2{\cdot}25}{2}$, $\therefore\ v_2 = 1{\cdot}06v_1$.

Again, discharge $Q = \frac{\pi}{4} \cdot d^2v$,

and also $$Q = \frac{\pi}{4}d^2v_1 + \frac{\pi}{4}d_2^2v_2 = \frac{\pi}{4}d^2v_1 + \frac{\pi}{4}d_2^2\, 1{\cdot}06v_1,$$

from which $$2^2 \cdot v = 2^2 \cdot v_1 + 2{\cdot}25^2 \cdot 1{\cdot}06v_1,$$

or $$v_1 = 0{\cdot}428v.$$

From (II) $$\frac{h_1}{h} = \frac{h_1}{130} = \frac{v_1^2}{v^2} = \frac{(0{\cdot}428v)^2}{v^2} = 0{\cdot}183,$$

and therefore h_1 = reduced friction head = 23·8 ft.

Now $$\frac{\text{reduced coal consumption}}{\text{original coal consumption}} = \frac{h_1 + 178}{h + 178} = \frac{201{\cdot}8}{308} = 0{\cdot}655$$

Hence *annual saving in coal* = 3200 (1 − 0·655) = *1100 tons.*

EXAMPLE 83.

A 15-cm. diameter cast-iron pipe has a length of 2000 metres; the whole of the water entering at one end is drawn off uniformly along the pipe by side branches at the rate of 1 litre per second per 50 metres of pipe. If the pressure at the inlet end is 14·5 kg./sq. cm., what would be the pressure at the closed end?

Solution :—

Discharge at inlet end $= \frac{2000}{50} = 40$ lit./sec.

$$\text{Velocity at inlet end} = \frac{\frac{40}{1000}}{\frac{\pi}{4} \cdot (0{\cdot}15)^2} = 2{\cdot}26 \text{ m./sec.} = v_i.$$

As points further and further along the pipe are considered, the velocity in the pipe will progressively diminish, due to the withdrawal of water through the side branches. The changes in velocity and pressure will thus be of the kinds indicated in the diagram.

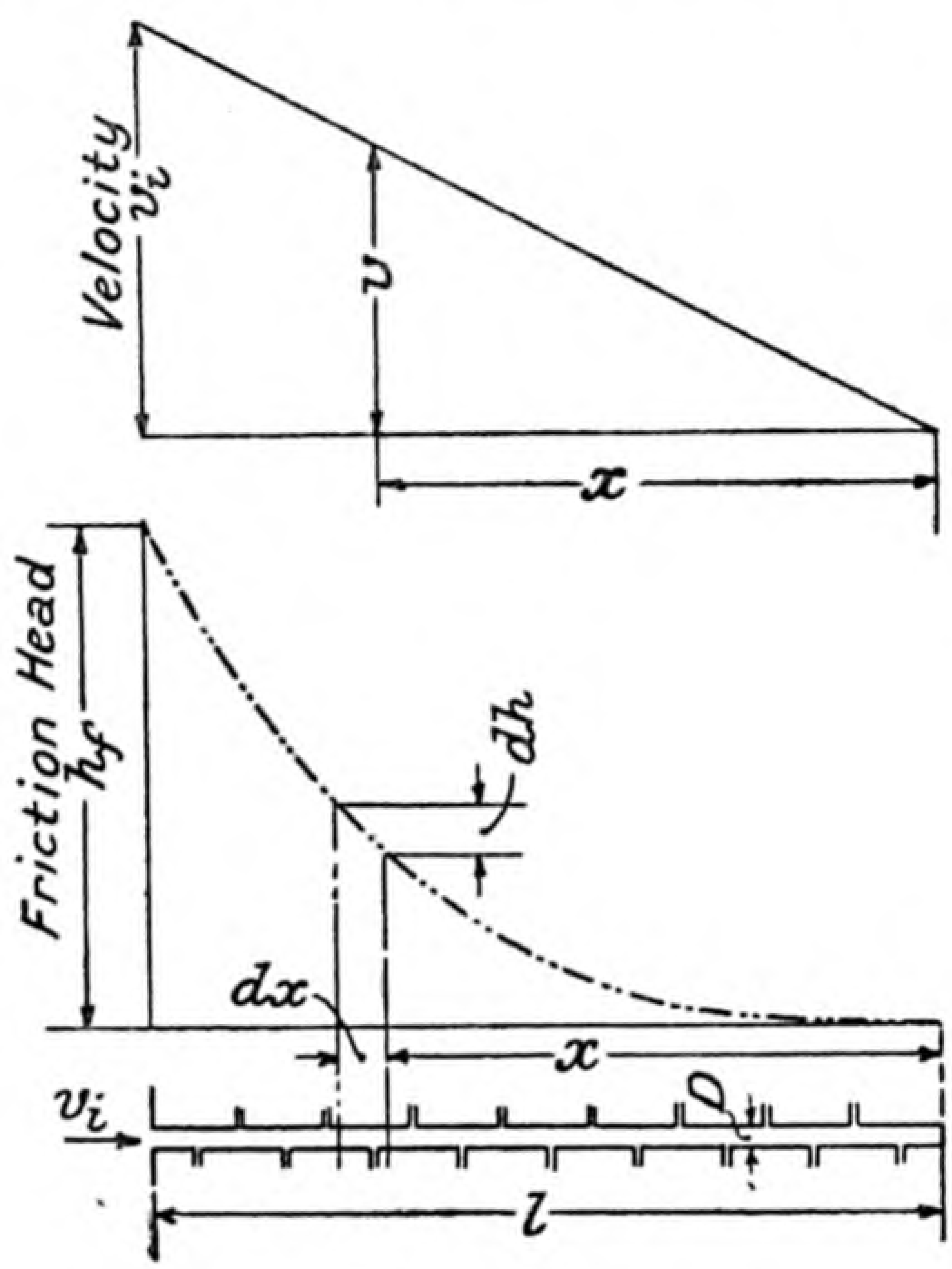

Considering a short section of pipe of length dx, in which the friction loss is dh, we can write

$$dh = \frac{4f \cdot dx}{D} \cdot \frac{v^2}{2g}. \quad \text{But } v = v_i \cdot \frac{x}{l},$$

therefore
$$dh = \frac{4f}{D \cdot 2g} \cdot \frac{v_i^2 x^2}{l^2} \cdot dx.$$

Integrating, h_f = total friction loss in length l

$$= \int dh = \frac{4fv_i^2}{D \cdot 2g \cdot l^2} \cdot \left[\frac{x^3}{3}\right]_{x=0}^{x=l}$$

$$= \frac{1}{3} \cdot \frac{4fl}{D} \cdot \frac{v_i^2}{2g}$$

= one-third of the friction loss H_f that would be incurred if the whole of the discharge flowed through the pipe instead of escaping through the side branches.

This loss can now be evaluated in the customary way. Using, for example, formula 9·9, $v = f_4 m^{\frac{2}{3}} i^{\frac{1}{2}}$, and inserting known values, we find

$$2{\cdot}26 = 94 \times \left(\frac{0{\cdot}15}{4}\right)^{\frac{2}{3}} \left(\frac{H_f}{2000}\right)^{\frac{1}{2}}, \text{ from which } H_f = 92{\cdot}2 \text{ m.}$$

Actual friction loss h_f when side branches are in operation $= \frac{1}{3}H_f$ $= 30{\cdot}7$ m.

Equivalent pressure drop $= 30{\cdot}7 \times 0{\cdot}1 = 3{\cdot}07$ kg./sq. cm.

Therefore *pressure at closed end of pipe* $= 14{\cdot}5 - 3{\cdot}07$
$= 11{\cdot}4$ *kg./sq. cm.*

(*Note.*—It is not economical to use a parallel pipe for water distribution, as is done here, for towards the closed end the pipe is much bigger than t need be. Preferably, the pipe should be successively reduced in diameter, so that the virtual slope had an almost constant value.)

EXAMPLE 84.

The plan shows the trace of an irrigation channel carried along the flank of a main valley; the discharge is 500 lit./sec., and the water slope is 1 in 3000. In order to cut out the long loop where the channel crosses a lateral valley it is proposed to substitute an inverted siphon AB. What should be its diameter, and what maximum pressure must it sustain?

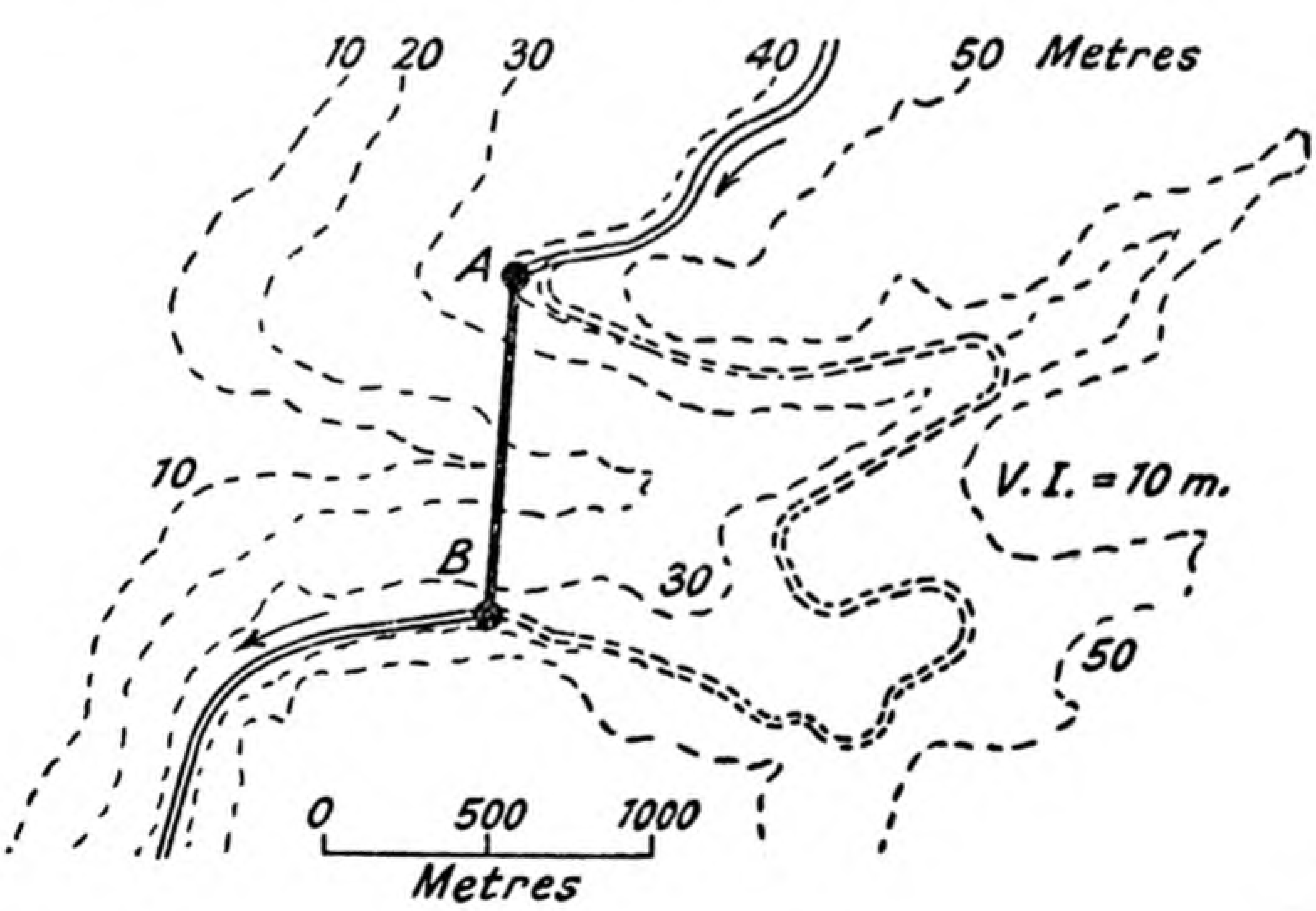

Solution:—

Length of loop (shown in broken lines) = 5000 metres, therefore fall in water surface between A and B is 5000/3000 = 1·67 m.

Length of siphon = 1020 m. Hence virtual slope $i = \frac{1{\cdot}67}{1020}$ $= 0{\cdot}00164$.

Concrete or reinforced concrete will be a suitable material, so a value of Kutter's $N = 0{\cdot}013$ will be on the safe side.

Using Manning's formula, § 158, we have

$$v = \frac{1}{0{\cdot}013}\left(\frac{d}{4}\right)^{\frac{2}{3}}(0{\cdot}00164)^{\frac{1}{2}}$$

$$= 1{\cdot}24d^{\frac{2}{3}}.$$

But $q = Av$, or $0{\cdot}5 = \frac{\pi}{4}d^2 \,.\, 1{\cdot}24d^{\frac{2}{3}}$, from which $d^{\frac{8}{3}} = 0{\cdot}514$.

By successively taking the square root and then cubing (all on the slide-rule), we find

$$d = \text{diameter of siphon} = \mathit{0{\cdot}78\ m.}$$

As the channel itself, even if concrete-lined, will have a cross-section greater than that of the pipe, it will almost certainly be advantageous to eliminate 5 k. of it by the use of the siphon. The contour lines show that the maximum head at the bottom of the siphon will be about 30 metres, or 3 kg./sq. cm., and the reinforcement of the siphon barrel can be worked out accordingly.

Example 85.

At a vertical bend in a turbine pipe-line, where the inclination changes from 23° 30′ to 52° 10′, there is to be an anchorage as shown in the diagram. At a distance of 20 ft. below the anchorage there is an expansion joint; at a distance 940 ft. above the anchorage there is another expansion joint (distances measured along pipe axis). The pipe diameter is 42 ins.; pipe thickness is 1 in.; mean water velocity is 8·5 ft./sec.; maximum pressure, under worst conditions of water hammer, is 645 lb./sq. in. Estimate the total thrust the anchorage must be designed to resist.

Solution :—

The total length of pipe, between the expansion joints, can be regarded as a single mass maintained in equilibrium under the effect of the following forces :—

(i) The weight W_p of the length of 960 ft. of pipe.

(ii) The static thrust P_t on the bend (§ 21).

(iii) The resultant dynamic thrust on the bend (§ 119).

(iv) The frictional resistance between the pipe and the saddles and expansion joints.

(v) The reaction exerted by the anchorage.

Neglecting item (iv), we can write

W_p=weight of pipe$=\dfrac{960\times 12\times 3{\cdot}14\times 1\times 42{\cdot}5\times 0{\cdot}28}{2240}=193$ tons.

W_a=component of weight acting axially along pipe

$$= W_p \sin 23^\circ\, 30' = 77 \text{ tons.}$$

$P=$ total hydrostatic thrust on plane normal to pipe axis

$$=\frac{\frac{\pi}{4}\times 42^2\times 645}{2240}=398 \text{ tons.}$$

P_t=resultant hydrostatic thrust on bend

$$= P\sqrt{2(1-\cos(52^\circ\, 10' - 23^\circ\, 30'))} = 197 \text{ tons.}$$

W=weight of water flowing per sec. $= wav = 5100$ lb./sec.

P_d=resultant dynamic thrust

$$= \frac{W}{g}\,.\,v\,.\,\sqrt{2(1-\cos(52^\circ\, 10' - 23^\circ\, 30'))}$$

$$= 669 \text{ lb.} = 0{\cdot}3 \text{ ton, which is negligibly small.}$$

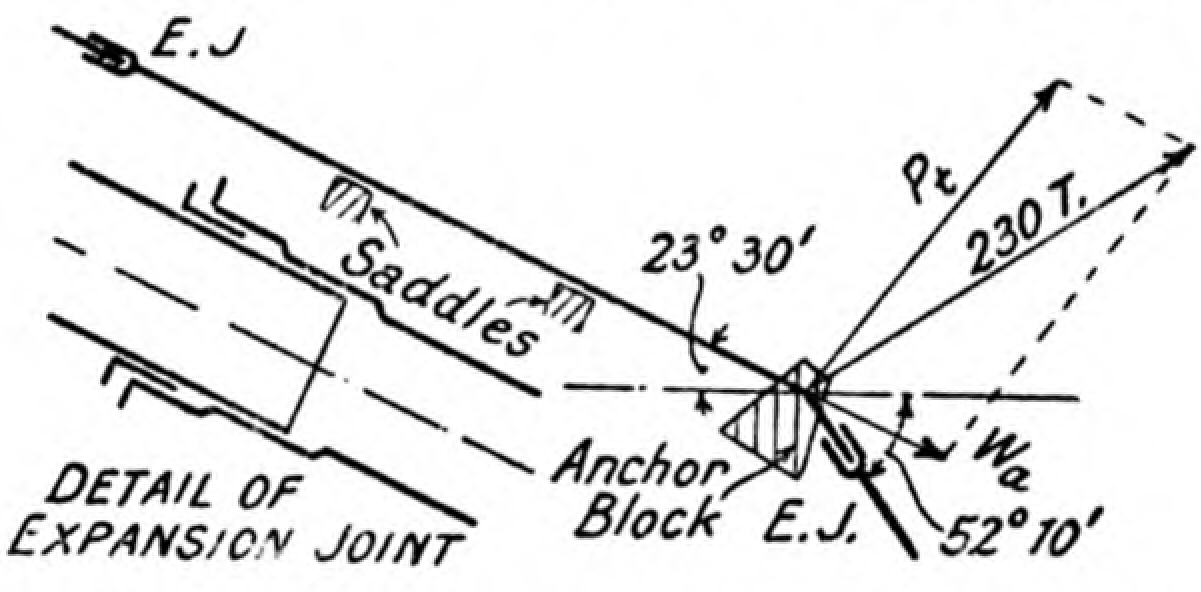

The total resultant force on the anchorage, or the resultant of W_a and P_t, can be found graphically as in the diagram ; it amounts to

230 tons.

The weight of the anchorage, and the manner in which it is keyed into the mountain side, must enable it to exert an equal and opposite reaction. Finally the value of W_a tons must be corrected by making suitable allowances for sliding friction, item (iv) above. Probably the worst conditions will occur when the pipe is expanding or lengthening under temperature changes.

Example 86.

The steel supply pipe for a Pelton wheel is 4850 ft. long, 36 ins. diameter, and 1·2 ins. thick. The gross head is 1035 ft. (i.e. static head above nozzle), and when the nozzle is fully open the area for flow is 0·32 sq. ft. Calculate the maximum pressure in the pipe-line when the needle is moved from the fully-open to fully-shut position in 6·7 secs. The movement of the needle is such that the area of opening is reduced at a uniform rate.

Solution. (i) Neglecting friction in pipe.

Let t = time in secs. from beginning of closing movement,

U = velocity of jet (ft./sec.) at time $t = C_v\sqrt{2gh_e} = 7{\cdot}87\sqrt{h_e}$,

h_e = effective head at nozzle at time t (ft.),

a_n = area of opening of nozzle at time $t = 0{\cdot}32\left(\dfrac{6{\cdot}7 - t}{6{\cdot}7}\right)$ sq. ft.,

a_p = area of pipe = 7·08 sq. ft.,

v_p = velocity in pipe (ft./sec.). Now velocity in pipe near nozzle

$$= U \times \frac{a_n}{a_p} = \frac{7{\cdot}87\sqrt{h_e}}{7{\cdot}08} \,.\, 0{\cdot}32\left(\frac{6{\cdot}7 - t}{6{\cdot}7}\right)$$

$$= 0{\cdot}0531(6{\cdot}7 - t)\sqrt{h_e} \ \ldots \qquad \text{(I)},$$

v_0 = velocity of pressure waves along pipe

= 4140 ft./sec. (§ 116, assuming E = 30,000,000 lb./sq. in.
K = 300,000 lb./sq. in.).

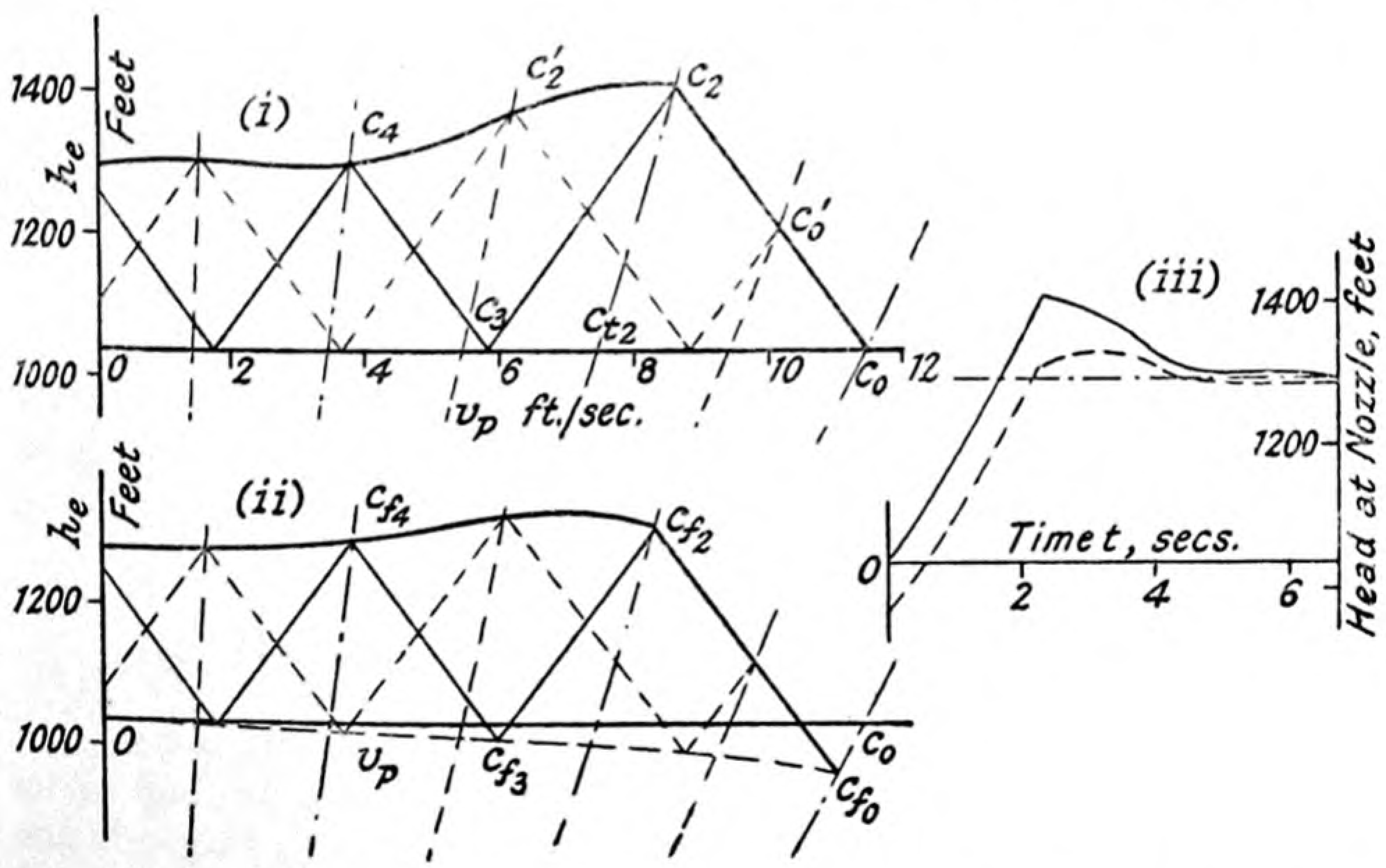

The head-velocity diagram can now be constructed, on the lines of Fig. 164 (iii), § 176; but the head axis is now graduated in units of total head or gauge head (static + inertia head), instead of in terms of inertia head only. At time 0 sec., the effective head h_e will be identical with the static head H = 1035 ft., and the corresponding value of v_p, from equation (I), is 11·46 ft./sec. With this information the first point on the diagram c_0 can be plotted. From point c_0 the line c_0c_2 can also be drawn, having a slope v_0/g = 128·3 secs. (diagram (i)).

At this stage the procedure departs slightly from what was described in § 176. There we knew what the pipe velocity was when the first return wave arrived at the valve, and point c_2 could be located accordingly. Now we do not know. But we *do* know what is the connection between time, head, and velocity: it is given by equation (I) above. The interval needed for the pressure wave to make a return trip along the pipe is

$$2 \,.\, dt = 2l/v_0 = 2 \times 4850/4140 = 2{\cdot}34 \text{ secs.}$$

Inserting in equation (I) this value $t = 2{\cdot}34$, we derive the equation $v_p = 0{\cdot}232\sqrt{h_e}$.

It is now easy to choose two or three values of h_e, extract corresponding values of v_p, plot the points, and sketch in the parabola $c_{t_2} \,.\, c_2$ as in the diagram. Since we are sure that the point c_2 will be somewhere along this parabola, and also somewhere along line c_0c_2, the intersection at once establishes its position. In a similar manner point c_4 is located by inserting in equation (I) the value $t = 4dt$, and so on.

The graph $c_0c_2c_3c_4$ . . . records the observations made by the first "observer." By sending out another imaginary patrolman after an interval dt from zero time, the graph $c'_0c'_2$ . . . is obtained. Finally, from the enveloping curve $c_0c'_0c_2c'_2c_4$ . . . we can clearly see that point c_2 represents the maximum head at a point near the valve, and as this will certainly be the lowest point in the pipe-line it is safe to scale off this head = 1405 ft. The *maximum pressure* is thus *610 lb./sq. in.*

(ii) *Allowing for pipe friction.*

The following approximate method is usually sufficiently accurate: If the velocity v_p at any moment were uniform throughout the length of the pipe, then the friction loss in the pipe (taking $f = 0{\cdot}005$) would be

$$h_f = \frac{4 \,.\, f \,.\, 4850}{3} \cdot \frac{v_p^2}{64{\cdot}4} = 0{\cdot}50 \,.\, v_p^2 \;\ldots \qquad \text{(II)}$$

Therefore at the selected moment the true head at the nozzle will be less by this amount than what it has hitherto appeared to be (solution (i) above). Nevertheless, equation (I) is still valid; hence at time $t = 0$ the state of the water near the valve will be represented by the point c_{f_0} at the intersection of the parabolas plotted from equations (I) and (II). We therefore use this point as the zero point of the head-velocity diagram, and we proceed as though the horizontal axis in Fig. (i) had been curved into the parabolic form $0c_{f_2}c_{f_0}$ in Fig. (ii). Otherwise the method is the same. It yields a lower value for the maximum pressure, viz. *580 lb./sq. in.*

(iii) If it is desired to plot pressure changes on a time basis, this can readily be done as in Fig. (iii). Here the full line relates to solution (i), the broken curve to solution (ii), while the horizontal

broken line describes the ideal case of uniform retardation with inelastic and frictionless pipe walls and water column. The respective values of maximum inertia head (in relation to static head) are: 370 ft.; 300 ft.; 260 ft.

(*Note.*—It will be realised that a complication hitherto disregarded would be the fluctuation of water-level in the surge-tank, § 255.)

EXAMPLES *for Solution:*—

87. What would be the discharge in gallons per minute through an old cast-iron pipe 21 ins. diameter and 5 miles long, if the pressure drop due to friction is 28 lb./sq. in. and Kutter's rugosity coefficient is 0·018? Ans. 1960 galls./min.

88. A pipe 31·9 m. long and 20 cm. diameter connects two reservoirs; the difference in level between the two water surfaces is 6·6 m. At inlet the pipe projects into the reservoir. The pipe coefficient is 0·007. Midway along the pipe is a partially-closed sluice valve, the area of the valve opening being 72 sq. cms. and its coefficient of contraction being 0·68. What would be the discharge through the system? Ans. 60 lit./sec.

89. In designing a high-pressure pipe line it was necessary to decide whether to use (*a*) a single large pipe, or (*b*) two smaller pipes in parallel. The total discharge was to be Q, and the virtual slope i. Assuming in the two cases identical stresses in the pipe walls and identical roughness coefficients, use formula 9-6 to find the ratio between the total weight of metal required for the single pipe and that required for the double pipes. Ans. 0·84.

90. It is required to conduct 200 gallons per min. of water from a point A through a distance of 4520 ft. to a point B. The only material available is 2150 ft. run of 4-inch pipe and 6000 ft. of 3-inch pipe. Accordingly, the 4-inch pipe is laid from A as far as it will go, then the 3-inch pipe is continued onwards to B, and finally the remainder of the 3-inch pipe is laid in parallel, backwards from B, until the end of it is connected up to the 4-inch pipe. Estimate the head loss between A and B, neglecting secondary losses and taking $f = 0{\cdot}006$ for the 4-inch pipe and 0·007 for the 3-inch pipe. Ans. 194 ft. head.

(*Note.*—The head loss could be reduced by cross-connecting the end of the 4-inch pipe to the 3-inch pipe lying alongside it. But the arrangement giving the least head loss would be: 4-inch pipe singly; then two lengths of 3-inch pipe in parallel; then three lengths of 3-inch pipe in parallel.)

91. Two parallel water mains of length L, identical in all respects, conduct a total discharge Q from one reservoir to another, the difference in level between the water surfaces being assumed to be constant. Cross-connections as in Fig. 147 are provided at distances $L/6$ apart. If two adjacent cross-connections are used to divert the whole flow through one pipe for a length $L/6$, so that

the corresponding length $L/6$ of the other pipe may be repaired, what would be the percentage reduction in discharge, neglecting secondary losses ? Ans. 18·2 per cent.

92. The following figures relate to a bitumen-lined steel pipe-line ABC carrying water :—

Elevation of points above datum :

$A = 244$ ft. : $B = 175$ ft. : $C = 171$ ft.

Lengths : $AB = 1070$ ft. : $BC = 765$ ft.

Diameters : $AB = 12$-ins. : $BC = 10$-ins.

Gauge pressures in pipe : at point A, 35·5 psi ;
at point C, 81·5 psi.

What would be the discharge through the system, and the gauge pressure at point B ? Ans. 1950 g.p.m. ; 70·5 psi.

(*Note.*—A suggested procedure is first to assume likely values of the pipe coefficients ; then to check the result by the use of Fig. 140, § 157.)

93. A siphon pipe 10 cms. diameter is to be used to conduct water over a bank from a pond or basin to another pond at a lower level. The inlet or rising leg of the siphon is 354 m. long, and the outlet or falling leg is 34 m. long. At its highest point the pipe axis is 2·40 m. above the water level in the upstream pond, and 15·9 m. above the level in the downstream pond. Assuming a pipe coefficient of 0·0075, calculate the maximum possible discharge through the siphon. What would be the discharge if a pipe of the same total length and diameter as the siphon pipe were passed through the bank instead of over it ? Ans. 9·5 lit./sec.
11·8 ,,

94. A canal is to be carried under another canal by means of an inverted siphon consisting of three reinforced concrete pipes each 32 m. long ; the total discharge is 14 cu. m./sec., and the loss of head is not to exceed 12 cms. Determine the diameter of the pipes if (*a*) they have sharp-edged inlets and outlets, and (*b*), they have bell-mouthed inlets, and outlets flared to 1·3 times the pipe diameter. Ans. (*a*) 2·25 m.
(*b*) 1·76 m.

95. A pumping installation is to be designed for forcing oil of S.G. 0·94 from a well to a storage centre. The pipe-line will be 8-inch diameter and 80 miles long, and at no point must the pressure exceed 800 lb./sq. in. when the normal discharge of 150 tons/hour is passing. The pipe is laid horizontally, and the oil enters and leaves it at atmospheric pressure ; the pipe coefficient is 0·008.

To overcome the frictional resistance of the pipe, there is to be a pumping station near the inlet and identical ones spaced at equal intervals along the line. The pump efficiency may be taken as 55 per cent. What would be the least number of pumping stations needed, and what would be the total power input at each station ?
Ans. 4 stations ; 510 h.p.

CHAPTER X.

EXAMPLE 96.

Calculate the discharge in a trapezoidal earthen canal of 26 ft. bed width, 6 ft. depth, surface slope 1 ft. per mile, side slopes 1 to 1. Take Kutter's $N = 0{\cdot}0225$.

Solution :—

Area of section $= A = (26 + 6)\,6 = 192$ sq. ft.

Wetted perimeter $= P = 26 + (2\sqrt{2} \times 6) = 42{\cdot}9$ ft.

Hydraulic mean depth $= m = \dfrac{A}{P} = 4{\cdot}49$ ft.

Surface slope $= i = \dfrac{1}{5280}$.

From Fig. 167, it is found that when $m = 4{\cdot}49$ and $i = \dfrac{1}{5280}$, $C = 86$ (foot units), hence $v =$ mean velocity $= C\sqrt{mi}$

$$= 86\sqrt{4{\cdot}49 \cdot \frac{1}{5280}}$$
$$= 2{\cdot}51 \text{ ft./sec.}$$

Therefore *discharge* $= Av = 192 \times 2{\cdot}51 =$ *481 cusecs.*

Alternative Solution :—

Using Manning's formula,

$$v = \frac{1{\cdot}486}{N} \cdot m^{\frac{2}{3}}\, i^{\frac{1}{2}} = \frac{1{\cdot}486}{0{\cdot}0225} \cdot 4{\cdot}49^{\frac{2}{3}} \cdot \left(\frac{1}{5280}\right)^{\frac{1}{2}} = 2{\cdot}48 \text{ ft./sec.,}$$

$q = 192 \times 2{\cdot}48 =$ *476 cusecs.*

EXAMPLE 97.

Compare the cross-sections of (*a*) an unlined, (*b*) a concrete-lined canal, to convey 4 cu. m./sec. on a longitudinal slope of 1 in 6400. The bed-width is to be equal to the depth, and the side slopes are 4 : 3.

Solution :—

Area of section $= A = d + \frac{4}{3}d^2 = 2{\cdot}33d^2$.

Wetted perimeter $= P = d + 2\sqrt{d^2 + (\frac{4}{3}d)^2} = 4{\cdot}33d$.

Hydraulic mean depth $= m = \dfrac{2{\cdot}33d^2}{4{\cdot}33d} = 0{\cdot}54d$.

Taking $N = 0{\cdot}024$ for the unlined earth canal (*a*), then

Discharge $= q = Av = 2{\cdot}33d^2 \cdot \dfrac{1}{0{\cdot}024} \cdot (0{\cdot}54d)^{\frac{2}{3}}\left(\dfrac{1}{6400}\right)^{\frac{1}{2}} = 4{\cdot}0$

from which $d^{\frac{8}{3}} = 5{\cdot}0$, or $d = 1{\cdot}82$ m. (This can all be worked on the slide-rule.)

$$\text{Cross-section} = 2{\cdot}33\ (1{\cdot}82)^2 = \mathit{7{\cdot}73\ sq.\ metres.}$$

Taking $N = 0{\cdot}012$ for the smoothly-rendered concrete-lined canal, (*b*), then

$$d = 1{\cdot}42 \text{ m., and } A = \mathit{4{\cdot}70\ sq.\ metres} \text{ (see diagram).}$$

Even allowing for the additional excavation to accommodate the concrete lining, which may be 10 cm. thick, there will certainly be a saving of 30 per cent. of excavation in favour of the concrete-lined canal. But it is to be noted that the gross area of excavation may be very different from the net cross-sectional area of the actual waterway; this depends upon the level of the water surface in relation to the natural ground surface. Three possibilities are shown in the diagram: (*c*) the water level is just sufficiently below ground level for the natural earth to form the banks, (*d*) the water surface is above ground level, and thus the spoil removed from the canal must be used to form the banks, (*e*) the canal is considerably below ground level, and thus forms the lowest part of a deep cutting.

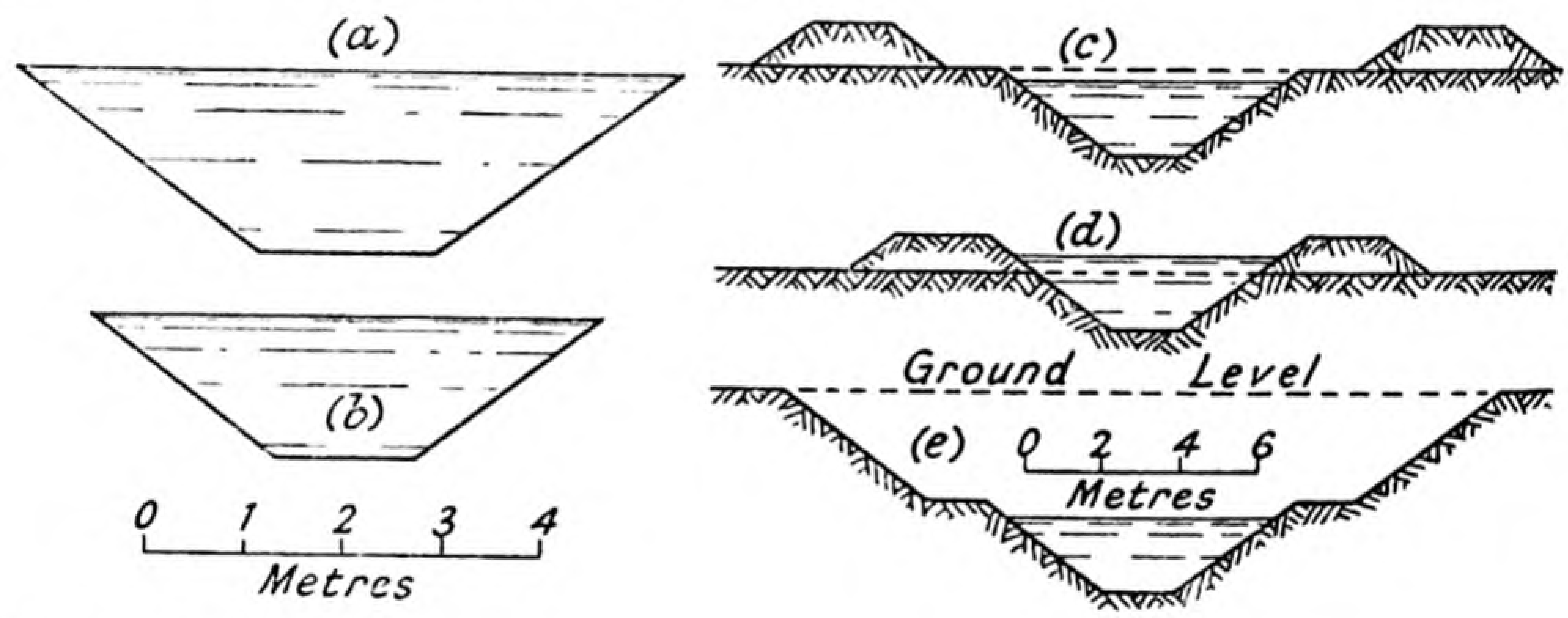

EXAMPLE 98.

A river 130 ft. wide and 10 ft. deep has a natural bed and surface slope of 1 in 12,000. Estimate roughly the length of backwater curve produced by an afflux of 6 ft.

Solution :—

For the desired approximate solution, the river may be assumed to be of rectangular section. The following values are then obtained: $A = 1300$ sq. ft., $P = 150$ ft., $m = 8{\cdot}67$ ft. Taking Kutter's $N = 0{\cdot}030$, and inserting these values in Manning's formula, we find that

$$v = 1{\cdot}91 \text{ ft./sec.}$$

and $$q = 2490 \text{ cusecs.}$$

At a point immediately upstream of the afflux, the water depth is now $10 + 6 = 16$ ft. instead of 10 ft., with the result that at this point we find: $A_1 = 2080$ sq. ft., $P_1 = 162$ ft., $m_1 = 12{\cdot}84$ ft.,

and $$v_1 = \frac{q}{A_1} = \frac{2490}{2080} = 1{\cdot}197 \text{ ft./sec.}$$

Inserting these modified values in Manning's formula, thus,

$$1{\cdot}197 = \frac{1{\cdot}486}{0{\cdot}030} \,.\, 12{\cdot}84^{\frac{2}{3}}\sqrt{i_1},$$

enables the modified water slope $i_1 = 0{\cdot}0000194$ to be obtained.

From Fig. 173 it is seen that approx. length of backwater curve

$$= \frac{2h}{i - i_1} = \frac{2 \times 6}{0{\cdot}000083 - 0{\cdot}000019} = 187{,}000 \text{ ft.}$$
$$= \textit{about 36 miles.}$$

Alternative Solution :—

Using formula 6-2, the values to be inserted are those prevailing upstream of the afflux, viz. $i = 0{\cdot}000083$, $v_1 = 1{\cdot}197$ ft./sec., $m_1 = 12{\cdot}84$ ft., $d_1 = 16$ ft., and

$$C = \frac{1{\cdot}486}{N} \,.\, m_1^{\frac{1}{6}} = \frac{1{\cdot}486}{0{\cdot}030} \,.\, 12{\cdot}84^{\frac{1}{6}} = 76,$$

whence $$\frac{\delta d}{\delta l} = \frac{0{\cdot}000083 - \dfrac{1{\cdot}197^2}{76^2 \times 12{\cdot}84}}{1 - \dfrac{1{\cdot}197^2}{32{\cdot}2 \times 16}} = \frac{0{\cdot}000083 - 0{\cdot}000019}{1 - 0{\cdot}0028}.$$

Length of backwater curve $= L = 2h \,.\, \dfrac{\delta l}{\delta d} = \textit{187,000 ft.}$

(*Note.*—These figures show that the term $\dfrac{v^2}{gd}$, which in this instance $= 0{\cdot}0028$, may safely be neglected, especially when the final result does not pretend to be more than quite a rough approximation.)

EXAMPLE 99.

What would be the discharge over a clear-overfall " ogee " weir 8·6 ft. high, of 180 ft. crest length, under a head of 4·47 ft.? The conditions are assumed to be geometrically similar to those represented in Fig. 175 (II).

Solution :—

The ratio between the height of the actual weir and the height of the type weir shown in the diagram is $\dfrac{8{\cdot}6}{1{\cdot}64} = 5{\cdot}24$.

Therefore the head over the type weir corresponding to the operating head of 4·47 ft. on the actual weir $= \dfrac{4{\cdot}47}{5{\cdot}24} = 0{\cdot}854$ ft.

From Fig. 176, the equivalent value of C_W, which is applicable both to the type weir and to the actual weir, is 3·70 ; hence

$$Q = \textit{discharge over actual weir} = C_W h^{\frac{3}{2}} \times 180$$
$$= 3{\cdot}70 \times 4{\cdot}47^{\frac{3}{2}} \times 180 = \textit{6280 cusecs.}$$

EXAMPLE 100.

A discharge of 18·4 cu. m./sec. flows over a weir 1·2 m. high, of 10·0 m. crest length, which is geometrically similar to the type I weir (Figs. 175 and 177). If the downstream water level is 68 cms. above the crest level, what afflux would be produced ?

Solution :—

The first step is to find the clear overfall upstream depth h, viz. the head that would be required to carry the given discharge over the weir under clear overfall conditions.

In the equation $q_s = C_W h^{\frac{3}{2}}$, some tentative value of C_W must be chosen—from Fig. 176, a value $C_W = 1{\cdot}70$ seems reasonable. The equation then becomes

$$\frac{18{\cdot}4}{10} = 1{\cdot}70\ h^{\frac{3}{2}}, \text{ from which } h = 1{\cdot}05 \text{ m. (nearly).}$$

The corresponding head over the type weir $= 1{\cdot}05 \times \dfrac{0{\cdot}5}{1{\cdot}2} = 0{\cdot}437$ m.

On referring again to Fig. 176, it is found that the true value of C_W at this head is 1·76. Inserting this corrected value in the equation, we have

$$1{\cdot}84 = 1{\cdot}76\ h^{\frac{3}{2}},$$

from which true value of $h = 1{\cdot}03$ m.

Now the actual downstream depth is given as 68 cms. $= 0{\cdot}68$ m. $= h_d$.

The ratio $\dfrac{h_d}{h}$ is thus $\dfrac{0{\cdot}68}{1{\cdot}03} = 0{\cdot}66$, or 66 per cent.

Turning now to Fig. 178, we find that when h_d is 66 per cent. of h, then the actual upstream depth h_u is 105 per cent. of h, or that the *afflux* h_L is 39 per cent. of h

$$= 0{\cdot}39 \times 1{\cdot}03 = 0{\cdot}40 \ m.$$

It will be observed that drowning the weir to a downstream depth of 68 cms. has only increased the upstream head over the weir by 5 per cent. of 1·03 m. = 5 cms.

EXAMPLE 101.

The head regulator of a canal has four openings each 3 m. wide, the water flowing between the upper and the lower gates. In order to give a desired discharge in the canal, the gates are set with a vertical opening of 1·10 m., the head on the regulator (i.e. the afflux) being then 0·40 m. If the upstream water level now rises 0·25 m.,calculate by how much the upper gates must be lowered in order tomaintain the canal discharge unaltered.

Solution :—

Original combined area of sluice openings $= A = 3 \times 4 \times 1{\cdot}10 = 13{\cdot}2$ sq. m.

Original discharge $= Q = C_d A\sqrt{2gh} = C_d \times 13{\cdot}2 \times 4{\cdot}43\sqrt{0{\cdot}4}$
$= 36{\cdot}9\ C_d$.

If the canal discharge is to remain unchanged, the canal water surface will also undergo no change. The rise in the upstream water level will thus increase the head or afflux from 0·4 to $(0{\cdot}4 + 0{\cdot}25) = 0{\cdot}65$ m. Meantime C_d may safely be assumed to have suffered no serious variation. If D_1 = new height of opening, we may now write

$$Q = C_d A_1 \sqrt{2gh_1}, \text{ or } 36{\cdot}9\, C_d = C_d(3 \times 4 \times D_1)\,.\,4{\cdot}43\sqrt{0{\cdot}65}$$

from which $D_1 = 0{\cdot}86$ m.

The upper gates must thus *be lowered by* $(1{\cdot}10 - 0{\cdot}86) =$ *0·24 m.*

Example 102.

A bridge having three piers each 8 ft. thick is built across a channel 80 ft. wide, in which the discharge is 1650 cusecs. Estimate what the afflux would be when the downstream depth is (*a*) 3 ft., (*b*) 10 ft.

Solution :—

(*a*) It is first necessary to ascertain whether or not the wide-crested weir formula 4-6 is applicable. Inserting appropriate values, we have (neglecting velocity of approach)

$$1650 = 0{\cdot}92 \times 0{\cdot}385 \times (14 \times 4)\sqrt{64{\cdot}4}\, d_u^{\frac{3}{2}}$$

from which $d_u = 4{\cdot}75$ ft. Since d_d, = 3 ft., is less than $\frac{2}{3}d_u$, evidently wide-crested weir flow will actually take place.

The approximate velocity of approach will be $\dfrac{1650}{4{\cdot}75 \times 80} = 4{\cdot}34$ ft./sec., and the head of approach $= \dfrac{4{\cdot}34^2}{64{\cdot}4} = 0{\cdot}29$ ft. Therefore corrected upstream depth $= 4{\cdot}75 - 0{\cdot}29 = 4{\cdot}46$ ft., and *afflux* $=$ 4·46 ft. − 3·00 ft. $=$ *1·46 ft.*—say about 1·5 ft.

(*Note.*—In view of the considerable difference between the present conditions and those in which the velocity of approach corrections mentioned in § 56 are strictly applicable, it is safer to deduct only the head of approach 0·29, and not $1{\cdot}5 \times 0{\cdot}29$.)

(*b*) When the downstream depth is 10 ft., the velocity in the downstream channel is $\dfrac{1650}{10 \times 80} = 2{\cdot}06$ ft./sec., and the velocity head $= h_{vd} = \dfrac{2{\cdot}06^2}{64{\cdot}4} = 0{\cdot}066$ ft.

Hence $$C'_d = 1{\cdot}29 - 3{\cdot}2\,.\left(\frac{0{\cdot}066}{10}\right) \quad . \; . \; . \; . \quad \text{(from § 196)}$$
$$= 1{\cdot}27.$$

This value may now be substituted in the formula

$$q = C'_d bd_d\sqrt{2g(d_u + h_{vu} - d_d)},$$

thus: $$\frac{1650}{4} = 1{\cdot}27 \times 14 \times 10\sqrt{64{\cdot}4(d_u + 0{\cdot}066 - 10)}\text{'}$$

from which $d_u = 10{\cdot}02$ ft. The *afflux* thus only amounts to
$$10{\cdot}02 - 10{\cdot}00 = \mathit{0{\cdot}02\,ft.}$$

EXAMPLES *for Solution*:—

103. A trapezoidal earthen canal having a bed slope of 8 centimetres per kilometre and side slopes of 3 to 2 (3 horizontal to 2 vertical), is to carry a discharge of 35 cu. metres/sec.; the bed width is to be three times the water depth. Assuming average conditions, determine the dimensions of the canal, using (*a*) Kutter's, (*b*) Manning's, and (*c*) Bazin's formula.

Ans. (*a*) depth 3·42 m., bed width 10·25 m.
(*b*) ,, 3·49 ,, ,, 10·47 ,,
(*c*) ,, 3·46 ,, ,, 10·36 ,,

104. A concrete culvert 4 ft. square in section is found to discharge 69 cusecs when running as an open channel with a water depth of 3 ft. 9 ins. What would be the approximate discharge when the culvert runs full, the virtual slope remaining the same?

Ans. 62 cusecs.

105. A dam built across a river in order to form a reservoir has twenty under-sluices each 1·5 m. wide. On a certain day the water surface of the reservoir has an area of 65 sq. kilometres, and its level is 11·6 m. above the bottom of the sluices; the natural flow of the river into the reservoir is 280 cu. m./sec. What sluice opening would be required (all the gates having the same setting) to ensure that one-half the river discharge was stored in the reservoir, and that the other half was passed through the sluices? Assume free-flow conditions, taking C_d and $n = 0{\cdot}7$. By how much would the reservoir level rise in 24 hours?

Ans. 0·45 m.; about 18·6 cms.

106. A total discharge of 1770 cu. ft./sec. is to be taken along a trapezoidal waterway on a slope of 1 : 12,000; the side slopes are 1 : 1, and the most economical cross-section is to be used, taking $N = 0{\cdot}0225$. Calculate the total cross-section of the waterway if (i) a single canal is used, (ii) two identical canals working in parallel are preferred. Ans. 660 sq. ft.; 780 sq. ft.

107. A brick-lined channel has side slopes inclined at 60° to the horizontal, the sides being tangential to a cylindrical "invert" of 1·48 ft. radius forming the bottom of the channel. If the water

surface slope is 4·5 ft. per mile, and the water depth is 1·74 ft., what would be the discharge ?

Ans. Kutter : 13·3 cusecs.
Bazin : 14·2 ,,
Barnes : 13·6 ,,

108. A main irrigation canal running parallel with a river is 56 miles long, 72 ft. bed-width, 16 ft. deep, with side slopes of 4 : 3. The value of N is 0·025. The water slope of the river is 1 in 8000, and the canal slope must be arranged to give a canal discharge sufficient to irrigate 536,000 acres. Each acre requires 740 cubic feet of water per day. At the tail of the canal the water surface must be 16 ft. above the river surface level at that point, in order to command the irrigated area ; the head of the canal takes off from the river immediately upstream from a diversion barrage. What should be the minimum afflux created by the barrage ?

Ans. $7\frac{1}{2}$ ft.

109. A sluice used for emptying a reservoir works under an *effective* head of 50 ft. when the reservoir is full, and in these conditions it discharges 142 cu. ft./sec. The corresponding surface area of the reservoir is 360,000 sq. ft. ; and after the level has fallen by successive intervals of 6 ft. the surface areas are 280,000, 170,000, and 60,000 sq. ft. respectively. Estimate approximately how long it will take to lower the water level from top level to 18 ft. below top level.

Ans. $8\frac{1}{2}$ hours.

110. Using the approximate form $v_o = 0{\cdot}79d^{\frac{2}{3}}$ in place of the usual Kennedy formula $v_o = 0{\cdot}84d^{0{\cdot}64}$, taking N in Manning's formula as 0·025, and assuming that the canals are so wide in relation to their depth that $d = m$ (approx.) ; then on these assumptions, show that non-silting and non-scouring canals in India should have a bed slope of $\frac{1}{5700}$ and in Egypt should have a slope $\frac{1}{12800}$.

111. A regulator having three openings each 2·5 m. wide is built across the canal whose characteristics are shown in Fig. 168 ; the gates are set so as to leave an opening between the bottom of the gates and the floor of 0·8 m. Estimate the afflux when the water depth downstream of the regulator (under conditions of uniform flow) is (*a*) 2·0 m., (*b*) 2·5 m.

Ans. (*a*) 0·51 m.
(*b*) 1·23 ,,

CHAPTER XI.

Example 112.

The discharge into the tank containing a cylindrical overflow weir (Fig. 212) is 8 lit./sec., and the outlet valve, which discharges into the atmosphere, is regulated to give an outflow of 5 lit./sec. The diameter of the weir is 35 cms., and the weir crest is 96 cms. above the outlet valve. If now the discharge into the tank is inadvertently allowed to rise to 10 lit./sec., what will be the flow through the outlet valve, assuming its setting and the setting of the weir to remain unchanged ?

Solution :—

Effective length of weir crest $= \pi \times 35 = 109{\cdot}9$ cms.

The flow over the weir is the difference between the inflow to and the outflow from the tank, viz. $8 - 5 = 3$ lit./sec. Taking a weir coefficient of 0·62 for use in formula 4-5, $Q = \frac{2}{3}C_d b\sqrt{2g}h^{\frac{3}{2}}$, we obtain

$3 \times 1000 = \frac{2}{3} \cdot 0{\cdot}62 \times 109{\cdot}9 \times 44{\cdot}3 \times h^{\frac{3}{2}}$, from which $h = 1{\cdot}31$ cm.

The water surface in the tank being thus 1·31 cm. above the weir crest, the head producing flow through the outlet valve is

$$96 + 1{\cdot}31 = 97{\cdot}31 \text{ cms.}$$

When the discharge into the tank rises to 10 lit./sec., the flow through the outlet valve will still remain at *approximately* 5 lit./sec., hence the flow over the weir will now be $10 - 5 = 5$ lit./sec. (approx.). The corresponding head over the weir will be

$$1{\cdot}31 \times \left(\frac{5}{3}\right)^{\frac{2}{3}} = 1{\cdot}85 \text{ cms.,}$$

and the head producing flow through the outlet valve will be

$$96 + 1{\cdot}85 = 97{\cdot}85 \text{ cms.}$$

Since the discharge through the valve is proportional to the square root of the head upon it, the *modified discharge* is

$$5\sqrt{\frac{97{\cdot}85}{97{\cdot}31}} = 5{\cdot}013 \textit{ lit./sec.}$$

Thanks to the overflow weir, therefore, an increase of 25 per cent. in the inflow to the tank only produces an increase of 0·25 per cent. in the outflow.

(*Note.*—It is probable that with small flows the weir coefficient will be much greater than 0·62, because with very low heads the nappe no longer springs clear, but clings to the downstream side of the weir (Fig. 42). If this happens, however, its only result will be still further to improve the effect of the overflow weir.)

Example 113.

A storage reservoir is to be formed by building a dam across a valley, so impounding the waters of a stream. Provision must be made for spilling over the crest of the dam the maximum flood discharge of the stream, which is estimated at 2800 cusecs, and under no circumstances can the reservoir level be allowed to rise to more than 946 ft. above datum.

The length of spillway available is 130 ft. When the water level is 946 ft. above datum, the water surface area is 1230 acres; when the level is 940 ft. above datum, the area is 1100 acres.

Estimate the additional volume of water that may be stored by using automatic siphon spillways in place of a plain spillway; and suggest suitable dimensions for the siphons.

Solution :—

For the plain spillway we may provisionally adopt the value 3·2 for the weir coefficient C_W in the equation (10-2)

$$Q = C_W b h^{\frac{3}{2}}. \qquad (\S\ 188.)$$

Hence $2800 = 3{\cdot}2 \times 130 \times h^{\frac{3}{2}}$, from which $h =$ head required to carry maximum flood discharge over full length of spillway $= 3{\cdot}6$ ft. Consequently the crest of the spillway must be set at a level $946 - 3{\cdot}6 = 942{\cdot}4$ ft. above datum.

For the siphon spillway a priming depth of 0·5 ft. may reasonably be assumed; hence the crest of the spillway must be set at a level $946 - 0{\cdot}5 = 945{\cdot}5$ ft. above datum.

The volume of water stored in the reservoir is that contained in the reservoir when the flood water has run off and the water surface is flush with the crest of the spillway. Thus the additional water that may be stored by the use of the siphon spillway is that contained between the levels 945·5 and 942·4, which is found to be approximately *160,000,000 cu. ft.* = 3670 acre-ft.

In fixing the dimensions of the siphons, the coefficient of discharge C_d may be taken as 0·65, and the operating head h as 20 ft. Then from the formula $q = C_d a\sqrt{2gh}$, we have

$$2800 = 0{\cdot}65\ .\ a\sqrt{64{\cdot}4 \times 20},$$

from which $a =$ combined area of siphons $= 120$ sq. ft.

Probably 10 siphons, each having a cross-section of 3 ft. by 4 ft., would be satisfactory. The total length of spillway would thus be less than half the length of the plain weir type of spillway.

EXAMPLES *for Solution :—*

114. A reservoir is to be constructed to control the stream whose hydrograph is plotted in Fig. 204, and excess water is to be discharged through a circular bell-mouth spillway, § 190. What should be the diameter of the spillway? Ans. About 60 ft.

(*Note.*—This provisional figure merely purports to show the magnitude of these structures. The value, 60 ft., is based on the maximum average flow of 8000 cusecs; but for short periods the flow might be far higher than that.)

115. It is desired to draw water from a collecting gallery sunk through very porous limestone down to a horizontal bed of hard (assumed impermeable) limestone. The gallery is to be parallel with a river, and 900 ft. away from it; the bottom is 8 ft. below river water level, and the draw-down is not to exceed 2 ft. when 4200 gallons of water per day are being pumped from the gallery. The permeability factor is 3 ft./hour. What should be the length of the gallery? Ans. 600 ft.

116. Estimate the largest and the smallest effective diameters of the needle for the float-controlled module shown in Fig. 220 (I), if the uniform rate of flow is 18 lit./sec., the maximum head to be destroyed in the module is 1·4 m. and the minimum head is 0·6 m. Determine also the diameter of the orifice through which the needle moves. Take $C_d = 0{\cdot}62$, and assume that the smallest needle diameter is 0·75 times the largest diameter. Ans. 9·21 cms.
6·90 „
12·47 „

117. A module of the type shown in Fig. 219 is required to pass a uniform discharge of 60 cusecs which must be maintained throughout a range of downstream water level of 2·8 ft. Determine the depth and width of the gate opening, the necessary upstream depth over the floor of the sluiceway, and the maximum and minimum loss of head sustained by the water. Assume that the minimum downstream level is half-way up the gate opening. Ans. 2·0 ft.
2·17 „
5·0 „
4·0 „
1·2 „

118. Referring to the float-operated valve shown in Fig. 209, use the following data to estimate approximately the minimum diameter of the inlet pipe in which the butterfly valve is fitted, and also the radius of the crank on the valve spindle.

Discharge	0·5 cusecs.
Maximum head, above water level in float chamber, on valve	7 ft.
Minimum head, above water level in float chamber, on valve	2 ft.
Inclination of valve to pipe axis in fully open position	30°
Inclination of valve to pipe axis in fully closed position	60°
Coefficient of discharge of valve	0·7
Maximum variation in float chamber water level .	½ in.

The fulcrum of the horizontal lever is mid-way between the two end pivots. Ans. About 5¼ ins.
„ 2½ „

CHAPTER XIII.

EXAMPLE 119.

Calculate how many jets would be required for a Pelton wheel which is to develop 12,200 B.H.P. under 264 m. net head, at a speed of 500 r.p.m., assuming that the jet diameter is not to exceed 1/9 × wheel diameter. State also the diameter of the jets, the diameter of the wheel, and the quantity of water required, taking the overall efficiency as 87 per cent.

Solution :—

$$\text{Water horse-power} = \frac{\text{B.H.P.}}{\text{efficiency}} = \frac{12{,}200}{0{\cdot}87}$$

$$= \frac{WH}{75} = \frac{W \times 264}{75}$$

from which W = weight of water required = 3990 kg./sec., and Q = *volume of water required* $= \frac{3990}{1000} = 3{\cdot}99$ *cu. m./sec.*

Velocity of jets $= U = C_v\sqrt{2gH} = 0{\cdot}98 \times 4{\cdot}43\sqrt{264} = 70{\cdot}6$ m./sec.

Velocity of wheel $= v = \phi\sqrt{2gH} = 0{\cdot}45 \times 4{\cdot}43\sqrt{264} = 32{\cdot}4$ m./sec.

$$= \frac{\pi DN}{60} = \frac{3{\cdot}14 \times D \times 500}{60}$$

from which D = *diameter of wheel* = *1·24 m.*

If $\quad \frac{d}{D} = \frac{\text{diam. of jet}}{\text{diam. of wheel}} = \frac{1}{9}$, then $d = \frac{1{\cdot}24}{9} = 0{\cdot}1378$ m.

and $\quad a$ = area of one jet $= \frac{\pi}{4}(0{\cdot}1378)^2 = 0{\cdot}0149$ sq. m.

Now $\quad A$ = total jet area required $= \frac{Q}{U} = \frac{3{\cdot}99}{70{\cdot}6} = 0{\cdot}0564$ sq. m.

Hence number of jets $= \frac{0{\cdot}0564}{0{\cdot}0149} = 3{\cdot}78$.

The next highest whole number is 4, therefore *4* jets are needed, each having a diameter of

$$\sqrt{\frac{0{\cdot}0564}{4 \times \frac{\pi}{4}}} = 0{\cdot}134 \ m.$$

The actual ratio $\frac{d}{D}$ is thus $\frac{0{\cdot}134}{1{\cdot}24} = \frac{1}{9{\cdot}25}$, which is within the prescribed limits.

Example 120

When running at full load, a Pelton wheel develops 280 B.H.P. under an effective head of 960 ft., with an overall efficiency of 82 per cent. Estimate what B.H.P. the wheel would develop at the same speed and head, if the discharge were reduced by 20 per cent., (i) by the use of a needle or spear in the nozzle, (ii) by the use of a sluice valve in the supply pipe, the nozzle remaining fully open.

Solution :—

Let Q = discharge at full load. Then under conditions of needle regulation (i), since ϕ remains unchanged, the efficiency will not

sensibly change, and the B.H.P. will fall in proportion to the discharge.

$$\text{Hence reduced B.H.P.} = 280 \times \frac{0{\cdot}8\,Q}{Q} = \textit{224} \text{ (approx.).}$$

Under condition (ii), the discharge will be proportional to $\sqrt{h_n}$, where h_n is the head at the nozzle. At full load, therefore,

$$Q = C_d a\sqrt{2g\,.\,960}\,;$$

at reduced load, $0{\cdot}8Q = C_d a\sqrt{2gh_n}$, from which $h_n = 614$ ft. The difference between 960 and 614 = 346 ft. has been destroyed in the throttle valve.

Since the nozzle area remains unchanged, the jet velocity U will fall in proportion to the discharge; but the wheel velocity has not altered, thus the value of ϕ based on the *head at the nozzle* has risen from, say, 0·46 to $\frac{0{\cdot}46}{0{\cdot}8} = 0{\cdot}575$. From Fig. 289 it is seen that this disturbance in the ratio of wheel speed to jet speed reduces the efficiency to 94 per cent. of its maximum value.

The true overall efficiency of the wheel will now only be $0{\cdot}82 \times \frac{614}{960} \times \frac{94}{100} = 0{\cdot}492$, and the reduced B.H.P. will be

$$280 \times \frac{0{\cdot}8\,Q}{Q} \times \frac{0{\cdot}492}{0{\cdot}82} = \textit{134.}$$

Example 121.

Estimate the main dimensions and the blade angles for an inward flow turbine to suit the following conditions: Net head = 205 ft., speed = 700 r.p.m., output = 450 B.H.P.

Assume that: Hydraulic efficiency = 94 per cent.; overall efficiency = 85 per cent.; flow ratio $\psi = 0{\cdot}15$; ratio of wheel width to diameter at entry $= n = 0{\cdot}1$; inner diameter of runner $= \frac{1}{2} \times$ outer diameter.

Solution :—

Overall efficiency

$$= \eta_m = 0{\cdot}85 = \frac{\text{B.H.P.}}{\text{W.H.P.}} = \frac{450}{\dfrac{W\,.\,H}{550}} = \frac{450}{\dfrac{W \times 205}{550}}$$

from which W = weight of water = 1420 lb./sec., and

$$Q = \text{discharge} = \frac{1420}{62{\cdot}4} = \textit{22·8 cusecs.}$$

Since flow ratio $= 0{\cdot}15 = \dfrac{Y}{\sqrt{2gH}}$,

then velocity of flow $= Y = 0{\cdot}15 \times 8{\cdot}03\sqrt{205} = 17{\cdot}2$ ft./sec., and

area for flow $= \dfrac{Q}{Y} = \dfrac{22{\cdot}8}{17{\cdot}2} = 1{\cdot}326$ sq. ft.

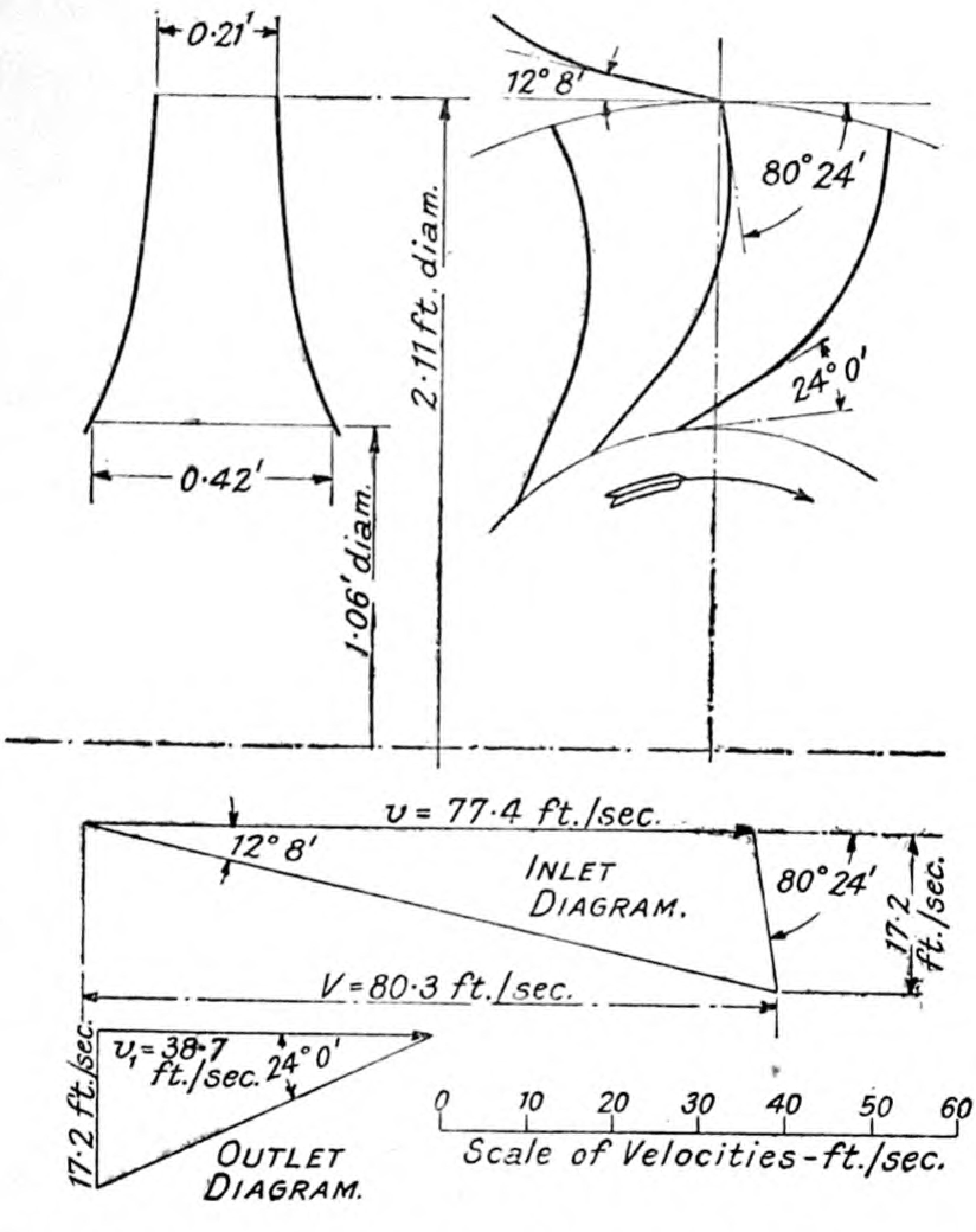

Assuming that $\frac{1}{20}$ of the circumferential area of the runner is blocked by the thickness of the blades, then area for flow

$= 0{\cdot}95 \,.\, \pi D \times 0{\cdot}1 \times D = 1{\cdot}326$, and $D = 2{\cdot}11$ *ft.* = *runner diameter.*

Runner *width* $= 0{\cdot}1 \times D = 0{\cdot}21$ *ft.*

Rim velocity v $= \dfrac{\pi DN}{60} = \dfrac{3{\cdot}14 \times 2{\cdot}11 \times 700}{60} = 77{\cdot}4$ ft./sec.

Also hydraulic efficiency $= \eta_h = \dfrac{Vv}{gH} = \dfrac{V \times 77{\cdot}4}{32{\cdot}2 \times 205} = 0{\cdot}94$,

whence V = velocity of whirl $= 80{\cdot}3$ ft./sec.

Now $\frac{Y}{V} = \frac{17 \cdot 2}{80 \cdot 3} = 0 \cdot 214 = \tan 12° \; 8'$, or *guide blade angle* $= 12° \; 8'$.

Also $\frac{Y}{V - v} = \frac{17 \cdot 2}{80 \cdot 3 - 77 \cdot 4} = 5 \cdot 93 = \tan 80° \; 24'$, or *inlet wheel blade angle* $= 80° \; 24'$.

Since $v_1 = \frac{1}{2} v$, $\frac{Y}{v_1} = \frac{17 \cdot 2}{\frac{77 \cdot 4}{2}} = 0 \cdot 445 = \tan 24° \; 0'$, or *outlet wheel blade angle* $= 24° \; 0'$.

Alternatively, the velocity diagrams may be drawn to scale and the angles obtained by direct measurement. (See diagram.)

(It will be noticed that a runner of the double-outlet type has been drawn, the water escaping axially in both directions.)

Example 122.

Two inward flow turbine runners have the same diameter, viz. 0·6 m., and the same efficiency; they work under the same head and they have the same velocity of flow, viz. 6 m./sec. One of the runners, A, revolves at 520 r.p.m., and has an inlet blade angle of 65°. If the other runner, B, has an inlet blade angle of 110°, at what speed should it run?

Solution :—

Rim velocity of runner $A = v_a = \frac{\pi D N_a}{60} = \frac{3 \cdot 14 \times 0 \cdot 6 \times 520}{60}$

$= 16 \cdot 31$ m./sec.

Since inlet blade angle of $A = 65°$, $\tan \alpha = \tan 65° = 2 \cdot 144$

$$= \frac{Y}{V_a - v_a} = \frac{6}{V_a - 16 \cdot 31}$$

whence $V_a = 19 \cdot 11$ m./sec.

Because the two runners work at the same efficiency, then

$$\frac{V_a v_a}{gH} = \frac{V_b v_b}{gH}, \text{ or } \frac{19 \cdot 11 \times 16 \cdot 31}{gH} = \frac{V_b v_b}{gH},$$

rom which $V_b \, . \, v_b = 312$ . . . . . (I)

Again, since inlet blade angle of runner $B = 110°$,

$$\tan 110° = -\,2 \cdot 75 = \frac{Y}{V_b - v_b} = \frac{6}{V_b - v_b}$$

from which $V_b - v_b = -\,2 \cdot 18$ . . . . . (II)

Solving equations I and II, we find that $v_b = 18 \cdot 8$ m./sec. = rim velocity of runner $B = \frac{3 \cdot 14 \times 0 \cdot 6 \times N_b}{60}$,

from which N_b = *speed of runner* B = *600 r.p.m.*

(Note this important connection between speed and blade angle. Under given conditions, an increase in speed necessitates an increase in the inlet wheel blade angle.)

EXAMPLES *for Solution* :—

123. An inward flow reaction turbine has a wheel 2 ft. diameter and 2 inches wide at the outer rim, the inner diameter being 0·65 times the outer diameter. The wheel blade angles at inlet and outlet are 95° and 14° respectively ; the velocity of flow is uniform throughout the wheel ; 8 per cent. of the circumferential area of the runner is blocked by the blade thicknesses.

If the head on the turbine is 176 ft., the hydraulic efficiency 88 per cent., and the overall efficiency 81 per cent., determine the speed and output of the turbine, and the quantity of water it would require.

Ans. 680 r.p.m.
179 h.p.
11·1 cusecs

124. For the turbine described in Example 121, plot to scale graphs between (i) distance travelled along absolute path by an element of water, and (ii) absolute velocity, total energy, and pressure-head. Assume that 2 per cent. of the working head is lost in the guides, and 2 per cent. in the runner blades.

(*Note.*—The graphs required are of the same nature as those plotted in Fig. 235 and 262 (ii).)

125. In Pelton wheel installations a small auxiliary nozzle is sometimes fitted, from which a jet of high-pressure water can be directed when required on to the *backs* of the buckets, thus acting as a brake and bringing the wheel quickly to rest. Estimate the time required to stop the wheel by this means, under the following conditions :

Diameter of braking nozzle	2·8 ins.
Head at nozzle	1560 ft.
Original velocity of buckets	146 ft./sec.
Corresponding kinetic energy of wheel and all revolving parts	11,200,000 ft. lb.

Assume that the dynamic thrust on the buckets is equivalent to that on flat radial blades. Ans. 16 secs.

126. A Francis turbine working under a head of 178 m. is fed through a pipe-line 965 m. long and 0·65 m. diameter, the mean velocity in the pipe at full load being 1·9 m./sec. To prevent excessive water-hammer effects when the servo-motor closes the gates during reduction of load, a relief valve in the spiral casing can be automatically opened in such a way as to limit the inertia pressure to 2·0 kg./sq. cm. Estimate the quantity of water that would be wasted through the relief valve if full load were suddenly thrown off the machine and the gates were completely closed in 3 secs. Neglect the elasticity of the water column, and assume that during the period of gate closure one-half of the total water coming down the pipe flows through the gates. Ans. 2150 litres.

127. In a Pelton wheel the water is turned in the buckets through an angle of 165°, the diameter of the wheel is 2·8 ft., and the jet velocity is 160 ft./sec. Draw to scale the outlet velocity diagrams for about 6 wheel speeds, ranging from zero to maximum, and use these diagrams to plot the following graphs :—

(i) Between wheel velocity and dynamic thrust on buckets.

(ii) Between wheel velocity and hydraulic efficiency. Neglect friction and similar losses.

128. In a high-head turbine installation a pressure tunnel 6·0 miles long, of sectional area 82 sq. ft., conducts the water from a reservoir to the head of the pipe-line, where it terminates in a surge tank whose spillway is 50 ft. above reservoir level. The steel pipe to each turbine is 2280 ft. long and 6 ft. diameter. The static head at the turbine nozzles is 950 ft., and the machines have an overall efficiency (including pipe losses, etc.) of 80 per cent.

Supposing that one unit only is working at an output of 14,100 h.p., estimate the minimum time in which its nozzle may be closed (assuming uniform retardation in the pipe-line), to ensure that water will just *not* spill over from the surge tank ? What would be the maximum pressure in the pipe ? Ans. 39·0 secs. ; 438 psi.

129. A propeller turbine runner has an outer diameter of 4·5 m. and an inner diameter of 2·0 m., and it is to develop 28,000 h.p. when running at 140 r.p.m. under a head of 21·8 m. The hydraulic efficiency is 94 per cent. and the overall efficiency is 88 per cent. Determine the inlet and outlet blade angles, measured at the mean radius. Ans. 148° 30′ ; 20° 0′.

130. The following data relate to the draft tube for a Kaplan turbine of the type shown in Figs. 242 (IV) and 243 : area of circular inlet or throat = 254 sq. ft. ; area of rectangular outlet = 1170 sq. ft. ; inlet velocity = 30 ft./sec. ; efficiency of draft tube = 0·7 ; elevation of inlet plane above tail-race level = 2 ft.

Use this information to determine :—

(i) the vacuum or negative head at the draft tube inlet,

(ii) the power wasted in the draft tube,

(iii) the power thrown away into the tail-race.

Ans. 11·8 ft. ; 3000 h.p. ; 570 h.p.

131. A power plant intended for peak-load operation is to develop 105,000 h.p. for 2 hours only each day. Water is stored in a reservoir having the following characteristics :—

Height of Reservoir Water Surface above Turbines (ft.).	Water Surface Area (acres).
162 (reservoir full)	81·5
156	64·1
150	50·6
144	40·8
138	33·2
132	26·0

At the beginning of each generating period the reservoir is full, and after the reservoir has been refilled by the stream which supplies the plant, the excess water is discharged over a spillway. The average gross efficiency of the plant may be taken as 0·83.

If the natural discharge of the stream is 810 cusecs, what would be (*a*) the lowest level of the water in the reservoir at the end of the generating period, (*b*) the total volume of water discharged over the spillway per day? Ans. 143 ft.; 400 acre-feet.

132. Calculate the cross-sectional area of the head-race and tail-race canals required for a low-head power scheme in which the output is 12,000 B.H.P., the efficiency of the turbines is 85 per cent., and the gross head, from head of inlet canal to tail of outlet canal, is 72 ft. The head-race canal is 4·3 miles long, the tail-race canal is 2·8 miles long, both are concrete lined, of the most economical section, with 1 : 1 side slopes. Give two solutions, assuming (*a*) that 5 per cent. of the gross head is lost in the canals, (*b*) that 10 per cent. of the gross head is lost. Ans. (*a*) 400 sq. ft.
(*b*) 320 ,,

133. A low-head turbine installation is embodied in a barrage built across a river. In the power-house there are three turbines each of 15,000 B.H.P.; the overflow spillway has four vents each 18 m. wide, the water spilling over the tops of the gates.

On a certain occasion the discharge of the river is 550 cu. m./sec., the three units are working at their full output under a head of 9·4 m., and the four spillway gates are set all at the same level. If, now, one of the units is shut down, the other two running as before, make an estimate of the amount by which all the gates must be lowered in order to maintain the upstream river level unaltered.
Ans. 0·6 metre.

134. A turbine installation derives its water from a stream whose discharge varies with the season. During the rainy season, which can be taken to last for three months, the discharge of the stream can be assumed to average 420 cusecs; but during the dry season, lasting for 9 months, the flow is only equivalent to 110 cusecs.

In order to allow the power station to generate energy at a uniform rate, a reservoir is formed at the head of the pipe-line so that the entire stream flow may be utilised; the mean reservoir level is 650 ft. above turbine level. There are three steel pipes connecting the reservoir to the turbines, each 4200 ft. long; the friction loss in these pipes is 3 per cent. of the gross head. The turbine efficiency is 0·87.

Estimate: (*a*) the capacity of the reservoir; (*b*) the diameter of the pipes; (*c*) the B.H.P. output of the turbines.

Ans. (*a*) 42000 acre-feet.
(*b*) 3·2 ft.
(*c*) 11700 H.P.

CHAPTER XIV

EXAMPLE 135.

A model of a Francis turbine, built to a scale of 1/5, when tested in the makers' works, was found to develop 4·10 B.H.P. at a speed of 360 r.p.m. under a head of 1·80 m. Estimate the equivalent speed and power of the full-size turbine when working under a head of 5·80 m.

Solution :—

Speed of model under 5·8 m. head $= 360\sqrt{\dfrac{5\cdot8}{1\cdot8}} = 646$ r.p.m.

Since under a given head the rim speeds of the model and of the full-size turbine are identical, the *speed of revolution* of the full-size turbine under 5·8 m. head $= 646 \times \frac{1}{5} =$ *129 r.p.m.*

Power of model under 5·8 m. head $= 4\cdot10\left(\dfrac{5\cdot8}{1\cdot8}\right)^{\frac{3}{2}} = 23\cdot7$ B.H.P.

Since under a given head, power varies as (diameter)^2, then *power* of full-size turbine under 5·8 m. head $= 23\cdot7 \times 5^2 =$ *593 B.H.P.*

As a check, we may calculate the specific speed of the model, $= \dfrac{360\sqrt{4\cdot10}}{1\cdot8^{\frac{5}{4}}} = 350$, and compare it with the specific speed of the full-size turbine $= \dfrac{129\sqrt{593}}{5\cdot8^{\frac{5}{4}}} = 350$. The two values agree, as they ought to do.

This simplified solution may now be corrected to take into account *scale effect* (§ 279), thus :—

If the model efficiency on test had been found to be $\eta_m = 0\cdot76$, then the prototype efficiency could be extracted from the equation

$$\frac{1-\eta_m}{1-\eta_M} = (n)^{\frac{1}{4}}, \quad \text{or} \quad \frac{1-0\cdot76}{1-\eta_M} = (5)^{\frac{1}{4}}$$

from which $\eta_M =$ prototype efficiency $= 0\cdot84$.

The true output of the prototype or full-scale turbine could therefore be expected to be about

$$593 \times \frac{0\cdot84}{0\cdot76} = \textit{656 B.H.P.}$$

EXAMPLE 136.

Calculate the diameter, the speed, and the specific speed of a propeller turbine runner to develop 8500 B.H.P. under a head of 15·8 ft., having given that : Speed ratio ϕ based on outer diameter $= 2\cdot10$; flow ratio $\psi = 0\cdot65$; diameter of boss $= 0\cdot35 \times$ external diameter of runner ; overall efficiency = 88 per cent.

Solution :—

$$\text{Overall efficiency} = 0{\cdot}88 = \frac{\text{B.H.P.}}{\text{W.H.P.}} = \frac{8500}{\frac{W \times 15{\cdot}8}{550}},$$

from which W = weight of water = 337,000 lb./sec.,

and $Q = \text{discharge} = \dfrac{337000}{62{\cdot}4} = 5400$ cusecs.

Flow ratio $\psi = 0{\cdot}65 = \dfrac{Y}{\sqrt{2g \times 15{\cdot}8}}$,

from which Y = velocity of flow = 20·7 ft./sec.

Area for flow $= \frac{\pi}{4}D^2 - \frac{\pi}{4}(0{\cdot}35\,D)^2 = 0{\cdot}690\,D^2$.

This area also $= \dfrac{Q}{Y} = \dfrac{5400}{20{\cdot}7} = 261$ sq. ft.,

from which D = *runner diameter = 19·5 feet.*

Speed ratio $\phi = 2{\cdot}10 = \dfrac{v}{\sqrt{2g \times 15{\cdot}8}}$,

from which v = velocity of outer edges of runner blades = 67·0 ft./sec. But v also

$$= \frac{3{\cdot}14\,DN}{60} = \frac{3{\cdot}14 \times 19{\cdot}5 \times N}{60},$$

from which N = rotational *speed of runner = 66 r.p.m.*

Specific speed of runner

$$= N_s = \frac{N\sqrt{P}}{H^{\frac{5}{4}}} = \frac{66\sqrt{8500}}{15{\cdot}8\sqrt[4]{15{\cdot}8}} = 193 \text{ (foot units)}.$$

Example 137.

In a proposed hydro-electric installation a number of Francis turbines are to be disposed along a barrage, as in Fig. 268; the head is 8·3 m. and the speed of the turbines is 75 r.p.m. It is stipulated that the distance between the vertical axes of the units must not be less than 3·5 × the outside diameter of the runners.

Calculate the maximum B.H.P. that can be generated per metre length of barrage.

Solution :—

For the duty in question, runners of type III (Fig. 282) would be suitable. Since their specific speed is 400, we find by inserting known values in the equation

$$N_s = \frac{N\sqrt{P}}{H^{\frac{5}{4}}}, \text{ or } 400 = \frac{75\sqrt{P}}{8{\cdot}30^{\frac{5}{4}}},$$

that P = output of each turbine = 5660 B.H.P.

By measurement of the drawing of the specific runner III in Fig. 282 we find that its outside diameter is about 0·3 m. Since this specific runner develops 1 h.p. under 1 m. head, it will develop $1 \times 8{\cdot}3^{\frac{3}{2}} = 23{\cdot}9$ h.p. at 8·3 m. head.

The diameter of runner D that will develop 5660 h.p. at 8·3 m. head can now be obtained from the relationship $\frac{(0{\cdot}3)^2}{D^2} = \frac{23{\cdot}9}{5660}$, viz. $D = 4{\cdot}62$ *m.*

The spacing between the turbine axes must therefore be $4{\cdot}62 \times 3{\cdot}5 = 16{\cdot}15$ m., and the B.H.P. generated per metre length of barrage $= \frac{5660}{16{\cdot}15} = 350$ *B.H.P.*

EXAMPLE 138.

A barrage incorporating a turbine power-house is built across a river in which the hydraulic conditions are as follows :—

State of River.	Water Level above Datum (Feet).	
	Upstream of Barrage.	Downstream of Barrage.
Flood conditions	52·6	34·0
Low stage conditions	51·2	18·4

The turbines proposed have a uniform speed under all conditions of 83·3 r.p.m. ; under a head of 26 ft. they develop at their maximum efficiency of 86 per cent. a horse-power of 3750, and their performance under other heads may be deduced from Fig. 295.

Calculate the output of each turbine, and the discharge required, under flood conditions and under low stage conditions.

Solution :—

There are two steps in the solution of this problem : (1) finding the new B.H.P. under the altered head, assuming that the efficiency is unchanged ; (2) making the necessary correction for the change in efficiency that is bound to accompany a change in the value of $N/\sqrt{H}$.

Under flood conditions the head H on the turbines is

$$52{\cdot}6 - 34{\cdot}0 = 18{\cdot}6 \text{ ft.}$$

Since the power under 26 ft. head is given as 3750, the power under 18·6 ft. head, if the value of $N/\sqrt{H}$, and therefore of the efficiency, remained the same, would be

$$3750 \times \left(\frac{18{\cdot}6}{26}\right)^{\frac{3}{2}} = 2270 \text{ B.H.P.}$$

But actually the unit speed, or speed under 1 ft. head $= \dfrac{N}{\sqrt{H}}$, has changed from $\dfrac{83\cdot3}{\sqrt{26}} = 16\cdot34$, to $\dfrac{83\cdot3}{\sqrt{18\cdot6}} = 19\cdot35$, viz. an increase of 18·2 per cent.

Now inspection of Fig. 295 shows that an increase in unit speed from 100 per cent. to 118·2 per cent. is accompanied by a fall in horse-power from 100 per cent. to 97·5 per cent.; hence the true *power* of the turbine under 18·6 ft. head is

$$2270 \times \frac{97\cdot5}{100} = \mathit{2210\ B.H.P.}$$

In a similar way we observe that the change in unit speed has brought down the efficiency to 95 per cent. of its maximum value, hence the efficiency under 18·6 ft. head is $0\cdot86 \times 0\cdot95 = 81\cdot7$ per cent. Consequently the weight of water required per turbine can be obtained from the relationship:—

$$0\cdot817 = \frac{2210}{\dfrac{W \times 18\cdot6}{550}}, \text{ or } W = 800{,}000 \text{ lb./sec.},$$

and *discharge per turbine* $= \dfrac{800{,}000}{62\cdot4} = \mathit{12{,}800\ cusecs.}$

Similarly, under low stage conditions, the head on the turbines $= 51\cdot2 - 18\cdot4 = 32\cdot8$ ft., and the power under this head, assuming unchanged efficiency $= 3750 \times \left(\dfrac{32\cdot8}{26}\right)^{\frac{3}{2}} = 5310$. But due to the change in unit speed from $\dfrac{83\cdot3}{\sqrt{26}} = 16\cdot34$, to $\dfrac{83\cdot3}{\sqrt{32\cdot8}} = 14\cdot54$, viz from 100 per cent. to 89 per cent., the power at a given head is found from Fig. 295 to fall from 100 per cent. to 95 per cent. and the efficiency falls from 100 per cent. of its maximum value to 98 per cent.

Hence true *output* at 32·8 ft. head $= 5310 \times \dfrac{95}{100}$
$= \mathit{5040\ B.H.P.}$,

and *discharge* at 32·8 ft. head

$$= \frac{5040 \times 550}{32\cdot8 \times 0\cdot86 \times 0\cdot98} \times \frac{1}{62\cdot4} = \mathit{16{,}100\ cusecs.}$$

(*Note.*—These results illustrate the point that the turbines would develop most power, and would require most water, just at the period at which there is the least amount of available water coming down the river. On the other hand, when the flood brings down a surplus of water, the output of the turbines is actually diminished because of the diminution in the afflux and in the working head.

The actual working of the problem could be much simplified by the direct use of a graph such as Fig. 300.)

EXAMPLE 139.

In a low-head water power project the turbines have to work for 7 hours per day at 100 per cent. of full load and for 17 hours per day at 40 per cent. of full load. Compare the total volume of water required per day, under equal conditions of head, output, etc., by (*a*) Kaplan turbines, (*b*) Francis turbines, and (*c*) Propeller turbines.

Solution :—

From Fig. 303, it is seen that the probable efficiencies of the various turbines will be somewhat as follows :—

	Kaplan.	Francis.	Propeller.
η_m = efficiency at full load . .	87 per cent.	87 per cent.	87 per cent.
η'_m = efficiency at 40 per cent. full load	91 per cent.	74 per cent.	61 per cent.

Let P = full load output of each turbine, under head H. Then discharge per second at full load

$$=\frac{550\,P}{H \times \eta_m} \times \frac{1}{62{\cdot}4} \text{ (foot units)}$$

and discharge per second at 40 per cent. of full load

$$=\frac{550 \times 0{\cdot}4\,P}{H \times \eta'_m} \times \frac{1}{62{\cdot}4}.$$

Therefore total volume of water required per day by Kaplan turbine.

$$=\left(7 \times 3600 \times \frac{550\,.\,P}{H \times 0{\cdot}87} + \frac{17 \times 3600 \times 550 \times 0{\cdot}4\,P}{H \times 0{\cdot}91}\right)\frac{1}{62{\cdot}4}$$

$$=K\left(\frac{7}{0{\cdot}87} + \frac{0{\cdot}4 \times 17}{0{\cdot}91}\right) = 15{\cdot}52\,K.$$

Similarly, total daily volume required by Francis turbine = $17{\cdot}24\ K$, and total daily volume required by propeller turbine = $19{\cdot}19\ K$,

The Francis turbine thus requires *11 per cent.* more water than the Kaplan turbine, and the propeller turbine requires *23 per cent.* more water than the Kaplan turbine.

(*Note.*—As in practice the station would no doubt contain two, three or more units, the Francis and propeller turbines would not be placed at such a disadvantage as the above results seem to show (§ 277).

Nevertheless, because of the fact that under given conditions of speed and head a Kaplan turbine can develop three or four times the power of a Francis turbine, there is a strong inducement to use a minimum number of large Kaplan units, and thus the superiority of this type, as demonstrated above, remains very real.)

EXAMPLES *for Solution* :—

140. Calculate the specific speed of a Francis turbine runner in which the speed ratio $\phi = 1{\cdot}05$, the flow ratio $\psi = 0{\cdot}25$, and the width of runner at the outer periphery is 1/4 of the outer diameter. The overall efficiency may be taken as 0·80. Ans. 61 (foot).
271 (metric).

141. A Pelton wheel works under a head of 120 m., and the mean diameter of the wheel is 1·15 m. During a brake test, in which the needle valve is kept fully open, it is found that when the wheel is brought completely to rest the torque on the shaft is 300 kg. metres. Estimate the speed and power of the wheel when running under its normal working conditions. Ans. 360 r.p.m. ; 75 h.p.

142. The quantity of water available for a hydro-electric station is 9200 cusecs under a head of 5·6 ft. Assuming the speed of the turbines to be 50 r.p.m., and their efficiency 82 per cent., determine the least number of machines, all of the same size, that will be needed if (i) Francis turbines whose specific speed must not exceed 105 (foot units), (ii) Kaplan turbines whose specific speed must not exceed 180, are chosen. What would be the individual output of the units in the two cases ?

Ans. (i) 15 turbines of 318 h.p. each.
(ii) 5 ,, ,, 955 ,, ,,

143. When running under a steady head of 20·7 ft., with full gate opening, at variable speed, a Francis turbine was found to give the following performance :—

Speed (r.p.m.).	B.H.P. Output.	Overall Efficiency. per cent.
400	100	84 per cent. (max.)
160	51	53
80	28	32
0	0	0

Use these figures to make a close estimate of the discharge flowing through the turbine, at zero speed, under the stipulated conditions. Ans. 33 cusecs.

144. Measure the projected blade area of the three runners shown in Fig. 282, and estimate for each wheel the ratio

$$\frac{\text{mean differential head } h_d}{\text{total head } H}$$

(h_d = head difference between back and front face of blade). You may assume that each runner has 14 blades.

Ans. About 0·2, 0·2, 0·33.

145. The draft-tube of a Kaplan turbine has an inlet diameter of 8·1 ft., and the inlet is set 7·5 ft. above tail-race level. When the turbine is developing 2100 h.p. under a net head of 19·6 ft., it is

found that a vacuum gauge connected to the draft-tube inlet indicates a negative head of 13·0 ft. If the turbine efficiency is 86 per cent., what would be the draft-tube efficiency ?

Then estimate what the reading of the vacuum gauge would be if the turbine output were reduced, by normal gate- and runner-blade regulation, to 1050 h.p. The net head remains unchanged at 19·6 ft., and the speed also remains constant.

Ans. 0·78 ; 8·9 ft.

146. A propeller turbine is to develop 950 B.H.P. under a head of 2·4 m., and its runner is to be geometrically similar to a type runner 1 m. diameter which develops 21 h.p. when running at 131 r.p.m. under a head of 1 m. Determine the speed, diameter, and specific speed of the actual runner required. If the head were increased to 3·8 m., what should be the speed of the actual runner in order to maintain the same efficiency as before ? Neglect scale effect.

Ans. 58·3 r.p.m.
3·5 m.
600 (metric).
73·4 r.p.m.

147. An impulse turbine working at full nozzle opening operates at a maximum efficiency of 0·87 when running at 450 r.p.m. under a head of 700 ft. If the speed were now held steady, and the head varied through a range 500 ft. to 900 ft., how would the efficiency respond ? To show this relationship, plot a curve between head and efficiency. You may assume that the basic performance curves have the ideal shape shown in Fig. 288.

Ans. At 500 ft., $\eta = 84{\cdot}0$ per cent.
At 900 ft., $\eta = 85{\cdot}7$ „

148. The mean relative velocity in the runner passages of a particular turbine can be expressed in the form $V_r = 1{\cdot}4\sqrt{2gH}$, and the dynamic head deficiency or depression head x can be written $x = 0{\cdot}2\left(\dfrac{V_r^2}{2g}\right)$. The velocity at entry to the draft tube is $0{\cdot}6\sqrt{2gH}$, and the efficiency of the draft tube is 0·67. What would be the minimum value of the cavitation factor σ at which it would be safe to run this turbine ? Ans. About 0·6.

149. A Francis turbine situated at an altitude of 4280 ft. above sea-level works under a head of 240 ft. and develops 6000 h.p. at 390 r.p.m. The flow ratio ψ based on the velocity at the entrance to the draft tube is 0·20 ; the efficiency of the draft tube is 60 per cent. Calculate (i) the maximum permissible height of the turbine above tail-water level, (ii) the negative head at the entrance to the draft tube, assuming that the turbine is set at its highest level.

Ans. 11 ft.
17 ft. of water.

150. In designing a propeller turbine installation, it is desired to choose the best position of the turbine relative to the tail-race level. The conditions are: total head = 45 ft. output = 22,000 B.H.P.; turbine efficiency = 0·89. Two possibilities are to be studied: (i) with the turbines 6 ft. above tail-race level, (ii) with the turbines 6 ft. below tail-race level.

Estimate in the two cases: (*a*) the maximum permissible speed of turbine, (*b*) the velocity energy of the water entering the draft-tube, expressed as a percentage of the total head.

Ans. 41 r.p.m.; 0·13.
50 r.p.m.; 0·21.

CHAPTER XV.

Example 151.

A single-acting single-cylinder plunger pump runs at 45 r.p.m.; the bore and stroke are 5 ins. and 12 ins. respectively; the suction pipe is 4 ins. diameter and 52 ft. long. Calculate the maximum permissible suction lift, assuming no vacuum vessel on the suction pipe to be fitted.

Solution :—

From § 290, inertia pressure at end of stroke

$$= p_i = 0{\cdot}000147\, LRN^2 \,.\left(\frac{D}{d}\right)^2$$

$$= 0{\cdot}000147 \times 52 \times 0{\cdot}5 \times 45^2 \times \left(\frac{5}{4}\right)^2 = 12{\cdot}1 \text{ lb./sq. in.}$$

Therefore available pressure for lifting water into pump

$$= \text{atmospheric pressure} - 12{\cdot}1 = 14{\cdot}7 - 12{\cdot}1 = 2{\cdot}6 \text{ lb./sq. in.}$$

Equivalent head $= 2{\cdot}6 \times \dfrac{144}{62{\cdot}4} = \mathit{6{\cdot}0\,ft.}$

(*Note.*—In practice cavitation would occur with a smaller lift than this not only because of the effect of the connecting-rod, but because of the liberation of air and water vapour under low pressures. But notice on the other hand that friction in the pipe can quite correctly be ignored, because under the conditions here specified, the water column in the suction pipe is at rest when the suction stroke begins.)

Example 152.

A three-throw pump having rams 12 ins. diameter by 24 ins. stroke is required to lift 1100 gallons of water per minute against a static head of 380 ft. The friction loss in the suction pipe is estimated at 4 ft., and in the delivery pipe at 56 ft. The pipe velocity is 3 ft./sec. The overall efficiency of the pump is 90 per cent., and the slip is 2 per cent.

Calculate the speed at which the pump should run, and the power required to drive it.

Solution :—

Discharge of pump per revolution

$$= 0{\cdot}98\left(\frac{\pi}{4} \times 1^2 \times 2 \times 3\right) = 4{\cdot}61 \text{ cu. ft.}$$

Discharge required per minute $= \dfrac{1100 \times 10}{62{\cdot}4}$

$= 176{\cdot}5$ cu. ft.

Hence *speed of pump* $= \dfrac{176{\cdot}5}{4{\cdot}61} = 38{\cdot}2$ *r.p.m.*

Total head against which pump works $= 380 + 4 + 56 + \left(\dfrac{3^2}{64{\cdot}4}\right)$

$= 440$ ft.

Horse-power input $= \dfrac{1100 \times 10 \times 440}{33{,}000 \times 0{\cdot}90}$

$=$ *163 S.H.P.*

EXAMPLE 153.

Estimate the dimensions of the rotors of a gear-wheel pump for the following duty: liquid, oil of viscosity 1500 secs. Redwood No. 1 ; discharge, 90 g.p.m. ; speed, 750 r.p.m. ; pressure generated ; 150 psi. What power input would be required ?

Solution :—

Discharge per revolution $= \dfrac{90 \times 1728}{6{\cdot}23 \times 750} = 33{\cdot}3$ cu. ins.

Reasonable assumptions for this pump would be :

Overall efficiency $= 0{\cdot}6$: Volumetric efficiency $= 0{\cdot}9$. Number of teeth per rotor $= 12$: Ratio $l/D = \dfrac{\text{length}}{\text{diameter}} = 1{\cdot}5$.

From § 303, value of D/C corresponding to 12 teeth $= 1{\cdot}18$.

$\therefore$ True discharge per rev. $= 33{\cdot}3$

$$= 0{\cdot}90 \times 0{\cdot}95 \times 3{\cdot}14 \times \frac{D}{1{\cdot}18}\left(D - \frac{D}{1{\cdot}18}\right) \times 1{\cdot}5D$$

from which $D =$ *rotor diameter* $= 4{\cdot}0$ ins.

and $l =$ *rotor length* $= 6{\cdot}0$ ins.

$$\text{Power output} = \frac{Qp}{33{,}000} = \frac{90}{6{\cdot}23} \cdot \frac{150 \times 144}{33{,}000} = 9{\cdot}45 \text{ h.p.}$$

$\therefore$ *Power input* $= \dfrac{9{\cdot}45}{0{\cdot}60} =$ *15·8* h.p.

EXAMPLE 154.

In a hydraulic ram installation the supply pipe is 6 cms. diameter and 4 metres long; the waste valve is 13 cms. diameter, it has an effective lift of 6·4 mm., it weighs 1·4 kg., and it makes 123 beats per minute. Estimate the discharge through the delivery pipe against a delivery head (above water level in supply reservoir) of 8 metres, neglecting all losses.

Solution :—

Area of base of waste valve $= \frac{\pi}{4} \times 13^2 = 133$ sq. cms. Upward pressure needed to close valve $= \frac{1 \cdot 4}{133} = 0 \cdot 0105$ kg./sq. cm. Equivalent head $= h_b = 0 \cdot 0105 \times 10 = 0 \cdot 105$ metres of water.
Maximum velocity past waste valve just before closure

$$= \sqrt{2gh_b} = 4 \cdot 43\sqrt{0 \cdot 105} = 1 \cdot 44 \text{ m./sec.}$$

Area past waste valve $= \pi \times 13 \times 0 \cdot 64 = 26 \cdot 2$ sq. cms.

Area of supply pipe $= \frac{\pi}{4} \cdot 6^2 = 28 \cdot 3$ sq. cms.

Therefore maximum velocity in supply pipe

$$= 1 \cdot 44 \times \frac{26 \cdot 2}{28 \cdot 3} = V = 1 \cdot 33 \text{ m./sec.}$$

In order to find the time in which the column in the supply pipe is brought to rest, we use formula 7-1, § 115, where h = retarding head = 8 m., L = length of supply pipe = 4 m., V = 1·33 m./sec.,

whence $$8 = \frac{4 \times 1 \cdot 33}{9 \cdot 81 \times t}, \text{ or } t = 0 \cdot 0678 \text{ secs.}$$

During this period water is flowing straight through from the supply pipe to the delivery pipe, with a mean velocity $= \frac{1}{2} \times$ maximum velocity V (assuming uniform retardation); thus the quantity of water flowing past the delivery valve per beat = mean velocity $\times$ pipe area $\times\ t$

$$= \frac{1 \cdot 33}{2} \times 100 \times \frac{28 \cdot 3}{1000} \times 0 \cdot 0678 = 0 \cdot 127 \text{ litre.}$$

Therefore *discharge per minute* of useful water

$$= 0 \cdot 127 \times 123 = \mathit{15 \cdot 6\ litres.}$$

Alternative Solution :—

At the moment of closure of the waste valve, the kinetic energy of the water column in the supply pipe is

$$\frac{WV^2}{2g} = \frac{\frac{28 \cdot 3 \times 400}{1000} \times (1 \cdot 33)^2}{19 \cdot 6} = 1 \cdot 02 \text{ kg. m.}$$

The weight of water that could be lifted through a height of 8 m. by this amount of energy is $\frac{1{\cdot}02}{8} = 0{\cdot}127$ kg., and thus discharge per minute $= 0{\cdot}127 \times 123 =$ *15·6 kg.*

(*Note.*—The dynamic thrust on the under-side of the waste valve, which has been neglected in the above solutions, might easily be much greater than the static thrust if the design of the valve box is favourable.)

EXAMPLES *for Solution :—*

155. A plunger pump works against a total static head of 96 m., and when running at 42 r.p.m. it is required to force 45 lit./sec. of water along a delivery pipe 25 cm. diameter and 130 m. long. There are no air vessels ; the pipe coefficient is 0·006 ; the slip is 3 per cent. ; the elasticity of the pipe walls and water column can be neglected ; the stroke of the plungers is twice the diameter.

If the number of cylinders chosen were 1, 2, 3, and 4, calculate in each case (i) the plunger diameter, (ii) the maximum pressure in the pipe. Ans. 34·8, 27·6, 24·1, 21·9 cm. ;
26·4, 18·0, 13·0, 14·3 kg./sq. cm.

156. It is desired to show by a series of graphs the behaviour of a single-acting ram pump. These graphs are :—

Abscissae : Stroke of ram, or distance from dead-centre.

Ordinates : (i) Velocity of water in delivery pipe.
(ii) Acceleration of water in delivery pipe.
(iii) Thrust on connecting rod.

The ram has a diameter of 14 cms. and a stroke of 22 cms. ; the pump runs at 85 r.p.m. ; the static delivery head is 34 metres ; the delivery pipe is 12 cm. diameter and 42 metres long ; the suction head and the length of the suction pipe are negligibly small.

Making simplifying assumptions, draw the graphs to scale.

157. A rotating-cylinder pump (§ 300 (ii)) is used in connection with a hydraulic transmission system in which the pump is to deliver 45 h.p. at a pressure of 500 lb./sq. in., when the speed is 200 r.p.m. and the housing E makes an inclination of 70° with the axis. The specific gravity of the oil is 0·95, the slip is 3 per cent., and the pitch diameter on which the cylinders are set is five times the cylinder diameter ; there are eleven cylinders.

Calculate the diameter of the cylinders. Ans. 2·27 ins.

158. A gear-wheel pump is required to deliver 4 lit./sec. of oil of S.G. 0·94 when running at 700 r.p.m. ; the suction pressure is 0·2 kg./sq. cm. (negative), and the delivery pressure is 6·0 kg./sq. cm. The overall efficiency is 48 per cent., and the volumetric efficiency is 90 per cent. The length of the gear-wheels or rotors is 2 × maximum diameter, and in shape they are geometrically similar to those shown in Fig. 340. What should be their outside diameter, and what would be the power input to the pump ?

Ans. 7 cms. ; 6·9 h.p.

159. Two duplex double-acting pumps identical with those shown in Fig. 325, § 294 (iii), are working in parallel; they deliver oil of S.G. 0·84 and viscosity 45 secs. Redwood into a pipe-line 98 miles long and 12 ins. diameter. Neglecting slip, and regarding the pipe as hydraulically smooth, estimate the pressure required to overcome frictional resistance. Ans. 865 lb./sq. in.

160. For forcing oil along a short pipe-line it is proposed to use a duplex direct-acting (non-rotative) steam pump; its steam pistons are 8-in. diam., and its pump pistons are 6-in. diam. The mean effective steam pressure available in the steam cylinders is 170 psi., and the pump efficiency is 65 per cent. = W.H.P./I.H.P. The oil to be pumped has the following characteristics :—

Tempr., deg. F.	60	100	140	180
Viscosity in poises	3·66	0·74	0·30	0·15
Mean S.G.	—	0·92	—	—

The static lift to be overcome is 30 ft. and the conditions are such that laminar flow always prevails in the pipe.

When the oil temperature is 75° F., it is found that a pressure of 310 psi. is required at the pump to force 66 g.p.m. through the pipe. But in practice the pump must maintain a rate of flow of 93 g.p.m., and accordingly the oil must be heated to make it flow freely enough. What temperature would be required?

Ans. 95° F.

161. The following particulars relate to a hydraulic ram installation :—

Supply head (above waste valve)	5·2 ft.
Length of supply pipe	14 ft.
Diameter of supply pipe	4 ins.
Effective area past waste valve when fully open	7 sq. ins.
Head in valve box required to close waste valve	0·4 ft.
Delivery head (above waste valve)	25 ft.

Neglecting frictional and eddy losses, determine the waste water per minute, the useful water lifted per minute, and the number of beats per minute. Ans. 36·8 gals./min.
·79 gals./min.
200 beats/min.

162. In a direct-acting steam pump the steam piston is 14 ins. diameter and the pump bucket is 8 ins. diameter. The steam pressure is 140 lb./sq. in., and the pump forces oil of S.G. 0·92 against a static pressure of 150 lb./sq. in. The delivery pipe is 6 ins. diameter and 1160 ft. long. If no air vessel were fitted, what would be the acceleration of the column of oil in the delivery pipe at the beginning of the stroke? The elasticity of the liquid and of the pipe-walls may be ignored. Ans. 19·6 ft./sec./sec.

163. A hydraulic ram is to be designed to suit the following conditions :—

> Supply head (above waste valve) $= 7{\cdot}2$ ft. : delivery head (above waste valve) $= 32$ ft. : useful water lifted per minute $=$ 190 lbs. : length of supply pipe $= 19{\cdot}0$ ft. : Rankine efficiency (assumed) $= 62$ per cent. : lift of waste-valve $= 1/10 \times$ diameter of waste-valve ; maximum velocity in supply pipe $=$ maximum velocity past waste-valve $= 7$ ft./sec.

Disregarding friction, etc., estimate : (i) the diameter of the supply-pipe ; (ii) the diameter of the waste-valve ; (iii) the rate of acceleration and rate of retardation in the supply pipe.

Ans. (i) 4·2 ins. ; 6·6 ins. ; 12·2 and 42 ft./sec.^{2}

164. An air lift pumping plant is required to raise 1200 gallons of water per minute against a static head of 190 ft. ; the submerged length of the rising main is 300 ft., and the overall efficiency of the plant, viz. $\dfrac{\text{water horse-power}}{\text{compressor B.H.P.}}$, may be taken as 30 per cent.

Estimate the volume of free air per minute (air at atmospheric pressure) that must be handled by the air compressor, having given that 0·25 B.H.P. is required to compress 1 cu. ft. of free air per minute to 130 lb./sq. in. pressure. Ans. 920 cu. ft./min.

165. A pumping station at A is provided for forcing 1700 tons of oil per day along a horizontal pipe-line AB: the points A, B, are at the same elevation and are 46 miles apart. The oil issues at the outlet end, B, at atmospheric pressure. When the pumps are working steadily throughout the 24 hours they are found to absorb 135 h.p., their efficiency being 82 per cent.

It is now desired to pump additional oil into the pipe at point C, midway between A and B, and at the same elevation. A new pumping station is therefore installed at C, identical with the original station at A. Consequently the quantity of oil to be delivered at point B each day is double what it was before.

It is required to compare alternative methods of operating the system : (i) allowing all the pumps to run uniformly throughout the 24 hours, (ii) allowing one pumping-station to run for 12 hours daily, at double its original rate of discharge, and then to stop this station and allow the other pumping station to run for the remaining 12 hours, at double the original rate.

If the pumps themselves are driven by oil-engines using 0·45 lb. of fuel-oil per B.H.P. hour, estimate the daily fuel consumption in the two alternative systems, (i) and (ii). Make suitable simplifying assumptions, e.g. that the pump efficiencies and the pipe coefficient remain unchanged. Ans. 8000 lb. ; 10700 lb.

CHAPTER XVI.

EXAMPLE 166.

A centrifugal pump having an *effective* blade angle at outlet of 45° is required to lift against a head of 20 m., the speed of the shaft being 700 r.p.m. and the velocity of flow, 2·0 m./sec. Calculate the diameter of impeller required if (i) the whole of the energy corresponding to velocity of whirl at exit is wasted, (ii) 40 per cent. of this energy is converted into useful pressure energy. Neglect friction.

In case (ii) state also the width of the mouth of the impeller if the discharge is 150 lit./sec. Blade thickness may be disregarded.

Solution :—

In case (i) the whole of the head of 20 m. must be generated in the impeller. Consequently formula 16-2 is applicable; inserting appropriate values, we have

$$20 = \frac{v^2 - 2^2(\sqrt{2})^2}{19 \cdot 6}, \text{ from which } v = \text{rim velocity}$$
$$= 20 \cdot 0 \text{ m./sec.}$$

But $$v = \frac{3 \cdot 14 \times D \times N}{60}, \text{ or } 20 \cdot 0 = \frac{3 \cdot 14 \times D \times 700}{60},$$

from which D = impeller diameter = *0·546 m.*

In case (ii) the head H_1 produced in the impeller need now be less than 20 m., because after leaving the impeller the water receives a further increase of pressure head equal to $0 \cdot 4 \left(\frac{V^2}{2g}\right)$.

Hence $$H_1 = \frac{v_1{}^2 - Y^2 \operatorname{cosec}^2 45°}{2g} = 20 - 0 \cdot 4 \left(\frac{V^2}{2g}\right),$$

or $$\frac{v_1{}^2 - 2^2(\sqrt{2})^2}{19 \cdot 6} = 20 - \frac{0 \cdot 4 (v_1 - Y \cot \gamma)^2}{19 \cdot 6}$$
$$= 20 - \frac{0 \cdot 4 (v_1 - 2 \times 1)^2}{19 \cdot 6},$$

from which $v_1 = 17 \cdot 4$ m./sec., and $D_1 =$ *0·475 m.*

(*Note.*—Comparing the values of the ideal efficiency $\frac{gH}{Vv}$, we find that in

case (i) $$\eta_i = \frac{9 \cdot 8 \times 20}{18 \cdot 0 \times 20 \cdot 0} = 0 \cdot 54,$$

whereas in case (ii), $$\eta_i{}' = \frac{9 \cdot 8 \times 20}{15 \cdot 4 \times 17 \cdot 4} = 0 \cdot 73.)$$

In case (ii), required area of impeller mouth $= \frac{Q}{Y}$

$$= \frac{0 \cdot 150}{2}$$
$$= 0 \cdot 075 \text{ sq. m.}$$

But area also $= 3{\cdot}14 \times D \times B$
$= 3{\cdot}14 \times 0{\cdot}475 \times B.$

Equating, $B = \dfrac{0{\cdot}075}{3{\cdot}14 \times 0{\cdot}475} = 0{\cdot}05$ m. or *5·0 cms.* = impeller width.

EXAMPLE 167.

A centrifugal pump lifts water against a static head of 119 ft., of which 13 ft. is suction lift. The suction and delivery pipes are both 6 ins. diameter; the head loss in the suction pipe is 6·8 ft. and in the delivery pipe, 23·2 ft. The impeller is $15\frac{1}{2}$ ins. diameter and 1 in. wide at the mouth; it revolves at 1200 r.p.m., and its effective exit blade angle is 35°.

If the manometric efficiency of the pump is 82 per cent., and the overall efficiency is 70 per cent., what discharge would you expect, and what horse-power would be needed to drive the pump? What would be the pressure head indicated at the suction and delivery branches of the pump?

Solution:—

If V_p = velocity in pipes, discharge $Q = \dfrac{\pi}{4}\left(\dfrac{6}{12}\right)^2 V_p$
$= 0{\cdot}196\ V_p$ cusecs.

Also Q = area of impeller mouth × velocity of flow

$$= 3{\cdot}14 \times \left(\frac{15{\cdot}5}{12}\right) \times \left(\frac{1}{12}\right) \times Y \text{ (neglecting blade thickness)}$$

$$= 0{\cdot}338\ Y.$$

Equating, $0{\cdot}196\ V_p = 0{\cdot}338\ Y$, or $Y = 0{\cdot}58\ V_p$.

$$\text{Rim velocity} = v = \frac{3{\cdot}14\ DN}{60} = \frac{3{\cdot}14 \times \frac{15{\cdot}5}{12} \times 1200}{60} = 81{\cdot}2 \text{ ft./sec.}$$

$$\text{Manometric head} = H_m = 119 + 6{\cdot}8 + 23{\cdot}2 + \frac{V_p^2}{2g} = 149{\cdot}0 + \frac{V_p^2}{2g}.$$

But also $$H_m = \eta_h \frac{Vv}{g} = \frac{0{\cdot}82\,(v - Y\cot\gamma)v}{32{\cdot}2}$$

$$= \frac{0{\cdot}82\,(81{\cdot}2 - 0{\cdot}58\ V_p \times 1{\cdot}428)81{\cdot}2}{32{\cdot}2}.$$

Equating the two values of H_m, we have

$$149{\cdot}0 + \frac{V_p^2}{64{\cdot}4} = \frac{0{\cdot}82\,(81{\cdot}2 - 0{\cdot}83\ V_p)\ 81{\cdot}2}{32{\cdot}2}.$$

Solving this equation, $V_p = 10{\cdot}0$ ft./sec.

Hence *discharge* $= 0{\cdot}196 \times 10{\cdot}0 = 1{\cdot}96$ *cusecs.*

$$\textit{Shaft horse-power} = \frac{QwH_m}{550 \times \eta_m} = \frac{1{\cdot}96 \times 62{\cdot}4 \times \left(149{\cdot}0 + \dfrac{10^2}{64{\cdot}4}\right)}{550 \times 0{\cdot}70}$$
$$= 48.$$

Since velocity head $= \dfrac{10^2}{64{\cdot}4} = 1{\cdot}5$ ft., $H_m = 150{\cdot}5$ ft.

Thus at pump *suction*, negative head $= 13 + 6{\cdot}8 + 1{\cdot}5 = 21{\cdot}3$ *ft.*; at pump *delivery*, positive head $= 150{\cdot}5 - 21{\cdot}3 = 129{\cdot}2$ *ft.*

EXAMPLE 168.

Draw up a provisional design for a centrifugal pump impeller for the following duty: effective head = 60 ft.; discharge = 400 g.p.m.: speed = 1450 r.p.m.

Solution:—

The specific speed works out at 23 (foot), which is acceptable for this single-stage pump. Suitable design characteristics would be: ϕ = speed ratio = 1·00; ψ = flow ratio = 0·105; d/D = ratio of inner diam. to outer diam. = 0·45; hydraulic efficiency = 0·87; overall efficiency = 0·73.

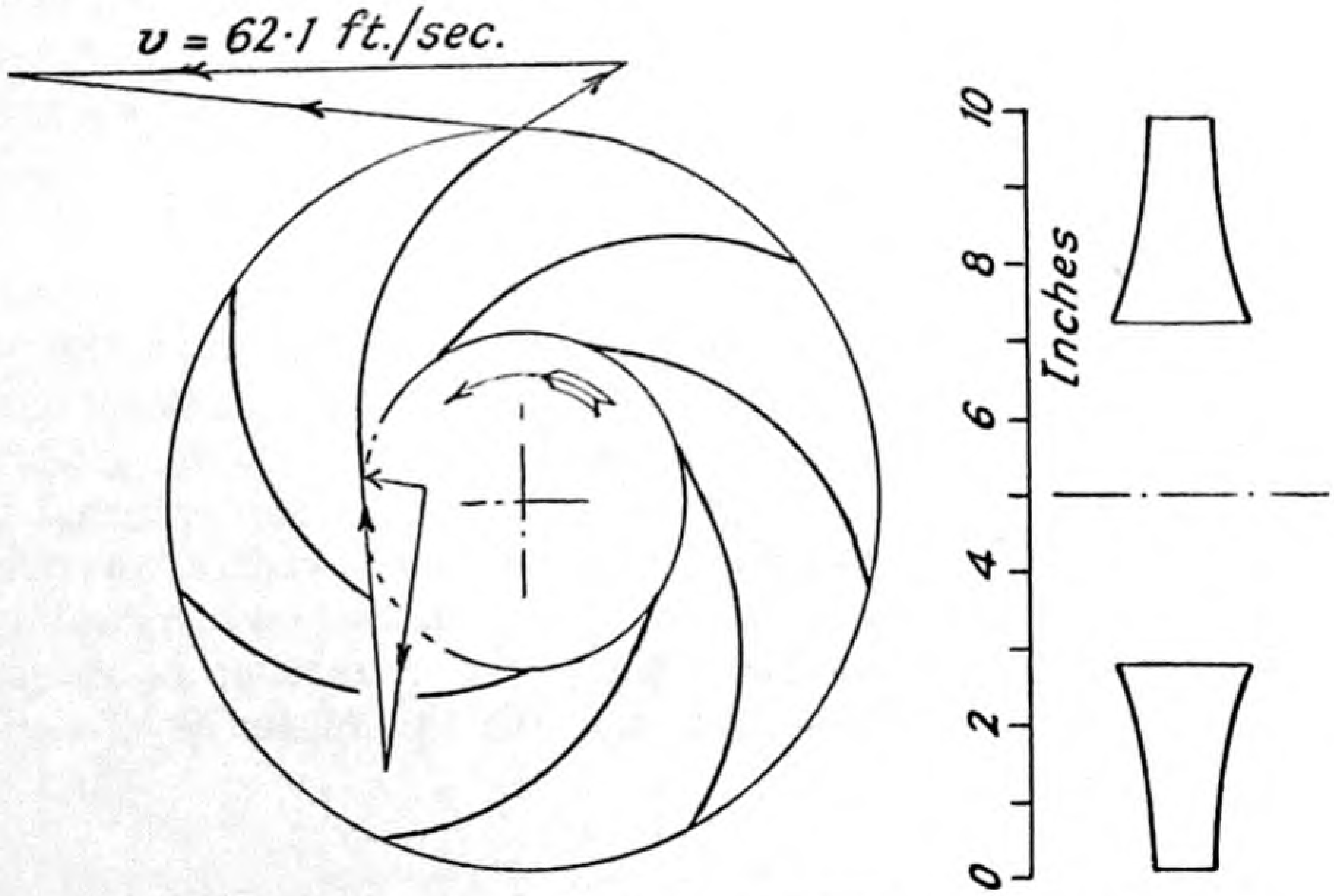

Since v = outer rim speed $= \phi\sqrt{2gH} = \pi DN/60$,

then $1{\cdot}00 \times 8{\cdot}03 \times \sqrt{60} = 3{\cdot}14 \times D \times 1450/60$,

from which D = *impeller diameter* = 0·82 ft.

Also Q = discharge = 400/374 = 1·07 cu. ft./sec.

$$= \pi DBY = 3{\cdot}14 \times 0{\cdot}82 \times B \times 0{\cdot}105 \times 8{\cdot}03 \times \sqrt{60}$$

from which B = *impeller width* = 0·064 ft.

Effective head $= H = \eta_h V_n v/g$

$$= 60 = 0{\cdot}87\,.\,\frac{V_n \times 62{\cdot}1}{32{\cdot}2},$$

from which V_n = true outlet whirl velocity component = 35·7 ft./sec. But, because of the "slip" described in § 320, the blades must be designed to give an ideal whirl component V which is greater than V_n. For present conditions an appropriate value of V_n/V is 0·7, and therefore $V = 35{\cdot}7/0{\cdot}7 = 51{\cdot}0$ ft./sec.

$$\text{Impeller outlet blade angle} = \gamma = \cot^{-1}\left(\frac{v - V}{Y}\right).$$

Now $\qquad v = \phi\sqrt{2gH} = 62{\cdot}1$ ft./sec.

$\qquad\qquad Y = \psi\sqrt{2gH} = 6{\cdot}52$ ft./sec.,

from which $\qquad \gamma =$ *outlet blade angle* $= 30° \; 23'$.

From the expression $\tan\beta = Y/v_1 = 6{\cdot}52/27{\cdot}9$, we find

$$\beta = \textit{inlet blade angle} = 13° \; 8'.$$

Accepting 7 as a suitable number of blades, they could then be drawn as in the diagram.

$$\textit{Power input to pump} = \frac{1{\cdot}07 \times 62{\cdot}3 \times 60}{550 \times 0{\cdot}73} = 10{\cdot}0 \text{ h.p.}$$

Corrections to these provisional figures would include: (i) allowance for thickness of metal forming blades, (ii) increase in flow area to allow for leakage loss, § 321, i.e. the impeller must pump *more* water than the designed flow.

EXAMPLE 169.

An electrically-driven centrifugal pump which has the characteristics shown in Fig. 376 is delivering 288 lit./sec. of water against an external head of 25·0 m. when running at 980 r.p.m. It is now desired to reduce the discharge to 120 lit./sec., the external head remaining the same. Determine the minimum B.H.P. of the driving motor under the new conditions, if (i) the motor is a constant speed A.C. machine running at 980 r.p.m., the reduction in discharge being carried out by throttling, and (ii) the motor is a variable speed machine.

Solution :—

(i) When the pump running at 980 r.p.m. is throttled down so as to deliver only 120 lit./sec., we find from Fig. 376 that the head generated is 37·5 m., and that the efficiency is 73 per cent. The S.H.P. input to the pump, and therefore the B.H.P. output of the motor, is thus

$$\frac{WH_m}{75\eta_m} = \frac{120 \times 37{\cdot}5}{75 \times 0{\cdot}73} = \mathit{82{\cdot}2}.$$

(Note that although only 25 m. head is required, the pump is *bound* to generate 37·5 m. head if we allow it to deliver the stated discharge at the stated speed. The surplus head of 12·5 m. must all be destroyed in the throttle valve on the delivery pipe.)

(ii) When using a variable speed motor, the motor and pump would be slowed down until the pump was delivering just the right quantity at the right head, viz. until its head-discharge characteristic passed through the point $H = 25$ m., $Q = 120$ lit./sec. This speed is found from Fig. 376 to be 805 r.p.m., the equivalent pump efficiency being 75 per cent. Hence the motor B.H.P. is now

$$\frac{120 \times 25}{75 \times 0{\cdot}75} = 53{\cdot}4.$$

EXAMPLE 170.

Two centrifugal pumps are installed in a pumping station for lifting water against a dead or static head of 18·5 metres and forcing it through 2180 metres of 50 cms. diameter new asphalted cast-iron piping. Calculate the discharge through each pump, and the output of the driving motors, when (*a*) one pump only is working, (*b*) the two pumps are working in parallel. The sets run at 960 r.p.m., and the pump performance is represented in Fig. 376.

Solution :—

It is first necessary to calculate the friction loss in the pipe corresponding to various rates of discharge. The virtual slope i can be read off directly from the abac (Fig. 141) and the information tabulated thus :—

Discharge in Pipe, and Discharge per Pump when One Pump Working (lit./sec.).	Discharge per Pump when Two Pumps Working (lit./sec.).	$i = \frac{h_f}{2180}$.	Friction Head $= h_f$ (metres).
50		0·00014	0·3
100	50	0·0005	1·1
150		0·0012	2·6
200	100	0·002	4·4
250		0·003	6·5
etc.			etc.

Neglecting velocity head, H_m = manometric head $= 18{\cdot}5 + h_f$; curves can therefore be plotted between discharge per pump and manometric head, as shown in the diagram, by the broken lines (*a*) and (*b*).

The actual pumping conditions will be represented by the intersections of these lines with the appropriate head-discharge pump characteristic, for then the internal head generated will exactly balance the external head required.

The following information can at once be read off :—

(*a*) *One pump working* : $Q = 268$ lit./sec.

$H_m = 26{\cdot}1$ m.

$\eta_m = 72$ per cent.

(*b*) *Two pumps working*: $Q = 195$ lit./sec. per pump.

$H_m = 33{\cdot}8$ m.

$\eta_m = 79$ per cent.

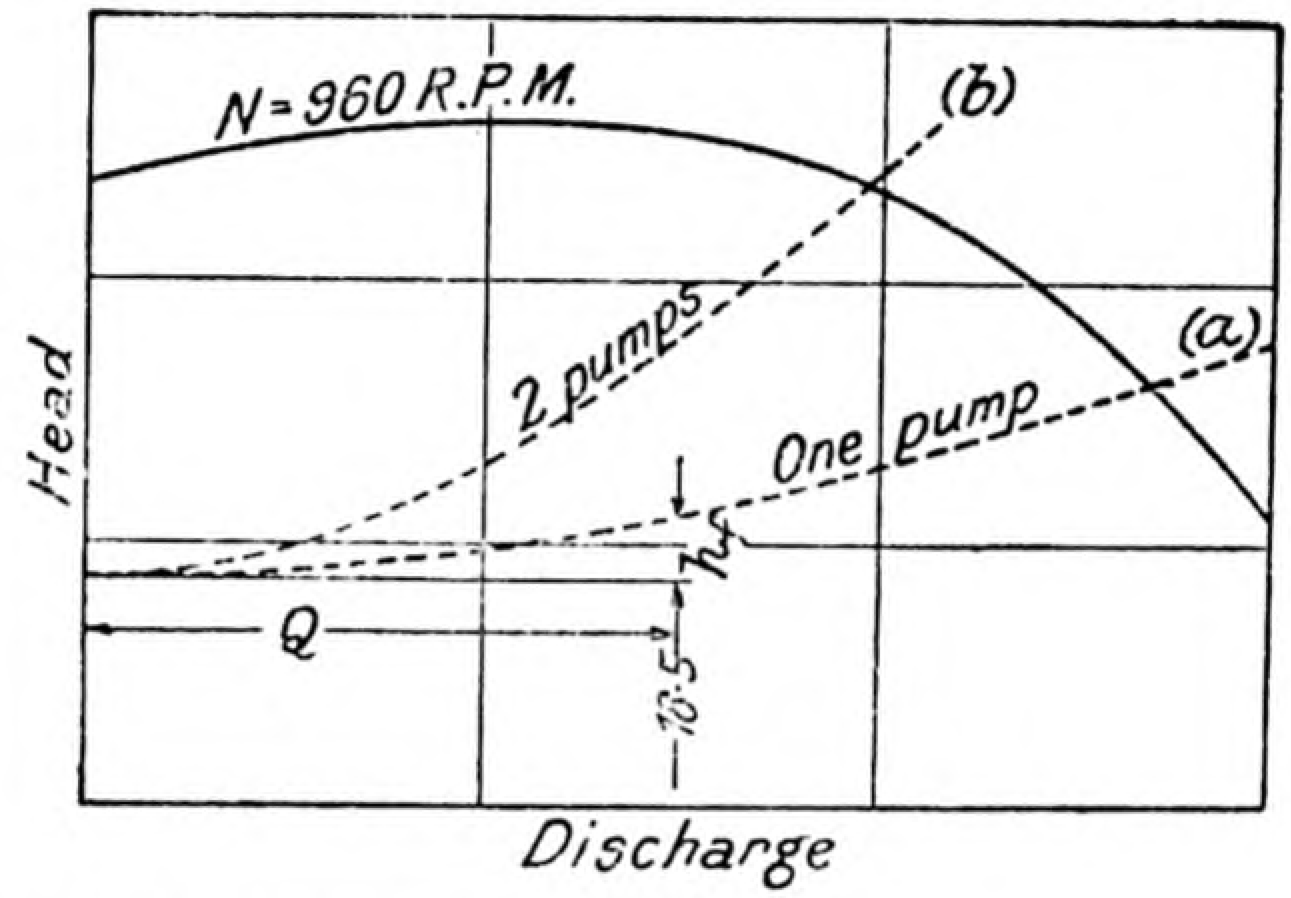

The corresponding motor outputs are

One pump working, 130 B.H.P.

Two pumps working, 111 B.H.P. per motor.

(Note that switching in the second pump only increases the total discharge by 46 per cent., but increases the power demand by 70 per cent.)

Example 171.

Estimate the diameter and the number of the impellers required for a multi-stage pump to lift 800 gals./min. against a total head of 560 ft., at a speed of 750 r.p.m.

Solution :—

The specific speed of the impellers will be about 18 (foot).

Substituting appropriate values in the expression

$$N_s = 0{\cdot}0174\,\frac{N\sqrt{Q}}{H^{\frac{3}{4}}},\ \text{we have } 18 = \frac{0{\cdot}0174 \times 750\sqrt{800}}{H^{\frac{3}{4}}},$$

from which H = head per stage = 56·1 ft.

Thus *number of stages* $= \dfrac{560}{56{\cdot}1} = $ *10.*

Fig. 380 shows that for an impeller of $N_s = 18$, the value of $\dfrac{H}{D^2}\left(\dfrac{1000}{N}\right)^2$ at the useful part of the characteristic is about 45.

Inserting known values,

$$\frac{56}{D^2} \cdot \left(\frac{1000}{750}\right)^2 = 45,$$

from which D = *impeller diameter* = 1·49 ft. = say *1·5 ft.*

As a check, the discharge of a similar impeller 1 ft. diameter running at 1000 r.p.m. may be worked out. This is

$$\frac{Q}{D^3}\left(\frac{1000}{N}\right) = \frac{800}{(1 \cdot 5)^3} \cdot \frac{1000}{750} = 317,$$

which agrees with the value found from Fig. 380.

Again, the value of

$$\phi = \frac{v}{\sqrt{2gH}} = \frac{\dfrac{3 \cdot 14 \times 1 \cdot 5 \times 750}{60}}{8 \cdot 03\sqrt{56}}$$

$$= 0 \cdot 98, \text{ which is a reasonable figure}$$

Examples *for Solution :—*

172. Calculate the specific speed of a centrifugal pump under the following conditions: speed = 980 r.p.m.; diameter of impeller = 28 cms.; width of impeller = 6 cms.; effective outlet blade angle = 30°; discharge = 120 lit./sec.; hydraulic efficiency = 86 per cent.
Ans. 180 (metric).

173. A single-stage centrifugal pump is built to give a discharge Q when working against a manometric head of 56 ft. On test, however, it is found that when the specified discharge Q is flowing through the pump, the head generated is 61 ft. As the shaft speed cannot be altered, it is necessary to turn down the impeller in the lathe to a smaller diameter. If the original diameter was $13\frac{1}{2}$ ins., what should be the corrected diameter to enable the pump to meet its specification?
Ans. about 13 ins.

174. A pumping installation is to be built up from the following elements: (*a*) a horizontal oil engine developing 55 B.H.P. at 320 r.p.m., fitted with a belt pulley, 85 cms. diameter; (*b*) two identical centrifugal pumps which are to be coupled in series; each has a 15 cm. diameter belt pulley, and each impeller is 21 cm. outside diameter and 3 cms. wide at the mouth; (*c*) a countershaft having pulleys of suitable sizes, through which the engine drives the pumps. The total head through which the water must be lifted, including friction, etc., is 60 m.

Make estimates of (i) the quantity of water delivered, (ii) the pump speeds, (iii) the diameters of the countershaft pulleys.
Ans. 40 lit./sec.; 2400 r.p.m; 30 and 40 cm.

175. If the characteristics of pump B reproduced in Fig. 377 relate to a pump speed of 2600 r.p.m., plot the characteristics for this pump at a speed of 2000 r.p.m., using the relationships of § 330. Head, power, and efficiency should be plotted against discharge.

176. The cast-iron suction pipe of a centrifugal pump is 6 in. diameter and is made up as follows: Foot-valve and strainer, 7 ft. 6 ins. of straight pipe, 90° bend, 32 ft. of straight pipe, 90° bend; 18 ft. of straight pipe. Estimate the maximum permissible height of the pump axis above the suction well water level, if the pump is to lift 530 gals./min. of water at 120° F. Assume that the loss of head in the foot-valve and strainer is three times the velocity head in the pipe. The absolute pressure at the suction flange is to be 1·9 lb./sq. in. above the vapour pressure.

Ans. 20 ft.

177. In designing a centrifugal pump to deliver a discharge of 60 lit./sec. against a total manometric head of 80 metres, it is stipulated that the shaft speed is to be 1470 r.p.m., the flow ratio is 0·15, and the speed ratio is 1·05, these values relating to the *head per stage*. Draw to the same scale outline diagrams of the impellers required, if (i) a single-stage pump, (ii) a three-stage pump, is chosen. Then, for the two designs, compare the horse-power loss in disc friction on the sides of the impellers.

Ans. (i) D = 54·3 cm., B = 6 mm.; (ii) D = 31·3 cm., B = 18 mm.
Ratio = 5·2 to 1.

178. At an oil-field near the sea, the crude oil from the wells is stored in tanks near the shore, from which it can be transferred to tanker ships moored near by. The oil, of S.G. 0·89, normally flows by gravity from the shore tanks to the ship tanks under a mean head of 8·6 metres, through a pipe system which is equivalent to a pipe 775 metres long and 8-in. diameter, having a pipe coefficient "f" of 0·0075.

What would be the rate of flow of oil in metric tons per minute?

Also estimate the rate of flow if it were augmented by putting in circuit a booster pump having the following characteristics :—

Discharge (lit./sec.)	0	20	40	60	80	100
Manometric head (metres)	11·8	12·0	11·6	10·0	8·4	6·0

Ans. 2·13 : 3·12 tons/min.

179. A centrifugal pump is to be so designed that the clearance, slip, or leakage loss between the impeller and the casing is 3 per cent. of the discharge, which is 330 gals. per min. The impeller is of the side-inlet type, Fig. 359 (I), the diameter (d) of the eye is 6 ins., and the axial length of the clearance space is 0·7 in. The head difference between the delivery and suction sides of the clearance is 39·5 ft., and in computing the leakage through the space you may use the Darcy formula 5-7, taking a coefficient f of 0·01. In this formula the value $2(a)$ is substituted in place of the pipe diameter, where (a), Fig. 359 (I), is the radial clearance required. What must this distance be? Ans. about 0·008 in.

180. A centrifugal pump and a gear-wheel pump, each running at its own fixed speed, can be arranged to work either in series or

in parallel. The discharge of the gear-wheel pump is 5·5 lit./sec., and the discharge of the centrifugal pump can be found from the relationship :—

$$H = 7 - 0{\cdot}08Q^2,$$

where H is the head generated in metres, and Q is the discharge in lit./sec.

State the total discharge through the system, when (*a*) the two pumps work in series against a total head of 21 metres, (*b*) the two pumps work in parallel against a head of 3·2 metres.

Ans. 5·5 lit./sec. : 12·4 lit./sec.

181. The pump whose performance is shown in Fig. 377 is to be used for lifting water from a lower to an upper tank, both tanks being rectangular, 30 ft. long and 15 ft. wide. When pumping begins, the difference in level between the water surfaces is 75 ft.; how long will it take to transfer 50,000 gallons from one tank to the other? Pipe friction losses, etc., may be taken to average 4 ft. head.

Ans. about 85 minutes.

182. A centrifugal pump is fixed 3·5 metres above the water level in the suction well. When running at a speed of 1950 r.p.m. against closed throttle (valve in delivery pipe closed), it generates a manometric head of 21·4 metres of water.

If now the pump is run at the same speed *before* being primed, viz. with the pump and pipes filled only with *air*, and with the delivery valve open, estimate how far the water will rise up the suction pipe.

Ans. 2·6 cms.

183. A centrifugal pump has an impeller 11·4 ins. diameter running at 960 r.p.m., with an effective outlet blade angle of 28°. The velocity of flow (assumed uniform throughout the system) is 6·5 ft./sec.; the static suction lift is 9·1 ft. The energy losses, in feet head of water, are: in suction pipe, 2·0 ft.; in impeller, 1·6 ft.; in volute casing, 2·9 ft.

From these particulars, estimate the readings of vacuum or pressure gauges placed, (i) at inlet to the pump; (ii) at impeller outlet, (in clearance space between impeller and volute); (iii) at pump outlet or delivery flange.

Ans. (i) $-$ 11·7 ft.; (ii) $+$ 19·6 ft.; (iii) $+$ 36·2 ft.

184. A 6-stage centrifugal pump takes in water at atmospheric pressure and discharges it against a head of 930 ft. The 6 impellers resemble that shown at (I), Fig. 359; the diameter (*d*) is $6\frac{3}{8}$ ins., the outer diameter is $15\frac{3}{4}$ ins., and the shaft diameter is $2\frac{3}{8}$ ins. The balancing disc, Fig. 368, has an outside diameter of $7\frac{7}{8}$ ins., and the cross-sectional area of the leakage passage is 0·05 sq. in. This passage may be treated as an orifice having a coefficient of discharge of 0·3.

Estimate the total axial thrust on the shaft that must be resisted by the balancing disc, and the quantity of balancing water that would leak past the disc.

Ans. 4·9 tons; $7\frac{1}{2}$ gals./min.

CHAPTER XVII.

EXAMPLE 185.

In order to increase the discharge in a gravitational water main, a booster pump of the propeller type is installed. Under the natural head of 67 ft. the flow in the main is 16,800 gallons per minute; when the pump is working the discharge is required to be 20,000 gallons per minute. Estimate the speed and diameter of the pump, and the power needed to drive it.

Solution :—

Since the discharge in a pipe varies roughly as $\sqrt{\text{friction loss}}$, we may write

$$\frac{16800}{20000} = \frac{\sqrt{67}}{\sqrt{h}},$$

from which h_t = total friction loss when pump is working = 95 ft.

Of this total head of 95 ft. the pump itself must supply $95 - 67 = 28$ ft. (see Fig. 152). Thus the duty of the pump is equivalent to lifting 20,000 gals./min. against a head of 28 ft.

Assuming a specific speed of 180 (foot), an overall efficiency η_m of 70 per cent., and a speed ratio ϕ of 2·1, we have

$$N_s = 180 = 0{\cdot}0174 \, . \frac{N\sqrt{Q}}{H^{\frac{3}{4}}} = 0{\cdot}0174 \frac{N\sqrt{20000}}{28^{\frac{3}{4}}},$$

from which N = *speed of pump = 890 r.p.m.*

Also
$$\phi = \frac{v}{\sqrt{2gH}} = 2{\cdot}1 = \frac{\dfrac{3{\cdot}14 \times D \times 890}{60}}{8{\cdot}03\sqrt{28}},$$

from which D = *diameter* of propeller = *1·91 ft.*

Finally, *horse-power*

$$= \frac{QwH}{33000 \times \eta_m} = \frac{20000 \times 10 \times 28}{33000 \times 0{\cdot}70} = 242 \text{ B.H.P.}$$

EXAMPLE 186.

The characteristics reproduced in Fig. 397 relate to a propeller pump running at a constant speed of 970 r.p.m. Estimate the speed at which the pump must be driven to enable it to deliver 1500 g.p.m. against a manometric head of 25 ft. What should be the power input?

Solution :—

The 970 r.p.m. curve from Fig. 397 is first reproduced as in the accompanying diagram. Then, having established the point A representing the specified conditions, viz. $q = 1500$, $H_m = 25$, it is

necessary to draw the iso-efficiency curve passing through this point. This can be done by locating another point B close to the given q-H characteristic, having co-ordinates q_b and H_b, such that

$$\frac{52}{H_b} = \left(\frac{1500}{q_b}\right)^2.$$

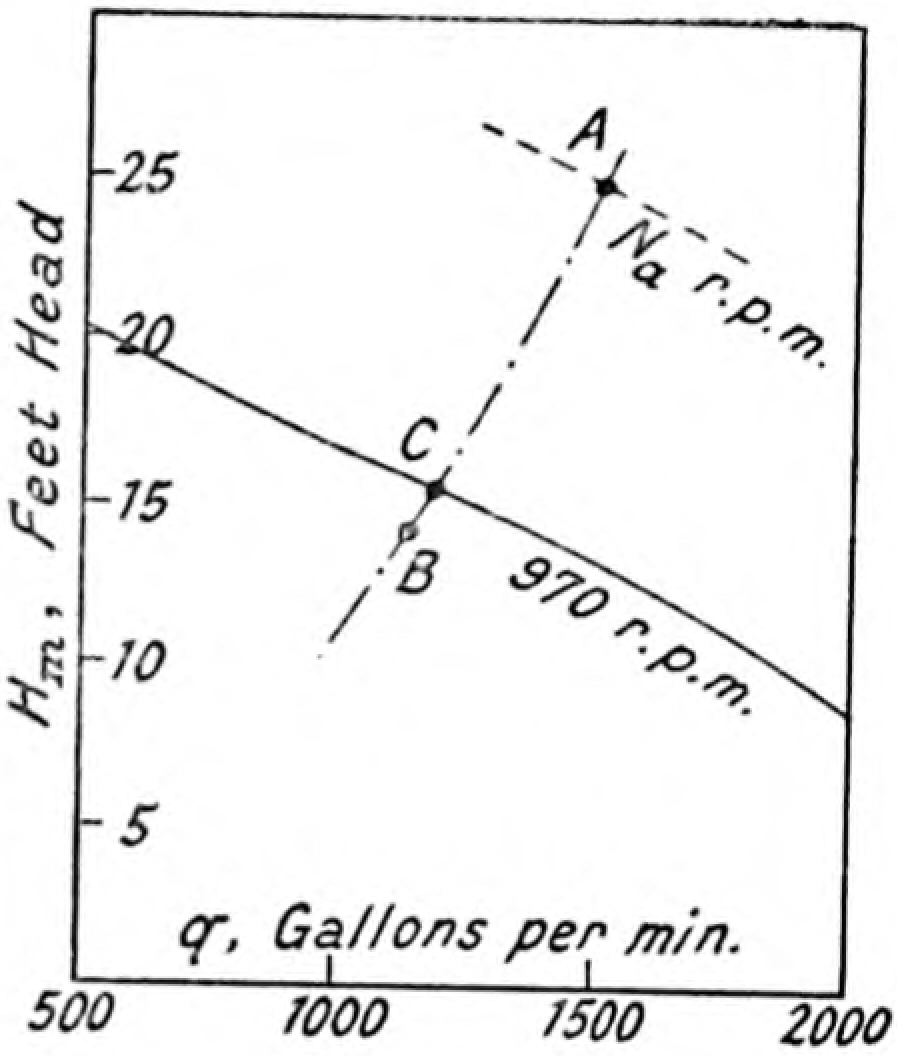

The parabola passing through A and B can now be sketched in, and the point C established at its intersection with the q-H curve (970 *r.p.m.*). We can directly apply to points A and C the relationship

Head $\propto$ (speed) ^{2} . (§ 330)

that is

$$\frac{25}{15{\cdot}5} = \left(\frac{Na}{970}\right)^2,$$

from which

$$N_a = \textit{required speed} = \textit{1230 r.p.m.}$$

Also efficiency corresponding to point C is 55 per cent. (from Fig. 397), and this value also applies to point A. Hence

$$\textit{S.H.P. input} = \frac{25 \times 1500 \times 10}{33{,}000 \times 0{\cdot}55} = \textit{20·6}.$$

(This useful method, which is applicable to all types of rotodynamic pumps, may be compared with the procedure when a complete series of head-discharge curves is available, § 327.)

Example 187.

Sea water of S.G. 1·03 is to be circulated through condensers by a propeller pump 47 in. diameter. It is found that a scale model of the pump, 9·8 in. diam., gives its best efficiency when pumping 1300 g.p.m. of fresh water against a head of 12·7 ft. at a speed of 2060 r.p.m.

What should be the speed of the full-size pump to deliver 90 tons per minute, and what pressure-difference would it generate ?

Solution :—

Using the relationships of § 331, and converting the above values to feet and cubic feet per second, we have

$$\frac{Q}{ND^3} = \frac{q}{nd^3}$$

or

$$\frac{52{\cdot}4}{N \times (3{\cdot}92)^3} = \frac{3{\cdot}48}{2060 \times (0{\cdot}817)^3}$$

from which N = *speed of full-size pump* = 279 r.p.m.

Similarly $$\frac{H}{N^2D^2} = \frac{h}{n^2d^2}$$

or $$\frac{H}{(279)^2 \times (3{\cdot}92)^2} = \frac{12{\cdot}7}{(2060)^2 \times (0{\cdot}817)^2}$$

from which H = head generated by full-size pump = 5·37 ft.
and p = *pressure difference*
$= 5{\cdot}37 \times 0{\cdot}434 \times 1{\cdot}03 = \mathit{2{\cdot}40}$ psi.

(*Note.*—Because of the scale effect (§ 279), the true pressure might be slightly greater than this.)

EXAMPLE 188.

Compare the general dimensions of alternative types of pump for forcing 50,000 barrels of oil per day against a pressure-difference of 1000 psi. The two types are (i) triplex double-acting reciprocating pump, (ii) multi-stage centrifugal. What power input would they need ?

Solution :—

(i) The reciprocating pump would comprise three lines of parts as Fig. 320 (*e*), § 292, the three cranks being set at 120°. Suitable additional data would be : speed = 50 r.p.m. : ratio (bore/stroke) = 1/3 : slip = 3 per cent. : overall pump efficiency = 90 per cent.

$$Q = \text{discharge per min. in cubic feet} = \frac{50{,}000 \times 5{\cdot}615}{24 \times 60} = 195{\cdot}2$$

$$= 0{\cdot}97 \times 50 \times 6 \times \frac{\pi}{4}D^2 \times 3D,$$

from which D = *plunger diam.* = 0·66 ft. or 7·92 ins.
L = *stroke* = 23·8 ins.
By scaling the diagram, Fig. 320 (*e*), it will be seen that the overall length of the pump would be at least 20 ft.

$$\text{Power output} = \text{W.H.P.} = \frac{195{\cdot}2 \times 1000 \times 144}{33{,}000} = 852 \text{ h.p.}$$

Power input = S.H.P. = 852/0·90 = *947 h.p.*

(ii) For the centrifugal pump, provisional data might be : Speed = 2000 r.p.m. ; specific speed = 22 (foot) : speed ratio = 0·95 : overall efficiency = 60 per cent. ; S.G. of oil = 0·92.

Total head = 1000 × 2·31/0·92 = 2520 ft.

By the method of Example 171, it is found that *Head per stage* = 210 ft.

Whence *Number of stages* = 12.

$$\text{Rim velocity} = v = 0{\cdot}95 \times 8{\cdot}03 \times \sqrt{210} = \frac{3{\cdot}14 \times D \times 2000}{60},$$

from which D = *impeller diameter* = 1·06 ft.

The pump would thus be something of the order of 8 ft. long and $2\frac{1}{2}$ ft. diameter.

Power input = S.H.P. = 852/0·60 = *1420* h.p.

Further comparisons might be: since both pumps would presumably be driven by oil engines, the reciprocating pump would require step-down gearing and the centrifugal pump would need step-up gears. If used for oil pipe-line service, an important difference would be that the centrifugal pump could be interposed directly in the pipe-line, thus serving as a booster pump; but the reciprocating pump must draw from its own oil reservoir. Evidently much more information would be necessary before a final choice could be made.

EXAMPLES *for Solution* :—

189. The rotor of a propeller pump has a mean diameter of 2·15 metres, and it revolves at 85 r.p.m. At the mean diameter the blade angle at inlet is 11°, and at outlet 14°. The manometric efficiency may be assumed to be 85 per cent. Draw to scale velocity diagrams at inlet and outlet, and from them calculate: (i) the manometric head generated, (ii) the speed ratio based on the mean diameter, and (iii) the flow ratio based on the mean diameter.

Ans. 1·74 m.
1·635
0·317

190. For forcing water along a 2 ft. diameter pipe, 5460 ft. long, two pumps are under consideration; one is a centrifugal pump, and the other is a propeller pump, their characteristics being showr Fig. 412. They both have the same normal discharge, 10·8 cus and normal head, 20 ft. The static head is 8 ft., and the p coefficient is 0·006. Make an estimate of (i) the time taken w each pump to accelerate the water column to its full speed, fr the moment when flow begins after the pump is started, (ii) the maximum pressure during the starting period. Ass e that the pump has reached its normal working r.p.m. be re flow begins.

44

Ans. (i) 83 secs., 39 secs.; (ii) 9·4 lb./sq. in., 22·6 lb./s in.

191. (i) The conditions in a centrifugal pump and pipe system are as follows: discharge = 930 U.S. gals. per min.; manometric head = 150 ft.; speed = 2950 r.p.m.: water velocity at impeller inlet = $0{\cdot}15\sqrt{2\,g.\,(\text{head per impeller})}$; energy loss in suction pipe, etc. = 6 ft.; barometric pressure is equivalent to 32 ft. of water; vapour pressure is equivalent to 3·5 ft. of water. The value of the cavitation factor σ' can be taken from the expression

$$\sigma' = \frac{4{\cdot}0 \times N_s^{\frac{4}{3}}}{10^6}$$

where N_s represents the nominal specific speed in U.S. units, viz. :

$$N_s = \frac{(\text{r.p.m.})\sqrt{\text{U.S. g.p.m.}}}{(\text{head in feet})^{\frac{3}{4}}}.$$

What would be the limiting static suction lift in these conditions ?

(ii) Now estimate what the static suction lift would be if a 2-stage pump were used for the same duty, the impellers being of the same specific speed as before, but running at a reduced rotational speed. What would be this reduced speed ?

Ans. (i) 3 ft.
(ii) 12·7 ft. : 1760 r.p.m.

(Note that the improvement in the suction capacity of the pump is gained at a high cost ; for the 2-stage pump has two impellers, both of which are *larger* than the original single stage impeller.)

192. For a specified duty—55 tons of water per minute against a head of 7 ft.—it is desired to compare the probable speeds and overall dimensions of a centrifugal pump and a propeller pump. Give an estimate of these values, assuming that the maximum diameter of the centrifugal pump casing is $2\frac{1}{2}$ times the impeller diameter, and that the maximum diameter of the propeller pump casing is $1\frac{1}{4}$ times the propeller diameter.

Ans. 150 r.p.m.
7′ 9″.
400 r.p.m.
2′ 8″.

193. A horizontal engine-driven pump is to be arranged in a siphonic circuit as indicated in Fig. 400 (I) ; the static lift is 12 ft. and the pump axis is to be set 4 ft. above the water surface in the outlet channel. The discharge is 120 tons/min. What would be the recommended maximum speed of the unit, and what type should it be ?

Ans. 330 r.p.m. ; propeller pump.

194. A low-lift pumping plant comprises three screw pumps, each driven by a Diesel engine. At the point of maximum efficiency each unit delivers 35 c.f.s. against a head of 26 ft. when running at 520 r.p.m. ; but the engines have a limited range of speed variation. On a certain occasion the total output of the station is 87 c.f.s., against the constant head of 26 ft. ; and it is desired to know what number of sets should be in operation, all running at the same speed, to ensure the minimum total S.H.P. input. What would this minimum input be ? The pump performance may be deduced from Fig. 405, assuming a maximum efficiency of 79 per cent.

Ans. Either two pumps at 565 r.p.m., or three pumps at 500 r.p.m., would require the same total input, viz. 330 h.p.

195. Compare the general dimensions of two types of boiler feed pump for the following duty : pressure difference to be generated = 200 psi : discharge = 100,000 pounds per hour : water temperature = 120° F.

The two types are: (i) Single-stage centrifugal pump, direct-driven by steam turbine. Its specific speed might be about 18 (foot units). (ii) Direct-acting steam driven pump, making 20 double strokes per minute, having a stroke/bore ratio of 3·0.

Ans. (i) Impeller about 4·8 ins. diam., running at 8000 r.p.m.
(ii) Pump cylinder about 8 in. × 24 in., giving an overall height of pump of about 9 ft.

CHAPTER XVIII.

EXAMPLE 196.

Certain machinery is worked from a weight-loaded accumulator through a pipe 2000 ft. long and 4 ins. diameter. The accumulator has a ram 11 ins. diameter and 12 ft. stroke, loaded with 32 tons; it is supplied with water by a three-throw pump running at 42 r.p.m., the plungers having a diameter of 2 ins. and a stroke of 14 ins. The slip may be estimated at 4 per cent.; the pipe coefficient is 0·008.

If the machinery absorbs 50 W.H.P., calculate the longest period during which it may be operated continuously.

Solution :—

$$\text{Pressure in accumulator} = \frac{32 \times 2240}{\frac{\pi}{4} \times \left(\frac{11}{12}\right)^2} = 108{,}600 \text{ lb./sq. ft.}$$

$$\text{Equivalent head } H = \frac{108600}{62\cdot4} = 1740 \text{ ft. of water.}$$

$$\text{Frictional loss in pipe, } h = \frac{4fl}{d} \cdot \frac{V_p^2}{2g}$$

$$= \frac{4 \times 0\cdot008 \times 2000}{\left(\frac{4}{12}\right)} \cdot \frac{V_p^2}{64\cdot4} = 3V_p^2.$$

$$\text{Also } W = \text{weight of water per sec.} = \frac{\pi}{4} \cdot \left(\frac{4}{12}\right)^2 . V_p \times 62\cdot4 = 5\cdot44\, V_p.$$

Effective head at machines $= H - h = 1740 - 3V_p^2$

Water horse-power at machines

$$= \frac{W(H-h)}{550} = \frac{5\cdot44 . V_p(1740 - 3V_p^2)}{550}$$

$= 50$, whence $V_p = 2\cdot95$ ft./sec., and $W = 16\cdot05$ lb./sec.

Corresponding volume per sec. *leaving* accumulator

$$= Q = \frac{16\cdot05}{62\cdot4} = 0\cdot257 \text{ cusecs.}$$

Now quantity of water *entering* accumulator = discharge of pump

$$= \frac{42}{60} \cdot 0{\cdot}96 \cdot \frac{2^2 \times 14 \times \frac{\pi}{4}}{1728} \times 3 = 0{\cdot}0513 \text{ cusecs.}$$

Hence net loss of water from accumulator $= 0{\cdot}257 - 0{\cdot}0513$
$= 0{\cdot}206$ cusecs.

Therefore time to empty accumulator = time during which machinery may be operated continuously

$$= \frac{\left(\frac{11}{12}\right)^2 \times \frac{\pi}{4} \times 12}{0{\cdot}206}$$

$$= \mathit{38{\cdot}5\ secs.}$$

(*Note.*—The pump W.H.P. is $\frac{0{\cdot}0513 \times 62{\cdot}4 \times 1740}{550} = 10{\cdot}1$. With the help of the accumulator the power delivered to the machines, *for short periods*, is nearly five times as great.

The frictional loss in the pipe $= 3V_p{}^2 = 26{\cdot}1$ ft. Hence efficiency of transmission $= \frac{1740 - 26{\cdot}1}{1740} = 0{\cdot}985$.)

EXAMPLE 197.

Calculate the saving in power that could be effected by interposing a hydraulic slip coupling between the A.C. motor and the centrifugal pump referred to in Example 169.

Solution :—

Here it is assumed that the quantity of oil fed into the coupling (§ 361) is just sufficient to enable the pump to run at its most suitable speed, viz. 805 r.p.m., the motor speed remaining at 980 r.p.m. As shown in Example 169, the power input to the pump is now 53·4 h.p., and since the efficiency of the coupling is $\frac{805}{980} = 0{\cdot}822$ (§ 362), the motor output will be $53{\cdot}4/0{\cdot}822 = 65{\cdot}0$ h.p.

When running direct-coupled to the pump, the output of the A.C. motor was seen to be 82·2 h.p., hence the *saving in power* by using the coupling is $82{\cdot}2 - 65{\cdot}0 =$ *17·2 h.p.*

The loss of $65{\cdot}0 - 53{\cdot}4 = 11{\cdot}6$ h.p. in the coupling itself would be regarded as unobjectionable for the intermittent duty contemplated, provided that means were provided for dissipating the equivalent heat. It will be noted that the coupling is really acting as a not very efficient variable speed-reduction mechanism.

EXAMPLE 198.

By means of a barrage built across a river, a discharge of 5630 cusecs under a head of 23·6 ft. is made available for generating power in a hydro-electric station. For 2 hours each day, however, a peak load of 11,000 K.W. must be met, necessitating the construction of a high-head pumped-storage system. If the average head between the upper and the lower storage basins is 380 ft., calculate their capacity, and state also the output of the high-head turbines.

Solution :—

$$\text{W.H.P. of low-head turbines} = \frac{WH}{550} = \frac{5630 \times 62{\cdot}4 \times 23{\cdot}6}{550}$$
$$= 15{,}100.$$

Assuming an overall efficiency of the station of 80 per cent., the useful output $= 15{,}100 \times 0{\cdot}80 \times 0{\cdot}746 = 9000$ K.W. Hence power to be delivered by high-head turbines = peak load − 9000

$$= 11{,}000 - 9000 = 2000 \text{ K.W.},$$

viz. *output of high-head turbine sets* $= \dfrac{2000}{0{\cdot}746} =$ *2680 h.p.*

Now W.H.P. of high-head turbines $= \dfrac{2680}{0{\cdot}75} = 3580$ (assuming an overall efficiency of 75 per cent.) ; but W.H.P. also

$$= \frac{W_o H_o}{550} = \frac{W_o \times 380}{550}.$$

Equating, we obtain W_o = weight of water per second

$$= \frac{3580 \times 550}{380} = 5180 \text{ lb./sec.}$$

Since this discharge is required continuously for 2 hours per day, the necessary *capacity of the storage basins*

$$= \frac{5180 \times 2 \times 3600}{62{\cdot}4} = \textit{598,000 cu. ft.}$$

(*Note.*—It is, of course, assumed that the *average* load on the main low-head station is less than the maximum output of 9000 K.W., so that at periods of low demand there may be a surplus of energy available for refilling the upper storage basin.)

EXAMPLES *for Solution :—*

199. A three-throw ram pump has rams 3-in. diameter × 16-in. stroke ; it runs at 130 r.p.m., with a slip of 4 per cent. The pump supplies a hydraulic transmission system in which the *mean* pressure is 2500 psi ; there is an air-loaded accumulator having 6 interconnected steel bottles, each 12-in. diameter × 16 ft. high, of which one may contain either air or water, while the others always contain air.

Estimate: (i) The maximum continuous period during which energy at the rate of 1200 h.p. may be drawn from the system; (ii) the highest and the lowest pressure in the system during this period; (iii) the power required to drive the pump.

Ans. (i) 9·6 secs.; (ii) 2730 psi, 2270 psi; (iii) 380 h.p.

200. Estimate the maximum thrust that an electro-hydraulic thrustor could exert, in the following conditions: diameter of impeller = 3·2 ins.; speed of impeller = 2950 r.p.m.; outer diameter of ram = 9·2 ins.; inner diameter of ram = 3·5 ins.; S.G. of oil = 0·89. Ans. About 650 lbs.

201. In an installation of hydraulic cranes, each crane is fed with water at a pressure of 50 kg./sq. cm. and is required to lift a load of 5 metric tons at a speed of 18 metres per minute, through a total height of 12 metres. The system of ropes and pulleys is to give a multiplication of 6. Assuming an efficiency of 60 per cent., estimate the stroke and diameter of the rams.

There are six cranes in the installation, and the working cycle of each one (hoisting and lowering) occupies 90 seconds. If it is assumed that all six might be making the working stroke at the same instant, calculate the minimum capacity of the pump feeding the installation, and the minimum capacity of the accumulator.

Ans. 2 m., 36 cms., 13·3 lit./sec., 670 lit.

202. A vane-type hydraulic motor, having the proportions shown in Fig. 339, § 302, is to develop 12 h.p. at a speed of 1000 r.p.m. when supplied with oil at 750 psi. If the rotor length is equal to the rotor diameter, and if the overall efficiency is 70 per cent., what should be the dimensions of the rotors?

Ans. 2·80 ins. length and diameter. (Note how much smaller this motor is than an electric motor of the same speed and output.)

203. In a testing machine for concrete, etc., the load is applied to the specimen by a ram 9 ins. diameter working in a cylinder to which pressure oil is admitted. The oil is derived from a small pump cylinder into which a plunger is forced by a handwheel and screw: the wheel is 2 ft. 6 ins. diameter and the screw is $\frac{1}{4}$ in. pitch.

Allowing a maximum tangential force on the handwheel of 60 lbs., and assuming an overall efficiency of 20 per cent., determine the necessary diameter of the pump plunger in order to exert a load of 50 tons on the specimen. Ans. 1·81 ins.

204. In a certain factory there are to be 30 hydraulic presses having the following characteristics: stroke, 18 cms.; thrust to be maintained during first half of stroke, 6 tons; thrust during second half of stroke, 25 tons; time taken by working stroke, at uniform speed, 6 seconds; number of strokes per hour per press, 190; efficiency of press, based on pressure *inside cylinder*, 0·8.

Two systems are under consideration, (*a*) to install an electrically-driven central pumping station, with accumulator, which feeds

the presses through a pipe network ; (*b*) to provide an individual motor-driven pump for each press without accumulator, making 30 self-contained units in all. The overall efficiency of the pumping sets,

$$\frac{\text{hydraulic energy output}}{\text{electrical energy input}},$$

may be taken as 76 per cent. for (*a*) and 40 per cent. mean and 56 per cent. maximum for (*b*).

Compare the average and the maximum E.H.P. input to the two systems, in the most unfavourable conditions.

Ans. (*a*) 156 h.p., mean and max. ; (*b*) 185 h.p. mean, 680 h.p. max.

205. A direct hydraulic press has a ram 7·5 in. diameter which is required to exert a thrust of 120 tons. It is supplied with oil—no accumulator being used—by a five-cylinder reciprocating pump running at 1470 r.p.m. The pump plungers have a diameter of 1·000 in. and a stroke of 0·250 in. The bulk modulus of the oil is 250,000 psi.

Estimate the speed at which the press ram would move, and state the S.H.P. input to the pump. Ans. 30·8 ins./min. ; 23 H.P.

206. The following relationship exists between the water level and the capacity of a hydraulic storage reservoir :—

Height of water surface above datum (feet).	*Capacity of reservoir (acre-feet).*
390	102 (reservoir full)
360	42
330	15
300	3
270	0 (reservoir empty)

Water can be pumped up into the reservoir from a low-level lake in which the level remains steady at 85 feet above datum, and it can generate power by flowing back into the lake through a pipe-line and turbines. If the overall efficiency of pipe, turbines and generators is 70 per cent., estimate the time during which the stored water could maintain a continuous output of 1200 E.H.P.

Ans. About 22 hours.

207. A weight-loaded accumulator has a ram 10-in. diameter, and the weight of the total moving load is 98 tons. At a given moment the accumulator is supplying 135 h.p. to a hydraulic machine some distance away : then the control valve of the machine is suddenly closed. Because of the elasticity of the water in the system, the ram continues to descend for a short time after valve closure, and the pressure in the pipe momentarily rises. Estimate what would be the maximum pressure in the present instance, having given that the total volume of water in pipes and accumulator is 8 cu. ft. Disregard friction, and the elasticity of the pipe walls.

Ans. 3240 psi.

CHAPTER XIX.

EXAMPLE 208.

A single column mercury manometer is to be used to indicate the quantity of water in a tank 4·0 m. long and 2·6 m. wide; the diameter of the gauge glass is 8 mm., and of the mercury container 5 cms. How many litres of water in the tank would be represented by 1 cm. on the scale of the manometer?

Solution :—

Inserting appropriate values in the formula of § 372 (iii), we obtain h = fall in surface level in the tank corresponding to a fall of 1 cm. in the mercury column of the manometer

$$= 1\left[13{\cdot}6 + 12{\cdot}6\left(\frac{\frac{\pi}{4}\,.\,8^2}{\frac{\pi}{4}\,.\,50^2}\right)\right] = 13{\cdot}92 \text{ cms.}$$

$$\text{Equivalent volume of water} = \frac{400 \times 260 \times 13{\cdot}92}{1000} = \textit{1450 litres.}$$

EXAMPLE 209.

In determining the rate of flow of water in the laboratory, a measuring tank is used which has a cross-sectional area of 0·460 square metres; the depth of water is measured by a glass-tube gauge in conjunction with a vertical scale graduated in millimetres, and time is measured by a stop-watch. The duration of each experiment, viz. time during which water is collected in the tank, is about one minute.

Estimate the maximum error in gauging the rate of discharge q if q were of the order of (i) 4·5 lit./sec., (ii) 0·5 lit./sec.

Solution :—

The two main observational errors will be :

(*a*) error in observing time and in switching at beginning and end of test, § 382,

(*b*) error in reading glass-tube gauge.

In regard to (*a*), an error of 1/5 sec. at beginning and end, or 0·4 secs. total, might be allowed.

In regard to (*b*), unless the observers are very experienced, it would be well to allow an error of 0·5 mm. for each reading, or 1·0 mm. in all.

Considering now test (i), difference in level during test

$$= \frac{60 \times 4{\cdot}5}{46} = 5{\cdot}87 \text{ dm. or } 58{\cdot}7 \text{ cms.}$$

$$\frac{\text{Estimated discharge}}{\text{True discharge}} = \frac{60 + 0{\cdot}4}{60} \times \frac{58{\cdot}7 + 0{\cdot}1}{58{\cdot}7} = 1{\cdot}008,$$

or percentage error = about *0·8 per cent.*

Similarly in test (ii), difference in level during test = 6·52 cm.,

and $$\frac{\text{Estimated discharge}}{\text{True discharge}} = \frac{60 + 0{\cdot}4}{60} \times \frac{6{\cdot}52 + 0{\cdot}1}{6{\cdot}52} = 1{\cdot}022.$$

$\therefore$ percentage error = about 2·2 per cent.

EXAMPLE 210.

A Venturi meter is to be interposed in a pipe 25 cms. diameter, in which the maximum flow is 130 lit./sec., and the pressure head is 6 m. of water. Calculate the minimum diameter of throat to ensure that a negative head will not be formed in it.

What discharge would be passing through the meter when the double column differential mercury gauge connected to it showed a deflection of 20 cms. ?

Solution :—

The minimum diameter of throat will be that which gives zero pressure head in the throat. The differential head when the maximum flow passes through the meter is thus 6 − 0 = 6 m.

Using appropriate values in the equation

$$Q = C_d A \sqrt{\frac{2gh}{\left(\frac{A}{a}\right)^2 - 1}},$$

we obtain

$$\frac{130}{1000} = 0{\cdot}985 \times \frac{\pi}{4}(0{\cdot}25)^2 \sqrt{\frac{19{\cdot}62 \times 6}{\left(\frac{A}{a}\right)^2 - 1}},$$

from which $\frac{A}{a} = 4{\cdot}15$. But $\frac{A}{a} = \left(\frac{25}{d}\right)^2$, hence d = *throat diameter* = *12·25 cms.*

When the differential head of *mercury* is 20 cms., the differential head of *water* generated in the meter is

$$0{\cdot}20\,(13{\cdot}6 - 1) = 2{\cdot}52 \text{ m}.$$

Now since the discharge varies as the square root of the differential head of water, and since a discharge of 130 lit./sec. produced a differential head of 6·0 m., the discharge corresponding to a head of 2·52 m. is evidently

$$130\sqrt{\frac{2{\cdot}52}{6{\cdot}0}} = \textit{84·2 lit./sec.}$$

EXAMPLE 211.

From the observations plotted in Fig. 464, calculate (i) the discharge in the 8-inch pipe, (ii) the ratio of the velocity at the pipe axis to the mean velocity.

Supposing the observations to have been taken with a "Pitometer" having the characteristics shown in Fig. 450, what would be the reading on the U-tube differential gauge when the orifices were set at the pipe axis ? The exact S.G. of the liquid in the U-tube was determined by disconnecting the gauge and balancing the liquid against unequal columns of water, as shown in the accompanying figure.

Solution :—

(i) By direct scaling from the velocity curves it is found that the mean velocities in the six rings are respectively

$$3{\cdot}75,\ 4{\cdot}19,\ 4{\cdot}40,\ 4{\cdot}50,\ 4{\cdot}54 \text{ and } 4{\cdot}52 \text{ ft./sec.};$$

the mean velocity over the whole pipe section is thus 4·32 ft./sec.

The area of the pipe is $\left(\frac{8}{12}\right)^2 \cdot \frac{\pi}{4} = 0{\cdot}349$ sq. ft.,

hence *discharge* $= 0{\cdot}349 \times 4{\cdot}32 =$ *1·51 cusecs.*

(Actually the effective area is slightly less than 0·349 sq. ft., on account of the area of the Pitometer itself.)

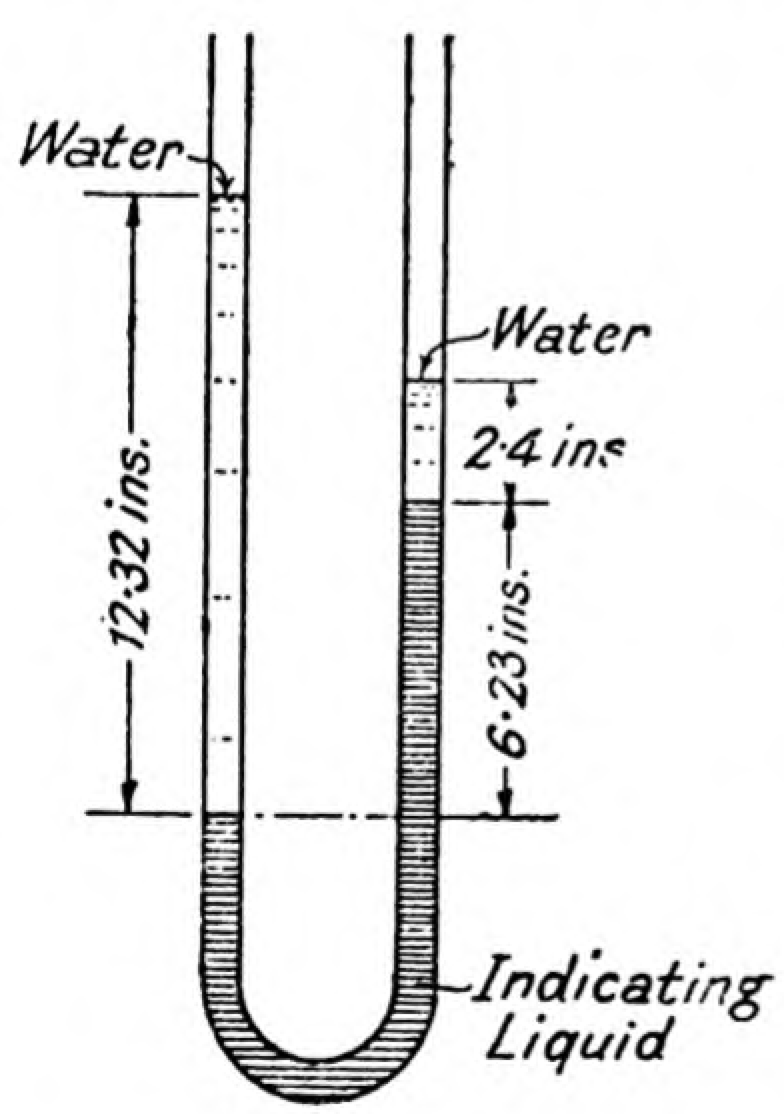

(ii) From Fig. 464 the velocity at the pipe axis is 4·49 ft./sec., hence the ratio

$$\frac{\text{velocity at pipe axis}}{\text{mean velocity}} = \frac{4{\cdot}49}{4{\cdot}32} = \mathit{1{\cdot}04},$$

which is much less than the ratio under normal conditions of velocity distribution.

From the accompanying figure we observe that a column of water 12·32 ins. high in the left-hand limb of the U-tube is balanced by 2·40 ins. of water plus 6·23 ins. of indicating liquid in the right-hand limb. Thus 6·23 ins. of indicating liquid would balance $12{\cdot}32 - 2{\cdot}40 = 9{\cdot}92$ ins. of water : evidently, therefore, the specific gravity of the liquid is $\frac{9{\cdot}92}{6{\cdot}23} = 1{\cdot}59$.

The velocity at the pipe axis being 4·49 ft./sec. (see above), the corresponding Pitometer coefficient C is found from Fig. 450. to be 0·86, and the differential head of water h, obtained from the relationship $4{\cdot}49 = 80{\cdot}6\sqrt{64{\cdot}4\,.\,h}$, is 0·423 ft. Inserting this value in the equation $h = h_2\,(1{\cdot}59 - 1)$, we finally obtain

$$h_2 = \textit{deflection} \text{ or differential head in U-tube}$$
$$= \mathit{0{\cdot}72\ ft.}$$

Examples *for Solution* :—

212. The flow of water to a piece of experimental apparatus in a laboratory is gauged by weirs in parallel as shown in Fig. 456; the rectangular weir is 30·00 cms. wide and 25·00 cms. high, the triangular weir has an angle of 90°; both are sharp-edged. Determine the total discharge when the head over the triangular weir is 14·03 cms. and the head over the rectangular weir is 12·96 cms.

Ans. 37·35 lit./sec.

213. In order to gauge the flow in a 6-inch pipe, a sharp-edged orifice plate is clamped between two adjacent flanges, and upstream and downstream connections are arranged in the plane of the plate. The measured mean diameter of the pipe is 5·98 ins., and of the orifice, 4·00 ins.

Calculate the discharge in the pipe when the differential head of mercury in a double column manometer is 8·35 ins.

Ans. 525 gallons per minute.

214. During a discharge determination by the salt titration method, the salt solution was fed into the stream at the dosing station at the rate of 3·22 lit./sec. The samples taken from the river and from the dosing station were prepared for titration, or "adjusted," as follows :—

(i) Samples of natural river water, taken upstream of the dosing station, were evaporated to 1/350 of their original volume.

(ii) Samples of the injected salt solution were diluted with seventy times their volume of distilled water.

(iii) Samples of dosed river water from the downstream sampling station were evaporated to 1/100 of their original volume.

The respective volumes of silver nitrate solution required to titrate 5 c.c. of each of the three "adjusted" samples were as follows : (i) 9·20 c.c. ; (ii) 14·62 c.c. ; (iii) 12·80 c.c.

Determine the discharge of the stream. Ans. 32·8 cu. m./sec.

215. In a compound manometer which is used for measuring the head of water in an overhead tank, the indicating column does not itself consist of water but of a liquid of specific gravity such that the movement of the indicating column exactly keeps pace with the movement of the water level in the tank, viz. when the water level falls 1 ft., the head of the indicating column also falls 1 ft.

If the area of the glass gauge tube containing the indicating liquid is 0·11 sq. in., and the area of the upper and lower mercury containers is each 12·6 sq. ins., what should be the specific gravity of the indicating liquid?

If the total range of level in the overhead tank is 7 ft., and the highest water level is 45 ft. above the top of the indicating column, what should be the approximate vertical distance between the two mercury containers?

Ans. 0·778.
3 ft. 8 ins.

216. An oil of S.G. 0·915 was found to flow through a U-tube viscometer under the specified conditions in 432 secs.; the time of flow through the same viscometer for a liquid of known viscosity 0·068 poises was 141 secs., this liquid having an S.G. 1·06.

Calculate the viscosity of the oil, (i) in poises, (ii) in foot units, and (iii) in Redwood units.

Ans. (i) 0·180 poises.

(ii) $0{\cdot}000376 \dfrac{\text{lb. sec.}}{\text{sq. ft.}}$

(iii) 84 secs. Redwood.

217. The maximum discharge of a stream is estimated to be about 2·5 cu. m./sec., and the corresponding water depth is 1·0 metre. It is proposed to build across the stream a gauging weir having a crest length of 2 metres. Two types are under consideration, (*a*) a suppressed sharp-edged rectangular weir, (*b*) a wide-crested or flat-topped weir, in which the permissible submergence is 66 per cent. of the working head. The respective coefficients of discharge may be taken as 0·66 and 0·98. What would be the minimum afflux or rise in surface level, at maximum discharge, created by the two weirs?

Ans. (*a*) about 0·84 m., (*b*) about 0·28 m.

BIBLIOGRAPHY

The following brief bibliography may help readers who require more detailed information or alternative methods of treatment. When consulting Engineering Societies' publications, it is worth remembering that the material contained in the Discussions (often printed in a later volume) may be nearly as valuable as the original paper. Titles of periodicals frequently mentioned are abbreviated thus :—

Proc. Inst. C.E. = Proceedings of the Institution of Civil Engineers.
Jour. Inst. C.E. = Journal of the Institution of Civil Engineers.
Proc. I. Mech. E. = Proceedings of the Institution of Mechanical Engineers.
Proc. A.S. Civ. E. = Proceedings of the American Society of Civil Engineers.
Trans. A.S.M.E. = Transactions of the American Society of Mechanical Engineers.
Engg. = *Engineering* (London).
The Engr. = *The Engineer* (London).
Z.V.D.I. = Zeitschrift des Vereines Deutscher Ingenieure.

PART I

Chapter I

§ No.

3 (1) *The Physics of Solids and Fluids*, by Ewald, Poschl, and Prandtl (McGraw-Hill).

5 (2) *Some Problems of Fluids for Hydraulic Power Transmission*, by A. E. Bingham (Proc. I.Mech.E., Vol. 165, 1951, p. 254).

5 (3) *New Method for Bulk Modulus Determination*, by S. Logan Kerr, etc. (Trans. A.S.M.E., Vol. 72, 1950, p. 1143).

9 (4) *Viscosities and Densities of Lubricating Oils*, by C. M. Murphy, etc. (Trans. A.S.M.E., Vol. 71, 1949, p. 561).

9 (5) *The Effect of Pressure on the Viscosity of Liquids and especially Oils* (The British Hydromechanics Research Association, Technical Note 16, September, 1949).

10 (6) *Evaporation from a free water surface*, by G. H. Hiscox (Proc. A.S. Civ. E., Vol. 70, Oct., 1944, p. 1297). See also *Report on Standard Methods of Measurement of Evaporation* (Jour. Inst. Water Engrs., Vol. II, 1948, p. 257).

11 (7) *Water Analysis*, by J. Alfred Wanklyn (Kegan Paul, Trench).

11 (8) *Entrainment of Air in Flowing Water*; A Symposium (Proc. A.S. Civ. E., Vol. 68, Sept., 1942, p. 1100).

11 (9) *Deformation and Flow;* An Elementary Introduction to Theoretical Rheology, by Marcus Reiner (H. K. Lewis & Co.).

CHAPTER II

§ No.

21 [10] *Stresses in Tubes due to Internal Pressure*, by J. S. Blair (Engg., Vol. 170, Sept., 1950, p. 218).

22 [11] *Bending Moments in the Walls of Rectangular Tanks*, by Dana Young (Proc. A.S. Civ. E., Vol. 67, Nov., 1941, p. 1683).

38 [12] *A Textbook of Fluid Mechanics for Engineering Students*, by J. R. D. Francis (Edward Arnold).

CHAPTER III

§ No.

39 [13] *The Turbulent Spreading of a Water Jet*, by A. M. Binnie (Engg., Vol. 153, 1942, p. 503).

39 [14] *Diffusion of Submerged Jets*, by M. L. Albertson, etc. (Proc. A.S.Civ.E., Vol. 74, 1948, p. 1571).

40 [15] *On Dimensional Analysis and the Presentation of Data in Fluid-flow Problems*, by E. R. Van Driest (Trans. A.S.M.E., Vol. 68, 1946, p. A34).

CHAPTER IV

§ No.

42 [16] *Hydraulics*, by F. C. Lea (Edward Arnold).

43 [17] *Ausflussmessungen mit scharfkantigen Blenden*, by K. Jaroschek (Z.V.D.I., Vol. 83, 11th Feb., 1939, p. 170).

48 [18] *The Use of a Vertical Pipe as an Overflow for a Large Tank*, by A. M. Binnie (Proc. Roy. Soc. A., Vol. 168, 1938, p, 219).

51 [19] *Scale Models in Hydraulic Engineering*, by Jack Allen (Longmans, Green & Co.).

58 [20] *Tests of Broad-crested Weirs*, J. G. Woodburn (Proc. A.S. Civ. E., Vol. 56, 1930, p. 1583).

59 [21] *Submerged Thin-plate Weirs*, by F. T. Mavis (Engineering News-Record, New York, 7th July, 1949, p. 65).

60 [22] *Construction of the Flow Net for Hydraulic Design*, by H. Alden Foster (Proc. A. S. Civ. E., Vol. 70, May, 1944, p. 647).

CHAPTER V

§ No.

62 [23] *The Mechanism of Energy Loss in Fluid Friction*, by B. A. Bakhmeteff and William Allan (Proc. A.S. Civ. E., Vol. 71, 1945, p. 129).

63 [24] *On the two Manners of Motion in Water*, by Osborne Reynolds (Proc. Royal Institution, 1884).

69 [25] *Streamline Flow through Curved Pipes*, C. M. White (Proc. Roy, Soc. A., Vol. 123, 1929).

69 [26] *The Resistance of the Flow of Water along Smooth Rectangular Passages, etc.*, J. Allen and N. D. Grunberg (Phil. Mag., Vol. XXIII, Mar., 1937, p. 490).

§ No.

69 [27] *An Experimental Study of the Flow of Water in Pipes of Rectangular Section*, S. J. Davies and C. M. White (Proc. Roy. Soc., Vol. CXIX, 1928, p. 92).

70 [28] *Strömungsgesetze in rauhen Rohren*, by J. Nikuradse (Z.V.D.I. Forschungsheft, 361, 1933). For translation, see N.A.C.A. Technical Memorandum 1292, Nov., 1950.

71 [29] *Fluid Mechanics for Hydraulic Engineers*, by Hunter Rouse (McGraw-Hill).

72 [30] *An Examination of Turbulent Flow with an Ultramicroscope*, A. Fage and H. C. H. Townend (Proc. Roy. Soc. A., Vol. 135, 1932).

73 [31] *On the Static Pressure in Fully-developed Turbulent Flow*, A. Fage (Proc. Roy. Soc., A., Vol. 155, p. 576).

75 [32] *The Mechanics of Turbulent Flow*, by B. A. Bakhmeteff (Princeton University).

78 [33] *On Transition from Laminar to Turbulent Flow in the Boundary Layer*, by A. Fage and J. H. Preston (*Proc. Roy. Soc. A*, No. 973, 12th June, 1941, Vol. 178, p. 201).

79 [34] *Roughness Factors in Fluid Motion through Cylindrical Pipes and through Channels*, by Jack Allen (Jour. Inst. C.E., April, 1943, p. 91).

81 [35] *Friction losses in Turbulent pipe-flow*, by L. E. Prosser, etc. (Proc. I. Mech. E., Vol. 165, 1951, p. 88).

82 [36] *Turbulent Flow in Pipes, etc.*, C. F. Colebrook (Jour. Inst. C.E., Feb., 1939, p. 133).

87 [37] *Conversion of Kinetic to Potential Energy in Flow Expansions*, by A. A. Kalinske (Proc. A.S. Civ. E., Vol. 70, Dec., 1944, p. 1545).

87 [38] *The Loss of Head in Pipe Fittings*, by S. T. Bonnington (The British Hydromechanics Research Association, Publication No. TN 403, 1950).

88 [39] *The Use of Cascades at Sharp Elbows in Water Pipes*, by A. M. Binnie, etc. (The Engr., Vol. 190, 1950, p. 232).

89 [40] *Technische Stromungslehre*, by Bruno Eck (Springer-Verlag, Berlin).

95 [41] *Conformity between Model and Prototype—a Symposium* (Proc. A.S. Civ. E., Vol. 68, Oct., 1942, p. 1267, and succeeding volumes).

96 [42] *Micromeritics; the technology of fine particles*, by J. M. Dallavalle (Pitman Publishing Corporation, New York).

97 [43] *Flow through Granular Media*, B. A. Bakhmeteff and N. V. Feodoroff (Trans. A.S.M.E., Vol. 59, 1937, p. A97).

97 [44] *An Investigation into the Laws of Flow of fluids through Beds of Granular Material*, by H. E. Rose (Proc. I.Mech.E., Vol. 153, 1945, pp. 141 and 154) (*see also* Vol. 160, 1949, p. 493).

98 [45] *Flow through Granular Media*, L. P. Hatch (Trans. A.S.M.E., Sept., 1940, p. A109).

CHAPTER VI

§ No.

99 [46] *Historic Development of the Theory of Flow in Canals and Rivers*, by S. Leliavsky (The Engr., Vol. 191, 1951, pp. 466, etc.).

100, 102 [47] *Streamline and Turbulent Flow in Open Channels*, J. Allen (Phil. Mag., Vol. XVII, June, 1934, p. 1081).

100 [48] *The Hydraulics of Steady Flow in Open Channels*, by S. M. Woodward and C. J. Posey (John Wiley & Sons).

102 [49] *Flow in a Channel of Definite Roughness*, by Ralph W. Powell (Proc. A.S. Civ. E., Vol. 70, Dec., 1944, p. 1521).

103 [50] *Velocity Distribution in Open Channels*, by V. A. Vanoni (Civil Engineering, New York, June, 1941, Vol. 11, p. 356).

112 [51] *Experimental Investigation of Turbulence Diffusion*, by E. R. Van Driest (Trans. A.S.M.E., Vol. 67, 1945, p. A91).

CHAPTER VII

§ No.

118 [52] *Final Report of Joint Surge Conference* (Middle East Pipe-Lines, Ltd., New York).

121 [53] *Umlenkung eines freien Flussigskeits strahles an einer ebenen Platte*, W. Schach (Z.V.D.I., Vol. 80, 11th Jan., 1936, p. 57).

126 [54] See ref. (33), § 78.

127 [55] *Modern Developments in Fluid Dynamics*, edited by G. Goldstein (Clarendon Press, Oxford).

127 [56] *Dynamics of Real Fluids*, by E. G. Richardson (Edward Arnold & Co.). See also *Essentials of Fluid Dynamics*, by L. Prandtl (Blackie & Son).

131 [57] *Cavitation Characteristics and Infinite Aspect-ratio Characteristics of a Hydrofoil section*, by J. W. Daily (Trans. A.S.M.E., Vol. 71, 1949, p. 267).

131 [58] *Hydrodynamic Design of 48 in. Water Tunnel*, by D. Ross, etc. (Engg., Vol. 166, 1948, p. 68).

134 [59] *Cavitation Mechanics and its Relation to the Design of Hydraulic Equipment*, by R. T. Knapp (Proc. I.Mech.E., Vol. 166, 1952, p. 150).

134 [60] *Theory of stress due to collapse of Vapour bubbles in a Liquid*, by R. S. Silver (Engg., Vol. 154, 1942, p. 501).

134 [61] *Cavitation in Hydraulic Structures: a Symposium* (Proc. A.S. Civ. E., Vol. 71, 1945, p. 999; also Vols. 72 and 73).

135 [62] *Cavitation-free Inlets and Contractions*, by Hunter Rouse and M. M. Hasan (Mechanical Engineering, March, 1949, p. 213).

137 [63] *The Hydraulic Jump in Sloping Channels*, by C. E. Kindsvater (Proc. A.S. Civ. E., Vol. 68, Nov., 1942, p. 1473).

BIBLIOGRAPHY

CHAPTER VIII

§ No.

141 (64) *Flow of Water Around Bends in Pipes*, D. L. Yarnell and F. A. Nagler (Proc. A.S. Civ. E., Vol. 60, Aug., 1934, p. 792).

145 (65) *Fluid Mechanics of Turbo-Machinery*, by G. F. Wislicenus (McGraw-Hill Book Co.).

148 (66) *Hydraulics and its Applications*, A. H. Gibson (Constable).

148 (67) *Resistance to Rotation of Disks in Liquids*, by A. H. Church and S. A. Gertz (A.S.M.E. paper, No. 49, A 103, 27th Nov., 1949).

PART II

CHAPTER IX

§ No.

149 (68) *The Colorado River Aqueduct* (The Engr., Vol. CLXI, 1936, p. 263). See also *Engineering News-Record*, Vol. 121, 24th Nov., 1938, p. 637.

150 (69) *Stresses in a Restrained Pipe-line*, by A. J. S. Pippard (Jour. I.C.E., Jan., 1951, p. 170).

150 (70) *The Optimum Diameter of a Pipe-line* (Le Genie Civil, Paris, 10th Oct., 1948, p. 367).

151 (71) *Prestressed Concrete Pipes*, by G. A. P. Ooykaas (Jour. Inst. Water Engineers, Vol. 6, 1952, p. 85).

152 (72) *Vyrnwy Aqueduct—Fourth Instalment Pipe-line*, by W. F. White (Jour. Inst. Water Engineers, Vol. IV, 1950, p. 13).

152 (73) *The Laying of a Steel Pipe-line*, by C. A. Serpell (Jour. Inst. Water Engineers, Vol. III, 1949, p. 17).

152 (74) *Joints for Pipe Lines* (Glenfield Gazette, No. 181, Jan.-Mar., 1941, p. 13).

153 (75) *Pipe Resistance*, by T. E. Beacham (E. & F. N. Spon, Ltd.).

155 (76) *Friction Factors for Pipe Flow*, by L. F. Moody (Trans. A.S.M.E., Vol. 66, 1944, p. 671).

155 (77) *Manual of British Water-Supply Practice* (The Institution of Water Engineers : W. Heffer & Sons, Ltd., Cambridge).

157 (78) *Hydraulic Flow Reviewed*, A. A. Barnes (E. & F. N. Spon).

157 (79) *New Formulæ for Water Flow in Pipes*, by J. S. Blair (Proc. I.Mech.E., Vol. 165, 1951, p. 74).

159 (80) *The Institution of Civil Engineers Velocity Formulæ Commttiee* (Jour. I.C.E., Dec., 1948, p. 173).

159 (81) *Considerations on Flow in Large Pipes, etc.*, James Williamson (Jour. Inst. C.E., April, 1939, p. 451).

159 (82) *Friction losses in the High-Pressure Pipe-line of the Lucendro Power Station, Switzerland* (Sulzer Technical Review, No. 4. 1949, p. 1).

§ No.

159 (83) *Friction losses in a large tunnel*, by G. H. Hickox (Proc. A.S. Civ. E., Vol. 73, 1947, p. 451).

159 (84) *The Flow of Water in Unlined, Lined and Partly Lined Rock Tunnels*, by C. F. Colebrook. (Proc. Inst. C. E., Vol. 11, Sept., 1958, p. 103).

160 (85) *Crude-oil flow Characteristics experienced in Large-diameter Lines*, by L. E. Anderson (Trans. A.S.M.E., Vol. 72, 1950, p. 659); see also *Large Pipeline Projects*, by A. C. Hartley (The Chartered Mechanical Engineer, March, 1959, p. 101).

160 (86) *Pipe-line flow of Solids in Suspension*, by W. E. Wilson (Proc. A.S. Civ. E., Vol. 67, Oct. 1941, p. 1434).

160 (87) *Turbulent Transfer Mechanism and Suspended Sediment in Closed Channels*, by Hassan M. Ismail (Proc. A.S. Civ. E., Vol. 77, Feb. 1951).

160 (88) *Hydraulic Transport of Solid Material in Pipes*, by R. C. Worster and D. F. Denny (Proc. I.Mech.E., Vol. 169, 1955, No. 32, p. 563).

161 (89) *The Reduction of Carrying Capacity of Pipes with Age*, C. F. Colebrook and C. M. White (Jour. Inst. C.E., Nov., 1937, p. 99).

161 (90) *The Relining of Water Mains in Situ*, by Alan Atkinson (Jour. Inst. Water Engineers, Vol. IV, 1950, p. 293).

165 (91) *Graphical Solution of Flow Problem in Pipe Networks*, by R. K. Harding and G. F. Mort (Jour. Inst. Water Engrs., Vol. III, 1949, p. 538).

166 (92) *The Design and operation of a True Siphon for a Sewerage System*, by D. J. McCulloch (Jour. Inst. C.E., Feb., 1945,p. 197).

171 (93) *Control of Flow by Gates and Valves*, by H. D. Morgan (Proc. Inst. C. E., July, 1957, Vol. 7, p. 537). See also *Some Aspects of Valve Engineering in Water Supply*, by P. L. Boucher (Journal Inst. Water Engrs., Vol. 6, Oct., 1952.)

175 (94) *Water-Hammer Effects in Power Conduits: accidents due to water-hammer*, by C. Jaeger (Jour. Inst. C.E., Feb., 1948, p. 334).

176 (95) *Water-Hammer in Pipes, etc.*, R. W. Angus (Proc. I. Mech. E., Vol. 136, 1937, p. 245). See also *Waterhammer Analysis*, by J. Parmakian (Prentice-Hall, Inc., New York).

178 (96) *Mechanical Engineering in the Oil Industry*, by A. C. Hartley (Proc. I. Mech. E., Vol. 157, 1947, p. 325).

178 (97) *The Trans-Arabian Pipe-line "Tapline"*, by V. S. Swaminathan (The Engr., Vol. 193, 1952, p. 556).

CHAPTER X

§ No.

179 (98) *Hydraulics of Open Channels*, by B. A. Bakhmeteff (McGraw Hill).

179 (99) *Use of Canal Linings in American Irrigation Schemes* (The Engr., Vol. 195, 1953, p. 199).

§ No.

180 (100) *High-Velocity Flow in Open Channels: a Symposium* (Proc. A.S. Civ. E., Vol. 75, 1949, p. 971). See also *Flow round Bends in Stable Channels*, by C. A. Mockmore (Proc. A.S. Civ. E., Vol. 69, 1943, p. 335).

181 (101) *Determination of Kutter's N for Sewers partly filled*, by C. Frank Johnson (Proc. A.S. Civ. E., Vol. 69, 1943, p. 187).

182 (102) *Stream and Channel Flow*, by E. E. Morgan (Chapman & Hall, Ltd.).

182 (103) *Alignment Charts for the Design of Sewers and other Open Channels*, by Frank Law (Jour. Inst. C.E., Nov., 1942, p. 56).

185 (104) *Integrating the Equation of Non-Uniform Flow*, by M. R. Von Seggern (Proc. A.S. Civ. E., Vol. 75, 1949, p. 105).

187 (105) *A Handbook of Applied Hydraulics*, by C. V. Davis (McGraw Hill Co.). See also *The Claerwen Dam*, by H. D. Morgan, etc. (Proc. Inst. C.E., Vol. 2, May, 1953, p. 249).

188 (106) *Experiments on Spillway Discharge of the Keokuk Dam*, F. A. Nagler and A. Davis (Proc. A.S. Civ. E., Vol. 55, 1929, p. 305).

189 (107) *Submerged Weir Discharge Studies*, by J. R. Villemonte (Eng. News-Record, 25th Dec., 1947, p. 866).

190 (108) *Model Tests of the Bellmouth Spillway and Outfall Fassidiri Project*, by E. S. Crump (Proc., Inst. C.E., Vol. 1, 1952, Part II, p. 573).

190 (109) *The Gorge Dam*, W. J. E. Binnie and H. J. F. Gourley (Jour. Inst. C.E., Mar., 1939, p. 179).

192 (110) *The Flow of Water under a Sluice Gate*, by A. M. Binnie (Quart. Journ. Mech. and Applied Math., Vol. 5, part 4 (1952)).

192 (111) *The Flow of Water through Groups of Sluices*, H. Addison (The Inst. C.E. Selected Engineering Papers, No. 105, 1931).

194 (112) *Further Experiments on the Discharge of Models of Sluices*, H. E. Hurst (Government Press, Cairo).

194 (113) *Supplementary Notes on Flow through Model Sluices*, H. Addison (Jour. Inst. C.E., Feb., 1938, p. 53).

195 (114) *Modern Types of Movable Dams* (The Engr., Vol. CLX, Nov., 1935, p. 471).

195 (115) *Discharge coefficients of Taintor Gates*, by R. E. Horton. (Eng. News Record, Vol. 112, Jan., 1934, p. 10).

197 (116) *Irrigation Principles and Practice*, by Orson W. Israelson (John Wiley: Chapman & Hall).

197 (117) *Irrigation and Hydraulic Design*, by S. Leliavsky (Chapman & Hall).

199 (118) *Design of Channel Expansions*, by Hunter Rouse, etc. (Proc. A.S. Civ. E., Vol. 75, 1949, p. 1369).

200 (119) *Formulæ for the Transportation of Bed Load*, by H. A. Einstein (Proc. A.S. Civ. E., Vol. 67, 1941, p. 351).

200 (120) *The Suspension of Solids in a Turbulent Stream*, E. G. Richardson (Proc. Roy. Soc. A., Vol. CLXII, 1937, p. 583).

§ No.

201 (121) *Equilibrium of Grains on the Bed of a Stream*, by C. M. White (Proc. Roy. Soc., Vol. 174A, 1940, p. 322).

201 (122) *An Investigation of the Stability of Bed Material in a Stream*, by Jack Allen (Jour. Inst. C.E., Mar., 1942, p. 1).

201 (123) *Flow in Alluvial Channels with Sandy Mobile Beds*, by Gerald Lacey (Proc. Inst. C. E., Feb., 1958, Vol. 9, p. 145).

201 (124) *Silt Transportation and its relation to Regime Channel Sections*, by W. M. Griffith (Jour. Inst. C.E., April, 1944, p. 107).

201 (125) *The Silting of Impounding Reservoirs*, by T. S. R. Winter (Jour. Inst. C.E., Dec., 1950, p. 65).

201 (126) *Future of Lake Mead and Elephant Butte Reservoir*, by J. C. Stevens (Proc. A.S. Civ. E., Vol. 71, 1945, p. 603, also Discussion in Vol. 72).

201 (127) *The Protection of Dams, Weirs, and Sluices against Scour*, R. V. Burns and C. M. White (Jour. Inst. C.E., Nov., 1938, p. 23). See also *Irrigation and Hydraulic Design*, by S. Leliavsky (Chapman & Hall, Ltd.).

202 (128) *The Emerson Barrage*, F. F. Haigh (Jour. Inst. C.E., Dec., 1941, p. 107).

202 (129) *The Effect of the Form of Cross-section on the Capacity and Cost of Trunk Sewers*, T. Donkin (Jour. Inst. C.E., Dec., 1937, p. 261).

Chapter XI

§ No.

204 (130) *Flood Estimation and Control*, by B. D. Richards (Chapman & Hall).

207 (131) *Multiple-Purpose Reservoirs: A Symposium* (Proc. A.S. Civ. E., Vol. 75, 1949, p. 287).

207 (132) *Methods of using Long-term Storage in Reservoirs*, by H. E. Hurst (Proc. Inst. C. E., Sept., 1956, Vol. 5, p. 519).

208 (133) *Drawdown Test to determine Effective Radius of Artesian Well*, by C. E. Jacob (Proc. A.S. Civ. E., Vol. 72, 1946, p. 629).

209 (134) *Water Supply in the Middle East Campaigns*, by H. Addison and F. W. Shotton (Water and Water Engineering, Vol. 49, 1946, p. 427).

210 (135) *The Movement of Water in the Middle and Lower Chalk of the River Dour Catchment*, by D. H. B. Reynolds (Jour. Inst. C.E., Dec., 1947, p. 73).

212 (136) *Hydraulic Laboratory Practice* (The American Society of Mechanical Engineers).

214 (137) *Siphon Spillways*, A. H. Naylor (Edward Arnold).

214 (138) *Determination of Pressures within a Siphon Spillway*, by I. M. Nelidov (Proc. A.S. Civ. E., Vol. 71, 1945, p. 297).

217 (139) *Water Supplies to the Smaller Provincial Towns of Egypt*, R. H. L. Pennell and H. Addison (Proc. Inst. C.E., Vol. 219, 1924-25, p. 73).

BIBLIOGRAPHY

Chapter XII

§ No.

219 (140) *Strömungsmaschinen*, by C. Pfleiderer (Springer-Verlag).

222 (141) *Hydraulic Seals*, by T. E. Beacham and F. H. Towler (Proc. I. Mech. E., Vol. 160, 1949, p. 532).

223 (142) *The Friction of Flexible Packings*, by D. F. Denny (Proc. I. Mech. E., Vol. 163, 1950, p. 98); see also *Packed Glands for High Pressures; an analysis of Fundamentals*, by J. L. Thomson (Proc. I. Mech. E., Vol. 172, 1958, p. 471).

223 (143) *The Mechanical Seal: Its Construction, Application and Utility*, by C. E. Schnitz (Trans. A.S.M.E., Vol. 71, 1949, p. 635).

Chapter XIII

§ No.

225 (144) *A Century of Water Turbines*, by J. Moser (Escher-Wyss News, Vol. 15/16, 1942-43, p. 101). See also *Origins of Water Power*, by Paul N. Wilson (Water Power, Aug., 1952, Vol. 3, p. 308).

228 (145) *Problems Encountered in the Design and Operation of Impulse Turbines*, Roy S. Quick (Trans. A.S.M.E., Vol. 62, Jan., 1940, p. 15).

228 (146) *Efficiency Analysis of Pelton Wheels*, by Robert Lowy (Trans. A.S.M.E., Vol. 66, 1944, p. 527).

228 (147) *Investigation of the Number of Buckets on the Performance of a Pelton Wheel*, by H. F. Taygun (Bulletin of the Hydraulic Institute of the Federal Technical High School, Zurich, No. 1, 1946).

229 (148) *Hydro-Electric Power—Design and Operation of Power House and Equipment*, by E. B. Strowger (Fourth World Power Conference, London, 1950, Section H/2, Paper No. 2).

229 (149) *Mechanical Features of the Glanville Impulse Turbine*, by Arnold Pfau (Trans. A.S.M.E., Vol. 66, 1944, p. 513).

232 (150) *The Lochaber Water Power Scheme* (The Engr., Vol. CLXI, 1936, p. 507).

240 (151) *Nantihala Turbine*, by J. P. Crowdon, etc. (Trans. A.S.M.E., Vol. 68, 1946, p. 687).

242 (152) *Flow Characteristics in Elbow Draft Tubes*, C. A. Mockmore (Proc. A.S. Civ. E., Vol. 63, 1937, p. 251).

244 (153) *Water Turbine Governors*, by N. G. Dennis (Proc. I. Mech. E., (B), 1952–53. Vol. 1B, No. 9, p. 379). See also *Water Turbine Governors and the Stability of Hydro-Electric Plant*, by N. G. Dennis (Water Power, Vol. 5, Feb. to May, 1950).

248 (154) *Laminar Flow Aerofoil Theory and the Application of Analogous Methods to the Design of Kaplan Turbine Blades*, by S. P. Hutton (Proc. I. Mech. E., 1950, Vol. 163, p. 81).

249 (155) *The Development of the Kaplan Turbine*, J. R. Finniecombe (Engg., Vol. 150, Nov., 1940, p. 381).

250 (156) *Kaplan Turbine Blading*, by M. Nechleba (Fourth World Power Conference, London, 1950, Sect. H/3, Paper No. 3).

§ No.

251 (157) *Hydro-Electric Engineering Practice*, edited by J. Guthrie Brown (Blackie).

252 (158) *North of Scotland Hydro-Electric Schemes* (The Engr., Vol. 190, 1950, p. 28 *et seq.*). See also *Civil Engineering Aspects of Hydro-Electric Development in Scotland*, by A. A. Fulton (Proc. Inst. C. E., May, 1952, p. 248).

252 (159) *Hydro-Electric Engineering*, by G. Gerard (Sir Isaac Pitman).

252 (160) *Underground Hydro-Electric Plants*, by J. D. Lewin (Engg., Vol. 169, 1950, p. 225).

252 (161) *Present trends in the design of Pressure Tunnels and Shafts for Underground Hydro-Electric Power Stations*, by Charles Jaeger. (Proc. Inst. C. E., March, 1955, Vol. 4, p. 116).

252 (162) *A New Swiss Low-Head Station* (Water Power, Vol. 3, No. 3, Feb., 1951, p. 45).

253 (163) *Water-Hammer Problems in Connection with the Design of Hydro-Electric Plants*, by E. B. Strowger (Trans. A.S.M.E., Vol. 67, 1945, p. 377).

254 (164) *Technische Hydraulik*, by C. Jaeger (Verlag Birkhauser, Basel).

254 (165) *Surge Tanks*, J. D. Watson (The Engr., Vol. CLXIV, 1937, p. 731).

255 (166) *Oscillations in Closed Surge Tanks*, by A. M. Binnie (Trans. A.S.M.E., 1943, Vol. 65, p. A183).

256 (167) *Galloway Hydro-Electric Development* (Jour. Inst. C.E., April, 1938, p. 323).

256 (168) *The Development of the River Rhone* (The Engr., Vol. 190, 1950, p. 549).

257 (169) *Design Developments—Structures of the Tennessee Valley Authority: A Symposium: Design of Hydro-Electric Stations* (Proc. A.S. Civ. E., Vol. 71, 1945, p. 1209).

258 (170) *Tidal Power: Its Development and Utilisation*, by B. D. Richards (Jour. Inst. C. E., April, 1948, p. 104).

258 (171) *French Tidal Projects* (Water Power, Vol. 2, No. 1, 1950, p. 14).

258 (172) *Report on the Severn Barrage Scheme* (Ministry of Fuel and Power, 1944).

CHAPTER XIV

§ No.

267 (173) *Characteristic Design Factors for Water Turbines*, J. R. Finniecombe (Engg., Vol. 152, July, 1941, p. 21).

268 (174) *The Hydraulic Turbine in Evolation*, by Pierre Danel (see The Chartered Mechanical Engineer, Dec., 1958, p. 460, also Proc. I. Mech. E., 1959).

268 (175) *Francis or Pelton Wheels* (Schweizerisches Bauzeitung, 68, No. 32, 1950, p. 429). See also *Pelton or Francis Turbines for High Heads*, by R. C. Collet (Water Power, Vol. 3, No. 3, Feb., 1951, p. 63).

§ No.

269 (176) *A Better Method of Representing and Studying Water-Turbine Performance*, by R. R. Sutherland (Trans. A.S.M.E., Vol. 68, 1946, p. 675).

278 (177) *Le Replacement des Essais de Reception, etc.*, by E. Seitz and C. Keller (Fourth World Power Conference, London, 1950, Sect. H/3, Paper No. 2).

279 (178) *Acceptance Tests of Water Turbines*, by H. Gerber (Escher Wyss News, Vol. 17/18, 1944-45, p. 23).

279 (179) *The Increase in Efficiency of Reaction Turbines*, by E. Muhlemann (Schweizerisches Bauzeitung, 66, No. 24, 1948, p. 331).

280 (180) *Cavitation of Hydraulic Turbine Runners*, R. E. B. Sharp (Trans. A.S.M.E., Vol. 62, Oct., 1940, p. 567).

281 (181) See ref. (154), § 248.

282 (182) *The Importance of Cavitation in the Development of High-pressure Kaplan Turbine Blading*, by J. Osterwalder (Escher Wyss News, Vol. 19/20, 1946-47, p. 17).

283 (183) *Fundamental Economics in Hydro-Electric Design*, by C. M. Roberts (Jour. Inst. C.E., April, 1951, p. 115).

283 (184) *The Control of Hydro-Electric Plant*, by A. C. H. Frost and W. Brittlebank (The Engr., Vol. 190, 1950, p. 569).

Chapter XV

§ No.

284 (185) *Pumps*, F. A. Kristal and F. A. Annett (McGraw-Hill).

284 (186) *Pumping Machinery*, by H. R. Lupton (Jour. Inst. C.E., Feb., 1949, p. 291); see also *Modern Trends in Waterworks Pumping Machinery*, by T. Irvine Hudson (Proc. I. Mech. E., 1957, Vol. 171, p. 647).

284 (187) *Hydraulic Machinery: Positive-Displacement Pumps, etc.*, by H. R. Lupton, etc. (Proc. I. Mech. E., Vol. 157, 1947, p. 330).

287 (188) *Experiments on an Archimedean Screw*, H. Addison (The Inst. C.E., Selected Engineering Papers, No. 75, 1929).

287 (189) *Discharge Tests of an Archimedean Screw*, by A. C. Donaldson (Proc. I. Mech. E., Vol. 157, 1947, p. 93).

290 (190) *Pressure Surges and Vibration in Reciprocating Pump Piping*, by J. W. Squire (Trans. A.S.M.E., Vol. 71, 1949, p. 317).

290 (191) *Pressure Calculations for Oil Engine Fuel-Injection Systems*, E. Giffen and A. W. Rowe (Proc. I. Mech. E., Vol. 141, 1939, p. 519).

294 (192) *Large-capacity High-Pressure Pumping Plant*, by F. H. Roberts (Proc. I. Mech. E., Vol. 155, 1946, p. 453).

294 (193) *Oil-Pipe Line Pumps for Iraq* (The Engr., Vol. 187, 1949, p. 266).

294 (194) *Recent Developments in High-Speed Reciprocating Pumps*, F. H. Towler and J. M. Towler (The Engr., Vol. CLXIV, 1937, p. 711).

294 (195) *A Concrete Pump* (The Engr., Vol. 187, 1949, p. 556).

296 (196) *Problems in Modern Deep-Well Pumping*, C. J. Coberly (Trans. A.S.M.E., Vol. 60, 1938, p. 561).

§ No.

298 (197) *Improvements in Reciprocating Plunger Pumps* (Brit. Pat. 650,060).

298 (198) *Regulating the Delivery of Reciprocating Pumps* (Sulzer Technical Review, 1940, No. 4, p. 14).

299 (199) *A History of Rotary Engines and Pumps* (The Engr., Vol. CLXVII, 1939).

299 (200) *Displacement Pumps and Motors,* by R. Hadekel (Sir Isaac Pitman).

301 (201) *Variable-stroke Pumps for Power Transmission—Some Design Considerations,* by T. E. Beacham. (Conference on Hydraulic Servo-Mechanisms, p. 17; The Institution of Mechanical Engineers, 1953).

303 (202) *High Pressure Gear Pumps,* by T. E. Beacham (Proc. I. Mech. E., Vol. 155, 1946, p. 417).

305 (203) *Positive-Displacement Pumps and Fluid Motors,* by Warren E. Wilson (Sir Isaac Pitman).

305 (204) *Some Characteristics of Rotary Pumps in Aviation Service,* by R. J. S. Pigott (Trans. A.S.M.E., Vol. 66, 1944, p. 615).

307 (205) *An Analytical and Experimental Study of the Hydraulic Ram,* W. M. Lansford and W. G. Dugan (University of Illinois Engineering Experiment Station, No. 326, 1941).

309 (206) *The Automatic Hydraulic Ram,* by J. Krol (Proc. I. Mech. E., Vol. 165, 1951, p. 53).

309 (207) *Hydraulic Machinery,* D. W. Mead (McGraw-Hill).

310 (208) *The Water Jet Pump,* J. E. Gosline and M. P. O'Brien (University of California Press, 1934).

311 (209) British Patent 492,474.

311 (210) British Patent 580,792.

311 (211) See ref. (187), § 284.

CHAPTER XVI

§ No.

313 (212) *Centrifugal and other Rotodynamic Pumps,* by Herbert Addison (Chapman & Hall, Ltd.).

315 (213) See ref. (65), § 145.

318 (214) *Centrifugal and Axial-Flow Pumps,* by A. J. Stepanoff (John Wiley & Sons, Inc.; Chapman & Hall, Ltd.).

319 (215) *Die Kreiselpumpen,* C. Pfleiderer (Julius Springer, Berlin).

320 (216) *The Influence of the Number of Impeller Blades, etc.,* W. J. Kearton (Proc. I. Mech. E., Vol. 124, 1933, p. 481).

320 (217) *Investigations concerning Flow Conditions in a Centrifugal Pump,* by J. F. Peck (Proc. I. Mech. E., Vol. 164, 1951, p. 1).

320 (218) *Head and Flow Observations on a High-efficiency Free Centrifugal Pump Impeller,* by W. C. Osborne and D. A. Morelli (Trans. A.S.M.E., Vol. 72, 1950, p. 999).

321 (219) *Leakage Loss and Axial Thrust in Centrifugal Pumps,* Alexey J. Stepanoff (Trans. A.S.M.E., Vol. 54, 1932, p. 65).

§ No.

322 (220) *Centrifugal and other Non-positive Pumps*, by R. Pennington (Proc. I. Mech. E., Vol. 157, 1947, p. 340).

325 (221) *Hydraulic Efficiency of Rotodynamic Pumps*, by G. G. MacDonald (Trans. Inst. Engineers and Shipbuilders of Scotland, Vol. 94, 1950-51, p. 77).

325 (222) *Centrifugal Pump Characteristics*, T. Y. Sherwell and R. Pennington (Proc. I. Mech. E., Vol. 123, Dec., 1932, p. 621).

330 (223) *The Law of Similitude for Flow Problems: Its Experimental Verification, etc.* (Sulzer Technical Review, 1947, No. 1, p. 15).

331 (224) *Dimensional Analysis and the Performance of Centrifugal Pumps*, J. Jennings (The Engr., Vol. CLXVII, 19th May, 1939, p. 614).

332 (225) *The Influence of Viscosity on Centrifugal Pump Performance*, by A. J. Ippen (Trans. A.S.M.E., Vol. 68, 1946, p. 823).

332 (226) *Use of Scale Models*, R. W. Allen (Engg., Vol. CXLVI, 26th Aug., 1938, p. 243).

333 (227) *Graphical Analysis of Pressure-Surge in Pumping Systems*, by H. R. Lupton (Jour. Inst. Water Engrs., Vol. 7, No. 2, March, 1953, p. 87).

333 (228) *Controlling Pine-Line Surges by Means of Air Vessels*, by J. S. Blair (Proc. I. Mech. E., Vol. 153, 1945, p. 1).

333 (229) *Elements of Graphical Solution of Water-hammer Problems, etc.*, by A. J. Stepanoff (Trans. A.S.M.E., Vol. 71, 1949, p. 515).

333 (230) *Water-Hammer in Pumping Mains* (Engg., Vol. CXLIII. 1937, p. 64).

335 (231) *Observations of Cavitation in Radial Centrifugal Pumps*, by R. Dziallas (Z.V.D.I., 20th Jan., 1945, No. 3/4, p. 41). See also Engineers' Digest, 1946, p. 251.

336 (232) *Cavitation in Centrifugal Pumps*, by A. J. Stepanoff (Trans. A.S.M.E., Vol. 67, 1945, p. 539).

336 (233) *Instruction and Research in Hydraulic Laboratories*, by Herbert Addison (Proc. I. Mech. E., Vol. 1B, 1952–53, No. 9, p. 401).

337 (234) *Centrifugal Pumps for Steam Power Stations*, by R. Pennington (Proc. I. Mech. E., 1952, Vol. IB, No. 4, p. 129).

338 (235) *Recent Land Drainage Pumping Stations*, by G. McLeod (Jour. Inst. Water Engrs., Vol. 4, 1950, p. 469).

338 (236) *The Design of Large Pumping Installations for Low and Medium Heads*, by G. A. Wauchope and H. P. Humphreys (Proc. I. Mech. E., 1951, Vol. 65, p. 229).

338 (237) *Kreiselpumpen zum Fordern von Schlamm und Abwasser*, R. Dziallas (Z.V.D.I., Vol. 81, 1937, p. 258).

338 (238) *The Evolution of the Waterworks Booster Pump*, by J. P. Hallam (Trans. Inst. Water Engrs., Vol. 49, 1944, p. 242).

339 (239) *Modern Methods of Raising Water from Underground Sources*, R. S. Allen and W. E. W. Millington (Proc. I. Mech. E., Vol. 120, 1931, p. 337).

§ No.

339 (240) *Submersible Pumps and Motors*, by W. L. Gardiner (Water and Water Engineering, Vol. 51, Nov., 1948, p. 531).

340 (241) See ref. (233), § 336. See also *Water-Ring Self-Priming Pumps*, by E. Crewdson (Proc. I.Mech.E., 1956).

CHAPTER XVII

§ No.

341 (242) *A Study of the Theory of Axial-flow Pumps*, by G. F. Wislicenus (Trans. A.S.M.E., Vol. 67, 1945, p. 451).

342 (243) *The Design of Propeller Pumps and Fans*, M. P. O'Brien and R. G. Folsom (University of California Press, Berkeley, 1939).

347 (244) *Velocity Distribution in Rotodynamic Pump Casings*, by H. Addison and Ramadan Sadek (The Engr., Vol. 186, 1948, pp. 459, 484).

348 (245) *The Cavitation Limit in Centrifugal Pumps and Water Turbines*, by C. Pfleiderer (Z.V.D.I., Vol. 92, 11th Aug., 1950, p. 629). See also The Engineers' Digest, Vol. 12, Jan., 1951, p. 9.

348 (246) *On Cavitation in Centrifugal Pumps*, C. von Widdern (Escher-Wyss News, Jan.-Mar., 1936, p. 14).

349 (247) *Operating-cost Analysis of Electrified Oil Lines*, W. H. Stueve (Trans. A.S.M.E., Vol. 59, 1937, p. 247).

349 (248) *The Reconstruction of Brimsdown "A" Power Station* (The Engr., Vol. CLXVII, 1939, p. 643).

349 (249) *Relation Between the Starting Torques of Pumps and Electric Motors* (Sulzer Technical Review, 1934, No. 4, p. 20).

350 (250) *The Economics of Pumping*, by G. W. Fuller (Jour. Inst. Water Engrs., Vol. II, 1948, p. 418).

350 (251) *The Pump Users' Handbook*, compiled by H. Addison (Sir Isaac Pftman).

350 (252) *Renewal and Extension of Pumping Machinery for the Metropolitan Water Board*, by M. R. James (Jour. Inst. C.E., Oct., 1946, p. 432).

CHAPTER XVIII

§ No.

352 (253) *Glenfield-Lockheed Remote Control* (Engg., Vol. 151, 1941, p. 43).

352 (254) *Oil Hydraulic Power and its Industrial Applications*, by Walter Ernst (McGraw-Hill Book Co.).

353 (255) *Fluid Pressure Mechanisms*, by H. G. Conway (Sir Isaac Pitman). See also *Conference on Hydraulic Machines* (The Institution of Mechanical Engineers, 1954).

353 (256) *Problems of the Gear Motor*, by M. Haubenhofer (Schweizerisches Bauzeitung, 24th July, 1948, p. 411).

353 (257) *A Hydraulic Motor* (The Eng., Vol. 195, 1953, p. 114).

354 (258) *Hydraulic Accumulators in Heavy Industry*, by J. G. Firth (Proc. I.Mech.E., 1956).

355 (259) *The Parallel Development of Hydraulic Presses in the United States and Great Britain*, by F. H. Towler (Trans. A.S.M.E., July, 1949, p. 501).

§ No.

356 (260) *Hydraulics in Agricultural Engineering,* by H. J. Hamblin (Engg., Vol. 173, 1953, pp. 605, 637).

356 (261) *Principles of Servo-Mechanisms,* by G. S. Brown and D. P. Campbell (John Wiley : Chapman & Hall).

356 (262) *Conference on Hydraulic Servo-Mechanisms* (The Institution of Mechanical Engineers, 1953).

356 (263) *Powered Flying Controls : Some Design Considerations,* by F. J. Bradbury and S. M. Parker (Proc. I. Mech. E., Vol. 1B, No. 4, 1952, p. 99).

356 (264) *Some Recent Advances in Mechanical Engineering on Shipboard,* by T. A. Crowe (Proc. I. Mech. E., Vol. 158, 1948, p. 264).

357 (265) *Recent Developments in the Use of Hydraulic Power,* H. C. Town (Proc. I. Mech. E., Vol. 143, May, 1940, p. 129).

357 (266) *Hydraulic Handbook* (Trade and Technical Press, Ltd.).

358 (267) See ref. (2), § 5.

358 (268) *Hydraulic Systems and Oils* (Shell Petroleum Co.).

358 (269) *Pipe Joints for Hydraulic Power Transmission,* by B. Cooke (Proc. I. Mech. E., Vol. 164, 1951, p. 308).

358 (270) *Control Valves for Direct-Hydraulic Presses,* by F. H. Towler and J. M. Towler (Proc. I. Mech. E., (B) 1952-53, Vol. 1B, No. 9, p. 420).

359 (271) *The Modern Direct-Hydraulic System,* by F. H. Towler (Proc. I. Mech. E., Vol. 154, 1946, p. 178). See also The Engr., Vol. 179, 1945, p. 400.

360 (272) *Some Problems in the Transmission of Power by Fluid Couplings,* H. Sinclair (Proc. I. Mech. E., Vol. 139, 1938, p. 83).

364 (273) *Torque Converters or Transmissions,* by P. M. Heldt (Nyack, N.Y.).

364 (274) *Progress in the Design of the Lysholm-Smith Torque-Converter,* H. F. Haworth and A. Lysholm (Proc. I. Mech. E., 1935, Vol. 130, p. 193). See also *Development of the Lysholm-Smith Torque Converter,* by A. Lysholm (Trans. A.S.M.E., Vol. 66, 1944, p. 343).

364 (275) *Automatic Transmissions in America,* by Charles A. Chayne (Proc. I. Mech. E., A.D. 1952-53, part 1, p. 9).

365 (276) *Large Capacity Hydraulic Dynamometer* (The Engr., Vol. 195, 1953, p. 560).

366 (277) *Pumped-Storage Stations,* by Arthur Koepchek (Water Power, Vol. 1, No. 6, 1949. p. 232). See also *Pump Storage Systems,* by A. Voska (Water Power, Vol. 2 ; 1950, pp. 137, 209).

368 (278) *La Construction en Italie . . . de Pompes pour Installations d'Accumulation,* by Guido Uccelli (Fourth World Power Conference, London, 1950, Section H/3, Paper No. 4).

368 (279) *The Hydraulic Storage Pumps of the Etzel Hydro-Electric Power Scheme* (Sulzer Technical Review, 1951, No. 3, p. 1).

§ No.

368 [280] *Reversible Pump Turbine* (Water Power, Vol. 5, May, 1953, p. 197).

369 [281] *Interesting Extension to a Swiss Hydraulic Power Plant* (Sulzer Technical Review, 1944, No. 1, p. 14).*

369 [282] *The Hydro-Electric Commission* (Hobart, Tasmania).

CHAPTER XIX

§ No.

[283] *Hydraulic Measurements,* H. Addison (Chapman & Hall).

370 [284] *A Monograph of Viscometry,* by Guy Barr (Oxford University Press).

371 [285] *Viscometry,* by A. C. Merrington (Edward Arnold).

371 [286] British Standard Specification No. 188, *Determination of Viscosity in Absolute Units.*

377 [287] *Mechanical Water-level Recording Instruments,* A. Linford (Civil Engineering, Vol. XXXVI, June, 1941, p. 491).

380 [288] *Pitot-Tube Practice,* E. S. Cole (Trans. A.S.M.E., Vol. 57, Aug., 1935, p. 281).

380 [289] *Measurement of Velocity and Pressure in 3-dimensional Flow,* by F. F. Krisam (Proc. A.S. Civ. E., Vol. 69, Sept., 1943, p. 22).

381 [290] *Effect of Turbulence on the Registration of Current Meters,* D. L. Yarnell and F. A. Nagler (Proc. A.S. Civ. E., Vol. 55, Dec., 1929, p. 2611).

385 [291] *Flow over Sharp-edged Weirs: Effect of Thickness of Crest,* by A. H. Jameson (Jour. Inst. C.E., Nov., 1948, p. 36). See also *Weirs for Flow Measurement in Open Channels,* by F. V. A. Engel and W. Stainsby (Water and Water Engineering, April-August, 1958).

385 [292] *A Weir with Flow proportional to Head,* by Edward Gerald Smith (Eng. News Record, Vol. 131, 29th July, 1943, p. 198). See also *Sutro Weir Investigations furnish Discharge Coefficients,* by E. Soucak, etc. (Eng. News Record, Vol. 117, 12th Nov., 1936, p. 679).

386 [293] *Flow Measurement and Meters,* by A. Linford (E. & F. N. Spon, Ltd.).

387 [294] *Discharge Measurements by Means of Venturi Tubes,* by A. L. Jorissen (Trans. A.S.M.E., Vol. 73, 1951, p. 403).

387 [295] *The Coefficients of Herschel Type Cast-Iron Venturi Meters,* by W. S. Pardoe (Trans. A.S.M.E., Vol. 67, 1945, p. 339).

388 [296] *British Standard 1042: 1943. Code for Flow Measurement* (The British Standards Institution). See also *Flow Measurement with Orifice Meters,* by R. F. Stearns, etc. (D. van Nostrand Co. Inc., N.Y.).

388 [297] *Fluid Meters* (The American Society of Mechanical Engineers).

BIBLIOGRAPHY

§ No.

389 (298) *The Use of Pipe Bends as Flow Meters,* H. Addison (Engg., Vol. CXLV, 4th Mar., 1938, p. 227).

393 (299) *Water Meters for Domestic and Small Trade Supplies* (Water and Water Engineering, Vol. 51, Nov., 1948, p. 506).

393 (300) *Some Experiences with Water Meters,* by H. Addison (The Engr., Vol. 173, 1942, p. 391).

395 (301) *Flow Measurement in Pipeline* (Water Power, Vol. 1, 1949, p. 199). See also Water Power, Vol. 4, 1952, p. 210.

395 (302) *New Equipment for Salt-Velocity Flow Measurement,* by W. H. P. Leslie and J. J. Hunter (Mechanical Engineering Research Laboratory, Fluids Report No. 62, March, 1959). See also *Comparison of Flow-measuring Techniques at Kinlochleven Hydro-Electric Station,* by F. A. L. Winternitz (Mechanical Engineering Research Laboratory, Fluids Report No. 65, March, 1958).

396 (303) See ref. (149), § 229.

397 (304) *Stream Flow,* by N. C. Grover and A. W. Harrington (Chapman & Hall, Ltd.).

397 (305) *The Measurement of the Discharges of the River-Basins, etc.,* by R. F. Wileman and H. W. Clark (Jour. Inst. C.E., April, 1946, p. 267).

398 (306) *Discharge by Surface Floats,* W. M. Griffith (Jour. Inst. C.E., Feb., 1941, p. 284).

400 (307) *A New Method of Gauging . . . by Means of a Submerged Weir,* by E. S. Crump (Proc. Inst. C.E., March, 1952, p. 283).

400 (308) See ref. (19), § 51.

400 (309) *The Venturi Flume,* F. V. A. E. Engel (The Engr., Vol. CLVIII, 1934, pp. 104, 131).

400 (310) *A Venturi Flume for Measuring the Flow of the River Derwent,* by W. W. Emms (Jour. Inst. Water Engrs., July, 1948, Vol. II, p. 392).

402 (311) See Trans. A.S.M.E., Vol. 54, 1932, HYD. 54-3, p. 27.

SOME BRIEF BIOGRAPHICAL NOTES

These notes are in no sense comprehensive; they are only intended to suggest how much the art and practice of Hydraulic Engineering owes to the efforts of mathematicians, scientists and engineers in many countries.

ALLIEVI, L. (-1942). Italian scientist, who, from 1895 onwards, made many contributions to the study of water-hammer in pipes.

ARCHIMEDES (287-212 (?) B.C.). Celebrated Greek philosopher and inventor. It is said that he devised the Archimedean screw for emptying the hold of a ship, but that he held such mechanisms in very low esteem.

BAZIN, Henri-Emile (1829-1917). French engineer, noted for his experiments on the Burgundy canal, near Dijon, and for his experimental work on weirs. He carried forward the work begun by H. Darcy.

BERNOULLI, Daniel (1700-83). Born at Basle, he came of a renowned Swiss mathematical family. His numerous writings included a treatise on Hydrodynamics.

BORDA, Jean Charles (1733-99). Officer in the French Army and Navy, a mathematician and nautical astronomer, he conducted also researches in Hydrodynamics.

BRAMAH, Joseph (1749-1814). Born in Yorkshire, he invented the Bramah lock, perfected the sluice-valve, and invented the beer pump as used in inns and hotels. He patented the hydraulic press in 1795, using for the first time the "U"-leather packing.

CHEZY, Antoine de (1718-98), French engineer and mathematician. Among other high offices he held in Paris was that of Director of the Polytechnic School. In the formula for open-channel flow that bears his name, he expounded in 1775 a new principle that was hitherto unrecognised.

CORIOLIS, Gustave Gaspard (1792-1843). French mathematician, best known for his work on Mechanics.

DARCY, H. P. G. (1803-58). This French engineer, the Inspector-General of the Paris waterworks, conducted an extensive series of experiments on the flow of water in pipes.

EULER, Leonhard (1707-83). Renowned Swiss mathematician, who studied at Basle and taught at St. Petersburg and Berlin.

FRANCIS, James B. (1815-92). Born in England, this engineer went to the United States in 1833, where he made large-scale experiments on the flow along channels and over weirs, and developed the inward-flow turbine that now bears his name.

FROUDE, William (1810-79). English scientist and engineer, who first began the practice of towing models of ships in tanks constructed for the purpose. He experimented also on flat surfaces towed through water, and on screw propellers.

SOME BRIEF BIOGRAPHICAL NOTES

KAPLAN, Victor (1876-1934). Austrian engineer and professor at Brunn. He patented the adjustable-blade turbine in 1913, and put into service the first practical Kaplan turbine in 1919.

KUTTER, W. R. (1818-88), Swiss geometer, who in 1870 published a new formula for the flow in pipes and channels.

MANNING, Robert (1816-97), Irish engineer, who spent his professional life in Dublin. In 1889, he presented before the Institution of Civil Engineers of Ireland his paper on " The Flow of Water in Open Channels and Pipes ".

PELTON, Lester Allen (1829-1908), American engineer and inventor, who in 1850 began gold-mining in California. In his efforts to improve the machines then in use in the gold-fields, he finally evolved the type of impulse turbine that now bears his name. This design was patented in 1880.

PITOT, Henri (1695-1771), French scientist and engineer. He carried out many important works, including a celebrated aqueduct, in southern France; he studied the manœuvring of ships; and he was responsible for making known the principle of the Pitot-tube.

POISEUILLE, Jean-Louis-Marie (1799-1869), French doctor, anatomist, and physiologist. In connection with his studies on the flow of blood through veins and arteries, he made experiments on which he based laws of friction in capillary tubes. These laws, first enunciated in 1844, were later confirmed analytically. The *Poise*, the unit of viscosity, is named after him.

REHBOCK, Theodor von (1864-1950). Born in Amsterdam, he became, in 1899, professor at the Karlsruhe (Germany) Technical High School, where he organised extensive hydraulic laboratories.

REYNOLDS, Osborne (1842-1912). Born at Belfast, Northern Ireland, he became the first Professor of Engineering at Owens College (later the University of Manchester). There he demonstrated the difference between laminar and turbulent flow in pipes, he applied the principles of geometrical and dynamical similarity to the flow in models of tidal estuaries, and investigated the principles of lubrication.

STOKES, Sir George Gabriel (1819-1903). While Lucasian Professor of Mathematics at Cambridge, he propounded many important principles and theories in physics, electricity, and hydromechanics.

THOMA, D. (1881-1943), German hydraulic engineer, professor at the Munich Technical High School.

VENTURI, Giovanni Battista (1746-1822), Italian scientist, engineer and diplomat, who conducted hydraulic research and construction in Italy and France. But the metering device that bears his name was introduced in 1887 by the American engineer Clemens Herschel, who gave it the title " Venturi meter " out of respect for Venturi's earlier achievements.

INDEX

The numbers refer to *Paragraphs* (§§) unless otherwise stated.

The numbers refer to *Paragraphs* (§§) unless otherwise stated.

INDEX

The numbers refer to *Paragraphs* (§§) unless otherwise stated.

The numbers refer to *Paragraphs* (§§) unless otherwise stated.

INDEX

The numbers refer to *Paragraphs* (§§) unless otherwise stated.

The numbers refer to *Paragraphs* (§§) unless otherwise stated.

INDEX

The numbers refer to *Paragraphs* (§§) unless otherwise stated.

The numbers refer to *Paragraphs* (§§) unless otherwise stated.

INDEX

The numbers refer to *Paragraphs* (§§) unless otherwise stated.

The numbers refer to *Paragraphs* (§§) unless otherwise stated.